

# **RIKEN Accelerator Progress Report**

2008

vol. **42**

BOOK & CD-ROM

独立行政法人理化学研究所 仁科加速器研究センター  
**RIKEN Nishina Center for Accelerator-Based Science**



**RIKEN Accelerator Progress Report** 2008

vol. **42**

BOOK & CD-ROM

独立行政法人理化学研究所 仁科加速器研究センター  
**RIKEN Nishina Center for Accelerator-Based Science**  
**Wako, Saitama, 351-0198 JAPAN**

**Chairperson of the Editorial Committee**

**H. En'yo**

**Editorial Committee**

<b>H. Okuno</b>	<b>K. Yoneda</b>
<b>S. Nishimura</b>	<b>K. Morimoto</b>
<b>A. Kohama</b>	<b>M. Wada</b>
<b>T. Kubo</b>	<b>H. Sato</b>
<b>Y. Kobayashi</b>	<b>T. Tada</b>
<b>T. Kambara</b>	<b>T. Abe</b>
<b>Y. Uwamino</b>	<b>K. Yazaki</b>
<b>K. Ishida</b>	<b>T. Ichihara</b>
<b>S. Michimasa</b>	
<b>Y. Sakata</b>	<b>Y. Iwata</b>

**All rights reserved. This report or any part thereof may not be reproduced in any form (including photostatic or microfilm form) without written permission from the publisher.**

**All reports are written on authors' responsibility and thus the editors are not liable for the contents of the report.**

# GRAVURES & HIGHLIGHTS OF THE YEAR

K. Morita <i>et al.</i> .....	i
Decay properties of $^{266}\text{Bh}$ and $^{262}\text{Db}$ produced in the $^{248}\text{Cm} + ^{23}\text{Na}$ Reaction – Further confirmation of the $^{278}113$ decay chain –	
SLOWRI Collaboration (M. Wada <i>et al.</i> ) .....	vii
RF multipole devices play important roles in SLOWRI experiments: Hyperfine spectroscopy of $^7\text{Be}^+$ and new type of ion crystals in an RF octupole ion trap (PP. 18 and 230)	
T. Ohnishi <i>et al.</i> .....	viii
Discovery 20 new isotopes by in-flight fission of 345 MeV/u $^{238}\text{U}$	
T. Nakagaewa <i>et al.</i> .....	ix
Status of the RIKEN 28GHz Superconducting ECR ion source	
S. Ishii, Y. Hayashi, H. Ryuto, N. Fukunishi, and T. Abe .....	xi
A new cultivar "Nishina Zaou" induced by heavy ion beam irradiation	
T. Suda <i>et al.</i> .....	xii
Demonstration of electron scattering using the SCRIT prototype	
D. Kaji <i>et al.</i> .....	xiii
Production and decay properties of $^{263}\text{Hs}$	
A. Takamine <i>et al.</i> .....	xiv
Precision optical transition measurements for $^{7,9,10,11}\text{Be}^+$ ions	
D. Kameda <i>et al.</i> .....	xv
Observation of new neutron-rich short-lived isomers among fission products of 345 MeV/nucleon $^{238}\text{U}$	
Y. Funaki, T. Yamada, H. Horiuchi, G. Röpke, P. Schuck and A. Tohsaki ...	xvi
$\alpha$ -Particle Condensation in $^{16}\text{O}$ Studied with a Full Four-Body Orthogonality Condition Model Calculation	
K. Hashimoto, T. Sakai, and S. Sugimoto .....	xvii
Holographic Baryons : Static Properties and Form Factors from Gauge/String Duality	
R. Koyama <i>et al.</i> .....	xviii
Nondestructive monitoring system of RF fields and beam-phase/intensity for stable operation of RIBF	
C. Torii <i>et al.</i> .....	xx
A series of asexual mutants and partial deletion of the Y-chromosome by heavy ion beam in <i>Silene latifolia</i>	

### 《Selection process of gravures and highlights》

Gravures and highlights will be selected in two-steps process. In the first step, referee will recommend manuscript for gravure or highlight. With the above recommendation, the editors will then give secondary recommendation.

After the following 1 and 2 are comprehensively considered, the editor-in-chief will draft a manuscript idea which will be thoroughly discussed by the editors for the final decision:

1. Approval based on the editor's judgement as an expert/non-expert in the field (thereby agreeing with the referee's recommendation)
2. Additional recommendation based on the editor's expertise.

## Decay properties of $^{266}\text{Bh}$ and $^{262}\text{Db}$ produced in the $^{248}\text{Cm} + ^{23}\text{Na}$ reaction – Further confirmation of the $^{278}113$ decay chain –

K. Morita, K. Morimoto, D. Kaji, H. Haba, K. Ozeki, Y. Kudou, N. Sato,<sup>\*1,\*2</sup> T. Sumita,<sup>\*3</sup> A. Yoneda, T. Ichikawa,<sup>\*4</sup> Y. Fujimori,<sup>\*5</sup> S. Goto,<sup>\*6</sup> E. Ideguchi, Y. Kasamatsu,<sup>\*7,\*8</sup> K. Katori, Y. Komori,<sup>\*9</sup> H. Koura,<sup>\*7</sup> H. Kudo,<sup>\*10</sup> K. Ooe,<sup>\*9</sup> A. Ozawa,<sup>\*11</sup> F. Tokanai,<sup>\*5</sup> K. Tsukada,<sup>\*7</sup> T. Yamaguchi,<sup>\*12</sup> and A. Yoshida

[ $^{266}\text{Bh}$ ,  $^{262}\text{Db}$ ,  $\alpha$ -decay, spontaneous fission, gas-filled recoil ion separator, position-sensitive focal plane detector]

A nuclide,  $^{266}\text{Bh}$ , is the great-granddaughter of  $^{278}113$  that is produced in the  $^{209}\text{Bi} + ^{70}\text{Zn}$  reaction<sup>1,2)</sup>. Thus far, only five atoms have been assigned to  $^{266}\text{Bh}$  by direct production<sup>3,4)</sup> partly because of the small production cross section and of the difficulty in finding proper target/beam combinations. Most of the heaviest odd-odd nuclei exhibit rather complicated decay properties. Therefore, it is difficult to obtain a clear assignment of heavy odd-odd nuclides such as  $^{266}\text{Bh}$ . In the present work, we performed an experiment with the aim of obtaining an unambiguous assignment of  $^{266}\text{Bh}$  by a genetic link. The main purpose of this work is to provide further confirmation of the production and identification of the isotope  $^{278}113$ . For this purpose, we used a gas-filled recoil ion separator (GARIS) coupled to a position-sensitive focal plane detector (PSD).  $^{266}\text{Bh}$  was produced for the first time in the  $^{248}\text{Cm} + ^{23}\text{Na}$  reaction.

The experiment was performed at the RIKEN Linear Accelerator (RILAC) Facility. A schematic view of the experimental setup is shown in Fig. 1. A photo picture of GARIS is shown in Fig. 2

A  $^{248}\text{Cm}_2\text{O}_3$  target having a thickness of  $350 \mu\text{g}/\text{cm}^2$  was prepared by electrodeposition onto a titanium backing foil ( $0.91 \text{ mg}/\text{cm}^2$ ). Six pieces of the target were mounted on a rotating wheel having a diameter of 10 cm. During irradiation, the wheel was rotated at 1000 rpm.

A  $^{23}\text{Na}$  beam was extracted from RILAC. Beam energies of 126, 130 and 132 MeV were used. The corresponding beam energies at the middle of the target were 121, 124 and 126 MeV respectively. The  $^{23}\text{Na}$  beam had a pulsed structure. All the measurements

were performed only in the beam OFF period. The typical beam intensity was 1 particle- $\mu\text{A}$  on average, and it was 4.4 particle- $\mu\text{A}$  in the beam ON period.

GARIS was used to collect evaporation residues (ERs) and separate them from the beam particles and other unwanted charged particles. GARIS was filled with helium gas at a pressure of 33 Pa. The  $B\rho$  of GARIS was set at 2.07 Tm for beam energies of 132 and 130 MeV to maximize the yield of  $^{266}\text{Bh}$ . At beam energies of 126 MeV and a part of 132 MeV,  $B\rho$  was set at 2.19 Tm to reduce the counting rate of the focal plane detector to one half.

ERs were transported to the focal plane of GARIS where the PSD was set. The arrangement of the focal plane detector is shown in Fig. 1.

An example of a singles spectrum is shown in Fig. 3. The spectrum was obtained from one strip in one run with a beam dose of  $3.1 \times 10^{17}$ . In the energy region below 8 MeV,  $\alpha$  lines from long-lived transfer products are observed, while in the region from 8 to 12 MeV, only one event that was assigned to an  $\alpha$  decay of  $^{266}\text{Bh}$  was detected.

The reduction in the number of transfer products and target recoils at the focal plane, that is achieved by using the physical pre-separator, GARIS and the high spatial resolving power of the PSD, enables a low background  $\alpha$ -SF correlation measurements. The  $\alpha$ -SF correlation measurement would be difficult to perform using only the gas-jet technique.

Other experimental details are described in the original paper. We performed offline analyses to search for mother-daughter correlations, i.e.  $\alpha$ - $\alpha$  and  $\alpha$ -SF events, based on the position in PSD, energy, and time difference.

We have assigned total of 32 correlations to true ones. Four of the events are  $\alpha_1$ - $\alpha_2$ - $\alpha_3$  correlations, one is an  $\alpha_1$ - $\alpha_2$ -SF, nine are  $\alpha_1$ - $\alpha_2$  and eighteen are  $\alpha_1$ -SF correlations. The maximum correlation time was set to 300 s.

A two-dimensional representation of the time- and position-correlated events is shown in Fig. 4. The horizontal and vertical axes represent the mother and daughter energy, respectively. The lower and upper panels (Figs. 4-a and 4-b) show the  $\alpha$ - $\alpha$  and  $\alpha$ -SF correlations, respectively.

The excitation energies of the compound nucleus,

† Condensed from the article in J. Phys. Soc. Jpn. **78**, 064201 (2009)

\*1 Department of Physics, Tohoku University

\*2 Present address: Japan Atomic Energy Agency

\*3 Faculty of Science and Technology, Tokyo University of Science

\*4 Present address: Yukawa Institute for Theoretical Physics, Kyoto University

\*5 Department of Physics, Yamagata University

\*6 Center for Instrumental Analysis, Niigata University

\*7 Japan Atomic Energy Agency

\*8 Present address: RIKEN Nishina Center

\*9 Department of Chemistry, Osaka University

\*10 Department of Chemistry, Niigata University

\*11 University of Tsukuba

\*12 Department of Physics, Saitama University

$^{271}\text{Bh}$ , at the middle of the target were calculated to be 44.4, 48.1 and 49.9 MeV for beam energies of 126, 130 and 132 MeV, respectively, by using a theoretical mass for  $^{271}\text{Bh}$ <sup>5)</sup>. The energies were selected to maximize the  $5n$  evaporation channel in the  $^{248}\text{Cm} + ^{23}\text{Na}$  reaction. Because the ER cross sections of these asymmetric reactions in the heaviest region exhibit a broad peaks around the optimum energies that produce the maximum yields, the isotope  $^{267}\text{Bh}$ , which is a product of the  $4n$  evaporation channel of the reaction, could be produced in considerable amounts, especially at lower excitation energies. We focused on these two isotopes in the analyses. The direct productions of  $^{262}\text{Db}$  and  $^{263}\text{Db}$  were not considered because of the reaction in the sub-barrier energy region.

### $\alpha$ - $\alpha$ correlations

In the correlations shown in Fig. 4-a, eight points are plotted in Group C. The mother energies of these events range from 8.40 to 8.74 MeV, and those of the corresponding daughters range from 8.57 to 8.80 MeV. We assigned these events to the  $^{262}\text{Db} \rightarrow ^{258}\text{Lr} \rightarrow$  decay. The obtained  $T_{1/2}$  in this work agrees very well with the adopted value<sup>6)</sup>. It should be noted that the  $\alpha$  energies obtained in this work are approximately 40–60 keV higher than the adopted energies<sup>6)</sup>. This is most probably attributable to the summing of  $\alpha$ -energy and a conversion electron or  $\gamma$ -ray energy, which is emitted simultaneously with the  $\alpha$ -decay in the cases of odd and odd-odd nuclei<sup>7)</sup>.

Because of a shift in energy and the limited energy resolution caused by the summing effect, one event in Group C could be assigned to the decay of  $^{263}\text{Db} \rightarrow ^{259}\text{Lr} \rightarrow$  as well as that of  $^{262}\text{Db} \rightarrow ^{258}\text{Lr} \rightarrow$ , referring the reported half-life and  $\alpha$ -decay energy of  $^{263}\text{Db}$ <sup>8)</sup> and those of  $^{259}\text{Lr}$ <sup>9)</sup>, respectively.

Three of the eight correlations in Group C are the second part ( $\alpha_2$ - $\alpha_3$ ) of the triple correlations ( $\alpha_1$ - $\alpha_2$ - $\alpha_3$ ). All the preceding correlations ( $\alpha_1$ - $\alpha_2$ ) are in Group A, as shown in Fig. 4-a, along with four additional  $\alpha_1$ - $\alpha_2$  correlations. Because of the genetic correlation to the  $^{262}\text{Db} \rightarrow ^{258}\text{Lr} \rightarrow$  decay, these three triple correlation events in Group A are conclusively identified as the correlations of  $^{266}\text{Bh} \rightarrow ^{262}\text{Db} \rightarrow ^{258}\text{Lr} \rightarrow$  decays. The other four correlations are identified as those of the  $^{266}\text{Bh} \rightarrow ^{262}\text{Db} \rightarrow$  decay or the  $^{266}\text{Bh} \rightarrow (^{262}\text{Db} \rightarrow \text{missing}) ^{258}\text{Lr} \rightarrow$  decay partly because the daughter energies agree well with the adopted decay energies of  $^{262}\text{Db}$  and  $^{258}\text{Lr}$  considering the above mentioned summing effect. The mean time differences between the  $\alpha_1$  and  $\alpha_2$  decays of the seven correlations in this group are calculated to be  $34^{+20}_{-10}$  s. The corresponding  $T_{1/2}$  is  $24^{+14}_{-7}$  s. This value is attributable to a mixture of the  $^{266}\text{Bh} \rightarrow ^{262}\text{Db} \rightarrow$  and  $^{266}\text{Bh} \rightarrow (^{262}\text{Db} \rightarrow) ^{258}\text{Lr} \rightarrow$  decays. Including this mixture effect, the value agrees well with the adopted half-lives

of  $^{262}\text{Db}$  and  $^{258}\text{Lr}$ . The observed  $\alpha$ -decay energies of  $^{266}\text{Bh}$  range from 9.05 to 9.23 MeV. The correlations observed and assigned here agree well with those reported by Wilk *et al.*<sup>3)</sup> and Qin *et al.*<sup>4)</sup>.

One  $\alpha_1$ - $\alpha_2$  correlation of the triple  $\alpha$  correlation exists in Group B, as shown in Fig. 4-a. The corresponding  $\alpha_2$ - $\alpha_3$  correlation exists in Group C, suggesting that the correlations in Group B also correspond to the decay  $^{266}\text{Bh} \rightarrow ^{262}\text{Db} \rightarrow ^{258}\text{Lr} \rightarrow$ . The energies of  $\alpha_2$  and  $\alpha_3$  agree well with the reported values for  $^{262}\text{Db}$  and  $^{258}\text{Lr}$  mentioned above. The observed  $\alpha$  energy of  $^{266}\text{Bh}$  assigned here is 8.83 MeV. Although the value just coincides with the decay energy of  $^{267}\text{Bh}$  reported by Wilk *et al.*<sup>3)</sup>, because of the observed decay characteristics, we assigned the correlated event to the decay of  $^{266}\text{Bh} \rightarrow ^{262}\text{Db} \rightarrow ^{258}\text{Lr} \rightarrow$ .

One additional correlation exists in Group B, as shown in Fig. 4-a. This could be also assigned to the decay of  $^{266}\text{Bh} \rightarrow ^{262}\text{Db} \rightarrow ^{258}\text{Lr} \rightarrow$  because of the similarity with the energies and decay times of the correlation assigned above. However, based on the  $\alpha_1$ - $\alpha_2$  correlation analysis, assignment to the decay of  $^{267}\text{Bh} \rightarrow (^{263}\text{Db} \rightarrow) ^{259}\text{Lr} \rightarrow$  is also possible if the summing effect is considered. Therefore, this correlation could not be assigned conclusively.

$\alpha_1$ - $\alpha_2$  of one  $\alpha_1$ - $\alpha_2$ -SF triple correlation is classified in a circle marked by D in Fig. 4-a. Here, the mother and daughter energies and the time difference between these decays, along with the followed SF decay, are fully consistent with the decay of  $^{267}\text{Bh} \rightarrow ^{263}\text{Db} \rightarrow ^{259}\text{Lr}$  (SF)<sup>3,9)</sup>. We then assign this correlation to the decay originating from  $^{267}\text{Bh}$ .

### $\alpha$ -SF correlations

The three correlated events in Group E in Fig. 4-b correspond to the  $\alpha_1$  energies of Group A (9.05–9.23 MeV). The corresponding half-life  $T_{1/2}$  deduced from the three events agrees well with that of  $^{262}\text{Db}$ . Therefore, we assign these correlated events to SF decays of  $^{262}\text{Db}$  fed by 9.05–9.23 MeV  $\alpha$ -decays of  $^{266}\text{Bh}$ .

Eight correlations are observed in Group F in Fig. 4-b. No  $\alpha$ -decays are observed in the  $\alpha_1$ - $\alpha_2$  correlations in this energy range, as shown in Fig. 4-a. The observed  $T_{1/2}$  is slightly longer than the reported  $T_{1/2}$  values of both  $^{262}\text{Db}$  and  $^{263}\text{Db}$ . Two  $\alpha$ -decay events having an energy of around 8.96 MeV were reported by Qin *et al.*<sup>4)</sup>, and these are assigned to the decay of  $^{266}\text{Bh} \rightarrow ^{262}\text{Db} \rightarrow$ . However, their experimental setup was not sensitive to the  $\alpha$ -SF correlations. The  $\alpha$ -decays having an energy of around 8.96 MeV observed in the present work fed a state in the daughter that decays mainly by SF with  $T_{1/2}$  of  $59^{+32}_{-15}$  s. This  $\alpha$ -decay could be tentatively assigned to the  $^{266}\text{Bh} \rightarrow ^{262}\text{Db}$  (SF) decay. However, the possibility of assignment to the  $^{267}\text{Bh} \rightarrow ^{263}\text{Db}$  (SF) decay could not be excluded. It should be noted that half the correlations were observed at the lowest incident energy.

One correlation exists in Group G, as shown in Fig. 4-b, along with the  $\alpha_1(-\alpha_2)$ -SF correlation that was assigned to the decay of  $^{267}\text{Bh} \rightarrow ^{263}\text{Db} \rightarrow ^{259}\text{Lr} \rightarrow$  in the present study. The  $\alpha_1$  energy and the SF decay time agree well with those of the correlation. Then, it is natural to assign this correlation to the decay of  $^{267}\text{Bh} \rightarrow ^{263}\text{Db}$  (SF) or  $^{267}\text{Bh} \rightarrow ^{263}\text{Db} \rightarrow ^{259}\text{Lr}$  (SF). However, we have assigned one correlation having almost the same  $\alpha_1$  energy to the decay of  $^{266}\text{Bh}$  (Group B in Fig. 4-a), suggesting that the correlation might still be assigned to the decay of  $^{266}\text{Bh}$ .

Three correlations exist in Group H in Fig. 4-b. The deduced  $T_{1/2}$  of the SF decay is  $44^{+55}_{-15}$  s. One decay chain having a decay energy of 8.73 MeV was assigned to the decay of  $^{267}\text{Bh}$  by Wilk *et al.*<sup>3)</sup>. These correlations can possibly be assigned to the decay of  $^{267}\text{Bh} \rightarrow ^{263}\text{Db}$  (SF) or  $^{267}\text{Bh} \rightarrow (^{263}\text{Db} \rightarrow) ^{259}\text{Lr}$  (SF).

Two correlations exist in Group I in Fig. 4-b. The  $\alpha$ -decay energy of the mother is approximately 8.43 MeV. One of these correlations is the  $\alpha_2$ -SF part of the triple  $\alpha_1$ - $\alpha_2$ -SF correlation. We have assigned this correlation to the decay of  $^{267}\text{Bh} \rightarrow ^{263}\text{Db} \rightarrow ^{259}\text{Lr}$  (SF). The other correlation could also be the decay of  $^{263}\text{Db} \rightarrow ^{259}\text{Lr}$  (SF). We could tentatively assign these correlations to the decay mentioned above although the deduced SF half-life of  $^{259}\text{Lr}$  is slightly longer than the adopted value.

Two correlations exist in Group J in Fig. 4-b. We could not assign these correlations.

### 9.05–9.23 MeV $\alpha$ decay of $^{266}\text{Bh}$

An isotope of the 107th element,  $^{266}\text{Bh}$ , which decays by  $\alpha$ -emission with an energy ranging from 9.05 to 9.23 MeV, was conclusively identified by the present study. A state in the daughter nuclei  $^{262}\text{Db}$ , fed by the  $\alpha$ -decay, decays by  $\alpha$ -emission and SF. In the observed decay chains of the isotope of the 113th element,  $^{278}113$ , studied by the RIKEN group<sup>1,2)</sup>, one of the great-granddaughters decayed by  $\alpha$ -emission with a decay energy of 9.08 MeV and decay time of 2.47 s, followed by SF. The assignment was based on an experimental result of the work done by Wilk *et al.*<sup>3)</sup> that reported one atom of  $^{266}\text{Bh}$  assigned by the sequential  $\alpha$  decays  $^{262}\text{Db} \rightarrow ^{258}\text{Lr} \rightarrow$ . The present work provided further confirmation of the assignment of  $^{266}\text{Bh}$  observed in a decay chain originating from  $^{278}113$  by demonstrating the observation of the same decay energy, as well as the observation of SF decays following the relevant  $\alpha$ -decay of  $^{266}\text{Bh}$ . A decay chain, which is attributed to be the one originating from the isotope  $^{266}\text{Bh}$  obtained in the present work is shown in Fig. 5, together with the one from the isotope  $^{278}113$  produced in the  $^{209}\text{Bi} + ^{70}\text{Zn}$  reaction.

Although a decay time analysis was performed in the macro beam OFF period, because of the small counting statistics, we could only state that the half-life is longer than 1 s.

This research was partly supported by a Grant-in-Aid for Specially Promoted Research, 19002005, from the Ministry of Education, Culture, Sports, Science and Technology, Japan.

### References

- 1) K. Morita et al.: J. Phys. Soc. Jpn. **73** 2593 (2004).
- 2) K. Morita et al.: J. Phys. Soc. Jpn. **76** 045001 (2007).
- 3) P. A. Wilk et al.: Phys. Rev. Lett. **85** 2697 (2000).
- 4) Z. Qin et al.: Nuclear Physics Review **23** 400 (2006), (Chinese journal in English).
- 5) P. Möller et al.: Atomic Data and Nuclear Data Tables **59** 185 (1995).
- 6) R. Dressler et al.: Phys. Rev. C **59** 3433 (1999).
- 7) M. Asai et al.: Phys. Rev. Lett. **95** 102502 (2005).
- 8) J. V. Kratz et al.: Phys. Rev. C **45** 1064 (1992).
- 9) K. E. Gregorich et al.: Phys. Rev. C **45** 1058 (1992).

## RIKEN Gas-filled Recoil Ion Separator GARIS

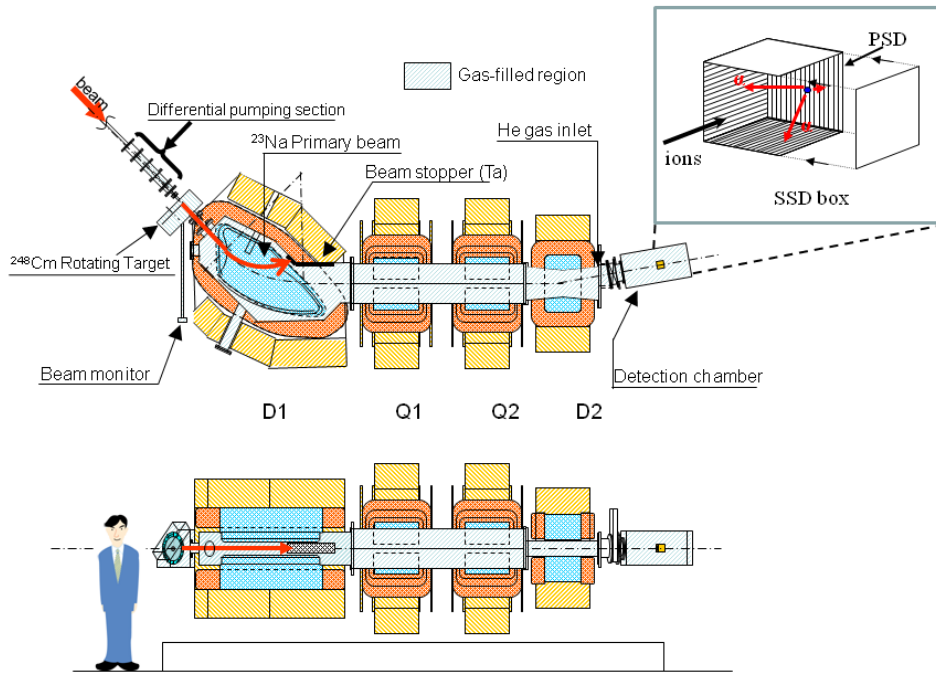


Fig. 1. Schematic view of the experimental setup.

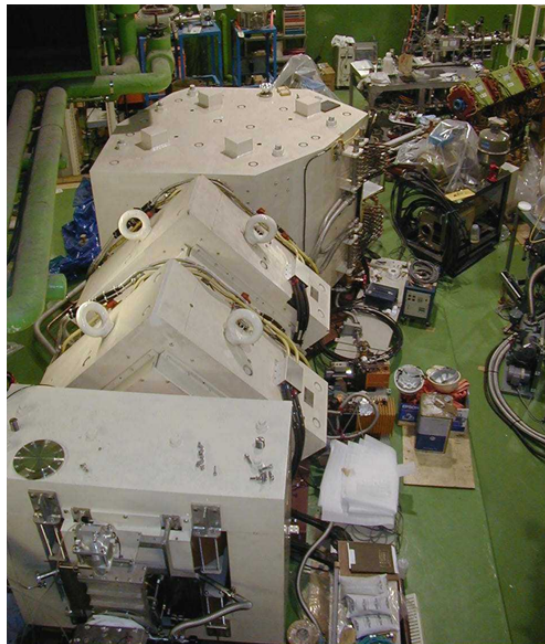


Fig. 2. Photo picture of GARIS.

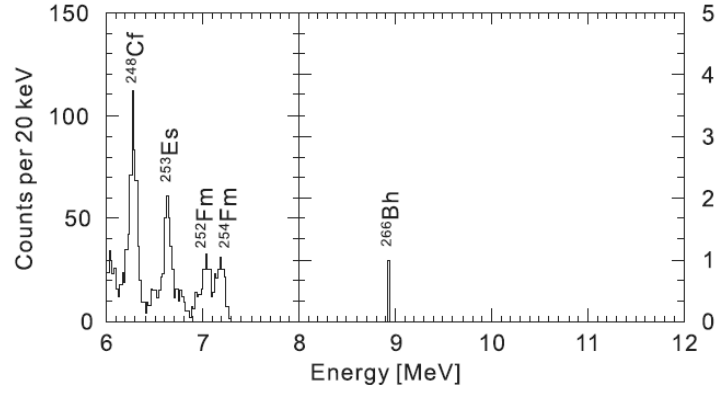


Fig. 3. Example of a singles spectrum. The 7th strip among 16 (0-15) in the PSD was used. The measurement time was 16.4 h for a beam dose of  $3.1 \times 10^{17}$ .

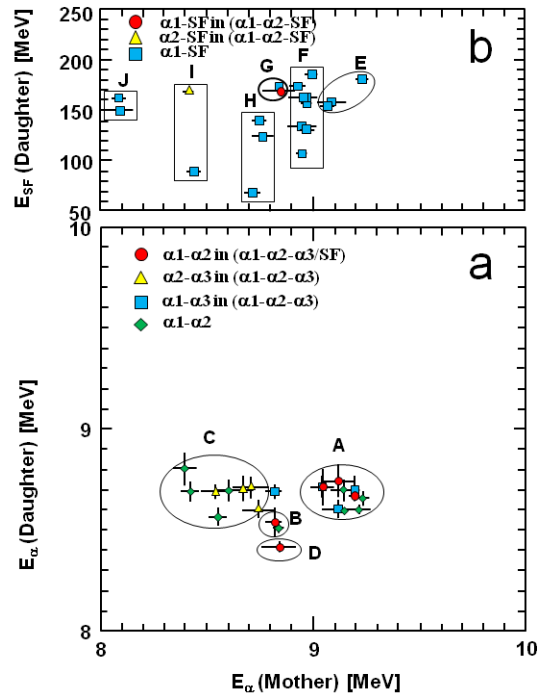


Fig. 4. Two-dimensional representation of time- and position-correlated events. The lower panel (a) shows the  $\alpha$ - $\alpha$  correlations. The upper panel (b) shows the  $\alpha$ -SF correlations. The time window was set to 300 s.



## RF multipole devices play important roles in SLOWRI experiments: Hyperfine spectroscopy of ${}^7\text{Be}^+$ and new type of ion crystals in an RF octupole ion trap (PP. 18 and 230)

SLOWRI Collaboration

Developments of a universal slow RI-beam facility (SLOWRI) are in progress. At the prototype SLOWRI, radioactive Beryllium ions provided from the projectile fragment separator RIPS at  $\approx 1$  GeV were decelerated by an energy degrader and RF ion guide gas cell and trapped in a linear RF quadrupole ion trap. They were further cooled by laser radiation down to  $1 \mu\text{eV}$ . This large kinetic energy reduction, a factor of  $10^{-15}$ , allowed for precision hyperfine structure spectroscopy (Fig. 1).

In this experiment, one of the key devices is an RF octupole ion beam guide made of carbon fiber reinforced plastic (Carbon-OPIG) (Fig. 2). This device transports slow ions extracted from an RF-carpet towards an ion trap through five differential pumping sections, from 1 mbar to  $10^{-9}$  mbar.

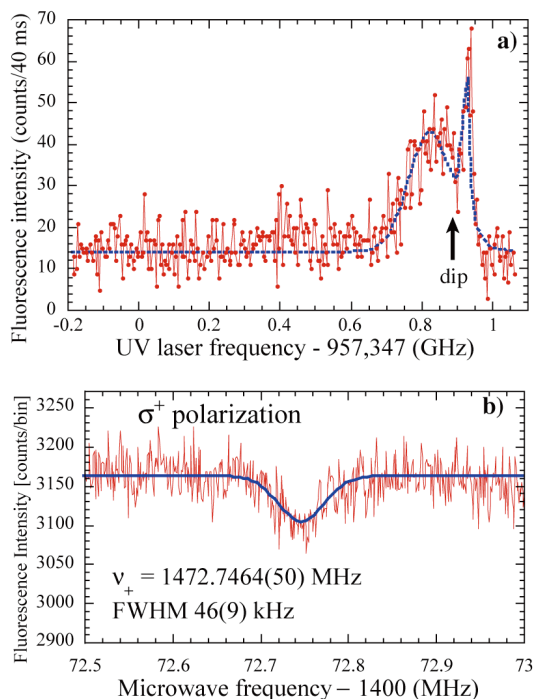


Fig. 1. Laser cooling spectrum (a) and microwave resonance spectrum (b) of  ${}^7\text{Be}^+$ .

A linear RF octupole ion trap (Fig. 3) was also tested off-line with  $\text{Ca}^+$  ions at Sophia university. Due to the unique pseudo potential form in the octupole trap, ion Coulomb crystals with large concentric shells containing large number of ions were observed for the first time.

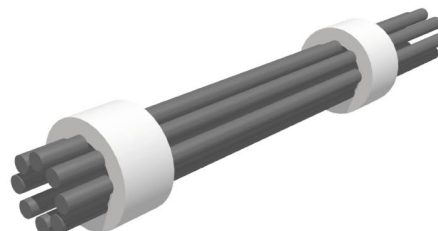


Fig. 2. Carbon-OPIG. Transverse DC electric field due to resistive rods transports ions even in 1 mbar pressure region.

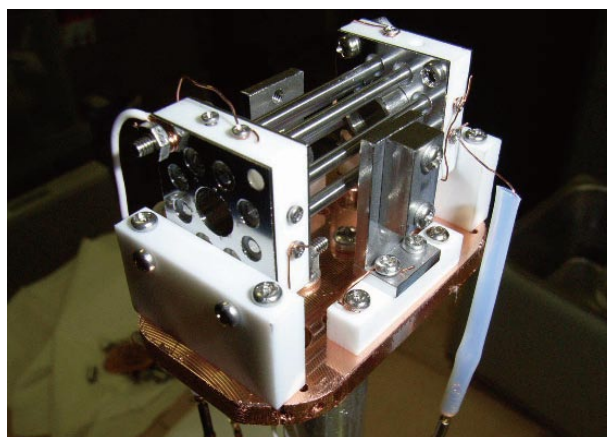


Fig. 3. Linear RF octupole ion trap. High order multipole field produces large quasi-field free region in the middle of the trap.

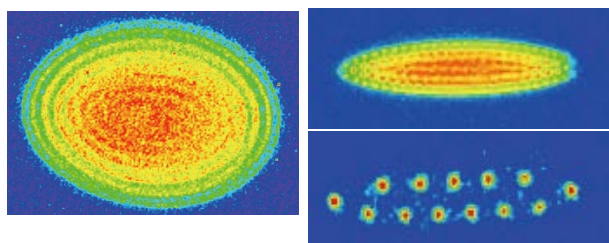


Fig. 4. Observed ion crystal images in the trap. Different type of crystals were formed depending on the trap conditions. A small potential hill at the center of the trap due to field penetration from the axial trapping potential produced large concentric shell structures.

## Discovery of 20 new isotopes by in-flight fission of 345MeV/u $^{238}\text{U}$

T. Ohnishi, N. Inabe, T. Kubo, K. Kusaka, A. Yoshida, K. Yoshida, M. Ohtake, N. Fukuda, H. Takeda, D. Kameda, K. Tanaka, Y. Yanagisawa, H. Watanabe, H. Otsu, Y. Kondo, Y. Gono, H. Sakurai, T. Motobayashi, H. Baba, T. Ichihara, Y. Yamaguchi, M. Takechi, S. Nishimura, H. Ueno, A. Yoshimi, T. Nakao,<sup>\*1</sup> M. Matsushita,<sup>\*2</sup> K. Ieki,<sup>\*2</sup> N. Kobayashi,<sup>\*3</sup> K. Tanaka,<sup>\*3</sup> Y. Kawada,<sup>\*3</sup> N. Tanaka,<sup>\*3</sup> S. Deguchi,<sup>\*3</sup> Y. Sato,<sup>\*3</sup> T. Nakamura,<sup>\*3</sup> K. Yoshinaga,<sup>\*4</sup> C. Ishii,<sup>\*4</sup> H. Yoshii,<sup>\*4</sup> N. Uematsu,<sup>\*4</sup> Y. Shiraki,<sup>\*4</sup> T. Sumikama,<sup>\*4</sup> J. Chiba,<sup>\*4</sup> E. Ideguchi,<sup>\*5</sup> T. Yamaguchi,<sup>\*6</sup> I. Hachimura,<sup>\*6</sup> T. Suzuki,<sup>\*6</sup> T. Moriguchi,<sup>\*7</sup> A. Ozawa,<sup>\*7</sup> T. Ohtsubo,<sup>\*8</sup> M. Famiano,<sup>\*9</sup> A. S. Nettleton,<sup>\*10</sup> B. M. Sherrill,<sup>\*10</sup> S. Manikonda,<sup>\*11</sup> and J. A. Nolen<sup>\*11</sup>

A new-isotope-search experiment has been performed by using the reaction of  $^{238}\text{U}$  (345MeV/u) +Be and Pb. Almost 20 isotopes were newly identified owing to significant improvement in the intensity and stability of the primary  $^{238}\text{U}$  beam after the last new-isotope-search in 2007.<sup>1)</sup>

The  $^{238}\text{U}$  beam accelerated up to 345 MeV/u by using RILAC-RRC-fRC-IRC-SRC was irradiated onto production targets and produced isotopes were collected and selected at the first stage of the BigRIPS. New isotopes with a wide range of A and Z were covered by three measurements with the BigRIPS settings optimized for isotopes with  $Z=20\sim 36$  (G1),  $Z=37\sim 46$  (G2) and  $Z=47\sim 54$  (G3). For each group, the target and Bp were determined by Monte-Carlo simulation of LISE++.<sup>2)</sup> The determined targets were Be 5.1 mm for G1, Be 3.0 mm for G2 and Pb 0.95 mm for G3. For G3 a 0.3 mm Al stripper was also located after the target to increase fully stripped isotopes. The Bp values are 7.902 Tm for G1, 7.931 Tm for G2, and 7.706 Tm for G3. Al degraders (1.29 mm for G1, 2.18 mm for G2, 2.56 mm for G3) were located at F1 to eliminate unwanted isotopes and reduce the total trigger rate.

Particle identification (PID) was performed at the second stage of the BigRIPS using PPACs at F3, F5 and F7, plastic scintillators at F3 and F7 and an ion chamber at F7. To confirm PID we also measured  $\gamma$ -rays from known isomers ( $^{95}\text{Kr}$  for G1 and G2 and  $^{136}\text{Sb}$  for G3) using Ge detectors located at F11 in the ZeroDegree spectrometer. For G3 only an Al degrader was inserted at F5 to cut hydrogen-like ions produced in the degrader at the first stage.

Figure 1a~c shows preliminary result of A/Q vs. Z plots for G1, G2 and G3. Three isotopes in G1 ( $^{81}\text{Cu}$ ,  $^{84}\text{Zn}$ ,  $^{87}\text{Ga}$ ), 14 isotopes in G2 ( $^{103}\text{Rb}$ ,  $^{106}\text{Sr}$ ,  $^{111}\text{Zr}$ ,  $^{114}\text{Nb}$ ,  $^{116,117}\text{Mo}$ ,  $^{119}\text{Tc}$ ,  $^{121,122}\text{Ru}$ ,  $^{123,124,125}\text{Rh}$ ,  $^{127,128}\text{Pd}$ ) and 3 isotopes in G3 ( $^{138}\text{Sn}$ ,  $^{140}\text{Sb}$ ,  $^{145}\text{I}$ ) can be clearly seen. Detailed analysis is in progress.

<sup>\*1</sup> Department of Physics, The University of Tokyo

<sup>\*2</sup> Department of Physics, Rikkyo University

<sup>\*3</sup> Department of Physics, Tokyo Institute of Technology

<sup>\*4</sup> Department of Physics, Tokyo University of Science

<sup>\*5</sup> Center for Nuclear study, The University of Tokyo

<sup>\*6</sup> Department of Physics, Saitama University

<sup>\*7</sup> Institute of Physics, University of Tsukuba

<sup>\*8</sup> Department of Physics, Niigata University

<sup>\*9</sup> Physics Department, Western Michigan University

<sup>\*10</sup> Michigan State University (MSU)

<sup>\*11</sup> Argonne National Laboratory (ANL)

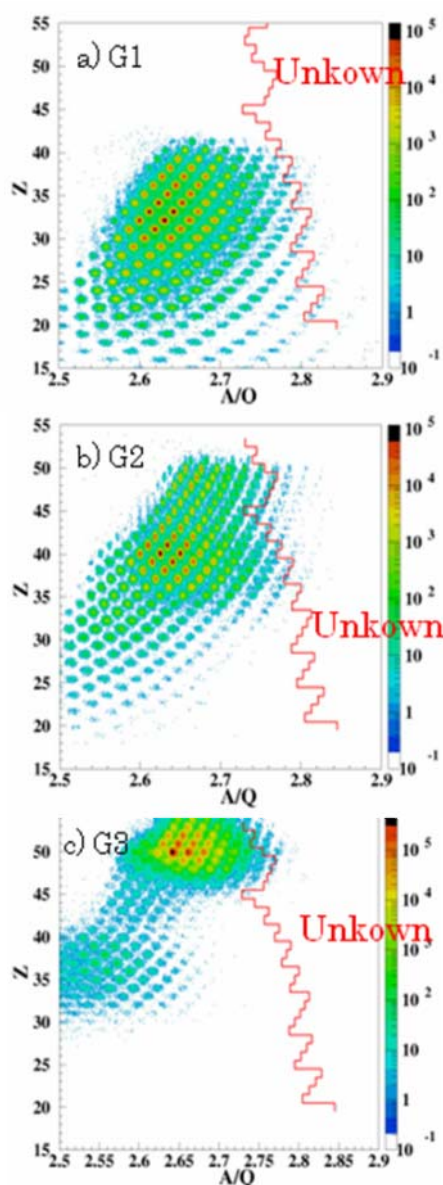


Figure1. A/Q vs Z polts. a) for G1, b) for G2 and c) for G3

### References

- 1) T. Ohnishi et al.: Jpn. J. Phys. Soc. Jpn. **77**, 083201 (2008).
- 2) O. B. Tarasov and D. Bazin: a manual of the code LISE++ available at <http://www.nsl.msu.edu/lise/>.

## Status of the RIKEN 28GHz Superconducting ECR ion source

T. Nakagawa, Y. Higurashi, J. Ohnishi, H. Okuno, K. Kusaka, M. Kidera, E. Ikezawa, M. Fujimaki, Y. Sato, Y. Watanabe, M. Komiyama, M. Kase, A. Goto, O. Kamigaito, and Y. Yano

Since the middle of the 1990s, RIKEN has been constructing a new accelerator facility called the Radio Isotope Beam Factory (RIBF)<sup>1)</sup> and a 345MeV/u U beam was successfully produced in 2007. However, to meet the requirements of the RIBF project (primary beam intensity of 1  $\mu$ A on target), we still need to increase the beam intensity of heavy ions. For this reason, we began construction of a new superconducting ECR ion source (SC-ECRIS) with an operational frequency of 28 GHz in 2007.

Before designing the ECRIS, we intensively studied effects of the key components of ECRIS (magnetic field, RF power, etc.) on plasma conditions and beam intensity. In the 1990s, it was found that a high mirror ratio of magnetic field gives the increase of beam intensity for higher charge states of heavy ion (High B mode operation).<sup>2)</sup> This is mainly due to a strong confinement of plasma. Since we observed in 2001 that the minimum strength of mirror magnetic field ( $B_{\min}$ ) strongly affects the beam intensity,<sup>3)</sup> we have systematically studied this effect. In this study, we observed that an optimum  $B_{\min}$  ( $(B_{\min})_{\text{opt}}$ ) exists for maximizing the beam intensity and it is almost constant ( $0.7\sim 0.9B_{\text{cet}}$ ).<sup>4)</sup> To investigate the mechanism, we used the laser ablation technique to obtain important plasma parameters (electron density, electron temperature and ion confinement time)<sup>5)</sup> and observed that  $B_{\min}$  strongly affects microwave absorption in the resonance zone.<sup>6)</sup> In order to investigate the plasma chamber size effect on the beam intensity of highly charged heavy ions, we compared the beam intensity produced from several high performance ECRISs which have different chamber size. In this comparison, we recognized that the chamber diameter should be larger than 10 cm to produce an intense beam of highly charged U ions.<sup>6)</sup>

Based on these considerations, we designed the new SC-ECRIS for the RIKEN RI beam factory project. To produce intense beam of  $\text{U}^{35+}$  ions, we will need to satisfy the following conditions

- 1) Magnetic field configuration: Maximum mirror magnetic field strength on RF injection side ( $B_{\text{inj}}$ )  $> 3.5$  T, maximum radial magnetic field strength ( $B_r$ )  $> 2$  T, maximum magnetic field strength at beam extraction side ( $B_{\text{ext}}$ )  $> 2$  T,  $B_{\min} \sim 0\sim 1$  T.
- 2) Plasma chamber size: Diameter  $> 10$  cm,
- 3) Microwave : Frequency, 28 GHz, power  $> 10$  kW (1 kW/L)
- 4) Size of resonance zone: There is no clear evidence of an ECR zone size effect on the beam intensity. If the size affects the beam intensity, we can increase the beam intensity by increasing size of the ECR zone. To clarify this effect, we adopted a special coil arrangement.

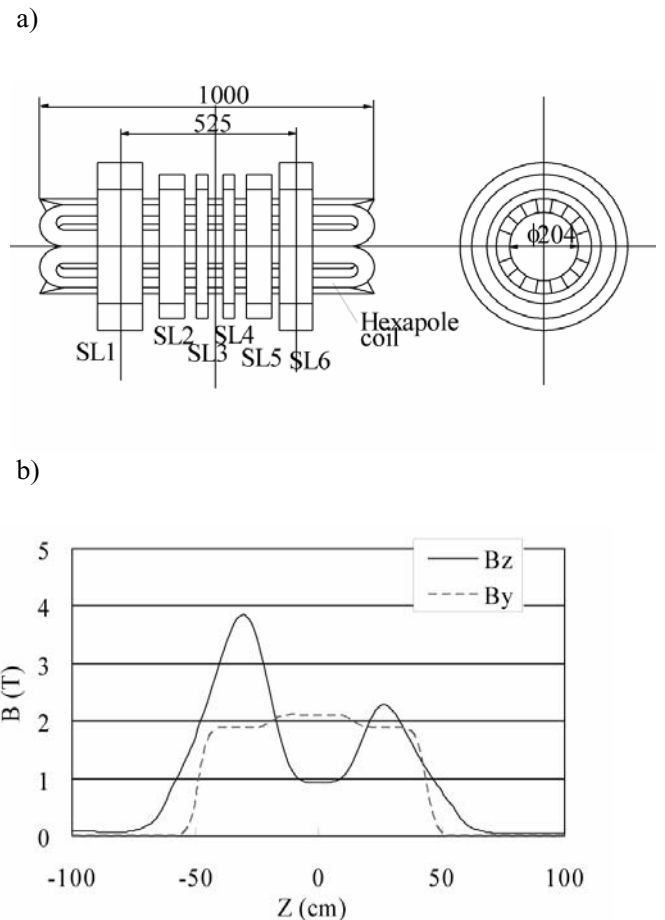


Fig. 1 a) Arrangement of the superconducting coil assembly. b) Axial ( $B_z$ ) and radial ( $B_y$ ) magnetic field strength

Figure 1a) shows the arrangement of the superconducting coil assembly. The coils are composed of six solenoid coils (SL1 ~ SL6) and one hexapole coil (HX). Figure 1b) shows the axial and radial magnetic field. Magnetic field strength was calculated by using the 3d-code "TOSCA". The peak fields on the RF injection side and beam extraction side are 3.8 T and 2 T, respectively. The minimum magnetic field can be changed from 0 T to 1 T. Four solenoid coils (SL2~SL5) work to produce a flat magnetic field in the central region for increasing the size of the ECR surface. The detailed structure and excitation test are described in Ref. 7. Figure 2 shows the ECR zone size vs.  $B_{\min}$ . Using this arrangement, we can produce large surface of ECR zone and change the surface size of the ECR zone without changing the field gradient.

Figure 3 shows a schematic drawing of the SC-ECR ion source. The inner diameter and length of the plasma chamber are 15 and 50 cm, respectively. The plasma chamber wall is made of Al to donate cold electrons to the

plasma and decrease plasma potential. It should be noted that Al is very resistant to plasma etching. A biased electrode is installed to obtain the same effect as that of the Al chamber wall. All the surfaces in contact with the plasma are water-cooled to minimize the temperature effects caused by plasma and microwave heating at high microwave power.

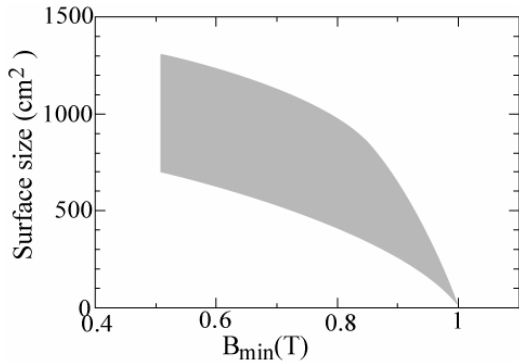


Fig. 2 ECR zone size vs.  $B_{\min}$

The expected total current from the ion source for production of  $15 \mu\text{A}$  of  $\text{U}^{35+}$  ion beam is higher than 10mA. Under this condition, we have to supply a very high extraction voltage (higher than 30 kV) to achieve good emittance (unnormalized emittance of  $\sim 150\pi \text{ mm} \cdot \text{mrad}$ ) for matching the acceptance of the RFQ linac. The ion

source will be equipped with a movable accel-decel extraction system not only to improve extraction conditions, but also to compensate for the space charge effect. After extraction at the maximum voltage of 40 kV, the solenoid coils are used to focus the beam. Design of the 90-degree analyzing magnet is based on the LBL magnet<sup>8)</sup>. The vertical gap is 150 mm and bending radius is 510 mm. These devices are installed on the high voltage terminal (maximum terminal voltage; 100 kV). The  $\text{U}^{35+}$  beam ( $\sim 130 \text{ q keV}$ ) will be transported to the first acceleration tank of Riken heavy ion linac through new beam line<sup>9)</sup>. By end of March, 2009, we will finish installing all devices (SC-ECRIS, analyzing magnet etc.) on the high voltage terminal and try to produce the first plasma with 18 GHz microwaves.

### References

- (1) Y. Yano: Nucl. Instrum. Methods B 2007 in press.
- (2) T. Antaya et al, Rev. Sci. Instrum. 65, 1723(1994).
- (3) H. Arai et al, Nucl. Instrum. Method. A491, 9(2002).
- (5) M. Imanaka et al, Nucl. Instrum. Method. B237, 647(2005).
- (6) T. Nakagawa et al, Rev. Sci. Instrum. 67, 02A327 (1996).
- (7) J. Ohnishi et al, : in this report.
- (8) D. Leitner et al, : 18th Int. Conf. Cyclotron and their Applications, Giardini Naxos, Sept. 2007, p265.
- (9) Y. Watanabe et al, : in this report.

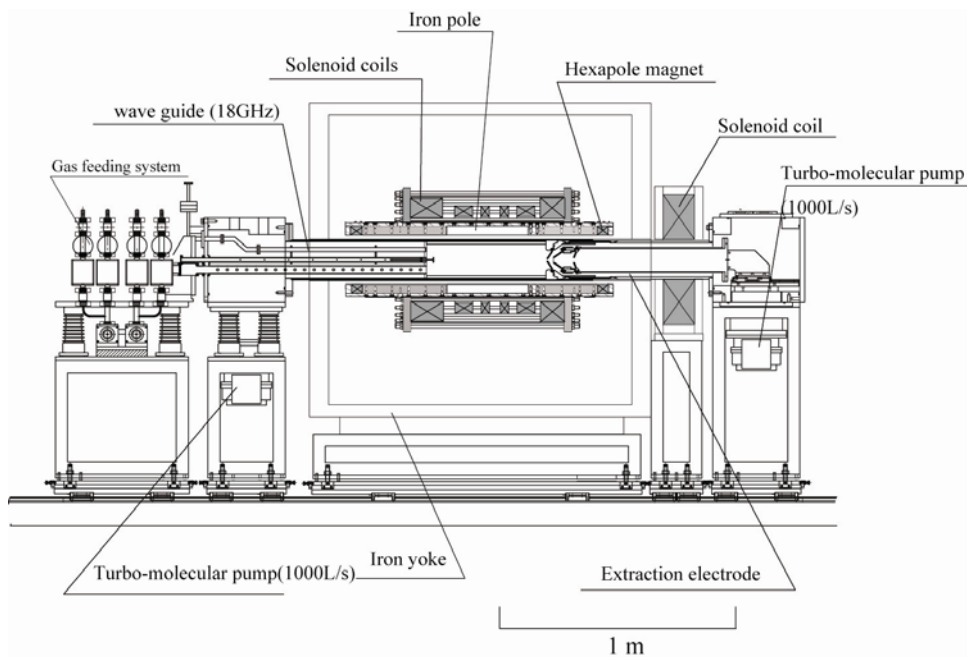


Fig.3. Schematic drawing of the RIKEN Sc-ECRIS

## A new cultivar “Nishina Zaou” induced by heavy ion beam irradiation

S. Ishii\*<sup>1</sup>, Y. Hayashi, H. Ryuto\*<sup>2</sup>, N. Fukunishi, and T. Abe

*Prunus lannesiana* ‘Gioiko’ is the only Japanese ornamental cherry variety that has a double flower with 10 to 12 petals. The color of flower changes from pale green to light purple during blooming time. Recently, heavy ion beams are recognized as an effective mutagen for plant breeding. A broad spectrum and a high frequency of mutation induction by heavy ion beam have proved in the case of rose<sup>1)</sup>. Some new cultivars of ornamental flowers induced by heavy ion treatment have been successfully developed and released to the market. In this report we describe the induction of a new cultivar of Japanese ornamental cherry using heavy ion beam irradiation.

The scions (approximately 150mm in length) of Gioiko were used for irradiation treatment. The doses of carbon beam irradiation (<sup>12</sup>C<sup>6+</sup>, 135MeV/u, LET 22.6keV/μm) were 10, 15 and 20Gy. The irradiated scions were grafted on the rootstock (*Prunus lannesiana* ‘Viridis’). Survival rate, a period from grafting scions on the rootstock to the first bloom, flower phenotypes (petal color, petal number and size of flower) were observed.

The survival rate decreased according as the increase of doses (Fig.1). At 20Gy irradiation, no plant survived. A flower colour mutant was isolated at 10Gy irradiation (Fig.2). The colour of mutant flower was pale yellow at the beginning of blooming time and then changed to yellowish pink. The color of the rims of petals was whitish green. The flower diameter was 40-50mm, which was 1.5 times larger than that of the original variety. The petal number was 7-8. The period from grafting to the first bloom of mutant line was one year but 3years in original variety (Fig.3). Reduction of the period from grafting to the first bloom is useful character for both breeding and commercialization of the new cultivar. These characters of this mutant line

were confirmed to be stable in the following season. This new cultivar was named “Nishina Zaou” by Dr. Noyori; the president of RIKEN in 2007. Nishina Zaou was released to the market in Nov. 2008.

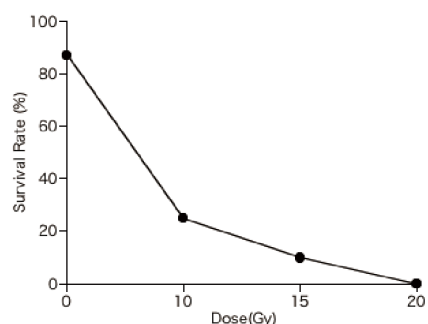


Fig. 1 Effect of C-ion irradiation on survival rate

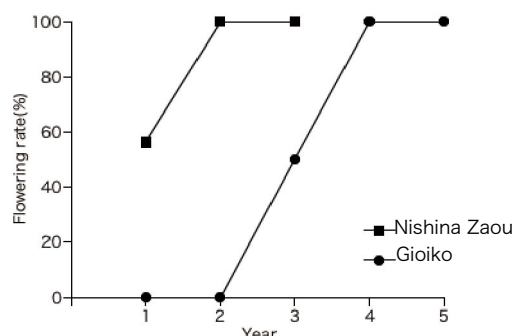


Fig. 3 Effect of C-ion irradiation on the period from grafting to the first bloom

### Reference

- 1) Y. Hara et al.:RIKEN Accel. Prog. Rep. **36**, 135 (2003).

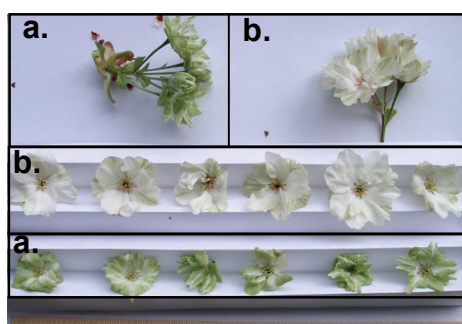


Fig. 2 Flower colour mutant.  
 a: Original flower (Gyoiko). b: Mutated flower.  
 c: Nishina Zaou planted in RIKEN (Wako). The scion was grafted in 2007, and the flower bloomed in April 2008.



\*1 JFC Ishii Garden

\*2 Photonics and Electronics Science and Engineering Center, Kyoto University

# Demonstration of electron scattering using the SCRIT prototype

T. Suda, T. Emoto, K. Ishii<sup>1</sup>, K. Kurita<sup>1</sup>, A. Kuwajima<sup>2</sup>, T. Tamae<sup>2</sup>, M. Wakasugi, and S. Wang

[SCRIT, elastic electron scattering, angular distribution]

We have continued SCRIT R&D studies at KSR this year. We have newly installed a large plastic scintillator for cosmic-ray rejection and an online luminosity monitoring system<sup>1</sup>). In this report, some progress we made this year are briefly presented.

Figure 1 shows electron energy spectra for the scattering angle of  $40^\circ$ . Figure 1a) and b) show those obtained the last year<sup>2</sup>) and this year, respectively. The solid (dotted) line denotes the spectrum with (without) the Cs ion injection. Clear difference between those with and without Cs ions  $80 \leq E_e \leq 120$  MeV are due to the elastic scattering events from the trapped Cs ions. The events above  $E_e \geq 120$  MeV have been attributed to those due to cosmic rays. It is seen that the cosmic ray events are well suppressed in Fig.1b), which enables us to identify elastic events reliably.

Figure 2 shows the change of event rate of elastic scattering in the 60-ms trapping time, equivalently the time dependence of the luminosity. Since the electron beam current,  $\sim 80$  mA, and its cross section are both almost constant, this figure shows the time dependence of the number of the trapped Cs ions on the electron beam. The line in the figure is a guide for the eye. One can conclude that the number of the trapped Cs ions decreases about 30 % during the trapping cycle.

Figure 3 denotes the angular distributions of the measured elastic scattering events already presented in Ref.<sup>2</sup>). The solid line in the figure represents a dis-

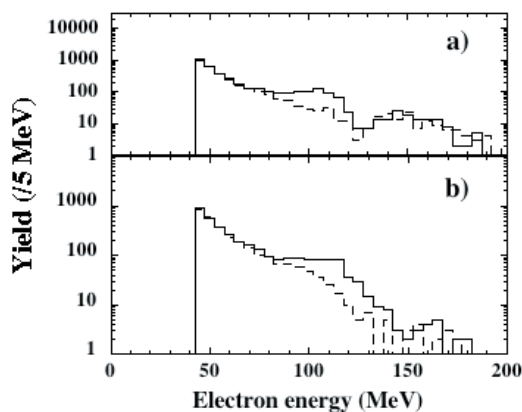


Fig. 1. The energy spectra for scattered electrons at  $\theta=40^\circ$  measured in the previous measurement<sup>2</sup>), a), and for this year, b). The solid (dashed) line shows the spectrum with (without) the Cs ion.

<sup>\*1</sup> Rikkyo University

<sup>\*2</sup> Tohoku University

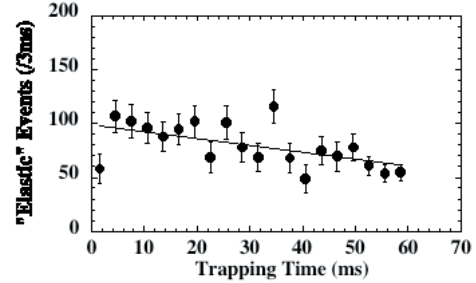


Fig. 2. Distribution of the elastic events as a function of the trapping time. The line is a guide for the eye.

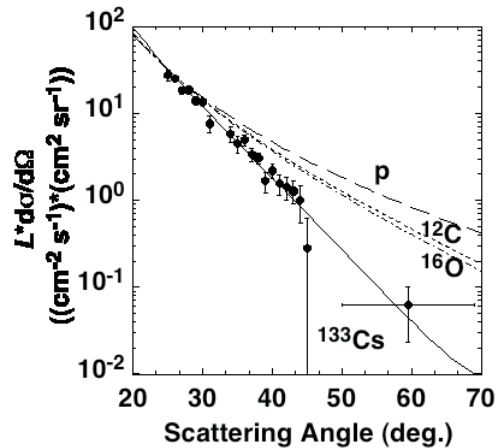


Fig. 3. The angular distribution of the elastic events. See the text for the lines.

torted wave calculation for elastic scattering off  $^{133}\text{Cs}$ . The dashed (dotted, dot-dashed) line represents the angular distribution of the elastic scattering for proton (carbon and oxygen), which are normalized to the data at a scattering angle of  $25^\circ$ . They are considered to be the main components of the residual gases in the ring to focus on the difference in angular dependence such as  $\text{H}_2$  and  $\text{CO}$ . The angular dependence clearly shows that the measured events are those of elastically scattered electrons from the trapped  $^{133}\text{Cs}$ <sup>3</sup>).

## References

- 1) S. Wang *et al.* : RIKEN Accel. Prog. Rep. 42 (2008).
- 2) SCRIT collaboration : T. Emoto *et al.* : RIKEN Accel. Prog. Rep. 41 (2007).
- 3) T. Suda *et al.* : submitted to Phys. Rev. Lett..

## Production and decay properties of $^{263}\text{Hs}^\dagger$

D. Kaji, K. Morimoto, N. Sato,<sup>\*1</sup> H. Haba, T. Ichikawa, E. Ideguchi,<sup>\*2</sup> H. Koura,<sup>\*3</sup> Y. Kudou, A. Ozawa,<sup>\*4</sup> K. Ozeki, T. Sumita,<sup>\*5</sup> T. Yamaguchi,<sup>\*6</sup> A. Yoneda, A. Yoshida, and K. Morita

[ $^{263}\text{Hs}$ , new isotope, hassium, GARIS]

A new neutron deficient hassium ( $Z=108$ ) isotope of  $^{263}\text{Hs}$  was identified via two different reactions of  $^{206}\text{Pb}(^{58}\text{Fe},n)$  and  $^{208}\text{Pb}(^{56}\text{Fe},n)$  by using the gas-filled recoil separator GARIS.

Projectiles of  $^{58}\text{Fe}$  and  $^{56}\text{Fe}$  with the charge state  $13^+$  were extracted from the 18-GHz ECR ion source and accelerated by RILAC (RIKEN Linear Accelerator). Beams of  $^{58}\text{Fe}$  with 287.7 MeV and  $^{56}\text{Fe}$  with 280.4 MeV were extracted from RILAC. Absolute accuracy of beam energy measurement was  $\pm 0.3$  MeV. The typical beam intensities on the target were  $4.5 \times 10^{12} \text{ s}^{-1}$  for  $^{58}\text{Fe}$  and  $2.3 \times 10^{12} \text{ s}^{-1}$  for  $^{56}\text{Fe}$ . The target was prepared by the vacuum evaporation of metallic  $^{206}\text{Pb}$  and  $^{208}\text{Pb}$  on a  $30 \mu\text{g}/\text{cm}^2$  carbon backing foil. The target thicknesses were  $400 \mu\text{g}/\text{cm}^2$  for  $^{206}\text{Pb}$  (enrichment of 99.3%) and  $440 \mu\text{g}/\text{cm}^2$  for  $^{208}\text{Pb}$  (enrichment of 98.4%). A thin carbon protection layer of approximately  $10 \mu\text{g}/\text{cm}^2$  covered the target surface on the downstream side. Sixteen targets were mounted on a  $\phi 30$  cm wheel, which rotated at 3000 rpm, to withstand the irradiation of high intensity beams. The reaction products were separated in flight from the beams by GARIS, and were guided into a detector box installed at the focal plane of GARIS. The separator was filled with helium gas at a pressure of 86 Pa. The magnetic rigidity  $B\rho$  was set to 2.05 Tm for  $^{263}\text{Hs}$  measurement, which was estimated using empirical data.<sup>1)</sup> The evaporation residue (ER) and its successive radioactive decays were measured by a system of time-of-flight (TOF) detectors and a silicon position-sensitive detector (PSD) array<sup>2)</sup> installed at the focal plane of GARIS. Identification of the products was based on the genetic correlations of mother and daughter nuclei. The singles counting rate of the PSD at the typical beam intensity was approximately 5 cps. The main components of the signals were due to target recoils and scattered beam particles. The counting rate of the decay signals (anti-coincidence with timing counters) was approximately 0.3 cps.

During 25-h irradiation of  $^{206}\text{Pb}$  with the  $^{58}\text{Fe}$  beam and 46-h irradiation of  $^{208}\text{Pb}$  with the  $^{56}\text{Fe}$  beam, 8

decay chains and 1 decay chain, respectively, were observed. No spontaneous fission was detected in the measurements followed directly after the ER implantation in the PSD. The properties of decay events obtained by irradiation of  $^{58}\text{Fe}$  on  $^{206}\text{Pb}$  match well with those by irradiation of  $^{56}\text{Fe}$  on  $^{208}\text{Pb}$ . All decay chains were assigned to subsequent decays from  $^{263}\text{Hs}$ . The decay data obtained in this work is summarized in Fig. 1. Three groups of  $\alpha$ -decay energies for  $^{263}\text{Hs}$  are identified. The mean  $\alpha$ -decay energies for the 3 groups are 10.82, 10.55, and 10.37 MeV, respectively. The half-life of  $^{263}\text{Hs}$  is determined to be  $0.60^{+0.30}_{-0.15}$  ms. In this experiment, the total beam doses for  $^{58}\text{Fe}$  and  $^{56}\text{Fe}$  were  $4.1 \times 10^{17}$  ions and  $6.2 \times 10^{17}$  ions, respectively. The production cross sections corresponding to the 8 decay chains and 1 decay chain have been deduced to be  $21^{+10}_{-8}$  pb and  $1.6^{+3.7}_{-1.3}$  pb by assuming the transmission of the system to be 80%.

The details of this experiment have described elsewhere.<sup>3,4)</sup>

### References

- 1) D. Kaji, Dr. Thesis, Graduate School of Science and Technology, Niigata University, Niigata (2003).
- 2) K. Morita, K. Morimoto, D. Kaji et al.: Eur. Phys. J. A 21, 257 (2004) .
- 3) D. Kaji, K. Morimoto, N. Sato et al.: J. Phys. Soc. Jap. 78, 035003 (2009).
- 4) N. Sato, Dr. Thesis, Graduate School of Science and Faculty of Science, Tohoku University (2009).

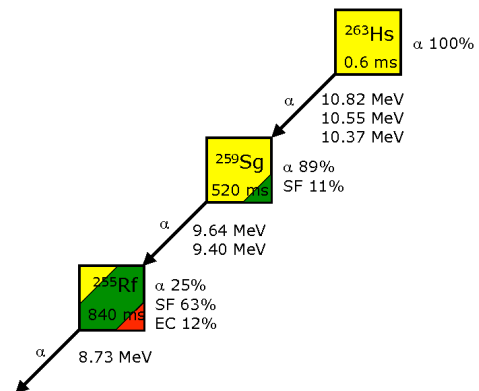


Fig. 1. Summary of decay chains observed in irradiation of  $^{206}\text{Pb}$  and  $^{208}\text{Pb}$  targets with  $^{58}\text{Fe}$  and  $^{56}\text{Fe}$  projectiles. Measured energies, decay times, and branching ratio are indicated in the figure.

<sup>†</sup> Condensed from the article in J. Phys. Soc. Jap. 78, 035003 (2009)

<sup>\*1</sup> Department of Physics, Tohoku University

<sup>\*2</sup> Center for Nuclear Study, University of Tokyo

<sup>\*3</sup> Advanced Science Research Center, Japan Atomic Energy Agency

<sup>\*4</sup> University of Tsukuba

<sup>\*5</sup> Faculty of Science and Technology, Tokyo University of Science

<sup>\*6</sup> Department of Physics, Saitama University

# Precision optical transition measurements for ${}^{7,9,10,11}\text{Be}^+$ ions

A. Takamine, M. Wada, T. Sonoda, T. Nakamura, K. Okada\*<sup>1</sup>, P. Schury, H. Iimura\*<sup>2</sup>, Y. Yamazaki, Y. Kanai, T. M. Kojima, A. Yoshida, T. Kubo, S. Ohtani\*<sup>3</sup>, I. Katayama\*<sup>4</sup>, H. Wollnik\*<sup>5</sup>, and H. A. Schuessler\*<sup>6</sup>

[neutron halo, charge radius, laser spectroscopy]

We have developed an online ion trap for precision atomic spectroscopy where unstable Be ions are stored for a long time and laser-cooled down to a very low temperature<sup>1,2</sup>). This is an ideal condition to perform double resonance spectroscopy to determine the absolute optical transition energies to deduce the isotope shifts of the optical transitions. From the isotope shifts, we can systematically determine the nuclear charge radii of Be isotopes.

The finite mass and size of a nucleus influence the electron binding energies of an atom. In the case of light nuclei such as Be, the field shift due to the size of a nucleus is as small as 10 MHz, whereas the optical transition energy is about  $10^9$  MHz and the mass contribution is about  $10^3$  MHz. The determination of charge radii requires not only theoretical calculations for the mass shift and other effects, such as QED effects, with sufficiently high accuracies but also the relative accuracies of the measurements must be as high as  $10^{-9}$ .

To measure the optical transition energy, we used the optical-optical double resonance (OODR) spectroscopy method<sup>3</sup>). In the cooling process, ions are optically pumped between the states  $2^2S_{1/2}$  (largest  $F$ ) and  $2^2P_{3/2}$  and strong laser-induced fluorescence is observed. If the optical pumping is imperfect, some fraction of the population remains in the other states. Under such a condition, if we use a weak probe laser resonant to the  $2^2S_{1/2}$  (smaller  $F$ )– $2^2P_{3/2}$  transition, a part of the population in the smaller  $F$  state is transferred to the larger  $F$  state. Then, an increase in the laser-induced fluorescence signal is observed. The cooling probe lasers alternately irradiated the trapped ions, using electro-optic modulators and polarizers to avoid the power broadening and shift effects. In this way, we can obtain a symmetric Lorentzian profile for the  $2^2S_{1/2}$ – $2^2P_{3/2}$  transition with a width close to the natural line width. The probe laser frequency was simultaneously measured by a clockwork optical femtosecond frequency comb (Menlo Systems FC1500)<sup>4</sup>). Then we can determine the absolute frequency of energy transitions with extremely high accuracy.

Typical OODR spectra are shown in Fig. 1 fitted with Lorentzian profiles to determine the res-

onance frequencies. Using the results compensated from the hyperfine splittings constant and the Zeeman splittings, the absolute transition frequencies in the  $2^2S_{1/2} \rightarrow 2^2P_{3/2}$  transition of  ${}^{7,9,11}\text{Be}^+$  were obtained to be 957 347 372.2(1.6) MHz, 957 396 620.6(2.7) MHz and 957 428 168.9(2.5) MHz respectively. Although the same method is not applicable for the even-even nucleus  ${}^{10}\text{Be}$ , we carefully measured the cooling transition at zero magnetic field and obtained a sharp symmetric spectrum (Fig. 1). From this spectrum, we determined the  $S_{1/2} \rightarrow P_{3/2}$  transition energy of  ${}^{10}\text{Be}^+$  as 957 413 949.8(0.5) MHz. The uncertainties of these values are mainly due to poor statistics.

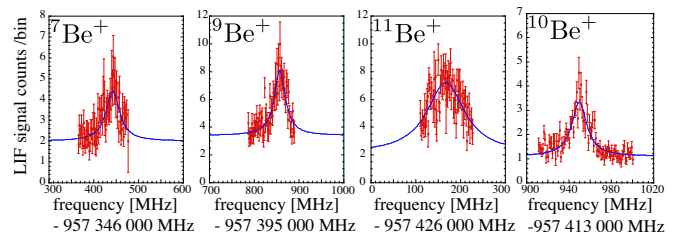


Fig. 1. OODR spectra of  $2^2S_{1/2} \rightarrow 2^2P_{3/2}$  transition for  ${}^{7,9,11}\text{Be}^+$  and laser cooling spectrum for  ${}^{10}\text{Be}^+$ .

The experiment is still in progress to achieve more accurate and reliable data. However, we preliminary evaluate the charge radii of Be isotopes as shown in Fig. 2.

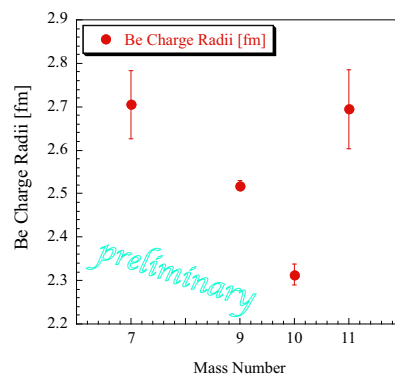


Fig. 2. Preliminary evaluated charge radii of Be isotopes.

\*<sup>1</sup> Department of Physics, Sophia University  
 \*<sup>2</sup> Japan Atomic Energy Research Association  
 \*<sup>3</sup> ILS, University of Electro-Communications  
 \*<sup>4</sup> Institute of Particle and Nuclear Studies, KEK  
 \*<sup>5</sup> II. Physikalisches Institut, Justus-Liebig-Universität  
 \*<sup>6</sup> Department of Physics, Texas A&M University

## References

- 1) T. Nakamura *et al.*: Phys. Rev. A **74**, 052503 (2006).
- 2) K. Okada *et al.*: Phys. Rev. Lett. **101**, 212502 (2008).
- 3) D. J. Wineland *et al.*: Opt. Lett. **5**, 245 (1980).
- 4) T. Udem *et al.*: Nature **416**, 233 (2002).

# Observation of new neutron-rich short-lived isomers among fission products of 345 MeV/nucleon $^{238}\text{U}$

D. Kameda, T. Nakao,<sup>\*1</sup> T. Kubo, T. Ohnishi, K. Kusaka, A. Yoshida, K. Yoshida, M. Ohtake, N. Fukuda, H. Takeda, K. Tanaka, N. Inabe, Y. Yanagisawa, H. Watanabe, H. Otsu, Y. Kondo, Y. Gono, H. Sakurai, T. Motobayashi, H. Baba, T. Ichihara, Y. Yamaguchi, M. Takechi, S. Nishimura, H. Ueno, A. Yoshimi, M. Matsushita,<sup>\*2</sup> K. Ieki,<sup>\*2</sup> N. Kobayashi,<sup>\*3</sup> K. Tanaka,<sup>\*3</sup> Y. Kawada,<sup>\*3</sup> N. Tanaka,<sup>\*3</sup> S. Deguchi,<sup>\*3</sup> Y. Sato,<sup>\*3</sup> T. Nakamura,<sup>\*3</sup> K. Yoshinaga,<sup>\*4</sup> C. Ishii,<sup>\*4</sup> H. Yoshii,<sup>\*4</sup> N. Uematsu,<sup>\*4</sup> Y. Shiraki,<sup>\*4</sup> Y. Miyashita,<sup>\*4</sup> T. Sumikama,<sup>\*4</sup> J. Chiba,<sup>\*4</sup> E. Ideguchi,<sup>\*5</sup> A. Saito,<sup>\*5</sup> T. Yamaguchi,<sup>\*6</sup> I. Hachiuma,<sup>\*6</sup> T. Suzuki,<sup>\*6</sup> T. Moriguchi,<sup>\*7</sup> A. Ozawa,<sup>\*7</sup> T. Ohtsubo,<sup>\*8</sup> M. A. Famiano,<sup>\*9</sup> A. Nettleton,<sup>\*10</sup> B. Sherrill,<sup>\*10</sup> S. Manikonda,<sup>\*11</sup> and J. Nolen,<sup>\*11</sup>

[In-flight fission, neutron-rich nuclei, short-lived isomer]

The BigRIPS separator provides intermediate energy radioactive isotopes (RI) that are identified event by event by their mass,  $A$ , and charge state,  $Q$ , in flight. In the 2008 search for new isotopes using in-flight fission of a 345 MeV/nucleon  $^{238}\text{U}$  beam, the intensities of the cocktail RI beams were around or below 1 k particles/s. The situation has allowed us to observe isomeric decays of the products, whose halfives are around a microsecond, in the neutron-rich region far from stability. During the new isotope search, we observed more than ten new isomers in detecting  $\gamma$  rays gated on the isotopes which were identified by using the so-called particle identification plot of  $A/Q$  versus proton number. Of these, this report describes the isomeric states of the neutron-rich Br isotopes,  $^{94}\text{Br}$  and  $^{95}\text{Br}$ , which were one of the intense isomers observed.

The  $\gamma$ -rays emitted from the isomeric states were detected using three clover-type Ge detectors located at the end of the ZeroDegree spectrometer. To stop the Br beams close to the detectors, an aluminum stopper was installed at the end of the beam line. The thickness of the stopper, 8.1 g/cm<sup>2</sup>, was chosen to stop almost all of the products in the new isotope search setting. The detail of the setup is described elsewhere. We accumulated the  $\gamma$  rays triggered by the particles with a 20  $\mu\text{s}$  time window. The beam condition of the Br isotopes is shown in Table 1.

Figure 1 shows the  $\gamma$ -ray energy spectra observed for  $^{94}\text{Br}$  and  $^{95}\text{Br}$ . To reduce  $\gamma$  background due to beam irradiation, which appears as a prominent peak in the  $\gamma$  time spectrum, the events around the peak were excluded. We have observed two strong peaks at 91.7 and 202.3 keV for  $^{94}\text{Br}$  and a strong peak at 537.9 keV for  $^{95}\text{Br}$ . In the insets, the decay curves

gated by these  $\gamma$  rays are presented. In  $^{94}\text{Br}$ , the preliminarily obtained halfives for the 91.7 and 202 keV  $\gamma$  rays are 713(71) ns and 655(46) ns, respectively. The agreement within the errors suggests that these  $\gamma$  rays come from an identical isomeric state. In  $^{95}\text{Br}$ , a preliminary halfife of the 538 keV  $\gamma$  rays was obtained as  $T_{1/2} = 4.0(12) \mu\text{s}$ . Further analysis is now in progress.

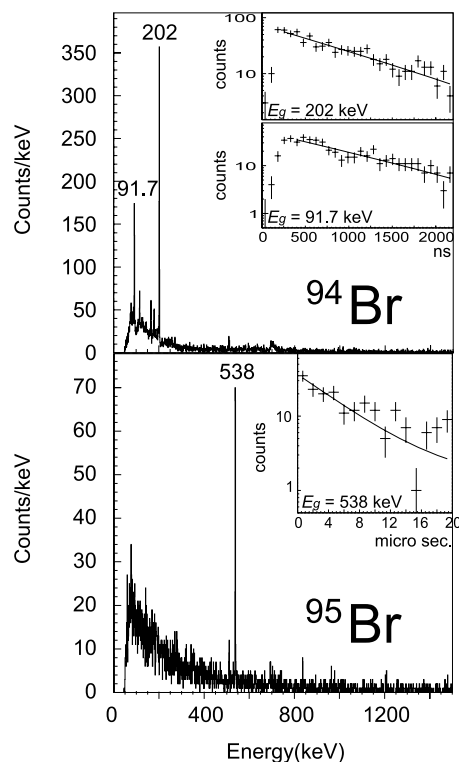


Fig. 1.  $\gamma$ -ray energy spectra for  $^{94}\text{Br}$  and  $^{95}\text{Br}$

\*1 Department of Physics, The University of Tokyo  
 \*2 Department of Physics, Rikkyo University  
 \*3 Department of Physics, Tokyo Institute of Technology  
 \*4 Department of Physics, Tokyo University of Science  
 \*5 Center for Nuclear Study, The University of Tokyo  
 \*6 Department of Physics, Saitama University  
 \*7 Institute of Physics, University of Tsukuba  
 \*8 Department of Physics, Niigata University  
 \*9 Physics Department, Western Michigan University  
 \*10 Michigan State University  
 \*11 Argonne National Laboratory

Table 1. Beam condition for the Br isotopes.

	$^{94}\text{Br}$	$^{95}\text{Br}$
production target	Be 5 mm	
charge state	35(fully stripped)	
yield in stopper	$2.1 \times 10^5$	$4.0 \times 10^4$

# $\alpha$ -Particle Condensation in $^{16}\text{O}$ Studied with a Full Four-Body Orthogonality Condition Model Calculation<sup>†</sup>

Y. Funaki, T. Yamada<sup>\*1</sup>, H. Horiuchi<sup>\*2</sup>, G. Röpke<sup>\*3</sup>, P. Schuck<sup>\*4</sup> and A. Tohsaki<sup>\*2</sup>

[Nuclear structure, Cluster model, Alpha particle]

It is well established that  $\alpha$ -clustering plays a very important role in the structure of light nuclei.<sup>1,2</sup> The importance of the  $\alpha$ -cluster formation has also been discussed in infinite nuclear matter, where  $\alpha$ -particle type condensation is expected at low density,<sup>3</sup> quite analogous to the recently realized Bose-Einstein condensation of bosonic atoms in magneto-optical traps.<sup>4</sup> Regarding  $\alpha$ -particle condensation in finite nuclei, only the Hoyle state, i.e. the  $0_2^+$  state in  $^{12}\text{C}$  has clearly been established thus far. Several past papers<sup>2</sup> and also more recent papers<sup>5-7</sup> have by now established beyond any doubt that the Hoyle state, only having about one third of saturation density, can be described, to good approximation, as a product state of three  $\alpha$ -particles, condensed into the lowest mean field  $0S$ -orbit.<sup>8,9</sup>

In this short note we present a result of the exploration of the  $4\alpha$  condensate state by solving a full Orthogonality Condition Model (OCM) four-body equation of motion without any assumption with respect to the structure of the  $4\alpha$  system. Here we take the  $4\alpha$  OCM with Gaussian basis functions,<sup>10</sup> the model space of which is large enough to cover the  $4\alpha$  gas, the  $\alpha+^{12}\text{C}$  cluster, as well as the shell-model configurations. The OCM is extensively described in Ref. 11.

As a result of the calculations, we can reproduce the full spectrum of  $0^+$  states up to about 15 MeV, and tentatively make a one-to-one correspondence of those states with the six lowest  $0^+$  states of the experimental spectrum. In view of the complexity of the situation, the agreement is considered to be very satisfactory (see Fig. 1 in Ref. 12).

The  $0^+$  spectrum of  $^{16}\text{O}$  up to about 15 MeV is now essentially understood, including the  $4\alpha$  condensate state. This is a remarkable improvement in our knowledge of the structure of  $^{16}\text{O}$ . The structures of the  $0_2^+$  state at 6.05 MeV and  $0_3^+$  state at 12.05 MeV are well established as having the  $\alpha+^{12}\text{C}(0_1^+)$  and  $\alpha+^{12}\text{C}(2_1^+)$  cluster structures, respectively.<sup>13,14</sup> These structures of the  $0_2^+$  and  $0_3^+$  states have been confirmed in the present calculation. We also mention that the ground state is described as having a shell-model configuration within the present framework, the calculated rms value, 2.7 fm, agreeing with the observed rms value

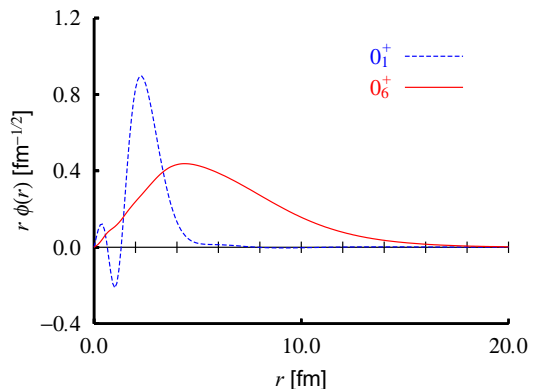


Fig. 1. (Color online) The radial parts of single- $\alpha$  orbits with  $L = 0$  belonging to the largest occupation number, for the ground and  $0_6^+$  states.

(2.71 fm). We find that the  $0_6^+$  state, calculated to be about 2 MeV above the  $4\alpha$  threshold, has a very large rms radius of about 5 fm and has a rather large occupation probability of 61% of four  $\alpha$  particles sitting in a spatially extended single- $\alpha$   $0S$  orbit (see Fig. 1). The wave function has a large  $\alpha+^{12}\text{C}$  amplitude only for  $^{12}\text{C}^*$ , i.e. the Hoyle state. These results are strong evidence of the  $0_6^+$  state, which is a new theoretical prediction, for the existence of the  $4\alpha$  condensate state, i.e. the analog to the Hoyle state in  $^{12}\text{C}$ . Further experimental information is very much requested to confirm this novel interpretation of this state.

## References

- 1) K. Wildermuth and Y. C. Tang, *A Unified Theory of the Nucleus* (Vieweg, Braunschweig, 1977).
- 2) For example, K. Ikeda *et al.*, Prog. Theor. Phys. Suppl. No. 68, 1 (1980), and references therein.
- 3) G. Röpke *et al.*, Phys. Rev. Lett. **80**, 3177 (1998).
- 4) F. Dalfovo *et al.*, Rev. Mod. Phys. **71**, 463 (1999).
- 5) A. Tohsaki *et al.*, Phys. Rev. Lett. **87**, 192501 (2001).
- 6) Y. Funaki *et al.*, Phys. Rev. C **67**, 051306(R) (2003); Eur. Phys. J. A **24**, 321 (2005); Eur. Phys. J. A **28**, 259 (2006); Nucl. Phys. News Lett. **17**(04), 11 (2007); Phys. Rev. C **77**, 064312 (2008).
- 7) M. Chernykh *et al.*, Phys. Rev. Lett. **98**, 032501(2007).
- 8) H. Matsumura *et al.*, Nucl. Phys. A **739**, 238 (2004).
- 9) T. Yamada *et al.*, Euro. Phys. J. A **26**, 185 (2005).
- 10) M. Kamimura, Phys. Rev. A **38**, 621 (1988).
- 11) S. Saito, Prog. Theor. Phys. **40**, 893 (1968).
- 12) Y. Funaki *et al.*, Phys. Rev. Lett. **101**, 082502 (2008).
- 13) Y. Suzuki, Prog. Theor. Phys. **55**, 1751 (1976).
- 14) K. Fukatsu *et al.*, Prog. Theor. Phys. **87**, 151 (1992).

<sup>†</sup> Condensed from the article in Phys. Rev. Lett. **101**, 082502 (2008).

<sup>\*1</sup> Laboratory of Physics, Kanto Gakuin University

<sup>\*2</sup> Research Center for Nuclear Physics, Osaka University

<sup>\*3</sup> Institut für Physik, Universität Rostock, Germany

<sup>\*4</sup> Institut de Physique Nucléaire, France

# Holographic Baryons : Static Properties and Form Factors from Gauge/String Duality †

K. Hashimoto,\*<sup>1</sup> T. Sakai,\*<sup>2</sup> and S. Sugimoto,\*<sup>3</sup>

[Static properties of nucleons, Superstring theory]

In this paper, we study properties of baryons by using a holographic dual of QCD on the basis of the D4/D8-brane configuration, where baryons are described by a soliton. Recent progress in string theory makes it possible to compute various physical quantities of strongly coupled QCD at low energy, at large  $N_c$ . We first determine the asymptotic behavior of the soliton solution, which allows us to evaluate well-defined currents associated with the  $U(N_f)_L \times U(N_f)_R$  chiral symmetry. Using the currents, we compute static quantities of baryons such as charge radii and magnetic moments, and make a quantitative test with experiments. It is emphasized that not only the nucleon but also excited baryons, such as  $\Delta$ ,  $N(1440)$ ,  $N(1535)$  etc., can be analyzed systematically in this model. We also investigate the form factors and find that our form factors agree well with the results that are well-established empirically. With the form factors, the effective baryon-baryon-meson cubic coupling constants among their infinite towers in the model can be determined.

We use a model of holographic QCD<sup>1)</sup> obtained in superstring theory, and calculate static quantities of the nucleon and excited baryons. In the model, The baryons are described as quantized instantons in five dimensional Yang-Mills-Chern-Simons (YMCS) theory. By defining the chiral currents properly at the spatial infinity in the fifth dimension and by solving the YMCS equations of motion with the instanton profile and Green's functions, we obtain the explicit expression for the chiral currents depending on the baryon state. From the currents we computed various static quantities of proton/neutron, such as charge radii, magnetic moments, axial coupling and axial radius. See the summary table below. The Goldberger-Treiman relation is naturally derived. These quantities can be computed for excited baryons in the same manner, which are our theoretical prediction for the excited baryons. We also calculated the nucleon form factors (and also that for excited baryons). It was shown that the electric and magnetic form factors of the nucleon are roughly consistent with the dipole behavior observed in experiments. Electric as well as magnetic charge radii of the baryons and their cou-

Table 1. Various static observables of nucleons, computed in our model. For a comparison, we quote results of the Skyrminion<sup>2)</sup>.

	our model	Skyrmion	experiment
$\langle r^2 \rangle_{I=0}^{1/2}$	0.742 fm	0.59 fm	0.806 fm
$\langle r^2 \rangle_{M, I=0}^{1/2}$	0.742 fm	0.92 fm	0.814 fm
$\langle r^2 \rangle_{E,p}$	$(0.742 \text{ fm})^2$	$\infty$	$(0.875 \text{ fm})^2$
$\langle r^2 \rangle_{E,n}$	0	$-\infty$	$-0.116 \text{ fm}^2$
$\langle r^2 \rangle_{M,p}$	$(0.742 \text{ fm})^2$	$\infty$	$(0.855 \text{ fm})^2$
$\langle r^2 \rangle_{M,n}$	$(0.742 \text{ fm})^2$	$\infty$	$(0.873 \text{ fm})^2$
$\langle r^2 \rangle_A^{1/2}$	0.537 fm	-	0.674 fm
$\mu_p$	2.18	1.87	2.79
$\mu_n$	-1.34	-1.31	-1.91
$ \frac{\mu_p}{\mu_n} $	1.63	1.43	1.46
$g_A$	0.73	0.61	1.27
$g_{\pi NN}$	7.46	8.9	13.2
$g_{\rho NN}$	5.80	-	$4.2 \sim 6.5$

Table 2. Our prediction for excited nucleons.

	n,p	N(1440)	N(1535)
$\langle r^2 \rangle_{E,p}$	$(0.742 \text{ fm})^2$	$(0.742 \text{ fm})^2$	$(0.699 \text{ fm})^2$
$\langle r^2 \rangle_{E,n}$	0	0	0
$\langle r^2 \rangle_{M,p}$	$(0.742 \text{ fm})^2$	$(0.742 \text{ fm})^2$	$(0.699 \text{ fm})^2$
$\langle r^2 \rangle_{M,n}$	$(0.742 \text{ fm})^2$	$(0.742 \text{ fm})^2$	$(0.699 \text{ fm})^2$
$\langle r^2 \rangle_A^{1/2}$	0.537 fm	0.537 fm	0.435 fm
$\mu_p$	2.18	2.99	2.18
$\mu_n$	-1.34	-2.15	-1.34
$ \frac{\mu_p}{\mu_n} $	1.63	1.39	1.63
$g_A$	0.734	1.07	0.380
$g_{\pi BB}$	7.46	16.7	6.32
$g_{\rho BB}$	5.80	5.80	4.51

plings to mesons are calculated from the form factors.

As shown in the first table, we have found a good agreement with experiments, for various quantities of baryons. The numerical values presented here as our result should be treated with care, since it was obtained for large value of the 't Hooft coupling and  $N_c$ .

## References

- 1) T. Sakai and S. Sugimoto, Prog. Theor. Phys. **113**, 843 (2005), Prog. Theor. Phys. **114**, 1083 (2005).
- 2) G. S. Adkins, C. R. Nappi and E. Witten, Nucl. Phys. B **228**, 552 (1983).

† Condensed from the article in Prog. Theor. Phys. **120**, 1093-1137 (2008)\*<sup>1</sup> Theoretical Physics Laboratory, RIKEN\*<sup>2</sup> Department of Physics, Ibaraki University\*<sup>3</sup> Institute for the Physics and Mathematics of the Universe, University of Tokyo

## Nondestructive monitoring system of RF fields and beam-phase/intensity for stable operation of RIBF

R. Koyama\*<sup>1</sup>, M. Fujimaki, N. Fukunishi, M. Hemmi, O. Kamigaito, M. Kase, N. Sakamoto, K. Suda, T. Watanabe, K. Yamada, and Y. Yano

We have developed a nondestructive monitoring system of RF fields and beam-phase/intensity in order to obtain stable operation of RI beam factory (RIBF). We have previously reported on a similar system for RILAC region in the last fiscal year<sup>1)</sup>, but we have extended the system throughout the RIBF in this fiscal year. The layout of the RIBF during a 345 MeV/nucleon uranium acceleration is shown in Fig. 1. In the uranium acceleration, ions are produced by 18GHz-ECRIS, and accelerated by the injection linacs (RFQ and RILAC) and four ring cyclotrons (RRC, fRC, IRC, and SRC). In addition, we have an injection buncher and four re-bunchers as shown in Fig. 1. Two charge strippers are placed downstream of the RRC and the fRC.

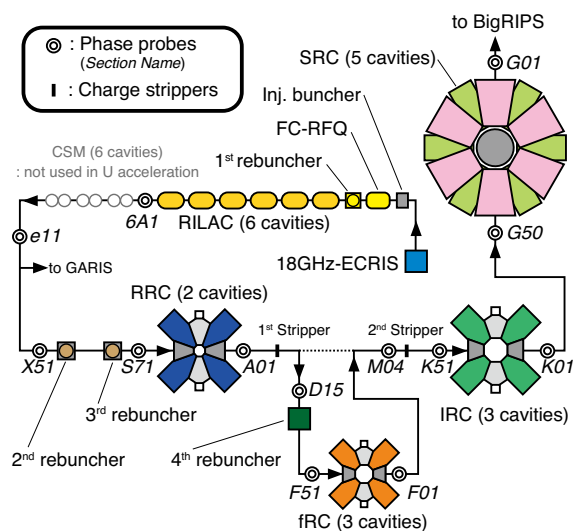


Fig. 1. Layout of RIBF during a 345 MeV/nucleon uranium acceleration.

In such a multi-stage acceleration system, one of the most important factors for stable operation is to maintain the matching of beam-phases between accelerators. However, drifts of beam-phases have frequently been observed, which may be the result of fluctuation of RF-fields, fluctuation of the magnetic field, etc.. Hence, it is important to monitor beam-bunch signals constantly, and we have developed a monitoring system using the commercial RF lock-in amplifier (LIA) model SR844 manufactured by Stanford Research Systems. In addition, the system for monitoring the RF-fields has also been developed to investigate their stability

\*1 SHI Accelerator Service, Ltd.

and the correlation with beam-phases and intensities. Both beam-bunch signals and the RF-fields monitoring system are divided into 5 sections, which are around RILAC, RRC, fRC, IRC, and SRC. Each section has a monitoring system with basically the same configuration shown in Fig. 2. The beam-bunch and RF-fields signals are analyzed by the LIA (via switching modules in some sections). All the systems are controlled by the developed LabVIEW program. Independently with our monitoring system, the temperatures of air and cooling water are also monitored using DC100 controlled by DARWIN DAQ32 from YOKOGAWA Electric Corporation.

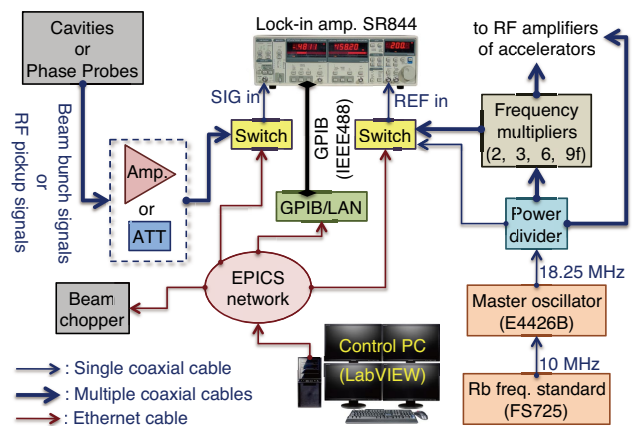


Fig. 2. Block diagram of developed monitoring system.

Our system constantly monitors fluctuations in voltages and phases of a total of 25 RF-cavities and also in beam-bunch signals detected nondestructively by 13 phase probes (PPs, shown as double circles with their section names in Fig. 1.) placed at beam transport lines during 345 MeV/nucleon uranium acceleration. In the other acceleration modes such as 345 MeV/u calcium acceleration using RILAC-RRC-IRC-SRC (skip the fRC), slight changes are made to the configuration of the monitoring system. Using this system, we have started to investigate the stability of our accelerator complex and relations between fluctuations of RF-fields of accelerators and observed instabilities of beam-phases and intensities. In this report, two notable examples are presented.

One is the correlation between RF and air temperature. Since it was known that there was some relation between the output fluctuation of the power divider (1f-PD) and the air temperature according to previous research<sup>2)</sup>, we investigated the relation between

them more precisely by putting a thermometer near the 1f-PD. This 1f-PD has been used for distributing the reference signal from a master oscillator to each low level module of all RIBF accelerators. Fig. 3-a shows the RF fluctuations observed on November 17, 2008, where fRC3f-PD is the power divider with frequency tripler for fRC main RF, fRC-W and E are the acceleration RF of two main cavities of fRC, and Air-temp. is the air temperature near the 1f-PD. The phase shifts by manual tunings are indicated by arrows. It is found that an air temperature fluctuation

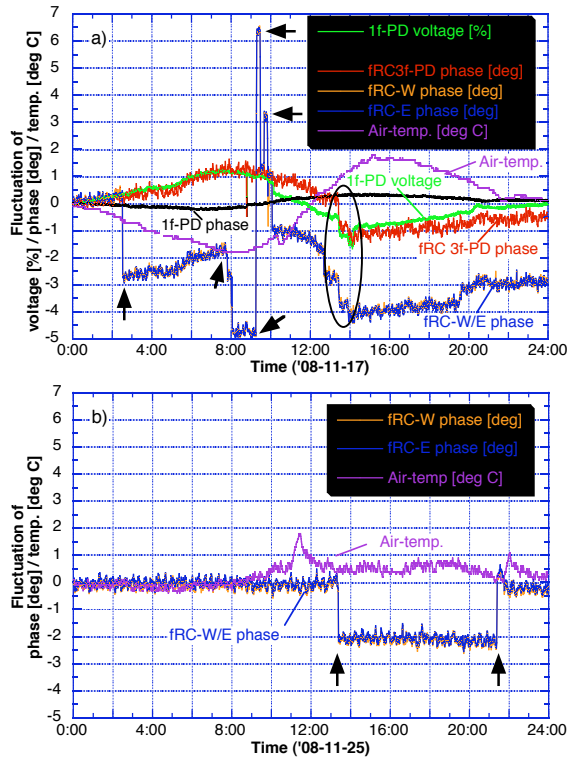


Fig. 3. RF fluctuations of power dividers and fRC. Arrows indicate the phase shifts due to manual tunings.

around 1f-PD of  $19.7 \pm 2$  °C caused phase and voltage fluctuations of 1f-PD and fRC3f-PD, and finally caused phase fluctuations of fRC-W and E of  $\pm 3^\circ$  (excluding the phase shifts by manual tunings). The phase shifts of fRC-W and E caused by the sudden voltage reduction of 1f-PD were also observed independently of the air temperature fluctuation as indicated by the closed circle in Fig. 3-a. The phase stabilities of fRC-W and E were improved as shown in Fig. 3-b after installing the directional couplers instead of the 1f-PD, and after starting air conditioning using a heat pump system.

The other example is the correlation between RF/beam-intensity and cooling water temperature. The periodic fluctuation of extraction intensity of RRC detected by PP-A01 was observed on December 9, 2008. Since the incident intensity of RRC detected by PP-S71 was relatively stable we investigated the RF of the RRC, and it was found that there was a

correlation between them as shown in Fig. 4-a. Additionally, we investigated the cause of fluctuation of RRC-RF, and it was found that it had a correlation with the cooling water temperature of RRC-cavities as shown in Fig. 4-b. The cooling water temperature of RRC-RF system is controlled by regulating the temperature of secondary cooling water by automatically controlling the fans and spray pumps of the cooling tower. We stopped this temperature regulation system because the period of the fluctuation of the cooling water temperature was synchronized with the on/off control of the fans and spray pumps. The stability of beam intensity at PP-A01 was significantly improved after stopping the regulation system as shown in Fig. 4-c, while the stability of RRC-RF was little improved. Hence the fluctuation of beam intensity at PP-A01 can be considered to be caused by the fluctuations somewhere else in origin such as the magnetic field of RRC main magnet, which also has a great influence on the beam quality, and uses same secondary cooling water.

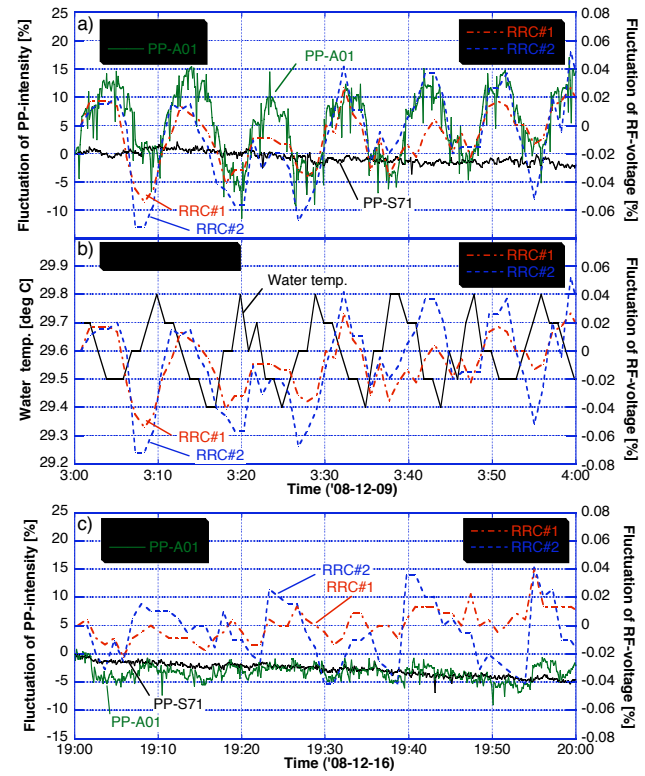


Fig. 4. Stability of extraction beam intensity of RRC.

As our next step, we plan to integrate the temperature monitoring system into our developed monitoring system in order to comprehend the correlations online for more prompt countermeasures.

References

- 1) R. Koyama et al.,: RIKEN Accel. Prog. Rep. **41**, 99 (2008).
- 2) R. Koyama et al.,: Proceedings of PASJ5-LAM33, August 2008, Higashi-Hiroshima-shi, Hiroshima, WP007.

## A series of asexual mutants and partial deletion of the Y-chromosome by heavy ion beam in *Silene latifolia*

Chihiro Torii,\* Kotaro Ishii,\* Kiyoshi Nishihara, Kahori Yamanaka,\* Naoko Ishi,\* Ayako Koizumi,\* Yusuke Kazama, Tomoko Abe and Shigeyuki Kawano\*

Sexual dimorphism is controlled by genes on the differential arms of the Y chromosome in *Silene latifolia*. They are divided into four functional regions: (1) a region causing suppression of gynoecium development, often called the gynoecium suppressing functional (GSF) region; (2) a region causing stamen development, also called the stamen promoting functional (SPF) region; (3) a region containing the gene necessary for late anther development, known as the male fertility functional (MFF) region; and (4) a recombining pseudoautosomal region. We have isolated a new series of Y-chromosome deletion mutants, expressed as asexual flowers.

Seeds and anthers were irradiated with a 135 MeV/u carbon-ion beam within a dose range of 20 - 200 Gy. The irradiated seeds were sown in pots, and after one month, viable plants were counted. The survival rates of the seeds irradiated at up to 75 Gy ranged from 100% to 85%. The survival rates of seeds irradiated at more than 75 Gy decreased as the irradiation dose increased. Irradiated pollen was used to fertilize female plants of the same inbred K line. After one month, seeds were collected and sown in pots. The germination rate of seeds generated from pollen irradiated at a dose of 20 Gy was more than 50%, but fell to 3% with a dose of 60 Gy.

Eleven asexual mutants, F01a, I02, G04, G01, G02, I01, G06a, I03h, F02a, G05 and G03, were obtained from the plants derived from irradiated pollen and compared with K034, our previously reported asexual mutant with two types of flowers, asexual and female-like flower.<sup>1)</sup> Flowers of *S. latifolia* have 10 stamens and a suppressed gynoecium as an undifferentiated rod (Fig. 1a). Asexual flowers of the eleven asexual mutants had rudimentary or various

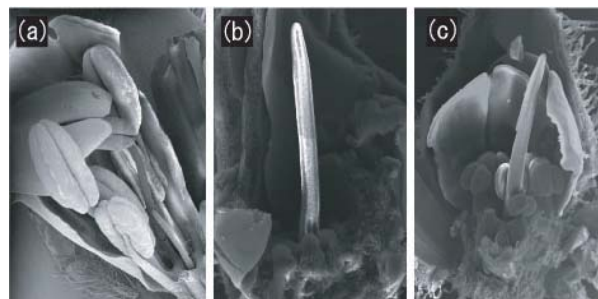


Fig. 1. SEM observations of male flowers of *S. latifolia*. (a) wt male, (b) G06a and (c) F02a.

developing stamens and a suppressed gynoecium (Fig. 1b and c). The number of stamens were always 10 and the two-flower type such as in K034 did not appear among them.

To determine whether the eleven asexual mutants have a Y chromosome, PCR analysis was performed using Y-specific sequence-tagged site (STS) markers (MK17, *SlssY*, Bgl10, *DD44Y*, Bgl16, MS4, ScD05, *SIAP3Y*, ScQ14, MS7 and MS2). K034, which has two flower phenotypes, possessed the Y chromosome carrying two deletions (MS4, Bgl10, *DD44Y*, Bgl16 and ScQ14) in the gynoecium-suppressing and stamen-promoting functional regions (Y<sup>d</sup>). Five mutants, F01a, I02, G04, G01 and G02, possessed a Y chromosome carrying a deletion of GSF in common. Another five mutants, I01, G06a, I03h, F02a and G05, possessed a common deletion of SPF. The last mutant, G03, only possessed a deletion of MFF.

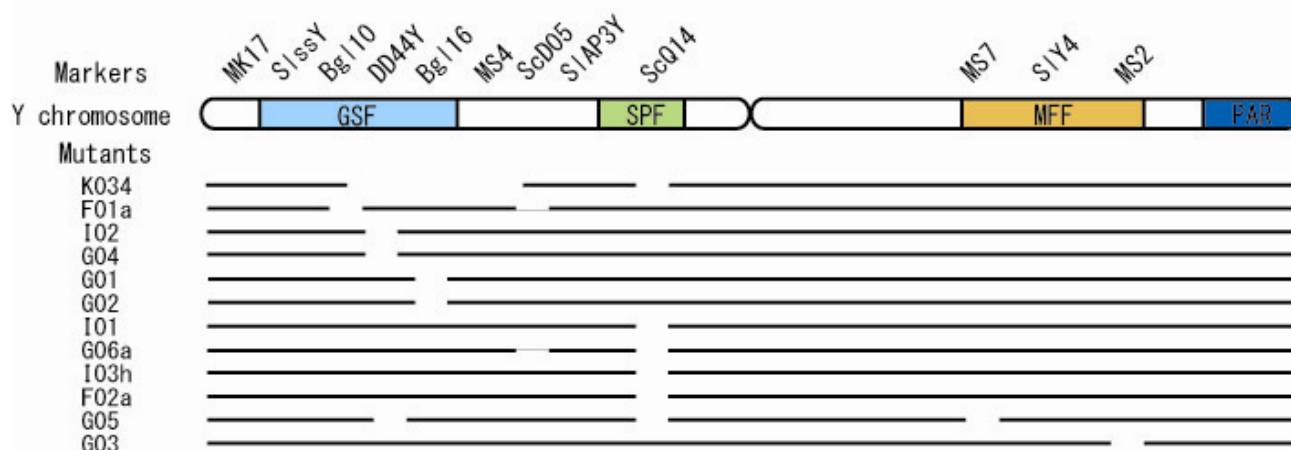


Fig. 2. Schematic representations of the entire Y chromosome of *S. latifolia* and the results of PCR of sequence-tagged site (STS) markers using each genomic DNA isolated from K034 and the series of asexual mutants obtained in this work. Bars for each mutant name represent markers. Blanks indicate the marker was missing.

### References

1) Koizumi, A. et al.: *Plant Cell Physiol.* **48**, 1450 (2007).

\* Department of Integrated Biosciences, Graduate School of Frontier Sciences, University of Tokyo

# C O N T E N T S

Page

## GRAVURES & HIGHLIGHTS OF THE YEAR

Decay properties of $^{266}\text{Bh}$ and $^{262}\text{Db}$ produced in the $^{248}\text{Cm} + ^{23}\text{Na}$ reaction — Further confirmation of the $^{278}113$ decay chain — .....	i
RF multipole devices play important roles in SLOWRI experiments : Hyperfine spectroscopy of $^7\text{Be}^+$ and new type of ion crystals in an RF octupole ion trap (PP. 18 and 230) .....	vii
Discovery of 20 new isotopes by in-flight fission of $345\text{MeV/u } ^{238}\text{U}$ .....	viii
Status of the RIKEN 28GHz Superconducting ECR ion source .....	ix
A new cultivar “Nishina Zaou” induced by heavy ion beam irradiation .....	xi
Demonstration of electron scattering using the SCRIT prototype .....	xii
Production and decay properties of $^{263}\text{Hs}$ .....	xiii
Precision optical transition measurements for $^{7,9,10,11}\text{Be}^+$ ions .....	xiv
Observation of new neutron-rich short-lived isomers among fission products of $345\text{ MeV/nucleon } ^{238}\text{U}$ .....	xv
$\alpha$ -Particle Condensation in $^{16}\text{O}$ Studied with a Full Four-Body Orthogonality Condition Model Calculation .....	xvi
Holographic Baryons : Static Properties and Form Factors from Gauge/String Duality.....	xvii
Nondestructive monitoring system of RF fields and beam-phase/intensity for stable operation of RIBF .....	xviii
A series of asexual mutants and partial deletion of the Y-chromosome by heavy ion beam in <i>Silene latifolia</i> .....	xx
<b>I. PREFACE</b> .....	1
<b>II. RESEARCH ACTIVITIES I (Nuclear-Particle Physics)</b>	
<b>1. Nuclear Physics</b>	
$\gamma$ Spectroscopy beyond the Island of Inversion .....	3
Inclusive Coulomb breakup of $^{22}\text{C}$ and $^{31}\text{Ne}$ .....	4
Measurement of interaction cross sections for neutron rich Ne Isotopes .....	5
Angular distributions for low-lying states in the $^{32}\text{Mg}(p, p')$ reaction .....	6
One-neutron removal reactions of $^{18}\text{C}$ and $^{19}\text{C}$ on a proton target .....	7
Inelastic proton scattering on the neutron-rich nucleus $^{58}\text{Ti}$ .....	8
Inelastic scattering studies of $^{16}\text{C}$ reexamined .....	9
Lifetime measurements of excited states in $^{17}\text{C}$ .....	10
Investigation of the $^{30}\text{S}(p,\gamma)^{31}\text{Cl}$ reaction via Coulomb dissociation .....	11
Inelastic scattering of proton-rich nucleus $^{23}\text{Al}$ .....	12
Large proton contribution to the $2^+$ excitation in $^{20}\text{Mg}$ studied by intermediate energy inelastic scattering .....	13

Coulomb excitation and proton inelastic scattering of $^{36}\text{Ca}$ .....	14
Attempt to produce the 3rd chain of $^{278}\text{113}$ .....	15
New decay properties of $^{264}\text{Hs}$ , $^{260}\text{Sg}$ , and $^{256}\text{Rf}$ .....	16
Precision measurement of the hyperfine constant of $^{11}\text{Be}$ .....	17
Precision hyperfine structure spectroscopy of laser-cooled radioactive $^7\text{Be}^+$ -ions produced by projectile fragmentation .....	18
Half life measurement of $^{46}\text{Cr}$ .....	19
$^{30}\text{S}$ Beam Development with CRIB .....	20
Study of astrophysically important states in $^{26}\text{Si}$ via the $p(^{25}\text{Al},p)^{25}\text{Al}$ elastic scattering.....	21
Measurement of the ground-state electric quadrupole moment of $^{33}\text{Al}$ .....	22
Electric quadrupole moment of proton-rich $^{23}\text{Al}$ .....	23
Production of $^{58}\text{Cu}$ through the charge exchange reaction of $^{58}\text{Ni}$ .....	24
The first T-violation experiment using polarized $^8\text{Li}$ at KEK-TRIAC.....	25
Current status of SAMURAI .....	26
Plan of measurement of $\vec{d}p$ scattering at RIBF .....	27
Probing Asymmetric Nuclear Matter at RIBF .....	28
The development of the Gamma ray detectors in BigRIPS and Zerodegree spectrometer.....	29
Measurement of double helicity asymmetry in direct photon production in $p + p$ at $\sqrt{s} = 200\text{GeV}$ .....	31
W-physics with Inclusive Muons in PHENIX: Detailed Feasibility Studies .....	32
Measurement of Collins Asymmetry in $e^+e^-$ Annihilation at Belle.....	33
Precision Measurements of Hadron Multiplicities in $e^+e^-$ Annihilation at BELLE .....	34
Measurement of Interference Fragmentation Functions at Belle.....	35
Double Helicity Asymmetry of Inclusive Charged Hadrons in $pp$ Collisions at $\sqrt{s} = 62.4\text{ GeV}$ at PHENIX .....	36
PHENIX local polarimeter analysis in polarized proton-proton collisions at $\sqrt{s} = 200\text{GeV}$ from RHIC Run-8 .....	37

## 2. Nuclear Physics(Theory)

Covalent isomeric state in $^{12}\text{Be}$ induced by two-neutron transfers .....	39
Isoscalar monopole transitions in $^{10,12}\text{Be}$ .....	40
A smoothing method of discrete breakup $S$ -matrix elements in the theory of continuum-discretized coupled channels .....	41
Elastic and total reaction cross sections of oxygen isotopes in Glauber theory .....	42
Shell-model description of beta-decays for pfg-shell nuclei .....	43
Skyrme-QRPA calculation for exotic modes in neutron-rich Mg isotopes close to the drip line .....	44

Evolution of the spin-orbit splitting in $^{48}\text{Ca}$ probed by the spectroscopic factor .....	45
Density functional for description of novel pairing properties in nuclei far from $\beta$ -stability .....	46
Two-neutron and two-proton correlations in nuclear surface .....	47
Calculation of nuclear photoabsorption cross section using the finite amplitude method for Skyrme functionals .....	48
Linear Response Calculations With Skyrme TDHF+BCS .....	49
Development of QRPA code with an FAM method .....	50
Spectroscopic Factors in Asymmetric Nuclei From Realistic Interactions .....	51
Ab-initio Green's Functions Calculations of Atoms .....	52
Thermodynamical ensemble treatments of nuclear pairing in a multilevel model .....	53
BCS-BEC transition in finite systems .....	54
$t$ -band and tilted axis rotation in $^{182}\text{Os}$ .....	55
Origin of the narrow, single peak in the fission-fragment mass distribution for $^{258}\text{Fm}$ .....	56
Neutron vortices in neutron stars .....	57
Direct reactions of antiproton and the black-sphere picture .....	58
Light $\Xi$ hypernuclei in four-body cluster models .....	59
$p\Xi^0$ force studied with lattice QCD .....	60
Hadro-Chemistry for High Momentum Probes of Heavy Ion Collisions .....	61

### 3. Hadron Physics

Absolute luminosity determination using the vernier scan technique at $\sqrt{s} = 62.4$ GeV .....	63
Cross Section For Prompt Photon Production in Proton-Proton Collisions at $\sqrt{s} = 62.4$ GeV .....	64
Double spin asymmetries of open heavy-flavor production in forward rapidity with polarized p + p collisions at $\sqrt{s}=200\text{GeV}$ .....	65
Measurement of transverse single-spin asymmetry with $J/\Psi$ in polarized p+p collisions at $\sqrt{s} = 200$ GeV ...	66
Study of $J/\psi$ spin alignment in proton-proton collisions at $\sqrt{s} = 200$ GeV in RHIC PHENIX experiment ...	67
Measurement of direct photon using a virtual photon method in $\sqrt{s} = 200$ GeV p+p collisions at RHIC-PHENIX .....	68
Longitudinal Double Spin Asymmetry for Inclusive Jet Production in Polarized p+p Collisions at 200 GeV ...	69
Measurement of Transverse Single Spin Asymmetry of Open Heavy Flavor in Polarized p+p Collisions at PHENIX .....	70
Reaction Plane Dependence of Neutral Pion Production at $\sqrt{s_{NN}}=200$ GeV Au+Au Collisions at RHIC-PHENIX .....	71
A study of $\omega$ meson production in $\sqrt{s_{NN}}=200\text{GeV}$ A+A collisions at PHENIX .....	72
High $p_T$ Charged Pion Cross Section, Using PHENIX Central Arms .....	73

Multiplicity Measurement in the Proton-Proton Collisions at the LHC .....	74
Recent progress in precision pionic atom spectroscopy at RIBF .....	75
<b>4. Hadron Physics(Theory)</b>	
Glueball Decay in Holographic QCD .....	77
Quark Mass Deformation of Holographic Massless QCD .....	78
Phenomenology of small $\chi$ physics. ....	79
An explanation of the NuTeV anomaly .....	80
EMC effect for parity-violating DIS .....	81
The study of multiquark states based on $1/N_c$ classifications .....	82
Non-Fermi-liquid magnetic susceptibility of quark matter .....	83
Temperature dependence of quarkonium correlators .....	84
Heavy-quark bound states in an anisotropic hot QCD plasma .....	85
Improved non-perturbative renormalization in lattice QCD .....	86
(2+1)-flavor DWF QCD and chiral perturbation .....	87
Nucleon form factors in (2+1)-flavor dynamical DWF QCD .....	88
Eta meson from two flavor dynamical domain wall fermions .....	89
<b>5. Particle Physics</b>	
$O(\alpha_s)$ matching in static heavy and DW light quark system .....	91
Thermal Noise in AdS/CFT .....	92
Extended MQCD and SUSY/non-SUSY duality .....	93
Kerr/CFT correspondence and five-dimensional BMPV black holes .....	94
Toward a Proof of Montonen-Olive Duality via Multiple M2-branes .....	95
D-brane States and Annulus Amplitudes in $OSp$ Invariant Closed String Field Theory .....	96
Gauge invariant overlaps for classical solutions in open string field theory .....	97
Schnabl's solution and boundary states in open string field theory .....	98
Comments on gauge invariant overlaps for marginal solutions in open string field theory .....	99
Electroweak symmetry breaking in $SO(5) \times U(1)$ gauge-Higgs unification with top and bottom quarks .....	100
Vacuum energy of two-dimensional $N = (2, 2)$ super Yang-Mills theory .....	101
Restoration of supersymmetry on the lattice: Two-dimensional $N = (2, 2)$ supersymmetric Yang-Mills theory .....	102
Some physics of the two-dimensional $N = (2, 2)$ supersymmetric Yang-Mills theory: A lattice Monte Carlo study .....	103
<b>6. Development of Accelerator Facility</b>	
Acceleration Tests of $^{238}\text{U}$ and $^{48}\text{Ca}$ in RIBF .....	105

Construction of the MEBT (Middle-Energy Beam Transport) line for new 28GHz Superconducting ECR Ion Source (SC- ECRIS) .....	107
New beam line for the AVF-RRC-SRC acceleration .....	109
Construction of the IRC-bypass beam transport line .....	111
Refinement of SRC for acceleration of high intensity beam in 2008 .....	113
Completion of Superconducting Magnet for the 28 GHz ECR Ion Source.....	115
Production of highly charged Na ion beams from the RIKEN 18 GHz ECRIS .....	117
Production of a highly charged Ge beam form the RIKEN 18 GHz ECRIS .....	118
Improvement of rf-system for cyclotrons at RIBF .....	120
Stability of RF system at RILAC in RIBF .....	122
Open-stub filter for fRC main amplifier .....	124
High-power test of four-rod cw RFQ for new injector to RI-beam factory.....	126
Design of a water-cooling device for the rf shield of an SRC rf resonator .....	127
The heating effect of cryogenic vacuum pump of SRC rf resonator .....	129
The effect of vacuum pressure on transmission efficiency of RILAC.....	131
Development of polymer-coated carbon stripper foils.....	133
Offline test of a gas charge stripper for uranium beams .....	135
Practical use of beam current monitor with HTS current sensor and HTS SQUID at RIBF .....	137
Development of ion beam core monitor .....	139
Radiation monitoring in the SRC using an ionization chamber. ....	141
Performance Tests of Old Power Supplies in RIBF.....	143
A Linux Cluster with Redundant Design for Accelerator Operation .....	145
Computer modelling of the nitrogen, oxygen, and proton acceleration in RIKEN AVF cyclotron.....	147
Low Energy Beam Transport of 127 kV U <sup>35+</sup> on 100 kV Cockcroft .....	148
Space Charge effects in the RILAC II .....	150
Medium Energy Beam Transport System from the New Superconducting ECR Ion Source to RILAC.....	152
Emittance measurement of a singly charged heavy ion beam produced by laser for use in RHIC-EBIS .....	154
Preparation for Beam Analysis Experiment for EBIS-RFQ Linac .....	155

## 7. Instrumentation

Status of the BigRIPS and ZeroDegree Project .....	157
Commissioning of ZeroDegree spectrometer .....	159
Beam intensity monitors for BigRIPS separator .....	161
Manipulation and performance of ionization chambers for BigRIPS experiments.....	163
SHARAQ Project — Progress in 2008 — .....	165

Magnetic field measurement for the dipole magnets of the SHARAQ spectrometer .....	167
Large acceptance transport in the high resolution beam line for SHARAQ spectrometer .....	169
Development of low-pressure multi-wire drift chambers for BigRIPS and high-resolution beam line .....	171
Development of Low-Pressure Multi-Wire Drift Chamber with Stripped Cathodes .....	173
Performance evaluation of low-pressure multiwire drift chamber .....	175
Focal-Plane Detector for SHARAQ Spectrometer .....	177
Gas-filled recoil ion separator GARIS-II .....	179
Designing of ionization chamber for super-heavy elements .....	181
The Potential of a new LaBr <sub>3</sub> (Ce) Based $\gamma$ -Ray Spectrometer for Fast-Beam Experiments at the RIBF .....	182
Beta-counting systems for decay-spectroscopy projects .....	183
Beam test of double-sided silicon-strip detector for decay spectroscopy .....	184
Development of thick solid hydrogen target .....	186
Parasitic production of slow RI-beam from a projectile fragment separator by ion guide Laser Ion Source (PALIS) .....	187
A Portable Multi-Reflection Time-of-Flight Mass Spectrograph for SLOWRI .....	189
Development of an absolute laser frequency counting system .....	191
Development of fluorescence detection system for nuclear laser spectroscopy in He II .....	193
Production of polarized Ag atoms by optical pumping in superfluid helium .....	194
“Hybrid-RF” sequence in $\beta$ -NQR for $Q$ -moment measurement of short-lived nuclei .....	195
Online luminosity monitor for the SCRIT experiment .....	196
Long-time measurement of fluctuation of magnetic field .....	197
Network and Computing Environment for RIKEN Nishina Center .....	198
RIBF DAQ for Day-one Experiments .....	199
PHENIX silicon vertex tracker project .....	201
Spin physics capability with silicon vertex tracker for PHENIX .....	202
Silicon Pixel Detector for the PHENIX Vertex Tracker .....	203
Development and production status of a fine-pitch and low-material-budget readout bus for the PHENIX pixel detector .....	205
Development of quality assurance software for the silicon pixel ladder in the PHENIX Vertex Tracker .....	207
Development of an encapsulation procedure for the first PHENIX pixel ladder in the production version .....	209
Implementation of charge sharing and clustering in simulator of PHENIX silicon vertex tracker .....	211
Beam test of the PHENIX silicon pixel detector for 120GeV proton .....	212
Performance test of silicon stripixel detector for PHENIX vertex tracker .....	214
High Momentum Trigger Electronics Upgrade of PHENIX Muon Arms for Sea Quark Polarization	

Measurement at RHIC .....	216
Development of the MuTRG-ADTX boards for the PHENIX muon trigger upgrade .....	217
Development and evaluation of the MuTRG-MRG and DCMIF boards for the PHENIX muon trigger upgrade.....	218
A fast, momentum sensitive muon Trigger for PHENIX using resistive plate counters .....	219
DAQ system Upgrade for optical alignment system of PHENIX Muon Tracker .....	221
CCJ Operation in 2007-2008 .....	223

### III. RESEARCH ACTIVITIES II (Material Science and Biology)

#### 1. Atomic and Solid State Physics(ions)

Microdose damage observed in power MOSFETs with trench structures .....	225
Structure of ePTFE irradiated with a 5 MeV/nucleon $^{14}\text{N}$ beam .....	226
Study of polymer reformed by ion-irradiation .....	227
Site change of hydrogen in Nb due to interaction with oxygen .....	228
Development of a multi-coincidence SIMS analyzer for study on potential sputtering of solid surfaces interacting with highly charged ions .....	229
Ion Coulomb crystals in a cryogenic linear RF octupole ion trap .....	230
Excitation spectrum of In atoms in superfluid helium .....	231

#### 2. Atomic and Solid State Physics(muon)

Installation of a new laser system for laser-irradiated pump-probe type $\mu\text{SR}$ experiments at RIKEN-RAL muon facility .....	233
Muons for Spintronics: Spin Exchange Scattering of Muonium with Laser-Induced Polarized Conduction Electrons in $n$ -Type GaAs .....	234
Discovery of Spin-Dependent Response of Negative Muonium ( $\text{Mu}^-$ ) to Laser Induced Polarized Electrons in $n$ -Type GaAs under Zero Field .....	235
Measurement of the Chemical Reaction Rate of Muonium with Stimulated Raman-Pumped $\text{H}_2^*(v=1)$ .....	236
Progress in design and development of counter system for new $\mu\text{SR}$ spectrometer at RIKEN-RAL .....	237
$\mu\text{SR}$ study around a quantum critical point in heavy fermion compounds $\text{Ce}_2\text{RhIn}_{8-x}\text{Sn}_x$ .....	238
On the exotic magnetic ground state in bond-disordered quantum spin system $\text{IPA-Cu}(\text{Cl},\text{Br})_3$ .....	239
Microscopic investigation of the crossover from impurity-induced order to pressure-induced order in $\text{Tl}(\text{Cu}_{1-x}\text{Mg}_x)\text{Cl}_3$ by muon-spin-rotation/relaxation .....	240
Quantum critical behavior in highly random systems $\text{Tl}_{1-x}\text{K}_x\text{CuCl}_3$ probed by zero- and longitudinal-field muon spin relaxation .....	241
Changes of spin dynamics in multiferroic $\text{Tb}_{1-x}\text{Ca}_x\text{MnO}_3$ .....	242
$\mu\text{SR}$ study of the spin-lattice cooperative phenomenon of $\text{RbCoBr}_3$ .....	243

$\mu$ SR studies on strongly correlated cubic Tm and Pr compounds with orbital degrees of freedom in the crystal-field ground state .....	244
$\mu$ SR study of heat transport due to spins in 2-leg spin-ladder system $\text{Ca}_9\text{La}_5\text{Cu}_{24}\text{O}_{41}$ .....	245
$\mu$ SR study of Heusler compounds $\text{Ru}_{2-\chi}\text{Fe}_\chi\text{CrSi}$ .....	246
Superconductivity in one-dimensional CuO double chains .....	247
$\mu$ SR study on ferromagnetism of rubidium clusters in zeolite A .....	248
$\mu$ SR Investigation of the Spin Dynamics of Central Fe Ions of Hemeproteins .....	249
Structural transition in $\text{Mo}_3\text{Sb}_7$ probed by muon spin relaxation .....	250
Dynamics of Amorphous Polymers near Glass Transition by $\mu$ SR .....	251
Muon spin rotation and relaxation on the one-dimensional cobalt(II)-radical coordination polymer magnet .....	252
Gas-Pressurized $\mu$ SR Setup at the RIKEN-RAL Muon Facility .....	253
High pressure magnetic study on a molecular conductor, $(\text{DMe-DCNQI})_2\text{Cu}$ .....	254
$\mu$ SR Studies of Cyanide Bridged Magnets .....	255
$\mu$ SR study of structure dependent electron radical dynamics in polythiophene and its derivatives .....	256
Lithium and muon diffusion in layered lithium-ion battery materials .....	257
Proton conductor II .....	258
Muon transfer studies in solid $\text{D}_2$ with implanted alkali and alkaline-earth ions .....	259
Feasible study of molecular effects on the muon transfer process .....	260
Muon beam density enhancement effect with tapered tubes .....	261

### 3. Radiochemistry and Nuclear Chemistry

Precision measurement of the half-life of $^{90m}\text{Nb}$ using a gas-jet transport system .....	263
Biodistribution of Riken multitracer (MT) and MT-EDTMP, MT-DOTMP in mice .....	264
Preparation of a rotating $^{248}\text{Cm}$ target for GARIS .....	265
Production of $^{261}\text{Rf}$ for chemical studies using the gas-jet transport system coupled to GARIS .....	266
Production of RI Tracers for chemistry of transactinide elements .....	267
Extraction of mendelevium (III) and lanthanides (III) from hydrochloric acid solutions to carbon tetrachloride with 2-thenoyltrifluoroacetone .....	268
Studies on solvent extraction behavior of molybdenum and tungsten for solution chemistry of seaborgium (element 106) .....	269
Adsorption of Nb, Ta and Pa on anion-exchanger in $\text{HF}/\text{HNO}_3$ solutions: Model experiments for the chemical study of Db .....	270
Development of an electrochemistry apparatus for the heaviest elements .....	271

### 4. Radiation Chemistry and Biology

Ion irradiation in a micro-volume of a cell with a micro beam system for cell irradiation using a tapered	
---	--

glass capillary with end-window .....	273
$\gamma$ -H2AX Foci Formation After Argon Beam Irradiation to the Cultured Animal Cell .....	274
Trichostatin A facilitates the phosphorylation of histone H2AX after X-ray irradiation in normal human fibroblast .....	275
Cell-killing effect of low dose of high-LET heavy ions (II) .....	276
Carbon-ion induced mutation frequencies and spectra in double strand break repair-deficient mutants of <i>Neurospora crassa</i> .....	277
Efficient visualization of microbial mutations using DNA two-dimensional electrophoresis display .....	278
Characterization of floral homeotic mutant, <i>Meshibedarake</i> , induced by C-ion beam irradiation .....	279
Identification of deletion mutation induced by C-ion beam irradiation in a tobacco white flower mutant .....	280
Expression analysis of anthocyanin-synthesis related genes in a torenia sector mutant produced by ion beam irradiation .....	281
Reduced expression of <i>flavonoid 3',5'-hydroxylase</i> gene in a red-flowered torenia mutant obtained by heavy-ion beam irradiation .....	282
Characterization of the GA-synthesis deficient mutants produced by heavy-ion-irradiation .....	283
Effect of the heavy-ion beam irradiation on survival rates and sex-reversal mutation in <i>Silene latifolia</i> .....	284
LET-dependent effect of C-ion beam irradiation on mutation induction in Rice. ....	285
Isolation of C-ion induced mutants of strawberry cultivar "Satsumaotome" .....	286
An early flowering mutant of strawberry cultivar "Satsumaotome" induced by C-ion irradiation .....	287
Breeding of a new Japanese barnyard millet variety with low amylose content and short-culm, by heavy-ion beam irradiation .....	288

#### IV. OPERATION RECORDS

##### 1. Operation of RIBF

Planning of RIBF operation .....	289
PAC Meetings for Nuclear Physics, and Material and Life Science .....	290
RILAC operation .....	291
AVF operation .....	293
Charged Distribution of Radioisotopes Produced at AVF Cyclotron .....	295
The operations of the RIBF ring cyclotrons.....	296
Status of RIBF control system and beam interlock system .....	298
Water Cooling System of Accelerator for RIBF .....	300
Radiation Safety Management at RIBF .....	302
Radiation field measurement around BigRIPS with a uranium beam .....	304
Operation of Cryogenic System for the Superconducting Ring Cyclotron .....	305

Oil contamination of the cryogenic system for SRC .....	307
Present status of the BigRIPS cryogenic plant.....	309
Present status of liquid-helium supply and recovery system .....	311
<b>V. RECORDS OF LABORATORIES, GROUPS, AND TEAMS (Activities and Members)</b>	
Events of Nishina Center & CNS from Jan. 2008 to Mar. 2009 .....	313
Accelerator Division	
Accelerator Development Group	
Accelerator Team .....	314
Ion Source Team .....	316
Accelerator Operation Group	
RILAC Team .....	317
Cyclotron Team .....	318
Beam Dynamics and Diagnostics Team .....	319
Cryogenic Technology Team .....	320
Nuclear Physics Research Division	
Heavy Ion Nuclear Physics Laboratory .....	321
Radioactive Isotope Laboratory .....	329
Superheavy Element Laboratory .....	333
Theoretical Nuclear Physics Laboratory .....	335
Experimental Installations Development Group	
SLOWRI Team.....	339
SAMURAI Team .....	342
Polarized RI Beam Team .....	343
Rare RI-ring Team .....	345
SCRIT Team.....	347
Experimental Installations Operation Group	
GARIS Team .....	348
BigRIPS Team .....	349
Computing and Network Team .....	351
Detector Team .....	352
User Liaison and Support Division	
User Liaison and Support Group	
User Support Office .....	354
Industrial Cooperation Team .....	355

Sub Nuclear System Research Division	
Radiation Laboratory .....	356
Advanced Meson Science Laboratory .....	362
Theoretical Physics Laboratory .....	369
Strangeness nuclear physics Laboratory .....	373
Accelerator Applications Research Division	
Accelerator Applications Research Group	
Radiation Biology Team .....	374
RI Applications Team .....	377
Safety Management Group .....	379
RIKEN-BNL Research Center	
Theory Group .....	381
Experimental Group .....	384
Center for Nuclear Study, Graduate School of Science, University of Tokyo. ....	388
TORIJIN (Todai-RIKEN Joint International Program for Nuclear Physics) Term .....	392
<b>VI. LIST OF PUBLICATIONS &amp; PRESENTATION .....</b>	<b>393</b>
<b>VII. LIST OF PREPRINTS .....</b>	<b>529</b>
<b>VIII. LIST OF SYMPOSIA .....</b>	<b>531</b>
<b>IX. LIST OF SEMINAR .....</b>	<b>535</b>
<b>X. AUTHOR INDEX</b>	

## **I. PREFACE**

## Preface

This volume No. 42 of RIKEN Accelerator Progress Report compiles the yearly research activities conducted in 2008 by the laboratories and the groups of RIKEN Nishina Center for Accelerator-Based Science, or simply RIKEN Nishina Center (RNC) which was inaugurated on April 1, 2006. It also contains progress reports submitted by users of RI Beam Factory (RIBF) and RIKEN-RAL (Rutherford and Appleton Laboratory, UK) Muon Facility (RRMF) which is operated by RNC, and is open to the international community.

The outstanding achievements of this year are selected by the editorial committee, and presented in “Frontispiece” and “Highlights of the Year”.

The RIBF project has made some amazing progress, and the RIBF is exhibiting its tremendous potentiality of RI beam production.

In December, with the Zero Degree Spectrometer (ZDS) which was successfully commissioned in November, the first PAC-approved day-1 experiments were performed. Twenty kinds of new very neutron-rich isotopes in the atomic-number range from 29 to 53 as well as more than ten kinds of new neutron-rich short-lived isomers were discovered among fission products of 345MeV/u  $^{238}\text{U}$ . This outcome was achieved in only ten days owing to the significant improvement in the intensity and stability of the primary  $^{238}\text{U}$  beam, the intensity of which was 0.3 pA. It was an order of magnitude stronger than in the 2007 experiment but remains yet as weak as a part of 3,300 of its goal. Among those newly discovered isotopes,  $^{128}\text{Pd}$ , which is more neutron-rich than  $^{125,126}\text{Pd}$  discovered last year, is remarkable because we have reached neutron-magic nuclide in Pd isotopes for the first time, and it may probably be one of the origin nuclides in the second r-process peak of the solar isotope abundance. It is anticipated that its mass and life-time will be measured precisely using our state of the art experimental installations in the near future.

We have achieved the intensity of 345 MeV/u  $^{48}\text{Ca}$  beam of 170 pA, nearly one fifth of its maximum intensity goal to the wonder and the admiration of the foreign veteran experimentalists. This world’s strongest  $^{48}\text{Ca}$  beam has led to the discovery of new neutron-hallow nuclides as well as a new very largely deformed nuclide in spite of a very short machine time allocation.

At the same time, 2008 was the year of long, hard struggle for RIBF with a major machine trouble in the helium refrigerators for the SRC and the BigRIPS. These refrigerators were heavily oil-contaminated due to the weak oil elimination power of their oil-driven helium gas compressors. Our cryogenic group persistently negotiated with the manufacturer, and in the end they admitted serious defects in their system. Thus the manufacturer repaired all

oil-contaminated parts, and improved oil elimination capacity by adding more oil eliminators, all free of cost. Now the refrigerators are working very stably.

Our GARIS group performed an excellent experiment to firmly establish the evidence of their discovery of the new super heavy element 113 in 2004. They studied decay properties of an isotope  $^{266}\text{Bh}$  and its daughter nucleus  $^{262}\text{Db}$  produced by the  $^{248}\text{Cm}$  ( $^{23}\text{Na}$ , 5n) reaction.  $^{266}\text{Bh}$  was clearly identified from the correlation of the known nuclide  $^{262}\text{Db}$ . The obtained  $\alpha$  energies and the mean life of  $^{266}\text{Bh}$  are consistent with those observed in the  $^{278}113$ . The paper was published in the JPSJ and sent to the chairperson of the joint working team of the IUPAC and IUPAP. We are looking forward to the confirmation of our right to name the new element 113. I personally prefer Japonium Jp. The GARIS group also discovered a new neutron deficient isotope of  $^{263}\text{Hs}$  by two different reactions of  $^{206}\text{Pb}$  ( $^{58}\text{Fe}$ , n) and  $^{208}\text{Pb}$  ( $^{56}\text{Fe}$ , n).

In November 4-5, RRMF Advisory Council consisting of 7 members chaired by Prof. A. Taylor, director of ISIS, facility was held in the RIBF building. The followings are the digest of their conclusions and recommendations: the RRMF provides unique instruments which serve a dynamic user community and produce excellent science; condensed matter and molecular science and ultra-slow muon source development should be prioritized; the council recommends extension of the RIKEN-RAL agreement beyond 2010 by at least another 7½ years to 2018.

In November 17-18, RBRC-SRC (RIKEN BNL Research Center Scientific Review Committee) consisting of 6 members chaired by Prof. W. Busza, MIT was held at BNL. The followings are the digest of their conclusions and recommendations: the physics issues addressed by the RBRC are among the most important in sub-nuclear physics, the results obtained to date are highly significant and of long term value; a major strength of the RBRC research program is its focus on one broad topic, QCD; its experimental program and theory program including the lattice computation program are all aimed at understanding the structure and properties of QCD matter; and that there is good reason to believe that prospects are there for the RBRC to continue being a highly successful scientific enterprise with potential for major scientific discoveries.

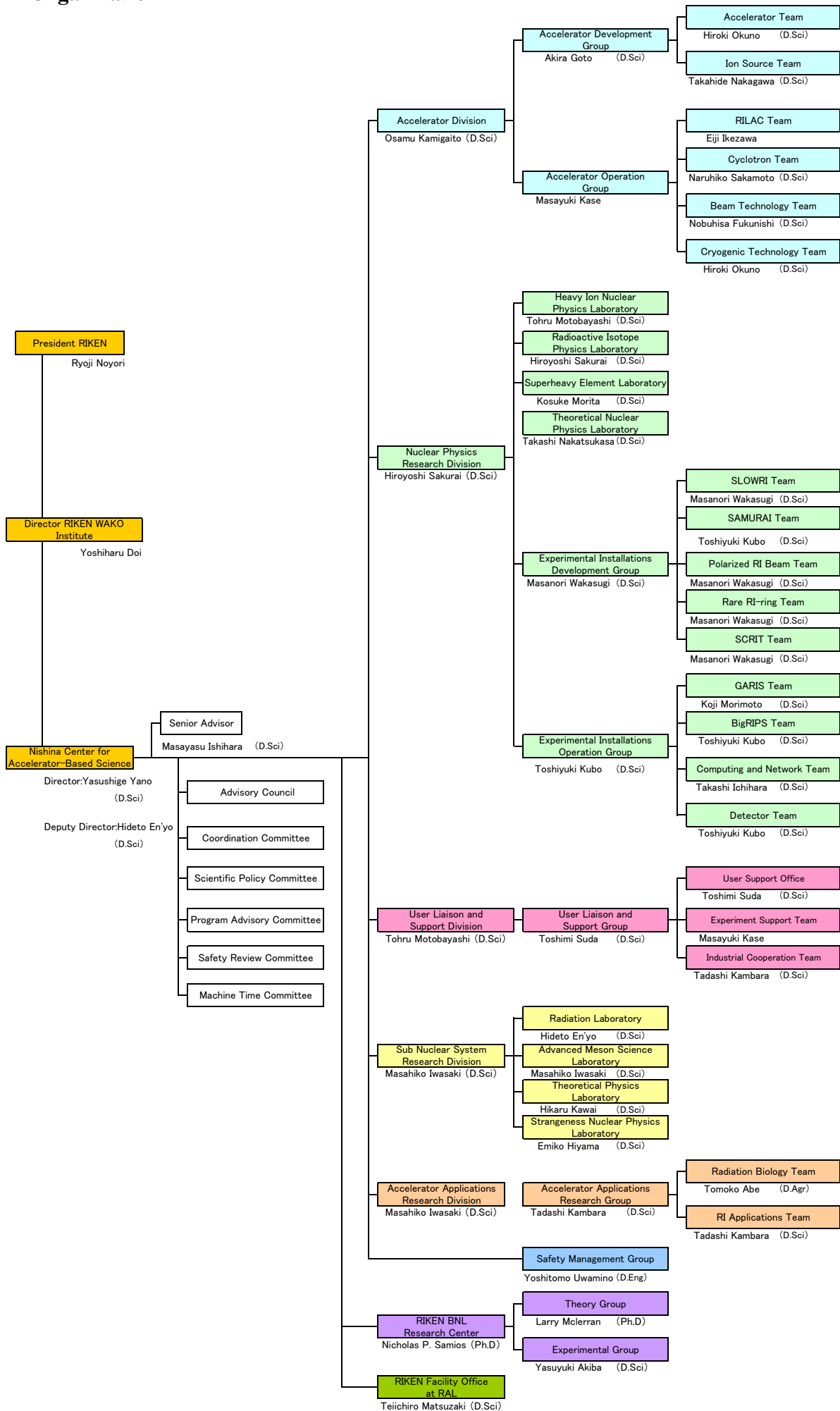
Nishina Center Advisory Council consisting of 14 members including Prof. A. Taylor, Prof. W. Busza chaired by Prof. S. Gales, director of GANIL will be held on January 15-17. Prof. Gales will report on the review when attending RIKEN Advisory Council (RAC) in April.

Yasushige Yano

*Director,*

*RIKEN Nishina Center for Accelerator-Based Science*

# Organization



## **II. RESEARCH ACTIVITIES I**

**(Nuclear-Particle Physics)**

## **1. Nuclear Physics**

## $\gamma$ Spectroscopy beyond the Island of Inversion

H. Scheit, N. Aoi, H. Baba, D. Bazin,<sup>1</sup> P. Doornenbal, N. Fukuda, H. Geissel,<sup>2</sup> R. Gernhäuser,<sup>3</sup> J. Gibelin,<sup>4</sup> Y. Hara,<sup>5</sup> C. Hinke,<sup>3</sup> N. Inabe, K. Itahashi, S. Itoh,<sup>6</sup> D. Kameda, S. Kanno, Y. Kawada,<sup>7</sup> N. Kobayashi,<sup>7</sup> Y. Kondo, R. Krücken,<sup>3</sup> T. Kubo, K. Kusaka, K. Li,<sup>8</sup> S. Michimasa,<sup>9</sup> T. Motobayashi, T. Nakamura,<sup>7</sup> T. Nakao,<sup>6</sup> S. Nishimura, T. Ohnishi, M. Ohtake, N. Orr,<sup>4</sup> H. Otsu, H. Sakurai, Y. Satou,<sup>7</sup> S. Shimoura,<sup>9</sup> T. Sumikama,<sup>10</sup> H. Takeda, E. Takeshita, S. Takeuchi, K. N. Tanaka,<sup>7</sup> K. Tanaka, Y. Togano, H. Wang,<sup>7</sup> M. Winkler,<sup>2</sup> Y. Yanagisawa, K. Yoneda, A. Yoshida, and K. Yoshida

[Nuclear structure, Island of Inversion, neutron-rich nuclei, in-beam  $\gamma$ -ray spectroscopy]

Despite strong theoretical and experimental interest in the rapid nuclear structure changes in and near the Island of Inversion no spectroscopic information is available on the low-lying states of even-even Ne and Mg isotopes beyond neutron number 20 and 24, respectively, and reduced transition probabilities,  $B(E2; 0_{gs}^+ \rightarrow 2_1^+)$  values, are only known up to neutron numbers 18 and 22, respectively. This is due to inadequate intensities of beams of these nuclei at presently operating radioactive nuclear beam facilities. This situation has changed with the commissioning of the RIBF, where very intense and high-energy secondary beams can be exploited to study nuclei that have so far been inaccessible.

The first in-beam  $\gamma$  spectroscopic study, demonstrating the potential of the new facility, has been performed in December 2008. A primary  $^{48}\text{Ca}$  beam with an average intensity of about 150 particle nA and an energy of 345 MeV/u was impinging on a 20 mm (3.7 g/cm<sup>2</sup>) thick rotating Be target located at the F0 focus of the BigRIPS<sup>(1)</sup> fragment separator. The produced secondary beams were separated using the standard  $B\rho$ - $\Delta E$ - $B\rho$  method employing a 15 mm thick wedge shaped Al degrader at the F1 dispersive focus of the BigRIPS separator. The momentum acceptance was  $\pm 3\%$ . The beam particles were identified event-by-event using the standard  $\Delta E$ -TOF- $B\rho$  method. The time of flight (TOF) was measured between two thin (1 mm and 3 mm) plastic scintillators located at the F3 and F7 achromatic foci (separated by a flight path of about 47 m), the energy-loss was determined with an ion-chamber<sup>2</sup> also located at the F7 achromatic focus and the  $B\rho$  was deduced from a position measurement at the dispersive F5 focus of BigRIPS. The figure shows the charge number  $Z$  versus the ratio of mass number to charge number  $A/Q$ . An excellent charge number and mass number resolution was observed. The location of  $^{32}\text{Ne}$  is indicated in the figure.

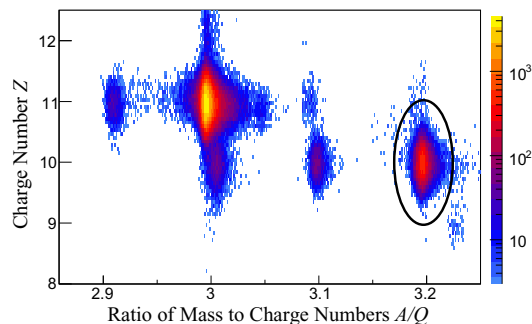


Fig. 1: Shown is the deduced charge number ( $Z$ ) versus the ratio of mass number to charge number ( $A/Q$ ) before the secondary target.  $^{32}\text{Ne}$  is indicated.

These secondary beams were then transported to the F8 secondary target position where a spot size of about  $13 \times 17 \text{ mm}^2$  (FWHM) was realized. To induce inelastic excitations a 14.1 mm (2.54 g/cm<sup>2</sup>) thick (natural) carbon target was used. The secondary  $^{32}\text{Ne}$  beam with an intensity of about 5 particles/s had an energy of about 225 MeV/u at the center of the secondary target. The emitted de-excitation  $\gamma$  rays were detected by the DALI2  $\gamma$  spectrometer<sup>3</sup> with a full energy peak efficiency of about 20% and an expected resolution after correcting the large Doppler shift of about 10% for a 1 MeV  $\gamma$  transition. For the particle identification and track reconstruction after the secondary target the newly commissioned Zero Degree Spectrometer (ZDS) was employed, which had an acceptance of about 80% for elastically scattered  $^{32}\text{Ne}$ . As before, the  $\Delta E$ -TOF- $B\rho$  method was applied to unambiguously identify the particles event by event.

After a total measuring time of only 7 hours a  $\gamma$  transition in  $^{32}\text{Ne}$  could be clearly identified not only after inelastic excitation, but also after one proton removal from  $^{33}\text{Na}$ . The data are currently under analysis.

This constitutes the first observation of a new  $\gamma$  transition in an in-beam experiment at the RIBF and demonstrates the great potential it offers for nuclear structure research in general and  $\gamma$  ray spectroscopy in particular. This measurement campaign will be continued in the fall of 2009, when the full intensity of the  $^{48}\text{Ca}$  beam can be utilized.

- 1) T. Kubo *et al.*, Nucl. Instr. Meth. B 204, 97 (2003)
- 2) H. Otsu, M. Takeuchi *et al.*, this report
- 3) S. Takeuchi *et al.*, RIKEN Acc. Rep. 36, 148 (2003)

\*1 NSCL, Michigan, USA

\*2 GSI, Darmstadt, Germany

\*3 Tech. Univ. München, Germany

\*4 LPC Caen, France

\*5 Department of Physics, Rikkyo University

\*6 Department of Physics, University of Tokyo

\*7 Department of physics, Tokyo Institute of Technology

\*8 Peking University, China

\*9 Center for Nuclear Study, The Univ. of Tokyo

\*10 Tokyo University of Science

## Inclusive Coulomb breakup of $^{22}\text{C}$ and $^{31}\text{Ne}$

T. Nakamura,<sup>\*1</sup> N. Kobayashi,<sup>\*1</sup> Y. Kondo, N. Aoi, H. Baba, S. Deguchi,<sup>\*1</sup> N. Fukuda, J. Gibelin,<sup>\*2</sup> N. Inabe, M. Ishihara, D. Kameda, Y. Kawada,<sup>\*1</sup> T. Kubo, K. Kusaka, A. Mengoni,<sup>\*3</sup> T. Motobayashi, T. Ohnishi, M. Ohtake, H. Otsu, N.A. Orr,<sup>\*2</sup> A. Saito,<sup>\*4</sup> S. Shimoura,<sup>\*4</sup> H. Sakurai, Y. Satou,<sup>\*1</sup> T. Sumikama,<sup>\*5</sup> M. Takechi, H. Takeda, E. Takeshita, S. Takeuchi, K.N. Tanaka,<sup>\*1</sup> K. Tanaka, N. Tanaka,<sup>\*1</sup> Y. Togano, Y. Yanagisawa, K. Yoneda, A. Yoshida and K. Yoshida

[Halo nuclei, Coulomb breakup]

Soft  $E1$  excitation is a unique property of halo nuclei. This property, in turn can be applied to search for a halo state by measuring such an enhancement of  $E1$  reduced transition probability  $B(E1)$ . As has been done for a number of halo nuclei<sup>1-5</sup>, Coulomb breakup is a suitable tool for this purpose.

Present work aims at identifying new halo nuclei in the neutron-drip line region of C and Ne isotopes by the Coulomb breakup. The candidate nuclei we have chosen are  $^{22}\text{C}$  and  $^{31}\text{Ne}$ , which are heavier than the heaviest known neutron halo nucleus  $^{19}\text{C}$ . This work can be a key to understand how the halo nuclei are located along the neutron drip line towards heavier nuclei.  $^{22}\text{C}$  is a Borromean nucleus where the two body constituents  $^{21}\text{C}$  nor  $nn$  system are unbound, with the estimated  $2n$  separation energy of only 419(935) keV<sup>6</sup>. On the other hand,  $^{31}\text{Ne}$  can be composed of the  $^{30}\text{Ne}$  core coupled to the loosely bound  $p$ -orbit neutron<sup>7</sup> as the estimated  $1n$  separation energy is only 332(1069) keV. The inversion of conventional shell order of  $0f_{7/2}$  and  $1p_{3/2}$  can be attributed to the deformation and loosely bound nature<sup>8</sup>.

The present experiment used the *inclusive* Coulomb breakup where we measured the  $1n(2n)$  removal cross sections of  $^{31}\text{Ne}(^{22}\text{C})$  on Pb target. Although the best way to study soft  $E1$  excitation is the direct observation of  $B(E1)$  energy spectrum by the *exclusive* full kinematical measurement, we have performed an inclusive measurement instead as the latter yield is much larger than the former one. We also measured the same reaction on C target to evaluate the nuclear breakup component in the reaction on the Pb target.

The inclusive measurement already provides a significant signal for an enhancement of  $E1$  strength at low excitation energies if a nucleus has a neutron halo. This can be easily seen by the fact that the inclusive Coulomb breakup cross section is written as an energy integral of the  $B(E1)$  multiplied by the  $E1$  virtual photon number ( $N_{E1}(E_X)$ ). Since  $N_{E1}(E_X)$  is a steep decreasing function of  $E_X$ , the enhancement of  $B(E1)$

at low energy is magnified by the photon numbers. Namely, the  $B(E1)$  at excitation energies  $E_X \sim 1$  MeV alone can contribute to the cross section by an amount of more than 500 mb.

The experiment was performed as one of a series of experiments called "Day-One Campaign" at RI beam factory (RIBF) at RIKEN. The  $^{22}\text{C}$  and  $^{31}\text{Ne}$  secondary beams were produced through the projectile fragmentation of  $^{48}\text{Ca}$  beam at 345 MeV/nucleon on a thick Be target. Typical  $^{48}\text{Ca}$  beam intensity was 60 pnA. The secondary beams were separated and focused upon the end point F8 of BigRIPS<sup>9,10</sup>, where the secondary targets of lead (3.37 g/cm<sup>2</sup> for  $^{31}\text{Ne}$  and 6.74 g/cm<sup>2</sup> for  $^{22}\text{C}$ ) and carbon (2.54 g/cm<sup>2</sup> for  $^{31}\text{Ne}$  and 4.02 g/cm<sup>2</sup> for  $^{22}\text{C}$ ) were installed. The mean energy of the  $^{22}\text{C}$  and  $^{31}\text{Ne}$  beams in the Pb target were 230 MeV/u and 234 MeV/u with a typical intensity of 6 cps and 5 cps respectively. Note that these secondary beam intensities are about  $10^3$ – $10^4$  times more than those previously obtained<sup>11</sup>.

For extracting the  $1n(2n)$  removal cross sections of  $^{31}\text{Ne}(^{22}\text{C})$ , the beam particle incident on the target, and the fragment particle following the breakup were identified and counted event by event. For the beam particle, the TOF between F3 and F7 (achromatic foci),  $\Delta E$  at F7, and position information at F5 (dispersive focus) were combined to determine  $A$  and  $Z$  of the particle. The fragment particle was analyzed and identified by the Zero-degree spectrometer (ZDS). The configuration of BigRIPS/ZDS can be seen in Fig. 1 of Ref.<sup>10</sup>. The off-line analysis for extracting the Coulomb breakup cross sections for  $^{31}\text{Ne}$  and  $^{22}\text{C}$  is now in progress.

### References

- 1) T. Kobayashi et al.: Phys. Lett. B **232**, 51 (1989).
- 2) T. Nakamura et al.: Phys. Lett. B **331**, 246 (1994).
- 3) T. Nakamura et al.: Phys. Rev. Lett. **83**, 1112 (1999).
- 4) N. Fukuda et al.: Phys. Rev. C **70**, 054606 (2004).
- 5) T. Nakamura et al.: Phys. Rev. Lett. **96**, 252502 (2006).
- 6) G. Audi et al.: Nucl. Phys. A **729**, 337 (2003).
- 7) REN Zhong-Zhou et al.: Commun. Theor. Phys. **35**, 717 (2001).
- 8) I. Hamamoto, Phys. Rev. C **69**, 041306(R) (2004).
- 9) T. Kubo: Nucl. Instrum. Methods Phys. Res., Sect. B **204**, 97 (2003).
- 10) T. Ohnishi et al.: J. Phys. Soc. **77**, 083201 (2008).
- 11) H. Sakurai et al.: Phys. Rev. C **54**, 2802(R) (1996).

<sup>\*1</sup> Department of Physics, Tokyo Institute of Technology

<sup>\*2</sup> LPC-ENSICAEN, IN2P3-CNRS et Université de Caen, France

<sup>\*3</sup> International Atomic Energy Agency, NAPC/Nuclear Data Section, Austria

<sup>\*4</sup> CNS, University of Tokyo

<sup>\*5</sup> Department of Physics, Tokyo University of Science

## Measurement of interaction cross sections for neutron rich Ne Isotopes

T. Ohtsubo<sup>\*1</sup>, M. Takechi, M. Fukuda<sup>\*2</sup>, T. Kuboki<sup>\*3</sup>, T. Moriguchi<sup>\*4</sup>, T. Sumikama<sup>\*5</sup>, H. Geissel<sup>\*6</sup>, S. Momota<sup>\*7</sup>, N. Aoi, N. Fukuda, I. Hachiuma<sup>\*3</sup>, N. Inabe, Y. Ishibashi<sup>\*4</sup>, Y. Itoh<sup>\*4</sup>, D. Kameda, K. Kusaka, M. Lantz, M. Mihara<sup>\*2</sup>, Y. Miyashita<sup>\*5</sup>, K. Namihira<sup>\*3</sup>, D. Nishimura<sup>\*2</sup>, H. Ohishi<sup>\*4</sup>, Y. Ohkuma<sup>\*1</sup>, T. Ohnishi, M. Ohtake, K. Ogawa<sup>\*4</sup>, A. Ozawa<sup>\*4</sup>, Y. Shimbara<sup>\*1</sup>, T. Suda, S. Suzuki<sup>\*1</sup>, T. Suzuki<sup>\*3</sup>, H. Takeda, K. Tanaka, R. Watanabe<sup>\*1</sup>, M. Winkler<sup>\*6</sup>, T. Yamaguchi<sup>\*3</sup>, Y. Yanagisawa, Y. Yasuda<sup>\*4</sup>, K. Yoshinaga<sup>\*5</sup>, A. Yoshida, K. Yoshida, and T. Kubo

[BigRIPS, reaction cross section, nuclear structure, unstable nuclei]

Measurement of interaction cross sections ( $\sigma_I$ ) with fast radioactive isotope beams at relativistic energies allows us to determine nuclear matter radii ( $\langle r_m^2 \rangle^{1/2}$ ) for the unstable nuclei via Glauber model analysis. The formation of a neutron halo in heavier Ne isotopes, where a level inversion of the  $1f-2p$  orbitals is predicted<sup>2)</sup>, is expected. Evidence of thick neutron skin in neighboring  $^{20}\text{N}$  has also attracted our interest<sup>3)</sup>. The low production rate, however, has so far prevented measuring their  $\sigma_I$ . The combination of a high intensity primary beam and the next generation fragment separator (BigRIPS)<sup>4)</sup> has made such nuclei accessible. Therefore, we have measured  $\sigma_I$  of neutron rich neon isotopes  $^{29-32}\text{Ne}$  as well as those in the region of the island of inversion at 250 MeV/nucleon to determine  $\langle r_m^2 \rangle^{1/2}$  of those nuclei.

A schematic drawing of the experimental setup is shown in Fig. 1. The setup is essentially the same as that of our previous experiment at GSI<sup>5)</sup>. We employed the transmission method to measure  $\sigma_I$ . A primary beam of 345 MeV/nucleon  $^{48}\text{Ca}$  with an intensity of 100 pA bombarded a Be production target at F0. Produced fragments were pre-separated at the first stage of BigRIPS. The Al wedge-shaped degrader was placed at F1. A 3.6 g/cm<sup>2</sup> thick carbon target was located at F5. The first (F3-F5) and second (F5-F7) halves of the second stage of BigRIPS were used to identify the incident and outgoing secondary beams with the  $B\rho - \Delta E$ -TOF method, respectively. We used the standard detectors<sup>6)</sup> at F3, F5 and F7. We replaced standard plastic scintillators with wider ones (240 × 100 mm) with 1mm and 3mm thicknesses at F5 and F7, respectively. These scintillation detectors provided both TOF and  $\Delta E$  information.

An example of a particle identification plot is displayed in Fig. 2.  $^{32}\text{Ne}$  intensity was around 5 cps. We accumulated roughly  $5 \times 10^4$  events of  $^{32}\text{Ne}$ , which corresponds to 1 % accuracy in  $\sigma_I$ . The data analysis to determine  $\sigma_I$  is now under way.

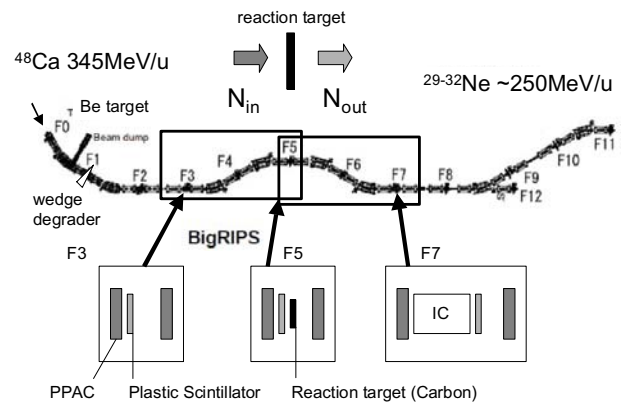


Fig. 1 Experimental setup at BigRIPS. Particle identification of incident and outgoing particles was performed by the  $B\rho - \Delta E$ -TOF method with particle detectors at F3, F5 and F7.

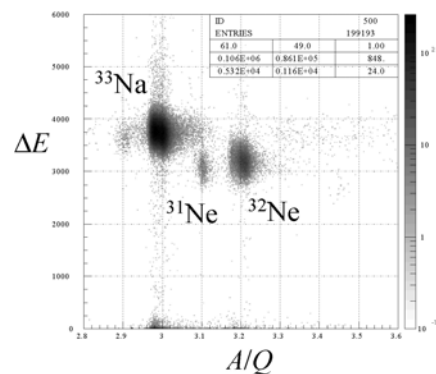


Fig. 2 Typical TOF- $\Delta E$  spectrum for the second stage of BigRIPS.

### References

- 1) A. Ozawa, T. Suzuki and I. Tanihata: Nucl. Phys. A **693**, 32 (2001).
- 2) W. Pöschl, D. Vretenar et al: Phys. Rev. Lett. **79**, 3841 (1996), J. Meng et al.: Prog. Part. Nucl. Phys. **57**, 470 (2006).
- 3) O.V. Bochkarev, et al.: Eur. Phys. J. A **1**, 15 (1998).
- 4) T. Kubo: Nucl. Instr. & Methods B **204**, 97 (2003).
- 5) T. Yamaguchi et al.: Phys. Rev. C **77**, 034315 (2008).
- 6) T. Ohnishi et al.: J. Phys. Soc. Japan **77**, 083201 (2008).

<sup>\*1</sup> Graduate School of Science, Niigata University  
<sup>\*2</sup> Department of Physics, Osaka University  
<sup>\*3</sup> Department of Physics, Saitama University  
<sup>\*4</sup> Institute of Physics, University of Tsukuba  
<sup>\*5</sup> Department of Physics, Tokyo University of Science  
<sup>\*6</sup> GSI, Germany  
<sup>\*7</sup> Faculty of Engineering, Kochi University of Technology

## Angular distributions for low-lying states in the $^{32}\text{Mg}(p, p')$ reaction

S. Takeuchi, N. Aoi, H. Baba,<sup>\*1</sup> T. Fukui,<sup>\*2</sup> Y. Hashimoto,<sup>\*3</sup> K. Ieki,<sup>\*4</sup> N. Imai,<sup>\*5</sup> H. Iwasaki,<sup>\*6</sup> S. Kanno, Y. Kondo, T. Kubo, K. Kurita,<sup>\*4</sup> T. Minemura,<sup>\*5</sup> T. Motobayashi, T. Nakabayashi,<sup>\*3</sup> T. Nakamura,<sup>\*3</sup> T. Okumura,<sup>\*3</sup> T. K. Onishi,<sup>\*6</sup> S. Ota,<sup>\*2</sup> H. Sakurai, S. Shimoura,<sup>\*1</sup> R. Sugou,<sup>\*4</sup> D. Suzuki,<sup>\*6</sup> H. Suzuki, M. K. Suzuki,<sup>\*6</sup> M. Takashina,<sup>\*7</sup> E. Takeshita, M. Tamaki,<sup>\*1</sup> K. Tanaka, Y. Togano, and K. Yamada

[nuclear structure, in-beam  $\gamma$ -ray spectroscopy]

Proton inelastic scattering on the neutron-rich nucleus  $^{32}\text{Mg}$  has been experimentally studied at  $E_{\text{lab}} = 46.5$  MeV/nucleon in inverse kinematics.<sup>1,2)</sup> The energies of excited states in  $^{32}\text{Mg}$  were obtained by measuring de-excitation  $\gamma$  rays. Five new states were identified by  $\gamma$ - $\gamma$  coincidence analysis as shown in Fig. 1. Measured angular distributions of the scattered  $^{32}\text{Mg}$  suggest  $\Delta L = 2$  and 4 for the excitation to the 885- and 2321-keV state, respectively, as reported in Ref<sup>1,2)</sup>. For other excited states, angular distributions were also obtained in the present experiment. Cross sections of excitations to the 5167- and 5204-keV states are found to be 2.9(4) and 2.7(4) mb, which are relatively larger than other states. In the present study, angular distributions were analyzed by DWBA calculations using ECIS97 code<sup>3)</sup>.

Figure 2 shows measured angular distributions of the excitation to the 5167- and 5204-keV states indicated by dots with statistical error-bars, and calculated curves indicated by solid, dashed, dotted-dash, and dotted curves representing transferred angular momentum ( $\Delta L$ ) of 1, 2, 3, and 4, respectively. DWBA calculations were examined using KD02 optical potential<sup>4)</sup> assuming the one-phonon excitation in the harmonic vibrational model. In the calculations, each curve was normalized to the measured cross section, adjusting amplitude parameter  $\beta_\lambda$ . Comparing with each reduced- $\chi^2$  value for each excited state, candidates of spins were  $J = 2$  and 3.

Angular distributions of the 5167- and 5204-keV states are similar to each other. Considering the uncertainty of the  $\gamma$ -ray energy determination, there is a possibility of the same excited state for the 5167- and 5204-keV states. Assuming the one excited state instead of the 5167- and 5204-keV states, the excitation energy could be 5186(28) keV and the cross section is 5.6 mb which is larger than the one of the 2321-keV state (3.7(6) mb). Possible spin assignment for the 5187-keV state may be  $J$  of 3, considering the angular distribution and decay scheme. The amplitude

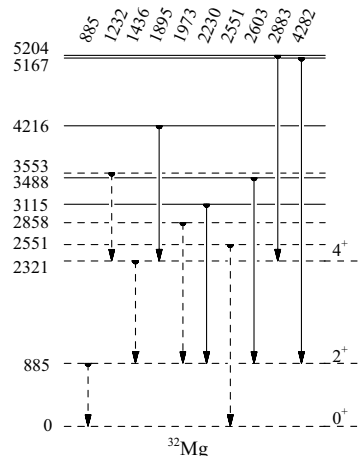


Fig. 1. Reconstructed level scheme of  $^{32}\text{Mg}$  deduced from the present studies of the  $^{32}\text{Mg}+p$  inelastic scattering. Solid lines and arrows show new levels and transitions, respectively.

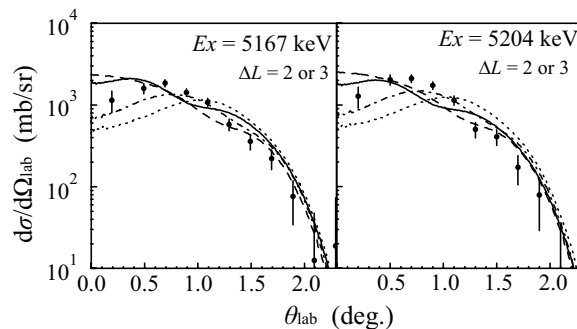


Fig. 2. Angular distributions for the excitation to the higher states around energies of 5 MeV in  $^{32}\text{Mg}(p, p')$  reaction.

$\beta_3$  of this excitation is found to be 0.171, indicating a possibility of a  $3^-$  state.

### References

- 1) S. Takeuchi et al.: J. Phys.:Conf. Ser. **49**, 153 (2006).
- 2) S. Takeuchi et al.: RIKEN Accel. Prog. Rep. **41**, xvi (2008).
- 3) J. Raynal: unpublished *coupled-channel code ECIS97*.
- 4) A. J. Koning, J. P. Delaroche, Nucl. Phys. A **713**, 231 (2003).

<sup>\*1</sup> Center for Nuclear Study, University of Tokyo

<sup>\*2</sup> Department of Physics, Kyoto University

<sup>\*3</sup> Department of Physics, Tokyo Institute of Technology

<sup>\*4</sup> Department of Physics, Rikkyo University

<sup>\*5</sup> Institute of Particle and Nuclear Studies, High Energy Accelerator Research Organization (KEK)

<sup>\*6</sup> Department of Physics, University of Tokyo

<sup>\*7</sup> Research Center for Nuclear Physics (RCNP), Osaka University

# One-neutron removal reactions of $^{18}\text{C}$ and $^{19}\text{C}$ on a proton target<sup>†</sup>

Y. Kondo, T. Nakamura,<sup>\*1</sup> Y. Satou,<sup>\*1</sup> T. Matsumoto, N. Aoi, N. Endo,<sup>\*2</sup> N. Fukuda, T. Gomi, Y. Hashimoto,<sup>\*1</sup> M. Ishihara, S. Kawai,<sup>\*3</sup> M. Kitayama,<sup>\*2</sup> T. Kobayashi,<sup>\*2</sup> Y. Matsuda,<sup>\*2</sup> N. Matsui,<sup>\*1</sup> T. Motobayashi, T. Nakabayashi,<sup>\*1</sup> K. Ogata,<sup>\*4</sup> T. Okumura,<sup>\*1</sup> H. J. Ong,<sup>\*5</sup> T. K. Onishi,<sup>\*5</sup> H. Otsu, H. Sakurai, S. Shimoura,<sup>\*6</sup> M. Shinohara,<sup>\*1</sup> T. Sugimoto, S. Takeuchi, M. Tamaki,<sup>\*6</sup> Y. Togano,<sup>\*3</sup> and Y. Yanagisawa

[Nuclear structure, momentum distribution, unstable nuclei]

We have studied the one-neutron removal reactions of  $^{18}\text{C}$  at 81 MeV/nucleon and  $^{19}\text{C}$  at 68 MeV/nucleon on a liquid hydrogen target to clarify the microscopic structure of these nuclei. Transverse-momentum distributions of the core fragments and partial cross sections were measured using coincidences with  $\gamma$  rays. These were compared to theoretical calculations based on the continuum-discretized coupled-channels (CDCC) method<sup>1)</sup> involving shell model spectroscopic factors calculated by the WBP effective interaction.<sup>2)</sup>

The experiment was performed at the RI Beam Factory operated by RIKEN Nishina Center and CNS, University of Tokyo. Secondary beams of  $^{18}\text{C}$  and  $^{19}\text{C}$  were produced via projectile fragmentation of a primary  $^{22}\text{Ne}$  beam at 110 MeV/nucleon on a Be target. The secondary beams were purified by RIPS and were transported to a cell of a cryogenic liquid hydrogen target,<sup>3)</sup> which is part of CRYPTA (cryogenic proton and  $\alpha$  target system). The average thickness of the liquid hydrogen was 120 mg/cm<sup>2</sup>. The incident ion, outgoing core fragment, and de-excitation  $\gamma$  rays were detected in coincidence to obtain the transverse momentum distribution and partial cross section for populating each individual state in the core nucleus. The details of the experimental setup can be found in Ref. 4.

In the one-neutron removal reaction of  $^{18}\text{C}$ , we observed two peaks at 0.21 and 0.33 MeV in the energy spectrum of the  $\gamma$  rays emitted from the outgoing core fragment  $^{17}\text{C}$ . By comparing the obtained transverse momentum distributions with the CDCC calculations, it was found that the distribution for the 0.21-MeV state is described well by the calculation for neutron removal from the  $1s$  orbital in  $^{18}\text{C}$ , whereas that for the 0.33-MeV state is consistent with neutron removal from the  $0d$  orbital. We thus confirm  $J^\pi = 1/2^+$  for the 0.21-MeV state and  $J^\pi = 5/2^+$  for the 0.33-MeV state as deduced in the previous  $^{17}\text{C}(p, p')$  experiment.<sup>5)</sup>

In the one-neutron removal reaction of  $^{19}\text{C}$ , three  $\gamma$  transitions were observed. The measured transverse

momentum distribution of  $^{18}\text{C}$  in coincidence with the 2.4-MeV  $\gamma$  ray, corresponding to the population of the 4.0-MeV state, is well reproduced by the CDCC calculation by assuming the  $0d$ -neutron removal. This result leads to the  $J^\pi$  assignment of the 4.0-MeV state in  $^{18}\text{C}$ . Because  $0d_{5/2}$ -neutron removal from  $^{19}\text{C}(1/2^+)$  populates the  $J^\pi = 2^+, 3^+$  states of  $^{18}\text{C}$  and  $0d_{3/2}$ -neutron removal produces the  $J^\pi = 1^+, 2^+$  states, the 4.0-MeV state can be assigned as  $J^\pi = (1, 2, 3)^+$ . The  $1^+$  assignment is excluded from the following discussion. The cross section for  $0d_{3/2}$ -neutron removal is expected to be small because the occupation number of the  $\nu d_{3/2}$  orbital in the ground state of  $^{19}\text{C}$  is expected to be small. In fact, the CDCC calculation with a shell-model spectroscopic factor  $C^2S_{\text{th}} = 0.086$  predicts a cross section of only  $\sigma_{\text{th}} = 1$  mb, which is much smaller than the experimental value  $\sigma_{\text{exp}} = 35(4)$  mb, indicating the inadequateness of the  $1^+$  assignment. Hence, we adopt the  $J^\pi = (2, 3)^+$  assignment for the 4.0-MeV state.

In the present study, we have demonstrated the usefulness of the one-neutron removal reaction on the proton target. It is found that the observed transverse-momentum distributions reflect the orbital angular momentum of the removed neutron, as in the well-studied longitudinal-momentum distributions measured with Be and C targets. We also demonstrated that CDCC analysis is a powerful tool for one-neutron removal from exotic nuclei by a proton target.

## References

- 1) M. Kamimura et al.: Prog. Theor. Phys. Suppl. **89**, 1 (1986).
- 2) E. K. Warburton and B. A. Brown: Phys. Rev. C **46**, 923 (1992).
- 3) H. Ryuto et al.: Nucl. Instrum. Methods A **555**, 1 (2005).
- 4) Y. Kondo et al.: Phys. Rev. C **79**, 014602 (2009).
- 5) Z. Elekes et al.: Phys. Lett. B **614**, 174 (2005).

<sup>†</sup> Condensed from the article in Phys. Rev. C. **79**, 014602 (2008)

<sup>\*1</sup> Department of Physics, Tokyo Tech

<sup>\*2</sup> Department of Physics, Tohoku University

<sup>\*3</sup> Department of Physics, Rikkyo University

<sup>\*4</sup> Department of Physics, Kyushu University

<sup>\*5</sup> Department of Physics, University of Tokyo

<sup>\*6</sup> Center for Nuclear Study (CNS), University of Tokyo

# Inelastic proton scattering on the neutron-rich nucleus $^{58}\text{Ti}$

H. Suzuki, N. Aoi, E. Takeshita, S. Ota,<sup>\*1</sup> S. Takeuchi, H. Baba,<sup>\*1</sup> S. Bishop,<sup>\*2</sup> T. Fukui,<sup>\*3</sup> Y. Hashimoto,<sup>\*4</sup> E. Ideguchi,<sup>\*1</sup> K. Ieki,<sup>\*5</sup> N. Imai,<sup>\*6</sup> H. Iwasaki,<sup>\*7</sup> S. Kanno, Y. Kondo, T. Kubo, K. Kurita,<sup>\*5</sup> K. Kusaka, T. Minemura,<sup>\*6</sup> T. Motobayashi, T. Nakabayashi,<sup>\*4</sup> T. Nakamura,<sup>\*4</sup> T. Nakao,<sup>\*7</sup> M. Niikura,<sup>\*1</sup> T. Okumura,<sup>\*4</sup> H. J. Ong,<sup>\*8</sup> T. K. Onishi,<sup>\*7</sup> H. Sakurai, S. Shimoura,<sup>\*1</sup> R. Sugo,<sup>\*5</sup> D. Suzuki,<sup>\*7</sup> M. K. Suzuki,<sup>\*7</sup> M. Tamaki,<sup>\*1</sup> K. Tanaka, Y. Togano, and K. Yamada

[Nuclear structure,  $^{58}\text{Ti}(p,p'\gamma)$ , inelastic scattering, unstable nuclei]

The structure of the neutron-rich nucleus  $^{58}\text{Ti}$  was investigated via proton inelastic scattering using the technique of in-beam  $\gamma$ -ray spectroscopy. A new region of deformation is suggested in the neutron-rich Cr isotopes around  $N = 40$ .<sup>1,2)</sup> It is interesting to study whether the deformation develops further in nuclei with more neutrons or less protons. We have studied the collectivity of  $^{58}\text{Ti}$  ( $N = 36$ ) for the first time.

A  $^{58}\text{Ti}$  beam was produced by fragmentation of a 63 MeV/nucleon  $^{70}\text{Zn}$  beam with a mean intensity of 150 pnA onto a  $^9\text{Be}$  target of 95 mg/cm<sup>2</sup> thickness, using the same experimental arrangement described in Ref.<sup>2)</sup> The  $^{58}\text{Ti}$  nuclei were separated by the RIKEN Projectile-fragment Separator (RIPS).<sup>3)</sup> The intensity of  $^{58}\text{Ti}$  was 1.5 cps. These nuclei bombarded a liquid hydrogen target<sup>4)</sup> of 72 mg/cm<sup>2</sup> thickness. The energy of  $^{58}\text{Ti}$  at the middle of the secondary target was 40 MeV/nucleon. The de-excitation  $\gamma$  rays from the inelastically scattered  $^{58}\text{Ti}$  nuclei were detected by the NaI(Tl) scintillator array DALI2<sup>5)</sup> surrounding the secondary target. The scattered particles were identified using the “TOF mass analyzer for radioactive isotope beam experiments” (TOMBEE)<sup>6)</sup> placed downstream of the secondary target.

The Doppler-shift corrected  $\gamma$ -ray energy spectrum measured in coincidence with inelastically scattered  $^{58}\text{Ti}$  is shown in Fig. 1 (a). A strong peak at 1046(11) keV, and weak peaks at 1376(18) keV and 1835(27) keV were observed for the first time. The 1046-keV peak was assigned to the  $2_1^+ \rightarrow 0_{g.s.}^+$  transition, because the first  $2^+$  state is most strongly populated by proton inelastic scattering on even-even nuclei.

The energy of the first  $2^+$  state [ $E_x(2^+)$ ] in  $^{58}\text{Ti}$  is compared with those of other even-even Ti isotopes and Cr isotopes in Fig. 1 (b). The  $E_x(2^+)$  value of  $^{58}\text{Ti}$  is slightly smaller than that of  $^{56}\text{Ti}$ . On the other hand,  $E_x(2^+)$  of  $^{56}\text{Ti}$  is significantly smaller than that of the sub-shell closed nucleus  $^{54}\text{Ti}$  with  $N = 32$ . This indicates that the increase of the collectivity from  $^{56}\text{Ti}$

to  $^{58}\text{Ti}$  is much smaller than that from  $^{54}\text{Ti}$  to  $^{56}\text{Ti}$ . In contrast,  $E_x(2^+)$  of the Cr isotopes decrease continuously from  $N = 34$  to  $N = 38$ , indicating continuous enhancement of the collectivity toward  $N = 38$ . The larger  $E_x(2^+)$  values of Ti isotopes than those of Cr isotopes suggest the weaker collectivity of Ti isotopes. Therefore, the development of the deformation region found in the neutron-rich Cr isotopes does not extend to  $^{58}\text{Ti}$ .

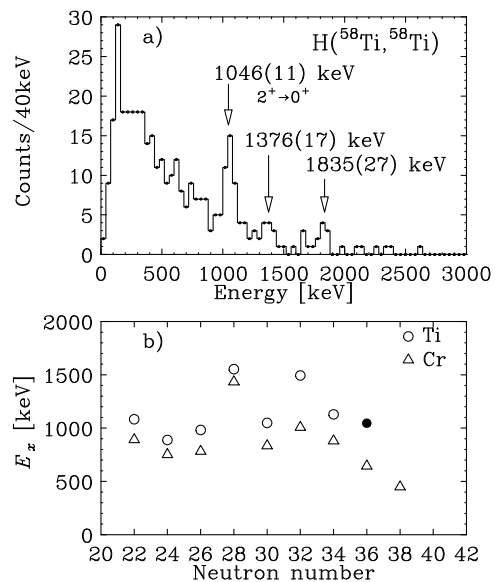


Fig. 1. (a) Doppler-shift corrected  $\gamma$ -ray energy spectrum for the proton inelastic scattering on  $^{58}\text{Ti}$ . (b) Plot of the excitation energies of the  $2^+$  states as a function of the neutron number for Ti isotopes (circles) and Cr isotopes (triangles). The filled circle indicates the result from the present work.

## References

- 1) O. Sorlin et al.: Eur. Phys. J. A **55**, 16 (2003).
- 2) N. Aoi et al.: Phys. Rev. Lett. **102**, 012502 (2009).
- 3) T. Kubo et al.: Nucl. Instrum. Methods B **70**, 309 (1992).
- 4) H. Ryuto et al.: Nucl. Instrum. Methods A **555**, 1 (2005).
- 5) S. Takeuchi et al.: RIKEN Accel. Prog. Rep. **36**, 148 (2003).
- 6) N. Aoi et al.: RIKEN Accel. Prog. Rep. **38**, 176 (2005).

\*1 Center for Nuclear Study, University of Tokyo

\*2 Faculty of Physics, Technische Universität München

\*3 Department of Physics, Kyoto University

\*4 Department of Physics, Tokyo Institute of Technology

\*5 Department of Physics, Rikkyo University

\*6 High Energy Accelerator Research Organization (KEK)

\*7 Department of Physics, University of Tokyo

\*8 Department of Physics, Osaka University

# Inelastic scattering studies of $^{16}\text{C}$ reexamined<sup>†</sup>

Z. Elekes,<sup>\*1</sup> N. Aoi, Zs. Dombrádi,<sup>\*1</sup> Zs. Fülöp,<sup>\*1</sup> T. Motobayashi, and H. Sakurai

[nuclear structure, unstable nuclei, inelastic scattering]

$^{16}\text{C}$  nucleus has been in the forefront of nuclear structure studies in the past years due to several reasons. Its extended neutron distribution was suggested from a reaction cross section measurement<sup>1)</sup>. Another interesting phenomenon in the chain of carbon isotopes, opposite deformations between protons and neutrons<sup>2)</sup>, which inspired several experimental works, were proposed in the mid-nineties by Antisymmetrized Molecular Dynamics (AMD) calculations. In addition, the anomalous long lifetime of the first  $2^+$  excited state and a corresponding hindered E2 strength was measured by recoil shadow method in RIKEN<sup>3)</sup>. Similar small  $B(E2)$  value and a strong dominance of neutron over proton excitations were concluded by analyzing the angular distribution of  $^{16}\text{C}$  nuclei inelastically scattered on a  $^{208}\text{Pb}$  target<sup>4)</sup>. This seemed to be confirmed by a proton inelastic scattering measurement in inverse kinematics<sup>5)</sup>. This year, the results of two new experiments aimed at redetermining the lifetime of the first  $2^+$  excited state have become available. RIKEN published a revised data<sup>6)</sup> and Lawrence Berkeley National Laboratory has reported a value close to this new result<sup>7)</sup>. These studies suggest a shorter lifetime and a corresponding larger  $B(E2; 0_{gs}^+ \rightarrow 2_1^+)$  between 10-20  $\text{e}^2\text{fm}^4$ .

In this paper, we present a reanalysis of the inelastic scattering experiments populating the  $2_1^+$  state using  $^{208}\text{Pb}$ <sup>4)</sup> and hydrogen targets<sup>5)</sup>. Since the Pb and H targets probe the neutron and proton distributions with different sensitivities, both mass and charge, and consequently, the neutron and proton deformation lengths ( $\delta_n$  and  $\delta_p$ ) can be extracted by comparing the integrated cross sections of the two processes in a simultaneous way.

As a first step, a pair of neutron and proton deformation lengths has been chosen.  $\delta_M^{Pb}$ ,  $\delta_M^{pp}$ ,  $\delta_C^{Pb} = \delta_C^{pp} = \delta_p$  are matter and Coulomb deformation lengths for the two probes, respectively.

$$(Z \cdot b_n^{Pb} + N \cdot b_p^{Pb}) \cdot \delta_M^{Pb} = N \cdot b_n^{Pb} \cdot \delta_n + Z \cdot b_p^{Pb} \cdot \delta_p \quad (1)$$

$$(Z \cdot b_n^{pp} + N \cdot b_p^{pp}) \cdot \delta_M^{pp} = N \cdot b_n^{pp} \cdot \delta_n + Z \cdot b_p^{pp} \cdot \delta_p \quad (2)$$

where  $b_n^{Pb}$ ,  $b_p^{Pb}$ ,  $b_n^{pp}$  and  $b_p^{pp}$  are the neutron and proton sensitivity parameters.

$\delta_{M,C}^{Pb}$ ,  $\delta_{M,C}^{pp}$  are the input parameters in the coupled channel code ECIS97 which were used to retrieve calculated cross sections  $\sigma_{cal}^{Pb}$  and  $\sigma_{cal}^{pp}$ . The difference

between the calculated and experimental cross sections has been quantified in a  $\chi^2$  value so that we ended up with a set of data ( $\delta_n, \delta_p, \chi^2$ ). This procedure was repeated with varied initial ( $\delta_n, \delta_p$ ) parameters and the results are visualized in a contour plot of  $\chi^2$  values. From the contour plot, the neutron and proton deformation lengths could easily be determined at  $\delta_n = 1.37 \pm 0.12$  (stat) fm,  $\delta_p = 0.90 \pm 0.13$  (stat) fm. The corresponding proton and neutron transition strengths are:

$$B(E2; 0_{gs}^+ \rightarrow 2_1^+)/e^2 = M_p^2 = 15.2 \pm 4.4 \text{ (stat) fm}^4 \quad (3)$$

$$M_n^2 = 98 \pm 17 \text{ (stat) fm}^4. \quad (4)$$

The total systematic uncertainties due to optical model parameters have been determined at  $\Delta\delta_n = 0.095$  fm,  $\Delta\delta_p = 0.13$  fm,  $\Delta M_n^2 = 14$   $\text{fm}^4$ ,  $\Delta M_p^2 = 4.4$   $\text{fm}^4$ . Another source of uncertainty comes from the sensitivity parameters of the probes. The values are not precisely known, and therefore, the dependence of the final data on them has been tested by introducing a 20% change in the  $(\frac{b_n}{b_p})^{pp}$  ratio, which alters the  $(\frac{b_n}{b_p})^{Pb}$  value consequently. This resulted to the following systematic errors:  $\Delta\delta_n = 0.025$  fm,  $\Delta\delta_p = 0.025$  fm,  $\Delta M_n^2 = 3.6$   $\text{fm}^4$ ,  $\Delta M_p^2 = 0.8$   $\text{fm}^4$ .

The presently determined  $B(E2) = 15.2$   $\text{e}^2\text{fm}^4$  value is close to the results coming from the two new lifetime measurements<sup>6,7)</sup> of  $13.0 \pm 1.0$  (stat)  $\pm 3.5$  (syst)  $\text{e}^2\text{fm}^4$  and  $20.8 \pm 3.7$   $\text{e}^2\text{fm}^4$  and are consistent with each other taking into account the error bars. However, they are much smaller than  $82.3$   $\text{e}^2\text{fm}^4$  which is expected using a global fit by Raman<sup>8)</sup> based on the Grodzins rule<sup>9)</sup>. On the other hand, our extracted neutron strength of  $98$   $\text{fm}^4$  is about 6 times larger than the proton, which shows the dominance of neutron over proton excitations in  $^{16}\text{C}$  nucleus.

## References

- 1) T. Zheng et al.: Nucl. Phys. A **709**, 103 (2002).
- 2) Y. Kanada-En'yo et al.: Phys. Rev. C **55**, 2860 (1997).
- 3) N. Imai et al.: Phys. Rev. Lett. **92**, 062501 (2004).
- 4) Z. Elekes et al.: Phys. Lett. B **586**, 34 (2004).
- 5) H.J. Ong et al.: Phys. Rev. C **73**, 024610 (2006).
- 6) H.J. Ong et al.: Phys. Rev. C **78**, 014308 (2008).
- 7) M. Wiedeking et al.: Phys. Rev. Lett. **100**, 152501 (2008).
- 8) S. Raman et al.: Atom. Data Nucl. Data Tabl. **78**, 1 (2001).
- 9) L. Grodzins: Phys. Lett. **2**, 88 (1962).

<sup>†</sup> Condensed from the article in Phys. Rev. C **78**, 027301 (2008)

<sup>\*1</sup> Institute of Nuclear Research of the Hungarian Academy of Sciences

## Lifetime measurements of excited states in $^{17}\text{C}^\dagger$

D. Suzuki,<sup>\*1</sup> H. Iwasaki,<sup>\*1</sup> H. J. Ong,<sup>\*2</sup> N. Imai,<sup>\*3</sup> H. Sakurai, T. Nakao,<sup>\*1</sup> N. Aoi, H. Baba, S. Bishop, Y. Ichikawa, M. Ishihara, Y. Kondo, T. Kubo, K. Kurita,<sup>\*4</sup> T. Motobayashi, T. Nakamura,<sup>\*5</sup> T. Okumura,<sup>\*5</sup> T. K. Onishi,<sup>\*1</sup> S. Ota,<sup>\*6</sup> M. K. Suzuki,<sup>\*1</sup> S. Takeuchi, Y. Togano and Y. Yanagisawa

[Nuclear Structure,  $^{17}\text{C}$ , excited states, lifetime]

We report on  $\gamma$ -decay lifetime measurements conducted for low-lying excited states of the loosely-bound isotope  $^{17}\text{C}$ . The electromagnetic transition strengths were determined for the corresponding deexcitations from the lifetimes observed. The present study aimed to elucidate the low-lying structure of  $^{17}\text{C}$ .

The low-lying level scheme of  $^{17}\text{C}$  is known to exhibit a couple of unique features. The spin-parity of the ground state was confirmed to be  $3/2^+$ ,<sup>1)</sup> which contradicts the naïve shell model expectation that the ground state of an odd nucleus with  $N = 11$  should have spin-parity of  $5/2^+$ . A recent work<sup>2)</sup> further revealed two excited states located below the very low neutron emission threshold at 728 keV. These states are almost degenerate with excitation energies of about 220 keV and 330 keV, both deexciting directly to the ground state. In light-mass nuclei, manifestation of such a high degeneracy is exceptional around the ground state. Although spin-parity assignments of  $(1/2^+)$  and  $5/2^+$  have been made for the first and second excited states, respectively, a comprehensive understanding has not yet been achieved on the underlying structure.

Measurements were performed at the RIPS beamline. The upgraded recoil shadow method (RSM)<sup>5)</sup> was applied to the breakup reaction on  $^{18}\text{C}$  at 79 AMeV. Details on the RSM are found in Ref.<sup>5)</sup>.  $^{18}\text{C}$  ions were produced in projectile fragmentation reactions of 110-AMeV  $^{22}\text{Ne}$  primary beams with a typical intensity of 320 pA, impinging on a 1.02-g/cm<sup>2</sup>  $^9\text{Be}$  production target. The  $^{18}\text{C}$  beam had a typical intensity of  $2.3 \times 10^4$  counts per second with a purity of about 60%, and was directed onto a 370-mg/cm<sup>2</sup>  $^9\text{Be}$  reaction target set at the final focal plane of RIPS. Positions and incident angles of the secondary beam particles were recorded with two sets of parallel plate avalanche counters (PPACs)<sup>6)</sup> placed upstream of the reaction target. Outgoing particles were detected by a plastic scintillator hodoscope,<sup>7)</sup> located 3.8 m downstream of the target, facilitating particle identification with the TOF- $\Delta E$ - $E$  method. The scattering angle of the particle was determined by combining the hit position on the hodoscope with those on the PPACs for the in-

coming particles. An array of 130 NaI(Tl) detectors<sup>8)</sup> surrounded the reaction target to detect deexciting  $\gamma$  rays. A 5-cm-thick lead slab was installed close to the target to serve as the  $\gamma$ -ray shield, which is an essential part of the RSM. The slab had an area of  $24 \times 24$  cm<sup>2</sup> with a 5.4-cm-diameter hole in the center.

Deexcitation  $\gamma$ -rays from the two excited states were clearly observed. The  $\gamma$ -decay mean lifetimes were determined to be  $583 \pm 21(\text{stat}) \pm 35(\text{syst})$  ps for the first excited state and  $18.9 \pm 0.6(\text{stat}) \pm 4.7(\text{syst})$  ps for the second excited state. Based on a comparison with the empirical upper limits for the electromagnetic transition strengths, these decays were determined to be predominantly M1 transitions. The reduced M1 transition probabilities to the ground state were deduced to be  $(1.0 \pm 0.1) \times 10^{-2} \mu_N^2$  and  $(8.2_{-1.8}^{+3.2}) \times 10^{-2} \mu_N^2$ , respectively, for the first and second excited states.

The obtained results were compared with those of the stable isotone  $^{21}\text{Ne}$ . It is known that  $^{21}\text{Ne}$  has an anomalous ground state spin-parity of  $3/2^+$  due to its large prolate deformation. The comparison showed that the level properties of the  $5/2^+$  states are remarkably similar between the two isotones in terms of the excitation energy and the M1 strength to the ground state. The similarity suggests the enhanced collectivity in  $^{17}\text{C}$ , since the  $3/2^+$  and  $5/2^+$  states form a rotational band in  $^{21}\text{Ne}$ . On the other hand, as crossing from  $^{21}\text{Ne}$  to  $^{17}\text{C}$ , the  $1/2^+$  state shows a significant lowering of the state by about 2.5 MeV, accompanied by a strong hindrance of the M1 strength. Naïve Nilsson-model considerations prompted a conjecture that the anomalous behavior of the  $^{17}\text{C}$   $1/2^+$  state is related to enhancement of a spatially extended  $s$ -wave component anticipated for a loosely bound deformed orbital.

### References

- 1) J. P. Dufour et al.: *Z. Phys. A* **324**, 487(1986); H. Ueno et al.: *Nucl. Phys. A* **738**, 211(2004).
- 2) M. Stanoiu et al.: *Eur. Phys. J. A* **20**, 95(2004).
- 3) H. G. Bohlen et al.: *Eur. Phys. J. A* **31**, 279(2007).
- 4) Z. Elekes et al.: *Phys. Lett. B* **614**, 174(2005).
- 5) H. J. Ong et al.: *Phys. Rev. C* **78**, 014308(2008).
- 6) H. Kumagai et al.: *Nucl. Instr. and Meth. A* **470**, 562(2001).
- 7) S. Takeuchi et al.: *Phys. Lett. B* **515**, 255(2001).
- 8) T. Nishio et al.: *RIKEN Accel. Prog. Rep.* **29**, 184(1996); S. Takeuchi et al.: *RIKEN Accel. Prog. Rep.* **36**, 148(2003).

<sup>†</sup> Condensed from the article in *Phys. Lett. B* **666**, 222(2008).

<sup>\*1</sup> Department of Physics, University of Tokyo

<sup>\*2</sup> RCNP, Osaka University

<sup>\*3</sup> KEK

<sup>\*4</sup> Department of Physics, Rikkyo University

<sup>\*5</sup> Department of Physics, Tokyo Institute of Technology

<sup>\*6</sup> CNS, University of Tokyo

# Investigation of the $^{30}\text{S}(p, \gamma)^{31}\text{Cl}$ reaction via Coulomb dissociation

Y. Togano, T. Motobayashi, N. Aoi, H. Baba, S. Bishop, X. Cai,<sup>\*1</sup> P. Doornenbal, D. Fang<sup>\*1</sup> T. Furukawa, K. Ieki,<sup>\*2</sup> N. Iwasa,<sup>\*3</sup> T. Kawabata,<sup>\*4</sup> S. Kanno, N. Kobayashi,<sup>\*5</sup> Y. Kondo, T. Kuboki,<sup>\*6</sup> N. Kume,<sup>\*3</sup> K. Kurita,<sup>\*2</sup> M. Kurokawa, Y. G. Ma,<sup>\*1</sup> Y. Matsuo, H. Murakami, M. Matsushita,<sup>\*2</sup> T. Nakamura,<sup>\*5</sup> K. Okada,<sup>\*2</sup> S. Ota,<sup>\*4</sup> Y. Satou,<sup>\*5</sup> S. Shimoura,<sup>\*4</sup> R. Shioda,<sup>\*2</sup> K. N. Tanaka,<sup>\*5</sup> S. Takeuchi, W. Tian,<sup>\*1</sup> H. Wang,<sup>\*1</sup> J. Wang,<sup>\*7</sup> K. Yamada, Y. Yamada,<sup>\*2</sup> and K. Yoneda

[ $^{208}\text{Pb}(^{31}\text{Cl}, p)^{30}\text{S}$ ], nuclear astrophysics, Coulomb dissociation]

The stellar reaction  $^{30}\text{S}(p, \gamma)^{31}\text{Cl}$  was studied via Coulomb dissociation. This reaction occurs in the rapid proton ( $rp$ ) capture process of hydrogen burning on the surface of an accreting neutron star.<sup>1)</sup> The nucleus  $^{30}\text{S}$  is a candidate for the waiting point, which the reaction flow temporary stops at this nuclei, in the  $rp$  process.<sup>2)</sup> The  $^{30}\text{S}(p, \gamma)^{31}\text{Cl}$  reaction decreases the amount of  $^{30}\text{S}$ , and thus speeds the reaction flow of the  $rp$  process up. Therefore the strength of this reaction affects the resultant abundance and energy production in the  $rp$  process.  $^{31}\text{Cl}$  production in the  $rp$  process mainly depends on resonant capture via the first excited state in  $^{31}\text{Cl}$  at around 0.6 MeV.<sup>3)</sup> No direct measurement of the  $^{30}\text{S}(p, \gamma)^{31}\text{Cl}$  reaction has been made so far due to the short lifetime of  $^{30}\text{S}$  and the small cross section of the reaction. We overcome this difficulty by applying the Coulomb dissociation reaction,<sup>4)</sup> which can extract the cross section of the relevant stellar reaction with relatively low beam intensity. The aim of the present work is to determine the resonant capture reaction rate of  $^{30}\text{S}(p, \gamma)^{31}\text{Cl}$  through the first excited state in  $^{31}\text{Cl}$ .

The experiment was performed using a part of the RIBF accelerator complex operated by RIKEN Nishina Center and the Center for Nuclear Study, University of Tokyo. The secondary beam of  $^{31}\text{Cl}$  at 58 MeV/nucleon was produced by the fragmentation of a 115 MeV/nucleon  $^{36}\text{Ar}$  beam on a  $^9\text{Be}$  target. The fragments were selected by the RIPS with the help of an RF-deflector system.<sup>5)</sup> The typical  $^{31}\text{Cl}$  beam intensity was about 500 cps, which is about 8% of the total secondary beam intensity. The beam of  $^{31}\text{Cl}$  bombarded a 104 mg/cm<sup>2</sup>  $^{208}\text{Pb}$  target. The reaction products, the isotopes of  $^{30}\text{S}$  and protons, were measured by detectors located downstream of the target as shown in Fig. 1. The entire system was in vacuum. The emission angles of the products were measured by a position sensitive silicon telescope located 62 cm downstream of the target. The energy of  $^{30}\text{S}$  was also measured by the silicon telescope. The telescope con-

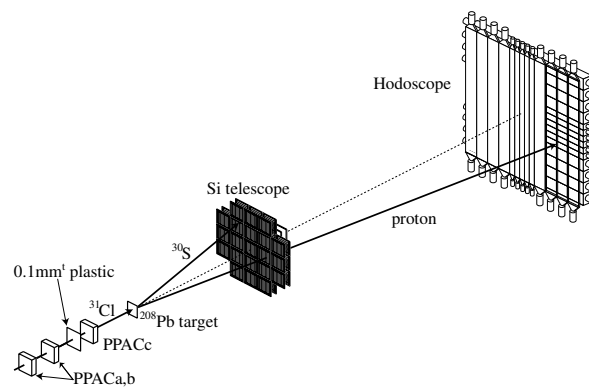


Fig. 1. A schematic view of the experimental setup.

sisted of four layer of detectors arranged in a  $5 \times 5$  matrix without 4 detectors at the corners of the first and second layer and a  $3 \times 3$  matrix for third and fourth layer. Each layer was composed of a silicon detector with an effective area of  $50 \times 50$  cm<sup>2</sup> and thickness of 500, 500, 325, and 500  $\mu\text{m}$ , respectively.  $^{30}\text{S}$  was stopped at the fourth layer, and identified using the  $\Delta E$  and  $E$  information. The energy of protons, which penetrated the silicon telescope, was determined with a plastic scintillator hodoscope placed 2.95 m downstream of the target by measuring the time-of-flight (TOF). The hodoscope had an active area of  $1 \times 1$  m<sup>2</sup>, consisting of thirteen 5-mm-thick  $\Delta E$ - and sixteen 60-mm-thick  $E$ -plastic scintillators. The outgoing proton was stopped in the  $E$  counters after passing through the  $\Delta E$  counters. The proton was identified by TOF,  $\Delta E$ , and  $E$  information. The relative energy between  $^{30}\text{S}$  and proton was obtained using the measured positions and energies of the products. An array of 160 NaI(Tl) scintillator DALI2<sup>6)</sup> was placed around the target to measure de-excitation  $\gamma$  rays from  $^{30}\text{S}$ . Analysis of the collected events is in progress.

## References

- 1) H. Schatz et al.: Phys. Rev. Lett. **86**, 3471 (2001).
- 2) J. L. Fisker et al.: Astrophys. J. **608**, L61 (2004).
- 3) C. Iliadis et al.: Astrophys. J. Suppl. Ser. **134**, 151 (2001).
- 4) G. Baur et al.: Nucl. Phys. **A458** 188 (1986).
- 5) K. Yamada et al.: Nucl. Phys. **A746**, 156c (2004).
- 6) S. Takeuchi et al.: RIKEN Accel. Prog. Rep. **36**, 148 (2003).

<sup>\*1</sup> Shanghai Institute of Applied Physics, CAS

<sup>\*2</sup> Department of Physics, Rikkyo University

<sup>\*3</sup> Department of Physics, Tohoku University

<sup>\*4</sup> Center for Nuclear Study (CNS), University of Tokyo

<sup>\*5</sup> Department of Physics, TITECH

<sup>\*6</sup> Department of Physics, Saitama University

<sup>\*7</sup> Institute of Modern Physics, CAS

## Inelastic scattering of proton-rich nucleus $^{23}\text{Al}$

T. Honda,<sup>\*1</sup> K. Okada,<sup>\*1</sup> Y. Togano, Y. G. Ma,<sup>\*2</sup> N. Aoi, H. Baba, X. Cai,<sup>\*2</sup> J. Chen,<sup>\*2</sup> D. Fang,<sup>\*2</sup> W. Guo,<sup>\*2</sup>  
 Y. Hara,<sup>\*1</sup> Z. Hu,<sup>\*3</sup> K. Ieki,<sup>\*1</sup> Y. Ishibashi,<sup>\*4</sup> Y. Itou,<sup>\*4</sup> N. Iwasa,<sup>\*5</sup> S. Kanno, T. Kawabata,<sup>\*6</sup>  
 H. Kimura,<sup>\*7</sup> Y. Kondo, K. Kurita,<sup>\*1</sup> M. Kurokawa, T. Moriguchi,<sup>\*4</sup> H. Murakami, H. Oishi,<sup>\*4</sup> S. Ota,<sup>\*6</sup>  
 A. Ozawa,<sup>\*4</sup> H. Sakurai, S. Shimoura,<sup>\*6</sup> R. Shioda,<sup>\*1</sup> E. Takeshita, S. Takeuchi, K. Yamada,  
 Y. Yamada,<sup>\*1</sup> Y. Yasuda,<sup>\*4</sup> J. Wang,<sup>\*3</sup> H. Wang,<sup>\*2</sup> T. Wendong,<sup>\*2</sup> K. Yoneda, and T. Motobayashi

[ $C(^{23}\text{Al}, p^{22}\text{Mg})C$ ,  $C(^{23}\text{Al}, ^{23}\text{Al}\gamma)C$ , Nuclear structure]

The neutron-deficient nucleus  $^{23}\text{Al}$  has attracted much attention since its discovery in 1969<sup>1)</sup>, because  $^{23}\text{Al}$  is a candidate for a proton halo system. The 1618 keV  $\gamma$  ray from the  $7/2^+$  state in  $^{23}\text{Al}^{2)}$ , whose energy is 1.5 MeV higher than the one proton separation energy of  $^{23}\text{Al}$  (122 keV<sup>3)</sup>) was observed. A candidate for a peak, which may be identical to the  $7/2^+$  state, was also observed as a particle decay events of  $^{23}\text{Al}$  in the Coulomb dissociation of  $^{23}\text{Al}$ .<sup>4)</sup> To clarify the structure of this state, the experiment was performed again, with the  $\gamma$  and the particle decays are measured simultaneously.

The experiment was performed using a part of the RIBF accelerator complex operated by the RIKEN Nishina Center and the Center for Nuclear Study, University of Tokyo. The present study was carried out as a by-product of the experiment of the momentum correlation function for  $^{23}\text{Al}$ .<sup>5)</sup> The secondary beam of  $^{23}\text{Al}$  at 72 MeV/nucleon was produced by projectile fragmentation of a 135 MeV/nucleon  $^{28}\text{Si}$  beam on a  $^9\text{Be}$  target. The fragments were selected by RIPS with the help of a RF-deflector system<sup>6)</sup> for purifying the secondary beam. The typical intensity and purity of the  $^{23}\text{Al}$  beam were 700 cps and 3%, respectively. The beam of  $^{23}\text{Al}$  bombarded a 355.4 mg/cm<sup>2</sup> C target. The outgoing  $^{23}\text{Al}$  and reaction products,  $^{22}\text{Mg}$  and a proton, were detected using a silicon telescope and a plastic scintillator hodoscope located at 62 cm and 2.95 m down stream of the target, respectively. The telescope consisted of five layers of 0.5-mm-thick silicon detectors, and identified  $^{23}\text{Al}$  and  $^{22}\text{Mg}$  using  $\Delta E$ - $E$  information. To obtain the scattering angles of the reaction products, silicon detectors which have strip electrodes with 5 mm pitch were used for the first and second layers. Single-element silicon detectors were used for the third, fourth and fifth layers. The hodoscope was constructed by three layers of plastic scintillators, which have an active area of  $1 \times 1$  m<sup>2</sup>,

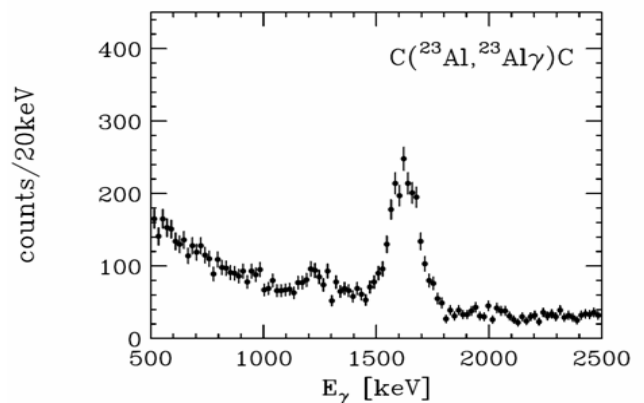


Fig. 1. Doppler-corrected energy spectrum of  $\gamma$  rays measured in coincidence with outgoing  $^{23}\text{Al}$ .

consisting of thirteen 5-mm-thick  $\Delta E$  counters, sixteen 60-mm-thick  $E1$  counters and thirteen 60-mm-thick  $E2$  counters. They detected protons which passed through the silicon telescope. The identification of protons was performed using  $\Delta E$ - $E$  information obtained from the hodoscope and time-of-flight information between the target and the hodoscope. The  $\gamma$  ray detector array DALI2<sup>7)</sup>, which was located around the target, was used to measure the de-excitation  $\gamma$  ray from the inelastically scattered  $^{23}\text{Al}$  and the reaction product  $^{22}\text{Mg}$ .

Figure 1 shows the Doppler-corrected energy spectrum of  $\gamma$  rays. A  $\gamma$  transition from the unbound excited state in  $^{23}\text{Al}$  was clearly observed in the present experiment. The energy of the prominent peak may correspond to the  $\gamma$  rays reported by Gade et al.<sup>2)</sup> The analysis of the particle decay events is now underway.

### References

- 1) J. Cerny, et al.: Phys. Rev. Lett. 22, 612 (1969).
- 2) A. Gade et al.: Phys Lett B 666 218-221 (2008).
- 3) G. Audi, et al.: Nucl. Phys. A 729, 337 (2003).
- 4) T. Gomi et al.: Nucl Phys. A758, 761c-764c (2005).
- 5) Y. G. Ma et al.: Proposal for Nuclear Physics Experiment at RI Beam Factory, unpublished.
- 6) K. Yamada et al.: Nucl. Phys. A746, 156c (2004).
- 7) S. Takeuchi et al.: RIKEN Accel. Prog. Rep. 36, 148(2003).

\*1 Department of Physics, Rikkyo University  
 \*2 Shanghai Institute of Applied Physics  
 \*3 Institute of Modern Physics, CAS  
 \*4 Department of Physics, Tsubota University  
 \*5 Department of Physics, Tohoku University  
 \*6 Center for Nuclear Study(CNS), University of Tokyo  
 \*7 Department of Physics, University of Tokyo

# Large proton contribution to the $2^+$ excitation in $^{20}\text{Mg}$ studied by intermediate energy inelastic scattering

N. Iwasa,<sup>\*1</sup> T. Motobayashi, S. Bishop, Z. Elekes,<sup>\*2</sup> J. Gibelin,<sup>\*3\*4</sup> M. Hosoi,<sup>\*5</sup> K. Ieki,<sup>\*3</sup> K. Ishikawa,<sup>\*6</sup> H. Iwasaki,<sup>\*7</sup> S. Kawai,<sup>\*3</sup> S. Kubono,<sup>\*8</sup> K. Kurita,<sup>\*3</sup> M. Kurokawa, N. Matsui,<sup>\*6</sup> T. Minemura H. Morikawa,<sup>\*3</sup> T. Nakamura,<sup>\*6</sup> M. Niikura,<sup>\*8</sup> M. Notani,<sup>\*9</sup> S. Ota,<sup>\*10</sup> A. Saito,<sup>\*8</sup> H. Sakurai, S. Shimoura,<sup>\*8</sup> K. Sugawara,<sup>\*5</sup> T. Sugimoto,<sup>\*6</sup> H. Suzuki,<sup>\*7</sup> T. Suzuki,<sup>\*5</sup> I. Tanihata,<sup>\*11</sup> E. Takeshita, T. Teranishi,<sup>\*12</sup> Y. Togano, K. Yamada, K. Yamaguchi,<sup>\*3</sup> and Y. Yanagisawa

[NUCLEAR REACTIONS:  $\text{Pb,C}(^{20}\text{Mg},^{20}\text{Mg}\gamma)$ , Coulomb excitation]

Manifestation of nuclear collectivity and shell closure in a wide range of nuclei has recently attracted a great deal of interest, as seen by the recent development of exotic-beam based experiments. The  $E2$  reduced transition probability  $B(E2)$  and the ratio of proton- to neutron-multipole matrix elements  $M_p/M_n$  for the  $0_{\text{gs}}^+ \rightarrow 2_1^+$  transition in even-even nuclei are fundamental quantities that measure the degree of nuclear collectivity. To determine  $B(E2)$  and  $M_p/M_n$  for  $^{20}\text{Mg}$ , we studied Coulomb excitation of the proton-rich nucleus  $^{20}\text{Mg}^*$ .

The experiment was carried out using a part of the RIBF accelerator complex operated by RIKEN Nishina Center and the Center for Nuclear Study, University of Tokyo. A radioactive  $^{20}\text{Mg}$  beam separated by RIPS with the help of the RF deflector<sup>1)</sup> impinged on a 226 mg/cm<sup>2</sup>-thick lead target. The average beam energy in the center of the target was 58A MeV. Measurement with a 118 mg/cm<sup>2</sup>-thick carbon target was also performed to evaluate the contributions of nuclear excitation. Scattered  $^{20}\text{Mg}$  were detected by an array of nine position-sensitive silicon telescopes. Particle identification was performed by the  $\Delta E$ - $E$  method. De-excitation  $\gamma$  rays from the reaction products were detected by sixty-eight NaI(Tl) scintillators (DALI)<sup>2)</sup>.

Figure 1 shows the energy spectra of  $\gamma$  rays after correcting for the Doppler shift, measured for the lead and carbon targets when both the beam particle and reaction products are identified as  $^{20}\text{Mg}$ . A strong  $\gamma$  line at 1.61(6)MeV is seen in the two spectra. Angular distribution of the scattered  $^{20}\text{Mg}$  measured in coincidence with the 1.61 MeV  $\gamma$  rays for the  $^{20}\text{Mg}+\text{Pb}$  inelastic scattering is consistent with the an-

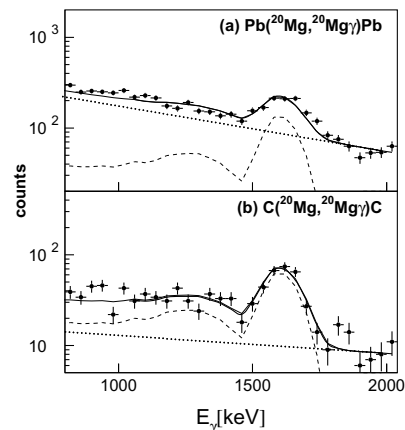


Fig. 1.  $\gamma$  energy spectra after correcting for the Doppler shift in (a)  $^{20}\text{Mg}+\text{Pb}$  and (b)  $^{20}\text{Mg}+\text{C}$  inelastic scattering. The solid curve represents the best fit by simulated line shape (dashed curves) and an exponential background (dotted curves).

gular momentum transfer  $\ell = 2$ , confirming  $2^+$  assignment to the 1.6 MeV state<sup>3)</sup>. To reproduce experimental cross section of the  $^{20}\text{Mg}+\text{Pb}$  inelastic scattering,  $B(E2;0^+ \rightarrow 2^+)$  was determined to be 177(32)  $e^2\text{fm}^4$ , yielding  $|M_p|=13.3(12)\text{fm}^2$ .

Assuming the isospin symmetry  $M_p(M_n)$  for a transition is equal to  $M_n(M_p)$  for the corresponding transition in the mirror partner. The  $M_p/M_n$  value of 2.51(25) for  $^{20}\text{Mg}$  was deduced, using the adopted  $B(E2)$  value of 28(2)  $e^2\text{fm}^4$  for  $^{20}\text{O}$  which is considerably larger than the “collective” limit,  $N/Z = 1.5$ . The extracted  $M_p/M_n$  value can be understood with a simple picture where the  $^{16}\text{O}$  core is inert and only four valence protons are responsible for the  $2^+$  excitation. In this picture, the  $M_p/M_n$  ratio for  $^{20}\text{Mg}$  should be equal to  $e_p/e_n$ , which results in the ratio 2.6 using standard effective-charge values  $e_p = 1.3e$  and  $e_n = 0.5e$ . This is in excellent agreement with the present result, and leads to a picture that the shell closure persists in  $^{20}\text{Mg}$ .

## References

- 1) K. Yamada et al.: Nucl. Phys. **A746**, 156c (2004).
- 2) T. Motobayashi et al.: Phys. Lett. **B346**, 9 (1995).
- 3) A. Gade et al.: Phys. Rev. **C76**, 024317 (2007).

\* Condensed from the article in Phys. Rev. **C78**, 024306 (2008).

<sup>\*1</sup> Department of Physics, Tohoku University

<sup>\*2</sup> ATOMKI, Hungary

<sup>\*3</sup> Department of Physics, Rikkyo University

<sup>\*4</sup> Institut de Physique Nucléaire, Orsay, France

<sup>\*5</sup> Department of Physics, Saitama University

<sup>\*6</sup> Department of Physics, Tokyo Institute and Technology

<sup>\*7</sup> Department of Physics, University of Tokyo

<sup>\*8</sup> Center for Nuclear Study, University of Tokyo

<sup>\*9</sup> Argonne National Laboratory, USA

<sup>\*10</sup> Department of Physics, Kyoto University

<sup>\*11</sup> RCNP, Osaka University

<sup>\*12</sup> Department of Physics, Kyushu University

## Coulomb excitation and proton inelastic scattering of $^{36}\text{Ca}$

N. Iwasa,<sup>\*1</sup> N. Kume,<sup>\*1</sup> Y. Togano, N. Aoi, H. Baba, S. Bishop, X. Cai,<sup>\*2</sup> P. Doornenbal, D. Fang,<sup>\*2</sup> T. Furukawa, Y. Hara,<sup>\*3</sup> T. Honda,<sup>\*3</sup> K. Ieki,<sup>\*3</sup> S. Kanno, T. Kawabata,<sup>\*4</sup> N. Kobayashi,<sup>\*5</sup> Y. Kondo, T. Kuboki,<sup>\*6</sup> K. Kurita,<sup>\*3</sup> M. Kurokawa, K. Li, Y.G. Ma,<sup>\*2</sup> M. Matsushita,<sup>\*3</sup> S. Michimasa,<sup>\*4</sup> H. Murakami, T. Nakamura,<sup>\*5</sup> K. Okada,<sup>\*3</sup> S. Ota,<sup>\*4</sup> Y. Satou,<sup>\*5</sup> H. Scheit, S. Shimoura,<sup>\*4</sup> R. Shioda,<sup>\*3</sup> T. Suzuki,<sup>\*6</sup> S. Takeuchi, K.N. Tanaka,<sup>\*5</sup> K. Tanaka, W. Tian,<sup>\*2</sup> H. Wang,<sup>\*2</sup> J. Wang,<sup>\*7</sup> K. Yamada, Y. Yamada,<sup>\*3</sup> K. Yoneda, and T. Motobayashi

[NUCLEAR REACTIONS:  $\text{Pb}, ^1\text{H}(^{36}\text{Ca}, ^{36}\text{Ca} \gamma)$ ,  $\text{Pb}, ^1\text{H}(^{36}\text{Ca}, ^{35}\text{K} p)$ , Coulomb excitation, ]  
[proton inelastic scattering

Coulomb excitation and proton inelastic scattering of the proton-rich nucleus  $^{36}\text{Ca}$  were studied to determine  $B(E2)$  and  $M_n/M_p$  for the  $0_{\text{gs}}^+ \rightarrow 2_1^+$  transition in  $^{36}\text{Ca}$ . Recently, the excitation energy of the first  $2^+$  state in  $^{36}\text{Ca}$  was determined using the  $^9\text{Be}(^{37}\text{Ca}, ^{36}\text{Ca}\gamma)$  reaction<sup>1)</sup>. The excitation energy, 3.015(16)MeV, is 0.44 MeV above the proton separation energy and 0.28 MeV lower than in the mirror nuclei  $^{36}\text{S}$ , and the extremely large mirror energy difference was discussed<sup>1)</sup>. To obtain further information on the nuclear structure of  $^{36}\text{Ca}$ , experimental determination of  $B(E2)$  and  $M_n/M_p$  is desired.

The experiment was carried out using a part of the RIBF accelerator complex operated by RIKEN Nishina Center and Center for Nuclear Study, University of Tokyo. A radioactive  $^{36}\text{Ca}$  beam was produced by fragmentation of a 100A MeV  $^{40}\text{Ca}$  beam in a 1-mm thick beryllium target and separated by RIPS. To improve the purity of  $^{36}\text{Ca}$ , an RF deflector was used<sup>2)</sup>. Particle identification of the secondary beam was performed event-by-event by measuring time of flight (TOF) and energy loss ( $\Delta E$ ). The TOF was measured using radio-frequency signal of the cyclotron and signal of a 0.1 mm-thick plastic scintillator placed at F3. The  $\Delta E$  was measured by a 0.1-mm-thick silicon detector. A 226 mg/cm<sup>2</sup>-thick lead target was bombarded by the secondary beam. The average beam energy in the center of the target was 58A MeV. Measurement with a 52 mg/cm<sup>2</sup>-thick liquid hydrogen target was also performed.

Scattering angle of reaction products,  $^{36}\text{Ca}$  or  $^{35}\text{K}+p$ , were measured by an array of 21 position-sensitive silicon telescopes arranged in a  $5 \times 5$  matrix, placed 0.62 m downstream of the target. Since  $^{36}\text{Ca}$  and  $^{35}\text{K}$  particles were stopped in the telescopes, particle identification was performed by the  $\Delta E$ - $E$  method. The breakup protons punched through the telescopes and were detected by a plastic scintillator hodoscope

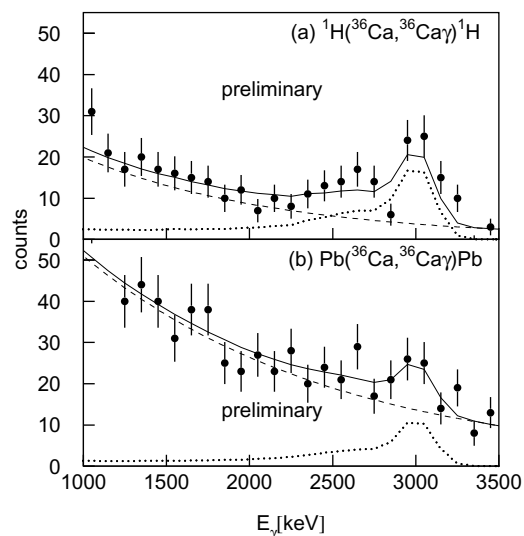


Fig. 1.  $\gamma$  energy spectra after correcting for the Doppler shift in (a)  $^{36}\text{Ca}+\text{Pb}$  and (b)  $^{36}\text{Ca}+^1\text{H}$  inelastic scattering. The solid curve represents the best fit including simulated line shape (dotted curves); an additional exponential background (dashed curves).

consisting of 5 mm-thick  $\Delta E$  and 60 mm-thick  $E$  layers, placed 2.95 m downstream of the target. De-excitation  $\gamma$  rays from the reaction products were detected using 160 NaI(Tl) scintillators (DALI2)<sup>3)</sup> surrounding the target.

Figure 1 shows the energy spectra of  $\gamma$  rays measured for the lead and liquid hydrogen targets when both the beam particles and reaction products are identified as  $^{36}\text{Ca}$ . The Doppler-shift correction is applied to obtain these spectra. A  $\gamma$  line at 3.0 MeV is seen in the two spectra. Further analysis of the data is in progress.

### References

- 1) P. Doornenbal et al.: Phys. Lett. **B647**, 237 (2007).
- 2) K. Yamada et al.: Nucl. Phys. **A746**, 156c (2004).
- 3) S. Takeuchi et al.: RIKEN Accel. Prog. Rep. **36**, 148 (2003).

\*1 Department of Physics, Tohoku University  
 \*2 Shanghai Institute of Applied Physics, China  
 \*3 Department of Physics, Rikkyo University  
 \*4 CNS, University of Tokyo  
 \*5 Department of Physics, Tokyo Institute and Technology  
 \*6 Department of Physics, Saitama University  
 \*7 Institute of Modern Physics, China

## Attempt to produce the 3rd chain of $^{278}113$

K. Morimoto, K. Morita, D. Kaji, T. Akiyama,<sup>\*1</sup> S. Goto,<sup>\*2</sup> H. Haba, E. Ideguchi,<sup>\*3</sup> K. Katori, H. Koura,<sup>\*4</sup> H. Kudo,<sup>\*2</sup> A. Ozawa,<sup>\*5</sup> K. Ozeki, N. Sato,<sup>\*6</sup> F. Tokanai,<sup>\*7</sup> T. Yamaguchi,<sup>\*1</sup> A. Yoneda, and A. Yoshida

[ $^{278}113$ , production and decay, gas-filled recoil ion separator]

In 2003 -2007, we performed an experiment to synthesize an element 113 by a  $^{209}\text{Bi} + ^{70}\text{Zn}$  reaction using a gas-filled recoil ion separator (GARIS) at RIKEN Nishina-Center. In a total of 241 days of net irradiation time experiment, two decay chains<sup>1,2)</sup> were observed and assigned from an isotope  $^{278}113$ . Both chains were connected to the known nuclei of  $^{266}\text{Bh}$ <sup>3)</sup> and  $^{262}\text{Db}$ <sup>3,4)</sup>, and ended by a spontaneous fission of  $^{262}\text{Db}$ . These latter two decay properties were consistent with reported values<sup>3,4)</sup>. The cross section of the  $^{209}\text{Bi}(^{70}\text{Zn},n)^{278}113$  reaction was determined to be  $31_{-20}^{+40}$  fb at that time.

In order to increase the number of statistics of the decay property, we continued to produce more decay chains. While the decay chains observed in the previous experiment ended in a spontaneous fission of  $^{262}\text{Db}$ , a  $^{262}\text{Db}$  would have the possibility to decay by alpha decay. Additionally  $^{258}\text{Lr}$ , the daughter nuclei of  $^{262}\text{Db}$ , is decaying by alpha decay. If the  $^{262}\text{Db}$  were observed in a sequential alpha decay, the decay chain would finally be connected to  $^{258}\text{Lr}$  and  $^{254}\text{Md}$  which have been well studied. Thus it would be a strong evidence for production of  $^{278}113$ .

The experiment was carried out from January 7 to March 31, 2008. The experimental conditions were identical to those used in the previous experiment. A  $^{70}\text{Zn}$  ion beam of 353 MeV was extracted from RILAC. Targets were prepared by the vacuum evaporation of metallic bismuth onto carbon backing foil of  $30 \mu\text{g}/\text{cm}^2$  thickness. The thickness of the bismuth layer was about  $450 \mu\text{g}/\text{cm}^2$ . The beam energy at the half-depth of targets was estimated to be 349.5 MeV. The reaction products were separated in-flight from the beam by GARIS and guided into a detector box. The detector box consists of five 16-strip silicon detectors. One of the detectors is a position sensitive detector (PSD) which was used as a stop detector. The separator was filled with helium gas at a pressure of 86Pa. The magnetic rigidity of GARIS was set to be 2.09 Tm for evaporation residue.

The net irradiation time was 83 days with a total dose of  $^{70}\text{Zn}$  was  $2.28 \times 10^{19}$ . The typical beam in-

tensity on the target was  $3.2 \times 10^{12}\text{s}^{-1}$ . The singles counting rate of PSD was about  $3 \text{s}^{-1}$  at typical beam intensity. In the present experiment no candidate for  $^{278}113$  was not observed. Combining the results of the present and previous experiments, the production cross section of  $^{278}113$  was determined to be  $22_{-14}^{+29}$  fb.

### References

- 1) K. Morita, K. Morimoto, D. Kaji et al.: J. Phys. Soc. Jap. **73**(2004) 2593.
- 2) K. Morita, K. Morimoto, D. Kaji et al.: J. Phys. Soc. Jap. **76**(2007) 045001-1.
- 3) P. A. Wilk, K. E. Gregorich et al.: Phys. Rev. Lett. **85** (2000) 2697.
- 4) Table of Isotopes 8th ed. 1998 Update, ed. R. B. Firestone (John Wiley and Sons, New York, 1998).

<sup>\*1</sup> Department of Physics, Saitama University

<sup>\*2</sup> Department of Chemistry, Niigata University

<sup>\*3</sup> Center for Nuclear Study, University of Tokyo

<sup>\*4</sup> Advanced Science Research Center, Japan Atomic Energy Agency

<sup>\*5</sup> University of Tsukuba

<sup>\*6</sup> Department of Physics, Tohoku University

<sup>\*7</sup> Department of Physics, Yamagata University

## New decay properties of $^{264}\text{Hs}$ , $^{260}\text{Sg}$ , and $^{256}\text{Rf}$

N. Sato,<sup>\*1</sup> H. Haba, T. Ichikawa, E. Ideguchi,<sup>\*2</sup> D. Kaji, H. Koura,<sup>\*3</sup> Y. Kudou, K. Morimoto, K. Morita, A. Ozawa,<sup>\*4</sup> K. Ozeki, T. Sumita,<sup>\*5</sup> T. Yamaguchi,<sup>\*6</sup> A. Yoneda, and A. Yoshida

[ $^{264}\text{Hs}$ ,  $^{260}\text{Sg}$ ,  $^{256}\text{Rf}$ , hassium, seaborgium, rutherfordium, GARIS]

Decay properties of  $^{264}\text{Hs}$  and its  $\alpha$ -decay daughter nuclei attract some interest because they are even-even superheavy nuclei. Productions and direct measurements of lifetime of only four atoms of  $^{264}\text{Hs}$  were reported previously<sup>1,2)</sup>. In this work, the production and decays of  $^{264}\text{Hs}$  are investigated using the  $^{208}\text{Pb}(^{58}\text{Fe},2n)$  and  $^{207}\text{Pb}(^{58}\text{Fe},n)$  reactions.

The  $^{58}\text{Fe}^{13+}$  ion beam was extracted from the RIKEN Linear Accelerator, RILAC. The beam energy at the middle of the target in the center of mass frame was set to be 227.2 MeV for  $^{208}\text{Pb}$  target and 220.5 MeV for  $^{207}\text{Pb}$ . The typical beam intensity was  $4.5 \times 10^{12} \text{ s}^{-1}$ .

Targets were prepared by vacuum evaporation of lead on carbon backing foil of  $30 \mu\text{g}/\text{cm}^2$  thickness. The target thickness was  $500 \mu\text{g}/\text{cm}^2$  for  $^{208}\text{Pb}$  (Enrichment 98.4%) and  $430 \mu\text{g}/\text{cm}^2$  for  $^{207}\text{Pb}$  (Enrichment 98.0%). The targets were covered by a  $10 \mu\text{g}/\text{cm}^2$  thick carbon to protect the target from sputtering.

The reaction products were separated in-flight from the beam by a gas-filled recoil ion separator, GARIS, and were guided into a detection system at the focal plane of GARIS. The details about separator and detector is reported elsewhere<sup>3,4)</sup>.

We observed three correlated events in irradiation of  $^{58}\text{Fe}$  on  $^{208}\text{Pb}$ , and eight events in irradiation of  $^{58}\text{Fe}$  on  $^{207}\text{Pb}$ . We assigned these eleven events to be the decays of  $^{264}\text{Hs}$ . In the eleven events, ten events were  $\alpha$ -decays while one was spontaneous fission decay. Alpha energies of  $10.80 \pm 0.08 \text{ MeV}$  ( $I_\alpha = 10\%$ ),  $10.61 \pm 0.05 \text{ MeV}$  ( $I_\alpha = 60\%$ ) and  $10.34 \pm 0.04 \text{ MeV}$  ( $I_\alpha = 30\%$ ) were observed. The decay time distribution obtained by this work are summarized in Fig. 1. A half-life was deduced to be  $0.90^{+0.40}_{-0.20} \text{ ms}$ . The production cross section was deduced to be  $8.5^{+7.7}_{-4.9} \text{ pb}$  for the  $^{208}\text{Pb}(^{58}\text{Fe},2n)^{264}\text{Hs}$  reaction and  $11^{+5}_{-4} \text{ pb}$  for  $^{207}\text{Pb}(^{58}\text{Fe},n)^{264}\text{Hs}$ .

In the decays of  $^{260}\text{Sg}$ , produced as decay daughter of  $^{264}\text{Hs}$  and its daughter nuclei  $^{256}\text{Rf}$ , we observed two groups. In this report, we describe short-lived nuclei as  $^a$ , and long-lived one as  $^b$ .  $^{260}\text{Sg}^a$  decays by spontaneous fission ( $b_{SF} = 60\%$ ) and  $\alpha$  emission ( $b_\alpha = 40\%$ )

with an energy of  $9.78 \pm 0.06 \text{ MeV}$  and a total half-life of  $4.1^{+3.3}_{-1.3} \text{ ms}$ .  $^{256}\text{Rf}^a$  is produced only by  $\alpha$ -decay of  $^{260}\text{Sg}^a$ , and decays by spontaneous fission ( $b_{SF} = 100\%$ ) with a half-life of  $12^{+21}_{-5} \text{ ms}$ . These decay properties agree well with the literature values, produced by the  $^{208}\text{Pb}(^{54}\text{Cr},2n)^{260}\text{Sg}$  and  $^{207}\text{Pb}(^{54}\text{Cr},n)^{260}\text{Sg}$  or  $^{208}\text{Pb}(^{50}\text{Ti},2n)^{256}\text{Rf}$  reaction<sup>5)</sup>.

On the other hand,  $^{260}\text{Sg}^b$  decays by  $\alpha$  emission with energies of  $9.51 \pm 0.06 \text{ MeV}$  ( $I_\alpha = 80\%$ ) and  $8.76 \pm 0.08 \text{ MeV}$  ( $I_\alpha = 20\%$ ) with a total half-life of  $180^{+150}_{-60} \text{ ms}$ .

$^{256}\text{Rf}^b$  decays by  $\alpha$  emission, too. Alpha energies of  $8.78 \pm 0.04 \text{ MeV}$  ( $I_\alpha = 80\%$ ) and  $8.47 \pm 0.04 \text{ MeV}$  ( $I_\alpha = 20\%$ ) were observed with a half-life of  $10.4^{+8.4}_{-3.2} \text{ s}$ . This state is produced only by  $\alpha$ -decay of  $^{260}\text{Sg}^b$ .

For  $^{260}\text{Sg}$  and  $^{256}\text{Rf}$ , the decay of such a long-lived state has not been reported. This experiment showed that  $^{260}\text{Sg}$  and  $^{256}\text{Rf}$  have long-lived state, which is created only by  $\alpha$ -decay of  $^{264}\text{Hs}$ . These are the first observations of isomerism in  $^{260}\text{Sg}$  and  $^{256}\text{Rf}$ .

### References

- 1) G. Münzenberg et al.: Z. Phys. A **324** 489 (1985).
- 2) Y. A. Akivali: Nucl. Data Sheets **87** 249 (1999).
- 3) D. Kaji et al.: RIKEN Accel. Prog. Rep. **42** (2009).
- 4) K. Morita et al.: Eur. Phys. J. A **21** (2004) 257.
- 5) B. Sulignano: Dr. Thesis, Johannes Gutenberg University (2007).

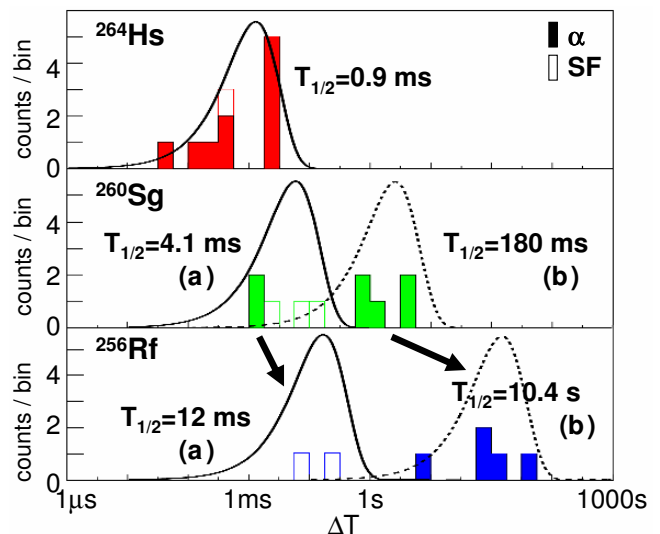


Fig. 1. Decay time distribution in logarithmic scale.

\*1 Department of Physics, Tohoku University

\*2 Center for Nuclear Study, University of Tokyo

\*3 Advanced Science Research Center, Japan Atomic Energy Agency

\*4 University of Tsukuba

\*5 Faculty of Science and Technology, Tokyo University of Science

\*6 Department of Physics, Saitama University

## Precision measurement of the hyperfine constant of $^{11}\text{Be}$

M. Wada, A. Takamine, K. Okada,<sup>\*1</sup> T. Nakamura, P. Schury, T. Sonoda, V. Lioubimov, Y. Yamazaki, Y. Kanai, T.M. Kojima, A. Yoshida, T. Kubo, I. Katayama,<sup>\*2</sup> S. Ohtani,<sup>\*3</sup> H. Wollnik,<sup>\*4</sup> and H.A. Schuessler,<sup>\*5</sup>

[hyperfine anomaly, neutron halo, laser spectroscopy]

The magnetic hyperfine structure (hfs) constant of the ground state  $^{11}\text{Be}^+$  ion has been measured at the prototype facility of SLOWRI at RIKEN. Energetic  $^{11}\text{Be}$  ions produced at the projectile fragment separator RIPS were decelerated and cooled by an RF-carpet ion guide<sup>1)</sup> and trapped in a linear RF trap. The stored  $^{11}\text{Be}^+$  ions were further cooled by laser irradiation to  $< 10$  mK and double resonance spectroscopy was performed to directly measure the magnetic hyperfine constant  $a$ .

The magnetic hfs constant of the  $s$ -state is a probe of the magnetization distribution of a nucleus which manifests itself under a local, *inhomogeneous* magnetic field due to a valence  $s$ -electron, while the nuclear magnetic moment is an integrated magnetization measured with a *homogeneous* external field. A comparison of the ratio of the hfs constant  $a$  to the nuclear  $g$ -factor  $g$  among isotopes yields the Bohr-Weisskopf effect<sup>2)</sup>, which should sensitively reflect the structure of the single neutron halo<sup>3)</sup>. In the naive picture shown in Fig. 1, the charge radius of  $^{11}\text{Be}$  is representative of the core size while the magnetization radius is representative of the radius of the extended halo neutron since the nuclear magnetization is mainly carried by the halo neutron. Combined with our isotope-shift measurements<sup>4)</sup>, we can clearly discern whether the valence neutron is really distributed with a large radius.

Figure 2 shows the fluorescence intensity for  $^{11}\text{Be}^+$  plotted as a function of the microwave frequency. A 313 nm laser radiation was used for the cooling and optical pumping of ions. If a resonant microwave radiation induces the hyperfine transition, the fluorescence intensity changes. From the spectrum the resonance frequency was determined to be 2667.434(10) MHz. We measured two transitions ( $|F, m_F\rangle = |0, 0\rangle \leftrightarrow |1, +1\rangle$  and  $|0, 0\rangle \leftrightarrow |1, -1\rangle$ ) at two different magnetic

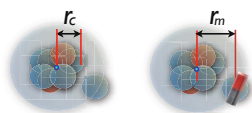


Fig. 1. Sketch of the charge ( $r_c$ ) and magnetization ( $r_m$ ) radii of neutron halo nucleus  $^{11}\text{Be}$ .

<sup>\*1</sup> Department of Physics, Sophia University

<sup>\*2</sup> Institute of Particle and Nuclear Studies, KEK

<sup>\*3</sup> ILS, University of Electro-Communications

<sup>\*4</sup> II. Physikalisches Institut, Justus-Liebig-Universität Giessen

<sup>\*5</sup> Department of Physics, Texas A&M University

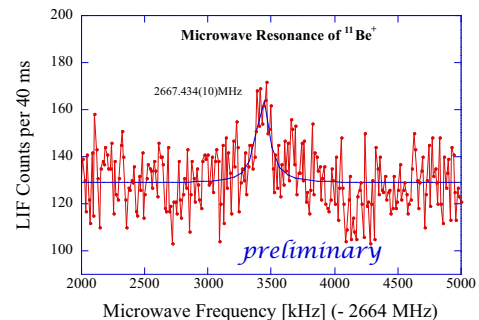


Fig. 2. Microwave resonance spectrum of  $^{11}\text{Be}^+$

fields, from which the magnetic hyperfine constant was determined to be  $a = -2677.308(2)$  MHz and the nuclear spin was confirmed to be  $I = 1/2$ .

The differential hyperfine anomaly  ${}^9\Delta^A$  which corresponds with the difference of the Bohr-Weisskopf effect with respect to the stable isotope  ${}^9\text{Be}$  is described as

$${}^9\Delta^A \equiv \frac{a_9/g_9}{a_A/g_A} - 1 \approx \epsilon_{\text{BW}}({}^9\text{Be}) - \epsilon_{\text{BW}}({}^A\text{Be}). \quad (1)$$

Fujita *et al.*<sup>5)</sup> predicted  ${}^9\Delta^A = 468$  ppm and 950 ppm, while Parfenova and Leclercq-Willaim<sup>6)</sup> calculated it to be 320 ppm and 221 ppm using various models. Though the theoretical values diverge depending on the nuclear models used, they all showed a very large anomaly as compared with  ${}^9\Delta^7$  and concluded that the anomaly is correlated with the large neutron spatial distribution. Experimentally, we preliminarily evaluated  ${}^9\Delta^A = 220 \pm 480$  ppm using the imprecise literature value of the nuclear magnetic moment  $\mu_I({}^{11}\text{Be}) = (-)1.6816(8) \mu_N$ <sup>7)</sup>. In the near future we will measure the Zeeman splittings of the hyperfine structure at a high magnetic field with a combined trap where we can determine the nuclear magnetic moments as well as the hyperfine constants with much higher accuracies as we have demonstrated<sup>8)</sup> for  ${}^9\text{Be}^+$ .

### References

- 1) M. Wada *et al.*: Nucl. Instrm. Meth. **B204**, 570 (2003).
- 2) A. Bohr and V. F. Weisskopf: Phys. Rev. **77**, 94 (1950).
- 3) M. Wada *et al.*: Nucl. Phys. **A626**, 365c (1997).
- 4) A. Takamine *et al.*: RIKEN Accel. Prog. Rep. **42**, xiv (2009).
- 5) T. Fujita *et al.*: Phys. Rev. C **59**, 210 (1999).
- 6) Y. Parfenova and Ch. Leclercq-Willaim: Phys. Rev. C **72**, 024312 (2005).
- 7) W. Geithner *et al.*, Phys. Rev. Lett. **83**, (1999) 3792.
- 8) T. Nakamura *et al.*: Opt. Comm. **205**, (2002) 329.

# Precision hyperfine structure spectroscopy of laser-cooled radioactive ${}^7\text{Be}^+$ -ions produced by projectile fragmentation

K. Okada,<sup>\*1</sup> M. Wada, T. Nakamura, A. Takamine, V. Lioubimov, P. Schury, Y. Ishida, Y. Yamazaki, Y. Kanai, T.M. Kojima, A. Yoshida, T. Kubo, I. Katayama,<sup>\*2</sup> S. Ohtani,<sup>\*3</sup> H. Wollnik,<sup>\*4</sup> H.A. Schuessler,<sup>\*5</sup>

[hyperfine constant, magnetic moment,  ${}^7\text{Be}$ , laser cooling]

We performed laser cooling and precision hfs spectroscopy of radioactive ions from projectile fragmentation, for the first time, at prototype SLOWRI. The first nucleus measured was  ${}^7\text{Be}$  which is a unique nucleus whose nuclear moments elude determination by the  $\beta\gamma$ -NMR method, since it emits no  $\beta$ -rays and emits  $\gamma$ -rays isotropically. Optical spectroscopy is therefore the only way to measure the nuclear moments.

${}^7\text{Be}$  ions produced at 1 GeV by projectile fragmentation were decelerated and cooled in an RF-carpet ion guide<sup>1,2)</sup> and trapped in an RF ion trap<sup>3)</sup>. They were further cooled by laser radiation to  $\mu\text{eV}$  and laser-microwave double-resonance spectroscopy<sup>5)</sup> was performed (Fig. 1)<sup>4)</sup>. A magnetic hfs constant of  $A = -742.77228(43)$  MHz and a nuclear spin of  $I = 3/2$  were determined from the microwave resonance frequencies with  $\sigma^+$  and  $\sigma^-$  radiations each at two low magnetic fields of 0.61 and 0.71 mT. The nuclear magnetic moment of  ${}^7\text{Be}$  was deduced from  $A$  to

Table 1. Nuclear magnetic moment of  ${}^7\text{Be}$  [ $\mu_N$ ]

Present experimental value	$-1.39928(2)$
Cohen-Kurath (8-16)POT <sup>8)</sup>	$-1.3787$
<i>Ab-initio</i> non-core shell model <sup>9)</sup>	$-1.138$
Variational quantum Monte Carlo <sup>10)</sup>	$-1.110(2)$

be  $\mu_I({}^7\text{Be}) = -1.39928(2)\mu_N$  where the small differential hyperfine anomaly ( ${}^7\Delta^9 < 10^{-5}$ ) was neglected while the uncertainty of  $\mu_I({}^7\text{Be})$  was evaluated from a theoretically derived  ${}^7\Delta^9$ . Spin expectation values  $\langle \Sigma\sigma_z \rangle = 0.94044(3)$  and  $\langle \Sigma l_z \rangle = 1.02978(1)$  were also deduced together with the magnetic moment of  ${}^7\text{Li}$ <sup>6)</sup>.

The magnetic moment was compared with theoretical calculations (Table 1). A simple shell model calculation with OXBASH using the Cohen-Kurath<sup>8)</sup> interaction shows good agreement, with a 1.5% discrepancy, while the *ab-initio* shell model calculation<sup>9)</sup> by Navrátil *et al.*, and the variational quantum Monte Carlo calculations by Pudliner *et al.*<sup>10)</sup> showed large discrepancies of about 20%. These modern calculations achieved good agreement for the magnetic moments of  $T = 0$  isoscalar nuclei, such as  ${}^{10}\text{B}$ , but not for  $T = 1/2$  isovector nuclei. This is considered to be due to two-body charge and current contributions, which are not included in the calculations; they largely cancel in the isoscalar nuclei, while they are noticeable in the isovector nuclei<sup>11)</sup>.

We have shown that high precision laser-microwave spectroscopy can be performed for radioactive ions produced at 1 GeV by projectile fragmentation. This guarantees that many new experiments on unexplored isotopes will be conducted using the same setup.

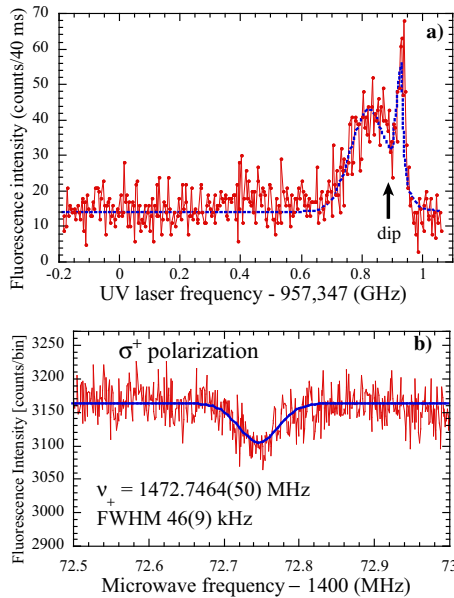


Fig. 1. (a) Laser cooling spectrum of  ${}^7\text{Be}^+$  ions and (b) microwave resonance detected by fluorescence intensity in the case of  $\sigma^+$  radiation.

<sup>\*1</sup> Department of Physics, Sophia University  
<sup>\*2</sup> Institute of Particle and Nuclear Studies, KEK  
<sup>\*3</sup> ILS, University of Electro-Communications  
<sup>\*4</sup> II. Physikalisches Institut, Justus-Liebig-Universität Giessen  
<sup>\*5</sup> Department of Physics, Texas A&M University

## References

- 1) M. Wada *et al.*: Nucl. Instrum. Methods Phys. Res. B 204, 570 (2003).
- 2) A. Takamine, *et al.*: Rev. Sci. Instr. 76, 103503 (2005).
- 3) T. Nakamura, *et al.*: Phys. Rev. A 74, 052503 (2006).
- 4) K. Okada *et al.*: Phys. Rev. Lett. **101**, 212502 (2008).
- 5) K. Okada *et al.*: J. Phys. Soc. Jpn **67**, 3073 (1998).
- 6) N. J. Stone: Atomic Data and Nuclear Data Tables, **90**, 75(2005).
- 7) T. Fujita *et al.*: Phys. Rev. C **59**, 210 (1999).
- 8) S. Cohen and D. Kurath: Nucl. Phys. 73, 1 (1965).
- 9) P. Navrátil *et al.*: Phys. Rev. C **68**, 034305 (2003).
- 10) B. S. Pudliner *et al.*: Phys. Rev. C **56**, 1720 (1997).
- 11) R. Schiavilla *et al.*: Phys. Rev. C **40**, 2294 (1989).

## Half life measurement of $^{46}\text{Cr}$

Y. Wakabayashi,<sup>\*1</sup> H. Yamaguchi,<sup>\*1</sup> T. Hashimoto,<sup>\*1</sup> S. Hayakawa,<sup>\*1</sup> Y. Kurihara,<sup>\*1</sup> S. Nishimura,  
D. N. Binh,<sup>\*1\*2</sup> D. Kahl,<sup>\*1</sup> M. Suga,<sup>\*3</sup> Y. Gono, Y. Fujita,<sup>\*3</sup> and S. Kubono<sup>\*1</sup>

[ $\beta$  decay, unstable nuclei]

For the rapid proton capture process (*rp*-process) in X-ray bursts and the core-collapse stage of supernovae, proton-rich *pf*-shell nuclei far from stability play important roles<sup>1)</sup>. Studies of the  $\beta$  and electron capture decays of these proton-rich *pf*-shell nuclei are of great astrophysical interest. These decays involved in the charged-current processes are predominated by the Fermi and Gamow-Teller (GT) transitions. Information on GT transitions can be derived directly from  $\beta$ -decay measurements. To determine the accurate  $B(\text{GT})$ , it is important to determine the feeding ratio and half-life of the  $\beta$ -decay accurately.

The purpose of the experiment is to measure the properties of  $^{46}\text{Cr}$ , namely, i) the total half-life of  $\beta$ -decay with an accuracy better than 10 %, ii) the decay branching ratios to the ground state (Fermi transition) and GT states accurately.

The experiment to measure the half life of  $\beta$  decay of  $^{46}\text{Cr}$  was performed using the low-energy RI beam separator (CRIB)<sup>2,3)</sup> of the Center for Nuclear Study (CNS), University of Tokyo. The  $^{46}\text{Cr}$  particles were produced by the  $^{36}\text{Ar} + ^{12}\text{C}$  fusion reaction. A natural C foil of  $0.56 \text{ mg/cm}^2$  was installed as the primary target. The  $^{36}\text{Ar}$  primary beam was accelerated to 3.6 MeV/nucleon by the AVF cyclotron, and degraded to 3.0 MeV/nucleon by a  $2.2\text{-}\mu\text{m}$ -thick Havar foil placed in front of the primary target to maximize production of  $^{46}\text{Cr}$  at lower energy. To separate  $^{46}\text{Cr}$  from the contaminants produced in the fusion reaction, the Wien filter (WF) was used at a high voltage of  $\pm 85 \text{ kV}$ . A microchannel plate (MCP) was placed at the final focal plane (F3) to monitor the beam position. We used a  $0.7\text{-}\mu\text{m}$ -thick aluminized Mylar covered by CsI for the window of the MCP. An ionization chamber (IC) was placed behind the MCP as a  $\Delta E$  detector. A double sided Si strip detector (DSSD) of  $500\text{-}\mu\text{m}$  thickness was set in the IC as an E and a  $\beta$ -ray detector. A Si detector of  $1.5\text{-mm}$  thickness was placed behind the DSSD for a  $\beta$ -ray detector. To measure  $\beta$ -delayed  $\gamma$  rays involved  $\beta$  decay, 3 clover and 1 coaxial Ge detectors were set around the IC. The beam was pulsed to measure the half life of the  $\beta$  decay of  $^{46}\text{Cr}$ . The durations of the beam-on and beam-off periods were 500 and 700 ms, respectively. Non-stop TDC (NSTDC) was used to measure half lives of fusion products.

Figure 1 shows a particle identification obtained

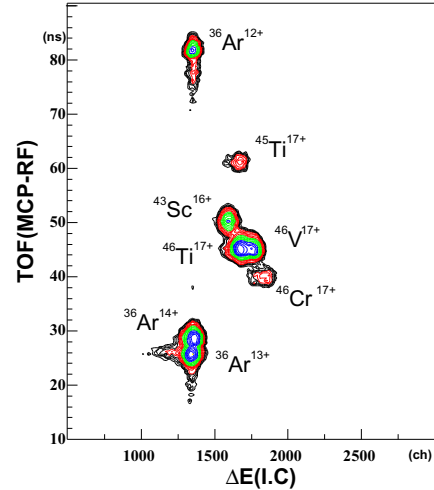


Fig. 1. RF- $\Delta E$  spectrum obtained by the IC and MCP placed at F3.

from the  $\Delta E$  and the time-of-flight (TOF) from the MCP and the RF signals.  $^{46}\text{Cr}$  was clearly separated from other products. In this experiment, the purity and the intensity of  $^{46}\text{Cr}$  were 2 % and 10 particle per second (pps) with the primary beam of 80 particle nA.

Figure 2 shows a decay spectrum of NSTDC between duration of beam off. This spectrum was made by only setting gates on more than 200 keV of DSSD, which is mainly dominated by the  $^{46}\text{V}$  decay. Further analysis is in progress to get a clean spectrum.

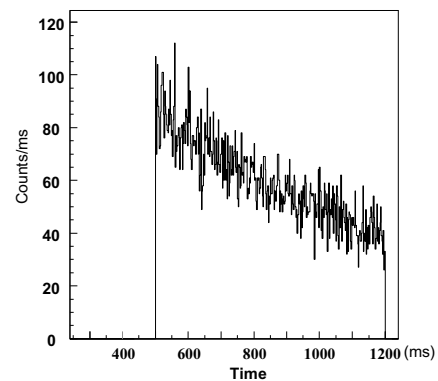


Fig. 2. Decay spectrum.

### References

- 1) K. Langanke and G. Martinez-Pinedo, Rev. Mod. Phys. **75**, 819 (2003).
- 2) S. Kubono et al., Eur. Phys. J. A **13**, 217 (2002).
- 3) Y. Yanagisawa et al., Nucl. Instrum. Methods Phys. Res. A **539**, 73 (2005).

<sup>\*1</sup> Center for Nuclear Study, University of Tokyo

<sup>\*2</sup> Institute of Physics and Electronic, Vietnam Academy of Science and Technology

<sup>\*3</sup> Department of Physics, Osaka University

## $^{30}\text{S}$ Beam Development with CRIB

D. Kahl,<sup>\*1,\*2</sup> A. A. Chen,<sup>\*1</sup> N. B. Dam,<sup>\*2</sup> J. Chen,<sup>\*1</sup> T. Hashimoto,<sup>\*2</sup> S. Hayakawa,<sup>\*2</sup> A. Kim,<sup>\*3</sup> S. Kubono,<sup>\*2</sup>  
Y. Kurihara,<sup>\*2</sup> N. H. Lee,<sup>\*3</sup> S. Michimasa,<sup>\*2</sup> S. Nishimura,<sup>\*4</sup> C. V. Ouellet,<sup>\*1</sup> K. Setoodeh nia,<sup>\*1</sup> Y.  
Wakabayashi,<sup>\*2</sup> and H. Yamaguchi,<sup>\*2</sup>

[Unstable nuclei, astrophysics]

The  $^{30}\text{S}(\alpha,p)$  reaction is a significant link in the rapid proton capture process in X-ray bursts on accreting neutron stars<sup>1)</sup>, but there are no experimental data to date. In order to perform a successful measurement of the  $^4\text{He}(^{30}\text{S},p)$  cross section at X-ray burst energies, Hauser-Feshbach calculations indicate we require a  $^{30}\text{S}$  beam of  $\sim 10^5$  particles per second (pps) at 32 MeV.

We conducted beam development experiments in 2006 and 2008 using the low-energy Center for Nuclear Study (CNS) radioactive ion beam (CRIB) separator facility<sup>2,3)</sup> of the University of Tokyo and located at the Nishina Center of RIKEN. We produce  $^{30}\text{S}$  via the  $^3\text{He}(^{28}\text{Si},^{30}\text{S})n$  reaction, by bombarding a cryogenic gas target<sup>4,5)</sup> of  $^3\text{He}$  at 90 K with beams of  $^{28}\text{Si}$ . We tested two primary beams:  $^{28}\text{Si}^{9+}$  (6.9 MeV/u and 130 pA);  $^{28}\text{Si}^{10+}$  (7.54 MeV/u and 10 pA); both beams were extracted from the CNS HyperECR ion source and accelerated by the AVF cyclotron. We tested three production target gas pressures (200, 300, 400 Torr), finding  $^{30}\text{S}$  yield was maximized at the highest  $^3\text{He}$  gas pressure.

RI Species	$E_{beam}$ (MeV)	Purity (%)	Intensity (pps @ 10 pA)
$^{30}\text{S}^{16+}$	30	30	500
$^{30}\text{S}^{14+}$	32	0.8	$1.2 \times 10^4$

Table 1. Selected results for  $^{30}\text{S}$  beams, using  $^3\text{He}$  at 400 Torr and the primary beam  $^{28}\text{Si}^{10+}$  at 7.54 MeV/u.

The  $^{30}\text{S}$  beam profile is monitored with delay-line PPACs and energy is measured with a Si detector at the target focus. Results are presented in Table 1 and Fig. 1. For both  $^{30}\text{S}$  experiments, the Wien filter potential was  $\pm 60$  kV, but it has achieved up to  $\pm 100$  kV, allowing higher  $^{30}\text{S}$  purity in future, which we like to be  $\geq 10\%$  due to the  $10^6$  Hz PPAC counting limit. We attempted to increase the purity of  $^{30}\text{S}^{14+}$  using a  $1.5 \mu\text{m}$  aluminized mylar degrader at the momentum dispersive focal plane, but the intensity on target decreased by 80% because the CRIB optics were not improperly retuned due to time constraints. It should be possible to accelerate  $^{28}\text{Si}^{9+}$  to 7.4 MeV/u at 130 pA, increasing the  $^{30}\text{S}^{14+}$  intensity by a factor of 13 to

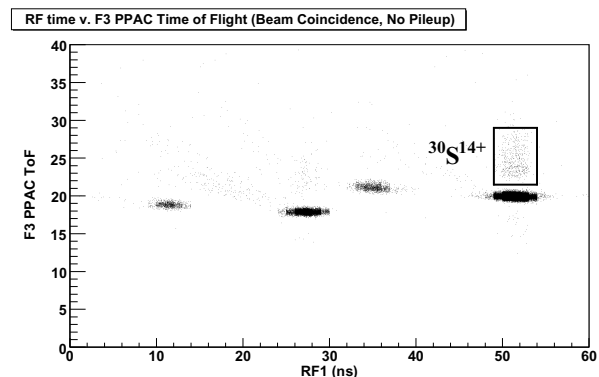


Fig. 1. RF-ToF spectrum using delay-line PPACs in the scattering chamber.  $^{30}\text{S}^{14+}$  is clearly separated.

above the requisite  $10^5$  pps. We also tested, but could not fully separate  $^{30}\text{S}^{15+}$  from the primary component  $^{28}\text{Si}^{14+}$  due to similar magnetic rigidity.

We measured the charge-state distribution of  $^{28}\text{Si}$  beam ions in carbon ( $550 \mu\text{g}/\text{cm}^2$ ) compared to Havar foil ( $2.2 \mu\text{m}$ ) (Table 2). For a  $^{28}\text{Si}$  beam of 3.4 MeV/u ( $\sim E_{beam}$  of  $^{30}\text{S}$ ), it was found that transmission of highly charged states of  $^{28}\text{Si}$  is improved through carbon foil compared to Havar foil with a ratio consistent with predictions of LISE++. It may be possible to preferentially populate higher charge states of  $^{30}\text{S}$  by use of a carbon stripper foil.

Target	Species	Normalized pps @ 10 enA
Havar	$^{28}\text{Si}^{12+}$	$1.075 \times 10^8$
Havar	$^{28}\text{Si}^{13+}$	$6.013 \times 10^7$
Havar	$^{28}\text{Si}^{14+}$	$3.901 \times 10^6$
Carbon	$^{28}\text{Si}^{12+}$	$1.758 \times 10^8$
Carbon	$^{28}\text{Si}^{13+}$	$1.300 \times 10^8$
Carbon	$^{28}\text{Si}^{14+}$	$4.365 \times 10^7$

Table 2. Intensity of selected charge states of  $^{28}\text{Si}$  after passing through Havar foil or carbon foil.

### References

- 1) J. L. Fisker, F.-K. Thielemann and M. Wiescher: ApJ. **608** (2004) L61.
- 2) S. Kubono *et al.*: Eur. Phys. J. A **13** (2002) 217.
- 3) Y. Yanagisawa *et al.*: Nucl. Instr. Meth. **A539** (2005) 74.
- 4) H. Yamaguchi *et al.*: Nucl. Instr. Meth. **A589** (2008) 150.
- 5) G. Amadio *et al.*: Nucl. Instr. Meth. **A590** (2008) 191.

\*1 Department of Physics & Astronomy, McMaster University, Canada

\*2 Center for Nuclear Study, University of Tokyo

\*3 Department of Physics, Ewha Womans University, Korea

\*4 RIKEN (the Institute of Physical and Chemical Research)

# Study of astrophysically important states in $^{26}\text{Si}$ via the $p(^{25}\text{Al},p)^{25}\text{Al}$ elastic scattering

J. Chen,<sup>\*1</sup> A. A. Chen,<sup>\*1</sup> S. Kubono,<sup>\*2</sup> H. Yamaguchi,<sup>\*2</sup> G. Amadio,<sup>\*2</sup> S. Cherubini,<sup>\*3</sup> M. La .Cognata,<sup>\*3</sup> H. Fujikawa,<sup>\*2</sup> S. Hayakawa,<sup>\*2</sup> N. Iwasa,<sup>\*4</sup> J. J. He,<sup>\*2</sup> D. Kahl,<sup>\*1</sup> L. H. Khieu,<sup>\*2</sup> Y. Kurihawa,<sup>\*2</sup> Y. K. Kwon,<sup>\*5</sup> J. Y. Moon,<sup>\*5</sup> M. Niikura,<sup>\*2</sup> S. Nishimura,<sup>\*6</sup> A. Odahara,<sup>\*7</sup> J. Pearson,<sup>\*1</sup> R. Pizzone,<sup>\*3</sup> A. Saito,<sup>\*2</sup> C. Signorini,<sup>\*8</sup> T. Teranishi,<sup>\*9</sup> Y. Togano,<sup>\*10</sup> and Y. Wakabayashi,<sup>\*2</sup>

Galactic  $^{26}\text{Al}$  in its ground state is produced by the proton capture on  $^{25}\text{Mg}$ . In nova explosions, the proton capture of  $^{25}\text{Al}$  competes with its  $\beta$  decay to supply the  $^{25}\text{Mg}$  and therefore bypasses the production of  $^{26g}\text{Al}$ , since the capture product  $^{26}\text{Si}$  decays quickly to  $^{26m}\text{Al}$  instead of its ground state. At even higher temperatures, such as in supernova explosions,  $^{26m}\text{Al}$  can be excited to the higher excited states by thermal excitation and then quickly de-excite to the ground state, thereby enhancing the production of  $^{26g}\text{Al}$ . The energy levels in  $^{26}\text{Si}$  in the Gamow window corresponding to these temperatures therefore need to be well understood in order to determine the  $^{25}\text{Al}(p,\gamma)^{26}\text{Si}$  reaction rate, and thus the production rate of  $^{26}\text{Al}$  in these explosive environments<sup>4-7</sup>.

A thick target method<sup>2,3</sup> was used to scan the center-of-mass energy from 0 to 3.38 MeV with the secondary beam of 3.52 MeV/nucleon  $^{25}\text{Al}$  impinging on the 6.58 mg/cm<sup>2</sup> CH<sub>2</sub> target, corresponding to a range of excited states from 5.515 MeV ( $^{25}\text{Al}+p$  threshold) to about 8.9 MeV. The  $^{25}\text{Al}$  beam was produced by the reaction  $^2\text{H}(^{24}\text{Mg},n)^{25}\text{Al}$ , with the purity of about 50% and intensity of about  $5 \times 10^5$  pps on target. The particle identification (PID) for the secondary beam was provided by two PPACs (Parallel Plate Avalanche Chamber) while PID for the scattered protons was provided by  $\Delta E$ -E telescopes as well as the TOF (time-of-flight) method.

The energy loss of the scattered proton traveling through the remaining part of the target must be taken into account. The total yields of background protons of different energies from a carbon target are normalized by the ratio of target thickness per energy bin and the ratio of the total number of beam events. Figure 1 shows a final proton spectrum after correcting the energy loss and subtracting the background protons.

For preliminary purpose to find the resonant energies, a Breit-Wigner fit was applied for each single peak in the proton spectrum. Figure 2 shows a sample fit.

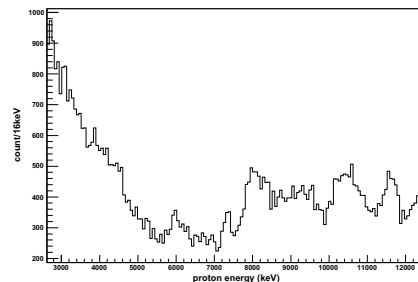


Fig. 1. Proton spectrum at  $\theta_{lab} = 0^\circ$  in the center of mass frame with energy loss corrected and background subtracted.

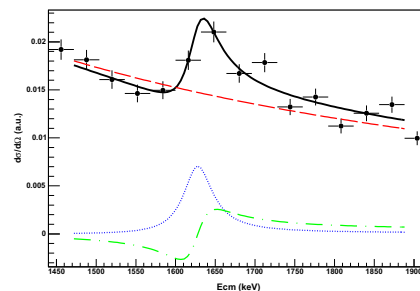


Fig. 2. A Breit-Wigner fit for the peak at  $E_{cm} = 1697\text{keV}$ , corresponding to the excited state  $E_x = 7156\text{keV}$ ,  $J^\pi = 2^+, ^7$  with the dashed line for the Coulomb part, dashed-dotted line for Coulomb-resonance interference and the dotted line for the pure resonant part.

An advanced R-Matrix<sup>8</sup> fit for the excitation function is being performed to extract physical parameters such as energy levels and proton widths. The results will be used as input for calculating the new  $^{25}\text{Al}(p,\gamma)^{26}\text{Si}$  reaction rate. The analysis is still in progress.

## References

- 1) R. C. Runkle, A. E. Champagne, and J. Engel, APJ **556** (2001) 970-978
- 2) S. Kubono, Nucl. Phys. A **693** (2001) 221-248.
- 3) A. H. Hernández *et al.*, NMB **143** (1998) 569-574
- 4) D. W. Bardayan *et al.*, Phys. Rev. C **65** (2002) 032801.
- 5) J. A. Caggiano *et al.*, Phys. Rev. C **65** (2002) 055801.
- 6) Y. Parpottas *et al.*, Phys. Rev. C **70** (2004) 065805.
- 7) D. W. Bardayan *et al.*, Phys. Rev. C **74** (2006) 045804.
- 8) A. M. Lane, and R. G. Thomas, Rev. Mod. Phys. **30** (1958) 257

<sup>\*1</sup> Dept. of Physics & Astronomy, McMaster Univ., Canada  
<sup>\*2</sup> Center for Nuclear Study, University of Tokyo, Japan  
<sup>\*3</sup> Dept. of Physics, University of Catania and INFN, Italy  
<sup>\*4</sup> Dept. of Physics, Tohoku University, Japan  
<sup>\*5</sup> Dept. of Physics, Chung-Ang University, South Korea  
<sup>\*6</sup> RIKEN(The Institute of Physical and Chemical Research)  
<sup>\*7</sup> Dept. of Physics, Rikkyo University, Japan  
<sup>\*8</sup> Dept. of Physics, University of Padova and INFN, Italy  
<sup>\*9</sup> Dept. of Physics, Kyushu University, Japan  
<sup>\*10</sup> Dept. of Physics, Nishinippon Inst. of Technology, Japan

# Measurement of the ground-state electric quadrupole moment of $^{33}\text{Al}$

H. Ueno, K. Asahi,<sup>\*1</sup> D.L. Balabanski,<sup>\*2</sup> J.M. Daugas,<sup>\*3</sup> M. Depuydt,<sup>\*4</sup> M. De Rydt,<sup>\*4</sup> L. Gaudefroy,<sup>\*3</sup> S. Grévy,<sup>\*5</sup> Y. Hasama,<sup>\*1</sup> Y. Ichikawa, D. Kameda, P. Morel,<sup>\*3</sup> T. Nagatomo, G. Neyens,<sup>\*4</sup> L. Perrot,<sup>\*6</sup> K. Shimada,<sup>\*7</sup> Ch. Stödel,<sup>\*5</sup> J.C. Thomas,<sup>\*5</sup> W. Vanderheijden,<sup>\*4</sup> N. Vermeulen,<sup>\*4</sup> P. Vingerhoets,<sup>\*4</sup> A. Yoshimi

[Nuclear structure, magnetic moment, unstable nuclei]

In the work currently being carried out, the ground-state  $Q$  moment of  $^{33}\text{Al}$  ( $I^\pi = 5/2^+$ ,  $T_{1/2} = 41.7(2)$  ms) has been measured by means of the  $\beta$ -ray detected nuclear magnetic resonance ( $\beta$ -NMR) spectroscopy<sup>1)</sup> incorporating the technique of fragmentation-induced spin-polarized radioactive isotope beams<sup>2,3)</sup>.

The experiment was carried out at the GANIL facility. A beam of  $^{33}\text{Al}$  was obtained from the fragmentation of  $^{36}\text{S}$  projectiles at  $E = 77.5A$  MeV on a 224 mg/cm<sup>2</sup>-thick  $^9\text{Be}$  target. In order to have  $^{33}\text{Al}$  spin-polarized, fragments emitted at angles  $\theta_{\text{Lab}} = (1 - 3)^\circ$  from the primary beam direction were accepted by the LISE spectrometer: the primary beam was deflected by  $2^\circ$  with respect to the target located at the spectrometer entrance. Also, a range of momenta  $p = (1.026 - 1.041)p_b$  was selected with a slit placed at the momentum-dispersive intermediate focal plane. Here  $p_b = 11.7$  GeV/ $c$  is the fragment momentum corresponding to the projectile velocity. Under the above conditions and with a primary  $^{36}\text{S}^{16+}$  beam current of  $I \sim 2$  e $\mu\text{A}$ , LISE provided the beam of  $^{33}\text{Al}$  with a purity  $\sim 75\%$  and an intensity of 1.3 k particles/s. Then, the spin-polarized  $^{33}\text{Al}$  were transported to a  $\beta$ -NMR apparatus located at the final focus of LISE, and were implanted in a stopper of  $\alpha\text{-Al}_2\text{O}_3$  single crystal of hexagonal structure. A static magnetic field  $B_0 \sim 500$  mT was applied to the stopper in order to preserve the spin polarization. The  $\alpha\text{-Al}_2\text{O}_3$  crystal was mounted in a stopper chamber so that the  $c$ -axis was oriented parallel to the  $B_0$  field. The stopper was kept in a vacuum and cooled to a temperature  $T \simeq 80$  K to suppress the spin-lattice relaxation of  $^{33}\text{Al}$  during the  $\beta$  decay.

The  $Q$  moment was measured based on the  $\beta$ -NMR technique, where resonance is observed through the change in the  $\beta$ -ray up/down ratio  $R$  measured with plastic scintillator telescopes located above and below the stopper. By taking a double ratio  $R/R_0$  where  $R_0$  is the value for  $R$  measured without an oscillating magnetic field  $B_1$ , the resonance frequency is derived from the position of a peak or dip deviating from unity. The obtained NMR spectra are shown in Fig. 1.

The experimental quadrupole coupling constant  $|eqQ/h|$  of  $^{33}\text{Al}$  can be determined from the peak positions in the spectra, with which the experimental  $|Q(^{33}\text{Al})|$  is deduced from the relation  $|Q(^{33}\text{Al})| = |Q(^{27}\text{Al}) \cdot eqQ/h(^{33}\text{Al})/eqQ/h(^{27}\text{Al})|$ , where  $Q(^{27}\text{Al})$  and  $eqQ/h(^{27}\text{Al})$  denote the  $Q$  moment of  $^{27}\text{Al}$  and the quadrupole coupling constant of  $^{27}\text{Al}$  in  $\alpha\text{-Al}_2\text{O}_3$ , respectively. Based on the least- $\chi^2$  fitting analysis adopted to the determination of  $|Q(^{31}\text{Al})|$ <sup>4)</sup>, a preliminary value  $|Q(^{33}\text{Al})| = 132(16)$  emb has been determined. The analysis is in progress.

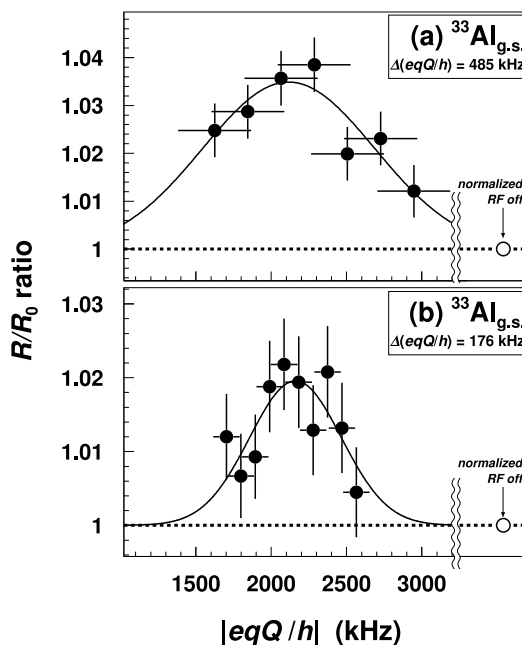


Fig. 1. NQR spectra obtained in an  $\alpha\text{-Al}_2\text{O}_3$  single crystal for the  $^{33}\text{Al}$  ground state by applying (a) wider and (b) narrower frequency windows of the  $B_1$  field. In the spectra, double ratios  $R/R_0$  are plotted as a function of the quadrupole coupling constant  $|eqQ/h|$ , where  $R_0$  is the value for  $\beta$ -ray up/down ratio  $R$  measured without the  $B_1$  field. The result of the least- $\chi^2$  fitting analysis is shown by solid curves.

<sup>\*1</sup> Department of Physics, Tokyo Institute of Technology

<sup>\*2</sup> INRNE, Bulgarian Academy of Sciences

<sup>\*3</sup> CEA/DIF/DPTA/PN

<sup>\*4</sup> K.U. Leuven, Instituut voor Kern-en Stralingsfysica

<sup>\*5</sup> Grand Accélérateur National d'Ions Lourds (GANIL)

<sup>\*6</sup> Institut de Physique Nucléaire d'Orsay

<sup>\*7</sup> Cyclotron and Radioisotope Center, Tohoku University

## References

- 1) K. Sugimoto et al.: J. Phys. Soc. Japan **21**, 213 (1966).
- 2) K. Asahi et al.: Phys. Lett. **B251**, 488 (1990)
- 3) H. Okuno et al.: Phys. Lett. **B335**, 29 (1994).
- 4) D. Nagae et al.: Phys. Rev. C **79**, 027301 (2009).

## Electric quadrupole moment of proton-rich $^{23}\text{Al}$

T. Nagatomo, Y. Hasama,<sup>\*1</sup> K. Asahi,<sup>\*1</sup> Y. Ichikawa, H. Iijima,<sup>\*1</sup> T. Inoue,<sup>\*1</sup> Y. Ishibashi,<sup>\*2</sup> H. Kawamura, K. Matsuta,<sup>\*3</sup> M. Mihara,<sup>\*3</sup> T. Minamisono,<sup>\*4</sup> T. Moriguchi, A. Ozawa, K. Suzuki,<sup>\*1</sup> T. Sumikama,<sup>\*5</sup> M. Uchida,<sup>\*1</sup> K. Yamada, A. Yoshimi and H. Ueno

[nuclear structure, spin-polarized RI beam, electric quadrupole moment,  $\beta$ -NMR/NQR]

Proton-odd nuclei in the  $sd$ -shell near the proton-drip line have much smaller proton-separation energies compared with stable nuclei. In particular, for  $^{23}\text{Al}$  ( $I^\pi = 5/2^+, ^1$ )  $T_{1/2} = 470\text{ms}$ ), the separation energy is extremely small as 125(25) keV, and so  $^{23}\text{Al}$  is considered to be a candidate of the proton-halo nucleus. Recently, a large reaction cross section, although error was still large, was reported<sup>2,3)</sup> and the authors suggested halo-like structure of  $^{23}\text{Al}$ . Note that there is at least one candidate of the proton-halo like nucleus whose spin-parity is not  $1/2^+$ , e.g.  $^8\text{B}^4)$  in the  $p$  shell. In this work, the  $Q$  moment of  $^{23}\text{Al}$  has been measured by  $\beta$ -ray detected Nuclear Quadrupole Resonance method ( $\beta$ -NQR method) to extract information about nuclear matter density distribution.

The experiment was carried out by utilizing the RIKEN Projectile Fragment Separator (RIPS) at the RI Beam Factory operated by RIKEN Nishina Center and CNS, University of Tokyo. Nuclear spin-polarized  $^{23}\text{Al}$  nuclei were produced by bombardment of  $^{24}\text{Mg}$  ions on a 2.5 mm-thick  $^9\text{Be}$  target. The  $^{24}\text{Mg}^{12+}$  ions were accelerated up to 100 MeV/nucleon and the intensity of the primary beam was typically  $\sim 800$  enA on the target. The production process,  $^{24}\text{Mg} + ^9\text{Be} \rightarrow ^{23}\text{Al} + \text{X}$ , is considered as a composite process of the pick-up and the projectile fragmentation processes. The fragments which are emitted into the angle from  $0.4^\circ$  to  $5.4^\circ$  relative to the primary beam with the momentum below  $1.05 p_0$ , where  $p_0 = 8.76$  GeV/ $c$  is the peak in the distribution, were selected by RIPS, and the degree of polarization of  $^{23}\text{Al}$  was measured as 1.2% by the  $\beta$ -NMR method. A wedge-shaped degrader (221 mg/cm<sup>2</sup>) was used for the energy loss separation, and then the  $^{23}\text{Al}$  ions were transported to the  $\beta$ -NQR apparatus and were implanted into a  $\alpha\text{-Al}_2\text{O}_3$  plate together with inseparable fragments such as  $^{22}\text{Mg}$  and  $^{21}\text{Na}$  which became low energy- $\beta$ -ray emitters. By  $\beta$ -ray energy separation, the purity was achieved to  $\sim 74\%$  in  $\beta$ -ray counts and the counting rate was typically  $\sim 100$  cps. Static magnetic field  $B_0 = 0.458\text{T}$  was applied on the crystal parallel to the polarization axis in order to preserve the polarization and to induce the Zeeman splitting. Electric field gradient  $q = V_{zz}$  at

the implantation site of  $^{23}\text{Al}$  in  $\alpha\text{-Al}_2\text{O}_3$  interacts with the  $Q(^{23}\text{Al})$  as a perturbation which is characterized by a quadrupole coupling constant  $eqQ/h$ . In  $\beta$ -NQR method, using plastic-scintillation-counter telescopes which are placed above and below the crystal relative to the polarization, the asymmetrical  $\beta$ -ray emission were detected as a up/down counting ratio. Oscillating magnetic field  $B_1$  was applied perpendicular to the  $B_0$ . When applied frequencies corresponds to the  $eqQ$ -perturbed Zeeman splitting, the polarization was resonantly changed, in other words, the up/down ratio was resonantly changed at the  $eqQ/h$ .

Obtained NQR spectrum is shown in Fig. 1. In Fig. 1, the  $\beta$ -ray asymmetry was expressed as the up/down ratio normalized by the up/down ratio without  $B_1$  field as a function of  $eqQ/h$ . From the peak position of the resonance and comparison with  $^{27}\text{Al}$  of which the  $Q$  moment<sup>5)</sup> and the quadrupole coupling in  $\alpha\text{-Al}_2\text{O}_3$ <sup>6)</sup> are well studied, the  $Q$  moment of the  $^{23}\text{Al}$  is determined as  $|Q| \sim 170$  emb from the preliminary analysis. Detailed analysis is in progress.

### References

- 1) A. Ozawa et al.: Phys. Rev. C **74**, 021301(R) (2006).
- 2) X.Z. Cai et al.: Phys. Rev. C **65**, 024610 (2002).
- 3) H.Y. Zhang et al.: Nucl. Phys. **A707**, 303 (2002).
- 4) T. Sumikama et al.: Phys. Rev. C **74**, 024327 (2006).
- 5) V.Kellö et al. : Chem. Phys. Lett. **304**, 414 (1999).
- 6) S.J. Gravina et al. :J. Mag. Reso. **89**, 515 (1990).

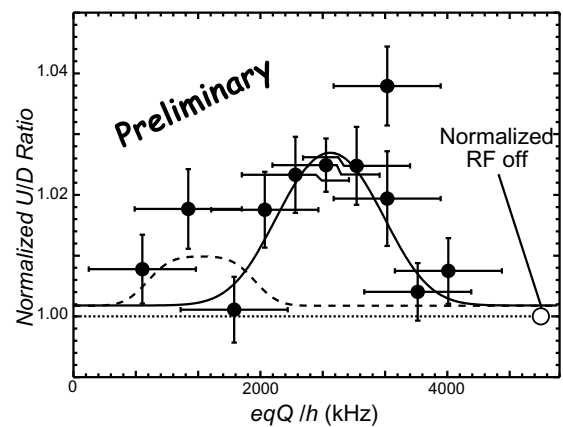


Fig. 1. NQR spectrum of  $^{23}\text{Al}$  in  $\alpha\text{-Al}_2\text{O}_3$  at room temperature. The solid line shows the result of preliminary analysis based on the least- $\chi^2$  fitting.

<sup>\*1</sup> Department of Physics, Tokyo Institute of Technology

<sup>\*2</sup> Department of Physics, University of Tsukuba

<sup>\*3</sup> Department of Physics, Osaka University

<sup>\*4</sup> Dept. for the Application of Nuclear Technology, Fukui University of Technology

<sup>\*5</sup> Department of Physics, Tokyo University of Science

## Production of $^{58}\text{Cu}$ through the charge exchange reaction of $^{58}\text{Ni}$

M. Mihara,<sup>\*1</sup> H. Ueno, T. Nagatomo, Y. Ichikawa, T. Moriguchi,<sup>\*2</sup> H. Oishi,<sup>\*2</sup> A. Ozawa,<sup>\*2</sup> M. Takechi, K. Yamada, A. Yoshimi, D. Nishimura,<sup>\*1</sup> M. Fukuda,<sup>\*1</sup> K. Matsuta,<sup>\*1</sup> T. Izumikawa,<sup>\*3</sup> T. Ohtsubo,<sup>\*4</sup> T. Kubo,<sup>\*4</sup> Y. Namiki,<sup>\*4</sup> Y. Ishibashi,<sup>\*2</sup> Y. Ito,<sup>\*2</sup> S. Momota,<sup>\*5</sup> D. Horikawa,<sup>\*5</sup> K. Suzuki,<sup>\*6</sup> I. Hachiuma,<sup>\*7</sup> K. Namihira,<sup>\*7</sup> T. Yamaguchi,<sup>\*7</sup> T. Suzuki,<sup>\*7</sup> Y. Hirayama,<sup>\*8</sup> T. Minamisono,<sup>\*9</sup> K. Sato,<sup>\*7</sup> T. Kuboki,<sup>\*7</sup> Y. Kobayashi, K. Asahi,<sup>\*6</sup> and K. Matsukawa<sup>\*10</sup>

[Charge exchange reaction, unstable nuclei]

Nuclei near the double magic nucleus  $^{56}\text{Ni}$  are of particular interest in investigating structure and interaction in the  $pf$ -shell region<sup>2)</sup>. The  $N=Z$  odd-odd nucleus  $^{58}\text{Cu}(I^\pi = 1^+, T_{1/2} = 3.2 \text{ s})$  with one proton and one neutron outside the  $^{56}\text{Ni}$  core is the best suited system for the study of proton-neutron interaction in a  $pf$  shell nucleus. We then plan to determine the electromagnetic moments of  $^{58}\text{Cu}$  by means of the  $\beta$ -NMR technique<sup>1)</sup>.

Also the short lived  $\beta$ -emitter  $^{58}\text{Cu}$  might be an attractive  $\beta$ -NMR probe for material science. For example in a Si device, a Cu impurity causes degradation of its performance because of the fast diffusivity and formation of deep impurity levels in the band gap<sup>3)</sup>.  $\beta$ -NMR studies with  $^{58}\text{Cu}$  as a microscopic probe should be able to provide unique information on the mechanism of Cu diffusion and the behavior of Cu-dopant complex (ex. Cu-B pair) in Si.

In this report, we present results for the production of  $^{58}\text{Cu}$  through a charge exchange reaction of  $^{58}\text{Ni}$ , as the first step of establishing a spin polarized  $^{58}\text{Cu}$  beam for  $\beta$ -NMR studies. A 95A MeV  $^{58}\text{Ni}$  beam was provided by the K540 RIKEN Ring Cyclotron and impinged on a 2-mm thick Be target. The  $^{58}\text{Cu}$  nuclei emitted at angles  $0.2^\circ$ – $4.5^\circ$  were separated by RIPS. An 85-mg/cm<sup>2</sup> thick curved Al plate was used at F1 as an achromatic degrader.

Particle identification was done with a standard particle detector system at RIPS. The momentum distribution for  $^{58}\text{Cu}$  was obtained as shown in Fig. 1 and the width is almost explained by energy spread due to the target thickness. The momentum of the peak for  $^{58}\text{Cu}$  is nearly the same as the momentum that corresponds to the primary beam velocity.

The size of the secondary beam was about 15 mm in diameter at the final focus point F3 where the  $\beta$ -NMR equipment is to be installed. Production of  $^{58}\text{Cu}$  was

also confirmed from the  $\beta$ -ray time spectrum measured at F3 as shown in Fig. 2.

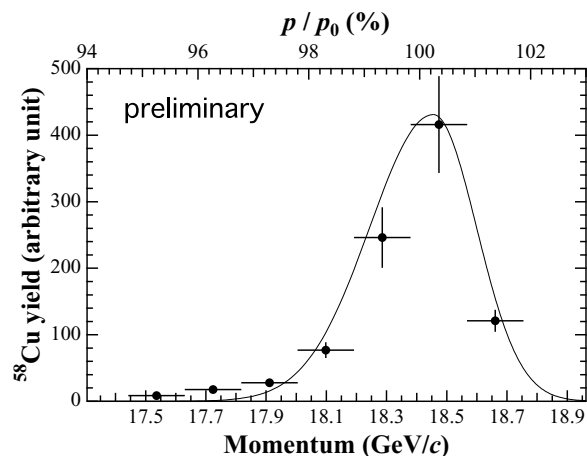


Fig. 1. Momentum distribution of  $^{58}\text{Cu}$  produced through the charge exchange reaction of  $^{58}\text{Ni}$  with a Be target.

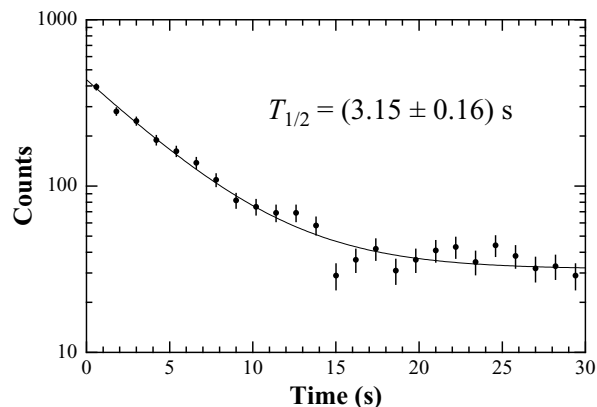


Fig. 2. Typical  $\beta$ -ray time spectrum for  $^{58}\text{Cu}$ .

\*1 Department of Physics, Osaka University  
 \*2 Department of Physics, University of Tsukuba  
 \*3 Radioisotope Center, Niigata University  
 \*4 Department of Physics, Niigata University  
 \*5 Faculty of Engineering, Kochi University of Technology  
 \*6 Department of Physics, Tokyo Institute of Technology  
 \*7 Department of Physics, Saitama University  
 \*8 Institute of Particle and Nuclear Studies, KEK  
 \*9 Department of Applied Nuclear Technology, Fukui University of Technology  
 \*10 Renesas Technology Corp.

### References

- 1) K. Asahi and K. Matsuta: Nucl. Phys. A **693**, 63 (2001).
- 2) M. Honma et al.: Phys. Rev. C **69**, 034335 (2004).
- 3) E.R. Weber: Appl. Phys. A **30**, 1 (1983).

# The first T-violation experiment using polarized $^8\text{Li}$ at KEK-TRIAC

H. Kawamura,<sup>\*1</sup> T. Akiyama,<sup>\*1</sup> M. Hata,<sup>\*1</sup> Y. Hirayama,<sup>\*2</sup> Y. Ikeda,<sup>\*1</sup> T. Ishii,<sup>\*3</sup> D. Kameda, S. Mitsuoka,<sup>\*3</sup> D. Nagae,<sup>\*3</sup> K. Ninomiya,<sup>\*1</sup> M. Nitta,<sup>\*1</sup> E. Seitaibashi,<sup>\*1</sup> T. Toyoda,<sup>\*1</sup> Y. X. Watanabe,<sup>\*2</sup> and J. Murata<sup>\*1</sup>

[ $\beta$  decay, spin polarization, symmetry]

The beta-decay rate function  $W$  can be expressed as

$$W \propto 1 + A \frac{\vec{J} \cdot \vec{p}}{E} + R \frac{\vec{J} \cdot (\vec{p} \times \vec{\sigma})}{E} \dots,$$

where  $\vec{J}$  denotes spin of the parent nucleus, and  $E$ ,  $\vec{p}$  and  $\vec{\sigma}$  indicate energy, momentum and spin of electrons, respectively.  $A$  is the beta-decay asymmetry parameter, and  $R$  is the coefficient we are interested in. Production of polarized nuclei, measurement of electron momentum, and measurement of electron transverse polarization are required to determine the  $R$  coefficient. If a non-zero  $R$  is observed, it means that time reversal symmetry is violated.

A physics experiment (RNB08K04) was performed in September 2008 using a polarized  $^8\text{Li}$  beam at KEK-TRIAC, and  $R$ -parameter measurement was performed. The detector setup is shown in Fig. 1. Regarding the Mott polarimeter, a multi-wire drift chamber has been developed as an electron tracking detector.<sup>1)</sup> The polarized  $^8\text{Li}$  is produced using the tilted-foil technique.<sup>2)</sup> In the present experiment, polystyrene ( $3\mu\text{g}/\text{cm}^2$ ) foil was used with a tilting angle of  $70^\circ$ . Systematic error of the detector system can be canceled by changing the foil angles every 5 minutes. A special beam stopper was developed at the Van de Graaff accelerator at Osaka University.<sup>3)</sup> A large platinum foil ( $t=20\mu\text{m}$ , annealed) was used to catch the diffrused beam efficiently. A magnetic field ( $>500$  Gauss) was applied using a pair of small permanent magnets in order to minimize the size of the entire stopper. It is known that transversely polarized electrons show up-down asymmetry in Mott scattering. Electron transverse polarization can be determined by obtaining the scattering angular distribution from the observed scattering tracks.

A new trigger system was developed for the September experiment. The previous trigger logic consisted of coincidence signals between scintillators. In the new system, the trigger purity (ratio of real scattered “V-tracks” events to all recorded events) is quite small. To improve the poor V-track efficiency, the hit signals from the drift chamber are included in the trigger logic. Using this new trigger system, the trigger rate can be reduced to 1/20 without losing real events.

We successfully reconstructed the tracks for the Mott scattered electrons. The value of the  $R$ -parameter was roughly estimated from the asymmetry

<sup>\*1</sup> Department of Physics, Rikkyo University, Tokyo

<sup>\*2</sup> Institute of Particle and Nuclear Studies, KEK, Ibaraki

<sup>\*3</sup> Advanced Science Research Center, JAEA, Ibaraki

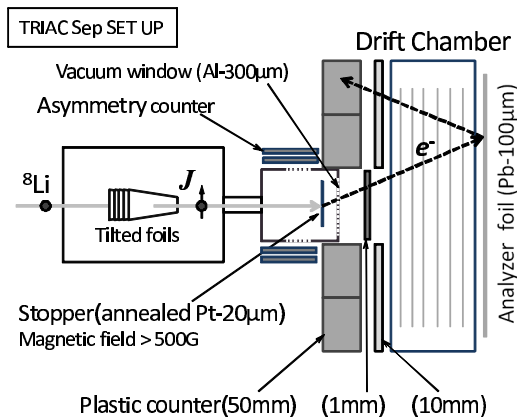


Fig. 1. Detector setup.

of the scattering angular distributions (Fig. 2), yielding  $R = 0.30 \pm 0.18$  (statistics only). This value is inconsistent with zero. More precise experiments are required to determine whether time reversal symmetry is violated or not.

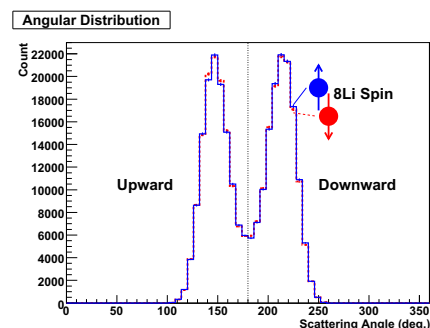


Fig. 2. Obtained angular distribution of Mott scattering.

Our future experiments will be performed at TRIUMF-ISAC. Since the beam intensity and polarization are greatly increased, a better result will surely be obtained. DAQ acceptance, however, must be improved with respect to the high count rate. It has already been approved by PAC in December 2008; No. S1183: MTV (Mott polarimetry for T-Violation experiment). We will be able to determine  $R$ -parameter with the highest precision.

## References

- 1) H. Kawamura et al.: RIKEN Accel. Prog. Rep. **41**, 177 (2008).
- 2) Y. Hirayama et al.: JAEA-Review, **046**, 28 (2007).
- 3) K. Narita et al.: OULNS Annual Report, 62 (2007).

## Current status of SAMURAI

K. Yoneda, N. Iwasa,<sup>\*1</sup> T. Kawabata,<sup>\*2</sup> T. Kobayashi,<sup>\*1</sup> T. Kubo, K. Kusaka,  
T. Motobayashi, T. Murakami,<sup>\*3</sup> Y. Nakai, T. Nakamura,<sup>\*4</sup> J. Ohnishi, H. Okuno, H. Otsu,  
H. Sakurai, H. Sato, Y. Satou,<sup>\*4</sup> K. Sekiguchi, and Y. Togano

This report describes the current status of SAMURAI. SAMURAI (Superconducting Analyzer for Multi-particles from Radio Isotope beam) is a large-acceptance multi-particle spectrometer to be constructed in RIBF. A schematic illustration of SAMURAI is shown in Fig. 1. The main part is a large-gap (80 cm) superconducting dipole magnet with maximum 7 Tm bending power for momentum analysis of heavy projectile fragments and projectile-rapidity protons with large momentum and angular acceptance. The large gap also enables measurement of projectile-rapidity neutrons with large angular acceptance in coincidence with heavy projectile fragments.

SAMURAI can be used in a variety of ways in experiments with the RI beams provided from BigRIPS. In the breakup experiments of neutron-rich and proton-rich nuclei, SAMURAI's large acceptance enables efficient heavy ion (HI)-neutron and HI-proton coincidence measurements required for invariant-mass spectroscopy. SAMURAI is also suitable for missing-mass spectroscopy, in which measurement of charged particles after the reaction provides not only tagging of the reaction channels but also helps explore the decay modes thanks to the multi-particle detection capability. SAMURAI is also used to scrutinize scattering reactions of light nuclei, such as polarized deuteron scattering on proton, in order to study fundamental nucleon-nucleon interactions including three nucleon force effects. We also plan to install a time projection chamber in the large gap of SAMURAI magnet, which is used mainly for reaction studies such as investigation of the density dependence of the asymmetry term of the nuclear equation of state.

The construction budget was approved in this fiscal year. The budget is funded for four years from this fiscal year, and covers the magnet and most of the detectors. Although construction is expected to finish in the fourth year, all contracts relating to the budget must be concluded in this fiscal year due to unavoidable clerical constraints. Therefore, we concluded the contracts for the superconducting dipole magnet, detectors of HI, neutrons, and protons, superconducting triplet quadrupole magnet for beam transport, and required peripheral equipments.

The superconducting dipole magnet is designed to have a maximum bending power of 7 Tm, providing a rigidity resolution of about 1/700 (rms) at 2.3 GeV/c,

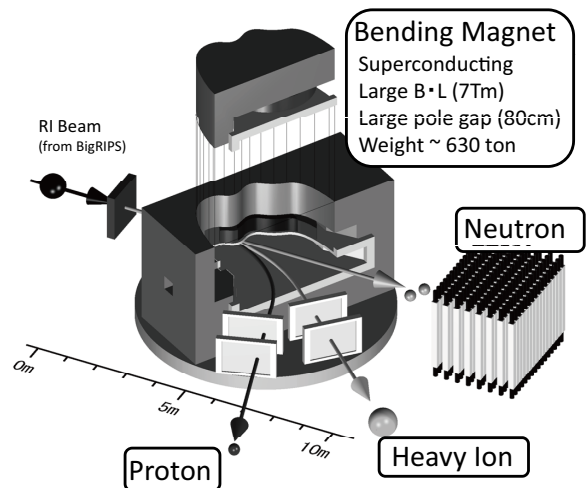


Fig. 1. Schematic image of SAMURAI system. SAMURAI consists of a large bending magnet with surrounding particle detectors. The magnet is a superconducting dipole magnet with a large bending power of 7 Tm and a large pole gap of 80 cm. The heavy ion detectors, neutron detectors, proton detectors, are installed around the magnet. The detector configuration changes depending on the experimental requirements.

particle identification up to  $A = 100$ , and a large pole gap of about 80 cm, providing vertical angular acceptance of projectile rapidity neutrons of  $\pm 5$  degrees. The current design is an H-type magnet with cylindrical poles 2 m in diameter, and round superconducting coils around both poles, each with magnetomotive force of about 2 MAT at maximum, resulting in 3 T central magnetic field. The outer size of the magnet, including the upper, lower, and side yokes, is about 6.8 m in width, 4.6 m in height, and 3 m in depth, and the total weight amounts to about 630 ton. Four field cramps are attached outside of the coils to reduce the fringe field, so that the detectors work beside the magnet. The entire magnet is placed on a rotatable stage to allow maximum flexibility in experimental configurations.

Magnet construction will start in October 2009, and finish early in 2011. The detectors will be constructed in parallel. After some tests and commissionings, the first SAMURAI experiment is scheduled to perform in summer 2011.

<sup>\*1</sup> Department of Physics, Tohoku University

<sup>\*2</sup> Center for Nuclear Study (CNS), University of Tokyo

<sup>\*3</sup> Department of Physics, Kyoto University

<sup>\*4</sup> Department of Physics, Tokyo Institute of Technology



## Probing Asymmetric Nuclear Matter at RIBF

T. Murakami,<sup>\*1</sup> S. Ebesu,<sup>\*1</sup> M. Sako,<sup>\*1</sup> E. Takada,<sup>\*2</sup> K. Ieki,<sup>\*3</sup> Y. Ikeda,<sup>\*3</sup> M. Matsushita,<sup>\*3</sup> J. Murata,<sup>\*3</sup>  
Y. Nakaya,<sup>\*3</sup> M. Nitta,<sup>\*3</sup> T. Toyoda,<sup>\*3</sup> H. Kawamura, Y. Nakai, S. Nishimura, and H. Sakurai

[EOS, centrality filter, pion range counter]

As reported in the last year progress report<sup>1)</sup> we have been developing a portable centrality filter and a pion range counter aiming to measure  $Y(\pi^-)/Y(\pi^+)$  yield ratios in central nucleus-nucleus collisions at intermediate energies. Detailed studies of pion production should provide meaningful constraints on the density dependence of the symmetry energy at high densities  $\rho > \rho_0$  where present constraints are least stringent.

This year we have increased the total number of plastics in the range counter to 12 as shown in Fig.1(left). As read-out phototubes we used either HAMAMATSU H1049-51's or H2431-50's with fast clipping of their anode signals. We have also completed the assembly of a centrality filter consisted of 60 slabs of  $5 \times 5 \times 78$  mm<sup>3</sup> plastic scintillators read by two HAMAMATSU H8500 flat-panel multianode-PMTs (Fig.1(right)).

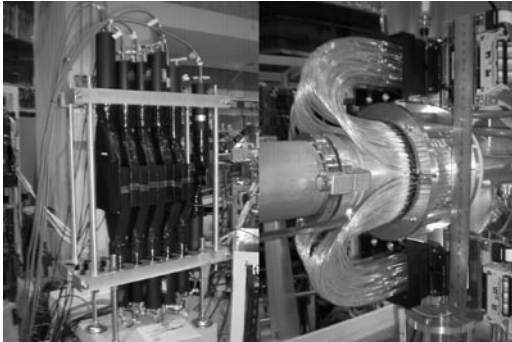


Fig. 1. Pictures of pion range counter(left) and centrality filter(right).

They are tested at HIMAC by measuring low-energy pion production in bombardments of 400 MeV/nucleon <sup>132</sup>Xe beam on In. The typical beam intensity was  $1 \times 10^6$  ppp and the target thickness was 330 mg/cm<sup>2</sup>. Signals are processed mainly by a FPGA module, QDC's and multi-hit TDC's and accumulated by a Linux PC.

Figure 2 shows a typical particle identification spectrum obtained with the 3rd and 4th elements of the pion range counter. Clear separations among electrons, pions, protons, deuterons, and tritons (from left to right) were observed in the spectrum. It should be noted that there are appreciable amount of back-

grounds around pion peak.

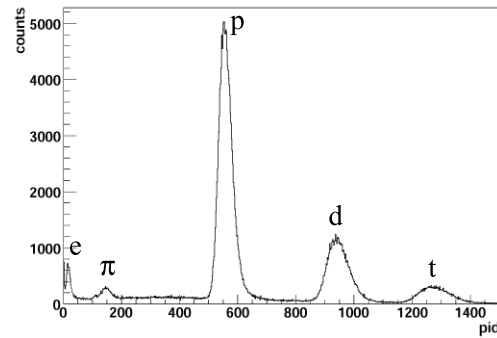


Fig. 2. Particle Identification Spectrum obtained by the pion range counter.

In Fig.3 we show a charged-particle multiplicity distribution associated with charged particles emitted toward 45° compared with an inclusive one. The charged particle-associated one seems strongly peaked at high multiplicity. Detailed analysis using these data is in progress.

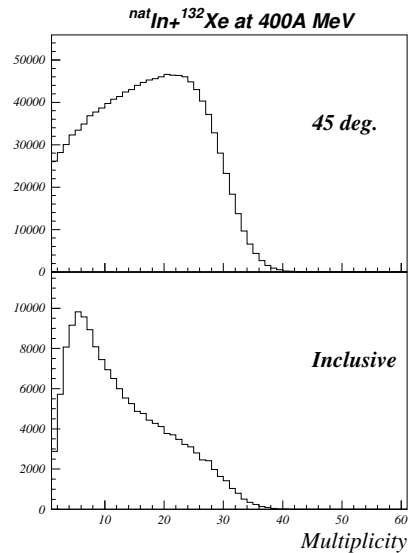


Fig. 3. Charged-particle multiplicity distributions for 45° charged particles in 400 MeV/N In+<sup>132</sup>Xe collisions (top). Inclusive one is also shown at the bottom.

<sup>\*1</sup> Department of Physics, Kyoto University, Kyoto, Japan

<sup>\*2</sup> Department of Accelerator and Medical Physics, NIRS, Chiba, Japan

<sup>\*3</sup> Department of Physics, Rikkyo University, Tokyo, Japan

### References

- 1) T. Murakami et al., RIKEN Accel. Prog. Rep. **41** (2008) 21.

## The development of the Gamma ray detectors in BigRIPS and Zerodegree spectrometer.

T.Nakao, <sup>\*1</sup> D.Kameda, T.Ohnishi, T.Kubo, K. Kusaka, K. Yoshida, A. Yoshida, M. Ohtake, N. Fukuda, H. Takeda, T. Tanaka, I. Inabe, Y. Yanagisawa, H. Watanabe, H. Otsu, Y. Kondo, Y. Gono, H. Sakurai, T. Motobayashi, H. Baba, T. Ichihara, Y. Yamaguchi, M. Takechi, S. Nishimura, H. Ueno, A. Yoshimi, M.Matsushita, <sup>\*2</sup> K. Ieki, <sup>\*2</sup> Y. Mizoi, <sup>\*3</sup> N. Kobayashi, <sup>\*4</sup> K. Tanaka, <sup>\*4</sup> Y. Kawada, <sup>\*4</sup> N. Tanaka, <sup>\*4</sup> S. Deguchi, <sup>\*4</sup> Y. Sato, <sup>\*4</sup> T. Nakamura, <sup>\*4</sup> K. Yoshinaga, <sup>\*5</sup> C. Ishii, <sup>\*5</sup> H. Yoshii, <sup>\*5</sup> N. Uematsu, <sup>\*5</sup> Y. Shiraki, <sup>\*5</sup> T. Sumikama, <sup>\*5</sup> J. Chiba, <sup>\*5</sup> E. Ideguchi, <sup>\*6</sup> S. Ota, <sup>\*6</sup> A. Saito, <sup>\*6</sup> Y. Sasamoto, <sup>\*6</sup> T. Uesaka, <sup>\*6</sup> S. Shimoura, <sup>\*6</sup> T. Yamaguchi, <sup>\*7</sup> T. Suzuki, <sup>\*7</sup> I. Hachiuma, <sup>\*7</sup> T. Moriguchi, <sup>\*8</sup> A. Ozawa, <sup>\*8</sup> T. Ohtsubo, <sup>\*9</sup> M. Famiano, <sup>\*10</sup> T. Nettleton, <sup>\*11</sup> B. Sherrill, <sup>\*11</sup> S. Manikonda, <sup>\*12</sup> and J. Nolen <sup>\*12</sup>

[BigRIPS, Zerodegree, Particle Identification, Isomer]

The observation of  $\gamma$ -rays emitted from isomeric states was very important for the particle identification in the BigRIPS experiment. In the same way, the observation of  $\gamma$ -rays is also important in the case of the Zerodegree spectrometer (ZDS). In this report, the present status of the development of the  $\gamma$ -ray Ge detector (Clover) in BigRIPS and ZDS is reported. The list of the isomeric states observed in the ZDS commissioning and new isotope search experiment, conducted in November 2008 (ZDS comm/Newiso exp.) is attached at the end of this report.

As in the previous report<sup>1)</sup>, two Clovers were installed at the 7th focal plane of BigRIPS (F7) as beamline detectors. This system was replaced by a more refined version. Figure 1 shows the picture of the system at F7. Three points are especially important for this new system. First, the additional chamber (Ge chamber) was installed in the downstream of F7 chamber. This chamber has two thin (1.5mm) aluminum windows for  $\gamma$ -ray measurement and a mechanism for the moveable beam stoppers. It became possible to transfer beams to the ZDS area maintaining the beamline vacuum. The moveable beam stopper mechanism is designed to put on two stoppers of different types. Second, the individual stages for two Clovers were installed at both sides of Ge chamber. Taking in and out the Clovers has become very easy because these stages were designed to introduce Clovers on the linear rails. These stages were for Clovers, but small portable type Ge detectors were also able to be installed. Lastly, the automatic Liquid Nitrogen filling device was re-

fined. The older version had a serious problem causing noises in signals on detectors' outputs. In the new version, this problem was overcome by replacing the thermometer, shielding on the electrical wires, etc. This device's ability has already been tested in the ZDS comm/Newiso exp. at the eleventh focal plane of ZDS (F11). Almost zero instances of noise were achieved.

In the case of ZDS, three Clovers were installed approximately 1500mm downstream of F11 chamber. Figure 2 shows the geometrical setup. This stage can install four Clovers in total, from both beamline sides of horizontal and vertical directions. In addition, the stage can be used not only for the F11 with 2m height beamline but also for the other focal planes with 1.7m height beamline such as F7 and F12. Two lead bricks were installed 190mm upstream of Clovers with a 100mm interval in order for the collimation so that the beams will not directly hit the Ge crystals.

In the ZDS comm/Newiso exp., two Al stoppers were prepared with different thicknesses in order to stop the produced charged particles efficiently. One has 10mm effective thickness along the beam axial direction, another has 30mm. In order to observe the  $\gamma$ -rays from three directions efficiently, stoppers have special shapes. Their typical figure is shown in fig. 3. As stoppers are completely symmetrical for horizontal direction and vertical direction, it is possible to obtain the same  $\gamma$ -ray photopeak efficiency for every Clover. In addition, a more effective rotation angle was performed than a 45 degree tilted stopper which had the same effective thickness along the beam axial direction. For this reason, it was possible to design the thickness of aluminum plate itself relatively thinner, and attenuation of  $\gamma$ -rays within the stopper was decreased. According to the Monte Carlo simulation using the Geant4 simulation program code (GEANT), 30% improvement of photopeak efficiency was obtained. The typical photopeak efficiency was 3% for 10mm stopper, and 2.3% for 30mm stopper for 1000keV  $\gamma$ -rays. The efficiency curve is shown in fig. 4. The dotted points represent the calibration result by the <sup>152</sup>Eu standard gamma source and curved lines represent the simula-

<sup>\*1</sup> Department of Physics, The Univ. of Tokyo

<sup>\*2</sup> Department of Physics, Rikkyo Univ

<sup>\*3</sup> Division of Electronics and Applied Physics, Osaka Electro-Communication Univ.

<sup>\*4</sup> Department of Physics, Tokyo Institute of Technology

<sup>\*5</sup> Department of Physics, Tokyo University of Science

<sup>\*6</sup> Center of Nuclear Study

<sup>\*7</sup> Department of Physics, Saitama University

<sup>\*8</sup> Department of Physics, University of Tsukuba

<sup>\*9</sup> Department of Physics, Niigata University

<sup>\*10</sup> Western Michigan University

<sup>\*11</sup> Michigan State University

<sup>\*12</sup> Argonne National Laboratory

tion result by the GEANT.



Fig. 1. The setup of the Clovers at F7.

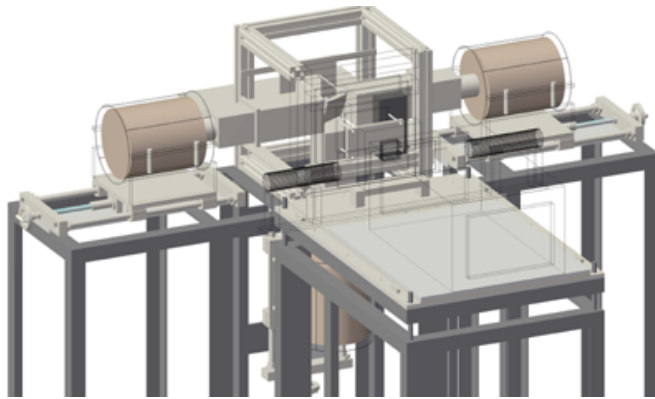


Fig. 2. Geometrical setup of the Clovers at F11.

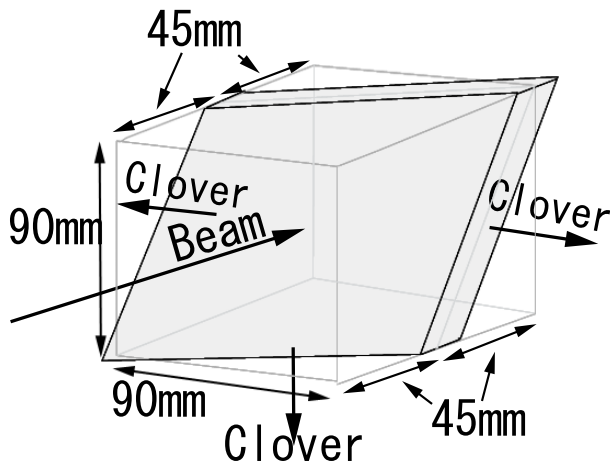


Fig. 3. The stopper shape. Cut under special direction to obtain complete symmetry for horizontal axis and z axis.

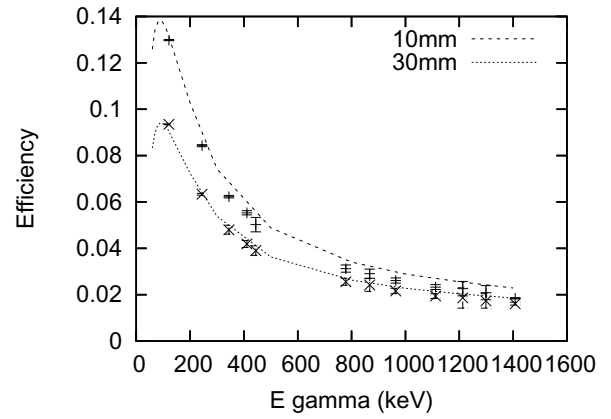


Fig. 4. The total photopeak efficiency curve of F11 three Clovers. The upper line for 10mm stopper and the lower line for 30mm stopper. The curved lines were the GEANT.

Table 1 shows the list of the known isomeric states which were observed in the latest experiment. Several indications of new isomeric states were also seen in that experiment. More precise analysis is now in development.

Table 1. The list of observed isomeric states in the experiment of the ZDS commissioning and the new isotope search in 2008 November.

Nucleus	$E_{\gamma}$ (keV)	Half Life(ns)
$^{54}\text{Sc}$	110	7000(5000)
$^{60}\text{V}$	99, 103	320(90)
$^{67}\text{Fe}$	367	43(30)
$^{76}\text{Ni}$	144, 354, 930, 992	590(180)
$^{78}\text{Zn}$	144, 730, 890, 908	319(9)
$^{92}\text{Br}$	97, 106, 155	—
$^{95}\text{Kr}$	84, 113	1400(20)
$^{96}\text{Rb}$	122, 240, 300	2000(100)
$^{98}\text{Sr}$	71, 144	25(2)
$^{100}\text{Sr}$	129, 288, 1202	85(—)
$^{117}\text{Ru}$	80, 101, 126, 184	—
$^{120}\text{Rh}$	98	—
$^{121}\text{Pd}$	134	—
$^{124}\text{Ag}$	75, 156, 304	—
$^{125}\text{Ag}$	714, 670	—
$^{127}\text{Cd}$	739, 771, 821, 909	—
$^{128}\text{Cd}$	237, 439, 537, 645, 783	—
$^{130}\text{Cd}$	128, 138, 539	220(30)
$^{129}\text{In}$	334, 359, 995, 1354	8500(500)
$^{130}\text{In}$	389	<6000
$^{129}\text{Sn}$	570, 1136, 1324	2400(200)
$^{130}\text{Sn}$	391	1600(150)
$^{131}\text{Sn}$	158, 173	300(20)
$^{132}\text{Sn}$	132, 300, 374, 4040	1980(50)
$^{134}\text{Sn}$	174, 347	80(15)
$^{136}\text{Sb}$	173	480(10)

#### References

- 1) T. Nakao et al.: RIKEN Accel. Prog. Rep. 41, 3 (2008)

# Measurement of double helicity asymmetry in direct photon production in $p + p$ at $\sqrt{s} = 200\text{GeV}$

R. Bennett,<sup>\*1</sup> and K. Okada,

The primary goal of the RHIC-PHENIX spin program is to measure the gluon spin component of the proton. The polarized  $p + p$  collider is the only way to access it in leading order interaction. Among many final states, the direct photon production is the simplest process and believed to be a golden channel. In contrast to the measurement of neutral pions,<sup>1)</sup> it is more sensitive to the sign of gluon polarization. The PHENIX detector<sup>2)</sup> has fine segmented electromagnetic calorimeters and is suitable for photon measurements. The direct photon cross section is measured and the NLO theoretical calculation describes the result.<sup>3)</sup>

In this report, double helicity asymmetry results are shown from the Run5 (2005,  $\int Ldt = 2.5\text{pb}^{-1}$ , pol=45%) and Run6 (2006,  $\int Ldt = 7.0\text{pb}^{-1}$ , pol=57%) data sets.

Because it is not possible to identify the direct photon on an event base, we calculate the asymmetry of the inclusive photons ( $A^{raw}$ ) and subtract the background asymmetry ( $A^{BG}$ ) using the following formula.

$$A^{sig} = \frac{A^{raw} - rA^{BG}}{1-r}, \quad \sigma_{A^{sig}} = \frac{\sqrt{\sigma_{A^{raw}}^2 + r^2\sigma_{A^{BG}}^2}}{1-r}.$$

To improve the purity (lower  $r$ ), a selection of events with small energy activities around the target photon (= isolation cut) is applied. The cut keeps more than 80% of direct photon events for the region of  $p_T$  higher than 7 GeV/c.<sup>3)</sup> The background asymmetry was estimated with  $\pi^0$  decay photons which pass the isolation cut in case the partner photon is missed. Fig.1 shows the double helicity asymmetries as a function of  $p_T$ . The curves are theoretically calculated based on the GRSV model.

Thanks to improvement in the figure of merit ( $\equiv LP^4$ ), the uncertainty is much reduced in Run6. The uncertainties do not change so much as a function of  $p_T$ , because the isolation cut is more effective in the high  $p_T$  region.

In leading order, the double helicity asymmetry ( $A_{LL}$ ) and the gluon polarization ( $\Delta G/G$ ) are connected by  $\Delta G/G = A_{LL}/A_1^p/\hat{a}_{LL}$ , where  $A_1^p$  is the proton spin asymmetry from polarized DIS experiments representing the quark polarization, and  $\hat{a}_{LL}$  is the helicity asymmetry in the partonic level. The kinematics are defined by the initial parton momentum and the angle of the outgoing photon.  $\Delta G/G$  is obtained by using a proper PDF set and requiring photons in the PHENIX acceptance. Fig. 2 shows the points from the Run5 and Run6 measurements and theoretical curves with different integrated gluon polarization

with a model at  $Q^2 = 10\text{GeV}^2$ .

In summary, we measured the double helicity spin asymmetry of direct photon production in  $p + p$  at  $\sqrt{s} = 200\text{ GeV}$ . The measurement from Run6 data is much improved over the previous Run5 result. According to the beam use request, we are going to accumulate  $25\text{pb}^{-1}$  with 70% polarization in a few years. With that data, the constraint on the gluon polarization in the proton will be improved significantly.

## References

- 1) S. S. Adler et al.: arXiv:0810.0694 (2008).
- 2) K. Adcox et al.: Nucl. Inst. Meth. A**499**, 469 (2003).
- 3) S. S. Adler et al.: Phys. Rev. Lett. **98**, 012002 (2007)

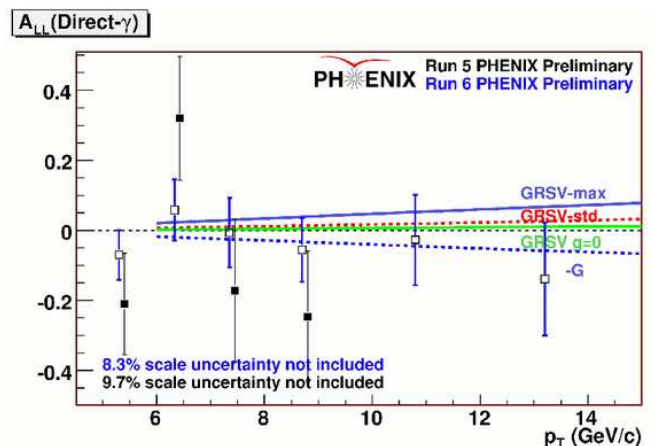


Fig. 1. Double helicity asymmetries of direct photon production. Curves are theoretical calculations.

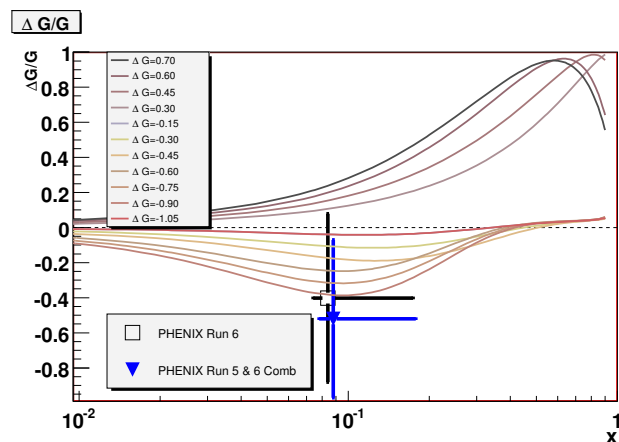


Fig. 2.  $\Delta G/G$  as a function of  $x_{Bj}$ . Theoretical curves correspond to different  $\Delta G$  values.

<sup>\*1</sup> SUNY, USA

# W-physics with Inclusive Muons in PHENIX: Detailed Feasibility Studies<sup>†</sup>

R. Seidl,<sup>\*1</sup> B. Meredith,<sup>\*2</sup> and M. Grosse-Perdekamp,<sup>\*2</sup>

[Spin physics, PHENIX, Parity violation]

W production will provide the first direct (flavor separated) measurement of the spin dependent quark and anti-quark-distributions for up- and down-quarks in the proton. The high energy scale set by the W-mass makes it possible to extract quark- and anti-quark polarizations from inclusive lepton spin asymmetries in W-production with minimal theoretical uncertainties<sup>1)</sup>. Real W production selects the quark flavors through their charge and it also selects only one helicity of nearly massless quarks due to the maximally parity violating weak interaction. Building the single spin asymmetry of count rates of Ws originating from protons with spin parallel and anti-parallel divided by their sum,  $A_L^W = \frac{1}{P} \times \frac{N^+(W) - N^-(W)}{N^+(W) + N^-(W)}$ , is then proportional to the helicity distribution  $\Delta q(x)$  as in

$$A_L^{W^+} = -\frac{\Delta u(x_1)\bar{d}(x_2) - \Delta\bar{d}(x_1)u(x_2)}{u(x_1)\bar{d}(x_2) + \bar{d}(x_1)u(x_2)}$$

and similarly for  $W^-$  by exchanging  $u$  and  $d$ .

The inclusive W measurement in PHENIX will be based on muons with  $P_T > 20$  GeV in the PHENIX forward arms<sup>2,3)</sup>. We have carried out detailed GEANT based Monte Carlo studies followed by full track reconstruction to evaluate the following backgrounds:

- punch through of high  $P_T$  hadrons through the magnet yoke upstream of the muon spectrometer and through the hadron absorber in the downstream muon identification system: these hadrons will be reconstructed with approximately correct high momentum.
- punch through of low  $P_T$ - hadrons through the magnet yoke and subsequent decay in the muon spectrometer magnet: these hadrons occasionally can be reconstructed incorrectly with high momentum.
- high momentum decay muons, and high  $P_T$  cosmic rays.

The simulations includes the full detector response with momentum smearing and realistic inefficiencies in reconstruction and acceptance. The momentum smearing is shown in Fig. 1 as function of the true generated transverse momentum. We have identified punch through hadrons that undergo decay as the dominant source of (false) high  $P_T$  background. Using optimized standard cuts that have been developed for single muon analysis in PHENIX we find a signal to background ratio of 1/3. Adding an additional hadron absorber of 30cm thickness improves the signal to background ratio to 3/1. Figure 2 shows the expected precision based on full detector simulation, smearing, 70%

polarization and 30cm of additional absorber as compared to current polarized parton parameterizations (see<sup>1)</sup> for an overview) as implemented in the RHIC-BOS<sup>4)</sup> generator. Additional studies are presently under way to develop a further optimized set of single muon cuts for  $P_T > 20$  GeV.

## References

- 1) G. Bunce et al: *Plans for the RHIC Spin Physics Program*, [http://spin.riken.bnl.gov/rsc/report/spinplan\\_2008/spinplan08.pdf](http://spin.riken.bnl.gov/rsc/report/spinplan_2008/spinplan08.pdf)
- 2) I. Nakagawa et al: *High Momentum Trigger Electronics Upgrade of PHENIX Muon Arms for Sea Quark Polarization Measurement at RHIC*, in this volume.
- 3) M. Grosse-Perdekamp, R. Seidl: *The PHENIX muon trigger RPC upgrade*, in this volume.
- 4) P. M. Nadolsky and C. P. Yuan, Nucl. Phys. **B666**, 31 (2003), hep-ph/0304002.

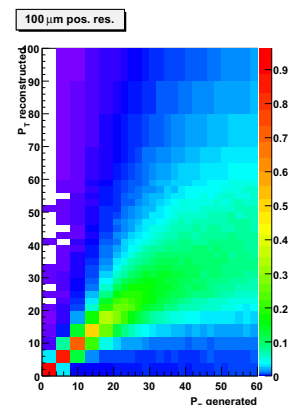


Fig. 1. Momentum smearing matrix for muons with nominal position resolution in the muon tracking system.

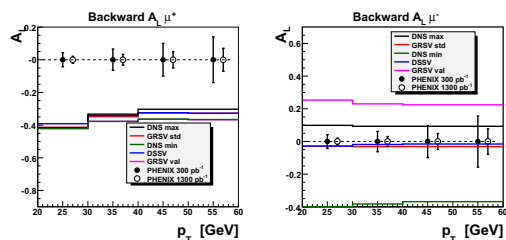


Fig. 2. Expected single spin asymmetries for inclusive leptons from W decays as a function of the reconstructed  $P_T$  at backward rapidities as described in the text.

<sup>\*1</sup> RIKEN BNL Research Center, USA

<sup>\*2</sup> University of Illinois at Urbana-Champaign, USA

# Measurement of Collins Asymmetry in $e^+e^-$ Annihilation at Belle.<sup>†</sup>

R. Seidl,<sup>\*1</sup> K. Hasuko,<sup>\*2</sup> M. Grosse Perdekamp,<sup>\*3</sup> and A. Ogawa,<sup>\*1,\*4</sup>

[Fragmentation, Transverse Spin, Collins Effect]

We have carried out the first measurement of spin dependent effects in the formation of hadrons from quarks that are transversely polarized. Spin effects were observed in the annihilation of electron-positron pairs into inclusive pairs of hadrons in Belle. Spin effects in quark fragmentation were first proposed by Collins<sup>1)</sup> in an attempt to describe the large spin asymmetries observed in proton-proton collisions with transverse polarization in the E704 experiment<sup>2)</sup>. Collins proposed that the asymmetries observed in E704 arise from struck quarks in hard scattering processes that have their spins aligned (or anti-aligned) with the transverse proton spin. Spin dependent effects in the fragmentation then would give rise to the left-right asymmetries observed in  $p+p \rightarrow \pi^+, \pi^0, \pi^-$  in E704. Collins predicted related spin asymmetries in deep inelastic scattering with leptons of transversely polarized targets. This effect was discovered by the HERMES collaboration at DESY<sup>3)</sup>. Boer, Jakob and Mulders first discussed azimuthal asymmetries from Collins fragmentation in hadron production in  $e^+e^-$  annihilation<sup>4)</sup>. A detailed description of the phenomenology of these asymmetries has been created by Boer<sup>5)</sup>. The present Belle experimental effort originates from a RBRC workshop on transverse spin asymmetries in 2000<sup>6)</sup>. At the workshop the plan was formulated to extract quark transversity distributions and Collins fragmentation functions from the global QCD analysis of spin asymmetries accessible in polarized semi-inclusive deep inelastic scattering, polarized proton-proton scattering and electron-positron annihilation.

We present here the final result of the Collins asymmetries observed at Belle. The measurement has been carried out on a data sample of  $\int L dt = 547 fb^{-1}$  of inclusive charged pion pairs:  $e^+e^- \rightarrow \pi + \pi + X$ . The analysis has been based on events with two-jet topology observing the azimuthal back-to-back correlation of two pions in opposite jet-hemispheres. The results for the Collins  $\cos(\phi_1 + \phi_2)$  coefficients,  $A_{12}$  observed in so-called hadron double ratios are shown in figure 1. For details refer to our results<sup>7)</sup> and<sup>8)</sup>.

The first combined analysis of Collins asymmetries from deep inelastic scattering and Belle has been recently carried out by Anselmino and collaborators<sup>9)</sup>. The resulting Collins fragmentation functions and quark transversity distributions are shown in figure 2.

It is found that quark transversity distributions in the proton are sizable and that there a significant spin effects in the fragmentation of transversely polarized quarks into pions.

## References

- 1) J. Collins: Nucl. Phys. Phys. B 396 (2003).
- 2) D. Adams et al.: Phys. Lett. B 264 (2001).
- 3) A. Airapetian et al.: Phys. Rev. Lett. 94:012002 (2005).
- 4) D. Boer, R. Jakob, P.J. Mulders: Nucl. Phys. B 504 (1997).
- 5) D. Boer: Nucl. Phys. B 806 (2009).
- 6) D. Boer and M. Grosse Perdekamp, Workshop on Future Transversity Measurements, (2000).
- 7) R. Seidl et al.: Phys. Rev. D 78:032011 (2008).
- 8) R. Seidl et al.: Phys. Rev. Lett. 96:232002 (2006).
- 9) M. Anselmino et al.: arXiv:0901.3078.

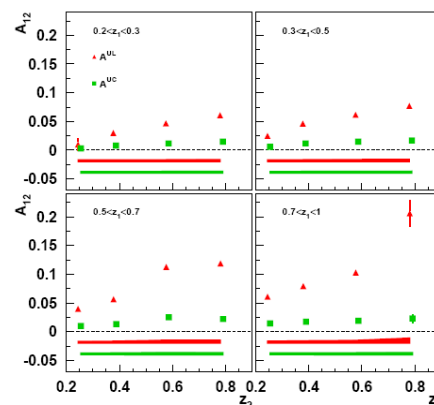


Fig. 1. Collins asymmetries observed in  $e^+e^- \rightarrow \pi\pi + X$  at Belle, see reference<sup>3)</sup>.

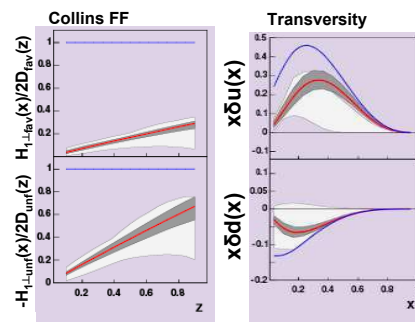


Fig. 2. Collins fragmentation function extracted from semi-inclusive deep inelastic scattering data and  $e^+e^- \rightarrow \pi\pi + X$  at Belle, see reference<sup>4)</sup>.

<sup>\*1</sup> Riken BNL Research Center, Upton, USA.

<sup>\*2</sup> Riken, Wako, Japan.

<sup>\*3</sup> University of Illinois, Urbana Champaign, USA.

<sup>\*4</sup> Brookhaven National Laboratory, Upton, USA.

# Precision Measurements of Hadron Multiplicities in $e^+e^-$ Annihilation at BELLE<sup>†</sup>

M. Leitgab,<sup>\*1</sup> K. Boyle,<sup>\*2</sup> M. Grosse Perdekamp,<sup>\*1</sup> R. Seidl,<sup>\*2</sup> A. Ogawa,<sup>\*3</sup> A. Vossen<sup>\*1</sup> and P. Francisconi<sup>\*1</sup>

[Precision hadron multiplicities, fragmentation functions, BELLE]

## 1 Measurement Description

This paper summarizes the status of precision measurements of  $\pi^{+,-}$ ,  $K^{+,-}$ ,  $\pi^0$  and  $\eta$  multiplicities in  $e^+e^-$  annihilation at a center of mass energy of 10.52 GeV at the BELLE experiment at KEK, Japan<sup>1)</sup>. The hadron multiplicities are measured as a function of  $z$  which is the hadron energy relative to half of the center-of-mass energy in electron-positron annihilation into quark-antiquark pairs. The measured multiplicity distributions are corrected for particle misidentification and acceptance effects.

## 2 Motivation

Multiplicity measurements at Belle are motivated by two recent studies describing the extraction of unpolarized fragmentation functions<sup>2),3)</sup>. Fragmentation functions describe hadron production from a final-state quark or gluon in processes such as hadron collisions, electron-positron annihilation and deep inelastic scattering of leptons on protons or nuclei. The present measurements are intended to provide high precision datasets as an input to the extraction of fragmentation functions, and thereby significantly lower the uncertainties of the extracted fragmentation functions. Precise knowledge of fragmentation functions is required for the extraction of the gluon helicity distribution from spin asymmetries measured in hadron collisions at the Relativistic Heavy Ion Collider (RHIC)<sup>4)</sup>.

## 3 Measurement Status and Outlook

For charged hadrons, experimental particle yields need to be corrected for particle misidentification. A detailed study to determine particle identification (PID) probabilities for  $e^{+,-}$ ,  $\mu^{+,-}$ ,  $\pi^{+,-}$ ,  $K^{+,-}$  and  $p, \bar{p}$  has been carried out. A linear model has been developed for the correction of measured yields for particle misidentification. This correction changes significantly the measured charged particle distributions at the order of 5 to 10% for pions and 10 to 35% for kaons. The yields of neutral hadrons  $\pi^0$  and  $\eta$  are measured via the two photon decay process.

Hadron multiplicities are presently extracted for

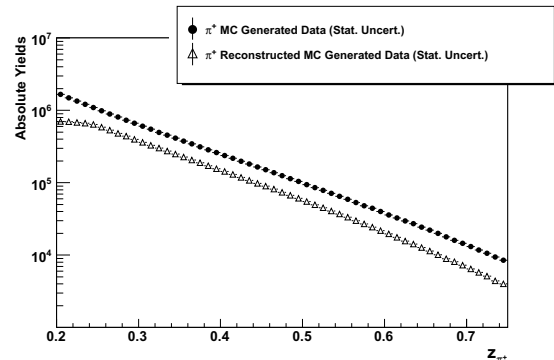


Fig. 1. Yields of  $\pi^+$  from Monte Carlo against the normalized hadron energy  $z_{\pi^+}$ . Closed circles show yields generated with PYTHIA. Open triangles indicate yields after detector response simulation and reconstruction. The difference between the plots shows the magnitude of the PID and acceptance correction.

normalized hadron energies  $z$  within  $0.2 < z < 0.75$  and a bin width of  $\Delta z = 0.01$ . Fig. 1 shows  $\pi^+$  yields against the normalized hadron energy  $z$ . Shown are the yields generated with the Monte Carlo event generator PYTHIA<sup>5)</sup> and the yields after a GEANT-based<sup>6)</sup> detector response simulation and reconstruction. Eventually, the measurement will be extended to higher values of  $z$  and the systematic uncertainty analysis for PID, momentum smearing and acceptance effects will be finalized. The leading uncertainty is expected to arise from the systematic uncertainties connected with the PID correction. The overall systematic uncertainties are expected to remain below 3% (5%) for  $\pi$  ( $K$ ) spectra at low to mid  $z < 0.6$ , and to increase with  $z$  up to 5% (17%) for  $\pi$  ( $K$ ) spectra, respectively.

## References

- 1) A. Abashian *et al.*; Nucl. Instrum. Methods **A** 479, (2002), pp. 117-232.
- 2) M. Hirai, S. Kumano, T.-H. Nagai, K. Sudoh; Phys. Rev. D 75, 114010 (2007).
- 3) D. de Florian, R. Sassot, M. Stratmann; Phys. Rev. D 75, 094009 (2007).
- 4) A. Adare *et al.*; Phys. Rev. D 76, 051106 (2007).
- 5) T. Sjöstrand *et al.*; Computer Phys. Commun. 135 (2001) 238.
- 6) Geant 4 Collaboration; Nucl. Instrum. Methods **A** 506, (2003), pp. 250-303.

<sup>\*1</sup> University of Illinois at Urbana-Champaign (UIUC), USA

<sup>\*2</sup> RIKEN BNL Research Center (RBRC), USA

<sup>\*3</sup> RIKEN BNL Research Center (RBRC)/ Brookhaven National Laboratory (BNL), USA

# Measurement of Interference Fragmentation Functions at Belle<sup>†</sup>

A. Vossen,<sup>\*1</sup> R. Seidl,<sup>\*2</sup> M. Grosse Perdekamp,<sup>\*1</sup> K. Boyle,<sup>\*2</sup> M. Leitgab,<sup>\*1</sup> P. Francisconi,<sup>\*1</sup> and A. Ogawa<sup>\*2,\*3</sup>

[Nucleon structure, Fragmentation, Interference fragmentation function, Transversity]

Measurements of azimuthal asymmetries in hadron pair correlations at Belle allow access to the chiral odd dihadron interference fragmentation function (IFF). The IFF describes the production of a hadron pair from a transversely polarized quark. The transverse spin of the fragmenting quark leads to an anisotropy in the azimuthal distribution of the final state hadron pair. This makes it possible to use IFF-processes as quark polarimeter. That makes it very important for the measurement of the so-called transversity distribution function which describes the transverse spin structure of the nucleon. Interference Fragmentation therefore offers an alternative way to access quark transversity distributions in hard scattering processes off transversely polarized nucleon targets<sup>1)</sup>. Recently, the single hadron Collins fragmentation process has been used for a first determination of quark transversity distributions and Collins fragmentation asymmetries have been measured in Belle<sup>2)</sup>. In comparison to Collins fragmentation, the IFF exhibits some favorable features that are unique to the fragmentation into two hadrons. Because the second hadron provides an additional degree of freedom, the asymmetry survives an integration over transverse momenta. This allows for collinear factorization, model independence and easier evolution of the results to center of mass energies of complementary fixed target experiments.

At Belle unpolarized electrons and positrons annihilate at a center of mass energy of 10.58 GeV for measurements on the  $\Upsilon(4S)$  resonance and 10.52 GeV for measurements of the continuum background. The produced quark - antiquark pairs will have antiparallel spin configurations with a transverse component proportional to  $\sin^2 \theta$ , where  $\theta$  is the angle between quark and electron axis in the center of mass system. The measurement is carried out in a sample with back to back di-jet geometry using a thrust selection of  $T > 0.8$ . The measurement consists of observing hadron pairs simultaneously in both jet-hemispheres and correlating the angular distribution of the hadron planes on both sides: If  $\mathbf{R}_j = \mathbf{P}_{h1}^j - \mathbf{P}_{h2}^j$ , with  $\mathbf{P}_{hi}^j$  the momentum vectors of the hadrons in hemisphere  $j \in \{1, 2\}$ , then the count rate is dependent on the azimuthal angle  $\phi_j$  between  $\mathbf{R}_j$  and the spin vector around the momentum of the fragmenting quark approximated by the thrust axis. The electron and positron beams in KEKB are unpolarized and therefore the  $\phi_j$  dependence of the hadron planes would

average out in an inclusive single hemisphere measurement. However, the correlation between  $\mathbf{R}_1$  and  $\mathbf{R}_2$  remains and leads to a dependence of the count rates on the angle  $\phi_1 + \phi_2$ . Figure 1 shows the projected sensitivities for charged pion pairs using the data collected off-resonance. The precision allows for significant asymmetries according to various model predictions<sup>3)4)5)</sup>. Furthermore on-resonance data, a factor 10 more abundant than the off-resonance data, will be used for this analysis. The anticipated Belle IFF results will improve the understanding of spin dependence in hadron formation and provide an important tool for the study of transverse nucleon spin structure.

## References

- 1) J. C. Collins, S.F. Heppelmann and G.A. Ladinsky: Nucl. Phys. B **420** (1994) 565.
- 2) R. Seidl et. al. [Belle Collaboration]: Phys. Rev. **D78** 032011 (2008) 0805.2975
- 3) R.L. Jaffe, X. M. Jin and J.A. Tang: Phys. Rev. **D57** (1998) 5920.
- 4) M. Radici, R. Jakob and A. Bianconi: Phys. Rev. **D65** (2002) 074031.
- 5) A. Bacchetta et. al.: JLAB-THY-08-917

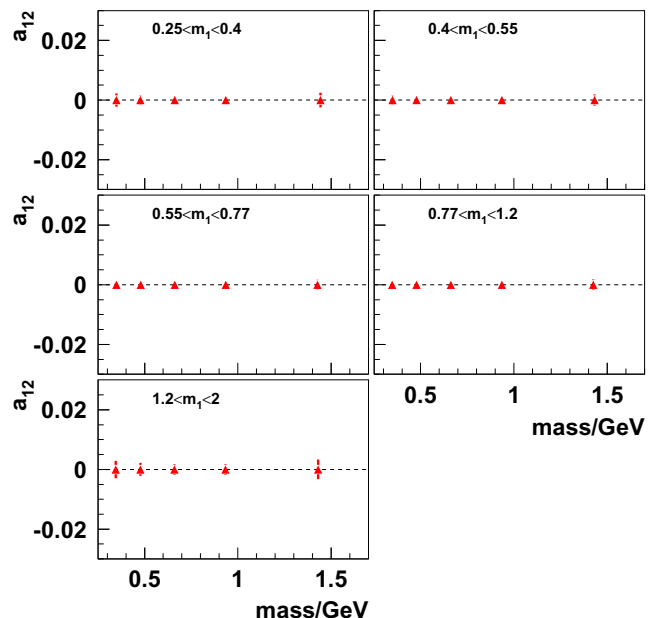


Fig. 1. Sensitivity projections for Belle measurements of charged pion IFF measurements using  $55 \text{ fb}^{-1}$ . The correlation asymmetries are shown as function of the pion pair invariant mass.

<sup>\*1</sup> University of Illinois at Urbana Champaign

<sup>\*2</sup> Riken BNL Research Center

<sup>\*3</sup> Brookhaven National Laboratory

# Double Helicity Asymmetry of Inclusive Charged Hadrons in $pp$ Collisions at $\sqrt{s} = 62.4$ GeV at PHENIX

D. Kawal,<sup>\*1,\*2</sup> and A. Datta<sup>\*2</sup>

[Double Helicity, Asymmetry, Longitudinal Polarization]

## Introduction

In 2006, the PHENIX collaboration at the Relativistic Heavy Ion Collider (RHIC) recorded  $\approx 50 \text{ nb}^{-1}$  of longitudinally polarized  $pp$  collisions at  $\sqrt{s}=62.4$  GeV/c. We have analyzed these data to extract the double longitudinal spin asymmetry,  $A_{LL}(pp \rightarrow h^\pm X)$  for unidentified, inclusive charged hadrons  $h^\pm$  at mid-rapidity,  $|\eta| < 0.35$ , with  $p_T$  from 0.5 to 4.5 GeV/c. The production of hadrons with  $p_T > 1$  GeV/c is dominated by quark-gluon scattering, and so is sensitive to the polarized gluon distribution,  $\Delta g(x)$ , for momentum fraction  $x \approx 0.05 - 0.2^1$ .

## Event Selection and Systematic Checks

We analyzed  $pp$  collisions selected with the minimum bias trigger for charged tracks in the PHENIX drift chamber (DC)<sup>2</sup>. These track were extrapolated to the outer pad chamber, PC3<sup>2</sup>, where we required closely matching hits. Fiducial cuts were applied, as were corrections for offsets of the beam and DC affecting the extraction of the particle  $p_T$  from the DC track angle.

Several backgrounds were present in this set of events. Electrons/positrons from  $\gamma$  conversion, ( $\gamma$  from  $\pi^0$  or  $\eta$  decay) were rejected by placing a veto on the PHENIX Ring Imaging Cherenkov<sup>2</sup>), which detects  $e^\pm$  above 20 MeV, and  $\pi^\pm$  above 4.7 GeV. Particles originating from long-lived particles ( $\pi^\pm$ ,  $K^\pm$ ,  $K_L^0$ ) decaying far ( $> 20$  cm) from the primary vertex, typically don't pass the tight DC-PC3 matching cuts. Short lived-particles ( $K_s^0$ ,  $\Lambda$ ,  $\Sigma$ ,  $\Xi$ , ...) decaying close to the vertex, yield particles that pass the cuts, and comprise  $\approx 7\%$  of the sample.

Each resulting double spin asymmetry was checked for errors by constructing the single spin, parity-violating asymmetry  $A_L$  (which was consistent with zero), randomizing the bunch polarizations, and by checking for the consistency of  $A_{LL}$  extracted separately from each detector arm, and from different fills.

## Results and Predictions From Theory

Preliminary results are shown in Fig. 1 with next-to-leading order perturbative QCD calculations based on different polarized gluon distributions<sup>3</sup>).

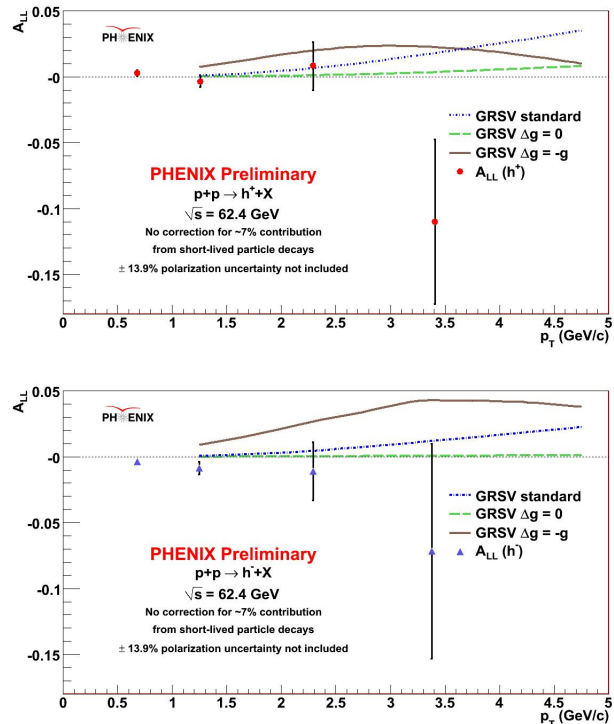


Fig. 1. GRSV predictions and preliminary results for  $A_{LL}(pp \rightarrow h^+ X)$  (upper) and  $A_{LL}(pp \rightarrow h^- X)$  (lower).

## Discussion

The statistical precision of the results is impressive, well below  $10^{-2}$  in the first two  $p_T$  bins. The results can be used to exclude the GRSV models,  $\Delta g(x) = -g(x)$  and  $\Delta g(x) = g(x)$  (which has  $A_{LL} > 0.1$  at  $p_T$  of 4 GeV/c, too big to show on the plot).

It is interesting to note that when  $qg$  scattering dominates, we expect  $A_{LL}^\pi \propto \Delta g(\Delta u D_u^\pi + \Delta d D_d^\pi)$ . Then, since  $\Delta d$  is large and negative,  $\Delta u$  is large and positive,  $D_u^{\pi^+} > D_d^{\pi^+}$ , and  $D_u^{\pi^-} < D_d^{\pi^-}$ , if  $\Delta g(x) > 0$  we'd expect  $A_{LL}^{\pi^+} > A_{LL}^{\pi^0} > A_{LL}^{\pi^-}$ . We can't discern such an ordering from this data, which is consistent with  $\Delta g$  being small and/or  $\Delta g(x)$  having a node.

## References

- 1) D. de Florian, W. Vogelsang and F. Wagner, Phys. Rev. D **76**, 094021 (2007).
- 2) K. Adcox et al. (PHENIX Collaboration), Nucl. Instr. and Meth. A **499**, 469-602 (2003).
- 3) M. Glück, E. Reya, M. Stratmann, and W. Vogelsang, Phys. Rev. D **63**, 094005 (2001).

<sup>\*1</sup> RIKEN-BNL Research Center, Brookhaven National Laboratory, Upton, NY, USA

<sup>\*2</sup> Department of Physics, University of Massachusetts, Amherst, MA, USA

# PHENIX local polarimeter analysis in polarized proton-proton collisions at $\sqrt{s} = 200\text{GeV}$ from RHIC Run-8

S. Dairaku\*<sup>1</sup> for the PHENIX Collaboration

[Spin, asymmetry]

In RHIC Run-8 proton-proton collisions, we were focused on transverse-spin physics, and thus collected data on transversely polarized proton-proton collisions. A local polarimeter was used to evaluate whether proton beams were transversely polarized in RHIC Run-8.

A local polarimeter was also used in previous RHIC Runs. One of the main goals of the PHENIX experiment is to determine the polarized gluon distribution function in a proton.<sup>1)</sup> To achieve this objective, we have used longitudinally polarized proton-proton collisions. We determine the polarized gluon distribution function by measuring double longitudinal-spin asymmetries during the production of various particles. In RHIC rings, proton beams are vertically polarized. Therefore, we need to change the direction of the beam polarization from the vertical direction to the longitudinal direction using spin rotator magnets. A local polarimeter is also used for evaluating how correctly the proton beams are longitudinally polarized when the spin rotator is on.

When the proton beams are vertically polarized, the local polarimeter can measure the significant single transverse-spin asymmetry ( $A_N$ ) for forward neutron production,<sup>2)</sup> which is calculated by

$$A_N \equiv \frac{\sigma_{\uparrow} - \sigma_{\downarrow}}{\sigma_{\uparrow} + \sigma_{\downarrow}} = \frac{1}{P} \frac{\sqrt{N_L^{\uparrow} N_R^{\downarrow}} - \sqrt{N_L^{\downarrow} N_R^{\uparrow}}}{\sqrt{N_L^{\uparrow} N_R^{\downarrow}} + \sqrt{N_L^{\downarrow} N_R^{\uparrow}}}, \quad (1)$$

where  $P$  is the absolute polarization value measured by the RHIC polarimeters, and  $N_{L(R)}^{\uparrow(\downarrow)}$  is the number of neutrons scattered to the left (right) when the direction of the beam polarization is vertically upwards (downwards). We identify forward neutrons using a zero degree calorimeter (ZDC) and measure the scattering direction of the neutrons with a shower maximum detector (SMD) by detecting the shower shape in the ZDC (see figure 1).

Figure 2 shows the azimuthal angle  $\phi$  dependence of the asymmetry  $A_N$  for forward neutron production for two RHIC rings (the so-called blue ring and yellow ring, respectively) from RHIC-Run8 data. We can see the clear sinusoidal shape and confirm that the proton beams are transversely polarized.

Figure 3 shows the asymmetry  $A_N$  for two RHIC rings versus a fill number which is defined as the period of time encompassing injection, acceleration, and stor-

age of beam in RHIC rings. It shows that the asymmetry  $A_N$  did not undergo a lot of changes from fill to fill and the transverse polarization of the proton beam was stable.

## References

- 1) G. Bunce et al.: Ann. Rev. Nucl. Part. Sci. **50**, 525 (2000).
- 2) Y. Fukao and M. Togawa et al.: Phys. Rev. B **650**, 325 (2007).

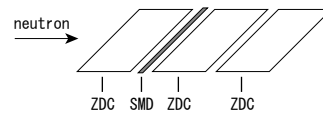


Fig. 1. Schematic layout of the ZDC and the SMD.

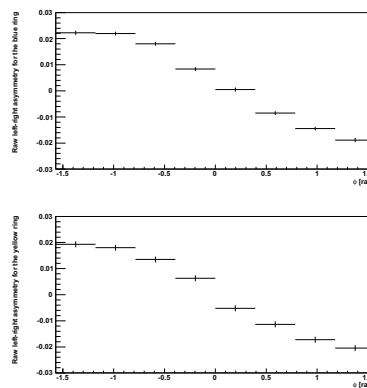


Fig. 2. Azimuthal angle  $\phi$  dependence of the asymmetry for forward neutron production for the blue ring in RHIC Run-8.

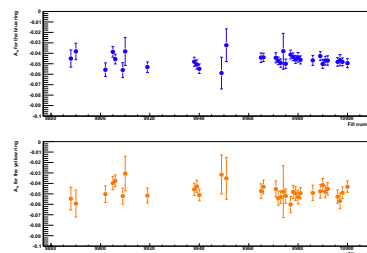


Fig. 3. Asymmetry for forward neutron production for each ring versus a fill number in RHIC Run-8.

\*<sup>1</sup> Department of Physics, Kyoto University, Japan

## **2. Nuclear Physics(Theory)**

# Covalent isomeric state in $^{12}\text{Be}$ induced by two-neutron transfers<sup>†</sup>

M. Ito,<sup>\*1</sup> and N. Itagaki,<sup>\*2</sup>

[Transfer reaction, molecular resonance, unstable nuclei]

The experimental techniques producing the slow RI beam are now under development in many facilities, and the scattering of a neutrons' drip-line nuclei,  $^8\text{He}$ , by an  $\alpha$  target has just been measured at GANIL<sup>1)</sup>. Since  $^8\text{He}$  has the  $\alpha+4N$  structure with four weakly bound neutrons and an  $\alpha$  cluster, during the collision, the valence four neutrons can easily be exchanged between two  $\alpha$ -particles. Therefore, the  $\alpha+^8\text{He}$  colliding system is the candidate manifesting an isomeric resonance excited by the neutron transfer coupling, and we investigated the resonance structures appearing in the excitation function of the  $\alpha+^8\text{He}$  scattering.

In order to investigate the  $\alpha+^8\text{He}_{g.s.}$  scattering, the reaction process should be treated consistently with the low-lying bound states of the compound system of  $^{12}\text{Be}$ , because the resonances correspond to excited states, which are embedded in the continuum above the particle decay threshold. In  $^{12}\text{Be}$ , the molecular orbitals (MO) model can successfully describe the low-lying states<sup>2)</sup>. In the present study, therefore, the MO configurations and the scattering process must be treated in a unified manner. For this purpose, we apply the generalized two-center cluster model (GTCM)<sup>3,4)</sup>, which can cover the low-lying MO configurations<sup>2)</sup> as well as the scattering states among the ionic ones, the  $X\text{He}+Y\text{He}$  ( $X, Y=4\sim 8$ ); hence, treating of resonant phenomena in slow scattering is possible.

In GTCM, the total wave function is given by

$$\Psi^{J^\pi(+)} = \sum_{\beta} \chi_{\beta}^{(+)} + \sum_{\nu} b_{\nu} \hat{\Psi}_{\nu}^{J^\pi} . \quad (1)$$

The first term stands for the ‘‘open channels’’ labeled by  $\beta$ , on which the scattering boundary condition is explicitly imposed<sup>3,4)</sup>. Here,  $\chi_{\beta}^{(+)}$  denotes the wave functions of two scattering nuclei. We consider three rearrangement channels,  $\alpha+^8\text{He}_{g.s.}$ ,  $^6\text{He}_{g.s.}+^6\text{He}_{g.s.}$  and  $^5\text{He}_{g.s.}+^7\text{He}_{g.s.}$  as open channels. The second term stands for the ‘‘intrinsic states’’, and the  $\hat{\Psi}_{\nu}^{J^\pi}$  labeled by an eigenvalue number  $\nu$ , is calculated by diagonalizing the total Hamiltonian with basis functions of the atomic orbitals (AOs).

The scattering matrices (S matrices) for the central collision of  $\alpha+^8\text{He}$  ( $J^\pi=0^+$ ) are shown in Fig. 1. In the S matrices calculated from the open channels (dotted curves), there are not any resonant peaks, but we can clearly confirm the formation of the sharp resonant

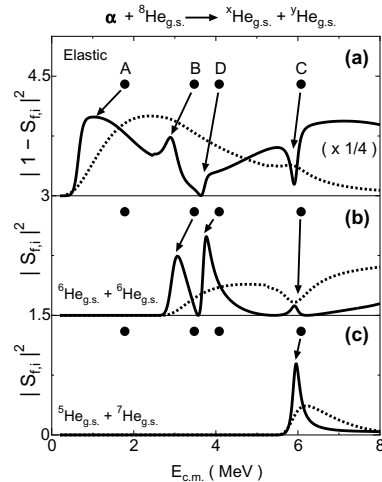


Fig. 1. S matrices for  $\alpha+^8\text{He}_{g.s.}$  ( $J^\pi=0^+$ ). See text for details.

peaks in the full solution (solid curves), in which the intrinsic states (solid circles) are coupled.

The resonances A~C have the ionic configuration of  $X\text{He}_{g.s.}+Y\text{He}_{g.s.}$ , while D has a characteristic structure, which is called the covalent SD state. In this configuration, two neutrons occupy the  $0p$ -wave AO, which is perpendicular to the  $\alpha-\alpha$  axis around each  $\alpha$ -cluster, like  $^5\text{He}+^5\text{He}$ , while the remaining two neutrons form the  $(\sigma^+)^2$  bonding. Due to the formation of the  $\sigma^+$ -bonding, the  $\alpha-\alpha$  distance is increased, and it corresponds approximately to hyperdeformation. The present calculation predicts the strong decays of the covalent SD state into  $^6\text{He}_{g.s.}+^6\text{He}_{g.s.}$ , which are supported by recent observation.<sup>5)</sup>

It is very interesting to compare the present results with the latest experiment at GANIL<sup>1)</sup>. This is the first study pointing out the formation of a covalent isomeric-state via a neutron-transfer reaction, which shall be generally observed in light neutron-rich nuclei and systematic studies are continually proceeding.

## References

- 1) M. Freer, N. Orr and A. W. Ashwood, Private communication (2008).
- 2) N. Itagaki and S. Okabe, Phys. Rev. C **61**, 044306 (2000), and references therein.
- 3) M. Ito, K. Kato and K. Ikeda, Phys. Lett. B **588**, 43 (2004); Makoto Ito, Phys. Lett. B **636**, 293 (2006); *ibid*, Mod. Phys. Lett. A **21**, 2429 (2006).
- 4) M. Ito, N. Itagaki, H. Sakurai, and K. Ikeda, Phys. Rev. Lett. **100**, 182502 (2008).
- 5) A. Saito, Private communication (2008).

<sup>†</sup> Condensed from the article in Phys. Rev. C **78**, 011602(R) (2008), Phys. Rev. Focus, Vol. 22, Story 4 (2008).

<sup>\*1</sup> Permanent address: Department of Pure and Applied Physics, Kansai University

<sup>\*2</sup> Department of Physics, University of Tokyo

# Isoscalar monopole transitions in $^{10,12}\text{Be}$

M. Ito,\*<sup>1</sup>

[Nuclear Structure, cluster model, unstable nuclei]

Recent studies strongly suggest that cluster structures can explain the strength of monopole transitions (MTR), in the energy region of  $E \leq 10$  MeV, which are observed as a discrete strength in the excitation energy. In fact, the enhancements of MTR are confirmed in the nuclear excitations of  $^{11}\text{B}^{(1)}$  and  $^{13}\text{C}^{(2)}$  by an  $\alpha$  target. In addition, a theoretical study clearly demonstrated that the cluster configurations in both the initial and final states strongly enhanced the MTR matrix elements in the  $N=Z$  systems, such as  $^{12}\text{C}$  and  $^{16}\text{O}$ .<sup>(3)</sup> Therefore, the MTR below  $E \sim 10$  MeV can be considered the guideline of the development of cluster structures, because naive shell models can never describe the enhanced MTR around this energy region.

On the contrary, in light neutron-excess systems, various molecular structures are discussed from the viewpoint of clustering phenomena, and hence investigations of MTR are quite important in the study of neutron-excess nuclei. In particular, strong MTRs are observed in a wide energy range of  $^{12}\text{Be}$ . In the transition to the low-lying  $0_2^+$  ( $E_x \sim 2.2$  MeV), an electric MTR is measured through the  $e^+e^-$  decays,<sup>(4)</sup> while in the continuum energy region above the  $\alpha$ -decay threshold, strong enhancements of MTRs are observed as discrete resonances, which finally decay into  $^6\text{He}_{g.s.} + ^6\text{He}_{g.s.}$  and  $\alpha + ^8\text{He}_{g.s.}$ .<sup>(5)</sup> In this report, we examine the nuclear structures of  $^{12}\text{Be} = \alpha + \alpha + 4N$  and discuss the enhancement of the monopole transition in connection to the intrinsic structures. We applied the generalized two-center cluster model in which the molecular orbital (MO) configurations and the atomic (ionic) ones with  $^x\text{He} + ^y\text{He}$  could be described in a unified manner.<sup>(6)</sup>

First, we calculated the energy spectra (left part in Fig. 1) and investigated the wave functions in individual levels to identify their intrinsic character. The MO configuration of  $(\pi_{3/2}^-)^2(\sigma_{1/2}^+)^2$  becomes the ground ( $0_1^+$ ) state, and the five levels are obtained as the excited states. We found that all the excited states can be characterized in terms of the excitation degree of freedoms. For instance, the  $0_2^+$  state has  $(\pi_{3/2}^-)^2(\pi_{1/2}^-)^2$ , and it corresponds to the two particle excitation mode from  $0_1^+$  with  $(\pi_{3/2}^-)^2(\sigma_{1/2}^+)^2$ . Furthermore, the  $0_3^+$  state corresponds to the cluster excitation mode from the  $0_1^+$  state, in which the relative motion between two  $\alpha$ -clusters is strongly excited.

Secondly, we calculated the matrix elements of isoscalar MTR,  $|\langle 0_f^+ | \sum_i^{12} r_i^2 | 0_1^+ \rangle|^2$ , and the result

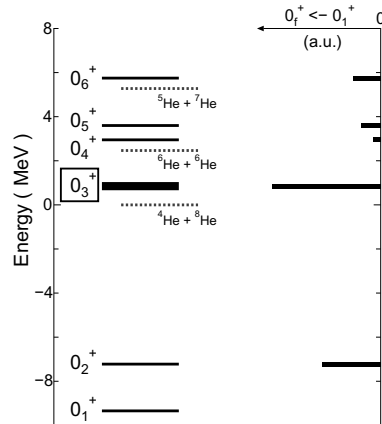


Fig. 1. Energy spectra (left) and monopole strength (right) in  $^{12}\text{Be}$  ( $J^\pi=0^+$ ). Dotted lines represent the threshold energy of the  $^x\text{He} + ^y\text{He}$  channels.

is shown at right in Fig. 1. As can be clearly confirmed in the figure, MTR to  $0_3^+$  is the largest of all the excited states, although an enhancement also occurs in the transition to  $0_2^+$ , which is consistent with the observed electric MTR.<sup>(4)</sup> Therefore, this result strongly suggests that the monopole transition is enhanced when the final state corresponds to the cluster excitation mode from the ground state.

We have also calculated the continuum discretized coupled-channels (CDCC) for the monopole breakup of  $^{10}\text{Be}$  into  $\alpha + ^6\text{He}$  by a  $^{12}\text{C}$  target.<sup>(7)</sup> This breakup reaction is mainly induced by a nuclear interaction from the target, and the multi-step of the continuum-continuum coupling is quite strong. We confirmed strong enhancement in the transition of  $0_1^+ \rightarrow 0_3^+$ . The final state corresponds to the cluster excitation mode from the  $0_1^+$  state. Therefore, the cluster excitation mode is strongly excited in the nuclear breakup reaction, which is consistent with the result in the analysis of MTR for  $^{12}\text{Be}$ .

## References

- 1) T. Kawabata et al.: Phys. Lett. B **646**, 6 (2007).
- 2) Y. Sasamoto et al.: Mod. Phys. Lett. A **31**, 2393 (2006).
- 3) T. Yamada et al.: Prog. Theor. Phys. **120**, 1139 (2008).
- 4) S. Shimoura et al.: Phys. Lett. B **654**, 87 (2007).
- 5) A. Saito et al.: AIP Conf. Proc. **891**, p.205 (2006).
- 6) M. Ito, N. Itagaki, H. Sakurai, K. Ikeda, Phys. Rev. Lett. **100**, 182502 (2008); M. Ito and N. Itagaki, Phys. Rev. C **78**, 011602(R) (2008), and references therein.
- 7) Makoto Ito, Mod. Phys. Lett. A **21**, 2429 (2006); *ibid*, Phys. Lett. B **636**, 293 (2006).

\*<sup>1</sup> Permanent address: Department of Pure and Applied Physics, Kansai University

# A smoothing method of discrete breakup $S$ -matrix elements in the theory of continuum-discretized coupled channels<sup>†</sup>

T. Matsumoto, T. Egami,<sup>\*1</sup> K. Ogata,<sup>\*1</sup> and M. Yahiro<sup>\*1</sup>

[Nuclear reaction, unstable nuclei]

The study on neutron-rich nuclei has become one of the central subjects in nuclear physics. Breakup reactions have played key roles in investigating such unstable nuclei. One of the most reliable methods for treating the breakup processes is the method of continuum-discretized coupled channels (CDCC)<sup>1</sup>. In CDCC, breakup continuum states of a projectile are described by a finite number of discretized states, which form a complete set within a finite model space. Consequently, the  $S$ -matrix elements calculated with CDCC,  $\hat{S}_i$ , are discrete in continuum, although the exact ones are continuous. Thus, one needs a way of smoothing  $\hat{S}_i$  in order to analyze real breakup processes.

In principle, this is possible by calculating the overlap functions between the exact continuum states and the discretized states. The overlap function called the smoothing factor can be easily calculated in three-body breakup reactions of two-body projectiles, but it is quite hard in four-body ones of three-body projectiles. Very recently, we have proposed a smoothing method applicable to four-body breakup reactions<sup>2</sup>), but it still requires heavy numerical calculations.

In this work, we present a simple formula that makes it possible to smooth  $\hat{S}_i$  accurately by using the complex scaling method<sup>3</sup>), which is a powerful tool for solving many body resonance and weakly bound states<sup>4</sup>). In the formula, the smoothing factor between the discretized state  $\hat{\phi}_i$  and the continuum one  $\psi$  with a positive energy  $\epsilon$  is calculated by

$$\begin{aligned} \langle \hat{\phi}_i | \psi \rangle &\approx \langle \hat{\phi}_i | \varphi_0 \rangle \\ &+ \sum_{jk} \langle \hat{\phi}_i | C^{-1}(\theta) | \phi_j^\theta \rangle \frac{1}{\epsilon - \epsilon_j^\theta} \langle \tilde{\phi}_j^\theta | V^\theta | \phi_k^\theta \rangle \langle \tilde{\phi}_k^\theta | C(\theta) | \varphi_0 \rangle, \end{aligned}$$

where  $C(\theta)$  and  $\varphi_0$  are the scaling transformation operator and the plane wave of constituent particles in the projectile, respectively. The complex scaled states  $\phi_i^\theta$  are obtained by diagonalizing the complex-scaled internal Hamiltonian  $H^\theta$  of the projectile with the  $L^2$ -type functions:  $\langle \tilde{\phi}_j^\theta | H^\theta | \phi_{j'}^\theta \rangle = \epsilon_j^\theta \delta_{jj'}$ , where  $\tilde{\phi}_j^\theta$  is a biorthogonal function of  $\phi_j^\theta$ . When the Gaussian basis functions are taken in the calculations of  $\hat{\phi}_i$  and  $\phi_j^\theta$ , the matrix elements  $\langle \hat{\phi}_i | C^{-1}(\theta) | \phi_j^\theta \rangle$  and  $\langle \tilde{\phi}_k^\theta | C(\theta) | \varphi_0 \rangle$  are analytically obtained. The matrix elements  $\langle \tilde{\phi}_j^\theta | V^\theta | \phi_k^\theta \rangle$  are also easily obtained by making a single integral. Thus, this formula is quite useful and applicable not only to three-body but also four-body breakup reactions.

Validity of the formula is tested for two kinds of three-body breakup reactions,  $^{58}\text{Ni}(d, np)$  at 80 MeV and  $^{12}\text{C}(^6\text{He}, ^2n^4\text{He})$  at 229.8 MeV. In the latter,  $^6\text{He}$  should be treated as the three-body  $n+n+^4\text{He}$  system. However, since our interest is the  $2^+$  resonance in the present test, we use the dineutron ( $^2n+^4\text{He}$ ) model that can describe the  $2^+$  resonance reasonably well.

Figure 1 shows the squared moduli of breakup  $S$ -matrix elements,  $S(k)$ , as a function of the relative momentum  $k$  between two constituent particles of the projectile. Here  $S(k)$  is defined as  $S(k) = \sum_i \langle \psi(k) | \hat{\phi}_i \rangle \hat{S}_i$ . The open circles are results calculated with the exact smoothing factors. The dotted, dashed, and solid lines correspond to results of the new smoothing method at the scaling angle  $\theta = 5^\circ, 10^\circ,$  and  $15^\circ$ , respectively. For both the cases, the breakup  $S$ -matrix elements smoothed with the formula tend to the exact ones as  $\theta$  increases. In a forthcoming paper, we will investigate the practicability of this formula for four-body breakup processes of three-body projectiles.

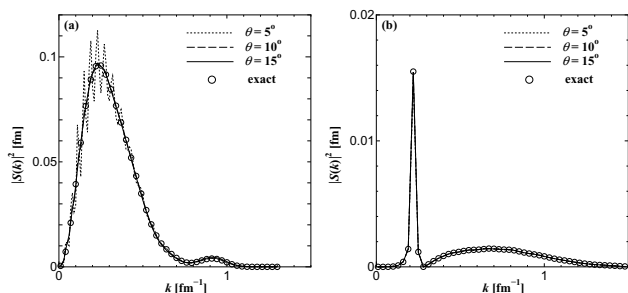


Fig. 1. The squared moduli of breakup  $S$ -matrix elements as a function of  $k$  for  $^{58}\text{Ni}(d, pn)$  at 80 MeV (left panel) and for  $^{12}\text{C}(^6\text{He}, ^2n^4\text{He})$  at 229.8 MeV.

## References

- 1) M. Kamimura, M. Yahiro, Y. Iseri, Y. Sakuragi, H. Kameyama and M. Kawai, Prog. Theor. Phys. Suppl. No. 89 (1986), 1 and references therein.
- 2) T. Egami, T. Matsumoto, K. Ogata and M. Yahiro, *arXiv:0812.3693 [nucl-th]*.
- 3) J. Aguilar and J.M. Combes, Commun. Math. Phys., **22**, 269, (1971). E. Balslev and J.M. Combes, Commun. Math. Phys., **22**, 280, (1971).
- 4) T. Myo, S. Aoyama, K. Katō, and K. Ikeda, Phys. Rev. C **63**, 054313 (2001). T. Myo, K. Katō, H. Toki, and K. Ikeda, Phys. Rev. C **76**, 024305 (2007).

<sup>\*1</sup> Department of Physics, Kyushu University

# Elastic and total reaction cross sections of oxygen isotopes in Glauber theory<sup>†</sup>

B. Abu-Ibrahim,<sup>\*1</sup> S. Iwasaki,<sup>\*2,\*3</sup> W. Horiuchi,<sup>\*2</sup> A. Kohama, and Y. Suzuki,<sup>\*4</sup>

[Nuclear reaction, total reaction cross sections, elastic scattering, unstable nuclei]

Studies on neutron-rich unstable nuclei have been attracting attention both experimentally and theoretically.<sup>1)</sup> These studies are motivated, for example, by that we want to understand the nuclear structure and excitation mode of neutron-rich nuclei as well as their role in forming heavy elements in stars. Binding energy, radius and density distribution, among others, are basic quantities for determining nuclear properties. Reactions of unstable neutron-rich nuclei with a proton target are, therefore, of current interest as they are at present a major means to probe the matter densities of exotic nuclei, particularly the region of the nuclear surface. If one appropriately selects incident energies, protons could be more sensitive to the neutron distributions than to the proton distributions of nuclei.

In this work, we systematically calculate the total reaction cross sections of oxygen isotopes,  $^{15-24}\text{O}$ , on a  $^{12}\text{C}$  target at high energies using the Glauber theory. We also study the differential elastic-scattering cross sections of  $p\text{-}^{20,21,23}\text{O}$  to examine the sensitivity of the diffraction pattern to the nuclear surface. The oxygen isotopes are described with the Slater determinants generated from a phenomenological mean-field potential containing central and spin-orbit potentials, which is an extension of our previous work for describing carbon isotopes.<sup>2,3)</sup> The strength of the spin-orbit potential is set to follow the standard value, whereas that of the central part is chosen so as to reproduce the separation energy of the last nucleon.<sup>2)</sup> This prescription is called the “ $S_n$  model” hereafter. It apparently ignores the pairing effect, which gives a larger separation energy for the even- $N$  nuclei than for the odd- $N$  nuclei. Therefore, this model tends to predict a too large size for the odd- $N$  isotope. To remedy this problem, we test another one, called the “ $\langle S_n \rangle$  model”, which fits the average separation energy for the nucleons in the last orbit. The agreement between theoretical and experimental results is generally good, especially in the  $\langle S_n \rangle$  model, but the sharp increase of the total reaction (interaction) cross sections from  $^{21}\text{O}$  to  $^{23}\text{O}$  remains an open question.

As a possible cross section that may depend on the

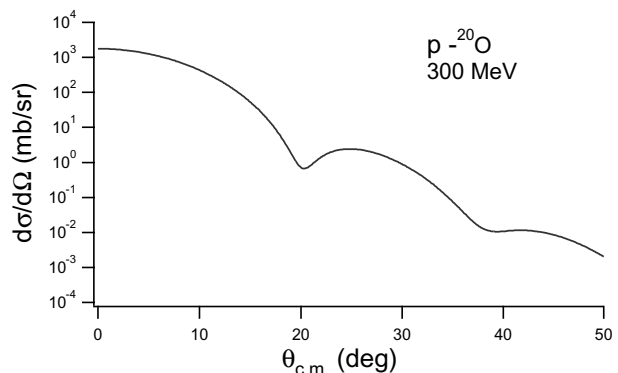


Fig. 1. Prediction of differential elastic-scattering cross section for  $p\text{-}^{20}\text{O}$  at  $E_p=300$  MeV. The curve represents the full calculation with the harmonic-oscillator shell-model wave function.

nuclear radius more sensitively than the reaction cross section, we examine the differential cross sections of the  $p\text{-}^{20,21,23}\text{O}$  elastic scatterings at the incident energy of  $E_p = 300$  MeV. For this purpose, we calculate the full Glauber amplitude using harmonic-oscillator wave functions. We prepare two amplitudes: One is obtained using the scale parameter of the wave function to reproduce the numerical result of each matter radius in the  $\langle S_n \rangle$  model, the other is obtained using the scale parameter to reproduce the empirical value of each total reaction (interaction) cross section. The differential cross sections calculated from the two amplitudes are found out to be not very different up to the second minimum of the angular distribution.

Finally, we predict the differential cross section for  $p\text{-}^{20}\text{O}$  elastic scattering (Fig. 1), which has recently been measured.<sup>4)</sup> Our prediction appears consistent with preliminary data. This implies that it is possible to calculate to a good approximation the total reaction and elastic scattering cross sections at high energies.

## References

- 1) A. Ozawa *et al.*: Nucl. Phys. **A 693**, 32 (2001).
- 2) W. Horiuchi, Y. Suzuki, B. Abu-Ibrahim, and A. Kohama: Phys. Rev. C **75**, 044607 (2007); Erratum: *ibid.* C **76**, 039903(E) (2007).
- 3) B. Abu-Ibrahim, W. Horiuchi, A. Kohama, and Y. Suzuki: Phys. Rev. C **77**, 034607 (2008).
- 4) S. Terashima *et al.*: RIKEN Accel. Prog. Rep. **40**, 18 (2007).

<sup>†</sup> Condensed from the article in J. Phys. Soc. Japan **78**, 044001 (2009).

<sup>\*1</sup> Department of Physics, Cairo University, Egypt

<sup>\*2</sup> Graduate School of Science and Technology, Niigata University

<sup>\*3</sup> Present address: Intertrade Co., Ltd.

<sup>\*4</sup> Department of Physics and Graduate School of Science and Technology, Niigata University

# Shell-model description of beta-decays for pfg-shell nuclei

M. Honma,<sup>\*1</sup> T. Otsuka,<sup>\*2,\*3</sup> T. Mizusaki,<sup>\*4</sup> and M. Hjorth-Jensen<sup>\*5</sup>

[NUCLEAR STRUCTURE, shell model, unstable nuclei]

The effective interaction is a key ingredient for successful shell-model calculations. Owing to recent developments in computers as well as novel numerical techniques, the applicability of the shell model is rapidly expanding. On the other hand, our knowledge of the effective interaction is still insufficient especially for cases where more than one major shell should be taken as an active valence space. Such a treatment is essentially important for describing neutron-rich nuclei.

We have developed an effective interaction<sup>1)</sup> for shell-model calculations in the model space consisting of valence orbits  $1p_{3/2}$ ,  $0f_{5/2}$ ,  $1p_{1/2}$  and  $0g_{9/2}$  assuming an inert  $^{56}\text{Ni}$  core (f5pg9-shell). It can be regarded as a first step for future extensions to the pf+sdg model space. Starting from a microscopic interaction (renormalized G-matrix)<sup>2)</sup> based on a realistic NN-potential, we have varied 45 linear combinations of Hamiltonian parameters (133 two-body matrix elements and four single-particle energies) by a least-squares fit to the 400 experimental binding and excitation energy data out of 87 nuclei with masses  $A=63-96$ . In the latest iteration, we have attained the rms error of 185 keV.

As an application of this interaction, we have evaluated the  $\beta$ -decay properties for  $N=50$  and 49 nuclei, aiming at the analysis of the r-process nucleosynthesis. For understanding the r-process, we need precise information of nuclear properties over a wide mass range under extreme conditions which is not accessible by current experiments. For this purpose, nuclear structure calculations based on the mean-field approximation have been widely used. Such methods are applicable to any nuclei in the nuclear chart, but are not necessarily accurate because only limited correlations can be treated. On the other hand, the shell model can treat any two-body correlations and can give accurate description of nuclear structure, if we can use suitably chosen model spaces and effective interactions.

Because of the strong energy dependence of the phase space factor, low-lying states mainly contribute to the  $\beta$ -decay half-life. The spin-flip decays  $\nu g_{9/2} \rightarrow \pi g_{7/2}$  and  $\nu f_{5/2} \rightarrow \pi f_{7/2}$  are both out of the present f5pg9-shell model space. Since we consider  $N=50$  and 49 neutron-rich nuclei, the former mode should appear at high excitation energy in the daugh-

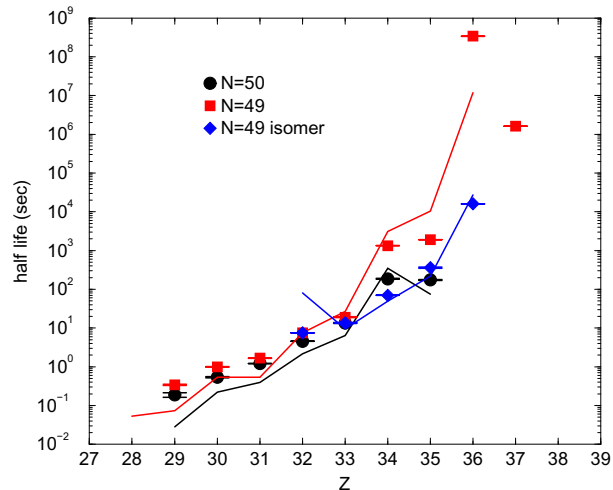


Fig. 1. Comparison of the  $\beta$ -decay half-life between the shell-model results (lines) and experimental data (symbols) for  $N=50$  and 49 nuclei. For  $N=49$  cases, the results for the low-lying isomer are also shown.

ter nucleus and may not be important. On the other hand, the latter mode may be important because it is predicted that, due to the strong repulsive interaction between the  $\pi f_{7/2}$  and the  $\nu g_{9/2}$  orbit through the tensor force<sup>3)</sup>, as neutrons occupy the  $g_{9/2}$  orbit, the effective single-particle energy gap above the proton  $f_{7/2}$  orbit decreases and the excitation from the  $Z=28$  core may be enhanced.

We have calculated the  $\beta$ -decay half-life for the allowed transitions by using the experimental  $Q$ -values and the same quenching factor  $q=0.6$  for the evaluation of the Gamow-Teller strength as in Ref.<sup>1)</sup>. Shell-model calculations have been carried out in a conventional way by using the code MSHELL.<sup>4)</sup> The results are shown in Fig.1. It can be seen that the shell-model results are in reasonable agreement with the experimental data for less neutron-rich nuclei ( $Z>30$ ) except for  $^{84}\text{Br}$ ,  $^{85}\text{Kr}$  and the isomer state in  $^{81}\text{Ge}$ , while for neutron-rich nuclei ( $Z<30$ ), the shell-model predictions systematically underestimate the experimental values. This result may indicate the importance of an explicit treatment of the  $Z=28$  core excitation.

## References

- 1) M.Honma et al.: J. of Phys.: Conf. Ser. **49**, 45 (2006).
- 2) M. Hjorth-Jensen et al.: Phys. Rep. **261**, 125 (1995).
- 3) T. Otsuka, et al.: Phys. Rev. Lett. **95**, 232502 (2005).
- 4) T. Mizusaki: RIKEN Accel. Prog. Rep. **33**, 14 (2000).

<sup>\*1</sup> Center for Mathematical Sciences, University of Aizu

<sup>\*2</sup> Department of Physics and Center for Nuclear Studies, University of Tokyo

<sup>\*3</sup> National Superconducting Cyclotron Laboratory, Michigan State University

<sup>\*4</sup> Institute of Natural Sciences, Senshu University

<sup>\*5</sup> Department of Physics and Center of Mathematics for Applications, University of Oslo

# Skyrme-QRPA calculation for exotic modes in neutron-rich Mg isotopes close to the drip line<sup>†</sup>

Kenichi Yoshida

[nuclear structure, density functional theory, unstable nuclei]

Presently, small excitation energies of the first  $2^+$  state and striking enhancements of  $B(E2; 0_1^+ \rightarrow 2_1^+)$  in  $^{32}\text{Mg}^{(1)}$  and  $^{34}\text{Mg}^{(2-4)}$  are being actively discussed in connection with the onset of quadrupole deformation, breaking of the  $N = 20$  spherical magic number, pairing correlation and continuum coupling effects. In order to get clear understanding of the nature of quadrupole deformation and pairing correlations, it is highly desirable to explore, both experimentally and theoretically, excitation spectra of these nuclei toward a drip line.

We apply the new calculation scheme of the deformed Quasiparticle-RPA on top of the Skyrme-Hartree-Fock-Bogoliubov mean field developed in Ref.<sup>(5)</sup> to the low-frequency excitation modes in neutron-rich Magnesium isotopes close to the drip line, and investigate the microscopic mechanism of the excitation modes uniquely appearing in deformed neutron-rich nuclei.

Figure 1 shows the low-lying excitation spectra for the  $K^\pi = 0^+$  modes appearing as the  $0_2^+$  states. Here excitation energies are evaluated by

$$E(I, K) = \hbar\omega_{\text{RPA}} + \frac{\hbar^2}{2\mathcal{J}_{\text{TV}}}(I(I+1) - K^2), \quad (1)$$

in terms of the vibrational frequencies  $\omega_{\text{RPA}}$  and the Thouless-Valatin moment of inertia  $\mathcal{J}_{\text{TV}}$  calculated microscopically by the QRPA as described in Ref.<sup>(6)</sup>. As can be seen in this figure, the appearance of the soft  $K^\pi = 0^+$  modes is quite sensitive to the neutron number, *i.e.*, the shell structure around the Fermi level of neutrons.

In Ref.<sup>(6)</sup>, we have discussed the generic feature of the

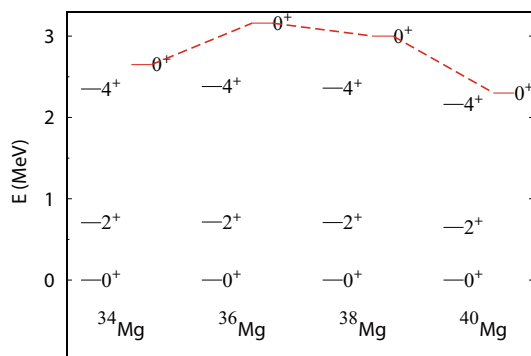


Fig. 1. Low-excitation energy spectra of  $^{34,36,38,40}\text{Mg}$ .

low-lying  $K^\pi = 0^+$  modes in deformed neutron-rich nuclei using a phenomenological mean field and QRPA model: In a deformed system where the up-sloping oblate-type and the down-sloping prolate-type orbitals exist near the Fermi level, one obtains a low-lying mode possessing enhanced strengths both for the quadrupole p-h transition and for the quadrupole p-p (pair) transition induced by the pairing fluctuations. The up-sloping and down-sloping orbitals have quadrupole moments with opposite signs. In the present calculation employing the SkM\* energy density functional, and the mixed-type pairing energy density functional, we obtain similar conclusions.

Furthermore, it is found that the low-lying collective modes in drip-line nuclei are characterized by the enhancement of excitation of neutrons. We summarize in Table 1 the ratio of the matrix elements for neutrons and protons normalized by that of the neutron and proton numbers,  $(M_\nu/M_\pi)/(N/Z)$ , for the lowest excitation modes. As the neutron drip line is approached, the contribution of the neutron excitation increases. This is understood as follows: In drip-line nuclei, the neutron two-quasiparticle (2qp) excitations predominantly take place outside of the nuclear surface. Therefore, the transition strengths of the 2qp excitation of neutrons become large. The proton p-h excitations, however, concentrate in the surface region. Consequently, coupling of the excitations between neutrons and protons becomes smaller, and the transition strengths of neutrons ( $M_\nu^2$ ) and protons ( $M_\pi^2$ ) become extremely asymmetric.

Table 1. Ratios of the neutron and proton matrix elements  $M_\nu/M_\pi$  divided by  $N/Z$ .

	$^{34}\text{Mg}$	$^{36}\text{Mg}$	$^{38}\text{Mg}$	$^{40}\text{Mg}$
$K^\pi = 0^+$	1.57	1.58	1.82	1.91
$K^\pi = 2^+$	1.41	1.41	1.55	1.79

## References

- 1) T. Motobayashi et al., Phys. Lett. **B346**, 9 (1995).
- 2) K. Yoneda et al., Phys. Lett. **B499**, 223 (2001).
- 3) J. A. Church et al., Phys. Rev. C **72**, 054320 (2005).
- 4) Z. Elekes et al., Phys. Rev. C **73**, 044314 (2006).
- 5) K. Yoshida and N. Van Giai, Phys. Rev. C **78**, 064316 (2008).
- 6) K. Yoshida and M. Yamagami, Phys. Rev. C **77**, 044312 (2008).

<sup>†</sup> Condensed from article in Eur. Phys. J. A (in press).

# Evolution of the spin-orbit splitting in $^{48}\text{Ca}$ probed by the spectroscopic factor

Y. Utsuno,<sup>\*1</sup> T. Otsuka,<sup>\*2\*3</sup> B.A. Brown,<sup>\*4\*3</sup> M. Honma,<sup>\*5</sup> and T. Mizusaki<sup>\*6</sup>

[Nuclear structure, shell model, unstable nuclei]

Evolution of the shell structure in unstable nuclei is attracting significant interest among radioactive beam facilities throughout the world. The disappearance of the  $N = 20$  magic number and the appearance of a new  $N = 16$  magic number were excellently described by shell-model calculations with the SDPF-M interaction,<sup>1)</sup> where the changing magic structure is caused by a strong  $T = 0$  monopole interaction between  $0d_{3/2}$  and  $0d_{5/2}$ . Recently, it has been pointed out that this strong monopole interaction between the particular orbits is an example of the evolution of the shell structure (referred to as “shell evolution”) caused by the tensor force.<sup>2)</sup> The present study aims to investigate dominance of the tensor force in shell evolution based on a shell-model calculation including an appropriate tensor force. The work was carried out in part as a RIKEN-CNS collaboration project on large-scale nuclear structure calculations.

We constructed a new  $sd$ - $pf$  shell interaction. Standard shell-model interactions were adopted as the intra-shell interactions: USD<sup>3)</sup> for the  $sd$  shell and GXPF1B (a small modification to GXPF1A<sup>4)</sup>) for the  $pf$  shell. We substituted a newly constructed interaction for the cross-shell part. Its tensor force is the  $\pi + \rho$  exchange potential with cutoff at 0.7 fm,<sup>2)</sup> and the central force is a single-range Gaussian force whose parameters are determined so as to give a monopole centroid similar to that of the GXPF1 interaction. Note that no direct fitting to experiment is adopted to determine the interaction.

While the central force is hardly responsible for the evolution of the spin-orbit splitting, the tensor force strongly reduces that of the proton as neutrons occupy the intruder orbit such as  $0f_{7/2}$ . We thus study the proton hole states in  $^{47}\text{K}$  to examine the dominance of the tensor force in the shell evolution. Since proton  $0d_{5/2}$  is located rather deeply there, its hole state does not concentrate on a single level but fragments into many levels. In such cases, the spectroscopic factor gives essential information on the single-particle (or

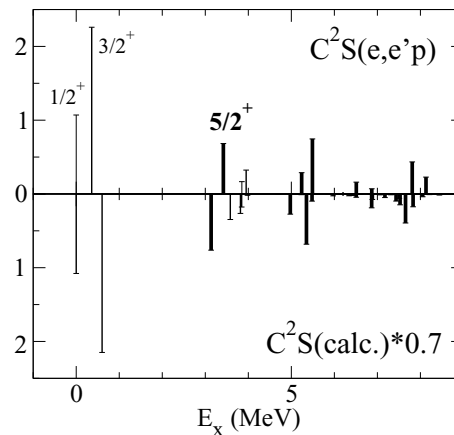


Fig. 1. Comparison of the distribution of spectroscopic factors for one-proton pickup from  $^{48}\text{Ca}$  between an  $(e, e'p)$  experiment<sup>5)</sup> (upper) and the shell-model calculation (lower). Overall quenching by 0.7 is included in the calculation. The spectroscopic factors of  $0d_{5/2}$  are presented by thick lines. Taken from<sup>6)</sup>.

hole) level. In Fig. 1, the distribution of spectroscopic factors for one-proton pickup from  $^{48}\text{Ca}$  is compared between experiment and the present calculation. Both the position of the  $5/2^+$  states and their spectroscopic factor strength are reproduced very well. If there is no tensor force in the cross-shell interaction, the spin-orbit splitting between proton  $d$  orbits becomes larger. Then, the agreement of the  $0d_{5/2}$  hole states is significantly worse so that the two major peaks at around 3 MeV and 5 MeV are reduced and the peak of around 9 MeV is enhanced. Hence, this result provides a clear evidence for the significance of the tensor force in shell evolution.

## References

- 1) Y. Utsuno, T. Otsuka, T. Mizusaki, and M. Honma: Phys. Rev. C **60**, 054315 (1999).
- 2) T. Otsuka, T. Suzuki, R. Fujimoto, H. Grawe, and Y. Akaishi: Phys. Rev. Lett. **95**, 232502 (2005).
- 3) B.A. Brown and B.H. Wildenthal: Ann. Rev. Nucl. Part. Sci. **38**, 29 (1988).
- 4) M. Honma, T. Otsuka, B. A. Brown, and T. Mizusaki: Eur. Phys. J. A **25** Suppl. 1, 499 (2005).
- 5) G.J. Kramer et al.: Nucl. Phys. A **679**, 267 (2001).
- 6) Y. Utsuno, T. Otsuka, B.A. Brown, T. Mizusaki, and M. Honma: Proc. 6th Japan-Italy Symposium on Heavy Ion Physics, to be published in AIP Conf. Proc. (AIP, 2009).

<sup>\*1</sup> Advanced Science Research Center, Japan Atomic Energy Agency

<sup>\*2</sup> Department of Physics and Center for Nuclear Study, University of Tokyo

<sup>\*3</sup> National Superconducting Cyclotron Laboratory, Michigan State University

<sup>\*4</sup> Department of Physics and Astronomy, Michigan State University

<sup>\*5</sup> Center for Mathematical Sciences, University of Aizu

<sup>\*6</sup> Institute of Natural Sciences, Senshu University

# Density functional for description of novel pairing properties in nuclei far from $\beta$ -stability

M. Yamagami, Y. R. Shimizu\*<sup>1</sup>, and T. Nakatsukasa

[Neutron-rich nuclei, pairing correlations, density functional theory]

Aiming for a universal description of pairing correlations in nuclei far from  $\beta$ -stability, we extend the energy density functional (DF) by enriching the density dependence of the isoscalar and isovector couplings in the particle-particle channel (pair-DF). We emphasize the necessity of the quadratic isovector density term<sup>1)</sup> in addition to the linear terms<sup>2)</sup> for description of pairing properties in nuclei with large neutron excess.

We propose a pair-DF of the following form;

$$H_{\text{pair}}(\mathbf{r}) = \frac{V_0}{4} \sum_{\tau=n,p} g_{\tau} [\rho, \rho_1] \{\tilde{\rho}_{\tau}(\mathbf{r})\}^2 \quad (1)$$

with

$$g_{\tau} [\rho, \rho_1] = 1 - \frac{1}{2} \frac{\rho(\mathbf{r})}{\rho_0} - \eta_1 \frac{\tau_3 \rho_1(\mathbf{r})}{\rho_0} - \eta_2 \left( \frac{\rho_1(\mathbf{r})}{\rho_0} \right)^2 \quad (2)$$

Here  $\tau = n$  (neutron) or  $p$  (proton), the strength  $V_0$ , and  $\rho_0 = 0.16 \text{ fm}^{-3}$  is the saturation density of symmetric nuclear matter.  $\rho$  ( $\rho_1$ ) is isoscalar (isovector) density. The  $\tau_3 = 1$  (n) or  $-1$  (p) in the linear  $\rho_1$  term is introduced so as to preserve the charge symmetry of the pair-DF.

The parameters  $\eta_1$  and  $\eta_2$  are optimized so as to reproduce the average dependence of pairing gaps on the mass number  $A$  and asymmetry parameter  $\alpha = (N - Z)/A$ :

$$\Delta_{n,\text{exp}}(\alpha) = (1 - 7.74\alpha^2) \Delta_n^{(A)} \quad (3)$$

$$\Delta_{p,\text{exp}}(\alpha) = (1 - 8.25\alpha^2) \Delta_p^{(A)}, \quad (4)$$

with  $\Delta_n^{(A)} = 6.75/A^{1/3} \text{ MeV}$  and  $\Delta_p^{(A)} = 6.36/A^{1/3} \text{ MeV}$ <sup>1)</sup>. For this purpose, we performed the extensive Hartree-Fock-Bogoliubov (HFB) calculation with Skyrme SLy4 force for 156 even-even nuclei around the region of  $A = 120 - 120$  and  $\alpha = 0.05 - 0.25$ . We showed that the parameters set  $(\eta_1, \eta_2) = (0.2, 2.5)$  not only gives a good description of the  $A$ - and  $\alpha$ -dependence<sup>1)</sup> (see Fig. 1, for neutron pairing gaps  $\Delta_n$ ), but also minimizes the r.m.s. deviation between the measured and calculated pairing gaps (Fig. 2). The r.m.s. deviation is defined by

$$\sigma_{\text{tot}} = \left[ \frac{1}{N_{\text{exp}}} \sum_{\tau} \sum_{N,Z} \left( \Delta_{\tau,\text{HFB}} - \Delta_{\tau,\text{exp}} \right)^2 \right]^{1/2}. \quad (5)$$

Here  $N_{\text{exp}} = 177$  is the number of existing data for pairing gaps in the region of the present investigation.

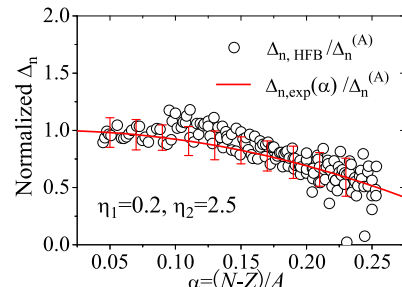


Fig. 1. Neutron pairing gaps obtained with  $(\eta_1, \eta_2) = (0.2, 2.5)$  are plotted as a function of  $\alpha$ . The pairing gaps are divided by  $\Delta_n^{(A)}$ . The  $V_0$  is fixed so as to reproduce the measured  $\Delta_n$  of  $^{156}\text{Dy}$ .

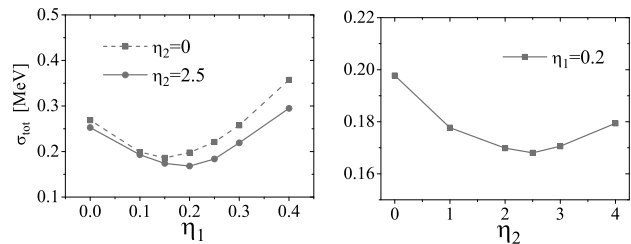


Fig. 2. (Left) The r.m.s. deviations are shown as a function of  $\eta_1$ . The results with either  $\eta_2 = 0$  or  $5/2$  are compared. (Right) The same but as a function of  $\eta_2$  with  $\eta_1 = 0.2$ . The  $V_0$  is fixed for each  $(\eta_1, \eta_2)$  so as to reproduce the measured  $\Delta_n$  of  $^{156}\text{Dy}$ .

The strength  $V_0$  is fixed so as to reproduce the measured  $\Delta_n$  of  $^{156}\text{Dy}$ . This enables us to reduce the computational efforts considerably compared to the determination of  $V_0$  by  $\chi^2$  fitting to the experimental data in the wide region of the nuclear chart. This choice gives  $\sigma_{\text{tot}} = 0.17 \text{ MeV}$ , which is close to  $\sigma_{\text{tot}} = 0.16 \text{ MeV}$  obtained with the optimized  $V_0$ , and much smaller than  $\sigma_{\text{tot}} = 0.34 \text{ MeV}$  with the standard choice reproducing the measured  $\Delta_n$  of  $^{120}\text{Sn}$ .

## References

- 1) M. Yamagami, Y. R. Shimizu, and T. Nakatsukasa: submitted to Phys. Rev. C (2008).
- 2) M. Yamagami and Y. R. Shimizu: Phys. Rev. C **77**, 064319 (2008).

\*<sup>1</sup> Department of Physics, Kyushu University

# Two-neutron and two-proton correlations in nuclear surface

Y. Kanada-En'yo,<sup>\*1</sup> N. Hinohara,<sup>\*1</sup> T. Suhara,<sup>\*2</sup>

[NUCLEAR STRUCTURE, Unstable nuclei, Cluster]

Two-neutron correlation in neutron-rich nuclei is presently one of the hot subjects in the physics of unstable nuclei. In two-neutron halo nuclei such as  $^{11}\text{Li}$ , the dineutron correlation was theoretically predicted in many works and was supported by experiments. The dineutron correlation, which is characterized by a strong spatial correlation of two neutrons in the  $^1S$  channel, is discussed also in light neutron-rich nuclei such as  $^8\text{He}^{1-3}$  and also in medium-heavy neutron-rich nuclei<sup>4,5)</sup> as well as asymmetric nuclear matter<sup>6,7)</sup>.

Our aim in this paper is to reveal how two neutrons can form in the nuclear surface. For this aim, we consider a very simplified model of quasi two-dimensional(2D) neutron systems which mimic a neutron layer in the surface where distribution of valence neutrons concentrates. We assume for simplicity that the transverse  $z$ -direction of the quasi-2D plane can be approximated by a frozen Gaussian packet,

$$\phi^{0s}(z) = \left(\frac{1}{\pi a^2}\right)^{1/4} \exp\left[-\frac{z^2}{2a^2}\right], \quad (1)$$

whereas the motion of the neutrons within the layer is free. Let us consider an two-neutron system in this quasi-2D space. By integrating the  $z$  coordinates, we can get the 2D Schrödinger equation with respect to  $r_\perp \equiv \sqrt{x^2 + y^2}$  for the  $S$ -wave relative wave function  $\Phi^{nn}(r_\perp, \chi_1, \chi_2)$ ,

$$\left(-\frac{\hbar^2}{m} \left(\frac{\partial^2}{\partial r_\perp^2} + \frac{1}{r_\perp} \frac{\partial}{\partial r_\perp}\right) + V^{2D}(r_\perp)\right) \Phi^{nn}(r_\perp, \chi_1, \chi_2) = E_{nn}^{2D} \Phi^{nn}(r_\perp, \chi_1, \chi_2), \quad (2)$$

$$\Phi^{nn} = \psi^{nn}(r_\perp) \otimes X_{S=0}(\chi_1, \chi_2), \quad (3)$$

$$V^{2D}(r_\perp) = \langle \phi^{0s}(z_1) \phi^{0s}(z_2) | V(r) | \phi^{0s}(z_1) \phi^{0s}(z_2) \rangle. \quad (4)$$

$\psi^{nn}(r_\perp)$  is the spatial wave function normalized as  $\int d^2r_\perp |\psi^{nn}(r_\perp)|^2 = 1$ , and  $X_{S=0}$  is the intrinsic-spin wave function for the spin-zero channel.

We calculated the two-neutron wave function in quasi-2D with the width  $a$  by using the Minnesota force which is an effective interaction adjusted to the experimental  $S$ -wave  $NN$  scattering lengths. It is known that a bound state in 2D can form at any arbitrarily small attraction. Since the  $^1S$  nuclear force is attractive at low energy, the two-neutron bound state is formed in quasi-2D with an arbitrary width  $a$ . Because the interaction  $V^{2D}(r_\perp)$  in 2D space becomes stronger for the smaller width  $a$  of the layer than the larger

one, energy and size of the two-neutron bound state decrease as the width  $a$  gets small. For example, in quasi-2D with  $a = 1$ , the energy  $E_{nn}^{2D}$  is  $-1.9$  MeV and the size  $\langle r_\perp^2 \rangle = 4.3$  fm. In Fig. 1, the calculated wave functions of the two-neutron and the two-proton states in quasi-2D are shown. The wave function  $\psi^{nn}(r_\perp)$  shows the prominent peak at small distance  $r_\perp$  region in quasi-2D with  $a = 1$  and  $a = 2$  fm. This indicates that the spatial correlation of two neutrons is enhanced in quasi-2D systems. We also calculated the wave function for an two-proton system in quasi-2D by adding the Coulomb force, and found that the two-proton correlation is still prominent if the layer is thin enough as  $a = 1 - 2$  fm.

The present results suggest that, if valence neutrons (protons) concentrate in the surface layer of neutron-rich (proton-rich) nuclei, spatial correlations of two neutrons (protons) in  $S = 0$  channel can be enhanced.

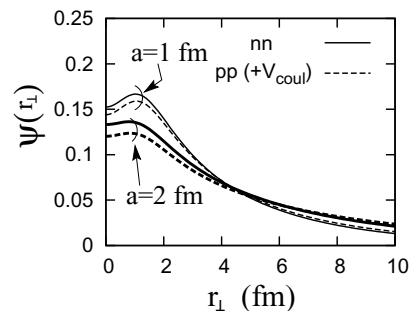


Fig. 1. Two-neutron and two-proton wave functions  $\psi^{nn}(r_\perp)$   $\psi^{pp}(r_\perp)$  in quasi-2D with the width parameter  $a = 1$  and  $a = 2$  fm calculated with the Minnesota force with and without the Coulomb force.

## References

- 1) Y. Kanada-En'yo, Phys. Rev. C **76**, 044323 (2007).
- 2) N. Itagaki, M. Ito, K. Arai, S. Aoyama and T. Kokalova, Phys. Rev. C **78**, 017306 (2008).
- 3) K. Hagino, N. Takahashi and H. Sagawa, Phys. Rev. C **77**, 054317 (2008).
- 4) M. Matsuo, K. Mizuyama and Y. Serizawa, Phys. Rev. C **71**, 064326 (2005).
- 5) N. Pillet, N. Sandulescu and P. Schuck, Phys. Rev. C **76**, 024310 (2007).
- 6) F. V. De Blasio, M. Hjorth-Jensen, O. Elgaroy, L. Engvik, G. Lazzari, M. Baldo and H. J. Schulze, Phys. Rev. C **56**, 2332 (1997).
- 7) M. Matsuo, Phys. Rev. C **73**, 044309 (2006).

<sup>\*1</sup> Yukawa Institute for Theoretical Physics, Kyoto University, Japan

<sup>\*2</sup> Department of Physics, Kyoto University, Japan

# Calculation of nuclear photoabsorption cross section using the finite amplitude method for Skyrme functionals

T. Inakura,<sup>\*1</sup> T. Nakatsukasa, and K. Yabana,<sup>\*2</sup>

[Nuclear structure, random-phase approximation, photonuclear reaction]

In the description of the dynamical properties in the nuclear response to external fields, the random-phase approximation (RPA) is a leading theory applicable to both low-lying states and giant resonances. The RPA is a microscopic theory, which can be obtained by linearizing the time-dependent Hartree-Fock (TDHF) equation, or equivalently, the time-dependent Kohn-Sham equation in density-functional theory. The linearization produces a self-consistent residual interaction,  $v = \delta^2 E[\rho]/\delta\rho^2$ , where  $E$  and  $\rho$  are the energy-density functional and the one-body density, respectively. The standard solution of the RPA is based on the matrix formulation of the RPA equation, which involves a large number of particle-hole matrix elements of the residual interaction,  $v_{ph',hp'}$  and  $v_{pp',hh'}$ . Since the realistic nuclear energy functional is rather complicate, it is a hard work to calculate all the necessary matrix elements. Although there have been numerous studies on HF-plus-RPA calculations, because of this complexity it has been a common practice to neglect some parts of the residual interactions. RPA calculations with the full self-consistency are becoming a current trend in nuclear structure studies, however, the applications to deformed nuclei are still scarce.

Recently, we have proposed a new practical method of solving the RPA equation, which we name the finite amplitude method (FAM)<sup>1)</sup>. The most advantageous feature of the present approach is that it does not require an explicit calculation of the residual interactions. Instead, the FAM estimates them using the operations of the single-particle Hamiltonian with the numerical differentiation. The numerical procedure is as follows. First, we calculate the ground state using the imaginary-time method, and obtain the single-particle orbitals and their eigenenergies:

$$h_0|\phi_i\rangle = \epsilon_i|\phi_i\rangle. \quad (1)$$

Then, we solve the following linear response equations by iteration.

$$\omega|X_i\rangle = (h_0 - \epsilon_i)|X_i\rangle + \hat{P}\{V_{\text{ext}} + \delta h\}|\phi_i\rangle, \quad (2)$$

$$-\omega|Y_i\rangle = \langle Y_i|(h_0 - \epsilon_i) + \langle\phi_i|\{V_{\text{ext}} + \delta h\}\hat{P}. \quad (3)$$

Here,  $V_{\text{ext}}$  indicates an external perturbative field, and  $\hat{P}$  the projection operator onto the particle space.  $|X_i\rangle$  and  $|Y_i\rangle$  are RPA forward and backward amplitudes, respectively,  $\delta h$  is the induced residual field, which is

evaluated with the FAM technique<sup>1)</sup>.

Figure 1 shows the accuracy of the FAM. Smearing the result of the diagonalization of the RPA matrix (vertical lines)<sup>2)</sup> with a width of 2 MeV, we obtain the solid curve. Circles indicate the results of the FAM. These two different calculations provide identical results. This proves that the numerical differentiation in the FAM for realistic Skyrme functionals is sufficiently accurate in practice. Note that the required computational resource for the diagonalization method is much larger than that for the FAM. As an example of the FAM results, we show in Fig. 2 the calculated photoabsorption cross sections for deformed <sup>24</sup>Mg and <sup>28</sup>Si. The systematic calculations of nuclear photoabsorption cross sections are under progress.

## References

- 1) T. Nakatsukasa, T. Inakura, and K. Yabana, Phys. Rev. C **76**, 024318 (2007).
- 2) H. Imagawa and Y. Hashimoto. Phys. Rev. C, **67**, 037302 (2003).

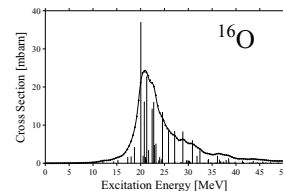


Fig. 1. Comparison of the photoabsorption cross sections for <sup>16</sup>O obtained with different methods. The SIII parameter set is used. See text for explanation.

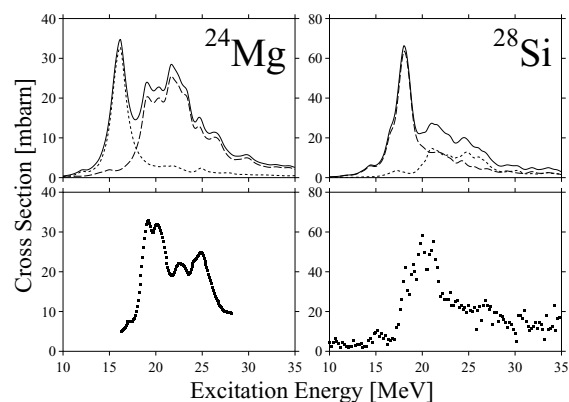


Fig. 2. Calculated photoabsorption cross sections in light deformed nuclei <sup>24</sup>Mg and <sup>28</sup>Si with experimental data.

<sup>\*1</sup> Institute of Physics, University of Tsukuba

<sup>\*2</sup> Center for Computational Sciences, University of Tsukuba

# Linear Response Calculations With Skyrme TDHF+BCS

S. Ebata,<sup>\*1</sup> T. Nakatsukasa T. Inakura,<sup>\*1,\*2</sup> Y. Hashimoto,<sup>\*2</sup> and K. Yabana<sup>\*1,\*2</sup>

[Nuclear structure, unstable nuclei]

The recent progress of radioactive facilities, such as RIBF in RIKEN, strongly demands a theoretical framework that is able to analyze and predict the properties of unknown nuclei. For this purpose, it should include the effects of deformation and pairing correlation, and should be capable of calculating not only the ground state but also the excited states. The Hartree-Fock-Bogoliubov plus quasi-particle random phase approximation (HFB+QRPA) is such a candidate, which is applicable to a wide range of nuclei from light to heavy ones. However, it requires a lot of effort for coding the programs as well as significant computational resources. The HFB+QRPA for deformed nuclei is currently still in preliminary stage.

We propose the time-dependent Hartree-Fock plus BCS (TDHF+BCS) in the three-dimensional coordinate-space representation, which can take into account the full effects of nuclear deformation, yet treating the pairing correlation in the BCS-like approximation.

TDHF+BCS equations are derived from the time-dependent variational principle<sup>1)</sup>. First, we set a time-dependent trial wave function as a BCS-like state

$$|\Phi(t)\rangle \equiv \prod_{l>0} (u_l(t) + v_l(t)\hat{c}_l^\dagger(t)\hat{c}_{\bar{l}}^\dagger(t))|0\rangle.$$

Here,  $\hat{c}_l^\dagger$  and  $\hat{c}_{\bar{l}}^\dagger$  are creation operators of canonical states. Note that the state  $\bar{l}$  is not necessarily the time-reversal state of the state  $l$ . Differentiating the Lagrangian,  $\mathcal{L}(t) = \langle\Phi(t)|\hat{H} - i\hbar\partial/\partial t|\Phi(t)\rangle$ , with respect to the single-particle states  $\phi_l, \phi_{\bar{l}}^*$  and the occupation probability parameters  $v_l, v_{\bar{l}}^*$ , we can derive the following equations for the single-particle states  $\phi_l(\mathbf{r}, t)$ , the occupation probabilities  $\rho_l \equiv |v_l|^2$ , and the pair densities  $K_l \equiv u_l v_l$ :

$$\begin{cases} i\hbar\dot{\phi}_l(\mathbf{r}, t) = (\hat{h}[\rho, \tau] - \varepsilon_l)\phi_l(\mathbf{r}, t), \\ i\hbar\dot{\rho}_l(t) = \Delta^* K_l(t) - \Delta K_l^*(t), \\ i\hbar\dot{K}_l(t) = K_l(t)(\varepsilon_l + \varepsilon_{\bar{l}}) + \Delta(2\rho_l(t) - 1), \end{cases}$$

where we used the normalization condition,  $u_l^2 + |v_l|^2 \equiv 1$ .  $\Delta \equiv G \sum_{l>0} K_l$  is the gap energy, the constant  $G$  is the strength of pairing interaction, and  $\varepsilon_l$  are the single-particle energies. The TDHF+BCS equations guarantee the conservation of the orthonormal property of single-particle states, the particle number, and the total energy. In the static limit, these equations agree with the well-known HF+BCS equations. With  $\Delta = 0$ , these are also equivalent to the TDHF equation.

We solve the TDHF+BCS equations in real time, and calculate the linear response of nuclei. In the linear-response calculation, we add an external field  $\hat{V}_{\text{ext}}(\mathbf{r}, t)$  which is weak and instantaneous in time,  $\hat{V}_{\text{ext}}(\mathbf{r}, t) \equiv -k\hat{F}\delta(t)$ ;  $k \ll 1$ .  $\hat{F}$  is a one-body operator, for example, the isovector dipole operator,  $\hat{D}_{\text{IV}} = (N/A)\sum_p \hat{z}_p - (Z/A)\sum_n \hat{z}_n$ . We calculate the time evolution of the expectation value of  $\hat{F}$ , and obtain the strength function  $S(\hat{F}; E)$  by using the Fourier transformation.

$$S(\hat{F}; E) = -\frac{1}{k\pi} \text{Im} \int_0^\infty dt (f(t) - f(0)) e^{iEt - \Gamma t/2},$$

$$f(t) \equiv \langle\Phi(t)|\hat{F}|\Phi(t)\rangle,$$

where  $\Gamma$  is a smoothing parameter.

Figure 1 shows the  $E1$  strength function for  $^{24}\text{Ne}$ , calculated with the SkM\* parameter set. In this calculation, the ground state of  $^{24}\text{Ne}$  is deformed to an oblate shape. The ground-state deformation is slightly smaller than that in the HF state without the pairing correlation. The strength function calculated with the TDHF+BCS turns out to be similar to that with the TDHF. For this nucleus, we have found that the effects of pairing correlation is weak for giant dipole resonance.

Currently, we are developing the TDHF+BCS code for parallel computing to facilitate the calculation of heavier nuclei. Following on from that, we will perform a systematic investigation of nuclear responses.

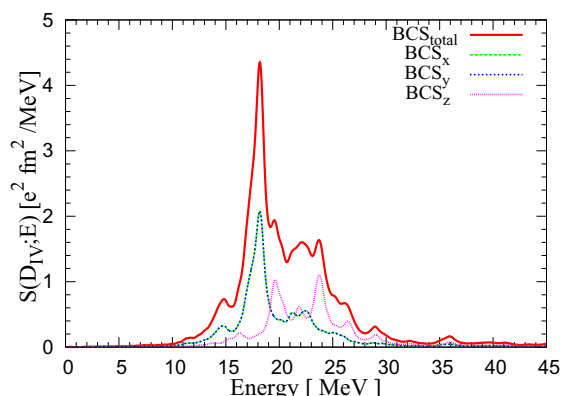


Fig. 1. The  $E1$  strength function for  $^{24}\text{Ne}$  calculated with the Skyrme functional of the SkM\* parameter set. The smoothing parameter of  $\Gamma = 1$  MeV is used.

## References

- 1) J. Błocki and H. Flocard: Nucl. Phys. **A 273**(1976), 45.

<sup>\*1</sup> Graduate School of Pure and Applied Sciences, University of Tsukuba

<sup>\*2</sup> Center for Computational Science, University of Tsukuba

## Development of QRPA code with an FAM method

P. Avogadro, T. Nakatsukasa

[Nuclear structure, QRPA]

QRPA is a technique successfully employed to study the low-lying excited states and giant resonances of a nucleus where pairing correlations cannot be neglected. The idea behind this study is to generalize the Finite Amplitude Method (FAM) for random phase approximation (RPA)<sup>1)</sup> to quasi particle RPA (QRPA). QRPA can be obtained as a limit for small amplitude oscillations from the Time Dependent Hartree Fock Bogoliubov equations (TDHFB)<sup>2)</sup>

$$i\hbar \frac{\partial \mathcal{R}}{\partial t} = [\mathcal{H}(t) + F(t), \mathcal{R}(t)] \quad (1)$$

where  $\mathcal{R}(t)$  is the generalized density matrix,  $\mathcal{F}(t)$  is the external perturbation field, which may include two particle transfer operators, and  $\mathcal{H}(t)$  is the HFB Hamiltonian:

$$\mathcal{H} = \begin{pmatrix} h & \Delta \\ \Delta^\dagger & -h \end{pmatrix}$$

In the frequency representation for small amplitude oscillations Eq. (1) becomes

$$\hbar\omega \mathcal{R}' = [\mathcal{H}', \mathcal{R}^0] + [\mathcal{H}^0, \mathcal{R}'] + [\mathcal{F}, \mathcal{R}^0] \quad (2)$$

Where

$$\mathcal{R}(t) = \mathcal{R}^0 + \mathcal{R}' e^{i\omega t} + h.c. \quad (3)$$

$$\mathcal{H}(t) = \mathcal{H}^0 + \mathcal{H}' e^{i\omega t} + h.c. \quad (4)$$

and the generalized density is:

$$\mathcal{R}' = \begin{pmatrix} \rho' & k' \\ \bar{k}' & -\rho' \end{pmatrix}$$

These equations not only involve the diagonalization of large matrices, but also calculation of the matrix elements is generally very difficult. In the past, analytic calculation of the self-consistent residual interaction has been truncated, so the results were not completely self-consistent. The variation of the HFB Hamiltonian is

$$\mathcal{H}' = \begin{pmatrix} \mathcal{H}'^{11} & \mathcal{H}'^{12} \\ \mathcal{H}'^{21} & \mathcal{H}'^{22} \end{pmatrix}$$

Calculation of the matrix  $\mathcal{H}'$  involves the evaluation of:

$$\frac{\partial^2 \mathcal{E}}{\partial \rho_{kl} \partial \rho_{ij}^*} \rho'_{kl}; \quad \frac{\partial^2 \mathcal{E}}{\partial k_{kl} \partial \rho_{ij}^*} k'_{kl}; \quad \frac{\partial^2 \mathcal{E}}{\partial \bar{k}_{kl} \partial \rho_{ij}^*} \bar{k}'_{kl} \quad (5)$$

where the derivatives are evaluated on the HFB ground state.

In the HF+RPA ( $\Delta = 0$ ), the FAM provides a feasible evaluation of  $\delta h$  by taking a numerical derivation

( $\eta$  being a small parameter)<sup>1)</sup>

$$\delta h(\omega) = \frac{1}{\eta} (h[\langle \psi' |, |\psi \rangle] - h[\langle \phi |, |\phi \rangle]) \quad (6)$$

which is correct with a proper choice of  $\langle \psi' |$  and  $|\psi \rangle$  as combinations of the single-particle orbitals and the forward- and backward-going amplitudes. This numerical derivation allows to obtain the RPA equations from a Hartree-Fock code with simple modifications. The RPA equations are then solved by using iterative methods. In QRPA, there is the second derivative of the energy respect not only to the normal density, but also the abnormal density. Currently we are developing a framework for the FAM, which can be applied to HFB+QRPA.

### References

- 1) T. Nakatsukasa, T. Inakura and K. Yabana: Phys. Rev. **C 76**, 024318 (2007)
- 2) J.P. Blaizot and G. Ripka: *Quantum Theory of Finite Systems*, The MIT press, Cambridge Massachussetts

# Spectroscopic Factors in Asymmetric Nuclei From Realistic Interactions

C. Barbieri,\*

Spectroscopic factors (SFs) for particle and hole states around closed shell nuclei are of particular interest since they carry important information regarding nuclear structure.<sup>1,2)</sup> Strong deviations from unity signal the onset of substantial correlation effects and imply the existence of non trivial many-body dynamics. Understanding how SFs change when moving close to the drip lines is important to constrain theoretical models for studying radioactive isotopes. The first information on these features has recently become available using one-nucleon knockout experiments in inverse kinematics. In general, it is found that SFs do change with proton-neutron asymmetry and the quenching of quasiparticle orbits (and hence correlations) become stronger with increasing separation energy.<sup>3)</sup>

Spectroscopic factors for both symmetric and asymmetric nuclei are being calculated within the framework of self-consistent Green's functions theory. Calculations are large scale and based on modern realistic nuclear forces. The Faddeev random phase approximation (FRPA) method is used to account for the interaction between nucleons and collective excitation of the nucleus.<sup>4,5)</sup> This is done by resumming Feynman diagrams such as the one depicted in Fig. 1. There, the  $\Pi(\omega)$  and  $g^{II}(\omega)$  propagators carry information on the collective motion of particle-hole (giant resonance) and two-particle or two-hole (pairing like) configurations. The effects of short-range correlations are also taken into account by using the G-matrix technique.

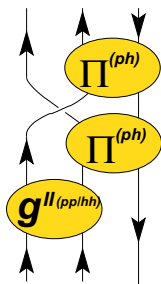


Fig. 1. Example of a diagram appearing in the all-orders summation generated by the FRPA method.

Figure 2 shows the first FRPA results for the spectroscopic factors of quasiparticles around  $^{16,28}\text{O}$  and  $^{40,60}\text{Ca}$ .<sup>6)</sup> These are based on the realistic chiral N3LO interaction.<sup>7)</sup> A dependence on proton-neutron asymmetry is indeed observed in the FRPA, with the spectroscopic factors becoming smaller with increasing nu-

cleon separation energy. A dispersive optical model analysis, which is constrained to data up to  $^{48}\text{Ca}$ , has also been extrapolated to proton rich Ca isotopes, with similar findings.<sup>8,9)</sup> However, for both analyses the change in magnitude is significantly smaller than the one deduced from direct knockout data.<sup>3)</sup>

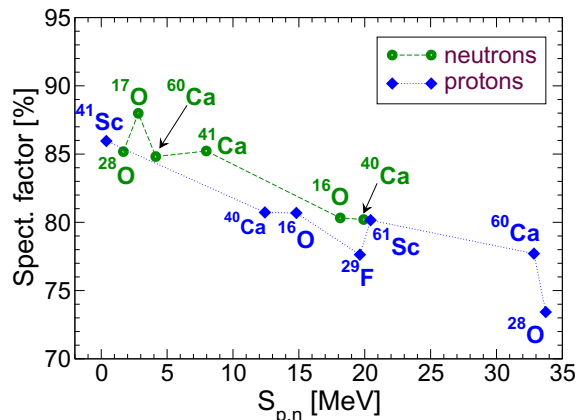


Fig. 2. SFs obtained from partially self-consistent FRPA.

All numbers are given as a fraction of the IPM value and refer to transitions from ground state to ground state. The points refer to knockout of a nucleon from the isotope indicated nearby. The lines are a guide to the eye.

Collective excitations, from Fig. 1 are the most important degrees of freedom governing the reduction of SFs.<sup>6)</sup> These are properly accounted for by the FRPA approach. However, realistic two-nucleon forces such as the one used here have a tendency to underestimate their importance. Hence, the dependence on asymmetry seen in Fig. 2 may become more substantial once FRPA calculations with improved forces are available.

## References

- 1) L. Lapikás, Nucl. Phys. **A553**, 297c (1993).
- 2) W. H. Dickhoff and C. Barbieri, Prog. Part. Nucl. Phys. **52**, 377 (2004).
- 3) A. Gade, et al., Phys. Rev. C **77**, 0044306 (2008).
- 4) C. Barbieri and W. H. Dickhoff, Phys. Rev. C **63**, 034313 (2001).
- 5) C. Barbieri, D. Van Neck and W. H. Dickhoff, Phys. Rev. A **76**, 052503 (2007).
- 6) C. Barbieri and W. H. Dickhoff, Int. J. Mod. Phys. A24, 2060, (2009).
- 7) D. R. Entem and R. Machleidt, Phys. Rev. C **68**, 041001(R) (2003).
- 8) R. J. Charity et al., Phys. Rev. Lett. **97**, 162503 (2006).
- 9) R. J. Charity et al., Phys. Rev. C **76**, 044314 (2007).

\* Theoretical Nuclear Physics Laboratory, RIKEN Nishina Center, Japan

# Ab-initio Green's Functions Calculations of Atoms

C. Barbieri,<sup>\*1</sup> and D. Van Neck,<sup>\*2</sup>

Density functional theory (DFT) allows for accurate calculations of ground states energies, while only single-particle (sp) equations must be solved. There is therefore a continuing interest in studying conceptual improvements and extensions to the DFT framework. An approach in this direction has been proposed in Ref.<sup>1)</sup> by developing a quasi-particle (QP)-DFT formalism, in which QP properties can be obtained along with ground state energies. Given the close relation between QP-DFT and the Green's functions (GF) formulation of many-body theory, we employ *ab initio* calculations in the latter formalism to investigate the structure of possible QP-DFT functionals. Recent advances in such calculations are reported below.

We employ the Faddeev random phase approximation (FRPA) expansion of the self-energy<sup>2,3)</sup>. This method explicitly accounts for coupling of electrons to particle-hole (ph) and two-particle (pp) or two-hole (hh) collective excitations of the system. The latter are obtained in the RPA framework. The FRPA method includes the *GW* approximation but goes further beyond since it accounts completely for exchange correlations at the 2p1h/2h1p level and it includes the propagation of pp/hh configurations.

	Hartree-Fock	FRPA	Exp. <sup>5,6)</sup>
He	-2.860 (+44)	-2.903 (+1)	-2.904
Be	-14.573 (+94)	-14.643 (+24)	-14.667
Ne	-128.547 (+281)	-128.917 (+11)	-128.928
Mg	-199.617 (+426)	-200.058 (-15)	-200.043

Table 1. Hartree-Fock and Faddeev-RPA binding energies (in Hartree) extrapolated from the cc-pVTZ and cc-pVQZ basis sets. The deviations from the experiment are indicated in parentheses (in mH). For Mg, the cc-pCV(TQ)Z bases were used.

Calculations were performed in the correlation consistent cc-pVTZ and cc-pVQZ gaussian bases for all atoms except for the ground state energies of Mg, for which the core-valence version cc-pCV(TQ)Z was used<sup>4)</sup>. The results were then extrapolated to the basis set limit according to  $E_X = E_\infty + AX^{-3}$ . Table 1 shows the results for the FRPA ground state energies and compares them to the experiment and the corresponding Hartree-Fock results. FRPA gives practically exact results for the two electron problem (He) and accounts for 96% of the correlation energy in the larger atoms. The atom of Be is an exception due to the pres-

<sup>\*1</sup> Theoretical Nuclear Physics Laboratory, RIKEN Nishina Center, Japan.

<sup>\*2</sup> Center for Molecular Modeling, Ghent University, Belgium.

	Hartree-Fock	FRPA	Exp. <sup>5,6)</sup>
He: 1s	0.918 (+14)	0.900 (-4)	0.904
Be: 2s	0.309 (-34)	0.322 (-21)	0.343
1s	4.733 (+200)	4.540 (+7)	4.533
Ne: 2p	0.850 (+57)	0.803 (+10)	0.793
1s	1.931 (+149)	1.795 (+13)	1.782
Mg: 3s	0.253 (-28)	0.277 (-4)	0.281
2p	2.281 (+161)	2.130 (+10)	2.12
Ar: 3p	0.590 (+11)	0.578 (-1)	0.579
3s	1.276 (+201)	1.065 (-10)	1.075
2p	9.570 (+410)	9.199 (+39)	9.160

Table 2. Ionization energies obtained from Hartree-Fock and the Faddeev-RPA method (in Hartree). All results are extrapolated from the cc-pVTZ and cc-pVQZ bases. The deviations from the experiment are given in mH.

ence of very soft excitations in the  $J^\pi=1^-, S=1$  channel which can drive the ph RPA equation to instability.

Ionization energies are shown in Tab. 2. The extrapolated results deviate from experiment by about 5 mH for the first ionization energies, while it increases to 10-15 mH for the separation of slightly deeper electron orbits. Schirmer and co-workers already pointed out the importance of a treatment that is consistent with at least third order perturbation theory<sup>7)</sup>. The present formulation of the FRPA fully includes of such correlations. At the same time, the explicit inclusion of RPA phonons holds the promise for successful applications to extended systems. Further work will be required to verify that this is indeed the case.

## References

- 1) D. Van Neck, S. Verdonck, G. Bonny, P. W. Ayers, and M. Waroquier, Phys. Rev. A **74**, 042501(2006).
- 2) C. Barbieri and W. H. Dickhoff, Phys. Rev. C **63**, 034313 (2001).
- 3) C. Barbieri, D. Van Neck and W. H. Dickhoff, Phys. Rev. A **76**, 052503 (2007).
- 4) C. Barbieri and D. Van Neck, arXiv:0901.1735v1 [physics.chem-ph], (2009).
- 5) NIST Atomic Spectra Database, NIST Standard Reference Database #78, <http://physics.nist.gov/PhysRefData/ASD/in-dex.html>
- 6) A. Thompson *et al.*, *X-ray Data Booklet* (Lawrence Berkeley National Laboratory, Berkeley, CA, 2001), and references cited therein.
- 7) O. Walter and J. Schirmer, J. Phys. B:At. Mol. Phys. **14**, 3805 (1981).

# Thermodynamical ensemble treatments of nuclear pairing in a multilevel model

N. Quang Hung, <sup>\*1</sup>and N. Dinh Dang

[NUCLEAR STRUCTURE, thermodynamic ensembles, superfluid-normal phase transition, thermal fluctuations, selfconsistent quasiparticle RPA, exact solution of pairing problem.]

The thermodynamic properties of infinite systems, such as superfluidity or superfluid-normal (SN) phase transition, are usually described by three principal ensembles, namely the grand canonical ensemble (GCE), canonical ensemble (CE) and micro canonical ensemble (MCE). The GCE consists of identically systems in thermal equilibrium, each of which shares its energy and particle number with an external heat bath. The CE is also in contact with the heat bath, but the particle number is fixed, whereas the MCE is an ensemble of thermally isolated system sharing the same energy and particle number. In thermodynamic limit, fluctuations of energy and particle number are zero, therefore three types of ensembles offer the same average values for thermodynamic quantities. However, the discrepancies between the predictions by these ensembles arise when thermodynamics is applied to small systems such as atomic nuclei or nanometer-size clusters.

In the present work, we carry out a systematic comparison of predictions for nuclear pairing properties obtained by averaging the exact solutions of the pairing problem<sup>1)</sup> in three principal thermodynamic ensembles as well as those offered by recent microscopic approaches to thermal pairing. For the latter, we choose the unprojected and particle-number projected versions of the FTBCS1+SCQRPA, which we recently developed in Ref.<sup>2)</sup>.

The numerical calculations are performed for the pairing gap, total energy, heat capacity, entropy, and microcanonical temperature within the doubly-folded equidistant multilevel pairing model. The results obtained show that the sharp SN phase transition, which is predicted by the conventional finite-temperature BCS (FTBCS) theory, is smoothed out in exact calculations within all three principal ensembles. The results obtained within the GCE and CE are very close to each other even for systems with small number of particles. As for the MCE, although it can be used to study the pairing properties of isolated systems at high excitation energies, there is a certain ambiguity in the temperature extracted from level density due to the discreteness of a small-size system. This ambiguity depends on the shape and parameter of the distribution employed to smooth the discrete level density. We found that, in this respect, the Gaussian distribution gives the best fit for both of the temperature and entropy to the canonical values. The predictions by

<sup>\*1</sup> On leave of absence from the Institute of Physics, Vietnam

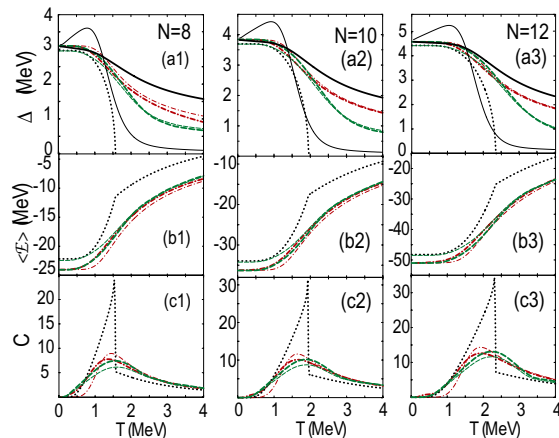


Fig. 1. Pairing gaps  $\Delta$ , total energies  $\langle \mathcal{E} \rangle$ , and heat capacities  $C$  as functions of temperature  $T$ , obtained within a doubly-folded equidistant multilevel pairing model for  $N = 8, 10$ , and  $12$  particles and pairing interaction parameter  $G = 0.9$  MeV. The dotted, thin dashed, thick dashed, thin dash-dotted and thick dash-dotted lines denote the FTBCS, FTBCS1+SCQRPA, FTLN1+SCQRPA, CE, and GCE results, respectively. The thin solid line shows the pairing gap obtained from the simple extension of the odd-even mass formula to  $T \neq 0$ , whereas the thick solid line represents the improved one.

the FTBCS1+SCQRPA and FTLN1+SCQRPA (i.e. FTBCS1+SCQRPA with Lipkin-Nogami's particle-number projection) are found in reasonable agreement with the GCE and CE results. The best agreement is seen between the FTLN1+SCQRPA and the GCE ones (See Fig. 1). We also suggest a novel formula to extract the pairing gap at finite temperature from the difference of total energies of even and odd systems, where the contribution of uncorrelated single-particle motion is subtracted. The new formula predicts a pairing gap in much better agreement with the canonical gap than the simple finite-temperature extension of the odd-even mass formula [See Figs. 1 (a1), (a2) and (a3)].

## References

- 1) A. Volya, B.A. Brown, and V. Zelevinsky: Phys. Lett. B 509 (2001) 37.
- 2) N. Dinh Dang and N. Quang Hung: Phys. Rev. C **77**, 064315 (2008).

# BCS-BEC transition in finite systems

N. Dinh Dang, N. Quang Hung, P. Schuck\*<sup>1</sup>

[NUCLEAR STRUCTURE, pairing, superfluid-normal phase transition, BCS theory, quasi-particle RPA, BCS-BEC transition]

Superfluidity and superconductivity in infinite systems are well described by the Bardeen-Cooper-Schrieffer (BCS) theory, which is a mean-field approach that shows the occurrence of pairing correlations forming the condensate. The collapse of the BCS pairing gap at a critical temperature  $T_c^{BCS}$  signals the transition from the superfluid phase to the normal one. In the normal state the mean-field theory cannot describe two-body correlations. Nozières and Schmitt-Rink (NSR)<sup>1)</sup> made an attempt to incorporate the effect of correlations on  $T_c$  in the electron-hole systems. In the weak coupling limit, the authors found the ordinary  $T_c^{BCS}$ . In the strong coupling limit, they found that the system is characterized by the non-interacting boson bound states that can undergo a Bose-Einstein condensation (BEC) at a specific critical temperature. NSR demonstrated a smooth transition from the strong to weak coupling limit (BCS-BEC transition).

However, NSR neglected the effect of the mean field created by the pairs. This effect is included in our selfconsistent quasiparticle random-phase approximation (SCQRPA)<sup>2)</sup>, which constitutes a fully selfconsistent extension of the NSR approach. The present study searches for the BCS-BEC transition in finite systems by using an exactly solvable doubly folded multilevel pairing model, for which the SCQRPA has been applied with success to describe the pairing correlations beyond the mean field. The model consists of  $\Omega$  equidistant levels with energies  $\epsilon_k = k-1$  (MeV) ( $k = 1, \dots, \Omega$ ), i.e. positive except for the bottom of the spectrum with  $\epsilon_1 = 0$ . These levels interact via a constant attractive pairing force. If the interaction is sufficiently strong, two fermions form a singlet bound pair, whose minimum energy is  $-\epsilon_1$  with  $\epsilon_1$  being the binding energy. The internal wave function  $\phi_k$  of the pair creation extends over a characteristic distance  $a_0 \sim \epsilon_1^{-1/2}$ . If two bound pairs have only a small overlap ( $|\phi_k| \ll 1$ ), they can be treated as a gas of structureless bosons. When this happens, the BCS equation reduces, in leading order, to the Schrödinger equation for a single bound pair, whose eigenvalue is the pair chemical potential  $\mu_P \equiv 2\lambda$ . Its zeroth order yields  $2\lambda = \epsilon_1$ , as for an ideal Bose gas. This means that  $\mu_P$  reaches the bottom of the single-particle spectrum. As  $\epsilon_1$  is chosen to be zero, this means  $\lambda$  vanishes. We found that, for a half-filled ( $N = \Omega$ ) or underfilled system ( $N < \Omega$ ) at zero tem-

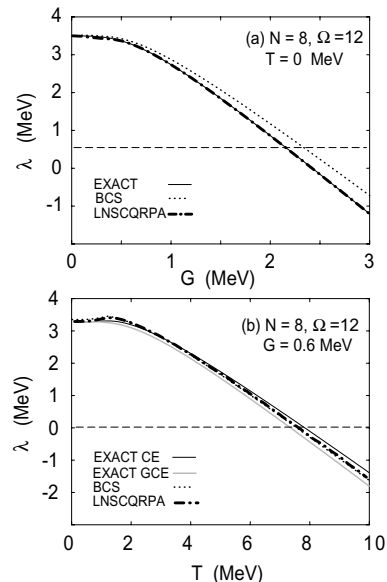


Fig. 1. Chemical potential  $\lambda$  for  $N = 8$  and  $\Omega = 12$  as a function of  $G$  at zero temperature  $T$  (a), and as a function of  $T$  at  $G = 0.6$  MeV (b) as predicted by the exact canonical and grand-canonical calculations as well as the BCS and LNSCQRPA theories.

perature ( $T = 0$ ),  $\lambda$  reaches zero at a certain value  $G = G_c$  (Fig. 1), higher than which it turns negative and continues to decrease with increasing  $G$ . We also found that at  $G < G_c$ , the chemical potential  $\lambda$  decreases with increasing  $T$ , and eventually crosses zero at  $T = T_c \gg T_c^{BCS}$ . The fact that the predictions by the SCQRPA with particle-number projection within the Lipkin-Nogami (LN) method (the LNSCQRPA) agree very well with the exact results up to a moderate temperature  $T$  shows that the SCQRPA is indeed a promising approach to study the BCS-BEC transition in finite systems. Several calculations to check if a finite system of pair fermions reaches that of bosons in the BEC limit within the SCQRPA at  $T \neq 0$  are now underway. Tests in realistic neutron-rich nuclei are being carried out as well.

## References

- 1) P. Nozières and S. Schmitt-Rink, J. Low Temp. Phys. **59**, 195 (1985).
- 2) N. Quang Hung and N. Dinh Dang, Phys. Rev. C **76**, 054302 (2007); Ibid **77**, 064315 (2008).

\*<sup>1</sup> Institut de Physique Nucléaire, Orsay, France

***t*-band and tilted axis rotation in  $^{182}\text{Os}$** Y. Hashimoto,\*<sup>1</sup> and T. Horibata \*<sup>2</sup>

We have proposed that there is a case where the *s*-band states become unstable against the tilting of a rotational axis in  $^{182}\text{Os}$ <sup>1)</sup>. We carried out intensive tilting calculations and found the so-called tilted axis rotational (TAR) states<sup>2)</sup> which are stable against the tilting of a rotational axis for each angular momentum state from  $J = 16\hbar$  to  $30\hbar$  in  $^{182}\text{Os}$ . Each of the TAR states seems to form a band which has nearly constant  $K \sim 7.5$ . This new band has lower energy than the *s*-band and appears as a yrast beyond  $J = 18\hbar$ <sup>3)</sup>. We expect this portion of new band structure may support Walker's long-standing prediction that the *t*-band is responsible for the occurrence of backbending in the  $A \sim 180$  region<sup>4)</sup>. In this article, we report some of our results on the band structure consisting of the TAR states.

The tilt angle  $\psi$  is measured from the x-axis and is perpendicular to the symmetry axis(z-axis) along the prime meridian. The wave function  $|\Phi(\psi)\rangle$  with tilt angle  $\psi$  is obtained by solving the 3D-CHFB equation with the pairing plus quadrupole Hamiltonian<sup>2)</sup>.

In Fig. 1, we plot the energies of the *s*-branches<sup>1)</sup> for several angular momentum states. The shapes of the *s*-branches vary smoothly for all tilt angles  $\psi$  from  $0^\circ$  to  $90^\circ$  as the angular momentum value is increased. Each curve has a minimum point (TAR state) and their positions shift gradually toward the smaller tilt angle region as the angular momentum increases.

The approximate  $K$  quantum number of each TAR state is estimated by calculating the projection of the angular momentum along the z-axis at the minimum point. In Table 1, we show the projections  $J \sin(\psi)$  of the angular momenta  $J$  from  $18\hbar$  to  $30\hbar$  which are shown in Fig. 1. Since the values of the projections are almost constant, it is expected that the family of the states at the minimum points of the *s*-branches form a band (TAR band).

We are now looking for the rest part of the band including a band head state ( $J = 8\hbar$ ) which must exist in the region just above the *g*-band below the  $J = 18\hbar$  band crossing point. This will require some more elaborate calculation techniques.

## References

- 1) Y.Hashimoto and T.Horibata: Phys.Rev.**C74**, 017301(2006).
- 2) T. Horibata and N. Onishi: Nucl.Phys.**A596**, 251-284(1996).
- 3) Y.Hashimoto and T.Horibata: Eur.Phys.J. A, accepted.
- 4) P.M. Walker et al.: Phys.Lett. **B309**, 17-22(1993).

\*<sup>1</sup> Graduate School of Pure and Applied Sciences, University of Tsukuba

\*<sup>2</sup> Faculty of Software and Information Technology, Aomori University

Table 1. Projection of angular momentum along z-axis at minimum points on the *s*-branches in Fig. 1

$J$	tilt angle $\psi$	$J \sin(\psi)$
18	$24^\circ$	7.3
22	$20^\circ$	7.3
24	$18^\circ$	7.6
26	$17^\circ$	7.6
28	$16^\circ$	7.7
30	$15^\circ$	7.8

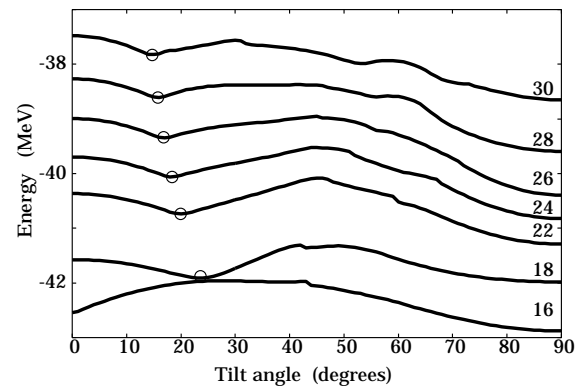


Fig. 1. Plot of energies of *s*-branches. Figures indicate the angular momentum  $J$ . Circles indicate minimum points of each curve.

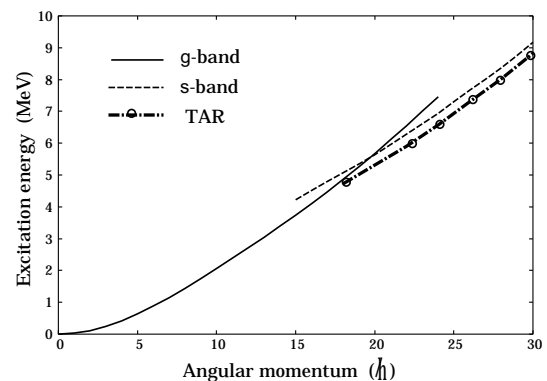


Fig. 2. Plot of energies of minimum points on *s*-branches in Fig. 1 (dash-dotted curve with circles labelled "TAR"). Circles on dash-dotted curve correspond to the position of minimum points labelled with circles in Fig. 1.

# Origin of the narrow, single peak in the fission-fragment mass distribution for $^{258}\text{Fm}^\dagger$

T. Ichikawa A. Iwamoto,<sup>\*1</sup> and P. Möller<sup>\*2</sup>

[Nuclear reaction, fission, Macroscopic-Microscopic model]

In spontaneous fission of Fm isotopes, the fragment mass distributions change abruptly from a double-peaked, broad, mass-asymmetric distribution for  $^{256}\text{Fm}$  to a single-peaked, very narrow, symmetric distribution for  $^{258}\text{Fm}$ .<sup>1,2)</sup> In addition, the kinetic-energy distribution of  $^{258}\text{Fm}$  can be expressed as the sum of a low-energy and a high-energy component, whose mean energies differ by about 35 MeV. The mechanism behind this phenomenon, referred to as the bimodal fission, is the strong nuclear shell effects that emerge when the mass-symmetric fission fragments are near the doubly magic nucleus  $^{132}\text{Sn}$ . The emergence of mass-symmetric divisions in  $^{258}\text{Fm}$  is thus qualitatively explained if one takes into account the emergence of a fission path strongly stabilized by the fragment shell effect,<sup>3)</sup> but quantitative understanding of the extremely narrow mass distribution has been less extensively studied.

So far, theoretical investigations have mainly focused on obtaining those fission paths by calculating the potential energy surface. In fact, theoretical models, such as the macroscopic-microscopic model,<sup>4)</sup> the constrained Hartree-Fock+BCS (HFBCS) model,<sup>5)</sup> and the constrained Hartree-Fock-Bogoliubov (HFB) model,<sup>6)</sup> have successfully described such shell-stabilized path, that is, a path leading to mass-symmetric divisions with compact scission configurations, referred to as the compact symmetric path. In this sense, the energy-minimum path leading to the compact symmetric fission has been well established, but the structure of a *potential valley* along the path has not been clarified. As long as the fragment mass yield curve is concerned, it is necessary to obtain the potential energy curve at the scission configurations as a function of the fragment mass number.

We discuss the origin of the narrowness of the single peak at mass-symmetric division in the fragment mass-yield curve for spontaneous fission of  $^{258}\text{Fm}$ .<sup>7)</sup> For this purpose, we employ the macroscopic-microscopic model and calculate a potential-energy curve at the mass-symmetric compact scission configuration, as a function of the fragment mass number, which is obtained from the single-particle wave-function densities. In the calculations, we minimize total energies by varying the deformations of the two fragments, with

constraints on the mass quadrupole moment, and by keeping the neck radius zero. The energies thus become functions of mass asymmetry. Using the obtained potential, we solve the one-dimensional Schrödinger equation with a microscopic coordinate-dependent inertial mass to calculate the fragment mass-yield curve, and estimate the mass yield curve originating from the compact symmetric valley.

An important point in the calculation is that the fragment masses are defined by the single-particle wave functions, rather than the macroscopic potential volumes. Using the Nilsson diagram at the scission point of the compact symmetric valley, we have shown that the mass numbers of two nascent fragments strongly depend on the single-particle configurations. In particular, the proton number of the fission fragments originating from the compact symmetric valley for  $^{258}\text{Fm}$  is strongly constrained to  $Z = 50$  due to the large shell gap. The calculated mass-yield curve is consistent with the extremely narrow experimental mass-yield curve. We obtain that the full width at half maximum for the fission fragments distribution originating from the compact symmetric valley is 3.6 u. For  $^{258}\text{Fm}$ , it would be interesting to measure the ratio of protons to neutrons on the mass-yield curve, because the neutron distribution may be wider than the proton distribution, because the mean fragment neutron number is not magic. This would be a very strong test of the mechanism behind the narrow mass distribution.

## References

- 1) D. C. Hoffman et al.: Phys. Rev. **C21**, 972 (1980).
- 2) E. K. Hulet et al.: Phys. Rev. Lett. **56**, 313 (1986).
- 3) D. C. Hoffman and M. R. Lane: Radiochim. Acta **70/71**, 135 (1995).
- 4) P. Möller, J. R. Nix, and W. J. Swiatecki: Nucl. Phys. **A469**, 1 (1987).
- 5) L. Bonneau: Phys. Rev. **C74**: 014301 (2006).
- 6) M. Warda, J. L. Egido, L. M. Robledo, and K. Pomorski: Phys. Rev. **C66**, 014310 (2002).
- 7) T. Ichikawa, A. Iwamoto, and P. Möller: Phys. Rev. **C79**, 014305 (2009).

<sup>†</sup> Condensed from the article in Phys. Rev. **C79**, 014305 (2009)

<sup>\*1</sup> Japan Atomic Energy Agency

<sup>\*2</sup> Los Alamos National Laboratory, USA

## Neutron vortices in neutron stars

P. Avogadro<sup>\*1</sup>, F. Barranco<sup>\*2</sup>, R.A. Broglio<sup>\*1\*3\*4</sup>, E. Vigezzi<sup>\*1</sup>

[neutron vortices, neutron stars, superfluidity, glitches]

Since their discovery neutron stars have proved to be an exceptional laboratory where many aspects of physics not on earth can take place. One aspect of neutron stars that still has to be fully explained is the phenomenon of “glitches”. A pulsar is a fast rotating neutron star whose period is very stable. The period decreases with time because of the constant energy emission of the star itself. During a glitch a pulsar undergoes a sudden angular velocity speed up, and then the frequency of the star undergoes a relaxation period after which the “normal” speed down rate is recovered. It has been proved that glitches are related to rearrangements of the structure of the star<sup>2)</sup> and one of the most promising models<sup>1)</sup> relates glitches to the superfluid present in the inner crust of the star. This superfluid is essentially decoupled from the rest of the star and acts as a reservoir of angular momentum. Since the angular momentum in a rotating superfluid is carried by the vortices that form therein investigation of the interaction between neutron vortices and the environment is of key importance in understanding the glitch phenomenon. According to a generally accepted picture, from the surface into the center of a neutron star the density increases and one encounters layers with a different structure. The outer crust of a neutron star is composed of heavy, neutron-rich nuclei, which get closer and closer until all neutron bound levels are filled and the drip line is reached. This represents the beginning of the inner crust, which extends from about  $4.6 \cdot 10^{11}$  g/cm<sup>3</sup> to about  $1.6 \cdot 10^{14}$  g/cm<sup>3</sup> (the saturation density in nuclei being  $n_0 = 2.8 \cdot 10^{14}$  g/cm<sup>3</sup>). The inner crust consists of a Coulomb lattice of nuclei embedded in a sea of free neutrons. The lattice step decreases with increasing density. We have limited ourselves to densities smaller than  $n_0/4$ , where nuclei can be assumed to be spherical. For such densities, the neutron sea should be superfluid, in keeping with the fact that the temperature of the neutron star should have dropped to about 0.01 MeV a few hundred years after its formation.

We have divided the inner crust into cylindrical cells where we have solved the Hartree Fock Bogoliubov equations with four different Skyrme interactions reproducing a vortex plus nucleus system. The result of the calculations shows that a vortex cannot form in the nuclear volume<sup>3)</sup> at least at low and medium density,

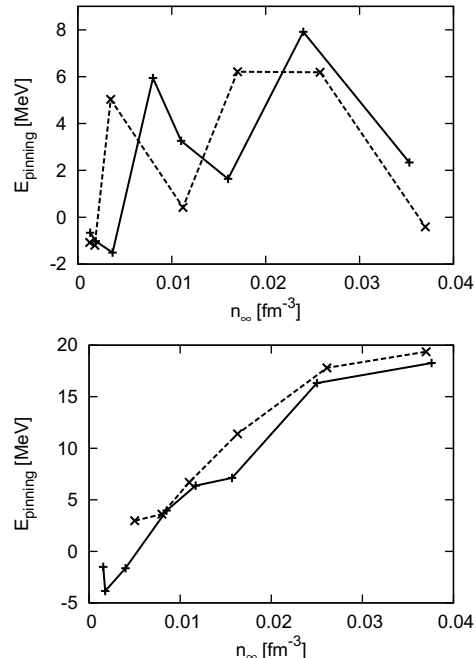


Fig. 1. Pinning energy for the SLy4 (solid) and SII (dashed) curves; (lower figure) the same but with SkM\* (solid) and SGII (dashed) curves.

while at high density the choice of the Skyrme interaction adopted may change this picture (in particular the SkM\* and SGII interaction lead to a vortex penetrating in the nuclear volume at high density, while for the SLy4 and SII interactions this is still forbidden). The impossibility a vortex penetrate the nuclear volume is shown by the complete suppression of the pairing gap in this region, which means that the region where the vortex and the nucleus are present is essentially no longer superfluid and thus the current flow is suppressed. The difference between the different Skyrme interactions is evident when calculating the energy to remove a vortex from a nucleus (the pinning energy) as shown in Fig [1].

### References

- 1) P.W. Anderson and N. Itoh, *Nature* **256** (1975).
- 2) B. Link, R.I. Epstein, and J.M. Lattimer, *Phys. Rev. Lett.* **83** (1999).
- 3) P. Avogadro, F. Barranco, R.A. Broglio, and E. Vigezzi, *Phys. Rev.* **C75** (2007).

† Condensed from the article in *Nucl. Phys. A* 811 378 (2008)

\*1 INFN, Milan

\*2 Universidad de Sevilla

\*3 Universita' degli studi di Milano

\*4 The Niels Bohr Institute

# Direct reactions of antiproton and the black-sphere picture

A. Kohama, K. Iida,<sup>\*1</sup> and K. Oyamatsu<sup>\*2</sup>

[Nuclear reaction, reaction cross section, nuclear radius, antiproton]

Nuclear size and mass are fundamental quantities characterizing the bulk properties of nuclei. Recently, for the purpose of deducing nuclear size from proton-nucleus elastic scattering and reaction cross sections, we proposed a model in which a nucleus is viewed as a “black” sphere of radius  $a$ .<sup>1,2)</sup> Here we assume that the target nucleus is strongly absorptive to the incident proton and hence acts like a black sphere. Another requirement for the black-sphere picture is that the proton wave length is considerably smaller than the nuclear size. For proton incident energies higher than about 800 MeV, these requirements are basically satisfied. We showed that, for proton beams incident on stable nuclei, the cross section of a black sphere of radius  $a$  ( $= \pi a^2$ ), which was determined by fitting the angle of the first peak calculated for proton elastic diffraction by a circular black disk of radius,  $a$ , to the measured value, is consistent with the measured total reaction cross section.<sup>2)</sup> Furthermore, we confirmed that the black-sphere picture is valid down to about 100 MeV of an incident proton kinetic energy.<sup>3,4)</sup>

This consistency suggests that the black sphere radius corresponds to a “reaction radius” inside which the reaction with incident protons occurs. Combining this fact with the notion of the “optical depth” of nuclei, which is defined by the ratio of the length of the proton trajectory inside the nucleus to the mean-free path of the proton, we constructed a formula for total reaction cross sections of proton-nucleus/nucleus-nucleus reactions, which is applicable for the reactions of wide region of mass and energy.<sup>3)</sup>

In this work, we extend this black-sphere picture to the processes of several hadronic probes, such as antiprotons, pions, kaons, with stable nuclei. Although the black-sphere picture is originally expected to provide a decent description of the reaction cross section for any kind of incident particle that tends to be attenuated in nuclear interiors, whether this extension could make sense or not is not obvious.

As a first step, we systematically analyze the data of antiproton elastic scattering and reaction cross section for stable nuclei at the antiproton incident energies of lower than about 1000 MeV. The numerical results of  $\sigma_{BS}$  for antiproton-carbon(copper) are plotted in Fig. 1. They are consistent with the empirical values of  $\sigma_R$  although the values of  $\sigma_{BS}$  as well as  $\sigma_R$  contains large uncertainties. These preliminary results are encouraging, and the analyses of the data for other

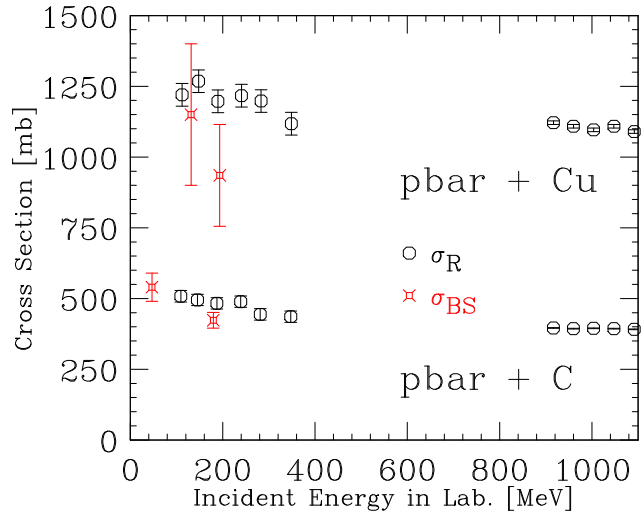


Fig. 1. Absorption cross section,  $\sigma_{BS}(= \pi a^2)$ , of an antiproton on a carbon(copper) target as a function of the incident kinetic energy of the antiproton. For comparison, we plot empirical data for the antiproton-carbon total reaction cross section,  $\sigma_R$  ( $\circ$ ), whose references are found in Ref.<sup>5)</sup>.

hadronic probes are in progress.

In the energy region under consideration, the total cross sections of antiproton-proton are about five times larger than those of proton-proton, which implies shorter mean-free path of an antiproton than that of a proton at the same kinetic energy and the same nuclear density. According to the results of Ref.<sup>3)</sup>, protons are only sensitive to the nuclear surface, where the optical depth to the proton is the order of one.<sup>3)</sup> Then, we can expect that an antiproton is sensitive to the outer surface of nuclei, where the optical depth to the antiproton is the order of one. This will open up a possibility of studying nuclear surface structure, which would control diffractive reactions, using several hadronic probes.

## References

- 1) A. Kohama, K. Iida, and K. Oyamatsu: Phys. Rev. C **69**, 064316 (2004).
- 2) A. Kohama, K. Iida, and K. Oyamatsu: Phys. Rev. C **72**, 024602 (2005).
- 3) K. Iida, A. Kohama, and K. Oyamatsu: J. Phys. Soc. Japan **76**, 044201 (2007).
- 4) A. Kohama, K. Iida, and K. Oyamatsu: Phys. Rev. C **78**, 061601(R) (2008).
- 5) C. J. Batty *et al.*: Adv. Nucl. Phys. **19**, 1 (1989).

<sup>\*1</sup> Department of Natural Science, Kochi University

<sup>\*2</sup> Department of Media Theories and Production, Aichi Shukutoku University

# Light $\Xi$ hypernuclei in four-body cluster models<sup>†</sup>

E. Hiyama<sup>1</sup>, Y. Yamamoto,<sup>\*1</sup> T. Motoba,<sup>\*2</sup> Th. A. Rijken,<sup>\*3</sup> and M. Kamimura

[hypernuclei, cluster model, hyperon-nucleon interaction]

In studies of nuclear interactions, two-body scattering data are the primary input for characterizing interaction models. However,  $S = -1$  hyperon (Y)-nucleon (N) scattering data are very limited because of experimental issues. For  $S = -2$  interactions such as  $\Lambda\Lambda$  and  $\Xi N$ , there are currently no scattering data. Therefore, the existing  $YN$  and  $YY$  interaction models have a substantial degree of ambiguity. Some  $YN$  scattering experiments will be performed at the Japan Proton Accelerator Research Complex (J-PARC) in the near future. Even in this facility, the possibility of performing  $\Xi N$  or  $\Lambda\Lambda$  scattering experiments is very limited or practically impossible. Hence, in order to obtain useful information on  $S = -2$  interactions, studies of many-body, hypernuclear structure are indispensable.

Our intention in this work is to investigate the possible existence of  $\Xi$  hypernuclei and to explore the properties of the underlying  $\Xi N$  interactions. Identification of  $\Xi$  hypernuclei in coming experiments at J-PARC will contribute significantly to understanding nuclear structure and interactions in  $S = -2$  systems, which can lead to an entrance into the world of multi-strangeness. In order to encourage new experiments seeking  $\Xi$  hypernuclei, it is essential to make a detailed theoretical investigation of the possible existence of bound states, despite some uncertainty in contemporary  $\Xi N$  interaction models. We investigate here the binding energies and structure of  $\Xi$  hypernuclei produced by  $(K^-, K^+)$  reactions on light targets on the basis of microscopic cluster models. One of the primary issues is how to choose the  $\Xi N$  interaction. For this purpose, we adopted  $G$ -matrix  $\Xi N$  interactions derived from the Nijmegen interaction models such as extended soft core model(ESC)<sup>1</sup> and Nijmegen model D (ND)<sup>2</sup>, which gives rise to substantially attractive  $\Xi$ -nucleus potentials in accordance with the experimental indications. The interactions are represented as  $k_F$ -dependent three-ranged Gaussian form potential.

In this report, the structure calculations in  ${}^7_{\Xi}\text{H}$  and  ${}^{10}_{\Xi}\text{Li}$  are performed within the framework of the microscopic four-body cluster models using the Gaussian Expansion Method, since these light  $\Xi$  hypernuclei can be described in the framework of four-body cluster model.

The calculated energies in the  $1/2^+$  ground state for  ${}^7_{\Xi}\text{H}(\alpha nn \Xi^-)$  and  $1^-$  and  $2^-$  state for  ${}^{10}_{\Xi}\text{Li}(\alpha \alpha n \Xi^-)$

using ESC are demonstrated in Fig.1 as a function of  $k_F$ .

In  $A=7$  hypernucleus, the four-body calculation predicts the existence of nuclear bound states in ESC case at reasonable  $k_F$  values of around  $0.9 \text{ fm}^{-1}$ . It is interesting to note that the addition of two neutrons to the  $\alpha \Xi^-$  system gives rise to about 1.3 MeV more binding energy. The same tendency is seen in ND.

In  $A=10$  hypernucleus, we have obtained the nuclear  $\Xi^-$  bound states as a result of careful four-body calculations with  $k_F \sim 1.0 \text{ fm}^{-1}$ . Furthermore, we have similar binding energies of the  $J = 2^-$  state for both the ESC and ND interactions.

## References

- 1) Th. A. Rijken and Y. Yamamoto, Phys. Rev. **C73**, 044008 (2006).
- 2) M. M. Nagels, T. A. Rijken, and J. J. deSwart, Phys. Rev. **D15**, 2547 (1977).

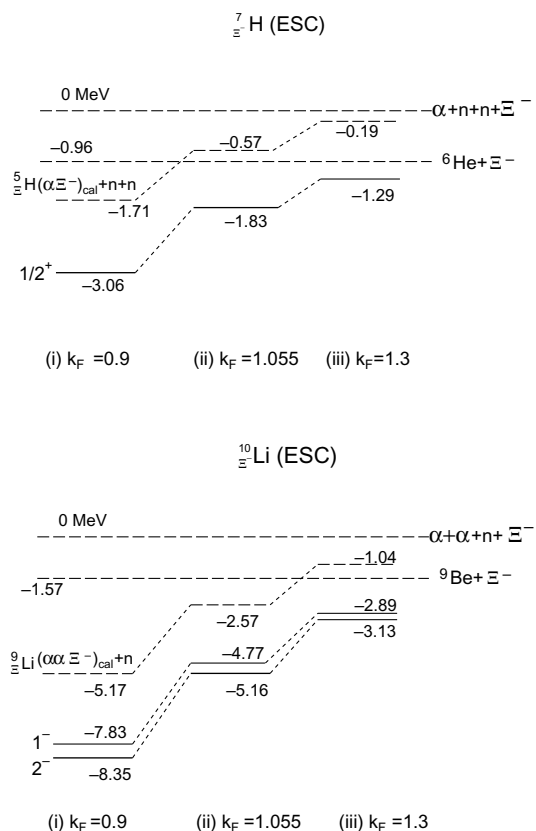


Fig. 1. Calculated energy levels of (a)  ${}^7_{\Xi}\text{H}$  and (b)  ${}^{10}_{\Xi}\text{Li}$  for three  $k_F$  values using ESC.

<sup>†</sup> Condensed from the article in Phys. Rev. C. **78**, 054316(2008)

<sup>\*1</sup> Physics Section, Tsuru University

<sup>\*2</sup> Laboratory of Physics, Osaka Electro-Communication University

<sup>\*3</sup> Institute for Theoretical Physics, University of Nijmegen

# $p\Xi^0$ force studied with lattice QCD<sup>†</sup>

H. Nemura, N. Ishii,<sup>\*1</sup> S. Aoki,<sup>\*2,\*3</sup> and T. Hatsuda<sup>\*4</sup>

[ Lattice QCD, Hyperon-nucleon interaction, Nuclear forces, Hypernuclei]

Study of the baryon-baryon interaction is an important subjects in the nuclear physics. The present hyperon-nucleon ( $YN$ ) and hyperon-hyperon ( $YY$ ) interactions have large uncertainties despite these interactions playing important roles in high density nuclear systems such as interior of neutron stars. For example, no reliable phase shift analysis of the  $\Lambda N$  scatter-

Table 1. Meson masses in the unit of MeV. The numbers in parenthesis show the errorbar in the last digit.

$\kappa_{ud}$	$N_{conf}$	$m_\pi$	$m_\rho$	$m_K$	$m_{K^*}$
0.1678	1283	368(1)	813(4)	554.0(5)	884(2)
0.1665	1000	511.2(6)	861(2)	605.3(5)	904(2)
Exp.		135	770	494	892

Table 2. Baryon masses in the unit of MeV. The numbers in parenthesis show the errorbar in the last digit.

$\kappa_{ud}$	$N_{conf}$	$m_N$	$m_\Lambda$	$m_\Sigma$	$m_\Xi$
0.1678	1283	1167(7)	1266(6)	1315(6)	1383(6)
0.1665	1000	1300(4)	1354(4)	1375(4)	1419(4)
Exp.		940	1116	1190	1320

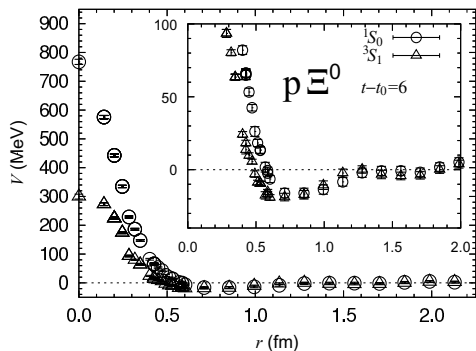


Fig. 1. The effective central potential for  $p\Xi^0$ , in the  $^1S_0$  (circle) and  $^3S_1$  (triangle), obtained from the wave function at time slice  $t - t_0 = 6$ . The hopping parameter  $\kappa_{ud} = 0.1678$  is used for the  $u, d$  quark. The inset shows its enlargement.

<sup>†</sup> Condensed from the article<sup>1)</sup>.

<sup>\*1</sup> Center for Computational Sciences, University of Tsukuba, Japan

<sup>\*2</sup> Graduate School of Pure and Applied Sciences, University of Tsukuba, Japan

<sup>\*3</sup> Riken BNL Research Center, Brookhaven National Laboratory, Upton, New York 11973, USA

<sup>\*4</sup> Department of Physics, University of Tokyo, Japan

ing has as yet been performed experimentally so that different phaseshifts have been predicted by different theoretical works. In principle, the interaction should be understood in terms of the dynamics of quarks and gluons, namely quantum chromodynamics (QCD).

We study the  $p\Xi^0$  force by using quenched lattice QCD. The Bethe-Salpeter amplitude is calculated for the lowest scattering state of the system so as to obtain the  $p\Xi^0$  potential. The numerical calculation is performed with  $\beta = 5.7$ , the lattice spacing of  $a = 0.1416(9)$  fm, on the  $32^3 \times 32$  lattice. The spatial lattice volume is  $(4.5 \text{ fm})^3$ . Two kinds of  $ud$  quark mass are used, corresponding to  $m_\pi \simeq 0.37$  GeV and 0.51 GeV. Tables 1-2 compare the hadron masses calculated from the lattice QCD with the experimental values. Figure 1 shows the effective central potential, obtained from the wave function at the time slice  $t - t_0 = 6$  with the hopping parameter  $\kappa_{ud} = 0.1678$ , corresponding to  $m_\pi \simeq 0.37$  GeV. The scattering length is obtained from Lüscher's formula.<sup>2)</sup> As is seen in Figure 2, the  $p\Xi^0$  interaction is both attractive at  $^1S_0$  and  $^3S_1$  channels, and the interaction in the  $^3S_1$  is more attractive than in the  $^1S_0$ . These attractive forces become stronger as the  $u, d$  quark mass decreases.

We are also calculating the  $p\Lambda$  potential by using  $(2+1)$ -flavor PACS-CS gauge configuration<sup>3)</sup>, which will be reported elsewhere.

## References

- 1) H.Nemura, N.Ishii, S.Aoki and T.Hatsuda, arXiv:0806.1094 [nucl-th].
- 2) M. Lüscher, Nucl. Phys. B **354**, 531 (1991).
- 3) S. Aoki, *et al.* [PACS-CS Collab.], arXiv:0807.1661 [hep-lat].

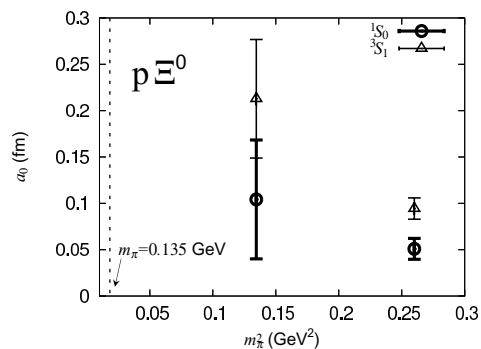


Fig. 2. The scattering lengths for  $p\Xi^0$  in the  $^1S_0$  (circle) and  $^3S_1$  (triangle) as a function of  $m_\pi^2$ . The dashed line shows the physical point at  $m_\pi = 0.135$  GeV.

# Hadro-Chemistry for High Momentum Probes of Heavy Ion Collisions<sup>†</sup>

R. J. Fries,<sup>\*1,\*2</sup> and W. Liu<sup>\*1</sup>

[Heavy ion collisions, quark gluon plasma]

Jet quenching, the suppression of hadrons emitted at high momentum  $p_T$ , has been one of the key discoveries in nuclear collisions at the Relativistic Heavy Ion Collider (RHIC). It has been interpreted as the energy loss of fast quarks or gluons traveling through quark gluon plasma. It is a main signature for the creation of a quark gluon plasma<sup>1</sup>). Energy loss is characterized by the transport coefficient  $\hat{q} = \mu^2/\lambda$ , the momentum transferred squared per mean free path  $\lambda$ .

In a series of papers in 2008 we have argued that measurements of the suppression and elliptic flow of identified hadrons at high transverse momentum  $p_T$  can lead to novel and complimentary information about the medium created in nuclear collisions. In principle, the mean free path  $\lambda$  can be extracted independent of  $\hat{q}$ . In simple terms, this is possible because the processes between jets and the medium which change the chemical composition are generally independent of the momentum transfer in the process.

We use a model in which a sample of leading jet partons is propagated through a fireball parameterization. Partons lose energy, described by a Fokker-Planck equation, at a rate fitting the single inclusive nuclear suppression ratio  $R_{AA}$ . In addition, the jet particles are subject to rate equations

$$\frac{dN^a}{d\tau} = - \sum_b \Gamma^{a \rightarrow b} N^a + \sum_c \Gamma^{c \rightarrow a} N^c \quad (1)$$

in which conversion rates  $\Gamma$  between flavors  $a, b, c$  are given by leading order elastic cross sections. We evolve samples of up, down and strange quarks as well as gluons and photons. Conversions of jets into photons have been discussed in the past<sup>2</sup>) and it was recognized that this might be an important contribution to the total photon yield. Heavy quarks are taken into account with slight modifications reflecting the mass threshold.

We first revisit the issue of the relative suppression of protons and pions. It was pointed out that protons fragment predominantly off gluon jets, while pions prefer quark jets. Quenching of gluons and quarks is related via a color factor 9/4 which leads to the naive expectation that protons should exhibit stronger quenching than pions at high  $p_T$ . This is not observed at RHIC. It was first pointed out by Liu, Ko and Zhang that this can be explained naturally if the flavor of a

jet parton is not conserved<sup>3</sup>). They can explain the proton/pion ratio with conversions of quarks into gluons and vice versa, essentially rendering the concept of a fixed jet flavor invalid. We confirm the results of Liu et al. and suggest a novel double ratio observable, the ratio of the  $R_{AA}$ s for protons and pions as a very sensitive quantity for conversion processes. We also find a rate for conversion photons which is consistent with the experimental results.

As a novel idea we propose to use strangeness as a signal for jet conversions and as a strong candidate for a measurement that could constrain the mean free path. Strangeness at RHIC energies is marginal in the jet sample,  $s/(u+d) \approx 5\%$  while it is chemically equilibrated in the plasma. The coupling between jets and medium will increase the amount of strange quark jets and should result in a relative enhancement of kaons compared to pions at high  $p_T$ . Finding and measuring the size of this enhancement would be an important step to quantify jet medium interactions.

At LHC, strangeness is already equilibrated in the initial jet sample due to the higher center of mass energy and the importance of initial flavor-blind  $g+g$  fusion process. Hence we predict no additional strangeness enhancement at LHC energies. We have a similar negative result for charm and bottom quarks at both RHIC and LHC energies. The reason for this is the lack of chemical equilibration of heavy quarks even in the bulk. Therefore the chemical gradient between jets and medium is small. Of course, this result is consistent with heavy quark measurements at RHIC.

Finally, we discuss the implications of flavor conversions for elliptic flow  $v_2$ . Conversion particles should lead to a negative contribution to  $v_2$ , as was first discovered for conversion photons<sup>4</sup>). We could show that this mechanism is also active for strange quarks at RHIC and should lead to an observable suppression of kaon  $v_2$  at high  $p_T$  compared to pion  $v_2$ .

## References

- 1) J. Adams *et al.* [STAR Collaboration], Nucl. Phys. A **757**, 102 (2005). K. Adcox *et al.* [PHENIX Collaboration], Nucl. Phys. A **757**, 184 (2005).
- 2) R. J. Fries, B. Müller, and D. K. Srivastava, Phys. Rev. Lett. **90**, 132301 (2003); Phys. Rev. C **72**, 041902 (2005).
- 3) W. Liu, C. M. Ko and B. W. Zhang, Int. J. Mod. Phys. E **16**, 1930 (2007).
- 4) S. Turbide, C. Gale and R. J. Fries, Phys. Rev. Lett. **96**, 032303 (2006).

<sup>†</sup> Condensed from the articles in Phys. Rev. C **77**, 054902 (2008), Phys. Rev. C **78**, 037902 (2008), arXiv:0805.3721

<sup>\*1</sup> Texas A&M University, College Station, USA

<sup>\*2</sup> RBRC, Upton, USA

### **3. Hadron Physics**

# Absolute luminosity determination using the vernier scan technique at $\sqrt{s} = 62.4$ GeV

Y. Goto, A. Bazilevsky<sup>\*1</sup>, and R. Bennett<sup>\*2</sup> for the PHENIX Collaboration

Measured cross sections in the PHENIX experiment<sup>1)</sup> are normalized to the integrated luminosity for the analyzed data sample,  $L$ , which is determined from the number of events triggered by beam-beam counters (BBCs) using an absolute calibration of the BBC trigger cross section obtained via the van der Meer or Vernier scan technique<sup>2)</sup>. In a scan, the transverse widths of the beam overlap are measured by sweeping one beam across the other in steps while monitoring the BBC trigger rate. This information and the bunch intensities of the two beams measured by Wall Current Monitors (WCMs) are used to compute the instantaneous machine luminosity  $L_{\text{machine}}$ <sup>2)</sup>. The BBC trigger cross section is the ratio of the BBC trigger rate when the beams are overlapping maximally to the effective luminosity  $L_{\text{eff}} = L_{\text{machine}} \cdot \epsilon_{\text{vertex}}$ , where  $\epsilon_{\text{vertex}}$  is the fraction of the number of collisions in PHENIX interaction region (IR) within BBC trigger vertex cut (usually  $|z| < 30$  cm).

In  $p+p$  collisions at  $\sqrt{s} = 62.4$  GeV, the BBC trigger efficiency vs  $z$  shape was estimated from the comparison with a “detector unbiased”  $z$ -vertex distribution obtained from the convolution of colliding bunch intensity profiles along the  $z$ -axis as measured by WCMs. The correction factor of  $0.83 \pm 0.08$  was obtained, resulting in  $\epsilon_{\text{vertex}} = 0.37 \pm 10\%$ . This approach is confirmed in  $p+p$  collisions at  $\sqrt{s} = 200$  GeV where zero degree calorimeters (ZDCs) have enough efficiency to measure the  $z$  vertex distribution. The efficiency of the ZDCs (located at  $z = \pm 18$  m) does not depend on collision vertex position in PHENIX IR, which was distributed with a sigma of 0.5–0.7m around  $z = 0$ . The vertex distribution obtained with the WCMs is well reproduced by the measurement with the ZDCs at  $\sqrt{s} = 200$  GeV (Fig. 1(a)).

Beam focusing in the IR leads to bunch transverse sizes that vary away from the collision point ( $z = 0$ ) as  $\sigma^2(z) = \sigma^2(z = 0) \times (1 + z^2/\beta^{*2})$ . This is so-called hourglass effect. The correction due to this effect for vernier scan data at  $\sqrt{s} = 62.4$  GeV with a betatron amplitude function at the colliding point of  $\beta^* = 3$  m was simulated with WCM data and calculated to be  $0.93 \pm 0.02$ . The applicability of our calculation technique is illustrated in Fig. 1 with the high statistics vernier scan data at  $\sqrt{s} = 200$  GeV.

Figures 1(b) and 1(c) shows the sensitivity of our data for the transversely displaced beams to crossing angle between colliding beams. Two peaks in Figs. 1(b) and 1(c) show overlap of diverged collid-

ing beams by the hourglass effect at large  $z$  in displaced collisions of the vernier scan. In all vernier scan measurements, the crossing angle was found to be less than 0.2 mrad, which translates to a negligible correction for  $L_{\text{machine}}$  at  $\sqrt{s} = 62.4$  GeV with a typical bunch length of  $\sim 1$  m and bunch transverse size of 1 mm.

Due to limited amount of data collected at  $\sqrt{s} = 62.4$  GeV, systematic uncertainties of vernier scan technique are thoroughly studied in abundant set of  $\sqrt{s} = 200$  GeV vernier scan data on bunch-by-bunch level. After all corrections discussed above, our BBC trigger cross section in  $p+p$  collisions at  $\sqrt{s} = 62.4$  GeV is found 13.7 mb with a systematic uncertainty of  $\pm 1.5$  mb ( $\pm 11\%$ ). A systematic uncertainty of 4% is assigned for the run-by-run error in the vernier scan analysis at  $\sqrt{s} = 200$  GeV, 10% for BBC trigger efficiency correction of  $\epsilon_{\text{vertex}}$ , and 2% for hour-glass correction.

## References

- 1) S. S. Adler *et al.*, Phys. Rev. Lett. **91**, 241803 (2003); A. Adare *et al.*, Phys. Rev. D **76**, 051106(R) (2007); A. Adare *et al.*, Phys. Rev. D **79**, 012003 (2009).
- 2) Y. Goto *et al.*: RIKEN Accel. Prog. Rep. **40**, 89 (2007); S. van der Meer, ISR-PO/68-31, KEK68-64; A. Drees and Z. Xu, PAC-2001-RPAH116.

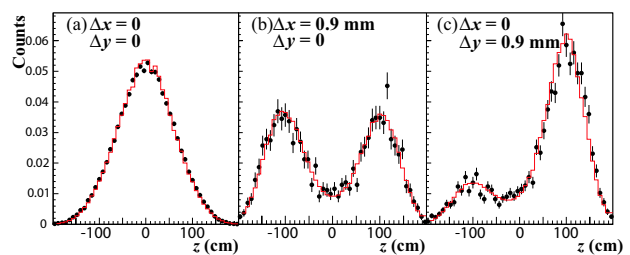


Fig. 1. Collision  $z$ -vertex distribution in PHENIX IR measured by ZDCs in a vernier scan at  $\sqrt{s} = 200$  GeV (points) and calculations from convolution of colliding bunch intensity profiles along  $z$ -axis and including the hourglass effect for bunches with typical length of 1 m and transverse size of 0.3 mm (histograms); a) beams are head-on; b) one beam is 0.9 mm displaced relative the other beam in horizontal direction and c) one beam is 0.9 mm displaced relative the other beam in vertical direction, calculations include bunch crossing angle in vertical projection of 0.15 mrad.

<sup>\*1</sup> Department of Physics, Brookhaven National Laboratory

<sup>\*2</sup> Department of Physics, Stony Brook University

# Cross Section For Prompt Photon Production in Proton-Proton Collisions at $\sqrt{s} = 62.4$ GeV

K. Sakashita,<sup>\*1</sup> T.-A. Shibata,<sup>\*1</sup> and K. Okada for the PHENIX Collaboration

Prompt photon production<sup>1)2)</sup> in high energy proton-proton collisions is expected to be useful to test the applicability of perturbative Quantum Chromodynamics (pQCD) to predict other quantities of interest, such as double helicity asymmetry  $A_{LL}$ . The  $A_{LL}$  is defined as;

$$A_{LL} = \frac{\sigma^{++} - \sigma^{+-}}{\sigma^{++} + \sigma^{+-}}. \quad (1)$$

$\sigma^{++(+)}$  is a cross section for particle production such as a prompt photon in the proton-proton collision with beam helicity pattern “+ + (+)”. Once the applicability of pQCD is confirmed, the framework of pQCD can be used to determine gluon spin contribution to the proton spin  $\Delta g$  from  $A_{LL}$ .

In proton-proton collisions, the prompt photon is mainly produced via quark-gluon collision and quark-anti-quark annihilation. The cross section for prompt photon production is defined as

$$E \cdot \frac{d^3\sigma}{dp^3} \sim \frac{1}{2\pi \cdot L \cdot p_T \cdot \varepsilon} \frac{\Delta N_\gamma}{\Delta p_T \cdot \Delta \eta} \quad (2)$$

where  $\Delta N_\gamma$  is yields per the unit of transverse momentum  $p_T$  and the unit of pseudo-rapidity  $\eta$ .  $L$  is the integrated luminosity, and  $\varepsilon$  is the correction factor described in the following paragraphs.

We measured the cross section for prompt photon production from proton-proton collisions at  $\sqrt{s} = 62.4$  GeV in a PHENIX experiment. The data was collected in 2006 with the PHENIX central arm spectrometer. The PHENIX central arm spectrometer consists of two arms which are placed almost back-to-back on their azimuth. Each arm covers pseudo-rapidity  $|\eta| < 0.35$  and 90 degree azimuthal angle. Photons with energy above 0.15 GeV are measured using the electromagnetic calorimeters (EMCal). Charged particles are identified with the pad chamber. The integrated luminosity is about  $0.065 \text{ pb}^{-1}$ , which corresponds to 894 M events. In this analysis,  $p_T > 2 \text{ GeV}/c$  photons are required to exist for each event in the offline analysis.

Prompt photons are extracted by subtracting background photons from inclusive photons. The background photons mainly come from  $\pi^0$  decay. Therefore, it is important to evaluate the  $\pi^0$  decay photons precisely. The  $\pi^0$  decay photons are categorized into two groups. If both of the photons are detected, they are called “two tag photons”. If only one of the two photons is detected, due to the limited acceptance of the EMCal, it is called a “one tag photon”. The  $\pi^0$  decay photons in the two tag photons are identified

with an invariant mass by reconstructing the four momenta of two photons. On the other hand, the  $\pi^0$  decay photons in the one tag photons are estimated using a fast Monte-Carlo simulation and the experimental data. Then, the contribution of decay photons from other particles such as  $\eta$ ,  $\omega$  and  $\eta'$  is also estimated.

The prompt photon yields are normalized with the integrated luminosity, and are corrected for the efficiency of EMCal etc. to obtain the cross section (Eq.2). Figure 1 shows the cross section with systematic uncertainties, and a comparison of the present data with the Next-to-Leading Order (NLO) pQCD calculation. The main systematic uncertainty at low  $p_T$  comes from extraction of  $\pi^0$  yields from the sample including misidentified particles. It means that it is not  $\pi^0$  but is accidentally regarded as  $\pi^0$ . The prediction of the NLO pQCD calculation at low  $p_T$  region is lower than experimental values. It suggests a need to take into account further higher order terms in the calculation. On the other hand, at high  $p_T$  region, both values agree with each other within the uncertainties of measurement and calculation.

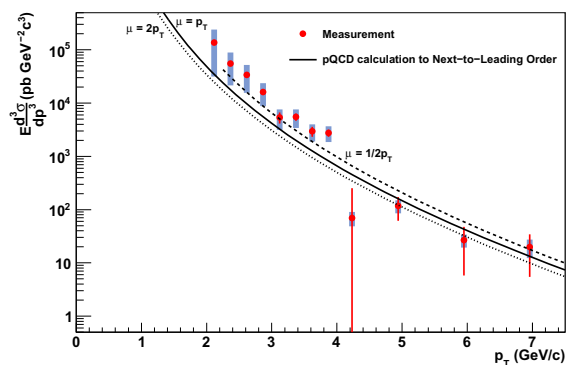


Fig. 1. The cross section for prompt photon production as a function of  $p_T$  with statistical uncertainties (red) and systematic uncertainties (blue) compared with the NLO-pQCD calculation. The three lines represent the calculation with different scales.

## References

- 1) S. S. Adler *et al.* [PHENIX Collaboration], Phys. Rev. Lett. **98**, 012002 (2007) [arXiv:hep-ex/0609031].
- 2) T. Horaguchi, Doctor Thesis, Tokyo Institute of Technology 2006.

<sup>\*1</sup> Department of Physics, Tokyo Institute of Technology

# Double spin asymmetries of open heavy-flavor production in forward rapidity with polarized p + p collisions at $\sqrt{s}=200\text{GeV}$

X. Wang,<sup>\*1</sup> H. Liu<sup>\*2</sup> and M. Liu<sup>\*2</sup>

[Open heavy flavor, spin, asymmetry]

Deep-inelastic scattering (DIS) experiments with polarized leptons and polarized nucleons have shown that the spins of quarks and anti-quarks account for only approximately 25% of nucleon spin.<sup>1)</sup> The rest of the proton spins must be carried by the gluons and orbital angular momentum. Measurements of the scale dependence of the inclusive nucleon spin structure function and recent semi-inclusive DIS data<sup>2)</sup> have shown the coarse constraint in the possible gluon spin contribution. Furthermore, heavy quark production in polarized p+p collision at RHIC energy is dominated by the gluon-gluon interaction, thus providing direct access to the (polarized) gluon distribution in the proton. Compared with the current double spin asymmetry of  $\pi$ <sup>03)</sup>, inclusive jet<sup>4)</sup> and photon measurement at RHIC, heavy flavor provides a very independent channel to study gluon polarization.

With the current PHENIX detector, open heavy flavor measurement in the muon arms is limited to indirect statistical measurement. Extraction of signal muons in this analysis is predicated upon successful estimation and statistical subtraction of all background sources which are defined to be tracks not resulting from the semi-leptonic decay of heavy flavor mesons. The "inclusive tracks" are defined as tracks penetrating the muon-identifier detector (MuID) and consist of muons from heavy-flavor decay, muons from decay of light hadrons (K and  $\pi$ ) and some light hadrons which punched through the MuID. The "hadron tracks" are defined as tracks stopping in the MuID and consist mostly of light hadrons according to our simulation studies.<sup>5)</sup>

Our strategy to extract the asymmetry of muons from the heavy-flavor decay is to 1) estimate background asymmetry with "hadron tracks", and 2) subtract the background asymmetry from the asymmetry of "inclusive tracks".

The asymmetries of "inclusive tracks" and "hadron tracks" are given as

$$A_{LL}^{incl/hadron} = \frac{1}{P_B \cdot P_Y} \frac{N_{incl/hadron}^{++} - R \cdot N_{incl/hadron}^{+-}}{N_{incl/hadron}^{++} + R \cdot N_{incl/hadron}^{+-}} \quad (1)$$

where  $P_B$  and  $P_Y$  are the polarization for blue and yellow beams respectively.  $N_{incl/hadron}^{++}$  ( $N_{incl/hadron}^{+-}$ ) is the number of "inclusive tracks" or "hadron tracks" from the same (opposite) helicity beam collisions.  $R = L^{++}/L^{+-}$  is the luminosity ratio of the same helicity

beam collision to the opposite helicity beam collision. The  $A_{LL}$  of signal muons from the heavy-flavor decay can be derived from

$$A_{LL}^{signal} = \frac{A_{LL}^{incl} - r \cdot A_{LL}^{BG}}{1 - r}, \quad (2)$$

$$\delta A_{LL}^{signal} = \frac{\sqrt{(\delta A_{LL}^{incl})^2 + r^2 \cdot (\delta A_{LL}^{BG})^2}}{1 - r} \quad (3)$$

where  $r$  is the background fraction and  $A_{LL}^{BG}$  is the background asymmetry for which  $A_{LL}^{hadron}$  are used.

The background fraction was calculated from the p+p run in the year 2005 single muon analysis.<sup>6)</sup> Figure 1 shows the double spin asymmetry results for muons from heavy flavor decays from the data for the runs in 2005 and 2006.

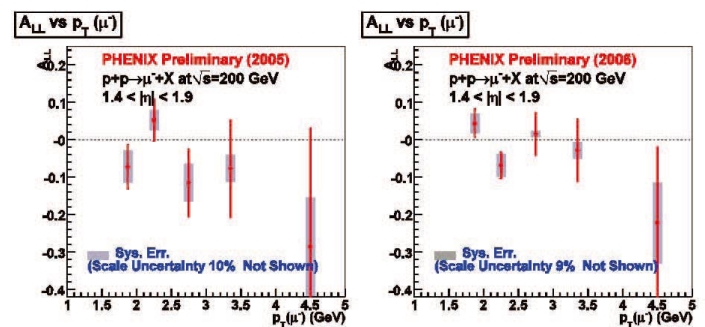


Fig. 1. Double spin asymmetry  $A_{LL}$  for  $\mu^-$  from heavy flavor decay as a function of  $p_T$  from p+p runs in 2005 and 2006, with averaged polarization 50% and 60%, respectively. Error bars show statistical errors and shaded error bands show systematic errors.

No nonzero  $A_{LL}$  has been observed at the current precision. Our results are limited by statistics. It is important to measure the  $A_{LL}$  of heavy flavor production for gluon polarization determination using an independent physics process with different systematic uncertainties and confirm the universality of the gluon polarization measurement.

## References

- 1) J. Ashman et al: Phys. Lett. B **206**, 364 (1988); Nucl. Phys. B**328**, 1 (1989); E. Hughes and R. Voss: Annu. Rev. Nucl. Part. Sci. 49, 303 (1999).
- 2) HERMES: Phys. Rev. Lett. **84**, 2584 (2000); COMPASS: Phys. Lett. B **633**, 25 (2006).
- 3) PHENIX collaboration: arXiv:(hep-ex)0810.0694, 2008
- 4) STAR collaboration: Phys. Rev. Lett. 100 (2008)232003
- 5) PHENIX collaboration: Phys. Rev. C 71, 034908 (2005).
- 6) D. Hornback: J. Phys. G35, 104113 (2008).

<sup>\*1</sup> New Mexico State University, Las Cruces, NM, USA

<sup>\*2</sup> Los Alamos National Laboratory, Los Alamos, NM, USA

# Measurement of transverse single-spin asymmetry with $J/\Psi$ in polarized p+p collisions at $\sqrt{s} = 200$ GeV

H. Al-Ta'ani,<sup>\*1</sup> H. Liu,<sup>\*2</sup> M. Liu,<sup>\*2</sup> G. Kyle,<sup>\*1</sup> and X. Wang,<sup>\*1</sup>

[Spin,  $J/\Psi$ , asymmetry]

The spin structure and its investigation of the proton has revealed itself to be extremely complex, and is an active area of ongoing research. Large transverse single-spin asymmetries in inclusive particle production at fixed target energies<sup>1)</sup> were observed in forward pion production by the E704 collaboration at FERMILAB ( $\sqrt{s} = 19.4$  GeV). Such large asymmetries were initially surprising due to the prediction of pQCD in leading order that these asymmetries should be small. Interest has recently grown with the discovery by STAR<sup>2)</sup> and BRAHMS<sup>3)</sup> that these asymmetries persist even at RHIC energies. Transverse single-spin asymmetries (SSAs),  $A_N$ , have the potential to be an important tool in understanding the quark and gluon spin distributions in a polarized proton. Precision measurement of SSAs in different kinematic regions with various particles and their QCD analysis may serve to quantify contributions from different mechanisms. In a theoretical model calculation by Feng Yuan, the SSA is found to be very sensitive to the production mechanism of heavy quarkonium, where the production has been studied using non-relativistic QCD (NRQCD) and the heavy quark pairs are produced at a short distance in color-singlet or color-octet configurations<sup>4)</sup>. According to this model, the SSA in ep scattering vanishes if  $J/\Psi$  is produced in the color-singlet channel but survives in the color-octet channel. However, in pp scattering the SSA vanishes if  $J/\Psi$  is produced through the color-octet channel but survives in the color-singlet channel.

The  $J/\Psi$ s have been measured with PHENIX muon spectrometers which cover the forward rapidity range of  $1.2 < |\eta| < 2.4$ . At RHIC energies, heavy flavor production is dominated by the gluon-gluon interaction; thus the Collins effect has minimum impact on  $A_N$  as the gluon's transversity is zero. Therefore, heavy flavor  $A_N$  in transversely polarized p+p collisions at the PHENIX experiment offers a good opportunity to gain information on transverse momentum dependent gluon distribution which can be described by gluon's Siverson function<sup>5)</sup>.

The left-right single-spin asymmetry  $A_N$  is calculated by:

$$A_N = \frac{1}{P_b} \frac{\sigma^\uparrow - \sigma^\downarrow}{\sigma^\uparrow + \sigma^\downarrow} = \frac{1}{P_b} \frac{\sqrt{N_L^\uparrow N_R^\downarrow} - \sqrt{N_L^\downarrow N_R^\uparrow}}{\sqrt{N_L^\uparrow N_R^\downarrow} + \sqrt{N_L^\downarrow N_R^\uparrow}}, \quad (1)$$

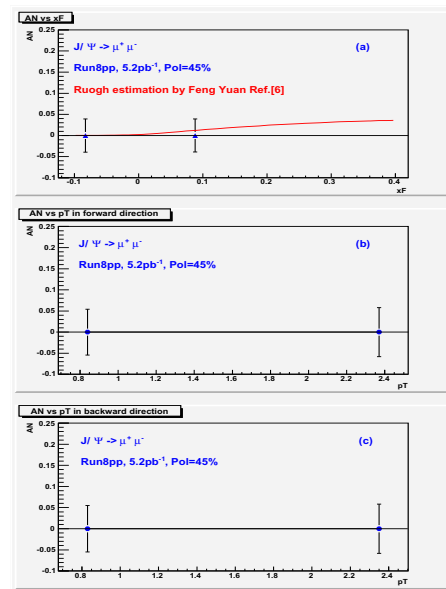


Fig. 1. Expected precision for  $A_N$  versus (a)  $x_F$ , (b)  $p_T$  in forward rapidity and (c)  $p_T$  in backward rapidity

where  $P_b$  is the beam polarization,  $\sigma^\uparrow$  ( $\sigma^\downarrow$ ) is the production cross section when the proton in the bunch is polarized up (down), and  $N^\uparrow$  ( $N^\downarrow$ ) is the  $J/\Psi$  yield from up (down) polarized bunches.

Here, we report our inclusive analysis with  $J/\Psi \rightarrow \mu^+ \mu^-$ . The expected statistical uncertainties of  $A_N$  in  $J/\Psi$  production for the data collected in 2008 ( $L = 5.2 \text{ pb}^{-1}$ ,  $P_b \sim 45\%$ ) are shown in Fig. 1 as a function of  $x_F$  and  $p_T$  in both forward and backward rapidities. The model calculation shown in Fig. 1 plot (a) assumes the gluon's Siverson function is  $0.5x(1-x)$  times the unpolarized gluon distribution and 30% of  $J/\Psi$  comes from feed down of  $\chi_c$ <sup>6)</sup>. Future high statistic measurement of  $A_N$  in  $J/\Psi$  production offers a good opportunity to study the heavy quarkonium production mechanism and gluon's Siverson function.

## References

- 1) D. L. Adams et al.: Phys. Lett. B **264**, 462 (1991); D. L. Adams et al.: Phys. Rev. D **53**, 4747 (1996).
- 2) J. Adams et al.: Phys. Rev. Lett. **92**, 171801 (2004).
- 3) I. Arsene et al.: Phys. Rev. Lett. **101**, 042001 (2008).
- 4) F. Yuan: Phys. Rev. D **78**, 014024 (2008). D.
- 5) Siverson: Phys. Rev. D **41**, 83-90 (1990).
- 6) F. Yuan: private communication.

<sup>\*1</sup> New Mexico State University, Las Cruces, NM, USA

<sup>\*2</sup> Los Alamos National Laboratory, Los Alamos, NM, USA

# Study of $J/\psi$ spin alignment in proton-proton collisions at $\sqrt{s} = 200$ GeV in RHIC PHENIX experiment

K. Shoji\* for the PHENIX Collaboration

[nucleon structure,  $J/\psi$ , spin alignment, polarization]

Non-relativistic quantum chromodynamics (NRQCD) calculations taking into account color octet models (COMs)<sup>1)</sup> have succeeded in describing the production cross section of heavy quarkonia measured by CDF and other experiments<sup>2,3)</sup>. However, the models can not reproduce experimental data with respect to  $J/\psi$  spin alignment<sup>4)</sup>. The CDF experiment reported small longitudinal polarization while NRQCD models predict transverse polarization at high transverse momenta. Understanding of heavy quarkonium production mechanism has not proceeded well due to the small number of experimental measurements.

The  $J/\psi$  spin alignment is determined experimentally by measuring decay angular distribution of leptons in the  $J/\psi$  rest frame. The angular distribution is parametrized with polar angle  $\theta$  which is the angle between lepton momentum in  $J/\psi$  rest frame and  $J/\psi$  momentum in the laboratory frame (helicity frame).

$$\frac{d\sigma}{d\cos\theta} \propto 1 + \lambda \cos\theta, \quad (1)$$

where  $\lambda = 0$  indicates non-polarization. Positive and negative values of  $\lambda$  correspond to transverse and longitudinal polarization, respectively.

A proton-proton collision experiment is in progress at the relativistic heavy ion collider (RHIC) operated at Brookhaven National Laboratory. The PHENIX experiment<sup>5)</sup> at the RHIC has muon spectrometers (Muon Arm) to detect  $J/\psi$  via  $\mu^+\mu^-$  channel. The PHENIX Muon Arm covers forward rapidity regions with  $1.2 < |\eta| < 2.2$  and  $\Delta\phi = 2\pi$ . Study of  $J/\psi$  spin alignment in proton-proton collisions at  $\sqrt{s} = 200$  GeV is ongoing with several ten thousands  $J/\psi$  events accumulated at the PHENIX Muon Arm. We have small acceptance in  $|\cos\theta| \sim 1$  because decay muons emitted backward in  $J/\psi$  rest frame are not boosted well enough to penetrate materials for hadron background rejection. Thus acceptance studies of a Muon Arm with a Monte-Carlo simulation have an important role in measuring  $J/\psi$  spin alignment.

Figure 1 shows simulated angular distributions of  $J/\psi$  decay muon at PHENIX Muon Arm. The simulation was performed for an unpolarized case ( $\lambda = 0$ ) and extreme cases ( $\lambda = \pm 1$ ).  $J/\psi$  events are generated as the simulation reproduces reconstructed  $J/\psi$  transverse momentum and rapidity distributions of real data. Expected statistical errors of real data are also shown on the points of  $\lambda = 0$ . The distribution of

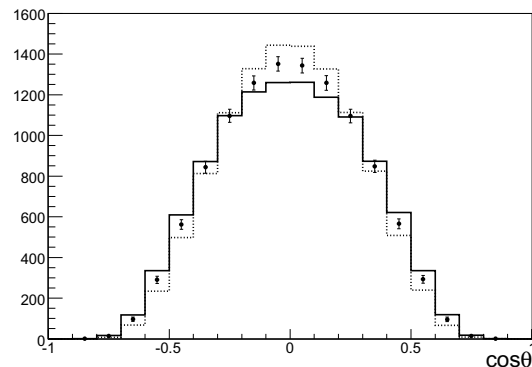


Fig. 1. Simulated angular distributions of  $J/\psi$  decay muon at the PHENIX Muon Arm. Simulation results from non-polarization ( $\lambda = 0$ ) are shown as black points with expected statistical errors of data. Solid and dashed histograms are for  $\lambda = +1, -1$ , respectively.

the transversely polarized case ( $\lambda = +1$ ) is broader than that of the longitudinal one ( $\lambda = -1$ ) as expected from the expression of (1).

From the acceptance study, we can expect that the statistical accuracy of

the current data set is enough to discuss  $J/\psi$  spin alignment.

Study of  $J/\psi$  spin alignment at RHIC PHENIX is ongoing. We hope to finalize the results soon. So far, an anisotropy in the helicity frame has been considered in this study. Recently, the necessity of analyzing data with respect to other frames, such as the Collins-Soper<sup>6)</sup> or the Gottfried-Jackson<sup>7)</sup> frame is being discussed because the proper polarization axis which is sensitive to a physics phenomenon is not known well. Moreover, measurements not only of polar angular distribution but also of azimuthal one are important. We will access these measurements in the future.

## References

- 1) G.T.Bodwin, E.Braaten, and G.P.Lepage, Phys. Rev. D **51**, 1125 (1995); **55**, 5853 (1997)
- 2) D.Acosta et al., Phys. Rev. D **71**, 032001 (2005)
- 3) A.Adare et al., Phys. Rev. Lett. **98**, 232002 (2007)
- 4) A.Abulencia et al., Phys. Rev. Lett. **99**, 132001 (2007)
- 5) K.Adcox et al., Nucl. Instr. Meth. A **499**, 469 (2003)
- 6) J.C.Collins and D.E.Soper, Phys. Rev. D **16** 2219 (1977)
- 7) K.Gottfried and J.D.Jackson, Nuovo Cimento **33** 309 (1964)

\* Department of Physics, Kyoto University

# Measurement of direct photon using a virtual photon method in $\sqrt{s} = 200$ GeV p+p collisions at RHIC-PHENIX

Y.L. Yamaguchi,<sup>\*1</sup> Y. Akiba,<sup>\*2</sup> T. Gunji,<sup>\*1</sup> and H. Hamagaki,<sup>\*1</sup>

[Direct photon, virtual photon method, Low  $p_T$ ]

Direct photon is a unique probe to investigate properties of Quark Gluon Plasma (QGP) since photons penetrate the dense and hot partonic matter created by heavy ion collisions. Special interest is given to thermal photons from the QGP which are considered to be the primary contributor at the low energy region in the inclusive photon spectrum.<sup>1)</sup>

A measurement of ‘real’ direct photon using an electromagnetic calorimeter is notoriously difficult below 4 GeV since systematic errors cannot be reduced due to the large hadron background, particularly  $\pi^0$ . Recently an alternative method using a ‘virtual’ direct photon measurement, i.e. a measurement of  $e^+e^-$  pairs from ‘virtual’ direct photon decays was demonstrated to provide the photon yield with less systematic error in both p+p and Au+Au collisions<sup>2)</sup> shown as Fig. 1. A clear excess over the binary scaled p+p result (shown

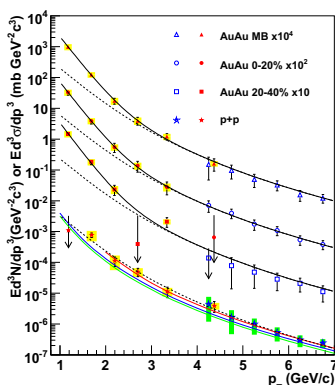


Fig. 1. The direct photon spectra in p+p and Au+Au collisions as a function of  $p_T$ .

by the dotted line) is seen in Au+Au collisions for  $1 < p_T < 3$  GeV/c, and a hydrodynamical calculation indicates that this excess comes from thermal radiation from QGP.<sup>3)</sup> Thus it is very important to measure the direct photon yield in p+p collisions more precisely for  $1 < p_T < 3$  GeV/c in order to evaluate the mean contribution of the thermal photons. The data on p+p collisions taken in 2006 is available and its statistics are about twice that of the one already analyzed. This report describes the current status of the analysis in  $\sqrt{s} = 200$  GeV p+p collisions at RHIC-PHENIX using the data taken in 2006.

All electrons and positrons in the same event are combined into pairs. The obtained  $e^+e^-$  pair mass

distribution contains several components from different sources, which are listed below.

- Virtual direct photon decays
- Hadron decays
- Photon conversions
- Combinatorial background
- Cross pairs from  $\pi^0, \eta \rightarrow 2\gamma(\text{or } \gamma e^+e^-) \rightarrow e^+e^-e^+e^-$

The pairs from photon conversions are removed by a cut on the orientation of the pair in the magnetic field<sup>4)</sup>. The combinatorial background is computed with a mixed-event technique and subtracted. The contributions from hadron decays are estimated using a hadronic cocktail simulation, which incorporates the measured yields of the hadrons at PHENIX. The effects on real data such as several efficiencies, geometrical acceptance and momentum smearing are considered in the cocktail simulation through the GEANT 3 based simulator of the PHENIX detector. The cross pairs are evaluated by comparing a like-sign pair distribution between the real and simulated one. Figure 2

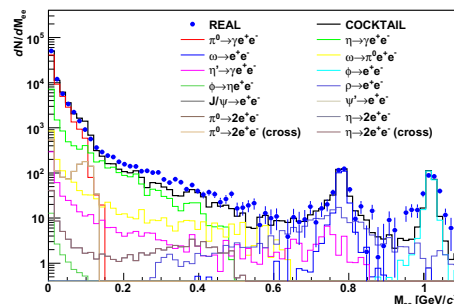


Fig. 2. Comparison of the  $e^+e^-$  pair mass distribution between the real and the cocktail simulation.

shows the comparison of the  $e^+e^-$  pair mass distribution between the real (blue symbols) and the cocktail simulation (black line). The real data is in good agreement with the cocktail simulation.

The virtual direct photon fraction to inclusive virtual photon yield will be evaluated from the excess over the cocktail simulation for several  $p_T$  regions and then the real direct photon yield will be determined from the obtained virtual direct photon fraction.

## References

- 1) S. Turbide, et al.: Phys. Rev. C **69**, 014903 (2004).
- 2) A. Adare, et al.: arXiv:0804.4168 [nucl-ex] (2008).
- 3) F. Liu, et al.: arXiv:0807.4771 [hep-ph] (2008).
- 4) A. Toia: arXiv:0711.2118 [nucl-ex] (2007).

<sup>\*1</sup> Center for Nuclear Study (CNS), University of Tokyo

<sup>\*2</sup> RIKEN (The Institute of Physical and Chemical Research)

# Longitudinal Double Spin Asymmetry for Inclusive Jet Production in Polarized p+p Collisions at 200 GeV

M. Sarsour for the STAR collaboration,\*<sup>1</sup>

[gluon polarization, jets, longitudinal double spin asymmetry, STAR]

The RHIC spin program uses polarized p+p collisions to study  $\Delta G$ , the integral of the gluon polarized distribution function,  $\Delta g(x, Q^2)$ . There are many processes where the gluon participates directly thus  $\Delta G$  can be probed directly and more precisely than previously attained. This contribution reports on the inclusive jet production asymmetry measurement at the Solenoid Tracker at RHIC (STAR) experiment<sup>1</sup>. The inclusive jets channel is an excellent tool to study the gluon polarization due to its large cross section and relative independence from fragmentation functions.

In 2005 we had an order of magnitude increase in the figure of merit over our previous measurements<sup>2</sup>) with coverage in jet  $p_T$  up to 30 GeV/c. This allowed us to perform a quantitative comparison of our measured results<sup>3</sup>) to global fits of polarized deep-inelastic scattering (DIS) data within the GRSV framework<sup>4</sup>) for various fixed values of  $\Delta G$ <sup>5</sup>). These comparisons showed that the global fits that predict very large  $\Delta G$  values and large  $A_{LL}$  are excluded<sup>3</sup>).

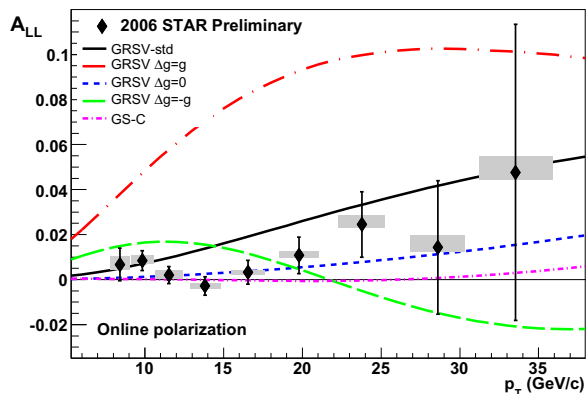


Fig. 1. Preliminary 2006  $A_{LL}$  for inclusive jet production at  $\sqrt{s} = 200$  GeV versus jet  $p_T$ , where the error bars are statistical and the gray bands indicate the systematic uncertainties.

Figure 1 shows preliminary 2006  $A_{LL}$  versus jet  $p_T$  corrected for detector response. The points with error bars are the data with statistical uncertainties. The gray shaded band represents the systematic uncertainties, excluding the 25% uncertainty on the beam polarization values. Figure 1 also shows NLO pQCD calculations which incorporate different scenarios for

$\Delta g(x)$ , including the best global fit to the inclusive DIS data (std)<sup>4</sup>). The other curves include maximally positive gluon polarization ( $\Delta g(x) = g(x)$ ) at the input scale, maximally negative gluon polarization ( $\Delta g(x) = -g(x)$ ), and zero gluon polarization ( $\Delta g(x) = 0$ ). In addition, it includes a prediction derived from GS-C<sup>6</sup>) which has a large positive gluon polarization at low  $x$ , a node near  $x \sim 0.1$ , and a negative gluon polarization at large  $x$ . The statistical uncertainties in the 2006  $A_{LL}$  measurements at high  $p_T$  are a factor of 3 to 4 smaller than they were in the 2005 data<sup>3</sup>), which leads to significantly more stringent constraints on gluon polarization models.

These results were included in a recent “global” NLO analysis, DSSV<sup>7</sup>), the first analysis to include inclusive DIS, semi-inclusive DIS, and RHIC pp collision data together. The result of this analysis showed that  $\Delta g(x, Q^2)$  is small in the accessible range of momentum fraction, with a possible node in the distribution near  $x \sim 0.1$ , basically evolving away at higher scales with the opposite phase from GS-C. A study of the DSSV  $\chi^2$  profile and the partial contributions  $\Delta\chi^2$  of the individual data sets shows that these STAR data provide the strongest limits on negative gluon polarization over the range  $0.05 < x < 0.2$  and also contribute significantly to the limits on positive gluon polarization over the same range.

In summary,  $A_{LL}$  measurements from inclusive jet data from 2005 and 2006 are reported. These results provide significant constraints on the gluon spin contribution to the proton spin when compared to NLO pQCD calculations. They play a significant role in the first global NLO analysis to consider DIS, SIDIS and RHIC data together.

## References

- 1) K. H. Ackermann *et al.* (STAR collaboration), Nucl. Instrum. Meth. A **499**, 624 (2003).
- 2) B. I. Abelev *et al.* (STAR collaboration), Phys. Rev. Lett. **97**, 252001 (2006).
- 3) B. I. Abelev *et al.* (STAR collaboration), Phys. Rev. Lett. **100**, 232003 (2008).
- 4) M. Glück, E. Reya, M. Stratmann and W. Vogelsang, Phys. Rev. D **63**, 094005 (2001).
- 5) M. Stratmann and W. Vogelsang (private communication), 2007.
- 6) T. Gehrmann and W. J. Stirling, Phys. Rev. D **53**, 6100 (1996).
- 7) D. de Florian, R. Sassot, M. Stratmann, and W. Vogelsang, Phys. Rev. Lett. **101**, 072001 (2008).

\*<sup>1</sup> Department of Physics and Astronomy, Georgia State University, Atlanta, GA 30303

# Measurement of Transverse Single Spin Asymmetry of Open Heavy Flavor in Polarized p+p Collisions at PHENIX

H. Liu<sup>\*1</sup>, M. Liu<sup>\*1</sup>, H. Al-Bataineh<sup>\*2</sup> and X.R. Wang<sup>\*2</sup> for the PHENIX Collaboration

[Spin, Asymmetry]

The transverse spin structure of the proton is still poorly understood. The measurement of transverse single spin asymmetries gives us an opportunity to probe the quark and gluon structure of transversely polarized nucleons. At RHIC energy, heavy flavor production is dominated by gluon-gluon fusion, so the Collins effect (transversity distribution in combination with spin-dependent fragmentation function) has minimum effects on transverse single spin asymmetry ( $A_N$ ) as the gluon's transversity is zero. The measurement of  $A_N$  in heavy flavor production is thus particularly sensitive to the gluon Sivers distribution (transversely asymmetric  $k_T$  gluon distributions) which is related to the orbital angular momentum of gluons inside the polarized protons.

In this report we present the first measurement of  $A_N$  in single muons from open heavy flavor decay production in transversely polarized p+p collisions at  $\sqrt{s}=200\text{GeV}$ . The muons are measured with muon spectrometers in full azimuthal coverage at forward rapidities ( $1.2 < |\eta| < 2.4$ ).

The single muons from semi-leptonic decay of open heavy flavor are measured through the statistical subtraction of background sources, with the remaining yield attributed to open heavy flavor decays. The sources of backgrounds are: (1) muons from light hadron decay before reaching the pre Muon Tracker (MuTr) absorber; (2) punch through hadrons which penetrate the 1.5m of steel absorber to reach the deepest layer of MuID; (3) background tracks which dominated by hadron which decay into a muon after reaching the MuTr. The detail of how to estimate the background contributions can be found in<sup>1)</sup>.

Transverse single spin asymmetry  $A_N$  is measured as

$$A_N = \frac{1}{P_b} \frac{\sigma^\uparrow - \sigma^\downarrow}{\sigma^\uparrow + \sigma^\downarrow} = \frac{1}{P_b} \frac{\sqrt{N_L^\uparrow \cdot N_R^\downarrow} - \sqrt{N_L^\downarrow \cdot N_R^\uparrow}}{\sqrt{N_L^\uparrow \cdot N_R^\downarrow} + \sqrt{N_L^\downarrow \cdot N_R^\uparrow}}, \quad (1)$$

where  $P_b$  is the beam polarization from CNI and jet polarimeter analysis,  $\sigma^\uparrow(\sigma^\downarrow)$  is the single muon production cross section from crossings with polarized bunch spin up(down),  $N^\uparrow(N^\downarrow)$  is the particle yield.

The measured  $A_N^{Incl}$  is corrected for the contribution of background by using

$$A_N^{Phys} = \frac{A_N^{Incl} - r \cdot A_N^{BG}}{1 - r}, \quad (2)$$

<sup>\*1</sup> Los Alamos National Laboratory, Los Alamos, NM, USA

<sup>\*2</sup> New Mexico State University, Las Cruces, NM, USA

$$\delta A_N^{Phys} = \frac{\sqrt{(\delta A_N^{Incl})^2 + r^2 \cdot (\delta A_N^{BG})^2}}{1 - r}, \quad (3)$$

where  $r = N^{BG}/N^{Incl}$  is the background fraction, and  $A_N^{BG}$  is the background asymmetry.

At RHIC energy, transverse single spin asymmetry in open charm production was suggested to probe gluon Sivers function<sup>2)</sup> and the trigluon correlation functions in the nucleon<sup>3)</sup>. The first measurement of  $A_N$  of single muons from open heavy flavor decay has been made as a function of  $x_F$  (Figure 1), and  $p_T$  in the forward and backward rapidities (Figure 2). The large uncertainty of background contribution dominates the systematic uncertainty. A direct comparison between the prediction for  $D$  mesons and muons from open heavy flavor (open charm and beauty) decay will be available soon. The observed asymmetries in single muon production are significantly smaller than the model prediction for  $D$  mesons with maximal gluon Sivers function in the same kinematics region ( $x_F$  and  $p_T$ ) given in ref.<sup>2)</sup>.

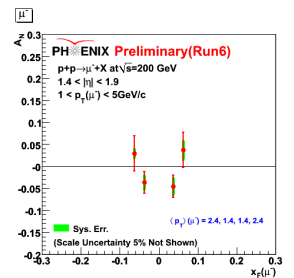


Fig. 1.  $A_N$  vs.  $x_F$  in single muon production.

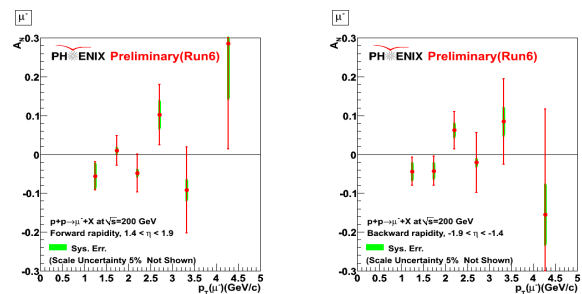


Fig. 2.  $A_N$  vs.  $p_T$  in single muon production in the forward (left) and backward (right) rapidities.

## References

- 1) S.S. Alder *et al.* : Phys. Rev. D **76**,092002(2007).
- 2) M. Anselmino *et al.* : Phys. Rev. D **70**,074025(2004).
- 3) Z.B. Kang *et al.* : Phys. Rev. D **78**,114013(2008).

# Reaction Plane Dependence of Neutral Pion Production at $\sqrt{s_{NN}} = 200$ GeV Au+Au Collisions at RHIC-PHENIX

Y. Aramaki\*<sup>1</sup>

[relativistic heavy ion collisions, jet quenching, elliptic flow]

It has been observed in central Au+Au collisions at Relativistic Heavy Ion Collider (RHIC) that the yield of neutral pion at high transverse momentum ( $p_T > 5$  GeV/c) is strongly suppressed compared to the one expected from  $p + p$  collisions scaled by the number of binary collisions. This suppression is considered to be due to the energy lost by hard scattered partons in the medium (jet quenching), which results in a decrease of the yield at a given  $p_T$ . Many theoretical models have been proposed to understand the parton energy loss mechanism. One of which is GLV method<sup>1)</sup> and it is one of the calculations that predicts that the magnitude of energy loss is proportional to square of the path length. Studying the path length dependence of energy loss should help in understanding of energy loss process.

Recently theoretical models (ASW<sup>2)</sup>, HT<sup>3)</sup> and AMY<sup>4)</sup>) to describe parton energy loss mechanism which involve the time-evolution of the medium produced at RHIC have been proposed. These models succeeded in reproducing the centrality dependence of  $R_{AA}(p_T)$ <sup>5)</sup>. Figure 1 shows the nuclear modification factor,  $R_{AA}(5 < p_T < 8$  GeV/c) as a function of azimuthal angle and the  $p_T = 15$  GeV/c of the ASW model curve which has largest variation in the above models. As shown in Fig. 1, even if we compare the curve with the  $p_T = 15$  GeV/c of the ASW model to data at much lower  $p_T$  ( $5 < p_T < 8$  GeV/c), these models are still unable to reproduce the azimuthal angle dependence of  $R_{AA}$ ,

Reaction plane detector was installed in RHIC-Year 2007 and reaction plane determination precision has been improved by a factor of two as compared to that in RHIC-Year 2004. Figure. 2 shows  $v_2(\pi^0)$  as a function of  $p_T$  for each 20 % centrality bin. The only two high  $p_T$  points above 10 GeV/c are measured with full statistics. Measured  $v_2(\pi^0)$  values are non-zero for all centrality bins. Two assumed functions are fitted to this data to understand the trend at high  $p_T$ . One is linear function ( $f(v_2) = a \cdot p_T + b$ ) and the other is constant value ( $f(v_2) = c$ ), where a, b and c are free parameters. At centrality bin range of 0-20 %, values of  $\chi^2/\text{NDF}$  for constant and linear function are 4.45/5 and 4.34/4, respectively. At centrality bin range of 20-40 %, values of  $\chi^2/\text{NDF}$  for constant and linear function are 4.39/5 and 1.49/4, respectively.

At centrality bin range of 40-60 %, values of  $\chi^2/\text{NDF}$  for constant and linear function are 2.23/5 and 2.21/4, respectively. These results indicate that the values of  $v_2(\pi^0)$  at most central and peripheral collisions tend to be constant while in mid-central collisions tend to decrease.

With the new data we will be able to measure the dependence of  $R_{AA}$  on azimuthal angle up to higher transverse momenta than ever before. We can also estimate the path length by measuring the azimuthal angle from reaction plane and mapping it into the shape of the participant region, which can be calculated by Glauber model for each impact parameter (centrality).

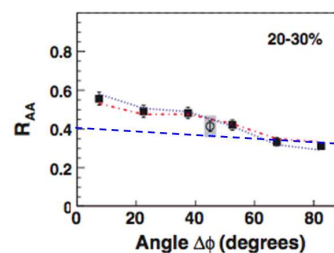


Fig. 1.  $R_{AA}(5 < p_T < 8$  GeV/c) as a function of azimuthal angle at centrality 20-30% and blue dashed line is ASW model curve at  $p_T = 15$  GeV/c.

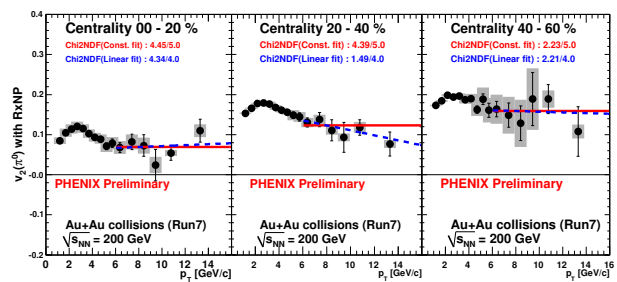


Fig. 2.  $v_2(\pi^0)$  as a function of  $p_T$  for each 20 % centrality bin. Red solid and blue dashed lines show constant and linear function, respectively. Red and blue lines are fitted to data from 6 GeV/c.

## References

- 1) M. Gyulassy *et al.*: Phys. Lett. **B538**, 282 (2002).
- 2) T. Renk *et al.*: Phys. Rev. **C75** 031902 (2007).
- 3) A. Majumder *et al.*: Phys. Rev. **C76** 041902 (2007).
- 4) G-Y. Qin *et al.*: Phys. Rev. **C76** 064907 (2007).
- 5) S.A. Bass *et al.*: J. Phys. **G35** 104064 (2008).

\*<sup>1</sup> Center for Nuclear Study, Graduate School of Science, University of Tokyo

# A study of $\omega$ meson production in $\sqrt{s_{NN}}=200\text{GeV}$ A+A collisions at PHENIX

M.Ouchida\*<sup>1</sup> for the PHENIX Collaboration

The measurement of hadrons under extreme conditions created by relativistic heavy-ion collisions is an intriguing study being carried out as part of the quest to observe the QCD phase transition, quark gluon plasma (QGP). PHENIX has provided systematic measurement of hadrons in Au+Au collisions suggesting that all meson production is suppressed due to jet quenching which is considered to be an effect of QGP<sup>1</sup> (Fig. 1 shows the nuclear modification factor of various particles; if there is no nuclear matter effect, the factor should be 1). Here, we contribute a measurement of  $\omega$  mesons ( $782\text{GeV}/c^2$ ) via the radiative decay mode ( $\omega \rightarrow \pi^0\gamma, \pi^0 \rightarrow 2\gamma$ ) in  $\sqrt{s_{NN}}=200\text{GeV}$  Au+Au collisions. It has been found that nuclear modification of  $\omega$  and  $\phi$  may be showing interesting behaviors, and this may be the onset of a dependence of quark energy loss on flavor and/or spin.

To support the study of  $\omega$  mesons in heavy-ion collisions, we have conducted an analysis of Cu+Cu collisions in  $\sqrt{s_{NN}}=200\text{GeV}$ . Since Cu+Cu collisions have lower multiplicity than Au+Au collisions and have different initial conditions, systematic measurement in this collision mode provide an important reference.

In addition to minimum bias (MB) trigger data, we used photon/electron trigger (ERT) data fulfilling high trigger condition of EMCal and RHIC, which are enriched with high-momentum photons to achieve better statistics for high momentum. The main challenge of this analysis is to handle the huge combinatorial background necessary for reconstructing particles from

the three-body decay mode. We introduce the same kinematical cuts such as momentum and energy range that are used for Au+Au analysis to establish the high  $S/\sqrt{B}$ . Fig. 2 shows an example of an invariant spectrum reconstructed by 3 gammas after subtracting two types of background: one is the combinatorial background reconstructed by the mixed event method and the other is from a resonance such as  $K_s^0(K_s^0 \rightarrow 2\pi^0)$ . Even though the statistics are limited, we can see the peak of  $\omega \rightarrow 3\gamma$  decays.

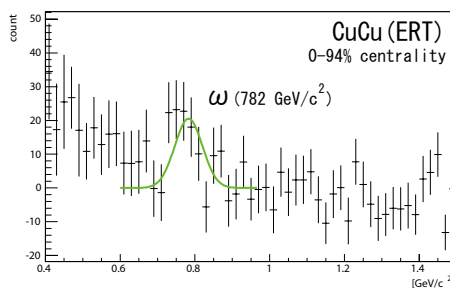


Fig. 2. Invariant Mass Spectra of  $3\gamma$  (after subtracting backgrounds) at  $6.5 < p_T(\omega) < 7.5$  [GeV/c] in ERT data set.

To evaluate the reconstructed efficiency, we performed a single  $\omega$  event simulation using event generators based on Monte Carlo codes. The PHENIX implementation of the GEANT-based simulation and the event particle tracking software system, PISA were used to consider the detector response. Trigger efficiency of ERT is estimated from a comparison of single  $\gamma$  energy spectra between the MB and ERT data set.

The analysis of  $\omega$  meson invariant yield in Cu+Cu is reaching the final stage. The behavior in  $R_{AA}$ , which is yet to be shown, is of great interest. We plan to publish the results of inclusive  $\omega$  meson measurement including the Cu+Cu results together with the Au+Au results shown in Fig.1. Although considerable statistical errors are unavoidable, a comparison between these analyses is quite meaningful for seeing the effect of different initial conditions provided by different beam species.

## References

- 1) A.Adare et al. : Phys. Rev. Lett. 101, 232301 (2008)
- 2) M.Naglis: nucl-ex/0809.3557

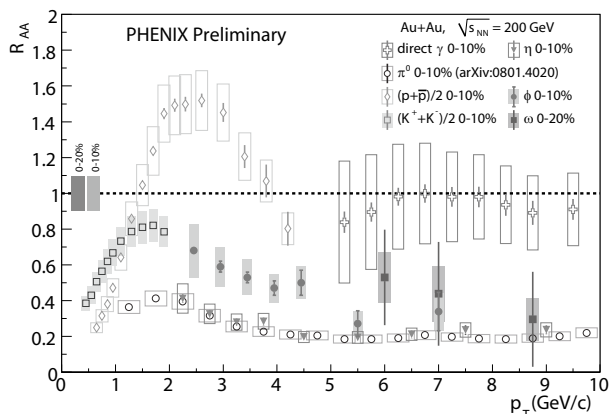


Fig. 1. Nuclear modification factor,  $R_{AA}$ , of various particles in central Au+Au collisions;<sup>2</sup> if there is no nuclear matter effect, the factor should be 1.

\*1 Hiroshima University

# High $p_T$ Charged Pion Cross Section, Using PHENIX Central Arms<sup>†</sup>

A. Morreale,<sup>\*1</sup>

[Nuclear structure, charged pions, cross sections, proton proton collisions]

## 1 Introduction

Inclusive  $\pi^\pm$  cross sections at high transverse momentum ( $p_T$ ) are of interest as these can be used to confirm that pQCD is an applicable framework to study spin asymmetries. Charged pion double helicity asymmetries from the 2006 run have been reported and compared with the latest theoretical predictions[3], which make use of fragmentation functions for charged separated species[2]. These asymmetry data will be useful in solving the puzzle of the origin of the proton's spin. In this report, we summarize the on-going effort to extract the charged separated pion cross sections for  $5 < p_T < 10$  GeV/c.

## 2 PHENIX Detection of high $p_T$ $\pi^\pm$

High  $p_T$   $\pi^\pm$  which are to be used for a cross section measurement, are selected from the reconstructed high quality charged tracks in the drift chamber(DC). Minimum bias triggered data is used. The  $\pi^\pm$  selection starts with applying an initial Čerenkov light emission threshold for the pions in the ring imaging Čerenkov detector (RICH)[1]. The reconstructed DC tracks are projected to the pad chambers (PC) and to the electromagnetic calorimeter (EMCal). The obtained hits in these detectors are compared to the actual associated hits. The standard deviations of the projected to the actual positions are evaluated as a function of momentum and incident angle; application of further cuts on these variables is known as pion track matching.

The main background for this analysis comes from secondary  $e^\pm$  from  $\gamma$  conversions, which occur far from the collision vertex. These particles will produce light in the RICH with high efficiency and will mimic high  $p_T$   $\pi^\pm$ , albeit with very low energy. The primary  $e^\pm$  to  $\pi^\pm$ , ratios are  $10^{-3}$ , thus  $e^\pm$  coming from the vertex pose small contamination.

## 3 Montecarlo Studies Compared to Data

The light emitting thresholds in the RICH are as follows:  $e^\pm$  17MeV/c,  $\pi^\pm$  4.7GeV/c,  $K^\pm$  16 GeV/c,  $p, \bar{p}$  30 GeV/c. Within a  $p_T$  of 5-10 GeV/c, only  $e^\pm$  and  $\pi^\pm$  will emit Čerenkov light. The RICH has different efficiencies for  $e^\pm$  and  $\pi^\pm$  as the opening angle is different for each species.  $e^\pm$  with their larger opening angle, will have recognizable ring or corona shaped light emission, while  $\pi^\pm$  will emit light over a disk.

Fig. 1 shows the typical turn on threshold behaviour for a  $\pi^\pm$ . Several monte carlo studies have been initiated, some which are omitted in this report due to page limitations. One such study shows that most  $e^\pm$  proceeding from  $\gamma$  conversions can be removed by applying a matching cut of  $2.5 \sigma$ : from roughly 8,000 simulated conversion  $e^\pm$  that mimic a high  $p_T$   $\pi^\pm$ , only about 72 will survive  $\pi^\pm$ , matching cuts. Zed, the z-coordinate at which the charged track crosses the drift chamber detector's reference radius (220 cm) is also studied. Conversion background has a strong zed dependance.  $\pi^\pm$ , have a flat zed distribution, while conversion  $e^\pm$ , will typically show high tails at high zed. [Fig. 2] A cut on this z coordinate, is also an effective way of removing background.

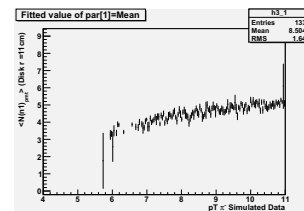


Fig. 1: Number of RICH photo multiplier tubes fired within a disk of 11 cm radius. The abscissa is the  $p_T$  of a simulated  $\pi^-$

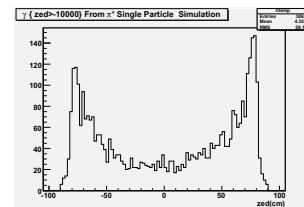


Fig. 2: Typical zed distribution of conversion  $e^\pm$  proceeding from  $\gamma$  conversions, note the high tails.

## 4 Conclusions

The studies reported represent a small sample of the ongoing effort to measure charged pion cross sections at high  $p_T$  in the PHENIX detector. RHIC p+p data from the year 2006 is used in this analysis.

## References

- 1) K. Adcox et al., *PHENIX central arm tracking detectors*, NIM A499 489-507, 2003
- 2) D. de Florian, et al., *Physical Review D*, Volume 75, American Physical Society, New York, 2007 pp. 114010. e-Print: hep-ph/0703242.
- 3) A. Morreale, *17th International Spin Physics Symposium*, AIP Conference Proceedings, AIP, New York, Volume 915, pp. 359-362, 2007.

<sup>\*1</sup> Department of Physics, University of California at Riverside

# Multiplicity Measurement in the Proton-Proton Collisions at the LHC<sup>†</sup>

S. Sano,<sup>\*1</sup> H. Hamagaki,<sup>\*1</sup> T. Gunji,<sup>\*1</sup> C. Garabatos<sup>2</sup> M. Ivanov<sup>2</sup> and J. Wiechula<sup>2</sup>

[Multiplicity, Color Glass Condensate (CGC), LHC]

Quantum Chromodynamics (QCD) predicts the color glass condensate (CGC) which is the consequence of the self interaction of the gluon<sup>1)2)</sup>. The hot and dense matter made at the Relativistic Heavy Ion Collider (RHIC) has the large elliptic flow in non-central Au+Au collision<sup>3)</sup>, and the values of  $v_2$ , anisotropy for the azimuthal angle distribution of generated particles, agree with the results in the calculation of the hydrodynamics of the ideal fluid, but not with the model including the effect of CGC<sup>4)</sup>. In order to research for the hydrodynamical property of the high energy matter, the investigation of the effect of the CGC is needed.

The parton saturation as a consequence of CGC will be more conspicuous in the LHC than the RHIC. In the first collision of proton-proton at the LHC, which will be done at 2009, the effect of CGC will be found in the multiplicity measurement<sup>5)</sup>. In this report, the status of the preparation for the measurement of  $dN/d\eta$  distribution of the charged multiplicity is described.

As the first step for the measurement of  $dN/d\eta$ , the estimation of the acceptance of the TPC for the charged particles was begun. These values are determined by the comparison of the input data from the event generator (MC event) to the event summary data (ESD) of the detector simulation and reconstruction. Data used to this analysis is Physics Data Challenge 2008 (PDC\_08), which simulates the p+p collisions at  $\sqrt{s} = 10$  TeV generated with Pythia 6 as the first physics for the LHC. The acceptance is assumed to be the function of pseudo-rapidity, vertex  $z$  position for the each track, and transverse momentum.  $dN/d\eta$  is calculated as

$$\frac{dN}{d\eta}|_{\eta=\eta'} = \int_{V_{z1}}^{V_{z2}} \int_{p_{T1}}^{p_{T2}} \sum_{event} \sum_{track} C(\eta', z, p_T) \times \left( \frac{dN}{dz dp_T d\eta} \right)_{ESD} dp_T dz \times C_{p_T, vz cut}(\eta') \quad (1)$$

where the summation is executed for the measured tracks and used events, the integration is executed for the region passed the vertex and  $p_T$  cutoff.  $C(\eta', z, p_T)$  is the correction factor obtained from the simulation as follows.

$$C(\eta, z, p_T) = \frac{N_{acc}(\eta, z, p_T)}{N_{gen}(\eta, z, p_T)} \quad (2)$$

$N_{acc}(\eta, z, p_T)$  and  $N_{gen}(\eta, z, p_T)$  are the number of

charged particles accepted and generated, respectively.  $C_{p_T, vz cut}(\eta')$  is the correction factor for the limited integration for  $p_T$  and the vertex  $z$  position. It is under development.

Calibration of the TPC using laser is also under development. The aim of the laser calibration is to measure the response of the TPC to the straight tracks at the known position. The distortion of the electric field at the edge of chambers, misalignment of the each sector, and the distortion of the drift velocity were measured. Figure 1 shows the distortion of the gain as a function of the distance from the edge of chambers of the TPC. The fit function shown in Fig 1 is used to the calibration code.

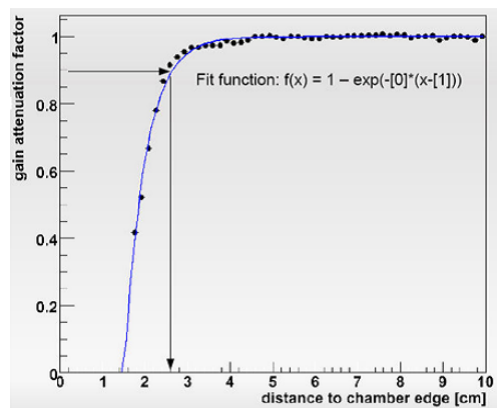


Fig. 1. The gain as a function of the distance from the edge of chambers of the TPC.

Estimation of the correction factor for the measurement of the charged multiplicity and the calibration of TPC will be developed until the first p+p collision at LHC scheduled on the September at 2009.

## References

- 1) L. V. Gribov, E. M. Levin, M. G. Ryskin, Phys. Rep. 100 (1983) 1.
- 2) L. McLerran, R. Venugopalan, Phys. Rev. D 49 (1994) 2233.
- 3) K. Adcox, et al, PHENIX Collaboration, Nucl. Phys. A 757 (2005) 184.
- 4) T. Hirano, U. Heinz, D. Kharzeev, R. Lacey, Y. Nara, Phys. Lett B 636 (2006) 299.
- 5) D. Kharzeev, E. Levin, M. Nardi, Nucl Phys A 747 (2005) 609.

<sup>\*1</sup> Center for Nuclear Study (CNS), University of Tokyo, Japan

<sup>\*2</sup> Gesellschaft für Schwerionenforschung (GSI), Germany

# Recent progress in precision pionic atom spectroscopy at RIBF†

K. Itahashi,\*<sup>1</sup> S. Itoh,\*<sup>1,\*2</sup> N. Fukunishi,\*<sup>1</sup> H. Outa,\*<sup>1</sup> H. Geissel,\*<sup>3</sup> M. Winkler,\*<sup>3</sup> H. Weick,\*<sup>3</sup> and R.S. Hayano\*<sup>2</sup>

for the pionic atom factory collaboration.

[hadron in medium, pionic atom, beam optics, spectroscopy]

## 1 Introduction

Spectroscopy of pionic atoms has been contributing to understanding of the origin of hadron masses<sup>1)</sup>. According to theories, the hadron masses dynamically grow as chiral symmetry of the surrounding media, the vacuum, is partially broken<sup>2)</sup>. The order of the symmetry breaking depends on the energy density of the vacuum and is parametrized by the magnitude of the quark condensate  $\langle \bar{q}q \rangle$ <sup>3,4)</sup>. At higher temperature or at higher density the quark condensate decreases and it becomes zero beyond certain limits.

The objective of the present experiment<sup>5)</sup> and those to follow is evaluation of the magnitude of the quark condensate at the normal nuclear density through precise experimental determination of the in-medium isovector interaction strengths between the pion and the nucleus<sup>5,6)</sup>. Previous results of pionic atom spectroscopy yielded first quantitative estimation of its reduction at the normal nuclear density to be about 33 % compared to that in the vacuum<sup>1,7-10)</sup>. This estimation is consistent with the theoretical prediction of about 30 %, and is supporting the theories. However, the value of 33 % definitely needs more careful and precise evaluation.

In the present experiment, we are going to measure missing mass of the  $^{122}\text{Sn}(d, ^3\text{He})$  reaction near the pion emission threshold using the BigRIPS<sup>11)</sup> in the RIBF<sup>12)</sup> as a spectrometer and to determine the binding energies and widths of the  $1s$  and  $2s$  pionic  $^{121}\text{Sn}$ . Accomplishment of this experiment will be a start point for systematic study of pionic atoms.

Here, we will briefly summarize the recent progress.

## 2 Beam optics

To achieve better precision, one of the most critical issues is the beam optics of the spectrometer BigRIPS. Since the momentum spread of the incident beam ( $\Delta p/p$ ) is as large as 0.1 %, its contribution to the experimental resolution is huge and is estimated to be about  $\sim 1$  MeV (FWHM), which is about 5 times larger than target value of 200 keV. Thus, to compensate for the momentum spread, we need to develop a dispersion matching beam optics between two sections; the beamline SRC–target and the spectrometer

target–F5 focal plane.

The dispersion matching condition in our experiment is described as

$$b_{16}s_{11} + b_{26}s_{12} + s_{16}t_{66} = 0 \quad (1)$$

with the transfer matrices

$$\begin{pmatrix} x_f \\ a_f \\ \delta_f \end{pmatrix} = STB \begin{pmatrix} x_0 \\ a_0 \\ \delta_0 \end{pmatrix}, \quad (2)$$

where

$$S = \begin{pmatrix} s_{11} & s_{12} & s_{16} \\ s_{21} & s_{22} & s_{26} \\ 0 & 0 & 1 \end{pmatrix}, B = \begin{pmatrix} b_{11} & b_{12} & b_{16} \\ b_{21} & b_{22} & b_{26} \\ 0 & 0 & 1 \end{pmatrix}$$

and T denotes ( $d, ^3\text{He}$ ) reaction at the target with  $t_{66} \sim 1.31$ , which is attributed to the relation between incident and outgoing momenta in the kinematics.

The largest difficulty to build above dispersion matching beam optics resides in the fact that the SRC is sitting in the most upstream of the system as a large optical element. Therefore, we need to study in detail the optics of the SRC first.

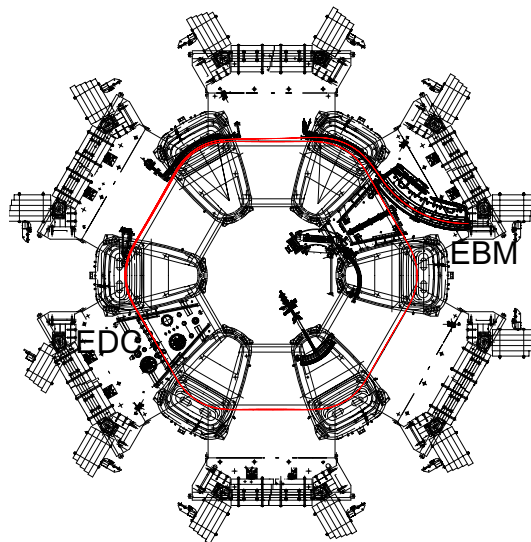


Fig. 1. Beam trajectories in the SRC.

We have performed a detailed calculation of the beam trajectories inside the SRC from EDC to EBM as shown in Fig. 1. At the EDC, the SRC is tuned to make an upright ellipsoid. Figure 1 shows the calculated beam trajectories in the SRC. Calculating the

\*<sup>1</sup> RIKEN Nishina Center, RIKEN

\*<sup>2</sup> Department of Physics, University of Tokyo

\*<sup>3</sup> GSI, Darmstadt

derivatives of the trajectories, we have obtained the first order transfer matrix from EDC to EBM. Thus calculated matrix is

$$\begin{pmatrix} a_{11} & a_{12} & a_{16} \\ a_{21} & a_{22} & a_{26} \\ a_{61} & a_{62} & a_{66} \end{pmatrix} = \begin{pmatrix} -1.00 & -0.34 & 7.69 \\ 2.97 & -0.01 & -25.4 \\ 0 & 0 & 1 \end{pmatrix}$$

The beamline optics between EBM and the target is calculated so as to decouple the optics near the intermediate focal plane after QDT11 to leave room for flexibility to adjust to the properties of the incident beam since we have little knowledge on them. The first quadrupole quartet is used for this purpose, and the quality of the adjustment is measured at the focus after the QDT11. The obtained matrix is

$$\begin{pmatrix} b_{11} & b_{12} & b_{16} \\ b_{21} & b_{22} & b_{26} \\ b_{61} & b_{62} & b_{66} \end{pmatrix} = \begin{pmatrix} -0.39 & 0 & 4.60 \\ -2.90 & -2.58 & 21.0 \\ 0 & 0 & 1 \end{pmatrix}$$

The calculated beam optics for the beamline is shown in Fig. 2

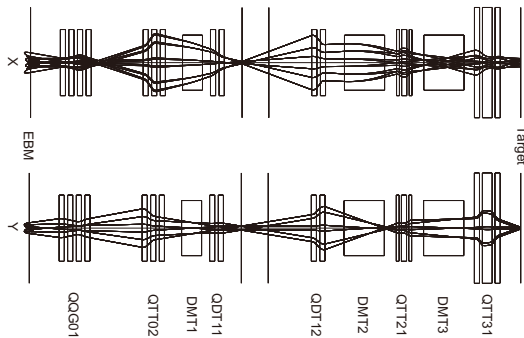


Fig. 2. Beam line optics from the SRC to the target.

The above obtained matrix is used for the optics calculation in the BigRIPS to fulfill Eq. 1

We are going to make a detailed test of the calculated beam optics in May, 2009.

### 3 Expected resolution

Based on the calculated beam optics, we have estimated the expected experimental resolution in FWHM depending on the emittance of the incident beam as shown in Fig. 3. The estimation is assuming the target thickness of 15 mg/cm<sup>2</sup>, which contributes about 140 keV [FWHM].

As shown in Fig. 3, the emittance of the incident beam is crucial in the present spectroscopy and we need to optimize the horizontal beam size at EBM.

#### References

- 1) K. Suzuki *et al.*, Phys. Rev. Lett. **92**, 072302 (2004).
- 2) Y. Nambu and G. Jona-Lasinio, Phys. Rev. **122**, 345 (1961).

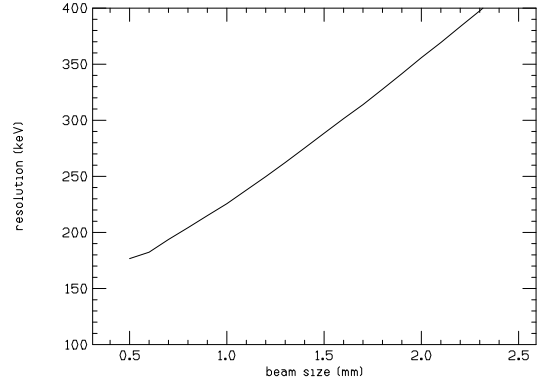


Fig. 3. Experimental resolution in FWHM depending on the horizontal beam size in  $\sigma$  at the EBM.

- 3) G. Drukarev and E. M. Levin, Nucl. Phys. **A511**, 679 (1990); **A532**, 695 (1991); Prog. Part. Nucl. Phys. **27**, 77 (1991).
- 4) W. Weise, Nucl. Phys. **A553**, 53 (1993) and references therein.
- 5) K. Itahashi *et al.*, RIBF proposal No.054 "Spectroscopy of Pionic Atom in <sup>122</sup>Sn(*d*, <sup>3</sup>He) Nuclear Reaction" (2008) and references therein.
- 6) E.E. Kolomeitsev, N. Kaiser, and W. Weise, Phys. Rev. Lett. **90**, 092501 (2003).
- 7) T. Yamazaki *et al.*, Z. Phys. A **355**, 210 (1996).
- 8) H. Gilg *et al.*, Phys. Rev. C **62**, 025201 (2001).
- 9) K. Itahashi *et al.*, Phys. Rev. C **62**, 025202 (2001).
- 10) H. Geissel *et al.*, Phys. Rev. Lett. **88**, 122301 (2002).
- 11) T. Kubo *et al.*, Nucl. Inst. Meth. B **204**, 97 (2003).
- 12) Y. Yano, Nucl. Inst. Meth. B **261**, 1009 (2007).

## **4. Hadron Physics(Theory)**

# Glueball Decay in Holographic QCD<sup>†</sup>

K. Hashimoto,<sup>\*1</sup> C.-I. Tan,<sup>\*2</sup> and S. Terashima<sup>\*3</sup>

[Glueballs, Hadron physics, Superstring theory]

Glueballs, as excitations of gauge-invariant composite operators in Yang-Mills theories, remain illusive. Although the existence of the glueballs (of various types, such as scalar glueballs and tensor glueballs) is expected, their experimental identification in the hadron spectra remains difficult. This difficulty is largely due to the inability to compute reliably couplings of glueballs to ordinary mesons in strongly coupled QCD. Lattice QCD predicts for the mass of the lightest scalar glueball to be around 1600-1700 MeV, but it doesn't yet provide information on the glueball couplings and decay products/widths, which are indispensable for their identification. The Large Hadron Collider (LHC) will likely yield a huge amount of hadronic data, which can lead to progress in revealing the mystery of glueballs.

In this paper, using holographic QCD based on D4-branes and D8-anti-D8-branes,<sup>1)</sup> we have computed couplings of glueballs to light mesons. We describe glueball decay by explicitly calculating its decay widths and branching ratios. Interestingly, while glueballs remain less well understood both theoretically and experimentally, our results are found to be consistent with the experimental data for the scalar glueball candidate  $f_0(1500)$ . More generally, holographic QCD predicts that decay of any glueball to  $4\pi_0$  is suppressed, and that mixing of the lightest glueball with  $q\bar{q}$  mesons is small.

The AdS/CFT (gauge/gravity) correspondence (duality) is one of the most important developments in string theory, and, holographic QCD refers to the application of AdS/CFT to QCD studies. The basic claim of the AdS/CFT correspondence is that correlation functions of gauge-invariant composite operators in large  $N_c$  gauge theories at strong 't Hooft coupling correspond to classical gravitational computations in higher dimensional gravity theories in curved backgrounds. The correspondence has been applied to (i) computation of glueball spectrum in large  $N_c$  pure Yang-Mills theory and to (ii)  $q\bar{q}$  meson spectra/dynamics in large  $N_c$  QCD, which we review briefly below. These efforts have been quite successful in reproducing lattice and experimental data of hadrons, even though the real QCD is recovered in the "CFT" side only when one incorporates various corrections in the large  $N_c$  and large 't Hooft coupling expansion.

Here we combine these two efforts, (i) and (ii), in order to calculate couplings between the glueballs and the  $q\bar{q}$  mesons, in the large  $N_c$  QCD.

The key merit of using holographic QCD is the fact that one not only can calculate the hadron spectra, but also can compute explicitly their *couplings*. It provides a more powerful method for constraining these couplings than the chiral perturbation technique. In particular, since glueballs are expected to be heavier than 1 GeV, derivative expansion in chiral perturbation becomes unreliable. Furthermore, current lattice calculations are not well suited for computing dynamical quantities such as decays and couplings. Our paper represents a first principle calculation for glueball decays, though in the approximation where the holographic duality is valid.

We compute the couplings between the glueballs and the  $q\bar{q}$  mesons in this setting. In the dual description through the AdS/CFT, they correspond to the supergravity fluctuations and the Yang-Mills fluctuations on the D8-branes, respectively. These two sectors are coupled in the combined system of supergravity plus D8-branes. We substitute the fluctuations (wave functions) of the supergravity fields (corresponding to the glueball) and the D8-brane massless fields (mesons) into the D8-brane action and integrate over the extra dimensions, to obtain the desired couplings. Combining sectors (i) and (ii) is important not only due to its phenomenological impact but also because this represents the first computation in holographic QCD of the couplings between the supergravity fluctuations and the fields on the probe D-branes.

Once the couplings are obtained, we can compute the decay widths for various decay channels of a glueball, and study its possible mixings. Because the whole  $q\bar{q}$  meson sector is combined into the D8-brane action, which is a higher-dimensional Yang-Mills lagrangian, several interesting mesonic features follow. For example, at the leading order (in the expansion of the large 't Hooft coupling), glueball decay to  $4\pi_0$  is prohibited. There is no direct  $4\pi_0$  coupling to the glueball, and, furthermore, glueball -  $\rho$  meson coupling also does not allow the  $4\pi_0$  decay mode. As for the mixing, we can show that the lightest glueball has no mixing with  $q\bar{q}$  mesons at the leading order of our expansion. These are our main predictions based on the holographic QCD.

<sup>†</sup> Condensed from the article in Phys. Rev. D **77**, 080061 (2008)

<sup>\*1</sup> Theoretical Physics Laboratory, RIKEN

<sup>\*2</sup> Department of Physics, Brown University

<sup>\*3</sup> Yukawa Institute for Theoretical Physics, Kyoto University

## References

- 1) T. Sakai and S. Sugimoto, Prog. Theor. Phys. **113**, 843 (2005), Prog. Theor. Phys. **114**, 1083 (2005).

# Quark Mass Deformation of Holographic Massless QCD<sup>†</sup>

K. Hashimoto,<sup>\*1</sup> T. Hirayama,<sup>\*2</sup> F.L. Lin,<sup>\*3</sup> and H.U. Yi<sup>\*4</sup>

[Quark mass, Hadron physics, Superstring theory]

AdS/CFT correspondence, gauge/gravity duality, has provided us with a new avenue to compute observables in strongly interacting gauge theories via weakly coupled gravitational descriptions. Recently in superstring theory, using particular kinds of D-branes, there proposed a holographic model of QCD by Sakai and Sugimoto<sup>1)</sup>, where the non-Abelian chiral symmetry and its spontaneous breaking is geometrically realized via a D4/D8/ $\overline{D8}$  configuration. The model predictions for the meson spectrum and the couplings between them compare well with experiments with a good accuracy. Baryons in this model were also investigated. Moreover, this holographic model has an ability of predicting possible glue-ball interactions to mesons. There are many other QCD observables that have been analyzed in this model, which show that the model is a good approximation to real QCD at least in low energy, large  $N_c$ -limit.

Despite its success in many aspects, this model has an apparent shortcoming that the pions are massless. This is because the quarks are massless from the construction. In our work, we propose deformations of the Sakai-Sugimoto model which correspond to the introduction of the quark mass. Our deformations have additional D-branes away from the original confining  $N_c$  D4-branes, which still have a reasonable field theory interpretation. The original Sakai-Sugimoto model is restored once these additional D-branes are moved to spatial infinity in the bulk. In the field theory view-point, our idea is rather similar to the extended technicolor model, where we have an additional sector to the original QCD, which contains new techni-quarks interacting via new technicolor interactions. The quarks/techni-quarks are massless at UV, but the chiral symmetry (the electroweak symmetry in this case) is spontaneously broken by a techni-quark condensate driven by the strong technicolor gauge interactions. QCD quarks get explicit bare mass term from the techni-quark condensate, through quark-techniquark interaction.

To realize this idea in our set-up, we introduce additional  $N'$  D4-branes (we call them D4'-branes) which are parallel to, but separated from the original  $N_c$  D4-branes of QCD gauge symmetry. The total gauge

symmetry is  $SU(N_c + N')$  when the D4'-branes are on top of the original D4-branes, and it is broken to  $SU(N_c) \times SU(N')$  by a Higgs mechanism via separating the D4' from the D4. Massive off-diagonal gauge bosons appear as strings suspended between the D4 and the D4'. We add  $N_f$  D8/ $\overline{D8}$ -branes as in Sakai-Sugimoto model to introduce massless quarks and techni-quarks, which are charged under the chiral symmetry  $U(N_f) \times U(N_f)$ . By assuming a strong technicolor  $SU(N')$  dynamics on the D4'-branes, which replaces the D4'-branes with the Witten's geometry, the chiral symmetry is spontaneously broken by adjoining the D8/ $\overline{D8}$ -branes there, as in the Sakai-Sugimoto model but with the technicolor instead of the QCD gauge group. This breaking will be mediated to the QCD sector of the  $N_c$  D4-branes by, for example, the massive gauge bosons coming from the open strings stretched between the D4 and the D4'-branes. This induces the bare masses for the QCD quarks.

From the Feynman graphs that would induce quark masses from a techni-quark condensate, we can easily identify the corresponding string worldsheets that mediate this phenomenon in our D-brane configuration in flat space. We consider a circle following D4-D8-D4'- $\overline{D8}$ -branes and a disk *worldsheet instanton* whose boundary is ending on this circle. It is responsible for the extended technicolor interactions coupling the quarks to the techni-quarks. Then we consider the strongly coupled field theory, or equivalently a weakly coupled gravity description, where we can identify the worldsheet instanton which has been responsible for the quark mass term. In the gravity description, where both D4 and D4'-branes are replaced by a near horizon geometry of a multi-center gravity solution, we have a closed loop on the surface of the probe D8-branes only, since the D8- and the  $\overline{D8}$ -branes are smoothly connected at two throats created by the D4- and the D4'-brane geometry. The previous worldsheet instanton in the weak coupling picture is now ending on this closed loop. The worldsheet instanton is a leading order contribution to the effective action of the D8-branes, since it is a planar diagram with a single boundary in the large  $N$  gauge theory. We show that this worldsheet instanton amplitude indeed induces the lowest mass perturbation for pions that is expected in the standard low energy chiral Lagrangian. We also show that the GOR relation is satisfied.

## References

- 1) T. Sakai and S. Sugimoto, Prog. Theor. Phys. **113**, 843 (2005), Prog. Theor. Phys. **114**, 1083 (2005).

<sup>†</sup> Condensed from the article in Journal of High Energy Physics **0807**, 089 (2008)

<sup>\*1</sup> Theoretical Physics Laboratory, RIKEN

<sup>\*2</sup> Physics Division, National Center for Theoretical Sciences, Hsinchu, Taiwan

<sup>\*3</sup> Department of Physics, National Taiwan Normal University

<sup>\*4</sup> The Abdus Salam International Center for Theoretical Physics, Trieste, Italy

## Phenomenology of small $x$ physics.

A. M. Stasto<sup>\*1,\*2,\*3</sup>

### Unitarity in Hadron collisions<sup>a)</sup>

The LHC machine will open a new kinematical regime for studying strong interactions in the hadronic collisions. Of particular interest is the contribution to the cross section from semihard jets. The perturbative QCD formula for minijet production constitutes an important ingredient in models describing the total cross section and multiparticle production in hadron-hadron scattering at high energies. Using arguments based on  $s$ -channel unitarity we set bounds on the minimum value of  $p_T$  for which the leading twist minijet formula can be used. For large impact parameters where correlations between partons appear to be small we found that the minimum value of  $p_T$  should be greater than 2.5 GeV for LHC energies and greater than 3.5 GeV for cosmic ray energies of about 50 TeV. We also argued that for collisions with values of impact parameters typical for heavy particle production the values of minimum  $p_T$  are likely to be considerably larger. We also analyzed and quantified the potential role of saturation effects in the gluon density. We found that although saturation effects alone are not sufficient to restore unitarity, they are likely to play an important role at LHC energies.

### Resummation at low $x$ and strong coupling<sup>b)</sup>

In recent years there has been large theoretical activity related to the duality between the string model in the anti de Sitter space and the conformal field theories. This duality offers a unique insight into the regime of the strong coupling constant in the gauge theory where standard perturbative methods fail. In particular case of the high energy scattering between the two hadrons the leading exchange is that of the Pomeron, a Regge trajectory with the quantum numbers corresponding to the vacuum. It was demonstrated that on the gravity side this scattering process is dominated by the exchange of the spin-two graviton. It is also known that the Pomeron in the perturbative theory can be computed using Feynman diagram technique, and it corresponds to the composite state of two reggeized gluons. It can be obtained as a solution to the evolution equation for the gluon Green's function at small values of Bjorken  $x$ . We have demonstrated that a particular resummation model for this evolution kernel for the gluon density at small  $x$  creates a

bridge between the weak and strong couplings. The resummation model embodies both DGLAP and BFKL anomalous dimensions at leading logarithmic orders, as well as a kinematical constraint on the real emission part of the kernel. In the case of pure gluodynamics the strong coupling limit of the Pomeron intercept is consistent with the exchange of the spin-two, colorless particle.

### Exact kinematics in the gluon cascades<sup>c)</sup>

It is well known that the kinematic effects constitute a large portion of the higher order corrections to the kernels in the small  $x$  evolution equations for the parton densities. They are also present in the computation of the higher order anomalous dimensions of the standard renormalization group approach. The problem of kinematic effects in the gluon and color dipole cascades has been addressed in the large  $N_c$  limit of  $SU(N_c)$  Yang-Mills theory. We investigated the tree level multi-gluon components of the gluon light cone wave functions in the light cone gauge keeping the exact kinematics of the gluon emissions. We focused on the components with all helicities identical to the helicity of the incoming gluon. The recurrence relations for the gluon wave functions were derived. In the case when the virtuality of the incoming gluon is neglected the exact form of the multi-gluon wave function has been obtained. Furthermore, we proposed an approximate scheme to treat the kinematic effects in the color dipole evolution kernel. The new kernel entangles longitudinal and transverse degrees of freedom and leads to a reduced diffusion in the impact parameter. When evaluated in the next-to-leading logarithmic (NLL) accuracy, the kernel reproduces the correct form of the double logarithmic terms of the dipole size ratios present in the exact NLL dipole kernel. Finally, we analyzed the scattering of the incoming gluon light cone components off a gluon target and the fragmentation of the scattered state into the final state. The equivalence of the resulting amplitudes and the maximally-helicity-violating amplitudes has been demonstrated in the special case when the target gluon is far in rapidity from the evolved gluon wave function.

### References

- 1) T. C. Rogers, A. M. Stasto and M. I. Strikman, Phys. Rev. D **77**, 114009 (2008) [arXiv:0801.0303 [hep-ph]].
- 2) A. M. Stasto, *Pomeron - Graviton duality*, [arXiv:0801.0437 [hep-ph]].
- 3) L. Motyka and A. M. Stasto, *Exact kinematics in the dipole and gluon cascade*, in preparation.

<sup>\*1</sup> Penn State University, University Park, PA 16802, USA

<sup>\*2</sup> RIKEN Center, BNL, Upton, NY 11973, USA

<sup>\*3</sup> Institute of Nuclear Physics, Kraków, Poland

a) Condensed from article<sup>1)</sup>.

b) Condensed from article<sup>2)</sup>.

c) Condensed from article<sup>3)</sup>.

# An explanation of the NuTeV anomaly<sup>†</sup>

W. Bentz,<sup>\*1</sup> T. Ito,<sup>\*1</sup> I. C. Cloët,<sup>\*2</sup> and A. W. Thomas<sup>\*3</sup>

[NUCLEAR PARTON DISTRIBUTIONS, Flavor dependence, Neutrino deep inelastic scattering]

The Paschos-Wolfenstein (PW) ratio is defined by<sup>1)</sup>

$$R = \frac{\sigma_{NC}^{\nu A} - \sigma_{NC}^{\bar{\nu} A}}{\sigma_{CC}^{\nu A} - \sigma_{CC}^{\bar{\nu} A}},$$

where  $A$  represents the nuclear target, and  $NC$  ( $CC$ ) indicates weak neutral current (charged current) interactions. This ratio was determined by the NuTeV collaboration in 2002<sup>2)</sup> by using an iron target, where the measured inclusive deep inelastic (anti-) neutrino cross sections are integrated over the Bjorken scaling variable ( $x_A$ ) and the energy transfer ( $y$ ). The ratio can be expressed in terms of nuclear valence quark distributions  $q_{A-} = q_A - \bar{q}_A$  by

$$R = \frac{g_v^u \langle x_A u_{A-} \rangle - g_v^d \langle x_A d_{A-} \rangle}{3 \langle x_A d_{A-} \rangle - \langle x_A u_{A-} \rangle} \equiv R_0 + \delta R$$

$$R_0 = \frac{1}{2} - \sin^2 \Theta_W$$

$$\delta R \simeq \left(1 - \frac{7}{3} \sin^2 \Theta_W\right) \frac{\langle x_A u_{A-} - x_A d_{A-} \rangle}{\langle x_A u_{A-} + x_A d_{A-} \rangle},$$

where  $\Theta_W$  is the Weinberg angle, and for the quark weak vector charges ( $g_v^q$ ) we follow the conventions of Ref.<sup>3)</sup>.  $\langle \dots \rangle$  implies integration over  $x_A$ , therefore the quantities in angle brackets are the fractions of the target momentum carried by the valence  $u$  and  $d$  quarks.  $R_0$  is the PW ratio for isospin symmetric matter, and is given solely in terms of the Weinberg angle.

If one can determine the correction term  $\delta R$  arising from the neutron excess, the PW ratio provides a unique way to measure the Weinberg angle. In the NuTeV analysis, this correction was determined by assuming that the target is composed of free nucleons. The result was<sup>2)</sup>  $R - \delta_f R = 0.2723$ , which implies  $\sin^2 \Theta_W = 0.2277$ . The deviation from the Standard Model value (world average<sup>4)</sup>)  $\sin^2 \Theta_W = 0.2227$  is a three-sigma discrepancy<sup>a)</sup>, and was often considered as an indication of physics beyond the Standard Model.

In our previous work<sup>5)</sup>, we used the quark-diquark description of the nucleon in the Nambu-Jona-Lasinio model combined with the mean field approximation for infinite nuclear matter, to evaluate the valence quark

distributions in isospin asymmetric nuclear environment. In this approach, which successfully describes the EMC effect<sup>6)</sup>, we found that the additional binding (symmetry energy) of  $u$  quarks in  $N > Z$  matter leads to an enhancement of medium modifications of the  $u$  quark distributions, and as a result the EMC effect increases as  $Z/N$  decreases from 1 to 0.6. Here we use our in-medium quark distributions for the same neutron excess as in the NuTeV experiment (5.74%) to investigate the influence of these isovector medium modifications on the PW ratio.

We use the Standard Model value of  $\sin^2 \Theta_W$ , and split the correction into three pieces:  $\delta R = \delta_f R + \delta_{\text{med}} R + \delta_{\text{csb}} R$ . The naive (“free”) and medium corrections are evaluated in our model, while the correction arising from charge symmetry breaking ( $m_d > m_u$ ) is taken from Ref.<sup>7)</sup>. Our results for  $R - \delta_f R = R_0 + \delta_{\text{med}} R + \delta_{\text{csb}} R$  are shown in Table 1 in comparison to the NuTeV result quoted above. The medium

$R_0$	+ med	+ csb	NuTeV
0.2773	0.2741	0.2724	0.2723

Table 1. Results for the PW ratio after naive isoscalarity corrections.

correction  $\delta_{\text{med}} R = -0.0032$  comes mainly from the vector-isovector nuclear mean field ( $\rho^0$ ), and only a small part from the Fermi motion of the nucleons. The final theoretical value, including medium modifications and charge symmetry breaking, is 0.2724, which explains the NuTeV result of 0.2723. Our conclusion is that the NuTeV measurement provides strong evidence that the nucleon is modified by the nuclear medium, and should not be interpreted as an indication for physics beyond the Standard Model.

## References

- 1) E.A. Paschos and L. Wolfenstein, Phys. Rev. **D 7** (1973) 91.
- 2) G.P. Zeller *et al.*, Phys. Rev. Lett. **88** (2002) 091802.
- 3) C. Amsler *et al.*, Phys. Lett. **B 667** (2008) 1.
- 4) D. Abbaneo *et al.*, arXiv:hep-ex/0112021.
- 5) W. Bentz, I.C. Cloët and A.W. Thomas, RIKEN Accel. Prog. Rep. **41** (2008) 66.
- 6) I.C. Cloët, W. Bentz and A.W. Thomas, Phys. Lett. **B 642** (2006) 210.
- 7) J.T. Londergan and A.W. Thomas, Phys. Lett. **B 558** (2003) 132.

<sup>†</sup> Condensed from an article by I.C. Cloët, W. Bentz, and A.W. Thomas, to be published.

<sup>\*1</sup> Department of Physics, Tokai University, Kanagawa, Japan

<sup>\*2</sup> Department of Physics, University of Washington, Seattle, WA, U.S.A.

<sup>\*3</sup> Jefferson Laboratories, Newport News, VA, U.S.A.

<sup>a)</sup> The result deduced by NuTeV is  $\sin^2 \Theta_W = 0.2277 \pm 0.0013(\text{stat.}) \pm 0.0009(\text{syst.})$ , while the world average is  $\sin^2 \Theta_W = 0.2227 \pm 0.0004$ .

# EMC effect for parity-violating DIS<sup>†</sup>

W. Bentz,<sup>\*1</sup> T. Ito,<sup>\*1</sup> I. C. Cloët,<sup>\*2</sup> and A. W. Thomas<sup>\*3</sup>

[NUCLEAR PARTON DISTRIBUTIONS, Flavor dependence, Parity violating deep inelastic  
electron scattering]

In the deep inelastic scattering (DIS) of longitudinal polarized electrons on unpolarized nuclear targets ( $A$ ), parity violating (PV) effects due to the interference between the photon exchange and  $Z^0$  boson exchange lead to a non-zero spin asymmetry  $A_{PV} = \frac{\sigma_R - \sigma_L}{\sigma_R + \sigma_L}$ . Here  $\sigma_{R,L}$  denote the double differential cross sections for DIS of right and left-hand polarized electrons. In the Bjorken limit, we have<sup>1)</sup>

$$A_{PV} = \frac{G_F Q^2}{4\pi\alpha\sqrt{2}} \left[ a_2(x_A) + \frac{1 - (1-y)^2}{1 + (1-y)^2} a_3(x_A) \right].$$

Here  $x_A$  is the Bjorken variable of the nucleus multiplied by the mass number  $A$ ,  $G_F$  is the Fermi coupling constant, and  $y = \nu/E$  is the energy transfer divided by the incident electron energy. The term  $a_2$  comes from the product of the electron weak axial current and the quark weak vector current, and is given by

$$a_2(x_A) = \frac{F_{2A}^{\gamma Z}(x_A)}{F_{2A}^{\gamma}(x_A)} = \frac{2 \sum_q e_q g_v^q q_{A+}(x_A)}{\sum_q e_q^2 q_{A+}(x_A)}.$$

Here  $q_{A+}(x_A) = q_A(x_A) + \bar{q}_A(x_A)$  are the nuclear parton distributions, and for the definitions of the nuclear structure functions ( $F_{2A}^{\gamma}$  and  $F_{2A}^{\gamma Z}$ ) and the quark weak vector couplings ( $g_v^q$ ) we follow the conventions of Ref.<sup>2)</sup>. The term  $a_3$ , which comes from the product of the electron weak vector current and the quark weak axial vector current, makes only a small contribution to the asymmetry, and will not be discussed here.

Because the structure functions  $F_{2A}^{\gamma Z}$  and  $F_{2A}^{\gamma}$  have different flavor dependences, they will receive different medium modifications in isospin asymmetric nuclear systems ( $N \neq Z$ ). This is clearly seen if we consider the isovector correction to first order:

$$a_2(x_A) \simeq \left( \frac{9}{5} - 4 \sin^2 \Theta_W \right) - \frac{12 u_{A+}(x_A) - d_{A+}(x_A)}{25 u_{A+}(x_A) + d_{A+}(x_A)},$$

where  $\Theta_W$  is the Weinberg angle. It follows that a measurement of  $a_2$  would give information on the flavor dependence of nuclear parton distributions. Conversely, if one can make reliable estimates of the isovector correction term, the spin asymmetry provides an independent method to determine the Weinberg angle.

Here we use the quark distributions in isospin asymmetric nuclear matter, calculated in our previous

work in the Nambu-Jona-Lasinio model<sup>3)</sup>, to show the isospin dependent medium modifications of the spin asymmetry term  $a_2$ . In Figs. 1 and 2,  $a_2^{\text{naive}}$  is the result without medium modifications (obtained by assuming that the target nucleus is composed of free nucleons), and  $a_2$  is our full model result. The Standard Model value  $\sin^2 \Theta_W = 0.223$  is used. The results, which refer to the NJL model associated with a low energy scale, do not change much under  $Q^2$  evolution in the valence quark region. We see that the medium modifications enhance the spin asymmetry for large  $x_A$ . The reason for this is that the isovector-vector mean field ( $\rho^0$ ) leads to an additional binding of  $u$  quarks, which results in a softening of  $u_A$  compared to  $d_A$  in the valence quark region<sup>3)</sup>.

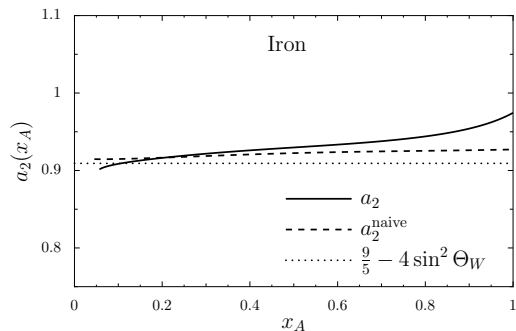


Fig. 1. Spin asymmetry  $a_1$  for  $Z/N = 26/30$ .

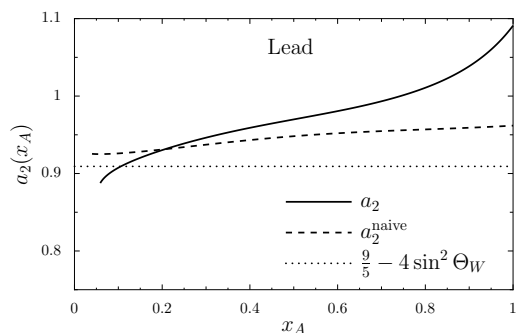


Fig. 2. Spin asymmetry for  $Z/N = 82/126$ .

## References

- 1) T. Hobbs and W. Melnitchouk, Phys. Rev. **D 77** (2008), 114023.
- 2) C. Amsler et al., Phys. Lett. **B 667** (2008), 1.
- 3) W. Bentz, I.C. Cloët and A.W. Thomas, RIKEN Accel. Prog. Rep. **41** (2008) 66.

<sup>†</sup> Condensed from an article by I.C. Cloët, W. Bentz, and A.W. Thomas, to be published.

<sup>\*1</sup> Department of Physics, Tokai University, Kanagawa, Japan

<sup>\*2</sup> Department of Physics, University of Washington, Seattle, WA, U.S.A.

<sup>\*3</sup> Jefferson Laboratories, Newport News, VA, U.S.A.

# The study of multiquark states based on $1/N_c$ classifications

Toru Kojo <sup>\*1</sup>[Multiquark,  $1/N_c$  expansion]

The hadron spectroscopy have provided a lot of clues to understand the dynamics of strong interaction, QCD. Nowadays, with concepts of color confinement and chiral symmetry breaking, the tendency of most hadrons, (conventional) mesons ( $q\bar{q}$ ) and baryons ( $qqq$ ), are well-classified by constituent quark picture. On the other hand, there exist exceptional hadrons as candidates of exotica, such as multiquark states with large number of quarks beyond two or three, meson-meson (baryon) molecules, and so on. Obviously we need new kinds of explanations, which would eventually unveil unexpected aspects of the theory. Fortunately recent experimental investigations provide an increasing number of data for exotica, e.g., pentaquark  $\Theta^+(1530)$ , exotic charmonia ( $X, Y, Z$ ),  $\Lambda(1405)$  as a candidate of meson-baryon molecule. Thus in the present situation, it may be possible to categorize exotica toward the construction of useful concepts for them in a similar way to using constituent quarks for conventional hadrons.

Among several candidates for exotica, in this work, we concentrate on the discussion of multiquark components, employing the  $\sigma$  meson ( $I = 0, J^{PC} = 0^{++}$ ) as an example. The  $\sigma$  has almost all important ingredients as the exotica: not only usual  $q\bar{q}$  (2q) component but hadronic states beyond the simple constituent quark picture such as glueball,  $\pi\pi$  molecule, and  $qq\bar{q}\bar{q}$  (4q) states. In this respect, the question always arising in theoretical studies of multiquark components is how to distinguish them from other hadronic states. To the best of our knowledge, there has been no simple and clearcut scheme to characterize the difference between them.

We try to solve this problem by introducing the classification scheme based on  $1/N_c$  ( $N_c$  is number of color) expansion<sup>1)</sup> for the hadronic states in the correlators made of quark gluon fields,

$$\Pi(q^2) = i \int d^4x e^{iqx} \langle T J_{4q}(x) J_{4q}^\dagger(0) \rangle \quad (1)$$

where  $\Pi$  calculated in terms of quarks and gluons includes all possible hadronic states generated by 4q operator. In quark-gluon side,  $\Pi$  can be classified by  $1/N_c$  as  $\Pi = \Pi^{(0)} + \Pi^{(1)} + \dots$ , and they are related to the properties of hadronic states order by order in terms of  $1/N_c$ . For instance, we can show that some hadronic states can appear at the leading order of  $1/N_c$ , while other states can not<sup>2)</sup>.

In this scheme, even if we consider hadronic states

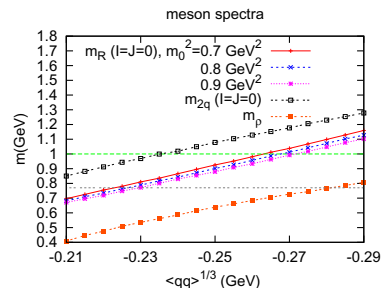


Fig. 1. The masses of 2q states in vector and scalar channel and 4q state as functions of quark condensate.

with the same quantum number, they can be distinguished by the choice of interpolating fields and by the order of  $1/N_c$  in such correlation functions. Then we can identify whose contributions in quark-gluon dynamics are responsible to those from the hadronic states of our interest. After such an identification, we can verify that the mixing diagrams of these states are suppressed by higher order of  $1/N_c$ , and concentrate on the hadronic states without mixing effects.

We apply this scheme to the case of the  $\sigma$  meson. It turns out that the obstacles to extract 4q components from 4q correlators, i.e., the contributions of instanton, glueball, and, in particular,  $\pi\pi$  scattering states can be identified and separated in terms of  $1/N_c$ , then we can concentrate on the remaining 2q and 4q contributions. The most remarkable point is that  $1/N_c$  classification defines 4q states as the states which appear in 4q correlator but can not be obtained from the  $\pi\pi$  scattering processes and 2q correlation functions. In this way, we can assign the hadronic states for proper quark-gluon diagrams in the computation<sup>3)</sup>.

After identification of quark-gluon graphs responsible to the 4q state, the actual computations of correlation functions in this work was done using QCD sum rule method. We calculate the masses of 2q states in the vector and scalar channels, and 4q state as function of quark condensate. The results in Fig.1 indicate that although 4q component can not explain the small empirical mass ( $\sim 500$  MeV) enough, still 4q configuration has smaller mass than 2q case by  $150\sim 200$  MeV despite the larger number of quarks participating in the dynamics. This explicitly indicates the existence of the nontrivial correlation for the mass reduction of the 4q system.

## References

- 1) G. 'tHooft, Nucl. Phys. **B724**, 61 (1974).
- 2) E. Witten, Nucl. Phys. **B160**, 57 (1979).
- 3) T. Kojo and D. Jido, arXiv:0807.2364 [hep-ph].

<sup>\*1</sup> RIKEN-BNL Research Center.

# Non-Fermi-liquid magnetic susceptibility of quark matter<sup>†</sup>

K. Sato\*<sup>1</sup> and T. Tatsumi\*<sup>1</sup>

[Magnetic susceptibility, Non-Fermi-liquid effect, QCD phase diagram]

Nowadays the phase diagram of QCD has been extensively studied theoretically and experimentally. In particular, magnetic properties of QCD or its magnetic instability is quite interesting, since it is related to the physics of compact stars, especially magnetars or primordial magnetic fields in the early universe. At high density but not high temperature, as expected in compact stars, the Fermi surface is a helpful concept. In recent papers, we have discussed the magnetic properties of quark matter by evaluating the magnetic susceptibility within Fermi-liquid theory. We have taken into account the anomalous self-energy for quarks due to the dynamic screening effect for the transverse gluons as well as the static screening effect given by the Debye mass for the longitudinal gluons.

In ref.1), we have studied the magnetic susceptibility at  $T = 0$ . We have seen that the transverse mode only receives the dynamic screening due to Landau damping, so that it still gives logarithmic singularities for the Landau-Migdal parameters, but that they cancel each other in the magnetic susceptibility to give a finite result. In refs. 2) and 3), we have also studied the magnetic susceptibility at finite temperature. The magnetic susceptibility at finite temperature is given by

$$\begin{aligned}
 & (\chi_M / \chi_{\text{Pauli}})^{-1} \\
 &= 1 - \frac{C_f g^2}{12\pi^2 E_F k_F} \left[ m(2E_F + m) - \frac{1}{2}(E_F^2 + 4E_F m - 2m^2) \kappa \ln \frac{2}{\kappa} \right] \\
 &+ \frac{\pi^2}{6k_F^4} \left( 2E_F^2 - m^2 + \frac{m^4}{E_F^2} \right) T^2 \\
 &+ \frac{C_f g^2}{72} \frac{(2k_F^4 + k_F^2 m^2 + m^4)}{k_F^3 E_F^3} T^2 \ln \left( \frac{\Lambda}{T} \right) + O(g^2 T^2). \quad (1)
 \end{aligned}$$

where  $\chi_{\text{Pauli}}$  is the Pauli paramagnetism,  $\chi_{\text{Pauli}} \equiv \bar{g}_D^2 \mu_q^2 N_c k_F \mu / 4\pi^2$ ,  $C_f = (N_c^2 - 1) / 2N_c$ , and  $\kappa$  is defined by  $\kappa = M_D^2 / 2k_F^2$  with the Debye mass  $M_D$ .  $\Lambda$  is a cut-off parameter and should be of  $O(M_D)$ .

The magnetic susceptibility at  $T = 0$  is given by the first and second terms in Eq. (1). The  $\kappa \ln \kappa$  term originates from the effective cut off of the longitudinal mode due to static screening. One can see that the magnetic susceptibility has  $T^2 \ln T$  dependence besides the usual  $T^2$  dependence. This anomalous temperature dependence comes from the dynamic screening effect for the transverse gluons and is an interesting *non-Fermi-liquid effect* in the magnetic susceptibility. It corresponds to the well-known  $T \ln T$  dependence in the specific heat<sup>4)</sup>. The divergence of  $\chi_M$  signals the magnetic instability of quark matter to the ferromagnetic phase. At low temperature,  $\ln(\Lambda/T) > 0$  so that

the  $T^2 \ln T$  term gives positive contribution to  $\chi_M^{-1}$ . Therefore, both  $T$ -dependent terms in Eq. (1) work against the magnetic instability. It may be interesting to note that the static screening gives the term proportional to  $M_D^2 \ln M_D^{-1}$ , while the dynamic screening gives the  $T^2 \ln T^{-1}$  term; the Debye mass  $M_D$  works as an infrared (IR) cutoff to remove the infrared singularity in the quasi-particle interaction exchanging the longitudinal gluons, whereas, at finite temperature, temperature itself plays a role of the IR cutoff through the dynamic screening for the quasi-particle interaction.

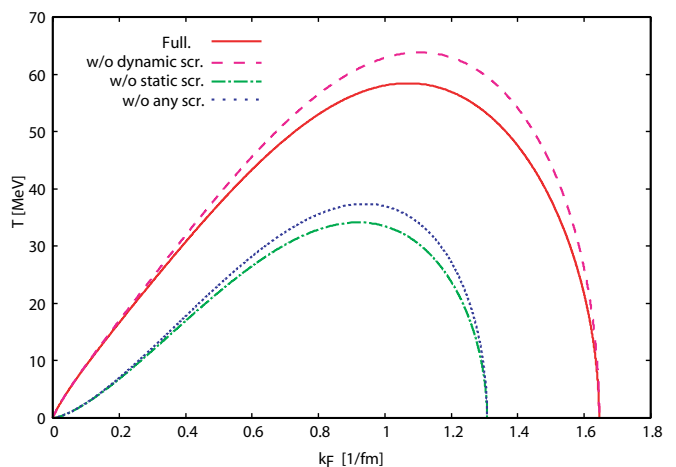


Fig. 1. Magnetic phase diagram in the density-temperature plane. The solid, dashed, dash-dotted, dotted curves show the results for the full expression Eq. (1), the one without the  $T^2 \ln T$  term, without the  $\kappa \ln \kappa$  term, and without both of the  $T^2 \ln T$  and  $\kappa \ln \kappa$  terms in Eq. (1).

We show a magnetic phase diagram of QCD on the density-temperature plane for  $\alpha_s = 2.2$  and  $m = 300 \text{ MeV}$  in Fig. 1. The four curves corresponds to the critical curves given by Eq. (1) under four different assumptions. The magnetic phase transition occurs on the critical curves: below the critical curves quark matter is in the ferromagnetic phase, while it is in the paramagnetic phase above them. One can see that static screening can enlarge the ferromagnetic region. As discussed in ref.1), it depends on the number of flavors whether the static screening works for ferromagnetism or not, which is peculiar to QCD. It also turns out that dynamic screening works against the magnetic instability and can reduce the ferromagnetic region in the phase diagram up to a point but this effect is not so large.

## References

- 1) T. Tatsumi and K. Sato, Phys. Lett. **B663** (2008) 322.
- 2) T. Tatsumi and K. Sato, Phys. Lett. **B672** (2009) 132.
- 3) K. Sato and T. Tatsumi, Nucl. Phys. **A826** (2009) 74.
- 4) See refs. [4-6,8,12-14] in ref. 2).

<sup>†</sup> Condensed from ref. 3)

\*<sup>1</sup> Department of Physics, Kyoto University

## Temperature dependence of quarkonium correlators

P. Petreczky,<sup>\*1</sup>

Quarkonium properties at finite temperature received considerable interest since the famous conjecture by Matsui and Satz that color screening will lead to quarkonium dissociation, which in turn can signal the onset of deconfinement in heavy ion collisions<sup>1</sup>. This problem has been studied using potential models with screened temperature dependent potential<sup>2</sup>. In-medium quarkonium properties are encoded in the corresponding spectral functions which in turn are related to meson (current-current) correlation functions in Euclidean time. Euclidean correlation functions can be calculated on the lattice. Therefore one can hope to learn something about in-medium quarkonium properties by studying the temperature dependence of meson correlators on the lattice. In particular, attempts to reconstruct quarkonium spectral functions using the Maximum Entropy Method (MEM) were presented in Refs.<sup>3-5</sup>. The study of the spectral functions using MEM indicated that 1S charmonia may survive in the deconfined phase till temperatures as high as  $(1.6 - 2.2)T_c$ <sup>3,4</sup>. This result is closely related to the small temperature dependence of the Euclidean correlator in the pseudo-scalar channel<sup>4,5</sup>. On the other hand the large temperature dependence of the scalar and axial-vector correlators has been interpreted as evidence for the expected dissolution of the P-state charmonium. However, it has been pointed out that zero mode contribution, i.e. the contribution from the spectral functions at very small frequencies could lead to large temperature dependence of the Euclidean correlators<sup>6,7</sup>. Therefore in order to understand quarkonium properties at finite temperature and their relation to collective effects, e.g. screening it is important to get a detailed understanding of the temperature dependence of the Euclidean correlators, including the role of the zero mode contribution. Here I discuss the temperature dependence of quarkonium correlators calculated in quenched approximation on isotropic lattices.

Since the width of the transport peak is very small<sup>6</sup>, the zero mode contribution is independent of the Euclidean time  $\tau$  to a good approximation. Therefore the zero mode contribution will not show up in the derivative of the correlation functions. To check this I calculated the ratio of the derivatives  $G^i(\tau, T)/G_{rec}^i(\tau, T)$ , where the reference correlator (the so-called reconstructed correlator) is defined as

$$G_{rec}^i(\tau, T) = \int_0^\infty d\omega \sigma^i(\omega, T^*) \frac{\cosh(\omega(\tau - 1/2T))}{\sinh(\omega/2T)}. \quad (1)$$

Here  $T^*$  is some reference temperature well below the

<sup>\*1</sup> Physics Department and RIKEN-BNL Research Center, Brookhaven National Laboratory, Upton, NY, USA

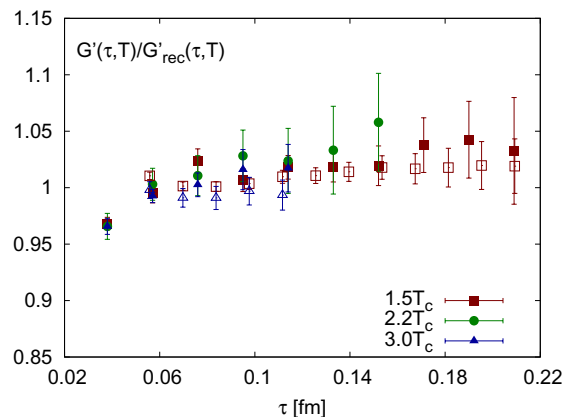


Fig. 1. The ratio of the derivatives  $G'(\tau, T)/G'_{rec}(\tau, T)$  in axial-vector channel. The results from anisotropic lattice calculations<sup>5</sup> are also shown (open symbols).

transition temperature  $T_c$ . Furthermore, the index  $i$  denotes different channel (e.g. vector, pseudo-scalar etc.). The numerical results for this ratio in the axial-vector channel are shown in Figure 1. As one can see from the figure the ratio is temperature independent to a very approximation and is close to unity. This means that almost the entire temperature dependence of the axial-vector correlator in the Euclidean time is given by the zero mode contribution and the expected dissolution of P states is not reflected in the correlators. The figure also shows that similar temperature dependence is found in calculation with anisotropic lattices. The temperature dependence of the scalar correlator follows the same pattern as the axial-vector correlator. A closer analysis of the zero mode contribution shows that it can be well described by a quasi-particle model, where the heavy quark masses receive a small thermal correction<sup>8</sup>. The details of the analysis are presented in a recent publication<sup>8</sup>.

### References

- 1) T. Matsui and H. Satz, Phys. Lett. B **178** (1986) 416
- 2) for recent review see Á Mócsy, arXiv:08110337 [hep-ph]
- 3) M. Asakawa and T. Hatsuda, Phys. Rev. Lett. **92** (2004) 012001
- 4) S. Datta, F. Karsch, P. Petreczky and I. Wetzorke, Phys. Rev. D **69** (2004) 094507
- 5) A. Jakovác, P. Petreczky, K. Petrov and A. Velytsky, Phys. Rev. D **75** (2007) 014506
- 6) P. Petreczky and D. Teaney, Phys. Rev. D **73** (2006) 014508
- 7) T. Umeda, Phys. Rev. D **75** (2007) 094502
- 8) P. Petreczky, arXiv:08100258 [hep-lat]

# Heavy-quark bound states in an anisotropic hot QCD plasma<sup>†</sup>

A. Dumitru,<sup>\*1</sup>

[Quarkonium, QCD, Plasma, Viscosity]

In Quantum Chromodynamics (QCD) with small  $t'$  Hooft coupling at short distances non-relativistic quarkonium states exist. At high temperatures, the deconfined phase of QCD exhibits screening of static color-electric fields which may lead to dissociation of quarkonium states. Inspired by the success at zero temperature, potential models have also been applied to understand quarkonium properties at finite temperature<sup>1</sup>.

Here, we assess the properties of quarkonium states in a QCD plasma which exhibits an anisotropy of the particle momenta,  $f(\vec{p}) = f_{\text{iso}}(p) - \xi \frac{p_z^2}{2pT} f_{\text{iso}}(p)(1 \pm f_{\text{iso}}(p))$ . This arises due to a locally anisotropic hydrodynamic expansion of a plasma with non-vanishing shear viscosity<sup>2</sup>):  $\xi = (10/T\tau)\eta/s$ , where  $\xi$  is the anisotropy parameter,  $T$  is the temperature,  $\tau$  is proper time (and  $1/\tau$  is the Hubble expansion rate), and  $\eta/s$  is the ratio of shear viscosity to entropy density.

We model the inter-quark potential in the deconfined phase as follows<sup>3</sup>):

$$V(r, T) = -\frac{\alpha}{r} (1 + m_D r) e^{-m_D r} + 2\frac{\sigma}{m_D} [1 - e^{-m_D r}] - \sigma r e^{-m_D r}. \quad (1)$$

Here,  $\sigma = 0.223 \text{ GeV}^2$  is the string tension and  $m_D(T)$  is the Debye screening mass. Eq. (1) interpolates from the Cornell potential at short distance to an exponentially Debye-screened string attraction at large  $r$ . For an anisotropic plasma the Debye mass  $m_D(T)$  is replaced by an angular dependent screening scale  $\mu(\theta; \xi, T)$  which can be obtained from the “hard thermal loop” resummed gluon propagator appropriate for an anisotropic plasma<sup>4</sup>). The potential now depends not only on the distance between the  $Q$  and the  $\bar{Q}$  but also on the angle  $\theta$  between their separation and the direction of anisotropy.

The binding energies follow from the three-dimensional Schrödinger equation, see Fig. 1. They decrease with temperature  $T$  but increase with the anisotropy  $\xi$ . This is due to the fact that in an anisotropic plasma the screening scale  $\mu(\theta)$  at a given temperature is smaller than the corresponding Debye mass  $m_D(T)$ , so screening is weaker.

Fig. 2 shows the binding energies of the  $1P$  states of bottomonium. The anisotropy leads to a preferred

polarization of the  $\chi_b$ , with about 50 MeV splitting between states with angular momentum  $L_z = 0$  and  $L_z = \pm 1$ , respectively. The experimental confirmation of such a polarization at RHIC or LHC may provide first evidence for a non-zero viscosity of QCD near  $T_c$ .

## References

- 1) Á. Mócsy, arXiv:0811.0337 [hep-ph].
- 2) eq. (6-40) in M. Asakawa, S. A. Bass and B. Müller, Prog. Theor. Phys. **116**, 725 (2007).
- 3) F. Karsch, M. T. Mehr and H. Satz, Z. Phys. C **37**, 617 (1988); A. Dumitru, Y. Guo, A. Mócsy and M. Strickland, arXiv:0901.1998 [hep-ph].
- 4) A. Dumitru, Y. Guo and M. Strickland, Phys. Lett. B **662**, 37 (2008).

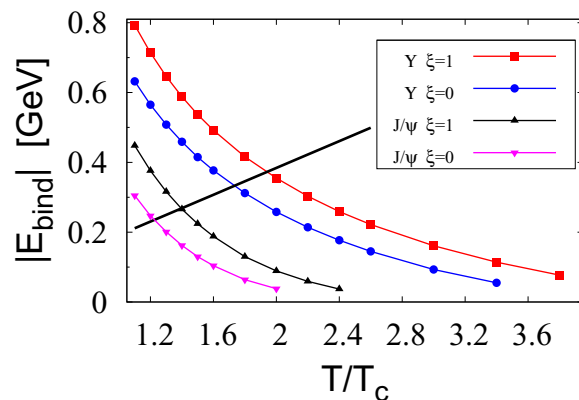


Fig. 1. Binding energies of the  $1S$  states of charmonium and bottomonium for two values of the plasma anisotropy parameter  $\xi$ . The straight line corresponds to a binding energy equal to the temperature.

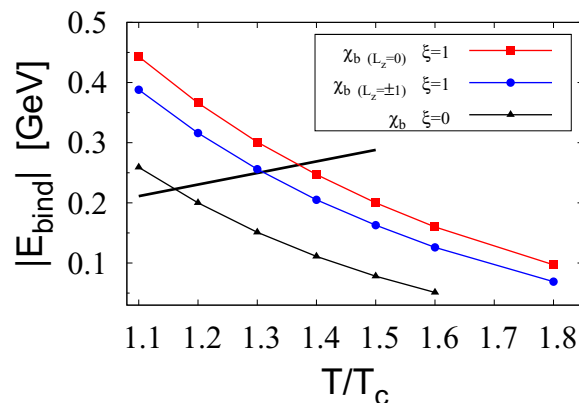


Fig. 2.  $1P$  state of bottomonium.

<sup>†</sup> Condensed from the article arXiv:0901.1998, preprint RBRC-774 (submitted to Phys. Rev. D)

<sup>\*1</sup> Department of Natural Sciences, Baruch College, New York and RIKEN-BNL Research Center (RIKEN fellow)

# Improved non-perturbative renormalization in lattice QCD<sup>†</sup>

Y. Aoki<sup>\*1</sup> [RBC and UKQCD collaborations]

Recent algorithmic developments and increasing power of supercomputers have made it possible to calculate basic physical quantities involving strong interaction from the first principles using lattice QCD with the light quark ( $u, d, s$ ) degree of freedom consistently taken into account. It often is the case that the calculated quantity needs renormalization to remove the ultraviolet divergence and/or to match to a theory with higher energy scale such as the Weinberg-Salam theory of electroweak interaction. Renormalization can be done by perturbation theory in principle. However, the lattice perturbation theory poorly converges, thus should be avoided. Instead, a non-perturbative renormalization (NPR) on the lattice should be used.

The most practical non-perturbative renormalization program is provided by RI/MOM scheme<sup>1)</sup>, where the renormalization condition is imposed in a regularization independent way to the amputated off-shell forward Green function of external quark states with the operator insertion. The external momentum sets the renormalization scale  $\mu^2 = p^2$ . This scheme has successfully applied to many lattice calculations, including the recent domain wall fermion simulations<sup>2)</sup>.

Although by using the RI/MOM-scheme NPR the systematic uncertainty from the use of lattice perturbation theory is eliminated, there still is a problem, which has only been revealed by the use of state-of-the-art chiral fermion (domain wall fermion) calculations. It is an unwanted contamination of the non-perturbative effect, and becomes another source of the systematic error. The mechanism of how this contamination occurs is associated with the momentum configuration. Possible small momentum flow in the internal loop, for the particular momentum configuration conventionally employed, triggers the contamination. We have come up with a solution of this problem by changing the kinematics of the external momentum to the ones that do not involve exceptional momenta (which have zero partial sum), thus, reduces the small momentum flow.

The quark mass renormalization  $Z_m$ , calculated through bilinear operator renormalization of scalar or pseudoscalar, is one of the worst cases that suffer from the contamination. In the calculation using domain wall fermions the reported strange quark mass renormalized in  $\overline{\text{MS}}$  scheme at  $\mu = 2 \text{ GeV}$  read<sup>3)</sup>,

$$m_s^{\overline{\text{MS}}} = 107.3(4.4)_{\text{stat}}(4.9)_{\text{syst}}(9.7)_{\text{ren}} \text{MeV}. \quad (1)$$

The largest error is the third, which arises from the renormalization, where there are two dominant contributions: (i) aforementioned contamination of un-

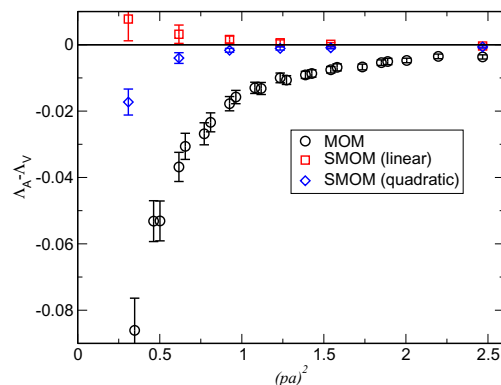


Fig. 1. Difference of axialvector and vector vertex function for the MOM and SMOM schemes. Chiral extrapolations with linear and quadratic in quark mass are shown for the SMOM scheme.

wanted non-perturbative effect. We estimate the corresponding uncertainty to be about 7%. (ii) The matching from the RI/MOM to the  $\overline{\text{MS}}$  scheme. The perturbative series in continuum theory for this matching is known to 3-loops but converges very poorly. The uncertainty is estimated to be about 6%.

We have constructed a new scheme called RI/SMOM scheme<sup>4)5)</sup> which makes use of non-exceptional momenta, thus is expected to reduce the systematic error from the contamination (i). We have performed a numerical test<sup>5)</sup> and the result is promising. Figure 1 shows the difference of the vector and axial vector vertex amplitude as a function of the squared renormalization scale. The original MOM scheme shows difference due to spontaneous chiral symmetry breaking, sizable at low energy region. The same quantity in the new SMOM scheme is very small: the non-perturbative contamination got reduced as expected. After all the systematic error of  $Z_m$  from the contamination is get reduced to the level less than 3%. It also appears from the perturbative calculation<sup>4)</sup> that the error (ii) shrinks a lot from the original scheme due to almost a factor 10 smaller one-loop correction. Thus, the new scheme is preferable by the two good reasons.

The concept of the new MOM scheme with non-exceptional momenta is quite general. It can be applied to other composite operators such as four quark operators for  $K^0 - \overline{K}^0$  mixing and  $K \rightarrow \pi\pi$  decays.

## References

- 1) G. Martinelli et al., Nucl. Phys. B445 (1995) 81.
- 2) Y. Aoki et al., Phys. Rev. D78 (2008) 054510.
- 3) RBC/UKQCD, C. Allton et al., Phys. Rev. D78 (2008) 114509.
- 4) C. Sturm et al. [RBC/UKQCD], (2009), arXiv:0901.2599.
- 5) Y. Aoki [RBC/UKQCD], (2009), arXiv:0901.2595.

<sup>\*1</sup> RIKEN-BNL Research Center

**(2+1)-flavor DWF QCD and chiral perturbation<sup>†</sup>**

C. Allton<sup>\*1</sup> D.J. Antonio<sup>\*2</sup> Y. Aoki<sup>\*3</sup> T. Blum<sup>\*3\*4</sup> P.A. Boyle<sup>\*2</sup> N.H. Christ<sup>\*5</sup> S.D. Cohen<sup>\*6</sup> M.A. Clark<sup>\*7</sup>  
 C. Dawson<sup>\*8</sup> M.A. Donnellan<sup>\*9</sup> J.M. Flynn<sup>\*9</sup> A. Hart<sup>\*2</sup> T. Izubuchi<sup>\*3\*10\*11</sup> A. Jüttner<sup>\*12</sup> C. Jung<sup>\*10</sup>  
 A.D. Kennedy<sup>\*2</sup> R.D. Kenway<sup>\*2</sup> M. Li<sup>\*5</sup> S. Li<sup>\*5</sup> M.F. Lin<sup>\*13</sup> R.D. Mawhinney<sup>\*5</sup> C.M. Maynard<sup>\*2</sup>  
 S. Ohta<sup>\*14\*15\*3</sup> B.J. Pendleton<sup>\*2</sup> C.T. Sachrajda<sup>\*9</sup> S. Sasaki<sup>\*3\*16</sup> E.E. Scholz<sup>\*10</sup> A. Soni<sup>\*10</sup> R.J. Tweedie<sup>\*2</sup>  
 J. Wennekers<sup>\*2</sup> T. Yamazaki<sup>\*17</sup> and J.M. Zanotti<sup>\*2</sup> for RBC and UKQCD Collaborations

[Quantum Chromodynamics, Hadron Physics]

Using QCDOC computers at RIKEN BNL Research Center, University of Edinburgh and Brookhaven National Laboratory, we performed a series of lattice quantum chromodynamics (QCD) calculations with two degenerate up and down quarks and one heavier strange quark fully dynamically represented by the domain-wall fermions (DWF) scheme<sup>1</sup>. The strange quark mass used turned out to be about 12 % heavier than the physical. The degenerate up and down mass were set to about 3/4, 1/2, 1/3 and 1/5 of the strange mass. The lattice cut off turned out to be about 1.7 GeV, and correspondingly the lattice spatial volume is about  $(2.7\text{fm})^3$ . These consist the most realistic set of lattice QCD numerical calculations ever performed.

The realistic strange mass and sufficiently light up and down mass aided by sufficiently large spatial volume allow detailed theoretical study of the role of flavor and chiral symmetries in hadron physics. We found the conventional SU(3) next-to-leading order (NLO) chiral perturbation theory (ChPT) that treats as if all three light quark flavors, strange, down, and up, have small mass compared to the chiral scale, fails. In other words we found the physical strange mass too heavy to be considered degenerate with the light up and down. This is an important discovery that calls into question many conventional analyses of hadronic phenomena that assumed the degeneracy of three light flavors. In contrast the SU(2) ChPT, that treat only the two lightest flavors of down and up degenerate, works.

In addition this work so far has resulted in three Phys. Rev. Letters publications: 1) a very accurate estimation of the kaon bag parameter<sup>2</sup>),  $B_K$ , of the in-

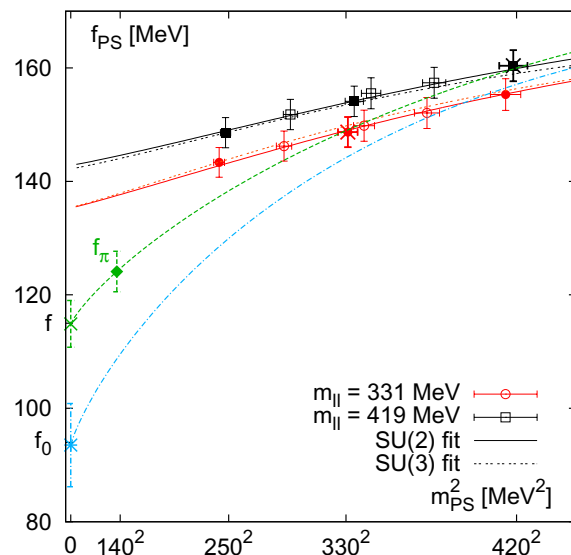


Fig. 1. SU(3) next-to-leading order (NLO) chiral perturbation theory (ChPT) fails, while SU(2) works: read ref.<sup>1)</sup> for details, especially its Fig. 18. Physical strange quark mass is too heavy for NLO ChPT to work.

direct CP-violating mixing of neutral kaon, 2) another very accurate estimation of the  $K_{l3}$  form factor<sup>3)</sup>, and 3) an unexpectedly large finite-size effect on nucleon isovector axial charge<sup>4,5)</sup>,  $g_A$ . The first two results impact accurate quantitative determination of the CKM quark mixing matrix and thus the human endeavor in search of physics beyond the standard model. The third points out a difficulty that still stands in our way toward full understanding of hadronic physics. We are working on a series of lattice QCD ensembles at higher cutoff of about 2.4 GeV to improve on our understanding of this rich physics.

We thank RIKEN, Brookhaven National Laboratory and US DOE, University of Edinburgh and UK PPARC for providing the facilities essential for the completion of this work.

## References

- 1) C. Allton *et al.*, Phys. Rev. D **78**, 114509 (2008).
- 2) D. Antonio *et al.*, Phys. Rev. Lett. **100**, 032001 (2008).
- 3) P. Boyle *et al.*, Phys. Rev. Lett. **100**, 141601 (2008).
- 4) T. Yamazaki *et al.*, Phys. Rev. Lett. **100**, 171602 (2008).
- 5) S. Ohta and T. Yamazaki, PoS LAT2008, 168 (2008).

<sup>†</sup> Condensed from Phys. Rev. D **78**, 114509 (2008)

<sup>\*1</sup> University of Swansea, UK

<sup>\*2</sup> University of Edinburgh, UK

<sup>\*3</sup> RIKEN BNL Research Center, USA

<sup>\*4</sup> University of Connecticut, USA

<sup>\*5</sup> Columbia University, USA

<sup>\*6</sup> Thomas Jefferson National Accelerator Facility, USA

<sup>\*7</sup> Boston University, USA

<sup>\*8</sup> University of Virginia, USA

<sup>\*9</sup> University of Southampton, UK

<sup>\*10</sup> Brookhaven National Laboratory, USA

<sup>\*11</sup> Kanazawa University

<sup>\*12</sup> Johannes Gutenberg-Universität Mainz, Germany

<sup>\*13</sup> Massachusetts Institute of Technology, USA

<sup>\*14</sup> Institute of Particle and Nuclear Studies, KEK

<sup>\*15</sup> SOKENDAI Graduate University of Advanced Studies

<sup>\*16</sup> University of Tokyo

<sup>\*17</sup> University of Tsukuba

# Nucleon form factors in (2+1)-flavor dynamical DWF QCD<sup>†</sup>

Y. Aoki,<sup>\*1</sup> T. Blum,<sup>\*2\*1</sup> H.-W. Lin,<sup>\*3</sup> S. Ohta,<sup>\*4\*5\*1</sup> S. Sasaki,<sup>\*6</sup> R.J. Tweedie,<sup>\*7</sup> T. Yamazaki,<sup>\*8</sup> and J.M. Zanotti<sup>\*7</sup> for RBC and UKQCD Collaborations

[Quantum Chromodynamics, Hadron Physics, Nucleon Structure]

The isovector form factors of nucleon are associated with the vector,  $V_\mu^+ = \bar{u}\gamma_\mu d$ , and axialvector,  $A_\mu^+ = \bar{u}\gamma_\mu\gamma_5 d$ , currents with up- and down-quark spinors  $u$  and  $d$ . Four form factors arise in matrix elements of these currents between proton and neutron states: the vector-current matrix element  $\langle p|V_\mu^+(x)|n\rangle$  gives rise to the vector,  $F_V$ , and induced tensor,  $F_T$ , form factors,

$$\bar{u}_p [\gamma_\mu F_V(q^2) + \sigma_{\mu\lambda} q_\lambda F_T(q^2)] u_n e^{iq\cdot x}.$$

$F_V$  is equivalent to  $F_1$  and  $F_T$  to  $F_2/(2M_N)$  in the isovector electromagnetic form factors. The axialvector-current matrix element,  $\langle p|A_\mu^+(x)|n\rangle$ , gives rise to the axialvector,  $F_A$ , and induced pseudoscalar,  $F_P$ , form factors,

$$\bar{u}_p [\gamma_\mu\gamma_5 F_A(q^2) + iq_\mu\gamma_5 F_P(q^2)] u_n e^{iq\cdot x}.$$

Here  $q$  denotes four-momentum transfer between the proton and neutron states. While the vector charge,  $g_V = F_V(0)$ , is not affected by the strong interaction because the vector current is conserved, the axial charge,  $g_A = F_A(0)$ , is affected: the ratio  $g_A/g_V$  deviates from unity,  $1.2695(29)^1$ . Calculation of this ratio and the other form factors requires adequate treatise of flavor and chiral symmetries of quarks. Conventional lattice fermion schemes, however, have difficulty with them. In contrast the domain-wall fermions (DWF) method that we, RIKEN-BNL-Columbia (RBC) collaboration that we, pioneered works very well<sup>2</sup>. The RBC and UKQCD collaborations jointly generated state-of-the-art lattice QCD ensembles with “(2+1) flavors” of quarks. The strange mass is fixed at a realistic value about 12% heavier than the physical and degenerate up- and down-quark mass varies down to about 1/5 of this strange mass<sup>3</sup>. Using these we reported unexpectedly large finite-size effect on the  $g_A/g_V$  ratio<sup>4</sup>.

In the present work we study the momentum-transfer dependence of all the four isovector form factors<sup>5</sup>. We found these form factors allow conventional dipole fitting and so extracting quantities such as anomalous magnetic moment or mean-squared charge radii. The signals and the dipole fits to them for conserved vector-current,  $F_V$  and  $F_T$ , are of very good

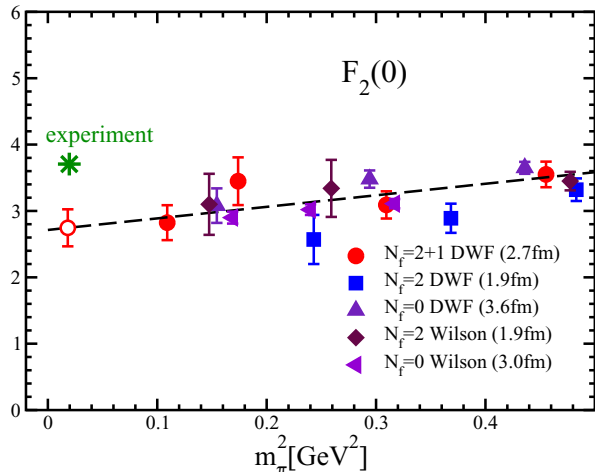


Fig. 1. Calculated isovector part of the nucleon anomalous magnetic moment compares well with the experiment.

quality: the extracted value of the anomalous magnetic moment,  $F_2(0)$ , as is shown in Figure 1, compares well with the experiment. The Dirac and Pauli mean-squared charge radii, however, significantly underestimate the corresponding experimental values. This can be explained by still too heavy up and down quark mass. Correspondingly we do not observe any logarithmic divergence toward the chiral limit that some models motivated by chiral perturbation predicts. The axialvector form factors,  $F_A$  and  $F_P$ , are of lesser statistical quality but provide us evidence that they suffer the same finite-size effect we observed in the axial charge,  $g_A$ <sup>4</sup>. Nevertheless we obtained good description of the Goldberger-Treiman relation. The extracted values for pion-nucleon coupling,  $g_{\pi NN}$ , and muon-capture coupling,  $g_P$ , also compare favorably with the experiments.

We thank the members of the RBC and UKQCD Collaborations. We also thank RIKEN, Brookhaven National Laboratory and the US DOE, Edinburgh University and the UK PPARC for providing the facilities essential for the completion of this work.

## References

- 1) C. Amsler *et al.*, *Physics Letters B* **667**, 1 (2008).
- 2) T. Blum *et al.*, *Phys. Rev. D* **69**, 074502 (2004); Y. Aoki *et al.*, *Phys. Rev. D* **72**, 114505 (2005); and references therein.
- 3) C. Allton *et al.*, *Phys. Rev. D* **78**, 114509 (2008).
- 4) T. Yamazaki *et al.*, *Phys. Rev. Lett.* **100**, 171602 (2008).
- 5) S. Ohta and T. Yamazaki, *PoS LAT2008*, 168 (2008).

<sup>\*1</sup> RIKEN BNL Research Center, BNL, USA  
<sup>\*2</sup> Physics Department, University of Connecticut, USA  
<sup>\*3</sup> Thomas Jefferson National Accelerator Facility, USA  
<sup>\*4</sup> Institute of Particle and Nuclear Studies, KEK  
<sup>\*5</sup> SOKENDAI Graduate University of Advanced Studies  
<sup>\*6</sup> Physics Department, University of Tokyo  
<sup>\*7</sup> School of Physics, University of Edinburgh, UK  
<sup>\*8</sup> Center for Computational Sciences, University of Tsukuba

Eta meson from two flavor dynamical domain wall fermions<sup>†</sup>T. Izubuchi<sup>\*1\*2\*3</sup> and K. Hashimoto<sup>\*2\*4</sup> for RBC and UKQCD Collaborations

[Quantum Chromodynamics, Hadron Physics]

We explore the spectrum of the flavor singlet pseudoscalar meson,  $\eta'$ , in two-flavor ( $N_f = 2$ ) lattice Quantum Chromo Dynamics (QCD). The continuum-like relation between the topology of the QCD vacuum and the  $U(1)_A$  anomaly, which prevents the  $\eta'$  meson from being a Nambu-Goldstone boson, is expected to hold in the domain wall fermions (DWF) used as a lattice quark field in this calculation.

We employ the ensemble of  $N_f = 2$  QCD vacuum<sup>1)</sup> generated with DWF quark actions. The lattice size is  $16^3 \times 32$ , the lattice scale is  $a^{-1} \approx 1.5$  GeV ( $a \approx 0.13$  fm), and the residual chiral breaking  $m_{\text{res}} = 0.00137(4)$  which is about an order of magnitude smaller than the up/down quark masses used in the simulations,  $m_f = 0.02 - 0.04$ , which correspond to  $m_\pi/m_\rho \approx 0.51 - 0.64$ . The number of vacuum samples are about 500-1,000.

To reduce the large statistical uncertainties of the  $\eta'$  meson propagator, we introduce a smeared quark operator,  $q_S$ , which is a superposition of the local quark operator  $q_L$  at neighboring space-time in a gauge-covariant manner. The shape of  $q_S$  in terms of  $q_L$  is Gaussian with its width being set to enhance the overlap to the quark wavefunction in the ground state hadrons.

The  $\eta'$  propagator, projected to the zero spacial momentum, consists of the connected,  $C_{\gamma_5}(t)$ , and the disconnected quark loop,  $D_{\gamma_5}$ , contributions:

$$\int d^3x \langle \eta'(\vec{x}, t) \eta'^{\dagger}(\vec{0}, 0) \rangle = C_{\gamma_5}(t) - N_f D_{\gamma_5}(t).$$

Here the Hermitian operator of the  $\eta'$  meson, is constructed by the quark operators,  $q_{I,f}$  and  $\bar{q}_{J,f}$  as,  $\eta'_I(\vec{x}, t) = \frac{1}{\sqrt{N_f}} \sum_{f=1}^{N_f} \bar{q}_{I,f}(\vec{x}, t) i\gamma_5 q_{I,f}(\vec{x}, t)$ , where  $f = 1, \dots, N_f$  is the flavor index, and  $I$  denotes whether we use the local quark field ( $L$ ) or the smeared field ( $S$ ), which controls the ground-state overlap. Both of the correlation functions,  $C_{\gamma_5}(t)$  and  $D_{\gamma_5}(t)$ , are calculated using the complex random  $\mathbf{Z}_2$  source.

The  $\eta'$  mass is extracted by fitting the propagator in following two ways, and the results are compared with each other to estimate systematic uncertainties: (A) Standard method: the propagator is fit to a single

$m_f$	$m_{\eta'}$	$t_0$	$t_{\min}$	$t_{\max}$	method
0.02	0.477(40)		2	5	(A)
	0.473(50)	2	$t_0 + 1$	6	(B)
0.03	0.571(60)		3	5	(A)
	0.600(44)	2	$t_0 + 1$	6	(B)
0.04	0.497(17)		2	5	(A)
	0.492(15)	2	$t_0 + 1$	5	(B)

Table 1.  $am_{\eta'}$  for each simulation points.

exponential dumping function in time distance from the source,  $C \cosh[m_{\eta'}(t - N_T/2)]$ , by assuming only the ground state propagates. (B) Variational method: the mass of the first excited state  $m_{\eta'^*}$  is also taken into account. Both the local ( $I, J = L$ ) and the smeared ( $I, J = S$ ) interpolation fields are used to construct  $2 \times 2$  correlation functions  $X_{IJ} \equiv \langle O_I O_J \rangle$  ( $I, J = S, L$ ). Eigenvalues of the normalized correlation matrix are then fit as a function of  $t$ :  $\lambda(t; t_0) = \frac{\cosh[(m(t - N_T/2)]}{\cosh[m(t_0 - N_T/2)]}$  to obtain the masses of the states.  $t_0$  is fixed to the point for the normalization.

The numerical values of  $m_{\eta'}$  and time ranges used in their fits are given in Table 1 for both method (A) and (B). We did not use a propagator from longer distance, where the statistics are too poor and the standard error analysis would not be reliable, although the inclusion of a few more data points does not change the fitted results for most of the masses. Method (B) produces flatter plateaux than that in method (A).

Then the masses are extrapolated using either of

$$m_{\eta'} = B_0 + B_1(m_f + m_{\text{res}}) \quad (\text{linear type}), \quad (1)$$

$$m_{\eta'}^2 = C_0 + C_1(m_f + m_{\text{res}}) \quad (\text{AWTI type}), \quad (2)$$

to estimate the mass of  $\eta'$  at the physical quark mass point. Our main estimation for the mass of  $\eta'$  at the physical quark mass point is obtained from the variational method (B) and chiral extrapolation using the lowest order of ChPT (2):

$$m_{\eta'}^{\text{phys}} = 819(127) \text{ MeV}, \quad (3)$$

which is close to the experimental value. One of the most obvious direction to remove various sources of the systematic errors in this first calculation using chiral quarks is to include the dynamical strange quark effect<sup>3)</sup>.

## References

- 1) Y. Aoki *et al.*, Phys. Rev. D **72**, 114505 (2005) [arXiv:hep-lat/0411006].
- 2) K. Hashimoto and T. Izubuchi, Prog. Theor. Phys. **119**, 599 (2008) [arXiv:0803.0186 [hep-lat]].
- 3) C. Allton *et al.*, Phys. Rev. D **78**, 114509 (2008).

<sup>†</sup> Condensed from Prog. Theor. Phys. **119**, 599 (2008)<sup>2)</sup>

<sup>\*1</sup> Brookhaven National Laboratory, USA

<sup>\*2</sup> RIKEN-BNL Research Center, USA

<sup>\*3</sup> ITP, Kanazawa University

<sup>\*4</sup> Radiation Laboratory, Nishina center, RIKEN

<sup>\*</sup> We thank RIKEN, Brookhaven National Laboratory and US DOE, University of Edinburgh and UK PPARC for providing the facilities essential for the completion of this work.

## **5. Particle Physics**

# $O(\alpha_s a)$ matching in static heavy and DW light quark system<sup>†</sup>

Tomomi Ishikawa\*<sup>1</sup> for RBC and UKQCD Collaborations

In the lattice QCD simulation, the Heavy Quark Effective Theory (HQET)<sup>1</sup> is widely used for treatment of the b quark. However, it has the following difficulties (and solutions).

- i The static propagator is too noisy. — This is basically because the static self-energy contains  $1/a$  power divergence. ALPHA collaboration introduced a static action with link smearing which improves the signal to noise ratio.<sup>2</sup>
- ii Non-perturbative matching with the continuum is needed. — If we include  $O(1/m_b)$  correction in the HQET formulation, the continuum limit cannot be reached by perturbative matching factor because of power divergence.<sup>3</sup>

As a first step in this project, the static approximation (lowest order of the HQET) is a valuable and important approach to the complete HQET. In the static limit, the perturbative matching procedure is justified. In this report we mainly focus on the  $O(a)$  improvement of operators, and then treat the matching factor between continuum HQET (CHQET) and lattice HQET (LHQET).

We use the Iwasaki gluonic action and the domain-wall (DW) fermion with light quark mass  $m_q$  for the light quark ( $q$ ) sector. In calculation of the matching factor, it is assumed that the extension of the 5th dimension is infinity, which means the light quarks have exact chiral symmetry. For the heavy quark ( $h$ ) sector, we use the static approximation with link smearing. The choices of the smearing are APE, HYP1 and HYP2.

Here we consider the static heavy-light quark bilinear and  $\Delta B = 2$  four-quark operator. The on-shell  $O(a)$  improved LHQET operators matched with CHQET have following form:

## Quark bilinear operator

$$O_\Gamma = Z(1 + bGm_q a) \left[ O_\Gamma^{(0)} + cGaO_\Gamma^{(1)} \right], \quad (1)$$

with  $O_\Gamma^{(0)} = \bar{h}\Gamma q$  and  $O_\Gamma^{(1)} = \bar{h}\Gamma\vec{\gamma} \cdot \vec{D}q$  with  $\Gamma = \{1, \gamma_\mu, \gamma_5, \gamma_\mu\gamma_5, \sigma_{\mu\nu}\}$ .  $Z$  is the overall matching factor;  $c$  and  $b$  are the  $O(pa)$  and  $O(m_q a)$  improvement coefficient, respectively; and they are all independent on  $\Gamma$ .  $G$  is defined by  $\gamma_0\Gamma\gamma_0 = G\Gamma$ .

## Four-quark operator ( $\Delta B = 2$ )

$$O_L = Z_L \left[ O_L^{(0)} + Z_L^{(1)} a O_{ND} + Z_L^{(m)} m_q a O_N \right], \quad (2)$$

with

$$O_L^{(0)} = 2[\bar{h}^{(+)}\gamma_\mu^L q][\bar{h}^{(-)}\gamma_\mu^L q], \quad (3)$$

$$O_{ND} = 2[\bar{h}^{(+)}\gamma_\mu^R(\gamma_i\vec{D}_i)q][\bar{h}^{(-)}\gamma_\mu^L q] \\ + 4[\bar{h}^{(+)}P_R(\gamma_i\vec{D}_i)q][\bar{h}^{(-)}P_L q] + \{(+)\longleftrightarrow(-)\}, \quad (4)$$

$$O_N = 2[\bar{h}^{(+)}\gamma_\mu^R q][\bar{h}^{(-)}\gamma_\mu^L q] \\ + 4[\bar{h}^{(+)}P_R q][\bar{h}^{(-)}P_L q] + \{(+)\longleftrightarrow(-)\}, \quad (5)$$

where  $h^{(+)}(h^{(-)})$  is the particle (anti-particle) of the static quark,  $\gamma_\mu^L = \gamma_\mu P_L$  and  $\gamma_\mu^R = \gamma_\mu P_R$ .  $Z_L$  is an overall matching factor, and  $Z_L^{(1)}$  and  $Z_L^{(m)}$  are the  $O(pa)$  and  $O(m_q a)$  improvement coefficient, respectively.

The matching factor and the  $O(a)$  improvement coefficients are calculated using one-loop perturbation theory. The calculation is performed by comparing the transition amplitude for the CHEQT and the LHQET. In order to extract the on-shell  $O(a)$  improvement coefficients, the amplitude is expanded in the external quark momenta around zero momentum and the light quark mass  $m_q$  around zero mass. The UV divergences in the continuum calculation are regulated by dimensional regularization and we use the  $\overline{\text{MS}}$  scheme for the renormalization. The IR divergences are regulated by introducing the gluon mass  $\lambda$ .

Now we roughly estimate these  $O(\alpha_s a)$  effects for physical quantities using the actual simulation data from the 2+1 flavor dynamical DW QCD project by RBC and UKQCD Collaborations ( $\beta = 2.13$ ,  $L^3 \times T \times L_5 = 16^3 \times 32 \times 16$ ,  $M_5 = 1.80$ ,  $m_{ud}a = \{0.01, 0.02, 0.03\}$ ,  $m_s a = 0.0359$ ) which appeared in Ref. 4). For this estimate the MF-improvement is taken into account. The coupling constant has the conservative range  $\alpha_s \sim 0.15 - 0.35$ . The conclusion is that the  $O(\alpha_s a)$  effect of the B meson decay constant  $f_B$  is  $3 - 8\%$ (APE) and  $5 - 12\%$ (HYP2); the effect of  $B^0 - \bar{B}^0$  mixing matrix element  $\mathcal{M}_B$  is  $9 - 24\%$ (APE) and  $15 - 36\%$ (HYP2); and the effect of the SU(3) breaking ratio  $\xi$  is less than 2%. Then, the  $O(a)$  improvement gives a non-negligible effect at one-loop perturbation. While perturbative matching has large ambiguities and its own limitations, we deduce that this conclusions is not largely changed even in non-perturbative matching.

## References

- 1) E. Eichten and B. R. Hill: Phys. Lett. B **234**, 511 (1990).
- 2) M. Della Morte, A. Shindler and R. Sommer: JHEP **0508**, 051 (2005) [arXiv:hep-lat/0506008].
- 3) J. Heitger and R. Sommer [ALPHA Collaboration]: JHEP **0402**, 022 (2004) [arXiv:hep-lat/0310035].
- 4) C. Albertus *et al.* [RBC and UKQCD Collaborations]: PoS **LAT2007**, 376 (2007).

<sup>†</sup> Condensed from the article in PoS (LATTICE 2008) 277.

\*1 RIKEN BNL Research Center

# Thermal Noise in AdS/CFT

Derek Teaney<sup>\*1,\*2</sup>

The AdS/CFT Correspondence is a useful tool to study the physics of strong coupling. In the field of heavy ion phenomenology, interest in the AdS/CFT correspondence began when Policastro, Son and Starinets<sup>1)</sup> and Kovtun, Son and Starinets<sup>2)</sup> determined the shear viscosity ( $\eta$ ) to entropy ( $s$ ) ratio of the  $\mathcal{N} = 4$  SYM plasma

$$\frac{\eta}{s} = \frac{1}{4\pi}. \quad (1)$$

This ratio is of order the ratio extracted from the RHIC results. The link between the correspondence and the experiments is tantalizing but circumstantial. Many more phenomenologically interesting observables may be computed within this framework and will clarify whether the predictions of  $\mathcal{N} = 4$  are qualitatively correct.

Recently, former Stony Brook student Jorge Casalderrey and I determined the diffusion coefficient of a heavy quark using the AdS/CFT correspondence<sup>5)</sup>

$$D = \frac{2}{\sqrt{\lambda\pi T}}. \quad (2)$$

This transport property may be relevant to the interpretation of the heavy flavor data at RHIC.

It is interesting that a diffusion coefficient can be predicted from the classical AdS/CFT correspondence. How can a stable linearized classical theory be the dual of a stochastic Brownian particle?

Indeed one of the most troubling aspects of the AdS/CFT correspondence is the apparent absence of the thermal noise. This seems at odds with the fluctuation-dissipation theorem and leads to some seemingly incorrect results from the correspondence. For instance, it predicts the absence of long-time hydrodynamic tails zero drag on mesons and the lack of Brownian motion of a quark string in AdS<sub>5</sub>. In many cases, the effect of thermal noise is suppressed either by large  $N$  or large  $\lambda$ , and therefore these inconsistencies with field theory intuition were rationalized as an artifact of these restrictive limits. In Ref.<sup>3)</sup> we overcame these difficulties by working through the simplest possible system which should exhibit drag and noise in AdS/CFT. This system is the Brownian motion of a heavy quark placed in the  $\mathcal{N} = 4$  SYM plasma.

In particular we worked out a bulk picture of fluctuations experienced by a heavy quark string in AdS<sub>5</sub>. A thermalized quark string in AdS<sub>5</sub> experiences drag

and noise. The physical picture that emerges when observing the quark is the following: In the long time limit, the motion can be regarded as stochastic. Then at each time step  $t_1, t_2, t_3 \dots$ , the quark string fluctuates to a new configuration which is perceived as a random force on the boundary. The average string is perceived as a drag and corresponds to the “trailing string” solution of Ref.<sup>6,7)</sup>.

Now work is in progress to compute the statistical fluctuations and diffusion of charmonium and other mesonic states in D-brane constructions. Although transport of these states is generally suppressed by  $1/N_c$ , the diffusion coefficient of a heavy meson was computed this year by appealing to the boundary fluctuation dissipation theorem<sup>4)</sup>. Given the bulk picture of fluctuations developed in Ref.<sup>3)</sup> a new understanding of this calculation is the following: The gravitational fields and dilatonic fields are continually fluctuating. Since these fluctuating gravitational and dilatonic fields shift the spectrum of the D7 brane excitations, gradients in these fields give rise to a net force on a mesonic normal modes of the D7 brane. This force jostles the heavy meson causing it to diffuse.

The work also suggest new direction for the study of fast quarks with AdS/CFT. For instance, it should be possible to compute the fluctuations of the average energy within a cone of a jet. Currently, the experimentalists are studying three particle correlations which probe this sort of physics. Many additional observables can be proposed and ultimately measured. There is much work to establish a good set fluctuation measures and to calculate these measures with kinetic theory and the AdS/CFT. Ultimately this analysis should establish the relevance or irrelevance of the AdS/CFT correspondence to the heavy ion reaction.

## References

- 1) G. Policastro, D. T. Son and A. O. Starinets, Phys. Rev. Lett. **87**, 081601 (2001) [arXiv:hep-th/0104066].
- 2) P. Kovtun, D. T. Son and A. O. Starinets, Phys. Rev. Lett. **94**, 111601 (2005) [arXiv:hep-th/0405231].
- 3) D. T. Son and D. Teaney, “Thermal Noise and Stochastic Strings in AdS/CFT,” arXiv:0901.2338 [hep-th]. *Submitted to JHEP*.
- 4) K. Dusling, J. Erdmenger, M. Kaminski, F. Rust, D. Teaney and C. Young, “Quarkonium transport in thermal AdS/CFT,” JHEP **0810**, 098 (2008) .
- 5) J. Casalderrey-Solana and D. Teaney, “Heavy quark diffusion in strongly coupled  $N = 4$  Yang Mills,” Phys. Rev. D **74**, 085012 (2006) .
- 6) C. P. Herzog, A. Karch, P. Kovtun, C. Kozcaz and L. G. Yaffe, JHEP **0607**, 013 (2006).
- 7) S. S. Gubser, Phys. Rev. D **74**, 126005 (2006).

<sup>\*1</sup> Department of Physics & Astronomy, Stony Brook University.

<sup>\*2</sup> D. Teaney was supported as a RIKEN-RBRC research fellow, by an Alfred P. Sloan Fellowship, and a OJI award from the U.S. Department of Energy DE-FG02-08ER41540.

# Extended MQCD and SUSY/non-SUSY duality<sup>†</sup>

K. Ohta<sup>\*1</sup> and T. -S. Tai<sup>\*2</sup>

[Geometric engineering, Calabi-Yau geometry, N=1 gauge theory]

Recently, Aganagic et al. proposed a SUSY/non-SUSY duality<sup>1)</sup> in Type IIB string compactification. In contrast to previous works where anti-branes are introduced by hand, the breakthrough was to turn on a holomorphic varying background NS-flux  $H_0$  through the non-compact Calabi-Yau (CY) three-fold. This soon suggests a way to realize various kinds of SUSY or non-SUSY vacua via adjusting parameters the NS-flux contains.

Let us briefly review their ideas. Because of the flux  $H_0 = dB_0$ , four-dimensional gauge theory, realized by wrapping D5-branes on vanishing two-cycles of a CY, acquires different gauge couplings at each  $P^1$  locus:  $\alpha = \frac{\theta}{2\pi} + \frac{4\pi i}{g_{YM}^2} = \int_{P^1} B_0(v)$ ,  $B_0 = B_{RR} + \frac{i}{g_s} B_{NS}$ , where  $v$  parameterizes a CY bearing, say, the  $A_1$ -type singularity as  $X : uz + w^2 - W'(v)^2 = 0$ . Note that  $W(v) = \sum_{k=1}^{n+1} a_k v^k$ , providing a non-trivial  $A_1$  fibration over  $v$ , corresponds to the tree-level superpotential breaking  $\mathcal{N} = 2$  down to  $\mathcal{N} = 1$ .

The proposed SUSY/non-SUSY duality is achieved by tuning coefficients of the  $v$ -dependent background  $B$ -field, which has the following expression  $B_0(v) = \sum_{k=0}^{n-1} t_k v^k$ . For generic  $t_k$ , SUSY is spontaneously broken at UV. This is accounted for by the fact that  $P^1$ 's may develop relatively different orientations at critical points  $W'(v) = \prod_{i=1}^n (v - v_i) = 0$  for  $\int B_{NS} \sim$  Kähler moduli of  $P^1$ . On the other hand, some specific choice of  $t_k$  can still make four supercharges preserved, i.e. all orientations of  $P^1$ 's are kept aligned. Trough geometric transition to dual CY manifolds, SUSY breaking effects can as well be captured qualitatively by studying strongly-coupled IR physics. Minimizing the effective superpotential there, one can further determine  $t_k$  from  $a_k$ <sup>a)</sup>.

Like the brane realization of meta-stable SUSY breaking vacua, our purpose in this paper is to translate things considered above into Type IIA/M-theory language. It is well-known that via a T-duality acting on  $X$  one instead obtains two NS5-branes in flat spacetime with D4-branes in between them. From the tree-level F-term  $\int d^2\theta \mathcal{F}_{UV}''(\Phi) \mathcal{W}_\alpha \mathcal{W}^\alpha + W(\Phi)$ , one can choose a vacuum  $\Phi = \text{diag}(v_1, \dots, v_2, \dots, \dots, v_n, \dots)$  such that the gauge group  $U(N)$  is broken to  $\prod_{i=1}^n U(N_i)$ . Then, it is seen that D4-branes, coming from IIB fractional D3-branes, remain at  $v_i$ 's. The size and orientation of  $P^1$ 's are translated, respec-

tively, to the length along the T-dual direction (bare gauge coupling) and sign of RR charge of  $i$ -th stack of D4-branes. Based on this Type IIA tree-level description<sup>b)</sup>,  $B_{NS}(v) < 0$  which naively means negative gauge couplings can be understood as two crossing NS5-branes that result in anti-branes. How spontaneously SUSY breaking vacua occur can therefore be visualized clearly in the presence of both D4- and  $\overline{D4}$ -branes as a consequence of the *extended* prepotential.

## References

- 1) M. Aganagic, C. Beem, J. Seo and C. Vafa: arXiv:0804.2489 [hep-th]

<sup>†</sup> JHEP 0809 (2008) 033

<sup>\*1</sup> Nishina Ctr., RIKEN

<sup>\*2</sup> Tohoku University

<sup>a)</sup> This fact can be interpreted from M-theory perspective.

<sup>b)</sup> As usual, we notice that tree-level field theory results match with classical brane pictures at the lowest order in  $\ell_s$  under  $g_s \rightarrow 0$ , i.e. brane bending and string interaction are not taken into account.

# Kerr/CFT correspondence and five-dimensional BMPV black holes<sup>†</sup>

H. Isono,<sup>\*1</sup> T. -S. Tai<sup>\*2</sup> and W. -Y. Wen<sup>\*1</sup>

[AdS/CFT correspondence, 5D rotating Black holes]

Considerable progress in deriving black hole entropy statistically has been made by resorting to state counting approaches. Among them, while Cardy's formula in conformal field theory (CFT) plays an indispensable role, this can be better understood in the context of AdS/CFT correspondence via string compactification and wrapped branes<sup>1</sup>. For example, a 2D  $\mathcal{N} = (0, 4)$  CFT living on an M5-brane wrapping spatially  $S^1 \times P_4$  ( $P_4 \subset CY_3$ ) was shown to be dual to a 5D black hole formed by M-lifting a Type IIA D0-D4 system which has an attractor geometry near the horizon<sup>2</sup>. The entropy in terms of Cardy's formula  $2\pi\sqrt{c_L L_0/6}$  agrees with Bekenstein-Hawking area law. Here  $c_L$  denotes the central charge and  $L_0$  is the eigenvalue of the left-moving Virasoro zero mode.

On the other hand, an alternative pioneered much earlier by Brown and Henneaux<sup>3</sup> is to take into account the asymptotic symmetry preserved at the boundary. They dealt with a 3D BTZ black hole, which asymptotically approaches  $AdS_3$  with  $SL(2, R)_L \otimes SL(2, R)_R$  isometry. There, two copies of Virasoro algebra emerge as a result of infinitely many Fourier modes of the boundary diffeomorphism  $\xi^\mu(x)\partial_\mu$ . The central term arising from commutators of Virasoro generators was thereby used to reproduce the entropy  $S_{BTZ} = 2\pi\sqrt{c_L L_0/6} + 2\pi\sqrt{c_R \tilde{L}_0/6}$ . Note that no dynamical detail about this dual non-chiral CFT was given though.

In much the same spirit of Brown-Henneaux, chiral auxiliary 2D CFTs dual to 4D extremal Kerr black holes have recently been proposed by Strominger et al.<sup>6</sup>. On the near-horizon geometry a crucial boundary condition is imposed such that the asymptotic symmetry group (ASG) includes ultimately two kinds of generators,  $K^t$  and  $K_n^\phi$ .

Quite remarkably, by further introducing Frolov-Thorne temperature  $T_{FT}$ <sup>7</sup>, Cardy's formula  $S = \frac{\pi^2}{3} c T_{FT}$  reproduces the macroscopic entropy perfectly. This aspect seems rather puzzling because it departs from our usual understanding instructed by BTZ black holes. There, neither their stringy derivation nor Brown-Henneaux method involves the underlying temperature  $T_{FT}$ .

In this article, we apply the above procedure to a well-known five-dimensional extremal supersymmetric charged spinning black hole constructed by Brecken-

ridge, Myers, Peet and Vafa (BMPV)<sup>9</sup>. Unlike Kerr-Newman black holes, this solution still exhibits unbroken supersymmetry even extremality is satisfied. As BTZ black holes mentioned above, the microscopic origin of BMPV entropy first roots in its D-brane realization. Nevertheless, the degeneracy counting that we will derive below will rely thoroughly on Virasoro algebra from ASG and Frolov-Thorne temperature. We remark that BMPV solutions have finite horizons and are asymptotically flat. Therefore, they are distinguished from another kind of 5D black holes formed by a M-theory lift of D0-D2-D6 systems.

## References

- 1) A. Strominger and C. Vafa, Phys. Lett. B **379** 99 (1996).
- 2) J. M. Maldacena, A. Strominger and E. Witten: JHEP **9712**, 002 (1997) .
- 3) J. D. Brown and M. Henneaux: Commun. Math. Phys. **104** 207 (1986).
- 4) G. Barnich and F. Brandt: Nucl. Phys. B **633** 3 (2002).
- 5) G. Barnich and G. Compere: J. Math. Phys. **49** 042901 (2008).
- 6) M. Guica, T. Hartman, W. Song and A. Strominger: arXiv:0809.4266 [hep-th].
- 7) V. P. Frolov and K. S. Thorne: Phys. Rev. D **39** (1989) 2125.
- 8) A. Strominger: JHEP **9802** 009 (1998).
- 9) J. C. Breckenridge, R. C. Myers, A. W. Peet and C. Vafa: Phys. Lett. B **391** (1997) 93.

<sup>†</sup> arXiv:0812.4440v2 [hep-th]

<sup>\*1</sup> Department of Physics and Center for Theoretical Sciences, National Taiwan University

<sup>\*2</sup> Nishina Ctr., RIKEN

# Toward a Proof of Montonen-Olive Duality via Multiple M2-branes<sup>†</sup>

K. Hashimoto,<sup>\*1</sup> T. -S. Tai<sup>\*1</sup> and S. Terashima<sup>\*2</sup>

[4D super Yang-Mills theory, 3D super-conformal Chern-Simons theory, Montonen-Olive duality]

Among recent developments on effective actions of multiple M2-branes, one of the surprising outputs is the non-abelian duality. In 3 dimensions, it has been known for more than a decade that the action of a single M2-brane can be dualized classically to that of a D2-brane: an abelian duality between scalar field theory and 3d electromagnetism. Based on Bagger-Lambert-Gustavsson model<sup>(2)(3)</sup> of multiple M2-brane, Mukhi and Papageorgakis have obtained a quite intriguing non-abelian duality<sup>(4)</sup>, a relation between field theories on multiple M2-branes and D2-branes. In this paper, we generalize their result and find a novel mechanism to prove the renowned Montonen-Olive (MO) duality conjectured<sup>(1)</sup> for 4d  $\mathcal{N} = 4$   $U(N)$  super Yang-Mills (SYM) theory.

The method of Mukhi et al. is as follows. First, one of the eight transverse fields is given a vacuum expectation value (vev)  $v$ , which turns out to provide mass terms for a non-dynamical part of gauge fields in Chern-Simons (CS) terms. Integrating massive modes out, one gets rightly a YM kinetic term of D2-branes. As pioneered by Aharony, Bergman, Jafferis and Maldacena (ABJM)<sup>(5)</sup>, following the renormalization group, certain  $\mathcal{N} = 3$  3d CSYM theories flow to  $\mathcal{N} = 6$  superconformal field theories (SCFTs) at IR fixed point, which precisely describe M2-branes probing  $\mathbf{C}^4/\mathbf{Z}_k$  ( $k > 2$ ) where  $k$  is the CS level. Equipped with these, the need for a vev then gets clarified geometrically, i.e. the M-theory circle is created in the above limit and D2-branes appear thereof. It is highly non-trivial that this mechanism requires CS terms which in turn give an orbifold moduli space.

Let us extend the step further to 4-dimensional theories. Let us summarize how  $\mathcal{N} = 4$  SYM, 3d SCFT and MO duality are related to each other. As is well known, the axio-dilaton  $\tau$  of Type IIB supergravity coincides with the gauge coupling of  $\mathcal{N} = 4$  SYM, realized on  $N$  coincident D3-branes at low energy. MO duality is then regarded as  $S$ -duality of Type IIB string theory. In terms of M-theory,  $\tau$  is interpreted as the complex structure of a two-torus formed by  $(x^9, x^{11})$  such that the  $S$ -duality gets readily identified with the  $SL(2, \mathbf{Z})$  modular transformation. Also, via duality chains, M2-branes transverse to the above two-torus with shrinking size and fixed  $\tau$  guarantee that D3-branes they are dual to are non-compact.

To get a torus, it is insufficient to just dwell in the

present ABJM model. We make use of a generalized version where the gauge group is  $\prod_{i=1}^{2n} U(N)_i$ . As shown in<sup>(6)</sup>, it is possible to prepare a IIB brane setup which flows to the theory we want at IR fixed point. Viewed from M-theory, this describes  $N$  M2-branes probing an abelian orbifold  $\mathbf{C}^4/\Gamma$  where  $\Gamma = \mathbf{Z}_n \times \mathbf{Z}_{kn}$ .

We turn on vevs  $(v, \tilde{v})$  of two scalars and make a torus using a crucial scaling limit which carries out the shrinking size with fixed  $\tau$ . Our field theory result shows that a 4d SCFT (SYM theory) emerges from a 3d SCFT (generalized ABJM model) as desired. Methods for uplifting dimensions are basically Taylor's T-duality<sup>(7)</sup> and deconstruction of extra dimensions<sup>(8)</sup>. With the SYM obtained, we go further to analyze MO duality. It is found that there are infinitely many equivalent SYMs derived from the same generalized ABJM action. But eventually they differ merely up to  $SL(2, \mathbf{Z})$  redefinition of  $\tau$ . This completes our proof of MO duality.

## References

- 1) C. Montonen and D. I. Olive: Phys. Lett. B **72**, 117 (1977).
- 2) J. Bagger and N. Lambert: Phys. Rev. D **77**, 065008 (2008).
- 3) A. Gustavsson: arXiv:0709.1260 [hep-th].
- 4) S. Mukhi and C. Papageorgakis: JHEP **0805**, 085 (2008).
- 5) O. Aharony, O. Bergman, D. L. Jafferis and J. Maldacena: JHEP **0810**, 091 (2008).
- 6) Y. Imamura and K. Kimura: JHEP **0810**, 040 (2008).
- 7) W. Taylor: Phys. Lett. B **394**, 283 (1997).
- 8) N. Arkani-Hamed, A. G. Cohen and H. Georgi: Phys. Rev. Lett. **86**, 4757 (2001).

<sup>†</sup> JHEP 0904 (2009) 025

<sup>\*1</sup> Nishina Ctr., RIKEN

<sup>\*2</sup> Yukawa Institute for Theoretical Physics, Kyoto University

# D-brane States and Annulus Amplitudes in $OSp$ Invariant Closed String Field Theory<sup>†</sup>

Y. Baba, N. Ishibashi,<sup>\*1</sup> and K. Murakami

[String field theory, D-branes, BRST symmetry]

D-branes have been studied for many years and used to reveal nonperturbative aspects of string theory. As Sen argued,<sup>1)</sup> D-branes can be realized as soliton solutions to the equation of motion in open string field theory. Now some of his conjectures have been proved analytically<sup>2)</sup> in Witten's open string field theory.

In previous works,<sup>3)</sup> we studied how D-branes can be realized in closed string field theory. A fairly clear answer to this question is given for noncritical strings. Fukuma and Yahikozawa<sup>4)</sup> showed that D-branes can be realized as solitonic operators which commute with the Virasoro and the  $W$  constraints for noncritical string theories. Hanada et al.<sup>5)</sup> showed how such solitonic operators can be realized in the string field theory for noncritical strings presented in Ref. 6). We showed<sup>3)</sup> that a similar construction is possible in the case of critical strings, using the  $OSp$  invariant string field theory. We constructed states with an arbitrary number of coincident D-branes in this theory. Imposing the condition that the states should be BRST invariant, we can determine the form of the states. In particular, the tension of the D-branes is fixed to be the correct value. We can calculate disk amplitudes using these states, and the results indeed coincide with those of first quantized string theory. A key to the proof of the BRST invariance of the above-mentioned D-brane states is the idempotency relation satisfied by the boundary state.<sup>7)</sup>

The purpose of this work is to extend our construction into the case where the parallel D-branes are located at different points from each other in space-time. Using such states with the D-branes, we would like to evaluate scattering amplitudes involving strings whose worldsheet have boundaries attached to D-branes contained in these states. In this report, we compute annulus amplitudes with closed string external lines, in the situation where the annulus is suspended between two parallel D-branes. We show that they coincide with the usual annulus amplitudes including the normalizations. This fact yields further evidence for our construction.

The BRST invariant state corresponding to one flat  $Dp$ -brane sitting at  $X^i = Y^i$  ( $i = p + 1, \dots, 25$ ) takes the form<sup>3)</sup>

$$|D(Y)\rangle\rangle = \lambda \int d\zeta \bar{O}_D(\zeta, Y)|0\rangle\rangle, \quad (1)$$

$$\bar{O}_D(\zeta, Y) = \exp \left[ A \int_{-\infty}^0 \frac{d\alpha}{4\pi} e^{\zeta\alpha} \langle B^\epsilon | \bar{\psi}(\alpha) \rangle + B\zeta^2 \right],$$

$$A = \frac{1}{2} \sqrt{\frac{\pi}{256} (8\pi^2)^{11-p}}, \quad B = \frac{2^{\frac{19+p}{2}} \epsilon^2 (-\ln \epsilon)^{\frac{p+1}{2}}}{\pi^{\frac{p-24}{2}} g},$$

where  $|B^\epsilon(Y)\rangle\rangle = e^{-\epsilon H} |B(Y)\rangle\rangle$  is a regularization (with an infinitesimal regularization parameter  $\epsilon$ ) of the boundary state  $|B(Y)\rangle\rangle$  for the  $Dp$ -brane located at  $X^i = Y^i$ ,  $H$  is the tree-level hamiltonian,  $g$  is the string coupling constant, and  $|\bar{\psi}\rangle\rangle$  is the creation operator of a string. We find that the state corresponding to  $N$  such  $Dp$ -branes located at  $X^i = Y_{(I)}^i$  ( $I = 1, \dots, N$ ) is given simply as

$$|D_N; Y_{(I)}\rangle\rangle = \lambda_N \prod_{I=1}^N \left( \int d\zeta_I \bar{O}_D(\zeta_I, Y_{(I)}) \right) |0\rangle\rangle, \quad (2)$$

if  $(Y_{(I)} - Y_{(J)})^2 \neq 0$  for  $I \neq J$ . In contrast to the case of coincident D-branes,<sup>3)</sup> we just have to consider the product of  $\int d\zeta \bar{O}_D$ 's. The idempotency relation<sup>7)</sup> is again a key to the proof of the BRST invariance of this state.

Following the prescription given in Ref. 8) to evaluate the S-matrix elements in the  $OSp$  invariant string field theory, we compute the annulus amplitudes mentioned above, by using the D-brane state (2). We find that the results in the first quantized string theory are reproduced with the correct normalization. The annulus amplitude is expressed as an integral over the moduli space of string worldsheet for the process. We notice that in this integral, the moduli space is covered completely and only once with the correct measure. This verifies the validity of our construction.

## References

- 1) A. Sen: Int. J. Mod. Phys. A **14**, 4061 (1999); JHEP **9912**, 027 (1999).
- 2) M. Schnabl: Adv. Theor. Math. Phys. **10**, 433 (2006).
- 3) Y. Baba, N. Ishibashi and K. Murakami: JHEP **0605**, 029 (2006); JHEP **0710**, 008 (2007).
- 4) M. Fukuma and S. Yahikozawa: Phys. Lett. B **396**, 97 (1997); ibid. B **393**, 316 (1997).
- 5) M. Hanada et. al.: Prog. Theor. Phys. **112**, 131 (2004).
- 6) N. Ishibashi and H. Kawai: Phys. Lett. B **314**, 190 (1993). A. Jevicki and J.P. Rodrigues: Nucl. Phys. B **421**, 278 (1994).
- 7) I. Kishimoto, Y. Matsuo and E. Watanabe: Phys. Rev. D **68**, 126006 (2003); Prog. Theor. Phys. **111**, 433 (2004).
- 8) Y. Baba, N. Ishibashi and K. Murakami: JHEP **0705**, 020 (2007).

<sup>†</sup> Condensed from the article in JHEP **0807** (2008) 046

<sup>\*1</sup> Institute of Physics, University of Tsukuba

# Gauge invariant overlaps for classical solutions in open string field theory<sup>†</sup>

T. Kawano,<sup>\*1</sup> I. Kishimoto and T. Takahashi<sup>\*2</sup>

[Nonperturbative techniques, string field theory, D branes, conformal field theory]

After the advent of Schnabl's analytic solution<sup>1)</sup> for tachyon condensation in Witten's cubic bosonic open string field theory, there have been a number of new developments in this field. A prominent feature is the potential height at the solution, which is equal to the tension of D25-brane as is consistent with Sen's conjecture. Here, we calculate other gauge invariant observables,<sup>2-4)</sup> which will be called gauge invariant overlaps, for Schnabl's solution with an analytic method and with level truncation approximation. We also compute these for the numerical solution<sup>5,6)</sup> initially obtained by Sen and Zwiebach in the level truncation approximation to compare with those for Schnabl's solution. The results are consistent with the expectation that these solutions may be gauge equivalent.

Gauge invariant overlap  $\mathcal{O}_V(\Psi)$  for an open string field  $\Psi$  is defined by

$$\mathcal{O}_V(\Psi) \equiv \langle V(i)f_{\mathcal{I}}[\Psi] \rangle, \quad f_{\mathcal{I}}(z) = \frac{2z}{1-z^2}, \quad (1)$$

where the CFT correlator is defined on the upper half plane and the operator  $V(i)$  inserted at the midpoint of the string field corresponds to an on-shell closed string state.  $\mathcal{O}_V(\Psi)$  is left invariant under the gauge transformation of the open string field theory:

$$\delta\Psi = Q_B\Lambda + \Psi * \Lambda - \Lambda * \Psi \quad (2)$$

with a gauge parameter string field  $\Lambda$ . Note that (1) vanishes for pure gauge solutions.

Schnabl's analytic solution<sup>1)</sup> can be expressed as

$$\Psi_\lambda = \frac{\lambda\partial_r}{\lambda e^{\partial_r} - 1} \psi_r|_{r=0} \quad (3)$$

with one parameter  $\lambda$ , where  $\psi_r$  is a particular string field based on the wedge state  $|r+2\rangle$ . We have computed  $\mathcal{O}_V(\psi_r)$  analytically and found that it is independent of  $r$ . Therefore, we conclude<sup>a)</sup>

$$\mathcal{O}_V(\Psi_\lambda) = \begin{cases} \frac{C_V}{2\pi i} & (\lambda = 1) \\ 0 & (\lambda \neq 1) \end{cases}. \quad (4)$$

( $C_V$  is determined by the normalization of  $V(i)$  in (1).) That is, the gauge invariant overlap for  $\Psi_\lambda$  becomes nontrivial only in the case  $\lambda = 1$ . Our result is consistent with the previous evaluation of the potential height and suggests that  $\Psi_{\lambda=1}$  represents a nonperturbative vacuum and  $\Psi_{\lambda \neq 1}$  gives pure gauge solutions.

<sup>†</sup> Condensed from the article in Nucl. Phys. B **803**, 135 (2008)

<sup>\*1</sup> Department of Physics, University of Tokyo

<sup>\*2</sup> Department of Physics, Nara Women's University

<sup>a)</sup> This result was also given by Ellwood.<sup>7)</sup>

We have also numerically computed  $\mathcal{O}_\eta(\Psi_\lambda)$  for  $|\lambda| \leq 1$  with the conventional  $L_0$ -level truncation approximation. Here  $V(i)$  in (1) corresponds to the dilaton state with zero momentum, which gives  $C_V = i$  in (4). For the interval  $-1 \leq \lambda < 1$ ,  $\mathcal{O}_\eta(\Psi_{\lambda,L})$  approaches zero as the level  $L$  is increased. For  $\lambda = 1$ ,  $\mathcal{O}_\eta(\Psi_{\lambda=1,L})$  approaches  $1/(2\pi) \simeq 0.159155$  as in Table 1. This is consistent with our analytic result in (4).

$L$	$\mathcal{O}_\eta(\Psi_{\lambda=1,L})$
0	0.138366
2	0.149284
4	0.156857
6	0.157395
8	0.158795
10	0.158765
12	0.159220
14	0.159159

Table 1.

We also computed the gauge invariant overlap for the numerical solution  $\Psi_N$  in the Siegel gauge, which is obtained by  $(L, 2L)$  and  $(L, 3L)$  truncation. The result is given in Table 2. The best approximation ( $(10, 30)$  truncation) gives 97% of  $1/(2\pi)$ . Therefore,  $\mathcal{O}_\eta(\Psi_N) \simeq \mathcal{O}_\eta(\Psi_{\lambda=1})$ . In addition to the matching of potential height, this gives further evidence for the gauge equivalence of  $\Psi_N$  with  $\Psi_{\lambda=1}$ , which implies that these two solutions give the same nonperturbative vacuum in the bosonic open string field theory.

$L$	$\mathcal{O}_\eta(\Psi_{N,(L,2L)})$	$\mathcal{O}_\eta(\Psi_{N,(L,3L)})$
0	0.114044	0.114044
2	0.139790	0.141626
4	0.147931	0.148325
6	0.151225	0.151369
8	0.152887	0.152976
10	0.154029	0.154080

Table 2.

## References

- 1) M. Schnabl: Adv. Theor. Math. Phys. **10**, 433 (2006).
- 2) B. Zwiebach: Mod. Phys. Lett. A **7**, 1079 (1992).
- 3) A. Hashimoto and N. Itzhaki: JHEP **0201**, 028 (2002).
- 4) D. Gaiotto, L. Rastelli, A. Sen and B. Zwiebach: Adv. Theor. Math. Phys. **6**, 403 (2003).
- 5) A. Sen and B. Zwiebach: JHEP **0003**, 002 (2000).
- 6) D. Gaiotto and L. Rastelli: JHEP **0308**, 048 (2003).
- 7) I. Ellwood: JHEP **0808**, 063 (2008).

# Schnabl's solution and boundary states in open string field theory <sup>†</sup>

T. Kawano,<sup>\*1</sup> I. Kishimoto and T. Takahashi<sup>\*2</sup>

[Nonperturbative techniques, string field theory, D branes, conformal field theory]

We discuss the fact that Schnabl's solution<sup>1)</sup> is an off-shell extension of the boundary state describing a D-brane in the closed string sector. This gives the physical meaning of the gauge invariant overlaps for the solution in our previous paper<sup>2)</sup> and supports Ellwood's recent proposal<sup>3)</sup> in the operator formalism.

The Schnabl solution for tachyon condensation  $\Psi_{\lambda=1}$  can be rewritten as

$$\begin{aligned}\Psi_{\lambda=1} &= \psi_0 + \sum_{n=0}^{\infty} (\psi_{n+1} - \psi_n - \partial_r \psi_r|_{r=n}) \\ &\equiv \psi_0 + \chi.\end{aligned}\quad (1)$$

Since it has been shown<sup>2,3)</sup> that  $\mathcal{O}_V(\psi_r)$  does not depend on  $r$ , it is evident that

$$\mathcal{O}_V(\Psi_{\lambda=1}) = \mathcal{O}_V(\psi_0).\quad (2)$$

This suggests that only the first term  $\psi_0$  contributes to the gauge invariant overlaps  $\mathcal{O}_V(\Psi_{\lambda=1})$ .

Recently, Ellwood has made the interesting proposal that the gauge invariant overlaps are related to the closed string tadpoles as follows<sup>3)</sup>

$$\mathcal{O}_V(\Psi) = \mathcal{A}_{\Psi}(V) - \mathcal{A}_0(V),\quad (3)$$

where  $\mathcal{A}_{\Psi}(V)$  is the disk amplitude for a closed string vertex operator  $V$  with the boundary condition of the CFT given by the open string field solution  $\Psi$ , and  $\mathcal{A}_0(V)$  is the usual disk amplitude in the perturbative vacuum. In fact, he has shown this to be the case for some analytic solutions. Since there are no D-branes after tachyon condensation, no closed tadpoles are available, and thus  $\mathcal{A}_{\Psi}(V) = 0$ . Therefore, the gauge invariant overlap for the tachyon vacuum solution gives the usual disk amplitude of the opposite sign with one closed string emitted. This suggests that, as expected, the analytic solution given by Schnabl is closely related to the boundary state describing a D-brane in the closed string perturbation theory.

Here, we will explicitly demonstrate this in the operator formalism of string field theory by using the Shapiro-Thorn vertex  $\langle \hat{\gamma}(1_c, 2) |$ , which maps an open string state to the corresponding closed string state. By using the open-closed string vertex  $\langle \hat{\gamma}(1_c, 2) |$ , as discussed in detail in our previous paper<sup>2)</sup> we can rewrite a gauge invariant overlap as

$$\mathcal{O}_V(\psi) = \langle \hat{\gamma}(1_c, 2) | \phi_c \rangle_{1_c} | \psi \rangle_2,\quad (4)$$

where  $|\phi_c \rangle_{1_c}$  is an on-shell state corresponding to the

vertex operator  $V$  of the closed string  $1_c$ , and  $|\psi \rangle_2$  is a state of the open string 2. For the analytic solution  $\Psi_{\lambda=1}$  (1), we have

$$\begin{aligned}\mathcal{O}_V(\Psi_{\lambda=1}) &= \langle \hat{\gamma}(1_c, 2) | \phi_c \rangle_{1_c} | \Psi_{\lambda=1} \rangle_2 \\ &= \langle \hat{\gamma}(1_c, 2) | \phi_c \rangle_{1_c} | \psi_0 \rangle_2 + \langle \hat{\gamma}(1_c, 2) | \phi_c \rangle_{1_c} | \chi \rangle_2\end{aligned}\quad (5)$$

and, as mentioned above (2), the second term on the right hand side is zero for the on-shell closed string state  $|\phi_c \rangle_{1_c}$ . For the first term on the right hand side,  $\langle \hat{\gamma}(1_c, 2) | \phi_c \rangle_{1_c} | \psi_0 \rangle_2$ , we can see that the open string tachyon state  $|\psi_0 \rangle = (2/\pi)c_1|0 \rangle$  is transformed via the vertex  $\langle \hat{\gamma}(1_c, 2) |$  into the boundary state  $\langle B |$ . In fact, we can obtain the relation

$$\langle \hat{\gamma}(1_c, 2) | \psi_0 \rangle_2 \mathcal{P}_{1_c} = \frac{1}{2\pi} \langle B | c_0^- \quad (6)$$

with the level matching projection  $\mathcal{P}_{1_c}$  for the closed string  $1_c$ , where the boundary state is the usual one:

$$\langle B | = \langle 0 | c_{-1} \bar{c}_{-1} c_0^+ e^{-\sum_{n=1}^{\infty} [\frac{1}{n} \alpha_n \cdot \bar{\alpha}_n + c_n \bar{b}_n + \bar{c}_n b_n]} \quad (7)$$

in the closed string perturbation theory. We thus find that

$$\mathcal{O}_V(\Psi_{\lambda=1}) = \frac{1}{2\pi} \langle B | c_0^- | \phi_c \rangle,\quad (8)$$

which is in precise agreement with Ellwood's result.

Since the second term on the right hand side of (5) does not necessarily vanish for off-shell closed string states, we may conclude that the transform of the analytic solution  $\Psi_{\lambda=1}$  via the Shapiro-Thorn vertex is an off-shell extension of the boundary state  $\langle B |$ . Although it seems more complicated to calculate  $\langle \hat{\gamma}(1_c, 2) | \phi_c \rangle_{1_c} | \chi \rangle_2$ , it would be interesting to find the relation of the off-shell boundary state with the equation of motion in closed string field theory<sup>5-8)</sup> or open-closed string field theory<sup>9)</sup>. We believe that our observation above may serve as an encouraging step in this investigation.

## References

- 1) M. Schnabl: Adv. Theor. Math. Phys. **10**, 433 (2006).
- 2) T. Kawano, I. Kishimoto and T. Takahashi: Nucl. Phys. B **803**, 135 (2008).
- 3) I. Ellwood: JHEP **0808**, 063 (2008).
- 4) J. A. Shapiro and C. B. Thorn: Phys. Lett. B **194**, 43 (1987).
- 5) M. Saadi and B. Zwiebach: Annals Phys. **192**, 213 (1989).
- 6) T. Kugo, H. Kunitomo and K. Suehiro: Phys. Lett. B **226**, 48 (1989).
- 7) T. Kugo and K. Suehiro: Nucl. Phys. B **337**, 434 (1990).
- 8) B. Zwiebach: Nucl. Phys. B **390**, 33 (1993).
- 9) B. Zwiebach: Annals Phys. **267**, 193 (1998).

<sup>†</sup> Condensed from the article in Phys. Lett. B **669**, 357 (2008)

<sup>\*1</sup> Department of Physics, University of Tokyo

<sup>\*2</sup> Department of Physics, Nara Women's University

# Comments on gauge invariant overlaps for marginal solutions in open string field theory <sup>†</sup>

I. Kishimoto

[Nonperturbative techniques, string field theory, D branes, conformal field theory]

We calculate the gauge invariant overlap<sup>a)</sup> for the marginal solution with nonsingular current given by Schnabl<sup>2)</sup> and Kiermaier-Okawa-Rastelli-Zwiebach<sup>3)</sup> (S/KORZ). The obtained formula is the same as that for the Fuchs-Kroyter-Potting/Kiermaier-Okawa (FKP/KO) marginal solution,<sup>4,5)</sup> which has already been computed by Ellwood.<sup>7)</sup> Our result is consistent with the expectation that these two types of solutions may be gauge equivalent. We also comment on a gauge invariant overlap for rolling tachyon solutions in cubic bosonic open string field theory.

The gauge invariant overlap  $\mathcal{O}_V(\Psi)$  is written as

$$\mathcal{O}_V(\Psi) = \langle \mathcal{I}|V(i)|\Psi \rangle, \quad (1)$$

where  $\langle \mathcal{I}|$  is the identity state and  $V(i)$  corresponds to an on-shell closed string state. Next, we can prove the following relations:

$$\langle \mathcal{I}|V(i)K_n = 0, \quad K_n \equiv L_n - (-1)^n L_{-n}, \quad (2)$$

$$\langle \mathcal{I}|V(i)(b_n - (-1)^n b_{-n}) = 0, \quad (3)$$

$$\langle \mathcal{I}|V(i)(c_n + (-1)^n c_{-n}) = 0. \quad (4)$$

Noting the above we can rewrite the S/KORZ marginal solution  $\Psi_{\lambda_m}^{\text{S/KORZ}}$  as

$$\begin{aligned} \Psi_{\lambda_m}^{\text{S/KORZ}} = & -\frac{1}{\pi} 2^{-\mathcal{L}_0} \left( e^{-\lambda_m \int_0^{2\pi} d\theta J_w(e^{i\theta})} - 1 \right) c_1 |0\rangle \\ & + O(K_1, \mathcal{L}_0 - \mathcal{L}_0^\dagger, \mathcal{B}_0 - \mathcal{B}_0^\dagger, c_n + (-1)^n c_{-n}). \end{aligned} \quad (5)$$

Here,  $J_w$  is a matter primary operator with dimension one on the unit disk  $|w| \leq 1$ , which has nonsingular OPE, and  $\lambda_m$  is a parameter which corresponds to a marginal deformation of the boundary CFT. The second term  $O(K_1, \mathcal{L}_0 - \mathcal{L}_0^\dagger, \mathcal{B}_0 - \mathcal{B}_0^\dagger, c_n + (-1)^n c_{-n})$  denotes some linear combination of terms comprising  $K_1, \mathcal{L}_0 - \mathcal{L}_0^\dagger, \mathcal{B}_0 - \mathcal{B}_0^\dagger$  and  $c_n + (-1)^n c_{-n}$ , where at least one of them is multiplied on the conformal vacuum  $|0\rangle$ .  $\mathcal{B}_0$  is the  $b$ -ghost zero mode on the sliver frame and  $\mathcal{L}_0 = \{Q_B, \mathcal{B}_0\}$ . Using this decomposition (5)<sup>b)</sup> and relations (2), (3) and (4), we can easily evaluate the gauge invariant overlap (1):

<sup>†</sup> Condensed from the article in Prog. Theor. Phys. **120**, 875 (2008)

<sup>a)</sup> See, our previous paper<sup>1)</sup> for technical details.

<sup>b)</sup> Similar decompositions are possible for the FKP/KO marginal solution  $\Psi_{\lambda_m, L}^{\text{FKP/KO}}$  and Schnabl's solution for tachyon condensation<sup>6)</sup>  $\Psi_{\lambda_m}^{\text{S}}$ . They give another approach to computing the gauge invariant overlap (1) for the solutions evaluated in earlier papers.<sup>1,7,8)</sup>

$$\begin{aligned} \mathcal{O}_V(\Psi_{\lambda_m}^{\text{S/KORZ}}) &= -\frac{1}{2\pi i} \left\langle c^w \bar{c}^w V_{w\bar{w}, m}(0, 0) \right. \\ &\quad \left. \times c^w(1) \left( e^{-\lambda_m \int_0^{2\pi} d\theta J_w(e^{i\theta})} - 1 \right) \right\rangle_{\text{disk}}. \end{aligned} \quad (6)$$

The result is the same as the formula<sup>7)</sup> for the FKP/KO marginal solution  $\Psi_{\lambda_m, L}^{\text{FKP/KO}}$ ,

$$\mathcal{O}_V(\Psi_{\lambda_m}^{\text{S/KORZ}}) = \mathcal{O}_V(\Psi_{\lambda_m, L}^{\text{FKP/KO}}), \quad (7)$$

for the same  $\lambda_m J$ . This is consistent with the expectation that  $\Psi_{\lambda_m}^{\text{S/KORZ}}$  and  $\Psi_{\lambda_m, L}^{\text{FKP/KO}}$  are gauge equivalent.

Let us consider the gauge invariant overlap  $\mathcal{O}_{V_\zeta}(\Psi)$  with  $V_m = \zeta_{\mu\nu} \partial X^\mu \bar{\partial} X^\nu$  ( $\zeta_{\mu\nu} V^\nu = V^\mu \zeta_{\mu\nu} = 0$ ) for Hellerman-Schnabl's solution<sup>9)</sup>  $\Psi_{\lambda_m}^{\text{HS}}$ , which is given by  $\Psi_{\lambda_m}^{\text{S/KORZ}}$  with the light-like rolling tachyon operator  $J = e^{\beta X^+}$ , ( $\beta \equiv 1/(\alpha' V^+)$ ), on the linear dilaton background  $\Phi(x) = V_\mu x^\mu$ , ( $V^+ > 0, 26 = D + 6\alpha' V_\mu V^\mu, \mu = 0, 1, \dots, D-1$ ). Applying our formula (6) for  $\Psi_{\lambda_m}^{\text{HS}}$  and using the formula of the CFT correlator,<sup>9,10)</sup> we can evaluate  $\mathcal{O}_{V_\zeta}(\Psi_{\lambda_m}^{\text{HS}})$  explicitly. On the other hand, for the tachyon vacuum solution  $\Psi_{\lambda=1}^{\text{S}}$ , we have

$$\mathcal{O}_{V_\zeta}(\Psi_{\lambda=1}^{\text{S}}) = -\frac{\alpha'}{4\pi i} \zeta_{\mu\nu} \eta^{\mu\nu} \int d^D x e^{-V \cdot x} \quad (8)$$

on this background. Then, we obtain the relation

$$\lim_{\lambda_m \rightarrow +\infty} \mathcal{O}_{V_\zeta}(\Psi_{\lambda_m}^{\text{HS}}) = \mathcal{O}_{V_\zeta}(\Psi_{\lambda=1}^{\text{S}}). \quad (9)$$

This is consistent with the late time limit of the light-like rolling tachyon solution:<sup>9)</sup>

$$\lim_{x^+ \rightarrow +\infty} \Psi_{\lambda_m}^{\text{HS}} = \lim_{\lambda_m \rightarrow +\infty} \Psi_{\lambda_m}^{\text{HS}} = \Psi_{\lambda=1}^{\text{S}}. \quad (10)$$

## References

- 1) T. Kawano, I. Kishimoto and T. Takahashi: Nucl. Phys. B **803**, 135 (2008).
- 2) M. Schnabl: Phys. Lett. B **654**, 194 (2007).
- 3) M. Kiermaier, Y. Okawa, L. Rastelli and B. Zwiebach: JHEP **0801**, 028 (2008).
- 4) E. Fuchs, M. Kroyter and R. Potting: JHEP **0709**, 101 (2007).
- 5) M. Kiermaier and Y. Okawa: arXiv:0707.4472 [hep-th].
- 6) M. Schnabl: Adv. Theor. Math. Phys. **10**, 433 (2006).
- 7) I. Ellwood: JHEP **0808**, 063 (2008).
- 8) T. Kawano, I. Kishimoto and T. Takahashi: Phys. Lett. B **669**, 357 (2008).
- 9) S. Hellerman and M. Schnabl: arXiv:0803.1184 [hep-th].
- 10) F. Larsen, A. Naqvi and S. Terashima: JHEP **0302**, 039 (2003).

# Electroweak symmetry breaking in $SO(5) \times U(1)$ gauge-Higgs unification with top and bottom quarks<sup>†</sup>

Y. Hosotani,<sup>\*1</sup> K. Oda,<sup>\*1</sup> T. Ohnuma,<sup>\*1</sup> and Y. Sakamura

[Extra dimension, gauge symmetry breaking]

The origin of electroweak symmetry breaking is still a mystery of elementary particle physics. In the standard model, it is broken by the vacuum expectation value of the Higgs field. However the Higgs boson has not been discovered yet, and searching to it is one of the main purposes of the Large Hadron Collider (LHC) experiment at CERN. Another aim of LHC is to discover evidence of new physics beyond the standard model. It is well known that the standard model has some theoretical problems, such as the gauge hierarchy problem. TeV-scale supersymmetry is one promising candidate for new physics that solves the gauge hierarchy problem. The supersymmetric models generically predict a relatively light Higgs boson. In the minimal supersymmetric standard model, for example, the Higgs mass is bounded below around 130 GeV, which is close to the experimental lower bound of 114 GeV. Under these circumstances, it is important to investigate candidates for new physics other than supersymmetry.

One important class of such candidates is extra dimensions. They are based on the idea that there are extra spatial dimensions other than the four-dimensional world we observe. Although these extra dimensions were originally introduced to explain the weakness of gravity compared to the other forces, they can also play an important role in solving other problems of the standard model. For instance, they can naturally realize the large hierarchy among the fermion masses, and can break gauge symmetries or supersymmetry by the boundary conditions along the extra dimensions. They also serve as a candidate for dark matter. For these reasons, models with extra dimensions have been studied extensively during the past decade.

Gauge-Higgs unification is an attractive idea for the origin of electroweak symmetry breaking in the context of extra dimensions. The basic idea is to identify the extra-dimensional components of the gauge field as the four-dimensional Higgs fields that break electroweak symmetry. This class of models has a theoretical advantage for the gauge hierarchy problem. The Higgs mass is protected against radiative correction by the higher dimensional gauge symmetry, and thus is insensitive to the ultra-violet cut-off scale of the models. Furthermore, these models provide interesting predictions for some masses and coupling constants in the four-dimensional effective theory because various quantities are related to each other due to the higher

dimensional gauge symmetry.

In spite of these virtues, the gauge-Higgs unification scenario on a flat geometry has some phenomenological problems. It predicts a Higgs particle which is too light, typically one order of magnitude lighter than the  $W$  boson, and the  $WWZ$  coupling may deviate significantly from that in the standard model. One way out of these problems is to consider this scenario in the Randall-Sundrum spacetime,<sup>1)</sup> which is a solution of the five-dimensional Einstein equation<sup>3)</sup> and is regarded as a slice of the five-dimensional anti-de Sitter space. Due to the warping geometry along the fifth dimension, it can explain the exponentially large hierarchy between the Planck and electroweak scales. Furthermore, the hierarchical pattern of the fermion masses can easily be realized in this spacetime by varying five-dimensional masses for fermions in an order one range compared to the five-dimensional Planck scale, which is the fundamental scale of the model. In our previous work,<sup>1,2)</sup> we have studied various coupling constants in the gauge-Higgs sector and pointed out that they can be deviated from the counterparts in the standard model.

In the present work, we construct an explicit model based on an  $SO(5) \times U(1)$  gauge theory in the Randall-Sundrum spacetime, focusing on the matter sector. The presence of fermions is vital to have electroweak symmetry breaking. The fermion content triggers electroweak symmetry breaking by quantum effects. Our model realizes observed matter content without any exotic light particles, and thus is a realistic model. One important prediction of this model is that the  $WWH$ - and the  $ZZH$ -couplings ( $H$  stands for the Higgs boson) vanish at the vacuum, which significantly affects Higgs production in collider experiments. This work leads to better understanding of the structure of gauge-Higgs unification models consistent with current experimental results.

## References

- 1) Y. Hosotani, S. Noda, Y. Sakamura and S. Shimasaki: Phys. Rev. D73, 096006 (2006).
- 2) Y. Sakamura and Y. Hosotani: Phys. Lett. B645, 442 (2007).
- 3) L. Randall and R. Sundrum: Phys. Rev. Lett. 83, 4690 (1999).

<sup>†</sup> Condensed from the article in Phys. Rev. D78, 096002 (2008)

<sup>\*1</sup> Department of Physics, Osaka University

# Vacuum energy of two-dimensional $\mathcal{N} = (2, 2)$ super Yang-Mills theory

I. Kanamori

[supersymmetry, spontaneous breaking, lattice simulation]

Numerical simulation on the basis of lattice formulation provides a very powerful tool for non-perturbative study of field theory. On the other hand, lattice formulation of supersymmetric systems is essentially difficult and thus its numerical simulation was regarded difficult as well. In a recent work<sup>1)</sup>, however, we successfully realized numerical simulation of a two-dimensional supersymmetric gauge theory,  $\mathcal{N} = (2, 2)$  super Yang-Mills theory. This report is based on one of its applications<sup>2)</sup>. Among non-perturbative phenomena in supersymmetric systems, one of the most important things is the spontaneous supersymmetry (SUSY) breaking. SUSY is not realized in the current universe and must be spontaneously broken if it is a relevant symmetry in nature. However, it is known that spontaneous SUSY breakings occur only non-perturbatively unless broken in a tree level. Therefore, non-perturbative analysis by simulation can be a powerful tool for spontaneous SUSY breaking.

In this report, we measure the vacuum energy density  $\mathcal{E}_0$ , which is an order parameter for SUSY breaking. We use the expectation value of the Hamiltonian density  $\mathcal{H}$  to measure  $\mathcal{E}_0$ <sup>3,4)</sup>. There are two important points in this procedure. The first one is that we must correctly choose the origin of  $\mathcal{H}$ . As a result of SUSY algebra,  $\mathcal{E}_0$  is zero if and only if SUSY is unbroken so we use the algebra to define  $\mathcal{H}$  as well. The second point is that we use the thermal boundary condition and take a zero temperature limit afterwards. The temperature can be regarded as an external field conjugate to  $\mathcal{H}$ .

The simulation was performed on RIKEN Super Combined Cluster (RSCC). We use Rational Hybrid Monte Carlo (RHMC) algorithm to generate the configurations<sup>5)</sup>. The complex phase of the Pfaffian of the lattice Dirac operator, which is neglected in the RHMC, is included as a reweighting factor in the measurement.

As shown in the previous work<sup>1)</sup>, we need to add a scalar mass term to the original lattice action in order to suppress fluctuations along the flat direction of the potential. We thus define the system by an extrapolation of  $\mu^2 \rightarrow 0$  after taking the continuum limit, where  $\mu$  is the scalar mass. In the extrapolation of  $\mu^2 \rightarrow 0$  we use a linear function of  $\mu^2$ , which fits very well to the data (Fig. 1). Although we use a lattice action with the scalar mass term to generate the configurations, we do not include the mass term to  $\mathcal{H}$ . In taking the continuum limit, we use 3–6 different lattice spacings. Since the gauge coupling  $g$  is dimensionful, we define

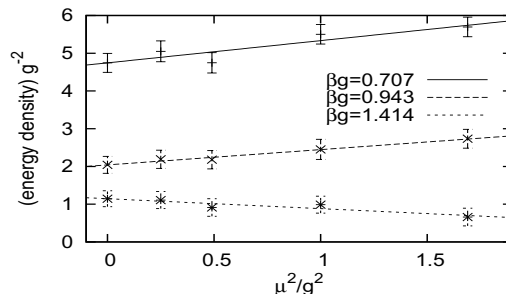
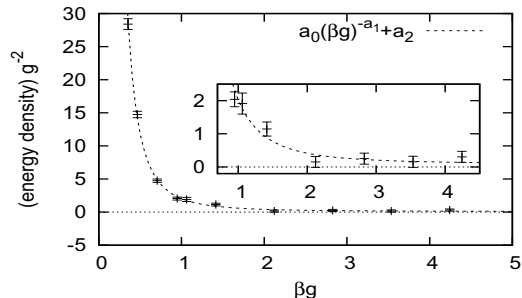


Fig. 1. Example of massless extrapolation.

Fig. 2. Energy density as a function of the inverse temperature  $\beta$ .

the continuum limit as the bare dimensionless coupling  $ag$  goes to 0, where  $a$  is the lattice spacing. The lattice is isotropic and the temperature is controlled through changing temporal lattice size.

In Fig. 2, we plot the temperature dependence of the energy density, after extrapolating the scalar mass to zero. By fitting by a power function of  $\beta$ , we obtain  $\mathcal{E}_0 = 0.09^{+10}_{-8} g^2$  as a value at  $\beta \rightarrow \infty$ , where errors denote statistical ones only. The obtained value is small compared with the typical scale of the system, and consistent with zero within the error. Although we cannot exclude a possibility of small non-zero vacuum energy, it seems to be consistent with no spontaneous SUSY breaking in this system. The full details including an analysis of the systematic errors will be presented in a forthcoming paper<sup>2)</sup>.

## References

- 1) I. Kanamori and H. Suzuki: Nucl. Phys. B **811** (2009) 420 [arXiv:0809.2856 [hep-lat]].
- 2) I. Kanamori: arXiv:0902.2876 [hep-lat].
- 3) I. Kanamori, H. Suzuki and F. Sugino: Phys. Rev. D **77** (2008) 091502 [arXiv:0711.2099 [hep-lat]].
- 4) I. Kanamori, F. Sugino and H. Suzuki, Prog. Theo. Phys. **119** (2008) 797 [arXiv:0711.2132 [hep-lat]].
- 5) I. Kanamori: PoS LATTICE2008 (2008) 232 [arXiv:0809.0655 [hep-lat]].

# Restoration of supersymmetry on the lattice: Two-dimensional $\mathcal{N} = (2, 2)$ supersymmetric Yang-Mills theory<sup>†</sup>

I. Kanamori and H. Suzuki

[supersymmetry, lattice gauge theory, Monte Carlo simulation]

It is widely believed that supersymmetry (SUSY) is an essential ingredient in particle physics beyond the Standard Model. Nonperturbative study of SUSY gauge theories from first principles is thus of great interest but it has always been elusive because the lattice formulation—only nonperturbative framework of gauge theories available to date—is irreconcilable with SUSY. Lattice structure explicitly breaks SUSY and one must generally fine-tune coefficients of relevant and marginal operators so that SUSY is recovered in the continuum limit. Such an intricate program is difficult to carry out practically within limited computational resources.

Given this situation, recently, for two- and three-dimensional extended SUSY gauge theories, lattice formulations that require no or a little fine tuning have been proposed. See Ref. 1) for a review. In these formulations, at least one fermionic symmetry that is a part of the full SUSY is manifested. This exact symmetry, combined with other lattice symmetries, (almost) prohibits relevant and marginal operators which break SUSY and other continuum symmetries. SUSY is then expected to automatically restored without or with a little fine tuning.

In the present study, we succeeded in numerically observing the restoration of SUSY in lattice formulation of the two-dimensional  $\mathcal{N} = (2, 2)$   $SU(2)$  SUSY Yang-Mills theory (SYM), proposed by Sugino.<sup>2)</sup> To our knowledge, this is the first demonstration of the SUSY restoration in lattice gauge theory.

As elucidated in the original paper, for some technical reasons, we need to introduce mass for the scalar fields that explicitly breaks SUSY. We also needed to adopt the thermal boundary condition that also explicitly breaks SUSY. With the present lattice setting, therefore, there are four possible sources for the SUSY breaking. That is, i) the scalar mass, ii) the thermal boundary condition, iii) the spontaneous SUSY breaking and iv) the lattice regularization itself. Among these, first three possess physical meaning but the last effect is unphysical and should be eliminated. In this paper, we will discuss if the last unphysical effect disappears in the continuum limit or not upon the restoration of SUSY.

Generic correlation functions are affected by the four breaking effects in a mixed manner. Can we then isolate or separate the last effect? For this, we should observe the SUSY Ward-Takahashi identities in the

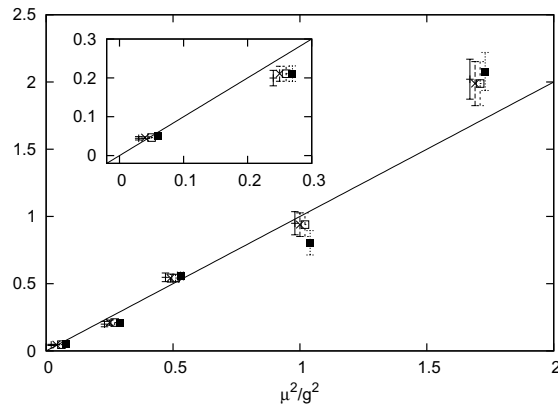


Fig. 1. The left-hand side of Eq. (1) as a function of the scalar mass squared  $\mu^2/g^2$ . Symbols: + for  $i = 1$ ,  $\times$  for  $i = 2$ ,  $\square$  for  $i = 3$  and  $\blacksquare$  for  $i = 4$ .

form of the partial conservation of the supercurrent (“PCSC” relation):

$$\frac{\partial_\mu \langle (s_\mu)_i(x)(f_0)_i(0) \rangle}{\langle (f)_i(x)(f_0)_i(0) \rangle} = \frac{\mu^2}{g^2}, \quad \text{for } x \neq 0. \quad (1)$$

In this expression,  $s_\mu$  is the supercurrent and  $f$  is a certain fermionic operator associated with the SUSY breaking scalar mass term.  $f_0$  is an arbitrary gauge invariant fermionic operator and we used a lowest dimensional one.  $\mu^2/g^2$  is the scalar mass squared. The spinor index  $i$  runs over 1, 2, 3 and 4. This relation explicitly incorporates the effect on the scalar mass, and holds independently of the boundary condition and the spontaneous SUSY breaking. This relation, however, does not hold if the regularization breaks SUSY and thus isolates the unphysical effect.

The plot in Fig. 1, that was obtained by the extrapolation of Monte Carlo data to continuum, beautifully shows that relation (1) certainly holds in the continuum limit. This result strongly indicates that the full SUSY is restored in the continuum limit and the target continuum theory (i.e., the two-dimensional  $\mathcal{N} = (2, 2)$   $SU(2)$  SYM with a soft SUSY breaking mass term) is realized as the continuum limit of the present lattice model.

## References

- 1) J. Giedt: PoS **LAT2006**, 008 (2006).
- 2) F. Sugino: J. High Energy Phys. **03**, 067 (2004).

<sup>†</sup> Condensed from the article in Nucl. Phys. B **811**, 420 (2009)

# Some physics of the two-dimensional $\mathcal{N} = (2, 2)$ supersymmetric Yang-Mills theory: A lattice Monte Carlo study<sup>†</sup>

I. Kanamori and H. Suzuki

[supersymmetry, lattice gauge theory, Monte Carlo simulation]

As reported elsewhere,<sup>1)</sup> we have obtained affirmative numerical evidence that the two-dimensional  $\mathcal{N} = (2, 2)$   $SU(2)$  supersymmetric Yang-Mills theory with a scalar mass term is realized as the continuum limit of a lattice model of Ref. 2). This result suggests the completely new possibility that the physical properties of a supersymmetric gauge theory (with a soft supersymmetry (SUSY) breaking mass) can numerically be studied. The aim of the present study is to illustrate this possibility.

As explored in Ref. 4), the correlation function between the  $U(1)_V$  current and the  $U(1)_A$  current in the present target theory in  $\mathbb{R}^2$  is expected to exhibit power-like behavior. This implies that there exists a massless bosonic state and that there is no mass gap. As Fig. 1 shows, our Monte Carlo results reproduce this power-like behavior fairly well for  $x_0 g \lesssim 1$ . (The blow-up at  $x_0 g \gtrsim 1$  is a reflection of the fact that our lattice is an approximation of a finite torus and not of  $\mathbb{R}^2$ .)

When the SUSY breaking scalar mass is small, we should have an approximately massless fermionic state corresponding to the above massless bosonic state, assuming that the spontaneous SUSY breaking does not occur. A SUSY Ward-Takahashi identity shows in

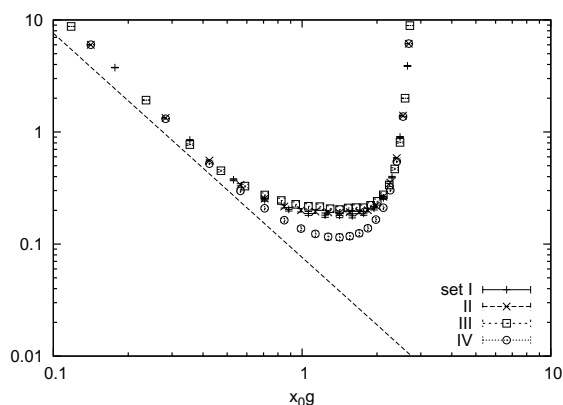


Fig. 1. Correlation function between  $U(1)_V$  current and  $U(1)_A$  current along the line  $x_1 = 0$  as a function of the coordinate  $x_0$ . For parameters in each configuration set, see Ref. 3). Broken line is the theoretical prediction for  $\mathbb{R}^2$ .<sup>3)</sup>

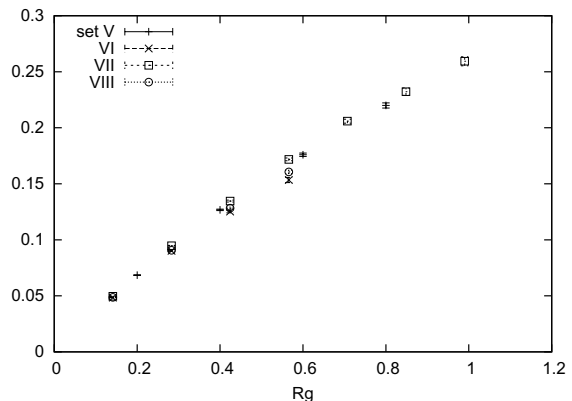


Fig. 2. Static potential energy  $V(R)/g$  between probe charges in the fundamental representation of  $SU(2)$ . For parameters in each configuration set, see Ref. 3.

which correlation function such a fermionic state appears in as an intermediate state. Our Monte Carlo results confirmed this reasoning on the basis of (approximate) SUSY fairly well.

Armoni, Frishman and Sonnenschein<sup>4)</sup> theoretically conjectured that a probe charge in the fundamental representation is screened in two-dimensional gauge theories containing a massless adjoint fermion. Our present target theory fulfills this criterion and thus it is of interest to observe the static potential between probe charges in the fundamental representation. Fig. 2 shows our result, obtained by a linear fit  $\ln\{W(R, T)\} = V(R)T + c(R)$  of the expectation value of the Wilson loop  $W(T, R)$  of size  $T \times R$ . Our result indicates that at least for  $Rg \lesssim 1$  the static potential increases almost linearly. This confining behavior appears distinct from the above conjecture, according to which the static potential asymptotically approaches a constant. We have to systematically explore, however, the static potential for  $Rg \gtrsim 1$  to determine the real asymptotic behavior.

## References

- 1) I. Kanamori and H. Suzuki, in this Report.
- 2) F. Sugino: *J. High Energy Phys.* **03**, 067 (2004).
- 3) H. Fukaya, I. Kanamori, H. Suzuki, M. Hayakawa and T. Takimi: *Prog. Theor. Phys.* **116**, 1117 (2007).
- 4) A. Armoni, Y. Frishman and J. Sonnenschein: *Phys. Lett.* **B 449**, 76 (1999).

<sup>†</sup> Condensed from *Phys. Lett. B* **672**, 307 (2009).

## **6. Development of Accelerator Facility**

Acceleration Tests of  $^{238}\text{U}$  and  $^{48}\text{Ca}$  in RIBF

Nobuhisa Fukunishi, Masaki Fujimaki, Akira Goto, Hiroo Hasebe, Yoshihide Higurashi, Eiji Ikezawa, Tadashi Kageyama, Masayuki Kase, Masanori Kidera, Misaki Komiyama, Makoto Nagase, Hironori Kuboki, Keiko Kumagai, Takeshi Maie, Takahide Nakagawa, Jun-ichi Ohnishi, Hiroki Okuno, Naruhiko Sakamoto, Kenji Suda, Hiroshi Watanabe, Tamaki Watanabe, Kazunari Yamada, Shigeru Yokouchi and Osamu Kamigaito

Beam acceleration tests performed in the period from April 2008 to December 2008 are summarized in Table 1. The major purpose of the tests in the stand-alone mode of the RIKEN heavy-ion linac (RILAC)<sup>1)</sup> is to investigate the lifetime of carbon foil strippers placed below RILAC. The tests indicate that the carbon foil lifetime is long enough for  $^{48}\text{Ca}$  with the maximum beam intensity extracted from the 18-GHz ECR ion source<sup>2)</sup>, which corresponds to 500 pA after extraction from the Superconducting Ring Cyclotron (SRC)<sup>3)</sup>. On the other hand, the lifetime is less than 6 hours for Kr and heavier ions with the maximum intensity of the ion source. Details of the carbon foil tests are summarized by Hasebe et al.<sup>4)</sup> in this report. The  $^{48}\text{Ca}$  test started on May 27<sup>th</sup> aiming to evaluate the beam intensity of the  $^{48}\text{Ca}$  beam. We successfully extracted 270 pA of  $^{48}\text{Ca}$  beam from the Intermediate-stage Ring Cyclotron (IRC)<sup>5)</sup> under the use of a beam attenuator which reduces the beam intensity by a factor of 1.8. According to the result, a beam service time of  $^{48}\text{C}$  beam was scheduled in December 2008.

Table 1 Summary of beam acceleration tests. The periods shown with the asterisk include beam service times, 18 days for  $^{238}\text{U}$  and 11 days for  $^{48}\text{C}$ , respectively.

Period	Particle	Accelerator used
4/08 – 5/02	$^{238}\text{U}$	RILAC to IRC
5/17 – 5/23	$^{86}\text{Kr}$	RILAC only
5/27 – 6/09	$^{48}\text{Ca}$	RILAC to IRC
6/26 – 7/10	$^{238}\text{U}$	RILAC to IRC
7/18 – 7/28	$^{136}\text{Xe}$	RILAC only
10/25 – 11/26*	$^{238}\text{U}$	RILAC to SRC
11/27 – 12/22*	$^{48}\text{Ca}$	RILAC to SRC

The uranium acceleration tests up to the IRC were performed to improve the transmission efficiency. The transmission efficiency of the whole accelerator complex of RIBF was limited to 2%, where charge stripping efficiencies are excluded<sup>6)</sup>. We investigated reasons for the poor transmission efficiency and made various improvements in this year. The essential points are as follows. First, we upgraded the vacuum system of RILAC and its low-energy beam transport system to avoid beam losses caused by electron capture reaction with residual gases<sup>7)</sup>. Secondly, the main differential probes of the fixed-frequency Ring Cyclotron (fRC)<sup>8)</sup> and the SRC were modified<sup>9)</sup>. The main differential probes measure turn patterns of the beams accelerated by our cyclotrons. Utilizing the fact that the turn pattern is very sensitive to the beam quality, we select appropriate voltages and phases of RF fields generated by the main and flattop cavities

installed in the cyclotrons. However, the secondary electrons emitted by uranium-ion bombardments and leakage RF fields from flattop cavities made it difficult to measure turn patterns precisely. These problems were solved just before the  $^{48}\text{Ca}$  test started on November 27<sup>th</sup>. One of the other remaining problems is that the energy spread of the uranium beams injected into the fRC exceeds what is acceptable. It is a result of the poor uniformities of the stripper foils used before the fRC acceleration. We tested various kinds of stripper foils in the tests. However, great progress was not made in this problem.

Hereafter, we will proceed to the acceleration tests using the whole RIBF accelerator complex. The transmission efficiencies of  $^{238}\text{U}$  and  $^{48}\text{Ca}$  beams are summarized in Table 2 compared with that of  $^{238}\text{U}$  in the previous year. Note that beam intensity monitors (Faraday cups and radial probes of the cyclotrons) include sizable errors (~20%), which is the reason why the transmission efficiencies in some sections in Table 2 exceed 100%. The transmission efficiency of the uranium beam was greatly improved as a result of the improvements mentioned above. The maximum intensity of the uranium beam delivered to the users was 0.4 pA. In addition, single turn extractions from all the cyclotrons, except for the SRC, were also established. On the other hand, tuning of the SRC was not satisfactory and the transmission efficiency was 66%. It is a consequence of the low quality nature of the uranium beam and of poor tuning of flat-topping RF fields.

Table 2. Transmission efficiencies obtained in the acceleration tests. The RIBF accelerator complex is divided into the sections shown in the table.

Section	$^{48}\text{Ca}$ (08/12/21)	$^{238}\text{U}$ (08/11/16)	$^{238}\text{U}$ (07/07/03)
IS - RILAC	55	40	29
RILAC - RRC		87	86
RRC	95	86	
RRC - fRC		101	41
fRC		87	88
fRC - IRC			75
RRC - IRC	106		
IRC	93	86	67
IRC - SRC	88	104	72
SRC	82	66	63
Total	37	16	2

The transmission efficiency of  $^{48}\text{Ca}$  was within the acceptable level to deliver 200-pA beams to users. The

reason for the relatively low transmission efficiency of SRC (82%) was that one of the accelerating cavities broke down during the test and the acceleration voltage was limited to be 75% of the design value.

Detailed analyses of the acceleration tests are in progress for better performance of our accelerator complex. Using the data obtained by beam profile monitors (wire monitor) installed in the beam transport lines, we can determine parameters of beam matrices ( $\sigma$ -matrix) which are relevant to estimating emittances of beams under the assumption that ions obey Gaussian distributions with elliptical shapes. Figure 1 is an example of the least-square fitting of beam widths measured by the profile monitors for the  $^{48}\text{Ca}$  beam.

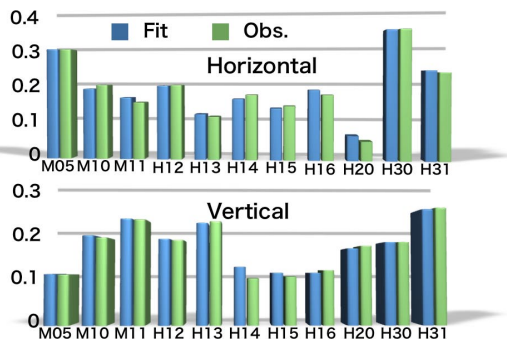


Fig. 1 Root-mean-square beam widths (cm) of the  $^{48}\text{Ca}$  beam (08/12/21) observed in the beam transport line from the second charge stripper to the IRC are shown compared with the fitting results based on  $\sigma$ -matrix analysis.

Similar analyses were done for other cases and the emittances estimated are summarized in Table 3. Note that the horizontal emittances were poorly determined compared with the vertical ones because correlation to the longitudinal motion under the presence of dipole magnets was not clearly separated due to lack of information. In that sense, the present analyses contain ambiguities, but are still useful.

Table 3 Emittances estimated by  $\sigma$ -matrix analyses. The emittance definition here is  $4\sigma$  emittance. The unit is  $\pi$  mm\*mrad. The abbreviations H and V stand for the horizontal and vertical direction, respectively. The horizontal emittance of  $^{48}\text{Ca}$  in the SRC-injection beam line was too sensitive to errors in the measurement.

	$^{238}\text{U}$ (08/11/07)		$^{48}\text{Ca}$ (08/12/21)	
	H	V	H	V
fRC injection	5.0	2.6	/	/
IRC injection	5 ~ 6	2.1	2.3	2.2
SRC injection	4	1.4	1.2 ~	1.7

For example, remarkable emittance growths in the horizontal direction are indicated in the case of uranium beam acceleration. The observed emittance growth of the fRC-injected beam originates from the mixing of the large longitudinal emittance into the horizontal one because the rebuncher<sup>10)</sup> between RIKEN Ring Cyclotron (RRC) and

the fRC is placed in a dispersive area. The uniformities of carbon foil strippers just after RRC acceleration are poor, which result in a large momentum spread. Hence, we plan to use thinner stripper foils and accelerate 69+ ions instead of 71+ with small modifications of the fRC. Furthermore, the matching conditions on dispersion were not precisely fulfilled for both the fRC and the IRC, which resulted in additional emittance growths. The emittances of the  $^{48}\text{Ca}$  beam were within what is acceptable.

Another example of the analyses is on turn patterns of the cyclotrons. Figure 2 shows a result of the  $^{238}\text{U}$  beam accelerated by the IRC. Close inspection of the turn pattern helps us to reduce ambiguities in determining the horizontal emittance that is not clearly separated from the longitudinal one within the  $\sigma$ -matrix analyses. The horizontal emittances listed in Table 3 were determined with the help of the present turn-pattern analyses.

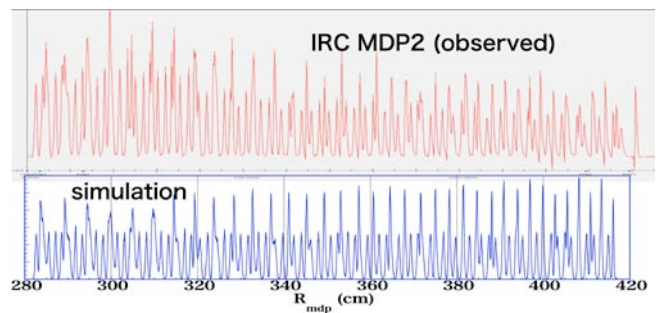


Fig. 2 IRC turn pattern of the  $^{238}\text{U}$  beam (08/11/26) compared with a numerical simulation.

As a summary, the transmission efficiency of uranium beam acceleration was greatly improved and the  $^{48}\text{Ca}$  beam with the maximum intensity of 170 pA was successfully extracted from the SRC. The fact that beam losses in the beam transport lines are well suppressed enables us to carry our detailed analyses on the beam dynamic aspect of RIBF, which revealed several problems that need to be solved. We plan to fix these problems in the next fiscal year.

#### References

- (1) M. Odera et al.: Nucl. Instrum. Methods **A227**, 187 (1984).
- (2) T. Nakagawa et al.: Nucl. Instrum. Methods **B 226**, 392 (2004).
- (3) H. Okuno et al.: Proc. 17<sup>th</sup> Int. Conf. On Cyclotrons and Their Applications, 373 (2004).
- (4) H. Hasebe et al.: in this progress report.
- (5) J. Ohnishi et al.: Proc. 17<sup>th</sup> Int. Conf. On Cyclotrons and Their Applications, 197 (2004).
- (6) N. Fukunishi et al.: RIKEN Accel. Prog. Rep. 41, ??? (2008).
- (7) S. Yokouchi et al.: in this progress report.
- (8) T. Mitsumoto et al.: Proc. 17<sup>th</sup> Int. Conf. On Cyclotrons and Their Applications, 384 (2004).
- (9) K. Yamada et al.: in this progress report.
- (10) T. Aoki et al.: Nucl. Instr. and Meth. **A 592**, 171 (2008).

## Construction of the MEBT (Middle-Energy Beam Transport) line for new 28GHz Superconducting ECR Ion Source (SC-ECRIS)<sup>†</sup>

Y. Watanabe, E. Ikezawa, Y. Sato, H. Okuno, T. Nakagawa, Y. Higurashi,  
J. Ohnishi, M. Fujimaki, N. Fukunishi, M. Kase, A. Goto and O. Kamigaito

The beam intensity of heavy ion must be increased for the RIBF project. J. Ohnishi, T. Nakagawa et al.<sup>1-2)</sup> started to construct a new superconducting ECR ion source (SC-ECRIS) with an operational frequency of 28 GHz in 2007. The superconducting coils were installed in the high voltage terminal at the end of 2008. All devices will be installed by the end of March 2009.

A Middle-Energy Beam Transport (MEBT) line is being constructed for the new 28 GHz Superconducting ECR Ion Source (28GHz SC-ECRIS).<sup>3-4)</sup> Figure 1 shows the schematic layout of the MEBT line for the 28 GHz SC-ECRIS. This beam line partly shares the existing beam line from the 18 GHz SC-ECR ion source. These magnets and the 1f-buncher/rebuncher are installed at the optimal positions of the minimum beam spots. The bending magnets (BM), quadrapole magnets (QM; DQ, TQ), steering magnets (ST), chambers, gate valves (GV), buncher and ducts used in this plan are as follows:

(1) BM; BM1, BM2 [used an injection line for the old

500 kV high voltage terminal]

(2) QM; QT011abc [from the CNS], QD012ab-022ab [from the RRC- CNS line], QDN2-1,2 [existing line]

(3) ST; SH012/SV012, SH013/SV013 [used an injection line for the old 500 kV high voltage terminal], SH03/SV03 [existing line]

(4) Chambers; Chamber011 [from the IRC line (H12a), Aluminum], Chamber012, 014 and 022 [New, Aluminum], Chamber013 and 021 [New, for CRP, stainless steel], Chamber 031 and 032 [existing line]

(5) GV; GV-011, 014 and 022 [New], GV-030, 031 [existing line]

(6) Buncher; Buncher [Modified, used an injection line for old 500kV high voltage terminal], Rebuncher [existing line]

(7) Ducts; Aluminum-Duct 10 [New, from the acceleration tube to the rebuncher], Stainless steel-duct 1 [New, from the RFQ to the rebuncher]

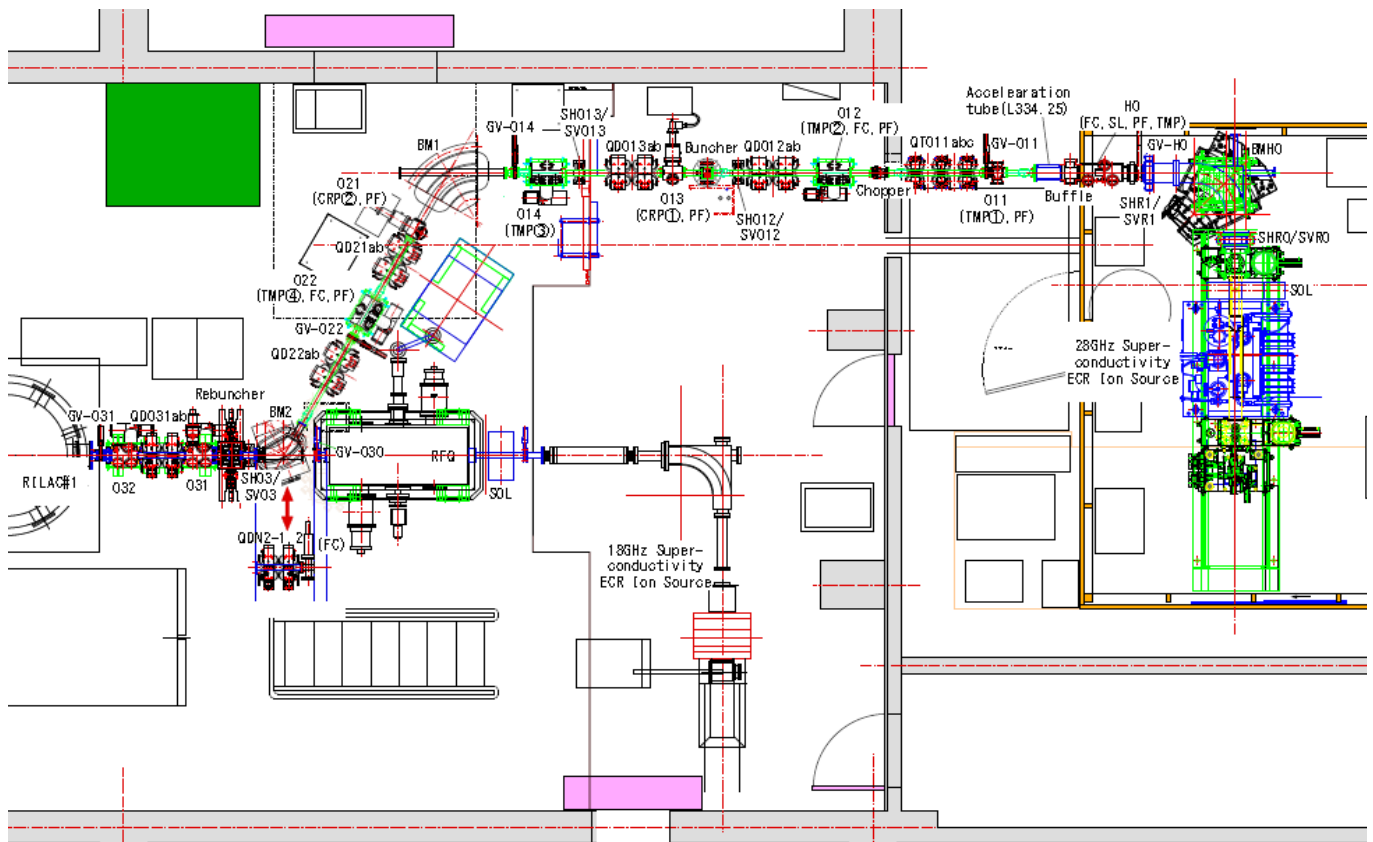


Fig. 1. Schematic layout of MEBT line.

Some new bases will be constructed for the installation of these devices (QT011abc, QD012ab-022ab, QDN2-1,2, SH//SV012, 013,03, Chamber011, 013, 021, Buncher and Rebuncher). We are also planning some arrangement and works before the construction of this line as follows:

- (1) Reinforcement of floor around BM1
- (2) Conveyance of SC-ECR ion source and its base
- (3) Arrangement of existing devices (Some operation control panels, power amplifier)
- (4) Removal of the DQ from the RRC-CNS line and installation in the MEBT line.

The following are notes and points on the design of the MEBT line:

- (1) Switching between the MEBT line and existing line is done simply by changing BM2 for the MEBT line and QDN2-1,2 for the existing line as shown in Figure 2.
- (2) The devices, ducts and bases between the RFQ and RILAC #1 for the existing line are used as much as possible and this reduces construction of new devices, ducts, and bases.

The MEBT line will finally be installed as shown in Figure 1. We are preparing for two newly constructed chambers and bases. The main outline of the future plan is as follows:

- ~ Feb. 2009, Final decision on the line arrangement
- ~ May. 2009, Some arrangement and work before construction of the line
- April ~ June 2009, Construction of the MEBT (Including cooling water, compressed air, cables and power supply)
- July 2009~, Beam test and machine study

#### References

- 1) J. Ohnishi, T. Nakagawa et al.: RIKEN Accel. Prog. Rep. 41, 86-87 (2007)
- 2) T. Nakagawa et al.: in this report.
- 3) Y. Sato, Y. Higurashi et al.: RIKEN Accel. Prog. Rep. 41, 88-89 (2007)
- 4) Y. Sato et al.: in this report.

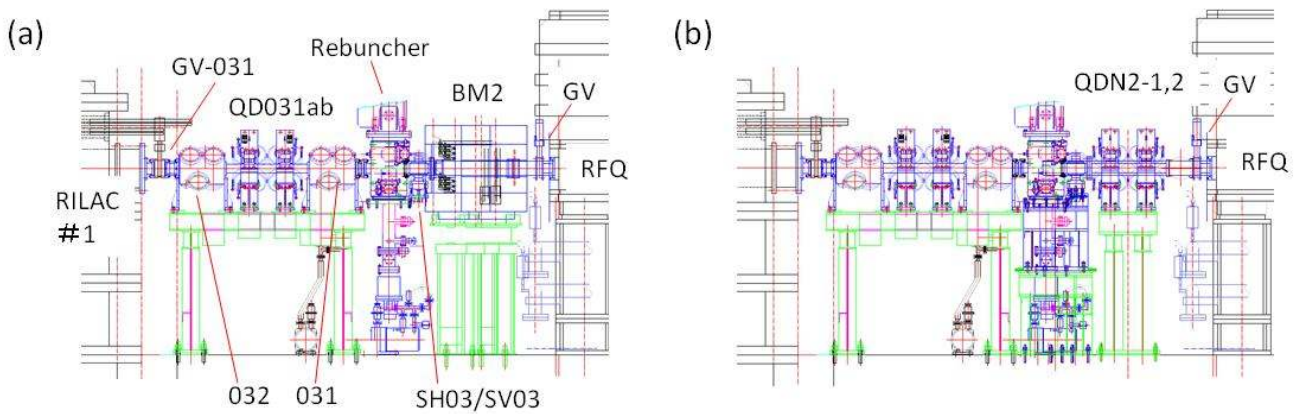


Fig. 2. Schematic layout from the RFQ to the RILAC #1. (a) MEBT line (b) Existing line.

## New beam line for the AVF-RRC-SRC acceleration

K. Kumagai, N. Fukunishi, T. Maie, S. Fukuzawa\*, Y. Watanabe, and M. Kase

Light ions accelerated in the AVF-RRC mode can be injected to the SRC directly because the injection radius of the SRC, 3.56 m, is the same as the extraction radius of the RRC. On the other hand, these beams cannot be accelerated in the IRC because the RRC needs to operate with a harmonic of five. In this AVF-RRC-SRC mode, the ions from deuteron to aluminum approximately can be accelerated to the maximum energy of 400 MeV per nucleon. In addition, the beams from the polarized ion source at the AVF are accelerated in the SRC.

To realize the acceleration mode, a new beam line was constructed to bypass the IRC. A schematic of this beam line is shown in Fig. 1. The beam line is from the DMH6 dipole to the DMG2. The DMH6 dipole was installed to diverge from the IRC injection beam line and two quadrupoles were moved down stream from the original positions. Part of this beam line will be used in the future to return the beams accelerated in the IRC to the experiment rooms in the Nishina building.

The beam line uses two horizontal and two vertical dipoles of 2.7 meters in radius, twenty quadrupoles and six sets of steering magnets that have both horizontal and vertical functions. The parameters of these magnets are listed in Table 1. Electric power cables for nine of the twenty quadrupoles were extended from the position of the quadrupoles on the injection and extraction beam lines of the IRC that are not used simultaneously. As a result, the power

supplies can be shared and it is economical for both equipment and cabling. Though the original magnetic field rigidity of the DMM1 dipole had been small for this operation mode, it has been increased by replacing the power supply for the previous investigation of the charge stripping of the uranium beam performed.

Figure 2 shows a diagram of the designed beam envelope between the RRC-EDC and the SRC-EIC including the new beam line. An extracted beam from the RRC is matched to be achromatic after the DMM1 dipole magnet. The sections from DMH6 to DMH7 and DMH8 to DMK9 are also designed to be achromatic. The beam transferred into the SRC room is strongly focused at the position of the polarimeter installed after the quadrupole triplet QTG92. The matching condition to the SRC injection was fulfilled using the quadrupole quartette QSG22 – QSG25.

Ten profile monitors, three faraday cups and a scintillation monitor were installed in the beam line as beam diagnostic equipment. Most of these components were transferred from injection and extraction beam lines of the IRC.

The first acceleration test in the AVF-RRC-SRC mode will be scheduled in February 2009. In this test, the new beam line will be commissioned and nitrogen ions with 90 MeV per nucleon extracted from the RRC will be sent to the SRC and accelerated to the energy of 250 MeV per nucleon.

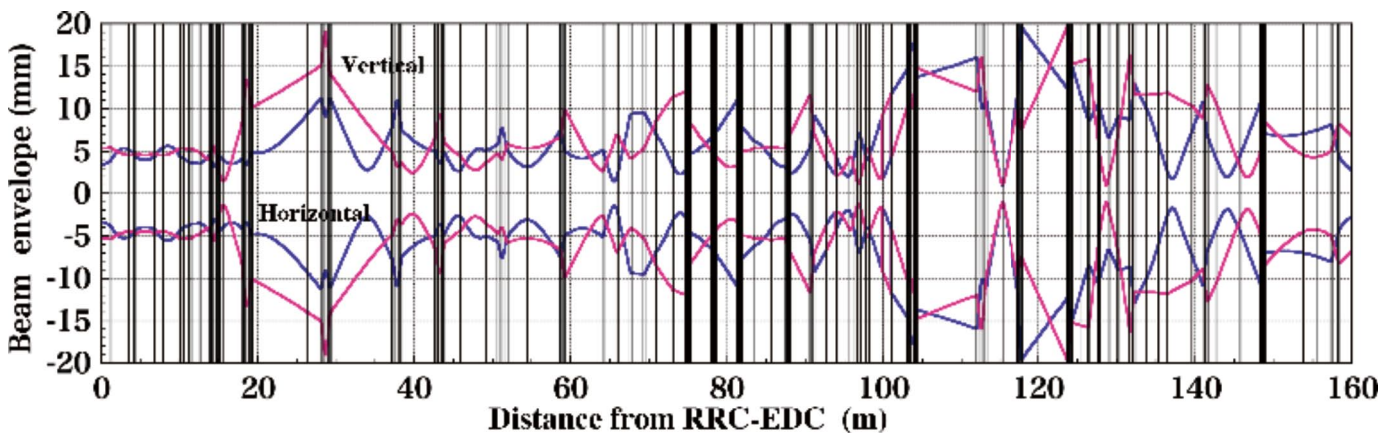


Fig.2. Beam envelope diagram. It shows distances from RRC-EDC until SRC-EIC. New beam lines are indicated from about 71 meters to 123 meters.

	Max fields	Gap, Bore	Core length	Eff. length	Max current	Number
[unit]	[T, T/m]	[mm]	[mm]	[mm]	[A]	
Dipole 45°	1.56 [T]	60	2120.5	2149.7	330	2
Dipole 25°	1.56 [T]	60	1178.1	1206.6	330	2
Quadrupole 220	15 [T/m]	70	220	250	158	15
Quadrupole 420	15 [T/m]	70	420	450	158	5

Table 1. Design parameters of magnets used for new beam line.

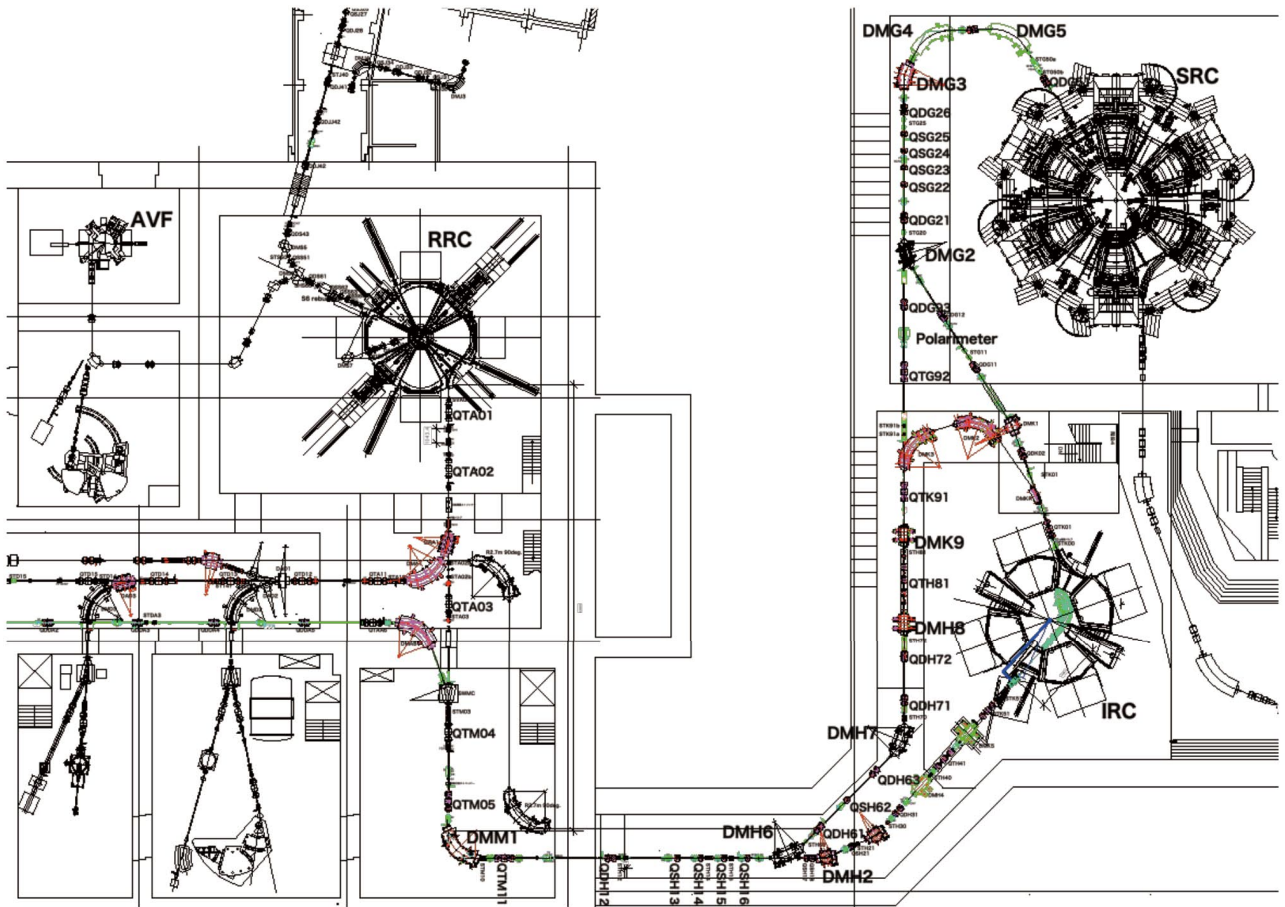


Fig.1. A schematic of beam lines from AVF-RRC to SRC.

\* SHI Accelerator Service, Ltd

## Construction of the IRC-bypass beam transport line†

Y. Watanabe, K. Sekiguchi, H. Suzuki, K. Kumagai, T. Maie, K. Yamada, M. Kase and N. Fukunishi

The new acceleration mode of AVF-RRC-SRC will provide the polarized deuteron beam with energies up to 440 MeV/u as well as light ion beams, e.g. nitrogen. Experiments with this mode are planned for May 2009.<sup>1)</sup>

For these experiments an IRC bypass beam transport line which skips the IRC was newly constructed in FY2008. This beam line partly shares the existing line which will be used for RIPS experiments in the RRC-IRC acceleration mode. Figure 1 shows photographs of the IRC bypass beam transport line after the construction. Figure 2 shows a schematic layout of the IRC bypass beam transport line.

The followings are lists of the beam line elements; dipole magnets (DM), quadrapole magnets (QM; DQ/SQ), steering magnets (ST), chambers, gate valves (GV), beam line polarimeters (Dpol, BigDpol) and ducts.

### 1. IRC-H zone [Fig. 1(a), (b) and Fig. 2]

- (1) DMH6 [New Chamber, a modified yoke],  
DMH7 [renamed DMH8; installed]
- (2) QSH17-18, QDH61-63, QDH71-72  
[installed]
- (3) STH14-15, STH60, STH70, STH72  
[installed]
- (4) Chamber; H16, H60, H61, H70 [New],  
H72 [from the RRC-CNS line],  
H80, H81 [New]
- (5) GV-H61 [New],  
GV-H80 [from the RRC-CNS line]
- (6) Al-Duct; 12 [New]

### 2. IRC-K zone [Fig. 1(b) and Fig. 2]

- (1) DMK9, DMK3 [installed]
- (2) QDK91 [installed]
- (3) STH91ab [from the RRC-CNS line]
- (4) Chamber; K90 [modified],  
K91 [from the RRC-CNS line]
- (5) GV-K91 [from the RRC-CNS line]
- (6) Beam line polarimeter, BigDpol
- (7) Al-Duct; 8 [New]

### 3. SRC-G zone [Fig. 1(c) and Fig. 2]

- (1) QTG92, QDG93 [installed]
- (2) Chamber; G93 [from the RRC-CNS line]
- (3) Beam line Polarimeter, Dpol
- (4) GV-G93 [from the RRC-CNS line]
- (6) Al-Duct; 4 [New]

The beam line polarimeters, Dpol and BigDpol, were installed at positions where beam size becomes small. The Faraday cups (FC) and profile (PF) monitors have been

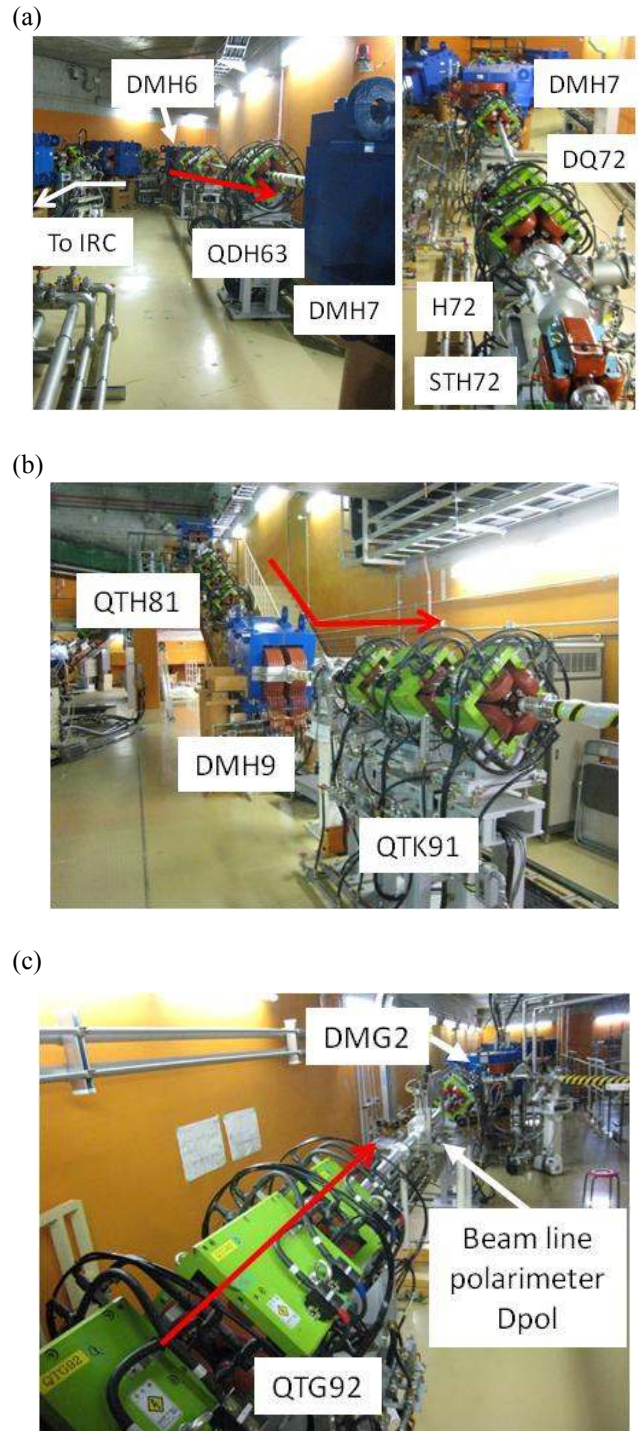


Fig. 1. Photographs of the IRC bypass beam transport line after arrangement. (a) IRC-H zone (b) IRC-H and K zone (c) SRC-G zone.

relocated from the skipped beam line in the IRC and SRC rooms. Because the dipole magnet DMH6 is used in both the IRC line and the IRC bypass beam transport line, we have made the following modifications. The upper yoke was removed and converted, and a chamber with branched flanges was newly constructed. Quadrupole magnets DQ/SQ were disassembled in order to install the Al-ducts. Alignment (Y level, pitching direction and yawing direction) of DM, QS/QD and the chamber was performed with precision of less than 0.1 mm in each straight line section.

Experiments using the new beam line will be performed after acceleration tests. We plan to conduct acceleration tests in AVF-RRC-SRC mode in Feb. 2009 and machine studies in May 2009.

**References**

- 1) K. Sekiguchi et al.: in this report.

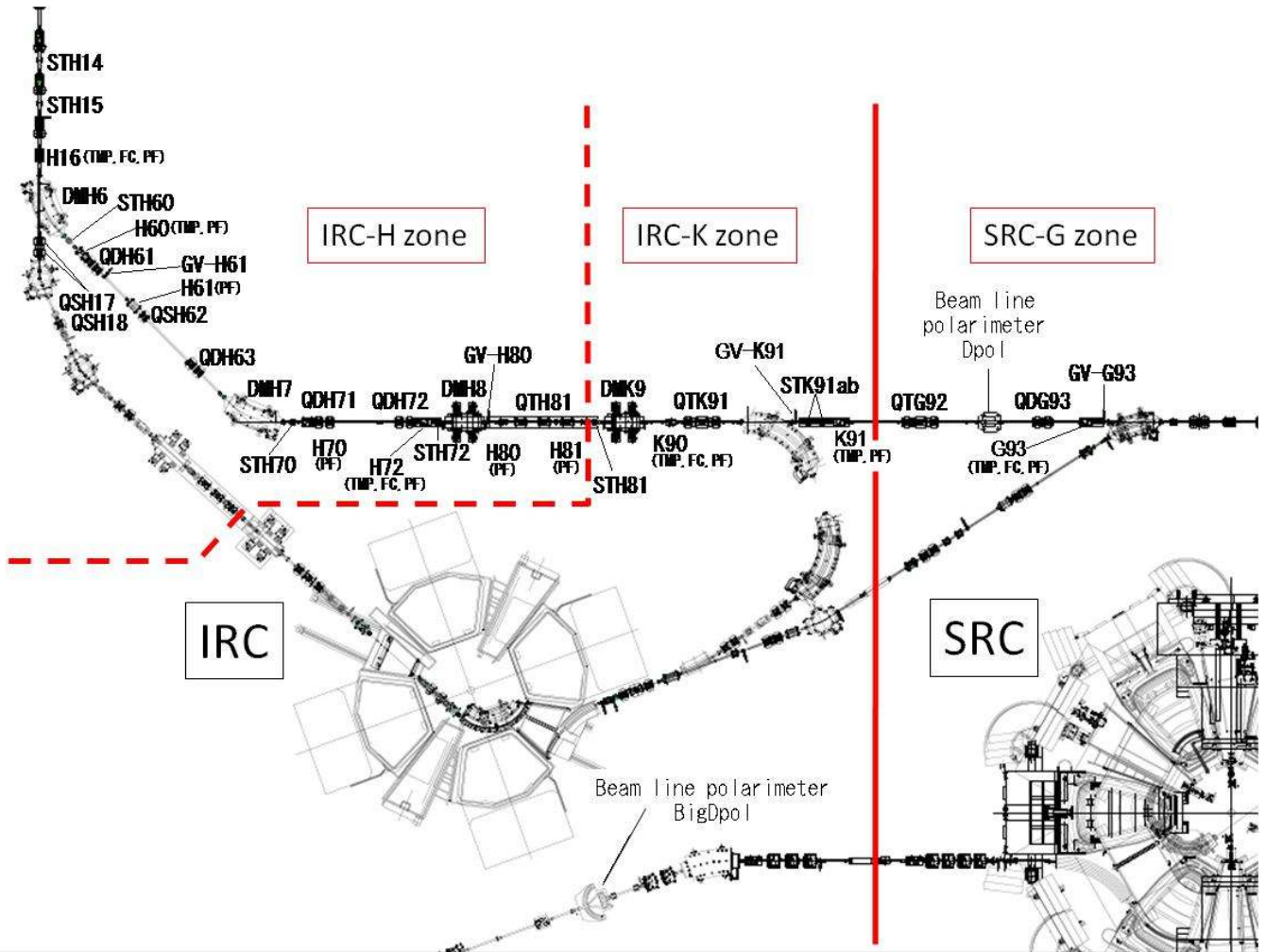


Fig. 2. Schematic layout of IRC bypass beam transport line.

## Refinement of SRC for acceleration of high intensity beam in 2008

K. Yamada, N. Fukunishi, M. Kase, J. Ohnishi, H. Okuno, N. Sakamoto, K. Suda, S. Yokouchi, and O. Kamigaito

The source of the problem in the SRC cryogenic system was found to be the contamination of the lubricant oil from screw compressors passing through the cascade of oil separators.<sup>1)</sup> The oil polluted the entire refrigerator. Consequently, the SRC was shutdown until August 2008 to rinse out the impurity. During the repair of the cryogenic system, various modifications were introduced to the SRC. The re-cooldown of the SRC started in September and the superconducting coils were ready to operate in October. The acceleration of  $^{238}\text{U}$  was performed immediately for the commissioning of the Zero-Degree Spectrometer and following new isotope search in November. Maximum beam intensity of 0.4 pA was achieved, which was ten times higher than the one in 2007. Following that, the first acceleration of  $^{48}\text{Ca}$  for the SRC was performed in December. The modifications and elaborate tuning of accelerators realized the world's most intense  $^{48}\text{Ca}$  beam that reached up to 200 pA on the Faraday cup located at the exit of the SRC. The details of modification and status for the SRC in 2008 are presented as follows.

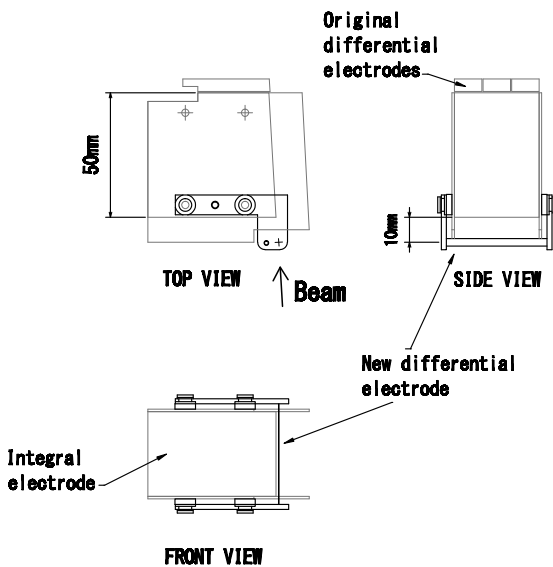


Fig. 1. Head assembly of the main differential probe mounted on SRC.

In order to improve the transmission efficiency of the SRC, a correct adjustment of RF voltage and phase is required, especially for flat-top acceleration cavity (FT). The goal is to observe proper information from the radial beam pattern by using the main differential probe (MDP) because the information gives a criterion

for the adjustment of RF. The radial beam pattern is measured by a differential electrode (the SRC has differential electrodes divided by three) mounted on behind an integral electrode with 0.5 mm overhang. Only the beam reaching the “0.5 mm” is counted at each radius. However, a lot of secondary electrons emitted from the MDP integral electrode had a great influence on the observation and the pattern could not be produced.<sup>2)</sup> In order to overcome the problem, a new differential electrode of 0.3 mm×3 mm tungsten ribbon was attached in front of the integral electrode at intervals of 10 mm as shown in Figure 1.

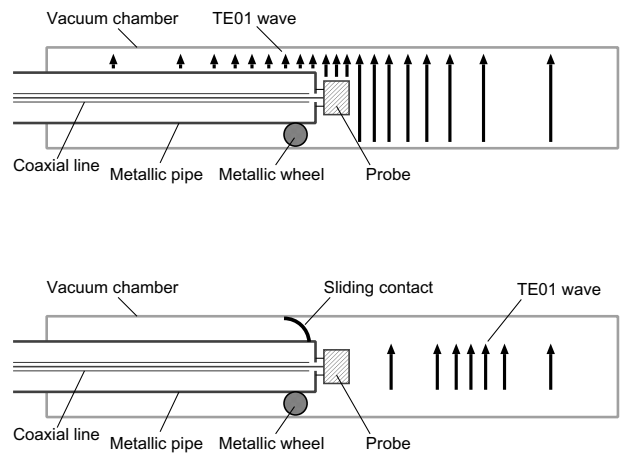


Fig. 2. Effect to disturb the propagation of TE01 microwave.

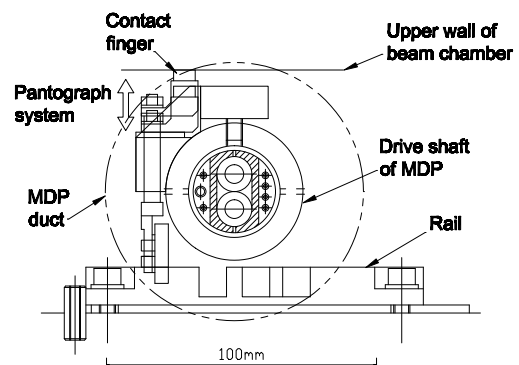


Fig. 3. Cross sectional view of the pantograph system for sliding contact.

Another problem we had in the MDP was that the beam signal was disturbed by the electromagnetic radiation from the FT resonator: the rf frequency is high enough for the electromagnetic wave to travel through the vacuum chamber. A schematic drawing of the

MDP in the chamber is shown in Figure 2. The driving shaft of the MDP is grounded by the metallic wheel on the chamber in the original configuration. Since the electromagnetic wave is TE01 mode, this asymmetric configuration allows the electric field to penetrate into the narrow gap between the shaft and the chamber, which induces the electric charge in the head of the probe. Therefore, we put an electric contact on the upper side of the shaft, as shown in Figure 2, in order to suppress the electric field around the probe head. A pantograph structure as illustrated in Figure 3 was adopted because the chamber face was not seamless. An adjustment for balance of the vertically located movable shorts in the FT is required simultaneously in order to reduce the leakage of microwaves. These modifications enabled us to measure the radial beam pattern for the entire region of the MDP with using the FT resonator as shown in Figure 4. Note that the low-level circuits of all RFs for the SRC were adjusted to stabilize the voltage and phase of resonators.<sup>3)</sup>

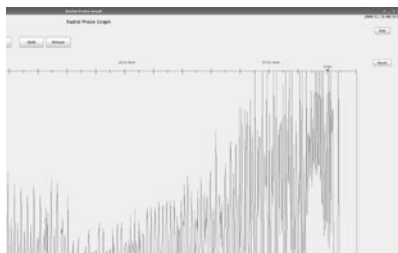


Fig. 4. Radial beam pattern of SRC for  $^{48}\text{Ca}$  beam in December 2008.

In the most cases, the major beam loss in cyclotron takes place on the septum of electrostatic deflector (EDC). For the acceleration of kilowatt beams, machine protection is required in order to avoid serious thermal damage caused by the large beam loss. For the protection during  $^{48}\text{Ca}$  beam acceleration, ten Type-E thermocouple gauges with ceramic tubes were mounted on the EDC septum to measure the temperature and switch off the beam if the maximum heat-up exceeded the criterion, which was set as 5 degrees in December 2008. This EDC protection worked well for the  $^{48}\text{Ca}$  beam. The temperature clearly responded to the beam loss and the extraction efficiency could be improved via tuning such as decreasing the temperature. Note that the temperature of EDC septum is also useful to us for adjusting the balance of the FT resonator because the temperature increases depending on the amount of RF leakage.

Additionally, several modifications were made to make maintenance easier, described as follows. Profile monitors (PF-SV1, SV2) mounted on the vacuum chamber of valley were converted to setback, so as not to block the detachment of EIC and EDC. Many

scaffolds were placed round in the SRC for the access to RF resonators when the magnetic shielding doors were closed. The mounting direction of a gate valve for assist-pumping TMP on the resonator no.2 was re-touched for easy access to the maintenance hatch.

Several problems occurred on the SRC in 2008, described as follows. The vacuum pressure was degraded when the high RF power was fed to the resonator. It was found that the temperature of cryopump was rose remarkably due to the extreme heating up of the RF shield attached in front of the pump due to RF irradiation.<sup>4)</sup> The problem was solved by mounting a water-cooling thermal baffle<sup>5)</sup> on the RF shield. Magnetic shields were covered on all cryopumps to prevent the degradation of performance from a stray field. The shaft of MDP emitted a loud noise and was scraped by its plain bearing. The bearing will be replaced to a roller type in March while the outer vacuum-duct of MDP will be modified to bellows for quick access to the head assembly. The angle settings of EDC, which determine the radius of curvature for beam extraction, were mechanically slid around the drive shaft, and we were not able to extract the uranium beam in a whole day until we readjusted them. The driving screw of EDC “ $\alpha$ ”-axis was cleaned and lubricated because it had hardened and was not able to drive. A directional coupler on the power feeding line of the RF resonator no.2 was burnt due to the excitation of third-harmonic mode. The contact fingers of the coarse tuning panel in the RF resonator no.3 burned out during the  $^{48}\text{Ca}$  experiment as a result of insufficient contact pressure because the shaft of the panel was not eccentric. The directional coupler in the wide-band driver amp of the FT resonator had the problem of a wire breaking.

A new beam acceleration scheme of AVF-RRC-SRC with IRC bypass beam line<sup>6)</sup> is scheduled for the spring of 2009 to perform the commissioning of SHARQA and some experiments using 250 MeV/u  $^{14}\text{N}$  or 250 MeV/u polarized deuteron beam. An acceleration study for the  $^{14}\text{N}$  beam was performed from February 5th to 9th. Additional beam diagnosis elements will be mounted on the SRC at the end of March because the existing elements cannot stop the deuteron beam.

#### References

- 1) T. Dantsuka et al., RIKEN Accel. Prog. Rep. **42**, 307 (2009).
- 2) K. Yamada et al., Proc. 18th Int. Conf. on Cyclotrons and their Applications, 325 (2008).
- 3) N. Sakamoto et al., RIKEN Accel. Prog. Rep. **42**, 120 (2009).
- 4) M. Nishida et al., RIKEN Accel. Prog. Rep. **42**, 129 (2009).
- 5) S. Yokouchi et al., RIKEN Accel. Prog. Rep. **42**, 127 (2009).
- 6) Y. Watanabe et al., RIKEN Accel. Prog. Rep. **42**, 111 (2009).

## Completion of Superconducting Magnet for the 28 GHz ECR Ion Source

J. Ohnishi, T. Nakagawa, Y. Higurashi, H. Okuno, K. Kusaka, and A. Goto

The superconducting magnet for the 28 GHz ECR ion source, under construction at a factory of the Mitsubishi Corporation since October 2007, was completed in December 2008. It consists of six solenoids SL1~SL6 and a set of sextupole coils as shown in Fig. 1. The maximum axial magnetic fields are 3.8 T on the RF injection side and 2.2 T on the beam extraction side. The sextupole magnetic field is approximately 2.2 T on the inner surface of the plasma chamber ( $r = 75$  mm). The radius of the room temperature bore is 86 mm. The coils use a NbTi-copper conductor and are bath-cooled in liquid helium. The maximum magnetic fields on the SL1 and the sextupole coils are 7.2 T and 7.4 T, respectively. The design details of the superconducting coils are described in Ref. 1 and 2.

The coil winding began in January 2008. The SL3 and SL4 use a conductor with a round shape of  $\phi 1.09$  mm and a copper/NbTi ratio of 6.5, while the other solenoids and the sextupole use a conductor with a rectangular shape of 0.82 mm x 1.15 mm and a copper/NbTi ratio of 1.3. Each of the six sextupole coils was dry-wound to work for turn

transitions and was vacuum impregnated with epoxy. The percolation of the epoxy into the inside of the windings was inspected and found to be successful by cutting a trial winding. On the other hand, each solenoid coil was wet-wound with warm epoxy and cured.

The six sextupole coils need to be fixed tightly because they are subjected to large magnetic forces from the solenoids. Figure 2 shows a cross section of the straight part of the sextupole between the SL1 and SL2. The six sextupole coils are assembled using titanium spacers with a triangular cross section and fixed with four layers of  $\phi 0.65$  mm stainless steel wires wound with very high tension of about 580 MPa. An iron pole of 330 mm in length is inserted in the central region of each coil to increase the sextupole field. A stainless steel disk with outer diameter of 250 mm and a thickness of 30 mm is inserted between the SL1 and the SL2 to fix the sextupole coils more tightly because the magnetic force in the azimuth direction is strongest there. The mechanical design here was carried out<sup>2)</sup> by combining 3D magnetic force calculation with Opera3D<sup>3)</sup> and mechanical calculation with ANSYS.<sup>4)</sup>

The final assembly of the sextupole coils and six solenoids is shown in Fig. 3. The ends of the sextupole coils are fixed with a stainless steel ring to support the large radial magnetic force acting on the current return sections. The six solenoids were assembled with stainless steel spacers and tightened with sixty-four long aluminum-alloy bolts that support a maximum repulsive force of approximately 800 kN among them.

Excitation tests of the completed coils were carried out in a commonly used cryostat in June 2008. First, the solenoids were tested one by one and all achieved the design currents without a quench. Next, the sextupole was tested. Table 1 shows the currents when a quench occurred in the sextupole.

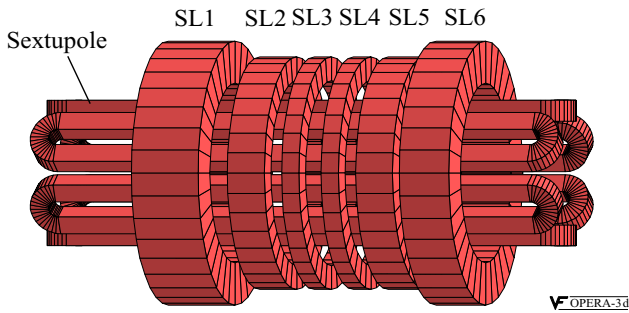


Fig. 1. Arrangement of the superconducting solenoid and sextupole coils.

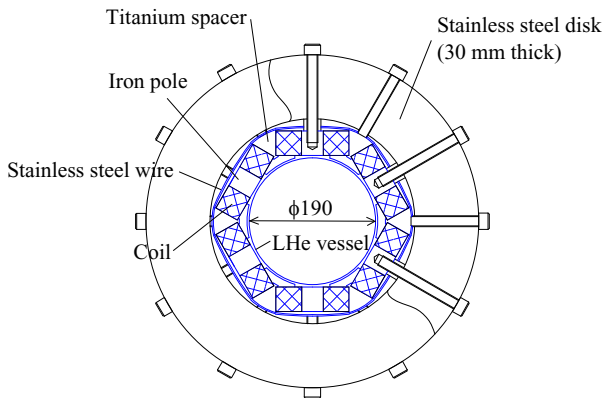


Fig. 2. Cross section of the straight part of the sextupole coils. A 30 mm thick stainless steel disk is inserted between the SL1 and the SL2.

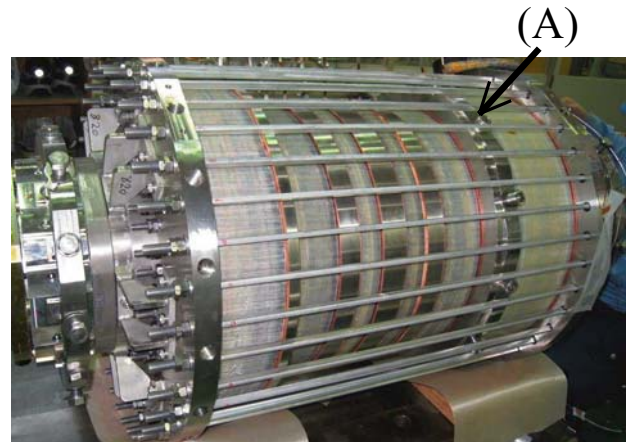


Fig. 3. Photograph of the coil assembly. (A) is a 30 mm thick stainless steel disk inserted between the SL1 and the SL2.

Table 1. Coil currents (Amps) when the sextupole quenched.

run #	sextupole	SL1	SL2	SL5	SL6
design	272	162	182	155	132
1	189				
2	255				
3	90	136	183		
4	65	136	183		
5	73	136	183		
6	114	136	183		
7	70	136	183		
8	77	136			
9	109				132
10	220				92
11	204			155	132
12	230			132	112
13(NQ)	272				
14	258	146	164		
15	234			135	114
16	238			136	116
17	235	127	143		

The sextupole also achieved the design current (271 A) after two quenches (189 A, 255 A) when no solenoids were excited. In all cases where the sextupole and one or two of the solenoids were excited at the same time, the sextupole quenched. The sextupole quenched at low currents ranging from 65 A (24%) to 115 A (42%) when SL1 and SL2 were excited at their design currents in advance (run #3-#7). The sextupole also quenched in a similar way when the SL6 was excited in advance (run #9, #11). The cause of these quenches was presumed to be coil motion at the ends of the sextupole, due to the voltage signals observed in some of these runs. In run #10, the SL6 was ramped after the sextupole was excited at 220 A. In run #12 and #14-#17, the solenoids and the sextupole were excited simultaneously, keeping a ratio of the currents so that the direction of the force acting on the sextupole coils did not change during the excitation. The quench current of the sextupole increased to more than 85% of the design value in this way. It was, however, difficult to reach the design current.

The results of these tests suggested that the support structure at the ends of the sextupole coils is not strong enough against the radial force toward the centre. Methods of remedying this problem were investigated, and performance was improved by increasing the thickness of the inside wall of the helium vessel for room temperature bore at both ends (see Fig. 2) and pressing the end parts of the sextupole coils against those points. After four months, we successfully achieved excitation of all the solenoids and the sextupole at the design currents after the sextupole quenched twice at current levels of 96% and 98%.

After this second excitation test, the cryostat for the 28 GHz ECR ion source was assembled with the superconducting coils in a short period of time and completed in December 2008. A photograph of the completed whole magnet is shown in Fig. 4. The cryostat is surrounded by yokes with thicknesses of 50 mm and 80 mm. Three cryocoolers (Sumitomo Heavy Industries) with two cooling stages each are installed at the top of the cryostat to



Fig. 4. Photograph of the completed superconducting magnet for the 28 GHz ECR ion source.

Table 2. Heat leak, capacity of the cryocoolers, and measured temperature at the stages of liquid helium and two radiation shields.

	LHe vessel	Inner shield	Outer shield
Heat leak (design)	0.14W@4.2K	18W@40K	127W@70K
RDK408D2	1W@4.2K		43W@45K
RDK408S x 2		18W@12K	86W@52K
Temperature (measured)*	4.2K**	14K	47K

\*Cryocoolers operated at 60 Hz.

\*\*Heater was powered at 1.2W to keep He pressure positive.

maintain approximately 330 liters of liquid helium. One (type RDK408D2) is used for re-condensing the liquid helium and cooling the outer of two radiation shields, and the other two (type RDK408S) are used for cooling of the inner and outer radiation shields. Nine current leads use high Tc superconducting material between the liquid helium vessel and the inner shield to reduce the heat leak to the liquid helium temperature. The designed values of the heat leak and capacity of these cryocoolers are listed in Table 2.

The magnet and cryostat were cooled down and tested. It took 1.5 days for pre-cooling with liquid nitrogen and pouring of liquid helium. The temperatures of the radiation shields in the steady state with the cryocoolers operating are listed in Table 2. The capacity of the cryocoolers was found to have a sufficient margin because the temperatures were lower than expected. The superconducting coils were excited again at the design currents after the sextupole coil had quenched once at the 96% current level.

After the operation test, the cryostat and magnet were warmed up and carried to RIKEN on December 19, 2008. The ion source of this magnet will start to operate in the spring of 2009.

#### References

- 1) J. Ohnishi et al.: RIKEN Accel. Prog. Rep. 41, 86 (2008).
- 2) J. Ohnishi et al.: Proc. EPAC2008 (2008), p. 433.
- 3) <http://www.vectorfield.com/>
- 4) <http://www.ansys.com/>

# Production of highly charged Na ion beams from the RIKEN 18 GHz ECRIS

Y. Higurashi, T. Nakagawa, M. Kidera, T. Aihara, M. Tamura, M. Kase, A. Goto and O. Kamigaito

In a series of experiments to search for super-heavy element in this case to verify the element with an atomic number of 113, an intense beam of Na ions was strongly needed at the end of 2008. The requirement was to produce an intense beam (~4 μA) of <sup>23</sup>Na ions as long as possible, with no break, in order to minimize experiment time. To meet this requirement, we conducted a test experiment to produce Na ions, and supplied an Na<sup>7+</sup> beam for the experiment.

To produce the Na beam, we used NaF rod (4x4x35mm<sup>3</sup>). The NaF rod was directly inserted into the ECR plasma of RIKEN 18 GHz ECRIS and heated up to obtain sufficient vapour pressure. The description and performance of the RIKEN 18 GHz ECRIS are reported in Ref.1.

Figure 1 shows the charge distribution of an Na ion. The ion source was tuned to produce Na<sup>7+</sup> ion beam. The RF power was 300W. The gas pressure was 5x10<sup>-7</sup>Torr. The extraction voltage was set to 11.7 kV. In this experiment, we used He gas as an ionized gas. Figure 2 shows the beam intensity of Na<sup>7+</sup> as a function of RF power. The beam intensity increased as RF power was raised to 48 μA.

mg. It is estimated that the consumption rate in this experiment was ~0.4 mg/h. The total weight of the rod is ~1.2 g. This means that, in principle, we can produce Na ions for 3000 h without inserting an additional rod.

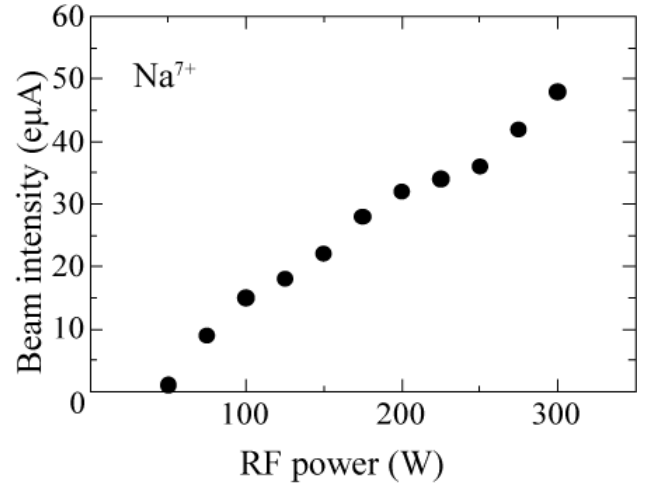


Fig. 2. Beam intensity of Na<sup>7+</sup> ions as a function of RF power.

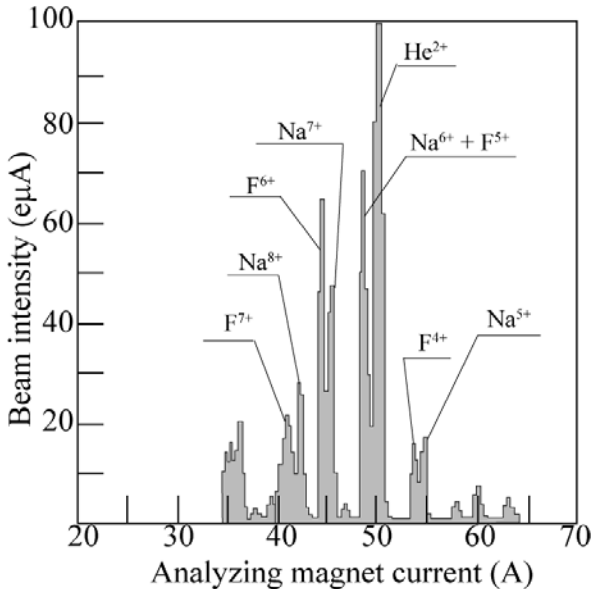


Fig. 1. Charge distribution of Na ions. The ion source was tuned for production of Na<sup>7+</sup>.

Figure 3 shows the 99% x and y-emittance of the Na<sup>7+</sup> beam under the same conditions for production of 48 eμA Na<sup>7+</sup> beam. The x and y emittance were 265 and 262 πmm · mrad, respectively.

Using this method, we successfully produced an average beam intensity of 45 eμA for 30 days for the experiment without any break. The total consumption of NaF was ~300

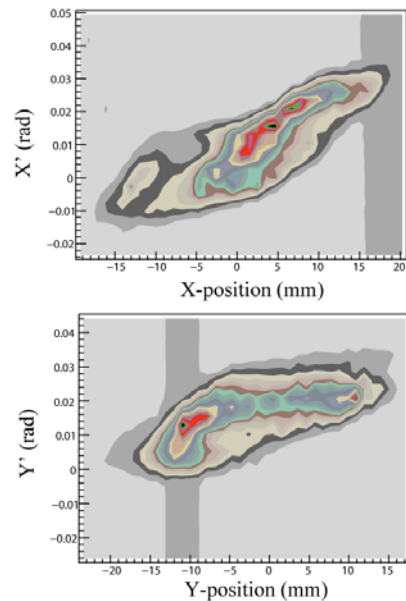


Fig.3. x and y emittance of the Na<sup>7+</sup> ion beam.

### References

- 1) T. Nakagawa et al., Nucl. Instrum. Methods. **B226**(2004)392

# Production of a highly charged Ge beam from the RIKEN 18 GHz ECRIS

Y. Higurashi, T. Nakagawa, M. Kidera, T. Aihara, M. Tamura, M. Kase, A. Goto, and O. Kamigaito

Recently, an intense  $^{76}\text{Ge}$  beam was strongly needed to search for a super-heavy element (atomic number 114) at RIKEN after producing the element which has an atomic number of 113.<sup>1)</sup> The requirement of this experiment was to produce an intense beam (1~2 pA) of  $^{76}\text{Ge}^{17+}$  ions as long as possible without break in order to minimize breaks in the experimental time. This is because the estimated cross section is very small (smaller than pb(  $10^{-36}$  cm<sup>2</sup>)).

One popular methods for producing highly charged heavy ions from a solid material is to use the oven in the plasma chamber of the ECR ion source<sup>2)</sup>. Using this method one can produce an intense beam of highly charged heavy ions at a low consumption rate ( lower than 1mg/h). However the main drawback of this technique is the limit on the material volume (~several 100 mg) which can be contained in the oven at present, when we install the oven in the small plasma chamber. If we assume a consumption rate of 1mg/h, the duration of the beam supply is several 100 h.

temperature.<sup>3)</sup> The advantage is that one can produce metallic ions in the same way as ion production with gaseous elements. This means that we can produce highly charged metallic ions for a very long period, without any break, if we can find a proper material for the MIVOC method.

For these reasons, we chose the MIVOC method for production of Ge ions. For production of Ge ions, we used trimethylgermanium ((CH<sub>3</sub>)<sub>3</sub>GeH) which has a high vapor pressure (~several 100 torr ) at room temperature.

Description and performance of the RIKEN 18 GHz ECR ion source are described in Ref. 4. Figure 1 shows a cross sectional view of the ion source and the microwave injection side. The material was placed in a chamber connected to the ECR plasma chamber by a gas-feeding tube via a variable leak valve. The gas flow rate was controlled by the variable leak valve. The inner wall of the

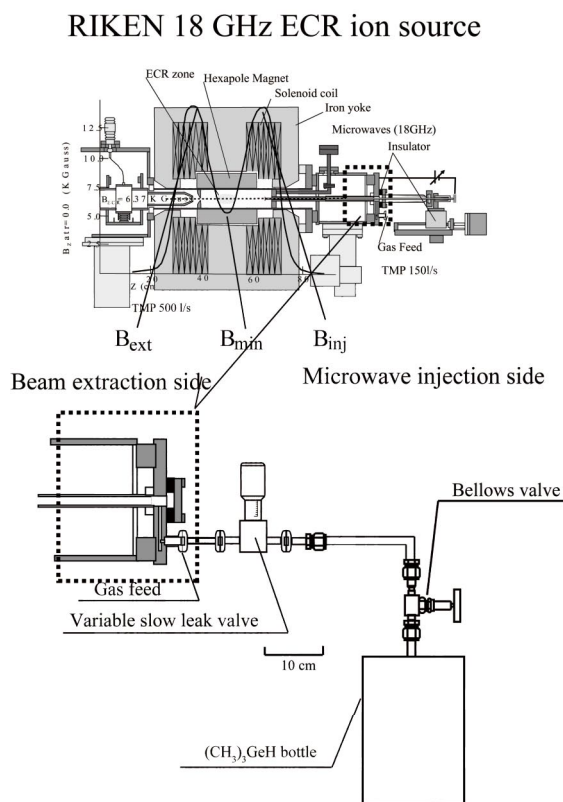
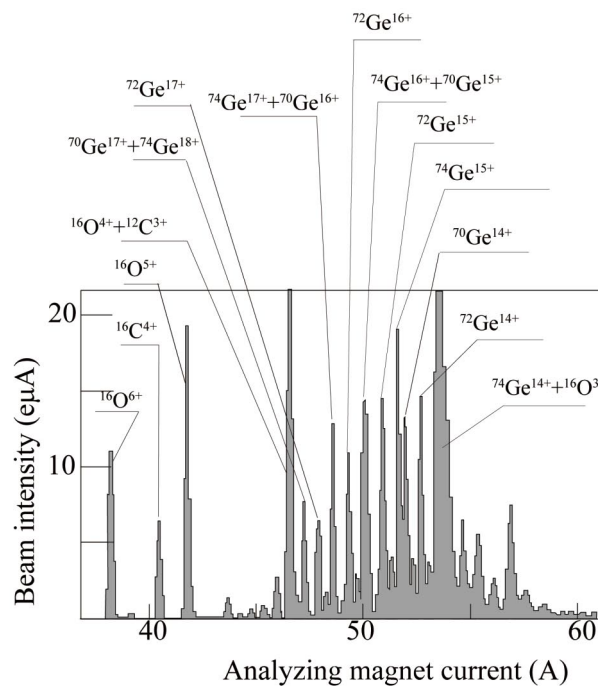


Fig. 1 Schematic drawing of the RIKEN 18 GHz.

A MIVOC method for the ECR ion source enables production of highly charged metal ions at room



plasma chamber was covered by a thin aluminum cylinder (1mm thickness).<sup>5)</sup>

Fig. 2. Charge state distribution of Ge ions.

Figure 2 shows the charge state distribution of the Ge ions. The RF power was 500 W. The gas pressure was  $8 \times 10^{-7}$  Torr. The maximum magnetic field strength on the microwave injection side, the minimum strength of the

mirror magnetic field, and the maximum magnetic field strength on the beam extraction side were 1.4, 0.49 and 1.2 T, respectively. The extraction voltage was 10 kV. Before producing Ge ions, we cleaned the inner wall of the aluminum cylinder with an oxygen plasma for 2 days. To stabilize the beam intensity we had to supply oxygen gas as a support gas. When adding the oxygen gas as a support gas, the beam intensity was very stable. Instability of beam intensity was within few %. As shown in Fig. 2, the charge distribution of Ge ions is very complicated, due to the existence of many kinds of stable isotopes ( $^{70}\text{Ge}$ ,  $^{72}\text{Ge}$ ,  $^{73}\text{Ge}$ ,  $^{74}\text{Ge}$  and  $^{76}\text{Ge}$ ). The isotope ratio of  $^{70}\text{Ge}$ ,  $^{72}\text{Ge}$ ,  $^{73}\text{Ge}$ ,  $^{74}\text{Ge}$  and  $^{76}\text{Ge}$  are 21, 27, 7.7, 36 and 7.6%, respectively. To estimate the beam intensity for each charge state, we chose the beam intensity of  $^{73}\text{Ge}$ , because only  $^{73}\text{Ge}$  was present in the one peak in the charge distribution. Based on these results, the beam intensity of highly charged Ge ions is estimated as shown in Fig. 3.

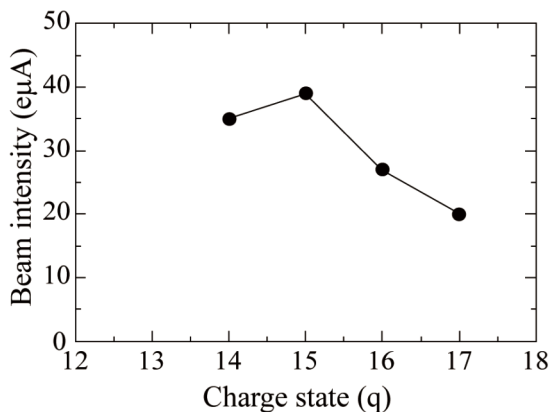


Fig. 3. Beam intensity of highly charged Ge ions.

Figure 4 shows the beam intensity of  $^{72}\text{Ge}^{17+}$  and  $^{76}\text{Ge}^{18+}$  as a function of RF power. It is estimated that 80% of the intensity of the  $^{72}\text{Ge}^{17+}$  and  $^{76}\text{Ge}^{18+}$  ion beam is  $^{72}\text{Ge}^{17+}$ . The beam intensity increases with increasing RF power. Figure 5 shows the beam intensity as a function of bias disc voltage.

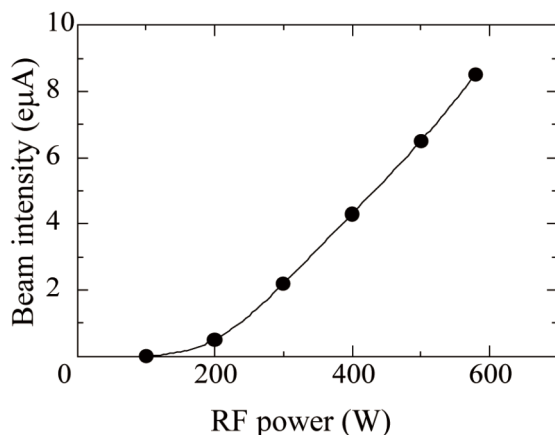
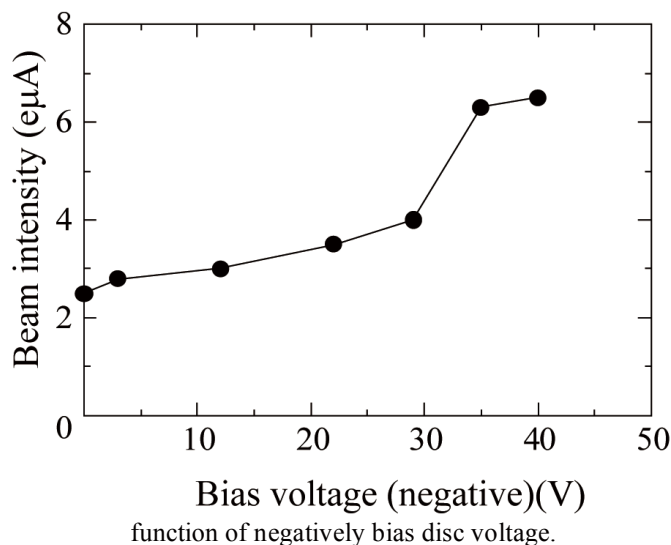


Fig. 4. Beam intensity of  $^{72}\text{Ge}^{17+}$  +  $^{76}\text{Ge}^{18+}$  ions as a function of RF power.

In conclusion, we successfully obtained higher than  $1\mu\text{A}$  of  $\text{Ge}^{17+}$  with the MIVOC method. This will be used for a super-heavy element ( $Z=114$ ) search experiment after producing  $(\text{CH}_3)_3^{76}\text{GeH}$ . In this experiment, we used a slit width of 8 mm, which is placed in front of the faraday cup. When using  $(\text{CH}_3)_3^{76}\text{GeH}$ , we can use a wider slit width ( $\sim 40\text{mm}$ ) because we do not need such good mass resolution. In this case, we may obtain higher intensity than with slit a width of 8mm.

Fig. 5. Beam intensity of  $^{72}\text{Ge}^{17+}$  +  $^{76}\text{Ge}^{18+}$  ions as a



#### References

- 1) K. Morita et al; J. Phys. Sci. Jpn. **73**(2004)2593.
- 2) R. Geller, Electron Cyclotron Resonance Ion Sources and ECR Plasma (IOP publishing, Bristol, 1996)382.
- 3) H. Koivisto et al, Nucl. Instrum. Methods B94(1994)291.
- 4) T. Nakagawa, Y. Higurashi, M. Kidera, T. Aihara, M.Kase and Y. Yano Nucl. Instrum. Methods B **226**(2004)392.
- 5) T. Nakagawa et al, Jpn. J. of Appl. Phys. **35**(1996)4077.

## Improvement of rf-system for cyclotrons at RIBF

N. Sakamoto, O. Kamigaito, K. Suda, R. Koyama, A. Goto, and M. Kase,

Improvements have been made to make the rf field much more stable and make the system itself much reliable. Deviations of the amplitude and phase of the acceleration voltage are required to be  $\pm 1 \times 10^{-1}$  and  $\pm 0.05^\circ$ , respectively. Stability of the voltage and the phase of acceleration field of rf cavities is one of the most important issues for reliable operation of cyclotrons. An unstable rf field causes emittance growth of the beams during acceleration because energy gain per turn varies according to the rf field deviations, and the radius of the beam orbit changes, resulting in beam losses especially at the extraction device. Stable rf means not only constant amplitude and locked phase with reference to the rf signal from the master oscillator but also minimum interruption to providing beams due to rf breakdown which occurs due to sparks on the cavity surface.

The unstable of the rf field can be categorized into modulation and drift. Modulations of voltage and phase are caused mainly by ripple in the d.c. power supplies of amplifiers. Power supply ripples have main frequency components of 300 Hz and appear as an amplitude modulation and a phase modulation with a frequency of 300 Hz. Modulation of the rf signal can be observed as a side-band spectrum by using a spectrum analyzer. For example, an amplitude modulation of  $\pm 5 \times 10^{-4}$  and a phase modulation of  $\pm 0.1^\circ$  correspond to spectrum levels of  $-72$  dBc and  $-61$  dBc, respectively. This modulation will be removed/minimized

by tuning a feed-back loop (i.e., choosing a gain and a time constant) while observing strength of the side-band spectrum. After careful tuning of the feedback loop the sideband of 300 Hz ripple was reduced to  $-76$  dBc.

On the other hand, drift of the rf voltage and phase occurs due to change in atmosphere temperature and change power supply. The temperature control oven system is equipped for the feed-back control. The temperature of the oven is controlled within  $|\Delta T| < 0.5^\circ\text{C}$ . In addition, an automatic voltage regulated power supply was introduced to the Auto Gain Control and Phase Lock Loop.

Finally the stability shown in Fig. 1 was achieved. Phase drift of only  $0.05^\circ$  of RES3 was observed over 14 hours. The others were well stabilized within 0.1% and  $0.1^\circ$ . Fig. 1 plots records of the amplitude and phase of 4 acceleration and 1 flattop cavities of the SRC during acceleration of  $^{14}\text{N}$  with an energy of 250 MeV/u ( $f = 27.4$  MHz). The gap voltage/rf power of acceleration cavities (RES1~4) and flattop cavity (FT) of the SRC were 440 kV/100 kW and 200 kV/12 kW, respectively. The measurements were made by using a new rf-monitor system.<sup>1)</sup> While the old vector voltmeter system had resolutions of 0.1 % and  $0.1^\circ$ , the voltage and phase resolutions of the new monitor are 0.01 % and  $0.02^\circ$ , respectively.

In the case of rf voltage control breakdown due to a spark, it is important to recover rf voltage as soon as possible, otherwise it takes more than half an hour to manually recover by adjusting tuner a few cm, due to thermal deformation of the cavity by a cooling water.

The low level system has an automatic recovery mode which turns the rf input to the rf amplifier into

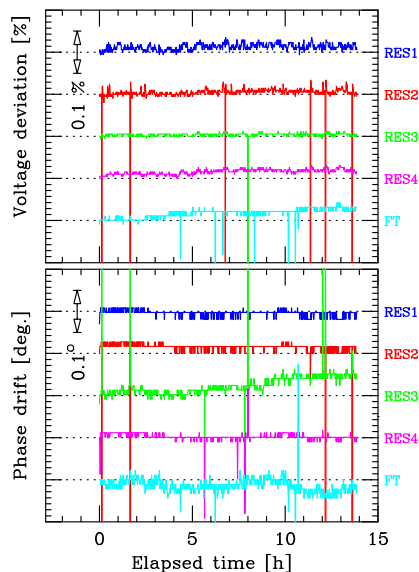


Fig. 1. Measured voltage(upper) and phase(lower) of cavities for SRC at the frequency of 27.4 MHz.

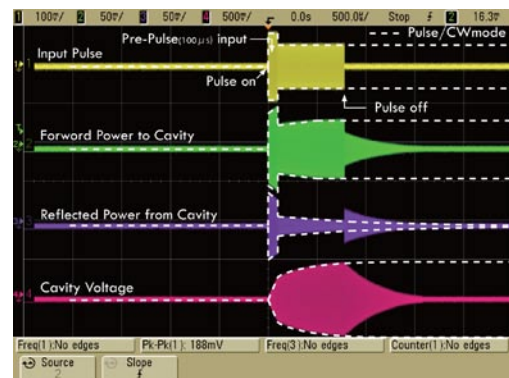


Fig. 2. Pre-pulse is introduced to pulse-mode to overcome multipactor of the cavity. a) envelope of input signal to amplifier. b),c) forward and reflected power at coaxial feeder line, respectively. d) pickup signal of cavity.

pulse mode. The pulse mode has very fast  $\Delta V/\Delta t$  of a few  $\mu s$ , and is crucial for overcoming the multipactor of the cavity in the recovery process. The rise-time of the cavity voltage is defined by the cavity and amplifier response. Therefore, in order to obtain fast pulse, large amplitude pre-pulse with a length of 100  $\mu s$  is introduced to the normal pulse to obtain a fast pulse. Fig. 2 shows the envelopes of the input pulse, forwarded power, reflected power and cavity pickup signal. It has been found that the fast  $\Delta V/\Delta t$  pulse successfully overcome the multipactor with a pre-pulse and consequently restores normal power to the safe level for power supplies of amplifier and the cavity itself. In automatic-recovery mode, the cavity voltage will be recovered along the dashed line within a few ms. Therefore no voltage down of RES4 was observed during the stability measurements shown in Fig. 1. It may be concluded that the pre-pulse excitation works very well. Fine tuning of the amplitude and length of the pre-pulse is in progress.

#### References

- 1) R. Koyama et al.: "RF fields and nondestructive beam-phase/intensity monitoring system for stable operation of RIBF", this report.

## Stability of RF system at RILAC in RIBF

K. Suda, R. Koyama,<sup>\*1</sup> O. Kamigaito, N. Sakamoto, N. Fukunishi, M. Fujimaki, T. Watanabe, K. Yamada, and M. Kase

The accelerating RF system of RILAC which is an injector to RRC in RIBF, must be highly stable as well as the four cyclotrons located downstream for a long term such as several weeks in order for us to provide high intensity heavy ion beams up to 1 pμA. If we maintain a deviation of beam phase before injection to RRC within  $\pm 1^\circ$  of accelerating RF of RRC, corresponding to 152 ps for  $^{48}\text{Ca}$  case ( $=2/36.5 \text{ MHz}/360 \text{ deg.}$ ), it is required to achieve RF stability of  $\pm 0.1\%$  in voltage and  $\pm 0.1^\circ$  in phase, since the coefficients of beam phase against RF of RILAC before injection to RRC are typically 0.5 – 1.0 nsec/% in voltage and 0.5 nsec/% in phase. For the purpose of determining the degree of stability, the RF voltage and phase were monitored as well as beam magnitude and phase using lock-in amplifiers (LIA) during the beam time of RIBF<sup>1)</sup>. Fig. 1 shows the long-term deviation of RF pickup voltages and phases in six tanks of RILAC observed during Uranium acceleration ( $f=18.25 \text{ MHz}$ ) in July 2008. The voltages for the last two tanks (#5 and #6) are rather stable within 0.05%, whereas that for the tanks #1 – #4 deviate more than 0.1%. The main reason for this difference is that Automatic Gain Control units (AGC) used to stabilize RF voltage for the last two tanks are newer than that for other tanks, and are designed well in order to provide better stability. On the other hand, phases are nearly monotonically increasing or decreasing, which is often observed at RILAC. The low-level circuits for phase stability (Automatic Phase Control units) are the same for all tanks. The corresponding beam phases monitored by

two phase probes (PP-e11, X51) located downstream of RILAC are shown in Fig. 2. A beam phase (arrival time) changes depending on deviations of RF voltage and phase. Therefore, if we assume deviation of RF is small enough, we can define the first order coefficient of beam phase against RF deviation. We determined the coefficients using following two different method.

- (1) Manually change RF voltage and phase for each tank, and measure the beam phase. (parameter change test)
- (2) Fitting beam phase data with RF voltage and phase deviation.

For the case of (1), we changed RF voltage by 0.09–0.3% and phase 0.21–0.53°. For (2), the function used for fitting is

$$\phi^{\text{beam}} = \sum_{i=1}^6 (a_i V_i^{\text{RF}} + b_i \phi_i^{\text{RF}}) + c$$

where  $\phi_{\text{beam}}$  is the beam phase,  $V_i^{\text{RF}}$  and  $\phi_i^{\text{RF}}$  are deviation of RF voltage and phase, respectively, and  $a_i, b_i, c$  are parameters. For comparison, data for fitting is separated into two: (2-a) initial 5.7 h, (2-b) last 6.5 h. In the fitting, a standard deviation of beam phase was assumed to be 0.015 ns taking noise level of PP into account. The fitting results of beam phase are shown in Fig. 2 as well as the values calculated by putting the parameters obtained in parameter change test into the fitting function. The results of fitting reproduce PP-data reasonably. Although an agreement with parameter change test is poor, fine structure is well reproduced. These results indicates that the fine structure of beam phase is actually caused by RF deviation. Fig. 3 compares the parameters obtained by parameter change test and by fitting. For the voltages of the last two tanks, parameters are significantly different between two methods. It seems that the fitting method can not determine these parameters because the RF voltages are nearly constant or not linear independent. Other than the last two tanks, the largest coefficient is that in the voltage of tank #2 ( $\sim 3 \text{ [ns/\%]}$ ). An improvement of a stability of beam phase was expected if AGC of tank #2 is upgraded to the same as that for the previous two tanks. Therefore, an upgrade of AGC was performed in September. A control system was also modified so that RF voltages for the first four tanks can be controlled in higher precision: from 1/3000 to 1/6000 for #1, #3 and #4, and #2 to 1/60000, the same as used in the previous two tanks. Fig. 4 shows the RF voltage and phase observed during

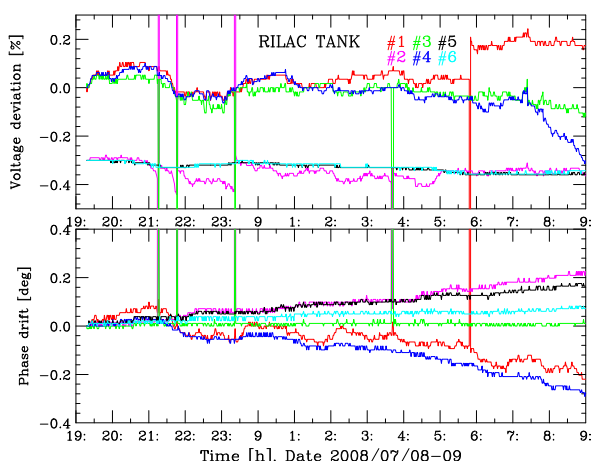


Fig. 1. RF voltage and phase of six tanks of RILAC. The voltage deviation (upper panel) for tank #2, #5 and #6 are shifted by  $-0.3\%$  for visibility.

<sup>\*1</sup> SHI Accelerator Service Ltd.

Uranium acceleration in November. A time dependent fluctuation of voltage in tank #2 became similar to that in the last two tanks as expected. However, the voltages for these three tanks started to decrease similarly at around 0:00 on the 17th. As a result, stability is within 0.15%, and is worse compared with that in July (Fig. 1). The corresponding beam phase and parameter fitting results are shown in Fig. 5 and 3, respectively. PP-data during beam test (13:15 – 13:45) were eliminated from fitting. From the fitting results, a fluctuation of beam phase from 8:00 to 18:00 seems to be mainly due to the RF voltage deviation of #3. RF pickup voltage and phase are summarized in Tables 1 and 2. Further analysis is still in progress.

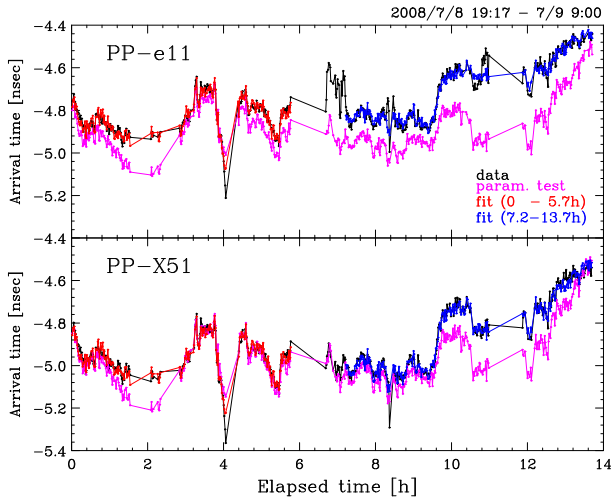


Fig. 2. Beam phase measured by two phase probes (PP-e11, X51) located downstream of RILAC. The data is compared with fitting results.

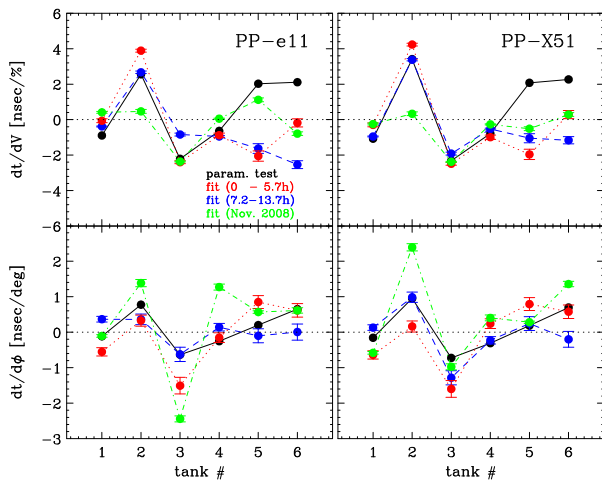


Fig. 3. Comparison of parameters obtained by parameter change test and fitting. Parameters  $a_i$  and  $b_i$  are shown in upper and lower panels, respectively.

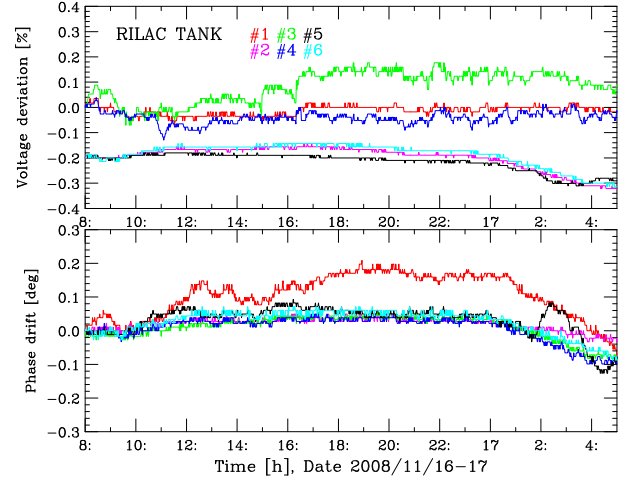


Fig. 4. RF voltage and phase of six tanks of RILAC. The voltage deviation for tanks #2, #5 and #6 are shifted by  $-0.2\%$  for visibility.

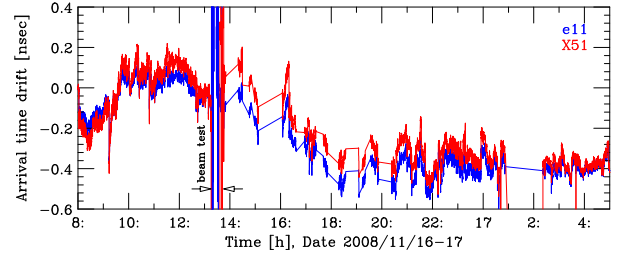


Fig. 5. Beam phase measured on 2008/11/16-17.

Table 1. RF pickup voltage and phase measured by LIA on 2008/07/08 19:17.

Tank #	1	2	3	4	5	6
Voltage [mV]	19.28	31.08	19.32	26.72	33.73	23.60
Phase [deg]	-81.72	-85.61	-80.00	-82.28	-71.16	-68.67
Phase(shifted)	0	-3.89	1.72	-0.56	10.56	13.05

Table 2. RF pickup voltage and phase measured by LIA on 2008/11/16 8:00.

Tank #	1	2	3	4	5	6
Voltage [mV]	18.99	30.47	19.00	25.84	33.29	23.47
Phase [deg]	-22.13	-30.36	-25.11	-28.16	-24.21	-20.66
Phase(shifted)	0	-8.23	-2.98	-6.03	-2.08	1.47

## References

- 1) R. Koyama et al., in this progress report.

## Open-stub filter for fRC main amplifier

O. Kamigaito, T. Chiba, Y. Chiba, N. Sakamoto, and K. Suda

The fixed-frequency ring cyclotron (fRC) in the RI-beam factory<sup>1)</sup> has two accelerating resonators operated at 54.75 MHz.<sup>2)</sup> Each resonator is fed by an rf amplifier based on a tetrode RS2058CJ with a grounded-grid configuration, and a maximum output power of 100 kW in the cw mode. The resonator and amplifier are connected by a 5 m coaxial waveguide (WX-120D). The typical input power for the acceleration of a uranium beam is 70 kW at a gap voltage of 450 kV.

There was a problem in these rf systems because the seventh harmonic component (383.25 MHz) became prominent in the resonators, as shown in Fig. 1, when the input power exceeded 40 kW. Apparently the harmonic component, transmitted from the amplifier, causes resonance of one of the resonant modes in the resonator coupled to the beam chambers. There are so many resonant modes in the frequency region above 350 MHz. In principle, the higher harmonic component should be as small as possible because the pickup signal from the resonator is rectified and used as input to the feedback loop of the amplitude.

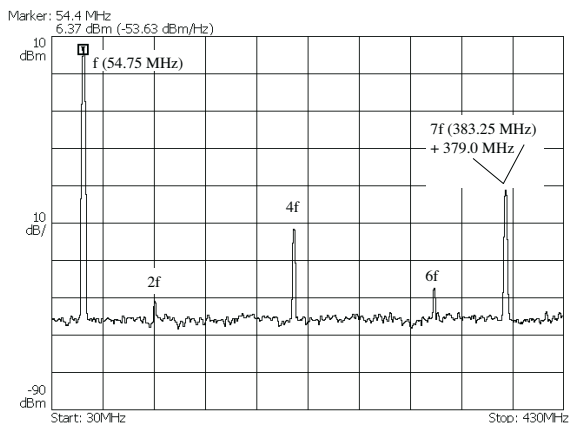


Fig. 1. Measured power spectrum of pickup signal of the accelerating resonator before installing the filter. Gap voltage was 440 kV. Although not shown clearly, the peak around the seventh harmonic component consists of two different components: 383.25 MHz and 379.0 MHz. The latter indicates self oscillations of the amplifier.

We first tried to suppress the harmonic component of the output power by re-adjusting the circuit parameters of the amplifier, but the improvement was quite limited. On the other hand, it seemed impossible to find an effective way to move the resonant modes far from the seventh harmonic frequency. Therefore, we decided to insert a notch filter in each waveguide, as illustrated below.

A schematic diagram of the filter is shown in Fig. 2,

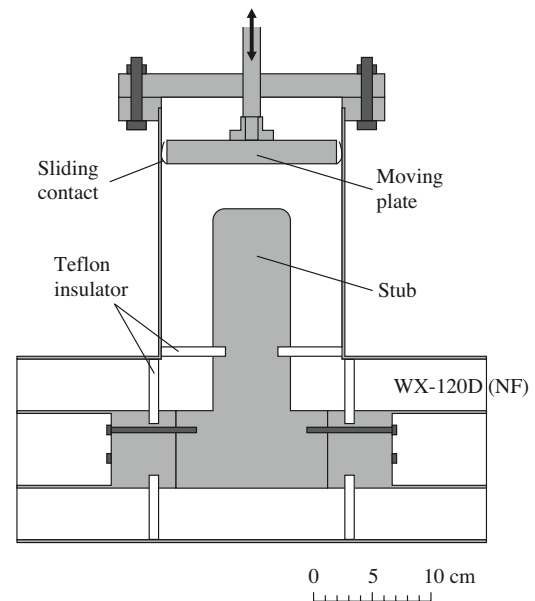


Fig. 2. Cross sectional view of the open-stub filter.

with an open stub added to a coaxial waveguide. The length of the open stub is chosen to be approximately equal to the quarter wavelength at 383.25 MHz so that the transmission through the coaxial line is zero at this frequency. Since the length of the stub is much smaller than the wavelength at 54.75 MHz, insertion loss at the fundamental frequency is very small.

The size of the transmission ports of the filter is based on WX-120D. In order to adjust the notch center precisely, a moving plate was added to the open end of the stub. The length of the stub and the stroke of the plate were optimized by using the computer program Microwave Studio.<sup>3)</sup> The thickness and position of the Teflon insulators were carefully taken into account in the calculation. All the components except for the inner conductor of the stub are made of copper, and the inner conductor is made of brass plated with copper.

The measured scattering parameter  $|S_{21}|$  of the filter is shown in Fig. 3. Transmission at 383.25 MHz can be completely suppressed by adjusting the position of the end plate. Insertion loss at the fundamental frequency is very small, as expected. The filter was inserted into the waveguide close to the output port of the amplifier, as shown in Fig. 4.

The measured power spectrum of the pickup signal after installing the filter is shown in Fig. 5. It is clear that the higher order components are significantly reduced.

The filters worked stably during the uranium acceleration performed in this year.

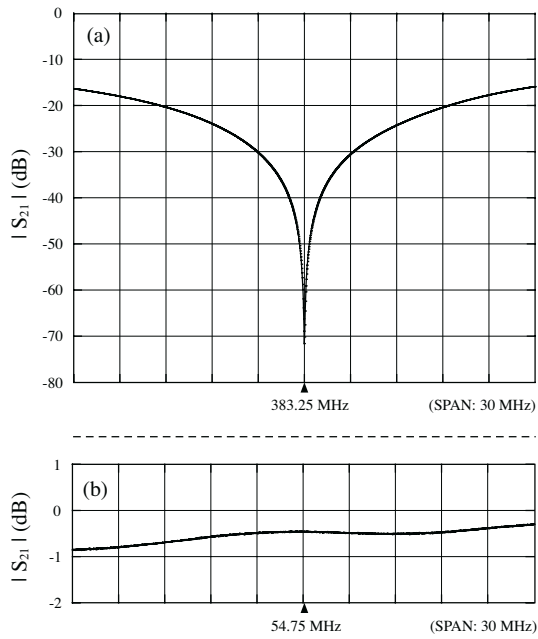


Fig. 3. Measured  $|S_{21}|$  of filter in the frequency region around the seventh order component (a) and around the fundamental component (b).

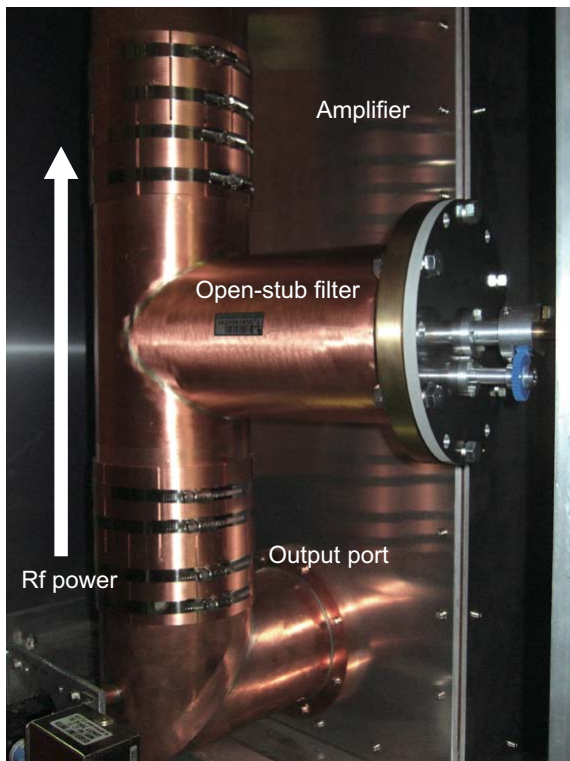


Fig. 4. Photograph of filter installed in the amplifier.

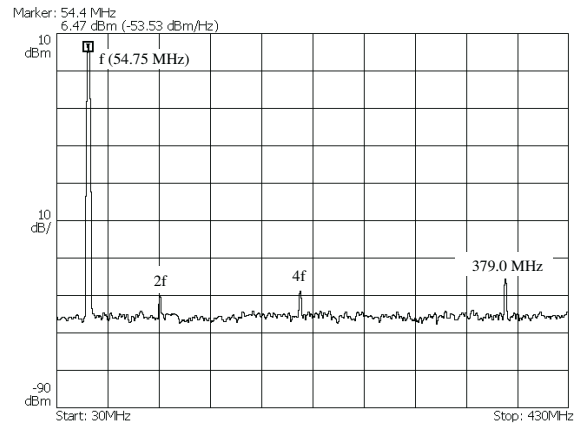


Fig. 5. Measured power spectrum of pickup signal of the accelerating resonator after installing the filter. Gap voltage was 440 kV. The resultant peak corresponds to a frequency of 379.0 MHz. The seventh harmonic component (383.25 MHz) disappeared completely.

Kase, A. Goto, and Y. Yano: Proc. 3rd Annual Meeting of Particle Accelerator Society of Japan and 31st Linear Accelerator Meeting in Japan, Sendai, Japan, August 2-4, 2006, p. 886.

3) <http://www.cst.de>

#### References

- 1) Y. Yano: Nucl. Instrum. Methods **B 261**, 1009 (2007).
- 2) N. Sakamoto, O. Kamigaito, S. Kohara, N. Inabe, M.

## High-power test of four-rod cw RFQ for new injector to RI-beam factory

E. Ikezawa, O. Kamigaito, H. Fujisawa, N. Sakamoto, K. Suda, K. Yamada, T. Aihara,\* T. Ohki,\*

H. Yamauchi,\* A. Uchiyama,\* K. Oyamada,\* M. Tamura,\* M. Kase, A. Goto, and Y. Yano

\* SHI Accelerator Service Ltd.

As reported in the last volume,<sup>1)</sup> an RFQ system<sup>2)</sup> consisting of a resonator, rf power amplifier system, and water-cooling system, has been brought to RIKEN to be recycled as part of the new injector<sup>3)</sup> for the RI-beam factory. High power tests of the resonator were carried out in 2008 as described below.

In February 2008, the water-cooling system was reassembled and new pipes were installed to supply de-ionized water for the resonator and the amplifier. The vacuum level in the resonator did not deteriorate in the presence of cooling water.

The rf amplifier mainly consists of two stages as shown in Fig. 1: the 5 kW driver stage based on a tetrode RS3021CJ, and the 50 kW final stage based on a tetrode RS2058CJ with a grounded grid configuration. A 500 W solid state amplifier is included in the driver stage. The amplifier was reassembled in the following way. First, in September 2008, the driver stage was brought to a factory and tuned to provide the designed power. At the same time, the program for the control unit was re-installed. Second, the final stage was reassembled at RIKEN and all the units including the DC power supply were connected with cables. Finally, the amplifier system was tested with a dummy load. We encountered no significant problems.

High power testing of the resonator started in December at 33.8MHz. So far, about 11 kW of power has been fed into the resonator in the cw mode. The estimated inter-vane voltage is 40 kV, which is sufficient for the acceleration of

the designed ions with  $M/q=6.8$  in the new injector. The vacuum stays at of  $1 \times 10^{-4}$  Pa during operation, and there seems to be no problem of heating. However, the vacuum pressure is insufficient for beam acceleration. In order to improve the vacuum pressure, two turbomolecular pumps of the RFQ will be replaced with cryogenic pumps.

The resonant frequency of the RFQ should be changed to 36.5 MHz when it is used in the new injector. We are planning to put block tuners in the resonator in this fiscal year. The calculation of the eigenmode has just started.

### References

- 1) O. Kamigaito et al.: RIKEN Acc. Prog. Report 41, 91 (2007)
- 2) H. Fujisawa: Nucl. Instrum. Methods A 345, 23 (1994).
- 3) O. Kamigaito et al.: in this issue.

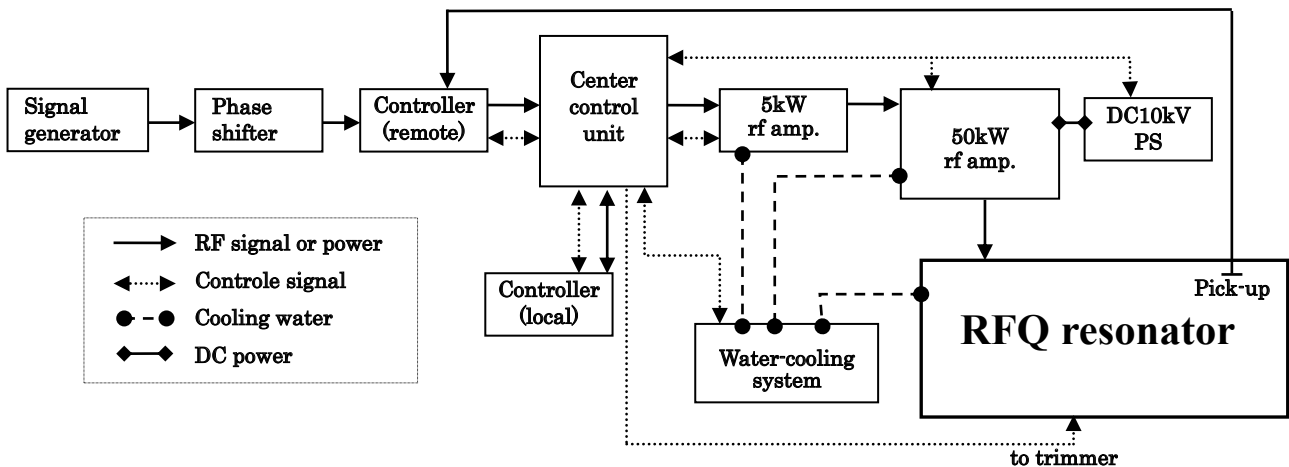


Fig. 1. Schematic block diagram of the RFQ system

## Design of a water-cooling device for the rf shield of an SRC rf resonator

S. Yokouchi, M. Nishida,\* K. Yadomi,\* K. Yamada, N. Sakamoto, H. Okuno, M. Kase, and A. Goto

It was required to design a device to prevent a cryogenic vacuum pump (the "cryopump") from being heated by thermal radiation from the rf shield of an SRC rf resonator.<sup>1)</sup> The rf shield faces the cryopump, and its temperature reached a maximum of about 180 °C due to wall loss during operation of the rf resonator at the maximum voltage of 600 kV. Although installation of a cooling baffle was considered between the rf shield and cryopump for thermal shield, direct cooling of the rf shield was selected for reasons of gas flow conduction, on the condition that the device was attached to the rf shield without welding or brazing.

The water-cooling device mainly consists of an insert flange and a water-cooling pipe as shown in Fig. 1. The insert flange is made of stainless steel, and mounted between the cryopump and the port flange. The water-cooling pipe is a single seamless pipe made of oxygen free copper (OFC), worked by bending. Inner diameter and length of the pipe are 5 mm and about 3.8 m, respectively. Clamps made of OFC are brazed to the straight portion of pipe at intervals of 10 mm to provide flexibility so that the water-cooling pipe can be easily attached to the rf shield. The rf shield is pressed tightly between the clamps and equalizing plates with sixty-two M5 screws to ensure good thermal contact (See detail "A" of Fig. 1). Total length of the clamps are 2.3 m, and total contact area with the rf shield is 0.021 m<sup>2</sup>.

The two ends of the water-cooling pipe are pulled out from the vacuum side into the atmosphere through two holes in the insert flange. Vacuum tightness is maintained by the shaft seal method using an O-ring in a groove with triangular cross section (See detail "B" of Fig. 1).

Wall loss of the rf shield is estimated to be roughly 2 kW. Under the assumption that all of this heat is removed by water flowing in the water-cooling pipe, various parameters were calculated so that the pipe flow velocity of water, pressure drop, and temperature increase were below 4 m/s, 0.15 MPa, and 10 °C, respectively. Table 1 shows the typical design parameters of the water-cooling pipe.

In heat transfer between the rf shield and water-cooling pipe, the temperature difference is caused by convective heat transfer at the inner wall of pipe, thermal conduction in the clamps, and thermal contact between the rf shield and clamps. Each temperature difference is approximately estimated assuming that the amount of heat transferred per unit time is 2 kW, and the water inlet temperature is 20 °C.

Table 1. Typical design parameters of water-cooling pipe for heat input of 2 kW.  $\lambda$  is calculated using Blasius equation.

Volume flow rate of water (L/min)	4.0
Pipe flow velocity of water (m/s)	3.4
Reynolds number $R_e$	18900
Coefficient of pipe friction $\lambda$	0.027
Pressure drop (MPa)	0.13
Temperature rise of water (°C)	7.2

The heat transfer coefficient is calculated to be 15 kW/m<sup>2</sup>°C for the design volume flow rate of 4.0 L/min using the Dittus-Boelter equation. Using this value, the logarithmic mean temperature difference, and the pipe wall temperature are estimated to be 7.3 °C and 31.5 °C, respectively.

The temperature difference in the clamps is calculated to be 3.6 °C. As a result the contact surface temperature of clamps with the rf shield is 35.0 °C.

The thermal contact resistance can be estimated using the Tachibana<sup>2)</sup> and Sanokawa<sup>3)</sup> equations. According to those equations, the resistance is proportional to solid hardness, inversely proportional to thermal conductivity and contact pressure, and slightly affected by solid surface roughness if both solids are made of the same material. For a hardness of 112 (HB) and a contact pressure of 7.1 MPa, the thermal contact resistance is calculated to be about  $6.8 \times 10^{-5}$  (m<sup>2</sup>°C/W). By using this result, the temperature difference is calculated to be 6.5 °C. Consequently the temperature around the top of rf shield is expected to be about 42 °C.

According to the manufacturer of the cryopump an allowable thermal load for a refrigerator of cryopump can be substituted for an allowable temperature of a surface with an emissivity facing the cryopump, and in the case of a surface with emissivity of 0.6 a permissible temperature of surface is below 58 °C.<sup>4)</sup> Assuming that emissivity of the rf shield is at the same level as copper oxide, which is commonly considered to be below ~0.6, the temperature of the rf shield is expected to be appreciably lower than that permissible.

Although the cryopump has a pumping speed of 10 m<sup>3</sup>/s for nitrogen gas, the effective pumping speed at the bottom of the rf shield should be considered from a practical standpoint. When connecting conducting elements (e.g. tubes, baffles, etc.) for molecular flow in series when the cross-sectional areas are different, it is convenient to use a transmission probability (a so-called Clausing's factor), and the relation is expressed

\* SHI Accelerator Service, Ltd.

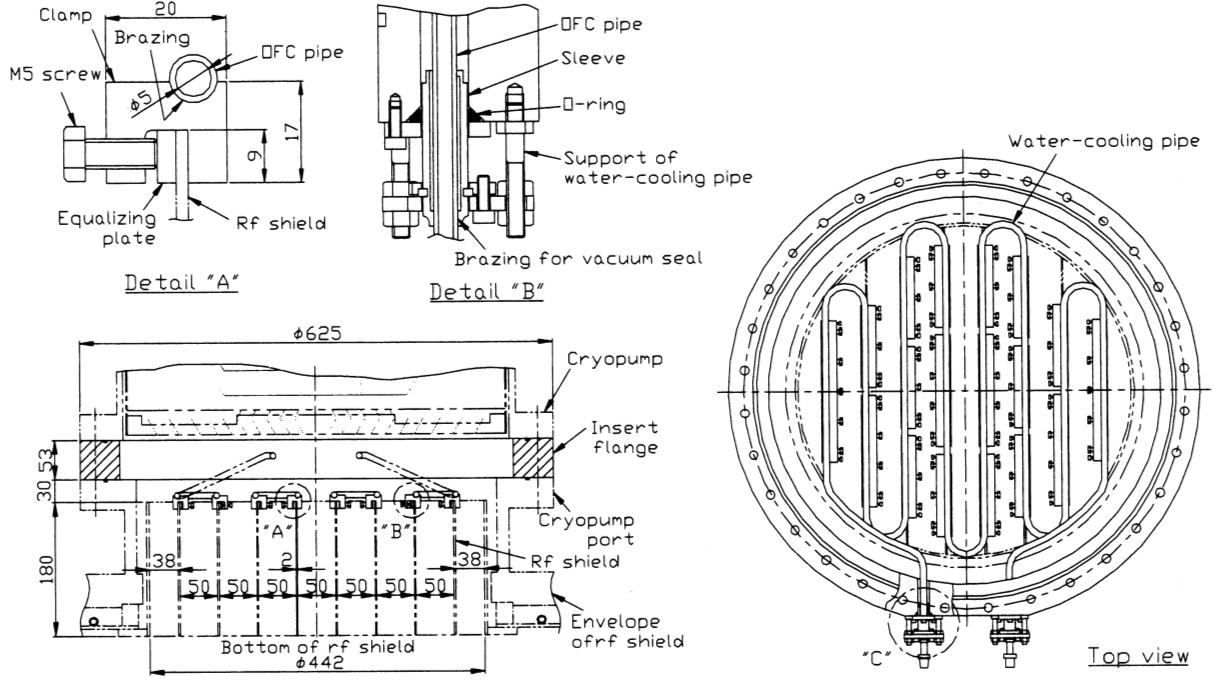


Fig. 1. Structural drawing of the water-cooling device.

by Eq. (1)<sup>5)</sup>

$$\frac{1}{A_1 W_{1n}} = \frac{1}{A_1} + \sum_{i=1}^n \frac{1}{A_i} \left( \frac{1}{W_i} - 1 \right) + \sum_{i=1}^{n-1} \frac{1}{A_i} \left( \frac{A_i}{A_{i+1}} - 1 \right) \delta_{i,i+1},$$

$$\delta_{i,i+1} = 1 \quad \text{for } A_{i+1} < A_i,$$

$$\delta_{i,i+1} = 0 \quad \text{for } A_{i+1} \geq A_i, \quad (1)$$

where  $n$  is the number of elements,  $W_{1n}$  is the total transmission probability passing through from the entrance of the first element to the exit of the  $n$ th element, and  $W_i$  and  $A_i$  are the transmission probabilities and cross-sectional areas of the individual elements, respectively. A pumping probability which denotes the ratio of the pumping speed to the conductance of the pump inlet has the same meaning as a transmission probability. Therefore, when a vacuum pump is connected to a chamber by conducting elements in series, the effective pumping probability is also derived from Eq. (1) by adding the vacuum pump as the last element. Table 2 shows the transmission probability and cross-sectional area of individual elements and the effective pumping probability without and with the water-cooling device. The effective pumping speed is obtained as the product of the conductance and effective pumping probability at the bottom of the rf shield, and the conductance for nitrogen gas at 20 °C is determined by multiplying 118 ( $\text{m}^3/\text{s}\cdot\text{m}^2$ ) by the cross-sectional area of the rf shield. The effective pumping speed with and without the water-cooling de-

vice for nitrogen gas at 20 °C are eventually calculated to be 4.6 and 4.1  $\text{m}^3/\text{s}$ , respectively.

Two water-cooling devices were manufactured and installed at the number 2 and 4 rf resonators in 2008, and the SRC vacuum is performing well.

#### References

- 1) N. Nishida et al.: RIKEN Accel. Prog. Rep. **42**, xxx (2009).
- 2) F. Tachibana: Jour. Jpn. Soc. Mech. Eng. **40**-397, 102 (1952).
- 3) K. Sanokawa: Trans. Jpn. Soc. Mech. Eng. **33**-251, 1131 (1967).
- 4) N. Suzuki: private communication.
- 5) R. A. Faefer: Vacuum **30**, 217 (1980).

Table 2. Transmission probability and cross-sectional area of individual elements, and effective pumping probability with and without the water-cooling device. Transmission probability of the water-cooling pipe was calculated as a rough estimate due to the labour involved.

Element	Transmission probability	Cross-sectional area ( $\text{m}^2$ )
Rf shield	0.358	0.153
Water-cooling pipe	0.703	0.177
Opening of cryopump port	0.941	0.177
Insert flange	0.907	0.212
Cryopump	0.415	0.204
Effective pumping probability		
without device	0.256	
with device	0.229	

## The heating effect of cryogenic vacuum pump of SRC rf resonator

M. Nishida,\* S. Yokouchi, K. Yadomi,\* K. Yamada, H. Okuno, N. Sakamoto, and M. Kase

The SRC has four rf resonators (RES1, RES2, RES3, and RES4). Each rf resonator is evacuated by three cryopumps (CP1, CP2, and CP3) whose nominal diameter is 500 mm as shown in Fig. 1. A vacuum pressure inside an rf resonator is kept as low as  $10^{-6}$  Pa when an rf voltage of the rf resonator is less than 500 kV. However, a vacuum pressure inside RES4 became high above a permissible level after its rf voltage was raised up to a design value of 600 kV. The variation of temperature inside every cryopumps and vacuum pressure of RES4 is shown in Fig. 2. A temperature of 80K baffle ( $T_1$ ), which was considered to be approximately 50 K higher than that of 1st stage of refrigerator, was also measured as well as that of 2nd stage ( $T_2$ ). The  $T_1$  and  $T_2$  of CP1 increased with time, and reached above 40 K and 200 K at  $t = 4$  hours, respectively. On the other hand, the  $T_1$  of CP2 and CP3 changed little with increase in time. The vacuum pressure increased steeply with time just after  $t = 0$ , and at  $t = 2$  hour fell rapidly to around  $1 \times 10^{-5}$  Pa. This drastic increase in pressure is considered to be caused by a large amount of hydrogen gas desorbed from an adsorption panel of CP1 due to increasing  $T_2$  above  $\sim 20$  K.

Wall loss has a peak value at the centre of rf resonator, and decreases with a distance from it. Since CP1 faces to the centre of rf resonator, input power to rf shield at CP1 port is larger than that to others. Therefore, this rf shield may be heated too much if it is not water-cooled sufficiently.

A check inside RES4 was carried out. As a result about half of screws, which fixed rf shield to copper plate (See Fig. 1(b)), turned out to be loose. After tightening these screws by a roughly 1/4 turn (re-tightening),  $T_1$  and  $T_2$  of CP1 were measured. The measured result is shown in Fig. 3. Although both  $T_1$  and  $T_2$  after re-tightening were lower than those before re-tightening, the  $T_1$  did not decrease below 130k equivalent to a permissible value of 80 K for 1st stage.

In order to decrease  $T_1$  below 130 K, it was concluded that an rf shield at CP1 had to be cooled to prevent CP1 from being heated by thermal radiation from it. A water-cooling device for an rf shield was designed.<sup>1)</sup> The device is chiefly composed of an insert flange of stainless steel and a cooling pipe of oxygen free copper which is built in the insert flange and clamps end face of the rf shield (See Fig. 4). Only two pieces of device were manufactured for RES2 and RES4, and installed at each CP1 port. Figure 5 shows  $T_1$ ,  $T_2$  and vacuum pressure for RES2 and RES4 after installing a water-cooling device. The  $T_1$ s were kept below a permissible temperature of 130 K, and the  $T_2$ s were

kept as low as 15 K. The vacuum pressures were kept approximately between 1 to  $2 \times 10^{-5}$  Pa, although small peaks were observed within  $t = 2$  hours. The devices for RES1 and RES3 are now in manufacturing, and will be installed in February 2009.

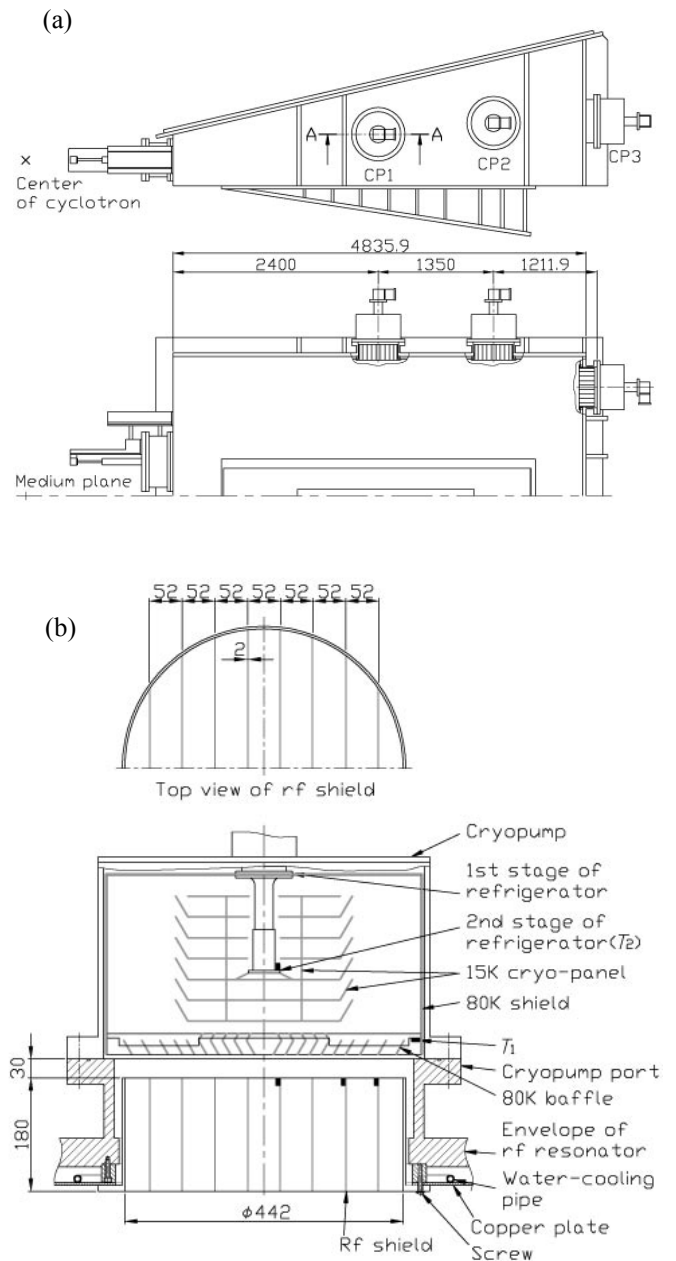


Fig. 1. (a) Layout of cryopumps installed for an rf resonator. (b) Cross-sectional view of A-A in (a) and top view of rf shield.

\* SHI Accelerator Service, Ltd.

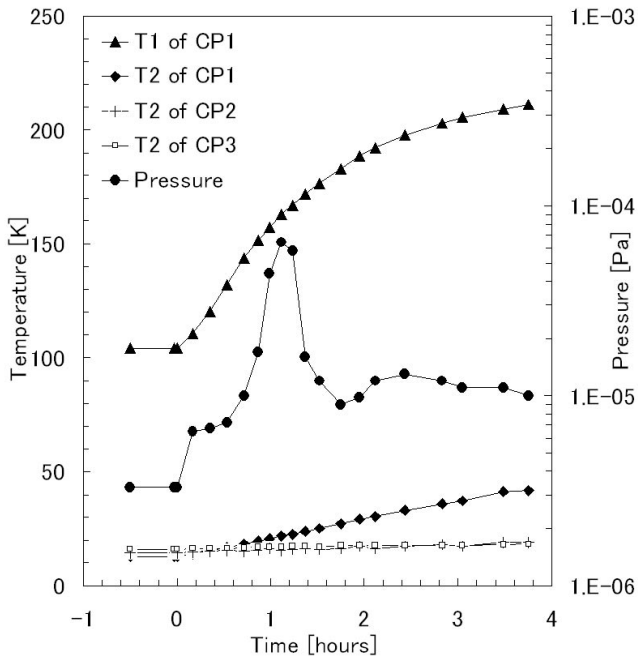


Fig. 2. The variation of temperature inside cryopumps, and vacuum pressure for RES4 after its rf voltage was set to 600kV at  $t=0$  in.

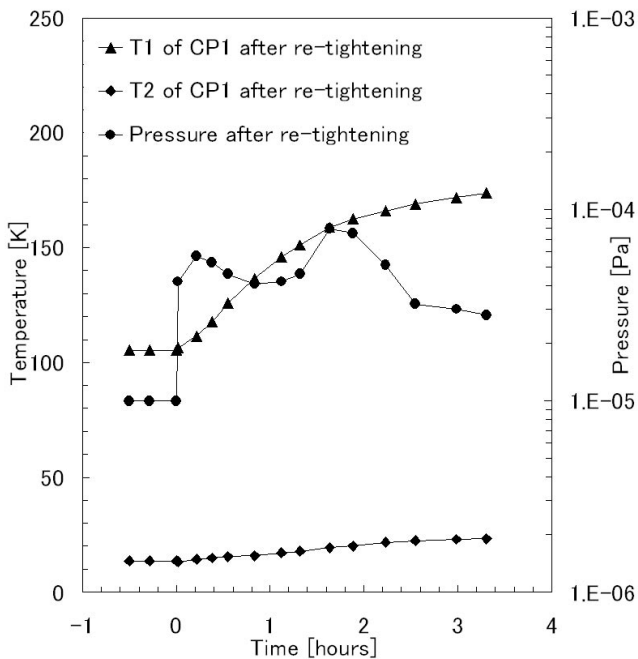


Fig. 3. The variation of temperature inside cryopumps, and vacuum pressure for RES4 after its rf voltage was set to 600kV at  $t=0$  after re-tightening.

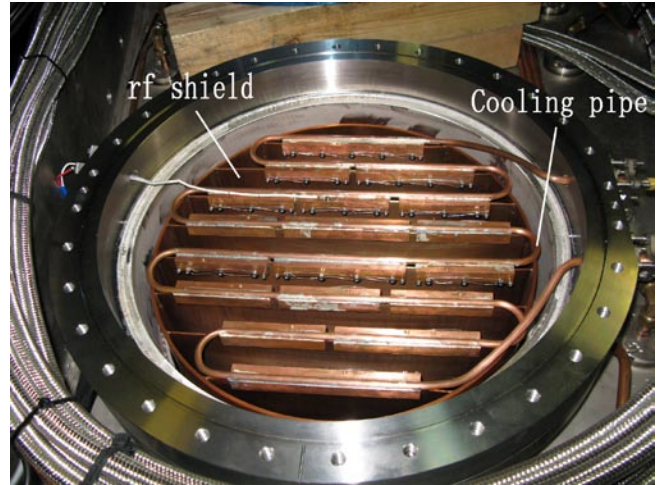


Fig. 4. Photograph of water-cooling device mounted at cryopump port flange.

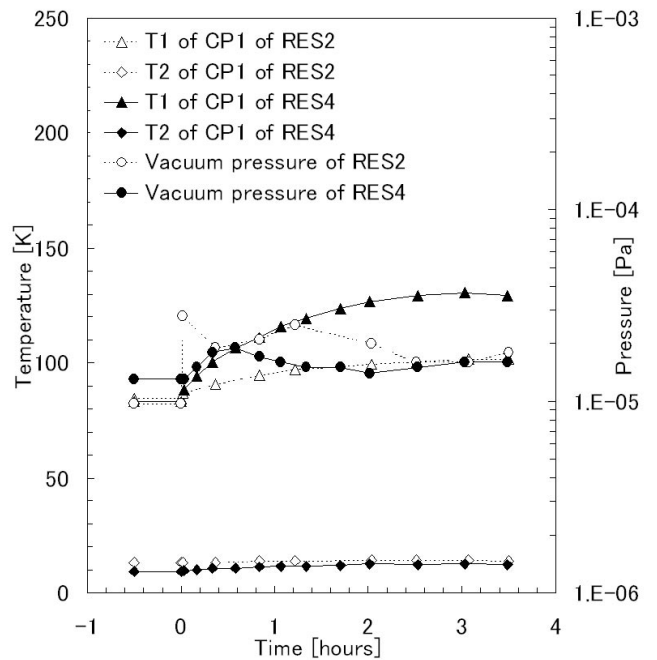


Fig. 5. The variation of temperature inside cryopumps, and vacuum pressure for RES2 and RES4 after each rf voltage was set to 600kV at  $t = 0$  after installing a water-cooling device. The solid lines represent the temperatures and pressure for RES4, and the dashed lines denote those for RES2.

#### References

- 1) S. Yokouchi et al.: RIKEN Accel. Prog. Rep. **42**, 226 (2009).

# The effect of vacuum pressure on transmission efficiency of RILAC

K. Oyamada,\* S. Yokouchi, N.Fukunishi, E. Ikezawa, and M. Kase

It is strongly required to improve the transmission efficiency of the RIKEN heavy-ion linac (RILAC) in order to obtain a higher beam intensity of uranium beam in the RI beam factory (RIBF).<sup>1)</sup> The transmission efficiency of  $^{35}\text{U}$  beam in RILAC was as low as 31% during the commissioning in early 2008, which is appreciably lower than typical transmissions, e.g. ~41% for  $^{56}\text{Fe}$ , and ~53% for  $^{64}\text{Zn}$ .

In the case of the acceleration and transport of a high-charge state heavy ion such as  $^{35}\text{U}$  in RILAC, the loss via the charge-exchange processes of the beam with residual gas in vacuum chambers may decrease the transmission efficiency. In fact, vacuum pressures of RILAC had been in the range of  $10^{-5}$  Pa. The vacuum required for the low energy  $^{35}\text{U}$  beam transport was estimated to be as low as  $10^{-6}$  Pa to keep the beam loss negligible. We investigated the effect of the vacuum pressure along the RILAC beam line on the overall transmission efficiency.

Figure 1 shows a layout of the RILAC. All the vacuum pumping system are shown in the figure. The whole beam lines are divided into fourteen sections; RFQ, rebuncher, six RILAC cavities and the beam lines between them. Each section is equipped with one or two vacuum pumping systems via an individual vacuum valve (VH). We measured the change in the overall transmission from RFQ to the CAVITY#6, when the vacuum pressure in section  $x$  was intentionally increased by closing the corresponding  $\text{VH}_x$  without changing the vacuum in neighboring sections.

The overall transmission efficiency of the RILAC that is defined as a ratio of the beam intensity at the location of e11 to that at the location of R1 is denoted by  $\eta_o$  which is obtained after sufficient beam tuning. Suppose that the initial transmission  $\eta_o$  is degraded to  $\eta_x$  as the vacuum pressure in section  $x$  is raised from the initial value  $p_{o_x}$  after  $\text{VH}_x$  is closed,

Since  $\eta_x/\eta_o$  denotes change in transmission of the vacuum section  $x$ , a beam loss ( $\lambda m_x$ ), which occurred additionally in the section is  $1 - \eta_x/\eta_o$ .  $\lambda m_x$  is considered to be approximately linear with respect to sufficiently small differences in the vacuum pressure,  $\Delta p_{m_x}$ , ( $=p_{m_x} - p_{o_x}$ ) assuming that both cross section and path length are constant. Therefore, an intrinsic beam loss ( $\lambda_x$ ) in the section  $x$  is calculated by  $\lambda_x = \lambda m_x \times (p_{o_x}/\Delta p_{m_x})$ .

Thus the estimated values from the measurements of  $\lambda_x$

at each section are plotted in Fig. 2. The beam loss in the upstream of RILAC was larger than that in the downstream expectedly. This result suggests that the vacuum effect on transmission efficiency is larger in the upstream of RILAC and that the improvement of the vacuum in the upstream is therefore more important. Although the  $\lambda_x$  in the section VAC12 looks large in Fig. 2, it was caused by a temporary increase in vacuum pressure during measurement and was certified to be normally as low as that in other sections in the downstream later.

Based on these results, the pumping systems for the three upstream sections, RFQ, 014, and CAVITY#1 were reinforced in the summer of 2008 as follows: one of the 1500 L/s TP's was replaced by a 2400 L/s CP in the RFQ, one new 220 L/s TP was added at the 014, and 2400 L/s TP was replaced to 13000 L/s CP in CAVITY#1. As for the rebuncher (REB), its vacuum system could not be improved under present circumstances. The estimation of effective pumping speeds for these three sections before and after the changes are summarized in Table 1. The changes in the vacuum pressures of the three sections are shown in Figure 3, and have improved corresponding to the increase in pumping speeds.

We received a transmission of ~40% during beam testing autumn 2008. This value for the transmission was improved by 10% from previous ones which can be explained by the measurement results in table 2. This improvement in transmission efficiency is thought to be mainly attributed to the reduction in the vacuum effect.

Section	Total pumping speed(L/s)		Improved ratio
	Before improvement	After improvement	
RFQ	1114	1672	1.5
014	216	376	1.7
CAVITY#1	4426	10585	2.4

Table 1. Comparison of total effective pumping speeds of CAVITY#1, RFQ, 014 and CAVITY#1 before and after the improvement of vacuum pumping system. Improved ratio represents the ratio of total effective pumping speed after the improvement to that which previously occurred.

\* SHI Accelerator Service, Ltd.

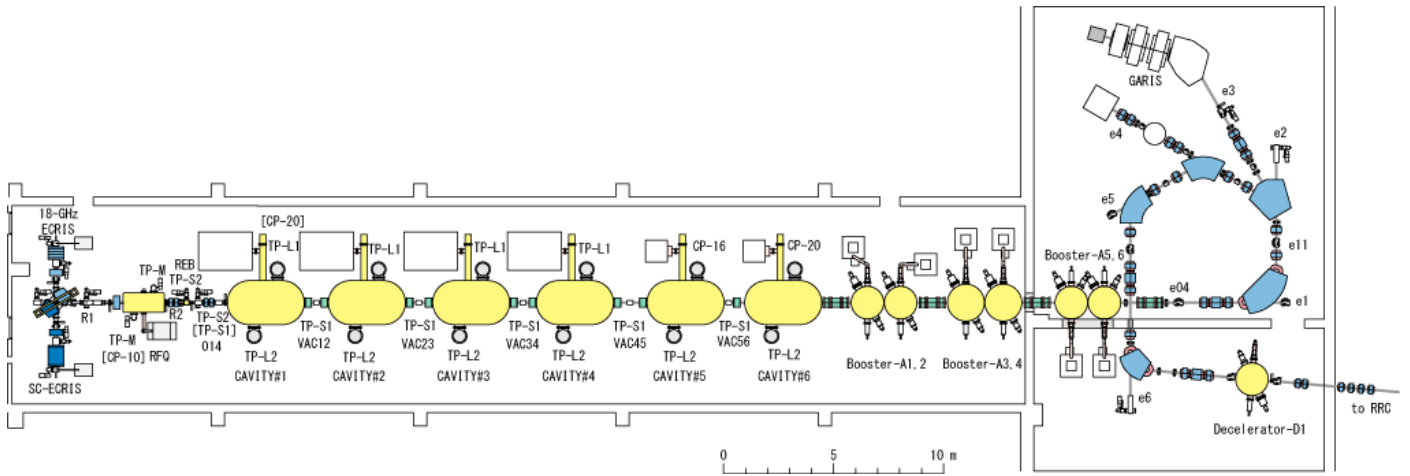


Fig. 1, Layout of the RILAC. TP denotes a turbomolecular pump, and the nominal pumping speeds of TP-, TP-L2, TP-M, TP- L1S1, and TP-S2 are 5000, 2400, 1500, 350, and 220 L/s respectively. CP- represents a cryopump, and the nominal pumping speeds of CP-20, CP-16, and CP-10 are 13000, 5000, and 2400 L/s respectively. Names in parentheses indicate those of the vacuum pumps replaced and name in brackets shows that of the vacuum pumps added in the improvement of the vacuum pumping system. The transmission efficiency of the RILAC is defined as the ratio of beam currents through e11 to that through R1.

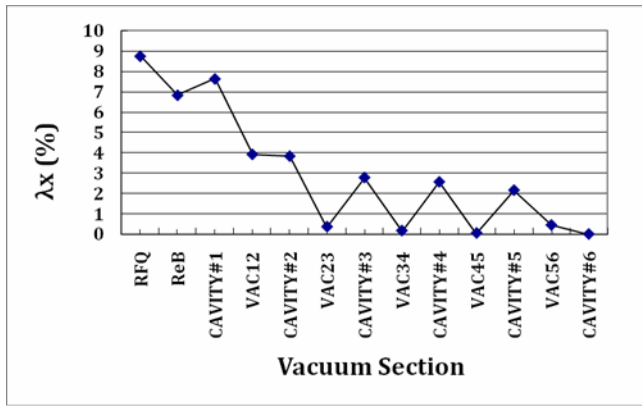


Fig. 2, Plot of intrinsic beam loss at each section

	$P0x(x10^{-6}Pa)$	$Pmx(x10^{-6}Pa)$	$\lambda x(\%)$	$D\lambda x(\%)$
RFQ	1.1E-05	4.7E-06	8.8	4.9
ReB	4.1E-05	2.9E-05	6.8	2.0
Cavity#1	7.2E-05	2.7E-05	7.6	4.8
Total				11.7

Table 2. The reduction of beam losses expected from improvement of vacuums in the three sections; RFQ, ReB, and Cavity#1. The result shows the transmission can be improved by a total of 12%.

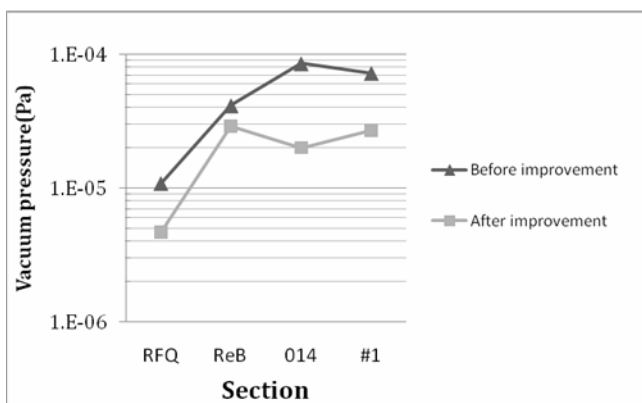


Fig. 3, Comparison of vacuum pressures of RFQ, REB, 014, and CAVITY#1 before and after the improvement of the vacuum pumping system when all GVs were open.

#### References

- 1) N. Nobuhisa et al.: RIKEN Accel. Prog. Rep. **41**, 85 (2008).
- 2) Y. Sato: private correspondence

## Development of polymer-coated carbon stripper foils

H. Hasebe, H. Okuno, H. Kuboki, N. Fukunishi, O. Kamigaito, A. Goto, M. Kase, and Y. Yano

Carbon foils (C-foils) are extensively used as charge strippers for heavy-ion beams at the RIKEN RI beam factory. As thicker C-foils became necessary, we started to develop polymer-coated carbon foils (PCC-foils)<sup>1)</sup> in 2005.

A beam test on the lifetime of C-foil with a fixed holder, with a racetrack-shaped hole of 14 mm x 23 mm, was performed in April 2008. The foil consisted of 5 poly-monochloro-para-xylene (Parylene) layers and 5 carbon layers. Multi-layer PCC-foils were irradiated with a 11 MeV/u  $^{238}\text{U}^{35+}$  beam at an intensity of 0.5 eμA that was delivered from the RIKEN ring cyclotron (RRC). The beam spot size was approximately 5 mm in diameter. The lifetime was determined by monitoring both the beam intensity of the stripped ions and the image of the C-foil on a TV display. Figure 1 shows photographs of two examples of multi-layer PCC-foils of 300 μg/cm<sup>2</sup> in carbon thickness after irradiation. Although the both foils were made in the same way, their lifetimes were substantially different; the foil in Fig. 1 (a) ruptured in a very short time and that in Fig. 1 (b) did not deteriorate even after 15 hours. Multi-layer PCC-foils are easily deformed by the heat due to beam irradiation because of the characteristics of Parylene.

Since the lifetime would become long if the Parylene was evaporated well or its polymer characteristics were lost, the final layer of the five Parylene layers was not deposited and the foils were put in an oven at 523 K (250 °C) for several hours before release off the glass substrate. PCC-foils made in this way stopped rupturing instantly, and all of them were usable for 6–24 hours in a beam study performed in July 2008. The beam condition in this beam study was the same as that of the previous test in April. These lifetimes are almost the same as those of C-foils (XCF-300) of the Arizona Carbon Foil Co. Inc.

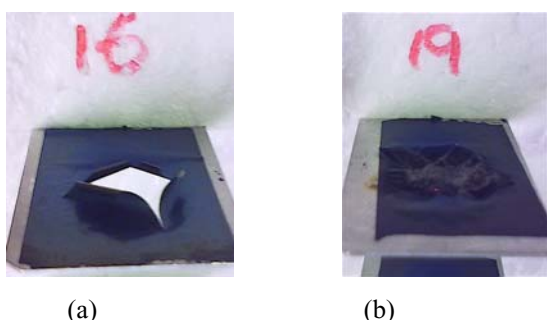


Fig. 1. Photographs of the 300 μg/cm<sup>2</sup>-thick multi-layer PCC-foils after irradiation with a  $^{238}\text{U}^{35+}$  beam: (a) PCC-foil that ruptured in a short time and (b) PCC-foil that was still usable after more than 15 hours.

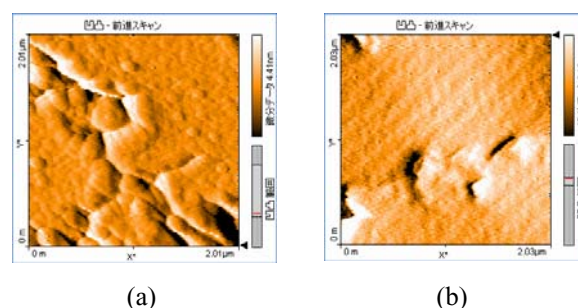


Fig. 2. AFM images of the surface of the substrate side of the 300 μg/cm<sup>2</sup>-thick multi-layer PCC-foil: (a) non-irradiated part and (b) irradiated part.

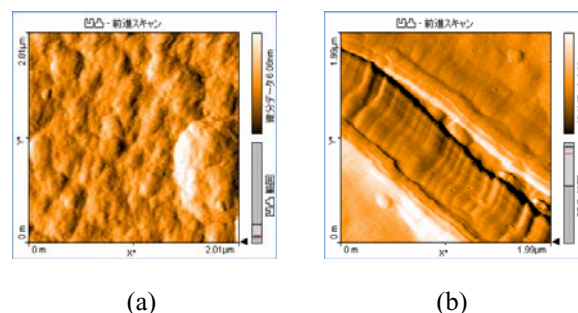


Fig. 3. AFM images of the surface of the evaporating source side of the 300 μg/cm<sup>2</sup>-thick multi-layer PCC-foil: (a) non-irradiated part and (b) irradiated part.

An Atomic Force Microscope (AFM)<sup>2)</sup> was introduced to observe the surface of thin C-foils. Figures 2 and 3 show the observed surface images of the non-irradiated part and the irradiated part of the 300 μg/cm<sup>2</sup>-thick PCC-foils, respectively. The imaged area size was 2 μm x 2 μm. The surface of the substrate side of the non-irradiated part, as shown in Fig. 2 (a), was observed to be flat with a small amount of rough area and to have crushed carbon mounds (200 – 300 nm in diameter). On the other hand, the surface of the evaporating source side, as shown in Fig. 3 (a), was observed to be quite rough and to have many carbon mounds attached. The surface of the PCC-foils after beam irradiation changed drastically. The surface of the substrate side of the irradiated part, as shown in Fig. 2 (b), was observed to have no carbon mounds but to be in a melted state. The surface of the evaporating source side, as shown in Fig. 3 (b), was also observed to have no carbon mounds but big cracks. The surface of the evaporating source side changed more drastically than that of the substrate side; this is the reason why we stopped depositing the final layer of the five Parylene layers.

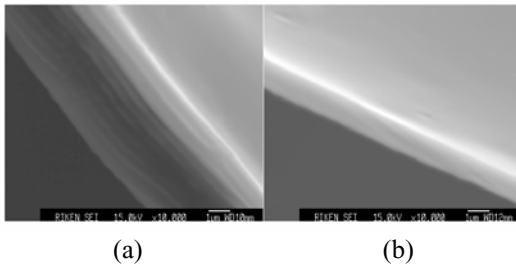


Fig. 4. SEM images of the cross section of the 500  $\mu\text{g}/\text{cm}^2$ -thick multi-layer PCC-foil: (a) non-irradiated part and (b) irradiated part.

A multi-layer PCC-foil of 500  $\mu\text{g}/\text{cm}^2$  in carbon thickness, which was used as a charge stripper in another beam study, was observed with an Scanning Electron Microscope (SEM)<sup>3)</sup> and an Electron Probe Micro Analyzer (EPMA)<sup>3)</sup>. The beam condition was the same as in the beam test on the lifetime of foils. Fig. 4 (a) and (b) show SEM images of the cross section of the PCC-foil at the non-irradiated part and irradiated part, respectively. The irradiated part was observed to be one layer with 1  $\mu\text{m}$  in thickness due to evaporation of Parylene, while the non-irradiated part was observed to be 10 layers with 3  $\mu\text{m}$  in total thickness. The reason for the drastic decrease in thickness is thought to be heat deformation by the beam. Fig. 5 (a) and (b) show results of qualitative analysis using the EPMA for the non-irradiated part and irradiated part, respectively. Peaks of Ar from the sputtering source and Cl from Parylene observed in the spectra for the non-irradiated part disappeared in that for the irradiated part.

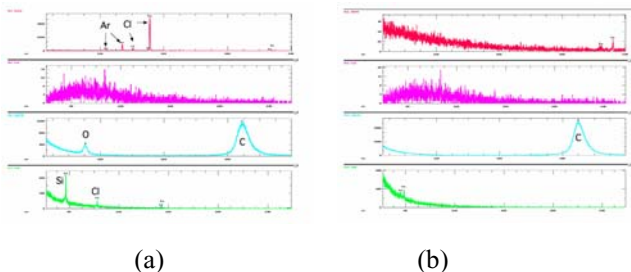


Fig. 5. Results of qualitative analysis using an EPMA for the 500  $\mu\text{g}/\text{cm}^2$ -thick multi-layer PCC-foil: (a) non-irradiated part and (b) irradiated part.

The lifetime of multi-layer PPC foils set in the rotating-cylinder stripper device<sup>4)</sup> was measured in May 2008. The foils were made of 5 layers of carbon plus 5 layers of Parylene (the final layer of Parylene was still deposited), with carbon thickness of 300  $\mu\text{g}/\text{cm}^2$  and diameter of 10 cm. The foils were rotated with a speed of 100–300 rpm and the beam was again a 11 MeV/nucleon  $^{238}\text{U}^{35+}$  beam with an intensity of 0.5  $\mu\text{A}$ . The measurement was performed for two foils: the first one was treated in the oven at 573 K (300 °C) for 2.5 hours before releasing it off the glass substrate and the second one was not treated. The result was that both foils ruptured in a time as short as 25 min. and 10 min, respectively. Figure 6 shows a photograph of the first foil after beam irradiation. A lot of holes were produced almost all along the beam-irradiated

ring area, and a big circular area inside the ring was torn off the foil when it was taken out from the device (see Fig. 7). The width of the beam-irradiated ring area was estimated to be approximately 5 mm, which corresponded to the beam spot size. A diamond-like C-foil manufactured by TRIUMF<sup>5)</sup> also ruptured in the same way after approximately 9 hours irradiation. The lifetimes of C-foils for the rotating-cylinder stripper device were found to be worse than or equivalent to those for the fixed holder, contrary to the expectation that the former would provide tens of times better performance than the latter. The rapid change in temperature in the beam-irradiated area due to the slow rotation speed might cause such results.

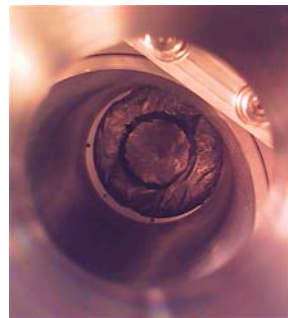


Fig. 6. Photograph of the 300  $\mu\text{g}/\text{cm}^2$ -thick multi-layer PCC-foil that was set in the rotating-cylinder stripper device and ruptured after 25-min beam irradiation. The ring area was discolored due to beam irradiation.

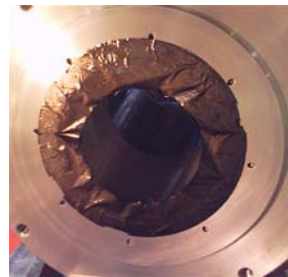


Fig. 7. Same as Fig. 6 except that the foil was removed from the device. A big circular area inside the ring was torn off the foil.

## References

- 1) H. Hasebe, H. Ryuto, N. Fukunishi, A. Goto, M. Kase, and Y. Yano: RIKEN Accel. Prog. Rep. **40**, 128 (2007).
- 2) Nanosurf AG, URL: <<http://www.nanosurf.com/>>.
- 3) K. Watanabe, RIKEN AD&SC
- 4) H. Ryuto, H. Hasebe, N. Fukunishi, S. Yokouchi, A. Goto, M. Kase, and Y. Yano: “Rotating charge strippers for acceleration of intense heavy-ion beams at RIKEN”, Nucl. Instrum. Methods Phys. Res. A **569**, 697 (2006).
- 5) TRIUMF Carbon Foil Laboratory

## Offline test of a gas charge stripper for uranium beams

H. Kuboki, H. Okuno, S. Yokouchi, T. Kishida, H. Hasebe, N. Fukunishi, O. Kamgaito, H. Ryuto,<sup>\*1</sup> M. Kase, A. Goto, and Y. Yano

Charge strippers play an essential role in a heavy-ion accelerator complex, since a high-charge state enables an acceleration of heavy-ion beams up to a high energy with small accelerators. The ions at a higher velocity are charge-stripped to a higher charge state<sup>1)</sup>. Therefore, the efficient acceleration of heavy-ion beams is realized by charge strippers placed between sequentially connected accelerators.

The RIKEN RI-beam factory (RIBF) is such a heavy-ion accelerator complex<sup>2)</sup>. At the RIBF, two stripper sections are used to accelerate uranium ions up to 345 MeV/nucleon<sup>3)</sup>. Figure 1 shows a schematic view of the RIBF. Heavy ions extracted from the

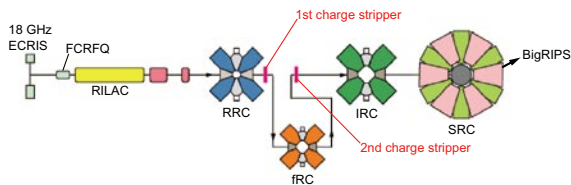


Fig. 1. Schematic view of the RIBF. The accelerators are shown with the ion source and the two charge strippers.

RIKEN 18 GHz ECR ions source<sup>4)</sup> are accelerated successively by the RIKEN heavy-ion linac (RILAC), the RIKEN ring cyclotron (RRC), the fixed-frequency ring cyclotron (fRC)<sup>5)</sup>, the intermediate-stage ring cyclotron (IRC)<sup>6)</sup>, and the superconducting ring cyclotron (SRC)<sup>7)</sup>. The two stripper sections are placed downstream of the first two cyclotrons, the RRC and the fRC. The beam energies incident on these two strippers are 11 and 51 MeV/nucleon, respectively. The first charge stripper strips uranium ions with a charge state of 35+ to 71+ which is the lowest charge state that enables uranium ions to be accelerated with the fRC. The second charge stripper strips  $U^{71+}$  ions to  $U^{86+}$  in order to accelerate uranium ions with the IRC. At present, carbon foils with a thickness of  $300 \mu\text{g}/\text{cm}^2$  and  $13.9 \text{ mg}/\text{cm}^2$  are used as the first and second charge strippers, respectively. The irradiation conditions at the two stripper sections are summarized in Table 1. Especially, the first stripper has two serious problems: 1) The foils have short lifetime (at most 24 hours) caused by heat load and mechanical stress of the irradiation. 2) The energy spread of the beam after the first charge stripper is estimated to be 0.55% ( $4\sigma$  value)<sup>8)</sup>, which is beyond the acceptance (0.2%) of the rebuncher<sup>9)</sup> placed between the RRC and the fRC.

We focus on a gas charge stripper as a new can-

didate to overcome two problems mentioned above, since a gas charge stripper has a very uniform thickness and is tolerant of heat load. One weak point is that a charge state lower than 71+ may be obtained due to the *density-effect*<sup>10)</sup>. In the case of gas strippers, the time between collisions is sufficient for excited projectiles to return to their ground states before entering into subsequent collisions. Since the cross section for ionization is larger when projectiles are in excited states than when projectiles are in the ground state, we may obtain charge states lower than that in the case of carbon foil strippers. A semi-empirical formula obtained by Sayer<sup>11)</sup> predicts that the charge state we can obtain using a gas charge stripper would be 63+. However, the data used to derive the formula does not match our case. Perumal et al.<sup>10)</sup> have also mentioned charge states of uranium ions stripped by gas charge strippers. The highest energy referred in Ref.<sup>10)</sup> has been 3.5 MeV/nucleon. Therefore, no one actually knows the charge states of uranium ions obtained by gas charge strippers at  $\sim 10$  MeV/nucleon.

We have developed a gas charge stripper using the windowless type gas target system<sup>12)</sup>. An overview of the gas charge stripper system for offline test is shown in Fig. 2. Figure 3 shows a schematic diagram together

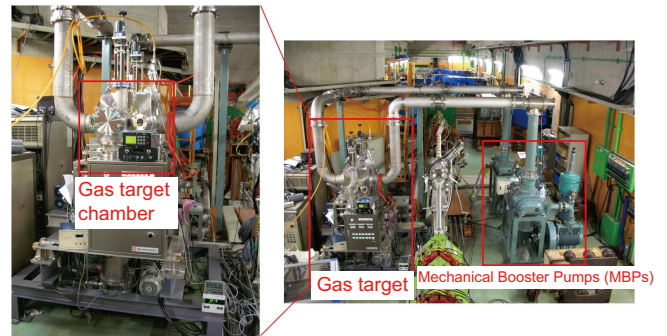


Fig. 2. Overview of the gas charge stripper system located at the D-room.

with its differential pumping system. The region in the target cell is defined as stage 1. The length of the target cell is 10 cm. The region outside of the target cell is defined as stage 2. Similarly, stage 3–5 denote the regions outside of stage 2–4, respectively. The pressure at each stage is indicated by  $P_1$ – $P_5$ , respectively. Since the gas charge stripper is operated in a beamline, the pressure  $P_1$  should be high and the pressure away from the target cell should fall as rapid as possible. We performed an offline test of the gas charge stripper with nitrogen gas injected into the target cell. The results

<sup>\*1</sup> Photonics and Electronics Science and Engineering Center, Kyoto University

Table 1. The irradiation conditions at the two stripper sections.

stripper	ion	energy (MeV/nucleon)	carbon thickness	beam intensity (pnA)	heat load (W)	spot diameter (mm)
1st	$^{238}\text{U}^{35+}$	11	$300 (\mu\text{g}/\text{cm}^2)$	14	0.50	5
2nd	$^{238}\text{U}^{71+}$	51	$13.9 (\text{mg}/\text{cm}^2)$	3.7	3.2	5

are shown in Fig. 4. The pressures  $P_2$ – $P_5$  are plotted as a function of  $P_1$ . We can obtain higher charge states

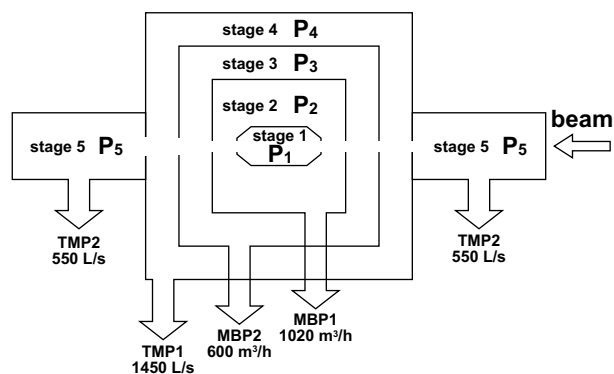


Fig. 3. Schematic diagram of the gas charge stripper with its differential pumping system<sup>12)</sup>. The target cell (stage 1) is located at the center. The length of the target cell is 10 cm. Other stages are also shown with pumping speeds of the attached pumps. Four apertures before the beam entrance into the target cell are 6 mm in diameter. The exit of the target cell and the exit of the stage 2 have also 6 mm diameter apertures. The exit of the stage 3 and 4 have 8 mm and 10 mm diameter apertures, respectively.

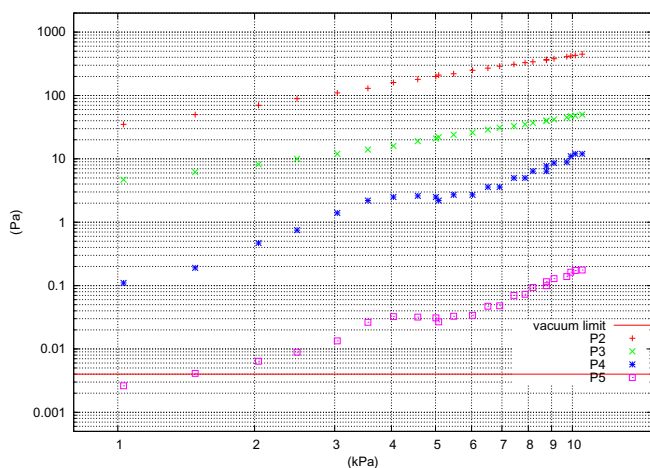


Fig. 4. The pressure at each stage is plotted as a function of  $P_1$ . Solid line shows the limit for an interlock ( $4 \times 10^{-3}$  Pa).

with a thicker charge stripper. However, in the case of carbon foils, the averaged charge state achieves equi-

librium at a thickness of  $500 \mu\text{g}/\text{cm}^2$ <sup>3)</sup>. With an assumption that the thickness for an equilibrium charge state using nitrogen gas is the same as that in the case of carbon foils, the thickness above  $500 \mu\text{g}/\text{cm}^2$  should be needed. The thickness estimated from the maximum pressure of 10.5 kPa was  $1.18 \text{ mg}/\text{cm}^2$ . However, a limitation of  $P_1$  is practically determined by  $P_5$ . The pressure  $P_5$  should be lower than  $4 \times 10^{-3}$  Pa which is the limit for an interlock. The results indicate that the pressure  $P_1$  should be maintained lower than 1.4 kPa ( $157 \mu\text{g}/\text{cm}^2$ ) to keep the pressure  $P_5$  under the limit.

We are planning to obtain data of the charge distribution with uranium beams at 11 MeV/nucleon in March 2009. To control  $P_1$  up to higher pressure, an additional stage (stage 6) and a couple of turbo molecular pumps will be introduced. A test with helium gas is also planned to investigate dependence on materials.

#### References

- 1) C. Scheidenberger et al., Nucl. Instr. and Meth. B **142**, 441 (1998).
- 2) Y. Yano, Nucl. Instr. and Meth. B **261**, 1009 (2007).
- 3) H. Ryuto et al., Proc. 2005 Particle Accelerator Conference, Knoxville, USA, 2005, p.3751.
- 4) T. Nakagawa et al., Nucl. Instr. and Meth. B **226**, 392 (2004).
- 5) T. Mitsumoto et al., Proc. 17<sup>th</sup> Int. Conf. on Cyclotrons and Their Applications, 384 (2004).
- 6) J. Ohnishi et al., Proc. 17<sup>th</sup> Int. Conf. on Cyclotrons and Their Applications, 197 (2004).
- 7) H. Okuno et al., Proc. 17<sup>th</sup> Int. Conf. on Cyclotrons and Their Applications, 373 (2004).
- 8) N. Fukunishi et al., RIKEN Accel. Prog. Rep. **41**, 81 (2007).
- 9) T. Aoki et al., Nucl. Instr. and Meth. A **592**, 171 (2008).
- 10) A.N. Perumal et al., Nucl. Instr. and Meth. B **227**, 251 (2005).
- 11) R.O. Sayer, Rev. de Phys. Appl. **12**, 1543, (1977).
- 12) T. Kishida et al., Nucl. Instr. and Meth. A **438**, 70 (1999).

## Practical use of beam current monitor with HTS current sensor and HTS SQUID at RIBF

T. Watanabe, Y. Sasaki, M. Kase, N. Fukunishi and Y. Yano

A highly sensitive beam current monitor with an HTS (high-temperature superconducting) SQUID (superconducting quantum interference device) and an HTS current sensor, that is, an HTS SQUID monitor, has been developed for use with the RIBF (RI beam factory) at RIKEN<sup>1-3</sup>). Unlike other existing facilities, the HTS SQUID monitor allows us to measure the DC of high-energy heavy-ion beams nondestructively in real time, and the beam current extracted from the cyclotron can be recorded without interrupting the beam user's experiments. Both the HTS magnetic shield and the HTS current sensor were dip-coated to form a  $\text{Bi}_2\text{-Sr}_2\text{-Ca}_2\text{-Cu}_3\text{-O}_x$  (Bi-2223) layer on 99.9% MgO ceramic substrates. In work conducted presently, all the fabricated HTS devices are cooled by a low-vibration pulse-tube refrigerator. These technologies enabled us to downsize the system. Prior to practical use at the RIBF, the HTS SQUID monitor was installed in the beam transport line of the RIKEN ring cyclotron to demonstrate its performance. As a result, a  $20 \mu\text{A}$   $^{40}\text{Ar}^{15+}$  beam intensity (63 MeV/u) was successfully measured with a 500 nA resolution. Despite the performance taking place in an environment with strong gamma ray and neutron flux radiation, RF background and large stray magnetic fields, the measurements were successfully carried out in this study. This year, the HTS SQUID monitor was upgraded to have a resolution of 100 nA. We will report the present status of the

monitor system.

Although the intensity of a sub-micro-ampere beam can be measured, a limit of a minimum current higher than two orders of magnitude is required for fainter beam measurement. The possibility of fabricating a new HTS current sensor and introducing high-permeability cores into the HTS SQUID through two holes has been investigated<sup>3</sup>). The cores are composed of 80% Ni and Mo, Re and Fe. A test using a simulated beam current shows a 50-fold improvement in gain, when the wire used as the simulated beam was wound directly on the high-permeability cores. However, we could not obtain the simulated beam current signal, when both the HTS SQUID and the HTS current sensor were used. The HTS SQUID sensor plays a role in detecting the beam current, from which we assumed the reason the signal could not be obtained was that the HTS current sensor could not reach a superconducting state. If the critical temperature of the HTS current sensor is lower than that of liquid nitrogen, the HTS current sensor was no longer be in a superconducting state. Then in order to cool the HTS current sensor and the HTS SQUID to below the temperature of liquid nitrogen, we chose a method using the cryostat of the HTS SQUID monitor by exchanging all components inside the cryostat. A new cooling mechanism inside the cryostat was designed and fabricated for these purposes. As a result, the HTS current sensor could reach superconducting state at a temperature of 68 K. On the other hand, because the HTS SQUID was designed to achieve the best performance at the temperature of the liquid nitrogen (77K), it could not operate properly at a temperature of 68K. Therefore, the examination to confirm whether these HTS components achieved high sensitivity is being postponed

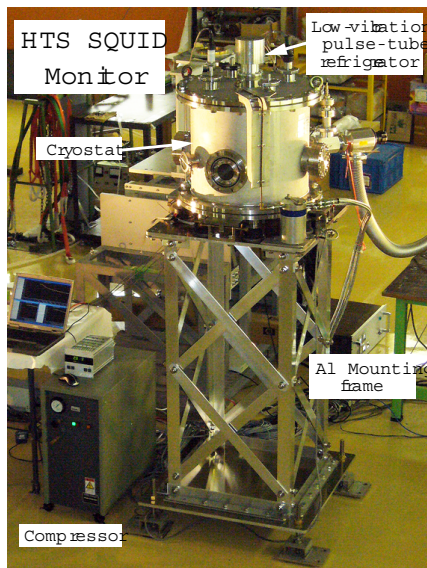


Fig. 1. The HTS SQUID monitor equipped with new HTS SQUID containing a high-permeability core and Al mounting frame was reassembled.



Fig. 2. Photograph of new HTS SQUID with two holes containing high-permeability core.

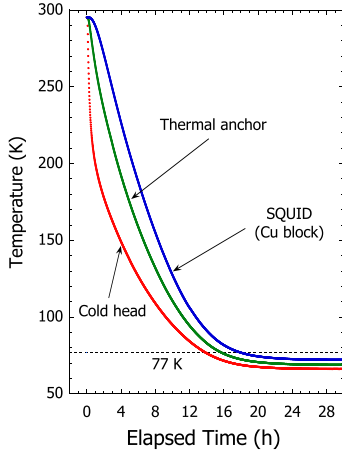


Fig. 3. Cooling processes recorded for over 30 h using silicon diode thermometers.

for the present.

Aiming for a practical use for accelerator operations at the RIBF, we reassembled the HTS SQUID monitor with the new HTS SQUID containing a high-permeability core and an aluminium mounting frame (Fig. 1). The previous frame made of iron was replaced with one made of aluminium with a relative permeability of 1. Figure 2 shows a photograph of the new HTS SQUID with two holes containing the high-permeability core. An HTS magnetic shield and the HTS current sensor, including the HTS SQUID, are cooled by a pulse-tube refrigerator which is a low vibration type and has a refrigeration power of 11 W at a temperature of 77 K. Figure. 3 shows the results of the cooling processes; temperatures of the cold head, the thermal anchor and the Cu block holding the HTS SQUID were recorded for over 30 h using silicon diode thermometers. The temperature of the HTS SQUID was found to reach the temperature of liquid nitrogen (77 K) after 16.5 h. The output voltage of the HTS SQUID controller as a function of the simulated beam current is plotted in Fig. 4. From these measurement

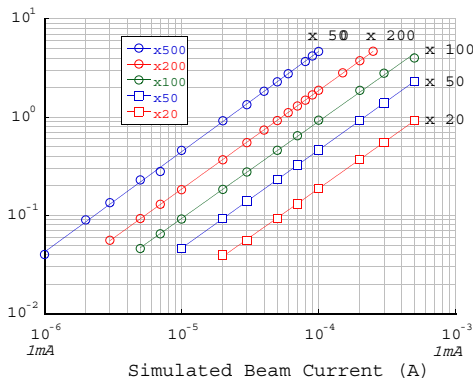


Fig. 4. Plot of output voltage of the HTS SQUID controller as a function of simulated beam current.

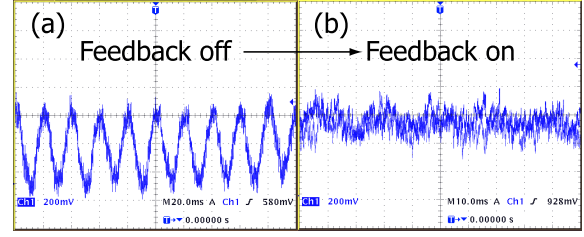


Fig. 5. Effect of removal of environmental noise by introducing the noise cancellation system.

results, the calibration equation obtained is

$$\begin{aligned} V_s &= S_{co} \times I_b \times G/500 \\ &= 46.60 \times I_b \times G/500, \end{aligned}$$

where  $S_{co}$ ,  $I_b$ ,  $V_s$  and  $G$  are the coupling efficiency ( $\text{mV}/\mu\text{A}$ ), the beam current ( $\mu\text{A}$ ), the output voltage of the HTS SQUID controller ( $\text{mV}$ ) and the gain, respectively. A test using a simulated beam current showed a 2-fold improvement in gain, because the coupling efficiency  $S_{co}$  of the HTS SQUID monitor was  $22.8 \text{ mV}/\mu\text{A}^1$ . The transfer of the magnetic field produced by the simulated beam current to the HTS SQUID was thus improved.

To obtain a better resolution for the measurement, we paid close attention to the reduction of noise. A noise-cut transformer which is completely isolated from the power circuit and not affected by AC source noise was introduced. Furthermore, all instruments were fixed onto a large aluminum plate and the grounds of the instruments were connected to the plate. The signal cables were wired carefully to reduce unnecessary loops as much as possible and all AC lines were covered with braided wires. The design of the noise cancellation system is based on a three-axis Helmholtz cage and feedback control engineering. Three-axis flux-gate sensors are placed near the equipment. A signal is fed through the proprietary controller to a compensation coil, producing precisely calibrated electromagnetic fields. The preliminary result in Figs. 5 (a) and (b) shows the effect of the removal of environmental noise by introducing the noise cancellation system. The data acquisition and control program being written by LabVIEW (National Instruments, Ltd.) is almost complete, but some modification is necessary.

The authors are grateful to E. Nemoto of JEOL DATUM, Ltd., for his cooperation regarding the noise cancellation system.

#### References

- 1) T. Watanabe et al., Supercond. Sci. Technol. **17** S450 (2004).
- 2) T. Watanabe et al.: Journal of Physics **43**, 1215 (2006).
- 3) T. Watanabe et al.: Journal of Physics **97**, 012248 (2008).

## Development of ion beam core monitor

H. Watanabe, S. Watanabe,<sup>\*1</sup> R. Koyama,<sup>\*2</sup> and M. Kase

A nondestructive ion beam core monitor has been developed to measure the intensity of a beam current. It is particularly useful if one can continuously monitor the ion beam current without interrupting the ion beam. The core monitor has been installed into the RIKEN ring cyclotron output beamline to measure ion beams. We report here the test experiments for nondestructive ion beam monitoring of the cyclotron using a toroidal transformer.

We used a Fast Current Transformer (FCT) manufactured by BERGOZ Instrumentation. The transformer, model FCT-082-05:1-H-INS, consists of a toroidal core made of cobalt-based nanocrystalline and amorphous alloys of 82 mm inner diameter and a five-turn coil wound by the proprietary multithread technique. The multithread winding is a technique of core winding whereby there are few turns around the core. Many parallel wires are wound, clockwise and anticlockwise. The principle of the transformer detector is shown in Fig. 1.

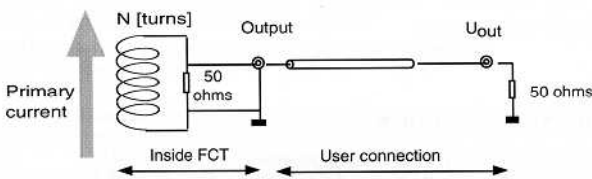


Fig. 1 Schematic diagram of core monitor.

The cyclotron beam is equivalent to a single-turn coil on the primary side of the transformer which induces a magnetic flux in the toroidal core, resulting in an induced current in the secondary coil. The bandwidth of the FCT is 32 kHz – 700 MHz and the typical rise time is 500 ps. The fast response of the detector allows us to observe the higher harmonics of the pulsed beam. Since the bunch width of the cyclotron beam is very short, it generates many harmonics and the higher order harmonics have almost the same power as the fundamental one (36.5 MHz). It is advantageous to observe higher order harmonics, since the ambient noise generally decreases with increasing frequency.

In order for the transformer to measure a current passing through its center, the wall current imaging the ion beam must be diverted around the outside of the device. The beam pipe of 63.5 mm diameter is electrically isolated by a PEEK sleeve of 4 mm width and the FCT is mounted close to the gap. A SUS304 box cover, shown in Fig. 2, forms the FCT electrostatic shielding as well as the electrical

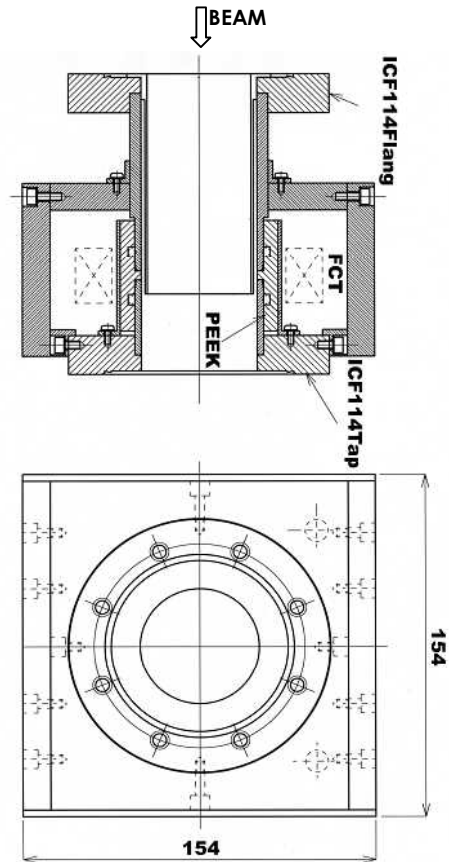


Fig. 2 Mechanical drawing of FCT box cover.

connection between the interrupted beam pipe outside the FCT. The signal from the FCT is sent to a low-noise preamplifier (model SA-230F5) produced by NF corporation. The gain of the preamplifier is 46 dB. The signals obtained from the preamplifier were measured by a spectrum analyzer.

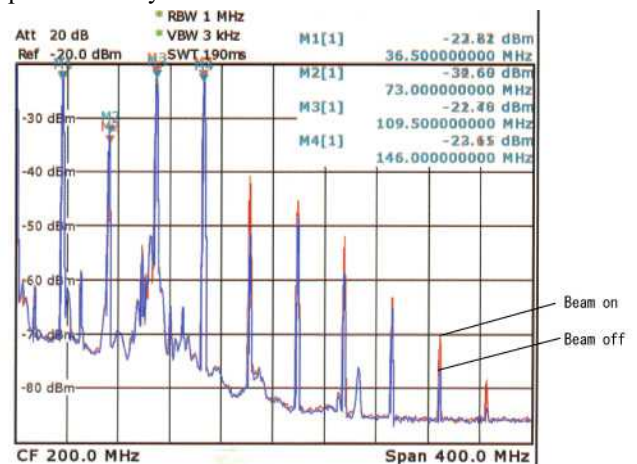


Fig. 3 Power spectrum of <sup>48</sup>Ca<sup>16+</sup> beam of 2.1 euA detected

<sup>\*1</sup> Center for Nuclear Study, University of Tokyo  
<sup>\*2</sup> SHI Accelerator Service, Ltd.

by the FCT.

The result is shown in Fig. 3. As expected, it is advantageous to observe higher order harmonics, since the ambient noise decreases with increasing frequency. In the future, beam current calibration will be done against a Faraday cup or an additional FCT one-turn coil which a standard current flows through.

## Radiation monitoring in the SRC using an ionization chamber.

M. Nakamura, H. Fukuda, K. Yamada and M. Kase

Recently, experiments of the RIBF using the SRC were successfully performed. Nevertheless, beam loss was still a serious problem from the first experiment. To detect the beam loss, we can monitor radiation generated by the interaction of ion beams with accelerator components. However, the radiation is too intense to use the usual detectors. Therefore, we have made an ionization chamber which has quite a simple structure and is solidly built. For this report, we tried to monitor radiation from the SRC during beam extraction using this ionization chamber.

The size of the ionization chamber was 400 mm x 250 mm x 80 mm. Two electrodes were included in the chamber. One electrode was for high voltage (HV), and the other was an ion collector for when radiation enters the ionization chamber. Al plates with 1.5 mm thickness were used for the electrodes. The size of the electrode was 200 mm x 360 mm. These two electrodes were placed at 25 mm interval. The chamber was not built as a vacuum chamber and was filled only with air. Hence, we can detect the ion current of air in this chamber, generated by radiations from the SRC.

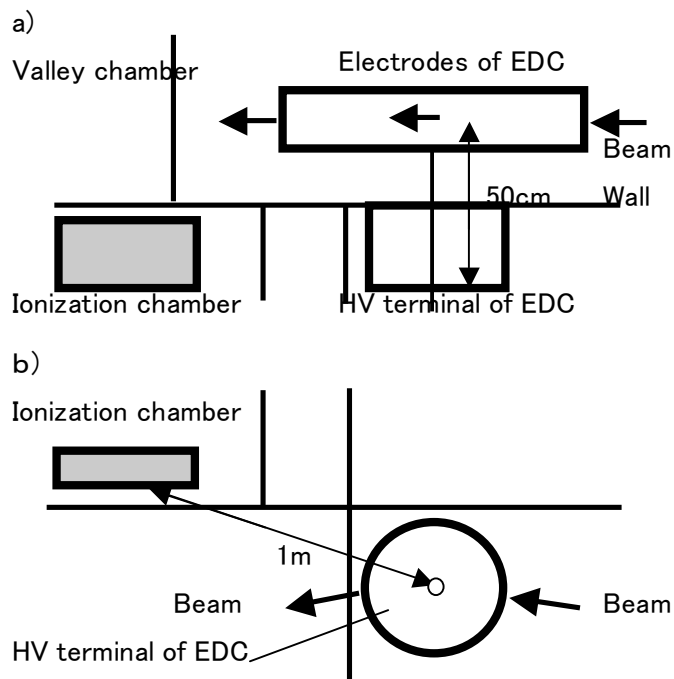


Fig. 1. Location of ionization chamber.  
a) Side view. b) View from lower part.

Strong radiation was generated from the septum of the electrostatic deflector (EDC) in the SRC when ion beams

were accelerated. The radiation could be strongly observed in the tangent direction of the ion beam. Therefore, the ionization chamber was set on the under side and in the diagonally forward direction of the EDC irradiated by the ion beam.

The location of ionization chamber is shown in Fig. 1 a) and b). The bottom of the HV terminal of the EDC was about 50 cm under the center of the EDC electrodes in the valley chamber. The bottom of the ionization chamber was set nearly as high as the bottom of the HV terminal (shown in Fig.1 a)). The distance between the center of the HV terminal and the ionization chamber was about 1 m (shown in Fig. 1 b)). A few stainless steel walls are present between the electrodes of the EDC and the ionization chamber.

FLUKE 415B was used for the power supply to the HV electrode. An ADVANTEST R8240 digital-electrometer was used for the monitor which transforms current between the two electrodes into voltage. A YOKOGAWA MX-100 was used for data acquisition of R8240 electrometer. Data was captured every 0.1 seconds.

We monitored radiation during RIBF operation from December 5 to 25, 2008. During this operation,  $^{48}\text{Ca}$  was accelerated to 345 Mev/nucleon. During this period, 1 kV voltage was always supplied to the HV electrode of the ionization chamber.

Figure 2 a) and b) show examples of the observed data recorded by the data-logger. In these figures, the horizontal axis shows the observation period and the vertical axis shows the voltage monitored by the electrometer. For the vertical axis of these figures, 0.01 V corresponds to 1 nA of current generated between the HV and collector electrodes. In the period shown in Fig. 2 a), the  $^{48}\text{Ca}$  beam was accelerated. In the period shown in Fig. 2 b), the ion beam was stopped. The difference between Fig. 2 a) and b) is clearly evident.

In Fig. 2 b), we can not observe any significant signals. On the other hand, in Fig. 2 a), we can observe about 14 nA of current at the maximum value and about 6-7 nA at the average value. These current values correspond to ion generation caused by radiation from the  $^{48}\text{Ca}$  beam interacting with SRC components (mainly, EDC).

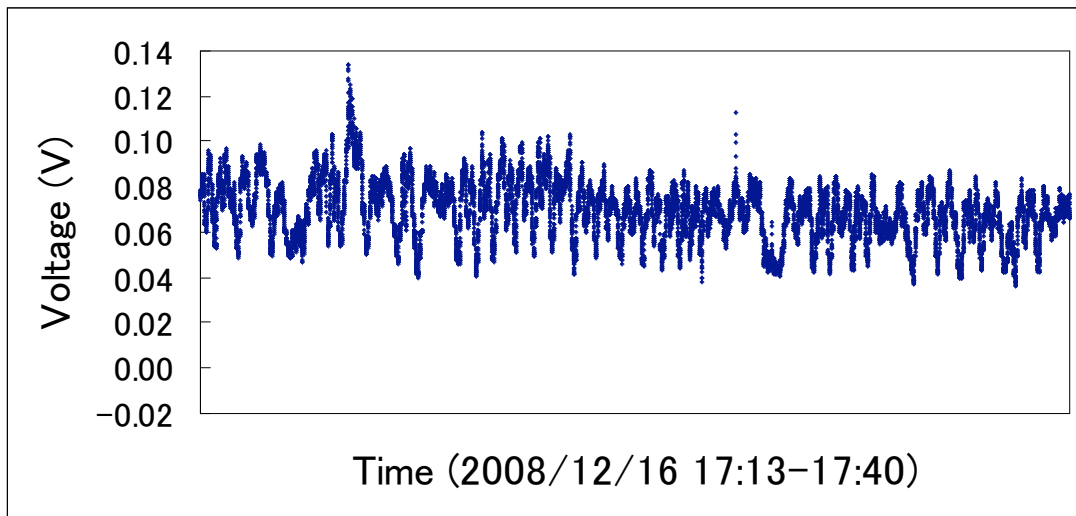
At this stage, the radionuclide observed by the ionization chamber can not be identified. However, considering the penetrating power of the radiation and ion-pair formation of air, we presume that protons entered chamber and ionized the air. If we assume the ion-current was made by 100 MeV/nucleon protons and ionization loss of protons was about 1 Mev, then 6-7 nA of current could be generated

by about  $6 \times 10^6$  protons/s.

In this experiment, we were at least able to observe the radiation from SRC using this “simply-made” ionization chamber. By detecting the voltage of the ionization chamber, we can also adjust the RIBF components (mainly,

EDC in SRC) at the best location and the beam-loss of RIBF smaller. For the next stage, we plan to set some ionization chambers in RIBF and monitor the beam-loss at these positions simultaneously.

a)



b)

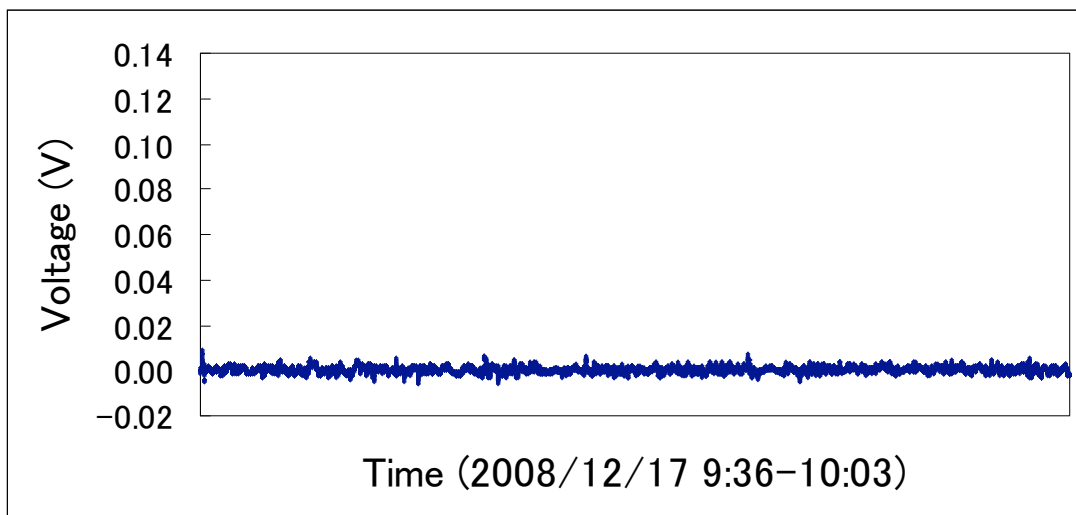


Fig. 2. Observed values of ionization chamber during RIBF commissioning.

a)  $^{48}\text{Ca}$  beam was emitted.      b) Ion beam was stopped.

## Performance Tests of Old Power Supplies in RIBF

Makoto Nagase, Nobuhisa Fukunishi, Seiji Fukuzawa<sup>\*1</sup>, Eiji Ikezawa, Keiko Kumagai, Kazuyoshi Yadomi<sup>\*1</sup>, Hiroshi Watanabe and Masayuki Kase

Magnet power supplies of RIKEN Ring Cyclotrons (RRC) and its beam transport system<sup>1)</sup> have been used for more than 20 years and we carried over these power supplies in RIBF accelerator complex. As a natural consequence of twenty years operation, we have experienced troubles on these power supplies several times, for example, leakage of water caused by corrosion of cooling water pipe.

As reported in Ref. 2, we started measurements on the accuracies, linearities and stabilities of these old power supplies last year. The main purpose of the measurements is to determine precisely the operation parameters of the magnets. These measurements also give us important information on deterioration of magnet power supplies. Hence, we continued measurements for a part of remaining old power supplies in 2008. Measurements were performed one by one during the periods in which beam services to RIBF users were not scheduled, because stability measurements require long time.

We employed high precision DC current transformers (DCCT)<sup>3,4)</sup> in the measurements as reported in Ref. 2. Accuracies of setting currents and long-term stabilities are directly measured by the DCCT employed. The linearity is estimated by increasing or decreasing the current with a constant rate as described in Ref. 2. The observed accuracies and stabilities are summarized in Table 1. The accuracies of the power supplies, which are defined as the differences between the setting currents and the actual output currents observed by the DCCT, were less than 1.7% for all the magnets except for the quadrupole magnet QTD12a. The reason of the observed large difference is that a trimmer potentiometer, which determines the maximum output current, was broken or accidentally moved to the improper value. For other magnets, observed accuracies are within the acceptable level.

Table 1. Summary of accuracy and stability tests performed in 2009.

SWMC	DCCT	303.8	-1.55%	9ppm/8H
QTA01a	Zeranin	263	-0.07%	10ppm/14H
QTA01b	Zeranin	262.8	0.11%	193ppm/14H
DAA1	DCCT	400	-0.28%	13ppm/13H
DMA1	DCCT	303.55	-1.41%	5ppm/4H
QTA11a	Zeranin	151.9	-1.25%	26ppm/13H
QTA11b	Zeranin	151.8	0.02%	189ppm/13H
QTA11c	Zeranin	151.5	-1.00%	17ppm/7H
QTD12a	Zeranin	152	5.29%	173ppm/7H
QTD12b	Zeranin	152.05	-1.04%	45ppm/7H
QTD12c	Zeranin	152.45	-0.34%	79ppm/7H
QTD13a	Zeranin	152.1	-0.41%	19ppm/7H
QTD13b	Zeranin	152.1	-0.14%	39ppm/7H
QTD13c	Zeranin	152	-0.46%	26ppm/10H
QTD14a	Zeranin	151.8	-0.32%	39ppm/10H
QTD14b	Zeranin	151.8	-0.27%	115ppm/13H
QTD14c	Zeranin	151.75	0.00%	152ppm/13H
QTD15a	Zeranin	152	-0.39%	30ppm/16H
QTD15b	Zeranin	151.81	-0.25%	131ppm/16H
QTD15c	Zeranin	151.81	-0.29%	30ppm/6H
QTD16a	Zeranin	151.82	0.81%	37ppm/6H
QTD16b	Zeranin	151.81	-0.43%	13ppm/16H
QTD16c	Zeranin	151.81	0.79%	23ppm/16H
QTD17a	Zeranin	151.85	-1.57%	21ppm/7H
QTD17b	Zeranin	152.3	-0.43%	49ppm/7H
QTD17c	Zeranin	152.1	-1.40%	35ppm/15H
QTD18a	Zeranin	152	0.14%	54ppm/15H
QTD18b	Zeranin	152.4	-1.64%	11ppm/8H
QTD18c	Zeranin	152.5	-0.72%	33ppm/8H
DAD4	DCCT	400	-0.23%	9ppm/4H
DMD4	DCCT	303.85	-1.53%	6ppm/4H

Magnet exited	Current sensor	Maximum current(A)	Error of current	Stability
QTF41a	Zeranin	151.87	-1.51%	51ppm/5H
QTF41b	Zeranin	151.83	-1.53%	39ppm/5H
QTF41c	Zeranin	151.94	-1.35%	15ppm/13H
QTF01a	Zeranin	151.8	-1.59%	35ppm/13H
QTF01b	Zeranin	151.8	-1.15%	37ppm/7H
QTF01c	Zeranin	151.9	-1.28%	67ppm/7H
DMDA	DCCT	303.75	-1.46%	8ppm/14H
DMAB	DCCT	300	0.12%	16ppm/14H

The stabilities of the power supplies are important for stable operation of RIBF accelerator complex. For dipole magnets (DMDA, DMAB, SWMC, DMA1, DAA1, DAD4, DMD4), the observed stabilities were less than 20 ppm during the measurements. This good performance was a result of the improvement of the current feedback system finished in 2005 as reported in Ref. 5. We adopted DCCT's as current sensors instead of old shunt resistors and also stabilized the temperature of the current-feedback system using Peltier coolers.

For quadrupole magnets, observed stabilities were less than 100 ppm during the measurements except for five quadrupole magnets (QTA01b, QTD12a, QTD14b, QTD15b). The worst one was 193 ppm for 14 hours in the

case of QTA01b. This value is acceptable for RIBF operation, but it means the power supply of QTA01b was very unstable compared with other old power supplies. For closer inspection, results of the stability measurements were shown in Fig. 1 compared with the result of QTA01a. Note that both power supplies are of the same design and were made at the same time. The observed instability for QTA01b may come from deterioration of circuit elements used in the current-feedback system, which is an example of aging problem

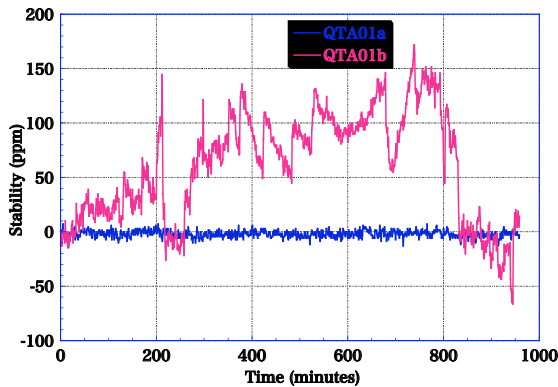


Fig. 1 Observed stabilities for QTA01a and QTA01b power supplies.

We also illustrate an example of a linearity test of the QTA01b power supply in Fig. 2. The maximum linearity error observed was 0.6A, which corresponds to 0.23%. It is also within the acceptable level.

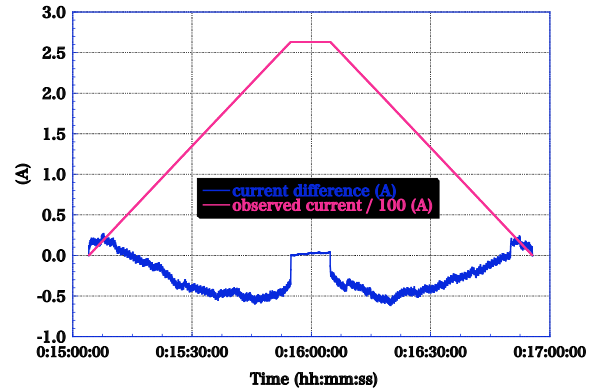


Fig. 2 Result of linearity test for QTA01b power supply. The current difference is defined as  $(I_{set} - I_{obs})$ ,  $I_{set}$  implies the setting current and  $I_{obs}$  the observed current measured by the DCCT. In the figure, the excitation current is also shown with the scaling factor of 1/100.

Results of a series of measurements performed in 2007 and 2008 will be used not only for the database of calculation-based operation but also for the basic information which determines a maintenance plan and replacements of deteriorated power supplies in the near future.

#### References

- (1) K. Hatanaka et al., Proc. 11<sup>th</sup> Int. Conf. On Cyclotrons and Their Applications, 384 (1986).
- (2) M. Nagase et al., Accel. Prog. Rep. 41, 103 (2008)
- (3) <http://www.pppower.co.uk/manuprod25.htm> (HITEC power protection)
- (4) <http://www.danfysik.com/> (DANFYSIK)
- (5) M. Nagase et al., Accel. Prog. Rep. 37, 273 (2003)

## A Linux Cluster with Redundant Design for Accelerator Operation

A. Uchiyama<sup>\*1</sup>, M. Kobayashi-Komiyama

The RIKEN RIBF control system is based on Experimental and Industrial Control Systems (EPICS). EPICS Input/Output Controllers (IOCs) control and monitor the devices through Ethernet using the control network. Our control system is consists of many server computers for various purposes; an operational log system based on Zope and PostgreSQL (Zlog)<sup>1</sup>, EPICS applications and DNS. Already more than five years have passed since their introduction into our system. In order to use them stably without any serious machine trouble, they should be replaced by new ones periodically. In this paper, we report on the replacement of servers in detail.

To store the EPICS application's programs, we have been using an exclusive server with a RAID 5 system. It has a lot of front-end applications for RILAC/AVF/RIBF operation, such as graphical user interface (GUI) and various measurement programs using channel access (CA). They are centralized to enable software management with ease, and every user connects their client PCs to the application server for beam tuning, beam monitoring and so on. As a result, if this application server has any problems in its control system, all of the accelerators will probably fail to operate. Our Zlog system, however, was implemented on another server computer. The parameters during beam tuning are very important to ascertain the condition of the beam, including essential information for beam analysis. Therefore, we cannot lose any data. For these reasons, we selected the servers which promote reliability, availability, and serviceability (RAS) for the replacement. The requirements of the new system are listed as follows.

- \* Installation of Redhat Enterprise Linux clones as its operating system.
- \* We need to consider the load balancing for its heavy system load.
- \* The service has to work without stopping during the experiment so as not to interrupt it, even if a serious problem occurs on the server, such as disk trouble.
- \* DNS should be available at any time.

Therefore, we decided to construct the new servers using Linux clustering with a redundant design. Figure 1 shows the system chart in this task.

We configured a new cluster with "active/active" mode for the EPICS applications server. It consists of two servers with load balancing using round robin DNS. The specifications are summarized in Table 1. Generally, round robin DNS is a technique for load balancing in some services, such as web service. In the system, clients can always connect to an available server of servers which share the same hostname. We confirmed that the telnet and ssh client included in CentOS 5.2 exhibit the same behavior as described above.

Besides, user data, for example the home directory, is shared by both the servers using DRBD<sup>2</sup>, Heartbeat<sup>3</sup> and NFS. Therefore, they can access the same data in both of the servers, and even if the other server has system failure, they can definitely connect to the alive server. As a result, the redundant system with load balancing was successfully designed and constructed for combination with round robin DNS and the shared user data.

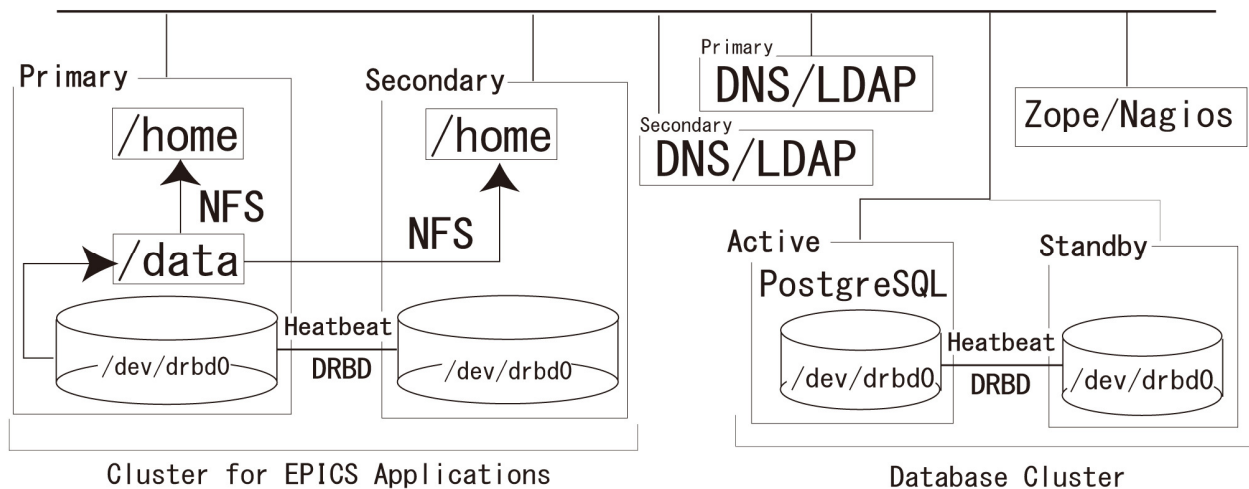


Figure 1. The system chart for this task.

<sup>\*1</sup> SHI Accelerator Service, Ltd.

OS	Scientific Linux 4.6
CPU	Dual-Core AMD Opteron 2212
Memory	2 GByte
Software	DRBD-0.7, Heatbeat-2.0.0, EPICS base-R3.14.7, MEDM

Table 1. Specifications of the system for EPICS applications.

Zlog is the operational log system developed at KEK for a control system based on EPICS.<sup>1)</sup> It consists of following three items; a log monitor server written by Python, a database on PostgreSQL, and the products made by Zope, which is the web application framework for user interface. In operating the system, registered parameters of various devices are monitored and recorded on the database by the log monitor server. Simultaneously, accelerator operators can search, view and input the operation log with the application running within the web browser. In our old Zlog system, Zope, PostgreSQL and log monitor service ran on the same hardware. However, it produced a heavy system load. Therefore, we introduced a new system with one server for Zope and two servers as a cluster for PostgreSQL and log monitor server. The specifications are summarized in Table 2. PostgreSQL cluster is configured with a high-availability (HA) system of “active/standby” using open-source DRBD and Heartbeat. In this HA system, the active node and standby node with RAID 1 system have shared storage using DRBD. Normally, the shared storage is mounted on an active node which runs the PostgreSQL and log monitor service. But if a problem in it is detected by Heartbeat, the standby node mounts the shared storage in place of active node during failover. At the same time, the services switch over to standby node automatically. As a result, the Zlog system is available to use continuously, even if problems in the system which take time for recovery occur.

Use	HA cluster (Active/Standby)	Zope
OS	CentOS 4.6	CentOS 5.2
CPU	Xeon L5410	Celeron 430
Memory	4 GByte	1 Gbyte
Software	DRBD-0.7, Heatbeat-2.0.0, PostgreSQL-8.0.19, log monitor server (at KEK), EPICS base-3.14.9	Zope-2.10.7, Nagios 3.06

Table 2. Specifications of the system for Zlog

In this task, we introduced two kinds of the clusters for Zlog and EPICS applications, to integrate management of the user environment, such as passwords, guides and login shells. OpenLDAP<sup>4)</sup> was installed in the same hardware of primary/secondary DNS for provide LDAP service. As a result of configuring two LDAP servers, the other LDAP server is available for use, even if one of the LDAP servers

has system failure. Generally, when a server encounters a system failure, and stops providing the service, a security alert will be sent by E-mail to the administrator. However, since our network is not connected with the Internet, we cannot receive E-mail. Therefore, open-source Nagios<sup>5)</sup> is used to provide the server monitoring system and the administrator can observe alive monitoring using a web browser at any time.

In December 2008, we started launching these clusters after a recovery test. As a result, we succeeded in implementation of RAS clusters for the key service of accelerator operation, constructed at a low-cost using open-source software only for increasing system availability.

Finally, the author would like to thank N. Yamamoto, K. Kamikubota, J. Odagiri in KEK, and S. Yoshida in the Kanto Information Service for their helpful suggestions, and K. Yoshii and T. Nakamura in Mitsubishi Electric System & Service Co. ltd. for constructing the Zlog system.

#### References

- 1) K. Yoshii et al.: Proc. ICALEPCS07, Knoxville, Tennessee, USA, 2007, p299-301
- 2) <http://www.drbd.org/>
- 3) <http://www.linux-ha.org/>
- 4) <http://www.openldap.org/>
- 5) <http://www.nagios.org/>

## Computer modelling of the nitrogen, oxygen, and proton acceleration in RIKEN AVF cyclotron

S. B. Vorozhtsov,<sup>\*1</sup> A. S. Vorozhtsov,<sup>\*1</sup> E. E. Perepelkin,<sup>\*1</sup> S. Watanabe,<sup>\*2</sup> S. Kubono,<sup>\*2</sup> and A. Goto

The project to upgrade the AVF cyclotron is being conducted by a collaboration of the Center for Nuclear Study (CNS) of the University of Tokyo, the Joint Institute for Nuclear Research (JINR, Dubna, Russia), and RIKEN.<sup>1)</sup> The present study is focused on the formulation of the new acceleration regimes and a beam extraction study in the AVF cyclotron by detailed orbit simulations. The new acceleration regimes include: the expansion of the acceleration energy region of light ions towards higher energies in the existing rf harmonics equal to 2, and the modification of the center geometry for the rf harmonics equal to 1 to make it possible to accelerate protons at several tens of MeV. The current status of the AVF Cyclotron computer model, used for calculations, is described elsewhere.<sup>2), 3)</sup>

The simulation of injection and acceleration of 7 MeV/nucleon  $^{14}\text{N}^{5+}$  ion beam was performed in order to obtain better calibration of the simulations vs. the recently conducted experiment.<sup>2)</sup> Assessment of losses from the buncher entrance until the initial 20th turn in the cyclotron was carried out. The estimation produced particle losses all along this passage at the level of  $\sim 66\%$  which corresponds to the measurement of 60-70 %.

The simulation of the  $^{14}\text{N}^{5+}$  extraction was also carried out by taking into account the 3D modeling results of electromagnetic fields of the extraction system. The extraction system consists of: harmonic coils (HC), an electrostatic deflector (ESD), a magnetic channel (MC) and a gradient corrector (GC). The layout of the extraction system is shown in Fig. 1. Upstream of the ESD the turn pattern showed that some overlapping of the bunches at the neighboring orbits took place. As a result, the beam was extracted with multi-turn extraction as shown in Fig. 2. The transmission efficiency through the ESD was approximately 80 %.

In order to increase the  $^{16}\text{O}^{7+}$  ion energy, which had been limited to less than about 10 MeV/nucleon due to the voltage available (below 50 kV), up to 11 MeV/u, changing the injection beam phase at the 1st acceleration gap from the original design value of  $-30^\circ\text{RF}$  to  $-8^\circ\text{RF}$  as well as the corresponding currents of the innermost trim coil was proposed. In this way the energy gain at the 1st turn was increased, permitting the beam to clear the channel immediately after passing through the exit of the inflector. In the actual beam test, 11 MeV/nucleon was successfully achieved with the presently available voltage of 49 kV.

The first attempt to simulate the acceleration of 60 MeV proton beam in the 1st rf harmonics mode was carried out. Clearly, with the realistic dee voltage of about 50 kV particles would be lost in the channel, since the existing

structure of the center region was designed for the 2nd harmonics, not for the 1st. Thus, the substantial redesign of the central electrode structure is needed to accelerate protons with reasonable values of the dee voltages. Nevertheless, to see how protons will be accelerated downstream of the channel, the rf phase excursion during the acceleration until the final energy was simulated using the realistic voltage of 50 kV. The simulation demonstrated a good quality of the magnetic field generated.

### References

- 1) S. B. Vorozhtsov et al.: RIKEN Accel. Prog. Rep. 41, 92 (2007).
- 2) S. B. Vorozhtsov et al.: Proc. XXI Russian Acc. Conf. (RuPAC2008), Zvenigorod, Russia, 2008, p.51-53.
- 3) E. E. Perepelkin and S. B. Vorozhtsov: Proc. XXI Russian Acc. Conf. (RuPAC2008), Zvenigorod, Russia, 2008, p.40-42.

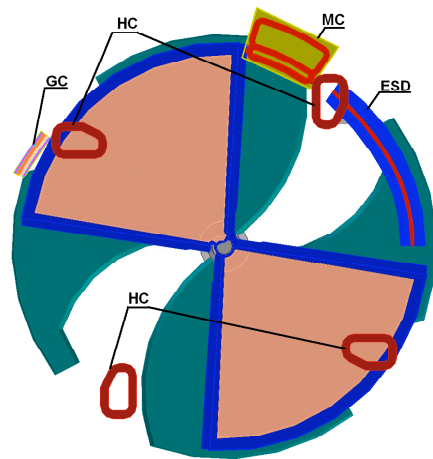


Fig. 1. Layout of the extraction system along with the harmonic coils.

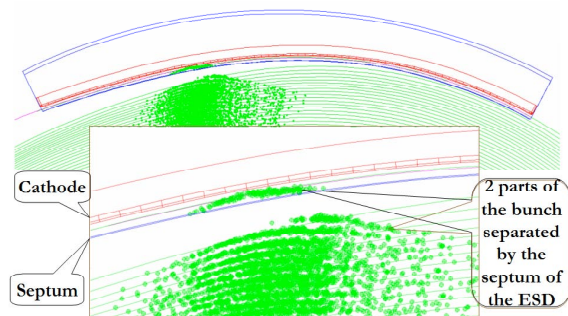


Fig. 2. Simulation of the beam bunches in the extraction region.

<sup>\*1</sup> Joint Institute for Nuclear Research, Dubna, Russia

<sup>\*2</sup> Center for Nuclear Study, University of Tokyo

## Low Energy Beam Transport of 127 kV $U^{35+}$ on 100 kV Cockcroft

Y. Sato,\*<sup>1</sup> M. Fujimaki, N. Fukunishi, A. Goto, Y. Higurashi, E. Ikezawa, O. Kamigaito, M. Kase, T. Nakagawa, J. Ohnishi, H. Okuno, and Y. Watanabe

We are going to construct a new beam line to inject 127 kV  $U^{35+}$  beams into the RILAC at RIKEN. The beam line from our new ECR ion source (ECRIS) to the RILAC has two sections, a low energy beam transport (LEBT) section and a medium energy beam transport (MEBT) section. The LEBT section is from the ECRIS to an acceleration tube, and it is on a 100 kV Cockcroft. The MEBT section is from the acceleration tube to the RILAC. The ECRIS has 27 kV higher voltage than the Cockcroft stage. Oxygen is used as supporting gas at the ECRIS. The ECRIS produces  $U^{35+}$ , other charged states of U ions, and O ions.

After passing a 90 degree analyzing magnet and a horizontal slit the  $U^{35+}$  beam is separated and goes into the acceleration tube. The acceleration tube connects the 100 kV Cockcroft stage and ground level. After the acceleration tube, the 127 kV  $U^{35+}$  beam is transported through 13.6 m MEBT up to the RILAC.

The LEBT consists of the 28 GHz superconducting ECRIS, a solenoid, a positioning box, a steerer upstream, the 90 degree analyzing bending dipole, a steerer downstream, a horizontal and vertical slit, diagnostics, and the acceleration tube (Fig. 1). It is

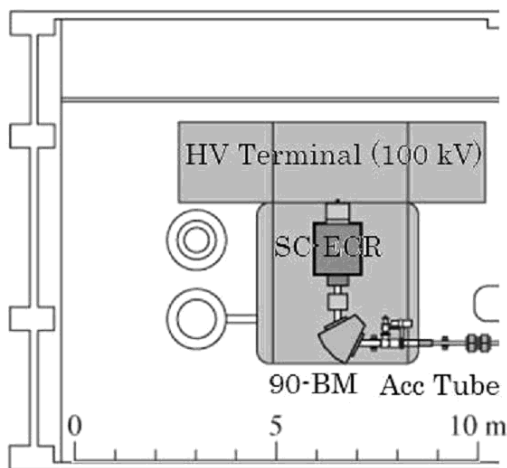


Fig. 1. Beam line of  $U^{35+}$  on 100 kV high voltage terminal. Acceleration tube connects the terminal and the ground.

1.4 m from an ECRIS plasma electrode to the bending dipole entrance. This dipole has a bending radius of  $\rho = 510$  mm, point to point focusing capability and sextupole components the same as the Venus type at LBNL<sup>1</sup>). The Horizontal slit position is 1.02 m down-

stream from the bending dipole exit.

We used FEMM<sup>2</sup>), IGUN<sup>3</sup>), OPERA and KOBRA<sup>4</sup>) codes for LEBT simulation. FEMM is a 2D electric field and magnetic field software. IGUN simulates plasma sheath of an ion source under cylindrical extraction voltage. OPERA is a 3D electric field and magnetic field software. KOBRA simulates 3D trajectory of ions under electric and magnetic fields, including space charge effect. The Solenoidal field of ECRIS and following solenoid was calculated by using FEMM. IGUN was used from the plasma electrode to the 2nd extraction electrode, with 100% space charge effect of total ion beam current 10 emA. We assumed that the ion current of the supporting gas O has the same ratio as RIKEN 18GHz ECRIS data<sup>5</sup>). KOBRA was used from the 2nd extraction electrode to the slit. This area was treated with 20% space charge effect, and the total ion beam current in simulation is 2 emA. The amount of space charge effect in the area is an unknown factor. It has been estimated from 1% to 20% by several groups<sup>1)4</sup>). The 3D magnetic field around the bending dipole was calculated with OPERA. The calculated 3D magnetic field was imported into the KOBRA simulation.

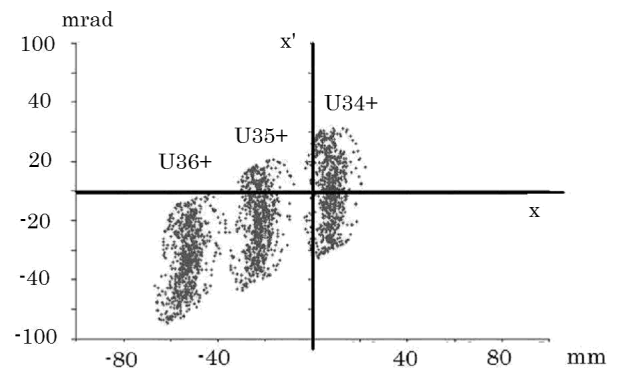


Fig. 2. Horizontal emittance diagram at 1020 mm after the analyzing dipole.  $U^{36+}$ ,  $U^{35+}$  and  $U^{34+}$  are in order from left.

By using the emittance diagrams at the slit are shown in Fig. 2 and 3, we can distinguish  $U^{35+}$  from other charged states of U ions. We are going to use this LEBT for uranium ions Fall in 2009 with a 18 GHz microwave source. From this measurement we will find the real amount of space charge effect. We can provide reasonable feedback to optimize our future LEBT, which will be constructed in FY2010.

\*<sup>1</sup> yoichisato@riken.jp

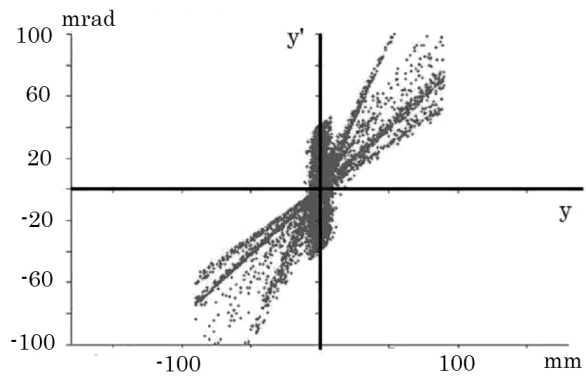


Fig. 3. Vertical emittance diagram at 1020 mm after the analyzing dipole.

#### References

- 1) D. Leitner, et. al. PAC 05, 179 (2005).
- 2) D. Meeker: in *Finite Element Method Magnetics, User's Manual* ‡ (<http://femm.foster-miller.net/Archives/doc/manual42.pdf>).
- 3) R. Becker and W. B. Herrmannsfeldt: Rev. Sci. Instrum. **63**, 2756 (1992).
- 4) P. Spaedtke and C. Muhle, Rev. Sci. Instrum. **71**, 820 (2000).
- 5) Y. Sato, H. Higurashi et. al.: RIKEN Accel. Prog. Rep **41**, 88 (2007).

## Space Charge effects in the RILAC II

H. Okuno, T. Fujinawa, M. Fujimaki, N. Fukunishi, A. Goto, Y. Higurashi, E. Ikezawa, O. Kamigaito, M. Kase, T. Nakagawa, J. Ohnishi, Y. Sato, Y. Watanabe, S. Yokouchi, Y. Yano

A new 28GHz superconducting ECR ion source has been constructed mainly to increase intensity of the uranium beam. The ion source is designed to have as large a plasma volume as  $1100 \text{ cm}^3$  [1, 2] and expected to produce  $\text{U}^{35+}$  ions at an intensity of more than  $15 \mu\text{A}$ , which is necessary to obtain  $1 \mu\text{A}$  beams from the SRC. This new ECR will take all the succeeding accelerators and beam transport lines to a space charge dominant regime, especially the front end section, which should be carefully looked at again to avoid emittance growth caused by space charge forces. The RILAC II, which is now in design, should allow efficient accelerations of ion beams from the powerful new ion source in order to avoid the emittance growths caused by their space charge forces. In this paper, preliminary results of the beam dynamics simulations for the RILAC II using TRACK codes [3] will be reported with brief discussions.

Figure 1 shows a plan for the new injector RILAC II which is designed to accelerate ions with a mass-to-charge ratio of 7, aiming at heavy ions such as  $^{84}\text{Kr}^{13+}$ ,  $^{136}\text{Xe}^{20+}$  and  $^{238}\text{U}^{35+}$ , up to an energy of 680 keV/nucleon. It consists mainly of the SC-ECR, an RFQ linac based on the four rod structure, a low energy beam line (LEBT) between extraction from the source and entrance to the RFQ and a drift-tube linac (DTL) based on three quarter-wavelength resonators (QWR) [4]. Using the TRACK code, we simulated beam dynamics in the LEBT, RFQ and DTL.

The LEBT, before charge selection, consists of an extraction region, a glaser solenoid focusing lens, and a 90 degree bending analyzing magnet for charge selection. The bending radius and edge angle of the

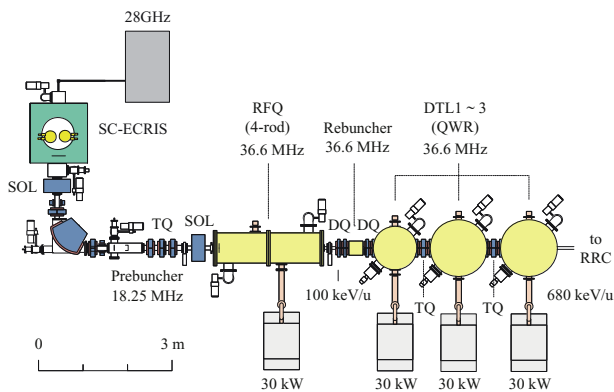


Fig. 1: A plan of the new injector RILAC II.

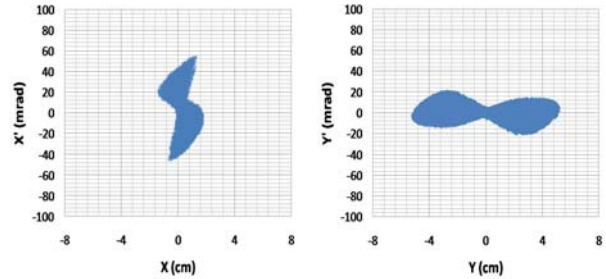


Fig. 2: Emittance plot of  $\text{U}^{35+}$  at the end of the LEBT in the case of 50% neutralization of the space charge forces.

bending magnet are selected to be 510 mm and 27 degree, respectively, to provide double focusing. First, the separation of  $\text{U}(34+)$ ,  $\text{U}(35+)$  and  $\text{U}(36+)$  at the selection point was checked at the 0 mA limit, showing good separation of the three charge states. However, more realistic simulations should include space charge forces from not only uranium ions themselves, but also the other ion species extracted from the ion sources.  $\text{U}(35+)$  and five  $\text{O}(2+, 3+, 4+, 5+, 6+)$  ions were simultaneously transported through the LEBT, assuming different neutralization factors by electrons from residual gases. The ion beam was assumed to consist of 0.5 mA of  $\text{U}^{35+}$ , 1.4 mA of  $\text{O}^{2+}$ , 2.5 mA of  $\text{O}^{3+}$ , 2.6 mA of  $\text{O}^{4+}$ , 1.9 mA of  $\text{O}^{5+}$  and 1.6 mA of  $\text{O}^{6+}$ . The calculation results show that emittance of the U beam grows with large distortion as the neutralization factor decreases. For example Fig. 2 shows an emittance plot in the horizontal and vertical direction in the case of 50 % neutralization. Fig. 3 summarizes the emittance versus the neutralization factor.

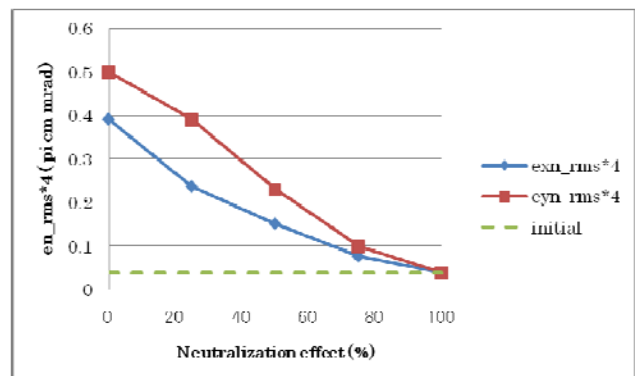


Fig. 3: Normalized emittance in the horizontal and vertical direction at the exit of the LEBT is listed versus neutralization factor of the space charge forces.

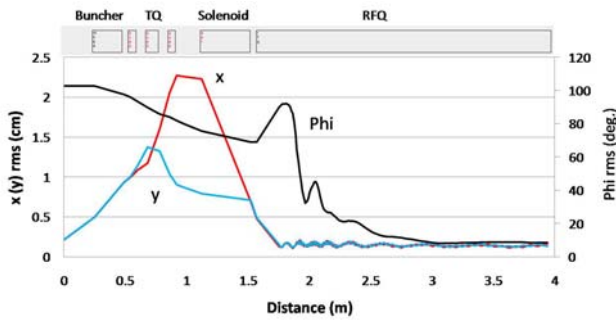


Fig. 4: Beam dynamics from the selection slits in the LEBT to the exit of the RFQ.

After the selection of the  $U^{35+}$  the ion beams are transported to the entrance of the RFQ. The components and the position of the section in the LEBT are shown in Fig. 4. They are designed by intensive study using TRANSPORT by Sato [6]. The field strength of each element was tuned so as to fit twiss parameters of the beams to the matching conditions at the entrance of the RFQ using TRACE3D [7]. A beam buncher is also installed in this section to make the beam bunch with 18.25 MHz which is the fundamental frequency of the RIBF accelerator complex. The voltage and position of the buncher should be optimized so as to maximize efficiency of beams trapped in the proper separatorix because the RFQ is operated in the second harmonic of the 18.25 MHz. Beam dynamics in the part of the LEBT after the selection slit and RFQ were simulated using TRACK code in order to estimate the trap efficiency in the cases of 0.0A and 0.5mA, changing the voltage of the buncher. An input file of its vane structure for TRACK was made by DESRFQ [8] code. Fig. 4 shows a result in the case of 0.5mA. Transmission and trap efficiency are listed in Table 1. Fig 5 shows bunch shapes which give the maximum transmission in the cases of 0.0mA and 0.5 mA. Even distorted bunch shape due to space charge forces can gives an efficiency of more than 80%.

Beam dynamics in the DTL were also simulated. The model of the DTL consists of the rf gaps and drift spaces with beam rebunchers and two quadrupole

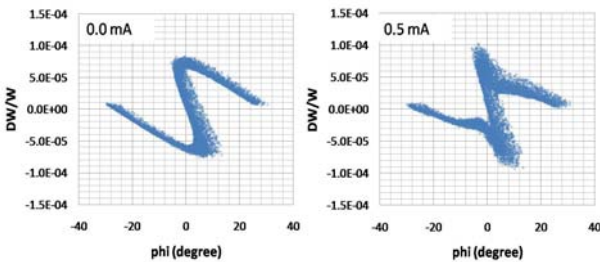


Fig.5: Longitudinal emittance plots at the entrance of the RFQ in the case of 0.0 mA and 0.5mA

	Transmission (%)	Trap efficiency (%)
0.0 mA	68.9	86.7
0.5 mA	50.2	81.1

Table 1: Transmission and trap efficiency of the ion beams from the selection slit to the exit of the RFQ.

doublets. Fig. 6 shows the simulation results in the case of 0.5 mA. The results for the both cases of 0 mA and 0.5 mA do not differ so much, indicating that 680keV/u is high enough to avoid the emittance growth caused by their space charge forces.

In summary, we simulated beam dynamics in the LEBT, RFQ and DTL for RILAC II using the TRACK code. Simulations for LEBT before the selection slit show that the neutralization factor of space charge force largely depends on emittance at the slit. Trap efficiency in the proper separatorix of the RFQ is not affected by the space charge force in the LEBT so much. We should, however, take care whether emittance growth at the exit of the RFQ has an affect on the transmission in the succeeding accelerator. This is under analysis. Simulations for the DTL showed that space charge effect in the DTL is not so large.

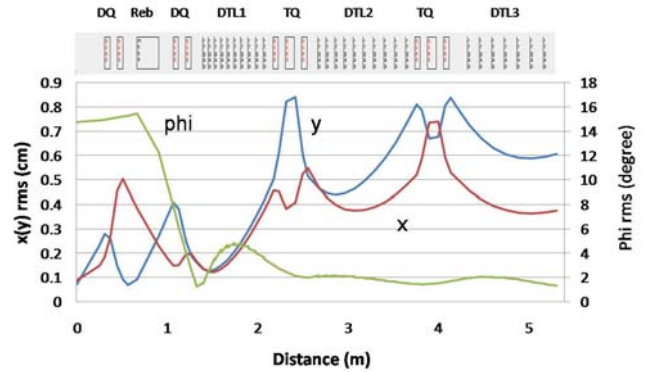


Fig. 6: Beam dynamics of the DTL with short MEBT including a re-buncher.

#### Reference

- [1] T. Nakagawa, *et. al.*, High Energy Physics and Nuclear Physics **31** (2007) 133.
- [2] J. Ohnishi, *et. al.*, High Energy Physics and Nuclear Physics **31** (2007) 37.
- [3] P.N. Ostroumov, V.N. Aseev, and B. Mustapha., Phys. Rev. ST. Accel. Beams **7**, 090101 (2004).
- [4] O. Kamigaito, *et. al.*, 3rd Ann. Meeting of PASJ and 31th Linac meeting in Japan, Sendai, (2006) 502.
- [5] H. Fujisawa, Nucl. Instrum. Methods **A345** (1994) 23.
- [6] Y. Sato, *et. al.*, in this proceedings.
- [7] K. R. Crandall, Los Alamos Report, No. LA-11054-MS, 1987.
- [8] A.A. Kolomiets, *et. al.*, ITEP report, 2001.

# Medium Energy Beam Transport System from the New Superconducting ECR Ion Source to RILAC

H. Okuno, T. Fujinawa, M. Fujimaki, N. Fukunishi, A. Goto, Y. Higurashi, E. Ikezawa, O. Kamigaito, M. Kase, T. Nakagawa, J. Ohnishi, Y. Sato, Y. Watanabe, S. Yokouchi, Y. Yano

The challenging superconducting coils for the new 28GHz ECR ion source [1] were successfully excited in 2008. [2] The ion source is designed to have as large a plasma volume as  $1100 \text{ cm}^3$ , so as to produce  $U^{35+}$  ions at an intensity of more than  $15 \mu\text{A}$ , which is necessary to obtain  $1 \mu\text{A}$  beams from the SRC. Beam tests will start in 2009. This new powerful ion source will be put on a 100kV deck so that extracted beams from the source can be directly injected to the RILAC, skipping the RFQ in the uranium acceleration in order to enjoy the high intensity uranium beams as soon as possible. The existing acceleration scheme requires low frequency operation of the RFQ pre-injector at 18.25 MHz and extraction voltage as low as 5 kV in the uranium acceleration. High power beams accelerated by the extraction voltage of 5 kV steadily grow up due to their space charge forces in the low energy transport line. This direct injection to the RILAC of extracted ion beams accelerated by the high voltage of 127 kV is expected to suppress the emittance growth in the low energy beam transport system because in general space charge effect is proportional to the cube of ion velocity. Furthermore this plan is easy for us to be realised because we can use the room for the former injector to the RILAC, 450kV Cockroft-Walton as shown in Fig. 1. Also, the existing operation will not be interrupted for long periods due to installation.

This project requires making the LEBT (Low Energy Beam Transport system), reformation of the HV terminal, the acceleration tube and the MEBT (Medium energy transport system), including the beam diagnosis and the vacuum system. The main component of the LEBT is the analyzing magnet

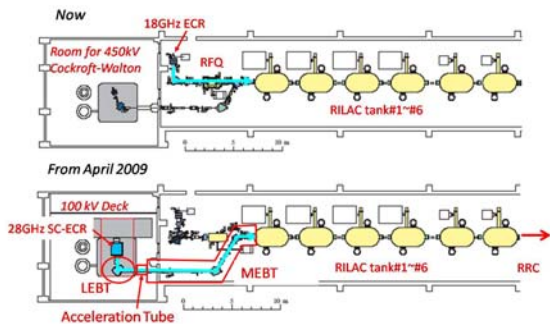


Figure 1: A plan of the new injector.

Table 1: Initial parameters and matching condition used in the simulations. Normalized emittance  $\epsilon_n$ , twiss parameters  $\alpha$  and  $\beta$  are listed in each section.

<b>(a) MEBT</b> Kinetic energy: 18.676 keV/u			
Ion: U35+			
	$\epsilon_n$ (cm mrad)	$\alpha$	$\beta$ (cm/rad)
Horizontal	0.041542	-0.6635	340
Vertical	0.041542	-0.6635	340
<b>(b) Matching condition with at the entrance of RILAC</b>			
Ion: U35+			
	$\epsilon_n$ (cm mrad)	$\alpha$	$\beta$ (cm/rad)
Horizontal		0.5743	22.69
Vertical		0.0872	132.3

which has the function of correcting aberrations in the horizontal and vertical direction. It was successfully fabricated after the study of the beam dynamics in the LEBT including space charge forces. [2] The reformation of the HV terminal including replacement of the insulating support rods, started before installation of the superconducting magnets for the 28GHz ECR ion source. A prehab room, which is necessary for the radiation control, was made after the installation of the ion source. Ion beams from ion sources accelerate by 100 kV through the acceleration tube, the detailed design of which is in progress. The

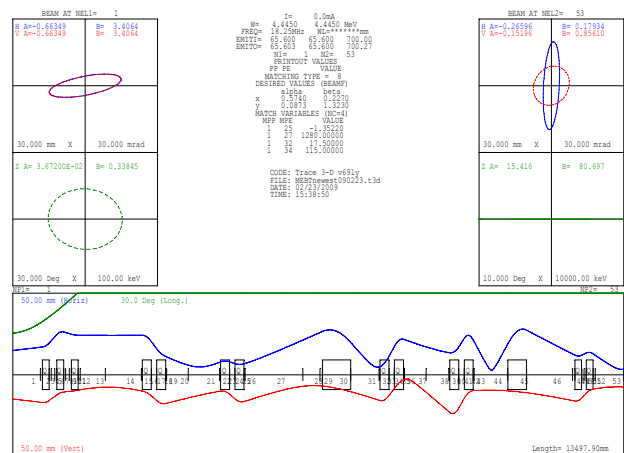


Figure 2 Beam envelope in the MEBT. Emittance plots at its entrance and exit are also shown in the upper parts.

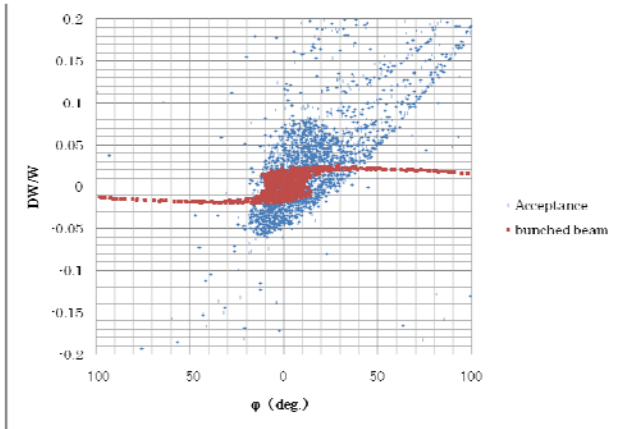


Fig.3 Longitudinal emittance plots at the exit of the MEBT with longitudinal acceptance of the RILAC.

detailed designs of MEBT are also in progress following the study of the beam dynamics [3,4].

The latter part of this report concentrates on the simulation of the beam dynamics in the MEBT and RILAC using TRACK [4]. Table 3 summarizes initial conditions at the entrance of the MEBT and matching conditions at the entrance of the RILAC.

After the ion beams from the LEBT are accelerated in the accelerating tube, they are transported to the entrance of the RILAC through the MEBT. In the MEBT DC beams from the ion source are bunched in the two 1<sup>st</sup> harmonics bunchers so that the RILAC can accept the beams effectively. The model consists of 13 quadrupole magnets and two 60 degree bending magnets. The first buncher is placed before the two bending magnets which allow doubly achromatic beam transportation and the last buncher is installed about 1 m before the entrance of the RILAC. This configuration is finalized following intensive study of beam dynamics using TRANSPORT [3]. The field gradients of the quadrupole magnets were obtained from the simulation using TRACE 3D [5] so that the Twiss parameters of emittance ellipses at the entrance of the RILAC match those of the acceptance ellipses.

Fig. 3 shows bunched phase plot from a simulation result using TRACK code. Longitudinal acceptance of the RILAC is also shown in the figure indicating that about 51% of the DC beams can be accepted by the RILAC. The RILAC consists of six variable-frequency cavities. The model treated the motion in the rf gaps with the impulse approximation; with sinusoidally varying voltage, it was assumed the ions gained kinetic energy at the midgap where they were exposed to the rf defocusing force at the same time. The validity of this approximation in such a low energy region should be checked by comparison with results using more realistic models. The model also includes the quadrupole magnets embedded in the drift tubes and inserted between the tanks. Fig. 4 shows the simulation results from the entrance of the MEBT to the exit of the RILAC in the case of 0mA. Total transmission efficiency of about 50% seems to be determined not by transversal but longitudinal acceptance.

In summary, beam dynamics simulations in the RILAC with MEBT were carried out using TRACK in order to check the matching conditions at the entrance of the RILAC and longitudinal acceptance in the RILAC. Simulation results in the case of 0 mA are consistent with the former studies on beam dynamics in the RILAC. Simulations including space charge forces in the case of non zero current are in progress.

#### Reference

- 1) T. Nakagawa, et. al., in this report.
- 2) J. Ohnishi, et. al., in this report.
- 3) Y. Sato, et. al., in this report.
- 4) Y. Watanabe, et at., in this report
- 4) P.N. Ostroumov, V.N. Aseev, and B. Mustapha., Phys. Rev. ST. Accel. Beams 7, 090101 (2004).
- 5) K. R. Crandall, Los Alamos Report, No. LA-11054-MS, 1987.

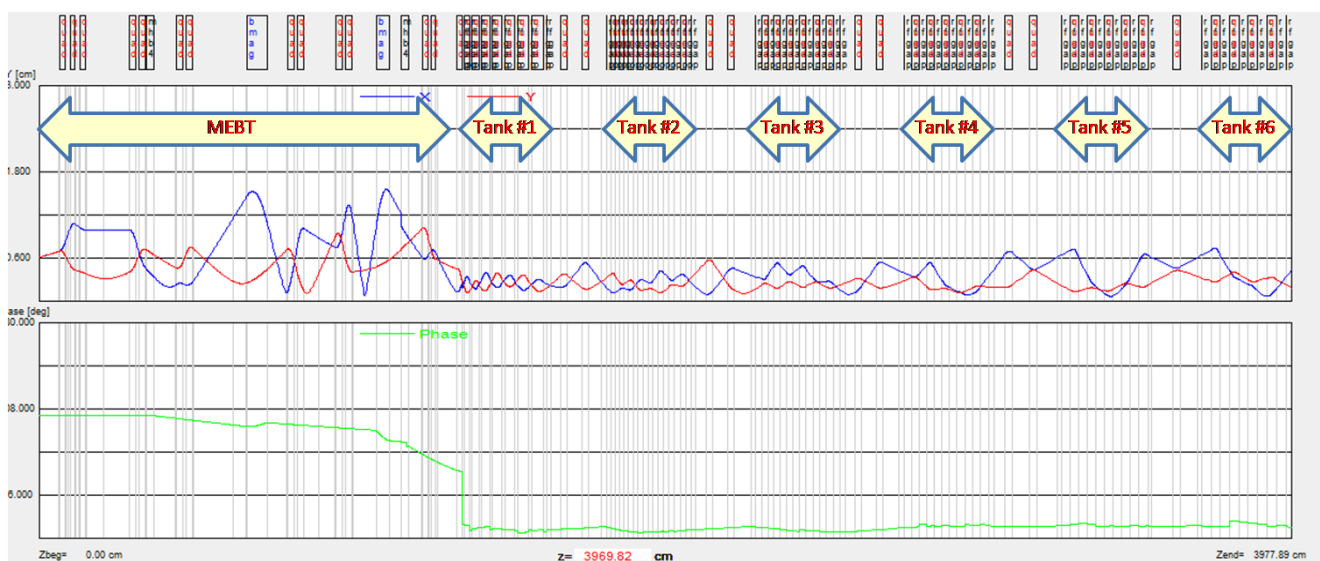


Fig.4 A simulation result for MEBT+RILAC.

## Emittance measurement of a singly charged heavy ion beam produced by laser for use in RHIC-EBIS

Takeshi Kanesue,<sup>\*1</sup> Jun Tamura,<sup>\*2</sup> Masahiro Okamura<sup>\*3</sup>

A Laser ion source (LIS) is a candidate for the primary ion source of the RHIC EBIS which is a future heavy ion injector for the Relativistic Heavy Ion Collider and NASA Space Radiation Laboratory.<sup>1)</sup> A low charge state, low emittance and high ion yield laser ion source using a high power Nd:YAG laser with a defocused laser beam is being studied as the primary ion source for the RHIC EBIS.<sup>2)</sup> During RHIC EBIS operation, the primary ion source provides singly charged ions and the RHIC EBIS enhances the charge state of ions. Since this EBIS will be capable of changing ion species on a pulse by pulse basis, the primary ion source is also required to change ions on a pulse by pulse basis.

A laser ion source produces ions by pulsed high power laser irradiation onto a solid state target. Ion species can be changed by controlling the laser path to other target species. The target is rapidly heated, vaporized and becomes a plasma called laser ablation plasma. Then the plasma expands adiabatically perpendicular to the target surface. Generally, a laser ion source is used for highly charged high current ion production with minimal laser spot size to achieve higher power density on the target. However, a laser ion source can be optimized for singly charged, low energy ion production suitable for providing seed ions for charge bleeding by decreasing the power density. Since the properties of laser produced plasma are different for different species, laser power density for singly charged ion production should be verified experimentally for each atomic species.

We measured plasma properties of C, Al, Si, Fe, Ta and Au targets using the second harmonics of Nd:YAG laser (532 nm wave length, up to 0.5 J / 6 ns). The relationship between power density and plasma total current was measured while changing laser power density by controlling laser spot size on the target. Results of this experiment show that singly charged ion dominant beams can be produced from all of the species mentioned above. For example, over 95 % of ions are singly charged ions below  $9 \times 10^8 \text{ W} / \text{cm}^2$  in case of Au. The details of this experiment are given in<sup>3)</sup>.

The emittance of the Au beam was measured using a pepper pot emittance monitor<sup>4)</sup>. Laser power density and extraction conditions were chosen to achieve sufficient particles as a primary ion source for this experiment based on singly charged ion production experiment. A laser power density of  $1.7 \times 10^8 \text{ W} / \text{cm}^2$  was used for this experiment. The plasma drifting length and extraction aperture diameter

were 1.60 m and 18 mm, respectively. The estimated number of particles, peak current and pulse duration were  $1.9 \times 10^{11}$ , 0.28 mA and 110  $\mu\text{s}$ , respectively.

The experimental set up was modified for emittance measurement experiment. A 25.4 cm long extraction column with a movable intermediate electrode was placed 1.6 m away from the target. A gridded lens,<sup>5)</sup> which is an electrical lens to focus the ion beam, was located downstream of the insulator. A pepper pot was located at a distance of 2.4 m from the target. The target chamber including the target and plasma drift chamber was biased to 16 kV to extract ions from the plasma.

Normalized RMS emittance was 0.025  $\pi \text{ mm mrad}$  after optimization of the gridded lens voltage, intermediate electrode position and voltage. This value is comparable to the hollow cathode ion source (HCIS) used as the primary ion source for the RHIC-EBIS test stand, although the current from the HSIS was typically several tens of micro amperes which is about an order of magnitude lower than that of LIS. Figure 1 shows the measured horizontal phase space diagram processed by software developed for the pepper pot. It was found that the laser ion source can be used as a primary ion source for the RHIC-EBIS.

We are grateful for the supports of E. Beebe and A. Pikin of Brookhaven National Laboratory.

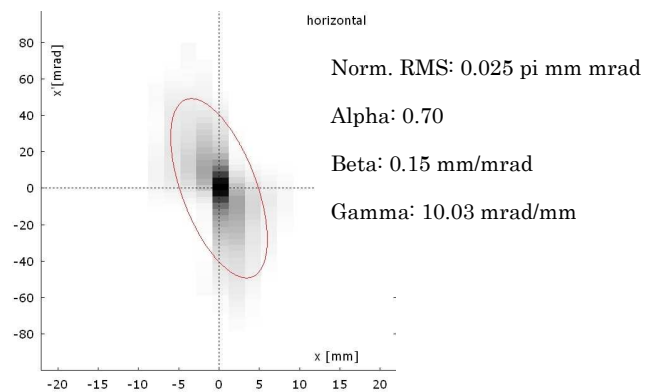


Fig. 1. Measured horizontal phase space using Au target with 16 kV extraction voltage

### References

- 1) J. Alessi, et. al.: Proc. of PAC07, Albuquerque (2007) p. 3782.
- 2) T. Kanesue et al.: Rev. Sci. Instrum. 79 (2008) 02B102.
- 3) T. Kanesue, et. al.: Proc. of EPAC08, Genoa (2008) p. 421.
- 4) A. Pikin, Brookhaven National Laboratory internal report C-A / AP #244.
- 5) A. Pikin, Brookhaven National Laboratory internal report C-A / AP #312.

<sup>\*1</sup> Department of Applied Quantum Physics and Nuclear Engineering, Kyushu University

<sup>\*2</sup> Department of Energy Sciences, Tokyo Institute of Technology

<sup>\*3</sup> Brookhaven National Laboratory, New York, USA

## Preparation for Beam Analysis Experiment for EBIS-RFQ Linac

J. Tamura,<sup>\*1</sup> M. Okamura,<sup>\*2</sup> and T. Kaneshue,<sup>\*3</sup>

We have prepared for an upcoming beam analysis experiment for a new RFQ linac which is part of an Electron Beam Ion Source (EBIS) based RHIC preinjector. The EBIS-RFQ (100 MHz, 4-rod cavity) was designed to accelerate  $\text{Au}^{32+}$  beam from an input energy of 17 keV/nucleon to 300 keV/nucleon. In the new preinjector system, multiple charge state ions are simultaneously injected into the RFQ.

To evaluate the output beam properties, we simulated a multiple charged ion beam acceleration using a particle-mesh method for space charge force calculation. At each step in time, this solves the Poisson equation from charge densities assigned to grid points from the particles, and then moves the particles. The RF electric field from vane electrodes was derived from the two-term potential function and the field in the radial-matching section was from the four-term potential function. Figure 1 shows a simulation result (longitudinal phase space at the end of the RFQ vane). Here  $\text{Au}^{31+}$  (3mA,  $17 \times 31/32$  keV/nucleon),  $\text{Au}^{32+}$  (4mA, 17keV/nucleon) and  $\text{Au}^{33+}$  (3mA,  $17 \times 33/32$  keV/nucleon) are injected into the RFQ. Then more than 98 % of the particles are accelerated to the designed output energy of 300 keV/nucleon, while unaccelerated particles maintain the velocity at the initial injection velocity. The bunch length is 60 degree (13 mm). There will be 1000-4000 bunches per pulse since the pulse width of a beam from EBIS is 10-40 us. The bunch shape will be measured with a fast Faraday cup installed just behind the RFQ. The ion current consists of particles which survived transversely (accelerated and unaccelerated).

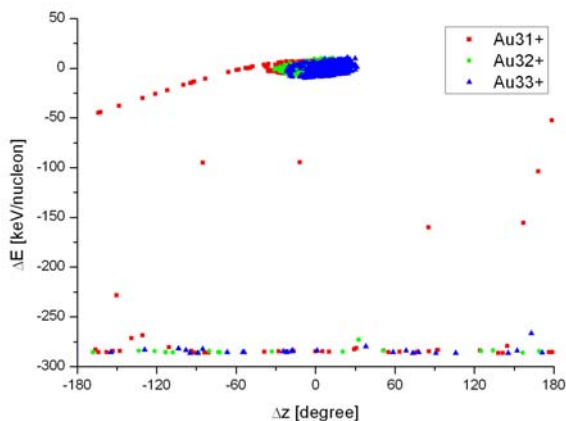


Fig. 1. Longitudinal phase space at the end of the RFQ vane. 180 degree is the length of 3.8 cm.  $dE = 0$  corresponds to the kinetic energy of 300 keV/nucleon.

The beam analysis line shown in Fig. 2 was designed using the TRACE-3D program. There are 5 quadrupole

magnets to control the beam condition and a dipole magnet to separate different charge state ions. Ion current only from accelerated particles can be measured with the fast Faraday cup installed between the quadrupole and dipole, since unaccelerated particles cannot pass through these quadrupole magnets. To separate  $\text{Au}^{32+}$  and the others using this dipole magnet ( $B \leq 1$  T, 45 degree deflection), more than 1 m distance from the magnet is necessary. In case of lighter species like Fe and Cu, less flight distance can be applied.

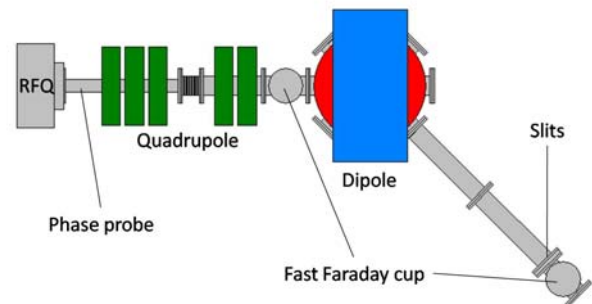


Fig. 2. Experimental set up of beam analysis line for EBIS-RFQ.

We measured resonant frequency of the RFQ cavity with a network analyzer by adjusting two tuners. When we pushed the tuner into the cavity, resonant frequency increased linearly. The full frequency range was from 100.574 MHz to 100.761 MHz. When we pushed one tuner into the cavity, the electric field near the tuner is decreased and the field near the other tuner is increased.

We will continue to improve the RFQ simulation code. This measurement will be completed by the end of March 2009.

<sup>\*1</sup> Department of Energy Sciences, Tokyo Institute of Technology

<sup>\*2</sup> Collider-Accelerator Department, Brookhaven National Laboratory

<sup>\*3</sup> Department of Applied Quantum Physics, Kyushu University

### References

- 1) A. Schempp et al.: "RFQ and IH Accelerators for the New EBIS Injector at BNL", Proceedings of PAC 2007, p. 1439.
- 2) J. Alessi et al.: "Status of the EBIS Project at Brookhaven", Proceedings of LINAC 2006, p. 385.
- 3) R. W. Hockney and J. W. Eastwood: "Computer Simulation Using Particles", (Taylor & Francis Group, New York, 1988).
- 4) Thomas P. Wangler: "RF Linear Accelerators", (WILEY-VCH, Weinheim, 2008).
- 5) K. R. Crandall: "RFQ Radial Matching Sections and Fringe Fields", Proceedings of LINAC 1984, p. 109.

## **7. Instrumentation**

## Status of the BigRIPS and ZeroDegree Project

T. Kubo, K. Kusaka, T. Ohnishi, K. Yoshida, A. Yoshida, N. Fukuda, M. Ohtake, Y. Yanagisawa, H. Takeda, N. Inabe, D. Kameda, K. Tanaka, H. Sakurai, T. Motobayashi, and Y. Yano

This report describes the status of the major research instruments in the RI beam factory (RIBF), such as the BigRIPS in-flight separator,<sup>1,2)</sup> the ZeroDegree spectrometer<sup>3)</sup> and the high-resolution beam line for the SHARAQ spectrograph.<sup>4)</sup> The BigRIPS and ZeroDegree were successfully commissioned in May 2007 and November 2008, respectively, while the high-resolution beam line is in the final stage of construction. Commissioning of the high-resolution beam line is scheduled for March 2009, together with SHARAQ.

Figure 1 shows a schematic layout of the major research instruments at RIBF along with the RIBF cyclotrons. The BigRIPS separator is composed of 14 superconducting triplet quadrupoles (STQ) having large apertures and 6 room-temperature dipoles, which are labeled as STQ1-14 and D1-6 in Fig.1. There are seven focuses indicated as F1-7. One of BigRIPS's major features is large acceptances, which were achieved by using the large-aperture quadrupoles. Thanks to this feature, not only projectile fragmentation of various heavy ions but also in-flight fission of uranium beams can be efficiently used as a production reaction for RI beams.

Another important feature is its two-stage structure. The first stage includes the components between the production target (F0) and F2, while the second stage spans those from F3 to F7. The section from F2 to F3 works as a matching

section. This feature allows deliver of tagged RI beams as well as use as a two-stage tandem separator. In the former mode, the first stage is used to produce and separate RI beams with an energy degrader, while the second stage works as a spectrometer to analyze and identify those RI beams. The momentum resolution of the second stage is high enough to identify RI beams without measuring total kinetic energies, even if some of them are not fully stripped. In the two-stage separator mode, an energy degrader is used at both stages to further purify the RI beams.

In each focus, there is a focal-plane chamber to accommodate various beam-line devices and detectors used for diagnostics and particle identification (PID). The PID scheme is based on the  $\Delta E$ -TOF- $B\rho$  method in which trajectory reconstruction is used to improve the resolution. The primary beams stops at a high-power beam dump located at the first dipole D1. The first stage is surrounded by radiation shields which weigh about 7000 tons.

The RI-beam delivery line following the BigRIPS is used not only to transport RI beams to experimental setups, but also as a forward spectrometer named ZeroDegree. It consists of 9 STQs and 2 dipoles, labeled as STQ15-23 and D7-8 in Fig.1. The magnets of ZeroDegree have essentially the same design as those of BigRIPS. The focuses are indicated as F8-F12. The section from F8 to F11 forms the ZeroDegree spectrometer, while that from F7 to F8

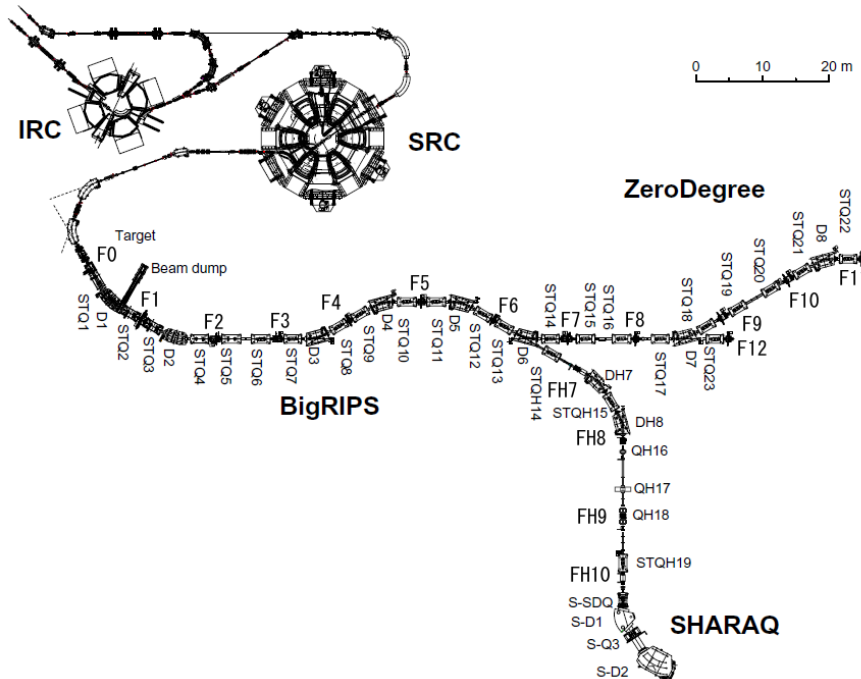


Fig.1. Schematic layout of RI Beam Factory in 2009.

works for matching. In each focus, there is a focal-plane chamber which accommodates beam-line detectors and devices similarly to BigRIPS. A secondary target is placed at F8, when the beam line is used as the ZeroDegree spectrometer for reaction studies with RI beams. The ZeroDegree analyzes and identifies projectile reaction residues, often in coincidence with  $\gamma$ -rays which are measured by a  $\gamma$ -ray array detector surrounding the target. Depending on the experimental requirements, the ZeroDegree can be operated in different optics modes, such as achromatic modes and dispersive modes. Figure 2 shows a recent photograph of the ZeroDegree spectrometer.



Fig. 2. Photograph of the ZeroDegree spectrometer.

The high-resolution beam line consists of the existing part (the section from F3 to D6) and the new part leading to the SHARAQ spectrograph (the section from D6 to the SHARAQ target position). The new part is composed of 2 room-temperature dipoles, 3 STQs, and 3 room-temperature quadrupoles, which are labeled as DH7-8, STQH14-15, STQH19, and QH16-18 in Fig. 1. The focuses are indicated as FH7-10. This beam line can be operated in a dispersive mode with high resolution, so that the dispersion matching conditions can be attained at the SHARAQ focal plane, allowing high-resolution measurement using the SHARAQ. Figure 3 shows a recent photograph of the high-resolution beam line under construction.



Fig. 3. Photographs of the high-resolution beam line.

Commissioning of the BigRIPS was carried out in May 2007 with a  $^{238}\text{U}$  beam at 345 MeV/u, and performance of the BigRIPS was successfully tested. High PID performance was obtained thanks to the trajectory reconstruction. Then a search for new isotopes was made using the  $^{238}\text{U}$  beam as a series of experiments, and the very neutron-rich new palladium ( $Z=46$ ) isotopes  $^{125}\text{Pd}$  and  $^{126}\text{Pd}$  were observed for the first time, although the uranium beam intensity was far from the goal and the observation time was

short. The discovery demonstrated not only the performance of the BigRIPS separator, but also the great potential of the RIBF. The details are described in Ref. 5.

Commissioning of the ZeroDegree was carried out in November 2008 with a  $^{238}\text{U}$  beam at 345 MeV/u, and the ion optics and PID performance were successfully tested for different ion-optics modes. Then we revisited the search for new isotopes using a  $^{238}\text{U}$  beam with  $\sim 40$  times larger intensity than in 2007, which demonstrated the overwhelming RI-beam production power at RIBF. Figure 4 shows the PID plot obtained using the BigRIPS. We were able to identify more than 20 new isotopes in the  $Z=30\sim 50$  region and also more than 10 new isomers. In particular we were able to observe the further neutron-rich palladium isotopes  $^{127}\text{Pd}$  and  $^{128}\text{Pd}$ , which means that we have reached an  $N=82$  magic number nucleus. Furthermore  $^{128}\text{Pd}$  is said to be one of the key nuclei in the r-process path. In December 2008 the ZeroDegree was used, for the first time, for a series of full-dress RI-beam experiments, where an intense  $^{48}\text{Ca}$  beam was employed for the production of RI beams and important results were obtained for very neutron-rich exotic nuclei.

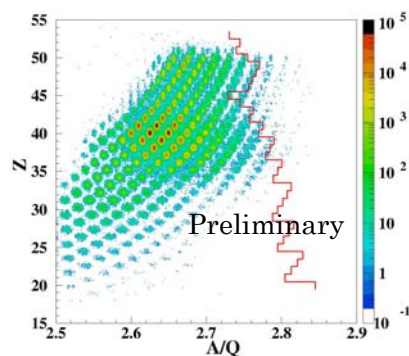


Fig. 4. Particle identification plot for fission fragments produced by  $^{238}\text{U}+\text{Be}$  reaction at 345 MeV/u.

The BigRIPS cryogenic plant, which is used to cool STQ1-5, suffered from an oil-contamination problem which caused a decrease in cooling power after an operation period of two months or so. This problem has been solved by upgrading the oil removal unit of the compressor and fully cleaning up the cold box.

We plan to fully install quick-release mechanisms using the pillow seal system in the beam line of the BigRIPS first stage in summer 2009. This will facilitate maintenance under high residual radiation.

More detailed reports on the project are given elsewhere in this progress report.

#### References

- 1) T. Kubo: Nucl. Instr. and Meth. **B 204**, 97 (2003).
- 2) T. Kubo et al.: IEEE Trans. Appl. Supercond., **17**, 1069 (2007).
- 3) Y. Mizoi et al.: RIKEN Accel. Prog. Rep. **38**, 297 (2005).
- 4) T. Kawabata et al.: RIKEN Accel. Prog. Rep. **41**, 129 (2008).
- 5) T. Ohnishi et al.: J. Phys. Soc. Japan **77**, 083201 (2008)

## Commissioning of ZeroDegree spectrometer

T. Ohnishi, T. Kubo, K. Kusaka, K. Yoshida, A. Yoshida, M. Ohtake, N. Fukuda, H. Takeda, D. Kameda, K. Tanaka, N. Inabe, Y. Yanagisawa, H. Watanabe, H. Otsu, Y. Kondo, Y. Gono, H. Sakurai, T. Motobayashi, H. Baba, T. Ichihara, Y. Yamaguchi, M. Takechi, S. Nishimura, H. Ueno, A. Yoshimi, T. Nakao <sup>\*1</sup>, M. Matsushita <sup>\*2</sup>, K. Ieki <sup>\*2</sup>, Y. Mizoi <sup>\*3</sup>, N. Kobayashi <sup>\*4</sup>, K. N. Tanaka <sup>\*4</sup>, Y. Kawada <sup>\*4</sup>, N. Tanaka <sup>\*4</sup>, S. Deguchi <sup>\*4</sup>, Y. Satou <sup>\*4</sup>, T. Nakamura <sup>\*4</sup>, K. Yoshinaga <sup>\*5</sup>, C. Ishii <sup>\*5</sup>, H. Yoshii <sup>\*5</sup>, N. Uematsu <sup>\*5</sup>, Y. Shiraki <sup>\*5</sup>, T. Sumikama <sup>\*5</sup>, J. Chiba <sup>\*5</sup>, E. Ideguchi <sup>\*6</sup>, S. Ota <sup>\*6</sup>, A. Saito <sup>\*6</sup>, Y. Sasamoto <sup>\*6</sup>, T. Uesaka <sup>\*6</sup>, S. Shimoura <sup>\*6</sup>, T. Yamaguchi <sup>\*7</sup>, T. Suzuki <sup>\*7</sup>, T. Moriguchi <sup>\*8</sup>, A. Ozawa <sup>\*8</sup>, T. Ohtsubo <sup>\*9</sup>, M. Famiano <sup>\*10</sup>, A. S. Nettleton <sup>\*11</sup>, B. M. Sherrill <sup>\*11</sup>, S. Manikonda <sup>\*12</sup>, and J. A. Nolen <sup>\*12</sup>

An RI-beam delivery line<sup>1)</sup> named the ZeroDegree spectrometer is located after the BigRIPS separator.<sup>2)</sup> The main purpose of this spectrometer is to analyze particles emitted by reaction of the RI beam with secondary targets. The ZeroDegree has different optics modes to handle various experimental condition requirements such as large angular acceptance or high momentum resolution for secondary-reaction experiments. In 2007, BigRIPS was successfully commissioned and the first experiment with BigRIPS was performed.<sup>3)</sup> After the improvement of optics calculation using the results obtained from the commissioning BigRIPS, we commissioned ZeroDegree using a uranium beam and RI beams in November 2008.

Figure 1 shows a schematic top view of BigRIPS and ZeroDegree. The labels STQn, Dn and Fn indicate the position of superconducting quadrupole triplets, room-temperature dipoles and focal planes, respectively. ZeroDegree consists of six superconducting quadrupole magnets (STQ17–22) and two room-temperature dipole magnets (D7–D8). The designs of these magnets are same as those of BigRIPS. In commissioning of ZeroDegree, three modes were examined: an achromatic large-acceptance (LA) mode, a dispersive mode, and a dispersive high-resolution (HR) mode. Their specifications are summarized in Table 1.

A <sup>238</sup>U beam was accelerated to an energy of 345 MeV/nucleon using an accelerator complex consisting of the linear accelerator RILAC and the four cyclotrons RRC, fRC, IRC, and SRC.<sup>4)</sup> The production targets were 7-mm-thick Be and 1.5-mm-thick Pb. Beam current was  $1.9 \times 10^9$  particle/sec on average. Fission fragments were collected and analyzed using BigRIPS. Tagged fragments were supplied to the RI delivery line

including ZeroDegree. During the commissioning experiment, the  $B\rho$  values of BigRIPS were set to 7.2 Tm and 7.4 Tm in order to examine the  $B\rho$  dependence of the properties of the optics. At the beginning of the beam line (F8) of ZeroDegree, a 2-mm-thick Pb secondary target was installed. Projectile fragments from the secondary target were analyzed and identified using ZeroDegree. To evaluate the performance of ZeroDegree more clearly, data without the secondary target at F8 was also obtained.

Particle identification in ZeroDegree is same as that in BigRIPS. It is performed using the measured  $B\rho$ , energy loss ( $\Delta E$ ), and time of flight (TOF). TOF was measured using two plastic scintillation counters placed on the first (F8) and final (F11) focal planes with a central flight length of 37 m. Thickness of the scintillation counters was 0.2 mm and their effective area was  $100 \times 100$  mm<sup>2</sup>. In the dispersive mode, the F11 focal plane changes to the dispersive focal plane. A long plastic scintillation counter with an active area of  $200 \times 100 \times 0.2$  mm<sup>3</sup> was installed at F11 to cover the wide position distribution in the dispersive and the dispersive HR modes. To measure  $\Delta E$ , an ionization chamber<sup>5)</sup> was installed at F11. The effective area of the ionization chamber was  $240 \times 150$  mm<sup>2</sup>. For precise  $B\rho$  measurement in the achromatic LA mode, the trajectory of the fragments was reconstructed from the positions and angles measured at two position-sensitive PPACs<sup>5)</sup> at the achromatic focal plane (F8) and two more at the dispersive focal plane (F9). For the other modes, two PPACs located at F11 instead of at F9 were used. Ion-optical transfer matrices calculated using the code COSY INFINITY<sup>6)</sup> were used in the reconstruction. The  $B\rho$  of each fragment was determined from the reconstructed trajectory, the magnetic fields measured using NMR probes, and the magnetic field-map data of dipole. To confirm the particle identification performed at ZeroDegree, delayed  $\gamma$  rays from isomeric states in some of the products were measured using three clover-type high-purity germanium detectors located at F11.<sup>7)</sup>

Fission fragments, produced in the <sup>238</sup>U+Pb reaction in BigRIPS with a  $B\rho$  setting of 7.395 Tm and a momentum acceptance of  $\pm 3\%$ , were delivered to ZeroDegree without the secondary target at F8.

<sup>\*1</sup> Department of Physics, The University of Tokyo  
<sup>\*2</sup> Department of Physics, Rikkyo University  
<sup>\*3</sup> Department of Engineering Science, Osaka Electro-Communication University  
<sup>\*4</sup> Department of Physics, Tokyo Institute of Technology  
<sup>\*5</sup> Department of Physics, Tokyo University of Science  
<sup>\*6</sup> Center for Nuclear Study, The University of Tokyo  
<sup>\*7</sup> Department of Physics, Saitama University  
<sup>\*8</sup> Institute of Physics, University of Tsukuba  
<sup>\*9</sup> Department of Physics, Niigata University  
<sup>\*10</sup> Physics Department, Western Michigan University  
<sup>\*11</sup> National Superconducting Cyclotron Laboratory, Michigan State University  
<sup>\*12</sup> Argonne National Laboratory

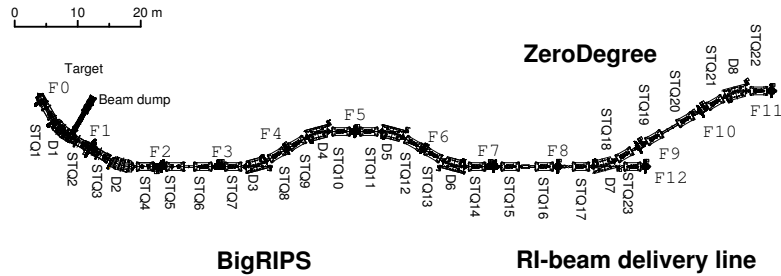


Fig. 1. Schematic top view of BigRIPS separator, RI-beam delivery line and ZeroDegree spectrometer. The labels STQn, Dn and Fn indicate the position of superconducting quadrupole triplets, room-temperature dipoles and focal planes, respectively.

Table 1. Basic specifications of the ZeroDegree spectrometer depending on the optics mode.

Mode	Achromatic large-acceptance mode	Dispersive mode	Dispersive high-resolution mode
Angular acceptance(mr)			
Horizontal	90	40	30
Vertical	70	60	30
Momentum acceptance(%)	6	4	2
Momentum resolution( $P/\Delta P$ )	1240	4100	6400

These fragments were identified again using ZeroDegree. Fig. 2a) and 2b) show two-dimensional plots of the atomic number  $Z$  versus the mass-to-charge ratio  $A/Q$  identified using ZeroDegree in the achromatic LA mode and dispersive mode, respectively. The typical relative root-mean-square (rms) resolution for  $Z$  and  $A/Q$  was 0.5% and 0.09% for the achromatic LA mode, and 0.6% and 0.076% for the dispersive mode. Since the calculated optical matrices are slightly different from the measured matrices, the resolution, especially the  $A/Q$  resolution, is worse than the expected values.

In summary, we commissioned ZeroDegree and measured its performance such as ion optics and particle identification capability. Further data analysis is in progress to extract more detailed features of ZeroDegree, for example, the performance of particle identification with the secondary target.

#### References

- 1) M. Mizoi et al.: RIKEN Accel. Prog. Rep. **38**, 297 (2005).
- 2) T. Kubo et al.: Nucl. Instr. and Meth. **B204**, 97 (2003).
- 3) T. Ohnishi et al.: J. Phys. Soc. Jpn. **77**, 083201 (2008).
- 4) Y. Yano: Nucl. Instr. and Meth. **B261**, 1009 (2007).
- 5) T. Ohnishi et al.: RIKEN Accel. Prog. Rep. **41**, 123 (2008).
- 6) K. Makino and M. Berz: Nucl. Instr. and Meth. **A558**, 346 (2006).
- 7) T. Nakao et al.: in this progress report.

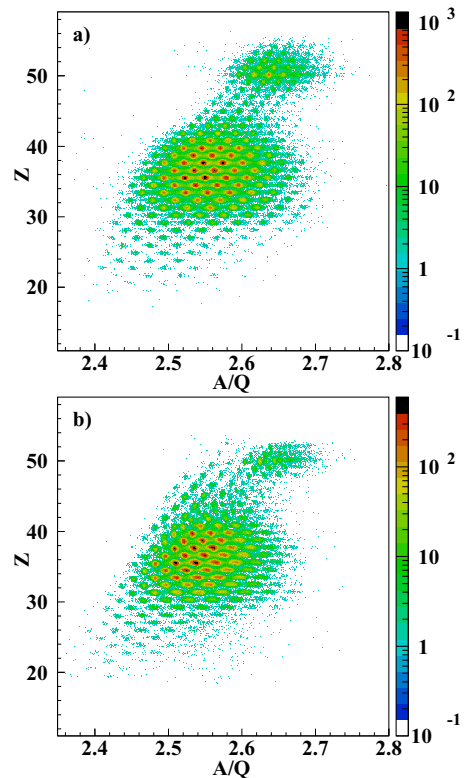


Fig. 2. Two-dimensional plot of  $Z$  versus  $A/Q$  identified using ZeroDegree. Fission fragments were produced in the  $^{238}\text{U}+\text{Pb}$  reaction at BigRIPS with a  $B\rho$  setting of 7.395 Tm and a momentum acceptance of  $\Delta P/P=\pm 3\%$ . The vertical axis is  $Z$ , while the horizontal axis is  $A/Q$ . Upper a) and lower b) figures show the results obtained with the achromatic large-acceptance and the dispersive modes, respectively.

## Beam intensity monitors for BigRIPS separator

Y. Yamaguchi, A. Yoshida, Y. Yanagisawa, K. Tanaka, T. Ohnishi, and T. Kubo

[scattering particle, beam current]



Fig. 1. Setup of beam intensity monitors at production target chamber.

To monitor the primary beam intensity on a production target of the BigRIPS separator<sup>1)</sup>, a scattered particle PLastic MONitor (PLmon), a Fast Current Transformer (FCT)<sup>2)</sup> and a Faraday Cup (FC) are installed at the production target chamber (Fig. 1). The FCT is fixed at the entrance beam duct, the FC is movable in front of the target and the PLmon is mounted on the top of the chamber at an angle of 120 degrees from the beam axis and 68 cm away from the target. The PLmon consists of three layers of plastic scintillators of 1 mm thickness, which detect scattered light charged particles from the target. The PLmon is designed for low intensity beams up to a few 100 electric nano-Ampere (enA). For higher intensity than that, the FCT should be used. These two detectors can continuously monitor the beam current during experiments. They should, however, be calibrated using the beam current measured by the FC at the beginning of each experiment. Here, we report the beam test results of these detectors.

The spectra of the PLmon were measured for three patterns of beam and target combinations as sum-

Table 1. The combinations of beams and targets for the PLmon measurement. The beam energy of U and Kr was 345 MeV/u and those maximum beam intensities are listed in units of enA. The count rate of the PLmon in single mode and in triple coincidence mode are also listed.

Pattern	Beam (enA)	Target	single/coin.
1	$^{86}\text{Kr}^{31+}$ (50)	Be (12 mm)	350k/68k cps
2	$^{238}\text{U}^{86+}$ (2.3)	Be (5 mm)	1.2k/0.2k
3	$^{238}\text{U}^{86+}$ (2.2)	Pb (1.5 mm)	1.2k/1.2k

marized in Table 1. They were measured under the triple coincidence condition of three layer scintillators. Figure 2 shows the energy-loss correlations between two scintillators in the PLmon. Although the beam is different, the spectra of pattern 1 and 2 looks similar. On the other hand, though the beam is the same, the spectra of pattern 2 and 3 look different. In pattern 3, it detected not only protons and deuterium but also tritium,  $^3\text{He}$  and/or  $^4\text{He}$ . This means that the kind of the scattered charged particle depends on the target material rather than the element of the incident beam. The energy distribution of these charged particles was measured roughly by inserting energy absorber plates made of aluminum in front of the first (pla1) scintillator. The minimum measurable energy was 10 MeV for protons, which was determined by a Kapton vac-

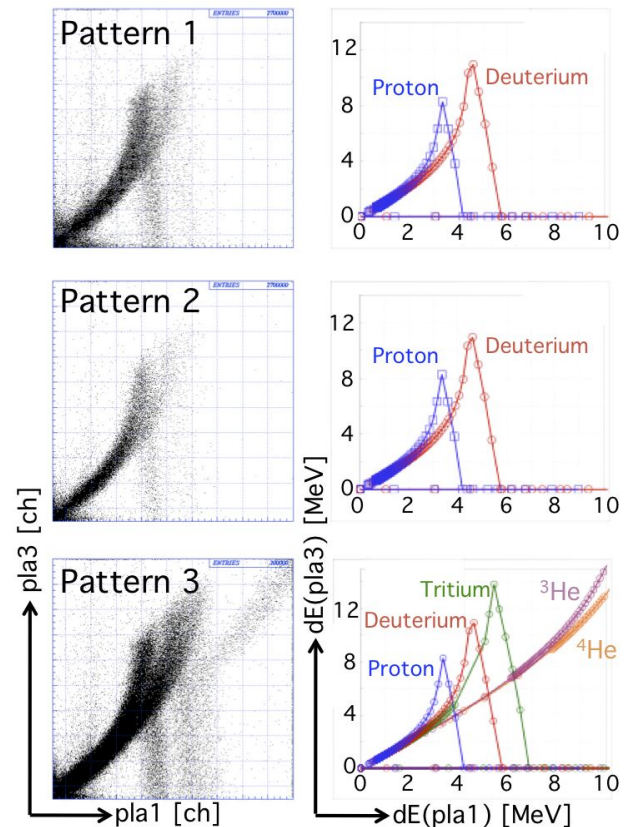


Fig. 2. Energy-loss correlations between the first (pla1) and the third (pla3) scintillator. Measured spectra (left side) and energy-loss calculations (right side) are compared for three patterns of beam and target combinations.

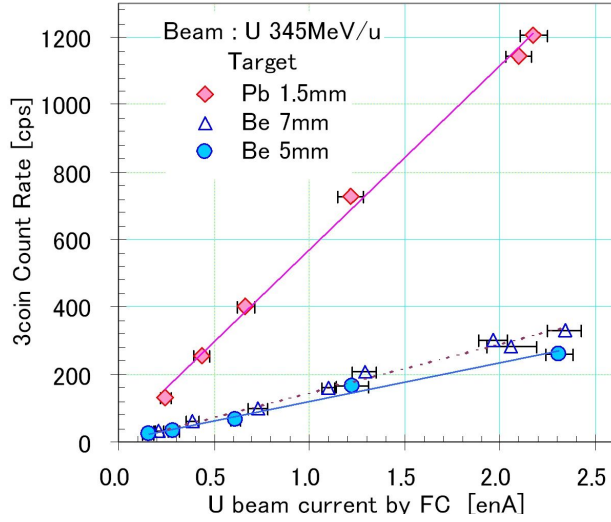


Fig. 3. Target dependence of the triple coincidence count rate of the PLmon.

uum foil of  $40 \mu\text{m}$  thickness placed at the mounting flange. We expected the energy of scattered protons in this backward angle to be up to a few 10 MeV, using a simulation code PHITS<sup>3)</sup>. It was, however, confirmed that protons with an energy of about 100 MeV were also scattered. However the rate of such high-energy protons is less than 1/10. This discussion is still ongoing. Figure 3 shows that the count rate of the PLmon had good linear correlation with the measured beam current using the FC in the range of 0.1 enA up to the maximum current listed in Table 1. The count rate also had a target dependence. The Pb target has

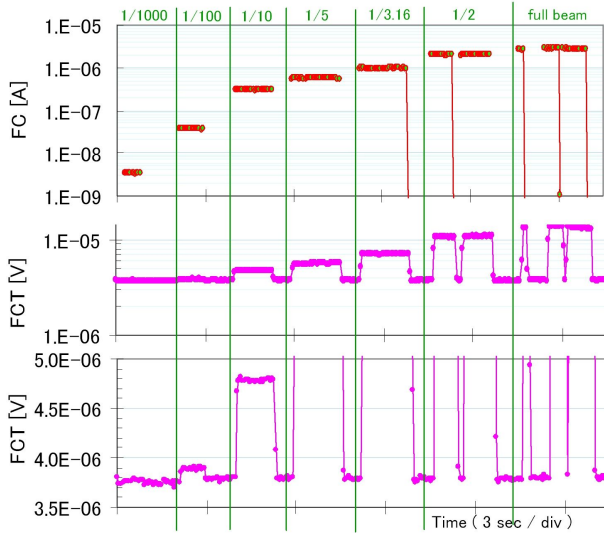


Fig. 4. Changing the  $^{48}\text{Ca}$  beam current, the FC beam current (upper) and the FCT signal (middle and lower) were compared. The background noise level of the FCT was  $3.7 \mu\text{V}$ .

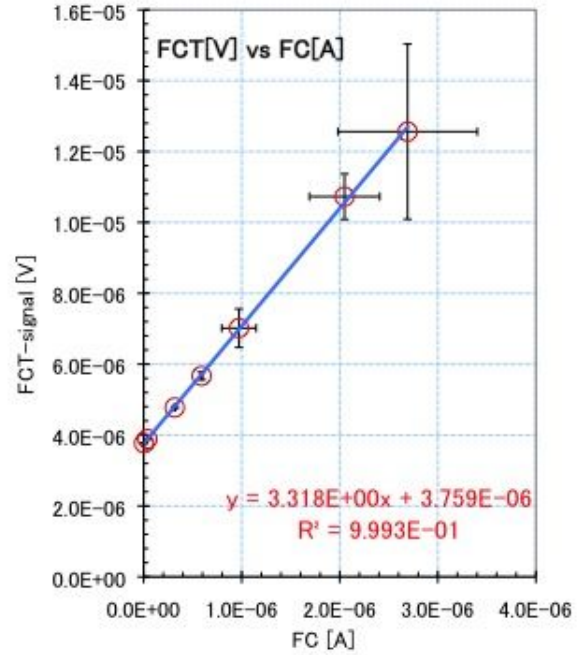


Fig. 5. Correlation between the FCT signal and the beam current measured by the FC.

a 3 times higher count rate than that of Be target. The PLmon was working without any problem in a few 10 enA. However, when the beam intensity was higher than a few 100 enA, the backgrounds increased and the scattered charged particle was not able to be counted precisely.

The FCT signal was measured using a high intensity beam of  $^{48}\text{Ca}^{20+}$ , 350 MeV/u. Figure 4 shows a comparison of measured FC current and FCT signal. The FCT signal is measured using a lock-in amplifier in the unit of volts. The FCT signal had good linear correlation with the measured FC current in the range of a few 10 enA up to  $3 \mu\text{A}$ . Its lower limit was determined by its noise level of  $3.7 \mu\text{V}$ . It is important to reduce the noise as much as possible. Figure 5 shows that the FCT signal had good linear correlation with the measured beam current using the FC in the range of a few 10 enA up to  $3 \mu\text{A}$ . The slope parameter  $3.3 \mu\text{V}/\mu\text{A}$  was slightly different from the nominal value of the FCT coil of  $5 \mu\text{V}/\mu\text{A}$ .

#### References

- 1) A.Yoshida et al: RIKEN Accel. Prog. Rep. **41**, vii (2008).
- 2) M. Wada et al.: RIKEN Accel. Prog. Rep. **38**, 170 (2005).
- 3) PHITS: <http://phits.jaea.go.jp/>

# Manipulation and performance of ionization chambers for BigRIPS experiments

H. Otsu, M. Takechi, Y. Kondo, T. Onishi, N. Fukuda, M. Lantz, K. Ozeki, S. Deguchi,<sup>\*1</sup> Y. Kawada,<sup>\*1</sup> T. Kuboki,<sup>\*2</sup> I. Hachiuma,<sup>\*2</sup> and K. Namihira,<sup>\*2</sup>

Ionization chambers used for BigRIPS experiments give information proportional to energy loss ( $\Delta E \propto \frac{Z^2}{\beta^2}$ ) of the flight particles. In order to deduce the  $Z$  information, it combined with Time Of Flight(TOF) information which is derived from a pair of fast response detectors such as plastic scintillators. In FY2008, two ion chambers were prepared and in effect operated for two sets of BigRIPS experiments using  $^{238}\text{U}$  and  $^{48}\text{Ca}$  primary beams in November and December respectively.

## Configuration of the ionization chamber

Each ionization chamber<sup>1)</sup> consists of the chamber itself, which contains inner gas, and a set of electrodes. The electrodes consist of 12 anodes sandwiched between 13 cathodes. The cathode electrodes are equivalent to ground voltage level. The original objective in reference<sup>1)</sup> was to tilt the electrodes up to  $30^\circ$  from perpendicular geometry which has been expected to prevent ionized pairs from recombining along drift directions. At this point, we selected the perpendicular setup as shown in fig. 1 where the electrodes were penetrated from around  $90^\circ$ . We have estimated a drawback of  $\Delta E$  resolution by the recombination effect being smaller than those of noise on signal from the electrodes or stability of circuits downstream. Effective

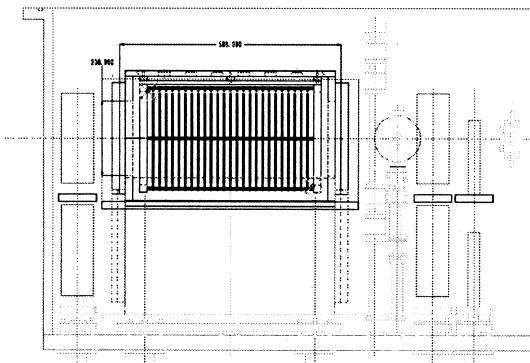


Fig. 1. Side view of the ionization chamber located at the F7 focal point on the BigRIPS beamline.

areas of electrodes are  $232\text{ mm}\phi$  for the F7 ionization chamber and  $260 \times 170\text{ mm}^2$  with edging by R10 for the F11 ionization chamber respectively. We describe them F7IC and F11IC following this. The electrode distances between the anode plate and the cathode

plate are 17 mm for F7IC and 20mm for F11IC. Path length for F7IC is 586 mm and that of F11IC is 660 mm, where the curve shapes of entrance and exit windows are neglected. Kapton foils are used for each of these windows. The thickness of the windows will be mentioned in the following paragraph. The geometry of F7IC is restricted by the boundary conditions interior within the F7 vacuum box.

The electrodes both for the anodes and the cathodes in F7IC are formed by a single face layer of evaporated aluminized Mylar with  $4\text{ }\mu\text{m}$  mounted on a frame. The other face was evaporated using a machine in the B52 room with evaporation thicknesses being 30 nm. The electrodes for F11IC were formed with a similar configuration but with a layer of aluminized Mylar of  $2\text{ }\mu\text{m}$ . Finally, it has been found that the electrode can be formed with a layer of Mylar film with  $2\text{ }\mu\text{m}$  thickness. Material thickness for F7IC is summed up to  $0.109\text{ g/cm}^2$  when used with P10 gas (Ar 90%+CH<sub>4</sub> 10%) at 650 Torr of pressure. Material thickness for F11IC is summed up to  $0.136\text{ g/cm}^2$  when used with P10 gas at 760 Torr of pressure.

## Performance of the ionization chamber

Signals from two neighboring anode plates were bundled inside the ionization chamber and 6 ch analog signals were read out. Each channel was followed by a pre-amplifier, CANBERRA 2004 for F7IC and TENNELEC TC-170 for F11IC. Pre-amplifier outputs were shaped by fast shaping amplifiers CANBERRA 2024 and acquired by peak hold ADCs for the recording of data. The pulse height from each channel was averaged over both arithmetically and geometrically and was found to be not so different from each other in the conditions for the last experiments. Figure 2 shows the result of the experiment for new isotope search in fission fragments from the  $^{238}\text{U}$  primary beam. The horizontal axis denotes a raw pulse height without a  $\beta$  correction while data are eliminated by just a narrow time range which corresponds to one isotope at each  $Z$ . Each peak represents the identified atomic number  $Z$ . In the on-line analysis of the  $^{238}\text{U}$  beam experiment,  $5\sigma$  separation was achieved in the  $Z \simeq 30$  for F11IC. As for F7IC, several mis-handlings worsened resolution to  $3\sigma$  separation. In the on-line analysis for the  $^{48}\text{Ca}$  beam experiment,  $5\sigma$  separation was achieved in  $Z \simeq 8$  for both F7IC and F11IC. For standard operation of ICs, a lower limit for the  $Z$  identification was found to be around  $Z = 5$  where the  $Z$  identification was realized even with plastic scintillators. A tolerance against beam intensity more than several of  $10^4\text{ Hz}$  has not yet

<sup>\*1</sup> Department of Physics, Tokyo Institute of Technology

<sup>\*2</sup> Department of Physics, Saitama University

been measured in the sequence of the experiments.

### Gas handling

It is very important to obtain constant pressure inside the ICs as pulse height is proportional to the amount of gas material along beam paths and energy loss of the penetrating particles should not fluctuate with gas pressure. The gas handler consists of a self-feedback system 640A (MKS Co.) with mass flow meter, baratron gauge, needle valve and rotary pump. The gas handler is the same with that for PPACs but the pressure range of the 640A is modified to cover up to 1000 Torr. Constant pressure had been achieved by applying a feedback of 640A. It should be noted that 640A actually has the two functions of open/close the valve and reducing conductance. The latter function responds quite quickly to deviation of pressure while the former function seems to require additional time, e.g. several minutes. As a result, pressure fluctuations may occur when 640A operates with opening and closing the valve.

In the experiment using the  $^{238}\text{U}$  beam, both the gas handlers for F7IC and F11IC operated by the open/close mode where comparatively amounts of gas flowed. Gas pressure fluctuated with a triangular wave form with time constant and repetition of order of 10 minutes. Therefore, output signal fluctuations were observed to be a maximum of 2%. Acquired data should be analyzed by correcting the alterations of pulse height for the experiment. This fluctuation might occurred according to difference of range of flow rate between the mass flow meter in the 640A and other devices including a gas regulator on gas bottles and the setting of the needle valve.

In the experiment in December, the gas flow quantity was quite limited by the needle valve and the solution was found so much that 640A does not enter the open/close mode but reduces only the conductance.

As a result, less than 2 Torr deviation was realized in comparison with more than 15 Torr for the previous experiment. So, we no longer require any treatment in

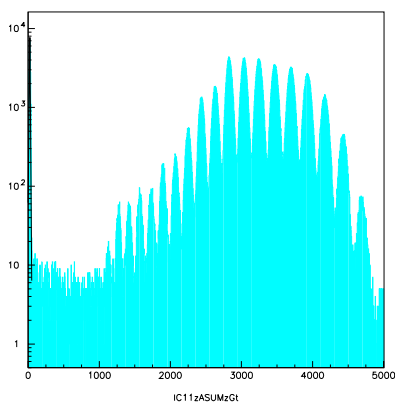


Fig. 2. Z identification by F11IC. Horizontal axis represents Z but the scale is arbitrary. The peak around channel 3900 corresponds to  $Z=32$ .

time chasing analysis in the experiment.

### Tore window incident

F11IC was prepared in August 2008 as the experiment had been scheduled in October at first. In the preparations, a tear in the vacuum tight window occurred in F11IC.

For shortage of gas substitution time, F11IC can be drawn to a vacuum and filled with high purity gases. For this method, entrance and exit windows were made of Kapton film with more than  $75\ \mu\text{m}$  of thickness. This thickness is relatively thick even though F11IC is located within atmospheric conditions rather than a vacuum as in the case of F7IC. To confirm whether this process is possible and feasible, vacuum tests were carried out twice without any devices inside the chamber. The vacuum achieved was less than 1 Torr sufficient to the substitution method. At that time, the Kapton sheet with  $75\ \mu\text{m}$  completely withstood any cracks or tears with the pressed surface shapes being fixed. After the tests, the devices inside F11IC were installed again and F11IC was set on the F11 focal plane. The exit window tear occurred when the vacuum in the chamber was drawn down to approximately 180 Torr. All 25 electrodes inside the chamber were also torn. A picture taken just after the incident is shown in figure 3. In addition, a plastic scintillator just downstream of F11IC was destroyed. We have not yet confined the reason of the problem. Possible reasons would be the rectangular shape of the exit window, the surface fixed shape after repeated testing, or possible defects in other source. The entrance and exit window of both F7IC and F11 IC were replaced with  $150\ \mu\text{m}$  Kapton film after the incident. F7IC is used in vacuum

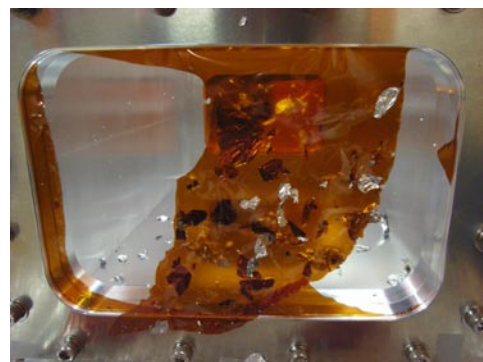


Fig. 3. Torn exit window just after the incident.

circumstance with the windows playing an important role to contain the gas inside. The same kind of incident would destroy not only the detectors inside the F7 vacuum chamber but also the vacuum system consisting of TMP, RP and vacuum gauges. Therefore, it is recommended the window film be replaced at each time experiment is conducted.

### References

- 1) K. Kimura, *et.al.*, Nucl. Instr. and Meth., A538(2005)608.

# SHARAQ Project — Progress in 2008 —

T. Uesaka,<sup>\*1</sup> A. Saito,<sup>\*2</sup> S. Michimasa,<sup>\*1</sup> K. Nakanishi,<sup>\*1</sup> S. Ota,<sup>\*1</sup> Y. Sasamoto,<sup>\*1</sup> K. Miki,<sup>\*2</sup> S. Noji,<sup>\*2</sup>  
 H. Miya,<sup>\*1</sup> H. Tokieda,<sup>\*1</sup> T. Kawabata,<sup>\*1</sup> H. Kurei,<sup>\*1</sup> N. Yamazaki,<sup>\*1</sup> A. Yoshino,<sup>\*1</sup> Y. Yanagisawa,<sup>\*3</sup>  
 T. Kubo,<sup>\*3</sup> T. Yoshida,<sup>\*4</sup> S. Shimoura,<sup>\*1</sup> and H. Sakai<sup>\*2</sup>

Construction of the SHARAQ spectrometer<sup>1)</sup> and the dedicated high-resolution beamline<sup>2)</sup> are coming to the final phase. This article provides an overview of progress in 2008.

## 1 Spectrometer

The SHARAQ spectrometer (Fig.1) consists of three quadrupole (Q1, Q2, and Q3) and two dipole (D1 and D2) magnets. All the magnets were installed in summer of 2007.

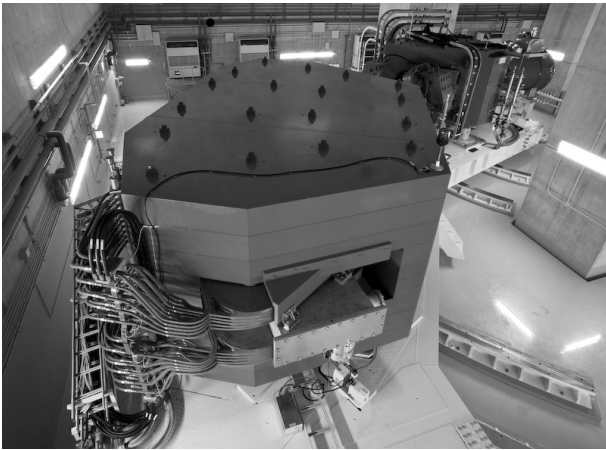


Fig. 1. Photograph of the SHARAQ spectrometer as of April 2008.

Magnetic field distributions of dipole magnets were measured in 2008. Accurate and precise knowledge of the magnetic field is extremely important for high-resolution ion-optical analysis in RI beam experiments. We have measured the magnetic field distribution for a large area of 1.3 m<sup>2</sup> each at the exit of D1 and the entrance and exit of D2. To scan this large area within a reasonable time, we used the search coil method<sup>4)</sup> for measurement. In addition to medium plane measurement, we also collected data for the off-medium plane of  $y=0-85$  mm, where  $y$  denotes distance from the medium plane. The details of the measurement are described in Ref.<sup>3)</sup>. Ion-optical calculation based on the measured field mapping will be used to predict transport matrix elements of the SHARAQ spectrometer.

Now that it is equipped with focal plane vacuum

chambers, the SHARAQ spectrometer is almost ready to accept heavy ion beams.

## 2 High-resolution beam line

Based on the detailed design in Ref.<sup>2)</sup>, we have finalized specifications of beamline devices, including two normal conducting dipole magnets with a 30° bending angle, vacuum chambers for beamline detectors, vacuum pumps, and DC power supplies. Four normal conducting quadrupole magnets and one superconducting triplet quadrupole magnets (STQ) were recycled. One of the normal conducting quadrupoles was renovated to enlarge the bore radius from 150 mm to 180 mm to enable acceptance of large-emittance secondary beams from BigRIPS. Construction of the beamline started in summer of 2008 and will be completed by the end of February 2009.<sup>5)</sup>

Several beamline modes should be prepared to enable versatile use of the SHARAQ spectrometer. We have investigated a new large momentum acceptance mode<sup>6)</sup>, in addition to dispersion matching and high-resolution achromatic modes for high-resolution missing mass measurements. In the large momentum acceptance mode, the beamline allows beam momentum spread of  $\Delta p/p = 2\%$ , which is about 6 times larger than that in the dispersion matching mode. Experiments with low-intensity rare isotope beams can be efficiently conducted in the large acceptance mode.

## 3 Focal plane detectors

Cathode readout drift chambers will be used as tracking detectors at the final focal plane of the SHARAQ spectrometer. They have an effective area of 550 mm (H)  $\times$  300 mm (V) to cover the focal plane. To minimize multiple scattering effects, operation at gas pressures as low as  $P_{\text{gas}} \sim 3-5$  kPa was investigated through simulations with GARFIELD. Based on the results, We examined expected performance of the CRDCs and specified the requirements for drift voltage, pad pattern, and readout electronics were specified.<sup>7)</sup> The CRDCs were fabricated in collaboration with the GANIL group and were transported to RIBF in December 2008.

## 4 Beam-line detectors

Thin tracking detectors working under a beam intensity of higher than 1 MHz are key devices in high-

\*1 Center for Nuclear Study (CNS), University of Tokyo

\*2 Department of Physics, University of Tokyo

\*3 RIKEN

\*4 Rikkyo University

resolution experiments with SHARAQ. They are used for tuning the beamline and tagging beam trajectories during measurements. Energy straggling and multiple scattering in the detector materials must be kept small so that the energy resolution of  $\Delta E/E < 1/7500$  and angular resolution of  $\Delta\theta < 1$  mrad required in SHARAQ experiments are not ruined. Low-pressure multiwire drift chambers (LP-MWDC) were developed as the beam-line detectors.<sup>8)</sup> In 2008, the detectors were irradiated with an accelerated  $\alpha$ -beam with an energy of 8.84 MeV.<sup>9,10)</sup> The energy deposit of the alpha particles is same as that of a 200-MeV/A nitrogen beam which will be used in a future experiment at SHARAQ. The results clearly demonstrated that LP-MWDC with an isobutane gas should work under a pressure as low as 10 kPa. It was also found that further improvements in the electronics are required for better determination of the energy loss of particles.

## 5 Towards commissioning

The commissioning of the SHARAQ spectrometer and the beamline is scheduled for March 2009. All the devices including magnetic systems and detectors will be tested there. One of the most important issues to be investigated in the commissioning run is evaluation of higher-order aberration of the beamline. A challenge of the SHARAQ project is to achieve high-resolution magnetic analysis with momentum resolution of  $p/\Delta p = 15000$  and angular resolution of  $\Delta\theta = 1$  mrad for large-emittance RI beams. Precise knowledge of higher order aberrations is especially important. We are planning to measure all the geometric and chromatic terms, causing image and angular broadening larger than 1 mm and 1 mrad. Efforts are being made to establish a method with which we can disentangle each contribution from the complicated phase space distributions.

## Acknowledgement

The authors would like to thank Al-. Zeller at Michigan State University for providing us with search coils for dipole field measurements. We would also like to express our gratitude to the members of the BigRIPS group for valuable suggestions and assistance on many occasions.

## References

- 1) T. Uesaka et al., Nucl. Instrum. Methods B **266**, 4218 (2008).
- 2) T. Kawabata et al.: Nucl. Instrum. Methods B **266**, 4201 (2008).
- 3) K. Nakanishi et al.: RIKEN Acc. Prog. Rep. **42** (2009).
- 4) J. A. Caggiano: Ph.D thesis, Michigan State University, (1999).
- 5) T. Kubo et al.: RIKEN Acc. Prog. Rep. **42** (2009).
- 6) Y. Sasamoto et al.: RIKEN Acc. Prog. Rep. **42** (2009).

- 7) S. Michimasa et al.: RIKEN Acc. Prog. Rep. **42** (2009).
- 8) A. Saito et al.: RIKEN Acc. Prog. Rep. **42** (2009).
- 9) K. Miki et al.: RIKEN Acc. Prog. Rep. **42** (2009).
- 10) H. Miya et al.: RIKEN Acc. Prog. Rep. **42** (2009).

# Magnetic field measurement for the dipole magnets of the SHARAQ spectrometer<sup>†</sup>

K. Nakanishi,<sup>\*1</sup> H. Kurei,<sup>\*1</sup> S. Michimasa,<sup>\*1</sup> K. Miki,<sup>\*1</sup> H. Miya,<sup>\*1</sup> S. Noji,<sup>\*1</sup> S. Ota,<sup>\*1</sup> A. Saito,<sup>\*1</sup> Y. Sasamoto,<sup>\*1</sup> S. Shimoura,<sup>\*1</sup> H. Tokieda,<sup>\*1</sup> T. Uesaka,<sup>\*1</sup> N. Yamazaki,<sup>\*1</sup> and A. Yoshino,<sup>\*1</sup>

[Fieldmapping, dipole magnet, spectrometer]

The SHARAQ (Spectroscopy with High-resolution Analyzer and RadioActive Quantum beams) spectrometer is a high resolution magnetic spectrometer designed for radioactive isotopes (RI) beam experiments at the RI Beam Factory (RIBF)<sup>1</sup>.

The SHARAQ spectrometer can analyze particles with magnetic rigidity of 1.8 - 6.8 Tm, corresponding to an energy of 40 - 440 MeV/nucleon for  $A/Z = 2$  particles. It is designed for momentum and angular resolutions of  $\delta p/p \sim 1/15,000$  and  $\delta\theta \sim 1$  mrad, respectively. The magnetic composition of the spectrometer is three quadrupole and two dipole magnets. The first dipole magnet (D1) is placed between first quadrupole doublet (SDQ) and singlet quadrupole (Q3) magnets.

The D1 and D2 dipoles have 230 mm and 200 mm gaps, respectively. They have maximum central fields of 1.5 Tesla. The bending radii are 4400 mm and bend angles are  $32.7^\circ$  in the D1 magnet and  $59.6^\circ$  in the D2<sup>2,3</sup>.

The beam transfer matrices describe how an ion's motion changes as it travels through the element. Thus, knowledge of transfer matrices requires precise and accurate information of the magnetic field data in the elements. The field data was intended to be used in the input parameters for COSY<sup>2</sup>.

The precision and accuracy goal of the mapping process was 0.1 mT at all points, namely  $\Delta B/B \sim 10^{-4}$ . This agreed the value of designed momentum resolution.

The field measurement technique was to pass a coil of wire through the magnetic field and measure the induced voltage,  $E = -d\Phi/dt$ , where  $\Phi$  is the magnetic flux through the coil. The field was determined along the path by time integral of the voltage. Field calibration measurements were made with hall probes.

The induction coils used for field measurement was lent from a spectrometer and beam physics team of the NSCL. They adopted it to the mapping for the S800 spectrometer<sup>3</sup>. The coil consisted of very fine wire, whose diameter was  $25 \mu\text{m}$ , spooled around a bobbin. The height of the bobbin was 12.7 mm, though the spool was only 9.53 mm tall. The wire was wrapped very tightly with a final diameter of 9.53 mm, a bore diameter of about 7 mm. The wires were copper, and given their diameter and resistance (about 6.7 k  $\Omega$ , whose turns of the coil was about 30,000.) providing a large voltage signal. For example, the induced voltage

is  $\sim 0.7$  V at a field gradient of 60 mT/mm with moving velocity of the coil at 75 mm/sec. There were five of these coils, one on the magnetic medium plane, the others above.

The mapper was designed to be put on the surface of the pole or vacuum chamber of the two dipoles. The frame was 50 mm thick plate made of an alloy of aluminum, 2347 mm across, with the a central radius of 4400 mm to match the one of the dipoles. An angular extent was  $28.73^\circ$ . The arc lengths of the D1 and D2 were over 2.5 m and 4.6 m, respectively, and the mapper couldn't be made to cover whole the magnetic field of dipoles because it was quite difficult to keep the flat level of its surfaces. Then, we decided to prepare the mapper to measure just around the magnet fringes separately. The whole distribution would be reconstructed via analyzed the data.

The coils ride on a cart which was mainly compounded from fiber glass epoxy resin (G10) and its size was 800 mm  $\times$  300 mm including aluminum hardware attachment. It had four plastic guide rollers, two on each side of the guide, to enable the cart to roll back and forth on an arc of fixed radius. The cart was fixed in the vertical direction by eight wheels which gripped the side edge, which was parted from underside, of the plate. The cart was propelled on the guide rail by a stainless steel chain connected to a servo motor. The chain make a loop between a gear and a sprocket and fixed to the cart at its center.

A diagram for the measurement system is shown in Fig.1. The positions and times of the field measure-

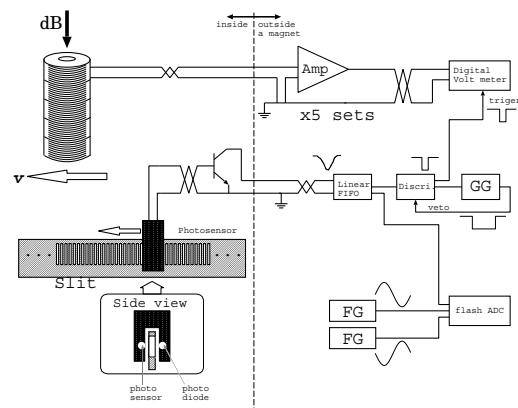


Fig. 1. Measurement system diagram

<sup>\*1</sup> Center for Nuclear Physics, University of Tokyo

ments were obtained by reading a small slit on a thin plate. The plate was put perpendicular on the top surface of the mapper. The size of each slit was 0.25 mm  $\times$  3.5 mm rectangular holes regularly spaced at a distance of 0.75 mm. A transmissive optical sensor, which contained a small infrared photodiode on one side of the slit plate, was used to detect the position of slit edge. The output of the transistor was supplied to the input of trigger for the data taking system. The timing of the output signals then translate into position information.

Simultaneously, the time intervals were deduced by a regular timing signals in every slit and accurate velocities were obtained. Fluctuations of output signals from the coils could be modified via the velocities at the every measurement point.

The production maps were taken at several current and field settings ranging from 0.15 to 1.5 Tesla for the D1 magnet and 0.17 to 1.66 Tesla for the D2, from 100 to 1000 Amps.

After the data correction, for example, off-set voltage at an amplifier output of each coil, cart velocity, coordinate and absolute magnetic field strength at the start and end point of the measurement, complete sets of the field distribution were obtained. The field distributions around magnet fringes forms not rectangular but continuous shape. From the analysis of the effective field boundaries (EFB) a substantial edge of the dipole magnets for the passing particles can be determined. From the entrance and exit points of the EFBs at the central rays in the dipoles, the effective field lengths (EFL) were also deduced at the excitation sets.

The relationship of the excitation current and the  $B\rho$  was obtained for each magnet is shown in Fig. 2. By using these results, the experimenter can set the magnet field for particles with a certain  $B\rho$  value.

Additionally, Fig. 3 describes the relationship between the EFL and the  $B\rho$  values of a passing particle at the D1 and D2 magnets, respectively. A drastically shifts can be recognised over 6 Tm while the EFLs are constant within 0.1% below. The calculation of the beam transport can be referred the relationship of the  $B\rho$  and the EFLs and one can describe the transfer matrices for an arbitrary situation.

#### References

- 1) T. Uesaka *et al.*, Nucl. Instr. and Meth. B 266 (2008) 4218.
- 2) T. Uesaka *et al.*, CNS Annual Report 2005.
- 3) G.P. Berg, Design Study of a New Dipole Magnet D2 for the SHARAQ Spectrometer, unpublished.
- 4) K. Makino, M. Berz, Nucl. Instr. and Meth. A 558 (2005) 346.
- 5) J.A. Caggiano, Doctoral dissertation, Department of Physics and Astronomy, Michigan State University (1999).

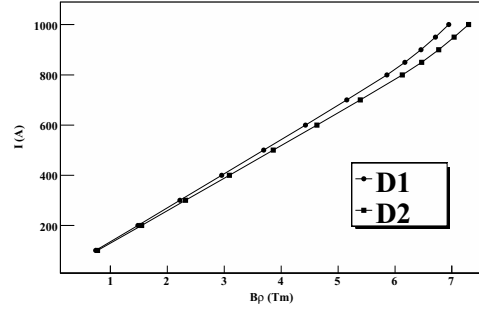


Fig. 2. The relationship of the excitation current and the  $B\rho$  value at the D1 and D2 magnets.

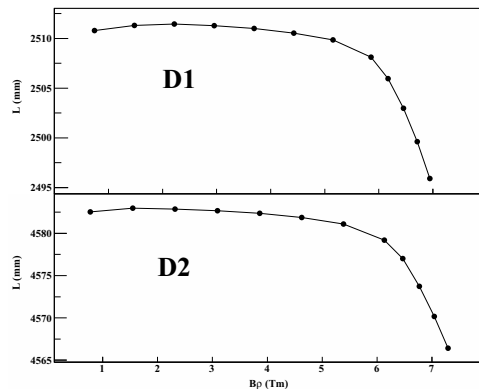


Fig. 3. The shifts of the effective field length (EFL) as a function of the  $B\rho$  value at the D1 and D2 magnets.

# Large acceptance transport in the high resolution beam line for SHARAQ spectrometer

Y. Sasamoto,<sup>\*1</sup> T. Kawabata,<sup>\*1</sup> T. Uesaka,<sup>\*1</sup> S. Shimoura,<sup>\*1</sup> T. Kubo, Y. Yanagisawa, H. Sakai,<sup>\*2</sup>  
N. Yamazaki,<sup>\*1</sup> and A. Yoshino,<sup>\*1</sup>

New missing mass spectroscopy with an RI beam is planned to be conducted at RIBF with the SHARAQ spectrometer<sup>1)</sup>. The SHARAQ spectrometer is designed to achieve a resolving power of  $p/\delta p = 1.5 \times 10^4$  and a high angular resolution of  $\delta\theta \sim 1$  mrad for particles with a maximum magnetic rigidity of  $B\rho = 6.8$  Tm.

To avoid loss of energy resolution due to the momentum spread of RI beams, the dispersion matching technique is applied to perform high resolution measurements<sup>2)</sup>. The maximum resolving power 15000 is achieved in the dispersion matching (DM) mode. However, in the DM mode, a large target is needed because the image size at the target is about as large as 10 cm. High resolution achromatic (HA) mode is also prepared. In the HA mode, the beam size of the target is about a few cm with keeping the half resolving power of the DM mode if the beam trajectories are measured at F6. The resolving power and acceptance for the DM and HA mode are summarized in Table 1. Now the high resolution beam line is under construction based on the ion optical design<sup>3)</sup>. In the commissioning run scheduled in March 2009, the measurements to determine the transfer matrix elements are planned.

Beam transports described above have the advantage of large resolving power at the cost of the small momentum acceptance of  $\pm 0.3\%$  as listed in Table 1. This is because the beam trajectories are spread out in accordance with the large dispersion of the beam line. In some experiments, more wider momentum acceptance transport mode is required for high intensity. The large acceptance (LA) achromatic mode is quite indispensable.

The beam trajectories of the LA mode obtained by the first order ion optical calculation using GIOS<sup>4)</sup> are shown in Fig. 1. The transfer matrix obtained by the calculation is summarized in Table 2. In the calculation, strengths of quadrupole magnets by F5 are equivalent to the BigRIPS standard transport<sup>5)</sup>. As shown in Fig.1, the beam is focused both horizontally and vertically at F6, FH7 and the Target, while the beam is focused only vertically at FH9. In this calculation, the momentum acceptance is limited by the beam size in STQ14, while the angular acceptance is limited by that in QH18.

The resolving power and acceptance are compared with other modes in Table 1. In the LA mode, mo-

mentum acceptance of  $\pm 2\%$  is achieved. On the other hand, the resolving power, which is the same value at F5 of BigRIPS standard is 1/10 of the DM mode. There is still some room for improvement in the LA transport. In the present calculation, polarities and locations of magnets are fixed to be the same as in the DM/HA mode. Due to the limitations, horizontal and vertical magnifications are not small enough in the LA mode. Investigation along these line is still in progress.

Transport mode	DM	HA	LA
Resolving power	15000	7500 (at F6)	1500 (at F5)
Momentum acceptance (%)	$\pm 0.3$	$\pm 0.3$	$\pm 2$
Angular acceptance			
horizontal (mrad)	$\pm 10$	$\pm 10$	$\pm 20$
vertical (mrad)	$\pm 30$	$\pm 30$	$\pm 20$

Table 1. Resolving power and acceptance for high resolution beam line for SHARAQ. Transport mode of DM, HA, and LA indicate the dispersion matching mode, high resolution achromatic mode and large acceptance mode respectively.

$(x x) =$	1.921	$(x a) =$	0.000
$(a x) =$	0.258	$(a a) =$	0.520
$(x \delta) =$	0.13		
$(y y) =$	5.001	$(y b) =$	0.002
$(b y) =$	6.612	$(b b) =$	0.225

Table 2. Transfer matrix elements of the large acceptance mode obtained from the first order calculation by GIOS<sup>4)</sup>. The units for the lengths and angles are meters and radian.

## References

- 1) T. Uesaka et al.: Nucl. Instrum. Meth. in Phys. Res. B266, 4218 (2008).
- 2) T. Kawabata et al.: Nucl. Instrum. and Meth. in Phys. Res. B266, 4201 (2008).
- 3) Y. Yanagisawa : Private correspondence.
- 4) H. Wollnik et al.: Ion-optics code GIOS, University of Giessen, Germany.
- 5) H. Takeda et. al.: RIKEN Accel. Rep. 41 (2008).

<sup>\*1</sup> Center for Nuclear Study, University of Tokyo

<sup>\*2</sup> Department of Physics, University of Tokyo

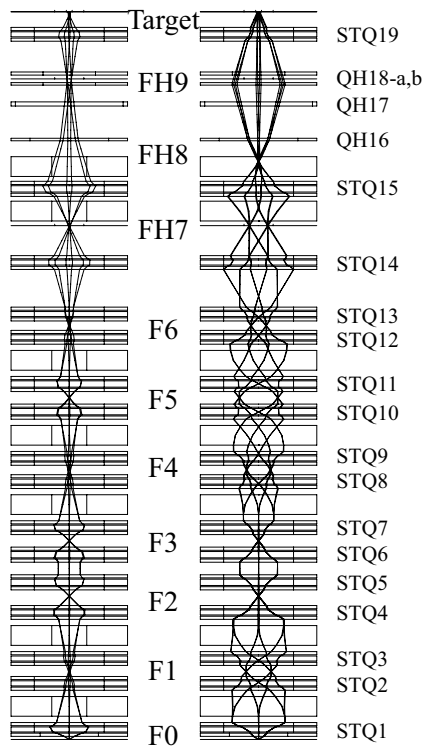


Fig. 1. Beam trajectories of the large acceptance mode from F0 to the SHARQA target. The left figure shows the trajectories in the vertical plane, and the right one shows that in the horizontal plane. The trajectories with  $x_0 = \pm 3$  mm,  $y_0 = \pm 3$  mm,  $\theta_0 = \pm 20$  and 0 mrad,  $\phi_0 = \pm 20$  and 0 mrad, and  $\delta_0 = \pm 2\%$  are also drawn.

# Development of low-pressure multi-wire drift chambers for BigRIPS and high-resolution beam line

A. Saito,<sup>\*1</sup> S. Shimoura,<sup>\*2</sup> K. Miki,<sup>\*1\*3</sup> H. Miya,<sup>\*2</sup> T. Yoshida,<sup>\*4</sup> T. Kawabata,<sup>\*2</sup> H. Kurei,<sup>\*2</sup> S. Michimasa,<sup>\*2</sup> K. Nakanishi,<sup>\*2</sup> S. Noji,<sup>\*1</sup> S. Ota,<sup>\*2</sup> Y. Sasamoto,<sup>\*2\*3</sup> H. Tokieda,<sup>\*2</sup> T. Uesaka,<sup>\*2</sup> and H. Sakai<sup>\*1</sup>

We are developing low-pressure multi-wire drift chambers (LP-MWDC's) that will be used at BigRIPS and the high-resolution beam line (HRBL) for experiments using the SHARAQ spectrometer.<sup>1)</sup> The SHARAQ spectrometer is designed to achieve a resolving power of  $p/\delta p \sim 1.5 \times 10^4$  and an angular resolution better than 1 mrad for charged particles with maximum magnetic rigidity of 6.8 Tm. The high-resolution beam line is designed to fulfill dispersion-matching conditions when combined with the SHARAQ spectrometer. The simultaneous achievement of lateral dispersion matching and angular dispersion matching conditions is crucially important in using the SHARAQ

spectrometer for RI beams, which necessarily entail a large momentum spread. Details of the dispersion-matching beam transport are described in an other report.<sup>2)</sup> Figure 1 shows the BigRIPS, HRBL, and the SHARAQ spectrometer. The LP-MWDC's are used at F3, F6, F-H7, F-H9, and F-H10. Event-by-event tagging and tracking are needed at F3 for monitoring image size and at F-H10 to measure the momentum vector of the RI beam.

There are some requirements for the tracking detectors. The thickness of the detectors should be as small as  $\sim 10^{-4}$  of the radiation length to reduce the effects of multiple scattering in the detectors to  $\sim 0.1$  mrad. The efficiency should be as large as possible even for

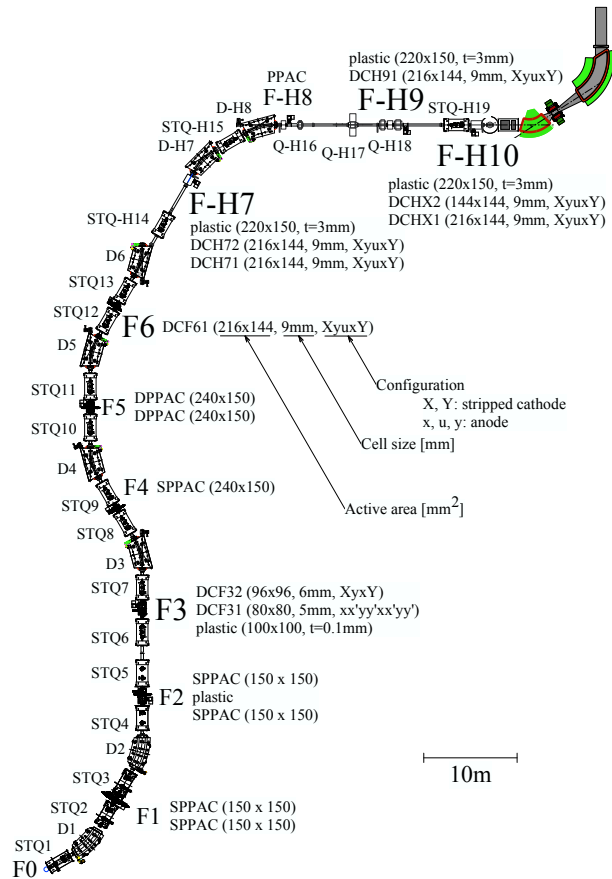


Fig. 1. LP-MWDC's in BigRIPS and high-resolution beam line.

Table 1. List of LP-MWDC's in BigRIPS and HRBL.

Focal Plane	Name	Active area [mm <sup>2</sup> ]	Cell size [mm]	Configuration
F3	DCF31	80×80	5	xx'yy'xx'yy'
	DCF32	96×96	6	XyuxY
F6	DCF61	216×144	9	XyuxY
	DCF71	216×144	9	XyuxY
F-H7	DCF71	216×144	9	XyuxY
	DCF72	216×144	9	XyuxY
F-H9	DCF91	216×144	9	XyuxY
F-H10	DCFX1	216×144	9	XyuxY
	DCFY1	144×144	9	XyuxY

X, Y: stripped cathode  
x, u, y: anode

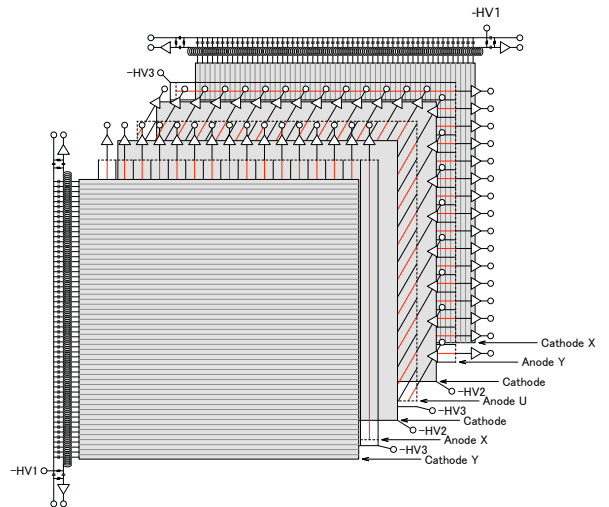


Fig. 2. Schematic view of DCHX2.

\*1 Department of Physics, University of Tokyo  
\*2 Center for Nuclear Study, University of Tokyo  
\*3 Department of Physics, Rikkyo University  
\*4 RIKEN Nishina Center

light RI beams such as  $^8\text{He}$  at 200 MeV/nucleon. Position resolution is required to be less than  $300\ \mu\text{m}$  in FWHM. The maximum counting rate should be 1 MHz for the dispersive beam transport. Energy loss information should be obtained by the tracking detectors for particle identification of the RI beam to reject in-flight  $\beta$ -decay events.

The LP-MWDC's are being developed in order to realize the performance described above. Low-pressure operation at around 10 kPa is needed to reduce multiple scattering in the detector to as low as 0.1 mrad. The list of the LP-MWDC's is shown in Table 1. Details of DCF31 and DCF32 are described in other reports.<sup>3,4)</sup> Figure 2 shows a schematic view of DCHX2. It includes three anode layers (x, u, and y) and two stripped cathodes (X and Y). The direction of the u wires is tilted by 30 deg. with respect to the x wires. The cathodes on the outside are stripped in vertical and horizontal directions (X and Y). The stripped cathodes give redundant position information, and the energy loss of the RI beam for particle identification. Signals from the stripped cathodes are read out using delay lines (DL's) which are used for the PPAC's.<sup>5)</sup> Three high voltages can be supplied individually to the stripped cathodes, other cathodes, and the field wires. Signals from DL's are amplified by a Kaizu 3356 preamplifier. Signals from the anode wires are amplified and discriminated by REPIC RPA-130/131 64-ch. preamplifier and discriminator cards. The timing signals from RPA-130/131 are digitized by CAEN V1190A/B multi-hit TDC's.

We performed two experiments to evaluate the LP-MWDC's. Both experiments were carried out in the E7B course of RIBF operated by RIKEN Nishina Center and CNS, University of Tokyo. The beam was  $\alpha$  at 8.8 MeV/nucleon which gives the same energy losses as  $^{12}\text{N}$  at 200 MeV/nucleon, which will be used in the experiments using the SHARAQ spectrometer. Details

of the first experiment are described in other reports.<sup>4)</sup> In the second experiment, we tested four LP-MWDC's, DCF31, DCHX2, DCHX1, and DCHX61. Figure 3 shows the experimental setup. The number of beams is counted by a  $100\text{-}\mu\text{m}$  thick plastic scintillator located upstream of the LP-MWDC's. The vacuum of the beam line and the counter gas of the LP-MWDC's are separated by  $50\text{-}\mu\text{m}$  thick aluminized mylar in front of DCF31. The configuration and the performance of DCF31 is described in another report.<sup>3)</sup> DCHX2, DCHX1, and DCF61 have the same configurations described above. DCHX1 was set to the opposite direction, i.e. YxvyX, in order to have the same setup as F-H10. An aluminum plate with "SHARAQ" character is located downstream of LP-MWDC's backed by a 5-mm thick plastic scintillator. Data was collected for gas pressures of 4, 5, 10, and 20 kPa. Data analysis to evaluate efficiencies and tracking resolutions is now in progress.

#### References

- 1) T. Uesaka et al.: Nucl. Instrum. Meth. in Phys. Res. **B266**, 4218 (2008).
- 2) T. Kawabata et al.: Nucl. Instrum. Meth. in Phys. Res. **B266**, 4201 (2008).
- 3) K. Miki et al.: RIKEN Accel. Prog. Rep. **42** (2009).
- 4) H. Miya et al.: CNS Ann. Rep. (2008);  
H. Miya et al.: RIKEN Accel. Prog. Rep. **42** (2009).
- 5) H. Kumagai et al.: Nucl. Instrum. Meth. in Phys. Res. **A470**, 562 (2004).

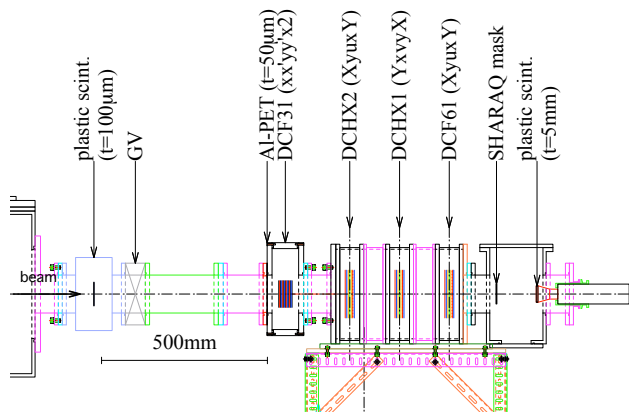


Fig. 3. Setup of the second experiment.

## Development of Low-Pressure Multi-Wire Drift Chamber with Stripped Cathodes

H. Miya,<sup>\*1</sup> S. Shimoura,<sup>\*1</sup> A. Saito,<sup>\*2</sup> T. Kawabata,<sup>\*1</sup> S. Michimasa,<sup>\*1</sup> H. Kurei,<sup>\*1</sup> K. Miki,<sup>\*2,\*3</sup> K. Nakanishi,<sup>\*1</sup> S. Ota,<sup>\*1</sup> Y. Sasamoto,<sup>\*1,\*3</sup> T. Uesaka,<sup>\*1</sup> and H. Sakai<sup>\*2</sup>

We are developing Low-Pressure Multi-Wire Drift Chambers with stripped cathodes (LP-MWDCs)<sup>1)</sup>. The LP-MWDC is used as a tracking detector in a high-resolution beam line<sup>2)</sup> for experiments using the SHARAQ spectrometer<sup>3)</sup>. The designed values such as the position resolution, efficiency and counting rate of the LP-MWDC are described in the previous report<sup>1)</sup>. The LP-MWDC is designed for operation at a low pressure of counter gas to reduce the amount of materials. High efficiencies are required for light RI beam such as  $^{12}\text{N}$ ,  $^{12}\text{B}$ , and  $^8\text{He}$  at 100–300 MeV/nucleon.

Figure 1 shows a schematic view of the LP-MWDC with stripped cathodes. The LP-MWDC consists of 2 anode layers and 4 cathode layers. The outside cathode layers are stripped and connected with the delay line. The signals from the cathodes are read out through the delay lines which were developed for RIKEN PPAC<sup>4)</sup>. The hit positions are determined both by the anode wires and stripped cathodes. Also, the position information of the cathode is used to resolve left-right ambiguity of the anodes. The counter gas is isobutane using as little as 20 kPa. The specifications are summarized in Table 1.

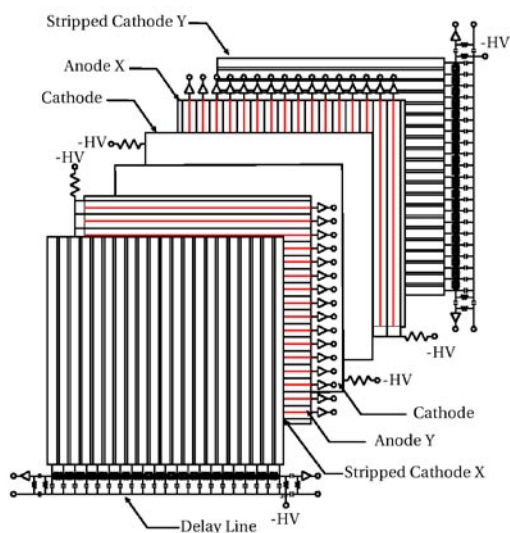


Fig. 1. Schematic view of the LP-MWDC with stripped cathodes

The LP-MWDC was tested for the  $\alpha$  beam at 8.8 MeV/nucleon. The energy-loss of the  $\alpha$  beam is com-

Table 1. Specification of the LP-MWDC with stripped cathodes

effective area	96×96 mm <sup>2</sup>
layer pattern	C <sub>X</sub> -A <sub>Y</sub> -C-C-A <sub>X</sub> -C <sub>Y</sub>
anode wire	20 μm <sup>φ</sup> , Au-W
potential wire	75 μm <sup>φ</sup> , Au-Cu
cell size	6×6 mm <sup>2</sup>
cathodes	Aluminized mylar, 1.5 μm <sup>t</sup>
strip width and pitch	2.4 mm and 0.1 mm
counter gas	isobutane, 4–20 kPa

parable to the  $^{12}\text{N}$  beam at 200 MeV/nucleon. Here, we report results of a test experiment for checking the detection efficiencies, position extraction and energy-loss resolution involved in a simulation condition.

The experiment was performed with the beam at the E7B course at RIKEN RIBF operated by RIKEN Nishina Center and CNS, University of Tokyo. The  $\alpha$  beam at 8.8 MeV/nucleon was supplied by the AVF Cyclotron. Figure 2 shows a schematic view of the experimental setup. A plastic scintillator, with the size of 5 mm<sup>t</sup> and 50×50 mm<sup>2</sup>, was placed at the downstream of the LP-MWDC as a trigger counter. The LP-MWDC was operated at the gas pressure between 4 kPa and 20 kPa. The timing signal of the anodes and cathodes were taken with a CAEN V1190A multi-hit TDC and a CAEN V792N QDC respectively.

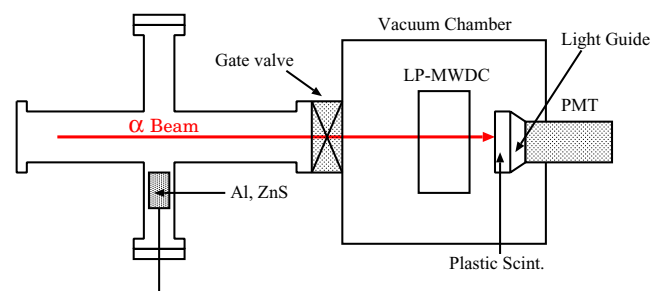


Fig. 2. Schematic view of the experimental setup

Figure 3 shows the detection efficiency of anode signals at a gas pressure of 20 kPa (open triangle), 15 kPa (closed square), 10 kPa (open square), 5 kPa (closed circle), and 4 kPa (open circle) as a function of the voltage applied to the cathodes and potential wires. The threshold levels of the anodes were evaluated to be 100 fC based on the energy loss of the  $\alpha$  beam and the gas multiplication factor<sup>5)</sup>. The efficiency of the

\*1 Center for Nuclear Study, University of Tokyo

\*2 Department of Physics, University of Tokyo

\*3 Riken Nishina center

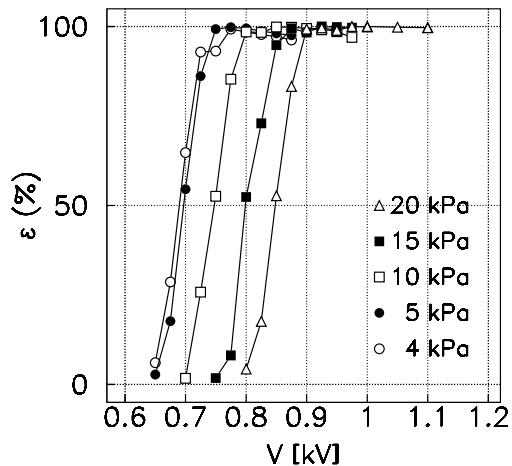


Fig. 3. The efficiencies of the anodes for gas pressures as a function of the applied voltage .

anodes reaches up to  $\sim 100\%$  at a low pressure in the range from 4 kPa to 20 kPa. The efficiency of the anodes satisfied the requirement.

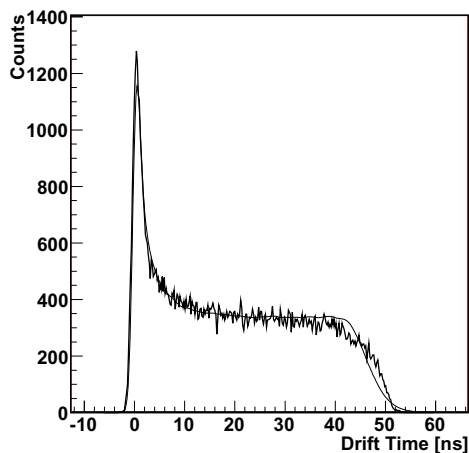


Fig. 4. Drift time distribution. The histogram is the distribution of the experimental data. The solid line is the distribution by folding the drift time obtained by means of Monte Carlo simulation.

Figure 4 shows the drift time distribution of the anode wire at 4.7 kPa and 850 V. The histogram is the experimental data, while the solid line is the distribution by folding the drift time distribution obtained by means of Monte Carlo simulation using the *GARFIELD* code<sup>5)</sup>. The distribution of the simulation is fitted to the experimental data. The function of space-time calibration is obtained with the simulation.

Figure 5 shows the charge distribution of the cathodes at 4.7 kPa. The energy-loss resolution evaluated from the data is found to be 40% in FWHM. The magnitude is compatible with an energy-loss difference for

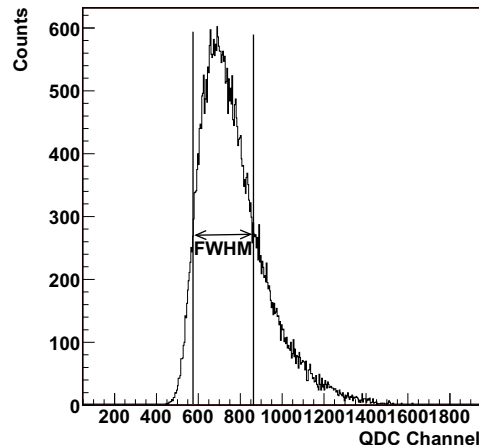


Fig. 5. Charge distribution of the cathodes.

Carbon and Nitrogen with the same velocity. Energy-loss resolutions at 10 kPa and 20 kPa are 20% and 30 %, respectively. The LP-MWDC should be operated at a higher gas pressure to obtain higher energy-loss resolution for the discrimination of the particles.

#### References

- 1) A. Saito et al.: RIKEN Accel. Prog. Rep. 40 (2007).
- 2) T. Uesaka et al.: Nucl. Instrum. Meth. in Phys. Res. **B266** (2008) 4218.
- 3) T. Kawabata et al.: Nucl. Instrum. Meth. in Phys. Res. **B266** (2008) 4201.
- 4) H. Kumagai et al.: Nucl. Instrum. Meth. in Phys. Res. **A470** (2004) 562.
- 5) A. Saito et al.: CNS Ann. Rep. (2008).
- 6) R. Vcenho : program *GARFIELD* - simulation of gaseous detectors <http://garfield.web.cern.ch/garfield/>

# Performance evaluation of low-pressure multiwire drift chamber

K. Miki,<sup>\*1,\*4</sup> A. Saito,<sup>\*1</sup> H. Miya,<sup>\*2</sup> S. Shimoura,<sup>\*2</sup> T. Kawabata,<sup>\*2</sup> H. Kurei,<sup>\*2</sup> S. Michimasa,<sup>\*2</sup> K. Nakanishi,<sup>\*2</sup> S. Noji,<sup>\*1</sup> S. Ota,<sup>\*2</sup> Y. Sasamoto,<sup>\*2,\*4</sup> T. Tokieda,<sup>\*2</sup> T. Yoshida,<sup>\*3</sup> T. Uesaka<sup>\*2</sup>, and H. Sakai<sup>\*1</sup>

## 1 LP-MWDC - DCF31

Low-pressure multiwire drift chambers (LP-MWDCs) have been developed<sup>1)</sup> as beam line detectors (BLDs) for the high-resolution measurement using the newly constructed spectrometer SHARAQ<sup>2)</sup> in RIBF. One of the largest physical motivations of SHARAQ is to explore unknown regions in nuclear physics via the exothermic charge exchange reaction using radioactive isotope (RI) beams. For the high-resolution measurement with RI beams, the following requirements are imposed on the BLDs:

- (1) position resolution better than  $300 \mu\text{m}$  (FWHM) for the precise ray tracing.
- (2) gas pressure as low as possible for sufficiently small energy straggling and multiple scattering effects.
- (3) efficiency close to 100% for the event-by-event tracking.

The performances of LP-MWDCs were tested by using an accelerated beam<sup>3)</sup>. In this article, we report on the performance evaluation for one of the LP-MWDCs, DCF31. DCF31 will be installed at BigRIPS-F3, which is the starting point of the high-resolution beam transport. The specifications and the schematic figure of DCF31 are shown in Table 1 and Fig. 1, respectively. Among the developed LP-MWDCs, DCF31 has the smallest cell size,  $5 \times 4.8 \text{ mm}^2$ , and therefore it can work at a relatively high rate. This feature is favorable for the use at F3, where the beam spot size is a few millimeters.

Table 1. Specifications of DCF31.

Number of planes	8 ( $X_1 X_1' Y_1 Y_1' X_2 X_2' Y_2 Y_2'$ )
Number of cells	16 cells/plane
Cell size	$5 \text{ mm}^w \times 4.8 \text{ mm}^t$
Sensitive Area	$80 \text{ mm} \times 80 \text{ mm}$
Anode wire	Au-W $12.5 \mu\text{m}$
Potential wire	Cu-W $75 \mu\text{m}$
Cathode foil	Al-PET $2 \mu\text{m}$
Operation Gas	pure isobutane

## 2 Experiment

The experiment was performed at the E7 experimental hall in RIBF. The  $\alpha$  beam was accelerated

<sup>\*1</sup> Department of Physics, University of Tokyo

<sup>\*2</sup> CNS, University of Tokyo

<sup>\*3</sup> Department of Physics, Rikkyo University

<sup>\*4</sup> RIKEN Nishina Center

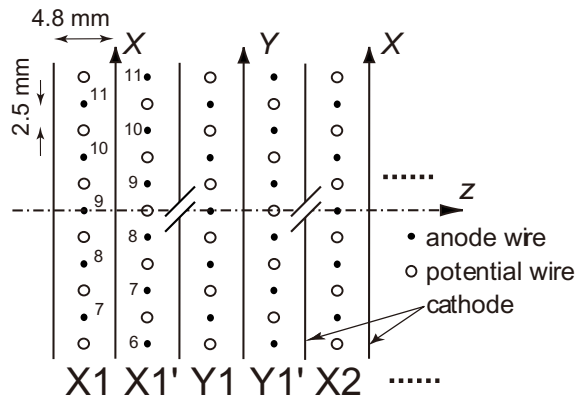


Fig. 1. The schematic view of DCF31.

up to 8.8 MeV/nucleon by the AVF Cyclotron and was transported to the E7B course. The  $\alpha$  beam at 8.8 MeV/nucleon gives the same energy loss in DCF31 as the  $^{12}\text{N}$  beam at 250 MeV/nucleon, which is a candidate for RI beam used in SHARAQ experiments. The transported  $\alpha$  beam was defocused around DCF31 so that the beam covered a large part of the sensitive area. The signals from anode wires were amplified and discriminated by the REPIC RPA-131 cards. Since the typical noise level was about 5 mV, the threshold of RPA-131 was set to 10 mV throughout the measurement. The timing information was digitized by the CAEN V1190A multi-hit TDC. The plastic scintillator with a thickness of 0.1 mm was installed about 60-cm upstream of DCF31. The signals from the photo multiplier tubes triggered the data acquisition system.

One problem is that the number of crosstalks with the neighbor cells increases as the applied high voltage (HV) increases. This problem was solved by taking the timing information for both of the leading and trailing edges by V1190A. The pulse width of the analog signal can be obtained from  $t_{\text{trail}} - t_{\text{lead}}$  as shown in Fig. 2. Since noise events have small pulse widths, they are clearly separated by gating on the pulse width as shown in Fig. 3.

## 3 Result

The obtained TDC spectrum is shown in Fig. 4. It has an ordinary shape which consists of a strong peak and a flat region. The width of the spectrum, corresponding to the drift time in a half-cell size, was about 40 nsec. This is consistent with the simulated value of 43 nsec by the program Garfield<sup>4)</sup>.

Figure 5 shows the efficiency curve obtained at gas

pressures of 5 kPa, 10 kPa and 20 kPa. The efficiency was estimated by  $Y_{X2}/Y_{\text{trigger}}$ , where  $Y_{X2}$  is the number of yields for X2 plane and  $Y_{\text{trigger}}$  is the number of triggered events. At 5 kPa, the applied HV tripped before the efficiency reached 100%. On the other hand, at 10 kPa and 20 kPa, it reached about 100% with the applied HV above 800 V and 900 V, respectively. Therefore the requirements (2) and (3) were met sufficiently.

The position resolution for each anode plane is estimated by the variance (residue) of the ray fitting. The overall position resolution for DCF31 is given using the half of it. The obtained resolution is shown in Fig. 6. The requirement (1) is satisfied above 8 kPa.

In summary, it was confirmed that the performance of DCF31 is satisfactory as a BLD at F3. DCF31 will be operated at a gas pressure of 10 kPa in the SHARAQ commissioning and in the subsequent experiments.

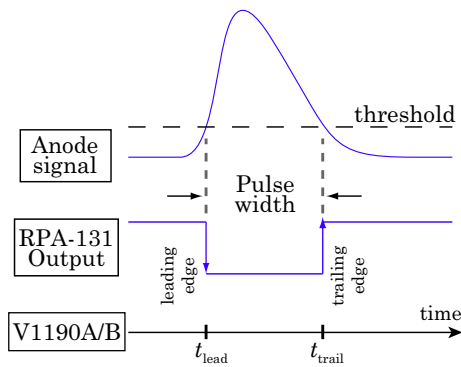


Fig. 2. Pulse width of the anode signal obtained by V1190A. It is given by  $t_{\text{trail}} - t_{\text{lead}}$ .

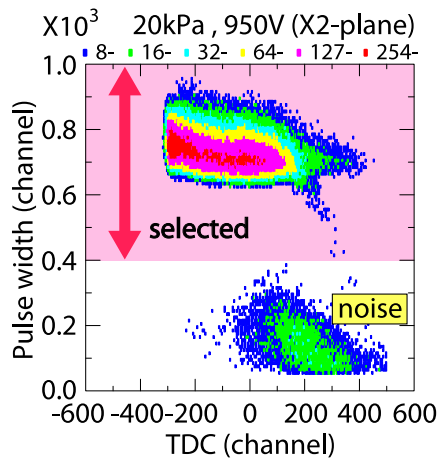


Fig. 3. Event selection by gating on pulse widths. Noise events have small pulse widths and are clearly separated from true signals.

## References

- 1) A. Saito et al.: RIKEN Accel. Prog. Rep. **40** (2007) 157.
- 2) T. Uesaka et al.: Nucl. Inst. Meth. **B266** (2008) 4218.
- 3) A. Saito et al.: in this report.
- 4) R. Veenhof: program GARFIELD - simulation of gaseous detectors - <http://garfield.web.cern.ch/garfield/>.

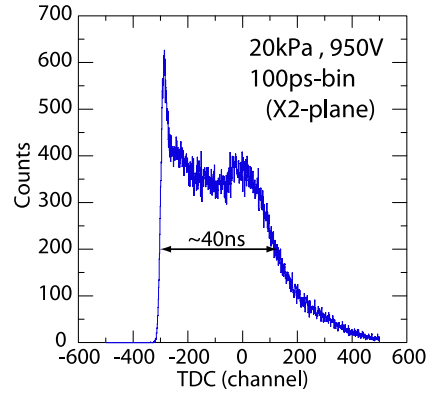


Fig. 4. Typical TDC spectrum obtained at 20 kPa and 950 V.

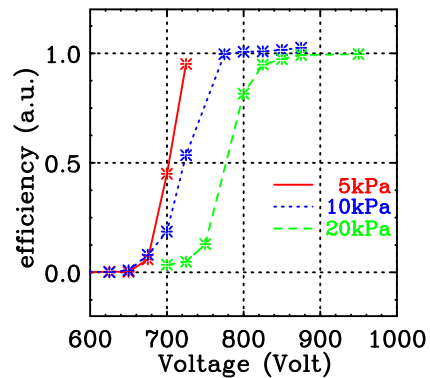


Fig. 5. Efficiency curve at 5 kPa, 10 kPa and 20 kPa. The efficiency is sufficiently high above 800 V (900 V) at 10 kPa (20 kPa), respectively.

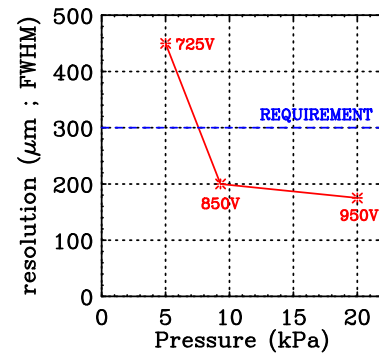


Fig. 6. Position resolution obtained for each of gas pressures. The requirement is satisfied above  $\sim 8$  kPa.

## Focal-Plane Detector for SHARAQ Spectrometer

S. Michimasa,<sup>\*1</sup> H. Tokieda,<sup>\*1</sup> S. Noji,<sup>\*2</sup> S. Shimoura,<sup>\*1</sup> T. Uesaka,<sup>\*1</sup> H. Sakai,<sup>\*2</sup> P. Roussel-Chomaz,<sup>\*3</sup>  
J-F. Libin,<sup>\*3</sup> P. Gangnant,<sup>\*3</sup> and C. Spitaels<sup>\*3</sup>

[SHARAQ spectrometer, cathode-readout drift chamber]

Constructions of the SHARAQ spectrometer<sup>1)</sup> and the high-resolution beam line<sup>2)</sup> are making progress in the RI Beam Factory (RIBF) at RIKEN. In order to realize high-resolution nuclear spectroscopy utilizing radioactive-ion probes, one of key devices is a tracking detector, located in the dispersive focal plane of SHARAQ, which is used to measure reaction Q values of induced reactions. Figure 1 shows a typical detector setup installed in the final focal plane of the SHARAQ spectrometer. The focal plane is located 3.04 m downstream from the exit of the SHARAQ-D2 magnet and is tilted at 35 degrees relative to the central orbit. The focal-plane detector system consists of a pair of tracking detectors, and a following plastic scintillator. The tracking detectors are used to measure the position and angle of particles and the plastic scintillator provides timing at the focal plane and energy deposit information. We have designed and manufactured the tracking detectors for SHARAQ by collaborating with an experimental group of GANIL.

The tracking detectors should fulfill the requirements necessary to successfully demonstrate the performance of the SHARAQ spectrometer, as summarized in Table 1. Eventually we adopted Cathode-Readout Drift Chambers (CRDCs)<sup>3)</sup> operated at low gas pressure as appropriate tracking detectors. Although similar types of tracking detectors are used as focal-plane detectors in several magnetic spectrometers<sup>4,5)</sup>, we have to achieve smaller multiple scattering and higher position resolution.

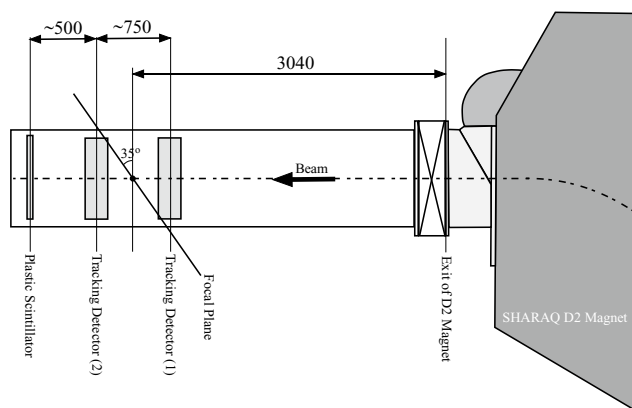


Fig. 1. Detector setup for the dispersive focal plane of SHARAQ.

\*1 Center for Nuclear Study, University of Tokyo

\*2 Department of Physics, University of Tokyo

\*3 GANIL, France

Table 1. Requirements for the focal-plane detectors.

Effective area	> 500 mm (H) × 300 mm (V)
Multiple scattering	≪ 1 mrad ( $\sigma$ )
Detection counting rate	> 10 <sup>3</sup> particles/sec
Position resolution	300 $\mu$ m (FWHM)
Detection efficiency	≈ 100%

Table 2. Specifications of the CRDC for SHARAQ.

Effective area	550 mm (H) × 300 mm (V)
Anode wire (A)	10 wires, 20 $\mu$ m $^{\phi}$
Potential wire (P)	11 wires, 75 $\mu$ m $^{\phi}$
Frisch grid wire (F)	21 wires, 75 $\mu$ m $^{\phi}$
Cathode pad (C)	2 mm (H) × 50 mm (T), 2 rows × 256 pads
Pitch of A-P and F-F	5 mm
Distance of A-C and A-F	3 mm
Mylar window	12 $\mu$ m
Foil used for field cage	2.5 $\mu$ m
Detector gas	Isobutane, 15–50 torr

Figure 2 shows the front view and cross section of the CRDC designed for the SHARAQ spectrometer, and its specifications are listed in Table 2. The effective area of the CRDC is 550 mm horizontally and 300 mm vertically. The total thickness of the CRDC is 219 mm, and the depth of the sensor space is 104 mm. In the sensor part, 10 anode wires and 11 potential wires are alternately placed. The potential wires and Frisch grid are arranged to make axially-symmetric electric fields in the vicinity of anode wires and to minimize position dependence in avalanche gains. The two rows of the cathode pads are arranged horizontally in the vicinity

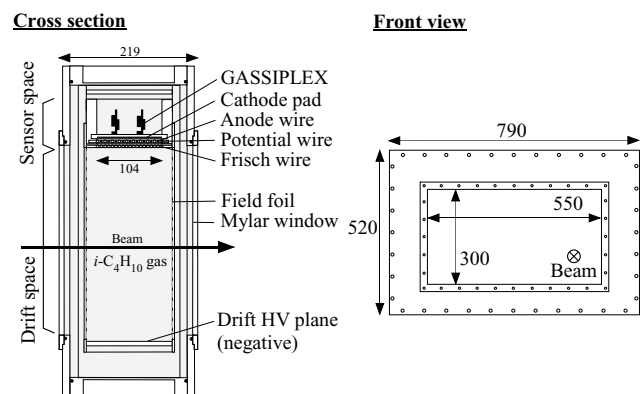


Fig. 2. Cross section and front view of SHARAQ CRDC. Front view is shown at half the scale of the cross section.

of the anode wires, and each row consists of 256 cathode pads arranged with a 2.2 mm pitch. Negative high voltage is applied in the drift space to form an electric field for electron drift. The field cage is made up of a drift high voltage (HV) plane and thin Mylar foils on which gold strips are evaporated. A strip on the Mylar foil is connected to the neighboring strips by resistances, and a parallel and constant electric field is provided by feeding voltage to the drift HV plane.

When a particle passes through the CRDC, secondary electrons produced by gas ionization move along the electric field produced by the field cage, and finally cause avalanches around the anode wires. The vertical hit position is deduced by the drift time of secondary electrons and the horizontal hit position is deduced by the charge distribution induced on the cathode pads. The maximum voltage for electron drift is designed to be more than 5 kV. Under this condition, the drift time for a 30 cm length in 15-torr isobutane gas is estimated to be approximately 6  $\mu$ s by using the GARFIELD code<sup>6)</sup>. The CRDC was designed for use in vacuum and for operation at low pressures of 15–50 torr. Low-pressure operation is effective not only for reducing the thickness of gas itself but also for reducing the thickness of Mylar windows sealing the detector gas. Multiple scattering at the CRDC is evaluated to be approximately 0.1 mrad ( $\sigma$ ) for  $^{12}\text{C}$  at 200A MeV.

The CRDC outputs two signals of avalanches on the anode wires and two multiplexed signals of charges induced on the cathode pads. The charge induced on the cathode pads is amplified, multiplexed and read out by using the GASSIPLEX chips developed at CERN<sup>7)</sup>. The GASSIPLEX chips are mounted close to cathode pads inside the detector for noise reduction as shown in Fig. 2. High-multiplexed performance allows us to transmit charge signals from 256 cathode pads by using only one cable. The multiplexed signals are read by a CAEN VME sequencer<sup>8)</sup> and a CRAM module<sup>9)</sup>. The readout process requires  $\sim 500 \mu$ s in total.

We have performed operation tests of the CRDCs with 15 torr and 30 torr isobutane using an  $\alpha$  source. The triggers for data acquisition were produced by anode signals from a CRDC itself. An induced charge signal obtained from the cathode pads is shown in Fig. 3. The histogram and curve are the obtained data and a Gaussian fit result, respectively. Although the Gaussian function, which is adopted in Ref.<sup>5)</sup> as an induced charge distribution, roughly reproduces our data, further study on the shape of the charge distribution is needed to measure particle positions more precisely. We have also studied the spark limit and avalanche gain of the anode wires. The CRDC operates stably with anode voltage as high as 1.0 kV although all cathode signals are above that range. It is reported in Ref.<sup>10)</sup> that the avalanche gain of isobutane increases by approximately 3 times as the anode voltage increases by 100 V. Therefore, by considering

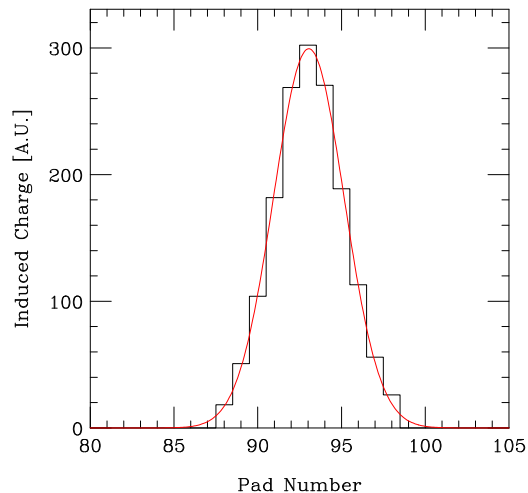


Fig. 3. An example of charge distribution data induced on the cathode pads. The curve shows a Gaussian fit result.

energy losses by an alpha particle from the source and an intermediate-energy heavy ion at CRDC, we estimate that similar charge distributions are obtained by the anode voltage of around 900 V for the case of 250A-MeV  $^{12}\text{C}$  particles.

In summary, we examined the setup configuration of the focal plane detectors that utilize high-resolution features of the SHARQA spectrometer.

A large-area and low-pressure CRDC is adopted as a tracking detector used in SHARQA due to its good position resolution and reduced multiple scattering. The CRDC operated well in 15 torr and 30 torr isobutane. This detector system will be used in the commissioning of the high-resolution beam line and the SHARQA spectrometer in March, 2009.

#### References

- 1) T. Uesaka et al.: Nucl. Instrum. Methods Phys. Res. B **266**, 4218 (2008).
- 2) T. Kawabata et al.: Nucl. Instrum. Methods Phys. Res. B **266**, 4201 (2008).
- 3) M.H. Tanaka et al.: Nucl. Instrum. Methods Phys. Res. A **362**, 521 (1995).
- 4) J. Yurkon et al.: Nucl. Instrum. Methods Phys. Res. A **422**, 291 (1999).
- 5) S. Pullanhiotan et al.: Nucl. Instrum. Methods Phys. Res. A **593**, 343 (2008).
- 6) R. Veenhof, GARFIELD, CERN Program Library W5050.
- 7) The GASSIPLEX is a re-designed chip of the AMPLEX by J.C. Santiard of CERN. The AMPLEX is described in E. Beuville et al.: Nucl. Instrum. Methods Phys. Res. A **288**, 157 (1990).
- 8) V551 C.A.E.N sequencer User Guide.
- 9) V550 C.A.E.N CRAM User Guide.
- 10) Yu.I. Davydov et al.: Nucl. Instrum. Methods Phys. Res. A **545**, 194 (2005).

# Gas-filled recoil ion separator GARIS-II

D. Kaji, K. Morimoto, N. Sato,\*<sup>1</sup> A. Yoneda, and K. Morita

[Gas-filled recoil ion separator, GARIS, superheavy, new element, hot fusion]

We designed a new gas-filled recoil ion separator GARIS-II. The construction of GARIS-II started in September 2008, and the spectrometer will be installed in the RIKEN linear accelerator (RILAC) facility in 2009.

## 1 Design concept

One of the world's most active gas-filled typed recoil separator GARIS<sup>1)</sup> is operating at RIKEN. The separator has been used as a powerful tool for nuclear decay spectroscopy of superheavy element (SHE) nuclides produced via Pb/Bi-based fusion reactions (cold fusion), e.g., the search for a new 113th element using the  $^{209}\text{Bi}(^{70}\text{Zn},n)^{278}113$  reaction.<sup>2,3)</sup> Recently, GARIS has gained some experience in more asymmetric actinide-based reactions (hot fusion) with the aim of studying physical and chemical properties of SHE.<sup>4)</sup> A gas-jet transport system coupled to GARIS as a pre-separator is a promising tool for next-generation SHE chemistry, i.e., identifying SHE nuclides under low background conditions with high efficiency of the gas-jet transport.<sup>5)</sup> However, we also encountered some difficulties in these hot fusion studies. First, transmission in GARIS becomes much lower for actinide-based asymmetric reactions,<sup>4)</sup> due to multiple scattering of the recoil ion by the filling gas atoms. Second, the background rate at the focal plane detector is 100~1000 times higher than the cold fusion case. Third, GARIS cannot transport recoil ions with  $Z > 110$  produced via

$^{248}\text{Cm}$ -based fusion reactions as considering an equilibrium charge state in a helium gas by our empirical data.<sup>6)</sup>

GARIS-II was designed on the basis of extensive experiences with construction, development, and operation of GARIS. The most interesting subjects studied by GARIS-II are chemical investigations of elements with  $Z \geq 104$ , nuclear reaction and nuclear structure studies of the SHE nuclides up to  $Z \sim 126$  produced via actinide-based fusion reactions, and understanding the operating principles of gas-filled typed recoil separators such as the equilibrium charge state with various filling gases. Specifications and technical requirement for experiments performed by GARIS-II are:

- To irradiate actinide targets with high intensity beams of  $^{18}\text{O}$  to  $^{70}\text{Zn}$  over at least  $2 \text{ p}\mu\text{A}$ , and to operate GARIS-II under this beam condition.
  - To install a differential pumping system.
  - To install a rotating target system.
  - To install a beam dump made of Ta plate with a water cooling.
  - To install a movable and fixed slit to reduce the background due to the primary beam.
- To transport SHE nuclides produced via hot fusion reactions and achieve much higher transmission than GARIS.
  - To be able to transport recoil ions with magnetic rigidity  $B\rho > 2.16$ .
  - To have a larger solid angle than GARIS.
  - To be able to use various filling gases, such as He and He/H<sub>2</sub> mixture.
  - To be able to use both stable targets and actinide targets, such as  $^{248}\text{Cm}$ ,  $^{238}\text{U}$ , and  $^{232}\text{Th}$  with thick thickness of  $T > 300 \mu\text{g}/\text{cm}^2$ .
  - To have a short total path length  $< 5.76 \text{ m}$ .
- To have high background suppression for unwanted projectiles and other by-products.
- To minimize the image size of the product at the focal plane.

## 2 Design and ion optical characteristics

GARIS-II consists of five magnets arranged in a  $Q_v$ - $D$ - $Q_h$ - $Q_v$ - $D$  configuration as shown in Figure 1. This configuration is the first design for the purpose of SHE study. The magnets are manufactured by Sumitomo Heavy Industries Ltd., according to specifications determined by RIKEN. Magnetic field model calcu-

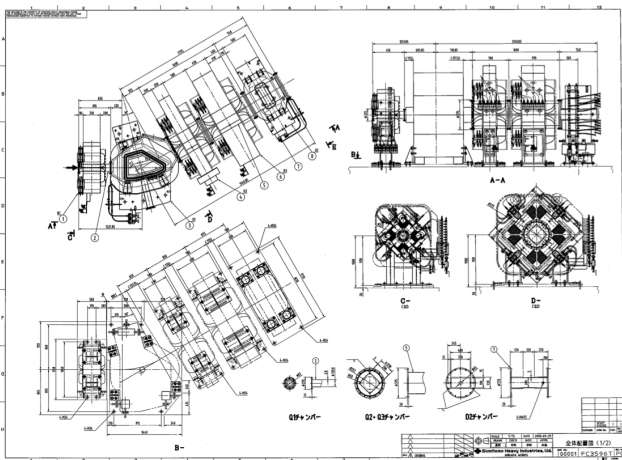


Fig. 1. Schematic of new gas-filled recoil ion separator GARIS-II.

\*<sup>1</sup> Department of Physics, Tohoku University

lations were performed to optimize the basic design of dipole and the quadrupole magnets using the simulation code OPERA.<sup>7)</sup> The characteristics of dipole and quadrupole magnets are shown in Tables 1 and 2, respectively. Ion optical characteristics were analyzed using the computer code TRANSPORT.<sup>8)</sup> The beam envelope in horizontal and vertical direction is shown in Figure 2 as a typical result for the case of the  $^{248}\text{Cm}(^{22}\text{Ne},5\text{n})^{265}\text{Sg}$  reaction. Q1 provides strong vertically focusing and this focusing power better matches D1 acceptance. D1 separates the primary beam immediately, and mainly reduces the background at the focal plane of the system. An exit angle of 30 degree provides a little horizontal focusing. D1 is an H-type dipole magnet. The beam dump is designed to reduce the background due to the primary beam. Q2 and Q3 act as horizontal and vertical focusing to the focal plane of the system. D2 separates unwanted transfer products and light charged particles

Table 3 provides a comparison between GARIS and GARIS-II in terms of the most important ion optical characteristics and its expected performance for typical hot fusion reactions of (A)  $^{248}\text{Cm}(^{18}\text{O},5\text{n})^{261}\text{Rf}$ , (B)  $^{248}\text{Cm}(^{22}\text{Ne},5\text{n})^{265}\text{Sg}$ , (C)  $^{248}\text{Cm}(^{26}\text{Mg},5\text{n})^{269}\text{Hs}$ , and (D)  $^{238}\text{U}(^{48}\text{Ca},3\text{n})^{283}\text{112}$ . Transmission was calculated while considering multiple scattering in target, angular spread by evaporation process, and multiple scattering in the filling gas. The solid angle is increased from 12.2 to 20.2 msr, approximately 1.7 times higher than GARIS. Therefore, transmission of GARIS-II is expected to be 2~4 times higher than GARIS. The number of magnetic elements is increased from 4 to 5, and the total path length of the separator is decreased

Table 1. Characteristics of dipole magnets

	D1	D2
Deflecting angle [deg]	30	7
Maximum field [T]	1.74	0.86
Pole gap [mm]	150	200
Radius of central ray [mm]	1440	2850
Entrance angle [deg]	0	7
Exit angle [deg]	30	-7
Max. AT/pole [AT]	285600	146160
Number of turns/pole	476	336
Max. current [A]	600	435

Table 2. Characteristics of quadrupole magnets

	Q1	Q2	Q3
Max. field gradient [T/m]	12.2	4.70	5.27
Pole length [mm]	330	250	450
Bore radius [mm]	75	150	150
Max. AT/pole [AT]	37800	59070	59070
Number of turns/pole	108	179	179
Max. current [A]	330	330	330

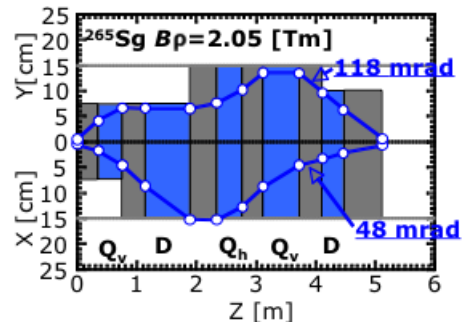


Fig. 2. Beam envelope of  $^{265}\text{Sg}$  ion calculated by TRANSPORT. Maximum horizontal and vertical angular acceptances are 48 and 118 mrad, respectively.

from 5.76 to 5.12 m. The separator vacuum chamber is filled with He (or He/H<sub>2</sub> mixture) from the the focal plane detector setup to the target region. The differential pumping system separates the helium filling from the high vacuum of the beam line. Continuous filling gas flow into the target chamber is regulated by a pressure/flow controller.

Table 3. Ion optical characteristics of GARIS-II and transmission anticipated for some types of hot fusions

Configuration	GARIS	GARIS-II
	DQ <sub>h</sub> Q <sub>v</sub> D	Q <sub>v</sub> DQ <sub>h</sub> Q <sub>v</sub> D
Ang. acceptance (X) [mrad]	±61	±48
Ang. acceptance (Y) [mrad]	±57	±118
Solid angle [msr]	12.2	20.2
Total path length [m]	5.76	5.12
Maximum $B\rho$ [Tm]	2.16	2.44
Possible SHE search [Z]	116	126
Dispersion [mm/%]	9.7	17.7
Transmission for reaction (A)	2%	8%
Transmission for reaction (B)	4%	16%
Transmission for reaction (C)	7%	28%
Transmission for reaction (D)	32%	75%

## References

- 1) K. Morita et al.: Nucl. Instr. and Meth. **B70**, 220 (1992).
- 2) K. Morita, K. Morimoto, D. Kaji et al.: J. Phys. Soc. Jpn. **73**, 2593 (2004).
- 3) K. Morita, K. Morimoto, D. Kaji et al.: J. Phys. Soc. Jap. **76**, 045001 (2007).
- 4) H. Haba, D. Kaji et al.: RIKEN Acc. Prog. Rep. **42**, (2009).
- 5) H. Haba, D. Kaji et al.: J. Nucl. Radiochem. Sci. **8**, 55 (2007).
- 6) D. Kaji, Dr. Thesis, Graduate School of Science and Technology, Niigata University, Niigata (2003).
- 7) <http://www.ces-kbk.com/sdi-sp/vf/index.htm>
- 8) K. L. Brown et al.: SLAC Report **No. 91** Rev. 1, 1974.

## Designing of ionization chamber for super-heavy elements

K. Ozeki, T. Sumita,<sup>\*1</sup> K. Morimoto, D. Kaji, N. Sato,<sup>\*2</sup> H. Haba, Y. Kudou, A. Yoneda, and K. Morita

In the field of super-heavy elements, the direct measurements of atomic number  $Z$  and mass number  $A$  of produced nucleus is a challenging task. One of the way to identify  $Z$  and  $A$  is to measure the energy loss per unit length  $dE/dx$ , and to measure total energy by stopping incident nucleus in a detector, respectively.  $A$  is derived from the combination of total energy and velocity of the nucleus. In the region of our interest ( $Z > 100$ ,  $A > 250$ ), the density of electron-hole pairs or primary electrons is too high in the semiconductor detector or even in a normal gas detector, because of large  $dE/dx$ . Too high density of electron-hole pairs provokes the recombination of electrons and holes. The number of electrons collected to electrodes comes to be unproportional to energy loss. As a result, the precise measurement of energy loss becomes almost impossible.

In this work, we make an attempt to operate the ionization chamber with low pressure to reduce the density of primary electrons. Our final aim is to measure the energy loss with a high degree of accuracy to identify  $Z$  and  $A$  of super-heavy elements.

Our detector is used for the nuclei with the total energy of several tens of MeV. Therefore, an amount of material other than gas filled in the effective area must be reduced as much as possible. For this purpose, anode and cathode electrodes are assembled parallel to the incident direction of nuclei. In addition, the anode electrode is segmented perpendicular to the incident direction of nuclei to measure  $dE/dx$ .

A prototype of the ionization chamber was previously constructed. As a result of operating tests using  $^{241}\text{Am}$  and electric field computations using a Garfield code<sup>1)</sup>, a structural defect was found — a parallel electric field could not be formed in the effective area. In such a deformed electric field, analog signals obtained from each segment of anode electrode do not reflect the energy loss in corresponding segmented area because a part of electrons drift into a segment other than the segment in which the electrons are generated originally. Thus, it is impossible to measure  $dE/dx$  correctly using this prototype ionization chamber.

Consequently, we redesigned a new ionization chamber. The electric fields under various geometries and applied voltages we could envision are computed to achieve parallel electric field in the effective area using the Garfield code.

Figure 1 shows optimized geometry of the ionization chamber and voltages applied to each constituent.

Computed electric fields using the Garfield code under previous and optimized geometries are also shown.

The voltages applied to anode and cathode electrodes are 450 V and 100 V respectively. The effective area is held at higher potential than surrounding wall of ground. A ratio of applied voltages must be kept even if applied voltages are changed from the requirements such as detection efficiency or counting rate.

The field wires are arranged in three columns at both upstream and down stream of the effective area. The distance between wires is 2.5 mm. The distance between wire columns is 5 mm. The voltage between neighboring wires is 5 V. The voltages applied to wires in the outer two columns are higher than those in the inner one column by a 5 V. A difference in potential between surrounding ground and field wires causes deformed electric field, especially in the vicinity of anode electrode. By applying higher voltage to the outer columns, parallel electric field in the effective area could be achieved.

Two columns of wires are arranged on the lateral sides of the effective area. Similarly, the voltages applied to wires in outer column are higher than those in the inner column.

A new prototype of ionization chamber with the geometry described above has been constructed. The operating tests using  $^{241}\text{Am}$  have just been started.

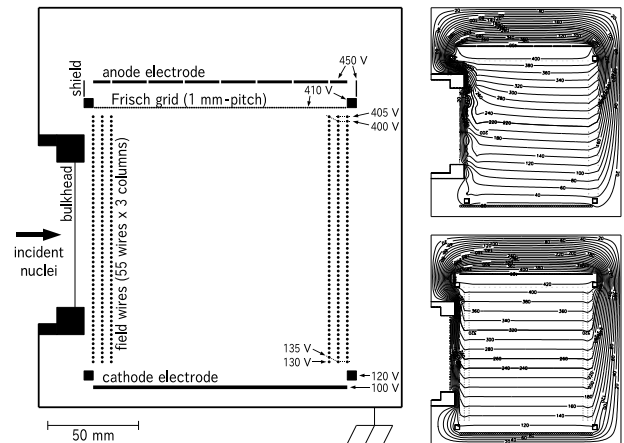


Fig. 1. Left: An optimized geometry of the ionization chamber and voltages applied to each constituent. Right: Computed electric fields under previous geometry (upper panel) and optimized geometry (lower panel).

### References

- 1) <http://garfield.web.cern.ch/garfield/>

<sup>\*1</sup> Faculty of Science and Technology, Tokyo University of Science

<sup>\*2</sup> Department of Physics, Tohoku University

# The Potential of a new $\text{LaBr}_3(\text{Ce})$ Based $\gamma$ -Ray Spectrometer for Fast-Beam Experiments at the RIBF

P. Doornenbal, H. Scheit, N. Aoi, T. Motobayashi, H. Sakurai, and S. Takeuchi

[Gamma-ray detection, high resolution scintillators]

Gamma-ray spectroscopy at intermediate and relativistic beam energies for present state-of-the-art spectrometers is hampered by either an energy resolution of only about 10 % if scintillation detectors are employed or by a very low full energy peak (FEP) efficiency for Ge-based arrays. For the former, the intrinsic energy resolution is the limiting factor, while Ge has an excellent energy resolution, but is a very expensive material. Thus, a Ge-based spectrometer covering the entire solid angle to obtain a high FEP efficiency would be extremely costly, in particular since pulse shaping algorithms have to be applied that keep the Doppler-broadening due to the detectors' opening angles small.

The new scintillation material  $\text{LaBr}_3(\text{Ce})$  possesses energy resolutions of 2 and 3 % (FWHM) at  $E_\gamma = 1333$  and  $662 \text{ keV}^{1)}$ , respectively, unprecedented for scintillators. Due to its highly reduced price per volume compared to Ge material and the high  $\gamma$ -ray absorption coefficient,  $\text{LaBr}_3(\text{Ce})$  is an excellent choice to build a  $4\pi$   $\gamma$ -ray spectrometer. This array is suited especially well for in-beam  $\gamma$ -ray spectroscopy if crystal geometries are chosen that minimize the Doppler broadening. To study the potential of a  $\text{LaBr}_3(\text{Ce})$  based spectrometer for the recently commissioned Radioactive Isotope Beam Factory (RIBF), simulations with the GEANT4 package are performed.

The aims for the complete array are set to an energy resolution of 3 % (FWHM) and a FEP efficiency of 40 % for 1 MeV  $\gamma$ -rays emitted at  $100 \text{ MeV}/u$ . The geometry of all single crystals is chosen to have an identical boxed-shape to ensure a high amount of flexibility for changes in the configuration of the complete array. The crystals are arranged in rings of the same polar angle in such a way that the opening angle induced Doppler broadening is kept constant for all detectors.

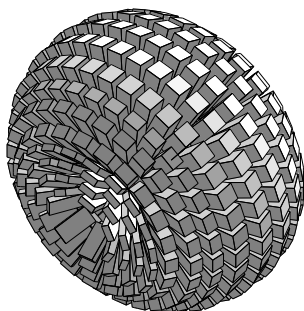


Fig. 1. Schematic Layout of  $\text{LaBr}_3(\text{Ce})$  array.

To reduce the Al housing material, part of the crystals are put into common housings of two and three crystals, respectively.

Taking these restrictions into account, different detector geometries have been investigated. Fig. 1 shows the configuration for crystal sizes of  $15 \times 40 \times 80 \text{ mm}^3$  and a total of 915 detectors. For this configuration, the simulated energy resolution and FEP efficiency for 1 MeV  $\gamma$ -rays emitted at  $100 \text{ MeV}/u$  are 3.1 % and 38 %, respectively, including the reconstruction of the total energy for add-back events.

These values have to be compared with present  $\gamma$ -ray detection arrays as DALI2<sup>2)</sup> and RISING<sup>3)</sup>. The DALI2 array was simulated in the configuration with 182 NaI(Tl) detectors, while for RISING the 15 Ge Cluster and 8 Ge Miniball detectors were taken into account. The comparison of the three arrays is given in Tab. 1. The gain of energy resolution is about a factor three compared to DALI2, while the FEP efficiency is higher. Compared to RISING, the energy resolution is about at the same level, while the gain in FEP efficiency is more than a factor six. A high efficiency is extremely important to pin down new level schemes with multiple decays from  $\gamma$ - $\gamma$  coincidences. Here, the advantage for two coincident 1 MeV  $\gamma$ -ray decays detected is about a factor 40 over RISING, demonstrating the high potential of a new  $\text{LaBr}_3(\text{Ce})$  based  $\gamma$ -ray detection array.

Table 1. Comparison of simulated energy Resolutions and FEP efficiencies  $\epsilon_{FEP}$  for 1 MeV  $\gamma$ -rays emitted at  $100 \text{ MeV}/u$  of the  $\gamma$ -ray detection arrays DALI2, RISING, and the  $\text{LaBr}_3(\text{Ce})$  based array.  $\epsilon_{FEP}^2$  corresponds to two 1 MeV  $\gamma$ -rays with both FEPs being detected.

Array	Energy resolution [%]	$\epsilon_{FEP}$ [%]	$\epsilon_{FEP}^2$ [%]
DALI2	8.4	30	9
RISING	2.5	6	0.36
$\text{LaBr}_3(\text{Ce})$	3.1	38	14

## References

- 1) Brilliance Scintillators Performance Summary, [www.detectors.saint-gobain.com](http://www.detectors.saint-gobain.com).
- 2) S. Takeuchi *et al.*, RIKEN Acc. Prog. Rep. 36, 148 (2003).
- 3) H.J. Wollersheim *et al.*, Nucl. Instr. Meth. in Phys. Res. **A537**, 637 (2005).

# Beta-counting systems for decay-spectroscopy projects<sup>†</sup>

S. Nishimura,<sup>\*</sup> N. Uematsu,<sup>\*1</sup> T. Sumikama,<sup>\*1</sup> S. Bishop,<sup>\*2</sup> J. Chiba,<sup>\*1</sup> K. Ieki,<sup>\*3</sup> C. Ishii,<sup>\*1</sup>  
M. Kurata-Nishimura, M. Matsushita,<sup>\*3</sup> Y. Miyashita,<sup>\*1</sup> H. Sakurai, Y. Shiraki,<sup>\*1</sup> H. Yoshii,<sup>\*1</sup> K. Yoshinaga,<sup>1</sup>  
and H. Watanabe

[Nuclear structure, unstable nuclei, beta-decay]

Beta-decay studies are unique and powerful probes of nuclear structure. The high sensitivity of beta counting systems is essential, especially to approach nuclei farthest from stability with extremely low production rates. We have developed two types of beta-counting systems to extract decay properties of rare-isotopes such as half-lives, level-schemes, and  $Q_\beta$  dedicated for fast beam experiments. The preparation status of decay spectroscopy projects will be reported.

## 1 DSSSD

A high resolution beta-counting system consisting of six double-sided silicon strip detectors (DSSSD : Micron Model W1-1000) has been developed. This system is designed for high efficiency beta-gamma spectroscopy. The position correlation of the implanted ions and associated decay beta-rays enables us to deduce the decay curves without pulsing the beam. Simultaneous measurements of heavy-ions and beta-rays require an extremely wide dynamic range of readout electronics. Thus, we have developed low noise readout electronics with the dynamic range from 20 keV to 4 GeV<sup>2</sup>. In addition, a freezer system was introduced to cool the DSSSD down to -25 degree to minimize the threshold energies as well as to reduce radiation damage in the DSSSD. The performance of the DSSSD system was tested using heavy-ion beams as reported in Reference<sup>3</sup>. This system can be used for high efficiency gamma-ray measurements associated with beta-decay and isomeric decay by incorporating Ge detectors. Five Clover type Ge detectors can be placed surrounding the DSSSD in close geometry. Three independent automatic refilling systems of liquid nitrogen have been developed for stable operation of the Ge-detector array.

## 2 CAITEN

Decay spectroscopy of rare-isotopes at a high counting rate of beams is challenging for a high statistics decay spectroscopy experiment. We have developed a novel system (CAITEN) comprised of two primary subsystems. One is a large cylindrical plastic scintilla-

tor (TPS:  $\phi 500\text{mm} \times 1000\text{mm}$ ,  $20\text{mm}^t$ ) as an active implantation target. The other is a twenty-four position-sensitive photomultiplier-tube (PSPMT: Hamamatsu H8500) array arranged inside the TPS<sup>1</sup>. The TPS consisting of  $4 \times 10^4$  pixel scintillators ( $5 \times 5 \times 20\text{mm}^3$ ) is designed to be rotated to measure the half-lives of many isotopes simultaneously. The positions of beta-rays are reconstructed by measuring the pulse height differences of the PSPMT's anode lines with a regressive-chain. Figure 1 shows the correlation between the position of beta source <sup>90</sup>Sr and the reconstructed position from the PSPMT with a rotation speed of TPS at 60 rpm. We confirmed an adequate position resolution of  $\sigma \sim 4\text{mm}$  after position calibration.

Reconstruction of decay curves for isotopes in a cocktail beam environment requires event matching of implanted ions with associated decays. We have developed new analysis frame (r2pro.cxx: Rawdata-To-Paw-ROot), which provides the platforms for CERN-LIB (cfortran)<sup>4</sup> and ROOT<sup>5</sup> users. Online monitoring will also be implemented in the code in order to have a consistent analysis frame.

## References

- 1) S.Nishimura, et al., Accel. Prog. Rep. 41 (2008) 149.
- 2) N.Uematsu, et al., Accel. Prog. Rep. 41 (2008) 151.
- 3) N.Uematsu, et al., in this progress report.
- 4) URL: <http://cernlib.web.cern.ch/cernlib>
- 5) URL: <http://root.cern.ch>

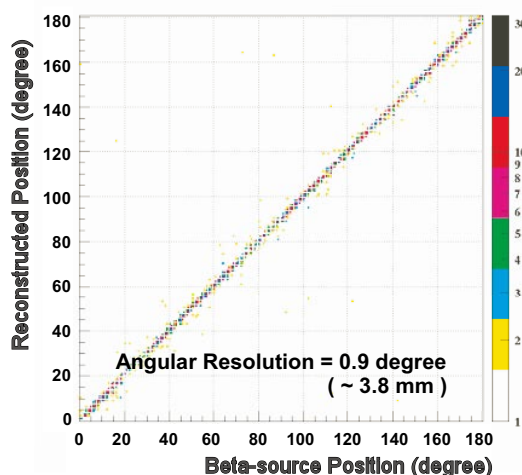


Fig. 1. Correlation between location of beta-source and reconstructed position using PSPMTs.

<sup>†</sup> supported by RIKEN President's Discretionary Fund and *kakenhi* grant (19340074).

<sup>\*1</sup> Tokyo University of Science

<sup>\*2</sup> TU München

<sup>\*3</sup> Rikkyo University

## Beam test of double-sided silicon-strip detector for decay spectroscopy

N. Uematsu,<sup>\*1</sup> T. Sumikama,<sup>\*1</sup> S. Nishimura, J. Chiba,<sup>\*1</sup> T. Hashimoto,<sup>\*2</sup> S. Hayakawa,<sup>\*2</sup> C. Ishii,<sup>\*1</sup> S. Kubono,<sup>\*2</sup> Y. Miyashita,<sup>\*1</sup> T. Murakami,<sup>\*3</sup> Y. Shiraki,<sup>\*1</sup> Y. Wakabayashi,<sup>\*2</sup> H. Watanabe, H. Yamaguchi,<sup>\*2</sup> H. Yoshii,<sup>\*1</sup> and K. Yoshinaga,<sup>\*1</sup>

Decay spectroscopy is one of the most powerful tool to study an exotic structure of unstable nuclei. Unstable nuclei with several hundreds MeV/nucleon provided by the BigRIPS are stopped in an active stopper at the end of the beam line.  $\beta$  and  $\gamma$  rays emitted from stopped nuclei are detected by double-sided silicon strip detectors (DSSDs) as the active stopper, of which thickness is 1 mm, and Clover-type Ge detectors surrounding the stopper, respectively.

A total energy of implanted nuclei is measured for particle identification by DSSD, and its  $\beta$  decay is detected by the same DSSD. The energy loss of a  $\beta$  ray is very small compared with the energy loss at implantation of unstable nuclei. The typical energy loss for  $\beta$  ray with several MeV is 300 keV in 1mm-thick silicon. The length passing through and also the energy loss in the DSSD changes as a function of the implantation depth and the emission direction of  $\beta$  ray. So the energy loss ranges down to 0 keV.

A new readout system of DSSD has been developed, which has a wide dynamic range from 20 keV to 4 GeV<sup>1)</sup>. The signal was divided into the two pre-amplifiers with low and high gains for several-GeV and down to 20 keV energy-loss detection, respectively. And we need to make a position correlation between the implantation and the emitted  $\beta$  ray in order to know the parent nucleus of  $\beta$  decay under the condition of a continuous and cocktail beam. Here, we report the test of this readout system using stable beam of  $^{132}\text{Xe}$  at HIMAC and unstable beam of  $^{18}\text{N}$  at CNS Radio Isotope Beam separator<sup>2)</sup> (CRIB).

The energy deposit in the DSSD with 1 mm thick is 4 GeV at a maximum for neutron-rich nuclei around  $^{110}\text{Zr}$ . In order to test the measurement of such a large energy deposit with DSSD, we have performed an experiment using a  $^{132}\text{Xe}$  beam with 400 MeV/nucleon at HIMAC. Since the  $^{132}\text{Xe}$  beam passed through the DSSD, not the total energy but the energy loss  $\Delta E$  in the DSSD was measured. Three kinds of  $\Delta E$  between 2 - 3 GeV were measured, where  $\Delta E$  was changed by degrading the beam energy using adjustable aluminum energy degraders. Figure 1 shows the  $\Delta E$  spectrum of 2.03 GeV and Fig. 2 shows the energy scale using  $\Delta E = 2.03, 2.18$  and  $2.83$  GeV. The measured scale was linear, but the extrapolation of the line to the

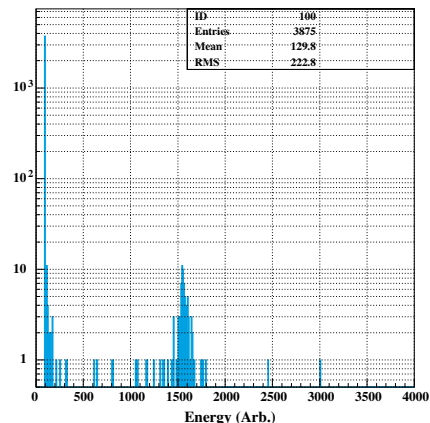


Fig. 1. Energy loss of  $^{132}\text{Xe}$  beam in the Si detector. Horizontal scale is arbitrary unit. Peak position corresponds to 2.03 GeV.

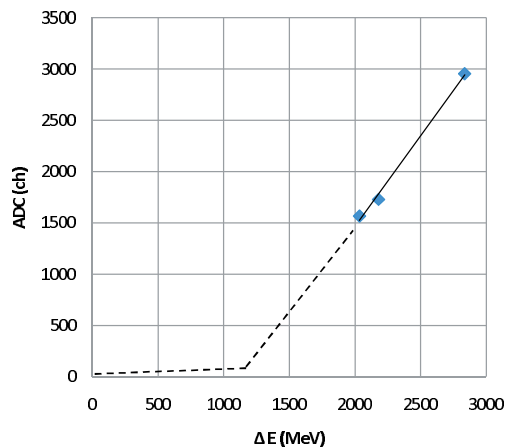


Fig. 2. Energy scale using three kinds of energy loss of  $^{132}\text{Xe}$ . Dashed line shows an extrapolation based on response for pulser.

lower energy deviated from the zero channel. This deviation was consistent with the result using a pulser as written in the previous report<sup>1)</sup>. When a signal is beyond a saturation of the high-gain preamplifier, the ratio of charge division changes and the energy scale of the readout system including the low-gain preamplifier is bended. The energy resolution was about 1.5 % as shown in Tab. 1. The resolution was not good due to the saturation of the high-gain preamplifier. This res-

<sup>\*1</sup> Department of Physics, Faculty of Science and Technology, Tokyo University of Science

<sup>\*2</sup> Center for Nuclear Study, University of Tokyo

<sup>\*3</sup> Department of Physics, Kyoto University

olution is, however, good enough to identify a charge state of an in-flight particle with  $Z = 40$ .

Table 1. Energy resolution in FWHM as a function of energy loss,  $\Delta E$ , in the DSSD.

$\Delta E$ (GeV)	FWHM (%)
2.03	$1.7 \pm 0.4$
2.18	$1.5 \pm 0.5$
2.83	$1.1 \pm 0.3$

We have tested the  $\beta$ -ray detection and the position correlation by using the unstable beam.  $^{18}\text{N}$  ( $T_{1/2} = 624$  ms) beam was produced through the reaction,  $^9\text{Be}(^{18}\text{O}, ^{18}\text{N})^9\text{B}$  and separated by CRIB, and the energy implanted in DSSD was 50 MeV. The total production rate was 14 cps and the purity of the  $^{18}\text{N}$  beam was 14%. Main contaminant was  $^{17}\text{N}$  ( $T_{1/2} = 4.17$  s) and its purity was 56%. Two 1mm-thick DSSDs were placed at F2 of CRIB. The  $^{18}\text{N}$  was implanted in the first DSSD. The implantation position was determined from a strip which have largest signal among strips. The strips of the second DSSD was connected together because this DSSD was used for the coincidence about  $\beta$  ray.

The  $^{18}\text{N}$  was implanted near the surface, therefore the  $\beta$  ray emitted to the direction of the surface was not detected. On the other hand, the  $\beta$  ray emitted to another surface was detected, of which a minimum energy loss was 300 keV. The energy-loss spectrum of  $\beta$  ray in DSSD was shown in Fig. 3. The coincidence spectrum with another DSSD was shown as the dashed line. The noise less than 200 ch and the energy loss of 300 keV around 400 ch were clearly separated. While the noise level at F2 of CRIB was higher than 20 keV, the lower noise level is expected at the BigRIPS beam line because the 20 keV was achieved at a cave around the BigRIPS in the previous test<sup>1)</sup>. The time spectrum of  $\beta$  decay under the position correlation between the implantation and the decay events was shown in Fig. 4. The half life was determined to be  $560 \pm 70$  ms, which was consistent with the known value  $624$  ms<sup>3)</sup>. The decay event of  $^{18}\text{N}$  was extracted purely against  $\beta$ -unstable contaminants.

In summary, we tested the DSSD with the newly developed readout system using the stable beam of  $^{132}\text{Xe}$  at HIMAC and the unstable beam of  $^{18}\text{N}$  at CRIB. The signal of 2 - 3 GeV energy loss of  $^{132}\text{Xe}$  beam was measured. The linearity and the resolution were checked. The  $\beta$  ray from  $^{18}\text{N}$  was measured by the DSSD where  $^{18}\text{N}$  was implanted. The decay event was extracted by the position correlation between the implantation and the  $\beta$  ray. The performance satisfied the requirement of the decay spectroscopy.

## References

- 1) N. Uematsu and S. Nishimura, RIKEN Accel. Prog. Rep. **41** (2008) 151.

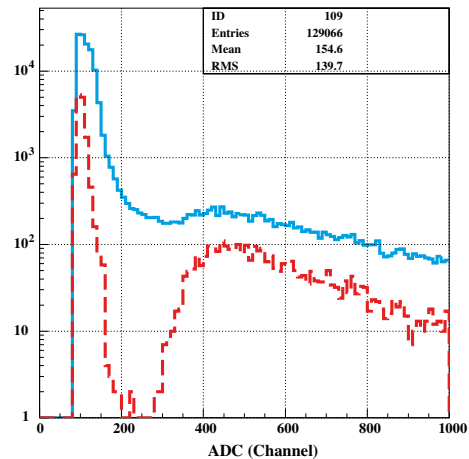


Fig. 3. Energy loss of  $\beta$  ray in the first DSSD. The dashed line shows the coincidence spectrum with the second DSSD. 400 ch was about 300 keV.

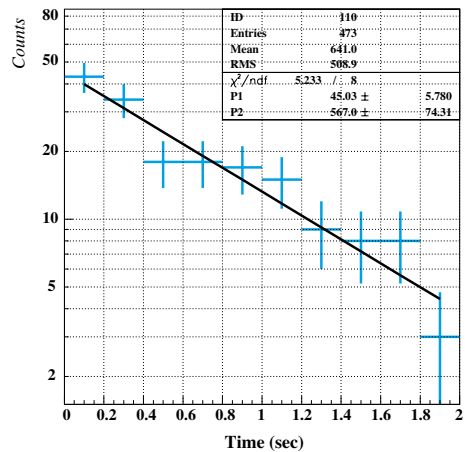


Fig. 4. Time spectrum from the implantation of  $^{18}\text{N}$  to the  $\beta$ -ray detection with the position correlation between the implantation and the  $\beta$  ray. The line shows the best fit of decay curve with no background component.

- 2) Y. Yanagisawa *et al.*, Nucl. Instr. Meth. A, **539** (2005) 74.
- 3) R.B. Firestone *et al.*, Table of Isotopes, 8th ed., A Wiley-Interscience Publication, (1996).

## Development of thick solid hydrogen target

T. Moriguchi,<sup>\*1</sup> A. Ozawa,<sup>\*1</sup> S. Ishimoto,<sup>\*2</sup> K. Tanaka, M. Takechi, Y. Yasuda,<sup>\*3</sup> Y. Ito,<sup>\*1</sup>  
K. Ogawa,<sup>\*1</sup> H. Ooishi,<sup>\*1</sup> and Y. Ishibashi<sup>\*1</sup>

We have developed a thick solid hydrogen target (SHT)<sup>1,2)</sup> to use for reaction cross-section measurements of unstable nuclei. Until now, a liquid hydrogen target (LHT) was used in the measurements at RIKEN<sup>3)</sup>. SHT has some advantages compared to LHT. (1) In SHT, distension of entrance and exit windows is less than that in LHT, and that allows us to make a target with a large area; thinner entrance and exit windows are also available with SHT. (2) In SHT, temperature control is not necessary. (3) Density of SHT is larger than that of LHT.

Figure 1 shows a schematic view of a target cell of SHT. The cell is made of a copper block, which allow us to make SHT with  $\phi 50$  mm diameter and 100 mm length. Thickness of this SHT corresponds to about  $0.9 \text{ g/cm}^2$ . Beam windows of SHT were made of kapton foils with  $25 \mu\text{m}$  thickness. To cool the target cell we used a cryocooler refrigerator, which has a cooling power of  $1.5 \text{ W}$  at  $4.2 \text{ K}$ . Hydrogen gas is put into the cell through an SUS tube, as shown in Fig. 1.

Figure 2 shows a schematic view of the vacuum chamber for SHT and the system to supply hydrogen gas. The SHT cell is surrounded by the thermal-radiation shield in the vacuum chamber ( $\sim 10^{-6}$  Torr). The thermal radiation shield made of copper shields the SHT cell from external heat. The cryocooler connected to the He compressor was used to cool the SHT cell. It takes 4 hours to reach about  $5 \text{ K}$ . Only the necessary amount of hydrogen gas is supplied into the H2 tank since the gas is flammable. Hydrogen gas was supplied into the SHT cell at a constant pressure (100 Torr) by a control valve. After starting the supply of gas to the SHT cell, it takes 150 minutes to complete

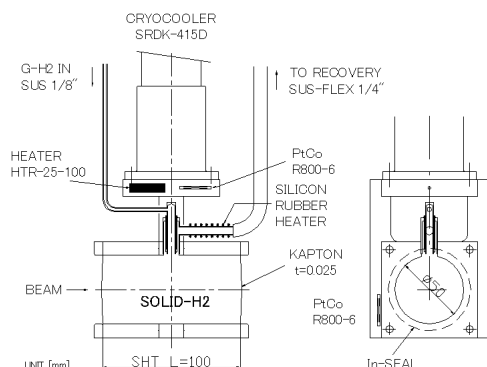


Fig. 1. Schematic view of SHT cell.

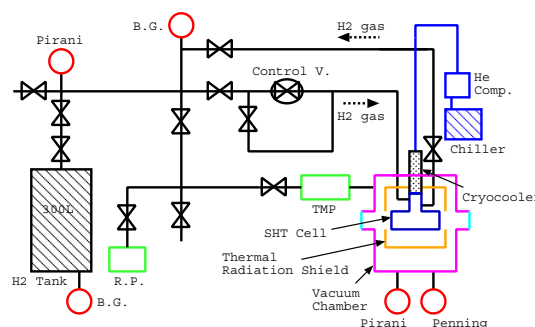


Fig. 2. Schematic view of system to supply hydrogen gas.

the SHT. Figure 3 shows a picture of a typical completed SHT. Dark shadows on the top of the figure are cracks which were produced just after completion of the SHT. If the gas pressure is high, more cracks are produced. On the other hand, if the gas pressure is low, hydrogen gas remains in the SHT as bubbles. The system is maintained at a constant optimal pressure of 100 Torr to minimize cracks and bubbles. The SHT can be melted by a heater, located at the top of the cell, and it returns to the H2 tank (see Fig. 2) gas. At the beginning of this recovery process, we also use a silicon rubber heater, which wraps the recovery tube in order to melt solid hydrogen inside the tube. Total time for recovery is about 30 minutes.

The present SHT system was installed at F11 of the zero degree spectrometer for Day-one experiment in December 2008. We checked homogeneity of SHT by using the secondary beam and measured the charge changing cross-section for some light neutron-rich nuclei. Analysis of the results is now in progress.



Fig. 3. Appearance of typical SHT.

### References

- 1) S. Ishimoto et al.: Nucl. Instr. and Meth. A **480**, 304 (2002).
- 2) S. Ishimoto et al.: Phys. Lett. A **299**, 622 (2002).
- 3) K. Tanaka et al.: RIKEN Accel. Prog. Rep. **39** 151 (2006).

<sup>\*1</sup> Institute of Physics, University of Tsukuba  
<sup>\*2</sup> KEK(High Energy Accelerator Research Organization)  
<sup>\*3</sup> Research Center for Nuclear Physics, Osaka University

## Parasitic production of slow RI-beam from a projectile fragment separator by ion guide Laser Ion Source (PALIS)

T. Sonoda, M. Wada, A. Takamine, K. Okada,<sup>\*1</sup> P. Schury, A. Yoshida, T. Kubo, Y. Matsuo, T. Furukawa, T. Wakui,<sup>\*2</sup> T. Shinozuka,<sup>\*2</sup> H. Imura,<sup>\*3</sup> Y. Yamazaki, I. Katayama,<sup>\*4</sup> S. Ohtani,<sup>\*5</sup> H. Wollnik,<sup>\*6</sup> H.A. Schuessler,<sup>\*7</sup> Y. Kudryavtsev,<sup>\*8</sup> P. Van Duppen,<sup>\*8</sup> and M. Huyse<sup>\*8</sup>

A new heavy ion accelerator facility and a projectile fragment separator, BigRIPS<sup>1)</sup> provide a wide variety of short-lived radioactive isotope (RI) ions without restrictions on their lifetime or chemical properties. The beams are however, not adequate for precision atomic spectroscopy. We therefore proposed a universal slow RI-beam (SLOWRI) facility as one of principal facilities of RIBF using a gas catcher cell with an RF-carpet ion guide<sup>2)</sup>. The R&D work for SLOWRI is successfully progressing and some spectroscopy experiments on Be ions have been performed<sup>3,4)</sup>. Beam time at such a modern accelerator facility, however, is always limited and operational costs are often high. We therefore propose an additional new method to drastically enhance the usability of such an expensive facility. At RIBF, a single primary beam produces thousands of isotopes simultaneously but only one isotope is used for an experiment while the other >99.99% of isotopes are simply thrown away. We propose a new method to collect such dead isotopes for a slow RI-beam by installing a laser ionization gas catcher in the vicinity of the first or second focal points of the fragment separator BigRIPS, which will provide parasitic RI-beams free of operational cost.

The fragment separator, BigRIPS, consists of a pair of magnetic separators with an energy degrader placed in between. A single isotope beam is, in principle, obtained by the two-stage separation. All contaminant ions with slightly different  $A/Z$  are stopped in the slit at the focal point of the first separator (F1) and dozens of isotopes in the vicinity of the desired isotope are stopped in the slit at the second focal point (F2). Our aim is to collect those isotopes lost in the slits. Due to space and accessibility constraints, a big gas cell like the one used in SLOWRI is not possible, so we must use a compact cell with a simpler mechanism. The proposed setup is shown in Fig. 1. We will place one or more compact gas cells on the side of the main beam path. Each gas cell will be filled with 1 bar Ar gas whereby most injected ions can be neutralized. A degrader located in front of the cell will adjust the beam energy to efficiently stop the ions inside the

cell. The neutralized atoms will be transported by gas flow toward the exit of the cell, where the atoms can be re-ionized by laser radiations. This uses the same principle as the conventional IGISOL<sup>5)</sup> for the transport and LISOL<sup>6)</sup> for the re-ionization scheme.

Although the size of the cell is limited, the high-pressure Ar will enable efficient stopping of energetic RI-beams. In order to ionize the neutralized RI-atoms efficiently, a multi-step resonance ionization method will be used with high power and high repetition rate pulsed lasers. Resonance ionization within a gas cell has been studied intensively at the Leuven<sup>6)</sup>, Mainz<sup>7)</sup>, and Jyvaskyla<sup>8)</sup> groups. The re-ionized RI ions from the gas cell will be transported by SPIG<sup>9)</sup> through multiple differential pumping stages to an electro-magnetic mass separator. Although the new method is not as universal as the original SLOWRI, the purity of ions can be extremely high. Separations by  $A/Z$  are made at BigRIPS, by  $Z$  via laser ionization, and by  $A$  at the mass separator. Fig. 2 shows one example of a part of available laser-ionized isotopes in an in-flight fission from  $^{238}\text{U}$  beam aiming for  $^{125}\text{Pd}$ , when the gas cell is placed  $X=75$  mm at the F1 slit. This intensity means the number of RI ions entering into the entrance of the gas cell whose diameter is 50 mm. The result may imply an adequate yield for even post acceleration.

One of the important issues in the gas catcher system is the extraction time to avoid the decay loss of short-lived isotopes. The proposed gas cell solely uses

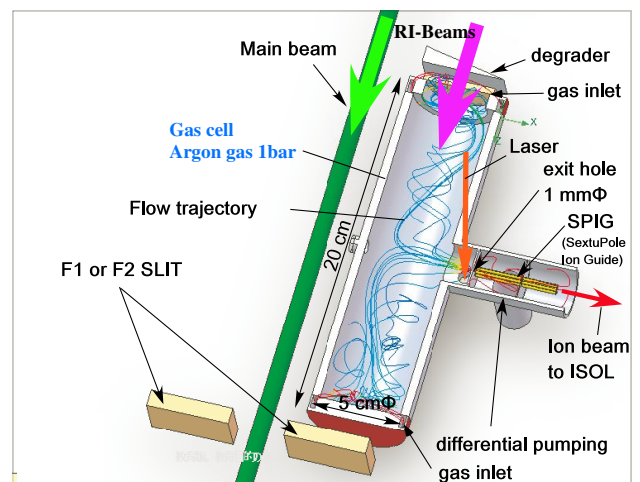


Fig. 1. Schematic image of the laser ionization gas catcher setup.

\*1 Department of Physics, Sophia University  
 \*2 Cyclotron and Radioisotope Center, Tohoku University  
 \*3 Japan Atomic Energy Agency (JAEA)  
 \*4 High Energy Accelerator Research Organization (KEK)  
 \*5 Institute for Laser Science, University of Electro-Comm.  
 \*6 II. Physikalisches Institute, University of Giessen  
 \*7 Department of Physics, Texas A&M University  
 \*8 Department of Physics, K.U. Leuven

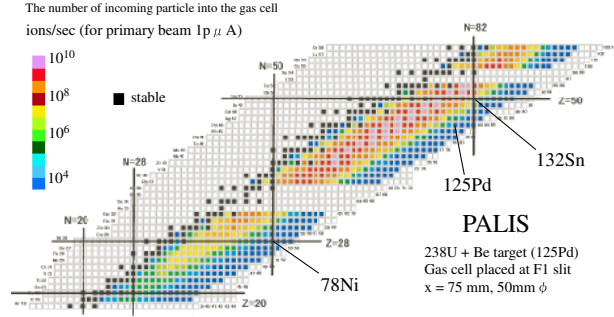


Fig. 2. A part of available laser-ionized isotopes in an in-flight fission from  $^{238}\text{U}$  beam aiming for  $^{125}\text{Pd}$ , when the gas cell is placed  $X=75$  mm at the F1 slit (the cell entrance is  $50\text{ mm}\phi$ ).

gas flow to guide stopped nuclei towards the exit hole of the cell. This extraction time is therefore determined by the volume of the cell and the conductance of the exit hole. The accessibility for short-lived nuclides was evaluated by using a flow calculation and a macroscopic simulation including diffusion loss. The evaluated total efficiency shown in Fig. 3 is obtained from a product of the total survival efficiency against decaying, the stopping efficiency and an assumed additional efficiency factor. This additional factor consists of the laser ionization efficiency and other possible loss, such as molecular formation and beam transport to SLOWRI. Based on experimental results at Leuven for Ni isotopes<sup>12)</sup>, this additional efficiency factor was evaluated to be 10%. The evaluated total efficiency suggests that more than 1% overall efficiency is still expected for nuclei with a half-life of longer than 1 s. The practical yield obtained by PALIS is a product of this total efficiency and the intensity shown in Fig. 2.

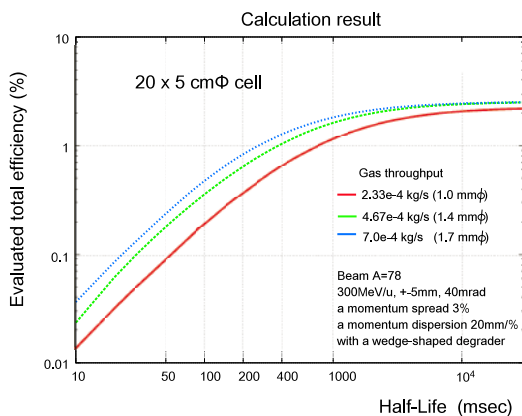


Fig. 3. Evaluated total efficiency of PALIS as a function of the half-life of the nucleus for different gas throughput.

Historically some distinct phenomena have been observed in the various gas catcher systems. The most serious problem is that the extraction efficiency from

the cell diminishes with increasing rates of incoming particles<sup>10,11)</sup>. This phenomenon can be explained as an effect of space charge in the cell. During the process of stopping in the gas cell, one incoming ion produces more than  $10^5$  ion-electron pairs and the electrons are removed quickly by the applied dc field, while the buffer gas ions remain in the cell for a longer period of time. The buffer gas ions distort the external field which is applied to transport the thermal ions towards the exit. The distorted electric field causes losses in the transport of RI-ions. The equilibrium space-charge density is proportional to the square-root of the beam intensity and the transport efficiency is roughly proportional to the reciprocal of the charge density<sup>11)</sup>. In the proposed scheme, however, the RI-ions are intentionally neutralized and transported exclusively by the gas flow. The effect of the space-charge must be minimal. A drastic efficiency enhancement for the high-intensity beam was observed using a laser ionization gas cell at LISOL Leuven<sup>12)</sup> (Fig. 4). A high efficiency is still preserved with  $10^{10}$  pps beam of  $^{58}\text{Ni}$ .

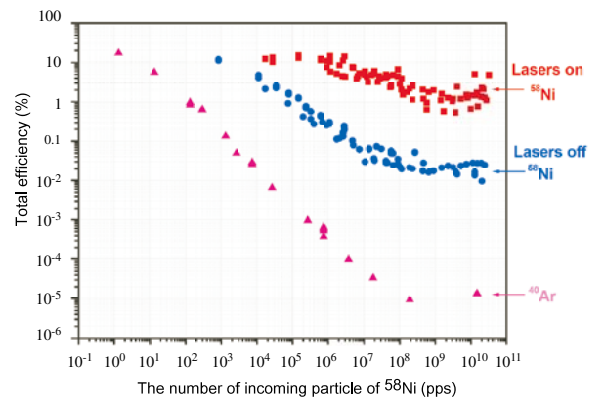


Fig. 4. Experimentally measured total efficiency of the laser ionization gas cell for  $^{58}\text{Ni}$  at Leuven<sup>12)</sup>.

We have presented a new experimental method to provide parasitic slow RI-beams from a projectile fragment separator without disturbing the primary RI-beam experiment. This is an additional option for RIKEN universal slow RI-beam facility, SLOWRI.

## References

- 1) T. Kubo, Nucl. Instr. Meth. B204 (2003) 97.
- 2) M. Wada et al., Nucl. Instr. Meth. B 204 (2003) 570.
- 3) T. Nakamura et al., Phys. Rev. A 74 (2006) 052503.
- 4) K. Okada et al., Phys. Rev. Lett. 101(2008) 212502.
- 5) J. Aysto, Nucl. Phys. A693 (2001) 477.
- 6) Yu. Kudryavtsev et al., Nucl. Phys. A701 (2002) 465.
- 7) K. Blaum et al. Nucl. Inst. Meth. B204 (2003) 331.
- 8) I.D. Moore et al., J. Phys. G31 (2005) s1499.
- 9) H. J. Xu, et al., Nucl. Inst. Meth. A333 (1993) 274.
- 10) K. Morita et al., Nucl. Inst. Meth. B26 (1987) 406.
- 11) A. Takamine et al., Rev. Sci. Inst. 76 (2005) 103503.
- 12) M. Facina et al., Nucl. Inst. Meth. B226 (2004) 401.

# A Portable Multi-Reflection Time-of-Flight Mass Spectrograph for SLOWRI<sup>†</sup>

P. Schury, K. Okada, V. A. Shchepunov,<sup>\*1</sup> T. Sonoda, A. Takamine, M. Wada, H. Wollnik,<sup>\*2</sup> and Y. Yamazaki

[Mass measurements, unstable nuclei, low energy beam]

We are continuing the development of a multi-reflection time-of-flight (MRTOF) mass spectrometer for use with radioactive ion (RI) beams. The MRTOF will be attached to its own dedicated gas stopping cell, allowing the system-as-designed to be portable. This will provide flexibility in commissioning the device by making it possible to use less-demanded RI sources, such as CRIB, while still being easily moved to other RI-beam sources at RIKEN – or even being relocated to another facility.

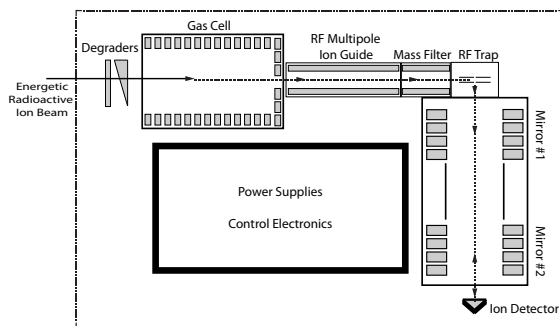


Fig. 1. Planned layout for the portable MRTOF system.

The system includes a gas cell for stopping relativistic ions, an ion trap to prepare ions for injection into the MRTOF and ion guide systems for transporting thermalized ions from the gas cell to the ion trap. The hatched box indicates that the entire system is portable.

Figure 1 provides a sketch of the system. Energetic ions will be slowed in a solid degrader and thermalized in a helium-filled chamber. Thermalized ions are injected into a radio-frequency (RF) multipole ion beam guide to be transported through a differentially pumped region after being extracted from the gas cell using a proven RF-carpet technique<sup>1)</sup>. An RF quadrupole mass filter will select for a specific ion mass number, removing non-isobaric ions. The isobaric ion ensemble will then be cooled in a low-pressure gas-filled RF ion trap before being injected into the MRTOF.

An early off-line prototype previously achieved a mass resolving power of  $R \approx 2 \times 10^5$ , with a measurement time of  $t \approx 7$  ms for  $A/q=28$  ions<sup>2)3)</sup>. However the efficiency at such a resolving power, while never quantified, was low. The on-line system, still under de-

velopment, is expected to be able to achieve even better resolving powers with a high efficiency. Efficiency improvement will result from reducing the emittance of ion pulse extracted from the trap and improving the vacuum level in the flight chamber; enhanced resolving power will result from achieving extremely high-stability voltage supplies for the MRTOF electrodes and reducing the energy and time spreads of ion pulses extracted from the ion trap.

To study the most exotic isotopes, the entire system must be highly efficient. To minimize space charge effects, a cryogenically cooled gas cell will be used. This will reduce gas impurities which might charge exchange with ionized helium. While the RF-carpet technique does not transport  $\text{He}^+$ , gas impurities ionized by exchange with helium ions can lead to a powerful source of impurity ions which can reduce extraction efficiency from the system due to space charge effects.

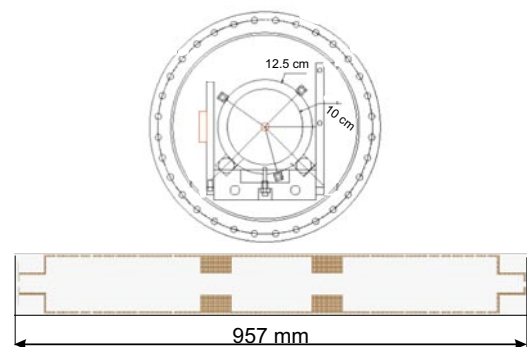


Fig. 2. (top) Mechanical drawing of MRTOF mounting, showing vacuum chamber, C-shaped mounting bracket, ceramic mounting rods and ring electrode. (bottom) Sketch showing electrodes for MRTOF.

As the total flight length may be as much as 1 km, the emittance strongly effects the the efficiency of the system. The energy spread of the ions directly effects of the maximum resolving power of the system. To address these issues, the ion trap will also be cryogenically cooled, which should lead to a reduction in the energy spread and emittance of the cooled ion cloud.

Figure 2 shows the mechanical layout of the MRTOF system. The system will be mounted on a heavy base of Titanium, with side-panels to minimize sagging effects. Titanium has been chosen because it has a low coefficient of expansion (9 ppm/K) which is well-matched the the coefficient of expansion for the ceramic insula-

<sup>\*1</sup> SRL, Manchester, England

<sup>\*2</sup> University of Gießen, Gießen, Germany

tors which will be used. This should help to minimize systematic effects from changes in the flight length. Additionally, Titanium has better vacuum properties while being much less magnetic than stainless steel.

A new ion trap of novel geometry is being developed for the MRTOF-MS. The trap uses a pair of printed circuit boards, each consisting of three strip electrodes. An RF signal applied to the outer electrodes creates a confining quadrupole pseudo-potential. The strips are segmented to allow an axial potential well for ion trapping. The ions are introduced into the trap parallel to the electrodes; after cooling, the ions are ejected perpendicular to the trap through a small ( $r = 100 \mu\text{m}$ ) hole in the central electrode. This geometry should produce very well-cooled ions without affecting the MRTOF-MS vacuum, leading to highly efficient operation. Figure 3 shows a photo of one of the printed circuit boards used to build the ion trap.

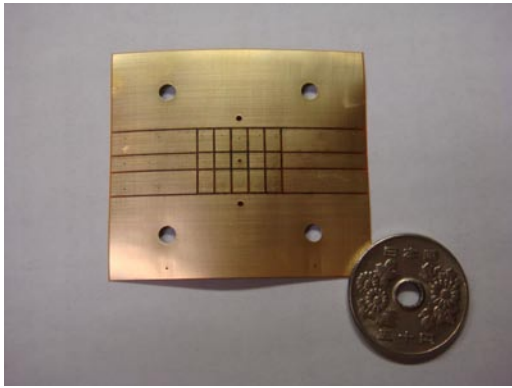


Fig. 3. Photograph of one of the printed circuit boards used to construct the ion trap. A ¥50 coin is shown for scale.

To optimize the voltage distribution and determine the maximum mass resolution which we can expect, a large number of simulations have been performed. These calculations have recently been reported<sup>4)</sup>. For minimally cooled ion clouds ( $R_0 = 100 \mu\text{m}$ ,  $T = 3000 \text{ K}$ ), calculations indicate that a mass resolving power of  $R_m \approx 5 \times 10^5$  can be achieved, as shown in Fig. 4. With such resolving powers it would be possible to resolve most long-lived isomeric states, making the device highly competitive with Penning trap mass spectrometry (PTMS). Furthermore, the fast measurement may allow the MRTOF-MS to exceed PTMS for sufficiently short-lived isotopes, as indicated in Fig. 5.

Development work for the portable MRTOF-MS is ongoing. The MRTOF electrodes and vacuum chamber have been sent for fabrication and are scheduled to arrive near the end of FY2008. The vacuum chamber and mounting for testing the new ion trap system has been sent for fabrication and is scheduled to arrive in February, 2009. At present, it is foreseen that construction of the system should be completed early in FY2009 with commissioning to begin thereafter.

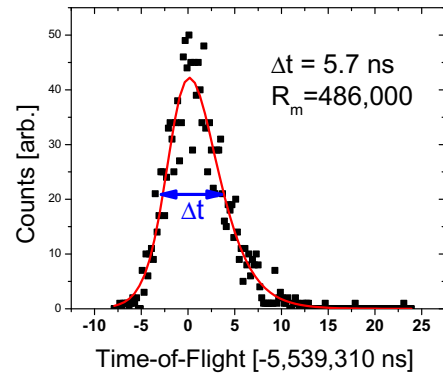


Fig. 4. Calculated time-of-flight pulse for  $A/q = 28$  ions after 518 laps in the MRTOF-MS, assuming a minimally cooled ion cloud ( $R_0 = 100 \mu\text{m}$ ,  $T = 3000 \text{ K}$ ) with an rise time of  $t_r = 1 \mu\text{s}$  for the MRTOF injection electrode. The full-width at 1% for this ion pulse represents  $\Delta m \approx \pm 75 \text{ keV}$  – indicating that the MRTOF-MS may be able to resolve *isomers*.

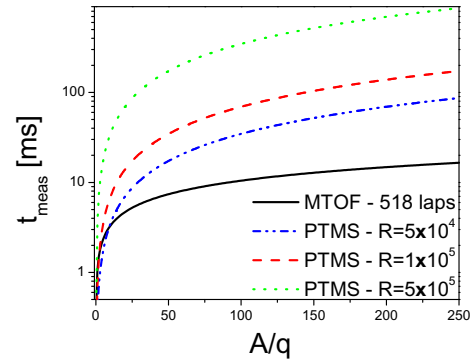


Fig. 5. Comparison of MRTOF and a 9.4T PTMS in terms of measurement time as a function of atomic mass. The resolving power for the MRTOF depends on many factors, however  $R = 5 \times 10^4$  should be easily achievable with 518 laps. Thus, it is clear that the MRTOF will require much shorter measurement times than PTMS.

#### References

- 1) M. Wada et al., Nucl. Instrum. Methods **B204**, 570 (2003)
- 2) Y. Ishida, M. Wada and H. Wollnik: Nucl. Instrum. Methods and Phys. Res. **B241**, 982 (2005).
- 3) Y. Ishida, M. Wada and H. Wollnik: RIKEN Accel. Prog. Rep. **40**, 150 (2007)
- 4) P. Schury, et al., *Multi-Reflection Time-of-Flight Mass Spectrograph for Short-Lived Radioactive Ions*, Proceeding of the 5th Conference on Exotic Nuclei and Atomic Masses

## Development of an absolute laser frequency counting system

M. Wada, A. Takamine, K. Okada,<sup>\*1</sup> P. Schury, T. Sonoda, V. Lioubimov, and H.A. Schuessler,<sup>\*2</sup>

Precision spectroscopy of atomic transitions is almost the exclusive method used to determine the nuclear charge radii of unstable nuclei. In such measurements, narrow-line-width continuous-wave lasers are often used and the wavelengths or frequencies of the laser radiations must be accurately known. Fortunately, nowadays a clockwork optical femtosecond frequency comb<sup>1)</sup> can provide an exact “scale” for laser frequency measurements. A common method to provide a laser radiation with an accurate frequency and a high stability is to “lock” the user’s laser frequency to the frequency comb. However, this method is not always applicable. For example, in our laser-laser double resonance spectroscopy experiments<sup>2)</sup>, we need to use two scannable laser radiations. Also in our collinear laser spectroscopy with parallel-antiparallel configuration<sup>3)</sup>, two laser radiations should be scanned simultaneously and independently. Although, it is possible to scan the frequency of a laser radiation locked to a frequency comb by scanning the repetition rate of the femtosecond laser, the scanning rate is slow and we need to have two frequency combs for two independent laser radiations. A frequency shifter based on an acousto-optic modulator can provide scanning capability from a fixed frequency laser, however the usability of such a device, especially for UV radiation, is limited.

We therefore used two commercial dye lasers with their own scanning and stabilization functions (using attached reference cavities) and *measure* the laser frequencies from the beat frequencies resulting from interference with a frequency comb. The dye laser frequency  $f_{\text{dye}}$  can be obtained using

$$f_{\text{dye}} = n f_{\text{rep}} \pm f_{\text{offset}} \pm f_{\text{beat}}, \quad (1)$$

where  $f_{\text{rep}}$  is the repetition rate of the femtosecond laser which is flexible around 250 MHz,  $f_{\text{offset}}$  is the offset frequency of the frequency comb which is usually fixed to 40 MHz, and  $f_{\text{beat}}$  is the beat frequency between the comb radiation and the dye laser radiation. The integer  $n$  and the polarity of  $f_{\text{offset}}$  can be obtained from other calibration sources, such as an wave meter and an iodine molecule cell. The polarity of  $f_{\text{beat}}$ , on the other hand, can be obtained from the trend of the beat frequency itself.

We have developed a system for counting the beat frequencies of dye laser radiations, which may fluctuate or jitter during measurements. It consists of a beat signal detection setup for two laser radiations, a filter circuit for counting the beat frequencies and software to reconstruct a spectrum as a function of the true laser

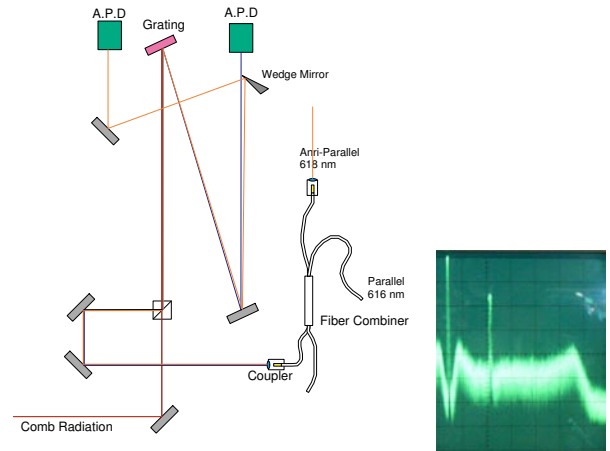


Fig. 1. Layout of the interaction region of the frequency comb radiation and the dye laser radiations (left) and beat signal of a dye laser observed in a spectrum analyzer scope. The left peak is a reference signal of the spectrum analyzer and the right peak is a beat signal.

frequency. Figure 1 (left) shows a schematic diagram of the detection scheme for two laser radiations in the case of collinear spectroscopy experiments. Two laser radiations were merged in a fiber combiner and interact with the comb radiation. Since the wavelengths of the two lasers are slightly different for the parallel and antiparallel beams, the interfered signals can be separated by a grating mirror and detected in two independent avalanche photo diodes, allowing the beat frequencies to be counted simultaneously. In the case of laser-laser double resonance spectroscopy for Be isotope ions, however the frequency difference between the two 626 nm radiations is too small to be separated by a grating. We saw two beat frequencies mixed in a spectrum analyzer scope, or we chopped the radiations and measure them alternately.

A typical beat signal observed in a spectrum analyzer is shown in Fig. 1 (right). It is often contaminated by higher harmonics and spurious signals. A filter circuit with many band-pass filters was used to eliminate such noise signals and count the true beat signal (Fig. 2). The circuit consists of amplifiers made of current-feedback operational amplifier devices AD8002, band-pass filter modules from Mini-Circuits, discriminators made of fast comparator devices MAX962, and pre-scalers made of AC393 or MC12026. The beat signals from all filter channels and fluorescence signals were counted simultaneously in a multi-input multi-channel scaler device made of PCI6607 interface cards. A short time interval of

<sup>\*1</sup> Department of Physics, Sophia University

<sup>\*2</sup> Department of Physics, Texas A&M University

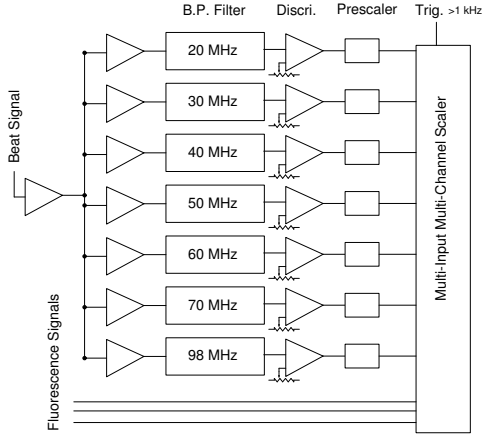


Fig. 2. Block diagram of the filter circuit for beat frequency counting.

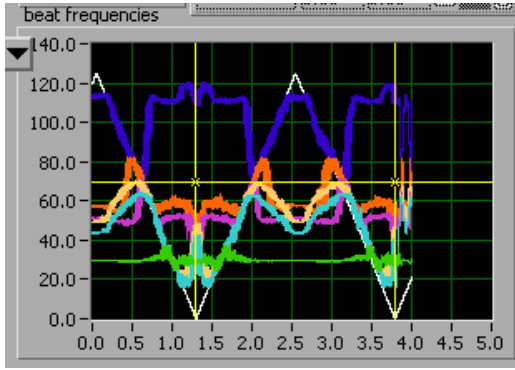


Fig. 3. Beat frequencies measured through multiple band pass filters during a laser scan

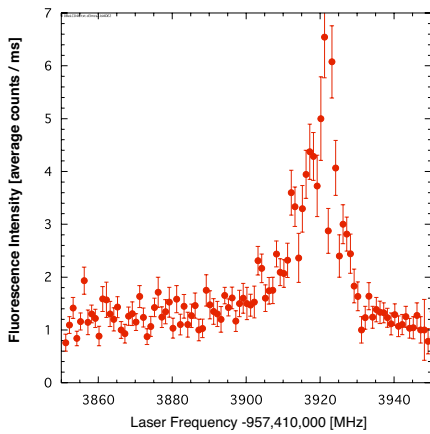


Fig. 4. Laser cooling spectrum of  $^{10}\text{Be}^+$  ions plotted as a function of the absolute laser frequency.

$t_{\text{bin}} < 1$  ms was used to track the relatively fast jittering of the dye laser frequency.

Figure 3 shows plots of the beat signal counts as a function of the scanning time. The observable range of the beat frequency covered as wide as from 15 MHz to 110 MHz while the vicinity of the turning points, 0 MHz and 125 MHz, are always suffered from the spurious signals. When the count values were not in the range of the band-pass filter, the beat frequencies are spuriously reported. This can be corrected for through the use of defined range table for each filter along with partial range overlap between the neighboring band-pass filters and correlation with the scan time.

Only with these consistency checks, can the absolute laser frequency be obtained through determination of the  $n$ -value, the polarity of  $f_{\text{offset}}$ , and the true beat frequency during each  $t_{\text{bin}}$ . This value can be stored along with the counts of the fluorescence signals detected during the time bin.

The number of the fluorescence count per  $t_{\text{bin}}$  may be small since a typical counting rate of the fluorescence signal is several kcps. We need to sum several time bins to show a spectrum. If one sums the spectrum according to the succeeding time bin, which is equivalent to measuring with a longer  $t_{\text{bin}}$  as used in ordinary laser spectroscopy, the effects of fluctuations and jitter become significant. To remove the effects of fluctuations and jitter, we should sum the spectrum according to the *measured* laser frequency which is tagged with the fluorescence count data for each time bin. In this *frequency-binning* process, however, the number of the measurements which belong to the same frequency bin is not constant. We defined the intensity in units of counts per  $t_{\text{bin}}$  as an average of the count number for all measurements which belong to the frequency bin while the statistical uncertainty is obtained from the total fluorescence counts in the frequency bin. In this way, we achieved a true frequency spectrum as shown in Fig. 4 even though the laser frequencies were not stable. It should be noted that such a method allows us to sum up multiple scans even if the laser scanning is not reproducible.

The frequency counting system has been used for precision spectroscopy of optical transition frequencies of  $^{7,9,10,11}\text{Be}^+$  ions. Development is in progress to achieve better performance. So far we use commercial counter interface cards for the multi-input multi-channel scaler, however we plan to use an FPGA based hand-made multiple counter interface to increase the number of input channels and the flexibility of the system.

#### References

- 1) T. Udem *et al.*: Nature **416**, 233 (2002).
- 2) A. Takamine *et al.*: RIKEN Accel. Prog. Rep. **42**, (2009).
- 3) V. Lioubimov *et al.*: RIKEN Accel. Prog. Rep. **41**, 189 (2008).

## Development of fluorescence detection system for nuclear laser spectroscopy in He II

A. Sasaki,<sup>\*1</sup> S. Hoshino,<sup>\*1</sup> T. Wakui,<sup>\*2</sup> T. Furukawa, M. Kazato,<sup>\*3</sup> K. Yamaguchi,<sup>\*3</sup> T. Kobayashi, A. Hatakeyama,<sup>\*4</sup> K. Fujikake,<sup>\*5</sup> Y. Matsuura,<sup>\*5</sup> A. Odahara,<sup>\*3</sup> T. Shimoda,<sup>\*3</sup> T. Shinozuka,<sup>\*2</sup> and Y. Matsuo

We are developing a fluorescence detection system for nuclear laser spectroscopy of RI atoms stopped in superfluid helium (He II). This project is called OROCHI (Optical RI-atom observation in condensed Helium as Ion-catcher) and aims to perform laser spectroscopy of unstable nuclei even with a production yield of 10 pps.<sup>1)</sup>

Detection efficiency must be maximized while minimizing background count rates in order to observe laser-induced fluorescence (LIF) from the low yield of unstable nuclei. Detection efficiency is maximized by using a Fresnel lens in close geometry with a cryostat. The Fresnel lens has a large diameter and short focal length. This introduces a large solid angle for collection of LIF. The background, which mainly originates from the excitation laser, can be reduced by using a wavelength filter, because the wavelength of fluorescence is sufficiently separated from that of excitation in He II.<sup>2)</sup> In this project, the fluorescence detection system is used not only to observe fluorescence from unstable nuclei, but also to detect emission light from a plastic scintillator, which is placed in the cryostat and used for adjusting the stop position of RI beam in He II.

Figure 1 shows the configuration of the fluorescence detection system. It consists of three Fresnel lenses, a spatial filter (SF), a wavelength filter, and a photomultiplier tube (PMT). The light emitted from atoms is collected and focused on the SF by the first Fresnel lens (FL1). The SF is used to reduce stray light. Light which has passed through the SF is collimated

with the second lens (FL2) so that the light enters at normal incidence to the wavelength filter for perfect separation of wavelength. The light is then focused on the photoelectric surface of the PMT by the third lens (FL3).

To optimize the configuration of the system, we performed an optical simulation for the wavelengths 793 nm for LIF of Rb atoms and 425 nm for emission light from the plastic scintillator. The highest light collection efficiency was found to be 6.8% for 793 nm and 5.1% for 425 nm, by calculating with various focal lengths and positions of lenses. It should be noted that light transmission efficiency for each lens was assumed to be 100% in the calculation.

A fluorescence detection system for 425 nm was built based on the simulation. The focal lengths of the lenses are 45 mm, 20 mm, and 70 mm for FL1, FL2, and FL3, respectively. All the optical elements are mounted in a black box. The position of lenses can be adjusted along three axes using micrometers. The spatial filter consists of two slits placed along the x and y axes of a surface perpendicular to the optical axis. The position and width of the slits can be tuned using micrometers. The detection system is mounted just below the cryostat. The light transmission rates for FL1, FL2, and FL3 have been measured using a laser and are 29.7%, 90.7%, and 89.7%, respectively. The transmission rate for FL1 is relatively low because FL1 is used to focus diverging light, even though the Fresnel lens used is designed to focus parallel light to a single point. The total light collecting efficiency of the system is estimated to be 1.2% based on the simulation and the transmission rate measured using the laser light.

In the beginning of January 2009, a test experiment on the fluorescence detection system was carried out in the E7 room of the RIKEN Accelerator Research Facility. In this experiment, a  $^2\text{H}$  beam of 9.1 MeV/u was passed through two aluminum rotatable degraders used to lower the beam energy and a plastic scintillator used to count the number of  $^2\text{H}$  particles. The  $^2\text{H}$  was then injected into a cryostat and stopped in another plastic scintillator placed on the optical axis of the detection system. The emitted light from the scintillator was collected and detected by the detection system. Analysis of the data is in progress.

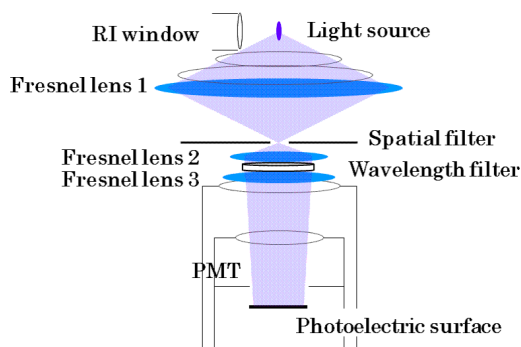


Fig. 1. Fluorescence detection system.

\*1 Department of Physics, Tohoku University  
 \*2 Cyclotron and Radioisotope Center, Tohoku University  
 \*3 Department of Applied Physics, Tokyo Univ. Agr. Tech.  
 \*4 Department of Physics, Osaka University  
 \*5 Department of Physics, Meiji University

### References

- 1) T. Furukawa et al.: RIKEN Accel. Prog. Rep. **41**, 153
- 2) Y. Takahashi, K. Sano, T. Kinoshita, and T. Yabusaki, Phys. Rev. Lett. **71**, 1035 (1993).

# Production of polarized Ag atoms by optical pumping in superfluid helium

T. Furukawa, K. Fujikake,<sup>\*1</sup> A. Hatakeyama,<sup>\*2</sup> Y. Matsuura,<sup>\*1</sup> A. Sasaki,<sup>\*3</sup>  
T. Kobayashi, T. Shimoda,<sup>\*4</sup> and Y. Matsuo

Polarized nuclei/atoms are one of most powerful tools for investigating nuclear properties, precise atomic structures, and fundamental physics. More specifically, our plan is to investigate nuclear electromagnetic properties such as nuclear spins and moments by measuring the atomic hyperfine or Zeeman structure of polarized atoms with laser-microwave/radiowave double resonance spectroscopy.

The optical pumping method is the most effective technique for producing high polarization of atoms, although the number of elements that can be optically pumped and polarized is limited. By using the optical pumping technique under superfluid helium conditions, we have achieved a large atomic polarization in Ag atoms for the first time. In this report, we describe details about optical pumping in superfluid helium.

The experimental setup is shown schematically in Fig.1. At the beginning of measurement, Ag atoms are laser-sputtered from an Ag metal sample disc placed approximately 1 cm above the helium surface, and are then introduced into the optical detection region in He II.<sup>1)</sup> Next, the introduced Ag atoms are optically pumped and polarized by irradiation with circularly polarized pumping laser light tuned to the  $^2S_{1/2} \rightarrow ^2P_{1/2}$  line of Ag atoms in He II.<sup>2)</sup> The circular polarization of pumping laser light is generated using a  $\lambda/4$  wave plate. In optical pumping, we apply a static magnetic field ( $\simeq 7$  Gauss) to hold the atomic polarization generated by optical pumping.

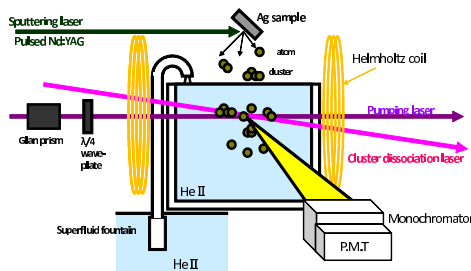


Fig. 1. Schematics of experimental setup

The polarization of optically pumped atoms is deduced from the measured laser-induced fluorescence (LIF) intensity of atoms with switching on and off the static magnetic field. It is to be noted that the LIF intensity  $I$  observed with irradiation by pumping light

is related to the polarization of Ag atoms as

$$I \propto N_{\text{atom}} \times (1 - P_l \times P_z), \quad (1)$$

where  $N_{\text{atom}}$  is the number of Ag atoms,  $P_l$  is the circular polarization of pumping laser light, and  $P_z$  is the electronic spin polarization of the atoms.<sup>3)</sup> Then LIF intensity is decreased gradually by increasing the polarization of atoms in optical pumping. From comparison of LIF intensity with and without the static magnetic field, the maximum polarization of Ag atoms in optical pumping is deduced to be more than 60%. The imperfection of achieved polarization is mainly due to the incomplete polarization of pumping laser light (70-80 %) because the wave plate we use is not suited for the wavelength of laser light. The atoms might be polarized much more if we used a wave plate suitable for the pumping laser wavelength.

Using the optically pumped Ag atoms, we have also measured the Zeeman splitting energy of the Ag atoms in He II using the laser-rf double resonance.<sup>3)</sup> Figure 2 shows the Zeeman resonance spectrum of stable  $^{107,109}\text{Ag}$  atoms in He II. We can deduce the nuclear spin of  $^{107,109}\text{Ag}$  from the peak position of the resonance spectrum<sup>3)</sup> as shown in the inset of Fig.2. Applying this optical pumping technique and double resonance technique to our project for nuclear laser spectroscopy in He II (named OROCHI), we can also measure the electromagnetic properties (nuclear spin, moment, and so on) of exotic Ag isotopes near the drip-line region which can not be measured with traditional methods.

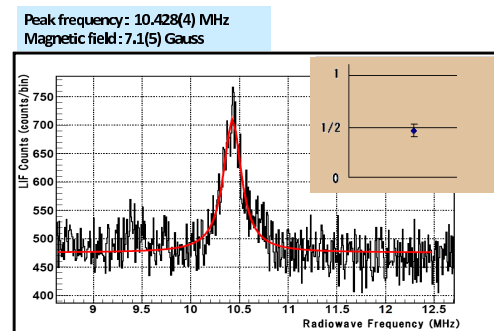


Fig. 2. Measured Zeeman resonance of  $^{107,109}\text{Ag}$  atoms in He II.

## References

- 1) T. Furukawa et al.: Phys. Rev. Lett. **96**, 095301 (2006).
- 2) Q. Hui: Doctoral thesis, Saitama Univ. (1997).
- 3) T. Furukawa: Doctoral thesis, Osaka Univ. (2007).

\*1 Inst. of Phys., Meiji University

\*2 Dept. of Appl. Phys., Tokyo Univ. Agr. Tech.

\*3 Dept. of Phys., Tohoku University

\*4 Dept. of Phys., Osaka University

# “Hybrid-RF” sequence in $\beta$ -NQR for $Q$ -moment measurement of short-lived nuclei

A. Yoshimi, H. Ueno, T. Nagatomo, K. Shimada,<sup>\*1</sup> Y. Hasama,<sup>\*2</sup> Y. Ichikawa, and K. Asahi<sup>\*2</sup>

The systematic measurement of electric quadrupole moments  $Q$  of unstable nuclei would provide important information for nuclear structure studies. In  $Q$ -moment measurement, it is crucial to realize highly efficient and rapid spin-flip using the AFP (Adiabatic Fast Passage) method. We have developed a new rf-application scheme called the “Hybrid-RF” method for AFP-NQR (Nuclear Quadrupole Resonance).

When measuring the  $Q$ -moment of unstable nuclei using the  $\beta$ -NQR technique,<sup>1)</sup> the nucleus is implanted in a crystal with an electric field gradient  $q$ . The resonance frequency for the implanted nucleus in a static magnetic field  $B_0$  splits into  $2I$  components due to  $eqQ$  interaction, and the transition frequency between the magnetic sublevels  $m$  and  $m + 1$  is given by

$$\nu_{m,m+1} = \nu_L - \nu_Q \frac{3(2m+1)(3\cos^2\theta_{c\text{-axis}} - 1)}{8I(2I-1)} \quad (1)$$

with  $\nu_Q = eqQ/h$ . Here  $\nu_L$  denotes the Larmor frequency and  $\theta_{c\text{-axis}}$  the angle between the  $c$ -axis in the crystal and the  $B_0$  field. An RF oscillating field  $B_1$  needs to induce all of the  $m \leftrightarrow m + 1$  transitions to get the full effect of NQR. Therefore each component of the RF frequencies should be adiabatically swept to meet the corresponding frequency  $\nu_{m,m+1}$  so that the population of  $m$  and  $m + 1$  are interchanged (AFP method).

We have previously used two methods in the RF sequence for the AFP-NQR experiment. In the first method (sequential-RF method), all  $\nu_{m,m+1}$   $B_1$  fields are applied sequentially. When  $I = 5/2$ , 15 RF steps are needed and the total RF application period takes as long as 100 ms. To perform AFP-NQR for short-lived nuclei, we developed a “Mixed-RF” method in which the frequencies for all  $2I$  components are swept at the same time.<sup>2)</sup> With this method the RF application period can be as short as order of ms. However the effective  $B_1$  field for each transition component in the mixed-wave field is reduced in inverse proportion to the number of components. Another difficulty with the mixed-RF method is that the population distribution does not change if  $\nu_L$  is slightly changed for some reason such as  $B_0$  drift according to a computer simulation. This is contrary to the sequential-RF scheme.

We have therefore introduced a new scheme, called the Hybrid-RF method, which is based on the sequential-RF and partially incorporates the mixed-RF method. With this method, some transitions which do not interfere each other are first induced at one time

by applying a mixed-RF wave. Another set of transitions are then induced by another mixed-RF wave. This sequence is continued until the population distribution is reversed. A possible sequence of this method in the case where  $I = 5/2$  is schematically shown in Fig. 1. The number of RF steps is 9 which is less than the 15 required in the sequential-RF method, and it is easier to satisfy the AFP condition than with the mixed-RF method. Since this method is based on sequential-RF, the full AFP-NQR effect is expected to detect if the  $\nu_L$  shifts slightly within the swept frequency windows.

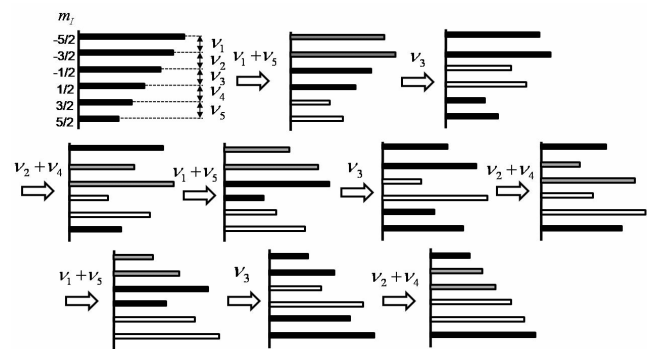


Fig. 1. Schematic diagram of hybrid-RF method showing how the population distribution is reversed.

We have tested the hybrid-RF method in an NQR-experiment with unstable nuclei  $^{31}\text{Al}$  ( $I = 5/2$ ,  $T_{1/2} = 644$  ms) whose  $Q$ -moment has been previously measured. The experiment was performed at GANIL. The  $^{31}\text{Al}$  nuclei were produced from the fragmentation of a  $^{36}\text{S}$  beam on a Be target.<sup>3)</sup> The beam of  $^{31}\text{Al}$  was spin-polarized by selecting its momentum and out-going angle, and implanted into an  $\alpha\text{-Al}_2\text{O}_3$  single crystal. AFP-NQR was performed using  $\beta$ -NMR. The applied  $B_0$  field was 5.000 kG, and the corresponding Larmor frequency was  $\nu_L = 5.824$  MHz. The applied hybrid-RF sequence was the same as in Fig. 1, where the total RF period was 72 ms and the  $B_1$  field was 3.0 G for each transition satisfying the AFP condition  $B_1 > 2\sqrt{\omega}/\gamma_{^{31}\text{Al}}$ . The measured asymmetry change with AFP-NQR was  $AP = 1.4(2)\%$ , which was found to be comparable with the value  $AP = 1.6(2)\%$  measured using the sequential-RF method.

## References

- 1) D. Kameda et al.: Phys. Lett. B **647** (2007) 93.
- 2) M. Takemura et al.: RIKEN Accel. Prog. Rep. **39** (2006) 145.
- 3) H. Ueno et al.: RIKEN Accel. Prog. Rep. **42** (2008).

<sup>\*1</sup> Cyclotron and Radioisotope Center, Tohoku University

<sup>\*2</sup> Department of Physics, Tokyo Institute of Technology

## Online luminosity monitor for the SCRIT experiment

S. Wang, T. Suda, T. Emoto, K. Ishii<sup>1</sup>, S. Ito, K. Kurita<sup>1</sup>, A. Kuwajiam<sup>2</sup>, T. Tamae<sup>2</sup>, M. Wakasugi and Y. Yano

In the last SCRIT experiment, a luminosity monitor was employed to monitor luminosity. It consists of three pieces of plastic scintillation detectors, including two “finger” detectors (10cm\*1cm\*0.5cm) and one “backup” detector (10cm\*5cm\*0.5cm). Two finger detectors were put in front of backup detector and the distance between two finger detectors is 1 cm. Luminosity monitor was put on the accelerator duct 4.5 m downstream from the center of SCRIT, as shown in Fig.1. For reducing the background, we made a coincident measurement between any one of those two finger detectors with backup detector.

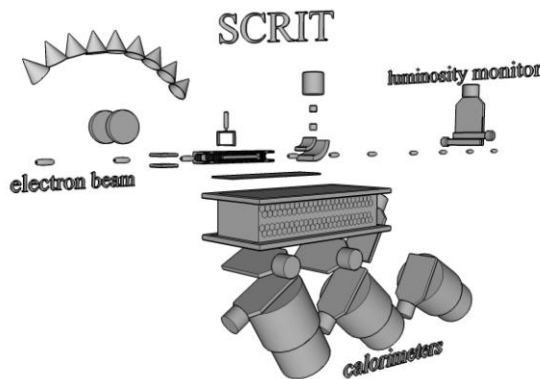


Fig.1 Sketch map of SCRIT.

Luminosity monitor utilizes forward elastic scattering where elastic cross section is huge. Two finger detectors can cover the scattering angle from 0.33 to 0.71 degree and from 0.58 to 0.86 degree. Considering Mott cross section and solid angle, the cross section of two finger detectors are 300 barn and 50 barn. Therefore, a short time measurement is needed to get enough statistics. Figure 2 shows the counting rate spectrum of one finger detector at beam current 71 mA.

The solid (dash) line is the spectra with (without) Cs ions trapped. The horizontal axis is the counting rate in the trapping time of 50 ms. Difference between two processes was only whether Cs ions were trapped or not. Therefore, the difference of two peaks should come from the events of trapped Cs ions.

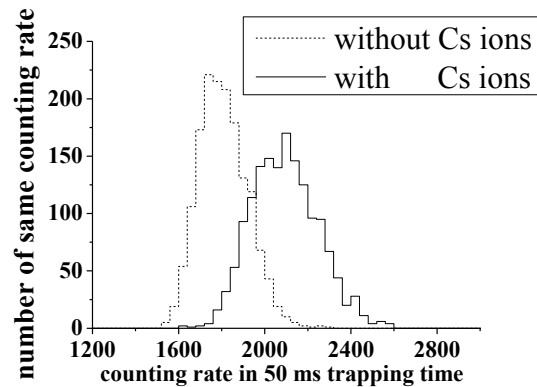


Fig.2 The counting rate spectrum.

From the counting rate difference and cross section, luminosity can be calculated from luminosity monitor, as shown in fig.3. The square points are the luminosity determined by elastic events from calorimeters and the circle points are the luminosity calculated from luminosity monitor. Two independent calculations got same results which suggest that this luminosity monitor can be used as an online luminosity monitor to monitor the luminosity during the experiment.

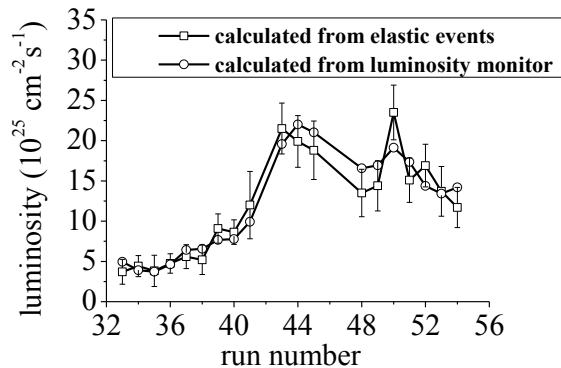


Fig.3 The calculated luminosity.

\*1 Rikkyo University  
\*2 Tohoku University

# Long-time measurement of fluctuation of magnetic field

Y. Yasuda,<sup>\*1</sup> A. Ozawa,<sup>\*1</sup> Y. Yamaguchi, I. Arai,<sup>\*1</sup> K. Y. Hara,<sup>\*1</sup> and T. Nakajima<sup>\*2</sup>

We are proceeding with research on uniformity and stability of a magnetic field of a sector magnet for constructing a storage ring in “Rare-RI Ring”. To achieve an isochronous condition in the storage ring with a relative accuracy of  $10^{-6}$ , a uniform and stable magnetic field in the storage ring is required. We performed a measurement of a magnetic field of a D8 magnet in a zero-degree forward spectrometer (ZDS) with a  $10^{-7}$  relative accuracy using newly produced NMR equipment<sup>1)2)</sup>. We performed the measurement of a fluctuation of the magnetic field for about 170 hours this time. We also measured the temperatures of the experimental room, yoke and coil surfaces and an output of a power supply by DCCT. The measurement was performed at around the center of the sector magnet in the median plane of the magnet. We started the measurement about 20 hours after the power of the magnet had been turned on.

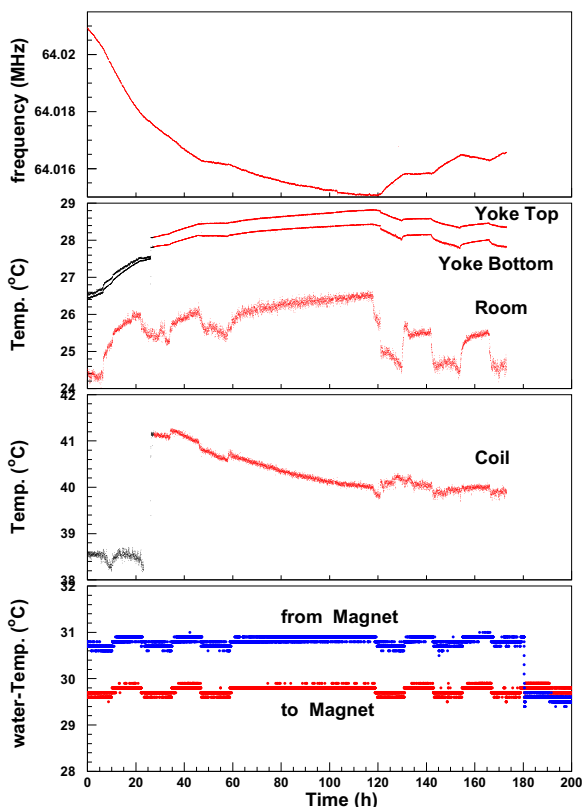


Fig. 1. Resonance frequency and temperatures

Figure 1 shows results of long-time measurement. The resonance frequency indicates the magnitude of the magnetic field. We also show temperatures of cooling water. The temperature lines of yoke and coil surfaces break at 27 hours since we improved attachment of Pt thermometers. The periodical fluctuation of the

temperature of the room is owing to the periodic operation of an air conditioner. It works from 08:00 to 20:00 in working day. The period from 60 to 120 hours was a weekend.

The fluctuation of the temperature of the room causes a fluctuation of the temperature of the yoke. From this measurement, definite correlation of the resonance frequency and the temperature of the yoke surface has been observed. Furthermore the resonance frequency ( $f$ ) has a strong linear correlation with the temperature of the yoke ( $T$ ). Its 1st order coefficient  $\frac{df}{dT}$  is  $-3.6 \times 10^{-3}$  MHz/K. It is  $-5.6 \times 10^{-5}$  1/K relatively and is the same order of magnitude as the rate of linear expansion of iron. Our result suggests that the fluctuation of the room temperature makes expansion and contraction of the iron of yoke and the expansion and contraction of the gap of the magnet affect the magnetic field.

Following this assumption, a calculation of heat conduction in an iron yoke in one dimensional space was performed. We thought it likely that a coil as a heat source and the heat flux conducts in the iron and radiates from the surface of iron. We made use of the measured room temperature as an input and chose the film heat transfer coefficient and thermal conductivity in the practical range. We show a calculated temperature of yoke surface with the temperatures of room and yoke surfaces in Fig. 2. The calculated line reproduces a characteristic of the fluctuation of the yoke surface. When unpractical parameters are used, it reproduces better. The poor reproduction might be on account of the limits of a one dimensional model.

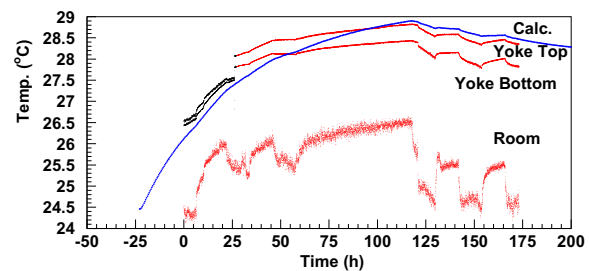


Fig. 2. The result of calculation.

For a period between 135 and 139 hours in Fig. 1, the resonance frequency and all temperatures became stable and the RMS of the frequency was  $2 \times 10^{-7}$  relatively. This implies that the magnetic field keeps its stability when the temperatures maintain their stability.

## References

- 1) ECHO ELECTRONICS CO., LTD., NMR EFM-15000R operating manual (2007).
- 2) Y. Yasuda *et al.* : RIKEN Accel. Prog. Rep. **41**, 141 (2007).

<sup>\*1</sup> Institute of Physics, University of Tsukuba

<sup>\*2</sup> ECHO ELECTRONICS CO., LTD.

# Network and Computing Environment for RIKEN Nishina Center

T. Ichihara, Y. Watanabe, and H. Baba

Our computing and networking team have been operating Linux/Unix NIS/NFS cluster systems<sup>1-2)</sup> at RIKEN Nishina Center.

Figure 1 shows the current configuration of the Linux/Unix servers at Nishina Center.

The host *RIBF* is used for the mail server and NFS server of the user home directory `/rarf/u/`. A 10 TB fiber-channel RAID with fiber-channel hard disk drive (FC-FC RAID) `/rarf/w/` has been connected to the *RIBFDATA01* server for data analysis. In addition, a 5.6 TB FC-FC RAID6 (`/rarf/d/`) has been newly added to *RIBFDATA01* to store raw data for the RIBF experiment starting in the fiscal year 2008. The *RIBF01* server is also newly installed and used together with the *RIBFDATA01*, for data analysis of the experiment at the RIBF. The RIBF Data Acquisition system (DAQ) has been developed and completed in the first phase.<sup>3)</sup>

Postfix is used for mail transport software and Dovecot is used for imap and pop services. These software packages enable secure and reliable mail delivery. The hosts *RIBFSMTP1* and *RIBFSMTP2* are mail front-end servers used for tagging spam mails and isolating virus-infected mails. Sophos Pure Message (PMX)<sup>4)</sup> was installed on those servers in March 2008 and has been working stably and correctly for those purposes.

The host *RIBF00* is used as an ssh login server from the outside and general-purpose computational server and a gateway to the RIBF intranet. Public-key authentication is used for ssh login to improve security.

The equipments of the Local Area Network (LAN) operated by the Advanced Center for Computing and Communication (ACCC) was replaced in January 2009. This made all Ethernet ports of the information wall sockets capable of the Gigabit Ethernet connection (10/100/1000BT).

Several wireless LAN access points (WLAP) in RIKEN Nishina Center have been added and switched to the new type WAPS-HP-A54G54<sup>5)</sup> which supports both 2.4 GHz 11g/11b and 5.2 GHz 11a protocols. Wireless application protocol (WAP) authentication is used to ensure the security instead of wired equivalent privacy (WEP) password authentication. In total, we have installed and operated 52 WLAP.<sup>6)</sup>

Eight temperature sensors were installed in the server rooms of the Nishina Bldg., RIBF Bldg. and in several experimental rooms of the RIBF Bldg. in September 2008. They are monitored via a web interface using the Cacti graphical tool developed by the CCJ<sup>7)</sup> team.

An anonymous ftp server, *FTP.RIKEN.JP*, is managed and operated at RIKEN Nishina Center. A 13

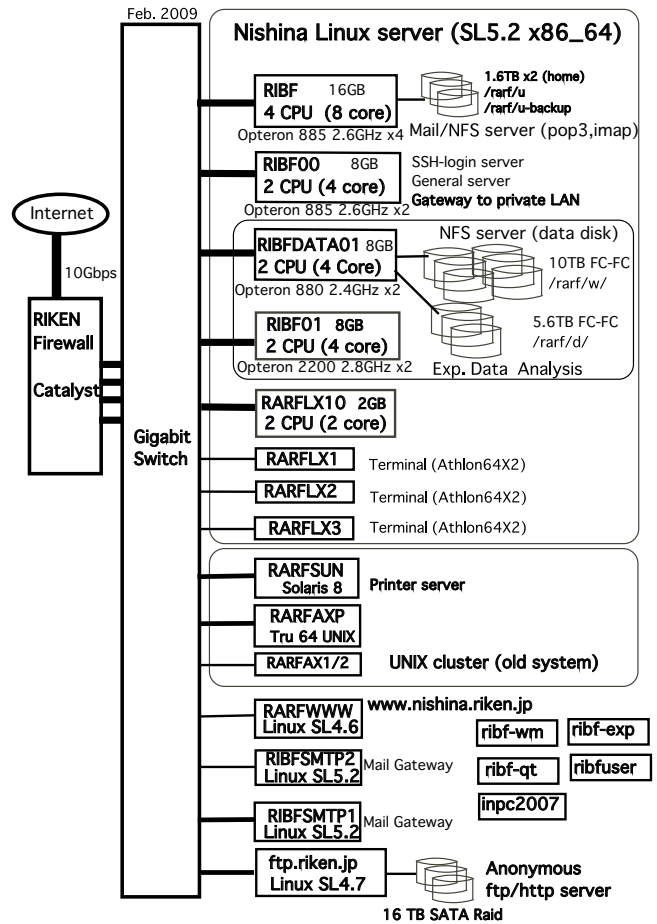


Fig. 1. Configuration of Linux/Unix servers.

TB SATA Raid system has been added to this server. Major Linux distributions are mirrored daily at the ftp server for research support.

Most of the users of Nishina Center have e-mail addresses of the following forms:

*username@ribf.riken.jp* or *username@riken.jp*.

The former represents an e-mail address of the mail server (*RIBF*) of RIKEN Nishina Center and the latter represents an e-mail address of the mail server (*POSTMAN*) of RIKEN ACCC.

## References

- 1) <http://ribf.riken.jp/>
- 2) T. Ichihara et al.: RIKEN Accel. Prog. Rep. 41, 154 (2008).
- 3) H. Baba et al.: In this report.
- 4) <http://www.sophos.com/products/enterprise/email/security-and-control/>
- 5) <http://buffalo.jp/products/catalog/item/w/waps-hp-am54g54/>
- 6) <http://ribf.riken.jp/comp/net/wireless.html>
- 7) S. Yokkaichi et al.: In this report.

## RIBF DAQ for Day-one Experiments

H. Baba, T. Ichihara, T. Ohnishi, S. Takeuchi, K. Yoshida, Y. Watanabe, S. Ota,\*<sup>1</sup> and S. Shimoura\*<sup>1</sup>

A RIBF data acquisition (DAQ) system<sup>1)</sup> has been developed to enable early RIBF experiments in the first several years. This system has the functions of network-distributed processing, on-line event building and analysis, hierarchical event building and parallel data readout from CAMAC and VME modules. Its event builder achieved a data processing capability of faster than 20MB/s<sup>2)</sup>.

Day-one experiments of RIBF-08, RIBF-28, RIBF-32, and RIBF-55 have recently been carried out with BigRIPS<sup>3)</sup> and ZeroDegree Spectrometer (ZDS) based on this DAQ system. The beam-line detectors<sup>3)</sup> installed at the focal planes of F1–F11 (Figure 1) were commonly used in these experiments, where the analog signals from a plastic scintillator and PPAC placed on the B2F experimental room were transported to the B3F measurement room via optical transceiver, and those from silicon (Si), germanium (Ge), and NaI(Tl) detectors and ion chamber (IC) were, on the other hand, converted to the digital values near the detectors. To accumulate digitized data, eleven front-end computers (FECs), which have the analog-to-digital converter modules, were installed at B2F and B3F. The allocations of the detector signals are listed in Table 1.

In addition to the eleven FECs, six servers were installed at B2F. Figure 2 shows the configuration of servers and FECs. *d02* is the master event builder for all FECs. Two local event builders *d01* and *ggdaq01*, installed for F11 Isomer Germanium, F8 NaI(Tl) detector array DALI2<sup>4)</sup>, respectively, allow us to acquire data independently of each other. As on-line analysis servers, *a02*, *a03* and *d03* were also installed.

The total number of signals of each event exceeds 1000, corresponding to the average data size  $\sim 1.6$  KB/event. The event rate depended on the beam intensity and the trigger condition. For example, with 1 kcps event rate, data transfer rate is 1.6 MB/s (5.8 GB/hour), which is five-times higher than those for typical RIPS experiments.

In spite of the higher data transfer rate, the dead time of the entire system is shorter than those of previously used DAQ systems<sup>5,6)</sup>. This is because of the following reason. The dead time of previous systems is linearly-proportional to the number of readout channels, which is  $\sim 2$  ms/event with this data transfer rate. In contrast to this, the dead time of RIBF DAQ depends only on the FEC having the longest dead time thanks to the scheme of the parallel-data readout and event builder. The list of the dead time for each FEC is shown in Table 2, where three dead times of *ccnet01*

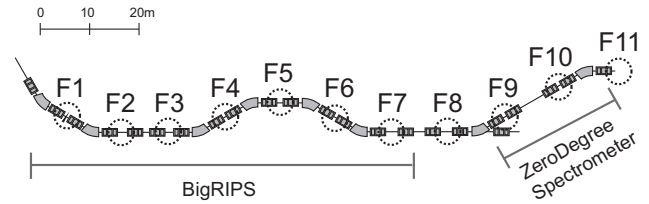


Fig. 1. The layout of the focal planes for BigRIPS and ZeroDegree Spectrometer.

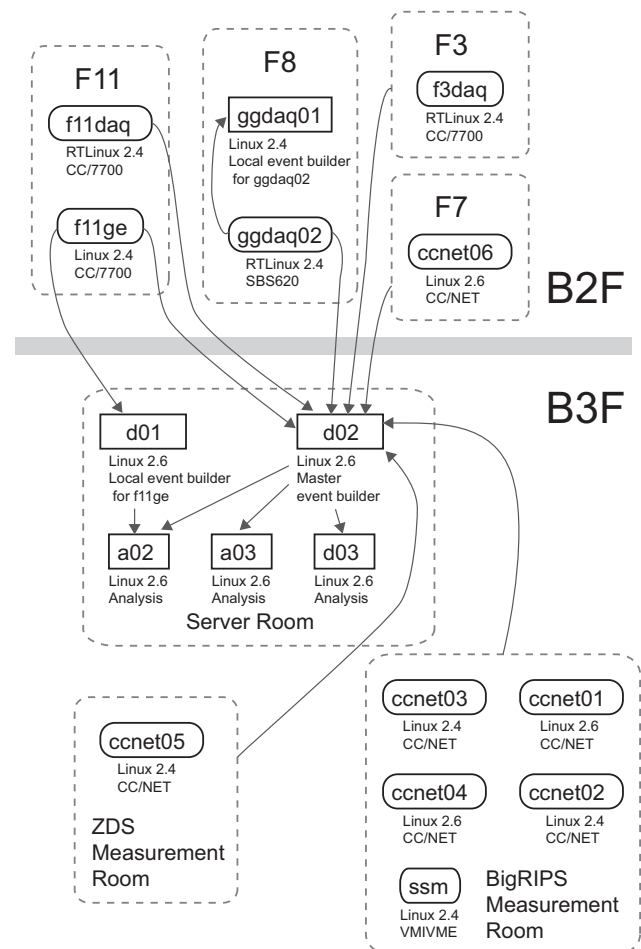


Fig. 2. The configuration of servers (rectangles) and FECs (ovals). Controllers of CC/NET and VMIVME are CPU-boards. CC/7700 and SBS620 are PCI-CAMAC and PCI-VME type controllers, respectively.

are shown separately. The detector configuration covered with *ccnet01* differs according to beam tuning and experiments. Their dead times for the whole DAQ system are 350 and 280  $\mu$ s/event, respectively. In these

\*<sup>1</sup> Center for Nuclear Study, University of Tokyo

Table 1. The allocations of the detector signals. *ccnet01-05* were installed on B3F measurement room. Other FECs were placed in B2F experimental room.

Detector	FEC
F1, F2, F3, F4, F6 Plastic and PPAC	⇒ <i>ccnet01</i>
F3 Si	⇒ <i>f3daq</i>
F5 Plastic and PPAC	⇒ <i>ccnet02</i>
F7 Plastic and PPAC	⇒ <i>ccnet03</i>
F7 Si, Ge and IC	⇒ <i>ccnet06</i>
F8 and F8' Plastic and PPAC	⇒ <i>ccnet04</i>
F8 NaI(Tl) detector array (DALI2)	⇒ <i>ggdaq02</i>
F9, F10, F11 Plastic and PPAC	⇒ <i>ccnet05</i>
F11 Si and IC	⇒ <i>f11daq</i>
F11 Ge	⇒ <i>f11ge</i>

Table 2. The dead time per 1 event for each FEC. Third configuration marked with a \* was prepared but not used. *ssm* was the front end for start/stop control and scaler. It did not affect the dead time of the system.

Name	Dead time	Remarks
<i>ccnet01(a)</i>	350 $\mu$ s	beam tuning (F1–F6)
<i>ccnet01(b)</i>	280 $\mu$ s	RIBF-08, 28, 32, 55 (F3–F6)
<i>ccnet01(c)</i>	130 $\mu$ s	RIBF-28, 32 (only F3)*
<i>ccnet02</i>	120 $\mu$ s	
<i>ccnet03</i>	130 $\mu$ s	
<i>ccnet04</i>	180 $\mu$ s	
<i>ccnet05</i>	230 $\mu$ s	
<i>ccnet06</i>	150 $\mu$ s	
<i>f3daq</i>	180 $\mu$ s	
<i>f11daq</i>	210 $\mu$ s	
<i>f11ge</i>	~200 $\mu$ s	depends on gamma-ray rate
<i>ggdaq02</i>	~200 $\mu$ s	depends on gamma-ray rate
<i>ssm</i>	—	start/stop control and scaler

cases, the bottleneck was the performance of *ccnet01*. The dead time of the system can be improved to as short as 230  $\mu$ s, which is limited by *ccnet05*, in the configuration of *ccnet01(c)* given in Table 2.

The dead time of each FEC depends on the number of readout channels, the conversion time of ADC, and the interrupt latency of the operating system. If the number of readout channels per FEC is small and the conversion times of all ADCs are short enough, it is possible to achieve a dead time of less than 100  $\mu$ s/event. The performances of CAMAC and VME controllers are important to reduce the dead time of FEC. Thus, a device driver for CC/NET has been newly developed. There are two hardware versions of CC/NET. The former version is running under Linux 2.4, whereas the latter is running under Linux 2.6. Their performances are summarized in Table 3. CC/NET has the functions of programmed input/output (PIO) block transfer mode and direct memory access (DMA) block transfer. The process time of these block transfer modes are determined

Table 3. The performance of the new CC/NET device driver. CC/NET has a block transfer mode only. The interrupt service routine (ISR) latency is the delay time coming from the period between the trigger signal reception and the actual start of the routine.

	Linux 2.4	Linux 2.6
Block PIO	3.6 $\mu$ s/ch + 2.4 $\mu$ s	2.6 $\mu$ s/ch + 1.7 $\mu$ s
Block DMA	1.2 $\mu$ s/ch + 9.9 $\mu$ s	1.2 $\mu$ s/ch + 6.7 $\mu$ s
ISR latency	21.7 $\mu$ s	30.0 $\mu$ s

by the number of readout channels and overhead time. The process time of CC/NET is much higher than other CAMAC controllers. The performances of other CAMAC and VME controllers such as TOYO CC/7700, Kinetic 3922, Wiener VMEMM, and SBS 620, have been reported in Ref. 7.

In summary the RIBF DAQ system has been developed and it functioned as designed in the day-one experiments. In spite of the large data transfer rate of 1.6 KB/event, the dead time was effectively suppressed to 280  $\mu$ s/event. The performance of the system is sufficiently high to cover most of RIBF experiments.

#### References

- 1) H. Baba et al.: RIKEN Accel. Prog. Rep. **41**, 155 (2008).
- 2) H. Baba et al.: IEEE Nuclear Science Symposium Conference Record 2008, 1384 (2008).
- 3) T. Kubo : Nucl. Inst. Meth. B **204**, 97 (2003).
- 4) S. Takeuchi et al.: RIKEN Accel. Prog. Rep. **36**, 148 (2003).
- 5) T. Ichihara et al.: IEEE Trans. Nucl. Sci. **36**, 1628 (1989).
- 6) H. Baba et al.: RIKEN Accel. Prog. Rep. **34**, 221 (2001).
- 7) H. Baba et al.: RIKEN Accel. Prog. Rep. **37**, 187 (2004).

## PHENIX silicon vertex tracker project

Y. Akiba, N. Cassano,<sup>\*1</sup> S. Chollet,<sup>\*2</sup> V. Cianciolo,<sup>\*3</sup> B. Deepack, A. Deshpande,<sup>\*1,\*4</sup> O. Drapier,<sup>\*2</sup> A. Drees,<sup>\*1</sup> H. En'yo, K. Fujiwara, F. Gastaldi,<sup>\*2</sup> R. Granier de Cassagnac,<sup>\*2</sup> Y. Haki,<sup>\*5</sup> K. Hashimoto,<sup>\*5</sup> R. Ichimiya, J. Kanaya, M. Kasai,<sup>\*5</sup> K. Kurita,<sup>\*5</sup> M. Kurosawa, A. Lebedev,<sup>\*6</sup> E. J. Mannel,<sup>\*7</sup> K. Nakano R. Nouicer<sup>\*8</sup> C. Ogilvie<sup>\*6</sup> H. Ohnishi, Y. Onuki, R. Pak,<sup>\*8</sup> C. Pancake,<sup>\*1</sup> P. Riedler,<sup>\*9</sup> E. Shafto,<sup>\*1</sup> M. Sekimoto,<sup>\*10</sup> W. Sondheim,<sup>\*11</sup> M. Togawa, A. Taketani, S. Watanabe,<sup>\*12</sup> and PHENIX VTX group

We are constructing a silicon vertex tracker (VTX) for the PHENIX experiment at RHIC. The primary purpose of the detector is to carry out precise measurements of heavy-quark production (charm and beauty) in  $A + A$ ,  $p(d) + A$ , and polarized  $p + p$  collisions. The main physics topics addressed by the VTX are as follows.

- Probing high-density partonic matter
  - Energy loss of heavy quarks (charm and bottom) in dense matter
  - Elliptic flow of heavy quarks in dense matter
  - Precise measurement of open heavy-quark production
  - Modification of jets by medium effects
- Measurements of gluon spin structure of nucleon
  - $\Delta G/G$  with heavy-quark production
  - $\Delta G/G$  with  $\gamma$ -jet measurement
- Nucleon structure in nuclei
  - Gluon shadowing over broad  $x$ -range

These are key measurements that are required for future RHIC programs, both for the study of QGP in heavy-ion collisions and for the measurement of the nucleon spin-structure functions.

The VTX detector consists of two inner layers of silicon pixel detectors<sup>1)</sup> and two outer layers of silicon strip detectors. The detector covers pseudo-rapidity  $|\eta| < 1.2$  and azimuth  $\Delta\phi \approx 2\pi$ . The project is funded by RIKEN, US DOE, and Ecole Polytechnique. The US side of the project was started in US FY07. The total budget is 4.7 M US dollars over four years (FY07-FY10).

The main points of progress this year are as follows.

- The first annual review of VTX was held at BNL in June 2008.

- Fabrication of the pixel buses<sup>2)</sup> is under way.
- Q/A of the pixel sensor module is on going.
- Development of a pixel detector assembly system is complete.<sup>3)</sup>
- A final prototype pixel ladder was fabricated with a production pixel bus and using the pixel assembly system.
- Q/A system for pixel ladders was developed.<sup>4)</sup>
- Performance of the pixel detector was tested at a beam test at FNAL.<sup>5)</sup>
- Development of the pixel read-out electronics is complete.<sup>7)</sup> Fabrication of the SPRIO read-out board is under way at Ecole Polytechnique. Fabrication of the pixel FEE boards has been started at Stony Brook.
- Q/A of the strip sensors is near completion.
- Signal to noise ratio of 10 has been achieved for the strip detector prototype based on a ROC3 read-out card in a bench test as well as in the FNAL beam test.<sup>6)</sup>
- Development of the read-out electronics for the strip system is underway. Prototypes of the RCC board, the LDTB board, the strip bus, and pre-production ROC will be produced soon.<sup>7)</sup>
- Fabrication of pixel staves (mechanical support+cooling) is on going at LBNL and will be completed soon.
- On the software side, update of simulation software of the VTX systems<sup>?)</sup> and physics simulation of VTX<sup>8)</sup> are on going.

### References

- 1) A. Taketani et al.: RIKEN Accel. Prog. Rep. **42**, 203 (2009).
- 2) K. Fujiwara et al.: RIKEN Accel. Prog. Rep. **42**, 205 (2009).
- 3) Y. Onuki et al.: RIKEN Accel. Prog. Rep. **42**, 209 (2009).
- 4) Y. Haki et al.: RIKEN Accel. Prog. Rep. **42**, 207 (2009).
- 5) M. Kasai et al.: RIKEN Accel. Prog. Rep. **42**, 212 (2009).
- 6) M. Togawa et al.: RIKEN Accel. Prog. Rep. **42**, 214 (2009).
- 7) K. Nakano et al.: RIKEN Accel. Prog. Rep. **42**, 211 (2009).
- 8) M. Kurosawa et al.: RIKEN Accel. Prog. Rep. **42**, 202 (2009).

<sup>\*1</sup> Stony Brook University, USA

<sup>\*2</sup> LLR, Ecole Polytechnique, CNRS-IN2P3, France

<sup>\*3</sup> Oak Ridge National Laboratory, USA

<sup>\*4</sup> RIKEN BNL Research Center, USA

<sup>\*5</sup> Rikkyo University, Japan

<sup>\*6</sup> Iowa State University, USA

<sup>\*7</sup> Columbia University, USA

<sup>\*8</sup> Brookhaven National Laboratory, USA

<sup>\*9</sup> European Organization for Nuclear Research, Switzerland

<sup>\*10</sup> High Energy Accelerator Research Organization, Japan

<sup>\*11</sup> Los Alamos National Laboratory, USA

<sup>\*12</sup> Tokyo Metropolitan College of Industrial Technology, Japan

# Spin physics capability with silicon vertex tracker for PHENIX

M. Kurosawa <sup>\*1</sup> for the PHENIX vertex collaborations

PHENIX is an experiment aiming to study the spin structure of nucleons and hot and dense matter at Brookhaven National Laboratory's Relativistic Heavy Ion Collider (RHIC). The PHENIX detector will be upgraded with the introduction of a silicon vertex tracker (VTX) to extend its physics capability<sup>1)</sup> in both the spin and heavy ion program. One of the roles of the VTX in the spin program is to determine x-dependence of  $\Delta G/G$  with  $\gamma$ -jet correlation over a wide x range. The  $\gamma$ -jet measurement is a good probe to determine x-dependence of  $\Delta G/G$  because the reaction is dominated by Compton  $qg \rightarrow \gamma q$  scattering. A detector with large acceptance and good position resolution is required in order to reconstruct the jet-axis in  $\gamma$ -jet measurement. The VTX has good position resolution ( $< 50 \mu\text{m}$ ) and covers a large acceptance in a pseudo-rapidity range  $\eta < 1.2$  and almost  $2\pi$  in azimuth.

In the future, integrated luminosity is expected to reach  $300 \text{ pb}^{-1}$  at  $\sqrt{s}=500 \text{ GeV}$ . This report describes the simulation results of a longitudinal double-spin asymmetry  $A_{LL}$  for  $\gamma$ -jet event with VTX detector at this expected luminosity.

The  $\gamma$ -jet production events were generated using the PYTHIA Monte Carlo program.<sup>2)</sup> Jet axis was reconstructed by using a simple cone algorithm.<sup>3)</sup> Direct photons were reconstructed with the finely segmented electromagnetic calorimeters in PHENIX detector.

With the current PHENIX detector, Bjorken x gluons ( $x_g$ ) are evaluated using only the transverse momentum of direct photon, as described by the following equation.

$$x_g = \frac{2P_T}{\sqrt{s}} \quad (1)$$

With the VTX detector,  $x_g$  can also be calculated by using jet axis information. The  $x_g$  is the smaller of  $x_1$  and  $x_2$  in the following equation.

$$x_1 = \frac{P_T}{\sqrt{s}}(e^{+\eta_{jet}} + e^{+\eta_\gamma}), \quad x_2 = \frac{P_T}{\sqrt{s}}(e^{-\eta_{jet}} + e^{-\eta_\gamma})$$

$$x_g = \min\{x_1, x_2\} \quad (2)$$

Figure 1 (a) and (b) show the scatter plot of true  $x_g$  from PYTHIA and reconstructed  $x_g$  with VTX and without VTX, respectively. Since the jet axis can not be measured without VTX, there are discrepancies between true  $x_g$  and reconstructed  $x_g$  within the region of low  $x(\gamma)$  in Fig. 1 (a). When measuring the jet axis with VTX, however, the reconstructed  $x_g$  is close to true  $x_g$  in Fig. 1 (b).

Figure 2 shows the simulated  $A_{LL}$  of gluon as a function of  $x_g$  assuming  $\Delta g = g$ ,  $\Delta g = -g$  and the GRSV

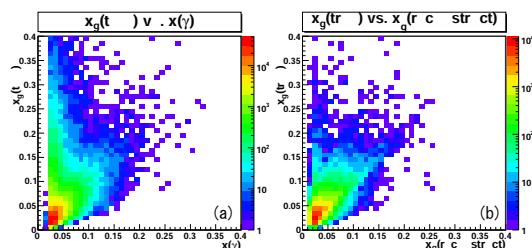


Fig. 1. Frame (a) and (b) show PYTHIA results comparing true  $x_g$  from PYTHIA and reconstructed  $x_g$  with VTX and without VTX, respectively.  $x_g(\text{true})$  is true  $x_g$ .  $x_g(\gamma)$  and  $x_g(\text{reconstruct})$  are obtained from Eq. 1 and Eq. 2, respectively.

standard model.<sup>4)</sup> The polarization of incident protons was assumed to be 70 %. Vertical error bars in the plot represent statistical and background subtraction errors. Horizontal error bars indicate reconstructed uncertainty of  $x_g$ .

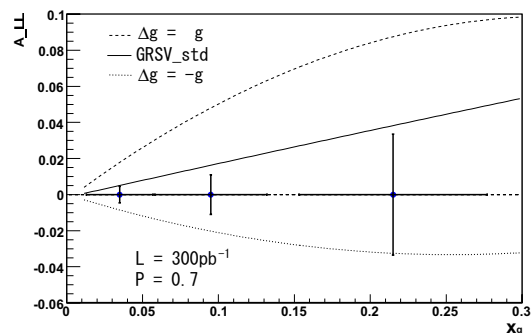


Fig. 2. Simulated  $A_{LL}$  of gluon as a function of  $x_g$ . Dashed, dot-dashed and solid lines correspond to  $A_{LL}$  assuming  $\Delta g = g$ ,  $\Delta g = -g$  and the GRSV standard model, respectively.

PYTHIA simulation of  $\gamma$ -jet production was performed under the conditions  $\sqrt{s} = 500 \text{ GeV}$  and  $L = 300 \text{ pb}^{-1}$ . Using VTX improved the x reconstruction especially in the lower  $x_g$  region. The  $A_{LL}$  was estimated as a function of  $x_g$ .

## References

- 1) Y. Akiba, et al.: Proposal for a Silicon Vertex Tracker (VTX) for the PHENIX Experiment (Brookhaven National Laboratory, Upton, NY, 2005).
- 2) T. Sjöstrand, S. Mrenna and P. Skands: *JHEP* 05, 026 (2006).
- 3) F. Abe et al.: *Phys. Rev.* D45, 2249 (1992).
- 4) M. Gluck, E. Reya, M. Stratmann and W. Vogelsang: *Phys. Rev.* D63 094005 (2001).

<sup>\*1</sup> Nishina RIKEN, RIKEN

## Silicon Pixel Detector for the PHENIX Vertex Tracker<sup>†</sup>

A. Taketani, Y. Akiba, N. Cassano,<sup>\*1</sup> S. Chollet,<sup>\*2</sup> B. Deepack, O. Drapier,<sup>\*2</sup> A. Dress,<sup>\*1</sup> H. En'yo, K. Fujiwara, F. Gastaldi,<sup>\*2</sup> R. Granier de Cassagnac,<sup>\*2</sup> Y. Haki,<sup>\*3</sup> K. Hasegawa,<sup>\*4</sup> H. Hasebe,<sup>\*4</sup> K. Hashimoto,<sup>\*3</sup> R. Ichimiya, J. Kanaya, M. Kasai,<sup>\*3</sup> M. Kawashima,<sup>\*3</sup> K. Kurita,<sup>\*3</sup> M. Kurosawa, E. J. Mannel,<sup>\*5</sup> K. Nakano, H. Ohnishi, Y. Onuki, R. Pak,<sup>\*6</sup> C. Pancake,<sup>\*1</sup> P. Riedler,<sup>\*7</sup> E. Shafto,<sup>\*1</sup> M. Sekimoto,<sup>\*8</sup> W. Sondheim,<sup>\*9</sup> M. Tabuki,<sup>\*10</sup> Y. Teshima,<sup>\*10</sup> M. Togawa, S. Watanabe<sup>\*11</sup>, and the PHENIX VTX group

The silicon Vertex tracker (VTX) will be installed in 2010 to PHENIX experiment at the Relativistic Heavy Ion Collider (RHIC) to enhance physics capability in both spin and heavy ion program. The VTX will be implemented very close to the collision points and cover  $\eta \leq 1.2$  and  $\phi \sim 2\pi$  by four layers of silicon sensors.<sup>1)</sup> It will be able to identify the heavy quark production from light quarks by measuring a displaced vertex due to the longer life time of charm and bottom quarks, whose  $c\tau$  ranges 100 to 400  $\mu\text{m}$ . The jet will be identified by measuring momentum of charged hadrons within its larger acceptance.

The VTX consists of pixel detectors on inner two layers and stripixel detectors on outer two layers, which are shown in Fig. 1. We, RIKEN group are in charge of 30 pixel ladders, which is the minimum replaceable module of the detector. This article describes the status of the pixel ladders.

The pixel ladder consists of four sensor hybrids, a support stave, and two readout bus. The pixel size of the sensor is  $50 \times 425 \mu\text{m}^2$ , which is shown in Fig 2 as small black box. One sensor has  $256 \times 32 \times 4$  and is connected to four ALICELHCB1 chips by the bump bonding technology. A signal from the sensor are converted to binary hit data through a preamplifier and a discriminator. These binary hit data as digital signal are transmitted to a Silicon Pixel Read-Out (SPIRO) board via an extender. The SPIRO board multiplex data from eight of ALUCLHCB1 chips, and transmits them to a Front End Module (FEM) thorough 1.6Gbps serial optical link.<sup>4)</sup> Up to the SPIRO will be implemented near collision points, so they must be compact, thin, and radiation hard. The FEM receives the hit information from multiple SPIRO boards and transmits them with format transformation to the PHENIX DAQ system.

The readout bus and the extender<sup>2)</sup> was made with polyimide-base flexible printed circuit. The bus that is 1.4cm wide, 25cm long, and 300  $\mu\text{m}$  thick, consists

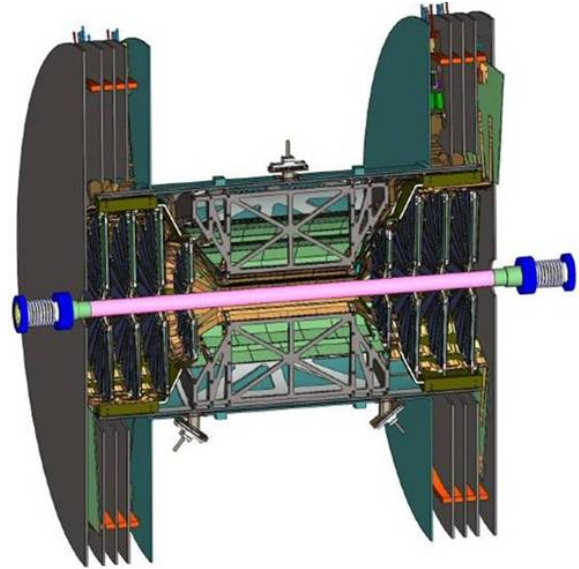


Fig. 1. PHENIX Vertex Tracker: Cut view on the Z- $\phi$  plane. The pink tube is a beam pipe. The two layers of pixel sensor and two layers of stripixel sensors are arranged in a concentric pattern.

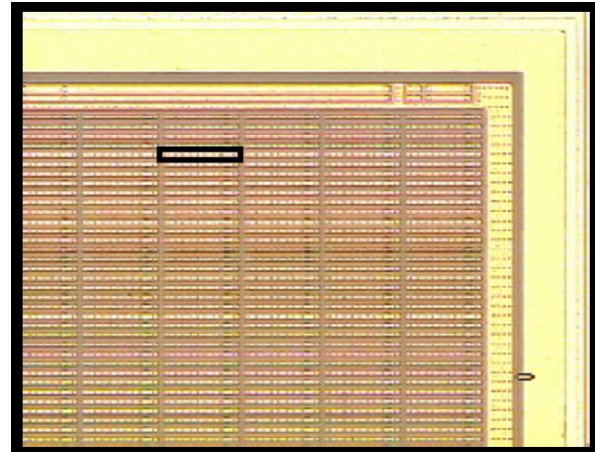


Fig. 2. Pixel sensor: One pixel is shown as black small box, whose size is  $50 \times 425 \mu\text{m}^2$ . The generated particles from the proton-proton collisions are boosted in the beam direction. The transverse momentum from beam axis has more physics information. It requires asymmetric spatial resolution to minimize the total number of readout channel.

<sup>\*1</sup> Stony Brook University, USA

<sup>\*2</sup> LLR, Ecole Polytechnique, CNRS-IN2P3, France

<sup>\*3</sup> Rikkyo University, Japan

<sup>\*4</sup> Tokyo Metropolitan College of Aeronautical Engineering, Japan

<sup>\*5</sup> Columbia University, USA

<sup>\*6</sup> Brookhaven National Laboratory

<sup>\*7</sup> European Organization for Nuclear Research, Switzerland

<sup>\*8</sup> High Energy Accelerator Research Organization, Japan

<sup>\*9</sup> Los Alamos National Laboratory, USA

<sup>\*10</sup> Tokyo Metropolitan College of Industrial Technology, Japan

of four signal layers, which include 186 signal lines, and two power layers. The bus and sensor hybrid are connected by bonding wires. The extender has two layers for signal lines, which are sandwiched by power layers and a thin shield layer. The connection between the bus and the extender are done by two fine pitch connectors. The cross talk on a trigger signal line was caused by the clock signal line, which was located on the back of the trigger line. These lines were isolated by the 50  $\mu\text{m}$  thick polyimide film. In addition to moving all lines from the backside of the trigger line, all backside lines were laid as cross-stitched. The extender with the new design was made and confirmed having no cross talks.

The four sensor-hybrids were lined up within 10 $\mu\text{m}$ , and then were glued to the support stave. Two readout buses were glued on them. After glue was cured, the sensor-hybrids and the buses were connected by the 25 $\mu\text{m}$  diameter aluminum bonding wires. Fig. 3 shows the full pixel ladder. Some of the wires have intermittent electrical current flow which is synchronized to the data taking triggers. The trigger rate is up to 20 KHz at the PHENIX DAQ environment. We observed wire vibration with resonance structure in the 1T magnetic field.<sup>3)</sup> The frequency of the resonance peak is around 5 KHz. So the wire may be broken in the real PHENIX environment. Therefore the wires are encapsulated by two types of glues. The low viscosity glue should encapsulate entire wires. The high viscosity glue is used for barriers preventing low viscosity one to flow out. The procedure for the encapsulation is established with the realistic pixel ladders.

The assembled pixel ladders have to be tested for functionality electrically with the extender, the SPIRO board and the FEM. The FEM was controlled by the PC with Microsoft Visual Basic environment. The original program was written for the hardware development. The functional test should be done automatically. We reorganized the original program.<sup>5)</sup> All configuration such as threshold of discriminating a signal from noises, pipeline delay length for the trigger tim-

ing, and so on are downloaded via JTAG control. The specified electric charge was injected into the preamplifier input and then hit data were retrieved. The threshold curve was obtained by scanning threshold of the discriminator. The threshold and noise characteristic of the each pixel channel were obtained. Also the sensor hybrid was irradiated by the  $\beta$ -ray from  $^{90}\text{Sr}$  source and then hit data were read out. The hit map was drawn and confirmed most of the pixels on the sensor were functional.

A telescope array of three pixel ladders were tested with 120 GeV/c proton beam at the Fermi National Accelerator Laboratory<sup>6)</sup> with stripixel ladders.<sup>7)</sup> The pixel ladders were connected to the FEM via SPIRO boards. The FEM sent data to the data acquisition system which emulated PHENIX data acquisition system. Event trigger was generated by the coincidence among two scintillation counters on upstream and downstream of the pixel telescope, and was required a hit on each three layers at minimum. The trigger rate was around 40Hz and 19K events were accumulated in the storage successfully.

In conclusion we have finished the development phase of the pixel ladders, confirmed their performance by using high energy proton beam. First mass production batch will be started in the early 2009.

#### References

- 1) Y.Akiba et al.:RIKEN Accel.Prog.Rep.**42**,xxx (2009)
- 2) K Fujiwara et al.:RIKEN Accel.Prog.Rep.**42**,xxx (2009)
- 3) Y.Onuki et al.:RIKEN Accel.Prog.Rep.**42**,xxx (2009)
- 4) E.J.Mannel et al.:RIKEN Accel.Prog.Rep.**42**,xxx (2009)
- 5) Y.Haki et al.:RIKEN Accel.Prog.Rep.**42**,xxx (2009)
- 6) M.Kasai et al.: RIKEN Accel.Prog.Rep.**42**,xxx (2009)
- 7) M. Togawa et al.:RIKEN Accel.Prog.Rep.**42**,xxx (2009)



Fig. 3. Assembled full pixel ladder: It consists from one carbon fiber stave, four sensor module, and two readout buses.

## Development and production status of a fine-pitch and low-material-budget readout bus for the PHENIX pixel detector

K. Fujiwara, A. Taketani, Y. Haki,<sup>\*1</sup> K. Hasegawa,<sup>\*2</sup> H. Hasebe,<sup>\*2</sup> S. Watanabe,<sup>\*2</sup> Y. Akiba, M. Kasai,<sup>\*1</sup> M. Kurosawa, Y. Onuki, H. En'yo, R. Ichimiya, K. Kurita, M. Sekimoto, M. Togawa, K. Nakano, J. Kanaya, D. Bista and PHENIX VTX group

The PHENIX detector system at the relativistic heavy ion collider (RHIC) at the Brookhaven National Laboratory will be upgraded by installing a four-layer silicon vertex tracker (VTX) by the summer of 2010.<sup>1)</sup> The VTX consists of two inner silicon pixel detectors and two outer silicon strip detectors. The VTX will enhance the physics capabilities to enable the investigation of new hot and dense nuclear matter in heavy-ion collisions and the structure of the proton spin in polarized proton-proton collisions at the RHIC by identifying heavy quarks via the measurement of the displaced vertex.<sup>1)</sup> Our group is responsible for developing and fabricating the Silicon Pixel ladder.

The signals from pixel sensors are processed using bump-bonded readout chips and converted to binary data. One readout chip has data of 32-bit  $\times$  256 depth. The binary data are transferred to a SPIRO board<sup>2)</sup> via fine-pitch and low-material-budget Pixel Bus. The signal on the SPIRO board is converted to a serial optical signal and transmitted to the PHENIX DAQ system. The Pixel Bus has been developed and is in the production phase. The status of the Pixel Bus is described in this report.

In principle the Silicon Pixel Detector has five constraints on the detector and the production sides:  $\sim 50 \mu\text{s}$  of detector readout time, avoidance of mechanical conflict with the neighboring detector sector, minimization of the multiple scattering and photon conversions, and ease of Pixel Bus production and handling on the production side. For the detector readout time, we have chosen to expand the parallel 32-bit data width in the original design of ALICE<sup>4)</sup> to 128-bits. First, we modified the digital PILOT chip, which has a  $2 \times 32$ -bit data bus width. The digital PILOT chip controls readout chips and multiplexes data from the chips.<sup>2)</sup> By using two digital PILOT chips for two sensor modules an approach, which is called a half-ladder,<sup>5)</sup> the Pixel Bus will have a 128-bit data bus width. Four readout chips ( $4 \times 32$ -bit data width) can be read in parallel on the half-ladder. However, this expansion requires a circuit with a layout four-times more dense than layout from the original ALICE design on the bus. Moreover, a bus width of 13.9 mm is required to avoid mechanical conflict with the neighborhood, a bus width of 13.9 mm is required. In order to minimize multiple scattering and photon conversion in the detector, the Pixel Bus has to be made as thin

as possible with available technology. Fourth, to facilitate production and handling of the bus, it should be made with Flexible Printed Circuit board (FPC) technology, in which the board is made from a conductor of copper and aluminum, and a polyimide insulator. Finally, two types of Pixel Bus are necessary for detector construction, i.e., the right side and left side bus. The difference between these buses is their signal and power connector positions. The circuit on the buses has exactly the same functionality. The right Pixel Bus has connectors on the right, the left Pixel Bus has them on the left. The development of such a fine-pitch FPC is a challenging but key component of the project.

We developed a new copper-aluminum-polyimide FPC that has a 128-bit data bus width. The Pixel Bus has the advantage of not only enabling a four-fold increase in the data bus width, but also reducing the material budget. For our bus, we are aiming for less than 0.28% of  $X/X_0$  in the radiation length. The bus has six layers that consist of copper, aluminum and polyimide films. It contains two signal layers, two via layers for manufacturing purposes, a power and a ground layer. Two fine pitch connectors on the bus are for connection with a Bus Extender connected to a SPIRO board. The connectors are for control and data signals. The bus contains 188 longitudinal lines in total. The size of the bus is  $13.9 \times 250 \text{ mm}^2$ . Hence, one signal and control line is  $30 \mu\text{m}$  in width and the interval between line and line is  $30 \mu\text{m}$  in minimum with  $3 \mu\text{m}$  thickness copper.<sup>7,8)</sup>

In the production phase, we have attempted to improve the bus production yield. We succeeded in increasing the yield from a very low level ( $< 10\%$ ) to  $\sim 80\%$  by two methods. The first method is a modification of the via process. A via is an interconnection between different layers, i.e., a through hole with copper plating. The second method is to reduce "Micro Short" between a line and a ground plane by using a new layout. The Micro Short means a bridge made by a residue of copper between a pattern and pattern.

In the via process, laser drilling is done by  $\sim 10$  times with a fine-adjusted laser output. Because in a via hole made by a laser by one time, a polyimide film is greatly melted by the generated heat and the reflection at the higher layer output. Consequently the via hole diameter is irregular in polyimide and copper regions. The irregular diameter region causes a defect in the Au plating process for the vias. The circular via hole is changed to an oval shape. This modification

<sup>\*1</sup> Department of Physics, Rikkyo University

<sup>\*2</sup> Tokyo Metropolitan College of Industrial Technology

allows the plating fluid to easily penetrate into the via hole.

In the new layout, the distance between a line and the ground layer increased by more than 100  $\mu\text{m}$  from the first design. With this layout, the residue of copper around the region is removed completely in the etching process, and the Micro Shorts on the bus disappear.

To evaluate performance, line resistance has been measured using an Agilent 4263B LCR meter and a micro-positioner with a probe needle. Figure 1 shows the measured resistance divided by the line length for the right and left side bus. The mean value is 0.174  $\Omega/\text{mm}$ ; the sigma is 0.017  $\Omega/\text{mm}$  for the right side bus; the mean value is 0.191  $\Omega/\text{mm}$ ; and the sigma is 0.011  $\Omega/\text{mm}$  for the left side bus. The calculated value is 0.13  $\Omega/\text{mm} \sim 0.17 \Omega/\text{mm}$ . Thus the fabrication quality is excellent.

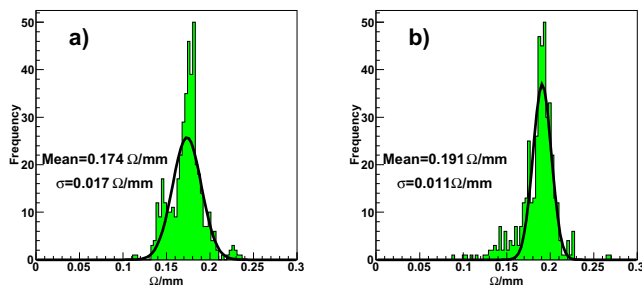


Fig. 1. Resistance distribution of the right and left Pixel Bus. a) is the right side bus, b) is the left side bus.

A half-ladder and a full-ladder were successfully fabricated using the buses.<sup>5)</sup> In 2008 we had access to a test beam to check the functionality at the Fermi National Laboratory. A telescope consisting of three layers of pixel ladders was used, and irradiation was done with a 120 GeV proton beam was irradiated.<sup>9)</sup>

A total 19542 events were collected and 7308 tracks were reconstructed.

In summary, we have successfully developed and produced a very fine pitch and low-material-budget read-out bus for the VTX upgrade. The production yield has been increased by improving the via process and line layout. This is shown by the measured resistance in the Pixel Bus. The pre-production ladder has been successfully fabricated, and performance was checked in the test beam at FNAL in 2008. Finally, the mass production of the Pixel Bus will start at the beginning of 2009.

## References

- 1) Y. Akiba: RIKEN Accel. Prog. Rep. **42**, 201 (2009).
- 2) R. Ichimiya: RIKEN Accel. Prog. Rep. **40**, 176 (2007).
- 3) R. Ichimiya: RIKEN Accel. Prog. Rep. **41**, 171 (2008).
- 4) A. Kluge et al.: Proc PIXEL 2002 Workshop (Monterey, CA) eConfC020909.
- 5) Y. Onuki: RIKEN Accel. Prog. Rep. **42**, 209, (2009).

- 6) K. Fujiwara et al.: Czech. J. Phys. **55** (12), (2005)
- 7) K. Fujiwara, Development of a silicon pixel tracker for an experiment of high energy heavy ion and polarized proton collisions, Doctoral dissertation, Niigata University, 2007.
- 8) K. Fujiwara, et al. "Fine Pitch and low Material Read-out Bus for the Silicon Pixel Detector in the PHENIX Vertex Tracker", IEEE Transactions on Nuclear Science, vol. 56, No.1, February 2009.
- 9) M. Kasai, et al.: RIKEN Accel. Prog. Rep. **42**, 212 (2009)

## Development of quality assurance software for the silicon pixel ladder in the PHENIX Vertex Tracker

Y. Haki<sup>\*1</sup>, K. Fujiwara, K. Hashimoto<sup>\*1</sup>, M. Kurosawa, A. Taketani, Y. Akiba, N. Apadula<sup>\*2</sup>, D. Bista, S. Chollet<sup>\*3</sup>, O. Drapier<sup>\*2</sup>, A. Dress<sup>\*3</sup>, R. Granier de Cassagnac<sup>\*3</sup>, R. Ichimiya, K. Kurita<sup>\*1</sup>, M. Kasai<sup>\*1</sup>, J. Kanaya, K. Nakano, Y. Onuki, C. Pancake<sup>\*2</sup>, M. Sekimoto<sup>\*4</sup>, E. Shafto<sup>\*2</sup>, M. Togawa,  
and the PHENIX VTX group

The PHENIX detector at RHIC-BNL will be upgraded with a silicon vertex tracker (VTX) surrounding a beam pipe with four cylindrical layers<sup>1</sup>. The inner two layers are silicon pixel detectors (SPDs) and the outer two layers are silicon strip detectors. As part of the plan upgrading the PHENIX VTX, the RIKEN group is developing the SPD. The SPD is made up of 30 ladders, each of which consists of a thermal plate, four sensor hybrids and two pixel buses<sup>2</sup>. A sensor hybrid is an assembly of a silicon pixel sensor and four read-out chips (ALICE1LHCb) which were bump-bonded with 20- $\mu\text{m}$ -diameter bumps to the sensor. The read-out chip has 8192 pixel cells arranged in 32 columns and 256 rows. The pixel size is 50  $\mu\text{m}$   $\times$  425  $\mu\text{m}$ . The pixel bus is a copper-aluminum-polyimide base flexible printed circuit board. A signal from the silicon pixel sensor is read out through the readout chip and the pixel bus. For the production of the ladder, a quality assurance (QA) test of the ladder is required to ensure that it can be implemented in the PHENIX. This report describes the development status of ladder QA software.

The set up of the ladder QA system is shown in Fig. 1. A half ladder is connected to a Silicon Pixel Interface Read Out module (SPIRO) board<sup>3</sup> with a flexible printed circuit board (the pixel bus and bus extender<sup>4</sup>). The SPIRO board supplies reference voltages to read out chips on the sensor hybrids, serializes data from two sensor hybrids on a half ladder and sends out the data to a front end module (FEM) via optical cables. The FEM sends out the data to a PC via USB1.1 data link.

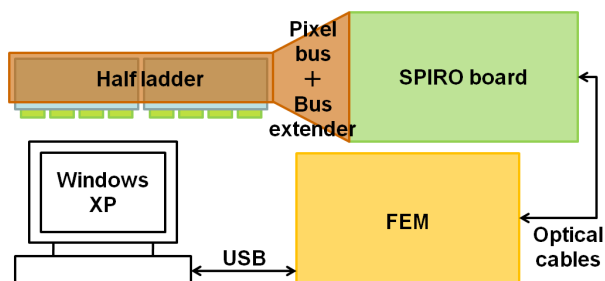


Fig. 1. Set up of ladder QA system.

The ladder QA software controls this equipment using a Visual Basic program and analyzes test results with the ROOT analysis tool<sup>5</sup> in the Microsoft Windows XP environment.

In the QA procedure, a chip is classified according to the threshold and the noise levels. As for the levels, we adopt mean levels calculated from the data for all of the pixels in the chip. The following method was applied to measure the threshold and noise levels for a pixel. A specific amount of charge was injected into the relevant preamplifier for a pixel 100 times. The efficiency of detecting the charge is the ratio of the event with a response. Nineteen different amounts of charge were examined in a similar way for measurement of the turning on curve as shown in Fig. 2, where the efficiency is plotted as a function of charge. The data was fitted with an error function (a line). The derivation of the function gives a gaussian distribution characterized by two parameters, mean and standard deviation. These two parameters correspond to the threshold and the noise levels for the pixel, respectively. The noise level is also used to identify a noisy pixel.

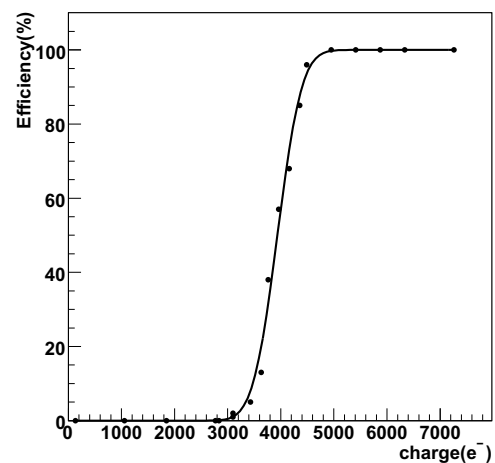


Fig. 2. A typical threshold curve obtained for a pixel. Horizontal axis is the charge value injected into the preamplifier input. Vertical axis is the efficiency for each injected charge.

In the present procedure, the data for pixels in the same row was taken simultaneously as shown in Fig. 3 (a). Therefore, the data for a whole chip has to be

<sup>\*1</sup> Department of Physics, Rikkyo University

<sup>\*2</sup> Department of Physics and Astronomy, Stony Brook University, USA

<sup>\*3</sup> LLR, Ecole Polytechnique, CNRS-IN2P3, France

<sup>\*4</sup> Institute of Particle and Nuclear Studies, KEK

transferred as many times as the number of rows. Based on the time we used to take the data for 320 pixels, it is estimated that this method takes  $\sim 17$  hours per one chip. Our goal is to finish the scan test for a chip in less than one hour. The reason it is time consuming is mainly due to the access time of 100 ms of USB1.1 link. Consequently, the threshold scan takes at least  $100 \text{ ms} \times 100 \text{ test pulses} \times 19 \text{ points} \times 256 \text{ rows} \sim 13 \text{ hours/chip}$ . However, if data is taken “column by column” instead of “row by row” as shown in Fig. 3 (b), time taking data is expected to be reduced by as much as a ratio of 256 to 32. Furthermore to reduce the amount of access, it is important that a data buffer is added in the FPGA on the FEM. For example, if 100 buffers are prepared, the data transmission via USB1.1 link will reduce one-hundredth. The data transmission time of 13 hours/chip is then reduced to 8 minutes. Through these improvements, we estimate that the data transmission time will be a few minutes/chip.

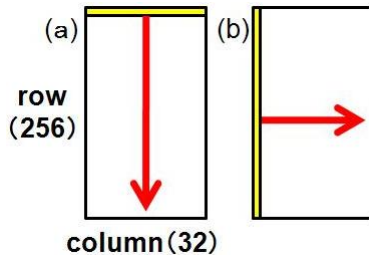


Fig. 3. The scanning directions are indicated by arrows. The number of rows and columns are 256 and 32, respectively. (a) The data for one row is taken one at a time. (b) The data for one column is taken one at a time.

In summary, the basic parts of the ladder QA software have been developed. The QA time will be improved, and as a result it will take a few hours in total for one half ladder. We expect that the QA software will be completed in advance of mass production of the half ladder.

#### References

- 1) Y. Akiba, et al.: RIKEN Accel. Prog. Rep. **42**, 201 (2009).
- 2) Y. Onuki, et al.: RIKEN Accel. Prog. Rep. **41**, 165 (2008).
- 3) R. Ichimiya, et al.: RIKEN Accel. Prog. Rep. **41**, 171 (2008).
- 4) K. Fujiwara, et al.: IEEE Trans. Nucl. Sci. **56**, 250 (2009).
- 5) <<http://root.cern.ch/>>.

## Development of an encapsulation procedure for the first PHENIX pixel ladder in the production version <sup>†</sup>

Y. Onuki, Y. Akiba, J. Asai, H. En'yo, K. Fujiwara, R. Ichimiya, M. Kasai,<sup>\*1</sup> K. Kurita,<sup>\*1</sup> M. Kawashima,<sup>\*1</sup> M. Kurosawa, K. Nakano, M. Sekimoto,<sup>\*2</sup> A. Taketani, M. Togawa, Y. Yamamoto<sup>\*3</sup> and PHENIX VTX Collaboration

The Relativistic Heavy Ion Collider (RHIC<sup>1</sup>) at Brookhaven National Laboratory (BNL) enables polarized  $p$ - $p$  collisions at  $\sqrt{s}$  up to 500 GeV and heavy nuclei at  $\sqrt{s_{NN}}$  up to 200 GeV. The Pioneering High Energy Nuclear Interaction eXperiment (PHENIX<sup>2</sup>) is one of the two main experiments at RHIC.

We have been constructing a silicon vertex tracker (VTX<sup>3</sup>) for the PHENIX which will enhance the physics capabilities of the PHENIX central arm detectors. The purpose is to measure the heavy flavor mesons which carry direct signals from Quark Gluon Plasma in heavy ion collisions and fundamental information on gluon polarization in polarized  $p$ - $p$  collisions.

The VTX consists of two types of silicon detectors: a pixel detector and a strip detector.<sup>4</sup> A pixel ladder is the basic unit of the pixel detectors. There are 10 and 20 pixel ladders in the first and second layer of the VTX, respectively. A pixel ladder is made of four sensor modules, two readout buses,<sup>5</sup> and a stave which provides mechanical support and cooling.

After assembly<sup>6</sup>, four sensor modules and two buses are connected electrically by wire-bonding. The 1848 Al wires, 25  $\mu\text{m}$  in diameter and roughly 4 mm long, are wedge-bonded at a 120  $\mu\text{m}$  pitch by a bonder machine, the K&S 8060.

We evaluated the effect of resonant vibration on bonding wires induced by Lorentz force<sup>7</sup> with mock circuits wire-bonded in 0.8 T magnetic field, corresponding to the actual environment where the VTX will be installed, using the magnet in the RIKEN Nishina Center. The ends of the bonding wire were connected to a GTL pulse generator and 50  $\Omega$  terminated register. A monochrome CCD video-camera equipped with a telephoto lens was located  $\sim 0.6\text{m}$  away from the circuit to prevent it from being influenced by magnetic fields. The vibration was observed as in Fig 1, where the horizontal thin lines are bonding wires which connect the ends of the left and the right electrodes. The vibration was recorded in a movie for 3 seconds in the AVI format with a capture board in the PC. GTL pulses were sent for 2 seconds (on signal) and nothing (off signal) was sent for 1 second.

On and off signal frames were integrated separately over the two-dimensional histograms of pixels for brightness. Next, each integrated two-dimensional histogram was sliced at the maximum resonant plane

of the bonding wire into a one-dimensional histogram. Each histogram, representing the cross-section of the resonant plane, was fitted with a Breit-Wigner function convoluted single Gaussian and a first-order polynomial function. In this fitting, the sigma of the convoluting Gaussian for the on signal histogram was fixed to the value of the sigma obtained by the fit for the off signal histogram. We defined the  $\text{FWHM}_{\text{on}}$  and  $\text{FWHM}_{\text{off}}$ , where the FWHM stands for the full width at half maximum of the fitted Breit-Wigner, obtained from the fitting the on signal and off signal histograms, respectively. The points in Fig 2 indicate the ratio of  $\text{FWHM}_{\text{on}}$  to  $\text{FWHM}_{\text{off}}$  at various frequencies, where the fitted empirical function  $f$  is defined by Eq (1) and described as a solid line with fitted parameters.

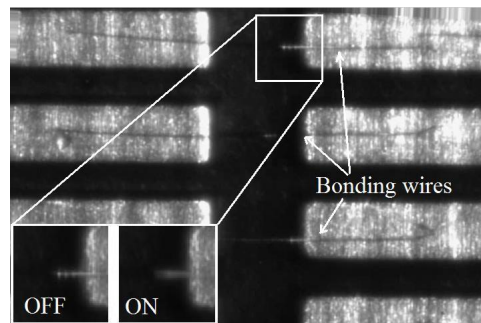


Fig. 1. Observed vibration of the bonding wire.

$$f = 1 + B.W. = 1 + \frac{(\gamma^2/4)H}{(\omega - \omega_0)^2 + (\gamma^2/4)} \quad (1)$$

The maximum vibration of the wire exists around 5.9 kHz which is close to the L1 trigger-rate in the PHENIX. Therefore, we concluded that the bonding wires should be encapsulated. An encapsulation method using two encapsulants, Sylgard 186 and 184, was developed using a dispensing robot. Dispensing just above the wires, the encapsulants can not stay around the wires. We solved this problem by forming a dam using Sylgard 186, which has a high viscosity, near the neck of the wires at the bus side. After curing, the ladder was tilted and filled with Sylgard 184 as shown in Fig.3.

We successfully assembled a first pixel ladder, shown in Fig 4, using the procedure in this report and the actual component in July, 2008. Table 1 shows a breakdown of the time required to assemble a ladder,

<sup>\*1</sup> Rikkyo University, Japan

<sup>\*2</sup> KEK, Japan

<sup>\*3</sup> University of Electro-Communications, Japan

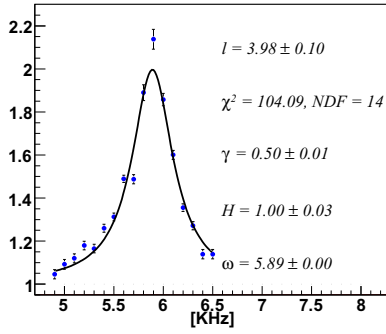


Fig. 2. Frequency dependence of the  $\text{FWHM}_{\text{on}}/\text{FWHM}_{\text{off}}$ , where  $l$  is the length of the bonding wire,  $\gamma$  is the FWHM,  $H$  is the height and  $\omega_0$  is the resonant frequency. The solid line indicates the fitted function  $f$ .

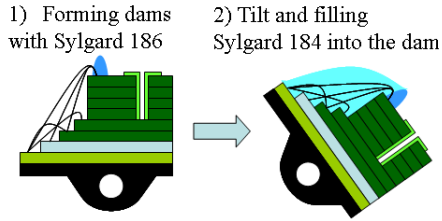


Fig. 3. Developed encapsulation method.



Fig. 4. Assembled pixel ladder in the container.

Procedure\Scheme	Past		Current	
	hour	day	hour	day
Sensor alignment	8×3	3	0.5	1
Q/A	→		0.5	
Gluing sensors	12×3		1	
Cure time	12×3		12	
Gluing buses	8×2	2	1	1
Cure time	12×2		12	
Q/A	→		0.5	
Wire-bonding	→	1	8	1
Forming dam	→	4	1×3	4
Cure time			12×3	
Filling encapsulant			1	
Cure time			12	
Total	161	10	87.5	7

Table 1. Assembly time of a ladder using current and past scheme.

comparing the current and the past assembly schemes. Past trial assemblies of half ladders were performed manually by skillful engineers. The time needed for wire-bonding is conservatively estimated at 8 hours, including tuning of the bonder machine for every ladder. The time for encapsulation is estimated at 52 hours which consists of forming the dam in three steps and the cure time. In total, 87.5 hours and 161 hours are required to assemble a ladder with the current and the past schemes, respectively. The number of the days to deliver a ladder is 7 days with the current scheme and 10 days with the past scheme. Most of the time is used to cure the adhesive and encapsulant in the ladder placed on the stave fixture. The waiting time can be reduced to use six stave fixtures and to pipeline the procedure in Table 1. Therefore, the total assembly time of 87.5 hours can be reduced to 27.5 hours, after subtracting the curing time of 60 hours. The number of days to deliver a ladder can be compressed to 2 days. The new pipeline assembly scheme can conservatively produce 40 ladders in four months.

We have confirmed that the current method produces ladders with higher precision and efficiency than the past assembly that required high cost and time.

#### References

- 1) H.Hahn et al.: Nucl. Instrum. Method Phys.A **499**, 245 (2003).
- 2) K.Adcox et al.: Nucl. Instrum. Methods Phys. Res. A **499**, 469 (2003)
- 3) PHENIX Collaboration, Proposal for a Silicon Vertex Tracker (VTX) for the PHENIX Experiment, BNL-72204R-2004.
- 4) J. Tojo et al.: IEEE Trans. Nucl. Sci. **51**, 2337 (2004); Z. Li et al.: Nucl. Instrum. Methods Phys. Res. A **541**, 21 (2005); Nucl. Instrum. Methods Phys. Res. A **535**, 404 (2004); Nucl. Instrum. Methods Phys. Res. A **518**, 300 (2004).
- 5) K. Fujiwara: Nuclear Science Symposium Conference Record, 2007. NSS apos;07.IEEE Volume 1, issue, Oct. 26 2007-Nov.3 2007 Page(s): 100-106; K. Fujiwara et al.: RIKEN Accel. Prog. Rep. **41**, 163 (2008).
- 6) Y. Onuki et al.: RIKEN Accel. Prog. Rep. **39**, 205 (2006); Y. Onuki et al.: RIKEN Accel. Prog. Rep. **40**, 171 (2007); Y. Onuki et al.: RIKEN Accel. Prog. Rep. **41**, 165 (2007).
- 7) G. Bolla et al.: Nucl. Instrum. Methods Phys. Res. A **518**, 277 (2005); A. R. Weidberg et al.: Nucl. Instrum. Methods Phys. Res. A **538**, 442(2005).

# Implementation of charge sharing and clustering in simulator of PHENIX silicon vertex tracker

K. Nakano, M. Togawa, M. Kurosawa and PHENIX VTX Group

The PHENIX experiment is being carried out at RHIC to investigate the property of hot and dense hadronic matter using heavy-ion collisions and the spin structure of the proton using polarized proton-proton collisions. The Silicon Vertex Tracker (VTX)<sup>1)</sup> is mandatory to improve the capabilities of the PHENIX experiment. It provides (1) a precise vertex measurement, which enables us to separate charm and bottom (heavy flavor) quarks, and (2) a charged-particle tracking with large acceptance, which enables us to measure charged particles to reconstruct the jet at mid-rapidity.

The VTX will be installed close to the collision point and cover a pseudorapidity region  $|\eta| < 1.2$  and a azimuthal angle  $\Delta\phi \approx 2\pi$ , where the acceptance of the PHENIX Central Arms is currently  $|\eta| < 0.35$  and  $\Delta\phi = 90^\circ \times 2^2$ ). The VTX consists of two pixel layers at inner and two stripixel layers at outer within 14 cm from the beams. One layer is segmented into 10 to 20 ladders, each of which covers a part of  $\phi$  angle. The sizes of pixels are  $50 \times 425 \mu\text{m}^2$  in pixel layer and  $80 \times 1000 \mu\text{m}^2$  in stripixel layer, where the longer side is parallel to the beam axis ( $z$ ). Stripixel channels are read out in two directions,  $x$ -strip (parallel to beam direction) and  $u$ -strip (tilted by  $\arctan(80/1000) = 4.6^\circ$ ), and all channels in each direction are summed up into one readout.

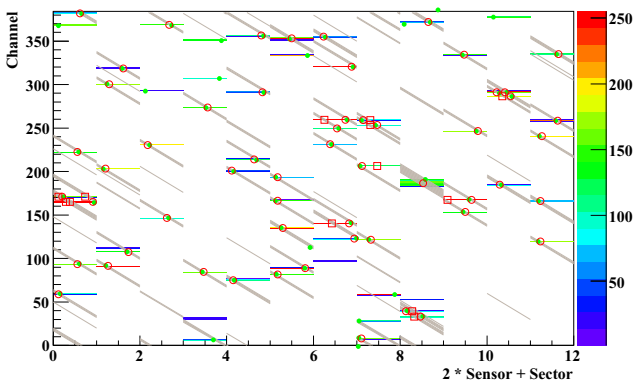


Fig. 1. An event display with a simulated event of most-central Au+Au collision. Only one stripixel ladder in the outer layer is shown ( $x$ -axis: 36 cm parallel to beam direction,  $y$ -axis: 3.43 cm). The **green filled circles** represent particle hit position; the **horizontal and tilted lines** represent  $x$  and  $u$  stripixels with above threshold energy respectively; the **red open circles and squares** show reconstructed hit position that does and does not have a corresponding particle hit, respectively.

In parallel to the detector construction, simulation studies based on the GEANT detector simulator are being carried out. It is indispensable to evaluate a realistic performance expected under the current detector configuration, such as position resolution and S/N. We implemented a realistic charge-sharing and clustering algorithms for it.

Charges deposited by a particle can be shared between neighboring strips particularly when the particle is incident non-vertically. The charge-sharing algorithm divides charges by the fraction of the path length in each strip. The clustering algorithm will deal with real data in the future as well as simulated data, and so far the clustering in stripixel layer has been implemented. Neighboring strips that have an ADC value above a threshold are gathered into a group. The position of a group is defined as the ADC-weighted positions of all strips in the group;  $x_{group} = \sum_i (ADC_i \cdot x_i) / \sum_i ADC_i$ . The same grouping is independently done with  $u$ -strips, and all crossing points of  $x$ -groups and  $u$ -groups are regarded as reconstructed hits. Figure 1 shows an example of the result of clustering, and Fig. 2 shows the position resolution, i.e. the difference between true and reconstructed hit positions. It is better than  $width/\sqrt{12}$  as expected when charges are shared with more than one strip.

The charge sharing and clustering that we implemented worked properly. Hereafter the efficiency of the clustering will be studied, which is not unity as it is observed that some particle hits in Fig. 1 do not have a corresponding reconstructed hit, and are optimized by adjusting the ADC threshold.

## References

- 1) M. Baker *et al.*, "Proposal for a Silicon Vertex Tracker for the PHENIX Experiment".
- 2) K. Adcox *et al.*, "PHENIX detector overview," Nucl. Instrum. Meth. A **499**, 469 (2003).

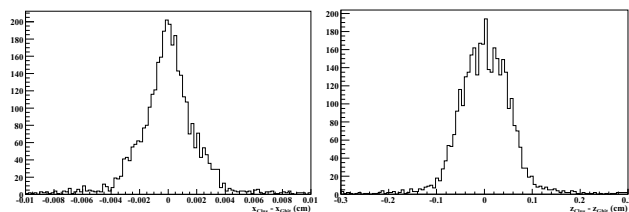


Fig. 2. Position resolution estimated with simulated events of most-central Au+Au collision, i.e. the difference between true and reconstructed hit positions. The **left** and **right** plots are of  $x$  and  $z$  directions respectively.

## Beam test of the PHENIX silicon pixel detector for 120GeV proton

M. Kasai,<sup>\*1</sup> K. Fujiwara, M. Kurosawa, A. Taketani, K. Kurita,<sup>\*1</sup> N. Apadula,<sup>\*2</sup> C. Pancake,<sup>\*2</sup> E. Mannel,<sup>\*3</sup> M. Togawa, A. Drees,<sup>\*2</sup> E. Shafto,<sup>\*2</sup> F. Gastaldi,<sup>\*5</sup> H. En'yo, K. Nakano, K. Hashimoto,<sup>\*1</sup> O. Drapier,<sup>\*5</sup> M. Sekimoto,<sup>\*4</sup> S. Chollet,<sup>\*5</sup> Y. Akiba, Y. Onuki, Y. Haki,<sup>\*1</sup> R. Ichimiya, W. Sondheim,<sup>\*6</sup> and PHENIX VTX group.

A Silicon Vertex Tracker (VTX) will be installed for PHENIX experiment at RHIC in 2010. The VTX will enhance the physics capabilities of the PHENIX central arm spectrometers by providing precision measurements of heavy-quark (charm and beauty) production in A+A, p(d)+A and polarized p+p collisions.

The VTX consists of pixel detectors at inner 2 layers (10 ladders [1,310,720 read-out channels] and 20 ladders [2,621,440 read-out channels]) and strip detectors at outer 2 layers (377,856 read-out channels) which cover pseudo-rapidity of  $|\eta| < 1.2$ , azimuth of  $\phi \sim 2\pi$ . Rikkyo University and RIKEN are responsible for the pixel ladders.

A pixel ladder consists of a stave which supports whole ladder mechanically and four pixel sensor modules<sup>3)</sup>, two read-out buses<sup>2)</sup> as shown in Figure 1. The stave including cooling structure is made from carbon fiber reinforced plastic. The sensor module<sup>3)</sup> is made from a pixel sensor, with pixel size of  $50\mu\text{m}$  in the  $z$  (row) direction and  $450\mu\text{m}$  in the  $\phi$  (column) direction, and four read-out chips connected by the bump bonding technique. The read-out bus is a copper-aluminum-polyimide base flexible printed circuit board. We established an assembly procedure for a pixel ladder and will start mass production in January 2009.<sup>1)</sup> We confirmed the performance of the pixel ladder by using high energy proton beam. In this report, we describe the tracking results of beam test with the pre-production pixel ladders.

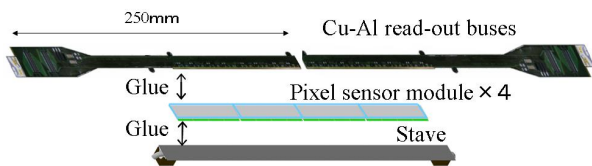


Fig. 1. Structure of a pixel full ladder

In August 2008, a beam test was carried out at Fermi National Accelerator Laboratory in order to check the data taking system (DAQ) and performance of prototype pixel detector. At the meson test beam area, 120GeV proton beam was used. The beam was de-

livered per 4 seconds. A spill had maximum  $\sim 2 \times 10^4$  counts.

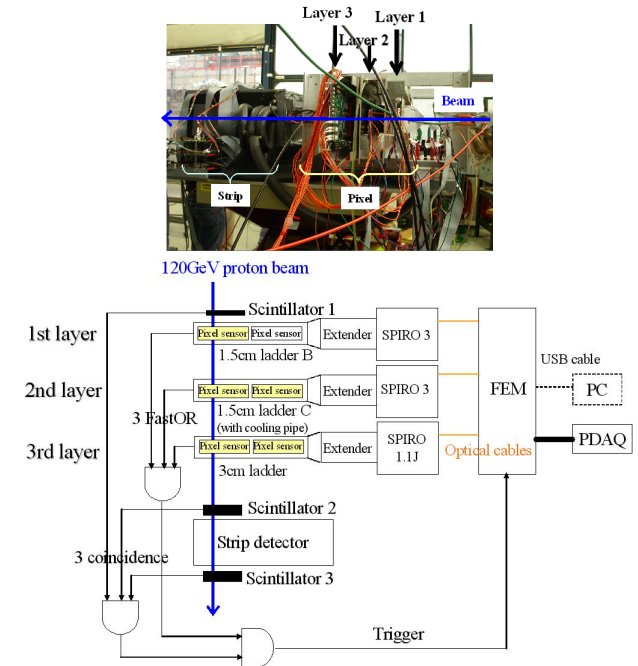


Fig. 2. Setup of beam test. The vertical distance between 1st layer and 2nd layer, 1st layer and 3rd layer were 46.5mm and 86.5mm, respectively.

The setup of beam test is shown in Figure 2. A telescope configuration of three pixel ladders was used. Each pixel ladder was connected to a Silicon Pixel Interface Read Out (SPIRO) board<sup>4)</sup>. Three SPIRO boards were fed to a Front End Module (FEM). Three scintillation counters were used as an event trigger and determination of the beam timing. The SPIRO board controls read-out chips and collects data and sends them to the FEM via optical cables. The FEM is a translator between detector specific electronics and PHENIX standard data acquisition modules that sends command signals to the SPIRO board and packs and transmits received data. The FEM has a USB interface for downloading the internal configuration from a local PC. Each readout chip has an all-hits-ORed output (FastOR), which will be fired even a single hit in the chip. The trigger is made of a coincidence of FastOR on the three layer and triple coincidence scintillation counter trigger. This system has been operated successfully.

The configuration of the telescope was changed third

\*1 Department of Physics, Rikkyo University

\*2 Stony Brook University, USA

\*3 Nevis Labs Columbia University

\*4 KEK

\*5 Ecole Polytechnique

\*6 LANL

time, A, B and C. The difference of the configuration was the position of 2nd layer along column direction.

Geometry	Trigger Rate	Number of Event	3 Hits
A	34	$8.9 \times 10^3$	$3.3 \times 10^3$
B	38	$6.0 \times 10^3$	$1.4 \times 10^3$
C	36	$4.6 \times 10^3$	$2.6 \times 10^3$

Table 1. Run List

DAQ system was able to set several values and take data without out of order. However, trigger rate was low and FastOR trigger has little problem. So Table 1 shows events of "3 Hits" were few, compared with "Number of Event". The "3 Hits" means a number of event which has hits on each three layer.

The track was reconstructed with hit information of each layer by using least-square method after the position alignment in offline analysis. Total of events with hits in three layers was  $7.3 \times 10^3$  events. A method of the track reconstructed was described in the following.

- (1) Mask noisy pixels. Noisy pixel defined that a pixel had more than 15 counts in beam profile of every chip.
- (2) Select event which has hit on each three layer. Every one event, draw lines by the least-squares fit methods with combination of all hits. When  $\chi^2$  is at a minimum, the hit positions become true positions in the event.
- (3) Get alignment parameters by offline analysis. Before beam test, three layers were aligned manually with a precision on the order of 1mm. A much more precise alignment was performed.
- (4) Iterate (1)~(3) until alignment parameters converge.
- (5) Obtain residual distribution after applying cut of beam angle. The data within the region of  $\sigma = \pm 2\text{mrad}$  ( $\sim \pm 0.12^\circ$ ) in beam angles distribution were used for residual distribution (Figure 3).

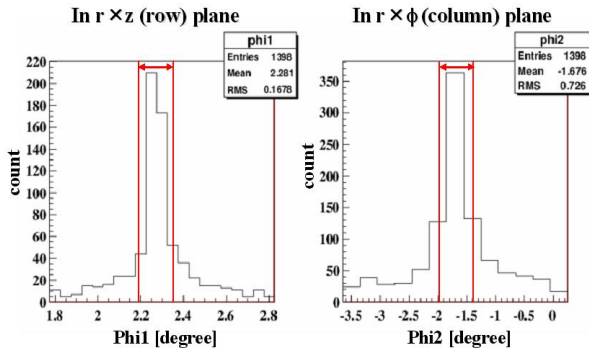


Fig. 3. Projected angular distribution of beam on column-beam (left) and row-beam plane (right). The region surrounded with lines is accepted region.

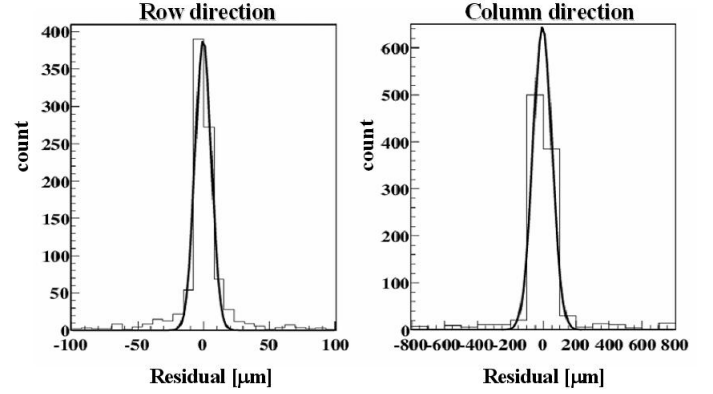


Fig. 4. Residual distributions in row and column directions on 1st layer.

These procedure was performed in every geometry. Finally, three residual distributions were sum up in each layer. The residual distribution in column and row direction on 1st layer are shown in Figure 4. The standard deviations of these residual distributions were calculated to be  $6 \pm 2 \mu\text{m}$  and  $58 \pm 11 \mu\text{m}$  in the row and column directions, respectively. The position resolution of sensor modules is determined mainly by the two factors. One is the intrinsic position resolution and the other is the effect of multiple scattering in the ladder components. The multiple scattering angle is given by the below equation<sup>5)</sup>.

$$\theta_0 = \frac{13.6 \text{ MeV}}{\beta c p} z \sqrt{\frac{X}{X_0}} \left[ 1 + 0.038 \ln\left(\frac{X}{X_0}\right) \right] \quad (1)$$

Here,  $p$ ,  $\beta c$ , and  $z$  are the momentum, velocity, and charge number of the incident particle, and  $X/X_0$  is the thickness of the scattering medium in radiation lengths.

A multiple scattering angle on 1st layer was estimated to be  $1.3 \mu\text{m}$ . The intrinsic resolutions in row and column directions were calculated to be  $14 \pm 6 \mu\text{m}$  and  $152 \pm 30 \mu\text{m}$ , respectively. The intrinsic resolution depends on pixel size (row :  $50 \mu\text{m}$  and column :  $425 \mu\text{m}$ ). We expect the resolution of the pixel sensor module are  $50/\sqrt{12} \approx 14 \mu\text{m}$  and  $425/\sqrt{12} \approx 123 \mu\text{m}$  in the row and column directions, respectively.

One thousand clear tracks were measured at beam test. The results of beam test at FNAL show good performance of the pixel detector for PHENIX experiment.

## References

- 1) Y. Onuki: Internal Journal of Modern Physics E Vol.16, Nos.7 and 8 (2007)
- 2) K. Fujiwara: RIKEN Accel. Prog. Rep. 41, 169 (2007)
- 3) M. Kurosawa: RIKEN Accel. Prog. Rep. 41, 173 (2007)
- 4) R. Ichimiya: RIKEN Accel. Prog. Rep. 41, 171 (2007)
- 5) Particle Data Group: Phys. Lett. B592, 245 (2004)

## Performance test of silicon stripixel detector for PHENIX vertex tracker

M. Togawa, Y. Akiba, V. Cianciolo,<sup>\*1</sup> A. Deshpande,<sup>\*2</sup> A. Dion,<sup>\*3</sup> A. Enokizono,<sup>\*1</sup> K. Fujiwara, M. Kasai,<sup>\*4</sup>  
K. Kurita,<sup>\*4</sup> M. Kurosawa,<sup>\*4</sup> E. Mannel,<sup>\*5</sup> R. Nouicer,<sup>\*6</sup> H. Pei,<sup>\*3</sup> A. Taketani and PHENIX VTX group

A silicon vertex tracker (VTX) for the PHENIX experiment<sup>1)</sup> at Brookhaven National Laboratory (BNL) has been developed to enhance physics capabilities<sup>2)</sup>. In this article, we report a recent performance test of a stripixel detector for the outer two layers of the VTX.

The stripixel sensor has two-dimensional position sensitivity only with single-sided processing. It consists of  $80 \times 1000 \mu\text{m}^2$  pixel structures with two interleaved p+ electrodes, and two-dimensional position sensitivity can be achieved by charge sharing between them with a projective readout by strips. One metal strip connects the pixels in a straight line (x read out), while a second strip connects at a 4.6 degree angle (u read out). The stripixel detector has been designed in collaboration with the BNL Instrumental Division<sup>3)</sup> and performance of the prototype detector was studied in static electrical tests, beam/source tests and radiation dose tests.<sup>4)</sup> The final design of stripixel was determined based on the results. Thickness is  $625 \mu\text{m}$ , for example.

Figure 1 shows the stripixel detector mounted on a prototype readout card (ROC). Signals from the stripixel detector are read out via SVX4 chips<sup>5)</sup> which are also mounted on the ROC. The ROC is connected to a prototype ROC control card (RCC) and a front-end module (FEM) compatible with the PHENIX DAQ system.

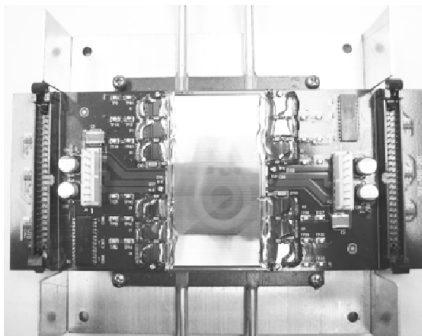


Fig. 1. Photograph of stripixel detector mounted on the ROC.

We tested performance of the whole read out system incorporating the stripixel detector with a beta source

and 120 GeV proton beam at Fermi National Accelerator Laboratory (FNAL). Important performance characteristics are,

- Signal to noise ratio (S/N)
- Detection efficiency
- Position resolution

In a typical silicon strip detector, detection efficiency is almost 100 %, and position resolution is dominated by the strip pitch. These two characteristics become worse with low S/N.

### Performance test with beta source

A beta source test was performed at the chemistry laboratory at BNL. We placed a beta source as close as possible to the stripixel detector, and data was collected by a scintillator trigger making with the detection of penetrated electron. The detector was placed in a dark box with flowing dry nitrogen and zero degree water running in cooling pipes. High voltage was supplied at 200 V.

Figure 2 (top left) shows ADC vs. channels with a beta source. Pedestal subtraction is applied event-by-event, and the pedestal value in each channel is determined by the average of the previous and next four channels. Then the corrected ADC is obtained, as shown in Fig. 2 (top right). We plan to implement this method in the FPGA and conduct zero suppression data collection. A clustering algorithm is used as follows to find a minimum ionization particle (MIP) peak. 1) If the ADC value is above two sigma of the pedestal width, the channel is tagged as hit. 2) If a hit continues to the next channel, they are combined so that the clustered ADC is sum and the clustered channel is calculated by centroid method. 3) A clustered ADC is required to be above 40 to decrease a fake cluster formed by noise. After clustering, we can see a clear MIP peak as shown in Fig. 2 (bottom). The S/N is defined as the most probable value of the MIP peak divided by the average pedestal width. We obtained S/N ratios of 9.3 and 9.7 for x and u, respectively.

### Performance test with 120 GeV proton beam

The proton beam was supplied at the Meson Test Beam Facility (MTBF) at FNAL as T984 experiment. A schematic view of the experimental setup is shown in Fig. 3. Three stripixel detectors were placed at 50 mm intervals as a hodoscope in the dark box and supplied

<sup>\*1</sup> Oak Ridge National Laboratory, USA

<sup>\*2</sup> Department of Physics and Astronomy, State University of New York-Stony Brook, USA

<sup>\*3</sup> Iowa State University, USA

<sup>\*4</sup> Department of Physics, Rikkyo University

<sup>\*5</sup> Columbia University, Nevis Laboratories, USA

<sup>\*6</sup> Brookhaven National Laboratory, USA

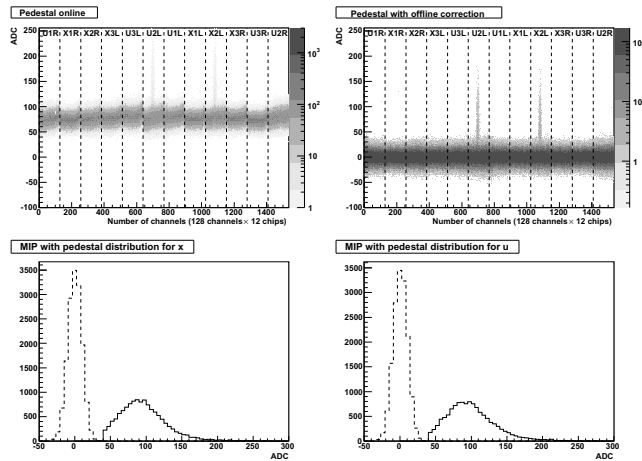


Fig. 2. Results of beta source test. Top) ADC vs. channel (left) and results after correction of pedestal subtraction (right). Bottom) Clustered ADC (solid line) and average pedestal (dotted line) distributions for x (left) and u (right).

with 200 V high voltage via RCC boards. The event trigger was coincidence of three scintillators placed upstream and downstream of the box and the “BEAM ON” signal coming from the accelerator. For analysis, we used the same algorithm as the beta source test and obtained results similar to Fig. 2. S/N ratios of 10.3 and 10.1 were obtained for x and u, respectively. The reason why S/N was higher in the beam test is that we tuned integration timing in the SVX4. We concluded they are consistent.

Figure 4 shows an event structure for one event with linear fit tracks. We can clearly see a penetrating event in raw ADC level and successfully reconstruct proton tracks with this S/N. With this tracking information, the residual distribution, correlated to the position resolution, can be obtained as the difference between the hit position and the expected position which are decided by the track with other two detectors. The residual distribution for the middle sensor in x read out is shown in Fig. 5 (left) and obtained as  $0.42 \times 80(\mu\text{m}) = 33.6(\mu\text{m})$  from the RMS value. The efficiency was determined by looking at the energy deposit in the detector at the expected channel which was also decided by other two detectors. The sum of ADC distribution in the expected channel  $\pm 2$  is shown in Fig. 5 (right). We extracted the efficiency as  $99.5 \pm 0.2\%$  with the hit definition of ADC above 40. Consistent results were obtained for u read out.

In summary, the stripixel detector integrating whole read out system satisfies the required performance with a S/N of about 10. Currently we are preparing for mass production with final feedback aiming for installation in 2010.

#### References

- 1) K. Adocox et al.: Nucl. Inst. Meth. **A499**, 469 (2003).
- 2) Y. Akiba et al.: RIKEN Accel. Prog. Rep. **42**, 201,

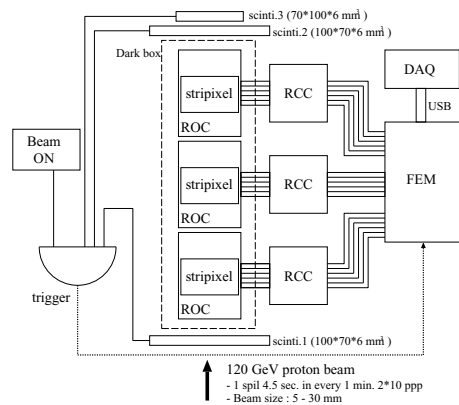


Fig. 3. Schematic view of the T984 setup.

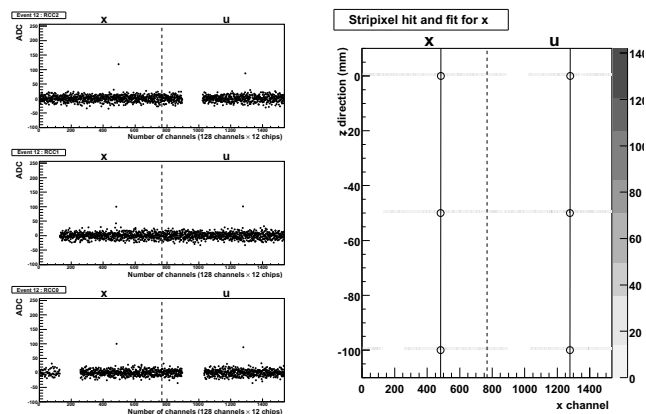


Fig. 4. Event structure for 120 GeV proton beam. Left) ADC vs. channel for all detectors. Right) Position in the beam direction vs. channel. Clustered channel positions are plotted as circle points and tracks by linear fit are shown as straight lines.

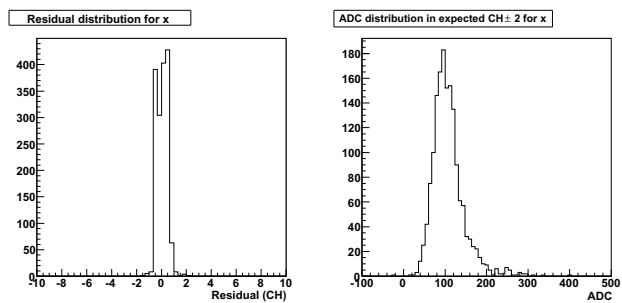


Fig. 5. Left) Residual distribution for the middle sensor. Right) Sum of ADC distribution at the expected channels by tracking. Both are for x.

- (2009); A. Taketani et al.: RIKEN Accel. Prog. Rep. **42**, 203, (2009).
- 3) Z. Li: Nucl. Inst. Meth. **A518**, 300 and 738 (2004).
- 4) J. Tojo et al.: RIKEN Accel. Prog. Rep. **36**, 252, (2003); RIKEN Accel. Prog. Rep. **37**, 251, (2004); IEEE Trans. Nucl. Sci. **51**, 2337 (2004); J. Asai et al.: RIKEN Accel. Prog. Rep. **38**, 235, (2005); RIKEN Accel. Prog. Rep. **39**, 203, (2006).
- 5) <http://www-cdf.lbl.gov/users/mweber/svx4>

# High Momentum Trigger Electronics Upgrade of PHENIX Muon Arms for Sea Quark Polarization Measurement at RHIC

I. Nakagawa, T. Mibe,<sup>\*1</sup> N. Saito,<sup>\*1</sup> S. Adachi,<sup>\*2</sup> H. Asano,<sup>\*2</sup> S. Ebesu,<sup>\*2</sup> K. Imai,<sup>\*2</sup> K. Karatsu,<sup>\*2</sup> T. Murakami,<sup>\*2</sup> K. Nakamura,<sup>\*2</sup> R. Nakanishi,<sup>\*2</sup> Y. Sada,<sup>\*2</sup> K. Shoji,<sup>\*2</sup> K. Tanida,<sup>\*2</sup> Y. Fukao, A. Taketani, T. Akiyama,<sup>\*3</sup> Y. Haki,<sup>\*3</sup> M. Hata,<sup>\*3</sup> Y. Ikeda,<sup>\*3</sup> K. Kurita,<sup>\*3</sup> J. Murata,<sup>\*3</sup> K. Ninomiya,<sup>\*3</sup> M. Nitta,<sup>\*3</sup> and E. Seitaibashi,<sup>\*3</sup>

[nucleon spin, W-boson, polarized parton distribution, Electronics, trigger]

Parity-violating production of the W boson with longitudinally polarized protons at RHIC provides a direct measure of the individual polarizations of the quarks and anti-quarks in the colliding protons. The high energy scale set by the W-mass makes it possible to extract quark and anti-quark polarizations from inclusive lepton spin asymmetries in W-production with minimal theoretical uncertainties. Sub-leading twist and higher-order terms in the perturbative QCD expansion are strongly suppressed, and a direct extraction without additional assumptions becomes possible. This program thus will break new ground in our detailed understanding of the proton's structure. The program is initiated by the first operation of RHIC polarized proton beams at its highest operational energy  $\sqrt{s} = 500$  GeV starting from 2009.

A new trigger on forward muons in PHENIX identifies and triggers on high momentum muons from W decay suppressing a large number of background low momentum muons coming from hadronic decays. Since the current muon trigger will fire on any muon above 2 GeV/c, it will not provide the required rejection factor for 500 GeV running, which is about 10,000. Two major upgrade projects are parts of this Muon Trigger; 1) Resistive Plate Chambers<sup>1)</sup>, 2) the muon tracker front-end-electronics (MuTr-FEE) upgrades<sup>2)</sup>. This report summarizes the introduction the latter and the installation to PHENIX during 2008 shutdown period.

The MuTr-FEE upgrade features additional fast readouts to the existing MuTr-FEE, which provides momentum sensitivity to the existing muon trigger beyond 2 GeV/c. There are three tracking stations of cathode strip (5mm pitch) chambers in the muon tracker for measuring the trajectory of particles in a magnetic field (with an integrated  $B - dl$  of approximately 0.75 Tesla-meters). A new amplifier discriminator (MuTRG-ADTX) board<sup>3)</sup> divides the signal into two paths; existing read out path and the digitization path for the fast trigger.

Figure 1 visualizes the principle of the momentum sensitive trigger. The hit signals from three tracking chambers (named station-1, 2, and 3, respectively from

the collision point) are immediately digitized and processed by MuTRG-ADTX and are sent to new merger boards (MuTRG-MRG)<sup>4)</sup>. The MuTRG-MRG board collects hit signals from multiple MuTRG-ADTXs and formats the data to meet the input format of the Local Level-1 (LL1) trigger module. The LL1 module receives data from MuTRG-MRG and then select the events which have  $\pm 1$  strip sagitta at station-2 from the linear interpolation between station-1 and station-3 hits, providing the trigger of only high transverse momentum track  $P_T > 10$  GeV/c.

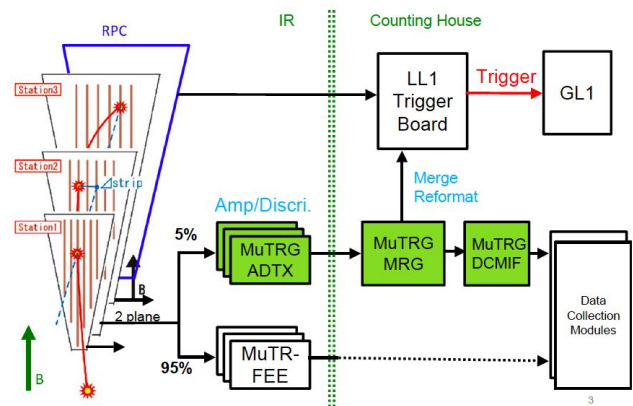


Fig. 1. The concept of momentum sensitive trigger using muon tracker cathode strip readouts.

The R&D, production of these new boards were nearly completed by the end of 2008. 192 MuTRG-ADTX boards were installed to the one of two muon arms in PHENIX and their commissioning starts as soon as Run09 beams are delivered. The installation to the remaining another half of the muon arm acceptance is scheduled during 2009 shutdown period.

## References

- 1) Conceptual Design Report for a Fast Muon Trigger (2007).
- 2) Technical Design Report on Amplifier-Discriminator board and Data Transfer board for the MuTr FEE upgrade (2008).
- 3) Y. Fukao, *et. al.*, RIKEN Accel. Prog. Rep. **42** (2009).
- 4) T. Mibe, *et. al.*, RIKEN Accel. Prog. Rep. **42** (2009).

<sup>\*1</sup> KEK, Tsukuba, Ibaraki, 305-08011, Japan

<sup>\*2</sup> Kyoto University, Kitashirakawa-Oiwakecho, Kyoto, 606-8502, Japan

<sup>\*3</sup> Rikkyo University, Rikkyo, 3-34-1, Nishi-Ikebukuro, Tokyo, 171-8501, Japan

## Development of the MuTRG-ADTX boards for the PHENIX muon trigger upgrade

Y. Fukao for the PHENIX MuTr FEE Upgrade Group

The contribution of sea quarks to proton spin is one of the mysteries in the study of the proton spin structure. The PHENIX experiment aims to directly probe the sea quark contribution through measurement of single helicity asymmetry in  $W$  boson production.  $W$  bosons are measured by detecting high-momentum muons from their decay, using the muon arms in the PHENIX detector.<sup>1)</sup> One of the greatest difficulties in measuring a  $W$  boson is that the trigger rate would be too high at the designed luminosity to record all events with  $W$  candidates. To collect  $W$  production events effectively, we are developing a new trigger system, which selects high-momentum muon tracks by performing rough momentum measurement online. An overview of the trigger system is provided elsewhere.<sup>2)</sup>

This report describes the development of an amplifier - discriminator - transmitter board (MuTRG-ADTX) for the existing muon tracking chamber (MuTr). Figure 1 is a picture of the MuTRG-ADTX board. MuTRG-ADTX is installed on MuTr and utilizes  $\sim 5\%$  of the charge induced in MuTr. The remaining 95% is used by the existing MuTr front-end electronics (MuTr-FEE) for precise offline position measurement. The input charge in MuTRG-ADTX is amplified and discriminated to provide a fast signal for the trigger. The digitized signals from 64 channels are serialized in an FPGA and sent to the downstream data merger board (MuTRG-MRG). Meanwhile, MuTRG-ADTX receives control signals and the beam clock from MuTRG-MRG. Optical fibers are used for the communication between them. Development of MuTRG-MRG is reported elsewhere.<sup>3)</sup>

In summer 2007, we installed prototype boards of MuTRG-ADTX to the actual MuTr in the PHENIX detector. They were tested with cosmic rays and sufficient performance was obtained.<sup>4)</sup> The prototype was composed of two separate boards – an analog signal part (amplifier + discriminator, AD part) and digital signal part (transmitter, TX part) – due to fears of possible noise from the TX part to the AD part. Based on the knowledge of grounding in the cosmic ray test, the AD and TX parts were combined into one board, MuTRG-ADTX. This modification also provides results in advantages in terms of costs, simplicity and easier installation. The combined MuTRG-ADTX board was again tested at PHENIX during RHIC 2008 run (Run08) and we confirmed that performance of MuTRG-ADTX was consistent with the prototype.

After a few minor modifications based on results of the test experiment, we started mass production of

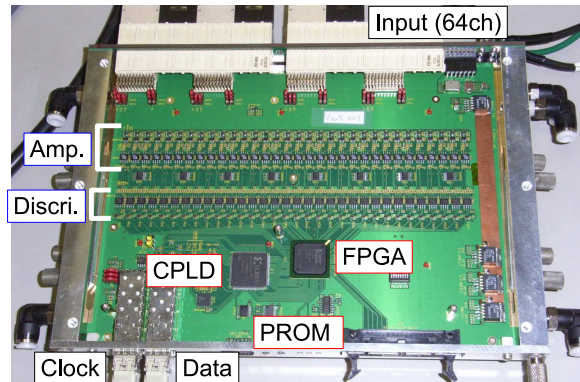


Fig. 1. MuTRG-ADTX.

MuTRG-ADTX. A total of 220 boards were produced in 2008. The boards were carefully examined before installation to the MuTr because access to MuTRG-ADTX is extremely difficult after installation. Check items for MuTRG-ADTX were : (1) signal reconstruction and efficiency, (2) fake hit rate to evaluate noise level, (3) cross talk between channels, (4) various slow controls including operation mode selection and threshold setting for the discriminator, (5) turn on curve of the trigger efficiency for each channel, (6) remote update of FPGA. In addition, noise increase and gain reduction on MuTr-FEE were checked for each MuTRG-ADTX board at the test bench. Finally, all produced boards passed the examination.

By the end of 2008, MuTRG-ADTX boards were installed for the north muon arm as scheduled, together with necessary infrastructure such as the low voltage power supply, cooling water system and optical signal lines between the beam interaction region and counting room. Tests of signal readout and slow controls were carried out for all installed MuTRG-ADTX boards, and we confirmed that the boards were fully operational. The impact of MuTRG-ADTX installation on MuTr-FEE, noise and gain, was measured and the effects were reasonable.

We plan to collect data on the new  $W$  trigger and evaluate its performance during the polarized proton run with  $\sqrt{s} = 500$  GeV in 2009 (Run09). Installation into the south muon arm is scheduled for summer 2009.

### References

- 1) PHENIX collaboration: Nucl. Instrum. Meth. **A499**, 537, (2003).
- 2) I. Nakagawa et al.: RIKEN Accel. Prog. Rep. **42** (2009).
- 3) I. Mibe et al.: RIKEN Accel. Prog. Rep. **42** (2009).
- 4) Y. Fukao et al.: RIKEN Accel. Prog. Rep. **41** (2008).

## Development and evaluation of the MuTRG-MRG and DCMIF boards for the PHENIX muon trigger upgrade

T. Mibe<sup>\*1</sup>, K.R. Nakamura<sup>\*2</sup>, K. Karatsu<sup>\*2</sup>, I. Nakagawa, Y. Fukao, H. Okada<sup>\*1</sup>, N. Saito<sup>\*1</sup>, A. Taketani, for the PHENIX MuTr FEE upgrade group<sup>1)</sup>

The parity violating single-spin asymmetry  $A_L$  of muons from the  $W$  decay in the 500 GeV polarized proton-proton collisions will be measured at the PHENIX in the future running. The PHENIX Muon Tracker Front End Electronics (MuTr FEE) needs to be upgraded to introduce momentum-sensitivity to the muon trigger by the fast measurement of the sagitta (a displacement of track position due to the magnetic field in three MuTr stations)<sup>1)</sup>.

In this report, development and evaluation of two key components of the trigger system, i.e. data merger board (MuTRG-MRG) and interface board to data-collection-module (MuTRG-DCMIF), are described.

The primary function of the MuTRG-MRG board is to receive data from the Amplifier-Discriminator-Transmission board (MuTRG-ADTX)<sup>2)</sup> boards and send reformatted data to the Local Level-1 Trigger board (LL1). The MuTRG-DCMIF board samples the merged data recorded in the MuTRG-MRG board, and send it to the Data Collection Module (DCM), a read-out port of the PHENIX data acquisition system, for the monitoring and diagnosis of the system. The requirements and specifications of the MuTRG-MRG and DCMIF boards are described elsewhere<sup>3)</sup>.

Prototype boards of the MuTRG-MRG and DCMIF boards were developed. They have optical transceivers with 16-bit serial links, 24-bit LVDS serial links, and VME J1 interfaces. The Xilinx Spartan3 FPGA is used to process the incoming data. The board power (3.3 V) is supplied through the VME64X backplane. Size of these boards is 9 U in height and 160 mm in depth with 10 layers (Fig. 1). These boards are installed in custom-made VME sub-racks in the PHENIX rack room. Each VME sub-rack accommodates sixteen MuTRG-MRG boards and two DCMIF boards. A full-size rack and its service for the VME sub-racks and optical patch panels have been installed in the PHENIX rack room.

Data communications as well as propagations of control signals have been individually tested at PHENIX under conditions as realistic as reasonably achievable during the RHIC machine shutdown in 2008. One of major test milestones was a successful data transmission from the MuTr cathode strip to the DCM with a full chain of the MuTRG electronics (MuTRG-ADTX,

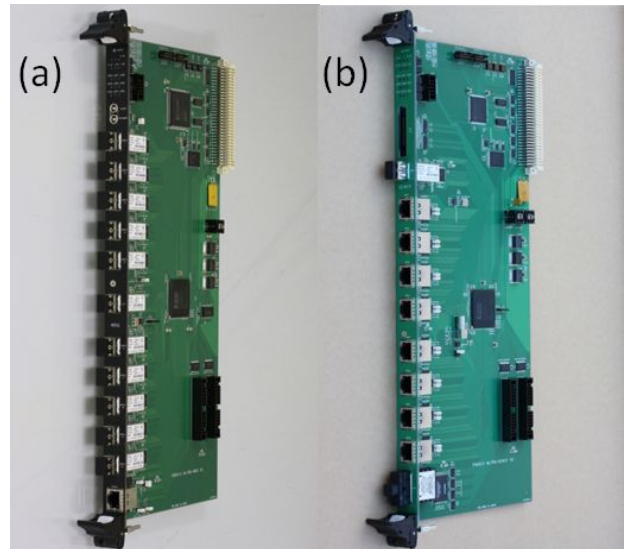


Fig. 1. (a) MuTRG-MRG board, (b) MuTRG-DCMIF board.

MRG, DCMIF) and the PHENIX standalone data acquisition system, including event building with existing MuTr subsystem.

The consistency of schedule and technical details for integration has been discussed by the internal PHENIX review committee. Upon positive feedbacks from the review, the boards production was started. In total 70 MuTRG-MRG boards and 12 MuTRG-DCMIF boards were produced. These board will be installed to PHENIX after quality assurance check-ups.

In summary, the prototypes of MuTRG-MRG and DCMIF boards have been developed. All individual functions of these boards were evaluated at PHENIX. With these boards, the MuTRG electronics were integrated to the PHENIX data acquisition system. Details of these achievements are described in the master's thesis<sup>4)</sup>.

### References

- 1) I. Nakagawa et al.: RIKEN Accel. Prog. Rep. **42** (2009).
- 2) Y. Fukao et al.: RIKEN Accel. Prog. Rep. **42** (2009).
- 3) K.R. Nakamura et al.: RIKEN Accel. Prog. Rep. **41** (2008).
- 4) K.R. Nakamura : Master's thesis, Kyoto University (2009).

<sup>\*1</sup> KEK, Tsukuba, Ibaraki, 305-08011, Japan

<sup>\*2</sup> Kyoto University, Kitashirakawa-Oiwakecho, Kyoto, 606-8502, Japan

<sup>\*3</sup> Rikkyo University, Rikkyo, 3-34-1, Nishi-Ikebukuro, Tokyo, 171-8501, Japan

<sup>\*4</sup> Seoul National University, Seoul, South Korea

# A fast, momentum sensitive muon Trigger for PHENIX using resistive plate counters<sup>†</sup>

M. Grosse-Perdekamp,<sup>\*1</sup> R. Seidl,<sup>\*2</sup> for the PHENIX Muon Trigger upgrade project

[Spin Physics, PHENIX, Trigger]

The parity violation of the weak interaction can be used to directly access the quark and sea quark helicities of the nucleon<sup>1)</sup>. Colliding longitudinally polarized protons at RHIC energies of  $\sqrt{s} = 500$  GeV one can produce real W bosons which will be detected through their charged decay lepton. The high mass of the W-boson makes it possible to isolate these decay leptons at high transverse momenta in the central and muon arms of the PHENIX detector. The existing muon trigger selects particles which pass through the muon arms including several layers of absorbing material. Presently, the muon yield is dominated by low momentum muons from hadron decays. At the expected luminosities for 500 GeV collisions at RHIC, the decay muon rate will far exceed the available bandwidth for data acquisition in Phenix. Figure 1 shows that a momentum sensitive first level trigger would be well suited to reject low momentum muons. For this purpose two detector upgrades are underway to create a momentum sensitive first level trigger which selects only high momentum muons. The first project is an upgrade of the front end electronics of the existing muon tracking stations to promptly feed muon tracking information to the trigger processor<sup>2)</sup>. The second detector upgrade adds two layers of resistive

plate counters (RPC) before and after the muon tracking system. The RPCs will be the only detectors with fast time response in the PHENIX muon spectrometers. The RPC can tag straight high momentum muon tracks in the first level trigger. The RPC timing will be critical in rejecting beam related backgrounds (prompt and thermal neutrons) in the trigger and backgrounds from cosmic ray muons in the offline analysis. Finally the timing information from the RPCs will be necessary to correlate W-candidates with the correct beam polarization information. The PHENIX muon trigger RPCs consist of double gas gaps sandwiching a signal plane with pick-up electrodes. The gas gaps are formed with bakelite plates, 2mm apart and externally coated with a thin layer of graphite for charge distribution. In order to keep the two plates at a constant distance (and thus at a constant electric field) polycarbonate spacers are located through the gap (see Fig. 2). The gas applied consists of 95% Freon, 4.5 % Isobutane and 0.5% SF<sub>6</sub>. The applied voltage is between 8.5 and 9.5 kV. The readout plane between the two gas gaps consists of large area printed circuit boards with copper strips. If a charged particle is traversing the gas volume an avalanche is created by the ionization. The amplification of the charge in the high electric field induces a detectable mirror charge on the pads outside the gas and electric field volume. The signal charge has a large dynamic range from 20 fC to 20 pC. The signal is being discriminated in front end electronics custom developed in CMS and are sent to TDCs.

\*1 University of Illinois at Urbana-Champaign, USA

\*2 RIKEN BNL Research Center, USA

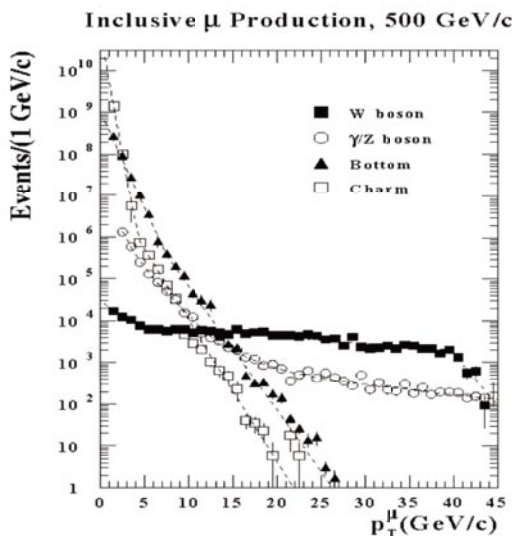


Fig. 1. Muon yields for different processes as a function of the transverse momentum of the muon.

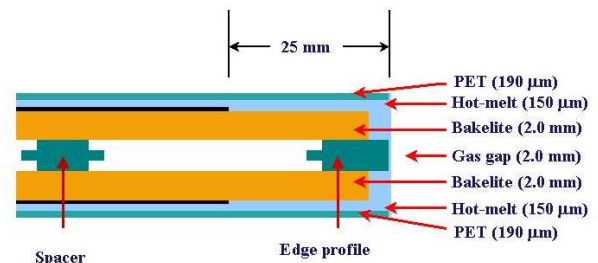


Fig. 2. Schematic view of a RPC gap showing two sheets of bakelite, the polycarbonate spacers, the are covered with graphite and the edge of such a gas gap.

## 1 Detector design

In order to obtain the maximum possible active area and to have a better matching with the existing muon tracking system the modules will be staggered in  $z$  in order to overlap inefficient areas in one detector module with an active area in the adjacent module. Two sets of detectors are being built. The first detector (RPC1) will be located downstream of the central magnet yoke just in front of Muon Tracker station 1. In order to maximize the acceptance in this detector octants will be staggered in azimuth around the beam axis to obtain full azimuthal coverage. The polar angle coverage is constraint by the PHENIX central magnet yoke and the in-sensitive boundaries of the RPC gas gaps. The resulting acceptance is only slightly less than the acceptance of the existing muon tracking system. The segmentation of the RPCs is between 200 and 480 pseudoradial strips over the full azimuthal angle and 4 segments in the polar angle. Upstream of RPC1 an additional 10-16cm thick lead absorber is planned which further increases the trigger rejection and reduces off-line backgrounds to the  $W$  measurements (see<sup>3</sup>). The second detector (RPC3) will be located behind the last muon ID steel absorbers at the intersection of the Experimental area and the RHIC accelerator tunnel. For the RPC3 detector station the inactive regions in the azimuthal direction coincide well with the size of the existing inactive regions in the PHENIX muon systems. For this reason the detector design focused on obtaining the optimum coverage along the polar angle direction. The RPC 3 detector stations will be formed from 16 half octants where each half octant will contain three detector modules. This configuration was driven given the maximum dimensions of gas gaps available from the gap production facility at Korea University. A sideview of the RPC detector locations can be seen in Fig. 3

## 2 Detector production

The production of the RPC detectors is organized around international cooperation within several

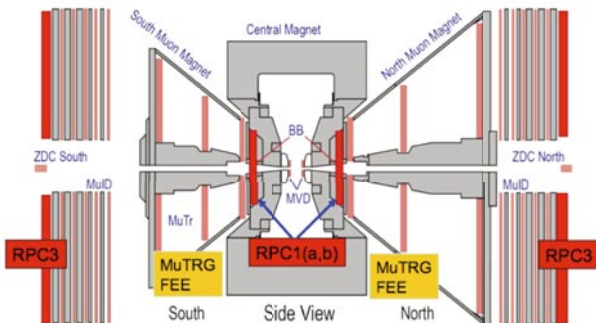


Fig. 3. Sideview of the PHENIX detector including the schematic locations of RPC stations 1 and 3.

PHENIX institutions and utilizing existing RPC technology from the CMS forward muon trigger detectors. Bakelite plates have been obtained from the CMS vendor in Italy. The plates were cut and cleaned in Italy and then shipped to Korea. From the raw bakelite plates the graphite coated gas gaps are being manufactured at Korea University. The module frames and the readout strips are produced in China under the supervision of the CIAE group in PHENIX. Both, module frames and gaps are shipped to BNL where they are tested and assembled into modules. The support structure will be build by an US manufacturer, test-assembled at UIUC before insertion of the modules at BNL and subsequent installation in the experiment. At all steps in the production chain the quality of the produced gaps will be closely monitored through leakage current measurements, efficiency measurements and environmental controls. The readout electronics has been developed at Nevis and is presently being produced. Fast custom trigger processors are being developed at Iowa State University.

## 3 Integration and Schedule

Two RPC prototypes that are close in dimension and design to the final RPC3 half octants have been installed in PHENIX and will be tested during run 9. The mass production of the final detector has been started in December 2008. As the RPC 3 detectors are sitting behind the muon identifier they have to be installed from the RHIC tunnel which requires technical support from the Collider Accelerator department of BNL. All services for RPC3 will be provided from the accelerator tunnel. The installation of the first RPC3 detector stations is planned for the summer of 2009. The station will be added to the PHENIX muon spectrometer north which already has been outfitted with new trigger electronics for the muon tracking chambers. The installation of the south side of RPC 3 will follow in 2010. The two smaller detector stations, RPC1, also will be installed in the summer of 2010. Subsequently, the full high momentum muon trigger will be available in PHENIX for run 11 when the first high luminosity polarized proton run at a center of mass energy of 500 GeV is anticipated.

### References

- 1) G. Bunce et al: *Plans for the RHIC Spin Physics Program*, [http://spin.riken.bnl.gov/rsc/report/spinplan\\_2008/spinplan08.pdf](http://spin.riken.bnl.gov/rsc/report/spinplan_2008/spinplan08.pdf)
- 2) I. Nakagawa et al: *High Momentum Trigger Electronics Upgrade of PHENIX Muon Arms for Sea Quark Polarization Measurement at RHIC*, in this volume.
- 3) R. Seidl et al.: *W-physics with Inclusive Muons in PHENIX: Detailed Feasibility Studies*, in this volume.

## DAQ system Upgrade for optical alignment system of PHENIX Muon Tracker

H. Kono<sup>\*1</sup>, K. Tsukada<sup>\*1</sup>, A. Taketani, J. Murata<sup>\*1</sup>, T. Akiyama<sup>\*1</sup>, Y. Fukao, M. Hata<sup>\*1</sup>, Y. Ikeda<sup>\*1</sup>,  
K. Karatsu<sup>\*2</sup>, T. Mibe<sup>\*3</sup>, I. Nakagawa, K. Nakamura<sup>\*2</sup>, K. Ninomiya<sup>\*1</sup>, M. Nitta<sup>\*1</sup> and N. Saito<sup>\*3</sup>

One of the major goals of the physics in the spin program at the RHIC-PHENIX experiment is to investigate the spin polarization of valence and sea quark ( $\Delta u$ ,  $\Delta d$ )<sup>1)</sup> in a proton separately by measuring W boson production asymmetry in the polarized proton-proton collision at the center of mass energy 500GeV.

The W boson is produced by collision of u and anti-d or d and anti-u and can be used for flavor decomposition of protons. The single spin asymmetry of the W production is shown as follows.

$$A_L^{pp \rightarrow W^+ X} = \frac{\Delta u(x_1)\bar{d}(x_2) - \Delta\bar{d}(x_1)u(x_2)}{u(x_1)\bar{d}(x_2) + \bar{d}(x_1)u(x_2)} \quad (1)$$

$$A_L^{pp \rightarrow W^- X} = \frac{\Delta d(x_1)\bar{u}(x_2) - \Delta\bar{u}(x_1)d(x_2)}{d(x_1)\bar{u}(x_2) + \bar{u}(x_1)d(x_2)} \quad (2)$$

In the case of  $x_2 \ll x_1$ , the equations of (1) and (2) can get into  $\Delta u/u$  and  $\Delta d/d$ . In the case of  $x_2 \gg x_1$ , those equations can get into  $\Delta\bar{d}/\bar{d}$  and  $\Delta\bar{u}/\bar{u}$ .

$$A_L = \frac{\sigma_- - \sigma_+}{\sigma_- + \sigma_+} \quad (3)$$

In the equation (3),  $\sigma_-$  is a cross-section in the collision between un-polarized and polarized protons with plus helicity.  $\sigma_+$  is that with minus helicity. Since both beams are polarized at the RHIC, one of two beams will be treated as un-polarized by taking the sum of positive and negative helicities. In this way,  $A_L$  can be evaluated for each beam simultaneously from a given collision. According to deep Inelastic Scattering experiment, the un-polarized distribution function of each quarks,  $u(x)$ ,  $d(x)$ ,  $\bar{d}(x)$  and  $\bar{u}(x)$  are reasonably well measured. Thus precision measurement of polarized distributions e.g.  $\Delta u$ ,  $\Delta d$ ,  $\Delta\bar{u}$  and  $\Delta\bar{d}$  are desired. They can be achieved via the W boson asymmetry measurement at RHIC. The W boson measurement is actually carried out by detecting muons' decay whose branching ratio is 10%. The muons from W decay have typically high momentum (transverse momentum  $P_t$  of 20GeV/c) due to heavy mass of W is 80GeV/c<sup>2</sup> and will be distinguished from dominant low momentum backgrounds.

A muon arm of the PHENIX consists of the Muon Identifier (MuID) and the Muon Tracker (MuTr). The MuID is designed to identify muons from hadron backgrounds using muons' penetration power through thick absorbers. The MuTr is for measuring momentums.

are mounted inside conical-shaped muon magnets. These stations are called "station-1", "station-2" and "station-3" starting from the near side of the collision point. Each station is symmetrically segmented into octants in azimuthal orientation. Each station is made of 2 or 3 gaps. An anode wire plane sandwiched by cathode signal planes forms a signal gap. The MuTr cambers are designed to provide a position resolution of 100–300 $\mu$ m, however this designed resolution has not been achieved with real data. The reason will be discussed in this report. An illustration of the MuTr is shown in Fig.1.

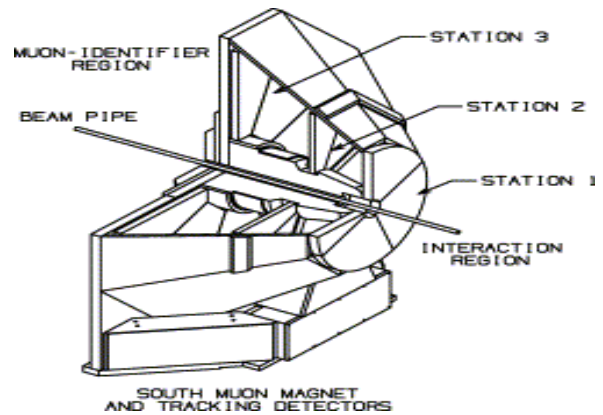


Fig.1: The illustration of the MuTr

A muon which enters into the MuTr is kicked toward the azimuthal direction by the radial direction magnetic field. We measure the momentum of a muon by using sagitta which is the deviation of a hit in station 2 from the straight line between hits in the station 1 and 3. The momentum of the muon is inversely proportional to the sagitta.

The muon from the W boson has higher momentum and its sagitta at the MuTr is quite small. The spectrum of single muon background drops sharply with its momentum, therefore the momentum resolution will affect the signal-to-noise ratio for the W asymmetry measurement.

However, each station moves 100-300 $\mu$ m because of the temperature excursion and the magnetic field. As a result, these displacements become one of the causes of the observed resolution which is 50-200% worse than the designed one.

The Optical Alignment System (OASys)<sup>2)</sup> measures the relative position movements among stations. There is a light source at the station-1, a lens at the station-2, and a CCD camera at the station-3. An image on the CCD camera reflects the relative movement among stations. Each octant, which covers 1/8 of each arm, has 7 sets of these as in Fig.2.

\*1 Rikkyo University

\*2 Kyoto University

\*3 High Energy Accelerator Research Organization, KEK

Three stations of cathode-strip readout tracking chambers

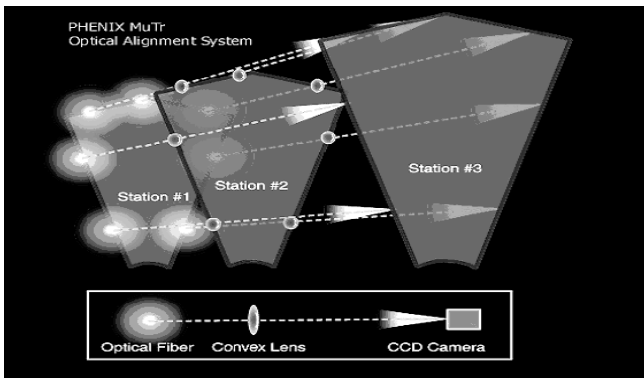


Fig.2: The image of Optical Alignment System (OASys)

OASys can track the relative movement among stations with accuracy of  $25\mu\text{m}^3$ . They can correct these positions and improve momentum resolution as a result

The Data Acquisition (DAQ) system of OASys consists of 112 CCD cameras, 2 multiplexers, 2 GPIB-Ethernet interfaces, 2 optical fibers, 2 pairs of fiber transmitter and receiver, an image capture board and a DAQ PC. The DAQ PC sends GPIB commands to the multiplexer via the Ethernet and the multiplexer selects the camera to capture the image. The video capture board obtains the spot image data from the selected camera, via an optical fiber to cut ground loop. The CCD camera transmits  $768 \times 498$  pixel. The video capture board, however, can receive  $640 \times 480$  pixel images. One longitudinal pixel corresponds to  $11\mu\text{m}$  and one lateral pixel corresponds to  $13\mu\text{m}$ . The diagram of the new DAQ system which was developed in 2008 is shown in Fig. 3.

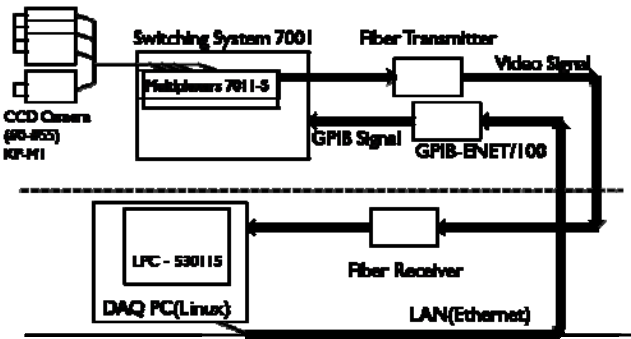


Fig. 3: Diagram of new DAQ system.

The previous DAQ system<sup>4)</sup> used two DAQ PCs which ran under Microsoft Windows operating system, National Instruments Labview and one analysis/storage Linux PC. The digitized images were previously transferred to the analysis PC via the network. However, this network service was terminated after a change in the network security policy in BNL.

The new DAQ system uses only one PC to collect data and to store the captured images. We employed the combination of a Linux operating system and a gcc compiler which is known to be very stable. As a consequence the new DAQ has been performing much more stably than the old one and is free of the data transfer problem. In addition, it

makes remote maintenance so simple.

In addition to the system change, a configuration file has been introduced for the system control. Some captured images on CCD cameras are obscure due to misalignment of the lens. However, the center positions of such images can be sharpened by integrated images. Due to the weak contrast images, captured images from the same camera are integrated in a digital fashion. The numbers to be integrated in digital images can easily be customized via the newly introduced configuration file.

The new DAQ system was commissioned during the OASys maintenance through the summer shut down period after Run08. In this maintenance period, major repair work was carried out for first time after several years since installation. One broken light source has been fixed, and many camera positions have been re-aligned. As a result, the number of available cameras increased from 30 to 98 out of a total 112.

A typical acquired image from the new system is shown in Fig.4. The spot of the image can authentically be recognized.

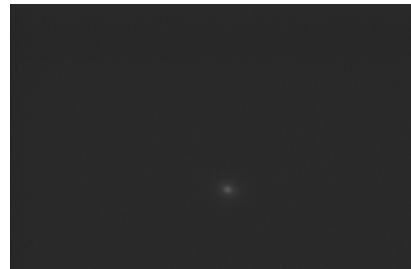


Fig. 4: An image on a CCD camera with the new DAQ system

The projection and fitted images should be prepared as the next step to extract the center position of spot image. An example which uses the image of Fig.4 is shown in Fig.5. The new DAQ system of OASys has been running stably from January 2009. It is expected to improve momentum resolution of the MuTr in coming 500GeV polarized proton run from March 2009.

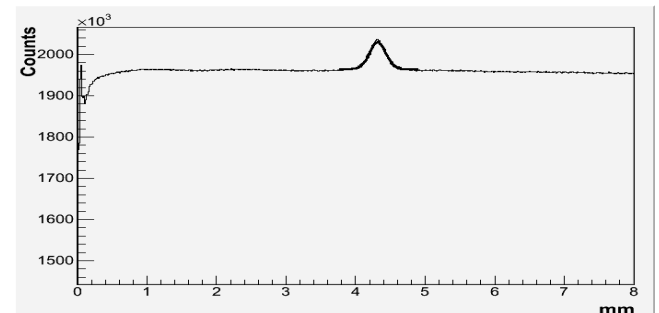


Fig.5. The projection and fitted image on X axis.

#### References

- 1) G. Bunce et al., Ann. ReV. Nucl. Part. Sci. 50, 525 (2000)
- 2) J. Murata et al.: Nucl. Instrum. Method Phys. Res. A500, 309(2003)
- 3) T. Watanabe: Master Thesis, TiTech (2004)
- 4) H. Kanoh: Master Thesis, TiTech(2005)

# CCJ Operation in 2007-2008

S. Yokkaichi, H. En'yo, Y. Goto, H. Hamagaki,\*<sup>1</sup> T. Ichihara, T. Nakamura, Y. Watanabe

## 1 Overview

The operation of CCJ<sup>1,2)</sup>, RIKEN Computing Center in Japan for the RHIC<sup>3)</sup> physics, started in June 2000 as the largest off-site computing center for the PHENIX<sup>4)</sup> experiment at RHIC. CCJ was initially planned to perform three roles in PHENIX computing, 1) as the simulation center, 2) as the Asian regional center and 3) as the center of spin physics. Recently, DST (Data Summary Tape) production from raw data has become more important, especially for the p+p data. Out of the many off-site computing facilities of PHENIX, only CCJ can handle the several hundreds of TB of raw data in use of HPSS (High Performance Storage System)<sup>5)</sup> for the time being.

A joint operation with RSCC (RIKEN Super Combined Cluster System)<sup>6)</sup> was started in March 2004. Most of our computing power is now provided by RSCC. On the other hand, the disk storage and service nodes are still located at the CCJ machine room in RIKEN Main Building and maintained by ourselves. Renewal of RSCC is on going and new CPUs will be available in August 2009.

Many analysis and simulation projects are being carried out at CCJ. They are shown on the web page: <http://ccjsun.riken.go.jp/ccj/proposals/>.

## 2 Current configuration

### 2.1 PC nodes

In June 2008, 112 PC nodes, which were purchased in 1999–2001, were retired and discarded. After that, we have approximately 80 PC nodes operated using Linux in the CCJ machine room. In these nodes, 54 nodes are used for calculation and the others are used for various services, e.g., data transfer, monitoring of nodes and network performances, database servers, log-in servers, WWW and mail server, and so on. Each calculation node has 1 GB of memory, 2 GB of swap area, 10–31 GB of local disks and dual CPUs (Pentium III 1.4 GHz and Pentium 4 2.0 GHz). Scientific Linux (SL) 4.4 is operated on the calculation nodes similarly to at RCF (RHIC Computing Facility)<sup>7)</sup>, which is the main analysis facility for PHENIX. At CCJ, upgrade from SL 3.0.5 was performed in April 2008.

Out of the calculation nodes, 36 nodes were augmented with 300 GB of local disk in March 2006, on which 10 TB of nDST (nano-DST) data are located in order to avoid the overhead of the data transfer from the data servers or HPSS. This "Data in local disk"

scheme is used by users with applause. These nodes were so old – purchased in March 2002 – that 14 times of system-disk crash occurred in 2008. The second-hand SCSI disks recycled from the retired servers and RAIDs were used for repairing.

Each RSCC calculation node has 2 GB of memory, 100 GB of local disk space and two Xeon 3.06 GHz processors. Out of the 1024 calculation nodes in RSCC, 128 nodes were dedicated to CCJ usage. In August 2008, the dedicated node was reduced to 64 because the congestion of the entire CPUs in RSCC. The dedicated nodes share the PHENIX software environment and can access the CCJ data servers as well as the nodes in the CCJ machine room. In order to run the PHENIX software, the operating system should be same as PHENIX, namely, SL 4.4 at present. This is why we need the 'dedicated nodes', in other words, we cannot share the CPU with the another RSCC users.

On the calculation nodes, the batch queuing system LSF<sup>8)</sup> is operated. Version 7.0 is used in CCJ, and 6.2 is used in the CCJ-dedicated nodes in RSCC.

Six temperature monitors were deployed in September 2008 and monitored by WEB using Cacti<sup>9)</sup> graphical tool, which was newly installed in 2008 and is also used to visualize the LSF performance and so on.

In February 2009, following success of the "Data on local disk" scheme, 18 nodes of new PC servers (HP ProLiant DL180 G5) were delivered. Each node has dual CPU (Quad-Core Xeon 2.66 GHz), two 146 GB SAS disks for the system, eight 1 TB SATA disks for the data storage, and 16 GB of memory. I/O bound jobs like the nDST analysis will be performed in the servers.

### 2.2 Data servers

We had a main server (SUN Fire V880) using Solaris 8 for the NIS/DNS/NTP servers and the NFS server for the users' home region on the 8 TB RAID. This machine was replaced by a new server machine, SUN Enterprise M4000 using Solaris 10 with the 10.5 TB of FC-RAID. The DNS, NIS, and NTP/NFS servers were replaced by the new machine in June 2008, October 2008, and January 2009, respectively. The home region is formatted by VxFS<sup>10)</sup> and served by NFS v3. The old server and RAID were discarded in Feb. 2009.

We have five data servers (SUN Fire V40z), which are operated by SL4. They serve five SATA-RAID systems (45 TB) and three FC-RAID systems (26 TB) which are formatted using XFS<sup>11)</sup>. In order to keep the total I/O throughput, *rcp* command is used to read the data on these servers instead of NFS.<sup>2)</sup>

In 2008, frequency of the hang-up of V40z servers

\*<sup>1</sup> CNS, University of Tokyo

was very low unlike the previous year.

### 2.3 HPSS

HPSS version 6.2 is used as a mass-storage system at CCJ and RSCC. As the first step of the renewal of RSCC, tape robots and HPSS servers were renewed in November 2008. A new robot and servers are located on CCJ machine room, instead of the RIKEN IT Building where the old system was located. Three UPSs (10.5 KVA each), additional power line and additional air-conditioning system for the robot and servers were newly equipped.

For the new HPSS core server and disk/tape movers, seven IBM p570 servers are operated using AIX 5.3. Twelve (six for CCJ) LTO-4 drives (120 MB/s I/O with 800 GB/cartridge), which are connected six (three for CCJ) tape movers, and 5000 LTO tapes (3000 for CCJ) are installed in the tape robot IBM TS3500, which can handle up to 10275 LTO tapes in current configuration. Since the old tapes cannot be used in the new tape drives, copying the data to the new tapes in the new robot was started in December 2008. Copying approximately 1.34 PB (2.02 M files) of CCJ data stored as of 1 January 2009 will be completed until the end of April 2009.

### 3 PHENIX software environment

Two AFS<sup>12)</sup> clients are operated using OpenAFS on Linux to share the software environment of the PHENIX experiment as analysis and simulation libraries, configuration files and so on. The total data size copied by AFS daily or weekly from BNL is approximately 330 GB as of January 2008. All the calculation nodes are served the software by NFS, not by AFS. Using a *rsync* server, the PHENIX software environment are also shared by PHENIX collaborators in Japan.

Three PostgreSQL servers are operated for the calibration database of PHENIX. The data size is approximately 60 GB as of January 2008. The data is copied daily from BNL.

### 4 WAN, data transfer and DST production

The SINET3 (maintained by NII<sup>13)</sup>) connects RIKEN Wako Campus to the Internet with 10 Gbps of bandwidth. Originally, two aggregated 1000BASE lines connected CCJ main switch (Catalyst 4506) and RIKEN Firewall with only 1.5 Gbps of bandwidth. For the data transfer between BNL, dedicated 10GBASE switch (Foundry FESX424) was deployed in CCJ and connected to RIKEN Main switch by a 10GBASE line in November 2007. Also for the transfer, dedicated four PC servers (HP ProLiant DL145 G3) which are operated by SL5 with a Grid environment (VDT<sup>14)</sup> 1.8.1) were deployed. Each server has two 1000BASE

network I/F, one is connected to the Foundry, and the other is connected to the Catalyst. The data from the BNL are transferred through the former line, and are written to the CCJ-HPSS through the latter line. Using the setup, a 360 MB/sec transfer rate from BNL to CCJ was achieved in the test.

In the PHENIX Run-8 (November 2007–March 2008), approximately 100 TB of p+p data were transferred using the data-transfer machines in February–March 2008. The data were sent from the PHENIX counting house in the 'semi-online' manner, namely, before they stored in RCF-HPSS, to avoid an overhead to read from the tape. As a sustained rate for a day, approximately 100 MB/s (8 TB/day) was achieved using gridFtp<sup>15)</sup>. Another 10–20 TB were also sent after the Run period. Thus the amount of Run-8 raw data stored in CCJ-HPSS is 117 TB in total. DST production was conducted mainly in August–October 2008 with the reduced 64 nodes in RSCC and 21 TB of analyzed data (nDST) were produced out of 117 TB of raw data, and sent to RCF.

### 5 Outlook

In 2009, one of the main task of CCJ is the data transfer of PHENIX run9 p+p raw data, which are expected to be 200-500 TB in the Run started January 2009. The DST production using the raw data is another task. To process such large amount of data, joint operation with the renewed RSCC after August 2009 is important.

Main network switch will be replaced in July 2009 by Catalyst 4900M, which have eight 10GBASE ports. Using this switch, a 10GBASE connection between CCJ and HPSS/renewed RSCC will be established.

The condor batch queuing system<sup>16)</sup>, which is already used in RCF, should be tested in the new PC servers. When it works well, LSF will be replaced.

### References

- 1) <http://ccjsun.riken.go.jp/ccj/>
- 2) S. Kametani et al., RIKEN Accel. Prog. Rep. 40, 197 (2007). S. Yokkaichi et al., RIKEN Accel. Prog. Rep. 41, 159 (2008).
- 3) <http://www.bnl.gov/rhic>
- 4) <http://www.phenix.bnl.gov>
- 5) <http://www.hpss-collaboration.org/>
- 6) <http://rsc.riken.jp>
- 7) <http://www.rhic.bnl.gov/RCF/>
- 8) <http://www.platform.com/products/LSF/>
- 9) <http://www.cacti.net/>
- 10) Veritas file system, provided by Symantec corporation.
- 11) <http://www.xfs.org/>
- 12) <http://www.openafs.org/>
- 13) <http://www.nii.ac.jp/>
- 14) <http://vdt.cs.wisc.edu/index.html>
- 15) <http://www.globus.org/grid/software/data/gridftp.php>
- 16) <http://www.cs.wisc.edu/condor/description.html>

**III. RESEARCH ACTIVITIES II**  
**(Material Science and Biology)**

## **1. Atomic and Solid State Physics(ions)**

# Microdose damage observed in power MOSFETs with trench structures

Y. Satoh,<sup>\*1</sup> A. Maru,<sup>\*1</sup> N. Ikeda,<sup>\*1</sup> S. Kuboyama,<sup>\*1</sup>  
 H. Ohzono,<sup>\*2</sup> O. Shimada,<sup>\*2</sup> H. Otomo,<sup>\*2</sup> H. Mutoh,<sup>\*2</sup> T. Kambara,<sup>\*3</sup> and M. Kase<sup>\*3</sup>

The power MOSFET is a frequently used device in power supply systems. Recently, a new type of power MOSFET with trench gate structures, shown in Fig. 1, has become available for commercial use. The vertical and straight current path in the trench gate structure makes it possible to decrease the size of a unit cell and increase the number of cells in a MOSFET chip, and this helps lower on-resistance and increase the efficiency of the power supply system.

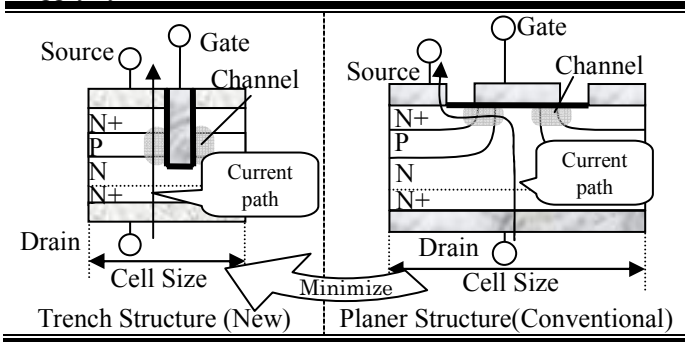


Fig. 1. Cross-section of power MOSFET structures.

However, it has been reported that the trench structure shows anomalously large degradation of electrical properties due to heavy ion irradiation.<sup>1)</sup> This degradation could have serious consequences in space systems, and thus therefore the heavy ion irradiation was performed using a cyclotron at RIKEN to investigate the criticality of the degradation. Kr ions were used, and their energy, LET, and range in Si were 5.5 GeV, 11 MeV-cm<sup>2</sup>/mg and 1.26 mm respectively.

The mechanism is a microdose effect, i.e., an extremely localized dose effect. As shown in Fig. 2, a heavy ion running through the gate oxide parallel to the channel makes an ion track parallel to the channel. This track induces a leak current path and the increase in leak current decreases threshold gate voltage ( $=\Delta V_{TH}$ ). This degradation

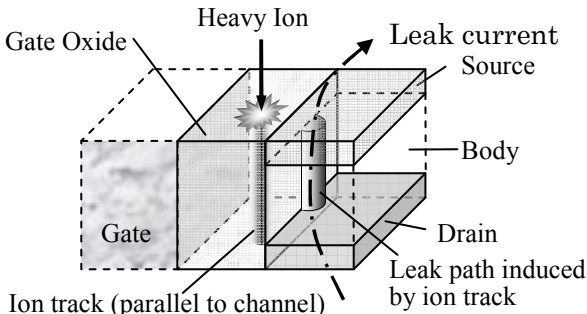


Fig. 2. Microdose effect

will cause a number problem for spacecrafts (e.g., switching failure).

We observed the incident angle dependence of  $\Delta V_{TH}$ . Fig. 3 shows the result.

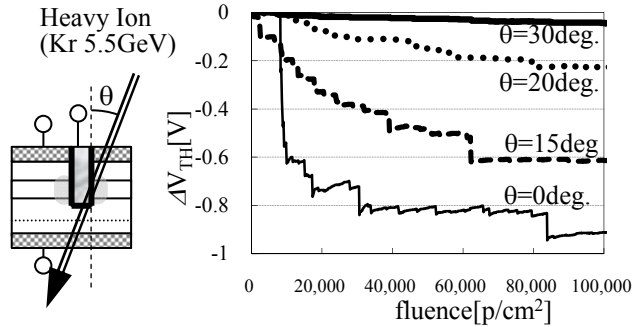


Fig. 3. Incident angle dependence of  $\Delta V_{TH}$ .

As the incident angle increases,  $\Delta V_{TH}$  decreases. Only extremely small  $V_{TH}$  shifting was observed over 30 degrees. These data show  $\Delta V_{TH}$  step down shifting events. The measured cross section of the degradation event is  $2.0 \times 10^{-3}$  [cm<sup>2</sup>].

LET > 1.0 [MeV/(mg/cm<sup>2</sup>)] particle flux was calculated with CREME96 code assuming altitude, inclination and geomagnetic condition of 700 km, 98.6 degrees and stormy, respectively. The result was  $5.4 \times 10^{-1}$  [p/m<sup>2</sup>/s/str]. The event rate in orbit was calculated using Eq.1. The critical angle is assumed to be 30 degrees utilizing Fig. 3, and the effective solid angle is  $2\pi\{1 - \cos(30[\text{deg.}])\}$ .

$$(5.4 \times 10^{-1} [\text{p} / \text{m}^2 / \text{s} / \text{str}]) \times (2 \times 10^{-7} [\text{m}^2]) \times 2\pi(1 - \cos(30[\text{deg.}])) = 9.1 \times 10^{-8} [\text{events} / \text{s}] \quad (\text{Eq.1})$$

This result means the event rate is about 130 day/event. Additionally, Fig. 3 shows that there is recovery from the microdose effect is due to the annealing effect in a few minutes. We can predict that the degradation events in trench structure will not be critical for space applications. Our next study will be an estimation of criticality, strictly for space use.

### References

1) James A.Felix, Marty R.Shaneyfelt, James R. Schwank, Scott M. Dalton, J.Brandon Wither: "Enhanced Degradation in Power MOSFET Devices Due to Heavy Ion Irradiation", *IEEE Trans. Nucl. Sci.*, Vol. 54, No. 6, pp. 2181-2189, Dec. 2007.

\*1 Japan Aerospace Exploration Agency  
 \*2 Ryoei Technica Corporation  
 \*3 RIKEN

## Structure of ePTFE irradiated with a 5 MeV/nucleon $^{14}\text{N}$ beam

Y. Suzuki, T. Kobayashi, K. Takahashi, T. Kambara, F. Saito,<sup>\*1</sup> T. Hyodo,<sup>\*1</sup> Y. Nagashima,<sup>\*2</sup> K. Okamura,<sup>\*3</sup>  
S. Uchikoshi,<sup>\*3</sup> N. Nakano,<sup>\*3</sup> A. Iwase,<sup>\*4</sup> D. Mano,<sup>\*5</sup> and Y. Shiga<sup>\*5</sup>

Amperometric gas sensors have been widely used in industrial applications and environmental monitoring for detecting hydrogen, hydrogen sulfide, nitrogen oxides, and other gases.<sup>1,2)</sup> However, superior sensitivity and selectivity of the sensor is a constant requirement. In this study, we tried to use ion beam irradiation of expanded polytetrafluoroethylene (ePTFE) membranes to improve gas permeability characteristics of the sensor electrode. We expect ion beam irradiation of the membrane to influence the permeability of gases, wettability of the membrane/electrolyte interface, and electrochemical reaction properties of gases at the gas/electrode/membrane interface.<sup>3,4)</sup> At first, surface analyses were performed to investigate mechanisms underlying the effects of ion beam irradiation on modification of ePTFE. The ePTFE membranes (Sumitomo Denkou, Japan) used had 0.3  $\mu\text{m}$  pore size, 34% porosity, and 0.2 mm thickness. The membranes were 30 mm square and were irradiated with 5 MeV/nucleon  $\text{N}^{7+}$  ions from the AVF cyclotron with fluences from  $1 \times 10^{12}$  to  $3 \times 10^{13}$  ions/ $\text{cm}^2$  at room temperature.

Ion beam irradiated and non-irradiated ePTFE were coated with gold in a plasma coater (SG-701, Sanyu Denshi, Japan). Microphotographs of field emission scanning electron microscopy (SEM) were obtained at a 5 kV acceleration voltage (JED6330F, JEOL, Japan). Figure 1 shows the SEM images of the non-irradiated ePTFE and the ion-irradiated ePTFE membrane with a fluence of  $3 \times 10^{13}$  ions/ $\text{cm}^2$ . The non-irradiated ePTFE has a micro porous structure consisting of nodes and fibrils of PTFE. The pore size of the ion-irradiated surface increased and the shape of the surface was more complicated compared to the non-irradiated ePTFE membrane.

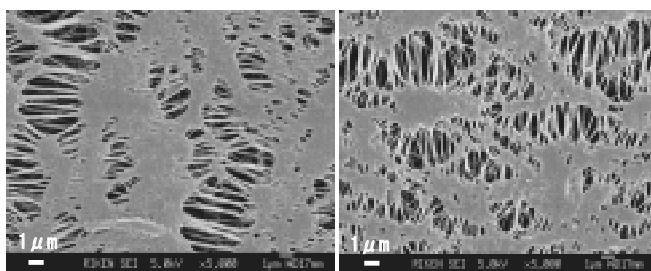


Fig. 1. SEM images of non-irradiated ePTFE (left) and ion-irradiated ePTFE membrane with a fluence of  $3 \times 10^{13}$  ions/ $\text{cm}^2$  (right).

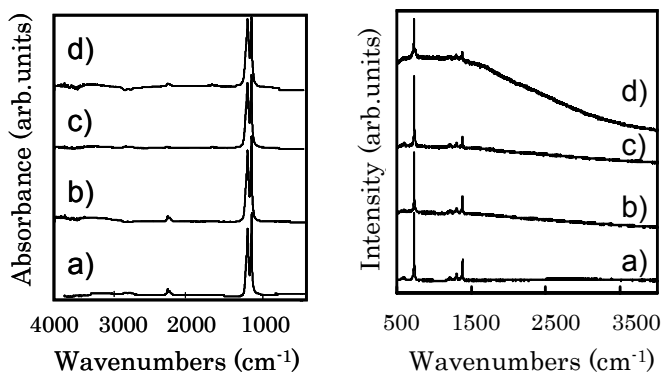


Fig. 2. IR (left) and Raman spectra (right) of non-irradiated (a) and ion beam irradiated ePTFE with fluences of  $1 \times 10^{12}$  (b),  $1 \times 10^{13}$  (c), and  $3 \times 10^{13}$  ions/ $\text{cm}^2$  (d).

The structures of ion beam irradiated layers were investigated using Fourier transform infrared spectroscopy (Nexus 470, Thermo Nicolet, USA) combined with attenuated total reflectance (FT-IR-ATR). In this analysis, the incident angle of light emitted from KBR on the specimens was  $45^\circ$ . The spectral range 400–4000  $\text{cm}^{-1}$  was analyzed and investigated by means of Raman spectroscopy (LABRAM, Jobin Yvon) with a 632.817 nm He-Ne laser. Figure 2 shows the IR spectra and Raman spectra of non-irradiated and N-ion beam irradiated ePTFE with fluences of  $1 \times 10^{12}$ ,  $1 \times 10^{13}$ , and  $3 \times 10^{13}$  ions/ $\text{cm}^2$ .

In the IR spectra, characteristic peaks are observed at 1150  $\text{cm}^{-1}$  and 1205  $\text{cm}^{-1}$  which are assigned as C-F bond. The absorbance peak of C-F was depressed with increased fluence of N-ions. The results of Raman spectroscopy at fluence of  $3 \times 10^{13}$  ions/ $\text{cm}^2$  shows a broad hump at 1300–1600  $\text{cm}^{-1}$  which corresponds to the formation of amorphous carbon. The characteristic peaks of  $\text{CF}_2$  (735  $\text{cm}^{-1}$ ) and C-C (1384  $\text{cm}^{-1}$ ) also decreased with increased fluence. In the ePTFE, the changes in internodal distance, density between nodes and the C-C radical were induced by 5 MeV/nucleon N-ion irradiation. We plan to study gas sensing properties of sensors using the ion-irradiated membranes in the next stage of development.

### References

- 1) T. Ishiji, T. Iijima, K. Takahashi, *Denki Kagaku* 64 (1996) 1304.
- 2) N. Nakano, S. Ogawa, *Sensors and Actuators B* 21 (1994) 51.
- 3) M. Iwase, A. Sannomiya, S. Nagaoka, Y. Suzuki, M. Iwaki, and H. Kawakami, *Macromol.* 37 (2004) 6892.
- 4) K. Okamura, T. Ishiji, M. Iwaki, Y. Suzuki and K. Takahashi, *Surface & Coatings Technology* 201 (2007) 8116.

\*1 University of Tokyo  
\*2 Tokyo University of Science  
\*3 Riken Keiki Co.Ltd.  
\*4 Osaka Prefecture University  
\*5 Meiji University

## Study of polymer reformed by ion-irradiation

F. Saito,<sup>\*1</sup> T. Hyodo,<sup>\*1</sup> Y. Nagashima,<sup>\*2</sup> Y. Suzuki

Reformation of ion irradiated polymer has been studied by positron annihilation measurements and electron resonance (ESR) measurements. Polymer chains are cleaved by ion irradiation, so that some of the scission sites remain as radicals and the others recombine or form crosslinks between polymer chains.

Positronium (Ps), a hydrogen-like bound state of an electron and a positron, is very sensitive to radicals. Ps has two states; para-Ps (p-Ps, spin singlet) annihilates with a mean lifetime of 125ps in a vacuum emitting two  $\gamma$  rays and ortho-Ps (o-Ps, spin triplet) annihilates with a mean lifetime of 142ns emitting three  $\gamma$  rays. When radicals exist, positronium formation is reduced since positrons and excited electrons are captured by radicals. Moreover, positronium quenches by spin conversion with an electron of a radical. By spin conversion, o-Ps becomes p-Ps. This effect is distinctive for o-Ps because of its long lifetime.

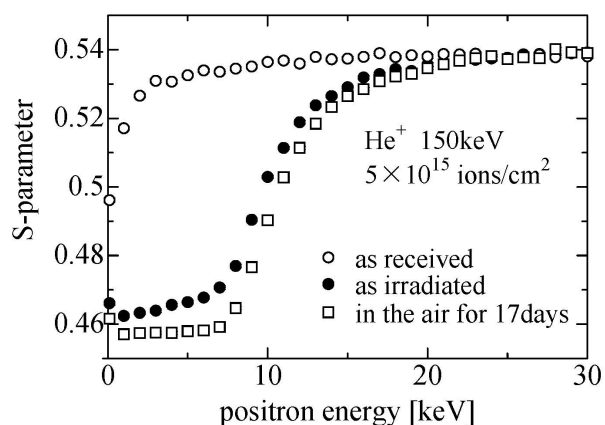


Fig.1 S-parameters of positron annihilation  $\gamma$  ray Doppler broadening peak obtained using a slow positron beam vs. incident positron energy

Figure 1 shows the S-parameters plotted against incident positron energy for the polystyrene irradiated by 150keV  $\text{He}^+$  ions with fluence of  $5 \times 10^{15}$  ions/cm<sup>2</sup> and that for the as-received sample<sup>1)</sup>. S-parameter is the shape parameter of positron annihilation  $\gamma$  ray Doppler broadening peak. The S-parameter for the as-received sample is almost constant, except below 2 keV. The S-parameter for the irradiated samples is lower than that for the as-received sample. The decrease of the S-parameter has been attributed to inhibition of Ps formation by radicals<sup>2)</sup>. We found that exposure of the sample to the air makes the S-parameter even lower.

<sup>\*1</sup> The University of Tokyo

<sup>\*2</sup> Tokyo University of Science

Figure 2 shows ESR spectra for the irradiated polystyrene. The intensity of the singlet peak decreases with time. It should be noted that the time constant for the decrease appears long.

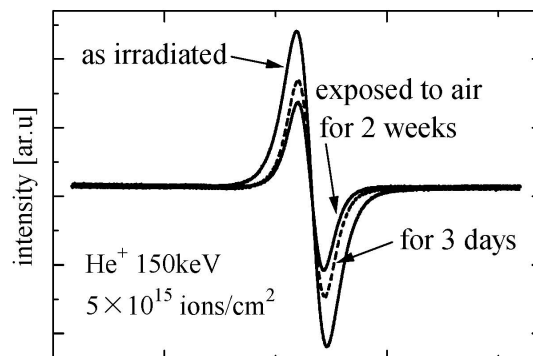


Fig. 2 ESR spectra for irradiated polystyrene exposed to air and as-irradiated

This data indicates that the decrease of the S-parameter by ion irradiation cannot be explained simply by the Ps formation inhibition by radicals<sup>3)</sup>. The inhibition may be due to the shielding of coulomb interaction between electron and positron by an abrupt increase of the electric conductivity of ion irradiated polymers<sup>4)</sup>. In order to elucidate this problem, the study of ePTFE irradiated by  $\text{N}^{7+}$  ions using the AVF cyclotron is in progress in RIKEN<sup>5)</sup>. Since the ions with energy of 5 MeV/nucleon penetrate deeply into the sample with the thickness of 0.2mm, conventional positron lifetime measurement and positron annihilation  $\gamma$  ray Doppler broadening measurement can be used in addition to slow positron beams measurement.

### References

- 1) Y. Kobayashi, I. Kojima, S. Hishita, T. Suzuki, E. Asari and M. Kitajima, Phys. Rev. B 52 (1995) 823
- 2) N. Djourelov, T. Suzuki, Y. Ito, K. Velitchkova and K. Kondo, Nucl. Instr. Meth. B, **225** (2004) 357
- 3) F. Saito, Y. Fujii, Y. Nagashima, T. Yotoriyama, A. Nakao, Y. Suzuki, M. Iwaki, I. Nishiyama, T. Hyodo, Phys. Stat. Sol. (c), **4** (2007) 3718.
- 4) I. H. Loh et al, Nucl. Instr. and Meth. B, **34** (1988) 337
- 5) Y. Suzuki, T. Kobayashi, K. Takahashi, T. Kambara, F. Saito, T. Hyodo, Y. Nagashima, K. Okamura, S. Uchikoshi, N. Nakano, A. Iwase, D. Mano and Y. Shiga, in this volume

## Site change of hydrogen in Nb due to interaction with oxygen†

E. Yagi,<sup>\*1</sup> K. Hirabayashi,<sup>\*2</sup> Y. Murakami,<sup>\*2</sup> S. Koike,<sup>\*3</sup> N. Higami,<sup>\*2</sup> T. Hayashi,<sup>\*2</sup> A. Takebayashi,<sup>\*2</sup> T. Yoshida,<sup>\*2</sup>  
C. Sugi,<sup>\*2</sup> T. Sugawara,<sup>\*4</sup> T. Shishido,<sup>\*4</sup> and K. Ogiwara

As to an interaction between hydrogen or deuterium and oxygen or nitrogen interstitial solutes in the group Va metals in the periodic table (V, Nb and Ta), H or D is trapped by O or N atoms to form O-H(D) or N-H(D) pairs. From the point of view of hydrogen diffusion, the jump rate of H(D) in those metals, especially in Nb, alloyed with oxygen or nitrogen has been investigated. The existence of O-H(D) or N-H(D) pairs allows measurement of the jump rate at low temperatures otherwise impossible, because hydride precipitation at low temperatures is suppressed due to trapping of H(D). The non-classical behaviour has been observed, and it has been interpreted to be tunnelling motion of trapped H(D) between equivalent two sites around its trapping centre O or N.<sup>1)</sup> As the configuration of the O(N)-H(D) pair, various models have been proposed, but it has not been clarified between which sites hydrogen makes tunnelling. In the present study, to obtain direct information on the lattice location of hydrogen in Nb alloyed with oxygen, channelling experiments were performed at room temperature utilizing a nuclear reaction  $^1\text{H}(^{11}\text{B}, \alpha)\alpha\alpha$  with a  $^{11}\text{B}$  beam of about 2 MeV.<sup>2,3)</sup> Hydrogen can be detected by measuring emitted  $\alpha$ -particles.

Specimens are single-crystal of Nb and Nb alloyed with oxygen of 0.3at.% ( $\text{NbO}_{0.003}$ ). Hydrogen was doped up to concentrations of 0.0027 and 0.023 in a hydrogen-to-metal-atom ratio for Nb specimens ( $\text{NbH}_{0.0027}$  and  $\text{NbH}_{0.023}$ ), and 0.003 and 0.019 for  $\text{NbO}_{0.003}$  specimens ( $\text{NbO}_{0.003}\text{H}_{0.003}$  and  $\text{NbO}_{0.003}\text{H}_{0.019}$ ). Figure 1 shows the channelling angular profiles obtained for  $\text{NbO}_{0.003}\text{H}_{0.003}$  and  $\text{NbO}_{0.003}\text{H}_{0.019}$ . The channelling angular profiles for both  $\text{NbH}_{0.0027}$  and  $\text{NbH}_{0.023}$  are similar to those for  $\text{NbO}_{0.003}\text{H}_{0.019}$ . It was demonstrated that hydrogen occupies tetrahedral (*T*) sites in pure Nb.<sup>3)</sup> From the comparison of the angular profiles of  $\alpha$ -particle yields with those calculated for various kinds of site occupancies, it was demonstrated that H atoms are located at sites displaced by 0.5-0.6 Å from *T* sites towards their nearest neighbour lattice point in  $\text{NbO}_{0.003}\text{H}_{0.003}$ , while in  $\text{NbO}_{0.003}\text{H}_{0.019}$  most of them are located at *T* sites and the remains are at the same sites as in  $\text{NbO}_{0.003}\text{H}_{0.003}$ . The separation between neighbouring equivalent displaced sites is about 0.82 Å. This magnitude is very close to the distance between two sites for hydrogen tunnelling, which was estimated from the result of inelastic neutron scattering experiment.<sup>1)</sup> The present result supports

the trapping of H by O atoms and the formation of O-H pairs. The number of H atoms trapped by one O atom was estimated to be approximately unity. As the location of trapped hydrogen in the O-H pair, there are possibilities of three types of displaced sites, site-a, site-d and site-j in Fig. 2, with different distances from the O atom but the same separation of about 0.82 Å between neighbouring equivalent sites. It is proposed that the site-a is most probable, which is different from hitherto proposed sites.

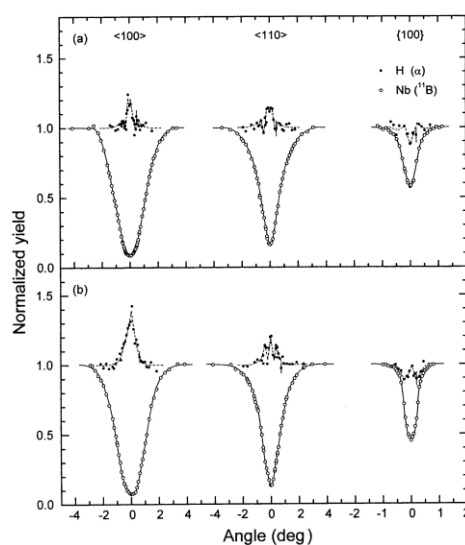


Fig. 1. Channelling angular profiles obtained for (a)  $\text{NbO}_{0.003}\text{H}_{0.003}$  and (b)  $\text{NbO}_{0.003}\text{H}_{0.019}$  specimens.

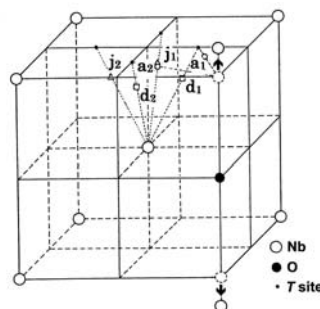


Fig. 2. Three types of probable sites for hydrogen trapped by oxygen.

### References

- 1) H. Wipf, A. Magerl, S. M. Shapiro, S. K. Satija, and W. Thomlinson: Phys. Rev. Lett. **46**, 947 (1981).
- 2) E. Yagi, T. Kobayashi, S. Nakamura, Y. Fukai, and K. Watanabe: J. Phys. Soc. Jpn. **52**, 3441 (1983).
- 3) E. Yagi, S. Koike, T. Matsumoto, T. Urai, and K. Ogiwara: Phys. Rev. B **66**, 024206 (2002).

† Condensed from the article in J. Phys. Soc. Jpn. **77**, 054802 (2008)

\*<sup>1</sup> RIKEN and The School of Sci. and Eng., Waseda University

\*<sup>2</sup> The School of Sci. and Eng., Waseda University

\*<sup>3</sup> Department of Physics, Tokyo University of Science

\*<sup>4</sup> Institute for Materials Research, Tohoku University

## Development of a multi-coincidence SIMS analyzer for study on potential sputtering of solid surfaces interacting with highly charged ions

K. Motohashi<sup>\*1</sup>, M. Flores, Y. Kanai, and Y. Yamazaki

The interaction between highly charged ions (HCIs) and solid surfaces has been attracting much attention because it induces effectively nanostructure formation<sup>1)</sup> and secondary particle emission<sup>2)</sup>. The secondary particle emission is also important as an initial process of nanostructure formation. The process is triggered by multi-electron capture by HCIs, and thus the process called “potential sputtering” is essentially different from any kinetic sputtering process. However, the details of potential sputtering by HCIs have not been clarified yet because of the experimental difficulty of separating it from the kinetic processes.

An experimental apparatus for studying the potential sputtering has been developed. The apparatus can simultaneously detect secondary electrons and secondary ions as well as scattered atoms and ions that captured electrons from the surface in off-normal incidence of HCIs<sup>3)</sup>. The velocity and charge state of scattered ions can also be analyzed with a Wien filter ( $E \times B$  filter) and a parallel plate analyzer, respectively. Therefore, the apparatus allows us to achieve coincidence experiments between time-of-flight secondary ion mass spectrometry (TOF-SIMS) and low-energy ion scattering spectroscopy (LEIS) of the scattered ions with a specific charge state. The coincidence measurement makes it possible to separate the potential sputtering from the kinematic ones. Further, it is also possible to achieve TOF-SIMS analysis of secondary ions in coincidence with that of secondary electrons<sup>4)</sup>.

Figure 1 shows a schematic illustration of the experimental setup at RIKEN. The charge state of HCI extracted from an electron beam ion source<sup>5)</sup> (EBIS) was analyzed by a magnet before this setup. After the adjustment of its trajectory and focus with an electrostatic lens (L) and four deflection plates ( $D_{1\perp}$ ,  $D_{1\parallel}$ ,  $D_2$ , and  $D_3$ ),

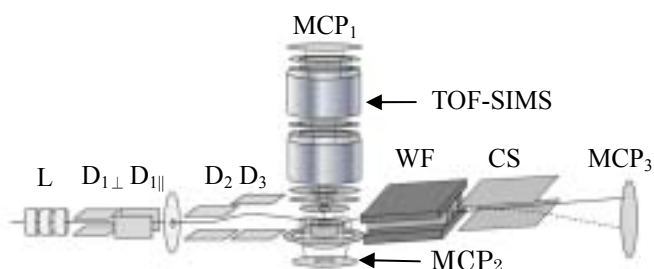


Fig. 1. Schematic illustration of the experimental setup developed to study the atomic processes of potential sputtering induced by highly charged ions.

L, lenses; D, deflection plates; WF, Wien filter; CS, charge separator; TOF-SIMS, time-of-flight secondary-ion mass spectrometer; MCP, multi-channel plate detectors

the HCI collides with a target surface at an off-normal or glancing angle. After its velocity and charge state are analyzed with the Wien filter and the parallel plates, ions scattered at the surface were detected by a two dimensional position sensitive detector (2D-PSD) denoted as MCP<sub>3</sub>. The time-of-flight of secondary ions (detected on MCP<sub>1</sub>) and the three waveforms from the MCP<sub>3</sub> were recorded event by event through a digital oscilloscope. The 2D position on the MCP<sub>3</sub> was obtained from the pulse heights of the waveforms.

The results of coincidence measurements between scattered ions and secondary ions in 2.5 keV Ar<sup>q+</sup> ( $q = 4$  and 6) incident on a GaN(0001) surface have already been reported<sup>3, 4)</sup>. It was found that kinetic processes between scattered Ar<sup>+</sup> and substrate atoms (Ga or N) on the surface play a role in the proton emission process<sup>6)</sup>.

The TOF-SIMS analysis can also be achieved by triggering with the signal of secondary electrons detected by MCP<sub>2</sub>. An example of the results is shown in Fig. 2 for Ar<sup>q+</sup> ( $q = 4 - 8$ ) hitting a dodecanethiol(C<sub>12</sub>H<sub>25</sub>SH)/Au(111) sample at 12° (tangential to the surface). The molecular ions fragmented from the alkane chain (CH<sub>2</sub>)<sub>11</sub> and the terminal functional group CH<sub>3</sub> were observed.

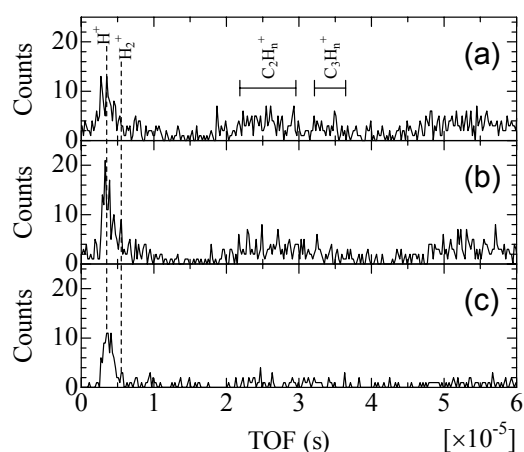


Fig. 2. TOF-SIMS spectra<sup>4)</sup> of a dodecanethiol/Au(111) surface interacting with slow (a) Ar<sup>4+</sup>, (b) Ar<sup>6+</sup>, and (c) Ar<sup>8+</sup> at 12° (tangential to the surface).

### References

- 1) A. S. El-Said *et al.*, Phys. Rev. Lett. **100** (2008) 237601.
- 2) M. Tona *et al.*, Phys. Rev. B **77** (2008) 155427.
- 3) K. Motohashi, e-J. Surf. Sci. Nanotech. **7** (2009) 21.
- 4) K. Motohashi *et al.*, J. Phys. Conf. Ser. (to be published).
- 5) K. Motohashi *et al.*, Rev. Sci. Instrum. **71** (2000) 890.
- 6) K. Motohashi, J. Phys. Conf. Ser. (to be published).

<sup>\*1</sup> Department of Applied Physics, Tokyo University of Agriculture and Technology

# Ion Coulomb crystals in a cryogenic linear RF octupole ion trap

K. Okada,<sup>\*1</sup> M. Wada, T. Takayanagi,<sup>\*1</sup> S. Ohtani,<sup>\*2</sup> H. A. Schuessler,<sup>\*3</sup>

Ion Coulomb crystals of laser-cooled ions are promising tools for quantum computing<sup>1)</sup>, studying ultra-cold ion-molecule collisions<sup>2)</sup>, tests of a possible variation of the fundamental physical constants<sup>3)</sup> and precision laser spectroscopy of unstable nuclear ions<sup>4)</sup>. A systematic study of ion Coulomb crystals was performed in Penning and Paul ion traps including its linear configurations so far. Laser cooling experiments in linear RF multipole ion traps and in particular an octupole trap have so far not been performed before our experiment<sup>5)</sup>. New features of Coulomb crystals not present in a linear Paul trap are expected in a higher order multipole trap due to the large almost field-free region in the middle of this trap.

Here we report the first observation of ion Coulomb crystals in a cryogenic linear RF octupole ion trap. Large and small Coulomb crystals of laser-cooled  $\text{Ca}^+$  ions have been observed. In addition we have systematically investigated the changes of the shapes of the crystals by varying the axial static voltages ( $V_{z0}$ ) and the asymmetric DC voltages ( $V_{dc}$ ).

The experimental setup is as follows. The octupole trap consists of eight cylindrical electrodes with a diameter of 2 mm. The distance from the center trap axis to the surface of the electrodes is a larger value ( $r_0 = 4.5$  mm) than the normal value ( $r_0 = 3$  mm) to increase the field of view. Although this trap configuration is not ideal, larger RF voltages reproduce an almost ideal effective potential. The vacuum chamber enclosing the ion trap is evacuated by a turbo molecular pump and an ion pump. In addition, the ion trap is mounted on a liquid-nitrogen vessel to obtain an ultra-high vacuum with  $P < 10^{-8}$  Pa. For laser cooling of  $\text{Ca}^+$  ions, two grating stabilized laser diodes ( $\lambda = 397$  nm and 866 nm) are used. Both the laser frequencies are locked to the temperature-controlled optical cavities. The laser-induced fluorescence (LIF) at 397 nm is observed by a cooled CCD camera at a right angle to the trap axis. The magnification of the lens system is  $6\times$ . A UV filter is used for the reduction of background photons.

Examples of the CCD images are shown in Fig. 1. For relatively small axial voltages, long prolate shapes of the ion crystals are observed when applying  $V_{dc}$ , while spherically symmetry shapes are observed for larger axial voltages (Fig. 1(a)). The clear shell structure can be recognized inside the crystals composed of  $\sim 400$  ions. The estimated interval between the shell is  $40\text{-}50$   $\mu\text{m}$ . Because of the small micromotion am-

plitudes in the central trap region, the clear shells are constructed. Single-ion sensitivity was also obtained as shown in Fig. 1 (b). The ions are not arranged like a string, but distributed in the oval with the ion-ion distance of about  $70$   $\mu\text{m}$ .

When a much larger number of ions are crystallized, the strange shape of the crystal emerges as shown in Fig.1 (c). The image was observed by setting the laser frequency to the position indicated by the arrow in the laser cooling spectrum of Fig. 1 (d). The number of ions is estimated to be  $N > 10^4$  using the uniform number density derived from the Coulomb crystal composed of a small number of ions such as Fig. 1(b). The ion temperature is estimated to be less than  $5$  mK from the residual Doppler width in the spectrum. Although the image is not clear, we recognize the dip along the trap axial direction. The reason of this interesting property is possibly attributed to the characteristic sum potential in the radial direction<sup>5)</sup>.

In summary, we have observed ion Coulomb crystals in the linear octupole ion trap for the first time. In the next step, the study of ultra-low energy ion-molecule collisions using a Stark decelerator is planned.

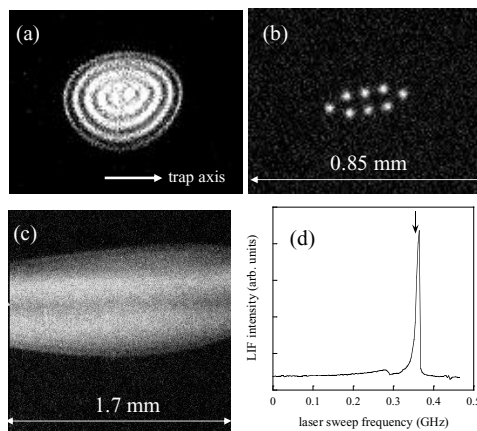


Fig. 1. Observed CCD images of the Coulomb crystal. The trapping parameters are  $f_{rf} = 6.04$  MHz,  $V_{ac} = 157$  V, and (a)  $V_{z0} = 3.40$  V,  $V_{dc} = 0.60$  V, (b)  $V_{z0} = 0.20$  V,  $V_{dc} = 0$  V, (c)  $V_{z0} = 0.80$  V,  $V_{dc} = 0$  V. The scale in the images of (a) and (b) is same.

## References

- 1) J. I. Cirac *et al.*: Phys. Rev. Lett. **74**, 4091 (1995).
- 2) S. Willitsch *et al.*: Phys. Rev. Lett. **100**, 043203 (2008).
- 3) U. Fröhlich *et al.*: Lecture Notes in Physics **648**, 297 (2004).
- 4) K. Okada *et al.*: Phys. Rev. Lett. **101**, 212502 (2008).
- 5) K. Okada *et al.*: Phys. Rev. A **75**, 033409 (2007).

<sup>\*1</sup> Department of Physics, Sophia University

<sup>\*2</sup> Institute for Laser Science, University of Electro-Communications

<sup>\*3</sup> Department of Physics, Texas A&M University

## Excitation spectrum of In atoms in superfluid helium

A. Sasaki,<sup>\*1</sup> T. Furukawa, K. Fujikake,<sup>\*2</sup> T. Kobayashi, A. Hatakeyama,<sup>\*3</sup> T. Shimoda,<sup>\*4</sup>  
H. Odashima,<sup>\*2</sup> and Y. Matsuo

Laser spectroscopy in superfluid He (He II) is useful for determining the spins and moments of unstable nuclei. We are planning to perform a systematic study of nuclear spins and moments of unstable nuclei stopped in He II, using laser-radiowave(RF)/microwave(MW) double resonance.<sup>1)</sup> Atomic polarization by optical pumping, however, has been achieved only with alkali and alkali-like elements, whose electronic energy level structure is rather simple.

On the other hand, non-alkali elements require a number of lasers of different wavelengths to achieve optical pumping due to their complicated energy level structures. To overcome this problem, we will use the unique spectral feature of atoms in He II. In general, the excitation spectra of atoms in He II are blue-shifted and significantly broadened from those in a vacuum due to interaction with surrounding He atoms.<sup>2)</sup> By using this characteristic, we expect that atomic polarization of non-alkali atoms by optical pumping can be achieved using a single laser.

Among non-alkali atoms, the Indium atom is an interesting candidate for generating atomic polarization. Indium has a proton number close to the magic number, while the electronic level structure of the third group elements such as In is not too complicated. To obtain a high atomic polarization, the wavelength of the excitation laser should be tuned to the absorption peak. However, a previously reported peak wavelength had large experimental uncertainties because the laser power correction was not sufficient. In this study, we measure the excitation spectrum of In in He II to obtain the absorption wavelength at the peak of the blue-shifted spectrum.

Figure 1 shows the experimental setup for spectrum measurement of In atoms in He II. The apparatus consists of a cryostat with quartz windows, a detection system, and three lasers. The bottom part of the cryostat contains liquid He. An open-top quartz cell is

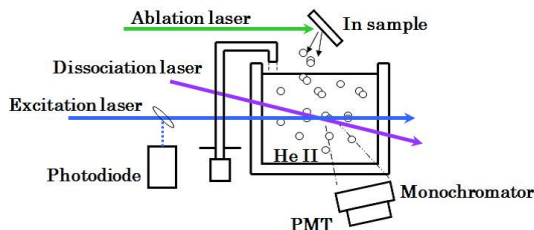


Fig. 1. Experimental setup.

placed above the liquid surface and is filled with He II by utilizing the fountain effect of He II. An In sample is irradiated by an ablation laser to introduce In atoms, ions, and clusters into He II. Because clusters are predominantly produced in laser ablation compared with atoms, the clusters are dissociated using a dissociation laser, typically producing  $10^6$  atoms in the observation region. The atoms that absorb the excitation laser light are excited from the ground  $P_{1/2}$  state to the  $S_{1/2}$  excited state, and emit fluorescence. The fluorescence is discriminated with a monochromator fixed at an In emission wavelength of 451 nm, and detected by a photomultiplier tube (PMT). The detection signal is captured by a gated integrator and recorded in a computer. In this experiment, pulsed dye lasers with four types of dyes are used to cover the excitation wavelengths from 350 nm to 390 nm. The spectrum observed using each dye is normalized for laser intensity. The normalized spectra are then combined with each other.

The obtained excitation spectrum of In atoms is shown in Fig. 2. The wavelength of the excitation peak observed at approximately 370 nm is found to be 5 nm longer than that previously reported.<sup>3)</sup> Atomic polarization will hence be produced efficiently by optical pumping in the vicinity of 370 nm. To determine the absorption peak position more precisely, we are planning to measure the excitation spectrum around the 370 nm wavelength in detail. An optical pumping experiment of In atoms using a 370 nm laser is also in progress.

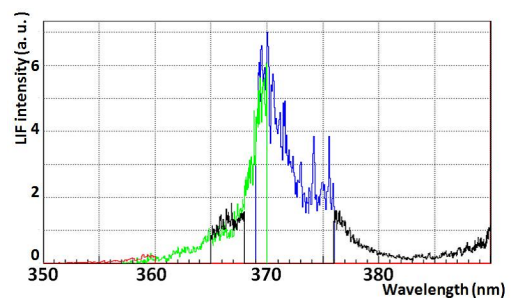


Fig. 2. Excitation spectrum of  $^{115}\text{In}$  in He II. The excitation peak is observed at approximately 370 nm. LIF intensity fluctuates due to fluctuation in the number of atoms in the ablation and dissociation processes.

### References

- 1) T. Furukawa et al.: Proc. International Nuclear Physics Conference (INPC2007), (Tokyo 2007) Vol. 2, pp. 624.
- 2) B. Tabbert et al.: J. Low. Temp. Phys. **109**, 653 (1997).
- 3) Q. Hui: Doctoral thesis, Saitama Univ. (1997)

\*1 Department of Physics, Tohoku University

\*2 Department of Physics, Meiji University

\*3 Department of Applied Physics, Tokyo Univ. Agr. Tech.

\*4 Department of Physics, Osaka University

## **2. Atomic and Solid State Physics(muon)**

## Installation of a new laser system for laser-irradiated pump-probe type $\mu$ SR experiments at RIKEN-RAL muon facility

P. Bakule,<sup>\*1,\*2</sup> Y. Matsuda,<sup>\*3</sup> H.W.K. Tom,<sup>\*4</sup> K. Yokoyama,<sup>\*4</sup> F.L. Pratt,<sup>\*2</sup> E. Torikai,<sup>\*5</sup> K. Shimomura,<sup>\*6</sup> and K. Nagamine<sup>\*4,\*6</sup>

Q-switched lasers (1-200 ns pulse duration) are ideally matched to pulsed muon sources (100 ns pulse duration) and yet so far there were only very few experiments that used lasers for synchronized sample excitations<sup>1,2</sup>). Use of laser pulses synchronized with muon implantation provides an extremely useful tool that extends the scope of  $\mu$ SR spectroscopy. Depending on the photon energy, the laser irradiation will cause coherent electron excitation or ionization in the studied sample or even affect the muonium state directly (e.g. convert diamagnetic  $\text{Mu}^-$  state to paramagnetic  $\text{Mu}$ ). Additionally, circularly polarized light can induce spin polarization of the excited electrons in the sample. The effects of the pump laser pulse on the sample can then be sensitively probed using  $\mu$ SR technique. The time difference between the muon implantation and the laser irradiation can be easily controlled on a nanosecond scale and such pump-probe experiments can then also provide measurement of the decay time constant of the generated excitation.

To allow routine use of such pump-probe technique we have built a dedicated laser room and laser beam delivery system next to the ARGUS  $\mu$ SR spectrometer (Fig. 1) at RIKEN RAL muon facility. The laser system was built by pooling equipment together in close collaboration between RIKEN, KEK, Yamanashi University, University of California and ISIS and is based on an optical parametric oscillator (Continuum Panther EX OPO) pumped by a Nd:YAG laser (Continuum Powerlite 9025). The OPO parameters are summarized in Table 1.

The laser, operating at 25 Hz, is fired at every second muon pulse (50 Hz) so that half of the data is taken with *laser-on* and half with *laser-off*. The output is linearly polarized and we have additionally built an optical setup for sample irradiation with left-hand and right-hand circularly polarized light including pulse-to-pulse control of the polarization.

The laser parameters, such as the wavelength, pulse energy and timing, are controlled in a user friendly manner consistent with the computer control of other

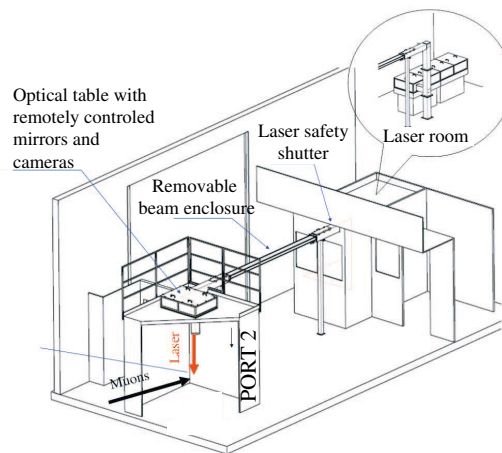


Fig. 1. Layout of the laser enclosure and beam delivery to  $\mu$ SR sample

Wavelength range (signal)	400 - 700 nm (3.1 - 1.8 eV)
Wavelength range (idler)	715 - 2500 nm (1.7 - 0.5 eV)
Pulse energy	1-70 mJ
Pulse duration	9 ns
Repetition rate	25 Hz
Polarization	Controlled pulse-to-pulse (linear, circular, elliptical)

Table 1. Summary of the OPO laser parameters

experimental parameters such as magnetic field or sample temperature.

The laser beam is steered onto the sample through a light-tight beam delivery system using broadband HR mirrors ( $R > 99\%$  over 350-1150 nm), some of which are remotely controlled. Samples are typically mounted in a vacuum chamber on mini-cryostat capable of reaching temperatures of about 15 K. Different mirror and sample configurations are possible where either the front or rear surface of the sample is irradiated.

The system can be also used for experiments at discrete Nd:YAG wavelengths (1064 nm, 532 nm, 355 nm) - see e.g. recent experiment on reaction dynamics of muonium<sup>3</sup>).

### References

- 1) E. Torikai et al: Physica B **289-290** (2000), p. 558.
- 2) K. Ghandi et al.: Phys. Chem. Chem. Phys. **9** (2007), p. 353.
- 3) P. Bakule et al.: Physica B **404** (2009), p.1013.

\*1 Advanced Meson Science Laboratory, RIKEN Nishina Center

\*2 ISIS Muon Facility, Rutherford Appleton Laboratory, United Kingdom

\*3 Graduate school of Arts and Sciences, University of Tokyo

\*4 Department of Physics and Astronomy, University of California, Riverside, USA

\*5 Yamanashi University, Faculty of Engineering, Kofu

\*6 Muon Science Laboratory, High Energy Accelerator Research Organization

# Muons for Spintronics: Spin Exchange Scattering of Muonium with Laser-Induced Polarized Conduction Electrons in *n*-Type GaAs

K. Yokoyama<sup>1</sup>, K. Nagamine<sup>1,2</sup>, K. Shimomura<sup>2</sup>, H.W.K. Tom<sup>1</sup>, R. Kawakami<sup>1</sup>, P. Bakule,  
Y. Matsuda<sup>\*</sup>, K. Ishida, K. Ohishi, F.L. Pratt<sup>3</sup>, I. Shiraki<sup>4</sup> and E. Torikai<sup>4</sup>

In order to develop materials and spin injection methods for spintronics, it is essential to establish the experimental methods by which to detect conduction electron polarization (CEP).

In the case of GaAs, because of a large spin-orbit interaction and a direct band gap, CEP can be produced through the electron excitation from a valence-band by circularly polarized (CP) laser and CEP detection is also performed with optical methods [1]. In contrast, for Si, Ge or Graphite, the optical methods can not be applied due to a small spin-orbit interaction and an indirect band gap.

Use of polarized ortho muonium (Mu, a bound state of positive muon ( $\mu^+$ ) and electron with spins aligned in the same direction) is a sensitive tool for CEP detection; the spin of the electron bound to  $\mu^+$  can be affected by a replacing it with a polarized conduction electron through an exchange scattering between the Mu electron and the electron in a conduction band. This muon method was proposed at KEK by Torikai et al. [2]. The present experiment is a feasibility study of the muon method to detect CEP in *n*-type GaAs whose properties are well known [1].

The experiment was conducted at Port 2 of the RIKEN-RAL Muon facility using a pulsed 4 MeV positive muon beam. The sample used was 360  $\mu\text{m}$  thick 50.8 mm diameter single crystalline GaAs with  $3 \times 10^{16} \text{ cm}^{-3}$  Si doping. The tunable laser light around 831 nm with a repetition frequency of 25 Hz was generated using a widely tunable OPO system pumped by 355 nm Nd:YAG laser. The linearly polarized laser was passed through an optical setup that converts the linearly polarized light to circularly polarized light illuminating the sample. Here, Pockel's cell (PC) is used for pulse-to-pulse control of switching between right-hand CP light ("R") and left-hand CP light ("L"). A laser pulse with a pulse length of 10 ns was arranged to irradiate the GaAs sample at 1  $\mu\text{s}$  after muon pulse.

The sample was placed in a strain-free manner by using a specially designed sample holder containing He gas.

The typical  $\mu\text{SR}$  time spectrum under 0.1 T at 15 K with laser irradiation is shown in Fig. 1, representing data under the conditions of "L" and "R" with reference to "Off". An exponential relaxation component corresponding to BC-Mu (Mu at body-center site) state observed in the "Off" data exists after laser irradiation, almost as it did in terms of amplitude and relaxation rate before irradiation. An insensitive response of BC-Mu to laser irradiation can be concluded.

<sup>4</sup>Medicine and Engineering, University of Yamanashi

<sup>\*</sup>Present address; Arts and Science, University of Tokyo

The "L-R" effect has a characteristic dependence on the external field. The effect which clearly exists below 0.1 T disappears above 0.2 T. There, the hyperfine magnetic field from the bound electron is decoupled by the external field so that the polarization change of the bound electron does not affect  $\mu^+$  polarization. Since the BC-Mu is now known to be insensitive, the muon state responding to the laser should be concluded as T-site Mu (Mu at tetrahedral site) state and/or  $\text{Mu}^-$  (bound state of  $\mu^+e^-$ ) state.

We then measured the dependence of the polarization effect on laser power by reducing laser power from 2.25 mJ down to 0.4 mJ. An increase of the "L-R" polarization effect with reference to "Off-On" effect was observed, which is consistent with the result of the increased spin life time against decrease of laser power in this power range observed in the optical measurement [1].

Also, by raising temperature, although the "On-Off" effect stays unchanged, the "L-R" effect began to disappear. The result is again consistent with decreased spin life time at higher temperature observed by the optical method [1].

In conclusion, the exchange scattering of the muonium was proved to detect CEP produced by circularly polarized lasers in *n*-type GaAs. Correct response of the signal was obtained, which is consistent with the CEP properties of the *n*-type GaAs sample known through the optical measurement [1]. The result of the present feasibility measurement for *n*-GaAs is encouraging for the muon method to be applied to CEP detection in many other spintronics materials such as Si, Ge, Graphite, etc.

## References

- [1] J.M. Kikkawa and D.D. Awschalom, Phys. Rev. Lett. **80**, 4313 (1998) and references therein.  
[2] E. Torikai et al., Physica B **289-290** (2000) 558-562.

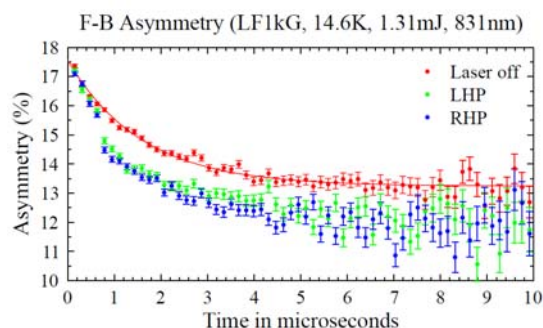


Fig. 1. The  $\mu\text{SR}$  time spectrum at 15 K and under 0.1 T with 3 laser conditions at 1  $\mu\text{s}$  after muon pulse; "Off" is shown by red points, "L" (Para) is shown by green points and "R" (Anti) is shown by blue points. A clear polarization effect can be seen.

<sup>1</sup>Physics Department, University of California, Riverside

<sup>2</sup>Muon Science Laboratory, IMSS, KEK

<sup>3</sup>ISIS, Rutherford Appleton Laboratory

## Discovery of Spin-Dependent Response of Negative Muonium ( $\text{Mu}^-$ ) to Laser Induced Polarized Electrons in $n$ -Type GaAs under Zero Field

K. Yokoyama<sup>1</sup>, K. Nagamine<sup>1,2</sup>, K. Shimomura<sup>2</sup>, H.W.K. Tom<sup>1</sup>, R. Kawakami<sup>1</sup>, P. Bakule, Y. Matsuda<sup>\*</sup>, K. Ishida, K. Ohishi, F.L. Pratt<sup>3</sup>, I. Shiraki<sup>4</sup> and E. Torikai<sup>4</sup>

In order to promote the spintronics, a use of spin-dependent exchange scattering between a polarized electron in ortho muonium (ortho-Mu,  $\mu^+e^-$ , a bound state of positive muon and an electron with the spins aligned in the same direction) to detect the conduction electron polarization (CEP) in semiconductors has been proposed at KEK by Torikai et al. [1]. Recently a feasibility study of the method was successfully carried out on a strain-free  $n$ -type GaAs ( $3 \times 10^{16} \text{ cm}^{-3} \text{ Si}$ ) by measuring a change in the  $\mu^+$  polarization in Mu against a relative directional change of the polarization under external longitudinal fields above 20 mT [2]. In  $n$ -type GaAs, CEP is produced by circularly polarized (CP) lasers due to a strong spin-orbit coupling and a direct band-gap. Observations consistent with the properties of the CEP known in optical experiments were obtained in the feasibility study [2].

On the other hand, the properties of muonium in undoped and doped GaAs have been thoroughly studied. The existence and properties of  $\text{Mu}^-$  ( $\mu^+e^-e^-$ , a diamagnetic bound state of  $\mu^+$  and the two electrons with a singlet coupling at the ground state) in  $n$ -type GaAs with Si doping concentration higher than  $10^{16}$  are known [3].

During the course of the feasibility experiment [2] conducted at Port 2 of the RIKEN-RAL, the present measurement was conducted by using a pulsed 4 MeV positive muon beam. A surprising spin-dependent response of the  $\text{Mu}^-$  was found.

The tunable laser light around 831 nm/1.49 eV with 25 Hz repetition frequency was generated using a widely tunable OPO system. As described [2], linearly polarized laser output was converted to CP light illuminating the sample. The Pockel's cell (PC) is used for pulse-to-pulse switching between right-hand CP light ("R") and left-hand CP light ("L"). A laser pulse with a pulse length of 10 ns was irradiated at 1  $\mu\text{s}$  after the muon pulse.

The obtained  $\mu\text{SR}$  time spectrum under zero field (ZF) at 15 K (Fig. 1) represents ZF muon spin relaxation data under the conditions of "L" and "R" with reference to "Off".

Combined with other high-statistics measurements, asymmetry amplitudes of the ZF "Off" at 15 K comprises  $\text{Mu}^-$  state with Gaussian relaxation (5.70(6) %) and 1/6 component of both BC-Mu (Mu at body-center site) with exponential relaxation (nearly 1.0 %) and T-Mu (Mu at tetrahedral site) with almost no relaxation (nearly 1.0 %).

In ZF "Off" (Fig. 1), major 5/6 components of full asymmetry of BC-Mu and T-Mu (amounting in total to 14 %) are missing due to hyperfine interaction in Mu and a nuclear hyperfine field on the remaining ortho Mu.

As for the polarization-dependent "L-R" effect, the following observations can be readily obtained: 1) the major component with Gaussian relaxation at "Off", which corresponds to the  $\text{Mu}^-$  state, does change against the change of CP of the laser irradiation; 2) As for the data under longitudinal fields above 20 mT [2], because of an unchanged exponentially decaying component before and after laser irradiation, the insensitive nature of the BC-Mu to the laser irradiation can be concluded. At the same time, the tail region of the relaxation function which represents a 1/6 component of T-Mu does not change. Thus, a major contribution to the ZF "L-R" effect may be concluded to be due to the  $\text{Mu}^-$  state.

In order to confirm the  $\text{Mu}^-$  dominance in "L-R" effect the polarization dependence of the TF rotation under 2 mT was measured with a laser timing set at 100 ns after the muon pulse. The shift of the laser timing was made in order to maximize the polarization effect in TF data. A clear "L-R" effect was observed in the amplitude of the remaining rotating component (0.30(4) %) with a phase shift corresponding to the time delay (0.24(8)  $\mu\text{s}$ ).

In order to understand the observed  $\text{Mu}^-$  response, a two-step process can be considered; (1) spin-independent one-electron removal collision between  $\text{Mu}^-$  and laser induced conduction electron followed by a formation of ortho Mu (50 %) and (2) spin-dependent ionization in between ortho Mu and polarized laser induced conduction electrons to produce  $\mu^+$  in a spin-dependent manner.

[1] E. Torikai *et al.*, *Physica B* **289-290** (2000) 558-562.

[2] K. Yokoyama *et al.* in this Progress Report (2009).

[3] K.H. Chow, B. Hitti and R. Kiefl, *Semiconductors and Semimetals*, **51a**, 137 (1997).

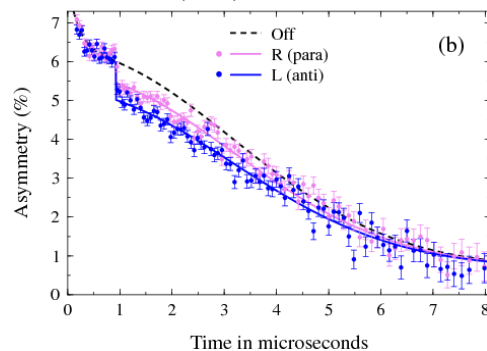


Fig. 1. Muon-spin-relaxation time spectrum under ZF in  $n$ -GaAs at 15 K with laser injection at 1  $\mu\text{s}$ , representing the polarization effect.

<sup>1</sup>Physics Department, University of California, Riverside

<sup>2</sup>Muon Science Laboratory, IMSS, KEK

<sup>3</sup>ISIS, Rutherford Appleton Laboratory

<sup>4</sup>Medicine and Engineering, University of Yamanashi

<sup>\*</sup>Present address; Arts and Science, University of Tokyo

# Measurement of the Chemical Reaction Rate of Muonium with Stimulated Raman-Pumped $\text{H}_2^*(v=1)^\dagger$

D.G. Fleming,<sup>\*1</sup> P. Bakule,<sup>\*2,\*4</sup> O. Sukhorukov,<sup>\*1</sup> Y. Matsuda,<sup>\*3</sup> F.L. Pratt,<sup>\*4</sup> P. Gumplinger,<sup>\*5</sup> T. Momose,<sup>\*6</sup> and E. Torikai<sup>\*7</sup>

Stimulated Raman pumping (SRP) is used to produce  $\text{H}_2$  in its first vibrational state, in order to measure, for the first time, the  $\text{Mu} + \text{H}_2^*(v=1) \rightarrow \text{MuH} + \text{H}$  reaction rate at room temperature, as a prototypical example of new directions in gas-phase muonium chemistry, utilizing the pulsed muon beam and a new dedicated laser system at the RIKEN/RAL Laboratory.

This experiment will provide new tests of reaction rate theory in the fundamental  $\text{H}_3$  system<sup>1,2)</sup> in three important ways:

- Since the pumped  $v=1$  state is not in thermal equilibrium, accurate TST calculations are not feasible, mandating rigorous 3D quantum rate calculations.
- The barrier to reaction is so much lower than for the GS, that rigorous calculations of the barrier height, including non-BO corrections, are required.
- At the temperatures of the experiment, quantum tunneling of Mu can be expected to play a major role, in contrast to the GS reaction, providing a further constraint on accuracy of the 3D quantum calculations needed.

The experiment utilizes the 2<sup>nd</sup> harmonic output of a Nd:YAG laser (532 nm) with pulse energies up to 500 mJ at a repetition rate of 25 Hz exciting up to  $8 \times 10^{17}$   $\text{H}_2$  molecules to  $v=1$  state. The muon stopping distribution in pure  $\text{H}_2$  at 50 bar has a variance  $\sigma$  of 11 mm and therefore the major difficulty in this experiment, compared to the standard SRP process, is to ensure a homogeneous excitation over a volume of several  $\text{cm}^3$  and a sufficient pressure of  $\text{H}_2^*(v=1)$  to ensure a measurable Mu relaxation rate. To optimize all of these requirements different optical setups have been constructed and tested.

<sup>†</sup> Condensed from the article in *Physica B*, **404**, 5-7 (2009); doi:10.1016/j.physb.2008.11.230

<sup>\*1</sup> TRIUMF and Department of Chemistry, University of British Columbia, BC., Canada

<sup>\*2</sup> Advanced Meson Science Laboratory, RIKEN Nishina Center, Wako, Saitama 351-0198, Japan

<sup>\*3</sup> Graduate school of Arts and Sciences, University of Tokyo, Komaba 3-8-1, Meguro, Tokyo 153-8902, Japan

<sup>\*4</sup> ISIS Muon Facility, Rutherford Appleton Laboratory, Harwell Science and Innovation Campus, Didcot, OX11 0QX, United Kingdom

<sup>\*5</sup> TRIUMF Laboratory, 4004 Wesbrook Mall, Vancouver, BC., Canada

<sup>\*6</sup> Depts. of Chemistry and Physics, University of British Columbia, Canada

<sup>\*7</sup> Yamanashi University, Faculty of Engineering, Kofu, Yamanashi 4008511, Japan

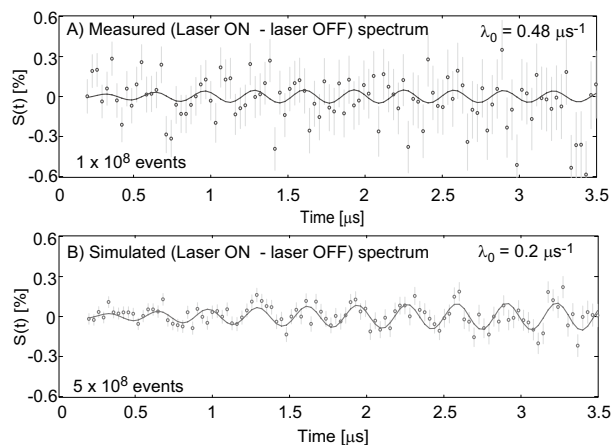


Fig. 1. A) experimental signal; B) simulated difference signal (see text)

The first result of this experiment gives a measured relaxation rate due to the laser excitation of  $\lambda^* = 0.085 \pm 0.051 \mu\text{s}^{-1}$ , consistent with theory but limited by both low statistics and particularly by a high background relaxation rate (about 5 times larger than  $\lambda^*$ ). The signal of interest in this experiment is the difference in  $\mu\text{SR}$  spectra for *laser ON* - *laser OFF* defined by  $S(t)$  in ref<sup>3)</sup>. Most variables in  $S(t)$  can be determined from the *laser OFF* experiments (muonium asymmetry  $A_{Mu}$ , background relaxation rate  $\lambda_0$ , muonium rotation frequency and phase) and the only parameters that need to be fitted are  $\lambda^*$  and the fraction  $f$  of Mu atoms that overlap with the laser pumped  $\text{H}_2^*(v=1)$  volume. Figure 1(A) shows a fit of  $S(t)$  to the experimental data for TF of 2.22 G,  $\lambda_0 = 0.48 \mu\text{s}^{-1}$ , muonium asymmetry  $A_{Mu} = (4.32 \pm 0.07)\%$  and  $f=0.4$  giving the above value for  $\lambda^*$ . The poor signal-to-noise ratio observed here should be significantly improved in the future experiments by reducing the background relaxation rate (originating mostly from magnetic field inhomogeneity) which damps the  $S(t)$  by a factor of  $\exp(-\lambda_0 t)$ . This is demonstrated in Fig. 1(B) showing simulated data assuming  $\lambda_0 = 0.20 \mu\text{s}^{-1}$  and improved statistics ( $5 \times 10^8$  events). The necessary improvement in the field inhomogeneity can be achieved through either unbalanced control of the existing Helmholtz coils or specifically designed compensation coil(s) placed around the sample cell.

## References

- 1) S.L. Mielke et al.: *Phys. Rev. Lett.* **91**, 6 (2003).
- 2) S.L. Mielke et al.: *J. Chem. Phys.* **122**, 22 (2005).
- 3) P. Bakule et al.: *Physica B* **404**, 5-7 (2009).

## Progress in design and development of counter system for new $\mu$ SR spectrometer at RIKEN-RAL

D. Tomono, T. Kawamata, Y. Hirayama<sup>\*1</sup>, M. Iwasaki<sup>\*1</sup>, I. Watanabe, K. Ishida and T. Matsuzaki

A new research project to explore various matters under multiple extreme conditions, such as high pressure, low temperature, etc. combined with  $\mu$ SR technique, has recently been launched using the high intensity beam at RIKEN-RAL. For this purpose, a high performance and multi-purpose spectrometer is being developed at the Port-4 area. A multi-segmented detector capable of measuring decay positrons with less signal pile-up, operating photomultiplier tube (PMT) remote from the magnetic field and mounting scintillators in the narrow space is essential for the setup and optimization of the performance of  $\mu$ SR spectrometers. Our recent feasibility test of the prototype counters<sup>1,2)</sup> showed that we can selectively observe positrons within 7 degrees from a muon stopping sample using spindle scintillator, wave-length shifting fibers, clear fibers and multi-anode PMT (MAPMT). Based on this test, a new counter system to fabricate the spectrometer has been designed and a data acquisition system was built in parallel.

Figure 1 shows pictures of counters and coils of the new spectrometer. The basic parts shown in Fig. 1 left, are longitudinal Helmholtz coils of 150 mm bore up to field of 0.4 T, transverse coils and 3 pairs of field cancellation coil. The polarization of muons stopped in a sample is determined by two counter assemblies located at the core of longitudinal coils, which were up-and downstream to the muon beam direction. The wavelength shifting fiber of 1.5 mm diameter (Kuraray Y-11(400)MS) is buried at the center of spindle counter ( $10 \times 10 \times 40$  or  $50 \text{ mm}^3$ )<sup>a)</sup> and tightly connected the clear fiber of 2.5 m length (Kuraray) as a light guide (Fig. 1 top-right). 16 clear fibers are bundled and connected to the MAPMT (H6568-10-200mod). The 606 counters are mounted in two special bases (Fig. 1 bottom-right). They are attached at the bore of the longitudinal magnet.

Figure 2 shows the muon decay time spectrum using practical 16 counters. Although a constant background component usually exists around  $10^{-3}$  of the statistics at  $t = 0$  due to the charged particles outside from the sample, it is not observed, at least, in less than  $3 \times 10^{-5}$  owing to direction sensitive mechanism<sup>1,2)</sup>.

A scheme of data acquisition system is briefly described in Fig. 3. The VME-based data acquisition with Linux software is built for data acquisition of the counters. The front end software (MACS/Windows<sup>3)</sup>)



Fig. 1. Pictures of counters and coils. (left) Counter base and coils. At the core of the longitudinal coil, a counter base is installed to mount scintillation counters. The 606 clear fibers mediate photons between counters and PMTs installed beneath coils. (top-right) Counters and optical fibers. (bottom-right) Counters mounted in the counter base.

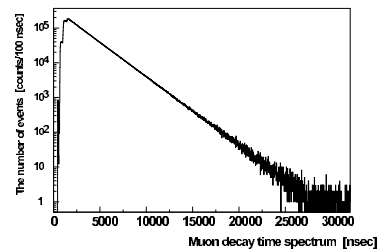


Fig. 2. Muon decay time spectrum. A constant background component is suppressed in less than less than  $3 \times 10^{-5}$  of the statistics at  $t=0$ .

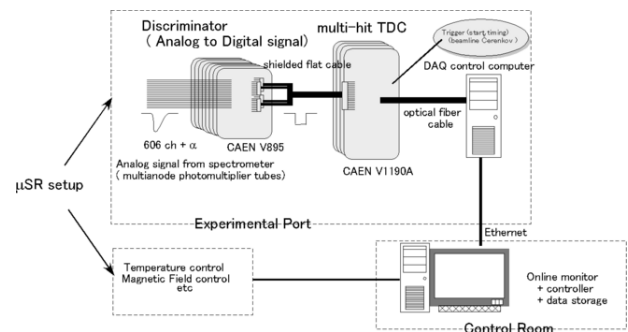


Fig. 3. Schematic figure of DAQ system. controls overall of the DAQ and slow-control system for temperature and magnet.

In summary, the new  $\mu$ SR spectrometer is designed and being constructed at RIKEN-RAL. The spectrometer installation at Port-4 and commissioning test are currently underway.

### References

- 1) Y. Hirayama, et al.: RIKEN Accel. Rep. **41** (2008).
- 2) D. Tomono, et al.: Nucl. Inst. Meth. A **600**(2009)44.
- 3) F. Pratt: RIKEN-RAL Report **4**(2001)26.

<sup>\*1</sup> also Department of Physics, Tokyo Institute of Technology

<sup>a)</sup> This scintillator is originally manufactured by TRIUMF group for the T2K near detector. We modified this scintillator for our requirements.

## $\mu$ SR study around a quantum critical point in heavy fermion compounds $\text{Ce}_2\text{RhIn}_{8-x}\text{Sn}_x$

K. Ohishi, T. Suzuki, R. H. Heffner,<sup>\*1,\*2</sup> T. U. Ito,<sup>\*1</sup> W. Higemoto,<sup>\*1</sup> and E. D. Bauer,<sup>\*2</sup>

Quantum phase transitions have attracted a great deal of attention on both the theoretical and experimental sides. Such transitions occur at zero temperature as a function of an external parameter (i.e., magnetic field, pressure or impurity concentration) which drives the system from an ordered to a disordered state. Heavy fermion compounds provide the opportunity to study such phenomena since the competition between ordering (via the RKKY interactions) and disordering (via the Kondo singlet formation) can easily be experimentally controlled.

The heavy fermion compound  $\text{Ce}_2\text{RhIn}_8$  is known as an antiferromagnet with  $T_N = 2.8$  K.<sup>1)</sup> Recently, it has been found that chemical substitution of Sn for In in  $\text{Ce}_2\text{RhIn}_{8-x}\text{Sn}_x$  depresses  $T_N$  with a critical concentration of about  $x \sim 0.5$ , suggesting the emergence of a quantum critical point.<sup>2)</sup> We have performed muon spin relaxation ( $\mu$ SR) measurements on several components of  $\text{Ce}_2\text{RhIn}_{8-x}\text{Sn}_x$  in order to investigate the evolution of magnetic order in this system.

In the previous report,<sup>3)</sup> we summarized the zero field (ZF)- $\mu$ SR results with  $x = 0.5$  and  $0.7$  above  $T \geq 0.3$  K. We found that the muon spin relaxation increased below  $0.5$  K with  $x = 0.5$ , while the muon spin precession signal was not observed. On the other hand, there was no increase in the relaxation rate with  $x = 0.7$  at low temperature. In order to study the observed relaxation below  $0.5$  K with  $x = 0.5$  in detail, we planned to perform ZF- $\mu$ SR experiments down to  $20$  mK. However, there was a problem with the dilution refrigerator (DR) so we could not perform  $\mu$ SR experiments with  $x = 0.5$  and  $0.7$  samples down to  $20$  mK. Hence, we changed the plan. Another important issue is to study the parent material as a reference for microscopically clarifying the systematic change of internal magnetic field with Sn-substitution. We have performed  $\mu$ SR experiments on  $\text{Ce}_2\text{RhIn}_8$  at temperatures from  $0.3$  K to  $5.0$  K on a single crystal flat plate with the  $c$  axis along the muon beam. The  $\mu$ SR measurements were conducted at the RIKEN-RAL Muon Facility in the Rutherford Appleton Laboratory, UK. In this report, we present preliminary results.

Figure 1 shows the ZF- $\mu$ SR time spectra at  $3.7$  K and  $0.3$  K. At higher temperatures above  $T_N$ , the time spectra consist of two components, i.e., one showing slow relaxation  $P_z(t)$  due to random local fields from nuclear magnetic moments, and the other mostly independent of time. More specifically, we have  $A(t) =$

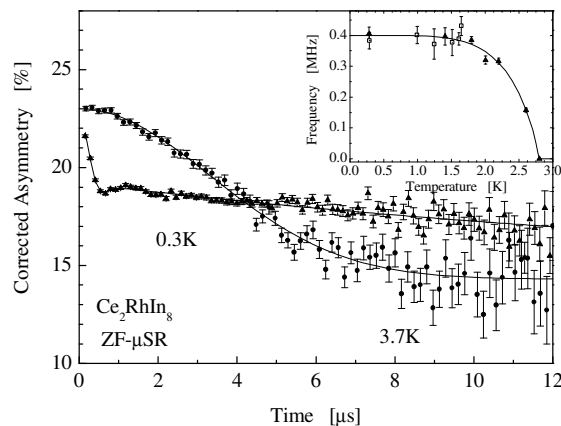


Fig. 1. ZF- $\mu$ SR time spectra in  $\text{Ce}_2\text{RhIn}_8$  at  $3.7$  K and  $0.3$  K. The solid lines are fits as described in the text. Inset shows the temperature dependence of muon spin precession frequency below  $T_N$ . The line is guide for the eyes.

$AP_z(t) + B$ , where  $A$  and  $B$  are the initial  $\mu$ -e decay asymmetry for the respective component, and  $P_z(t) = \exp(-\Delta^2 t^2)$  with  $\Delta/\gamma_\mu$  being the rms value of random local field (where  $\gamma_\mu = 2\pi \times 135.54$  MHz/T is the muon gyromagnetic ratio). The time spectra were well reproduced by the above formula with  $\Delta \simeq 0.214(5) \mu\text{s}^{-1}$  which is mostly due to  $^{113,115}\text{In}$  nuclear moments and is consistent with the previous results.<sup>3)</sup> The second “background” component is attributed to the silver sample holder and  $A/B$  is estimated to be  $0.589(14)$ . For  $T < T_N$ , we found that  $P_z(t) = (1 - s) \exp(-\sigma^2 t^2) \cos(2\pi f t + \phi) + s \exp(-\lambda t)$  reproduces the spectra, where  $\sigma$  and  $\lambda$  are the relaxation rates,  $f$  is the muon spin precession frequency under a local field  $H_{loc}$ ,  $\phi$  is the initial phase and  $s$  is the fraction. As shown in Fig. 1, a clear precession signal was observed below  $T_N$ . The volume fraction of the antiferromagnetic component at  $0.3$  K was estimated to be  $\sim 56\%$ . The temperature dependence of  $f$  is shown in the inset of Fig. 1. The  $f$  increases below  $T_N$  with the development of the internal magnetic field, while the temperature dependence of  $s$  does not show any change.

### References

- 1) J. D. Thompson et al.: J. Magn. Magn. Mater. **266-230**, 5 (2001).
- 2) E. D. Bauer: Unpublished results.
- 3) K. Ohishi et al.: RIKEN Accel. Prog. Rep. **41** (2008).

<sup>\*1</sup> Advanced Science Research Center, Japan Atomic Energy Agency

<sup>\*2</sup> Los Alamos National Laboratory, USA

# On the exotic magnetic ground state in bond-disordered quantum spin system IPA-Cu(Cl,Br)<sub>3</sub>

T. Goto,<sup>\*1</sup> T. Suzuki, S. Nakajima,<sup>\*1</sup> K. Doi,<sup>\*1</sup> I. Watanabe and H. Manaka<sup>\*2</sup>

The quantum spin system (CH<sub>3</sub>)<sub>2</sub>CHNH<sub>3</sub>-Cu(Cl<sub>x</sub>Br<sub>1-x</sub>)<sub>3</sub> abbreviated as IPA-Cu(Cl<sub>x</sub>Br<sub>1-x</sub>)<sub>3</sub> is a solid solution of two spin gap systems (CH<sub>3</sub>)<sub>2</sub>CHNH<sub>3</sub>-CuCl<sub>3</sub> and (CH<sub>3</sub>)<sub>2</sub>CHNH<sub>3</sub>-CuBr<sub>3</sub>, whose energy gaps are 14 K and 98 K respectively. So far, macroscopic experiments on this system have indicated that it becomes gapless and show a magnetic order at  $T_N=12-18$ K depending on  $x$  only when  $x$  is within the limited region between the two quantum critical points (QCPs) of  $x_C = 0.44$  and  $0.87$ , and otherwise it possesses a spin gap [1]. However, theoretical investigation by the quantum Monte Carlo method showed that the region of  $x < 0.44$  should be gapless though the occurrence of magnetic order is critical [2].

We have investigated by muon spin relaxation ( $\mu$ SR) the ground state of the two samples with  $x=0.40$  and  $0.45$ , which straddle the QCP  $x_C=0.44$ . Experiments were performed at both RAL and PSI. The incident muon beam was directed parallel with the  $b^*$ -axis of aggregation of crystals which were aligned and set onto the silver plate[2]. The muon spin relaxation in both the samples over the entire temperature and field region was described by a function containing two components expressed as

$$A_1 G_{KT}(\tau, \Delta) \exp(-t/\lambda_1) + A_2 \exp(-\tau/\lambda_2)$$

where  $G_{KT}$  is the Kubo-Toyabe function with parameters of a static field distribution width at the muon site  $\Delta$ , relaxation rates  $\lambda_1$  and  $\lambda_2$ , and component amplitudes  $A_1$  and  $A_2$ . The static field distribution width  $\Delta$  was around  $0.2$  ( $\mu\text{s}^{-1}$ ), temperature independent within the experimental resolution, and considered to be due to the nuclear contribution. The magnitude of  $\lambda_2$  always exceeded  $\lambda_1$  by more than ten times. These results mean that the sample is intrinsically in a microscopic phase separation of the two phases, namely, the magnetic region with microscopic island form corresponding to  $\lambda_2$ , and the singlet-like sea, which corresponds to  $\lambda_1$  and surrounds the former[3]. The amplitude fraction of  $\lambda_2$  was  $A_2 \approx 10\%$  in the sample  $x=0.40$  at 8 K, increased with decreasing temperature, and reached 0.4 below 4K and stayed constant down to 15 mK. With  $x=0.45$ ,  $A_2$  reached 0.36 at 2 K.

No muon spin rotation due to a static field by a magnetically ordered phase was observed in either sample. This fact supports the macroscopic experiments in the  $x=0.40$  case [1]. However, the relaxation rate of the fast component  $\lambda_2$  significantly increases with decreasing temperature and reaches an anomalously large value below 1 K. This means that a dynamical spin fluctuation with a large amplitude remains down to 15 mK. The frequency spectrum of this spin fluctuation was previously investigated at RAL in a limited temperature region down to

0.3 K, where we found that the spin fluctuation slows down with decreasing temperature [3]. This behavior was interpreted as the soft-mode toward a possible magnetic phase transition at absolute zero such as Bose-glass phase.

The exotic phase was first predicted theoretically by Fisher *et al.*[5] as a ground state of disordered Boson systems in which particles are in a gapless state and still are localized. The soft mode that corresponds to the Bose glass is expected to be distributed over a finite region in  $q$ -space, rather than to be restricted in a well-defined  $q$ -point as in conventional structural phase transitions. The fact that the muon is a local probe allows one to detect such an unconventional soft mode. The present experiment provides a further evidence of the possibility that the ground state of the system with  $x \leq 0.45$  is the Bose-glass, which is magnetic and still does not order at finite temperature.

Next, our observation of no magnetic order with  $x = 0.45$  down to 2 K, as shown in Fig. 1, indicates that the previously reported value of the quantum critical point  $x_C=0.44$  [1] should be modified to be at least larger than 0.45.

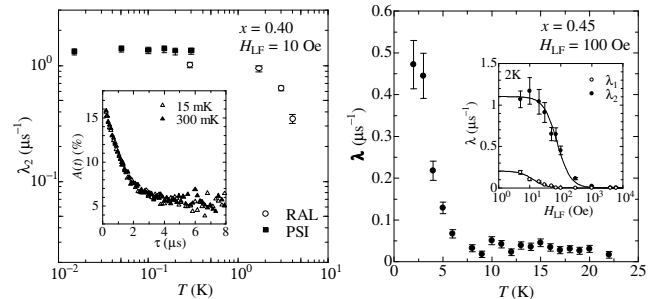


Fig. 1 Temperature dependence of the muon spin relaxation rate  $\lambda_2$  with  $x=0.40$  (left) and  $0.45$  (right). Insets of the each figure shows typical relaxation curves and LF decoupling respectively.

## References

- 1) H. Manaka et al. Phys. Rev. B63, 104408 (2001); *ibid* B66, 064402 (2002)
- 2) T. Nakamura, Phys. Rev. B71, 144401 (2005).
- 3) T. Goto *et al.* Phys. Rev. B74, 134423 (2006); *ibid* B78, 054422 (2008); K. Kanada et al., J. Phys. Soc. Jpn., 76, 064706 (2007).
- 4) M. P. A. Fisher et al., Phys. Rev. 40, 546 (1989).

<sup>\*1</sup> Sophia University,

<sup>\*2</sup> Department of Physics, University of Tokyo

# Microscopic investigation of the crossover from impurity-induced order to pressure-induced order in $\text{Tl}(\text{Cu}_{1-x}\text{Mg}_x)\text{Cl}_3$ by muon-spin-rotation/relaxation

T. Suzuki, I. Watanabe, F. Yamada,\*<sup>1</sup> Y. Ishii, K. Oishi, Risdiana, T. Goto,\*<sup>2</sup> and H. Tanaka,\*<sup>1</sup>

[spin gap, impurity, crossover, magnetic order, pressure]

In  $\text{TlCuCl}_3$  system, field-induced magnetic ordering has been investigated extensively, and the obtained results are qualitatively well described by the magnon Bose-Einstein condensation theory<sup>1)</sup>. Pressure-induced magnetic ordering has also been reported in  $\text{TlCuCl}_3$ . It is reported that the critical pressure  $P_c$  is 0.42 kbar, and that the pressure-induced ordered state is an antiferromagnetically ordered state of which the magnetic structure is the same with the case of the field-induced phase. In the impurity-introduced  $\text{Tl}(\text{Cu}_{1-x}\text{Mg}_x)\text{Cl}_3$  system, the magnetic phase transition to an ordered state is observed by magnetization and specific heat measurements. Recently, Imamura *et al.* reported the pressure-induced magnetically ordered phase by magnetization measurements in  $\text{Tl}(\text{Cu}_{1-x}\text{Mg}_x)\text{Cl}_3$ , and concluded that the change from the impurity-induced phase to the pressure-induced phase is the crossover<sup>2)</sup>. In order to clarify the microscopic difference between magnetic states induced by pressure and by impurity doping, we carried out muon-spin-rotation/relaxation ( $\mu\text{SR}$ ) measurements at the RIKEN-RAL Muon Facility using the newly installed gas-pressurized  $\mu\text{SR}$  setup<sup>3)</sup>.

The magnetic phase transition at ambient pressure is determined by the magnetization measurement to be  $T_N = 2.85$  K for  $x = 0.015$ . Figure 1 (a) shows Zero-field  $\mu\text{SR}$  (ZF- $\mu\text{SR}$ ) time spectrum under various pressures at 2.3 K. Each plot is shifted consecutively for clarity. All spectra are analyzed using the two component function of  $A(t) = A_1 e^{-\lambda_1 t} \cos(\omega t + \theta) + A_2 e^{-\lambda_2 t} G_z(\Delta, t)$ . The first term is the signal from samples, and the second term is that from the large pressure cell.  $\lambda_1$  and  $\lambda_2$  are the muon-spin-relaxation rate, and  $\omega$  is the muon-spin-rotation frequency.  $G_z(\Delta, t)$  is the static Kubo-Toyabe function. The ratio of the amplitude of signal from samples and the pressure cell  $A_1/A_2$  is 0.16. Fitted results are shown in Fig.1 as solid lines. Above 0.5 kbar, the muon-spin-rotation is observed although no rotational signal is observed in ambient pressure. The rotational signal indicates that a long-range coherent ordering appears above 0.5 kbar. The internal magnetic field  $H_{\text{int}}$  at the muon sites are deduced using the relation of  $H_{\text{int}} = \omega/\gamma_\mu$  (open circles in Fig. 2). To determine whether or not the fast relaxation originates from a static internal magnetic field,

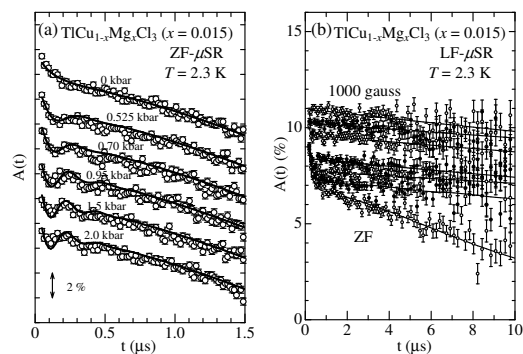


Fig. 1. (a) Time spectra of the ZF- $\mu\text{SR}$  at 2.3 K under pressures. (b) Time spectra of the LF- $\mu\text{SR}$  at 2.3 K in ambient pressure.

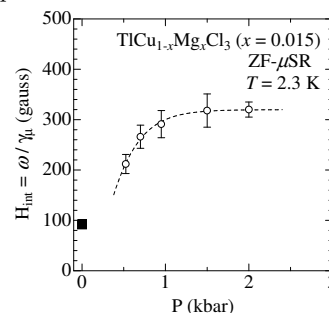


Fig. 2. Pressure dependence of the internal magnetic field at muon sites. Dashed line is guide for the eye.

the longitudinal-field muon-spin-relaxation (LF- $\mu\text{SR}$ ) measurements are carried out in ambient pressure using a usual cryostat. Time spectra of LF- $\mu\text{SR}$  at 2.3 K are shown in Fig.1 (b). The typical behavior in the presence of a static internal magnetic field at the muon sites is observed. By analysing this decoupling pattern under the assumption that  $H_{\text{int}}$  has a unique magnitude but random directions to LF,  $H_{\text{int}}$  at the muon sites is estimated to be 92 gauss at 2.3 K (a closed square in Fig.2). Deduced  $H_{\text{int}}$  from the rotation frequency and LF data are summarized in Fig. 2. From these results, we conclude that the crossover reported by Imamura *et al.*<sup>2)</sup> is the continuous change from a short-range order to a long-range coherent order without the quantum critical point.

## References

- 1) T. Nikuni *et al.* : Phys. Rev. Lett. **84** (2000) 5868.
- 2) H. Imamura *et al.* : Phys. Rev. B **74** (2006) 064423.
- 3) I. Watanabe *et al.* : Physica B: Physics of Condensed Matter (in press).

<sup>†</sup> Condensed from the article submitted to PRL

\*<sup>1</sup> Department of Physics, Tokyo Institute of Technology

\*<sup>2</sup> Department of Physics, Sophia University

# Quantum critical behavior in highly random systems $\text{Tl}_{1-x}\text{K}_x\text{CuCl}_3$ probed by zero- and longitudinal-field muon spin relaxation

T. Suzuki, F. Yamada,<sup>\*1</sup> I. Watanabe, T. Goto,<sup>\*2</sup> T. Kawamata, and H. Tanaka,<sup>\*1</sup>

[spin gap, magnon, soft mode, randomness]

In the mixed system  $\text{Tl}_{1-x}\text{K}_x\text{CuCl}_3$ , the spatial randomness of the local chemical potential is introduced through the difference of the value of the dominant intradimer interaction  $J$  between  $\text{TlCuCl}_3$  and  $\text{KCuCl}_3$ , because  $J$  corresponds to the local potential of magnons. Magnetization measurements suggest that the ground state is a magnetic state with finite susceptibility in the mixed system in zero field (ZF), although finite excitation gap remains<sup>1</sup>.

Recently, we have reported results of  $\mu\text{SR}$  measurements on  $\text{Tl}_{1-x}\text{K}_x\text{CuCl}_3$ . As for  $x = 0.20$ , the increase and the saturation of the muon spin relaxation rate  $\lambda$  were observed at low temperatures, which is possibly a precursor to the Bose-glass phase<sup>2</sup>. In the case of  $x = 0.44$  and  $0.58$ , the increase of  $\lambda$  is observed, which suggests the slowing down of the frequency of the Cu-3d spin fluctuations toward a spin frozen state below 20 mK in contrast to the predicted Bose-glass phase, and the root-exponential-like behavior of the time spectrum indicates that the origin of the relaxation is possibly the spatially-fixed fluctuating dilute moments<sup>3,4</sup>. However, the spin dynamics, which is the frequency spectrum of spin fluctuations, has not yet been clarified under the conditions that the randomness is enhanced with increasing the concentration of  $x$  and that the divergent increase of  $\lambda$  is observed. In order to investigate microscopic dynamical magnetic properties in highly random systems, we carried out the zero- and detailed longitudinal-field muon spin relaxation (ZF- and LF- $\mu\text{SR}$ ) measurements in  $\text{Tl}_{1-x}\text{K}_x\text{CuCl}_3$  with  $x = 0.51$  and  $0.60$  single crystals at the RIKEN-RAL muon facility.

Figure 1(a) shows the LF- $\mu\text{SR}$  time spectrum at each temperature in the longitudinal field of 3950 gauss. With decreasing temperature, the time spectrum becomes to show a faster relaxation down to 3 K, however, below 3 K, the spectrum shape goes back to those of higher temperature, i.e., the relaxation becomes slower. To discuss the temperature change of the spectrum and the muon spin relaxation rate  $\lambda$ , the LF- $\mu\text{SR}$  time spectra are analyzed using the stretched exponential function  $A(t) = A_0 \exp(-\lambda t)^\beta$ . Figure 1(b) shows the deduced relative temperature change of the muon spin relaxation rate  $\lambda$  in each longitudinal field. In 3950 gauss, peak structure in the relative

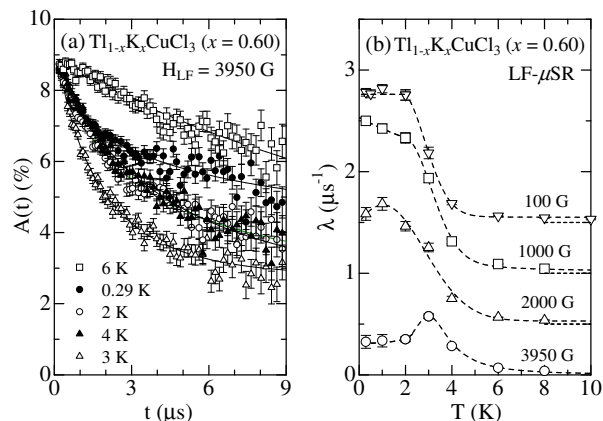


Fig. 1. (a) Time spectra of the LF- $\mu\text{SR}$  in 3950 gauss. Solid lines are fitted results. (b) Relative temperature change of the muon spin relaxation rate  $\lambda$  in each longitudinal field. Dashed lines are guide for the eye. Each plot is shifted upward consecutively by  $0.5 \mu\text{s}^{-1}$  for clarity.

temperature change of  $\lambda$  is observed at  $T \sim 3$  K. We have to notice here that a unit of  $\lambda$  is practically an arbitrary unit, because power  $\beta$  shows the large temperature dependence and the change of  $\beta$  affects the absolute value of  $\lambda$ . Thus, we can only discuss the relative change of  $\lambda$  in this case.

The temperature where the peak is observed decreases with decreasing the magnetic field. The muon spin relaxation rate  $\lambda$  in the LF corresponds to the wave-vector( $q$ )-integration of the generalized dynamical susceptibility. In other word, the  $H_{\text{LF}}$  dependence of  $\lambda$  corresponds to the frequency ( $\omega_{\text{LF}} = \gamma_\mu H_{\text{LF}}$ ) spectrum of spin fluctuations, where  $\gamma_\mu$  is the gyromagnetic ratio of the muon spin. Therefore, observed peak shift to lower temperatures with decreasing  $H_{\text{LF}}$  is the observation of the slowing down of Cu-3d spins fluctuation frequency, and is interpreted as the soft mode of spin waves toward a possible magnetic phase transition. In the case of  $x = 0.60$ , the change of  $\lambda$  saturates in low magnetic fields. This result indicates that ground state at the zero temperature is not magnetic, and the system is in the vicinity of the quantum critical point.

## References

- 1) A. Oosawa *et al.* : Phys. Rev. B **65** (2002) 184437.
- 2) T. Suzuki *et al.* : J. Phys. Soc. Jpn. **75** (2006) 025001.
- 3) T. Suzuki *et al.* : J. Phys. Soc. Jpn. **76** (2007) 074704.
- 4) T. Suzuki *et al.* : Physica B **404** (2009) 590-593.

<sup>†</sup> Condensed from the article : Phys. Rev. B, **79** (2009) 104409.

<sup>\*1</sup> Department of Physics, Tokyo Institute of Technology

<sup>\*2</sup> Department of Physics, Sophia University

# Changes of spin dynamics in multiferroic $\text{Tb}_{1-x}\text{Ca}_x\text{MnO}_3$

A. A. Nugroho,<sup>\*1</sup> Risdiana, M. Mufti,<sup>\*3</sup> T. T. M. Palstra,<sup>\*3</sup> I. Watanabe, and M. O. Tjia<sup>\*1</sup>

[Multiferroic, Relaxor, Ca-doped manganite]

Recently, an interesting effect was found in the Ca-doped  $\text{TbMnO}_3$  single crystal showing typical response of relaxor ferroelectric at 5% Ca doping level as revealed by the temperature dependent dielectric response as well as the neutron diffraction measurement on a single-crystalline sample<sup>1</sup>). This relaxor behavior was suggested to be related to the ferroelectric properties of this material well known to have a magnetic origin. The effect was further suggested to be associated with the weakening of the next-nearest neighbor superexchange interactions<sup>2</sup>). However, this suggested weakening decoupling has yet to be observed directly. The effect of Ca doping on the magnetic ordered state

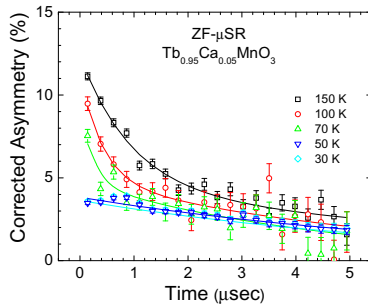


Fig. 1. Temperature dependence of the corrected asymmetric of zero-field fast muon relaxation in  $\text{TbCa}_{0.05}\text{MnO}_3$ .

was investigated here by a ZF- $\mu$ SR measurement carried out at various temperatures on the 5% Ca-doped single crystal at the RIKEN-RAL Facility in UK. The time spectra in Fig.1 show a fast depolarization behavior around 100 K. With decreasing temperature and hence increasing effective internal field, the initial depolarization process took place at a faster pace and became a sharp drop below about 50 K. This means that the spin fluctuations of Tb and/or Mn moments in this sample were weakened with decreasing temperature at a much faster rate as compared to the undoped case where the depolarization process remains observable at 40 K. This effect was further investigated by the measurement carried out at 10 K. Figure 2 shows the comparison between the effects of different Ca doping concentrations at that temperature. The same behavior is exhibited by the 5% Ca-doped sample at this temperature in contrast to the flat behaviors shown by the undoped and the 10% Ca-doped samples supposedly associated with homogeneous internal field.

Finally, the measurement was repeated at the same

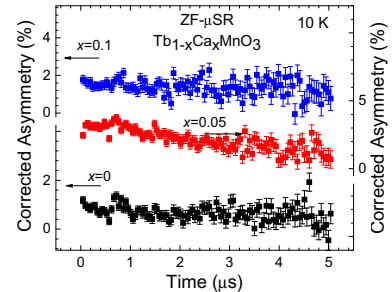


Fig. 2. ZF- $\mu$ SR spectra of  $\text{Tb}_{1-x}\text{Ca}_x\text{MnO}_3$  with  $x=0, 0.05$  and  $0.1$  at  $10\text{ K}$ .

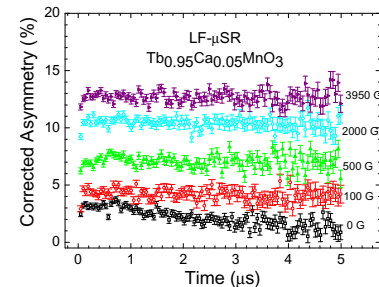


Fig. 3. LF- $\mu$ SR spectra at  $10\text{ K}$  for 5% Ca doped  $\text{TbMnO}_3$

temperature in various applied longitudinal fields (LF). The result presented in Fig.3 clearly shows a magnetic ordered state at  $10\text{ K}$ . Admittedly the correct decoupling field is difficult to estimate from the data because some non-intrinsic instrumental effects induced by LF resulted in unexpected shift in the baseline of the spectrum. However, a comparison of these time spectra with those obtained at  $10\text{ K}$  and zero LF, shows that the asymmetry lost in ZF was gradually recovered with increasing LF. However the less than complete recovery seems to indicate that the internal field is too large for the muon to be decoupled from it even at  $4\text{ kG}$ .

We note that no sign of coherent muon-spin precession was observed due to the limited time resolution of the pulsed muon beam, and additional investigations is needed using the dc muon beam with higher time resolution. Nevertheless, our current data do suggest the possible appearance of inhomogeneous internal field due to the 5% Ca-doped  $\text{TbMnO}_3$ , which is not inconsistent with the inhomogeneous nature of the spin alignment revealed by the neutron scattering measurement<sup>1</sup>).

## References

- 1) N. Mufti et al., Phys. Rev. B **78**, 24109 (2008)
- 2) T. Kimura et al., Phys. Rev. B **68**, 60403(R) (2003)

<sup>\*1</sup> FMIPA, Institut Teknologi Bandung, Indonesia

<sup>\*3</sup> Solid State Chemistry, Rijkuniversiteit Groningen, The Netherlands

# $\mu$ SR study of the spin-lattice cooperative phenomenon of RbCoBr<sub>3</sub>

T. Kawamata, Y. Nishiwaki,\*<sup>1</sup> T. Kato\*<sup>2</sup> and I. Watanabe[ $\mu$ SR, frustration]

In the frustration system, cooperative phenomena between different degrees of freedom have recently attracted interest. RbCoBr<sub>3</sub> is on the ABX<sub>3</sub>-type compounds which are well-known frustrated magnets. ABX<sub>3</sub>-type compounds have  $-BX_3-$  linear chains of infinitely connected face-shared BX<sub>6</sub> octahedral run along the *c*-axis. The chains form an equilateral triangular lattice in the *c*-plane, forming a triangle pillar.

RbCoBr<sub>3</sub>, which shows both magnetic and structural phase transitions, is a new compound in the ABX<sub>3</sub>-type system. Neutron scattering measurement showed a linear increase in the intensity of the (111) magnetic Bragg peak with decreasing temperature below the ferrimagnetic transition temperature,  $T_{N2} \sim 31$  K.<sup>1)</sup> This unusual result is successfully reproduced by a new spin-lattice model proposed by Nakamura *et al.*<sup>2)</sup> This model is introduced in the frustration of not only spin systems but also lattice systems, say "lattice frustration". The lattice frustration is new concept to discuss the structural phase transitions. Accordingly, RbCoBr<sub>3</sub> is a very unique compound with spin and lattice frustration, changing its spin and lattice alignments cooperatively to minimize the energy releasing frustrations. This study aims to understand the new spin-lattice cooperative phenomena in RbCoBr<sub>3</sub>. The  $\mu$ SR measurements were performed at the RIKEN-RAL Muon Facility.

Figure 1 shows the ZF- $\mu$ SR time spectra of RbCoBr<sub>3</sub>. With decreasing temperature, the depolarization of muon spins becomes fast. Clear muon spin rotation was observed below the partial disordered phase transition temperature,  $T_{N1} \sim 37$  K. Temperature dependence of the precession frequency obtained by Fourier analysis of the spectra is shown in Fig. 2. There are two branches below  $T_{N1}$ , one is the main component which can be observed down to low temperatures with the saturated frequency of about 4 MHz, and the other has higher frequency but broadens and seems to vanish below  $T_{N2}$ . The behavior of the main component, which is similar to the temperature dependence of the intensity of the  $(\frac{1}{3}\frac{1}{3}1)$  and  $(\frac{2}{3}\frac{2}{3}1)$  magnetic Bragg peaks,<sup>1)</sup> indicates the development of a magnetic ordered state. The broadening of the higher component is possibly caused by smearing of the muon-spin rotation due to the pulsed muon-beam structure and/or due to the limitations of the time resolution of detecting system. This is because the frequency of this higher component is close to the resolution limit of the

RIKEN-RAL Muon Facility ( $\sim 6$  MHz) with decreasing temperature. However, we definitely confirmed through  $\mu$ SR experiments using a dc muon beam at PSI that the higher component was broadening with decreasing temperature. The broadening below  $T_{N2}$  is expected to be caused by the random domain structures due to a structural phase transition at  $T_{N2}$  suggested by the spin-lattice model.<sup>2)</sup>

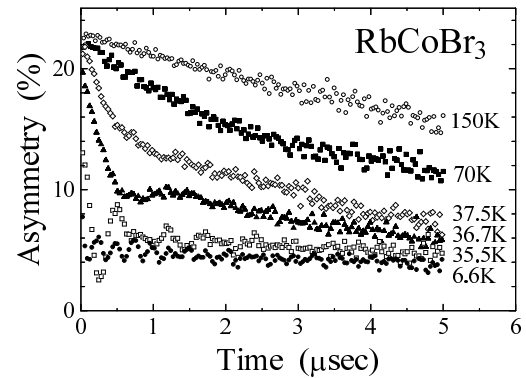
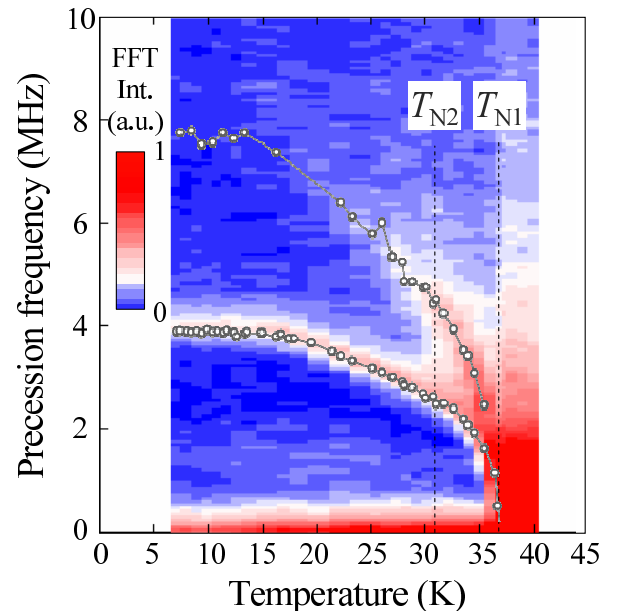
Fig. 1. ZF- $\mu$ SR time spectra of RbCoBr<sub>3</sub>.

Fig. 2. Temperature dependence of the precession frequency obtained by Fourier analysis. Open circles indicate the peak center frequency.

## References

- 1) Y. Nishiwaki et al.: J. Phys. Soc. Jpn. **77**, 104703 (2008).
- 2) T. Nakamura and Y. Nishiwaki: Phys. Rev. B **78**, 104422 (2008).

\*<sup>1</sup> Dept. of Physics, Tokyo Women's Medical University\*<sup>2</sup> Faculty of Education, Chiba University

# $\mu$ SR studies on strongly correlated cubic Tm and Pr compounds with orbital degrees of freedom in the crystal-field ground state

H.S. Suzuki,<sup>\*1</sup> S. Takagi,<sup>\*2</sup> T. Suzuki, I. Watanabe and T. Matsuzaki

Cubic non-Kramers rare earth compounds of TmAg<sub>2</sub>In and PrMg<sub>3</sub> exhibit strongly correlated electron behavior characterized by a huge broad anomaly in  $T$ -dependence of the specific heat below 1 K<sup>1</sup>). The crystal field ground states (CFGs) in both have orbital degrees of freedom, invoking that multipoles in CFGs are possibly related to their strongly correlated electron behaviors. Especially, the non-Kramers CFGs doublet  $\Gamma_3$  for PrMg<sub>3</sub> has no magnetic dipoles but electric quadrupoles and a magnetic octupole. In this study, we intend to clarify the ground state properties and the low energy dynamics at low- $T$  by utilizing the  $\mu$ SR technique.  $\mu$ SR measurements were carried out using AUGUS spectrometer at RIKEN-RAL Muon Facility. The ZF and LF spin relaxation function  $G_Z(t)$  was measured on the single crystals with the initial  $\mu^+$  spin polarization  $P_{\mu^+}$  along the cubic [001] axis.

For TmAg<sub>2</sub>In,  $G_Z(t)$  at low- $T$  was found to be fitted quite well by the two components exponential relaxation as  $G_Z(t) = A_1 \exp(-\lambda_1 t) + A_2 \exp(-\lambda_2 t)$  with a ratio of  $A_1 : A_2 = 2 : 1$  and  $\lambda_1 \gg \lambda_2$ . As shown in Fig. 1,  $\lambda_1$  exhibits a strong  $T$ -dependence, while  $\lambda_2$  is almost  $T$ -independent. At high- $T$ ,  $\lambda_1 \approx \lambda_2$  and the two components are not well discriminated. Under LF, the exponential relaxation is found not to be decoupled easily indicating the electric origin of the relaxation. Most probable stopping sites are (1/4, 1/4, 0) and its equivalent sites, which are the same as in the isomorphous compound of SmAg<sub>2</sub>In determined by TF  $\mu$ SR<sup>2</sup>). Recent specific heat measurement at ultra low- $T$  has revealed a phase transition at  $T_0 = 0.22$  K, suggesting that the increase of  $\lambda_1$  down to the lowest- $T$  of

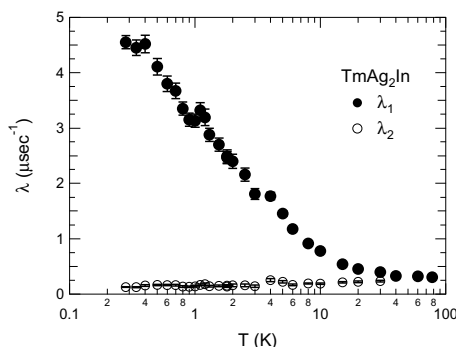


Fig. 1.  $T$ -dependence of the zero-field  $\mu^+$  relaxation rate  $\lambda_1$  and  $\lambda_2$  in TmAg<sub>2</sub>In.

<sup>\*1</sup> National Institute for Materials Science

<sup>\*2</sup> Physics Department, Graduate School of Science, Tohoku University

our measurement reflects the slowing down of fluctuating moments toward  $T_0$ .

Fig. 2 shows ZF and LF  $G_Z(t)$  in PrMg<sub>3</sub> at  $T = 0.28$  K. In the case of the non-magnetic CFGs, the hyperfine coupling between the nucleus and the Van Vleck susceptibility introduces the enhancement of the local magnetic field from the nuclear magnetic moments at low- $T$ <sup>3</sup>). As shown in Fig. 2, the experimental results can be described well up to LF of 200 Oe in terms of the dynamical Kubo-Toyabe (KT) model with two components, in which the local fields are *hyperfine-enhanced*. Here, the two components in  $G_Z(t)$  are presumed on the analogy with the results of TmAg<sub>2</sub>In with the similar structure to PrMg<sub>3</sub>. The *hyperfine-enhanced* factor used in the dynamical KT analysis is  $\sim 9$ , which is comparable with calculated one from the van Vleck term of PrMg<sub>3</sub> ( $\cong 7$ ). These mean the possibility of indirectly deducing  $1/T_1$  of <sup>141</sup>Pr nucleus from  $\mu$ SR. The fluctuation rate of the local field obtained by the dynamical KT analysis increases with decreasing- $T$  at low- $T$ . We may observe the slowing of the fluctuation of the quadrupole moments in 4f electrons through the <sup>141</sup>Pr nucleus, of which quadrupoles couple with those of 4f electrons.  $\mu$ SR studies to investigate lower- $T$  for both compounds are proposed in the continuation proposal.

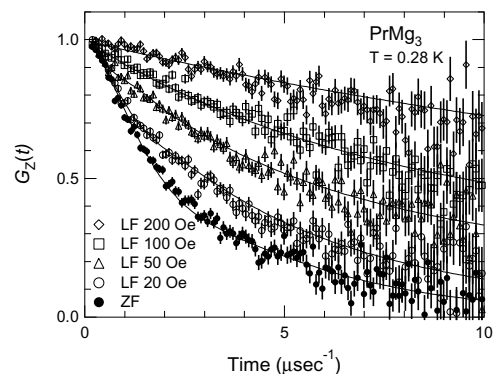


Fig. 2. ZF and LF depolarization of  $\mu^+$  in PrMg<sub>3</sub> at  $T = 0.28$  K. The solid lines denote the calculated results in terms of dynamical Kubo-Toyabe model.

## References

- 1) H. Tanida et al. : J. Phys. Soc. Jpn. **75**, 073705 (2006)
- 2) T. Ito: *Doctor thesis* (2008)
- 3) D.E. MacLaughlin et al.: Phys. Rev. B **61**, 555 (2000)

# $\mu$ SR study of heat transport due to spins in 2-leg spin-ladder system $\text{Ca}_9\text{La}_5\text{Cu}_{24}\text{O}_{41}$

T. Kawamata, I. Watanabe, T. Suzuki, Y. Tanabe\*<sup>1</sup> and Y. Koike\*<sup>1</sup>[ $\mu$ SR, heat transport due to spins]

In several low-dimensional quantum spin systems, it has been reported recently that the temperature dependence of the thermal conductivity exhibits anisotropic peaks or shoulders. In the 2-leg spin ladder system  $\text{Ca}_9\text{La}_5\text{Cu}_{24}\text{O}_{41}$ , for example, the temperature dependence of thermal conductivity along the  $c$ -axis parallel to the leg of the spin ladder exhibits a very large peak around 150 K.<sup>1,2)</sup> Some argue that the large peak is attributable to the thermal conductivity due to magnetic excitations, namely, the thermal conductivity due to spins. This suggestion is only supported by a few studies of the anisotropy and nonmagnetic impurities effects of the thermal conductivity. Therefore, the anisotropic behaviors of the heat transport due to spins have not yet been directly proved. In this study, we try to detect the change in spin dynamics caused by heat transport due to spins on 2-leg spin-ladder systems  $\text{Ca}_9\text{La}_5\text{Cu}_{24}\text{O}_{41}$  from  $\mu$ SR.

We performed the  $\mu$ SR experiments at the RIKEN-RAL Muon Facility at  $T = 150$  K with and without a temperature difference,  $\Delta T = 10$  K, along the  $c$ -axis. Three rectangular single-crystals of  $\text{Ca}_9\text{La}_5\text{Cu}_{24}\text{O}_{41}$ , with dimensions of  $\sim 1$  mm thickness,  $\sim 10$  mm width and  $\sim 30$  mm length, were mounted on our own sample holder as shown in Fig. 1. One side of the single-crystals was set on a silver plate as a heat sink and the opposite side was set on a silver plate with chip resistances as heaters. The  $\Delta T$  across the samples was measured with several Cernox thermometers.

The inset of Fig. 2 shows the typical  $\mu$ SR time spectra in the longitudinal fields (LF) up to 3950 G with and without  $\Delta T$  along the  $c$ -axis. The time spectra in low fields up to a few tens G are driven by the fluctuation of the nuclear dipoles, because the initial part of the time spectra decays with a Gaussian-like function. On the other hand, it is expected that time spectra in high fields are affected by the fluctuation of the Cu-3d spins, because the internal field can not be decoupled even by a high LF of 3950 G. All of the time spectra were analyzed using the function  $A_0 \exp(-\lambda t) G_{KT}(t)$ , where  $A_0$  is the initial asymmetry,  $\lambda$  is the relaxation rate of the muon spin polarization and  $G_{KT}(t)$  is the static Kubo-Toyabe function.<sup>3)</sup> The  $\lambda$  in low fields and high fields is expected to correspond to the fluctuating field created by the nuclear dipoles and the Cu-3d spins, respectively. Figure 2 shows the field dependence of  $\lambda$  with and without  $\Delta T$ . The values of  $\lambda$  with and without  $\Delta T$  are almost the same. This shows that

changes in the fluctuation of the Cu-3d spins due to heat transport are not detected by  $\mu$ SR. The possible reasons are: (1) fluctuation occurring too fast due to large exchange interaction,  $J$ , and/or (2) short mean free path of magnetic excitations due to diffusive heat transport in  $\text{Ca}_9\text{La}_5\text{Cu}_{24}\text{O}_{41}$ . For conclusive results, it will be necessary to perform an experiment on a  $S = 1/2$  antiferromagnetic spin system with small  $J$ , where the heat transport due to spins is ballistic.

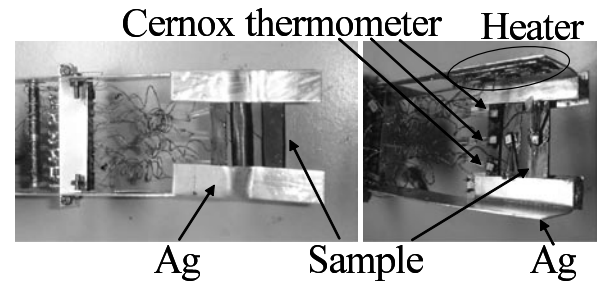


Fig. 1. Sample holder for measurements under temperature gradient.

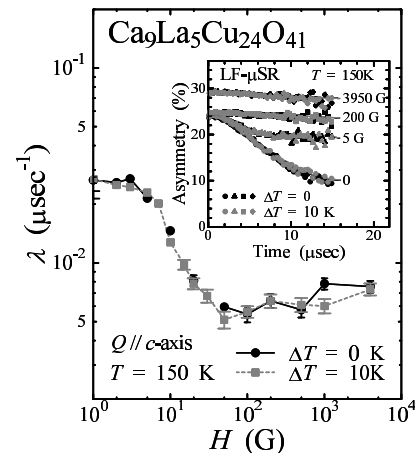


Fig. 2. Field dependence of relaxation rate,  $\lambda$ , with and without temperature difference,  $\Delta T = 10$  K, at  $T = 150$  K. Heat current,  $Q$ , flows along the  $c$ -axis. The inset shows the  $\mu$ SR time spectra of  $\text{Ca}_9\text{La}_5\text{Cu}_{24}\text{O}_{41}$  under the longitudinal fields with and without  $\Delta T$  at  $T = 150$  K.

## References

- 1) K. Kudo et al.: J. Phys. Soc. Jpn. **70**, 437 (2001).
- 2) C. Hess et al.: Phys. Rev. B **64**, 184305 (2001).
- 3) R. Kubo and T. Toyabe: in *Magnetic Resonance and Relaxation*, edited by R. Blinc (North-Holland, Amsterdam, 1967) p. 810.

\*<sup>1</sup> Department of Applied Physics, Tohoku University

## $\mu$ SR study of Heusler compounds $\text{Ru}_{2-x}\text{Fe}_x\text{CrSi}$

M. Hiroi,<sup>\*1</sup> T. Hisamatsu,<sup>\*1</sup> T. Suzuki K. Oishi Y. Ishii and I. Watanabe

Recently magnetic properties of the Heusler compounds  $\text{Ru}_{2-x}\text{Fe}_x\text{CrSi}$  were studied.<sup>1)</sup> It was found that the Fe-rich compounds are ferromagnetic. On the other hand the Ru-rich compounds with  $x = 0.1$  were found not to be ferromagnetic but to show a peak in magnetic susceptibility at 30 K which is likely to indicate an antiferromagnetic transition. Meanwhile, no anomaly in resistivity and specific heat to indicate phase transition was found. Moreover below  $\sim 15$  K separation of the magnetic susceptibility between zero-field cooling and field cooling process was found. This behavior suggests the appearance of a spin glass state. In order to clarify if a magnetic order develops or not, zero-field (ZF)  $\mu$ SR and longitudinal-field (LF)  $\mu$ SR measurements were performed for polycrystalline  $\text{Ru}_{1.9}\text{Fe}_{0.1}\text{CrSi}$ . The measurements were carried out at the RIKEN-RAL Muon Facility using a spin-polarized single-pulse positive surface muon beam. The time spectra, namely, the time evolution of the asymmetry parameters  $A(t)$  was measured down to 4.3 K.

Figure 1 shows ZF- $\mu$ SR time spectra of  $\text{Ru}_{1.9}\text{Fe}_{0.1}\text{CrSi}$  at various temperatures. Spectra below 40 K appear to consist of two components and their  $A(t)$  seem to be expressed as

$$A(t) = A_1 \exp(-\lambda_1 t) + A_2 \exp(-\lambda_2 t), \quad (1)$$

where  $A_i$  and  $\lambda_i$  ( $\lambda_1 > \lambda_2$ ) are initial asymmetry and

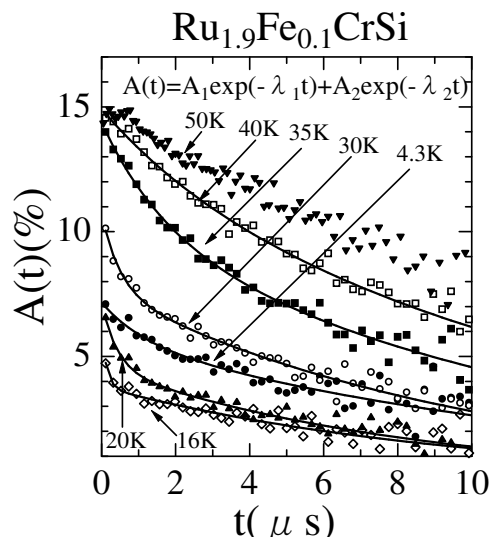


Fig. 1. ZF- $\mu$ SR spectra of  $\text{Ru}_{1.9}\text{Fe}_{0.1}\text{CrSi}$  at various temperatures. Solid lines are the fit of  $A_1 \exp(-\lambda_1 t) + A_2 \exp(-\lambda_2 t)$ .

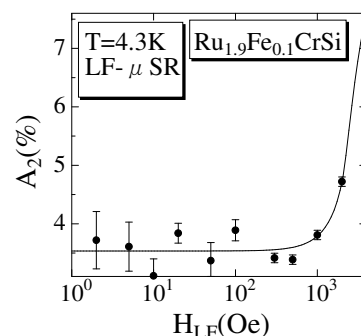


Fig. 2. Longitudinal field  $H_{\text{LF}}$  dependence of  $A_2$  at 4.3 K. The best fit by formula (2) is shown by the solid line.

muon spin relaxation rate for each component, respectively. As shown in Fig. 1 the time spectra are fitted well by Eq. (1). With decreasing temperature the initial asymmetry  $A(0)$  decreases and becomes smallest at  $\sim 16$  K. This behavior suggests the developments of a static internal field.

In order to examine if this behavior originates from a static internal field, LF- $\mu$ SR measurements were carried out at 4.3 K under longitudinal magnetic field  $H_{\text{LF}}$  up to 3950 Oe. These time spectra are also well fitted by Eq. (1). The tail of the spectra increases with increasing  $H_{\text{LF}}$ . These results mean that the observed depolarization of muon spins is caused by a static internal magnetic field  $H_{\text{int}}$ . Figure 2 shows  $H_{\text{LF}}$  dependence of  $A_2$  at 4.3 K. This represents the decouple of muon spins from  $H_{\text{int}}$  by  $H_{\text{LF}}$ . On the assumption that the magnitude of the internal field at each muon site is unique but its direction is random,  $H_{\text{int}}$  was estimated by the following formula:

$$A_2 = \frac{3}{4} - \frac{1}{4x^2} + \frac{(x^2 - 1)^2}{16x^3} \ln \frac{(x + 1)^2}{(x - 1)^2}, \quad (2)$$

where  $x = H_{\text{LF}}/H_{\text{int}}$ . The solid line of Fig. 2 is the best fit of Eq. (2) and  $H_{\text{int}} \sim 2100$  Oe was evaluated.

The present results shows the existence of a static internal field in  $\text{Ru}_{1.9}\text{Fe}_{0.1}\text{CrSi}$  at low temperatures. This is consistent with observed remarkable irreversibility in the magnetic susceptibility below  $\sim 15$  K, which indicates a spin glass state.

### References

- 1) M. Hiroi, K. Matsuda, and T. Rokkaku, Phys. Rev. B. **76** 132401 (2007) .

<sup>\*1</sup> Department of Physics, Kagoshima University

# Superconductivity in one-dimensional CuO double chains

F. Ishikawa,<sup>\*1</sup> Yuh Yamada,<sup>\*2</sup> A. Matsushita<sup>\*3</sup> I. Watanabe, T. Suzuki, and T. Matsuzaki

One of the most famous high-temperature superconductors discovered so far is  $\text{YBa}_2\text{Cu}_3\text{O}_{7-\delta}$ . When the Y-sites were replaced by different lanthanides, Pr alone showed neither superconductivity nor a metallic nature despite retaining a crystalline structure, whereas all the other elements showed superconducting transition temperatures of approximately 90 K. Thus, “Pr issues” were of particular interest in this research from the start.

The  $\text{Pr}_2\text{Ba}_4\text{Cu}_7\text{O}_{15-\delta}$  (Pr247) compound has both CuO double chains and CuO single chains, and shows metallic conductivity at low temperatures due to metallic conduction in the CuO double chains. Recently, we found that Pr247 compounds show superconductivity below 18 K after a reduction process by post-annealing in a vacuum.<sup>1,2)</sup> A nuclear quadrupole resonance experiment revealed that the superconductivity in Pr247 is realized at the CuO double-chain layers.<sup>3)</sup> We performed  $\mu\text{SR}$  experiments on superconductive and non-superconductive samples of Pr247 to obtain information on the superconductivity on Pr247.

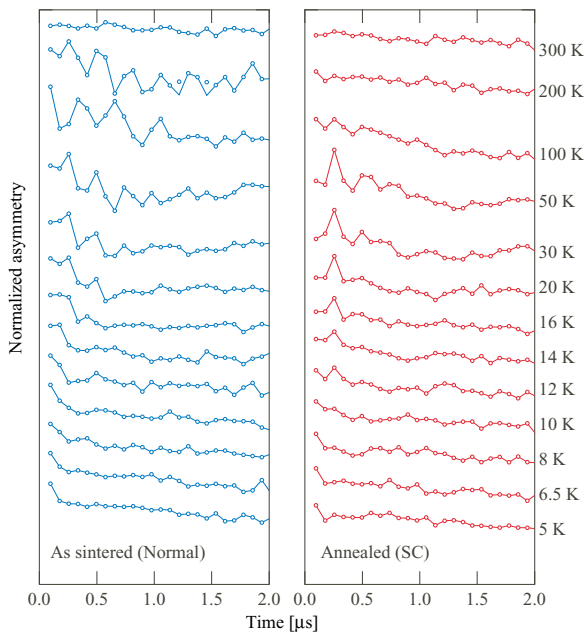


Fig. 1. Zero-field  $\mu\text{SR}$  spectra of the as-sintered and the annealed samples of Pr247.

The as-sintered sample examined in this study exhibits no superconductivity. We prepared an annealed sample by annealing the as-sintered sample for 72

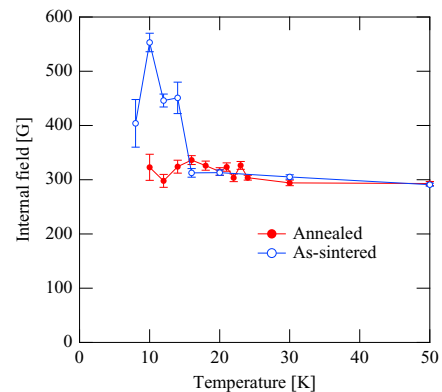


Fig. 2. Temperature dependence of the internal field in the as-sintered and the annealed Pr247 samples.

hours at 673 K in vacuum. The annealed sample with oxygen deficiency  $\delta = 0.38$  has a superconducting temperature  $T_c$  of 22 K with the superconductive volume fraction of 60%. Figure 1 shows zero-field  $\mu\text{SR}$  spectra on as-sintered and annealed samples of Pr247. Muon spin rotation is observed in both samples. However, the rotation signal of the as-sintered sample, which shows no superconductivity, is somewhat larger than that of the superconductive annealed sample.

Temperature dependence of the internal field is shown in Fig. 2. Below 16 K, the internal field of the as-sintered sample increased rapidly, while that of the annealed sample exhibited only a small change. We also measured another superconductive annealed sample, which has  $T_c = 14$  K with the superconductive volume fraction of 1.8%. In this sample, the profile of temperature dependence of the internal field is similar to that of the as-sintered sample. The increase in the internal field at low temperature is probably due to the magnetic ordering of Pr below the Néel temperature. These results indicate that suppression of the magnetic ordering of Pr has a close relationship with the appearance of superconductivity of Pr247.

## References

- 1) M. Matsukawa, Yuh Yamada, M. Chiba, H. Ogasawara, T. Shibata, A. Matsushita and Y. Takano: *Physica C* **411**, 101 (2004).
- 2) Yuh Yamada, A. Matsushita: *Physica C* **426-431**, 213 (2005).
- 3) S. Watanabe, Y. Yamada and S. Sasaki: *Physica C* **426-431**, 473 (2005).

<sup>\*1</sup> Graduate School of Science and Technology, Niigata University

<sup>\*2</sup> Department of Physics, Niigata University

<sup>\*3</sup> NIMS

# $\mu$ SR study on ferromagnetism of rubidium clusters in zeolite A<sup>†</sup>

T. C. Duan,<sup>\*1</sup> T. Nakano,<sup>\*1</sup> J. Matsumoto,<sup>\*1</sup> R. Suehiro,<sup>\*1</sup> I. Watanabe, T. Suzuki, T. Kawamata, A. Amato,<sup>\*2</sup> F. L. Pratt,<sup>\*3</sup> and Y. Nozue<sup>\*1</sup>

Alkali metal nanoclusters can be generated in the periodically arrayed spaces of zeolite crystals. Magnetically ordered states have been found in these systems without any magnetic elements<sup>1,2</sup>. Recently, we have newly found ferromagnetic properties in Rb clusters in zeolite A<sup>3</sup>. The mechanism of ferromagnetism seems different from that of K clusters.

Zeolite A has the LTA-type framework structure as shown in Fig. 1, where the  $\alpha$  and  $\beta$  cages with the respective inside diameters of  $\simeq 11$  and  $\simeq 7$  Å are alternatively arrayed in a CsCl structure. We used a highly Rb-exchanged zeolite A with chemical formula of  $\text{Rb}_{11}\text{K}_1\text{Al}_{12}\text{Si}_{12}\text{O}_{48}$ , where the host alkali cations ( $\text{K}^+$ ,  $\text{Rb}^+$ ) are distributed in the space of zeolite framework ( $\text{Al}_{12}\text{Si}_{12}\text{O}_{48}$ ). By loading guest Rb atoms into dehydrated zeolites the  $5s$ -electrons of the adsorbed Rb atoms are shared among guest  $\text{Rb}^+$  and host cations, and confined in the zeolite cages to form Rb clusters. Rb clusters show ferromagnetic properties at loading densities (the number of guest Rb atoms per formula unit),  $n$ , larger than 4.0<sup>3</sup>. At these high values of  $n$ , Rb clusters are in metallic state and clusters formed in both  $\alpha$  and  $\beta$  cages<sup>3</sup>. The basic properties of Rb clusters are different from that of K clusters where the clusters are formed only in the  $\alpha$  cages and the ferromagnetic property is explained by spin-canting of antiferromagnetism in an insulating state. For Rb clusters, a model of ferrimagnetism has been proposed<sup>3</sup>. In order to investigate the ferromagnetic properties in detail, we performed  $\mu$ SR measurements at RIKEN-RAL for Rb clusters in zeolite A with  $n = 5.8$ . This sample has the highest Curie temperature,  $T_C \sim 5$  K.

The internal field is confirmed to be almost static in LF- $\mu$ SR spectra below  $\simeq 4$  K. At  $T \leq 6$  K, ZF- $\mu$ SR spectra were fitted with a function sum of an exponential and a precession component

$$P(t) = A_1 \exp(-\lambda_1 t) + A_2 \exp(-\lambda_2 t) \cos \omega t + B, \quad (1)$$

where  $A_1$  and  $\lambda_1$  are the relaxation amplitude and the muon spin depolarization rate of the exponential component, and  $A_2$ ,  $\lambda_2$  and  $\omega$  are the the relaxation amplitude, the damping and the frequency of the muon spin precession component, respectively. The center and the distribution width of the internal field,  $B_{int}$  and  $\Delta B_{int}$ , respectively, are estimated from  $\omega$  and  $\lambda_2$ . Figure 2 shows temperature dependence of  $\lambda_1$ ,  $B_{int}$  and  $\Delta B_{int}$ . The exponential component dominates the decay, and the relaxation rate  $\lambda_1$  obviously increases

at lower temperature, similar to that of spontaneous magnetization. At  $T \sim 4$  K,  $B_{int} \simeq \Delta B_{int}$  reflects the breakdown of magnetic ordered state near  $T_C$ . The ratio of the relaxation term to the total asymmetry,  $(A_1 + A_2)/(A_1 + A_2 + B)$ , is estimated to be  $\sim 0.6$ . This value is high enough that the magnetic phase is in major part of the volume sample. K clusters in zeolite A are known to show very fast muon spin relaxation with an anomalous LF-dependence. This behavior is strongly related to the spin-canting mechanism. In the Rb clusters, however, such fast relaxation was not observed. This may indicate the different mechanism of ferromagnetism from that of K clusters.

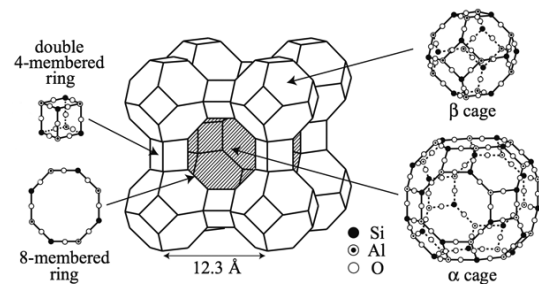


Fig. 1. Schematic illustration of the crystal structure of zeolite A.

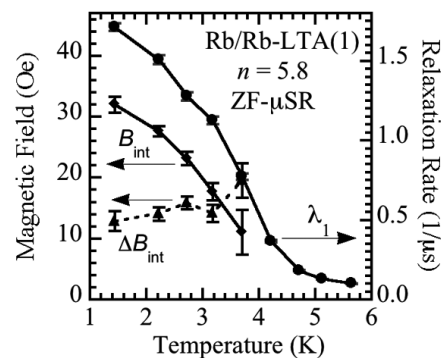


Fig. 2. Temperature dependence of muon spin relaxation rate, center and width of the internal field obtained from ZF- $\mu$ SR for Rb clusters in zeolite A with  $n = 5.8$ .

## References

- 1) Y. Nozue et al.: Phys. Rev. Lett. **68**, 3789 (1992).
- 2) V. I. Srdanov et al.: Phys. Rev. Lett. **80**, 2449 (1998).
- 3) T. C. Duan et al.: J. Magn. Magn. Mater. **310**, 1013 (2007); e-J. Surf. Sci. Nanotech. **5**, 6 (2007).

<sup>†</sup> Condensed from the article in Physica B **404**, 634 (2009).

<sup>\*1</sup> Department of Physics, Osaka University

<sup>\*2</sup> Paul Scherrer Institute, Switzerland

<sup>\*3</sup> Rutherford Appleton Laboratory, UK

## $\mu$ SR Investigation of the Spin Dynamics of Central Fe Ions of Hemeproteins

I. Watanabe, A. Kikuchi, T. Suzuki, T. Kawamata, A. Stoykov, <sup>\*1</sup> and R. Scheuermann, <sup>\*1</sup>

The main purpose of this study is to discover hints about relationships between the local structures of the central heme (Fe-protoporphyrin IX) and the functions of hemeproteins, which the largest single class of metalloproteins. Functions of hemeproteins are known to be not only to their 3D protein structures but also to the electronic state around their central Fe ions. In many cases, the electronic state of the central Fe ion is very sensitive to tiny changes in the surrounding protein environment. Thus, investigations of the electronic state of the central Fe ions from the microscopic viewpoint are quite important to understand functions of hemeproteins [1,2]. In order to simplify the study and avoid difficulties due to complexity of the protein environment, we have prepared Fe-porphyrin complexes as simple models of hemeproteins for the proposed  $\mu$ SR experiment.

In 2008, we obtained 6 days beam time at the ALC experimental area of the Paul-Scherrer Institut (PSI) in Switzerland to investigate the electronic states of the model-complexes of hemeproteins. This reports the results of the first attempt to investigate the electronic state of Fe(TPP)X (X= Imidazole, Cl) using high-field  $\mu$ SR measurements.

Figure 1 shows the samples prepared for the present  $\mu$ SR investigation. Sample-(a) is Fe(TPP)(Imidazole)<sub>2</sub> (TPP=tetraphenylporphyrin) and sample-(b) is Fe(TPP)Cl. The difference between the samples is the local structure around Fe spin. That is, there is a difference in the number of molecules attached to the central Fe ion. Valence values of Fe ions in samples is Fe(III). We applied high-field  $\mu$ SR to these two model samples at room temperature up to 4.5 T using the ALC superconducting magnet in order to observe the dynamics of the Fe(III) ion.

Figure 2 shows high-field  $\mu$ SR time spectra of each model complex at room temperature. Under the zero-field condition, both samples showed strong depolarization behavior due to the strong fluctuations of Fe spins. As the field was increased up to the maximum of 4.5 T, the fast depolarization behavior recovered. The simple exponential function,  $A_0 e^{-\lambda t}$ , was applied to analyze time spectra. The solid lines in Fig. 2 are the best-fit results using this analysis function. Figure 3 shows the LF dependence of the depolarization rate,  $\lambda$ , of each sample. The  $\lambda$  tends to be suppressed with increasing LF above about 2 T and there seems to be a cut-off in  $\lambda$  near the maximum field of 4.5 T. In order to obtain more detailed information on the fluctuating internal field at the muon site, the Redfield function was applied to the field dependence of  $\lambda$  [3].

The solid lines in Fig. 3-(a) and (b) are the best-fit

results using the Redfield function. As shown in Fig. 3-(a) and (b), the internal field at the muon site which is coming from the fluctuating Fe spins was of the order of 2 kG and its frequency was around 400 MHz. Interestingly, no difference was observed in the values of the internal field at the muon site or its fluctuation rate. This means that the dynamics of the central Fe spin are not affected by the axial ligands.

We plan to continue these measurements using other model samples which have different local structures and valence values of the central Fe spin in order to gather more information about the dynamics of the central Fe spin.

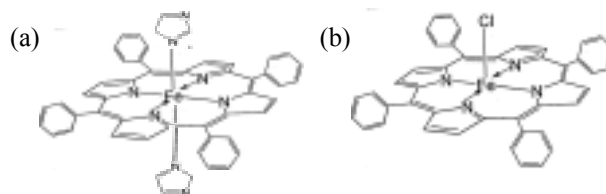


Figure 1: Model samples used in the current high-field  $\mu$ SR study; (a) is Fe(TPP)(Imidazole)<sub>2</sub> and (b) is Fe(TPP)Cl.

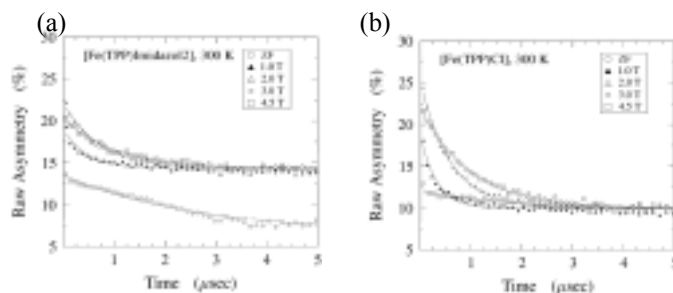


Figure 2: High-field  $\mu$ SR time spectra of (a) Fe(TPP)(Imidazole)<sub>2</sub> and (b) Fe(TPP)Cl obtained at various fields up to 4.5 T.

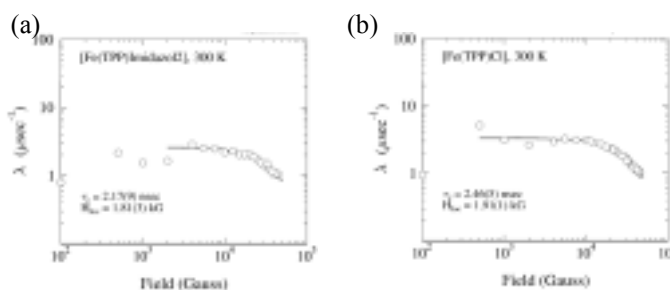


Figure 3: Field dependence of the dynamic muon-spin depolarization rate,  $\lambda$ , in (a) Fe(TPP)(Imidazole)<sub>2</sub> and (b) Fe(TPP)Cl. The solid lines are the best-fit results using the Redfield formula.

### References

- 1) C. More *et al.*, *Biospectroscopy* **S 3-18** (1999) 5.
- 2) U. Gonser *et al.*, *Science* **143**, 680 - 681, (1964).
- 3) C. P. Slichter, *Principles of Magnetic Resonance* (Springer-Verlag, Berlin, Heidelberg, 1978, 1990).

<sup>\*1</sup> Bulk Muon Group, PSI, Villigen, Switzerland.

# Structural transition in $\text{Mo}_3\text{Sb}_7$ probed by muon spin relaxation<sup>†</sup>

H. Nakamura,<sup>\*1</sup> Y. Tabata,<sup>\*1</sup> T. Koyama,<sup>\*2</sup> T. Kohara,<sup>\*2</sup> and I. Watanabe

[structural transition, valence bond crystal, frustration]

A metallic compound  $\text{Mo}_3\text{Sb}_7$ , with the cubic  $\text{Ir}_3\text{Ge}_7$  type structure (space group  $Im\bar{3}m$ ), is a superconductor with a critical temperature  $T_c \simeq 2.1$  K. The Mo sublattice (12e) is the 3D network of Mo-Mo dumbbells formed by nearest neighbors (NN). Next-nearest-neighbor (NNN) bonds form an octahedral cage at the body-centered position. The sufficiently short NN distance (3.0 Å) compared with the NNN distance (4.6 Å) makes us anticipate easy dimerization between NN pairs. Recently, Candolfi et al.<sup>1)</sup> recognized  $\text{Mo}_3\text{Sb}_7$  as an itinerant electron magnet and suggested the coexistence of superconductivity and spin fluctuations. Although no phase transition other than that at  $T_c$  was noticed in Ref. 1, Tran et al.<sup>2)</sup> recently reported the presence of another phase transition at  $T_S \simeq 50$  K, and proposed spin gap formation associated with Mo-Mo dimerization. Thus  $\text{Mo}_3\text{Sb}_7$  is now classified as a new material with another phase transition prior to superconductivity. We have found clear evidence of the symmetry breakdown at  $T_S$ ; a drastic change in the nuclear quadrupole resonance (NQR) spectrum and strong enhancement of the nuclear magnetic relaxation rates,  $1/T_2$  and  $1/T_1$ <sup>3)</sup>. X-ray analysis revealed that this is crystal symmetry transition from cubic to tetragonal<sup>3)</sup>.

To determine the magnetic state below  $T_S$ , we performed zero-field (ZF) and longitudinal-field (LF)  $\mu\text{SR}$  measurements at the RIKEN-RAL Muon Facility using a pulsed positive surface muon beam at 5–150 K under fields of 0 and 20 G<sup>3,4)</sup>. We found no evidence of magnetic order, in accordance with the spin-singlet formation suggested in Ref. 2. The feature of ZF relaxation shows Gaussian-like depolarization both below and above  $T_S$ , as shown in the inset of Fig. 1. The width of the static field distribution  $\Delta$  estimated by fitting the data to the commonly used damped Kubo-Toyabe (KT) function is sufficiently small of  $\Delta/\gamma_\mu \sim 1$  G ( $\gamma_\mu$  the muon gyromagnetic ratio), which is attributed to dipolar fields coming from randomly oriented nuclear spins. As seen in Fig. 1, with increasing temperature passing through  $T_S$ , the width of the field distribution  $\Delta/\gamma_\mu$  is reduced from  $\sim 2.1$  to  $\sim 0.5$  G via a thermal excitation process with activation energy of  $E_a/k_B \simeq 120$  K. We interpreted this temperature dependence as the motional narrowing of the nuclear dipolar field associated with the lattice dynamics from

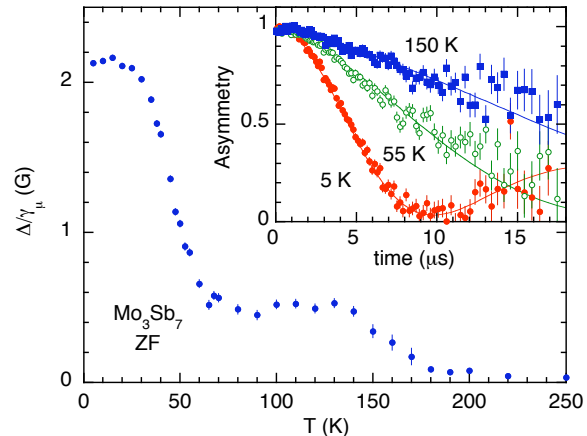


Fig. 1.  $T$  dependence of the ZF Kubo-Toyabe relaxation rate  $\Delta$  in  $\text{Mo}_3\text{Sb}_7$ . Inset shows typical examples of ZF- $\mu\text{SR}$  spectra. Solid curves indicate the fit by the damped KT function. (Cited from Ref. 3.)

tetragonal to cubic.

By applying LF, the Gaussian term is decoupled; the time evolution is roughly described by the single exponential functions as  $P_\mu(t) = \exp(-\lambda t)$  where  $\lambda$  is the relaxation rate. The relaxation rate  $\lambda$  shows a divergent behavior at  $T_S$ , which is qualitatively same as that of the nuclear spin-lattice relaxation rate  $1/T_1$  estimated in  $^{121}\text{Sb}$ -NQR experiment<sup>3)</sup>, although the enhancement of NQR- $1/T_1$  at  $\sim T_S$  looks much stronger. The critical behavior suggests that the phase transition is triggered by the instability in the Mo electronic system.

Thus, the temperature dependence of  $\Delta$  estimated in ZF- $\mu\text{SR}$ , corresponding to the nuclear spin-spin interaction, is relatively moderate and is attributed to the atomic motion in the three-dimensional crystal. On the other hand, the LF relaxation rate at  $\sim T_S$  is dominated by the critical phenomenon probably in the electronic system. Taking account of these facts, we propose long-range order of spin-singlet dimers, i.e., the formation of the valence bond crystal below  $T_S$ , possibly due to the frustration of interdimer antiferromagnetic interaction.

## References

- 1) C. Candolfi et al., Phys. Rev. Lett. 99, 037006 (2007).
- 2) V. H. Tran, W. Miiller, Z. Bukowski, Phys. Rev. Lett. 100, 137004 (2008).
- 3) T. Koyama et al., Phys. Rev. Lett. 101, 126404 (2008).
- 4) Y. Tabata et al., Physica B 404, 746 (2009).

<sup>†</sup> Condensed from the articles in Refs. 3 and 4, and published in RIKEN Research

<sup>\*1</sup> Department of Materials Science and Engineering, Kyoto University

<sup>\*2</sup> Graduate School of Material Science, University of Hyogo

# Dynamics of Amorphous Polymers near Glass Transition by $\mu$ SR

T. Kanaya,<sup>\*1</sup> R. Inoue,<sup>\*1</sup> I. Watanabe,<sup>\*2</sup> T. Matsuzaki,<sup>\*2</sup>

We have studied the dynamics of two glass-forming polymers (polybutadiene (PB) and polyisobutylene (PIB)) in a temperature range from 10 to 300 K using  $\mu$ SR covering the glass transition temperature  $T_g$ . PB and PIB have molecular weight and polydispersity of  $M_w=200,000$ ,  $M_w/M_n=1.2$  and  $M_w=800,000$ ,  $M_w/M_n=2$ , respectively. The glass transition temperatures  $T_g$  are 180 K and 200 K, respectively. The  $\mu$ SR measurements were done at the RIKEN-RAL Muon Facility. The temperature range of the measurements was 10 to 300 K for both the samples.

Figure 1 shows decays of asymmetry for PB and PIB at 300 K under longitudinal magnetic field of 100 G. The decays of PB were described in a single exponential function in the temperature range examined while those of PIB showed an additional slow decay component at high temperatures above  $\sim 200$  K. At the moment the origin of the slow component is not clear. We analyzed the decays fitting a single exponential function to the data. In one fitting procedure all parameters were free, and in another procedure we assumed the intensity of asymmetry was independent of temperature. The temperature dependence

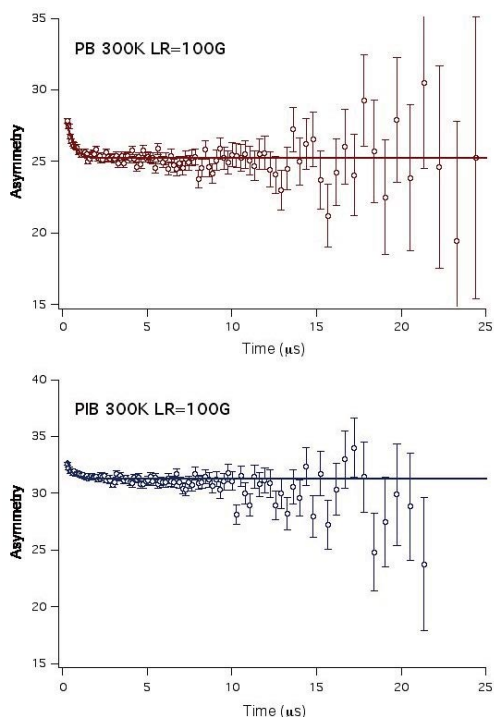


Figure 1. Decays of symmetry for PB and PIB at 100K.

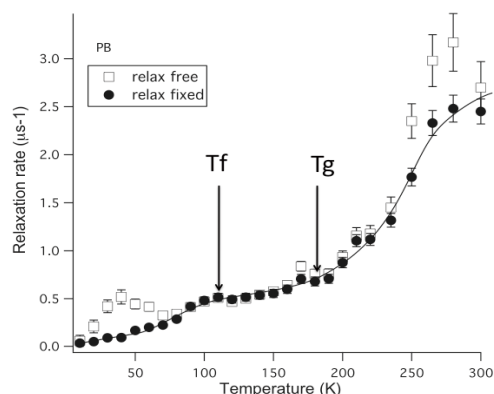


Figure 2. Temperature dependence of decay rate for PB. Solid curve was drawn by eye.

of the decay rate evaluated in both the procedures are shown in Figure 2 for PB. In the Figure, the open symbols show the results of the free parameter fits. The decay rate (or relaxation rate) begins to increase steeply with temperature above about the glass transition temperature  $T_g$  ( $\sim 180$  K), showing that the glass transition is clearly observed in the  $\mu$ SR experiment. This agrees with the previously reported data by Pratt et al.[1]. In a temperature range below  $\sim 80$  K the results of the two fitting procedures are very different. We see a maximum of the decay rate at around 40 K in the free parameter fits. However, when the amplitude of asymmetry is fixed, the decay rate monotonously increases with temperature. Judging from the previous data obtained by other methods such as inelastic neutron scattering [2], the monotonous increase in the decay rate is more physically reasonable. Hence, we employed the results obtained when the intensity of asymmetry was fixed. In the result the temperature dependence of the decay rate changes at around 100-120 K. This temperature corresponds to the onset temperature of the so-called pico-second fast process ( $T_f$ ), which was revealed in inelastic neutron scattering [2]. This observation strongly suggests that we can detect polymer motion in pico-second order in  $\mu$ SR measurements as well as motion in micro-second at  $T_g$ .

## References

- 1) F. L. Pratt et al., *Physica B* **326**, 34 (2003) and references herein.
- 2) T. Kanaya and K. Kaji, *Adv. Polym. Sci.*, **154**, 87 (2001).

<sup>\*1</sup> Institute for Chemical Research, Kyoto University

<sup>\*2</sup> RIKEN

# Muon spin rotation and relaxation on the one-dimensional cobalt(II)-radical coordination polymer magnet

Takayuki Ishida,<sup>\*1</sup> Yoshitomo Okamura,<sup>\*1</sup> and Isao Watanabe

The first single-chain magnet [Co(hfac)<sub>2</sub>•AnNN] was discovered by Gatteschi et al.<sup>1)</sup> (see Fig. 1a with R = CH<sub>3</sub>). The single-chain magnet nature is identified with magnetic hysteresis from a single-chain origin without any interchain interaction. On the other hand, we have reported the record coercivity ( $H_C = 52$  kOe at 6 K) for [Co(hfac)<sub>2</sub>•BPNN] (abbreviated hereafter as CoBPNN, R = *n*-C<sub>4</sub>H<sub>9</sub>).<sup>2)</sup> The phase diagram of CoBPNN was empirically depicted as: a hard magnet for  $T \leq 10$  K and a soft magnet for  $10 \text{ K} < T \leq 45$  K. Although a long-range order is likely to occur before it behaves as a hard magnet, no direct evidence for long-range order has yet been obtained, and the temperature at which the long-range order takes place still remains in question.

The  $\mu$ SR measurements on CoBPNN were carried out at the RIKEN-RAL Muon Facility in the UK. Fig. 1b shows the ZF- $\mu$ SR of CoBPNN. Above 28 K, monotonically decreasing relaxation curves were obtained, which corresponds to a paramagnetic phase. Upon cooling, the signal became the superposition of slow and fast relaxing signals. Below 28 K, a few cycles were found for  $t \leq 0.5 \mu\text{s}$ . The appearance of oscillation due to the muon Larmor precession clearly indicates the presence of an appreciable internal magnetic field due to a spontaneous magnetization. The coherency of the rotation implies a magnetically ordered state. The small amplitude of the oscillation may be related with the size of the magnetic domain.

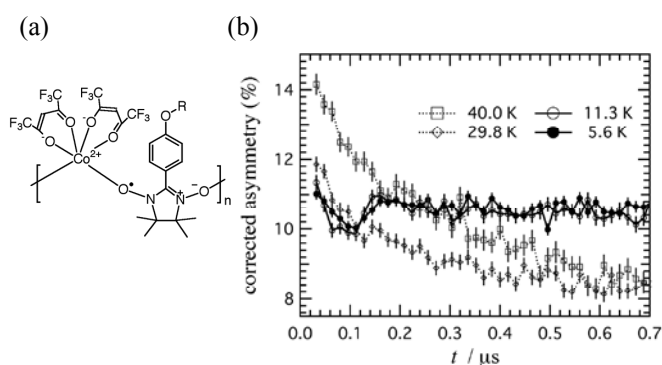


Fig. 1. (a) Structural formula of CoBPNN. (b) Temperature dependence of ZF- $\mu$ SR time spectra on CoBPNN in a temperature range from 40 K to 5 K.

We investigated detailed muon-spin relaxation in a wide temperature range to clarify whether the long-range order would take place at 28 K or somewhere else. The time spectra below 90 K were analyzed based on the following equation consisting of two components,  $A(t) = A_{\text{fast}}(0)\exp(-\lambda_{\text{fast}}t) + A_{\text{slow}}(0)\exp(-\lambda_{\text{slow}}t)$ . The relaxation rate

constant ( $\lambda_{\text{fast}}$ ) and the total initial asymmetry  $A(0)$  are plotted as a function of temperature (Fig. 2). A sharp cusp of  $\lambda_{\text{fast}}$  was found at 40 K and a plateau of  $A(0)$  below 40 K. An extremely slow decay and a constant  $A(0)$  imply completely frozen systems such as magnetically ordered systems. The temperature at the  $\lambda$  divergence is usually defined as a magnetic transition temperature. In our previous report,<sup>2)</sup> an apparent magnetic phase transition temperature of CoBPNN was estimated to be 45 K, which corresponds to 40 K in the present experiments. The present value is more reliable because the experiments were conducted at zero-field.

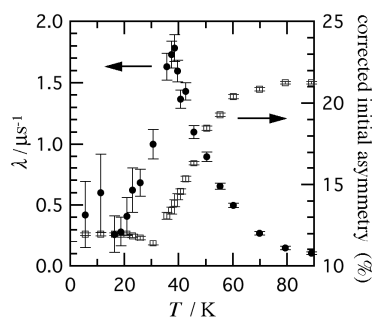


Fig. 2. Muon-spin relaxation in the ZF- $\mu$ SR on CoBPNN. Temperature dependence for the rate constant  $\lambda_{\text{fast}}$  and total initial asymmetry  $A(0) (= A_{\text{fast}}(0) + A_{\text{slow}}(0))$ .

Analysis according to the Arrhenius equation,  $\ln(2\pi\nu) = -\ln(\tau_0) - E_a/k_B T$ , gave  $E_a/k_B = 350$  K and  $\tau_0 = 6.8 \times 10^{-13}$  s obtained from the ac susceptibility measurements whose time scale was  $10^0 - 10^{-4}$  s.<sup>2)</sup> The temperature at which the dynamic process is sufficiently slow that  $\nu = 10^{-4}$  Hz (i.e.,  $\tau$  becomes hours) is 10 K from the extrapolation of this equation, which corresponds to the critical temperature for the hard magnet behavior. Similarly, if the dynamic process is assumed to be as fast as  $\nu = 10^6$  Hz, the freezing temperature would rise to 28 K. This calculation perfectly agrees with the  $\mu$ SR results. The temperature of 10 or 28 K is not essential for the magnetic ground state. On cooling, the magnetic hardness gradually grows in a unique phase below 40 K, which can be defined as the intrinsic magnetic phase transition temperature.

## References

- 1) A. Caneschi, D. Gatteschi, N. Lalioti, C. Sangregorio, R. Sessoli, G. Venturi, A. Vindigni, A. Rettori, M. G. Pini, and M. A. Novak: *Angew. Chem. Int. Ed. Engl.* **40**, 1760 (2001).
- 2) N. Ishii, Y. Okamura, S. Chiba, T. Nogami, and T. Ishida: *J. Am. Chem. Soc.* **130**, 24 (2008).

<sup>\*1</sup> Department of Applied Physics and Chemistry, The University of Electro-Communications

## Gas-Pressurized $\mu$ SR Setup at the RIKEN-RAL Muon Facility

I. Watanabe, Y. Ishii, T. Suzuki, T. Kawamata, and F.L. Pratt\*<sup>1</sup>

Pressure is an important parameter which allows the investigation of novel electronic states of solid-state materials. Since the muon-spin-relaxation ( $\mu$ SR) method can sense magnetic properties of materials in the zero-field (ZF) condition, the demand for a high-pressure  $\mu$ SR technique has been increasing recently in order to study magnetic properties and ground states of materials such as organic conductors and strongly correlated systems. The RIKEN-RAL Muon Facility is the only current facility which can provide a high-momentum double-pulsed muon beam up to 120 MeV/c.<sup>1)</sup> Thus, the development of a high-pressure  $\mu$ SR setup for the RIKEN-RAL Muon Facility is very important in offering a new experimental technique to  $\mu$ SR users working in materials science. The RIKEN  $\mu$ SR team has been collaborating with the ISIS high-pressure group at the Rutherford Appleton Laboratory (RAL) since 2005 in the development of a gas-pressurized high-pressure  $\mu$ SR setup. A gas-pressurized setup has the particular advantage over a clamp cell design in being able to change the pressure continuously without any change in the other sample conditions. This report provides detailed information on the design and development of the high-pressure system.

We finished the assembly of a high-pressure cell, a high-pressure pump and an intensifier in April 2008 and tested the system at the RIKEN-RAL Muon Facility.<sup>2)</sup> This is the first report on the test of the gas-pressurized system with a real muon beam at RAL. Designed values and photographs of each component have been reported already in the RIKEN Accel. Prog. Rep. 2006.<sup>3)</sup>

In order to confirm the signal-to-noise ratio (SN ratio) of the high-pressure set up, powdered  $\text{Fe}_2\text{O}_3$  was mounted in the cell and measured at room temperature. Iron moments in  $\text{Fe}_2\text{O}_3$  show an antiferromagnetically ordered state at room temperature. The appearance of a strong internal field at the muon site from the ordered iron moments causes the fast depolarization of the muon spin within the time resolution of the detecting system. Accordingly, the muon-spin asymmetry is lost when the injected muons stop in the  $\text{Fe}_2\text{O}_3$  powder.

Figure 1 shows the momentum dependence of  $A_0$ , the muon-spin asymmetry at  $t=0$ , measured in a transverse field (TF) of 20 G. The high-pressure cell used for this test was made of CuBe and has a flat wall, 8 mm thick, for the injection of the muon beam. This cell can be used up to the maximum pressure of 6.4 kbar.<sup>2,3)</sup> High-momentum backward-decay muons were tuned from 80 MeV/c to 100 MeV/c. Time spectra have been analyzed by using the function  $A(t) = A_0 G(\Delta, t) \cos(\omega t + \phi)$  for the time evolution

of the precessing part of the muon-spin asymmetry, where  $G(\Delta, t)$  is a Gaussian-shape damping factor of the muon-spin precession with a damping rate of  $\Delta$ . The  $\omega$  and  $\phi$  are the frequency and phase of the muon-spin precession, respectively. The  $A_0$  is about 25 % at 80 MeV/c and shows a sudden drop at around 89 MeV/c with increasing the muon momentum. The appearance of this sudden decrease of  $A_0$  means that injected muons pass through the muon window and stop at the sample position. Using the Lorentz-type fitting function the position of the minimum point of the sudden dip was determined to be 88.9 MeV/c. The SN ratio was estimated from the depth of the dip of  $A_0$  to be about 1:5. This means that about 1/6 of the injected muons stop at the sample position. Other signals come from the high-pressure cell. This SN value was not so bad and the signal from the sample was measurable. Thus, the current test using muon beams has proved that this system can be applied to real  $\mu$ SR at the RIKEN-RAL Muon Facility.

The asymmetry baseline decreases gradually with increasing momentum. The injected muons stop in deeper places of the cell when the momentum increases. In this case, the thickness of the wall of the cell seen from the muon toward the downstream side becomes thinner. Then, the absorption rate of positrons emitted from muons by the wall of the cell becomes smaller. This effect makes the total asymmetry smaller, because the backward-decay muon spin is directed to the downstream side of the muon path and the fraction of low-momentum positrons which have lower asymmetry increases at the forward counters located at the downstream side.

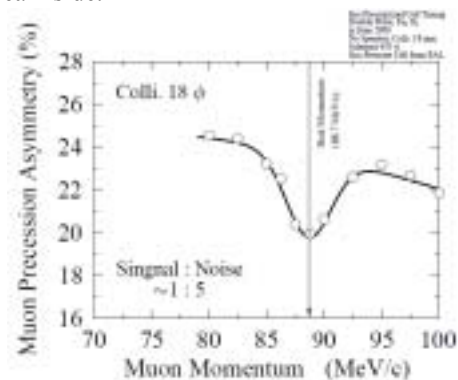


Fig. 1. Muon momentum dependence of the amplitude of the muon-spin precession in TF of 20 G measured at room temperature. The high-pressure cell was filled with  $\text{Fe}_2\text{O}_3$ .

### References

- 1) K. Nagamine et al.: *Hyperfine Interact.* **87**, 1091 (1994).
- 2) I. Watanabe et al.: *RIKEN Accel. Prog. Rep.* 2006.
- 3) I. Watanabe et al.: *Physica C* (in press).

\*<sup>1</sup> Muon Group, ISIS, Rutherford-Appleton Laboratory, UK.

# High pressure magnetic study on a molecular conductor, (DMe-DCNQI)<sub>2</sub>Cu

Y. Ishii, I. Watanabe, T. Suzuki, T. Kawamata, T. Matsuzaki and R. Kato

A series of anion radical salts, (DCNQI)<sub>2</sub>Cu, where DCNQI is *N,N*-dicyanoquinonediimine, have been extensively investigated because of their peculiar physical phenomena such as heavy-fermion-like behavior and the Metal-Insulator transition<sup>1)</sup>. The hybridization between the wide 1D  $2p\pi$  bands and the narrow  $3d$  bands is a key factor in understanding electronic properties of these systems. One of these salts, (DMe-DCNQI)<sub>2</sub>Cu, (DMe-DCNQI = 2,5-dimethyl-DCNQI) has an unusual pressure-temperature ( $P$ - $T$ ) phase diagram (Fig. 1). At ambient pressure, this material shows metallic behavior down to 450 mK. Peculiar to (DMe-DCNQI)<sub>2</sub>Cu, an insulating phase is induced by the application of pressure higher than 100 bar<sup>2)</sup>. This unusual  $P$ - $T$  phase diagram can be reproduced by the chemical pressure effect using selectively deuterated compounds<sup>3)</sup>. The fully deuterated sample of (DMe-DCNQI)<sub>2</sub>Cu, in which the chemical pressure corresponds to 512 bar, exhibits the antiferromagnetic ordering below 8 K<sup>4)</sup>.

Recently, we have developed a high-pressure  $\mu$ SR setup for the RIKEN-RAL Muon Facility<sup>5)</sup> and successfully observed a sign of pressure-induced magnetic ordering of (DMe-DCNQI)<sub>2</sub>Cu, which was predicted by the chemical pressure study, using this high-pressure setup.

Figure 2 shows typical zero-field  $\mu$ SR time spectra at 500 bar. At a low-temperature of 2 K, significant decrease of initial asymmetry due to a static magnetic

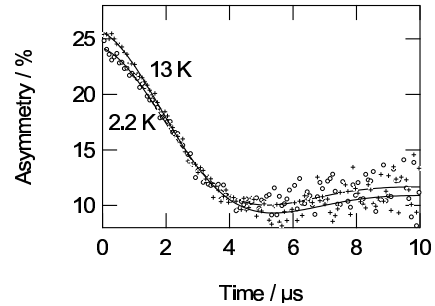


Fig. 2. Zero-field  $\mu$ SR time spectra of (DMe-DCNQI)<sub>2</sub>Cu at 500 bar for selected temperatures.

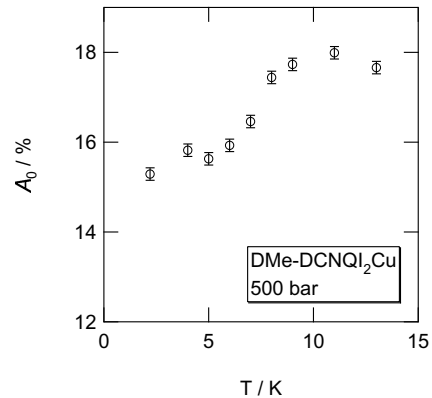


Fig. 3. Temperature dependence of a total relaxing  $A_0$ .

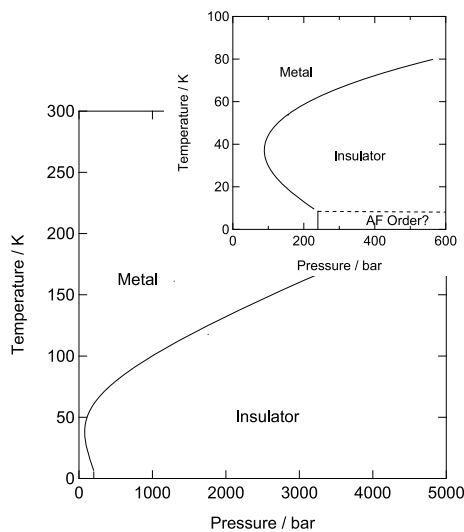


Fig. 1. Pressure - Temperature phase diagrams of (DMe-DCNQI)<sub>2</sub>Cu. The inset shows the magnification around the low-pressure region.

ordering is observed. The spectra are well fitted with a function:  $P(t) = A_0 \exp(-\lambda t) \cdot G_{KT}(\Delta, t) + B$ , where  $A_0$  is a total relaxation,  $\lambda$  is a muon relaxation rate,  $G_{KT}(\Delta, t)$  is Kubo-Toyabe function,  $\Delta$  is the distribution width of the internal field due to the nuclear dipoles and  $B$  is temperature independent background. Temperature dependence of  $A_0$  is shown in fig. 3. As shown in fig. 3, the decrease of  $A_0$  is observed below 8 K, which indicates this compound is an antiferromagnet with  $T_N = 8$  K. This  $T_N$  value is consistent with the chemical pressure study.

## References

- 1) H. Kobayashi et al.: Phys. Rev. **B 47** 3500 (1993).
- 2) S. Tomic et al.: J. Phys. C: Solid State Phys. **21** L203 (1988).
- 3) R. Kato et al.: Bull. Chem. Soc. Jpn. **73** 515 (2000).
- 4) M. Tamura et al.: Mol. Cryst. Liq. Cryst. **271** 13 (1995).
- 5) I. Watanabe et al.: Phys. **B** In Press.

# $\mu$ SR Studies of Cyanide Bridged Magnets<sup>†</sup>

F. Pratt,<sup>\*1</sup> S. Ohira-Kawamura,<sup>\*2</sup> W. Kaneko,<sup>\*3</sup> M. Ohba,<sup>\*3</sup> S. Kitagawa,<sup>\*3</sup> S. Blundell,<sup>\*4</sup> T. Lancaster,<sup>\*4</sup> and I. Watanabe

Molecular magnets form a broad class of materials<sup>1)</sup> that can often be engineered to have desired properties by careful chemical control. An example is the series of molecular magnets of the basic form  $[M_A(L)_2]_3[M_B(CN)_6]_2$ , abbreviated as  $M_A M_B(L)$ , in which the crystal structure is strongly influenced by the nature of the amine derivative ligands  $L^2)$ , leading to a range of 1D, 2D and 3D magnetic structures.  $\mu$ SR investigations of the relationship between the critical properties and the structural arrangement of the constituents have been made for various examples of these molecular magnets at RIKEN-RAL and PSI. Some properties of the four cyanide-bridged magnets on which we report  $\mu$ SR results here are listed in Table 1. Example data plots for the critical behaviour of the first three materials are shown in Fig.1. The muon precession frequency  $f(T)$  follows  $f(T)/f(0) = t^\beta$  and the longitudinal muon spin relaxation rate  $\lambda(T)$  follows  $\lambda(T)/\lambda(0) = t^{-w}$ , where  $t = |T - T_c|/T_c$ . From the measured critical behaviour the 3D ferromagnet NiFe(dipn)<sup>3)</sup> is seen to conform reasonably well to the Heisenberg model, whereas the cubic ferrimagnet MnMn(dien) has a significantly lower  $w$  value reflecting its antiferromagnetic nature. NiFe(en) has an unusual highly anisotropic rope-ladder structure and is seen to have critical behaviour closer to the Ising model.

Table 1. The cyanide-bridged magnets studied here.

	$S_A$	$S_B$	$T_c$	Structure
NiFe(dipn)	1	1/2	8.5 K	3D network
MnMn(dien)	5/2	1	25 K	Cubic
NiFe(en)	1	1/2	12.5 K	Rope-ladder
MnMn(R,S-pn)	5/2	1	21 K	Layered

When L is a chiral ligand, non-collinear interactions may be enhanced and magnetic ordering and magnetic fluctuations with well-defined chirality may be possible. This was investigated for MnMn(L) where L is one of two chiral enantiomers R-pn and S-pn or a racemic 1:1 mixture of R-pn and S-pn (Rac-pn)<sup>4)</sup>. The results for the ZF relaxation are shown in Fig.2 where a clear difference in behaviour is observed: in the racemic case the exponent  $w$  is found to be consistent with the N=2 non-collinear class, whereas in the chiral case a crossover to a weaker exponent is observed when  $T$  falls within 10% of  $T_c$ . Chiral spin correlations within the N=2 non-collinear class are expected to have the much weaker exponent  $w = 0.10$ , compared to  $w = 0.4$

<sup>†</sup> Condensed from the article in Physica **Bnn**, xxx (2009)

<sup>\*1</sup> Rutherford Appleton Laboratory, UK

<sup>\*2</sup> Ochanomizu University

<sup>\*3</sup> University of Kyoto

<sup>\*4</sup> University of Oxford, UK

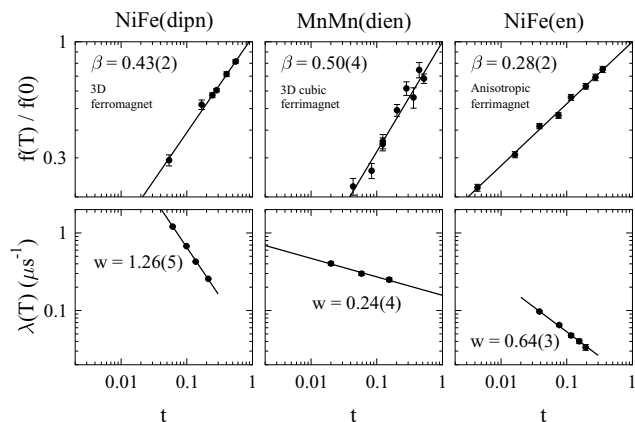


Fig. 1. Critical properties of some cyanide bridged magnets obtained from ZF  $\mu$ SR.

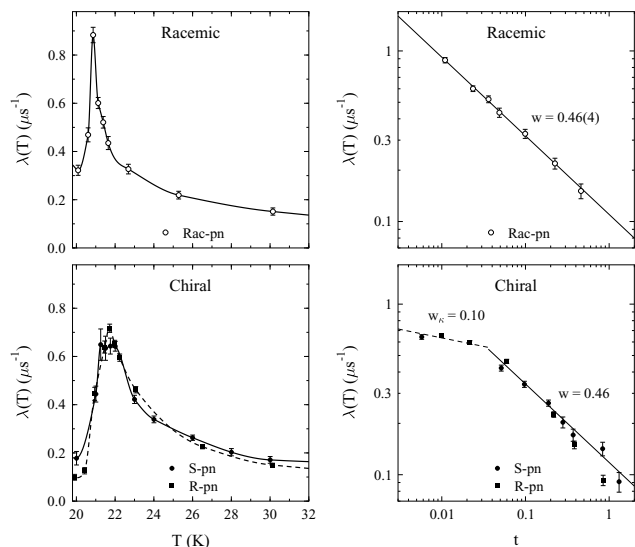


Fig. 2. Paramagnetic critical behaviour for MnMn(L) with racemic (L=Rac-pn) and chiral (L=R-pn,S-pn) ligands.

for normal spin correlations within the same class<sup>5)</sup>. The data therefore suggest that such chiral spin correlations become dominant near the transition in the case of the chiral compounds.

## References

- 1) S.J. Blundell and F.L. Pratt, J. Phys.:Condens. Matter 16 (2004) R771.
- 2) M Ohba and H. Okawa, Coord. Chem. Rev. 198 (2000) 313.
- 3) N. Yanai *et al*, J. Am. Chem. Soc. 129 (2007) 3496.
- 4) W. Kaneko *et al*, J. Am. Chem. Soc. 129 (2007) 248.
- 5) H. Kawamura, J. Phys. Soc. Jpn. 61 (1992) 1299.

# $\mu$ SR study of structure dependent electron radical dynamics in polythiophene and its derivatives

Risdiana,\*<sup>1</sup> Fitrilawati,\*<sup>2</sup> R. Hidayat,\*<sup>3</sup> and I. Watanabe\*<sup>1</sup>

The study of electronic states of organic materials of conducting polymers is one of exciting fields of material science worldwide because of their novel electronic properties and their functional applications. Among the materials being intensively studied are polythiophene (PT) based polymers. Compared with other systems of conducting polymers, the polythiophene form an important class with certain practical advantages. These include : they are easily synthesized and doped with various dopants; they are chemically, thermally and environmentally stable in air and moisture both in doped and undoped states; they are easily modified by side change substitution for property modifications and they have potential commercial applications.

The most notable properties of these materials are their electrical conductivity resulting from the delocalization of electrons in the polymer backbone via doping to the conjugated  $\pi$ -orbital. These properties are related to the charge carrier transport and its mobility along (intra) and perpendicular (inter) to the polymer chain.

The macroscopic electronic transport measurement of conducting study conducted on PT reported that the functional properties of these polymers depend strongly on their structures such as regio-regularity (regio-random or regio-regular) and the side-chain length of its alkyl substituent. However, none of the reported studies can clearly explain the properties because of the mechanism of the intra- and inter-chain charge transport.

Here, we propose to study the microscopic intrinsic charge transport along the chain and perpendicular to the chain in polythiophene (PT) based polymers with different structures by a muon-spin-relaxation ( $\mu$ SR) method to elucidate the intra- and inter-chain hopping mechanism.

We have carried out longitudinal field (LF)-  $\mu$ SR measurements in a polythiophene sample of Poly(3-hexylthiophene-2,5-diyl) with regio-regular structure. All of the time spectra are well fitted by the two-component function below:

$$A(t) = A_1 \exp(-\lambda_1 t) + A_2 \exp(-\lambda_2 t) \quad (1)$$

$A_1$  and  $A_2$  are the initial asymmetries and  $\lambda_1$  and  $\lambda_2$  are the depolarization rates for fast and slow components, respectively. According to Butler *et al.*,<sup>(1)</sup>, the LF dependence of the dynamical depolarization rate

reflects the dimensionality of the diffusion of the spin-excited state. That is, the depolarization rate is proportional to  $H^{-0.5}$  for 1 dimensional intra-chain diffusion and  $C \cdot H^{0.5}$  for 3 dimensional inter-chain diffusion.

Figure 1 shows the longitudinal-field (LF) dependence of the muon-spin depolarization rate ( $\lambda_1$ ) of regio-regular polythiophene of Poly(3-hexylthiophene-2,5-diyl) at temperatures of 300 K and 10 K. The solid line is the best fit, using the diffusion model mentioned above. In low temperatures of 10 K, the depolarization rate reflected intra-chain diffusion, meaning that at low temperatures the charge transport is dominated by mobility along (intra) the polymer chain. With increasing temperature, the charge carrier mobility changes from intra-chain to an inter-chain diffusion one. Similar behaviors are also observed at an LF dependence of  $\lambda_2$ . However the values of  $\lambda_2$  are two order magnitude smaller than that of  $\lambda_1$  indicating that the contributions of the second component to the muon spin relaxation are very small compared to the first component. The present results indicate that the dimensional cross over is observed in the regio-regular polythiophene. Compared to other conducting polymers such as PANI and PPV<sup>(2)</sup>, observation of dimensional cross over in the low temperatures indicated that the samples have more metallic behavior.

To obtain conclusive results, other polythiophene samples with different structures such as regio-random polythiophene and the polythiophene with different length of side groups should be used for the  $\mu$ SR measurements.

## References

- 1) M. A. Butler *et al.*, : J. Chem. Phys. **64** (1976) 3592.
- 2) F. L. Pratt: J. Phys. Condens. Matter **16** (2004) S4779.

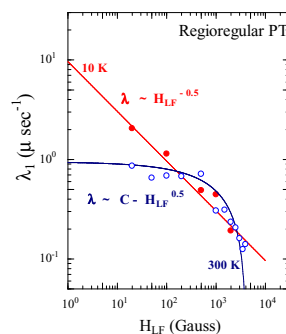


Fig. 1. The longitudinal-field dependence of  $\lambda_1$  of regio-regular polythiophene (PT) of Poly(3-hexylthiophene-2,5-diyl) at 10 K and 300 K.

\*<sup>1</sup> The Institute of Physical and Chemical Research (RIKEN)

\*<sup>2</sup> Department of Physics, Padjadjaran University, Indonesia

\*<sup>3</sup> Department of Physics, Bandung Institute of Technology, Indonesia

# Lithium and muon diffusion in layered lithium-ion battery materials

K. Mukai,<sup>\*1</sup> J. Sugiyama,<sup>\*1</sup> H. Nozaki,<sup>\*1</sup> M. Månsson,<sup>\*2</sup> I. Watanabe,<sup>\*3</sup> K. Ariyoshi,<sup>\*4</sup> and T. Ohuzku<sup>\*4</sup>

[muon, lithium-ion battery, diffusion]

Lithium cobalt dioxide  $\text{LiCoO}_2$ , in which the  $\text{Li}^+$  plane is sandwiched by the two adjacent  $\text{CoO}_2$  layers, has been extensively studied as a positive electrode material of lithium-ion batteries (LIB)<sup>1)</sup>. In order to increase/optimize the performance of the LIB, fundamental electrochemical properties should be given for all the LIB materials. Among them, the Li diffusion constant ( $D_{\text{Li}}$ ) plays a significant role on the battery performance. For non-magnetic compounds,  $D_{\text{Li}}$  is usually determined by  $^7\text{Li}$ -NMR. However, for the positive electrode material such as  $\text{LiCoO}_2$ <sup>2)</sup> and  $\text{LiMn}_2\text{O}_4$ <sup>3)</sup>, since the spin-lattice relaxation rate of  $^7\text{Li}$ -NMR is strongly affected by the  $3d$  electron-spins, it is difficult to estimate the correct  $D_{\text{Li}}$  by  $^7\text{Li}$ -NMR. Therefore, we have carried out the  $\mu\text{SR}$  experiments in order to examine the  $D_{\text{Li}}$  for the LIB materials.

Powder samples of  $\text{Li}_x\text{CoO}_2$  were prepared by an electrochemical reaction between Li and  $\text{LiCoO}_2$  in non-aqueous Li-ion cells. According to an ICP-AES analysis, the Li/Co ratios of the samples were determined to be 0.73 and 0.53. For the  $\mu\text{SR}$  experiments, powder samples were packed in a sealed aluminum sample cell in a He-filled glove-box, and then placed on a copper sample holder in a cryostat. The  $\mu\text{SR}$  spectra were measured in the surface muon beam line of the RIKEN-RAL Muon Facility at the ISIS.

The  $\mu\text{SR}$  spectra above 50 K for the  $\text{Li}_x\text{CoO}_2$  samples with  $x = 0.73$  and 0.53 were well fitted by a dynamic Kubo-Toyabe function  $G^{\text{DGKT}}$ ;

$$A_0 P_{\text{ZF}}(t) = A_{\text{KT}} G^{\text{DGKT}}(t, \Delta, \nu) \exp(-\lambda_{\text{KT}} t) + A_{\text{BG}}, \quad (1)$$

where  $A_0$  is the empirical maximum muon decay asymmetry,  $A_{\text{KT}}$  and  $\lambda_{\text{KT}}$  are the asymmetry and relaxation rate of the Kubo-Toyabe signal,  $\Delta$  is the static width of the local frequencies at the disordered sites, and  $\nu$  is the field fluctuation rate. As  $T$  increases from 50 K,  $\Delta$  for the both samples decreases monotonically up to 160 K, and then rapidly drops around 170 K [Fig. 1(a)]. The  $\nu(T)$  curves indicate an Arrhenius behavior in the  $T$  range between 170 and 320 K [Fig. 1(b)]. Although there are no magnetic transitions above 100 K by our previous  $\mu\text{SR}$  for  $\text{Li}_x\text{CoO}_2$ , the  $\chi(T)$  curves show a small anomaly around 160 K [Fig. 1(c)]. Furthermore, electrostatic potential calculations suggested that  $\mu$  are not located at the vacant Li site but at the vicinity of  $\text{O}_2^-$  ions. The increase in  $\nu$

above 150 K is, therefore, most unlikely due to  $\mu$  diffusion but is likely due to  $\text{Li}^+$  diffusion. In other words,  $\nu$  corresponds to the jumping rate of  $\text{Li}^+$  ions. The self-diffusion coefficient  $D_{\text{Li}}^{\text{self}}$  is, therefore, estimated by a simple random walk model;  $D_{\text{Li}}^{\text{self}} = NZs^2\nu$ , where  $N$  is the number of Li sites,  $Z$  the vacancy fraction, and  $s$  the jump distance. Using the jump distance of  $\sim 0.2$  nm (the nearest distance between Li-Li ions, i.e. lattice parameter of  $a_{\text{h}}$ ),  $D_{\text{Li}}^{\text{self}}$  is estimated to be about  $10^{-10} \text{ cm}^2\text{s}^{-1}$  at 250 K. This value is larger by two order of magnitude than that from the  $^7\text{Li}$ -NMR and is comparable with that of electrochemical measurement<sup>4)</sup>.

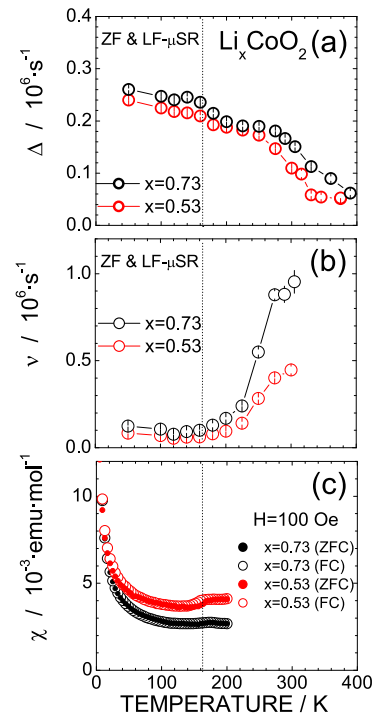


Fig. 1. Temperature dependences of (a) field distribution width ( $\Delta$ ), (b) field fluctuation rate ( $\nu$ ), and (c) susceptibility ( $\chi$ ) measured in the zero field-cooling (ZFC) and field-cooling (FC) mode with  $H = 100$  Oe, for the  $\text{Li}_x\text{CoO}_2$  with  $x = 0.73$  and 0.53.

## References

- 1) K. Mizushima *et al.*; Mater. Res. Bull. **15**, 783 (1980).
- 2) K. Nakamura *et al.*; Solid State Ionics **135**, 143 (2000).
- 3) V. M. J. Verhoeven *et al.*; Phys. Rev. Lett. **86**, 4314 (2001).
- 4) A. Van der Ven and G. Ceder; Electrochem. Solid-State Lett. **3**, 301 (2000).

<sup>\*1</sup> Toyota Central Research and Development Labs., Inc.

<sup>\*2</sup> Laboratory for Neutron Scattering, PSI

<sup>\*3</sup> Muon Science Laboratory, RIKEN

<sup>\*4</sup> Department of Applied Chemistry, Osaka City University

## Proton conductor II<sup>†</sup>

H. Nozaki,<sup>\*1</sup> Y. Ikedo,<sup>\*2</sup> J. Sugiyama,<sup>\*1</sup> M. Kawasumi,<sup>\*1</sup> and I. Watanabe

[Proton diffusion, fuel cell]

Perfluorinated sulfonic acid copolymers (F-polymers) such as Nafion are currently being used as an electrolyte for vehicle fuel cells (FC). However, these FC do not work above 373 K (100°C) because Nafion is sufficiently conductive only when it contains enough water. Therefore, we need to develop a new electrolyte with high proton conductivity which does not use water, in order to improve FC performance. In our previous  $\mu$ SR experiments, we measured several F-polymers with various sulfonic acid densities ( $D_s$ ).<sup>1,2)</sup> The result suggested that  $\mu^+$ s diffuse by thermally activated process, and their activation energy ( $E_a$ ) decreases with increasing  $D_s$ . In other words, higher  $D_s$  result in lower  $E_a$ ; that is, an F-polymer which works under dry conditions can be realized if we increase  $D_s$  above the critical value ( $D_c = 4.47 \times 10^{-3}$  eq/cm<sup>3</sup>). Here,  $D_c$  is defined as the value at which  $E_a = 0$ . Unfortunately, it is difficult to synthesize F-polymers with  $D_s \geq D_c$ . Among several proton-conducting polymers, a hydrocarbon (HC)-polymer is one candidate for an FC electrolyte. Here, we report  $\mu^+$ SR results on the HC-polymer to study the relationship between proton conducting behavior and  $D_s$ .

HC-polymer films based on sulfonated poly ether ether keton (PEEK) were dried in an Ar-filled globe-box at 110°C for 12 hours. Then the several films with  $\sim 24$  mm diameter were stacked in a sealed sample cell

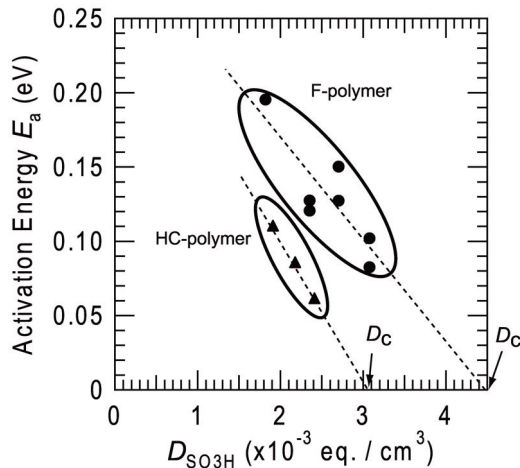


Fig. 1. Relationship between  $D_s$  and activation energy  $E_a$  for HC- and F-polymers. The dashed lines calculated by the least square method.  $D_c$  is defined as the crossing point of the horizontal axis and dashed line.

<sup>\*1</sup> Toyota Central Research and Development Labs. Inc.

<sup>\*2</sup> High Energy Accelerator Research Organization

made of titanium with a gold o-ring at Toyota CRDL, and then the cell was transferred to the UK and set onto the oven sample holder. The  $\mu^+$ SR experiment was carried out on the ARGUS surface muon beamline at the RIKEN Muon Facility at ISIS in the temperature range between 300 and 500 K.

According to the longitudinal field (LF)  $\mu$ SR measurements, it was found that 70  $\sim$  80% of  $\mu^+$  produce muonium. But the remaining 20  $\sim$  30% provided an exponentially relaxing signal in zero external field (ZF), which is thought to be caused by  $\mu^+$  diffusion between the nearest neighboring SO<sub>3</sub> groups. Therefore, the ZF- $\mu$ SR spectrum was fitted with the following equation;

$$A_0 P_{ZF}(t) = A_{\text{fast}} \exp(-\lambda_{\text{fast}} t) + A_{\text{slow}} \exp(-\lambda_{\text{slow}} t), \quad (1)$$

where  $A_0$  is the empirical maximum muon decay asymmetry,  $A_{\text{fast}}$  and  $A_{\text{slow}}$  are the asymmetries associated with the two components, and  $\lambda_{\text{fast}}$  and  $\lambda_{\text{slow}}$  are their relaxation rates. In Eq. (1), the first term corresponds to the signal from muonium, while the second term corresponds to the signal from  $\mu^+$  diffusion. Typical  $\lambda_{\text{fast}}$  and  $\lambda_{\text{slow}}$  values were 6  $\sim$  7 ( $10^6$  s<sup>-1</sup>) and 0.05  $\sim$  0.16 ( $10^6$  s<sup>-1</sup>), respectively.  $\lambda_{\text{fast}}$  has no temperature ( $T$ ) dependency within the error bar, favoring production of muonium. The  $T$  dependence of  $\lambda_{\text{slow}}$  is found to obey the Arrhenius law described by Eq. (2) above 300 K, indicating the existence of a thermally activated process, as in the case for the F-polymer.

$$\lambda_{\text{slow}} = A \exp\left(-\frac{E_a}{kT}\right) \quad (2)$$

where  $A$ ,  $E_a$  and  $k$  are the pre-exponential factor, activation energy and Boltzmann constant, respectively. The  $D_s$  dependence of  $E_a$  is shown in Fig. 1.  $E_a$  for the HC-polymer decreases systematically with increasing  $D_s$ . This is very reasonable due to the fact that the average hopping distance shortens with increasing  $D_s$ . Interestingly, when  $D_s$  is same,  $E_a$  for the HC-polymer is almost half the  $E_a$  of the F-polymer. Furthermore, the  $D_c$  of HC-polymer is estimated to be  $3.04 \times 10^{-3}$  eq/cm<sup>3</sup> which is lower than that of F-polymer. This suggests that HC-polymers may be a better material for a proton conducting electrolyte without water.

### References

- 1) J. Sugiyama et al.: KEK-MSL Report 2004, 20 (2004).
- 2) J. Sugiyama et al.: Riken-RAL Muon Facility Report 6, 62 (2004-2006).

# Muon transfer studies in solid D<sub>2</sub> with implanted alkali and alkaline-earth ions

P. Strasser,<sup>\*1</sup> A. Taniguchi,<sup>\*2</sup> S. Ohya,<sup>\*3</sup> T. Matsuzaki, K. Ishida, Y. Matsuda,<sup>\*4</sup> M. Iwasaki, and K. Nagamine<sup>\*5</sup>

[Muonic atom spectroscopy, solid hydrogen film, ion implantation]

We have proposed the cold hydrogen film method<sup>1)</sup> to expand muonic atom spectroscopy by utilizing nuclear beams, including, in the future, radioactive isotope (RI) beams, to produce radioactive muonic atoms. This method will enable the study of unstable nuclei by the muonic X-ray method at facilities where both intense  $\mu^-$  and RI beams will be available. The basic concept is to stop both  $\mu^-$  and nuclear beams simultaneously in a solid hydrogen film, followed by the application of the direct muon transfer reaction to higher  $Z$  nuclei to form radioactive muonic atoms. An experimental program to perform muonic X-ray spectroscopy with stable ions implanted in a solid hydrogen (H<sub>2</sub>/D<sub>2</sub>) film has been initiated at the RIKEN-RAL muon facility.

Promising results have already been reported from the first transfer experiment performed with isotopically separated <sup>88</sup>Sr and <sup>86</sup>Sr ions using a new surface ion source constructed and installed on the existing  $\mu A^*$  apparatus with the aim of using radioactive isotopes in the future.<sup>2)</sup> It can produce ions from alkali and alkaline-earth elements with high efficiency.

Last year we conducted further experiments and measured a target with isotopically separated <sup>87</sup>Sr ions. We utilized the same procedure as that used previously to implant argon and strontium ions. Figure 1 shows the delayed energy spectrum measured by the Ge detector with 1-mm pure D<sub>2</sub> and <sup>87</sup>Sr (solid line) ions implanted non-uniformly. The fitting curves obtained previously with <sup>88</sup>Sr (dotted line) and <sup>86</sup>Sr (dashed line) are also shown. A preliminary analysis shows that the measured isotope shifts are consistent with those observed in previous experiments using enriched strontium isotopes in very large quantities. This experiment was performed using natural strontium oxide (SrO) in the ion source, and only about  $4 \times 10^{16}$  ions of <sup>87</sup>Sr ions in the target. The set of measurements with strontium isotope ions is now completed. The data are being analyzed, and a publication should follow shortly.

The first measurement with barium isotopes was also performed with isotopically separated <sup>138</sup>Ba ions implanted into 1-mm thick solid deuterium film in a way similar to that used with strontium isotopes. Trans-

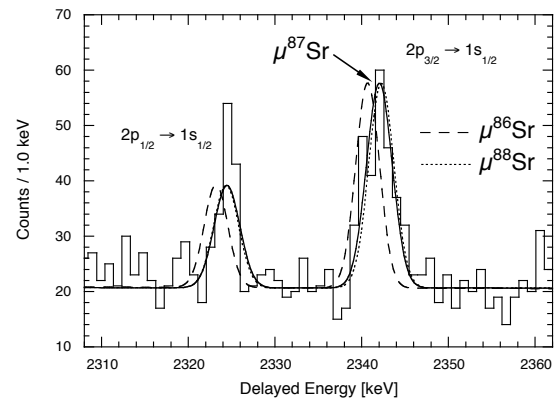


Fig. 1. Muonic <sup>87</sup>Sr delayed energy spectrum (solid line). Fitting curves for  $\mu^{88}\text{Sr}$  (dotted line) and  $\mu^{86}\text{Sr}$  (dashed line) measured previously are also shown.

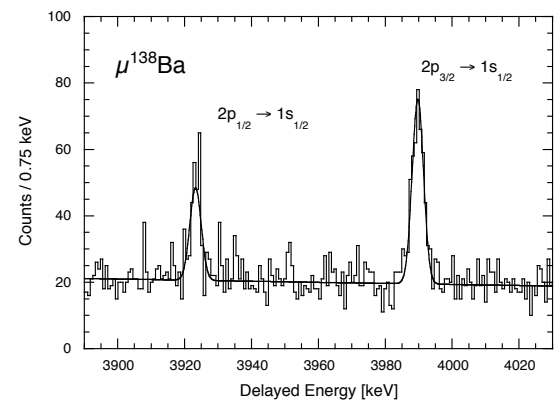


Fig. 2. Muonic <sup>138</sup>Ba delayed energy spectrum.

fer X-rays were successfully observed at around 4 MeV (see Fig. 2). The energies of muonic X-rays increase rapidly with the atomic number resulting in low detection efficiency. Our measurements are consistent with previous experiments performed using enriched Ba isotopes. The energy calibration is determined from muonic Pb X-rays at around 6 MeV measured in a separate run.

These experiments are still performed with a relatively large number of implanted ions because of the relatively low  $\mu^-$  beam intensity at a momentum of 27 MeV/c. Future muon facilities with higher muon flux would require fewer implanted ions. Further measurements are planned with rare-earth elements.

## References

- 1) P. Strasser et al.: AIP Conf. Proc. 793, 242 (2005).
- 2) P. Strasser et al.: RIKEN Acc. Prog. Rep. 41 (2007).

\*1 Muon Science Laboratory, IMSS, KEK

\*2 Research Reactor Institute, Kyoto University

\*3 Department of Physics, Niigata University

\*4 Graduate School of Arts and Sciences, University of Tokyo

\*5 University of California Riverside, CA, USA

## Feasible study of molecular effects on the muon transfer process

K. Ninomiya<sup>\*1</sup>, R. Nakagaki<sup>\*1</sup>, K. Kubo<sup>\*2</sup>, Y. Kobayashi, K. Ishida, T. Matsuzaki, H. Matsumura<sup>\*3</sup>, T. Miura<sup>\*3</sup>  
and A. Shinohara<sup>\*1</sup>

It is known that the muon capture phenomenon is influenced by the electron structure of a muon capturing molecule or atom when a free muon is captured on a muon atomic orbit directly. Our group has been studying on the molecular effects on the formation process of muonic atoms.

In this study, we focused on another muonic atom formation process; the muon transfer process. A muonic hydrogen atom ( $\mu\text{p}$ ) has a neutron-like property because of its small muon atomic orbit. So, it can penetrate the electron clouds of other atoms and the atomic muon then transfers to the deeper atomic muon level of the atom. This phenomenon is known as a "muon transfer process". In a muon transfer process, no molecular effects have been reported. We expect that some effects from valence electrons and/or molecular structure also exist in the muon transfer process because the size of muonic hydrogen is much larger than that of a neutron and the muon is transferred to an excited (i.e., large) muon atomic orbit.

We are going to study the molecular effects on the muon transfer process from muonic X-ray measurements for various molecules. If there are some influences on the muon transfer reaction from the electron structures of muon capturing molecules, different muonic X-ray spectra will be obtained from two samples that contain the same elements but have different molecular structures. We constructed a new system for muonic X-ray measurement (Fig. 1) at port-1 in RIKEN-RAL<sup>1)</sup>. The feasibility of X-ray measurement was studied with argon, hydrogen and mixture of these gases under the pulsed muon beam conditions.

First, the optimum measuring conditions; muon momentum, beamline magnet current, beam slits, the magnetic field in target position, sample gas pressures (10 or 30 bar) and the configuration of radiation shield, were studied by using argon gas samples. Muonic X-ray measurements for pure argon samples were carried out under the optimized measuring conditions, to obtain the muonic X-ray spectra for the direct muon capture process. We also determined optimum muon irradiation momentum for mixed gases (hydrogen 99.7% and argon 0.3%) by using pure hydrogen gas samples, and then carried out muonic X-ray measurements for the mixed gas samples. The obtained X-ray spectra for argon and mixed gas samples are shown in Fig 2. Obvious differences in X-ray spectra were found. For example, the ratio of  $\mu\text{Ar}(3-1)$  to  $\mu\text{Ar}(2-1)$  X-ray

intensity in a mixed gas sample ( $0.19 \pm 0.05$ ) is larger than that in a pure argon sample ( $0.05 \pm 0.01$ ). In the mixed gas samples, muonic argon X-rays were mainly detected in a time region delayed from the muon beam pulse because the transfer process occurs after muonic hydrogen formation. We determined the lifetime of muonic hydrogen atoms experimentally from timing spectra of muonic argon X-rays ( $170 \pm 130$  ns for 10 bar and  $90 \pm 60$  ns for 30 bar). These X-ray intensities and lifetimes reproduce the results of PSI experiment well<sup>2)</sup>.

In this study, we successfully obtained muonic X-ray spectra from muonic argon formed through a muon transfer process for 10 and 30 bar conditions. As the next step, we are planning to construct further effective systems (for example, by using more X-ray detectors) and use molecular gas samples for muon irradiations to examine the molecular effects on the muon transfer process

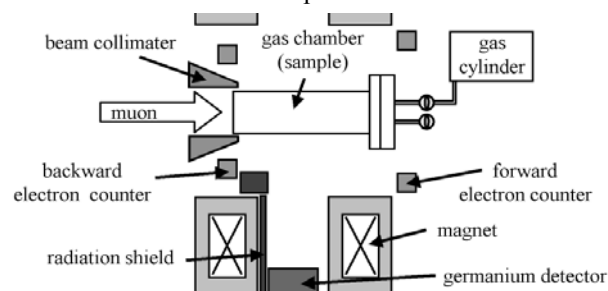


Fig. 1. Schematic view of the measuring system at port-1.

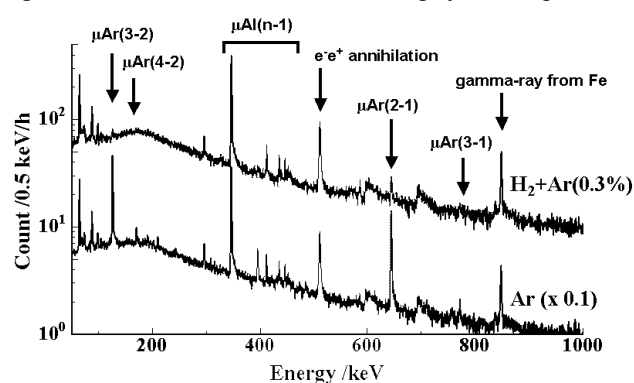


Fig. 2. Muonic X-ray spectra for Ar and  $\text{H}_2+\text{Ar}$  in 10 bar. The numbers in parenthesis represents the change in the muon principal quantum number. The sample chambers were made of aluminum and stainless steel. As a result muonic aluminum X-rays and gamma-rays from iron were also detected.

<sup>\*1</sup> Graduate School of Science, Osaka University

<sup>\*2</sup> Division of Natural Sciences, International Christian University

<sup>\*3</sup> Radiation Research Center, High Energy Accelerator Research Organization

### References

- 1) T. Matsuzaki, *et al.*, Nucl. Inst. Meth. **A465** (2001) 365
- 2) R. Jacot-Guillarmod, *et al.*, Phys. Rev., **A55** (1997) 3447

## Muon beam density enhancement effect with tapered tubes

D. Tomono, T.M. Kojima, T. Ikeda, K. Ishida, Y. Iwai, M. Iwasaki, Y. Kanazawa\*<sup>1</sup>, Y. Matsuda\*<sup>2</sup>, T. Matsuzaki, and Y. Yamazaki\*<sup>3</sup>

Charged particles can be effectively focused by a tapered glass tube, which deflects them at the inner wall surface and guides them to its outlet. Previous experiments confirmed this effect with a glass capillary for 2 MeV He<sup>+</sup> ions<sup>1)</sup> and for 8 keV Ar<sup>8+</sup> ions<sup>2)</sup>. Our recent experiment<sup>3)</sup> at RIKEN-RAL showed that a beam density of 54 MeV/c muons can be increased almost by a factor of two, when a tapered glass tube is inserted coaxially along the muon beam. This can be explained by a Coulomb scattering on the inner wall. This observation suggests a possibility exists to increase the number of available muons by optimizing the inner shape of collimators. For the practical application of  $\mu$ SR and other muon studies, detailed study of the density enhancement mechanism was performed using a continuous muon beam at TRIUMF, Canada.

The present experiment aims to understand two issues. One is to examine kinematics, such as kinetic energy distribution and angular distribution of the outgoing beam through tapered tubes, although at RIKEN-RAL, only the number of outgoing muons was measured due to the pulsed nature of the muon beam. The other is to observe the material dependence of the enhancement effects. Because of the larger reflection coefficient of the Coulomb scattering in a heavy material, Monte Carlo simulation shows that tapered tubes made of heavy materials, such as copper and gold, give larger density enhancement than glass tube. For simplicity, 1-dimensional scattering effects were measured using glass, Cu and Au-coated Cu plates rather than their tubes.

Figure 1 shows a schematic view of the setup at the M9B beam line, TRIUMF. All components are placed in a vacuum chamber so that low energy muons around 40 MeV/c cannot scatter or stop in the air. The incoming muon is identified by a 0.5 mm thick plastic scintillator (S1). A pair of vertical plates at a slightly narrowing angle are mounted around the beam axis, where some muons are scattered downstream, resulting in the beam being focused on a detector position. Muons stopped at the plates decay into positrons, which are identified by 5 mm thick plastic scintillators (S2-S7) surrounding the plates. The outgoing muon energy is measured by a 5mm thick and 16 mm $\phi$  lithium drifted silicon detector (SSD, ORTEC TL-045-200-5). Plastic scintillators (S8, S9) are surrounded to monitor decay positrons which come from muons stopped in SSD. Angular dependence of the muon energy distri-

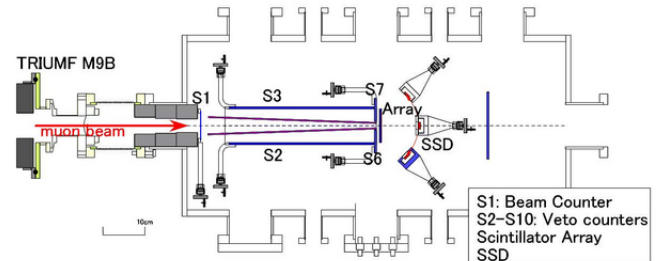


Fig. 1. A schematic view of the setup at M9B beam line.

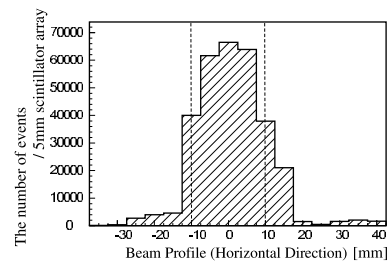


Fig. 2. A beam profile observed by the array counter of 5 mm segments, which is set 100 mm downstream of the plates outlet. The dashed line shows the outlet width.

bution is observed by SSD rotated around the outlet of plates. Angular dependence of the number of muons is observed by an array counter instead of SSD. It consists of 16 scintillators of 10 mm length and 5 mm square aligned in the vertical direction, and covers 10  $\times$  80 mm<sup>2</sup> area in total. The SSD or array is mounted 10 mm or 100 mm downstream of the outlet. The 5 mm thick large plastic scintillator (S10) is mounted downstream to identify muons which do not stop at SSD, array or any counters.

Figure 2 shows a preliminary result of the beam profile observed by the array counter set 100 mm downstream of the outlet when the Cu plates are placed at the center. It shows that most muons are focused at the outlet although some muons are scattered wider than the outlet width of 20 mm.

In summary, we performed the test experiment to observe beam density enhancement with various tapered plates made of metals and glass instead of the tapered glass tube. Accumulated data in the last beam time is being analyzed at present. The next beam time is scheduled in June in order to complete this measurement.

### References

- 1) T. Nebiki, et. al.: J. Vac. Sci. Tech. A **21**(2003)1671.
- 2) T. Ikeda, et. al.: Appl. Phys. Lett. **89**(2006)163502.
- 3) T.M. Kojima, et. al.: J. Phys. Soc. Jpn. **76**(2007)093501.

\*1 Department of Physics, Sophia University

\*2 Graduate School of Arts and Sciences, University of Tokyo

\*3 RIKEN and Graduate School of Arts and Sciences, University of Tokyo

### **3. Radiochemistry and Nuclear Chemistry**

# Precision measurement of the half-life of $^{90m}\text{Nb}$ using a gas-jet transport system

H. Kikunaga,<sup>\*1</sup> H. Fujisawa,<sup>\*1</sup> W. Yahagi,<sup>\*1</sup> K. Ooe,<sup>\*1</sup> R. Takayama,<sup>\*1</sup> A. Shinohara,<sup>\*1</sup>  
Y. Kasamatsu,<sup>\*2</sup> Y. Ezaki H. Haba K. Hirose,<sup>\*3</sup> and T. Ohtsuki<sup>\*3</sup>

The goal of our research is to clarify the effects of chemical structure on the decay constant of  $^{90m}\text{Nb}$ . Almost all  $^{90m}\text{Nb}$  nuclides decay via a 2.3-keV transition from the 124.7-keV level to the 122.4-keV level in  $^{90}\text{Nb}$ .<sup>1)</sup> Because of the high internal conversion coefficient and low transition energy, the probability of the transition is expected to vary with changes in the chemical structure affecting the electron density at the nucleus.

In the previous studies, the decay constant of  $^{90m}\text{Nb}$  was obtained with a radioactive equilibrium method<sup>2)</sup> or direct half-life measurement.<sup>3)</sup> However, it appears that strong activity from undesired nuclear reaction products interfered with the measurements. In order to precisely determine the short half-lives of  $^{90m}\text{Nb}$  in various chemical states, we employed an on-line gas-jet transport system in this study.

The isotope  $^{90m}\text{Nb}$  was produced in the nuclear reaction  $^{nat}\text{Zr}(p, xn)^{90m}\text{Nb}$  with a 14 MeV proton beam delivered from the RIKEN K70 AVF Cyclotron. Five  $^{nat}\text{ZrO}_2$  targets of about  $100 \mu\text{g cm}^{-2}$  thickness were prepared by electrodeposition onto an  $810 \mu\text{g cm}^{-2}$  aluminum backing foil. The targets were placed in a gas-jet chamber at intervals of 8 mm. The beam intensity was about  $8 \mu\text{A}$ . The 14 MeV proton beam entered the target stack at an energy of 13.8 MeV. The reaction products recoiling out of the targets were stopped in the helium gas, attached to KCl aerosol particles generated by sublimation of KCl powder at  $640^\circ\text{C}$ , and

continuously transported to the chemistry laboratory.

The reaction products were collected on a glass filter for 180 s and assayed by  $\gamma$ -ray spectrometry with a HP-Ge semiconductor detector. The accumulation of  $\gamma$ -ray spectrum for 1 min was started 1 min after the end of aerosol collection and then repeated 30 times successively. Next, the reaction products were deposited on a polyethylene terephthalate film to measure the half-life of  $^{90m}\text{Nb}$  in 20 M HF. After deposition for 30 s, they were dissolved in 20 M HF and subjected to  $\gamma$ -ray spectrometry. The accumulation of  $\gamma$ -ray spectrum for 6 s was started within 1 min after the end of the aerosol deposition and then repeated 15 times successively. In order to achieve adequate statistical precision, the procedure was repeated 120 times. The half-lives of  $^{90m}\text{Nb}$  were determined by the reference source method<sup>4)</sup> using  $^{137}\text{Cs}$  as a reference source.

A  $\gamma$ -ray spectrum measured for 5 min after the 180-s aerosol collection is shown in Fig. 1. The  $\gamma$  peaks of  $^{90g}\text{Nb}$  ( $T_{1/2} = 14.6$  h),  $^{90m}\text{Nb}$ ,  $^{52m}\text{Mn}$  (21.1 min),  $^{54m}\text{Co}$  (1.48 min),  $^{64}\text{Ga}$  (2.63 min), and  $^{91m}\text{Y}$  (49.7 min) are observed in the spectrum. The  $\gamma$ -peak of  $^{90m}\text{Nb}$  at 122 keV is clearly separated from the peak of  $^{90g}\text{Nb}$  at 133 keV, which is the closest to that of  $^{90m}\text{Nb}$ . No serious background was observed in the  $\gamma$ -ray spectrum for determination of the half-life of  $^{90m}\text{Nb}$ .

In the latter experiment, the  $\gamma$  peaks derived from the nuclear reaction products were observed only for  $^{90m,g}\text{Nb}$  except for the 511-keV line. The obtained half-life of  $^{90m}\text{Nb}$  in 20 M HF solution was  $18.97 \pm 0.03$  s, which is consistent with the literature value <sup>1)</sup> ( $18.81 \pm 0.06$  s) within  $2\sigma$ . Although thoroughly corrections for dead-time and pile-up have not yet been performed, measurements under the low-background condition with good precision were conducted. The present system will allow us to measure the half-life of  $^{90m}\text{Nb}$  with various chemical states.

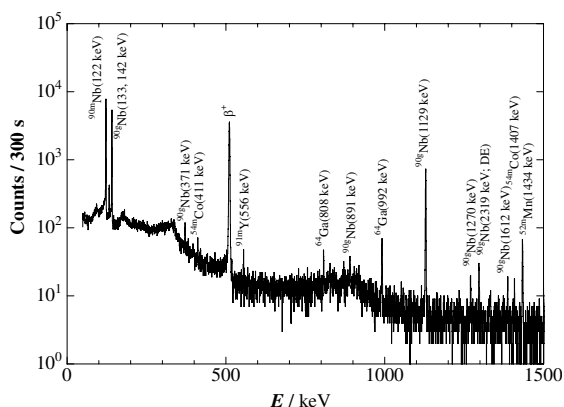


Fig. 1. Gamma-ray spectrum measured for 300 s after 180-s aerosol collection.

<sup>\*1</sup> Department of Chemistry, Osaka University

<sup>\*2</sup> Japan Atomic Energy Agency

<sup>\*3</sup> Laboratory of Nuclear Science, Tohoku University

## References

- 1) R. B. Firestone and V. S. Shirley: *Table of Isotopes, 8th ed.* (John Wiley and Sons, New York, 1996).
- 2) J. A. Cooper et al.: *Phys. Rev. Lett.* **15**, 680 (1965); A. Olin, *Phys. Rev.* **C1**, 1114 (1970).
- 3) J. S. Geiger et al.: *Can. J. Phys.* **47**, 949 (1969); W. Weirauch et al.: *Z. Phys.* **209**, 289 (1968) 289; A. Meykens et al.: *Z. Phys.* **A284**, 417 (1978).
- 4) M. A. L. Silva et al.: *Appl. Radiat. Isot.* **60**, 301 (2004).

## Biodistribution of Riken multitracer (MT) and MT-EDTMP, MT-DOTMP in mice

K. Washiyama,<sup>1</sup> R. Nakamura,<sup>2</sup> H. Koshida,<sup>2</sup> H. Haba, S. Enomoto, R. Amano<sup>1</sup>

In nuclear medicine, samarium-153 labelled ethylenediamine-tetramethylene phosphonic acid (EDTMP) and holmium-166 labelled 1,4,7,10-tetraazacyclododecane-1,4,7,10-tetramethylene phosphonic acid (DOTMP) have been used, respectively, in bone pain palliation for bone metastases<sup>1)</sup> and myeloablative treatment for multiple myeloma.<sup>2)</sup> Both phosphonates typically accumulate in bone. The usage of these radiolabelled phosphonates is dependent on the half-life, radiolabelled energy, and decay mode of selected nuclides. In order to examine the practical applicability of labelled phosphonates, it is important to investigate their metabolism. The Riken multitracer (MT) technique is highly efficient for comparison of many tracers under same conditions, and has been used to investigate the biodistribution of MT, MT labelled EDTMP and DOTMP in vivo.

Male 8-week-old ICR mice were grouped and administered with MT (in saline solution), MT-EDTMP, and MT-DOTMP. The blood, liver, kidney, small intestine, large intestine, femur, and brain were excised and weighed. The uptake rates of several nuclides (<sup>57</sup>Co, <sup>65</sup>Zn, <sup>75</sup>Se, <sup>83</sup>Rb, <sup>88</sup>Zr, <sup>88</sup>Y, <sup>101</sup>Rh) in tissues were determined by gamma-ray spectrometry.

In this study, the seven radionuclides in MT were used to determine the biodistribution of MT chelated with phosphonates in seven representative tissues. The MT were distributed in various tissues and showed a specific accumulation pattern for each chemical species. Figure 1 shows biodistribution of <sup>83</sup>Rb chloride, <sup>83</sup>Rb-EDTMP, <sup>83</sup>Rb-DOTMP, <sup>88</sup>Zr chloride, <sup>88</sup>Zr-EDTMP, <sup>88</sup>Zr-DOTMP in mice. In the case of MT-EDTMP and MT-DOTMP, most of the MT-phosphonates accumulated in bone except for <sup>75</sup>Se and <sup>83</sup>Rb phosphonates. Yttrium-88 and <sup>88</sup>Zr phosphonates showed particularly high uptakes in bone compared to other tissues. Zirconium-88 phosphonates also showed fast bone uptake and rapid clearance from other soft tissues. The biodistribution of <sup>75</sup>Se phosphonates, and <sup>83</sup>Rb phosphonates showed the same behavior as <sup>75</sup>Se chloride and <sup>83</sup>Rb chloride, respectively. This suggests that Se and Rb exist in free ion form rather than as a phosphonate complex in vivo. In conclusion, these results should provide useful information for nuclear medicine.

### References

- 1) P. Anderson and R. Nunez: *Expert Rev. Anticancer Ther.* **7**, 1517 (2007).
- 2) S. Giralt et al.: *Blood* **102**, 2684 (2003).

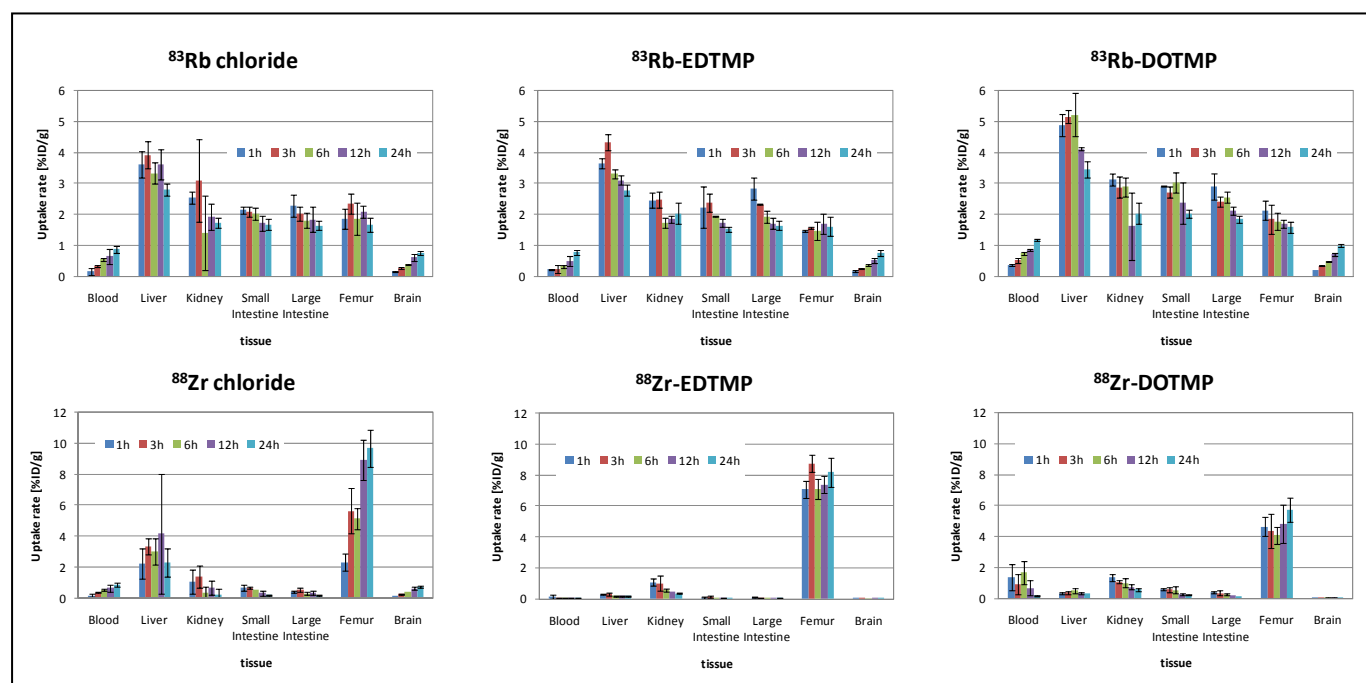


Fig.1 Biodistribution of <sup>83</sup>Rb chloride, <sup>83</sup>Rb-EDTMP, <sup>83</sup>Rb-DOTMP, <sup>88</sup>Zr chloride, <sup>88</sup>Zr-EDTMP, <sup>88</sup>Zr-DOTMP in mice

\*<sup>1</sup> Department of Forefront Medical Technology, Kanazawa University Graduate School of Medical Science

\*<sup>2</sup> School of Health Sciences, Faculty of Medicine, Kanazawa University

## Preparation of a rotating $^{248}\text{Cm}$ target for GARIS

Y. Kudou, H. Haba, K. Ooe,\*<sup>1</sup> D. Kaji, K. Morimoto, A. Shinohara\*<sup>1</sup> and K. Morita

We plan to study chemical properties of superheavy elements (SHEs, atomic numbers  $Z \geq 104$ ) by using a gas-jet transport system coupled to the RIKEN gas-filled recoil ion separator (GARIS) at the RIKEN Linear Accelerator Facility (RILAC).<sup>1,2)</sup> The SHE nuclides with long half lives (e.g.,  $^{261\text{a/b}}\text{Rf}$ : 68/3 s,  $^{265\text{a/b}}\text{Sg}$ : 9/16 s) used in chemical experiments are produced by hot fusion reactions using actinide targets such as  $^{238}\text{U}$ ,  $^{248}\text{Cm}$ , and  $^{249}\text{Bk}$ . Stable targets are much desired due to the extremely low-production cross-sections of SHEs on the order of nanobarn or picobarn. Actinide targets in an oxide form are stable in high-intensity heavy-ion bombardments for prolonged beam irradiation. Here, we report on a procedure to prepare a large and uniform  $^{248}\text{Cm}_2\text{O}_3$  target using a molecular plating method for irradiation using the rotating target system of GARIS.

Figure 1(a) shows a schematic view of the cell used for electrodeposition. A Ti backing foil of 2  $\mu\text{m}$  thickness placed on a water-cooled Ti block was used as a cathode, while a Rh plate of 0.1 mm thickness on another Ti block was used as an anode. A 10 mm thick Teflon<sup>®</sup> spacer perforated in the shape of a banana was sandwiched by electrodes sealed using 1 mm thick silicon rubber pieces perforated in the same banana shape. The active target area is 2.04  $\text{cm}^2$ .

Prior to preparation of the  $^{248}\text{Cm}$  target, the electrodeposition conditions were optimized by preparing  $^{\text{nat}}\text{Gd}$  targets. Gadolinium including  $^{88}\text{Y}$  as a yield tracer was purified by a cation-exchange method in HCl-methanol media. Six microliters of 0.1 M  $\text{HNO}_3$  containing 700  $\mu\text{g}$  of Gd were mixed with 5.5 mL of 2-propanol, and the electrodeposition cell was filled with the mixture. At an applied voltage of 1000 V, the deposition yields increased with electrodeposition time from 52% at 2 min to 100% at  $\geq 8$  min (Fig. 2a). The deposition yields also increased with increasing applied voltage: from 50% at 200V to  $\sim 100\%$  at 800 V during the 10 min electrodeposition (Fig. 2b). The uniform target layer is visually observed, and the average-target thickness was  $350 \pm 10 \mu\text{g cm}^{-2}$  for the targets electrodeposited for  $\geq 8$  min. The  $^{248}\text{Cm}$  targets were prepared after obtaining results for the  $^{\text{nat}}\text{Gd}$  targets. The isotopic composition of Cm used in this study was  $^{244}\text{Cm}$ : 0.024%,  $^{245}\text{Cm}$ : 0.13%,  $^{246}\text{Cm}$ : 3.17%,  $^{247}\text{Cm}$ : 0.04%, and  $^{248}\text{Cm}$ : 96.636%. Twenty microliters of 0.2 M  $\text{HNO}_3$  containing 610  $\mu\text{g}$  of  $^{248}\text{Cm}$  was mixed with 5.5 mL of 2-propanol, and the electrodeposition cell was filled the mixture. Electrodeposition was carried out by applying a voltage of 1000 V with an increasing current density from 9.8 to 11.8  $\text{mA cm}^{-2}$  for 10 min. During the electrodeposition, the Ti blocks were continuously water-cooled at 10  $^\circ\text{C}$ . After the electrodeposition, the target was dried by an infrared lamp. The  $^{248}\text{Cm}$  target

thickness of  $320 \pm 20 \mu\text{g cm}^{-2}$  averaged for the 6 targets was determined by  $\gamma$ -ray spectrometry on  $^{245}\text{Cm}$ , while referring to the isotopic composition of Cm. The average deposition yield was  $100^{+0}_{-3}\%$ . Figure 1(b) shows an illustration of the  $^{248}\text{Cm}$  target fixed to the target holder. The  $\alpha$  activities of the 7 points shown in Fig. 7(b) were measured to confirm the uniformity of the target. The  $\alpha$ -particles from the Cm isotopes were collimated with an aluminum slit of 1 mm diameter, and were detected with a Si detector. Standard deviations of the target thickness at the seven points were evaluated to be 11%.

The 6  $^{248}\text{Cm}$  targets were arranged on a rotating wheel of 10 cm diameter, and were irradiated by a 126-MeV  $^{23}\text{Na}$  beam with beam currents up to 1 particle  $\mu\text{A}$  (50% duty) to produce  $^{266}\text{Bh}$  via the  $^{248}\text{Cm}(^{23}\text{Na}, 5n)^{266}\text{Bh}$  reaction.<sup>3)</sup>

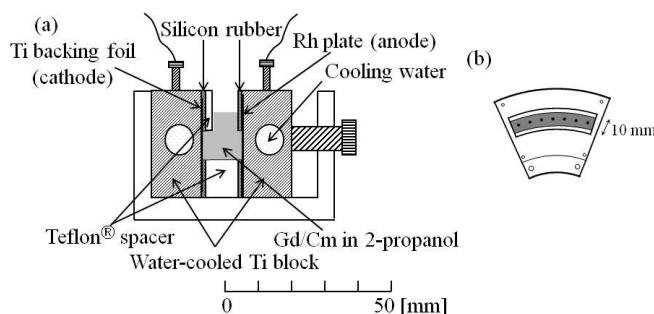


Fig.1. (a) Schematic view of the cell for electrodeposition. (b) Illustration of the Cm target fixed to the target holder. Uniformity of the target was estimated by  $\alpha$ -particle measurements at the seven points shown in the figure.

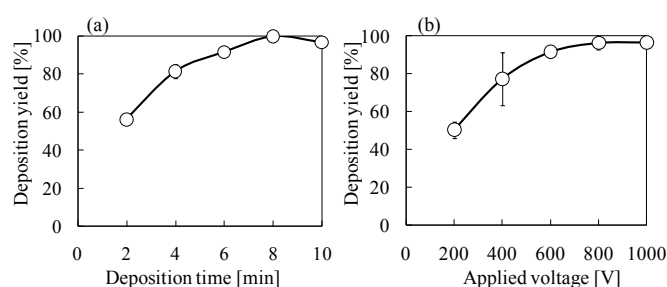


Fig. 2. Dependence of deposition yields of the  $^{\text{nat}}\text{Gd}$  target on (a) deposition time at an applied voltage of 1000V and (b) applied voltage at an electrodeposition time of 10 min.

<sup>1</sup> Graduate School of Science, Osaka University

### References

- 1) H. Haba et al.: J. Nucl. Radiochem. Sci. **8**, 55 (2007).
- 2) H. Haba et al.: J. Nucl. Radiochem. Sci. **9**, 27 (2008).
- 3) K. Morita et al.: J. Phys. Soc. JPN. **78**, 064201 (2009).

## Production of $^{261}\text{Rf}$ for chemical studies using the gas-jet transport system coupled to GARIS

H. Haba, D. Kaji, Y. Komori,<sup>\*1</sup> Y. Kudou, K. Morimoto, K. Morita, K. Ooe,<sup>\*1</sup> K. Ozeki, N. Sato, A. Shinohara,<sup>\*1</sup> and A. Yoneda

We have been developing a gas-jet transport system coupled to the RIKEN gas-filled recoil ion separator GARIS as a novel technique for superheavy element (SHE,  $Z \geq 104$ ) chemistry.<sup>1,2)</sup> The performance of the system has been investigated using  $^{206}\text{Fr}$ ,  $^{245}\text{Fm}$ , and  $^{255}\text{No}$  produced in the  $^{169}\text{Tm}(^{40}\text{Ar}, 3n)$ ,  $^{208}\text{Pb}(^{40}\text{Ar}, 3n)$ , and  $^{238}\text{U}(^{22}\text{Ne}, 5n)$  reactions, respectively.<sup>1,2)</sup> The results revealed that the GARIS/gas-jet system is a promising tool for next-generation SHE chemistry, i.e., identifying SHE nuclides under low background conditions with high efficiency of the gas-jet transport. Hot fusion reactions based on a  $^{248}\text{Cm}$  target should be considered for producing SHE nuclides with long half-lives for chemical experiments. Since the last experiment with  $^{255}\text{No}$ , we have developed a new gas jet chamber having a large focal plane window of 100 mm diameter to efficiently collect evaporation residues. A rotating target system for the  $^{248}\text{Cm}$  material was also installed. Recently,  $^{261}\text{Rf}$  produced in the  $^{248}\text{Cm}(^{18}\text{O}, 5n)$  reaction was successfully extracted to a chemistry laboratory after physical separation by GARIS.

A  $^{248}\text{Cm}_2\text{O}_3$  target of  $280 \mu\text{g cm}^{-2}$  thickness was prepared by electrodeposition onto a  $0.90 \text{ mg cm}^{-2}$  Ti backing foil.<sup>3)</sup> The  $^{18}\text{O}^{5+}$  ion beam was extracted from the RIKEN Linear Accelerator, RILAC. Beam energy was 95.5 MeV at the center of the target, and average beam intensity was  $4.8 \mu\text{A}$ . The reaction products of interest were separated in-flight from the beam and the majority of the nuclear transfer products by GARIS and then guided into the gas-jet chamber of 100 mm i.d.  $\times$  20 mm depth through a Mylar window of  $0.5 \mu\text{m}$  thickness, which was supported by a circular-hole grid with 78% transparency. GARIS was filled with He gas at a pressure of 33 Pa. The magnetic rigidity of GARIS was set at 1.73 Tm. In the gas-jet chamber, the reaction products were stopped in He gas, attached to KCl aerosols, and continuously transported through a Teflon capillary (2.0 mm i.d.  $\times$   $\sim$ 10 m length) to a rotating wheel system, MANON, for  $\alpha$  spectrometry. The He flow rate was  $2.0 \text{ L min}^{-1}$ , and the inner pressure of the chamber was 49 kPa. In MANON, the aerosols were deposited on 200-position Mylar foils of  $0.5 \mu\text{m}$  thickness placed at the periphery of a stainless steel wheel of 420 mm diameter. After aerosol collection, the wheel was stepped at 30-s intervals to position the foils between seven pairs of Si PIN photodiodes (Hamamatsu S3204-09). To evaluate the number of  $^{261}\text{Rf}$  atoms that passed through the Mylar window of GARIS, the gas-jet chamber was replaced with a detector chamber equipped with nine Si PIN photodiodes (Hamamatsu S3584-09,  $3 \times 3$  square arrangement).

Figure 1 shows the sum of  $\alpha$ -particle spectra measured in the seven top detectors of MANON. The 30-s aerosol collection was repeated 697 times. A beam dose of  $6.3 \times 10^{17}$  was accumulated. As shown in Fig. 1,  $\alpha$  peaks of  $^{261}\text{Rf}$  (65 s, 8.28 MeV)<sup>4)</sup> and its daughter  $^{257}\text{No}$  (24.5 s, 8.222 and 8.323 MeV)<sup>5)</sup> are clearly seen under the extremely low background condition, suggesting that the gas-jet transport of  $^{261}\text{Rf}$  was successfully conducted after the physical separation by GARIS. A total of 168  $\alpha$  events were registered in the energy range of interest, including 58 time-correlated  $\alpha$  pairs. The 7.687-MeV peak is due to  $^{214}\text{Po}$ , a descendant of the natural radioisotope  $^{222}\text{Rn}$  in the room. By comparing the spectrum measured with the focal plane Si detector, the gas-jet transport efficiency of  $^{261}\text{Rf}$  was evaluated to be  $52 \pm 12\%$ . On the other hand, the transport efficiency of GARIS was  $7.8 \pm 1.7\%$  for the focal plane of 100 mm diameter, referring to the cross section of 13 nb.<sup>6)</sup> The present results suggest that the GARIS/gas-jet system is a promising approach for exploring new frontiers in SHE chemistry: (i) the background radioactivities of unwanted reaction products are strongly suppressed, (ii) the intense beam is absent in the gas-jet chamber and hence high gas-jet efficiency is achieved, and (iii) the beam-free condition also allows for investigations of new chemical systems.

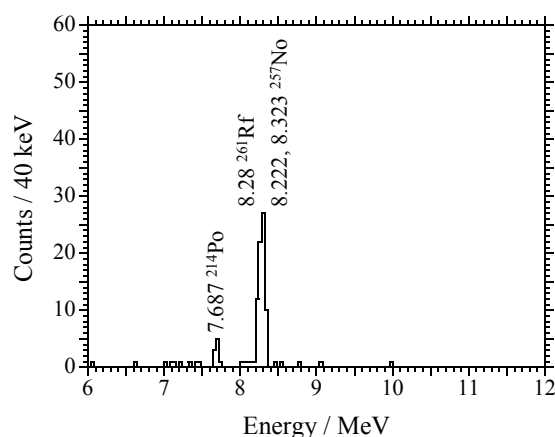


Fig. 1. Sum of  $\alpha$ -particle spectra measured in seven top detectors of MANON.

### References

- 1) H. Haba et al.: *J. Nucl. Radiochem. Sci.* **8**, 55 (2007).
- 2) H. Haba et al.: *J. Nucl. Radiochem. Sci.* **9**, 27 (2008).
- 3) Y. Kudou et al.: *RIKEN Accel. Prog. Rep.* **42** (in press).
- 4) R. B. Firestone and V. S. Shirley: *Table of Isotopes, 8th ed.* (John Wiley & Sons, New York, 1996).
- 5) M. Asai et al.: *Phys. Rev. Lett.* **95**, 102502 (2005).
- 6) Y. Nagame et al.: *J. Nucl. Radiochem. Sci.* **3**, 85 (2002).

<sup>\*1</sup> Graduate School of Science, Osaka University

## Production of RI Tracers for chemistry of transactinide elements

S. Goto,\*<sup>1</sup> T. Hasegawa,\*<sup>2</sup> H. Kudo,\*<sup>2</sup> Y. Ezaki,\*<sup>3</sup> and H. Haba,\*<sup>3</sup>

[Radioactive tracer, niobium, tantalum]

Since a transactinide element has a very short life and its production cross-section is very small, only a very little quantity — usually one atom — is handled for a chemistry experiment at a time. To investigate the chemical property of such transactinide element, many repetition experiments in terms of rapid chemistry method are necessary until sufficient statistics are obtained. In other words, it takes very long time to one experimental condition. Thus, the off-line experiment using a light homologue will be valid for an efficient on-line experiment. The aim of this work is to produce the non-carrier tracer for carrying out the off-line chemical experiments.

For the rapid chemistry experiments of Db, the radioactive isotopes  $^{95g}\text{Nb}$  ( $T_{1/2} = 35$  d) and  $^{179}\text{Ta}$  ( $T_{1/2} = 665$  d) were selected as a tracer in consideration of whether measuring their gamma-ray (or x-ray) is possible and whether the half life is measurable. The tracers were produced using the  $^{96}\text{Zr}(p, 2n)^{95g}\text{Nb}$ ,  $^{179}\text{Hf}(p, n)^{179}\text{Ta}$  and  $^{180}\text{Hf}(p, 2n)^{179}\text{Ta}$  reactions with RIKEN K70 AVF cyclotron. The  $^{\text{nat}}\text{Zr}$  foil ( $64.5$  mg  $\text{cm}^{-2}$ ) and the Hf foil ( $141$  mg  $\text{cm}^{-2}$ ) covered with aluminum foils were stacked and placed at the irradiation chamber. The Zr target was put on the beam upstream to make the proton energy optimal to the intended nuclear reactions. The proton beam energy was about 14 MeV. The irradiation time was 12 hours, and the average beam current was about  $15$   $\mu\text{A}$ . The activities of  $^{95g}\text{Nb}$  and  $^{179}\text{Ta}$  were 4.1 MBq and 3.0 MBq, respectively, after 21 days from the end of bombardment. Those were enough to perform the experiment for a few months.

Each tracer nuclide was separated from the target material using an anion-exchange method. The tracers have been used in different experiments to develop solvent extraction technique for 5th-group elements.

---

\*1 Center for Instrumental Analysis, Niigata University

\*2 Department of Chemistry, Niigata University

\*3 Nishina Center for Accelerator Based Science, RIKEN

## Extraction of mendelevium (III) and lanthanides (III) from hydrochloric acid solutions to carbon tetrachloride with 2-thenoyltrifluoroacetone

H. Fujisawa,<sup>\*1</sup> W. Yahagi,<sup>\*1</sup> K. Ooe,<sup>\*1</sup> R. Takayama,<sup>\*1</sup> H. Kikunaga,<sup>\*1</sup> T. Yoshimura,<sup>\*1</sup> N. Takahashi,<sup>\*1</sup> H. Haba, Y. Kudou, Y. Ezaki, A. Toyoshima,<sup>\*2</sup> M. Asai,<sup>\*2</sup> Y. Nagame,<sup>\*2</sup> S. Enomoto<sup>\*3</sup> and A. Shinohara<sup>\*1</sup>

Chemical properties of trivalent actinides have often been discussed by comparing actinides to lanthanides. The liquid-liquid extraction of trivalent actinides and lanthanides with  $\beta$ -diketonates has been studied thoroughly<sup>1)</sup>. However, there are very few reports on the investigation with a series of lanthanides and trivalent actinides in the same extraction conditions. In particular, the data of the elements with atomic number an above 100 are limited because those are produced only in heavy-ion induced nuclear reactions by using an accelerator.

We have performed extraction experiments of americium, curium, californium and fermium with 2-thenoyltrifluoroacetone (HTTA) as an extractant<sup>2)</sup>. In this experiment, liquid-liquid extraction of mendelevium (Md) was examined.

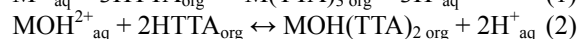
Mendelevium-255 was produced in the  $^{248}\text{Cm}(^{11}\text{B},4n)^{255}\text{Md}$  reaction using the K70 Cyclotron at RIKEN. The produced  $^{255}\text{Md}$  was transported to a chemistry laboratory and dissolved in 100  $\mu\text{L}$  of an HCl solution with a pH 2.85 to 3.53 containing 0.1 M  $\text{NH}_4\text{Cl}$ . The solution was mixed with an equal volume of 0.1 M HTTA- $\text{CCl}_4$  solution. Both phases were shaken for 20 min and centrifuged for 1 min. After phase separation, aliquots of 80  $\mu\text{L}$  of each phase were evaporated to dryness on hot tantalum discs and assayed for alpha activity.

Lanthanide extraction experiments were performed using the RIKEN multitracer. The tracer was stocked in an HCl solution with pH about 3.5. In a test tube, 90  $\mu\text{L}$  of HCl solution with various pH values containing 0.1 M  $\text{NH}_4\text{Cl}$ , 10  $\mu\text{L}$  of tracer stock solution and 100  $\mu\text{L}$  of 0.1 M HTTA- $\text{CCl}_4$  solution were mixed. The mixture was shaken for 20 min using a vortex mixer and then centrifuged for 3 min. After phase separation, each phase was assayed for gamma activity after which the pH value of the aqueous phase was measured.

The distribution ratio  $D$  is obtained by following equation:  $D = V_{\text{aq}}A_{\text{org}} / V_{\text{org}}A_{\text{aq}}$ , where  $V_{\text{aq}}$  and  $V_{\text{org}}$  is the volumes, and  $A_{\text{aq}}$  and  $A_{\text{org}}$  are the radioactivities of the aqueous and organic phases, respectively.

The  $\log D$  values of Md as a function of pH value in the aqueous phase are shown in Fig. 1. The gradient decreases with increasing pH value. The slope value changes at pH about 3.1. A similar tendency has been found in lanthanides and other actinides, Am, Cm and Cf. The phenomenon is

explained in terms of the formation of a hydroxyl species<sup>3,4)</sup>. The reactions of this extraction are explained by Eqs. (1) and (2).



The reaction described by Eq. (1) dominates at lower pH ( $\text{pH} < 3.1$ ). As the pH becomes higher ( $\text{pH} > 3.1$ ), the hydrolysis reaction of lanthanides and actinides occurs, that is, the reaction in Eq. (2) dominates. The  $\log D$  is described in Eq. (3). When the extraction behavior follows to the Eq. (1), the slope value derived from the linear correlation of  $\log D$  against pH value should be 3 according to the Eq. (3).

$$\log D = \log K_{\text{ex}} + 3\text{pH} + 3\log[\text{HTTA}]_{\text{org}} \quad (3)$$

As shown in Fig. 1, the linear correlation is found in the lower pH range ( $\text{pH} < 3.1$ ), thus, the equilibrium constant  $K_{\text{ex}}$  can be estimated, according to Eq. (3). However additional experiments under more various pH conditions are required for deriving a reliable  $K_{\text{ex}}$  values. The obtained  $K_{\text{ex}}$  allows us to discuss the reactivity of Md to HTTA.

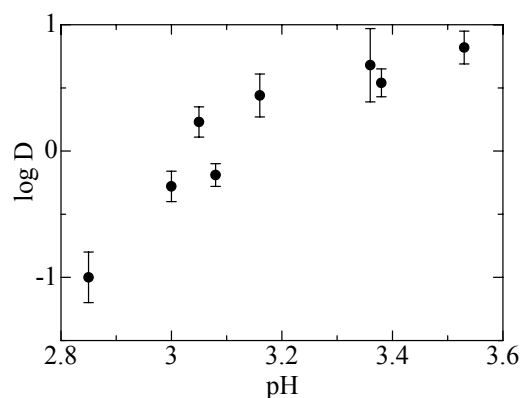


Fig. 1. The extraction behavior of mendelevium from hydrochloric acid solutions to carbon tetrachloride with 2-thenoyltrifluoroacetone

### References

- 1) A. M. Poskanzer and B. M. Foreman Jr.: *J. Inorg. Chem.* **16**, 323 (1961)
- 2) Y. Komori *et al.*: *OULNS Ann. Rep.* 2007, 109 (2008)
- 3) C. Keller and H. Schreck: *J. Inorg. Chem.* **31**, 1121 (1969)
- 4) P. K. Mohapatra and P. K. Khopkar: *Polyhedron* **8**, 2071 (1989)

<sup>\*1</sup> Department of Chemistry, Osaka University

<sup>\*2</sup> Japan Atomic Energy Agency

<sup>\*3</sup> Graduate School of Medicine, Dentistry and Pharmaceutical Sciences, Okayama University

## Studies on solvent extraction behavior of molybdenum and tungsten for solution chemistry of seaborgium (element 106)

K. Ooe,<sup>\*1</sup> W. Yahagi,<sup>\*1</sup> Y. Komori,<sup>\*1</sup> H. Fujisawa,<sup>\*1</sup> H. Kikunaga,<sup>\*1</sup> T. Yoshimura,<sup>\*1</sup> N. Takahashi,<sup>\*1</sup> H. Haba, Y. Kudou, Y. Ezaki, and A. Shinohara.<sup>\*1</sup>

Schädel et al. reported chromatographic behavior of seaborgium (element 106, Sg) in an aqueous solution.<sup>1,2)</sup> It was shown that the Sg ion elutes from a cation exchange column in 0.1 M HNO<sub>3</sub>/5 × 10<sup>-4</sup> M HF in the similar behavior as its lighter homologues, molybdenum (Mo) and tungsten (W)<sup>1)</sup> and Sg is adsorbed on the cation exchange column in 0.1 M HNO<sub>3</sub> in contrast to Mo and W.<sup>2)</sup> However, the chemical experiments of Sg have been limited to the chromatographic method. We have a plan to make a solvent extraction experiment for the chemical study of Sg. In this work, solvent extraction behavior of Mo and W was investigated as a comparative study of Sg. It is generally known that macro amounts of Mo and W form polyoxometalate in the aqueous solution below pH 8–9. However, it is required for the study of Sg to investigate the chemical behavior of mononuclear Mo and W because the production rate of Sg is the order of one atom per hour. To study the solvent extraction behavior of mononuclear Mo and W, the carrier-free isotopes produced by heavy-ion-induced nuclear reactions were used.

Molybdenum and tungsten isotopes, <sup>90</sup>Mo ( $T_{1/2} = 5.7$  h) and <sup>173</sup>W ( $T_{1/2} = 7.6$  min) were produced in the <sup>nat</sup>Ge(<sup>22</sup>Ne,xn)<sup>90</sup>Mo and <sup>nat</sup>Gd(<sup>22</sup>Ne,xn)<sup>173</sup>W reactions, respectively, using the RIKEN K70 AVF Cyclotron. Reaction products recoiling out of the target were stopped in a helium gas flow, attached to KCl aerosols generated by sublimation of KCl powder, and then transported to a chemistry laboratory. The aerosols with reaction products were collected on a polyester or Naflon sheet and were dissolved in 200 μL of 0.1–11 M hydrochloric acid. The concentrations of Mo and W tracers in the aqueous phase were about 10<sup>-13</sup> M. Equal volume of the 0.05 M tetraphenylarsonium chloride (TPAC)-chloroform or the 0.05 M Aliquat 336-chloroform solution was mixed with the aqueous phase. The mixture was shaken for 15 min in extractions of Mo with TPAC or 3 min in the other experiments. After centrifuging, the aliquots of the aqueous and organic phases were taken, and were subjected to  $\gamma$ -ray spectrometry using Ge detectors. Distribution ratios ( $D$ ) were obtained from radioactivities of each phase.

Figure 1 shows the distribution ratios of Mo and W as a function of hydrochloric acid concentration [HCl]. The both distribution ratios of Mo and W rise with the increase of [HCl], indicating that the chloride coordinated Mo and W complexes are formed. It has been reported that the extracted species of Mo and W are MoO<sub>2</sub>Cl<sub>3</sub><sup>-</sup> or MoO<sub>2</sub>Cl<sub>4</sub><sup>2-</sup> and WO<sub>2</sub>Cl<sub>3</sub><sup>-</sup>, WO<sub>2</sub>Cl<sub>4</sub><sup>2-</sup> or WOCl<sub>5</sub><sup>-</sup> respectively.<sup>3-5)</sup> The distribution ratio of Mo was also investigated in 11 M HCl

as a function of Aliquat 336 concentration to determine the chemical species of Mo. The results are shown in Fig. 2. The plots of log  $D$  vs. log Aliquat 336 concentration give a linear correlation with a slope of  $1.08 \pm 0.04$ . This indicates that the net charge of Mo chloride complex is -1. Therefore, the extracted species of Mo would be MoO<sub>2</sub>Cl<sub>3</sub><sup>-</sup>. In the near future, the speciation analysis of the extracted W species will be performed. The present results will be also utilized for determination of the experimental conditions for the future chemical studies of Sg.

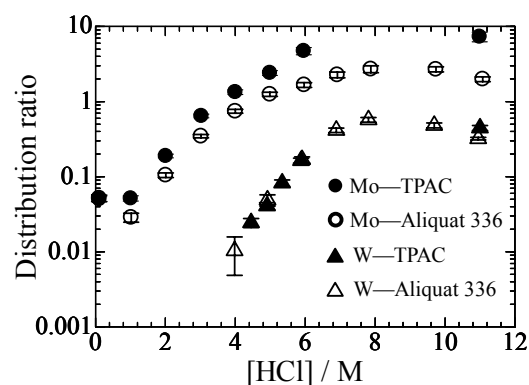


Fig. 1. Extractions of Mo and W from hydrochloric acid with 0.05 M TPAC-chloroform and 0.05 M Aliquat 336-chloroform solution.

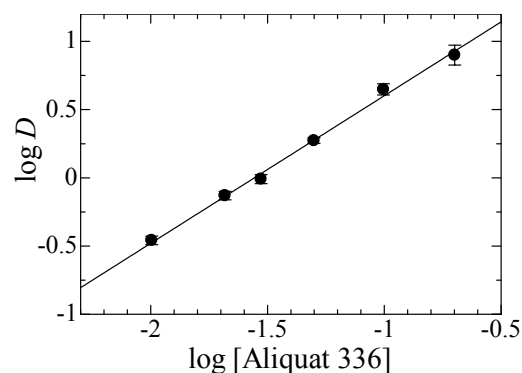


Fig. 2. The distribution ratio of Mo in 11 M hydrochloric acid as a function of Aliquat 336 concentration.

### References

- 1) M. Schädel et al.: *Radiochim. Acta* **77**, 149 (1997).
- 2) M. Schädel et al.: *Radiochim. Acta* **83**, 163 (1998).
- 3) K. A. Kraus et al.: *J. Am. Chem. Soc.* **77**, 3972 (1955).
- 4) R. Caletka and V. Krivan: *J. Radioanal. Nucl. Chem.* **142**, 373 (1990).
- 5) I. Nelidow and R. M. Diamond: *J. Phys. Chem.* **59**, 710 (1955).

<sup>\*1</sup> Graduate School of Science, Osaka University

# Adsorption of Nb, Ta and Pa on anion-exchanger in HF/HNO<sub>3</sub> solutions: Model experiments for the chemical study of Db†

Yoshitaka Kasamatsu,<sup>\*1</sup> Atsushi Toyoshima,<sup>\*1</sup> Hiromitsu Haba, Kazuaki Tsukada,<sup>\*1</sup> Kazuhiko Akiyama,<sup>\*2</sup>

Takashi Yoshimura,<sup>\*3</sup> and Yuichiro Nagame,<sup>\*1</sup>

Several model experiments aiming at the chemical study of Db in aqueous solution have been performed using the lighter homologues Nb and Ta, and the pseudo homologue Pa.<sup>1)</sup> Although some chemical experiments of Db have been studied,<sup>1)</sup> little is known about its chemical properties. For clear understanding of the chemical properties of Db, systematic investigations are strongly required. We plan to investigate the fluoride complexation of Db through anion-exchange experiments in HF/HNO<sub>3</sub>; the  $K_d$  values of Db will be systematically measured as a function of the ligand (F<sup>-</sup>) and the counter-ion (NO<sub>3</sub><sup>-</sup>) concentrations as those with Rf.<sup>2)</sup> The  $K_d$  values of Nb, Ta and Pa on the anion-exchange resin were previously determined as a function of the fluoride ion concentration ([F<sup>-</sup>]) in HF/HNO<sub>3</sub> at [NO<sub>3</sub><sup>-</sup>] = 0.1 M.<sup>3)</sup> In this work, the  $K_d$  values of these elements were measured as a function of [NO<sub>3</sub><sup>-</sup>] for further analysis on their fluoride complexation.

The radiotracers <sup>95</sup>Nb and <sup>179</sup>Ta were produced by the RIKEN K70 AVF cyclotron, and <sup>233</sup>Pa was separated from <sup>237</sup>Np. The experimental procedures are basically the same as those described in the previous report.<sup>3)</sup> The  $K_d$  values of Nb, Ta and Pa on the anion-exchange resin in HF/HNO<sub>3</sub> were determined as a function of [NO<sub>3</sub><sup>-</sup>] at constant [F<sup>-</sup>] =  $2.0 \times 10^{-4}$ ,  $3.0 \times 10^{-3}$  and  $1.0 \times 10^{-2}$  M.

Variations of the  $K_d$  values of Nb, Ta and Pa on the anion-exchange resin in HF/HNO<sub>3</sub> solutions are shown in Fig. 1 as a function of [NO<sub>3</sub><sup>-</sup>] at [F<sup>-</sup>] of (a)  $2.0 \times 10^{-4}$ , (b)  $3.0 \times 10^{-3}$  and (c)  $1.0 \times 10^{-2}$  M. Distinct difference in the anion-exchange behavior was observed among the elements. The slopes of the fitted linear lines in the log $K_d$  vs. log[NO<sub>3</sub><sup>-</sup>] plot are presented in Table 1. The net charges of the complexes were evaluated from the slopes for the elements under the following conditions, [F<sup>-</sup>] =  $2.0 \times 10^{-4}$  and  $3.0 \times 10^{-3}$  M ((a) and (b)). In the case of (c), the net charge cannot be evaluated due to the effect of HF<sub>2</sub><sup>-</sup>. Chemical species were deduced based on the evaluated net charges of the complexes and the knowledge concerning their chemical species in HF solutions as follows; 1) NbOF<sub>4</sub><sup>-</sup> would be present at [F<sup>-</sup>] =  $2.0 \times 10^{-4}$  and  $3.0 \times 10^{-3}$  M, 2) TaF<sub>6</sub><sup>-</sup> is dominantly present at [F<sup>-</sup>] =  $3 \times 10^{-3}$  M and Ta seems to be hydrolyzed at [F<sup>-</sup>] =  $2.0 \times 10^{-4}$  M, and 3) PaF<sub>6</sub><sup>-</sup> and PaF<sub>7</sub><sup>2-</sup> would be dominantly present at [F<sup>-</sup>] =  $2.0 \times 10^{-4}$  and  $3.0 \times 10^{-3}$  M, respectively.

† Condensed from the article in J. Radioanal. Nucl. Chem. **279**, 371 (2009)

\*<sup>1</sup> Japan Atomic Energy Agency

\*<sup>2</sup> Department of Chemistry, Tokyo Metropolitan University

\*<sup>3</sup> Department of Chemistry, Osaka University

Table 1. Slopes of the fitted linear lines in Fig. 1.

[F <sup>-</sup> ] / M	Slope		
	Nb	Ta	Pa
$2.0 \times 10^{-4}$	-1.0 ± 0.1	-0.5 ± 0.1	-1.2 ± 0.1
$3.0 \times 10^{-3}$	-1.3 ± 0.1	-1.2 ± 0.1	-1.8 ± 0.1
$1.0 \times 10^{-2}$	-1.5 ± 0.1	-1.3 ± 0.1	-2.0 ± 0.1

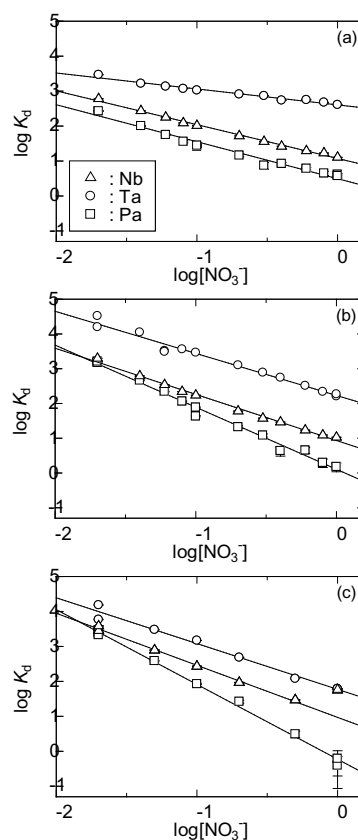


Fig. 1. Variations of the  $K_d$  values of <sup>95</sup>Nb, <sup>179</sup>Ta and <sup>233</sup>Pa on the anion-exchange resin.

## References

- 1) M. Schädel: *Angew. Chem. Int. Ed.*, **45**, 368 (2006).
- 2) A. Toyoshima, H. Haba, K. Tsukada, M. Asai, K. Akiyama, S. Goto, Y. Ishii, I. Nishinaka, T. K. Sato, Y. Nagame, W. Sato, Y. Tani, H. Hasegawa, K. Matsuo, D. Saika, Y. Kitamoto, A. Shinohara, M. Ito, J. Saito, H. Kudo, A. Yokoyama, M. Sakama, K. Sueki, Y. Oura, H. Nakahara, M. Schädel, W. Brüchle, and J. V. Kratz: *Radiochim. Acta* **96**, 125 (2008).
- 3) Y. Kasamatsu, A. Toyoshima, H. Toume, K. Tsukada, H. Haba, and Y. Nagame: *J. Nucl. Radiochem. Sci.*, **8**, 69 (2007).

## Development of an electrochemistry apparatus for the heaviest elements†

A. Toyoshima,<sup>\*1</sup> Y. Kasamatsu,<sup>\*1</sup> Y. Kitatsuji,<sup>\*1</sup> K. Tsukada,<sup>\*1</sup> H. Haba, A. Shinohara,<sup>\*2</sup> and Y. Nagame,<sup>\*1</sup>

It is of great importance to study oxidation states of the heaviest atoms and to determine their oxidation-reduction (redox) potential in aqueous solution. Theoretical calculations predict that oxidation states and redox potentials of the heaviest atoms are influenced by relativistic effects.<sup>1)</sup> Thus, electrochemical properties of the heaviest elements will give valuable information on relativistic effects. However, an electric current originating from a redox reaction of one of the heaviest elements is not measurable because of an atom-at-a-time situation. Thus, we developed an electrochemistry apparatus combined with a chromatographic separation technique available even to single atoms. This report describes the development of this electrochemistry apparatus.

Figure 1 shows a schematic diagram of the electrochemistry apparatus, which is based on an electrolytic cell.<sup>2,3)</sup> A solution containing the heaviest elements fed from the inlet passes through a working electrode made of glassy carbon fibers packed into a vycol-glass tube and flows out of the outlet. The surface of the fibers is chemically modified with a polyelectrolyte material of Nafion perfluorinated ion-exchange resin,<sup>4,5)</sup> so that the working electrode works just like a cation-exchange column. Ions are oxidized on the electrode according to their redox potentials, and the resulting oxidized species are separated from non-oxidized species by cation-exchange chromatography.

Test experiments were performed using the present apparatus for an oxidation reaction of  $10^{10}$  atoms of  $^{139}\text{Ce}$ . The radioisotope  $^{139}\text{Ce}$  was produced by the  $^{139}\text{La}(p,n)$  reaction at the RIKEN K70 AVF cyclotron. The produced  $^{139}\text{Ce}$  was chemically separated from the target material by a cation-exchange method and was then stored in 0.1 M  $\alpha$ -hydroxyisobutyric acid ( $\alpha$ -HIB) solution together with  $^{88}\text{Y}^{3+}$ ,  $^{88}\text{Zr}^{4+}$ , and  $^{175}\text{Hf}^{4+}$  which were mixed for comparison of their behavior as typical trivalent and tetravalent ions. We investigated elution behavior of these radiotracers from a chemically-modified electrode with applied potentials of 0.2 - 1.0 V versus an Ag-AgCl reference electrode. With an applied potential of 0.2 V, elution of  $^{139}\text{Ce}$  followed that of  $^{88}\text{Y}$ . This elution behavior of  $^{139}\text{Ce}$  shows that Ce is bound in the most stable trivalent state. At a higher potential of 1.0 V,  $^{139}\text{Ce}$  was eluted together with  $^{88}\text{Zr}$  and  $^{175}\text{Hf}$ . This indicates that  $^{139}\text{Ce}$  exists as a tetravalent ion. With intermediate potentials around 0.75 V, elution behavior of  $^{139}\text{Ce}$  varied from that of  $\text{Ce}^{3+}$  to that of  $\text{Ce}^{4+}$ . An electric potential of 0.75 V is almost equal to that determined by

cyclic voltammetry with 0.001 M Ce in 0.1 M  $\alpha$ -HIB. These results show that  $^{139}\text{Ce}$  in the trivalent state is successfully oxidized to the tetravalent state using the present apparatus on a tracer scale. Electrochemical oxidation of nobelium will be performed in the near future.

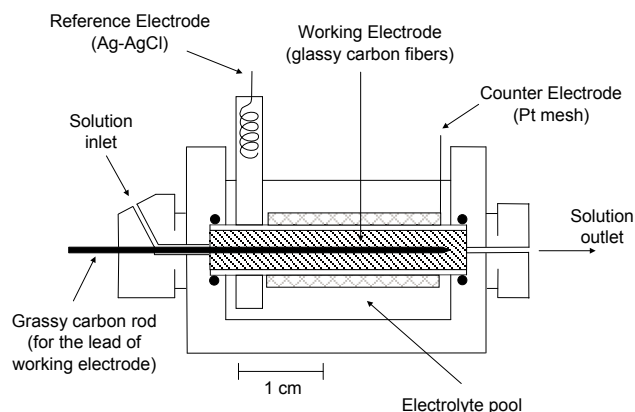


Fig. 1. Schematic diagram of developed electrochemistry apparatus.

### References

- 1) V. Pershina: *Theoretical Chemistry of the Heaviest Elements*, In *The Chemistry of Superheavy Elements* (Ed. M. Schädel, Kluwer Academic publishers, Dordrecht, 2003), p. 31.
- 2) S. Kihara, Z. Yoshida, H. Muto, H. Aoyagi, Y. Baba and H. Hashitani: *Anal. Chem.* **52** 1601 (1980).
- 3) H. Aoyagi, Z. Yoshida and S. Kihara: *Anal. Chem.* **59**, 400 (1987).
- 4) C. R. Martin and H. Freiser: *Anal. Chem.* **53**, 902 (1981).
- 5) M. W. Espensheid, A. R. Ghatak-Roy, R. B. Moore III, R. M. Penner, M. N. Szentirmay and C. R. Martin: *J. Chem. Soc., Faraday Trans.* **82**, 1051 (1986).

† Condensed from the article in *Radiochim. Acta* **96**, 323 (2008)

\*<sup>1</sup> Japan Atomic Energy Agency

\*<sup>2</sup> Department of Chemistr, Osaka University

## **4. Radiation Chemistry and Biology**

## Ion irradiation in a micro-volume of a cell with a micro beam system for cell irradiation using a tapered glass capillary with end-window

Y. Iwai, K. Maeshima, T. Ikeda, T. M. Kojima, M. Wada, Y. Kanai, T. Kobayashi, K. Ogiwara, M. Hamagaki, T. Nurusawa,\*<sup>1</sup> N. Imamoto, and Y. Yamazaki

Research and development of ion irradiation for micro-volume of living cell, has been in progress at RIKEN. Several research groups have been intensively working on the preparation of  $\sim$ MeV microbeams for biological applications.<sup>1-3</sup> In the conventional scheme, a well-focused energetic ion beam is extracted in air via a vacuum isolation window or micro-size aperture, and then injected into a biological cell in water. One of the drawbacks of these schemes is that a relatively large cylindrical volume is damaged along the beam trajectory in addition to the targeted point. To overcome this technical problem, we have developed a scheme using a tapered glass capillary with a thin window at its outlet.<sup>4</sup> This “cell surgery” scheme can realize pinpoint energy deposition and three-dimensional selection of the bombarded point by observing the outlet through a microscope with micron precision or better at an arbitrary position in a living cell.

The tapered glass capillary is  $\sim$ 50 mm long with inlet and outlet diameters of 0.8 mm and several micrometers, respectively. Figures 1(a) and 1(b) show an optical microscope image and a scanning ion microscope (SIM) image near the capillary outlet, respectively. The end-window is vacuum-tight and the outlet can be safely dipped in liquid. The transmitted beam can be injected into a liquid target at a well-defined position in front of the capillary.<sup>4</sup>

Figure 2 shows the design of a micro beam system for cell irradiation using a capillary installed downstream of the electrostatic tandem accelerator (Pelletron) at RIKEN. To irradiate a living cell in a petri dish, the system consists of three bending magnets, a transport beam line at 45 degrees, and a fluorescent and phase contrast microscope installed on a three-dimensional stage in a darkroom.

Figure 3(a) shows an image of an anchor HeLa cell nucleus labeled with a fusion protein of histone H2B and green fluorescent protein (GFP).<sup>5</sup> An ion beam

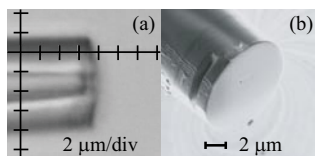


Fig. 1. (a) and (b) are a microgram of the capillary outlet and a diagonal image of the capillary outlet by SIM, respectively.<sup>4</sup>

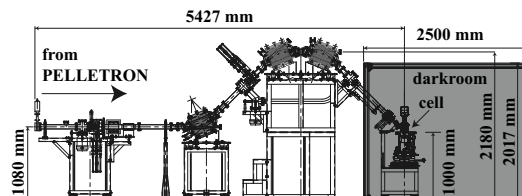


Fig. 2. Design of RIKEN micro beam system for cell irradiation. The system consists of three bending magnets, a transport beam line at 45 degrees, and a fluorescent and phase contrast microscope installed on a three-dimensional stage in a darkroom.

of 1 MeV  $H^+$  from PELLETRON was injected into a tapered glass capillary with an end-window of 8  $\mu$ m in thickness and outlet diameter of 5  $\mu$ m. Figures 3(b) and 3(c) show the fluorescence images of the nucleus before and after irradiation with transmitted current  $\sim$ 10 pA and  $\sim$ 20 s, respectively. We have demonstrated that a micro beam system for cell irradiation using a tapered glass capillary with a thin end-window can deposit energy in a micro volume of a cell. A tool enabling “surgery” in an arbitrary region of a living cell is now available, providing a technique for studying various functions of intracellular structures independently.

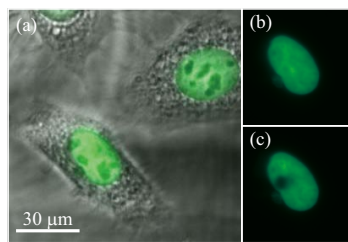


Fig. 3. Images of anchor HeLa cells nucleus labeled with histone H2B-GFP.<sup>5</sup> (b) and (c) are the fluorescence images before and after irradiation, respectively.

### References

- 1) G. Randers-Pehrson et al.: Radiat. Res. **156**, 210 (2001).
- 2) M. Folkard et al.: Nucl. Instrum. Methods Phys. Res. B **210**, 302 (2003).
- 3) Y. Kobayashi et al.: Nucl. Instrum. Methods Phys. Res. B **210**, 308 (2003).
- 4) Y. Iwai et al.: Appl. Phys. Lett. **92**, 023509 (2008). (<http://www-ap.riken.go.jp/nanobeam/index-enc.html>)
- 5) H. Kimura et al.: J. Cell Biol. **153**, 1341 (2001).

\*<sup>1</sup> Kochi University of Technology

## $\gamma$ -H2AX Foci Formation After Argon Beam Irradiation to the Cultured Animal Cell

K. Takagi<sup>\*1</sup>, T. Tsukada, M. Izumi, Y. Kazama, Y. Hayashi, and T. Abe

Histone 2AX(H2AX) is a member of histones, which composes a part of a core-histone of the chromatin. When DNA double strand break (DSB) is provoked, Ser139 residues of H2AXs surrounding the breaking point are phosphorylated to form phosphorylated H2AX ( $\gamma$ -H2AX) focus<sup>1)</sup>. Therefore, it is possible to assume  $\gamma$ -H2AX foci as landmarks of DSB.

To investigate the distribution of DSBs after the heavy ion-beam irradiation, Ar-beams ( $^{40}\text{Ar}^{+17}$ , 95 MeV/u) were irradiated to mouse fibroblast cell line BALB-3T3 cultured in the confluent condition. Beams of various LET values were irradiated to the cells at the same fluence (15 ions/100  $\mu\text{m}^2$ ). Thirty minutes after the irradiation, cells were fixed and localization of  $\gamma$ -H2AX was detected by the indirect immunofluorescence method. The fluorescence of cells was observed by laser-confocal microscopy.

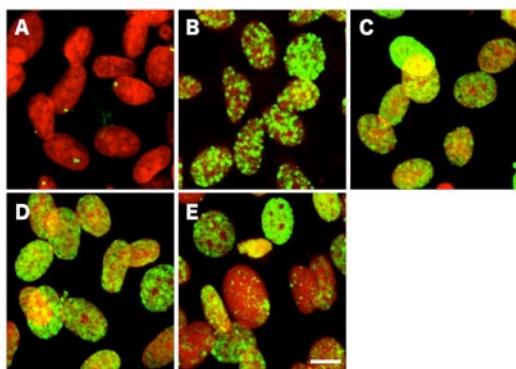


Fig. 1. Localization of  $\gamma$ -H2AX immunofluorescence in Ar-beams irradiated cells.

Red color depicts localization of nuclei, and yellow color indicates  $\gamma$ -H2AX localization. A: control, B: 313 keV/ $\mu\text{m}$ , C: 656 keV/ $\mu\text{m}$ , D: 1130 keV/ $\mu\text{m}$ , E: 1940 keV/ $\mu\text{m}$ . Bar = 10  $\mu\text{m}$ .

Figure 1 depicts the  $\gamma$ -H2AX immunofluorescence after the irradiation of Ar-beams of various LETs. In 313 keV/ $\mu\text{m}$  Ar-beam irradiated cells, large  $\gamma$ -H2AX foci were observed in the nuclei. The outline of the focus was obscured by diffused fluorescence. In 656 keV/ $\mu\text{m}$  and 1130 keV/ $\mu\text{m}$  beams,  $\gamma$ -H2AX fluorescence seemed to expand whole nuclear area. It was hard to distinguish clear foci structure in nuclei. Strange result was observed in 1940 keV/ $\mu\text{m}$  Ar-beam irradiated cells. Some cells revealed very large foci in the nuclei, others revealed pan-nuclear fluorescence, and revealed weak fluorescent signal.

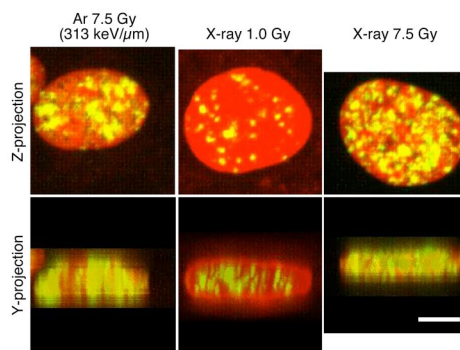


Fig. 2. Comparison of  $\gamma$ -H2AX foci between Ar- and X-ray irradiation. Bar = 5  $\mu\text{m}$ .

In 313 keV/ $\mu\text{m}$  Ar-beam irradiated cells, mean number of foci per 100  $\mu\text{m}^2$  nuclear area was  $19.4 \pm 5.6$  ( $n=30$ ). The value was close to the fluence of the beams. In 1.0 Gy X-ray irradiated cells, mean number of foci was  $14.8 \pm 8.6$  ( $n=20$ ). The mean volume of a focus was about 11 fold greater in Ar-irradiated cells than in X-ray irradiated cells ( $1.91 \mu\text{m}^3$  in Ar-irradiated cells vs.  $0.17 \mu\text{m}^3$  in X-ray irradiated cells). Figure 2 depicts a nucleus of 7.5 Gy Ar-beam (313 keV/ $\mu\text{m}$ ), 1.0 Gy X-ray (150 kV), and 7.5 Gy X-ray irradiated cell, respectively. In Ar-irradiated cell, many foci penetrated from top to bottom of the nucleus. On the other hand, they rarely penetrated the nucleus in the case of X-ray irradiation. At the same dose (7.5 Gy), X-ray-evoked foci were distributed within the whole nuclear area. These results suggest that high-LET Ar-beams cause multiple DSBs in the restricted nuclear volume along the beam track.

In the present report, we examined the effect of Ar-beam irradiation on localization of  $\gamma$ -H2AX in different LETs. We found that clear  $\gamma$ -H2AX foci were formed at LET value of 313 keV/ $\mu\text{m}$ . The number of the foci was close to the fluence of the beam. Many foci penetrated the nucleus and mean focus volume was much greater than in the case of X-ray irradiation, suggesting multiple DSBs along the beam track. At higher LET (656 and 1130 keV/ $\mu\text{m}$ ),  $\gamma$ -H2AX diffusely expanded in whole nuclear area, rather than formed clear focal structure. This was probably due to the expansion of affecting volume by one particle with increasing LET and/or the increase of actual fluence caused by the Ar-ion disruption. The localization of  $\gamma$ -H2AX was quite different from cell to cell at 1940 keV/ $\mu\text{m}$ . That might be due to the heterogeneous distribution of particles at this LET (very close to the Bragg's peak in this experiment).

### Reference

- 1) E. Rogakou *et al.* J. Biol. Chem. **273**, 5858, (1998)

\*1 The Wakasa Wan Energy Research Center

## Trichostatin A facilitates the phosphorylation of histone H2AX after X-ray irradiation in normal human fibroblast

M. Izumi

In eukaryotes, DNA is packaged into nucleosomes, which are in turn arranged in various higher order structures to form chromatin. The chromatin structures are regulated by histone modifications and chromatin-associated factors, and thereby contribute to the formation of domains within the genome, referred to as euchromatin and heterochromatin. The chromatin structures are involved in many aspects of DNA metabolism including DNA replication, recombination, and transcription. However, it is unknown how repair reactions and checkpoint responses after exposure to ionizing radiation are regulated by the chromatin structures.

Histone H2AX is a histone variant and is rapidly phosphorylated following double-strand breaks induced by ionizing radiation.<sup>1)</sup> Histone H2AX is phosphorylated in large chromatin domains flanking DNA double-strand breaks and seems to recruit DNA damage repair proteins including Mre11/Rad50/Nbs1 complex, Brca1, NFB1, 53BP1, cohesin complex and several chromatin remodeling factors.

I have been focusing on the relationship between chromatin structure and DNA damage response. My previous experiments showed that DNA double strand breaks induced reduction in the rate of DNA synthesis more efficiently in the heterochromatic region than in the euchromatic region.<sup>2)</sup> We also found that the foci of phosphorylated histone H2AX were not detected in the pericentric heterochromatin in the presence of DNA replication inhibitors, which induce phosphorylation of histone H2AX adjacent to DNA replication fork by ATR.<sup>3)</sup> These results suggest that the efficiency and the mechanism of DNA repair are affected by the chromatin structures.

To examine the roles of chromatin structure in DNA repair, we examined the damage response after cells were treated with trichostatin A (TSA), which is an inhibitor of histone deacetylase and alters the chromatin structures in this study. Human normal fibroblast NB1-RGB cells (population doubling level = 21) were irradiated with 10 Gy of X-ray after the pretreatment of 5  $\mu$ M TSA. Then the cell extracts were prepared in the presence of phosphatase inhibitors, and phosphorylated histone H2AX was detected by immunoblotting (Fig. 1). The phosphorylated histone H2AX rapidly increased after irradiation and decreased gradually. Pretreatment of TSA increased the phosphorylated histone H2AX by 2.5-fold 1 h after irradiation, and a substantial amount of the phosphorylated form remained 5 h after irradiation. This result suggests that "loosened" chromatin structure makes damage recognition easier and facilitates the damage response.

Now we are investigating whether TSA has the same effect on the damage response after heavy-ion irradiation. We are also trying to directly quantify the amount of DNA

damage and cell survival after the pretreatment of TSA.

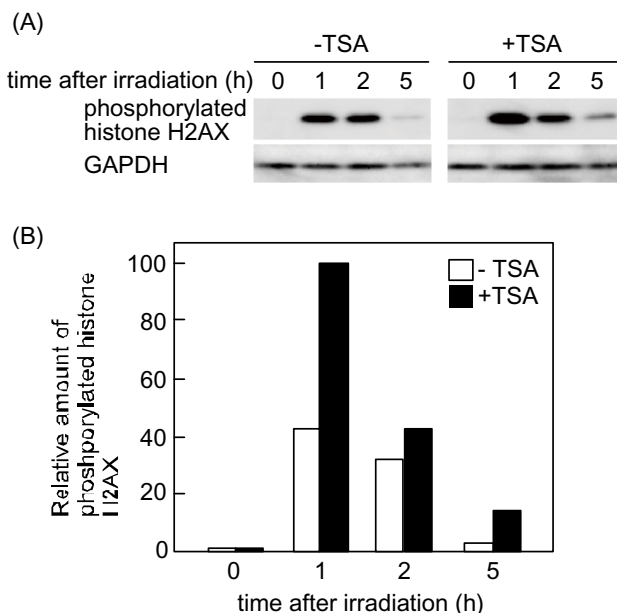


Fig. 1 Western blot analysis of phosphorylated histone H2AX after X-ray irradiation. A, human NB1-RGB cells provided by RIKEN cell bank were irradiated with 10 Gy of X-ray using Softex (Rigaku). Whole cell extracts were then prepared at indicated time points and subjected to immunoblotting. As a loading control, glyceraldehyde-3-phospho dehydrogenase (GAPDH) was detected. B, the intensity of each band was measured using luminoimage analyzer LAS3000 (Fuji Film) and normalized against the amount of GAPDH.

### References

- 1) C. Thiriet and J. J. Hayes: *Mol. Cell* **18**, 617 (2005).
- 2) M. Izumi: *RIKEN Accel. Prog. Rep.* **40**, 249 (2007).
- 3) M. Izumi, et al.: *RIKEN Accel. Prog. Rep.* **37**, 144(2004).

## Cell-killing effect of low dose of high-LET heavy ions (II)

M. Tomita,\*<sup>1</sup> T. Tsukada, and M. Izumi

Radiation-induced bystander responses are defined as responses in cells that have not been directly targeted by radiation but are in the neighborhood of cells that have been directly exposed.<sup>1)</sup> In a space environment, astronauts are exposed to low fluencies of high-LET radiation. In addition, normal cells surrounding a tumor also undergo exposure in heavy-ion cancer therapy. Therefore, bystander responses induced by a low dose of high-LET radiation are an important problem in radiation biology. In our study we aim to clarify the molecular mechanisms and biological implications of bystander responses induced by low doses of high-LET radiation. Previously, we reported that the cell-killing effect of high-LET iron (Fe) ions is significantly higher than that of low-LET X-rays under 0.2 Gy.<sup>2)</sup> Here we show the progress of results reflecting new data.

Figure 1 shows the clonogenic surviving fraction of normal human lung embryonic fibroblast WI-38 cells irradiated with 250 kV X-rays (2 keV/ $\mu\text{m}$ ) or 90 MeV/u Fe ions at 1000 keV/ $\mu\text{m}$ . WI-38 cells were plated on a 25 cm<sup>2</sup> cell culture flask for one week before irradiation to form confluent monolayers. The surviving fraction was determined by a colony formation assay. The radiosensitivity of WI-38 cells to Fe ions was higher than that to X-rays (Fig. 1A). Surviving fractions (*SFs*) at doses (*D*) above 0.1 Gy were fitted by the linear-quadratic model (L-Q model). Cell survival curves for cells irradiated with X-rays and Fe ions were

$$SF = \exp(-0.045D^2 - 0.40D)$$

and

$$SF = \exp(0.036D^2 - 0.81D)$$

respectively. The doses resulting in 10% cell survival ( $D_{10}$ ), calculated from the cell survival curves, were 4.02 Gy and 3.32 Gy for X-rays and Fe ions, respectively. The RBE relative to X-rays was 1.21. Figure 1B indicates the surviving fractions at doses of less than 0.5 Gy. At lower doses, the surviving fractions for Fe ions were much lower than those extrapolated from higher doses above 0.1 Gy using the L-Q model. These results suggest that high-LET Fe ions show low-dose hypersensitivity. In addition, the surviving fractions for Fe ions were much lower than those for X-rays. The values of  $D_{95}$  were 0.12 and 0.018 for X-rays and Fe ions, respectively. The RBE was 6.8 suggests that a low dose of high-LET radiation can induce cell death more efficiently than low-LET radiation.

The average size of the nucleus of WI-38 was 188  $\mu\text{m}^2$ . The average number of ion tracks per nucleus

was calculated as 0.11 in the nuclei of cells irradiated with 0.1 Gy of Fe ions. Thus, nonirradiated cells exist in the same population. Our present results suggest that a low dose of high-LET Fe ions shows low-dose hypersensitivity induced by bystander response.

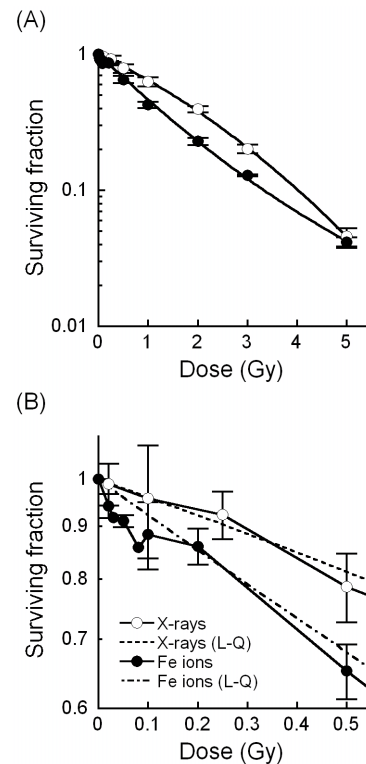


Fig. 1. Cell survival curves of normal human fibroblast WI-38 cells. Confluent monolayers of normal human fibroblast WI-38 cells were irradiated with 250 kV X-rays (2 keV/ $\mu\text{m}$ ) and 90 MeV/u Fe ions (1000 keV/ $\mu\text{m}$ ). Cells were harvested and plated 24 h after irradiation. Surviving fractions (*SFs*) were normalized to those for non-irradiated controls. A shows all *SFs* obtained in this study and cell survival curves calculated by the linear-quadratic (L-Q) model using *SFs* at doses above 0.1 Gy. B shows *SFs* at doses under 0.1 Gy. Error bars of the *SFs* represent the standard errors of the means (SEMs).

### References

- 1) K. M. Prise et al.: Radiat. Prot. Dosimetry **99**, 223 (2002).
- 2) M. Tomita et al.: RIKEN Accel. Prog. Rep. **4**, 220 (2008).

\*<sup>1</sup> Central Research Institute of Electric Power Industry

## Carbon-ion induced mutation frequencies and spectra in double strand break repair-deficient mutants of *Neurospora crassa*

L. Q. Ma,\* S. Tanaka,\* H. Inoue,\* Y. Kazama, H. Ichida, T. Abe and S. Hatakeyama\*

Our lab is interested in how homologous recombination (HR), non-homologous end-joining (NHEJ) and the MRX (Mre11-Rad50-Xrs2) complex coordinate to repair DNA damage arising from carbon-ion irradiation. To this end, we used the filamentous fungus *Neurospora crassa* to examine the killing and mutagenic effect of a carbon-ion beam on a wild type and three DSB repair-deficient mutant strains, *mus-52* (*YKU80*), *mei-3* (*RAD51*) and *uvs-6* (*RAD50*), which are deficient for NHEJ, HR and the MRX complex, respectively.

For each of the *N. crassa* strains examined, 8 ml of conidia ( $4 \times 10^6$  conidia/ml) were transferred to a 15 ml centrifuge tube that was subsequently irradiated with carbon-ions ( $^{12}\text{C}^{5+}$ ; 135 MeV/u) at doses of 25 to 400 Gy. Following irradiation, samples were plated on Fries' medium supplemented with 2% sorbose. For the wild type, *mus-52* and *mei-3* strains, each plate was inoculated with  $2 \times 10^3$  conidia, while for the *uvs-6* mutant, the inoculum size was doubled. After two days at 30°C, the survival rate for each dose of the carbon-ion beam was calculated using unirradiated plates as a control (Fig.1). Among the strains and doses tested, the *uvs-6* mutant always showed the highest sensitivity to the carbon-ion beam, suggesting that the MRX complex has an important role in protecting the cell from carbon-ion induced damage. Sensitivity of the *mus-52* mutant was higher than that of the wild type and *mei-3* strains for carbon-ion doses below 50 Gy. However, the *mus-52* mutant was less sensitive to the carbon-ion beam than the *mei-3* mutant and the wild type strain at doses over 100 Gy and 150 Gy, respectively. From these results, we speculate that DNA damage induced by higher doses of the ion beam (>100 Gy) are repaired mainly by HR, while damage sustained from lower doses (<50 Gy) are fixed through NHEJ.

The frequency of induced mutation was determined by measuring the rate of forward mutation occurring at the *ad-3A* (*adenine-3*) or *ad-3B* locus. Mutations at either of these loci can interfere with adenine biosynthesis, causing the accumulation of a metabolic intermediate that results in purple colonies. For each strain examined,  $5 \times 10^5$  irradiated but viable conidia were used to inoculate a 5 L Florence flask, which was cultured in the dark at 30°C with low aeration. After 1 week of growth under such conditions, each germinating conidium formed a bead-like colony in the liquid medium. The number of purple colonies that formed in each flask was used to calculate the frequency of mutation at the *ad-3* loci (Fig.2). At a dose of 100 Gy, the mutation frequency of the *mus-52* strain was ~2.8-fold lower than that of the wild type strain. Conversely, the *mei-3* strain had a ~3.0-fold higher frequency of mutation than wild type. These results suggest that an error free repair pathway (i.e. HR) predominantly functions in the *mus-52* strain, while mutations occurring in the *mei-3* strain are mainly repaired through an error prone and/or mutagenic pathway (i.e. NHEJ).

The purple colonies obtained above were characterized as *ad-3A* or *ad-3B* mutants through complementation tests using forced heterokaryons. To determine the type of mutation induced at each locus, genomic DNA was purified from each strain and the sequence of the *ad-3A* (924 bp) or *ad-3B* (2501 bp) gene was analyzed. Results obtained from three independent irradiation experiments are summarized in Figure 3. In the wild type strain, the most common mutation induced by the carbon-ion beam was a deletion of the 715<sup>th</sup> nucleotide of the *ad-3A* gene (Fig.3). On the other hand, carbon-ion irradiation of the *mei-3* strain frequently induced transitions between the 100<sup>th</sup> and 300<sup>th</sup> nucleotide of this gene. Exposure of *mus-52* to carbon-ions generated mutations within *ad-3B*, but not *ad-3A*. A complete comparison of the *ad-3B* mutation spectra from wild type and each of the DSB repair-deficient strains will soon be reported.

\*Laboratory of Genetics, Saitama University

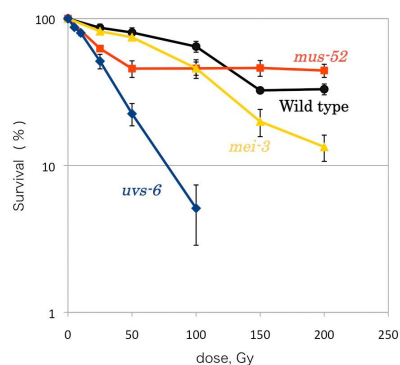


Fig. 1 Percent survival of strains irradiated with a carbon-ion beam.

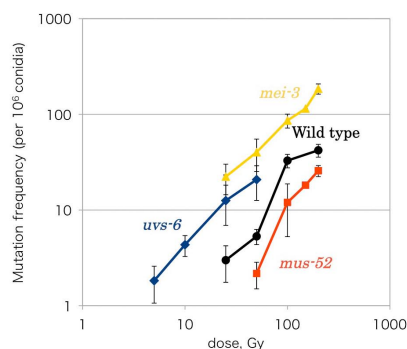


Fig. 2 Mutation frequency of the *ad-3* locus in carbon-ion irradiated strains.

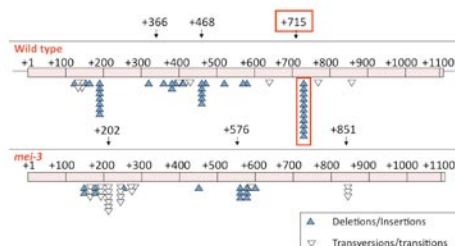


Fig. 3 Mutation spectrum of *ad-3A* in wild type and *mei-3* strains

## Efficient visualization of microbial mutations using DNA two-dimensional electrophoresis display

H. Ichida, T. Matsuyama, T. Koba,\*<sup>1</sup> and T. Abe

Recent advances in DNA sequencing technology have enabled the sequencing of entire genomes of several species of plants and microbes and the resulting data has allowed a comprehensive identification of microbial mutations induced naturally or artificially. To examine genome profiles, we used the method of restriction landmark genome scanning (RLGS), which is a two-dimensional DNA electrophoresis method in which restriction enzyme recognition sites are labeled with radioisotopes as landmarks and are visualized as spots on X-ray films.

This method has several major advantages compared with other DNA analysis methods: 1) almost 3,000 spots can be clearly visualized on film; 2) RLGS spots linearly reflect the copy numbers because there are no amplification steps and no bias in the detection step; 3) the recent development of a computer simulation-based analysis called *in silico* RLGS enables a comparison between two RLGS images, one obtained experimentally (real image) and the other by computer simulations based on whole genome sequences (*in silico* image); and 4) the cost per spot is several times lower than other techniques such as microarray and next-generation sequencing.

We obtained RLGS images of *Mesorhizobium loti* MAFF303099 with several enzyme combinations. The most important step in RLGS analysis is selecting landmark enzymes that produce well-focused and informative spot patterns. We used *AscI*, *BspEI*, and *NotI* as landmark enzymes and observed approximately 1071, 979, and 1025 spots respectively. When real and *in silico* images of *M. loti* MAFF303099 were compared, most of the spots matched the simulated images and we obtained profiles with almost complete linkage between RLGS spots and sequences (Fig. 1).

The ability of *in silico* RLGS analysis to comprehensively predict genome changes was examined. We found that the spots located between 500 and 15,000 bp in the first dimension and between 100 and 1000 bp in the second dimension always showed sufficient resolution and reproducibility with every enzyme combination used. The first-dimension coverage of *M. loti* MAFF303099 with the enzyme combinations of *AscI*-*MboI*, *BspEI*-*MboI*, and *NotI*-*MboI* was 42.3, 61.8, and 49.2% respectively. Overall, the first dimension coverage of the three enzyme combinations without duplication was 87.3%. This result clearly demonstrates that RLGS analysis combined with *in silico* profiling enables efficient and high-density scanning for mutations over the entire genome with good resolution.

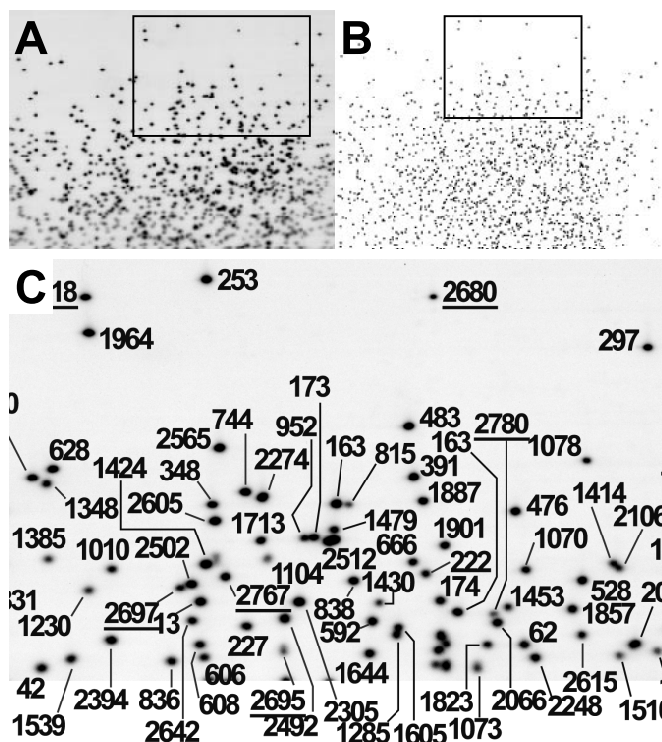


Fig. 1. Comparison between real and *in silico* RLGS images of *M. loti* MAFF303099. (A) Real RLGS image with *NotI* and *MboI*. (B) *In silico* RLGS image calculated based on the whole-genome sequence. (C) Boxed regions in A and B were compared and corresponding pairs of spots were shown on the real RLGS image with numbers (Non-underlined: chromosome, underlined: pMLa).

Computer simulation showed that RLGS analysis with three or four combinations of landmark enzymes covers 80% or more regions of the genomes in *Bradyrhizobium japonicum* USDA110, *Pseudomonas syringae* pv. *tomato* DC3000, *Xanthomonas oryzae* pv. *oryzae* MAFF311018. Therefore, *in silico* RLGS is applicable not only to *M. loti* but also other bacteria whose complete genome sequences are available and is universal technique to identify microbial mutations. We previously showed that accelerated heavy-ions cause insertions and deletions on microbial genomes<sup>1)</sup> suggesting that the combination of heavy-ion beam irradiation and *in silico* RLGS enables efficient induction and identification of microbial mutations.

### References

- 1) H. Ichida: *Mut. Res.* **639**, 101–107 (2008).

\*<sup>1</sup> Graduate School of Horticulture, Chiba University

## Characterization of floral homeotic mutant, *Meshibedarake*, induced by C-ion beam irradiation

Hinako Takehisa, Yusuke Kazama, Hiroyuki Ichida, Yoriko Hayashi, Sumiko Ohbu, Kazumitsu Miyoshi\*, Tomoko Abe

Previously, we examined the effects of heavy ion beams on plant-mutation induction in developing embryos, seeds, in vitro cultured cells, in anther culture and leaf cultures of tobacco.<sup>1)</sup> Generally, plants are regenerated from anther culture that have haploid genome. Therefore, the mutation induction in anther culture offers the possibilities of screening for recessive mutants in the first generation, selecting for novel genotypes from very large haploid populations, avoiding chimerism and rapidly fixing selected genotypes.

In this study, we identified a novel mutant “*Meshibedarake*” (*md* mutant) that promoted homeotic conversion of stamen into pistil structures in *N. tabacum* (cvs. Xanthi) (wild-type: Fig. A and *md* mutant: B). The *md* mutant was isolated from M<sub>1</sub> plants regenerated by anther cultures that were irradiated with C ions (135MeV/u, LET 23keV/μm) at dose of a 5 Gy. The *md* mutant was sterile, and was determined to be haploid by Flow Cytometer. Therefore, to identify the mutation gene of *md* mutant, we analyzed the detail phenotypes and mutation by using M<sub>1</sub> and clone plants. The *md* mutant showed dwarf-type and had small flower organs as with commonly haploid plant (Fig. C). In addition, the mutant had abnormal organs instead of normal stamens (Fig. D-F). However no obvious morphological changes could be observed in any other part of the flower organs (Fig. A-C). First, to determine the nature of the abnormal organs, we observed the epidermal cell of each flower organ by using scanning electron microscopy (SEM). The all organs except for abnormal organs of *md* mutant were typical of wild-type style. In the abnormal organs, the tip organs (Fig. D, white arrow head) had many trichomes as in the case of the stigma of wild type. Moreover, in the stigmatic organs, wild-type pollen could germinate and the pollen tube could grow as in the stigma of the wild type (Fig. G). The epidermal cell of bottom parts of the abnormal organs (Fig. D, gray arrow head) resembled that of the anthers of the wild type. These results indicate that the abnormal organs of *md* mutant were composed of fused organs between stigma and anther, and the mutant cause conversion of stamens into pistils.

The conversion of the stamen into the pistil in *Petunia* was known as loss of homeotic genes, *GLO*, *DEF* or *TM6*. Therefore, we attempted to identify the mutation gene of the *md* mutant by Southern blot analysis using these candidate genes as probes. The *md* mutant should lack signals that were detected in wild-type, only when the *DEF* gene was used as a probe (Fig. H). To identify the mutant sequence, we isolated the *DEF* gene

in wild type and the mutant. As a result, we detected deletion of over 4,244bp including *DEF* in the mutant genome. These results suggest that the conversion of the stamens into the pistils of *md* mutant is caused by the loss-of-function in the *DEF* gene. The *DEF* mutant of *Petunia* shows not only the conversion of stamen into pistil, but also the conversion of petal into sepal. The conversion like the *md* mutant had been observed only *N. tabacum*<sup>2)</sup>. These results indicate that *N. tabacum* has unique *DEF* function which was different from other Solanaceae plants including *Petunia*.

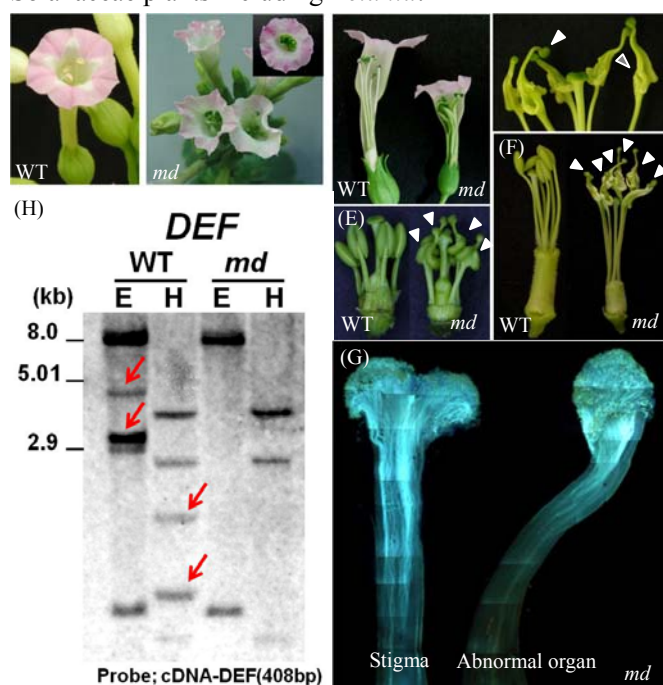


Figure. Phenotype of flower organs of wild-type (WT) and *md* mutant (A-G), and Southern blot analysis of WT and *md* mutant genomic DNA with a probe for a *DEF* gene (H). (A) and (B) WT and the *md* mutant flowers, respectively. (C) WT (left) and *md* mutant (right) flower. Petals have been removed partially. (D) Abnormal organs (five organs) and pistil (the center) of *md* mutant. White and gray arrow-heads indicate the tip organ and bottom organ of the abnormal organ, respectively. (E) Buds (sepal and petals have been removed) of WT and *md* mutant at bud-5mm and (F) -20mm stage. These white arrow-heads indicate the abnormal organs except for stamens. (G) Pollen tube growths in stigma and the abnormal (stigmatic) organs of *md* mutant. (H) Southern blot analysis of WT and *md* mutant genomic DNAs with a *DEF* probe. Two bands (red arrows) were not detected in *md* mutant genomic DNA after digested with *Eco*RI: E and *Hind*III: H, respectively.

### References

- 1) H. Saito et al.: RIKEN Accel. Prog. Rep. 40, 256 (2006)
- 2) J. Broadhvesti et al.: Plant J. 2, 991 (1992)

\* Akita. Prefectural University.

## Identification of deletion mutation induced by C-ion beam irradiation in a tobacco white flower mutant

Yusuke Kazama, Hinako Takehisa, Sumie Ohbu, Hiroyuki Ichida, Yoriko Hayashi and Tomoko Abe

Heavy-ion beam irradiation is widely accepted as a powerful tool for inducing deletion mutations with high efficiency. We are studying the size of deletions induced by heavy-ion beam irradiation in plant genomes, and previously reported a 985-bp and a 440-bp deletion in *Arabidopsis* mutants induced by irradiation with  $^{12}\text{C}^{6+}$  and  $^{14}\text{N}^{7+}$  ions, respectively.<sup>1),2)</sup> In this report, we determined a new deletion occurring in a tobacco white flower mutant, *xwf1* (Fig. 1), to obtain more insight into the deletion sizes.

The *xwf1* mutant was induced by  $^{12}\text{C}^{6+}$ -ion beam irradiation (135 MeV/nucleon, 23 keV/ $\mu\text{m}$ ) at a dose of 20 Gy.<sup>3)</sup> Flower colors are most often conferred by the structure of flavonoids. One of the flavonoids, cyanidin is the major component of colored anthocyanidins in the tobacco flower. Cyanidin is produced from dihydrokaempferol by the action of flavonoid 3' hydroxylase (F3'H), dihydroflavonol 4-reductase (DFR) and anthocyanidin synthase (ANS). We previously reported that the *xwf1* mutant did not accumulate cyanidin and pelargonidin but contains dihydrokaempferol and quercetin, which is a product of F3'H action.<sup>3)</sup> From the result, it was postulated that DFR or ANS may be defective in the *xwf1* mutant. Thus, we investigated whether the *xwf1* mutant has mutations in the *N. tabacum* *DFR* gene (*NtDFR*) or the *N. tabacum* *ANS* gene (*NtANS*).

Southern blot analysis was performed using the DNA fragment coding *DFR* gene as a probe (Fig. 2). Wild-type plant showed four hybridization signals after *Eco*RI or *Hind*III digestion, whereas the *xwf1* mutant lacked signals of 8-kb fragment produced by *Eco*RI digestion and of 1.5-kb fragment produced by *Hind*III digestion. This result indicates that the *xwf1* mutant would have a deletion mutation in the *NtDFR* gene. When the *NtANS* gene was used as a probe, no signal difference was observed between wild-type and the *xwf1* mutant.

To clarify the deleted region in the *xwf1* mutant, we determined genomic sequences of the *NtDFR* genes in *N. tabacum* cv. Xanthi. Tobacco is a natural allotetraploid derived from the interspecific hybridization of ancestral *N. sylvestris* and *N. tomentosiformis*. Thus, at least two copies per every gene exist in the tobacco genome. Two copies of the *DFR* gene, *NtDFR1* and *NtDFR2*, were previously identified in cv. SN1<sup>4)</sup> and in cv. SamsunNN. Two independent genomic fragments, 6,723 bp and 3,847 bp, including *NtDFR* genes were obtained by PCR-based cloning and sequencing (Fig. 3). Sequence homology search using the BLAST program on the GenBank database (<http://www.ncbi.nlm.nih.gov/>) revealed that the 6,723-bp and 3,847-bp fragments harbors a gene homologous to *NtDFR1* and *NtDFR2*, respectively. The size

of the *Hind*III fragment that disappeared in the *xwf1* genome in Southern hybridization analysis (Fig. 2) was corresponding to that of the *Hind*III fragment included in the 3,874-bp sequence. This result suggests that the deletion may occur in the *NtDFR2* gene. To ascertain the existence of the deletion in *NtDFR2*, PCR was performed by using *NtDFR2*-specific primers. The fragment containing the *NtDFR2* gene was amplified from the wild-type genomic DNA, but did not from the *xwf1* mutant genomic DNA (data not shown). These results indicate that the *xwf1* mutant has a deletion that is at least larger than 3,874 bp.



Fig. 1. Flowers of the wild-type tobacco cv. Xanthi and the *xwf1* mutant.

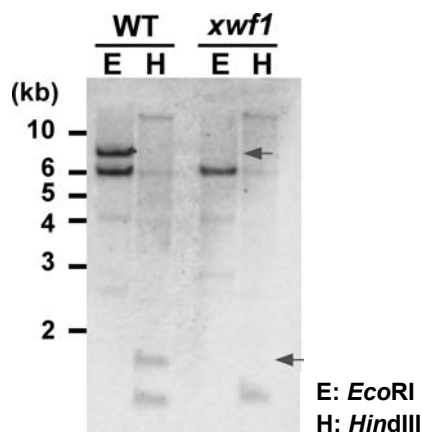


Fig. 2. Southern blot analyses using *NtDFR* gene as a probe. Arrows indicate signals lacking in the *xwf1* mutant.

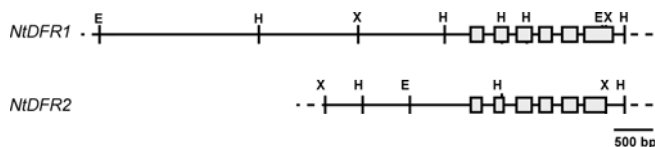


Fig. 3. Genome structures of two copies of *NtDFR* genes.

### Reference

- 1) Y. Kazama et al.: Biosci. Biotech. Biochem. **71**, 2864 (2007)
- 2) Y. Kazama et al.: Plant Biotech. **25**, 113 (2008).
- 3) Y. Kazama et al.: Plant Biotech. **25**, 105 (2008).
- 4) T. Nakatsuka et al.: Plant Cell Rep. **26**, 1951 (2007).

## Expression analysis of anthocyanin-synthesis related genes in a torenia sector mutant produced by ion beam irradiation

K. Sasaki\*, H. Yamaguchi\*, R. Aida\*, M. Shikata\*, T. Komatsu\*, Y. Hayashi, H. Ryuto, N. Fukunishi, T. Abe and N. Ohtsubo\*

We have previously reported that the application of heavy-ion beam irradiation to genetically modified torenia (*Torenia fournieri* Lind. 'Crown Violet'; Figure 1A) plants carrying anthocyanin biosynthesis-related transgenes could create various petal color and coloration, and concluded that the combination of ion beam irradiation and genetic engineering efficiently facilitates improvement of agrobiological and commercial traits within a short period

Among the mutants obtained, we chose a sector mutant, 40-53, for our analysis (Figure 1B-a and -b), because we were interested in the unique and novel phenotype in petal coloration, which has never seen before in torenia. The 40-53 mutant was obtained by the  $^{20}\text{Ne}$  (25 Gy) ion beam irradiation to CA411-3 (Figure 1A-b) carrying 35S::antisense-chalcone synthase (*CHS*) gene<sup>2)</sup>. In this mutant, a large part of the petal showed pale purple (Figure 1B-a, region  $\beta$ ), which is slightly fainter than the petals of CA411-3 plants, and a smaller part of petals showed dark purple (Figure 1B-a, region  $\alpha$ ) as in wild-type torenia (Figure 1A). We assumed that one of anthocyanin biosynthesis-related genes would be deficient in the mutant to be partially restored to dark purple color. To progress in the analysis of the mutant, we cloned 10 torenia anthocyanin biosynthesis-related genes, such as anthocyanin synthase 1 and 2 (*TfANS1* and *TfANS2*), chalcone isomerase (*TfCHI*), chalcone synthase 1 and 2 (*TfCHS1* and *TfCHS2*), dihydroflavonol 4-reductase (*TfDFR*), flavanone hydroxylase (*TfF3H*), flavonoid 3' hydroxylase (*TfF3'H1* and *TfF3'H2*) and flavonoid 3' 5'-hydroxylase (*TfF3'5'H*), and examined the expression of these genes by RT-PCR analysis using petals of  $\alpha$  and  $\beta$  regions in the mutant (Figure 1C). The results showed that the expressions of *TfCHS1* and *TfCHS2*, which were not detected in CA411-3 plants, were detected in region  $\alpha$  of the mutant. Unexpectedly, the expression of *TfDFR* was up-regulated in CA411-3, and down-regulated in region  $\alpha$  of the mutant. Expressions of the other genes were not significantly changed in the mutant.

Because the expression of *TfCHS1* and *TfCHS2* gene were restored in region  $\alpha$  of the mutant, we supposed that this phenotype was caused by a mutation, which released the gene silencing of the two genes by the antisense-*CHS*. Alteration of *TfDFR* expression from wild-type torenia would be explained by feedback effect under the control of the expression of *TfCHS* genes, because the *DFR* is downstream of the *CHS* on anthocyanin biosynthesis. Meanwhile, only a single base

mutation would not cause this sector phenotype, and we supposed that an unstable mutation which partially release the gene silencing on a phase of petal pigmentation and coloration, such as insertion of unknown transposable elements<sup>3)</sup> and alteration of methylation, would occur around the transgene. We are now trying to isolate and confirm the sequences of transgene including the whole T-DNA region in the mutant. We expect that we would be able to control not only petal color but also petal coloration of torenia plants in the future by elucidation of a gene mutation that causes the phenotype of the 40-53 mutant.

### Reference

- 1) K. Sasaki et al.: Plant Biotechnol. 25, 81 (2008)
- 2) R. Aida et al.: Plant Sci. 153, 33 (2000)
- 3) A. Hoshino et al.: J Plant Res. 122, 215 (2009)

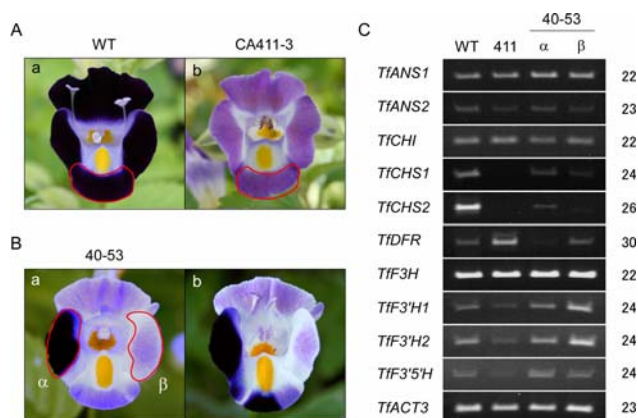


Figure 1. Analysis of 40-53 mutants obtained by heavy-ion beam irradiation. Photographs of WT (A-a), CA411-3 (A-b) and 40-53 mutants (B). (C) RT-PCR analysis of 10 anthocyanin-synthesis related genes, *TfANS1*, *TfANS2*, *TfCHI*, *TfCHS1*, *TfCHS2*, *TfDFR*, *TfF3H*, *TfF3'H1*, *TfF3'H2* and *TfF3'5'H* in petals of WT, CA411-3 and 40-53. In 40-53, dark purple region ( $\alpha$ ) and pale purple region ( $\beta$ ) were used for RT-PCR materials. The torenia actin gene, *TfACT3* (AB330989), was used as an internal control. PCR cycles were indicated on right sides of each column.

\* National Institute of Floricultural Science

## Reduced expression of *flavonoid 3',5'-hydroxylase* gene in a red-flowered torenia mutant obtained by heavy-ion beam irradiation

M. Shikata,<sup>\*1</sup> K. Sasaki,<sup>\*1</sup> R. Aida,<sup>\*1</sup> H. Yamaguchi,<sup>\*1</sup> Y. Hayashi, H. Ryuto, N. Fukunishi, T. Abe, and N. Ohtsubo<sup>\*1</sup>

Flower color is one of the most attractive characteristics of ornamental flowers. The color is principally determined by anthocyanins, a colored flavonoid pigment. Enzymes responsible for anthocyanin biosynthetic pathway, including dihydroflavonol-4-reductase (DFR) and flavonoid 3',5'-hydroxylase (F3'5'H), are well established, and the genes encoding them have been used for genetic engineering of flower color modification in petunias, roses, carnations and so on<sup>1)</sup>. We have previously generated the transgenic torenia DA416-20 with reduced activity of DFR by overexpressing an antisense gene<sup>2)</sup>. DA416-20 plants had light blue petals due to disturbed anthocyanin biosynthesis<sup>3)</sup>, while the wild type (*Torenia fournieri* Lind. cultivar 'Crown Violet') exhibits violet color (Fig. 1). We have further mutated DA416-20 plants by heavy-ion beam irradiation and have obtained various mutants with flower color variation<sup>4)</sup>. Disturbed anthocyanin biosynthesis might account for changed color. To test this hypothesis, we analyzed a mutant line 25-36 which had reddish flowers rather than blueish ones (Fig. 1). Blue color is derived from derphinidin-based anthocyanins, and a key enzyme for derphinidin biosynthesis is F3'5'H. Since cosuppression of the *F3'5'H* gene caused pink colored flowers in *Torenia hybrida*<sup>5)</sup>, 25-36 plants were expected that the *F3'5'H* gene expression was reduced. Therefore, we first isolated *TjF3'5'H* (*Torenia fournieri* *F3'5'H*) gene from wild-type torenia. Two cDNA sequences for *TjF3'5'H* were obtained. One encodes 520 aa protein which is comparable to the length of other plant F3'5'H, and another one encodes truncated protein (140 aa) because of frame-shift caused by 1 nucleotide deletion. We refer to them as type A and B, respectively. In addition, three nucleotides were different between two cDNAs. We performed quantitative real time PCR to compare the *TjF3'5'H* expression between wild-type and 25-36 plants. *TjF3'5'H* expression was extremely reduced to 1.3% of the wild type in the line 25-36, while it was not in DA416-20 and other DA416-20-based mutant lines (Fig.2). Sequence analysis revealed that wild-type plants expressed type A *TjF3'5'H*, while 25-36 exclusively accumulated type B *TjF3'5'H*. This result indicate that the reddish flower of 25-36 plants were due to impaired function of TjF3'5'H which is essential enzyme for blue color pigmentation. To investigate whether impaired expression of *TjF3'5'H* was caused by a mutation in this gene, we determined the genomic sequence of *TjF3'5'H* in wild-type and 25-36 plants. However, there was no mutation in the coding region of genomic sequence both of type A and B *TjF3'5'H* in the 25-36 mutant.

We are now trying to elucidate whether there is a mutation in the promoter region of *TjF3'5'H* gene and in the gene which regulates the *TjF3'5'H* expression directly or indirectly. Although it remains to be elucidated what caused reduction of the *TjF3'5'H* expression, we found that heavy-ion beam irradiation has disturbed anthocyanin biosynthesis to alter flower colors.

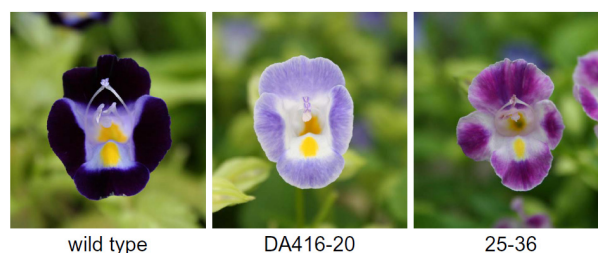


Figure 1. Altered flower color of torenia by molecular engineering.

Mutant line 25-36 was obtained by heavy-ion beam irradiation to DA416-20 plants which was harboring *DFR* antisense gene.

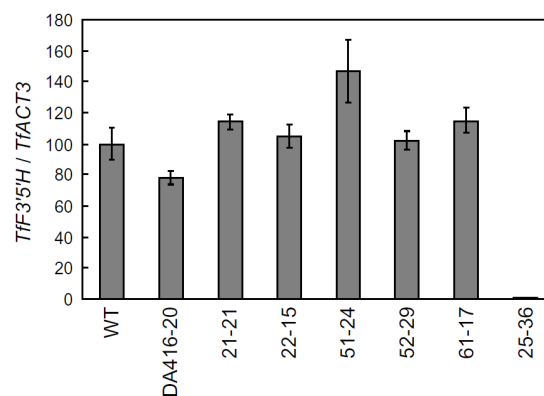


Figure 2. *TjF3'5'H* gene expression.

*TjF3'5'H* and *TjACT3* expression were analyzed by quantitative real-time RT-PCR. Line 21-21, 22-15, 51-24, 52-29, 61-17 and 25-36 are ion-beam induced mutants of DA416-20 background. Values are average  $\pm$  SD of three technical duplicates and are represented by relative value to wild type designated as 100.

### References

- 1) Y. Tanaka et al.: *Plant Cell Physiol.* 39. 1119-1126 (1998).
- 2) R. Aida et al.: *Plant Sci.* 153. 33-42 (2000).
- 3) R. Aida et al.: *Plant Sci.* 160. 49-56 (2000).
- 4) K. Sasaki et al.: *Plant Biotechnol.* 25. 81-89 (2008).
- 5) K. Suzuki et al.: *Mol. Breed.* 6. 239-246 (2000).

<sup>\*1</sup> National Institute of Floricultural Science, National Agriculture and Food Research Organization

## Characterization of the GA-synthesis deficient mutants produced by heavy-ion-irradiation

Yusuke Kazama, Ichiro Honda,<sup>\*1</sup> Kiyoshi Nishihara, Kaori Kikuchi,<sup>\*1</sup> Satoshi Matsuo,<sup>\*1</sup> Machiko Fukuda,<sup>\*1</sup> Shigeyuki Kawano<sup>\*2</sup> and Tomoko Abe

Mutants in plants are powerful tools for clarifying physiological mechanisms as well as developing new plant varieties in practical breeding programs. Recently, irradiation of plants with accelerated heavy-ion from a ring cyclotron was established as a new effective method to induce mutation. We already reported the effects of heavy-ion bombardment on mutagenesis in sweet pepper (*Capsicum annuum* L., cv. California Wonder) and isolated two dwarf (D, SD) and one xantha mutants from M<sub>1</sub> plants that were irradiated by Ne-ion beams at a dose of 10 Gy. Genetic analysis indicated that these mutants have monogenic recessive mutations in nuclear genes.<sup>1)</sup> In this report, we examined two dwarf (D, SD) mutants to clarify their physiological mechanism of dwarfism.

Reciprocal grafting between D or SD and a wild type (WT) indicated that both dwarfisms do not transmit between scion and stock. Some cases of these dwarfisms are caused by defects of gibberellin (GA) biosynthesis or its signal transductions. Thus, we performed a foliar application of GA<sub>3</sub> in the mutants. As a result, shoot elongations were induced in D, SD and WT, especially, that in D is clearer than those in others. We also examined endogenous GAs in their shoot (Fig. 1). As endogenous GAs, GA<sub>1</sub>, GA<sub>8</sub>, GA<sub>19</sub>, GA<sub>20</sub>, and GA<sub>44</sub> were identified. The levels of GA<sub>19</sub>, GA<sub>20</sub>, and GA<sub>44</sub> in SD were lower than that in WT, whereas in D plant, those of GA<sub>19</sub>, GA<sub>20</sub> and GA<sub>8</sub> were lower, but that of GA<sub>44</sub> were higher than that in WT. These results indicated that D and SD mutant may have a defect in the GA20-oxidase genes.

It is reported that four GA20-oxidase genes may exist in the tomato genome. Based on the sequence information of the tomato GA20-oxidase genes, we designed specific primers and carried out PCR-based cloning of pepper GA20-oxidase genes. Two partial cDNA sequences were obtained. Sequence homology search using the BLAST program on the GenBank database (<http://www.ncbi.nlm.nih.gov/>) revealed that both sequences are homologous to GA20-oxidase genes. Using one of them (1-kb fragment) as a probe, genomic Southern blot analysis was performed. Wild-type plant and SD mutant showed the same signal patterns after *Eco*RI or *Hind*III digestion, whereas D mutant showed different signal size after *Hind*III digestion (Fig. 2). This result indicates that a mutation may occur around a GA20-oxidase gene in D mutant. Sequencing analysis of GA20-oxidase gene in D mutant is in progress.

\*1 National Institute of Vegetable and Tea Science

\*2 Department of Integrated Bioscience, The University of Tokyo

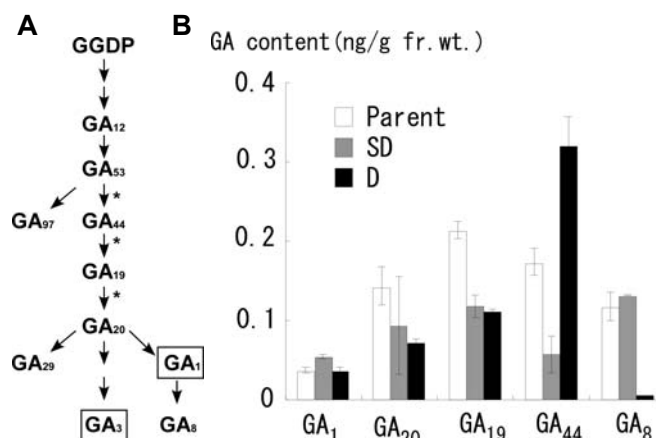


Fig. 1. (A) The GA biosynthesis pathways. Asterisk and box indicate GA20-oxidase-catalyzed reaction and bioactive GAs, respectively. (B) Endogenous GA contents in shoots (4-5 leaf stage). Bars indicate standard error.

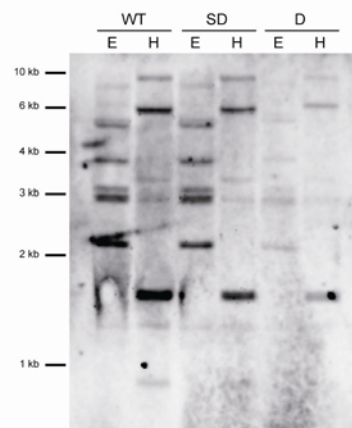


Fig. 2. Genomic Southern blot analysis of GA20-oxidase genes in the pepper dwarf mutants. An asterisk indicates band size shift detected in the D mutant. E: *Eco*RI, H: *Hind*III.

A part of this study was financially supported by the Budget for Nuclear Research of the Ministry of Education, Culture, Sports, Science and Technology, based on screening and counseling by the Atomic Energy Commission of Japan.

### Reference

- 1) Honda et al.: *Euphytica* **152**, 61 (2006)

## Effect of the heavy-ion beam irradiation on survival rates and sex-reversal mutation in *Silene latifolia*

K. Nishihara, Y. Kazama, S. Ohbu, A. Koizumi,\* K. Yamanaka,\* H. Ichida, Y. Hayashi, H. Ryuto, N. Fukunishi, S. Kawano,\* and T. Abe.

The Caryophyllaceae perennial herb *Silene latifolia* is a dioecious plant, which has a XY sex determination system. It is presumed that its Y chromosome has three functional regions; the gynoeceum-suppressing function (GSF), the stamen-promoting function (SPF), and the anther-maturing function.<sup>1)</sup> Though these regions are thought to contain sex-determination genes, those genes have not been identified yet. In the earlier studies on sex-determination of *S. latifolia*, many attempts to get Y-chromosome-deleted mutants were performed; e.g.  $\gamma$ -ray irradiation. Among these irradiated plants, the mutants that lack GSF showed hermaphroditic phenotype and the mutants that lack SPF represented asexual phenotype.<sup>2,3,4)</sup> This correspondence relationship supported the existence of sex-determination genes on each functional region. However, no more information was able to be received from these mutants, because most of them are sterile and ephemeral and are now defunct.

Recently, we obtained a novel hermaphroditic mutant by C ion beam irradiation.<sup>5)</sup> This mutant is fertile and, interestingly, can produce progenies by self-pollination. Genetic analyses have demonstrated that this mutant has a deletion in Y chromosome. Thus, the ion beam irradiated mutants would be used for isolating sex-determination genes by sequencing deleted regions in the Y chromosome. Mutations of the other regions of Y chromosome will be induced with ion-beam irradiation. Then, we planned to survey the appropriate conditions of irradiation to induce mutations on Y chromosome efficiently.

Dry seeds of *S. latifolia* were irradiated by Fe-ion beams (90 MeV/u, LET 624 keV/ $\mu$ m) at a dose range of 5 to 40 Gy. Wet seeds imbibed for 24h and 28h were irradiated by Fe-ion and C-ion beams (135 MeV/u, LET 23 keV/ $\mu$ m) at a dose range of 2 to 40 Gy and of 5 to 80 Gy, respectively. The effect of each ion beam was observed three weeks after sowing by measuring survival rates (Fig. 1). From the obtained survival curves, the lethal dose 50 (LD<sub>50</sub>) for dry seed was estimated at approximately 145 Gy of C-ion irradiation and 9 Gy of Fe-ion irradiation. The LD<sub>50</sub> value for imbibed seeds was estimated to be approximately 30 Gy of C-ion irradiation and 5 Gy of Fe-ion irradiation. As summarized in Fig. 1, the imbibed seeds showed more sensitivity to irradiation than the dry seeds. This difference of sensitivity could be brought about by the difference in the hydration state of DNA and/or free radicals.<sup>6,7)</sup> The Fe-ion beam had a stronger effect than the C-ion beam. The

difference in the effect is thought to be because the LET of Fe ions is higher than that of C ions.

Following on from this, we grew the imbibed seeds and screened mutants. We found some mutants including asexual mutants and hermaphroditic mutants among the plants irradiated with C ion at 10 Gy or 20 Gy and the plants irradiated with Fe ion at 4 Gy (Table 1). We deduced that imbibed seed irradiated C ion and Fe ion at 10 Gy and 4 Gy are effective in isolating mutants, respectively. However, we were not able to fix these mutants because they were conspicuously chimerical; for example, there was only one mutated flower in a plant.

These results indicated the possibility of ion beams being able to induce various mutations on Y chromosome. Now, we are screening mutants among Fe-ion-irradiated dry seeds.

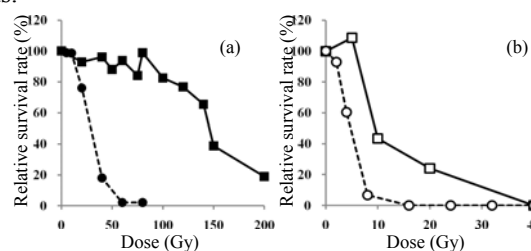


Fig. 1. Survival curve of ion-beam irradiated *S. latifolia*. (a) Survival curve of C-ion irradiated seeds. (b) Survival curve of Fe-ion irradiated seeds. The longitudinal axis indicates relative survival rate when the control is assumed to be 100. ■, □: survival rate of dry seeds, ●, ○: survival rate of imbibed seeds.

Ion	Dose (Gy)	No. of plants	Number of mutants		
			Asexual	Hermaphrodite	Variegated
C	0	94	0	0	0
	5	89	0	0	0
	10	85	2	1	1
	20	70	1	0	0
	40	16	0	0	0
	60	2	0	0	0
	80	2	0	0	0
Fe	0	101	0	0	0
	2	92	0	0	0
	4	61	0	1	1
	8	7	0	0	0

Table 1. Mutants induced with ion-beam irradiation on imbibed seeds of *S. latifolia*.

### Reference

- 1) M. Westergaard: Adv. Genet. **9**, 217 (1958).
- 2) A. Lardon et al.: Genetics **151**, 1173 (1999).
- 3) I. Farbos et al.: Genetics **151**, 1187 (1999).
- 4) S. Lebel-Hardenack et al.: Genetics **160**, 717 (2002).
- 5) K. Nishihara et al.: RIKEN Accel. Prog. Rep. **40**, 258 (2007).
- 6) Shikazono et al.: Radiat. Environ. Biophys. **41**, 159 (2002)
- 7) Qin et al.: Int. J. Radiat. Biol. **83**, 301 (2007)

\* Graduate School of Frontier Sciences, The University of Tokyo

## LET-dependent effect of C-ion beam irradiation on mutation induction in Rice.

Y. Hayashi, H. Takehisa, Y. Kazama, S. Ohbu, N. Fukunishi, H. Tokairin, S. Mituo<sup>\*1</sup>, S. Takada<sup>\*1</sup>, T. Sato<sup>\*2</sup> and T. Abe

Heavy ion beams have high linear energy transfer (LET) and produce more localized ionization than other radiation such as X-rays and  $\gamma$ -rays for the same dose. Therefore, a heavy ion particle is postulated to cause double strand break of DNA and induce mutation with low dose irradiation<sup>1)</sup>. LET of ion beams is an important factor affecting mutagenesis. In Arabidopsis, the lethality rate and flowering rate after ion beam treatment are affected by LET. Furthermore, there is an optimum LET value for mutation induction in M<sub>2</sub> plants of Arabidopsis<sup>2)</sup>. We examined the effect of LET values on mutation induction in rice.

Imbibed seeds of rice (*Oryza sativa* L. cv. Nipponbare) were exposed to C-ion accelerated to 135MeV/u by RRC. The dose range and the LET range of the C-ion beam were 7.5 to 40Gy and 23 to 60keV/ $\mu$ m respectively. The LET of the C-ion was selected using a range shifter that consists of twelve energy absorbers<sup>3)</sup>. The LET values were calculated at the surface of the seeds. After irradiation, seedlings were transplanted into the soil in pots, and grown in a greenhouse. One month after irradiation, plants were transplanted to a paddy field. M<sub>1</sub> plants were harvested approximately 6 months after irradiation. Survival rates and seed fertilities were surveyed in M<sub>1</sub> progenies. M<sub>2</sub> seeds were harvested separately from each M<sub>1</sub> plant. These seeds were sown on seedbeds and grown in a greenhouse for one month to observe mutations. The numbers of CDM (chlorophyll-deficient mutants): albina (albino); xantha (yellow); chlorina (pale green); striata (stripe) were observed.

The survival rate of M<sub>1</sub> plants decreased as the dose increased, and the survival curves differed according to the LET (Fig.1). In over all the fertility of M<sub>2</sub> seeds decreased as the dose increased. There was no significant difference with increased LET values (Fig.2). Mutation rates at 7.5Gy and 10Gy irradiation were low with any

values of LET. In the irradiation at 15 or 20Gy, the higher LET values such as 50 or 60keV/ $\mu$ m were effective in CDM induction (Table.1). These results show that increase of mutation rates could be achieved by controlling LET values in adequate dose irradiation. We are now investigating the effect of higher LET values using Ne ion beams on mutation induction in rice.

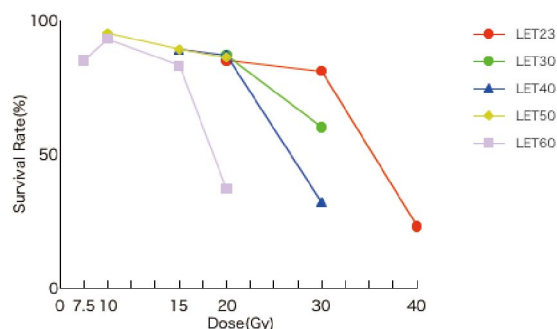


Fig. 1 Survival curves for various LET of C-ion irradiation

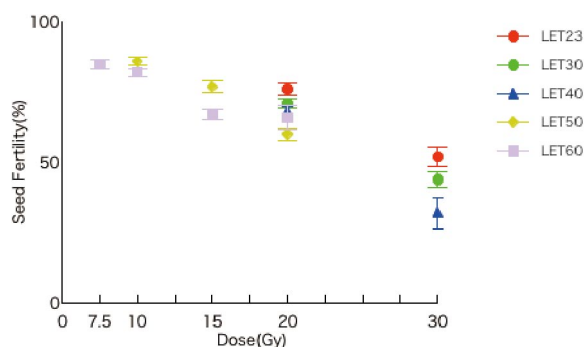


Fig. 2 Relationship between the seed fertility and the dose

### Reference

- 1) Y. Yokota et al.: Radiat Res. **167**,94(2007)
- 2) Y. Kazama et al.: Plant Biotechnology **25**, 113(2008)
- 3) H. Ryuto et al.: Plant Biotechnology **25**, 119(2008)

Table.1 Frequency of chlorophyll-deficient mutants (CDM) induced by C-ion beam irradiation

Dose (Gy)	LET (keV/ $\mu$ m)	Survival Rate (%)	Fertile M <sub>1</sub> lines	CDM				Total CDM	Frequency of CDM (%)
				albina	xantha	chlorina	striata		
7.5	60	85	127	2	2	0	0	4	3.2
10	50	95	142	2	2	0	0	4	3.3
	60	93	140	2	1	1	0	4	2.8
15	50	89	134	4	5	0	0	9	6.7
	60	83	249	7	2	4	2	15	6.2
20	23	85	127	1	1	1	0	3	2.4
	30	87	261	11	1	1	1	14	5.4
	40	87	260	7	3	2	2	14	5.4
	50	86	258	9	4	1	1	15	5.8
	60	37	56	1	1	2	0	4	7.1
30	23	81	121	2	2	1	1	6	5.0
	30	60	180	6	1	2	0	9	5.0
	40	32	47	1	0	0	0	1	2.1

Harvest from 2005 and 2007.

\*1 Faculty of Science, Tokyo University of Science

\*2 Graduate School of Life Sciences, Tohoku University

## Isolation of C-ion induced mutants of strawberry cultivar "Satsumaotome"

M. Ooe,\* T. Nagatani,\* Y. Takenoshita,\* H. Saito and T. Abe

Demand for strawberries in Japan rises at the end of the year. Although the strawberry cultivar 'Satsumaotome' developed by Kagoshima prefecture has large fruits and good eating quality, it is classified as a late-harvesting cultivar, and is not suitable for harvesting at the time with high demand. Recently, heavy-ion beams have been frequently utilized for breeding by artificially inducing mutations in various plant species.<sup>1)</sup> Therefore, we examined the possibility of applying heavy-ion beam irradiation to the development of strawberries, and selected earlier-flowering mutants derived from 'Satsumaotome'.

Multiple shoot cultures derived from the shoot apex were used in the irradiation treatments. Cultures were irradiated with C-ion beams whose LETs were controlled to ca. 23 or 48 keV/ $\mu\text{m}$  at the surface of the cultures. Shoots developed from their irradiated cultures were propagated via runner production after acclimatization, transplanted to pots and grown in a greenhouse. Culturing was done using the general method for 'Satsumaotome' in Kagoshima prefecture.

A decrease in survival rate was observed with increasing in dose; after 10 Gy and 45 Gy irradiation treatments with LETs of 48 and 23 keV/ $\mu\text{m}$ , respectively, the survival rate decreased to about half that of controls (Fig.1). Also, a decrease in plant growth was observed with increasing in doses; 10 Gy with 48 keV/ $\mu\text{m}$  and 40 Gy with 23 keV/ $\mu\text{m}$  produced many plants with decreased growth. Among the irradiation conditions with different LETs and doses, several interesting morphological alterations, in characteristics such as habits of growth and flowering, colors of leaf, pericarp and sarcocarp, and fruit shapes, were observed (data not shown). We selected mutation lines showing early flowering two years after the irradiation treatments (Table 1). Putative early flowering mutants were selected from all irradiation conditions tested. However, most selected lines also showed other differences from the originals. As a result, we selected two suitable early flowering mutants, which seem to retain the original fruit characteristic of 'Satsumaotome' after 20 Gy irradiation treatment with LET of 23keV/ $\mu\text{m}$  (Table 2).

Although fruit characteristics of the selected lines were similar to 'Satsumaotome', both mutants flowered 4 days earlier and their fruits ripened 7 days earlier than that of the originals.

The results obtained in this study revealed that C-ion beam irradiation may be effective for mutation induction of strawberries. Two putative early flowering mutants were continuously grown in the greenhouse and their detailed characterization is in progress.

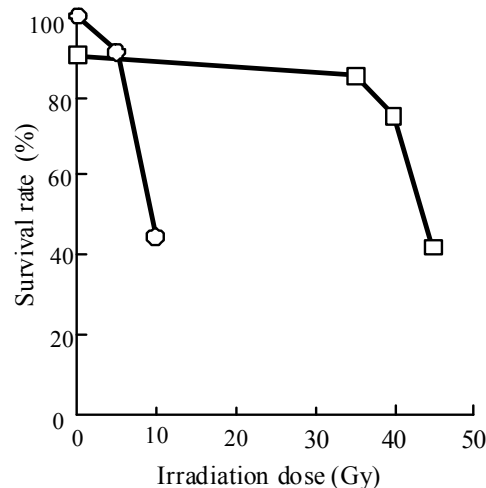


**Fig. 1.** Effect of C-ion beams on survival rate in 'Satsumaotome'. Data were recorded 20 weeks after the irradiations. LETs at the surface of samples were 23 ( $\square$ ) and 48 ( $\circ$ ) keV/ $\mu\text{m}$ .

**Table 1.** Effect of C-ion beam irradiation on the selection of early flowering lines in 'Satsumaotome'.<sup>a</sup>

LET <sup>b</sup> (keV/ $\mu\text{m}$ )	Dose (Gy)	No. of lines planted	Early flowering lines selected (%)
	0	78	0 (0)
23	10	196	5 (2.6)
	20	53	5 (9.4)
	30	126	6 (4.8)
48	5	149	5 (3.4)
	10	85	2 (2.4)

<sup>a</sup> Data were recorded two years after the irradiations.

<sup>b</sup> LETs were determined at the surface of irradiation samples.

**Table 2.** Characterization of early flowering mutants of 'Satsumaotome'.<sup>a</sup>

Lines	First Brix flowering (%)	First harvesting	Color of pericarp	Color of sarcocarp	
Satsumaotome	Nov. 8	Dec. 15	Light orange	White	9.7
B0401	Nov. 4	Dec. 8	Light orange	White	9.7
B0403	Nov. 4	Dec. 8	Light orange	White	10.3

<sup>a</sup> Data were recorded two years after the irradiations.

### References

- 1) M. Ooe: Nuclear Viewpoints 53(5) pp8-9,(2007)

\* Kagoshima Biotechnology Institute

## An early flowering mutant of strawberry cultivar "Satsumaotome" induced by C-ion irradiation

Y. Takenoshita,\* T. Nagatani,\* M. Ooe,\* H. Saito and T. Abe

The strawberry cultivar "Satsumaotome" registered by Kagoshima prefecture has large fruits and good eating quality. But it is a late flowering cultivar, so the yield to the end of the year is low. Therefore we aimed to develop early flowering mutants which retain the original excellent fruit characteristics of "Satsumaotome" by ion beam breeding.

We determined optimum doses of C-ion irradiation based on the survival rate of the cultured tissue. From the mutants irradiated with C-ion beams (LET 23 keV/μm, 20 Gy) in 2004, we found one promising line B0401 which has a flowering date by 5 days earlier than "Satsumaotome". We are currently investigating the detailed characteristics of B0401. To find a line with even an earlier flowering date than that of B0401, we tried individual selection and line selection from the population irradiated with ion beams in 2005.

In 2005, we irradiated with C-ion beams (LET 23 keV/μm) at doses up to 20 Gy, targeting in-vitro cultured multiple buds derived from the shoot apex of "Satsumaotome". After the irradiations, we cultured to isolate mutants from chimera, and finally obtained 98 nursery plants. In 2006, we selected 16 individuals from the 98 plants based on their vigor and disease tolerance. In 2007, we propagated the selected 16 individuals to 8 stocks respectively, and planted them in a field for line selection. We investigated the plant habit, day of flowering, size and shape of fruits, and color of fruit peel and flesh, and selected a promising line.

One line (B0518) had an earlier flowering date, and two lines (B0513 and B0516) had a later flowering date than "Satsumaotome" (Table 1). The flowering date of B0518 was 20 days earlier and its number of days to flowering was 17 days shorter than "Satsumaotome" (Table 1). In terms of fruit characteristics, we found two variants (B0513 and B0517) whose fruit shapes were "long-conical" and "round" respectively, and whose peel color was "deep red". B0518 was not different from "Satsumaotome" in terms of the size of the fruit, predominant shape of the fruit, color of peel, and color of flesh (Table 2). As a result, we found that B0518 is a promising early flowering line which retains the original excellent fruit characteristics of "Satsumaotome". Next year, we plan to perform a more detailed investigation of B0518 characteristics with the eventual aim of registration as a variety.

Following the previous promising line B0401, we have selected the early flowering promising line B0518 which retains the original excellent fruit characteristics of "Satsumaotome". From the results, we concluded that ion beam breeding is effective for developing early flowering mutant lines of the strawberry cultivar "Satsumaotome".

Table 1. Flowering characteristics of mutant lines in 2007

Line Cultivar	Dose (Gy)	Flowering date (month/day)	Number of	SEM
			days to flowering (day)	
B0501	10	11/23	52.0	1.4
B0504	10	11/27	54.9	0.8
B0505	10	11/24	52.8	0.7
B0506	10	11/21	50.1	1.5
B0507	10	11/22	54.5	4.4
B0509	20	11/23	51.3	0.3
B0510	20	11/21	49.1	0.7
B0511	10	11/26	53.8	1.1
B0512	20	11/24	51.3	2.5
B0513	20	12/13	75.0 **	4.2
B0514	20	11/23	51.0	2.2
B0515	20	11/20	47.9	1.4
B0516	20	12/27	85.1 **	0.1
B0517	20	11/28	55.8	1.6
<b>B0518</b>	<b>20</b>	<b>11/12</b>	<b>41.5 **</b>	<b>1.9</b>
B0519	20	11/24	50.6	2.2
Satsumaotome	—	12/1	58.4	1.0

Flowering date: 50% of plants at first flower

Number of days to flowering: Average number of days from planting to flowering

\*\* indicates a significant difference from "Satsumaotome" based on Tukey-Kramer's Test ( $p < 0.01$ )

Table 2. Fruit characteristics of mutant lines in 2007

Line	Fruit characteristics			
	Size	Predominant shape	Color of peel	Color of flesh
<b>B0518</b>	<b>large</b>	<b>conical</b>	<b>vivid red</b>	<b>whitish</b>
B0513	large	long-conical	deep red	whitish
B0517	large	round	deep red	whitish
Satsumaotome	large	conical	vivid red	whitish

\* Kagoshima Biotechnology Institute

## Breeding of a new Japanese barnyard millet variety with low amylose content and short-culm, by heavy-ion beam irradiation

S. Nakajo<sup>\*1</sup>, S. Hasegawa<sup>\*2</sup>, H. Yoshida<sup>\*1</sup>, S. Urushibara<sup>\*3</sup>, A. Abe<sup>\*3</sup>, T. Abe, N. Fukunishi, H. Ryutou<sup>\*4</sup> and Y. Oshimizu<sup>\*5</sup>

Japanese barnyard millet (*Echinochloa utilis* Ohwi et Yabuno) is considered to be one of the oldest cereal crops in Japan. In Iwate prefecture, Japanese barnyard millet has been cultivated as one of the main cereal crops, and as hay for horse feed, from ancient times. However, the millet cultivation area of Iwate has been rapidly decreasing since the late 1950's due to progress in upland field reclamation to paddy fields and the introduction of cold weather resistant rice varieties and industrial crops. For the last two decades, the nutritional value of millet has been reevaluated by home consumers. Due to this trend, the millet cultivation area and production of Iwate is increasing year by year. In particular, a large part of the national production of Japanese barnyard millet is produced in Iwate prefecture.

'Mojappe' is a local variety of Iwaizumi, a town located in the mountainous area of northern Iwate. It has good

quality for eating because of its sticky starch with low amylose content. The amylose content of 'Mojappe' is about 12 to 13%, half that of other ordinary non-glutinous barnyard millets.<sup>1), 2)</sup> 'Mojappe' was adopted as a variety recommended for good flavor in Iwate prefecture in 2005. However, it has been hard to expand the cultivation area of this variety as much as it expected, because its culm length is too long to harvest with a head-feeding combine. Therefore, we tried mutation breeding of 'Mojappe' for mechanized production by means of culm length shortening.

Dry-seeds of 'Mojappe' were irradiated by C-ions accelerated to 135 MeV/u at a dose of 20 Gy at the RIKEN RI-beam factory in November 2003. The LET (linear energy transfer) range was 23 keV/μm. After irradiation, M<sub>1</sub> seeds were sown in a greenhouse of the Iwate Agricultural Research Center (IARC) in December 2003. About 5 months after the sowing, M<sub>2</sub> seeds were obtained. In 2004, M<sub>2</sub> seedlings were transplanted in an upland field of IARC, Northern Region Agricultural Institute. Seventeen out of 906 M<sub>2</sub> plants were selected for culm length after the heading stage. Harvested seeds of 17 selected M<sub>2</sub> plants were grown in a greenhouse during the M<sub>3</sub> generation in wintertime. In 2005, 17 M<sub>4</sub> lines originating from the selected M<sub>2</sub> plants were grown in a paddy field, and finally, only one line was selected as the shortest culmed mutant line. During 2007-2008, this line was evaluated for its yield, culm length, amylose content and other agronomic characters together with another mutant lines derived from gamma-ray irradiation. Eventually, this line was designated as 'Hie-Iwate 2'.<sup>3)</sup>

'Hie-Iwate 2' is shorter than 'Mojappe', but taller than 'Daruma', the leading variety of Iwate (Fig.1). However, we confirmed that a head-feeding combine could harvest 'Hie-Iwate2' in a paddy field test in 2008. Additionally, we expect that 'Hie-Iwate 2' is suitable for mechanical hulling and sawing with its awnless kernel.

We will apply for a official registration of 'Hie-Iwate 2' to the Ministry of Agriculture, Forestry and Fisheries of Japan within 2009.



Fig. 1 Culm length of new variety.

### References

- 1) S. Hasegawa and M. Katsuta: Bull. Iwate. Agric. Res. Ctr. 5,53-62 (2005) (In Japanese with English summary).
- 2) S. Hasegawa and M. Katsuta: Breed. Res. 5 (suppl. 1) p.522 (2003) (in Japanese).
- 3) S. Nakajo et al.: Breed. Res. 10 (suppl. 1) p.181 (2008) (in Japanese).

<sup>\*1</sup> Iwate Agricultural Research Center (IARC), Northern Region Agricultural Institute  
<sup>\*2</sup> Iwate Central Agricultural Extension Center, Tono Extension Center  
<sup>\*3</sup> Iwate Agricultural Research Center (IARC)  
<sup>\*4</sup> Photonics and Electronics Science and Engineering Center, Kyoto University  
<sup>\*5</sup> Iwate Science Museum of Agriculture

## **IV. OPERATION RECORDS**

## **1. Operation of RIBF**

## Planning of RIBF operation

T. Suda, M. Kase, and T. Fujinawa

The operation of RIBF for FY2008 has been planned according to the approved budget for this fiscal year, plans for machine commissioning and construction and beam-time requests from experimenters.

According to the approved operation budget for five months, the operation plan of the new facilities, including the cyclotron cascade and BigRIPS/ZE, was made originally as :

- 1) Two months in the period of April to June,
- 2) Three months after the summer period.

No operation of the new facility was planned in the summer period, specifically from July to September, due to high electricity costs.

In February 2008, however, it turned out that there was a serious oil contamination problem in the refrigerators for SRC and BigRIPS. Detailed studies showed that its complete repair would take nearly half a year.

We, therefore, changed the operation schedule before summer. The time has been devoted into the developments of U and <sup>48</sup>Ca beams including the charge stripper development. As a result, the beam stability became remarkably better, and we were sure that the world's most intense <sup>48</sup>Ca beam would be provided for BigRIPS experiments when the refrigerators become ready.

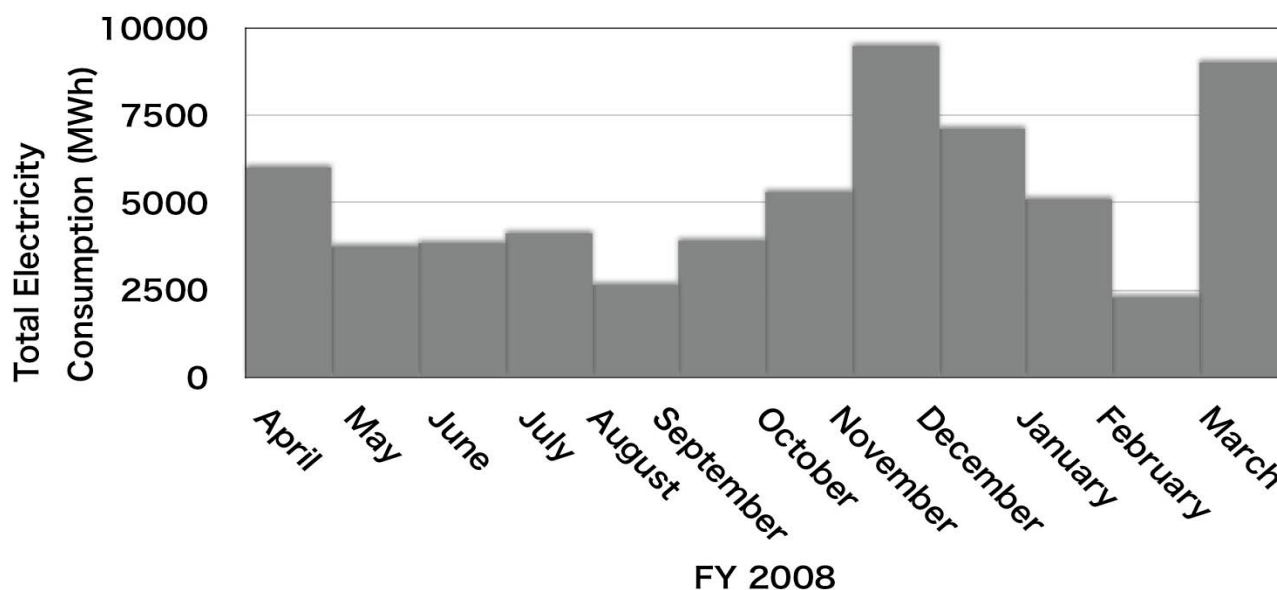
The refrigerators have been completely fixed up in August, and they became operational immediately. A series of BigRIPS experiments using U and <sup>48</sup>Ca have been conducted for nearly two months during November and October.

In addition, the first SHARAQ commissioning was carried out using <sup>14</sup>N beam in the late March. A new beam line skipping IRC was installed and used for this experiment.

A long-term super-heavy search experiment to strengthen the evidence of our discovery of Z=113, more specifically <sup>23</sup>Na + <sup>148</sup>Cm -> <sup>266</sup>Bh + 5n was done for one month in October, and more than 40 days from Jan. 1 to the middle of February.

The other experiments at the "old" facilities were also scheduled and performed as much as possible based on the requests from spokespersons of the PAC-approved proposals. Even in the summer period, mainly in the weekends experiments were carried out.

In total, the accelerator has been operating 198.3 days for 78 experiments. The commissioning of the new facility was for 81 days. As a reference, the electric consumption profile of Nishina Center for FY2008 is shown in Fig. 1.



# PAC Meetings for Nuclear Physics, and Material and Life Science

T. Suda, K. Ishida, and Y. Kobayashi

In 2007, RIKEN Nishina Center has established two Program Advisory Committees for reviewing submitted proposals in the fields of nuclear physics (NP-PAC) and material and life science (ML-PAC). Each PAC holds the meetings twice a year, and reviews the proposals.

The NP-PAC is co-organized by RIKEN Nishina Center and CNS, Univ. of Tokyo. The ML-PAC reviews experimental programs at RAL and RIBF.

## NP-PAC

The NP-PAC meetings were held Feb. 18-19 and Nov. 20-21 this year<sup>1)</sup>. The statistics of the meetings are shown in Tabel 1.

## ML-PAC

The ML-PAC meetings were held March 27-28, 2008 and Jan. 13-14 this year<sup>2)</sup>. The statistics of the meetings are shown in Tabel 2.

## PAC members

**NP-PAC** : *W. F. Henning (ANL, the chair )*, *J. Aysto ( Univ. of Jyväskylä )*, *W. Mittig ( MSU )*, *Karlheinz Langanke ( GSI )*, *W. Lynch ( MSU )*, *D. C. Radford ( ORNL )*, *W. Liu ( CIAE )*, *A. A. Ogloblin ( Kurchatov )*, *B. Fulton ( Univ. of York )*, *A. Ohnishi ( Kyoto Univ. )*, *K. Yabana ( Univ. of Tsukuba )*, *I. Hamamoto ( Lund Univ. )*, *K. Imai ( Kyoto Univ. )*, *T. Noro ( Kyushu Univ. )*, *H. Okamura ( RCNP )*, *H. Miyatake ( KEK )*, *H. Sakai ( Univ. of Tokyo )*

**ML-PAC** : *R. F. Kiefl ( UBC, the chair )*, *G. A. Beer ( Univ. of Victoria )*, *S. Ikeda ( KEK )*, *M. Iwasaki ( RIKEN )*, *R. Kato ( RIKEN )*, *K. Nagamine ( UC, Riverside )*, *N. Nishida ( Tokyo Tech. )*, *K. Nishiyama ( KEK )*, *F. Pratt ( RAL )*, *H. Takagi ( RIKEN )*, *J. Zmeskal ( Stefan Meyer Inst. )*, *F. Hanaoka ( Gakushuin Univ. )*, *T. Kameya ( Tohoku Univ. )*, *K. Komaki ( Univ. of Tokyo )*, *A. Shionohara ( Osaka Univ. )*

## References

- 1) <http://www.nishina.riken.jp/UsersGuide/NP-PAC>
- 2) <http://www.nishina.riken.jp/UsersGuide/ML-PAC/>

	3rd (Feb.18-19, 2008)				4th (Nov. 20-21, 2008)			
	Proposals		Days		Proposals		Days	
	requested	approved	Requested	approved	requested	approved	requested	approved
GARIS	0	0	0	0	0	0	0	0
CRIB	5	5	39	35.5	4	3	35	16
RIPS	6	5	53.5	29.5	2	2	19	19
BigRIPS/ZD /SHARAQ	7	6	70.7	44	6	4	58	30
TOTAL	18	16	163.2	109	12	9	112	65

Table 1. Statistics of the NP-PAC meetings held this year.

	3rd (March.27-28, 2008)				4th (Jan. 13-14, 2009)			
	Proposals		Days		Proposals		Days	
	requested	approved	Requested	approved	requested	approved	requested	approved
RAL	16	16	80	56	18	16	118	62
RIBF	3	3	30.5	25	3	3	43.5	25
TOTAL	19	19	110.5	81	21	19	161.5	87

Table 2. Statistics of the ML-PAC meetings held this year.

## RILAC operation

Eiji Ikezawa, Ohki Tomonori,\* Kase Masayuki, Takahide Nakagawa, Naruhiko Sakamoto,  
 Hiroki Okuno, Nobuhisa Fukunishi, Masaki Fujimaki, Makoto Nagase, Tadashi Kageyama, Shigeru Yokouchi,  
 Misaki Kobayashi-Komiyama, Masanori Kidera, Yoshihide Higurashi, Tamaki Watanabe, Kazunari Yamada,  
 Takeshi Maie, Hiroo Hasebe, Hironori Kuboki, Kenji Suda, Yutaka Watanabe, Toshimitsu Aihara,\*  
 Hiromoto Yamauchi,\* Akito Uchiyama,\* Kazuyuki Oyamada,\* Masashi Tamura,\*  
 Akira Goto, Osamu Kamigaito, and Yasushige Yano

\* SHI Accelerator Service Ltd.

Throughout this reporting period, RILAC has been in steady operation and has supplied various ion beams for various experiments and beam commissioning. Table 1 shows some statistics for RILAC operation from January 1 through December 31, 2008. The beam service time of RILAC accounted for 88% of the operation time of RILAC. The percentages of injection into RRC and the RILAC standalone were 43% and 57% of the total RILAC beam service time, respectively.

For beam commissioning and experiments of the RI Beam Factory (RIBF), 0.67 MeV/nucleon  $^{238}\text{U}$ , 2.68 MeV/nucleon  $^{86}\text{Kr}$ , and 2.68 MeV/nucleon  $^{48}\text{Ca}$  ion beams accelerated by RILAC were injected intensively into the

Table 1. Statistics for RILAC operation from January 1 through December 31, 2008.

Operation time of RILAC	4578.0 hr
Beam service time of RILAC	4025.0 hr
Mechanical trouble	72.5 hr
Beam service time of RILAC standalone	2312.5 hr
Beam transport to RRC	1712.5 hr

Table 2. Beam service time of RILAC standalone allotted to each beam course in the No. 1 target room of RILAC in 2008.

Beam course	Total time (hr)	%
e2	101.0	4.4
e3	2210.5	95.6
e4	1.0	0.0
Total	2312.5	100.0

RIKEN Ring Cyclotron (RRC) 6 times in total from April through December 2008.

Table 2 shows a summary of the beam service time of the RILAC standalone allotted to each beam course (e2, e3, and e4) in the No. 1 target room of RILAC in 2008. This year, the e2 and e3 beam courses were used for the study of accelerator mass spectrometry and for research experiments on the heaviest elements, respectively.

Research experiments on the heaviest elements have been carried out since 2002. This year, the research experiments were carried out for 86 days from January through April, 25 days in June, 9 days in September, and 3 days in December.

Table 3 shows statistics for the operation times of an 18 GHz ECR ion source (18G-ECRIS) and a superconducting

Table 3. Operation statistics for two ion sources (18G-ECRIS and SC-ECRIS) in 2008. These include preliminary work time. Operation times using SC-ECRIS are indicated in parentheses.

Ion	Mass	Charge state	Total time (hr)
O	18	5	164.0 ( 0.0 )
Ne	22	5	223.5 ( 0.0 )
Na	23	5, 7	289.0 ( 0.0 )
Ar	40	11	42.0 ( 0.0 )
Ca	48	10	919.0 ( 0.0 )
Fe	58	13	371.0 ( 0.0 )
Zn	70	16	2044.5 ( 0.0 )
Kr	86	18	147.5 ( 0.0 )
Xe	136	20	223.5 ( 0.0 )
Os	188	24	80.5 ( 0.0 )
U	238	35	1650.0 ( 0.0 )
Total			6154.5 ( 0.0 )

ECR ion source (SC-ECRIS) in 2008. The ion beams of 11 elements were used in various experiments, beam acceleration tests, and beam commissioning.

We carried out the following improvements and overhauls during this reporting period.

- 1) The beam transport line between the 18G-ECRIS and the analyzing magnet was modified.
- 2) Flow switches for the lower-limit detection in the No. 2 rf power amplifier were replaced with new ones.
- 3) In the rf system for the No. 2 rf power amplifier, an auto gain controller and a pickup detecting the rf signal of the cavity was improved.
- 4) Automatic voltage regulators for all low level systems of the rf power amplifier were installed.
- 5) Plate power supplies at the final stages of the rf systems were subjected to annual inspection.
- 6) Two turbomolecular pumps of the FC-RFQ cavity and the No.1 RILAC cavity were replaced with cryogenic pumps. A turbomolecular pump was installed additionally at the beam transport line between the FC-RFQ cavity and the No.1 RILAC cavity. The other vacuum pumps were subjected to annual inspection.
- 7) Electron suppressers of the faraday cup at the beam transport line between the RILAC cavities were improved.
- 8) All water pumps of the water cooling system were subjected to a simple inspection.
- 9) The power supplies for dipole magnets (DMe1, DMe3, DMe4, and DMe5) will be replaced with new ones, because they were worn out from many years of operation. Each new magnet power supply is of the switching type and has a network IO (NIO) interface.

We experienced the following mechanical problems during this reporting period.

- 1) A cavity of the FC-RFQ was splashed with water due to a small hole in the cooling pipe of the outer wall of the cavity, and we repaired the part.
- 2) In the rf power amplifier system of the No.1 RILAC, power supplies for the filament of the final vacuum tube and for the plate of the driving vacuum tube had problems, and we replaced them with spare ones.
- 3) In the rf power amplifier system of the No.5 RILAC, a wide band amplifier and a driving vacuum tube had problems, and we replaced them with spare ones.
- 4) In the rf power amplifier systems of the CSM-A3 and the CSM-A4, power supplies for the plate of the final vacuum tube had problems, and we repaired them.
- 5) In the rf power amplifier system of the CSM-A5, a power supply for the control grid of the final vacuum tube had a problem, and we replaced it with spare one.
- 6) A magnet power supply of the miller-coil for the

18G-ECRIS was splashed with water due to a leak of a cooling pipe at an upper floor, and we repaired it.

- 7) A hard disk drive of the file server for the EPICS crashed, and another server system was used as a substitute for it. Later, all hard disk drives for the EPICS were replaced with new ones.

For the RI Beam Factory project, a high voltage terminal of the Cockcroft-Walton injector was remodeled and a superconducting coil system for the 28 GHz ECR ion source was installed on it. Thus, an 8 GHz ECR ion source (NEOMAFIOS), which has been used at the Cockcroft-Walton injector for many years, was removed. The beam transport line of the Cockcroft-Walton injector will be installed in parallel with the existing injection line of the FC-RFQ linac with two ECR ion sources.

## AVF operation

M. Kase, T. Kageyama, N. Tsukiori<sup>\*2</sup>, Y. Ohshiro<sup>\*1</sup>, N. Fukunishi, T. Nakagawa, H. Okuno, N. Sakamoto, M. Fujimaki, M. Kidera, M. Kobayashi-Komiyama, Y. Higurashi, M. Nagase, S. Yokouchi, K. Yamada, H. Hasebe, K. Suda, H. Kuboki, T. Maie, K. Kobayashi<sup>\*2</sup>, M. Nishida<sup>\*2</sup>, Y. Kotaka<sup>\*2</sup>, S. Fukuzawa<sup>\*2</sup>, T. Nakamura<sup>\*2</sup>, R. Koyama<sup>\*2</sup>, K. Yadomi<sup>\*2</sup>, S. Ishikawa<sup>\*2</sup>, Makoto Hamanaka<sup>\*2</sup>, Kazuo Miyake<sup>\*2</sup>, Akira Goto, Osamu Kamigaito, and Yasushige Yano

<sup>\*1</sup> CNS: Center of Nuclear Study, Graduate School of Science, the University of Tokyo

<sup>\*2</sup> SHI Accelerator Service Ltd.

Table 1 shows the operation statistics of the RIKEN K70-MeV AVF cyclotron (hereafter denoted as AVF) in 2008 together with those in the preceding years. The total operation time in 2008 was almost the same as those in 2006 and 2007. The operation of AVF as the injector to RRC (AVF-RRC) has been at low level since 2006 because the RRC was frequently injected by RILAC for RIBF commissioning and experiments. The total operation time of 2008 in the AVF stand-alone increased by 8% compared with that in 2007 but did not reach the level of 2006.

About 60% of the total AVF operation time in 2008 was dedicated to CRIB experiments managed by CNS. Eleven experiments were carried out at the CRIB. Two kinds of solid material ion beams, Si and Li, were produced in the Hyper ECR ion source and delivered to the CRIB.

It is now the 7th year since the educational physics experiment for university students commenced based on the RIKEN-CNS collaboration agreement. Four sets of one-day experiments on the elastic scattering using a 6MeV/u  $\alpha$ -beam were performed in Autumn at

the vacuum chamber on the way to the CRIB.

The E7b beam line which is for general purposes was used six times in 2008. Four of them were for the experiments on the electrochemistry of seaborgium using boron, oxygen and neon beams on a <sup>248</sup>Cm target. Since 2008, a new category of beam time for the detector-development was allocated officially for the first time. Two test beam times for detector development were carried out in C03 and E7b.

The C03 target station was used six times for RI productions for charged distribution, which had been routinely performed since late 2007. Radio-nuclides of <sup>65</sup>Zn and <sup>109</sup>Cd are produced using a 14MeV proton beam and delivered to outside RIKEN via Japan Radioisotope Association. The experiments to study  $\alpha$ -fine structure of lawrencium isotopes were also performed at C03 using nitrogen beams on a <sup>248</sup>Cm target twice in November 2008.

In November, a problem related to the pumping of cooling water for ion source caused the cancellation of a scheduled experiment. This was eventually compensated in December.

Table 1. Statistical data of AVF operation in 2006 – 2008.

Year	2006	2007	2008
<b>Total operation time</b>	<b>3963 hr</b>	<b>3669 hr</b>	<b>3648 hr</b>
Beam tuning	853 hr (22 %)	767 hr (21 %)	686 hr (19 %)
Injection to RRC	1051 hr (27 %)	1235 hr (34 %)	1165 hr (32 %)
AVF stand-alone	2059 hr (52 %)	1667 hr (45 %)	1797 hr (49 %)
<b>Beam course (AVF stand-alone)</b>			
E7a (CRIB)	1275 hr (62 %)	1289 hr (77 %)	1119 hr (62 %)
E7b	257 hr (12 %)	0 hr (0 %)	228 hr (13 %)
C03	527 hr (26 %)	378 hr (23 %)	450 hr (25 %)

Some of the contact fingers of No.1 rf resonator were burnt due to trouble in the driving part of the air cylinders pressing on the coaxial part of the resonator. During the Summer overhaul period, the levels of the two rf dee electrodes were re-adjusted using a special

jig, since over the years they had sunk down from the median plane by 4 mm at the maximum over a long period of time.

Beam studies were performed on a few ion beams. First, the acceleration test for 14 MeV protons was

carried out aiming at obtaining higher intensities to meet the requirement for RI production. By precisely tuning the injection and extraction systems, an intensity of 30  $\mu\text{A}$  became available. Next the acceleration tests to increase the attainable maximum energies of  $^{16}\text{O}^{7+}$  and  $^6\text{Li}^{3+}$  ions were carried out. The maximum energies of these ions had been limited by the available dee voltages, which are lower than the required ones in correspondingly high frequencies. Recent simulations, however, showed that these energies could be increased even with these available voltages by adjusting the injection beam phase and the trim coils currents in the central region to enable a beam to clear the channel immediately after the exit of the inflector. In these tests, the maximum energies of  $^{16}\text{O}^{7+}$  and  $^6\text{Li}^{3+}$  ions were actually increased from 10 to 11 and from 9.5 to 11.2 MeV/nucleon

A new hot lab has quickly become necessary when the RI material produced at the C03 target station is treated chemically because the previous hot lab in the

basement of the Nishina Building was far too busy for the new RI distribution, for the preparation of uranium material in the ion source as well as for the ordinary radiochemical research. Taking into account of the convenience of the shortest distance of RI transportation, the site right above the C03 with a direct distance of 6 m in the polarized ion-source room was selected as the location of the new hot lab. In order to make the space for new hot lab, the previous 10GHz ECR ion source was replaced by the super-conducting ECR ion source that is more powerful and compact. The new ion source which belongs to CNS was installed in the Summer of 2008 after the 10 GHz ECR ion source which had been used for twenty years, was handed over to Tohoku University in June 2008. During the conversion of the ion sources, the Hyper ECR was the only ion source for AVF. Due to the shortage in preparation time, it failed to deliver enough intensities for the  $^{28}\text{Si}$  and  $^{58}\text{Ni}$  beam.

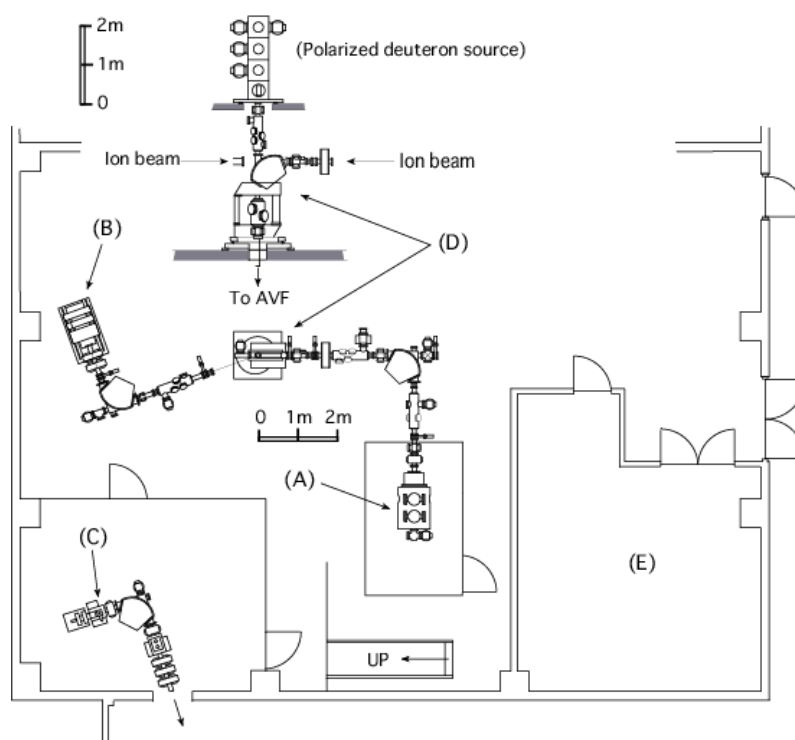


Fig. 1. The new layout of the polarized-ion-source room. The 14GHz super-conducting ECR ion source (A) was installed in place of the old 10GHz ECR ion source. A new hot lab (E) is just above of the C03 target station. (B) is Hyper-ECR ion source and (D) is the rotating magnet for switching the two ECR ion

sources. The polarized deuteron source, which is on second floor and is not shown in the figure, is same as before and is now ready for supply the 250 MeV polarized deuteron in the spring of 2009. (C) is the CAPRIS (ECR ion source) which is used for the atomic physics reserches

## Charged Distribution of Radioisotopes Produced at AVF Cyclotron

T. Kambara, H. Haba, Y. Ezaki, K. Takahashi, and H. Miyamoto

RIKEN Nishina center started fee-based distribution of radioisotopes (RI's) in order to contribute to the general public in Japan through accelerator technologies.

RIKEN has a long history of production and application of RI's at its cyclotrons since the first cyclotron was built in 1937. At the present AVF cyclotron, 19 nuclides with relatively long lifetime have been produced and used for experiments.<sup>1)</sup> Based on its historical background and accumulated know-how on RI production, RIKEN Nishina Center has started fee-based distribution of two nuclides,  $^{65}\text{Zn}$  ( $T_{1/2} = 244$  days) and  $^{109}\text{Cd}$  ( $T_{1/2} = 463$  days), to the general public. These nuclides were previously supplied by private companies but recently they terminated the supply, although there is still demand.

Distribution is carried out in collaboration with the Japan Radioisotope Association<sup>2)</sup> (JRIA), an organization of RI users and research workers which maintains a complete system from supply to disposal of RI's in Japan. Transactions are based on a Material Transfer Agreement between JRIA and RIKEN which went into effect in October 2007. Requests for RI's can be sent from inside of Japan through JRIA (FAX 03-5395-8055, E-mail: gyomu1@jrias.or.jp). The chemical form can be selected from solutions of hydrochloric acid, acetic acid, nitric acid or isotonic sodium chloride, between 0.1 mL and 3 mL. Details are found in the on-line ordering system J-RAM<sup>3)</sup> of JRIA. Normally the RI's are distributed 10-16 days after the acceptance of the order. In 2008, we accepted 6 requests for  $^{109}\text{Cd}$  and distributed total amount of 33 MBq, and 7 requests for  $^{65}\text{Zn}$  and distributed 34.7 MBq.

The nuclides are produced at a beam line of the AVF cyclotron dedicated to RI production,  $^{65}\text{Zn}$  is produced by the reaction  $^{65}\text{Cu}(p,n)$  with a metallic copper target and  $^{109}\text{Cd}$  by the reaction  $^{109}\text{Ag}(p,n)$  with a silver target. The beam energy from the AVF cyclotron is 14 MeV and intensity is about  $15 \mu\text{A}$ . The target is a stack of two disks with diameter of 10 mm and thickness of 0.125 mm each, purity of 99.99 % and natural isotopic composition. The target is cooled by water and He gas during irradiation which lasts about 2 days. After the irradiation,  $^{65}\text{Zn}$  is separated by an ion-exchange method and  $^{109}\text{Cd}$  by the AgCl precipitation and ion-exchange method.

Examples of the quantity and quality of the nuclides of our RI's are as follows: In the case of  $^{65}\text{Zn}$ , an amount of 73 MBq was produced in 41 hours of irradiation and 99 % of it was separated by the chemical processing, and in case of  $^{109}\text{Cd}$ , an amount of 16 MBq was produced in 36 hours of irradiation and the

chemical yield was 74 %. The impurities as well as the specific activities of the purified RI's were evaluated using ICP-MS. As an example, the specific activities of  $^{65}\text{Zn}$  and  $^{109}\text{Cd}$  were 410 and 340 kBq/ng, respectively.

The next nuclide candidates of fee-based distribution are  $^{75}\text{Se}$  ( $T_{1/2} = 120$  days) and  $^{88}\text{Y}$  ( $T_{1/2} = 107$  days) and the production and separation techniques are being developed.

We are also studying the production and application of short-lived RI's with a gas-jet transport system.<sup>4)</sup> The target chamber of the gas jet system is installed in front of the target for the production of  $^{65}\text{Zn}$  and  $^{109}\text{Cd}$ , so the long- and short-lived RI's are produced in parallel with the same beam.

### References

- 1) H. Haba and S. Enomoto: RIKEN Accel. Prog. Rep. **38**, 105 (2005).
- 2) <http://www.jrias.or.jp/index.cfm/1,html> (Japanese), <http://www.jrias.or.jp/index.cfm/11,html> (English).
- 3) <https://www.j-ram.net/jram/DispatchTopPage.do> (in Japanese).
- 4) T. Takabe, Y. Kitamoto, D. Saika, K. Matsuo, Y. Tashiro, T. Yoshimura, H. Haba, D. Kaji, and A. Shinohara: RIKEN Accel. Prog. Rep. **39**, 113 (2006).

## The operations of the RIBF ring cyclotrons

M. Kase, N. Fukunishi, E. Ikezawa, T. Nakagawa, H. Okuno, N. Sakamoto, M. Fujimaki, H. Hasebe, Y. Higurashi, T. Kageyama, M. Kidera, M. Kobayashi-Komiyama, H. Kuboki, K. Kumagai, T. Maie, M. Nagase, J. Ohnishi, Y. Ohshiro<sup>\*1</sup>, K. Suda, T. Watanabe, K. Yamada, S. Yokouchi, T. Ohki<sup>\*2</sup>, N. Tsukiori<sup>\*2</sup>, T. Aihara<sup>\*2</sup>, S. Fukuzawa<sup>\*2</sup>, M. Hamanaka<sup>\*2</sup>, S. Ishikawa<sup>\*2</sup>, K. Kobayashi<sup>\*2</sup>, Y. Kotaka<sup>\*2</sup>, R. Koyama<sup>\*2</sup>, K. Miyake<sup>\*2</sup>, T. Nakamura<sup>\*2</sup>, M. Nishida<sup>\*2</sup>, K. Oyamada<sup>\*2</sup>, M. Tamura<sup>\*2</sup>, A. Uchiyama<sup>\*2</sup>, K. Yadomi<sup>\*2</sup>, H. Yamauchi<sup>\*2</sup>,  
A. Goto, O. Kamigaito, and Y. Yano

<sup>\*1</sup> Center for Nuclear Study, the University of Tokyo

<sup>\*2</sup> SHI Accelerator Service Ltd.

The RIBF accelerator complex consists of four ring cyclotrons (RRC, fRC, IRC, and SRC) together with two injectors (RILAC and AVF). Although there are many acceleration modes, the RRC always works as the first booster ring cyclotron in every acceleration mode. Figure 1 shows how every ring cyclotron operated in 2008 on a basis of RRC Yearly operation-time, 3961 hr in 2008. About half of them were spent for the RIBF accelerations; 30% for the fixed-frequency acceleration mode of a <sup>238</sup>U beam with an energy of 345MeV/u and 20% for the variable-frequency acceleration mode of a <sup>48</sup>Ca beam with the same energy.

In early 2008, the BigRIPS experiments using the <sup>238</sup>U beam with 345MeV/u had been scheduled in spring. However trouble with oil contamination was found in February inside the BigRIPS and SRC cryogenic systems one after another and after following investigations, it turned out that the problem was so serious that it will take

several months to sweep all the problems completely. Then it was decided in April that the BigRIPS experiments were shifted in autumn.

During the improvement of the SRC cryogenic system, machine studies were performed for the <sup>238</sup>U and <sup>48</sup>Ca beam accelerations without the SRC, focusing on checking of stripper foils, improving beam monitors, conditioning many rf cavities, establishing precise isochronous magnetic field in each ring cyclotron, stabilizing all the parameters of the accelerators including the injector RILAC etc.

The experiments of BigRIPS were reshcheduled and carried out in November for <sup>238</sup>U beam and in December for <sup>48</sup>Ca. The beam parameters during the experiments are summarized in Table 1. In 2008, the acceleration parameters were dedicated for one frequency of 36.5 MHz in the IRC and the SRC, giving a final energy of 345MeV/u

Table 1 Beam parameters of RIBF experiments in 2008

Beam	Energy (MeV/u)	Period (days)	Beam intensity (pnA)	Supply eff. (%)
<sup>238</sup> U	345	18.3	0.1 - 0.4	75
<sup>48</sup> Ca	345	11.5	100 - 170	59

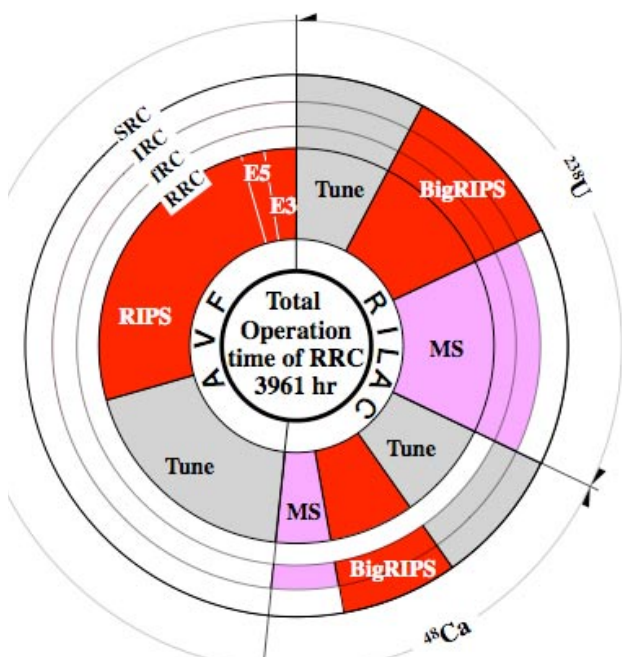


Fig. 1. The operation statistic in 2008 of every ring cyclotrons in the RIBF on basis of the RRC. The total operation time of RRC was 3961 hr, corresponding to 360 deg of the circle graph. “Tune” is the beam tuning for experiments, “MS” the machine study. The dark portions with white letters are the experiments, BigRIPS in RIBF and RIPS, E5, E3 in the Nishina Building.

only.

In the BigRIPS experiments, the  $^{238}\text{U}$  beam was used for the Zero Degree Spectrometer commissioning and also for the new isotope search, resulting in a discovery of more than twenty new isotopes. The  $^{48}\text{Ca}$  beam was used for the research for the nuclear structure and the gamma spectrometry. During the  $^{238}\text{U}$  beam time, the beam intensity became larger and larger and finally reached to 0.4pnA. The operation became gradually stable and in the last few days of the experiment, the beam stayed on the BigRIPS target more than 90% of the available time. On the other hands, during the  $^{48}\text{Ca}$  beam time, several problems occurred and frequently interrupted the experiments, although the beam intensity reached a value (170pnA) more than expected. The cooling system of the beam monitor was paralyzed twice, probably due to a high irradiation of fast neutrons on its flow sensors. The plate power supply to one of the rf amplifier for the SRC resonator, RES1 was turned off due to an error of interlock circuits. One of the SRC resonators, RES3, had a problem inside and became unusable during the second half of the beam time. A wide band amplifier for a flat-top system of SRC had a problem in its output directional coupler. The total interruption time amounted to more than eighty

hours.

About half of the RRC operation time was used on ordinary experiments in the Nishina Building as listed in Table 2. A total of 1000 hr was spent on six kinds of RIPS experiments, including the development of ion-trapping technology, which was performed four times. The experiments for the biological research were still so active that a total of 89 hr were spent on them by using the three kinds of beams  $^{12}\text{C}$ ,  $^{40}\text{Ar}$  and  $^{56}\text{Fe}$  ions and repeating 17 times on a regular basis in the E5 target room. In the E3 target room, the following experiments were carried out; the RI productions for multi-tracer, the simulation of single event in electronic devices against irradiation of cosmic ray, and the calibration of the radiation detector for cosmic ray.

In August, one of the RIPS experiments using  $^{28}\text{Si}$  beam was interrupted for a half day due to an instantaneous power failure caused by a thunderbolt hitting a power facility near by. In the RIPS experiments using a beam of solid ions,  $^{28}\text{Si}$  and  $^{58}\text{Ni}$ , the enough beam intensities could not be supplied under a lack of preparation time of ion source due to an exchange of AVF ECR sources.

Table2 The experiments using the RRC beams in 2008

Beam Course	No. of allocation	Beam & Energy	Total Hours	Proportion
E6(RIPS)	12	$^{13}\text{C}$ -135MeV/u $^{28}\text{Si}$ -135MeV/u $^{36}\text{Ar}$ -115MeV/u $^{40}\text{Ca}$ -90MeV/u $^{58}\text{Ni}$ -90MeV/u	987	85%
E5b	17	$^{12}\text{C}$ -135MeV/u $^{20}\text{Ne}$ -135MeV/u $^{40}\text{Ar}$ -95MeV/u $^{56}\text{Fe}$ -90MeV/u	81	7%
E3b	3	$^{14}\text{N}$ -135MeV/u $^{40}\text{Ar}$ -95MeV/u $^{84}\text{Kr}$ -70MeV/u	97	8%
Total			1165	100%

## Status of RIBF control system and beam interlock system

M. Kobayashi-Komiyama, A. Uchiyama,<sup>\*1</sup> T. Nakamura,<sup>\*1</sup> M. Fujimaki, J. Odagiri,<sup>\*2</sup> N. Yamada, H. Yamauchi,<sup>\*1</sup>  
M. Hamanaka,<sup>\*1</sup> N. Fukunishi and M. Kase

We report three developments of the RIBF control system. The first is development of useful software used in the recent fine tuning of the cyclotron complex. The second is performance testing of our beam interlock system (BIS). The third is introduction of a new EPICS-embedded system on F3RP61-2L. Our work is crucial for providing high power beams for RI-beam production at BigRIPS.

New software was developed to visualize data measured by differential probes installed in our cyclotrons. The radial pattern of the accelerating beam in the cyclotron is obtained by measuring beam current with a thin electrode called a differential probe. The radial distribution of the beam is strongly affected by cyclotron parameters such as the RF phase of flat-top cavities. The new radial-probe software has the following functions:

- Zooming in or out of the graph on both the X and Y

axes.

- Automatically indicating the numerical coordinates of the mouse pointer on the graph. This function is used to measure turn separation.
- Saving raw data in a numerical table format.
- Leaving the measured data on the graph in shadow. We use this function to compare the most recent data with previous or a stored data.
- Selecting whether to display or hide the data from each measurement finger of the radial probe.

Fig. 1 shows data measured by the IRC-MDP2 during a  $^{48}\text{Ca}$  experiment. Thanks to the new functions mentioned above, precise tuning of the RF phases and voltages of accelerating and one flattop cavities was done using the new radial probe graph software. This worked effectively to reduce beam losses in the cyclotrons during beam tuning.

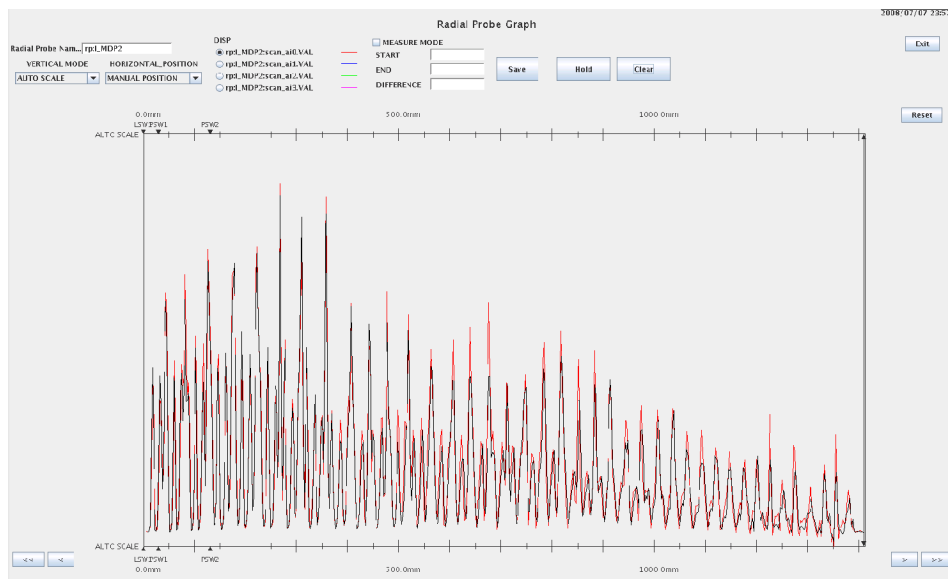


Fig. 1. Beam pattern in the IRC measured by IRC-MDP2 with reference data.

In addition, we created many new GUIs to support cyclotron operators. For example, we prepared a bar-graph type GUI to simultaneously show beam intensities lost at the selected baffle slits placed at the entrance or exit of magnetic or electric channels of cyclotrons. It was very helpful to know positions where beam losses took place. The information on beam intensity is also transferred to the BIS, whose purpose is to protect cyclotrons from serious beam losses.

The BIS is a beam interlock system to protect various devices in accelerators and their beam transport lines from irradiation by excess beam.<sup>1)</sup> It turns on a beam chopper placed at the exit of an ion source when the system senses a safety alarm signal from devices. To definitely ensure that a beam is shut off, the system simultaneously sends a signal to insert a Faraday cup located upstream of the sensed device. In the current state, many alarm signals are connected into the BIS: breakdown of RF control, errors of magnet power supplies, vacuum systems, temperature monitor system of SRC, doors of each experimental cave,

<sup>\*1</sup> SHI Accelerator Service Ltd

<sup>\*2</sup> High Energy Accelerator Research Organization (KEK)

and so on. In addition to digital alarm signals, the BIS can stop a beam by setting a threshold for analog data measured by beam baffle slits in cyclotrons. Three BIS were installed to the RILAC area, the RRC and fRC area, and the IRC and SRC area. The BIS is a system based on PLCs. Each BIS has 5 PLC stations except for RILAC one (3 stations). Optical fiber cables connect among them and 5 PLC stations constitute one loop structure. Each safety alarm signal and output signal is connected into the I/O module in each station. The BIS was introduced into the RIBF in 2005. The BIS debugging processes have been conducted in the three subsequent years. Recently the beam power from SRC was greatly increased, for example to 3 kW for a  $^{48}\text{Ca}$  beam. It is essential for each BIS to properly carry out its function of preventing destruction of cyclotrons by high beam power. This year we improved the circuit of a beam chopper used in BIS. During the experiments, all BIS worked perfectly, i.e.; the beam chopper and Faraday cups stopped the beam without exception after receiving alarm signals or signals caused by threshold-over beam losses. This implies that BIS is now finished. The remaining problem is that the programmed logic for the action of the beam chopper is not correct. The program for the action of the beam chopper will have to be improved in 2009.

Last are new developments this year in our EPICS-based control system. Many PLCs have been adopted in the RIBF control system. They implement various control logics on themselves and control devices such as radial probes of cyclotrons, vacuum systems of cyclotrons, and so on. Most are controlled or monitored in the EPICS-based control system. In order to control PLCs on EPICS, PLCs need to be connected with EPICS Input/Output Controllers (IOCs) through Ethernet connections to convert the communication protocols (EPICS Channel Access protocol and the proprietary communication protocol of each company's PLC). If it is possible to run EPICS IOC programs on the PLC CPUs themselves, that is a more cost-effective and convenient solution for us. The reason is that this eliminates the need to install a PC for running IOC programs, and was can just create control programs with EPICS sequencers only instead of creating ladder programs for PLCs and EPICS sequencers for IOC. At the beginning of this year, Yokogawa Electric Corporation developed a new CPU module running Linux which can function with a base module and I/O modules of FA-M3 PLC, F3RP61-2L.<sup>2)</sup> We started to develop embedded EPICS on F3RP61-2L in collaboration with the KEK control group and successfully complete the development in June.<sup>3)</sup> It is expected that introducing F3RP61-2L will make our control system simpler and easier to maintain. In July, we successfully controlled a test switch box with some push buttons and indicators using F3RP61-2L. Furthermore, we recently succeeded in setting and reading an analog value to a test system. Fig. 2 shows a PLC test system with a F3RP61-2L. In J-PARC (KEK), F3RP61-2Ls have been used to control power supplies and the motion of septum magnets and beam diagnostic devices in the slow extraction line of the J-PARC Main Ring. Encouraged by the results, we plan to

introduce the embedded EPICS on F3RP61-2L into the following newly installed and current systems:

- Control system of CNS super-conducting ECR ion source.
- Control system of a new super-conducting ECR ion source of RILAC II.
- Control system of the injection buncher, RFQ, and rebuncher of RILAC.
- Control system for motion control of Faraday cups of RILAC.<sup>4)</sup>

We have already made the system for the third system above, and will try to introduce it in February 2009. Furthermore, we have started developing control systems for the first two systems with the aim of using them in early 2009.



Fig. 2. F3RP61-2L (the second from left module) in a test system.

#### References

- 1) M. Komiyama et al.: Proc. 2nd Annu. Meet. Of Particle Accelerator Society of Japan and 30th Linear Accelerator Meet. In Japan, Tosu, 2005-7 (2005), p. 615.
- 2) <http://www.yokogawa.co.jp/rtos/Products/rtos-prdcpu9-ja.htm>
- 3) A. Uchiyama et al.: Proc. PCaPAC08, Ljubljana, Slovenia, 2008-10, p.145.
- 4) M. Komiyama et al.: Proc. 5th Annu. Meet. Of Particle Accelerator Society of Japan and 33rd Linear Accelerator Meet. In Japan, Hiroshima, 2008-8 (2008), p. 376.

## Water Cooling System of Accelerator for RIBF

T. Maie, K. Kusaka, T. Kageyama, E. Ikezawa, Y. Watanabe, H. Okuno and M. Kase

The water cooling system for the RI Beam Factory (RIBF) was newly constructed in 2004. Photographs of the water-pumps and the cooling towers are shown in Fig. 1, Fig. 2, Fig. 3, and Fig. 4. A block diagram of the water cooling system is shown in Fig. 5. There are seven categories as follows ; the No.1 cold-water circuit(CW-1), the No.2 cold-water circuit(CW-2), the No.2 Cooling-tower circuit (CT-2), the No.3 Cooling-tower circuit(CT-3), the No.4 Cooling-tower circuit(CT-4), the Sub-system and the cooling system for the fixed-frequency Ring Cyclotron (fRC).

The precise temperature control function adheres to the fRC Cooling system, supplying the controlled water at  $\pm 0.1$  degree to each main and trim coil.

The system was designed to save energy. In every water-pump in these systems, a highly effective motor with an efficiency of 93.5% is used, as shown in Fig.1, compared to a normal motor with an efficiency of 91%. In addition, the use of low-noise and low-vibration devices together with inverter circuits is also effective.



Fig.1. Photograph of the Water-pump with highly effective motor. ( JIS Standard C4212 )



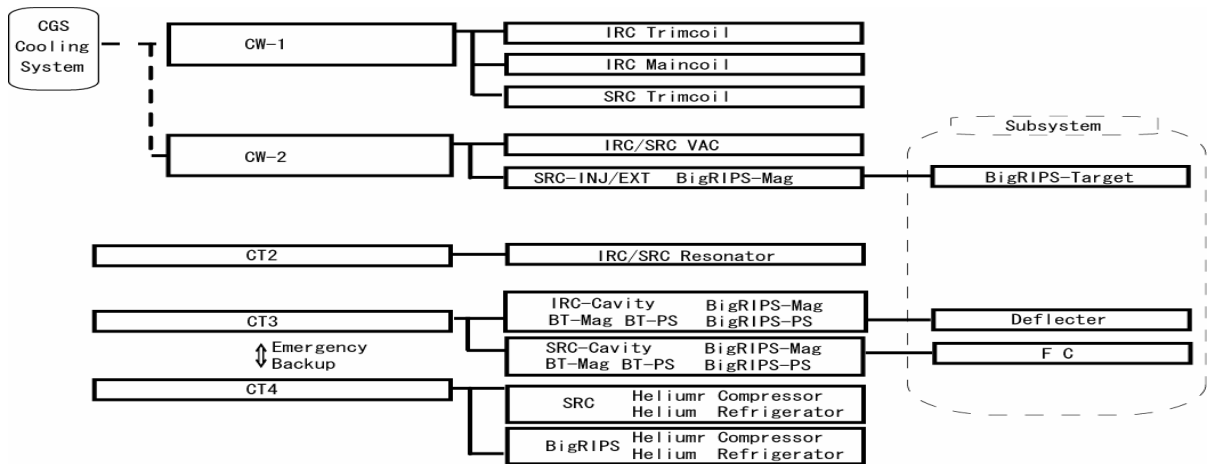
Fig. 2. Photograph of the Cooling Towers on the rooftop.



Fig. 3. Photograph of the Cooling water-pump on the first floor.



Fig.4. The Sub-system cooling pump. (IRC room on the second floor in the basement)



RRC: RIKEN RING Cyclotron, fRC: fixed-frequency Ring Cyclotron,  
 IRC: Intermediate-stage Ring Cyclotron, SRC : Superconducting Ring Cyclotron

Fig. 5. Schematic diagram of the Water-Cooling System of the Accelerator for RIBF

The total operation time of the water-cooling system in fiscal year 2008 was 120 days due to oil-contamination trouble in the SRC and BigRIPS helium refrigerators.

In December, during the beam time, the water pump (P-13) in the sub-system stopped twice due to a failure of its control circuit. It may have been by the high-level radiation of fast neutrons from a beam line. One of the system water-flow sensor which was being irradiated, made an error signal. The sensor will be moved far from the beam line in 2009.

Because the systems CT-2 and CT-3 supply water to

various equipment, there is frequently a lack of water flow in some equipment. Fine adjustment of water-flow division is always an important and hard task when new equipment is installed.

The construction of the cooling system for the new injector (RILAC II) was designed as shown in Fig. 6. The new system will use cold water from CGS system as much as possible.

### Cooling equipment for New injector (RILAC II)

Nishina Building cold water is used in place of a cooling tower.

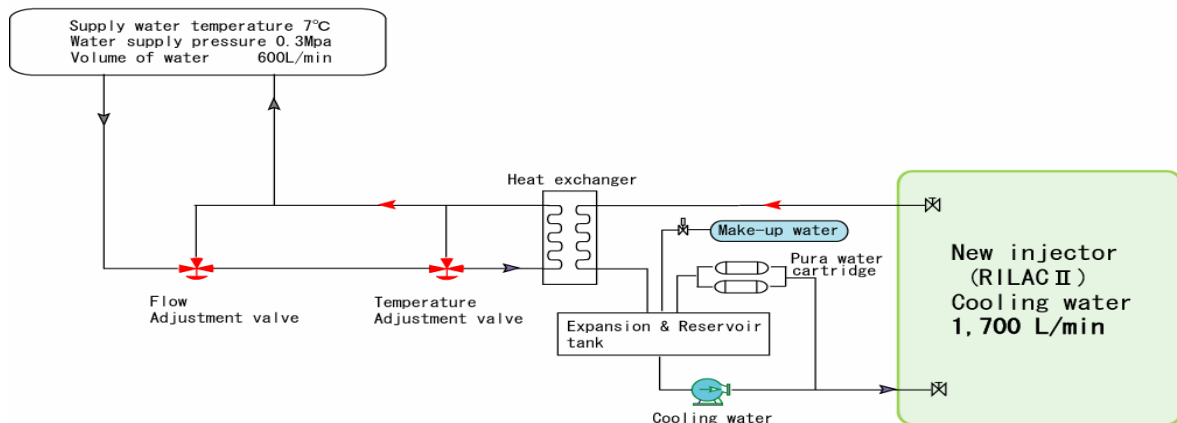


Fig. 6. Schematic diagram of the cooling system for RILAC II

## Radiation Safety Management at RIBF

Y. Uwamino, H. Sakamoto, R. Hirunuma Higurashi, H. Mukai<sup>\*1</sup>, A. Horigome, H. Fukuda, S. Fujita, T. Yamaki, K. Igarashi, K. Nakano and S. Iizuka

Residual radioactivity at the deflector of the AVF cyclotron was measured to be 12.5 mSv/h on December 4, 18 hours after an operation with a 6.2 MeV/u 300 pA <sup>20</sup>Ne beam. We did not have an opportunity to measure the RRC deflector in 2008. Figure 1 shows the variation in the dose rates at these deflectors since 1986. The beam intensity of AVF was increased for the radioisotope production and the dose rate increased again.

The residual radioactivity was measured along the beam lines after almost every experiment. Spots 1–31, marked with solid circles in Fig. 2, are the places where high dose rates were observed. Table 1 shows these dose rates together with the measurement dates, beam conditions and the decay periods following the end of an operation. The maximum dose rate was found to be 5.2 mSv/h at point 29 on the surface of G01 Faraday cup after SRC.

We continuously monitor the radiation in and around the RIBF facility by using neutron and gamma area monitors. The results at the site boundary (No. 1–4 posts) and at the computer room of the Nishina building which is the boundary of the radiation controlled area are shown in Fig. 3. The values are the average dose rates of each day including natural background radiation. No. 1 post is close to the Wako Daiyon Elementary School, No. 2 is in front of the Nishina building, No. 3 is close to Route 254 and No. 4 is close to the BSI Central Building. The computer room is on the ground floor immediately above a bending magnet that guides the beam from the RRC vault to the distribution corridor.

Due to the constant natural gamma radiation from the building structure, the gamma dose rate at the computer room is high and stable, the computer room's neutron dose, however, is low because of the shielding effect of the building against the cosmic neutrons and as a result of it being strongly affected by the accelerator operation.

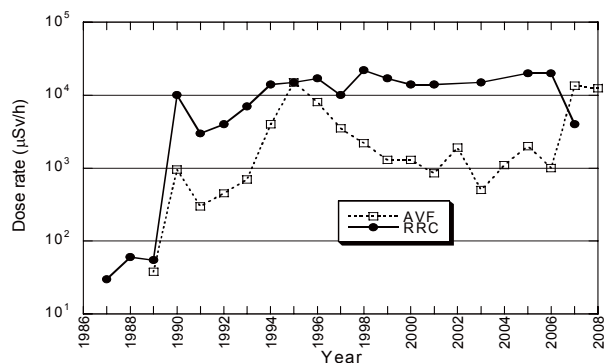


Fig. 1. Dose rate at the deflectors of RRC and AVF since 1986. Dose rates were not measured at RRC in 2002, 2004 and 2008.

No accelerator was operated between August 19 and September 13, and the dose rates at this period were assumed to be natural background. The net accumulated dose, i.e., the dose after the subtraction of background, at the computer room in 2008 was 3.5  $\mu$ Sv which was much lower than the legal limit (5 mSv/y). The annual dose since 1999 is shown in Fig. 4. The value increased until 2005 and decreased after that due to the operation condition of RRC.

The net dose rates at the site boundary are very small, because the influence of the accelerator operation is tiny, owing to the long distances and the thick shields. The net accumulated dose at any point was smaller than the detection limit, which was assumed to be one standard deviation; 8  $\mu$ Sv/y for gammas and 2  $\mu$ Sv/y for neutrons. In any case, the annual dose at the site boundary was much lower than the legal limit (1 mSv/y).

Table 1. Dose rates measured at beam lines in 2008. Points 1-31 indicate measured locations shown in Fig. 2.

Point	Dose rate ( $\mu$ Sv/h)	Date (M/D)	Particle	Energy (MeV/u)	Intensity (pA)	Decay period (h)
1	280	8/14	Si-27	135	6	173
2	1200	8/14	Si-28	135	6	173
3	550	8/14	Si-28	135	6	173
4	45	8/14	Si-28	135	6	173
5	550	6/10	Ca-48	114	68	24
6	42	6/10	Ca-48	114	68	24
7	40	6/10	Ca-48	114	68	24
8	13	6/10	Ca-48	114	68	24
9	18	6/10	Ca-48	114	68	24
10	25	8/14	Si-28	135	6	173
11	18	8/14	Si-28	135	6	173
12	40	8/14	Si-28	135	6	173
13	50	8/14	Si-28	135	6	173
14	40	8/14	Si-28	135	6	173
15	750	8/14	Si-28	135	6	173
16	150	8/14	Si-28	135	6	173
17	40	5/2	U-238	114	2	3
18	18	5/2	U-238	114	2	3
19	27	6/10	Ca-48	114	68	24
20	250	6/13	N-14	135	500	293
21	45	6/13	N-14	135	500	293
22	13	5/2	U-238	114	2	3
23	14	6/10	Ca-48	114	68	24
24	23	6/10	Ca-48	114	68	24
25	12	12/24	Ca-48	345	160	109
26	1300	6/10	Ca-48	114	68	24
27	700	6/10	Ca-48	114	68	24
28	130	12/24	Ca-48	345	160	80
29	5200	12/24	Ca-48	345	160	80
30	200	12/25	Ca-48	345	160	109
31	950	12/25	Ca-48	345	160	109

\*1 Japan Environment Research Corp.

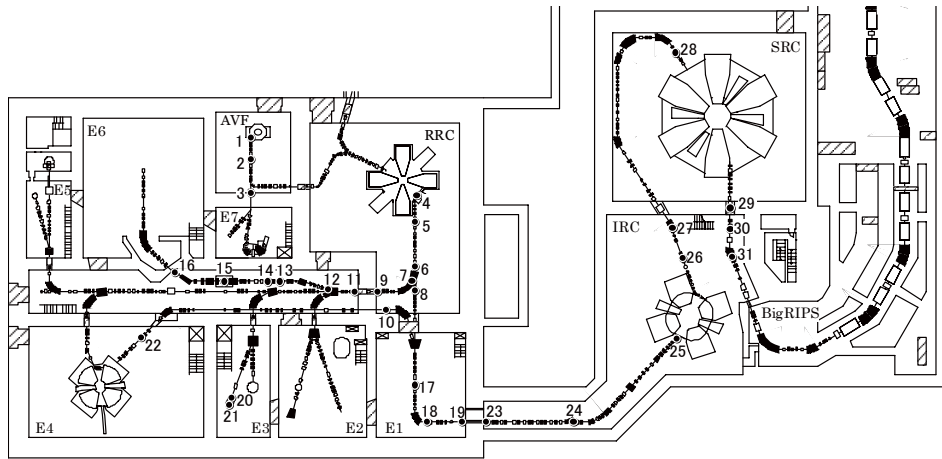


Fig. 2. Layout of beam lines at RIBF. Locations where high residual radioactivity was observed are indicated by solid circles, 1-31.

The water in the closed cooling systems at BigRIPS was sampled after the operation with an intense 345-MeV/u <sup>48</sup>Ca beam in December, 2008, and radionuclide concentrations were measured by using a liquid-scintillation counter and a Ge detector. The results are shown in Table 2. The concentration of the cooling water used at the side-wall beam dump was highest, but the sum total of the ratios of the concentrations to the legal limits for the drain water over all the radionuclides is still much smaller than unity. We will monitor these concentrations, and release the water before they exceed the legal limit.

Radiation surveys in and around the RIBF building were also performed by using hand-held detectors during the accelerator operation with the <sup>48</sup>Ca beam in December, 2008. At the boundary of the radiation controlled area, the highest dose rates of 0.7 μSv/h for neutrons and 0.2 μSv/h

for gammas were observed at the He compressor room on the 1st floor of RIBF accelerator building. In the radiation controlled area, streaming radiations through the air duct from IRC vault caused the highest dose rate of 210 μSv/h for neutrons and 40 μSv/h for gammas at the He refrigerator room on the 1st basement floor. The streaming from SRC vault was found to be as small as 1.5 μSv/h for neutrons and 4 μSv/h for gammas.

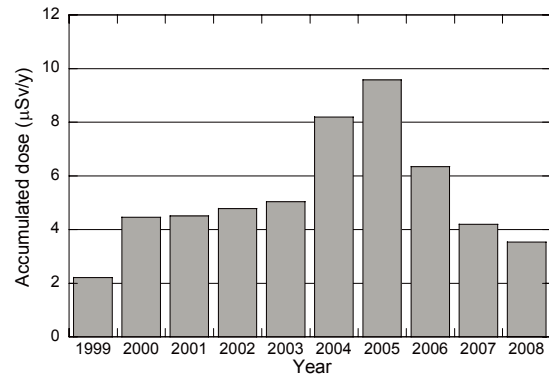


Fig. 4. Accumulated leakage radiations at the computer room of Nishina building since 1999.

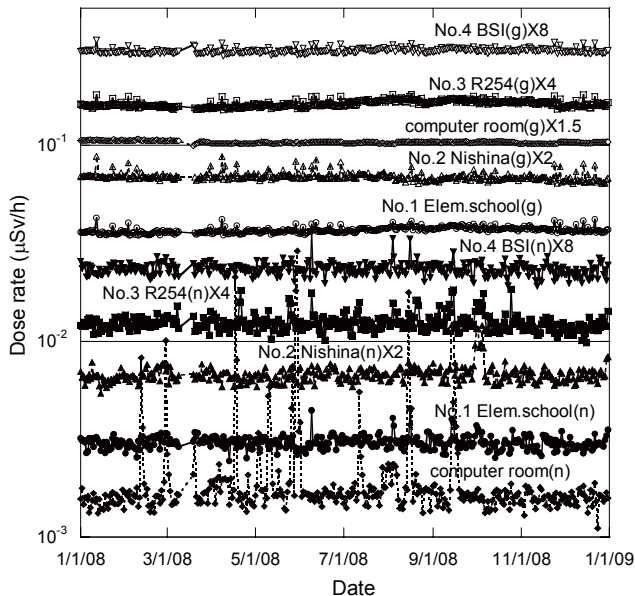


Fig. 3. Daily averaged dose rates in 2008 at the site boundary (No. 1 through No. 4) and at the computer room of the Nishina building. (g) and (n) represent gammas and neutrons, respectively, and “×2”, for example, means the values are multiplied by 2.

Table 2. Radionuclide concentration in cooling water of BigRIPS at January 7, 2009, the legal limits for drain water, and the ratio of the concentration to the limit.

cooling water	nuclide	concentration (Bq/cm <sup>3</sup> )	limit	ratio to limit
F0 target	H-3	- <sup>1)</sup>	60	-
Exit beam dump	H-3	1.7e-1 <sup>2)</sup>	60	2.9e-3
	H-3	3.5e-1	60	5.8e-3
	Be-7	9.5e-1	30	3.2e-2
	Co-57	6.4e-4	4	1.6e-4
	Co-58	3.7e-3	1	3.7e-3
Side-wall beam dump	Mn-52	5.3e-4	0.5	1.1e-3
	Mn-54	5.4e-4	1	5.4e-4
	Mn-56	7.8e-4	3	2.6e-4
	Na-22	5.8e-4	0.3	1.9e-3
	Ca-47	1.5e-3	0.5	2.9e-3
summation				4.8e-2

1) lower than detection limit. 2) read as  $1.7 \times 10^{-1}$

## Radiation field measurement around BigRIPS with a uranium beam

H. Mukai,\*<sup>1</sup> A. Horigome, H. Fukuda, H. Sakamoto, A. Yoshida, K. Yoshida and Y. Uwamino

To investigate the neutron field around BigRIPS, activation reaction rates of C, Al, Au and Bi samples were measured with a 345-MeV/u <sup>238</sup>U<sup>86+</sup> beam in November, 2008. Effective doses due to neutrons and photons were also measured with thermoluminescence dosimeters (TLDs), of which the neutron dosimeter was developed by us. The beam was stopped at the BigRIPS beam dump and maximum intensity was about 0.35 pA. The positions of samples and dosimeters are shown in Fig. 1. The circled numbers 1-9 are numbers of activation samples, and the letters A-G enclosed in squares indicate TLD dosimeters.

The induced radioactivity of samples was measured with Ge detectors, and the reaction rate,  $y$  ( $U^{-1}$  [sample atom]<sup>-1</sup>), was obtained with the following formula.

$$y = N_T \times 86 \times 1.602 \times 10^{-19} \left/ \left( N_S \int_0^T q(t) \times e^{-\lambda(T-t)} dt \right) \right.$$

Where  $N_T$  is the number of radionuclides at the end of irradiation,  $N_S$  is the number of atoms in the sample,  $T$  is the irradiation length,  $q(t)$  is the U beam current in amperes at time,  $t$ , and  $\lambda$  is the decay constant.

The results for the reaction rate,  $y$ , are shown in Table 1. Threshold reactions at positions 3 and 4 were below the detection limit, and the <sup>197</sup>Au(n,γ)<sup>198</sup>Au reaction rates were found to be only  $1.1 \times 10^{-29}$  and  $2.0 \times 10^{-28}$  for positions 3 and 4, respectively. Any activity at position 9 was not observed.

The dose equivalents measured with TLD dosimeters are shown in Table 2. Background radiation is not included in these values. It is difficult to estimate the error in these

values, but it seems to be more than several tens of % in the results for position B and the photon result for position E.

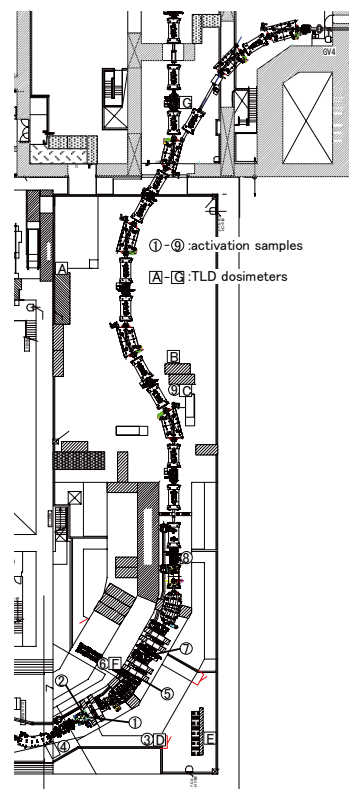


Fig. 1. Positions of samples and dosimeters around BigRIPS.

Table 1. Measured reaction rates per one <sup>238</sup>U<sup>86+</sup> ion per one atom of activation sample.

type of reaction	half life	E <sub>th</sub> (MeV)	position					
			1	2	5	6	7	8
<sup>12</sup> C(n,2nα) <sup>7</sup> Be	53.1d	28.5	6.5e-30 <sup>1)</sup>	<u>8.5e-32</u> <sup>2)</sup>	8.3e-30	- <sup>3)</sup>	-	-
<sup>12</sup> C(n,2n) <sup>11</sup> C	20.3m	20.3	1.7e-29	1.6e-31	1.8e-29	-	<u>2.0e-32</u>	-
<sup>27</sup> Al(n,α) <sup>24</sup> Na	15.0h	3.2	1.1e-29	4.0e-31	1.9e-29	-	<u>1.4e-32</u>	<u>3.3e-33</u>
<sup>197</sup> Au(n,γ) <sup>198</sup> Au	2.69d	-	2.5e-27	2.2e-27	4.6e-27	5.5e-29	1.0e-27	<u>7.3e-31</u>
<sup>197</sup> Au(n,2n) <sup>196</sup> Au	6.18d	8.1	2.5e-28	1.1e-29	3.5e-28	-	-	-
<sup>197</sup> Au(n,4n) <sup>194</sup> Au	1.64d	23.2	9.0e-29	2.5e-30	1.3e-28	-	-	-
<sup>209</sup> Bi(n,4n) <sup>206</sup> Bi	6.24d	22.6	1.2e-28	2.9e-30	1.1e-28	9.2e-33	1.6e-31	2.0e-32
<sup>209</sup> Bi(n,5n) <sup>205</sup> Bi	15.3d	29.6	1.4e-28	2.6e-30	1.3e-28	<u>1.1e-32</u>	1.9e-31	2.2e-32
<sup>209</sup> Bi(n,6n) <sup>204</sup> Bi	11.2h	38.1	7.0e-29	6.8e-31	5.3e-29	-	<u>5.2e-32</u>	2.0e-32
<sup>209</sup> Bi(n,7n) <sup>203</sup> Bi	11.8h	45.4	7.4e-29	5.2e-31	4.0e-29	-	<u>6.8e-32</u>	1.3e-32
<sup>209</sup> Bi(n,8n) <sup>202</sup> Bi	1.72h	54.2	7.5e-29	3.3e-31	4.7e-29	-	9.3e-32	<u>1.3e-32</u>
<sup>209</sup> Bi(n,9n) <sup>201</sup> Bi	1.80h	61.7	3.2e-29	<u>1.9e-31</u>	2.7e-29	-	-	-
<sup>209</sup> Bi(n,10n) <sup>200</sup> Bi	36.4m	70.9	3.0e-29	-	<u>2.3e-29</u>	-	-	-

1) Read as  $6.5 \times 10^{-30}$ . 2) Underline indicates error larger than 10%. 3) Lower than detection limit.

Table 2. Dose equivalent rate (μSv/h) at 1-pnA <sup>238</sup>U<sup>86+</sup> ion beam measured with TLD dosimeters.

type of radiation	position						
	A	B	C	D	E	F	G
neutron	- <sup>1)</sup>	0.080	11	260	1.4	2500	3.8
photon	-	0.56	1.4	30	0.32	160	-

1) Lower than detection limit.

\*<sup>1</sup> Japan Environment Research Corp.

# Operation of Cryogenic System for the Superconducting Ring Cyclotron

H. Okuno, T. Dantsuka, K. Yamada, M. Kase, O. Kamigaito and Y. Yano

2008 was a tough year for operation of the superconducting ring cyclotron (SRC) cryogenic system. Oil contamination of the helium refrigerator from the compressor forced us to stop operation for six months in order to clean up the oil-contaminated He refrigerator and to install two additional oil separators to the existing helium compressor units. A few drops of oil found at the seats of the low temperature valves in the helium refrigerator alerted us of the oil contamination in February. Further investigation of the inside of the refrigerator showed the contamination to be very severe and dispersed over the whole refrigerator. We decided that internal parts (pipes, heat exchangers etc.) should be cleaned with florine225 to remove the oil in the helium refrigerator. Clean-up of the heat exchangers in particular was very tough work. We took them to the clean factory to allow them to wash them in the various angles. Another important task was to increase oil separation capability by adding 2-stage oil separators. Details of the restoration are described in the report by Dantsuka [1].

Restoration of the cryogenic system lasted until the end of August and Saitama prefecture allowed us to produce high pressure helium gas after the test according to the high pressure gas safety regulation on August 28, 2008. We restarted the helium compressor in order to check performances of the oil separation systems where the 2-stage separators were newly installed. Measured data showed that oil contamination was lower than the level which the cold trap monitor can detect (40 ppb) while designed contamination is 20 ppb. Next, we performed stand-alone operation to check cooling capacity. Some filters were installed to block incoming oil impurities. Pressure drops may be

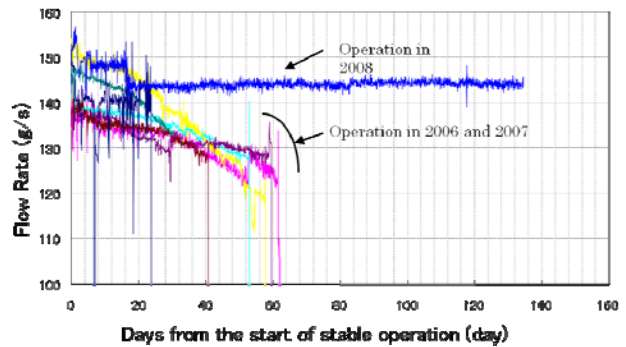


Fig. 2: Flow rate trends in the helium refrigerator.

generated at the filters, causing degradation of cooling power of the helium refrigerator. Measured cooling power was larger than that required for cooling of the SRC superconducting magnets. The two test results mentioned above let us proceed to the next stage of operation of the helium refrigerator in the connection with the superconducting magnets. After purification operation for about 1 week, we started cool-down operation of the superconducting magnets. Fig. 1 shows the cool-down curves with those obtained in the operation of 2005. It took about 22 days to cool-down the superconducting magnets from room temperature to 4.2 K, indicating no degradation of cooling power compared with first cool-down when the refrigerator contained no oil. After the end of cool-down operation, liquid helium was transferred to the

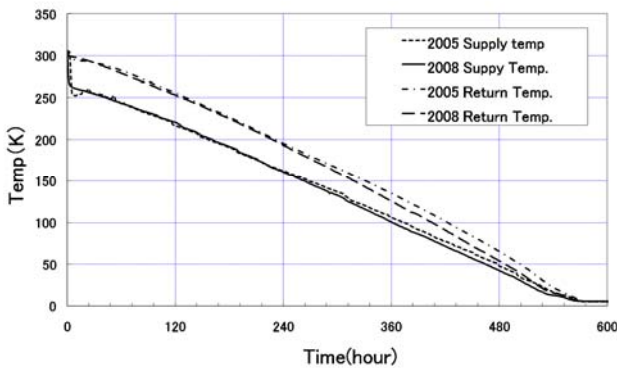


Fig. 1: Cool-down curves of the SRC superconducting magnets.

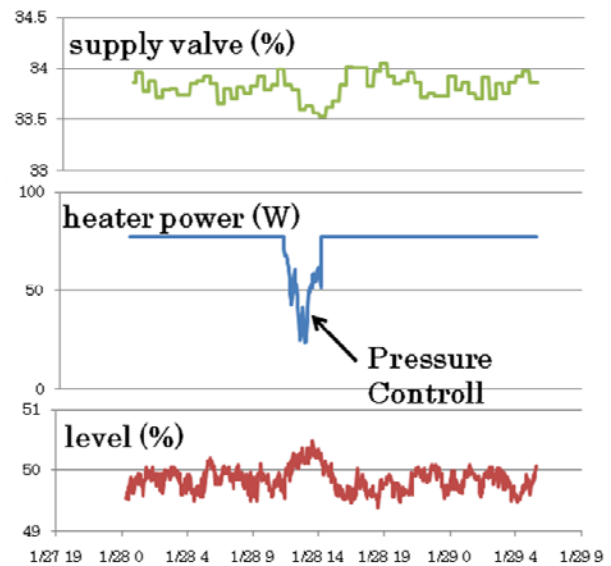


Fig. 3: Performance of the control of the liquid helium level.

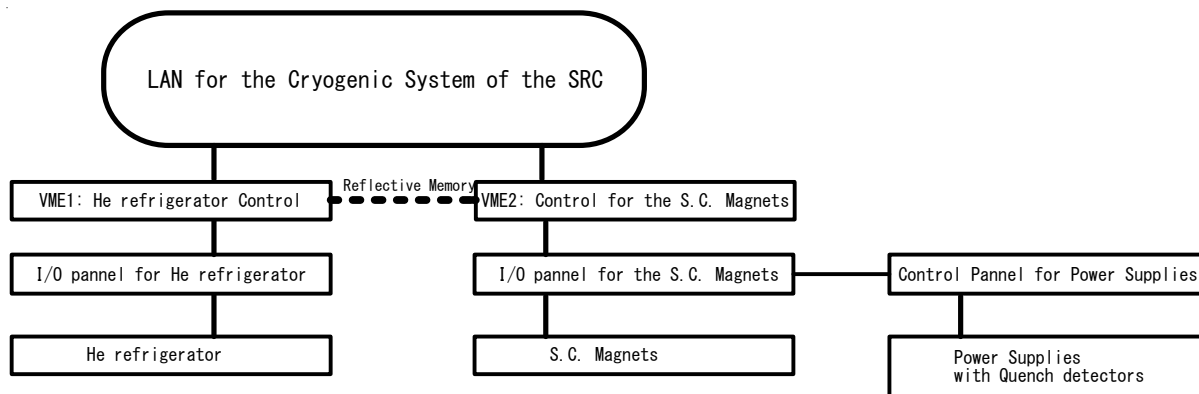


Fig. 4: Cryogenic control system for the SRC superconducting magnets and helium refrigerator.

helium vessel for the magnets and steady operation was attained on October 3, 2008. The superconducting magnets were excited to accelerate uranium and calcium beams in the SRC in November and December of 2008. At present (February 2009) stable steady operation is continuing without any severe trouble requiring us to stop the refrigerators. Fig. 2 shows the flow rate trend through the helium refrigerator with the trends during 2006-2007 operation. Long-term operation lasted more than 100 days, showing no sign of degradation of the flow rate, while operation in 2006 and 2007 was terminated around 60 days due to degradation. These trend graphs clearly suggest that this phenomenon occurred due to oil contamination in the refrigerators and the present refrigerator was very clean. In 2006-2007 we warmed up the refrigerator every two months to room temperature to recover cooling power. We understand now that the frequent warm-ups made the oil to disperse to all the pipes of the refrigerator.

In stable operation the thermal load to the superconducting magnets is almost constant. Slow feedback is enough to maintain the level of the liquid helium in the 2000 L reserve tank. The ratio of supply valve opening in the refrigerator to the magnet is automatically changed by the magnitude of  $-0.6 \times$  (level change) every 30 minutes. Fig. 3 shows good performance of the level control. A large change in the heat load occurs in excitation and de-excitation of the

superconducting magnets due to eddy current in the aluminum support for the superconducting trim coils. This change in the heat load can be compensated by changing the power of the heater in the helium vessel, thereby keeping pressure constant in the vessel. Fig. 4 shows that this pressure control moderates disturbances in the liquid level and temperature distribution inside the helium refrigerators. An interlock and alarm system were installed for safety of long-term operation. The figure shows the cryogenic control system of the helium refrigerator and superconducting magnets. The system consists of VME1 for control of the refrigerator and VME2 for control of the cryogenic parts of superconducting magnets. Each VME has a reflective shared memory connected with the other through optical fibers. This system can communicate with the power supply control panel where important information on the superconducting magnets is gathered. Table 1 lists conditions and actions of the interlocks which prevent serious trouble involving the magnets and the refrigerator. Monitoring oil contamination from the compressor is very important for preventing oil contamination of the helium refrigerator again. Cold trap measurement after the final stage is performed once every two months and oil contamination after each separator was measured once a month. Oil volume in the drain of the each separator is continuously monitored. Operation will continue until the end of the next June to check that oil separation system works well even after a 9 month period of long term operation.

Reference

- 1). T. Dantsuka, et. al. in this report.

Action	Condition
Fast shut down & isolation of the He refrigerator	Quench. Bad thermal insulating vacuum.
Slow shut down	Compressor or Turbine Trip. High or low liquid He level. High temp. of the S.C. coils. Low flow of gas He to P.L. High temp. of P.L. Low flow of the liquid He to the S.C. trim and SBM.

Table 1: Interlock list for the SRC superconducting magnets.

## Oil contamination of the cryogenic system for SRC

T. Dantsuka, H. Okuno and M. Kase

Operation of the He refrigerator for SRC was stopped in 2008 due to oil from the compressor contaminating the refrigerator. It took six months to investigate and recover from the problem. Subsequent operation started in September, and has been very stable thanks to a complete recovery process<sup>1)</sup>. This report describes details of the investigation and recovery.

The cryogenic system for SRC started operation in the autumn of 2005. The system successfully cooled-down the large superconducting magnets for SRC to carry out magnetic field measurements and beam commissioning from 2006 to 2007. However operation of the refrigerator itself was not very satisfactory, and it had to be stopped every two months due to degradation of cooling power. Investigation of impurities such as H<sub>2</sub>O and N<sub>2</sub> was carried out during operation, but did not suggest any reason why the cooling capacity degrades in such short period of two months. The cryogenic system for BigRIPS also had a similar problem. In February of 2008, however, a few drops of oil were found at the seat of the cryogenic valves in the He refrigerator for BigRIPS, and this gave us the key to solve the problem. The next day oil was also found in the SRC refrigerator, and investigation of the oil contamination was initiated.

First, we focused on the investigating how much oil is contained in the He refrigerator and where the oil

vacuum pump and so on. We opened the filter located just upstream of the first turbine as shown in Fig. 1 to check whether oil reached there by going through the 80K adsorber made from charcoal which protects against oil from the compressor. We found a mixture of the charcoal and oil there, strongly indicating that oil coming from the compressor is enough to overload 80K adsorber and the lower temperature stage of the He refrigerator. Next the 1<sup>st</sup> heat exchanger (HX) was inspected. A large amount of oil was found there, and it was very difficult to remove the oil with AK225 cleaner (HCFC-225ca) from the HXs because it has a complicated structure and sits in sideways. Less than ten percent of the oil contained in the 1<sup>st</sup> HX could be removed after much trial and error. So we decided cut the units of the 1<sup>st</sup> – 4<sup>th</sup> HXs from the refrigerator in April for cleaning in the factory, which would allow us to clean them in various sitting angles and access the lower temperature region of the He refrigerator. Fig. 2 shows the cleaning process for each heat exchanger unit in the factory. Cleaning enables us to know the correct volume of contamination of the oil and charcoal from the 80K adsorber. Inspection of the lower temperature region at the RIKEN site gave us the volume of the oil using NVR (Non Volatile Residue) technique. Finally it was found that about 400 cc of oil was contained in the helium refrigerator

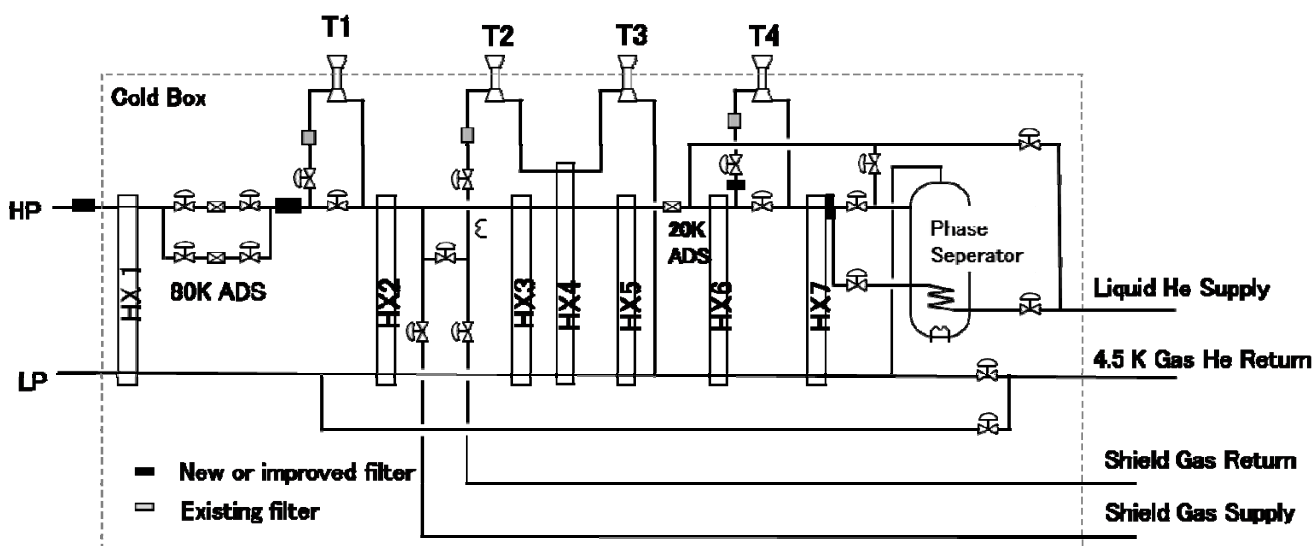


Fig. 1. Diagram of the SRC He refrigerator. T1-T4 stand for the first – fourth turbines, and HX1-7 stand for the 1<sup>st</sup>-7<sup>th</sup> heat exchangers. The new or improved filters are shown with the existing filters.

comes from. Infrared spectroscopy of the oil made it clear that it came from the screw compressor not the

and cleaning was carried out to reduce the contained oil up to about 4 cc. Replacement of charcoal in the 80



Fig. 2. Cleaning process of the heat exchangers in the factory.

K adsorber was a hard task due to the limited access to the inside. Filling charcoal into the vessel for the 80 K adsorber without spaces is important to prevent degradation of the charcoal, which can damage the seats of the cryogenic valves and the heat exchangers in the He refrigerators. This was successfully done after much try and error.

In parallel with the cleaning process, additional oil separators were designed after reconsidering the oil separation system in the compressor unit. Originally it consisted of four oil separators. The 1st is the demister type, the 2 and 3rd consist of coalescer elements and the 4th consists of charcoal and molecular sieves. We decided to add a coalescer element (the 1.5th separator) and a 5th separator made of charcoal as shown in Fig. 3. Estimated oil contamination is about 10 ppb which is smaller than the original design values by 10 ppb. Furthermore, filters to prevent incoming oil were installed before and in the inside of the helium refrigerator as shown in the Fig. 1. The recovery process, including many welding points for the pipe and covering super insulators, was the next important issue. Welding was an especially hard task in the limited space inside the refrigerator.

Permission to make the high pressure gas was given on Aug. 28, 2008 by Saitama Prefecture after the entire recovery process was complete. Tests of compressor running and stand-alone operation of the refrigerator were performed before we started to cool-down the superconducting magnets for SRC. The test results showed that cooling power in stand-alone operation was 1378.2 W at 4.5 K while initial cooling power was 1410.4 W in 2004. This degradation, which is allowable for cool-down of the SRC magnets, may arise from pressure drops caused by adding some filters to the high pressure lines of the refrigerators.

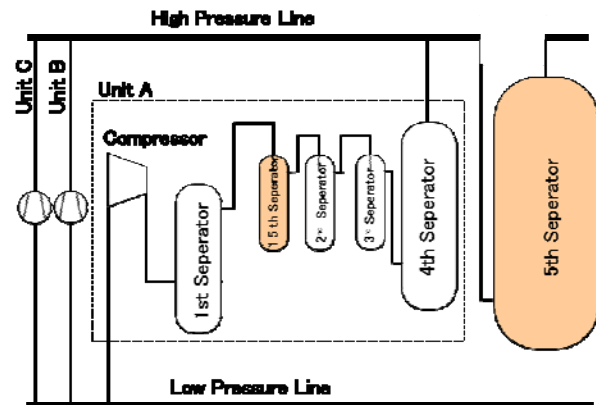


Fig. 3. Oil separators for the He compressors. The 1.5<sup>th</sup> and 5<sup>th</sup> separators were newly installed.

The process for cleaning and recovery gave us the opportunity to inspect the inside of the refrigerator, even though the main purpose was to remove oil from the refrigerator. First we found a large amount of metallic dust in the phase separator. We found that this dust comes from factory processes and left it untouched because the probability of it affecting the turbines and superconducting coils is thought to be very low. Second, we found a leak in the heat exchanger made of copper pipe placed in the phase separator. This unit improves the quality of the liquid helium before supplying it to the magnet. This leak is allowable for the present operation but we are afraid that it will become larger in long term operation, resulting in pressure in the pipe becoming the same as that in the phase separators, and causing the supply of liquid helium to stop. We will keep monitoring the leak by checking again after one year of operation.

#### References

- 1) H. Okuno et. al.: in this report.

## Present status of the BigRIPS cryogenic plant

K. Kusaka, M. Ohtake, T. Kubo, K. Yoshida, A. Yoshida, T. Ohnishi, Y. Yanagisawa, N. Fukuda, Y. Yano,  
M. Nobutoki,<sup>\*1</sup> H. Ito,<sup>\*2</sup> T. Sasaki,<sup>\*2</sup> N. Kakutani,<sup>\*2</sup> T. Tsuchihashi,<sup>\*2</sup> and K. Sato<sup>\*2</sup>

The five superconducting triplet quadrupoles (STQ1 – STQ5) in the first stage of the BigRIPS separator are cooled by a large liquid helium cryogenic plant. The main components are a Linde-TCF50S refrigerator (cold box), a Mayekawa 315 kW compressor unit, one 10 m<sup>3</sup> and two 100 m<sup>3</sup> helium buffer tanks, a 2000 L liquid helium Dewar vessel, and a 50-m-long transfer line.<sup>1)</sup> The whole cryogenic system, including the STQs was fabricated by Toshiba Corporation and Taiyo Nippon Sanso Corporation, and installed in the RIBF building at the beginning of 2004.

Test operation of the BigRIPS cryogenic plant was performed from March 2004 to June 2006.<sup>2,3)</sup> Stand-alone tests of the cold box and heat-load measurements of the transfer line were conducted until August 2005. The first cooling operation of the whole system was performed in October and November 2004 and took 20 days.<sup>2)</sup> The measurement results and the estimated excess cooling capacity are summarized in ref. 2 and ref. 3. The second cooling operation was performed in May and June 2006. Excitation tests of the STQs, and the simultaneous excitation of all the BigRIPS magnets were successfully performed during 43 days of continuous operation in the refrigerator mode.<sup>3)</sup>

Regular operation of the BigRIPS cryogenic plant started in October 2006. The cryogenic plant typically operates according to the following thermal cycle: purification of helium gas, pre-cooling, liquefaction, steady state operation in refrigerator mode, and warm-up.

The first operation cycle was from October 2006 to January 2007 (Cycle I). After 3 weeks of steady operation in the refrigerator mode, the heater power in the phase separator (PS), which corresponds to the excess of cooling capacity, started decreasing gradually. We stopped the refrigerator after 53 days of operation in the refrigerator mode, since we could not keep the liquid helium levels in the cryostats of STQs constant. We then warmed up the cold box separately and re-cooled the whole system after purification operation while taking great care regarding impurity concentration in the helium gas.<sup>3)</sup>

The second cycle was from January to April 2007 (Cycle II) in which the first RI beam has been successfully produced by the BigRIPS separator. However, we were again forced to stop the refrigerator after 59 days of steady state operation due to degradation of the cooling capacity.

We repeated two more thermal cycles prior to July 2007 in the same way as Cycle I and II in accordance with the BigRIPS beam time schedule. The third cycle (Cycle III) was from April to June 2007 and the fourth (Cycle IV) was

from June to July 2007. Commissioning experiments of BigRIPS separator were successfully performed in these periods. The cooling capacity decreased gradually in both cycles. The periods of steady operation in refrigerator mode were 39 days and 43 days in Cycle III and Cycle IV, respectively. As reported in ref. 3, we have measured the inorganic impurity concentrations in helium gas repeatedly in these cycles, but we could not find the reason for the cooling-capacity deterioration.

After a series of these operation cycles, we conducted maintenance on the oil-removal module of the compressor unit and some of the cryogenic valves in the cold box in early 2008. In February 2008 when the cryogenic valve at the entrance of the 80K adsorber (ADS) which leaked in Cycle IV was removed for maintenance, a small amount of oil was found on the valve sheet. The oil contamination in the cold box was investigated using fiber scopes and it was found that the heat exchangers and internal high pressure lines in the cold box were contaminated. The high pressure line between the compressor unit and the cold box was also investigated and oil was found in the strainer at the entrance of the cold box. The oil was identified by Fourier transform infrared (FTIR) spectroscopy analysis as coming from the compressor unit. We have concluded that the reason for the decreasing cooling capacity oil contamination in the heat exchangers.

The oil removal module of the compressor unit was then investigated using the oil check kit which is often used by the compressor manufacturer. The oil contamination level is measured by the size of oil spots on a prepared slide on which sampling helium gas was blown. Our main compressor is a 2-stage oil-flooded screw type with a flow rate of 73.5 g/sec and a discharge pressure of 1.60 MPaG. Compressor lubricant injected to the screws is separated from the discharged helium gas using a 4-stage oil removal module comprised of an oil vessel with a demister as a bulk oil separator, two coalescer vessels, and an adsorbent vessel which contains activated charcoal and molecular sieves. Residual oil at the exit of each separator stage was measured to be 3750, 100, 7.5, and 1.25 ppm (weight) in 2008, whereas it was 2500, 5, <0.25, and < 0.25 ppm (weight) in 2004. FTIR combined with the cold trap method was also performed in 2004 to measure oil contamination at the exit of the adsorbent vessel and the result was less than 40 ppb (weight). Since residual oil at the exit of the adsorbent vessel was too high, we decided not to perform cold trap measurement in 2008. The significant increase in oil contamination at the exits of the two coalescer vessels suggests an unusual change of the coalescer filters during long term operation, so we opened

\*1 Taiyo Nippon Sanso Corporation

\*2 Toshiba Corporation

the two coalescer vessels and investigated the coalescer filter elements and their seal rings. However, we could not find anything unusual in the coalescer vessels. Although we could not find a clear cause of the oil carry over, we came to the conclusion that the oil removal module must be improved.

We have decided to build an additional charcoal vessel and extra coalescer vessel in order to improve the performance of the oil removal module. The design of the new compressor unit is schematically shown in Fig. 1. The newly introduced third coalescer vessel is identical with the original two coalescer vessels and the design of the final charcoal vessel is based on the oil-removal unit in the RIKEN-RAL Muon facility. We expect the oil contamination to be 0.008-0.02 ppm after the improvement. We have also installed solenoid valves in the oil return lines to control the oil level in the coalescer vessels. By counting the valve actions we can estimate the oil separation performance of the coalescer filters.

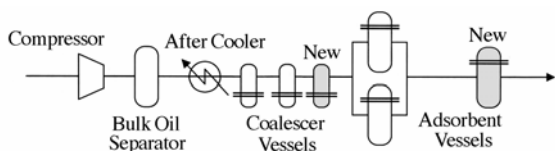


Fig. 1. Schematic diagram of the improved compressor unit.

While the additional charcoal vessel and coalescer vessel were being fabricated, we cleaned the cold box and the high pressure lines using the solvent HCFC225cb. In April 2008, the cold box was shipped to the factory where the transfer line was fabricated and all the heat exchangers were cleaned by cutting internal pipes and filling HCFC225cb. The filling solvent was drained and the amount of oil was evaluated using the non-volatile residue (NVR) method. We have repeated this process 9 to 11 times for each heat exchanger. Most of the pipes in the cold box except those in low pressure lines and the PS were also cleaned in the same manner. The total amount of remaining oil after cleaning was evaluated to be 0.34 mg (0.42 cc) using the NVR test. The remaining solvent HCFC25cb in the cleaned parts was then evaporated by sending warm N<sub>2</sub> gas. We confirmed whether the solvent HCFC25cb and water were dried from the cleaned parts by measuring HCFC25cb concentration in the outlet N<sub>2</sub> gas using the gas detector tubes and a dew point meter. All the parts were dried until HCFC25cb concentrations were less than the sensibility of the detector tube (1.4 ppm) and the dew point was in the range between -60.8 and -84.1 degree. The contaminated 80K- and 20K-ADSs and inlet filter of the turbine were replaced with improved new ones in which adsorbent charcoal was tightly filled. The cryogenic valves were disassembled and wiped to clean off possible oil contamination and the valve sheets were replaced with new ones.

Cleaning of the cold box took about 2.5 months and reassembly of the cold box at the factory was finished at the end of July 2008. Then the cold box was shipped to

RIKEN. The pipes of the high pressure lines from the compressor unit to the cold box were also cleaned by filling with HCFC225cb in early July. The new coalescer vessel and charcoal vessel were fabricated and shipped to RIKEN in mid July and installation was finished at the end of July. Reassembly of the whole system was finished in mid August and the series of test operations was finished in early September.

Stand alone operation of the cold box and cooling capacity measurement have been performed. After optimizing operation parameters such as temperature of helium gas at the entrance and exit of expansion turbines, the maximum cooling capacity was measured to be 496 W at 4.5 K at PS and 833 W at 80 K lines with a pressure of 1.35 MPaG at the entrance of the first expansion turbine T1. Converting the 80 K cooling capacity to the one at 4.5 K, the total cooling capacity is evaluated to be 543.1 W. Temperature of the discharge gas from the compressor unit, which depends on the temperature of cooling water was 32.7 degrees. Taking into account the discharge gas temperature dependence, the total cooling capacity of 543.1 W corresponds to 563.7 W with the discharge gas at 19.0 degrees, which is consistent with the result obtained in 2004 (560.5 W).<sup>2,3)</sup>

Continuous operation of the BigRIPS cryogenic plant started on September 11, 2008. After one week of purification operation, STQ1 - STQ5 were cooled from room temperature to 4 K in 18 days, and it took another 3 days to fill the cryostats with liquid helium. Steady state operation in refrigerator mode started on October 7 and we are planning to maintain continuous operation until June 2009. Figure 2 shows the flow rate of turbine T1 in the steady-operation period up to the end of January 2009 together with the flow rate for Cycle I-IV. After fixing the operation parameters on 70-th day in the refrigerator mode, the T1 flow rate has stayed almost constant, so that we have confirmed that improved oil removal module works well.

Performance of the oil removal module in the compressor unit has been checked by the cold trap method, and oil contamination at the exit of the compressor unit has been measured to be better than 10 ppb so far. Details on oil concentration measurement at each stage of oil separators will be reported in the near future.

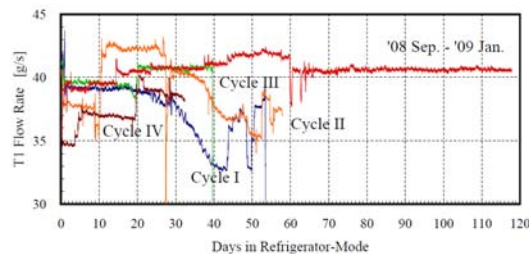


Fig. 2. T1 flow rates as functions of the operation period in refrigerator mode.

#### References

- 1) T. Kubo et al.: RIKEN Accel. Prog. Rep. **36**, 316 (2003).
- 2) T. Kubo et al.: RIKEN Accel. Prog. Rep. **38**, 289 (2005).
- 3) K. Kusaka et al.: RIKEN Accel. Prog. Rep. **41**, 244 (2008).

## Present status of liquid-helium supply and recovery system

K. Ikegami, H. Okuno, M. Nakamura, T. Maie, T. Dan s t uka, and M. Kase

A liquid-helium supply and recovery system,<sup>1)</sup> which can generate liquid helium at a rate of 200 L/h from pure helium gas, has been stably operating since the beginning of April 2001. The volumes of liquid helium supplied per year are listed in Table 1. The supplied volume has gradually increased from 2006 to 2007. The volume supplied to the low temperature physics laboratory in 2007 increased more than 10 kiloliter over 2006. The exploratory materials team in the category “other laboratories” began to use liquid-helium for the first time in March 2008. The laboratory for human brain dynamics in the brain science institute finished using liquid-helium at the end of September 2008.

The control system of the compressor for liquefying helium gas was tripped several times at the end of August and in the middle of November 2008 after the electricity stoppage plan. The cause of the trips is unknown and is now under examination.

A new recovery pipe was connected from the south side of the laser science laboratory to the recovery station behind the BSI east brain building at the end of October.

The purity of helium gas recovered from laboratories improved gradually after the completion of the system. The volume of recovered helium gas sent from each building on the Wako campus to the liquid-helium supply and recovery system has been measured. The recovery efficiency, defined as the ratio of the recovered helium gas to supplied liquid helium has been measured. Recovery efficiency for the south side of the Wako campus - such as the cooperation center building for the advanced device laboratory, the chemistry and material physics building, and nanoscience joint laboratory building - became more than 90%. Recovery efficiencies of the main research building and the laser science laboratory are very low. Average recovery efficiency measured from December 2005 to March 2008 is shown in Fig.1. Average recovery efficiency for two years has risen above 85%.

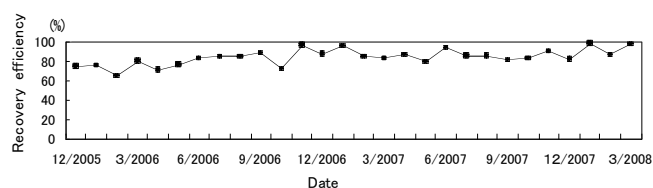


Fig. 1 Average recovery efficiency measured from December 2005 to March 2008.

At the end of April 2008, a hydrogen removal apparatus<sup>2)</sup> which has a weight of 1.7kg of the silver-zeolite “Ag-400” was installed in the system to adsorb hydrogen gas in recovery gases. The helium gas circulated in the system is returned to the gas bag of the system through the hydrogen removal apparatus without ejection in to the air. We expect that volume of purchased helium gas will decrease. Fig 2 is a diagram of the system installed in the hydrogen removal apparatus.

### Reference s

- 1)K. Ikegami et al.: RIKEN Accel. Prog. Rep. **34**, 349 (2001).
- 2)M. Nakamura et al.: RIKEN Accel. Prog. Rep. **41**, 111 (2007).

Year	2001	2002	2003	2004	2005	2006	2007
Laboratory & institute	Amount of supplied liquid helium ( ℓ )						
Magnetic materials laboratory	3392	7024	7713	11829	15672	16512	23282
Low-temperature physics laboratory	1270	3090	6966	9515	34713	29520	39855
Advanced device laboratory	9977	10849	9726	7401	11264	15017	14733
Condensed molecular materials laboratory	1939	1615	3079	5353	5912	7772	5331
Surface chemistry laboratory	1146	1676	4533	5007	5370	5486	3636
Brain science institute	6277	8144	5055	6292	7285	6956	6480
Other laboratories	3535	7730	14476	9487	15717	14767	15877
Total	27536	40182	51530	54884	95933	96030	109194

Table 1. Volumes of liquid helium supplied to laboratories per year from 2001 to 2007

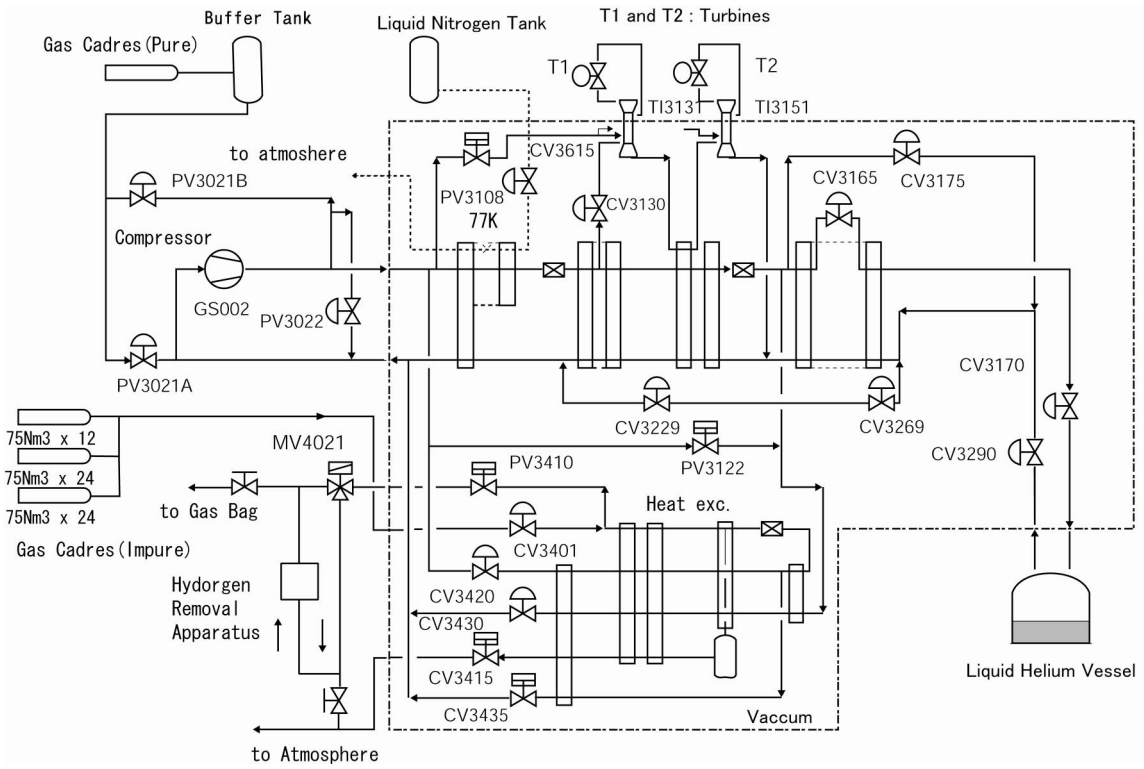


Fig. 2 Diagram of system installed in the hydrogen removal apparatus.

**V. RECORDS OF LABORATORIES,  
GROUPS, AND TEAMS  
(Activities and Members)**

## Events of Nishina Center & CNS from Jan. 2008 to Mar. 2009

2008

- 18, Jan. Tree Planting Ceremony of "Nishina Zao"  
 30, Jan. Conclusion of the Agreement "French-Japanese International Associated Laboratory for Nuclear Structure Problems" at CNRS, Paris  
 18-19, Feb. The 3rd Program Advisory Committee meeting for Nuclear Physics (NP-PAC)  
 27-28, Mar. The 4th Program Advisory Committee meeting for Materials and Life Science (MP-PAC)  
 19, Apr. RIKEN Wako Institute Open Day  
 22, Apr. RBRC Management and Steering Committee at BNL  
 Apr. The SCRIT team demonstrated the base technology of Self-Confining RI Ion Target  
 2, May A paper on development of SCRIT (Self-Confining RI Target) was issued in Phys. Rev. Lett.  
 3-4, May Science School for High School Students "A Starry Sky Tour/Travel among Elements"  
 17, Jun. Memorandum of Understanding (MOU) between Nishina Center and Indonesian Universities for Material Sciences using Muons at the RIKEN-RAL muon facility  
 25, Jul. A paper on the discovery of new Pd isotopes,  $^{125}\text{Pd}$  and  $^{126}\text{Pd}$ , was published in JPSJ online  
 Summer Maintenance and upgrade of the Liquid Helium Cryogenic Plants  
 26, Aug.-1, Sep. The 7th CNS-EFES (International Research Network for Exotic Femto Systems) summer school was held  
 Sep. The SLOWRI team performed the 1st laser cooling and precision spectroscopy  
 6, Oct. CNS (Univ. of Tokyo)-RIKEN Collaborative Research Liaison Council (annual meeting)  
 6, Oct. Lecture Commemorating 10th year of Collaborative Research on Heavy Ion Physics between the Univ. of Tokyo and RIKEN"  
 7-16, Oct. Peking University "Nishina School"  
 4-5, Nov. RIKEN-RAL Muon Facility International Advisory Committee  
 17-18, Nov. RBRC Scientific Review Committee at BNL  
 20-21, Nov. NP-PAC  
 22, Nov. RIBF International User Group Meeting  
 Nov. BigRIPS/Zero Degree Spectrometer (ZDS) Commissioning experiments  
 Nov.-Dec. Commissioning of the Zero-degree Spectrometer  
 9-21, Dec. Day One experiment in BigRIPS-ZeroDegree Spectrometer

2009

- 13-14, Jan. ML-PAC  
 15-17, Jan. Nishina Center Advisory Council (NCAC)  
 Dec.-Mar.  $^{266}\text{Bh}$  production experiment  
 Mar. SHARAQ (Spectroscopy of Hadronic Systems with Radioactive Quorum Beam) Commissioning

**Accelerator Division  
Accelerator Development Group  
Accelerator Team**

**1. Abstract**

We are developing the key hardware in upgrading the RIBF accelerator complex. Firstly we are developing the challenging superconducting coils for the new 28 GHz ECR ion source which is being developed in order to increase the intensity of uranium beam. We are designing LEBT (Low Energy Beam Transport) which transport the high power beam from the ion source to the next injector linac. Correct estimations of neutralization of space charge forces are hard task. Finally we are developing long-lived charge stripper foils which are installed to breed the ion charges for reduction of their magnetic rigidities. We are also developing gas or window-less liquid lithium strippers.

**2. Major Research Subjects**

- (1) Development of superconducting technology in acceleration system.
- (2) Development of the LEBT (Low Energy Beam Transport) and the new injector for the high power beams.
- (3) Development of charge strippers for high power beams (foil, gas, liquid)

**3. Summary of Research Activity**

- (1) Development of superconducting technology in acceleration system.

Ohnishi, J., Okuno, H.,

We are developing the challenging superconducting magnets for the 28GHz ECR ion source. We just started to study the possibility of the superconducting cavity in the RIBF accelerator complex.

- (2) Development of the LEBT (Low Energy Beam Transport) and the new injector for the high power beams.

Sato, Y., Okuno, H.,

We are developing the LEBT for the ion beams from the new 28GHz ion source. We are also studying space charge effects in the new injector for the RIBF accelerator complex.

- (3) Development of charge strippers for high power beams (foil, gas, liquid)

Hasebe, H., Kuboki, H., Yokouchi, S., Okuno, H.,

We are developing the long lived charge stripper for high power ion beams. Foils, gas and liquid for the strippers are being studied in parallel.

*Team Leader*

Hiroki OKUNO

*Members*

Jun-ichi OHNISHI

*Nishina center engineer*

Shigeru YOKOUCHI

*Technical staff I*

Hiroo HASEBE

*Contract Researcher*

Hironori KUBOKI

Yoichi SATO

*Visiting Scientists*

Noriyosu HAYASHIZAKI (Tokyo Institute of Technology)

Mitsuhiro FUKUDA (RCNP, Osaka Univ.)

Masatoshi ITO (CYRIC, Tohoku Univ.)

Yoshitaka IWASAKI (SAGA Light Source)

Satoshi KURASHIMA (JAEA, Takasaki)

Nobumasa MIYAWAKI (JAEA, Takasaki)

Hajime SAITO (SHI Accel. Serv. Ltd.)

*Research Consultants*

Yoshiaki CHIBA

Shoushichi MOTONAGA

*Students*

*Student trainees*

Hiroaki MATSUBARA (Grad Sch. Sci., Osaka Univ.)

**Accelerator Division  
Accelerator Development Group  
Ion Source Team**

**1. Abstract**

Our aim is to operate and develop the ECR ion sources for the accelerator-complex system of the RI Beam Factory. We focus on further upgrading the performance of the RI Beam Factory through the design and fabrication of a superconducting ECR heavy-ion source for production of high-intensity uranium ions.

**2. Major Research Subjects**

- (1) Operation and development of the ECR ion sources
- (2) Development of a superconducting ECR heavy-ion source for production of high-intensity uranium ions

**3. Summary of Research Activity**

- (1) Operation and development of ECR ion sources

T. Nakagawa, M. Kidera, Y. Higurashi, H. Haba, T. Kageyama and A. Goto

We routinely produce and supply various kinds of heavy ions such as zinc and neon ions for the super-heavy element search experiment as well as uranium ions for RIBF experiments. We also perform R&D's to meet the requirements for stable supply of high-intensity heavy ion beams.

- (2) Development of a superconducting ECR ion source for use in production of a high-intensity uranium beam

T. Nakagawa, J. Ohnishi, M. Kidera, Y. Higurashi, Y. Sato and A. Goto

The RIBF is required to supply uranium beams with very high intensity so as to produce RI's. We have designed and are fabricating an ECR ion source with high magnetic field and high microwave-frequency, since the existing ECR ion sources have their limits in beam intensity. The coils of this ion source are designed to be superconducting for the production of high magnetic field. We are also designing the low-energy beam transport line of the superconducting ECR ion source.

*Team Leader*

Takahide NAKAGAWA

*Members*

Hiromitsu HABA

Tadashi KAGEYAMA

*Contract Researcher*

Yoshihide HIGURASHI

Masanori KIDERA

*Visiting Scientists*

Takehiro MATSUSE (Fac. Text. Sci. Technol., Shinshu Univ.)

*Student Trainee*

Hiroyuki HIGASHIJIMA (Grad. Sch.. Sci., Rikkyo Univ.)

**Accelerator Division  
Accelerator Operation Group  
RILAC Team**

**1. Abstract**

The operation and maintenance of the RIKEN Heavy-ion Linac (RILAC) have been carried out. There are the two modes, the standalone mode, in which the beam is delivered directly to the low-energy beam user in the RILAC, and the injection mode, in which the RILAC beam is injected to the RIKEN Ring Cyclotron (RRC). The RILAC is composed of two ion sources, the frequency-variable RFQ linac, six frequency-variable cavities, and six energy booster cavities (CSM). The maintenance of these devices is important to keep the long-term stability of RILAC beams.

**2. Major Research Subjects**

- (1) The long term stability of the RILAC operation.
- (2) Improvement of efficiency of the RILAC operation.

**3. Summary of Research Activity**

The RIKEN Heavy-ion Linac (RILAC) is a frequency-tunable linac. The RILAC is composed of two Heavy-ion ECR ion sources, RFQ linac, six main cavities, and six energy booster cavities. Thousands hours are spent in a year for delivering many kinds of heavy-ion beams to various experiments.

The RILAC has two operation modes: the stand-alone operation delivering low-energy beams directly to experiments and the injection mode operation supplying beams into the RIKEN Ring Cyclotron (RRC). In the first mode, the RILAC supplies very important beam to the nuclear physics experiment of "the research of super heavy elements". In the second mode, the RILAC plays very important role as upstream end of the RIBF accelerators.

The maintenance is very important in order to keep the high quality performance of the RILAC. Improvements are always carried out for the purpose of more efficient operation.

*Team Leader*

Eiji IKEZAWA

*Member*

Yutaka WATANABE

*Research Consultants*

Toshiya CHIBA

Masatake HEMMI

Yoshitoshi MIYAZAWA

**Accelerator Division  
Accelerator Operation Group  
Cyclotron Team**

**1. Abstract**

Together with other teams of Nishina Center accelerator division, maintaining and improving the RIBF cyclotron complex. The accelerator provides high intensity heavy ions. Our mission is to have stable operation of cyclotrons for high power beam operation. Recently stabilization of the rf system is a key issue to provide 10 kW heavy ion beam. To analyze

**2. Major Research Subjects**

- (1) RF technology for Cyclotrons
- (2) Beam-RF correlation analysis
- (3) Operation of RIBF cyclotron complex.
- (4) Maintenance and improvement of RIBF cyclotrons.

**3. Summary of Research Activity**

Development of the rf system for a stable operation.  
Improvement and maintenance of rf cavities, deflection devices, beam lines.  
Introduction of precise monitoring system.  
Correlation analysis between rf and beam.

*Team Leader*

Masayuki KASE

*Members*

Naruhiko SAKAMOTO

*Research Associate*

Kenji SUDA

**Accelerator Division  
Accelerator Operation Group  
Beam Dynamics and Diagnostics Team**

**1. Abstract**

In order to realize the efficient acceleration in RIBF accelerator complex, beam-dynamics studies based on realistic computer simulations and related technology (beam diagnosis, computer control, power supplies and charge stripper) were developed.

**2. Major Research Subjects**

- (1) Improvement on the beam transmission along the multi-stage accelerator system.
- (2) Development of beam diagnosis.
- (3) Development of computer control.
- (4) Improvement on long-term stabilities of power supplies and magnets.
- (5) Development of charge stripper for high intensity heavy ion beam.

**3. Summary of Research Activity**

- (1) Development of the beam diagnostic technology.
- (2) Development of the charge-stripping foil.
- (3) Development of the computer control system of accelerator.
- (4) Investigation of beam behavior in accelerators.

*Team Leader*

Nobuhisa FUKUNISHI

*Members*

Masaki FUJIMAKI  
Sachiko ITO  
Keiko KUMAGAI  
Tamaki WATANABE

*Contract Technical Scientist*

Misaki KOBAYASHI-KOMIYAMA  
Kazunari YAMADA  
Hiroshi WATANABE  
Makoto NAGASE

*Visiting Scientists*

Hikomichi RYUTO (Photonics and Electronics Science and Engineering Center, Kyoto Univ.)  
Jun-ichi ODAGIRI  
Yuichiro SASAKI

*Research Consultants*

Jiro FUJITA

**Accelerator Division  
Accelerator Operation Group  
Cryogenic Technology Team**

**1. Abstract**

We are operating the cryogenic system for the superconducting ring cyclotron in RIBF. We are operating the helium cryogenic system in the south area of RIKEN Wako campus and delivering the liquid helium to users in RIKEN. We are trying to collect efficiently gas helium after usage of liquid helium.

**2. Major Research Subjects**

- (1) The high efficiency of the liquid helium production cycle.
- (2) Optimization of the large-scaled superconducting ring cyclotron.

**3. Summary of Research Activity**

We are operating the cryogenic system for the superconducting ring cyclotron in RIBF. Severe monitoring of the impurity is necessary to realize that. We are operating the helium cryogenic system located in the south area of Wako campus of RIKEN. We are producing liquid helium and supplying them to RIKEN inside users. For the purpose of efficient operation, we are trying to collect the gas after the use of liquid helium.

*Team Leader*

Hiroki OKUNO

*Members*

Masato NAKAMURA

*Nishina Center Engineer*

Takeshi MAIE

*Technical Staff-I*

Tomoyuki DANTSUKA

*Research Consultant*

Kumio IKEGAMI

Yutaka ODAJIMA

Ken-ichi KATO

## Nuclear Physics Research Division Heavy Ion Nuclear Physics Laboratory

### 1. Abstract

With fast RI beams provided by the RIBF cyclotron complex, we study exotic behavior of nuclei far from the stability valley, explosive nuclear burning in high-temperature and high-density environment in stars and early universe, and nuclear reactions related to solar neutrino production. For that purpose, we develop various experimental methods utilizing intermediate-energy inelastic scattering including Coulomb excitation, Coulomb dissociation, transfer- and fragmentation-reactions coupled with gamma- and particle-decay measurements. We perform also study of the three-nucleon forces by precise measurements of elastic scattering and breakup reactions of few-nucleon systems. New techniques including new laser-spectroscopy for exotic nuclei are also developed. Technical developments of radiation measurements such as semiconductor detectors and scintillation detectors, data processing methods, and construction of experimental equipment, together with theoretical studies on nuclear structure and nuclear reaction, are also made.

### 2. Major Research Subjects

- (1) Spectroscopy of unstable nuclei with direct reactions
- (2) Study of astrophysical nuclear reactions with fast beams of unstable nuclei
- (3) Three nucleon forces studied by intermediate-energy p+d scattering
- (4) Development of radiation detector systems with high performance
- (5) Development of laser spectroscopy for unstable nuclei
- (6) Theoretical studies on nuclear structure and nuclear reactions

### 3. Summary of Research Activity

#### 3.1. Spectroscopy using direct reactions with gamma-ray measurements

Proton inelastic scattering, Coulomb excitation, nucleon removal reactions on neutron- and proton-rich nuclei was studied by measuring gamma-rays in coincidence with the reaction products created in these reactions in inverse kinematics with fast RI beams. The evolution of shell structure, development of collectivity, and possible decoupling of proton- and neutron-motion are mainly studied.

#### (1) $^{32}\text{Ne}$ , $^{32}\text{Mg}$ , $^{34}\text{Si}$ —in island of inversion around $N=20$

Proton inelastic scatterings on  $^{32}\text{Mg}$  and  $^{34}\text{Si}$  were studied. The experiment was aimed at clarifying the nature of the "islands of inversion" around  $N=20$ . The  $4^+$  state was identified for the first time and several new excited states were found in  $^{32}\text{Mg}$  including a  $3^-$  state, the location of which indicates disappearance of the sd-pf shell gap. The anomalously hindered  $B(E2)$  value for the  $0^+-2^+$  transition in  $^{34}\text{Si}$  was compared with the neutron-transition multipole element extracted from the  $^{34}\text{Si}$  (p, p') result. The very neutron rich nucleus  $^{32}\text{Ne}$  was studied by the Coulomb excitation at the new facility of RIBF. The result indicates that this nucleus is in the island of inversion.

#### (2) $^{17,18}\text{C}$ —new method with transverse momentum measurement

One neutron removal reaction with a hydrogen target was studied with  $^{18}\text{C}$  and  $^{19}\text{C}$  beams. The transverse momentum distributions, where the final states were identified by their gamma-decays, were analyzed, and their spins and parities were determined. The result indicates the usefulness of the transverse-momentum associated with proton induced nucleon removal processes for the spin-assignment with the help of new approach for the reaction process, *i. e.* CDCC.

#### (3) $^{62,64}\text{Cr}$ —behavior of neutron-rich nuclei around $N=40$

Proton inelastic study with radioactive  $^{62}\text{Cr}$  and  $^{64}\text{Cr}$  beams has been performed at RIPS. Despite of the nature of magic nucleus observed in  $^{68}\text{Ni}$  with neutron number  $N=40$ , development of static deformation was observed by the deformation length and the  $4^+-2^+$  ratio for  $^{62}\text{Cr}$  and the location of the  $2^+$  state in  $^{64}\text{Cr}$ .

#### (4) $^{20}\text{Mg}$ —role of four protons around the $^{16}\text{O}$ core

Coulomb excitation of the proton-rich nucleus  $^{20}\text{Mg}$  was studied. Its B (E2) value for the  $2^+$  excitation was compared with that for the mirror nucleus  $^{20}\text{O}$ . The large ratio between the neutron- and proton-matrix elements is consistent with the known core polarization effect induced by the valence nucleons, showing that the anomalous decoupling phenomena observed in  $^{16}\text{O}$  is not observed in  $^{20}\text{O}$  and  $^{20}\text{Mg}$ .

### 3.2. Spectroscopy of unbound states using breakup and other reactions

#### (1) Invariant mass spectroscopy of nuclei in the vicinity of the neutron drip line

(a) Inelastic-scattering, one-neutron knockout, and charge exchange reactions of  $^{14}\text{Be}$  were measured for proton and  $^{12}\text{C}$  targets. The transition to the first  $2^+$  state of  $^{14}\text{Be}$  at  $E_x=1.55$  MeV was measured, which showed smaller deformation lengths compared to  $^{12}\text{Be}$ . The invariant mass spectrum of  $^{13}\text{Be}$  in the one-neutron knockout channel showed two peaks. The peak at higher energy around  $E_x=2$  MeV has a d-wave property, and the lower one is of p-wave nature which indicates obliteration of the  $N=8$  shell gap.

(b) Invariant mass spectra were obtained by the breakup and inelastic scattering of  $^6\text{He}$ ,  $^{17}\text{C}$ , and  $^{19}\text{C}$  on proton targets. New peaks were found for neutron-rich carbon isotopes.

#### (2) Invariant mass spectroscopy of proton-rich nuclei

Coulomb dissociation of the proton-rich nuclei  $^{23}\text{Al}$ ,  $^{27}\text{P}$ , and  $^{31}\text{Cl}$  on  $^{208}\text{Pb}$  were measured. Relative energy spectra for  $^{22}\text{Mg}+p$ ,  $^{26}\text{Si}+p$ , and  $^{30}\text{S}+p$  were obtained. The breakup cross sections were converted to the radiative proton-capture cross sections, which provide useful information for the astrophysical network calculation on the explosive nucleosynthesis in novae and X-ray bursts.

#### (3) Missing mass spectroscopy of very neutron-rich light nuclei

Experimental search for the exotic  $^7\text{H}$  system was performed in the  $d(^8\text{He}, ^3\text{He})^7\text{H}$  reaction using missing mass method. The excitation spectrum shows the peculiarity at  $\sim 2$  MeV that can not be reproduced by a reasonable phase space distributions and might indicate the existence of the  $^7\text{H}$  state at low excitation energy. Simultaneously, the strong peaks that corresponds to  $^7\text{He}$  and  $^{11}\text{Li}$  ground states were observed in the  $d(^8\text{He}, t)$  and  $d(^{12}\text{Be}, ^3\text{He})$  reaction channels.

### 3.3. Experimental studies on the three nucleon forces

(1) Necessity of the three-nucleon-force is shown to reproduce the deuteron-proton elastic scattering cross section. To further investigate the three-nucleon-force, spin transfer coefficients for deuteron-proton breakup reactions were measured. Experiments at higher energies using the new RIBF accelerator complex are being prepared for the first measurement in 2009.

(2) Many experiments have been performed to test experimentally Bell's inequality. However, tests using hadron systems are limited. We tested Bell's inequality in the proton-neutron system by measuring the spin-correlation between the proton-neutron pair in  $^1S_0$ -state which was produced by the  $^2\text{H}(d, pn)$  reaction.

### 3.4. "OROCHI" (Optical RI atom Observation in Condensed Helium as Ion-catcher) development

A novel nuclear laser spectroscopy technique for exotic nuclei trapped in superfluid helium, named as OROCHI (Optical RI-atom Observation in Condensed Helium as Ion-catcher), is being developed. We have carried out high precision measurement of Zeeman and hyperfine splittings of  $^{85,87}\text{Rb}$  and  $^{133}\text{Cs}$  atoms in superfluid helium, and successfully demonstrated that the nuclear spins and moments of unknown nuclei can be deduced by comparing their Zeeman and hyperfine splitting energies with those of known nuclei. We have also succeeded in optical pumping of non-alkali atoms such as Ag, which opens the door to the versatility of the OROCHI method. We are now ready to measure unknown spins and moments of exotic nuclei.

### 3.5. SCRIT development

We successfully finished feasibility studies of a novel experimental scheme, SCRIT (Self-Confining RI

Target), which makes it possible to study the internal structure of exotic nuclei by electron scattering. A prototype has been installed at the electron storage ring, KSR, of Kyoto University. We could measure electron scattering with Cs nucleus by the SCRIT scheme, and its principle has been verified. Construction of the system to be used in future experiments was started at RIBF.

### 3.6. SAMURAI

SAMURAI (Superconducting Analyzer for Multi-particle from Radio Isotope Beams) is a large-acceptance multi-particle spectrometer we will construct at RIBF. Its major part is of a large-gap superconducting magnet with 7 Tm of bending power. SAMURAI enables momentum analysis of heavy projectile fragments and projectile-rapidity protons with large angular and momentum acceptance. SAMURAI also affords projectile-rapidity neutron measurements with large angular acceptance in coincidence with heavy projectile fragments.

The construction budget has been approved, and is funded in four years from fiscal year 2008. The budget covers the superconducting dipole magnet and most part of detectors for heavy ions, neutrons, and protons. Our lab is, in particular, in charge of silicon strip detectors for protons and heavy ions and readout circuits requiring capability of broad dynamic range and high density signal processing. Our lab also partly takes care of the total arrangements of the SAMURAI collaboration group constituted by members from several institutes, each of which has unique physics interest.

Detailed design of the superconducting dipole magnet is to be finalized in fiscal year 2009. The magnet construction in RIBF will start early in 2010, and will complete early in 2011. The detectors are constructed in parallel. It is planned that the first SAMURAI experiment is performed in summer 2011.

### 3.7. Theoretical studies of nuclear physics

Most of the activities of theoretical nuclear physics have been moved to the Theoretical Nuclear Physics Laboratory led by T. Nakatsukasa.

Studies on nuclear structure at finite temperature are in progress: A self-consistent formulation of quasiparticle RPA including the effects of quantal and thermal fluctuations to study the properties of finite systems with pairing at finite temperature and angular momentum.

#### *Head*

Tohru MOTOBAYASHI

#### *Member*

Yukari MATSUO

Yoshiyuki YANAGISAWA

Nori AOI

Ken-ichiro YONEDA

Yasushi WATANABE

Toshimi SUDA

Akihisa KOHAMA

#### *Contract Researchers*

Nguyen Dinh DANG

Kimiko SEKIGUCHI (SAKAGUCHI)

#### *Senior Visiting Scientists*

Kengo OGAWA (Yamazaki Lab. In Riken)

Wolfgang MITTIG (GANIL)

Hisashi HORIUCHI (Osaka Univ. Nuclear Physics Center)  
Hiroyuki SAKURAGI (Grad. Sch. of Sci., Osaka City Univ.)

*Research Consultants*

Yasuo AOKI (univ. of Tsukuba)  
Hiroyuki MURAKAMI (Rikkyo Univ.)  
Toshimitsu YAMAZAKI

*Special Postdoctoral Researchers*

Masaki SASANO (Univ. of Tokyo)  
Yasuhiro TOGANO (Rikkyo Univ.)

*Junior Research Associates*

Kenjiro MIKI (Univ. of Tokyo)  
Masafumi MATSUSHITA

*Asia Program Associates*

Nguyen Quang HUNG (Hanoi Univ. of science)

*International Program Associates*

He WANG (Peking Univ., China)

*Visiting Scientists*

Kentaro YAKO (Univ. of Tokyo)  
Yosuke KONDO (Sch. Of Sci., Tokyo inst. Of Tech)  
Alexey KORSHENINNIKOV (Inst. Generall & Nucl. Phys., Kurchatov Inst., Russia)  
Evgueni NIKOLSKI (Russian Res. Center, Kurchatov Inst., Russia)  
Mototsugu MIHARA (Grad. Sch. of Sci., Osaka Univ.)  
Takuji IZUMIKAWA (Niigata Univ. RI Center)  
Tomotsugu WAKASA (Fac. of Sci., Kyusyu Univ.)  
Kyoichiro OZAWA (CNS, Grad. Sch. Sci., Univ. of Tokyo)  
Didier BEAUMEL (Paris-XI Univ., France)  
Shinichiro FUJII (Kyusyu Univ.)  
Yasuo MIAKE (Grad. Sch. of Pure and Applied Sci., Univ. of Tsukuba)  
Peter MOLLER (Los Alamos Nat. Lab., USA)  
Nasser KALANTAR (Univ. Groningen, The Netherlands)  
Michael FAMIANO (MSU, NSCL, USA)  
Kikuo KIMURA (Nagasaki Inst. of Applied Sci.)  
Kensaku MATSUTA (Sch. of Sci., Osaka Univ.)  
Zoltan ELEKES (ATOMKI, Hungary)  
Gabor KALINKA (Hungarian Academy Sci., Inst. Nucl. Res., Hungary)  
Takashi OHTSUBO (Dept. of Phys., Niigata Univ.)  
Jianjun HE (Chainese Academy of Science)  
Ben MOTTELSON (Copenhagen NORDITA, Denmark)  
Yohei MATSUDA (Dept. of Phys., Tohoku Univ.)  
Kazushige MAEDA (Dept. of Phys., Tohoku Univ.)  
Hiroshi SUZUKI (univ. of Tsukuba)  
Kevin Insik HAHN (Ewaha Womans Univ., Korea)  
Peter VON BRENTANO (Koln Univ., Germany)  
Atsushi HATAKEYAMA

Yanlin YE (Peking Univ., China)  
Julien GIBELIN (GANIL)  
Dorottya SOHLER (ATOMKI, Hungary)  
Yorick BLUMENFELD (Paris-XI Univ., France)  
Bo CEDERWALL (Royal Insti. Tech., Sweden)  
Takashi KIKUCHI (Fac. of Eng., Utsunomiya Univ.)  
Tetsuro KOMATSUBARA (Grad. Sch. of Pure and Applied Sci., Univ. of Tsukuba,)  
Hironobu IZIYAMA  
Filho LICHTENTHALER (The Univ. of Sao Paulo)  
Valdir GUIMARAES (The Univ. of Sao Paulo)  
Jingbin LU (Fac. of Sci., Kyusyu Univ.)  
Gerhardus Johannes MESSCHENDORP (Univ. of Groningen, Netherlands)  
Akos HORVATH (Eotvos Lorand Univ., Hungary)  
Takeshi KOIKE (Dept. of Phys., Tohoku Univ)  
Kimikazu SASA (Univ. of Tsukuba)  
Cai Xiangzhou CAI (SINAP)  
Alessandra GUGLIELMETTI (University of Milano)  
Marco MAZZOCCO (Univ. of Padova)  
Mauro ROMOLI (Institute Nazionale Fisica Nucleare Sezione de Napoli)  
Sunchan JEONG  
ManYee Betty TSANG (MSU, NSCL, USA)  
Franck DELAUNAY (CAEN)  
Andreas STOLZ (MSU, NSCL, USA)  
Zhihong LI  
Shoji SUZUKI (Inst. of Particle and Nuclear Studies, KEK)  
Silvio CHERUBINI (Catania Univ., Italy)  
Marco LA COGNATA (Catania Univ., Italy)  
Rosario Gianluca PIZZONE (Catania Univ., Italy)  
Young Kwan KWON  
Ken-Ichi FUSHIMI (Fac. of Integrated Arts and Sci., Univ. of Tokushima)  
Ichiro ARAI (Grad. Sch. of Pure and Applied Sci., Univ. of Tsukuba,)  
Tadaaki TAMAE (Lab. of Nucl. Sci., Dept. of Phys., Tohoku Univ.)  
Jonathan PEARSON (McMaster Univ., Canada)  
Alan CHEN (McMaster Univ., Canada)  
Masatoshi ITOH (Tohoku Univ.)  
Daniel BEMMERER (Tech. Univ. Berlin Inst., Germany)  
Adam KISS (Eotvos Lorand Univ., Hungary)  
Peter Georg BERG  
Henning ESBENSEN (Argonne Nat. Lab., USA)  
Weiping LIU (China Inst. Atomic Energy, China)  
Wei GUO (Shanghai Institute of Applied physics, China Academy of Science)  
Patricia ROUSSEL-CHOMAZ (GANIL)  
Chen LI (Peking Univ., China)  
David HINDE (Australia Nat. Univ., Australia)  
Renju THOMAS (Australia Nat. Univ., Australia)  
Mahananda DASGUPTA (Univ. of Bombay)  
Stefano ROMANO (Catania Univ., Italy)  
Wendong TIAN (Shanghai Institute of Applied physics, China Academy of Science)

Tomokazu SUZUKI (Osaka Univ.)  
Nelson Richard BOYD (Dept. of Phys., Ohio State Univ., USA)  
Yang SUN (Univ. of Notre Dame)  
Nicolas DE SEREVILLE  
Alain COC (Centre National de la Recherche Scientifique)  
Jarvis David DEAN (Oak Ridge National Lab.)  
Thomas PAPANBROCK (Univ. of Tennessee)  
Szily Alinka LEPINE (Univ. Sao Paulo)  
Zhendong WU (China Institute of Atomic Energy)  
Chengjian LIN (China Institute of Atomic Energy)  
Marco LA COMMARA (Univ. de Napoli)  
Claudio SPITALERI (Catania Univ., Italy)  
Marian Livius TRACHE (Texas A&M University, US)  
Aurora TUMINO (Catania Univ., Italy)  
ST John Alexander MURPHY  
Fairouz HAMMACHE (Institute de Physique Nucleaire D'Orsay)  
John Philip WOODS (Univ. of Edinburgh)  
Jiansong WANG (Institute of Modern Physics, Chinese Academy of science)  
Hongwei WANG (Institute of Modern Physics, Chinese Academy of science)  
Rudrajyoti PALIT (Tata Institute of Fundamental Research)  
Bing GUO (China Institute of Atomic Energy)  
Youbao WANG (China Institute of Atomic Energy)  
Zhengguo HU (Chinese Academy of Science)  
Meng WANG (Chinese Academy of Science)  
Jingen CHEN (Shanghai Institute of Applied physics, Nuclear Physics Division)  
Andrew Nigel ORR (Lab. Physique corpusculaire de CAEN, ENSICEAN)  
August Roman GERNHAUSER  
Shengquan YAN  
Moreno Francisco Miguel MARQUES (Caen)  
Fa. A BECK (Strasbourg Nucl. Inst., France)  
Masahiro NOTANI  
Kazuyoshi KURITA (Fac. of Sci., Rikkyo Univ.)  
Naohito IWASA (Dept. of Phys., Tohoku Univ.)  
Yoshiteru SATO (Seoul international Univ.)  
Takayuki YAMAGUCHI (Saitama Univ.)  
Yutaka WATANABE (Inst. of Particle and Nuclear Studies, KEK)  
Chongcheoul YUN (Chung-Ang Univ., Korea)  
Tadanori MINAMISONO (Fukui University of Technology)  
Yasuki NAGAI (RCNP, Osaka Univ.)  
Hiroyuki OKAMURA (RCNP, Osaka Univ.)  
Kichiji HATANAKA (RCNP, Osaka Univ.)  
Yoshihiro TAGISI (University of Tsukuba)  
Hideyuki SAKAI (Grad. Sch. of Sci., Univ. of Tokyo)  
Yoshitaka FUJITA (Grad. Sch. of Sci., Osaka Univ.)  
Hiroari MIYATAKE (Inst. of Particle and Nuclear Studies, KEK)  
Zsolt FULOP (ATOMKI, Hungary)  
Sadao MOMOTA (Kochi Univ. of Tech., Intelligent Mechanical Systems Eng.)  
Takeshi SUZUKI (Faculty of Eng., Saitama Univ.)

jun HASEGAWA (Tokyo Inst. of Tech., Res. Lab. for Nuclear Reactors)  
Tadayuki TAKAHASHI (JAXA)  
Yoshihide FUCHI (KEK)  
Kazuo IEKI (Fac. of Sci., Rikkyo Univ.)  
Shintaro NAKAYAMA (Fac. of Integrated Arts and Sci., Univ. of Tokushima)  
Tsuneyasu MORIKAWA (Fac. of Sci., Kyusyu Univ.)  
Harutaka SAKAGUCHI (Dept. of Applied Phys., Fac. of Eng., Univ. of Miyazaki)  
Seigo KATO (Fac. of Sci., Yamagata Univ.)  
Mitsunori FUKUDA (Sch. of Sci., Osaka Univ.)  
Masahiko TANAKA (KEK)  
Takashi NAKAMURA (Tokyo Inst. of Tech., Particle-, Nuclear-, and Astro-Phys.)  
Atsuko ODAHARA (Grad. Sch. of Sci., Osaka Univ.)  
Alberto MENGONI (Univ. of Tokyo)  
Atsushi TAMII (RCNP, Osaka Univ.)  
Takashi TERANISHI (Kyusyu Univ.)  
Tetsuro ISHII (JAEA)  
Zsolt DOMBRADI (ATOMKI, Hungary)  
Takashi MIYACHI (Adv. Res. Inst. Sci. Eng., Waseda Univ.)  
Takao SAKAGUCHI (BNL, USA)  
Le Hong Khiem  
Evgueni KUZMIN (Russian Res. Center, Kurchatov Inst., Russia)  
Ogloblin A. Alexey OGLOBLIN (Russian Res. Center, Kurchatov Inst., Russia)  
Mkrtychevich Gurgen TER AKOPYAN (JINR, Flerov Lab. of Nuclear Reaction, Russia)  
Shigeru ISHIMOTO (Inst. of Particle and Nuclear Studies, KEK)  
Shuwei XU  
Cosimo SIGNORINI (Univ. of Padova)  
Takashi WAKUI (Tohoku Univ. CYRIC)  
Tomoko MIYAGISHI (Natl. Inst. Radiol. Sci.)  
Nobuaki IMAI (Inst. of Particle and Nuclear Studies, KEK)  
Yukie MAEDA (Miyazaki Univ.)  
Tao ZHENG (Peking Univ., China)

*Intern*

Shuo WANG (Peking Univ., China)  
Kyoung Ho TSHOO (Suoal International Univ.)

*Student Trainees*

Keisuke ITOH (Saitama Univ.)  
Ryohei MATSUMIYA (Univ. of Osaka)  
Shumpei NOJI (Univ. of Tokyo)  
Kunihiko TAJIRI (Univ. of Osaka)  
Yoshiaki NAKAYAMA (Tokyo institute of Technology)  
Daiki NISHIMURA (Univ. of Osaka)  
Ayako SASAKI (Tohoku University)  
Kana TANAKA (Tokyo institute of Technology)  
Nobuyuki KOBAYASHI (Tokyo institute of Technology)  
Kousuke NAMIHIRA (Saitama Univ.)  
Isao HACHIUMA (Saitama Univ.)  
Sebastiana PUGLIA

Gabor KISS (Eotvos Lorand Univ., Hungary)  
Takashige HONDA (Rikkyo Univ.)  
Masayuki KAZATO (Univ. of Osaka)  
Anna TAKASHIMA (Osaka Univ.)  
Masaki SUGA (Osaka Univ.)  
Yosuke KAWADA (Tokyo institute of Technology)  
Naoki TANAKA (Tokyo institute of Technology)  
Shigeki DAGUCHI (Tokyo institute of Technology)  
Naoto KUME (Tohoku Univ.)  
Yuta HARA (Rikkyo Univ.)  
Yuichi MATSUURA (Meiji Univ.)  
Sayaka IZUMI (Tohoku Univ.)  
Hiroyuki OUCHI (Tohoku Univ.)  
Tomonori SUZUKI (Tohoku Univ.)  
Kensuke UCHIDA (Tohoku Univ.)  
Yuichi NAMIKI (Niigata Univ. RI Center)  
Yuki OHKUMA (Niigata Univ. RI Center)  
Shinji SUZUKI (Niigata Univ. RI Center)  
Kyoko YAMAGUCHI (Osaka Univ.)  
Kanao YAMAGUCHI (Univ. of Tsukuba)  
Toru SAITO (Miyazaki Univ.)  
Yosuke ITO (Univ. of Osaka)  
Yo KENMOKU (Univ. of Osaka)  
Masaaki TACHI  
Kensuke TANAKA  
Anna SHIBUSAWA  
Sotaro OSHIMA (Tohoku Univ.)  
Yunju LI  
Jun SU  
Shiwei XU (Chinese Academy of Science)  
Jun HU  
Masayuki NAGASHIMA (Niigata Univ. RI Center)  
Yuta MIURA (Tohoku Univ.)  
Yuki KATO (Meiji Univ.)  
Koutaro TAKAHASHI (Tokyo institute of Technology)  
Takayuki SAKO (Tokyo institute of Technology)  
Riyato KAMBAYASHI (Rikkyo Univ.)  
Takahiro NISHIGUCHI (Aoyama Gakuin University)

*Visiting Technician*

Henri Patrice GANGNANT  
Patrice Jean-Francois LIBIN  
Vincent Charles SPITAELS

*Secretary*

Emiko ISOGAI

## **Nuclear Physics Research Division Radioactive Isotope Laboratory**

### **1. Abstract**

This laboratory explores exotic nuclear structures and dynamics in unstable nuclei that have never been investigated before, such as those with largely imbalanced proton and neutron numbers. Our aim is to develop new experimental techniques utilizing fast RI beams to discover new phenomena and properties in unstable nuclei. Another important subject is the equation-of-state of asymmetric nuclear matter, and its association with the origin of elements and with neutron stars. For instance, we are making attempts to better understand underlying mechanism for exotic stability-enhancements of very neutron-rich fluorine isotopes, the large deformation of the nucleus  $^{34}\text{Mg}$  with  $N=22$  in spite of its vicinity to the  $N=20$  magic neutron number and anomalous collectivity in  $^{16}\text{C}$ . We are further extending these studies to medium- and heavy-mass regions by developing facilities, detectors and unique methods at RIBF, thereby leading on the challenging task to find new exotic phenomena. We also perform numerical simulations of nucleosynthesis under the environment of core-collapse supernovae, and moreover quest for footprints of supernovae and solar activities in the past, embedded in Antarctic ice core, in collaboration with Cosmic radiation laboratory and National Institute of Polar Research.

### **2. Major Research Subjects**

- (1) Study of structure and dynamics of exotic nuclei through developments of new tools in terms of reaction- and technique-based methodology
- (2) Research on EOS in asymmetric nuclear matter via heavy-ion induced reactions
- (3) Promotion of nuclear astrophysics in an interdisciplinary organization
- (4) Detector developments for spectroscopy and reaction studies

### **3. Summary of Research Activity**

- (1) Program based on missing mass method

Missing mass technique is promising for future radioactive isotope programs at RIBF. Detection of recoil particles from target is essential in excitation energy determination of particle unbound states without any assumption of particle- and gamma-decay processes, and also giving us transfer angular momentum from the angular distribution measurement. We have developed a solid hydrogen target as well as a detector system called ESPRI for proton- (in) elastic scattering. These systems have been employed for light mass nuclei available at the HIMAC facility. In addition, quasi-elastic scattering such as  $(p, 2p)$  reaction has been also performed with a  $(p2p)$  telescope at HIMAC. These programs are pilot programs for RIBF and being extended as RIBF programs. At low energies, spectroscopy on nuclei beyond the proton drip-line has been recently performed with MUST-2 at GANIL.

- (2) Program based on in-beam gamma spectroscopy

In the medium and heavy mass region explored at RIBF, collective natures of nuclei are one of important subjects, which are obtained through production and observation of high excited and high spin states. To populate such states, heavy-ion induced reactions such as fragmentation, fission are useful and development of in-beam gamma methods fit for the reactions is necessary. So far, we have developed two-step fragmentation method as an efficient method to identify and populate excited states, and lifetime measurements to deduce transition strength.

- (3) Decay spectroscopy

Beta- and isomer-spectroscopy is a traditional and efficient method for nuclear spectroscopy, especially for non-yrast levels. In the light mass region, several light-mass nuclei in both neutron-rich and proton-rich region have been investigated at RIPS through beta-gamma and beta-p coincidence technique. Concerning the medium and heavy mass region available at RIBF, we are developing two position-sensitive active-

stoppers to achieve low-background via position correlation; strip-silicon detectors and a cylindrical active stopper called CAITEN.

(4) Equation-of-state via heavy-ion central collisions

One of unsolved questions in projectile fragmentation at intermediate energies is target dependence of production cross sections for neutron-rich fragments. To seek for a possible mechanism we measured momentum distributions and cross sections of projectile fragments converted from a 90A MeV Ar-40 with Be and Ta targets. We found that differences between two targets are in production cross sections only. The cross section difference may stem from transfer/pick-up components or charge exchange ones. The similar measurements at the new facility could clarify which components are dominant. In addition, we observed in light mass fragments the acceleration phenomenon, which once had observed at GSI. These phenomena could give us an opportunity to study EOS of nuclear matter. Concerning RIBF programs, a detector for pions produced in heavy-ion collisions is being tested at the HIMAC.

(5) Interdisciplinary study for nuclear astrophysics

To understand the origin of elements beyond iron, interdisciplinary works are important in linking data from nuclear physics program. We are promoting simulation of nucleosynthesis in the r-process path, and investigation of Antarctic ice core to search for footprints of supernovae as well as solar activity in the past via mass spectrometer, to link data obtained from nuclear physics program.

*Head*

Hiro Yoshi SAKURAI

*Members*

Takashi ICHIHARA  
Takashi KISHIDA  
Yoichi NAKAI  
Shunji NISHIMURA  
Hideaki OTSU  
Heiko SCHEIT

*Nishina Center Researcher*

Yuko MOTIZUKI

*Research Associate*

Hiroshi WATANABE  
Satoshi TAKEUCHI

*Special Postdoctoral Researcher*

Maya TAKECHI  
Eri TAKESHITA  
Satoru TERASHIMA

*Senior Visiting Scientist*

Wolfgang MITTIG (GANIL, France)

*Visiting Scientists*

Sachiko AMARI (Washington Univ., USA)  
Koichiro ASAHI (Tokyo Institute of Technology)  
Sudhee BANERJEE (Variable Energy Cyclotron Center, India)  
Xiangzhou CAI (Shanghai Inst. Applied Physics, China)

Junsei CHIBA (Tokyo University of Science)  
Alfred DEWALD (Univ. Cologne Insti. Nucl. Phys.)  
Deqing FANG (Shanghai Inst. Applied Physics, China)  
Adrian GELBERG (Univ. zu KoelnInst. Fur Kern Physik, Germany)  
Wei GUO (Shanghai Inst. Applied Physics, China)  
Kaoru HARA (University of Tsukuba)  
Steven KARATAGLIDIS (Rhodes Univ., South Africa)  
Hiroyuki KOURA (JAEA)  
Yugang MA (Shanghai Inst. Applied Physics, China)  
Hideki MADOKORO (Mitsubishi Heavy Industries, Ltd)  
Masayuki MATSUO (Grad. Sch. of Sci. and Tech., Niigata Univ.)  
Tetsuya MURAKAMI (Kyoto Univ.)  
Jiro MURATA (Rikkyo Univ.)  
Tetsuo NORO (Kyusyu Univ. Fac. of Sci.)  
Akira ONO (Tohoku Univ.)  
Naohiko OTSUKA (International Atomic Energy Agency, Austria)  
YURI PENIONZHKEVICH (Flerov Lab. Nucl. Reactions, JINR, Russia)  
Simona SCHEIT (Univ. of Tokyo)  
Toshiyuki SUMIKAMA (Tokyo University of Science)  
Takahiro TACHIBANA (Waseda High Sch., Waseda Univ.)  
Kohji TAKAHASHI (Universite Libre de Bruxelles, Belgium)  
Noboru TAKIGAWA (Fac. of Sci., Tohoku Univ.)  
Oleg TARASOV (MSU, NSCL, USA)  
Ryouichi WADA (Texas A&M Univ., USA)  
Juzo ZENIHIRO (Grad. Sch. of Sci., Kyoto Univ.)  
Shuangquan ZHANG (Peking Univ., China)  
Yumin ZHAO (Shanghai Jiao Tong Univ.)

*Contract Researcher*

Yasuyuki GONO

*Students*

*Junior Research Associate*

Taro NAKAO

Mugumi NIKURA

Hitomi KIMURA

*Student Trainees*

Shoichiro EBESU (Kyoto Univ.)

Yuhei HASHIZUME (Tsukuba Univ.)

Maki HATA (Rikkyo Univ.)

Chihiro ISHII (Tokyo University of Science)

Yoshihiko IWAO (Kyoto Univ.)

Hiroaki MATSUMOTO (Kyoto Univ.)

Minori NIITA (Rikkyo Univ.)

Ken-ichiro OGAWA (Tsukuba Univ.)

Kensuke OKADA (Rikkyo Univ.)

Akio SHIRAKI (Tokyo Univ.)

Daisuke SUZUKI (Tokyo Univ.)

Hirotake TAKAHASHI (Shinsyu Univ.)  
Nobuya UEMATSU (Tokyo University of Science)  
Hideakira YOSHII (Tokyo University of Science)  
Kenta YOSHINAGA (Tokyo University of Science)

*IPA*

Kuoang LI (Peking Univ., China)

*Visiting Rsearcher*

Pieter DOORNENBAL (JSPS Fellow)

Mattias LANTZ (JSPS Fellow)

*Secretary*

Tomoko FUJII (Temporary staff)

## **Nuclear Physics Research Division Superheavy Element Laboratory**

### **1. Abstract**

The elements with their atomic number  $Z > 103$  are called as trans-actinide or superheavy elements. The chemical properties of those elements have not yet been studied in detail. Those elements do not exist in nature therefore, they must be produced artificially for the scientific study of those elements. In our laboratory, we have been studying the physical and chemical properties of the superheavy elements utilizing the accelerators in RIKEN and various methods of efficient production of the superheavy elements.

### **2. Major Research Subjects**

- (1) Search for new superheavy elements
- (2) Decay spectroscopy of the heaviest nuclei
- (3) Study of the chemical properties of the heaviest elements
- (4) Study of the reaction mechanism of the fusion process (theory)

### **3. Summary of Research Activity**

- (1) Searching for new elements

To expand the periodic table of elements and the nuclear chart, we will search for new elements.

- (2) Spectroscopic study of the nucleus of heavy elements

Using the high sensitivity system for detecting the heaviest element, we plan to perform a spectroscopic study of nuclei of the heavy elements.

- (3) Chemistry of superheavy elements

Study of chemistry of the trans-actinide (superheavy element) has just started world-wide, making it a new frontier in the field of chemistry. Relativistic effects in chemical property are predicted by many theoretical studies. We will try to develop this new field.

- (4) Study of a reaction mechanism for fusion process

Superheavy elements have been produced by complete fusion reaction of two heavy nuclei. However, the reaction mechanism of the fusion process is still not well understood theoretically. When we design an experiment to synthesize nuclei of the superheavy elements, we need to determine a beam-target combination and the most appropriate reaction energy. This is when the theory becomes important. We will try to develop a reaction theory useful in designing an experiment by collaborating with the theorists.

#### *Head*

Kosuke MORITA

#### *Members*

Hiromitsu HABA

Kouji MORIMOTO

#### *Special Postdoctoral Researcher*

Takatoshi ICHIKAWA

Daiya KAJI

Kazutaka OZEKI

Yuki KUDOU

#### *Contract Technical Scientist*

Akira YONEDA

*Visiting Scientists*

Kazuhiko AKIYAMA (Tokyo Metropolitan Univ.)  
Masato ASAI (Japan Atomic Energy Agency)  
Shin-ichi GOTO (Niigata Univ.)  
Kouichi HAGINO (Tohoku Univ.)  
Yoshitaka KASAMATU (Japan Atomic Energy Agency)  
Hisaaki KUDO (Fac. Sci., Niigata Univ.)  
Yuichiro NAGAME (Japan Atomic Energy Agency)  
Tetsuya MURAKAMI (Grad. Sch. Sci., Kyoto Univ.)  
Minoru SAKAMA (Tokushima Univ.)  
Atsushi SHINOHARA (Osaka Univ.)  
Tetsuya SATO (Japan Atomic Energy Agency)  
Keisuke SUEKI (Grad. Sch. Pure Appl. Sci., Univ. Tsukuba)  
Fuyuki TOKANAI (Dept. Phys., Yamagata Univ.)  
Atsushi TOYOSHIMA (Japan Atomic Energy Agency)  
Kazuaki TSUKADA (Japan Atomic Energy Agency)  
Akihiko YOKOYAMA (Dept. Chemi., Kanazawa Univ.)  
Takashi YOSHIMURA (Osaka Univ.)

*Research Consultants*

Takashi INAMURA  
Kenji KATORI  
Toru NOMURA

*Students*

*Junior Research Associate*

Nozomi SATO (Grad. Sch. Sci. Eng., Tohoku Univ.)

*Student Trainees*

Takayuki SUMITA (Tokyo Univ. of Science)  
Tomohiro NANRI (Dept. Chem., Kanazawa Univ.)  
Itsuro YAMAZAKI (Dept. Chem., Kanazawa Univ.)  
Atsushi ASANO (Dept. Chem., Kanazawa Univ.)  
Mikio ARAKI (Dept. Chem., Kanazawa Univ.)  
Kazuhiro OOE (Osaka Univ.)  
Yukiko KOMORI (Osaka Univ.)  
Daisuke SUZUKI (Dept. Chem., Kanazawa Univ.)  
Reona TAKAYAMA (Osaka Univ.)  
Masaki NISHIO (Dept. Chem., Kanazawa Univ.)  
Wataru YAHAGI (Osaka Univ.)  
Itsuro YAMAZAKI (Dept. Chem., Kanazawa Univ.)  
Hiroyuki FUJISAWA (Osaka Univ.)  
Takuma KAWASAKI (Niigata Univ.)

## **Nuclear Physics Research Division Theoretical Nuclear Physics Laboratory**

### **1. Abstract**

Nuclei are finite many-particle systems composed of protons and neutrons. They are self-bound in femto-scale ( $10^{-15}$  m) by the strong interaction (nuclear force) whose study was pioneered by Hideki Yukawa. Uncommon properties of the nuclear force (repulsive core, spin-isospin dependence, tensor force, etc.) prevent complete microscopic studies of nuclear structure. There exist number of unsolved problems even at present. In addition, radioactive beam facilities reveal novel aspects of unstable nuclei. We are tackling these old problems and new issues in theoretical nuclear physics, developing new models and pursuing large-scale calculations of quantum many-body systems. We are also strongly involved in research on other quantum many-body systems, to resolve mysteries in the quantum physics

### **2. Major Research Subjects**

- (1) Nuclear structure and quantum reaction theories
- (2) First-principle calculations with the density functional theory for many Fermion systems
- (3) Computational nuclear physics

### **3. Summary of Research Activity**

- (1) Finite amplitude method for nuclear response calculations

We have performed a systematic calculation of nuclear photoabsorption cross section for light nuclei. The calculation is fully self-consistent and is based on the time-dependent density-functional theory with the Skyrme functional. This is achieved using the finite amplitude method we have recently developed. The key feature of the method is to obtain the matrix elements of the random-phase approximation (RPA) in a simple way avoiding explicit calculation of induced residual fields. So far, even-even nuclei up to mass number  $A=80$  have been studied.

In addition, we have been working on extension of the finite amplitude method to nuclei where the pairing correlations are important. The basic equations have been derived and we are currently developing the computer program to calculate the linear response utilizing the finite amplitude method for the quasi-particle RPA.

- (2) Large amplitude dynamics in shape coexistence phenomena

Shape coexistence phenomena in proton-rich Se isotopes have been studied with the adiabatic self-consistent collective coordinate method. The canonical collective variables, mass parameter, and potential were determined self-consistently. The calculation indicates importance of the triaxial degrees of freedom for the tunneling dynamics between two quasi-vacua at prolate and oblate shapes. The collective Hamiltonian was requantized to calculate excitation spectra and transition properties for the first time. The shape mixing is hindered by coupling to the rotational motion to localize collective wave functions around prolate and oblate minima.

- (3) Reaction cross section of stable and unstable nuclei

We have studied the difference between the interaction cross section and the total reaction cross section for relativistic energies. We show that, for incident stable nuclei, the predicted difference is large enough to probe the nuclear structure, particularly in a mass region of less than around 40.

We have systematically calculated the total reaction cross sections of oxygen isotopes,  $^{15-24}\text{O}$ , on a  $^{12}\text{C}$  target at high energies using the Glauber theory. We have also studied the differential elastic-scattering cross sections of proton- $^{20,21,23}\text{O}$ . The agreement between theoretical and experimental results is generally good, and our prediction for proton- $^{20}\text{O}$  elastic scattering appears consistent with recent (preliminary) experimental data.

- (4) Low-lying collective modes in deformed unstable nuclei

Low-frequency modes of excitation in deformed neutron-rich nuclei have been studied by means of the self-consistent Hartree-Fock-Bogoliubov and the quasiparticle-random-phase approximation based on the Skyrme energy density functional and the pairing density functional. We have investigated soft  $K^\pi=0^+$  modes in neutron-rich Mg isotopes close to the drip line and have found that its strong collectivity is due to the coherent coupling between the beta vibration and the pairing vibration of neutrons.

(5) Density functional for description of novel pairing properties in nuclei far from stability

Our research focuses on the pairing properties in nucleonic systems under the extreme conditions; super neutron-rich nuclei ( $N > 2Z$ ) and stellar interiors. We developed an energy density functional for pairing correlations (pair-DF) toward description of pairing properties in nuclei across the mass table. Our pair-DF is an indispensable ingredient for reliable prediction of the ground states and dynamical properties in super neutron-rich nuclei around heavy and medium-heavy mass regions, which are the main research targets in the RIKEN RIBF. We have completed the extensive calculation from  $(N-Z)/A=0$  to 0.4 (neutron drip line region) for all even-even nuclei with  $N, Z > 40$ . From the analysis, we found the anomalous enhancement of pairing correlations in nuclei with large neutron excess, which can bring about various novel collective phenomena.

(6) Molecular structure of  $^{12}\text{Be}$  studied with the generalized two-center cluster model

We have developed the generalized two-center cluster model (GTCM), which can handle the ionic, atomic, and covalent configurations in general two center systems. We have applied the GTCM to a unified study on structures and reactions in  $^{12}\text{Be}$ . We have found that, above the alpha decay threshold, various chemical-bonding states coexist with a small energy interval. We also predicted that they were strongly populated through the two-neutron transfer reactions,  $\alpha+^8\text{He} \rightarrow ^6\text{He}+^6\text{He}$ , which has been measured very recently at GANIL.

(7) Quantum condensed state of alpha particles in nuclei

We have investigated the quantum condensate state in nuclei, composed of a finite number of alpha particles, which are weakly interacting like a gas and condensed into the lowest mean field 0S orbit. We find a dilute density state in  $^{16}\text{O}$  of strong alpha condensate character. The state is located at around the four-alpha breakup threshold as the sixth  $0^+$  state. This discovery in this work is of a great significance in triggering further investigation in heavier nuclei.

(8) Many-body green's function approaches to nuclear structure

Numerical codes for Green's function theory were extended to achieve large-scale calculations using modern realistic nuclear interactions. Ab-initio studies of medium mass nuclei (up to  $A=60$ ) are now being performed. Calculations for  $^{56}\text{Ni}$  have reproduced the known spectroscopic factors. Based on this success, the dependence of nuclear correlations on proton-neutron asymmetry is being investigated. The quenching of experimental spectroscopic factors is currently an open puzzle for drip-line nuclei. Analogous calculations have been performed for electronic systems (atoms) to aid in developments of density functional theory.

(9) Smoothing method of S-matrix elements in CDCC calculations

One of the most reliable methods for treating the breakup processes is the method of continuum discretized coupled channels (CDCC). In CDCC, the calculated S-matrix elements are discrete in continuum, although the exact ones are continuous. Thus, one needs a smoothing procedure of the S-matrix in order to analyze real breakup processes. For this purpose, we have proposed a simple formula by using the complex scaling method and the validity of the new smoothing method was confirmed by test calculations for three-body breakup reactions. In a future work, we will investigate the practicability of this formula for four-body breakup processes.

*Head*

Takashi NAKATSUKASA

*Members*

Akihisa KOHAMA

*Special Postdoctoral Researcher*

Makoto ITO

Yasuro FUNAKI

Kenichi YOSHIDA

Carlo BARBIERI

Paolo AVOGADRO

*Contract Researcher*

Masayuki YAMAGAMI

Takuma MATSUMOTO

*Senior Visiting Scientist*

Kenichi MATSUYANAGI

*Research Consultant*

Kiyomi IKEDA

Syuhei YAMAJI

Kosai TANABE

*Visiting Scientists*

Tsunenori INAKURA (Grad. Sch. of Pure and Applied Sci., Univ. Tsukuba)

Nicolas L. J. MICHEL (Dept. Phys., Kyoto Univ.)

Taiichi YAMADA (Kanto Gakuin Univ.)

Takenori FURUMOTO (Osaka City Univ.)

Nobuo HINOHARA (Yukawa Inst. Theoretical Phys.)

Makito OI (Univ of Surrey.)

Kazuo TAKAYANAGI (Sophia Univ.)

Akitsu IKEDA (Shizuoka Inst. Scie. Tech.)

Satoshi CHIBA (Japan Atomic Energy Agency.)

Wenhui LONG (Peking Univ.)

Michio HONMA (Aizu Univ.)

Masaaki KIMURA (Hokkaido Univ.)

Kazusuke OGATA (Kyushu Univ.)

Takayuki MYO (Osaka Univ.)

Kei IIDA (Kochi Univ.)

Ikuko HAMAMOTO (Lund Univ.)

Kazuhiro YABANA (Grad. Sch. of Pure and Applied Sci., Univ. Tsukuba)

Ryoichi SEKI (California Univ.)

Kazuko TANABE (Otsuma Women's Univ.)

Jun TERASAKI (Univ. North)

Toshitaka KAZINO (NAOJ)

Noritaka SHIMIZU (Univ of Tokyo)

Meng JIE (Peking Univ.)

Dao TIEN KHOA (Inst. Nucl. Scie. Tech.)

Takatoshi HORIBATA (Aomori Univ.)

Yasuhisa ABE (RCNP)

Akira KISHIMOTO (Japan Atomic Energy Agency.)

Kiyoshi KATO (Hokkaido Univ.)  
Masahisa OTA (Konan Univ.)  
Hiroyuki SAGAWA (Aizu Univ.)  
Takahiro WADA (Kansai Univ.)  
Akihiro SUZUKI (Suzuki Corporation)  
Shigeyoshi AOYAMA (Niigata Univ.)  
Yasuyuki SUZUKI (Niigata Univ.)  
Kazuhiro OYAMATSU (Aichi Shukutoku Univ.)  
Naoyuki ITAGAKI (Univ of Tokyo)  
Yoshiko ENYO (Yukawa Inst. Theoretical Phys.)  
Yutaka UTSUNO (Japan Atomic Energy Agency.)  
Kosuke SUMIYOSHI (Numzu National College of Technology)  
Masatoshi TAKANO (Waseda Univ.)  
Naoki TAJIMA (Univ of Fukui)  
Yoshihiro ARITOMO (JINR)  
Munetake ICHIMURA (The Open Univ of Japan)  
Yoshihumi SHIMIZU (Kyushu Univ.)  
Naotaka YOSHINAGA (Saitama Univ.)  
Chie KUROKAWA (Hokkaido Univ.)  
Hubert FLOCARD (INP-Orsay)  
Badawy SARHAN (Cairo Univ.)  
Satoshi SUGIMOTO (Juntendo Univ.)  
Toshio SUZUKI (Fukui Univ.)  
Masaaki TAKASHINA (RCNP)  
Kazuo MUTO (Tokyo Institute of Technology)  
Koji HIGASHIYAMA (Chiba Institute of Technology)  
Koichi HAGINO (Tohoku Univ.)  
Yumin ZHAO (Shanghai Jiao Tong Univ.)  
Steven KARATAGLIDIS (Rhodes Univ.)  
Masayuki MATSUO (Tohoku Univ.)  
Akira ONO (Tohoku Univ.)  
Noboru TAKIGAWA (Tohoku Univ.)

*Students*

*Junior Research Associates*

Shuuichiro EBATA (Grad. Sch. of Pure and Applied Sci., Univ. Tsukuba)  
Koichi SATO (Dept. Phys., Kyoto Univ.)

*Student Trainees*

Shouhei IWASAKI (Niigata Univ.)  
Takenori FURUMOTO (Osaka City Univ.)

*Secretary*

Shinko ODAI

**Nuclear Physics Research Division**  
**Experimental Installations Development Group**  
**SLOWRI Team**

**1. Abstract**

A next-generation slow radioactive nuclear ion beam facility (SLOWRI) which provides slow, high-purity and small emittance ion beams of all elements is being build as one of the principal facilities at the RIKEN RI-beam factory (RIBF). High energy radioactive ion beams from the projectile fragment separator BigRIPS are thermalized in a large gas catcher cell. The thermalized ions in the gas cell are guided and extracted to a vacuum environment by a combination of dc electric fields and inhomogeneous rf fields (rf carpet ion guide). From there the slow ion beam is delivered via a mass separator and a switchyard to various devices: such as an ion trap, a collinear fast beam apparatus, and a multi-reflection time of flight mass spectrometer. In the R&D works at the present RIKEN facility, an overall efficiency of 5% for a 100A MeV  $^8\text{Li}$  ion beam from the present projectile fragment separator RIPS was achieved and the dependence of the efficiency on the ion beam intensity was investigated.

First spectroscopy experiment at the prototype SLOWRI was performed on Be isotopes. Energetic ions of  $^7,^{10,11}\text{Be}$  from the RIPS were trapped and laser cooled in a linear rf trap and precision spectroscopy was performed. The evaluated ion temperature of <10 mK demonstrates that a reduction of more than 15 orders of magnitude for the kinetic energy of radioactive Be was achieved online. Precise investigation of the hyperfine structure will confirm the anomalous mean radius of the valence neutron of the so called neutron halo nucleus.

Other spectroscopy experiments using the slow RI-beams are also under progress in off-line setups. A collinear fast beam apparatus for nuclear charge radii measurements was build and tested with stable Ar<sup>+</sup> ion beams. A multi-reflection time-of-flight mass spectrograph was build for precise and fast measurements of short-lived radioactive nuclei. A high mass resolving power of 200,000 has been achieved with a 3 ms measurement period.

**2. Major Research Subjects**

- (1) Development and construction of the next-generation slow RI-beam facility
- (2) Precision hyperfine spectroscopy of trapped ions for magnetization distribution in a halo nucleus
- (3) Nuclear charge radii measurements using ion trap and collinear fast beam apparatus
- (4) Precision mass measurements of short-lived nuclei using a multi-reflection TOF mass spectrograph
- (5) Development of deceleration and cooling devices for energetic beams using gas cell and rf fields.
- (6) Atomic physics and fundamental symmetry research investigating nuclear decay of an isolated atom

**3. Summary of Research Activity**

- (1) Development of universal slow RI-beam facility

WADA, Michiharu, TAKAMINE, Aiko, SCHURY Peter, SONODA, Tetsu, OKADA, Kunihiro, KANAI, Yasuyuki, YOSHIDA, Atsushi, KUBO, Toshiyuki, YAMAZAKI, Yasunri, WOLLNIK, Hermann, SCHUESSLER, Hans, NODA, Koji, OHTANI, Shunsuke, KATAYAMA Ichiro

A next-generation slow radioactive nuclear ion beam facility (SLOWRI) which provides slow, high-purity and small emittance ion beams of all elements is being build as one of the principal facilities at the RIKEN RI-beam factory (RIBF). High energy radioactive ion beams from the projectile fragment separator BigRIPS are thermalized in a large gas catcher cell. The thermalized ions in the gas cell are guided and extracted to a vacuum environment by a combination of dc electric fields and inhomogeneous rf fields (rf carpet ion guide). From there the slow ion beam is delivered via a mass separator and a switchyard to various devices: such as an ion trap, a collinear fast beam apparatus, and a multi-reflection time of flight mass spectrometer. In the R&D works at the present RIKEN facility, an overall efficiency of 5% for a 100A MeV  $^8\text{Li}$  ion beam from

the present projectile fragment separator RIPS was achieved and the dependence of the efficiency on the ion beam intensity was investigated.

(2) Laser spectroscopy of trapped radioactive beryllium isotope ions

WADA, Michiharu, TAKAMINE, Aiko, SCHURY Peter, SONODA Tetsu, OKADA, Kunihiro, KANAI, Yasuyuki, YOSHIDA, Atsushi, KUBO, Toshiyuki, YAMAZAKI, Yasunori, WOLLNIK, Hermann, SCHUESSLER, Hans, NODA, Koji, OHTANI, Shunsuke, KATAYAMA Ichiro

As a first application of the prototype SLOWRI setup, we are applying hyperfine structure spectroscopy to the beryllium isotopes to determine in particular the anomalous radius of the valence neutron of the neutron halo nucleus  $^{11}\text{Be}$ , and to determine the charge radii of these beryllium isotopes through laser-laser double resonance spectroscopy of laser-cooled ions. Laser cooling is an essential prerequisite for these planned experiments. However, the exact resonance frequencies of the cooling transitions for radioactive beryllium isotopes are not known. In such light elements, the isotope shifts in the atomic transitions are larger than several 10 GHz and their dominant parts are due to complicated multi-electron correlations. Some theoretical works on the isotope shifts of the beryllium ion exist, however the values contradict each other at the level of accuracy needed.

The first laser spectroscopy experiments for beryllium isotopes were performed to measure the resonance frequencies of  $2s\ ^2S_{1/2} - 2p\ ^2P_{3/2}$  transition of  $^7\text{Be}^+$ ,  $^9\text{Be}^+$ ,  $^{10}\text{Be}^+$  and  $^{10}\text{Be}^+$  ions aiming at determining the nuclear charge radii. The hyperfine structure of  $^{11}\text{Be}^+$  and  $^7\text{Be}^+$  ions using the laser-microwave double resonance spectroscopy were also performed and  $A(^7\text{Be}^+) = -742.7723(4)$  MHz and  $A(^{11}\text{Be}^+) = -2677.308(2)$  MHz were determined for the first time. Precision measurements of the nuclear magnetic moments of these Be isotopes are in progress.

(3) Development of a multi-reflection TOF mass spectrograph

WADA, Michiharu, SCHURY Peter, TAKAMINE, Aiko, SONODA Tetsu, OKADA, Kunihiro, YAMAZAKI, Yasunori, WOLLNIK, Hermann,

The atomic mass is one of the most important quantity of a nucleus and has been studied in various methods since the early days of physics. Among many methods we chose a multi-reflection time-of-flight (MR-TOF) mass spectrometer. Slow RI beams extracted from the RF ion-guide are bunch injected into the spectrometer with a repetition rate of  $\sim 500$  Hz. The spectrometer consists of two electrostatic mirrors between which the ions travel back and forth repeatedly. These mirrors are designed such that energy-isochronicity in the flight time is guaranteed during the multiple reflections while the flight time varies with the masses of ions. A mass-resolving power of  $>200,000$  has been obtained with about 500 reflections in a 30 cm length spectrometer. This mass-resolving power should allow us to determine ion masses with an accuracy of  $10^{-7}$ . The advantages of the MR-TOF spectrometer are: 1) short measurement periods, typically 2 ms, which allows all neutron rich nuclei to be investigated, 2) the device is compact and its operation is simple, especially, it is independent from the all upstream devices, accelerators and fragment separators, 3) ions of more than isobars can be measured simultaneously, so that mass reference can easily be established in the mass spectra. In total, the number of measurable nuclides within a limited beam time would be larger than that can be achieved by other methods. It should be noted here also that this method can be used even during a low-duty parasite beam time. An on-line MR-TOF mass spectrograph with 80 cm length having an expected mass resolving power of 1,000,000 is under fabrication.

(4) Development of collinear fast beam apparatus for nuclear charge radii measurements

WADA, Michiharu, SCHUESSLER, Hans, IIMURA, Hideki, SONODA, Tetsu, SCHURY, Peter, TAKAMINE, Aiko, OKADA, Kunihiro, YAMAZAKI, Yasunori, WOLLNIK, Hermann,

The root-mean-square charge radii of unstable nuclei have been determined exclusively by isotope shift measurements of the optical transitions of singly-charged ions or neutral atoms by laser spectroscopy. Many isotopes of alkaline, alkaline-earth, noble-gases and several other elements have been measured by collinear laser spectroscopy since these ions have all good optical transitions and are available at conventional ISOL facilities. However, isotopes of other elements especially refractory and short-lived ones have not been

investigated so far.

In SLOWRI, isotopes of all atomic elements will be provided as well collimated mono-energetic beams. This should expand the range of applicable nuclides of laser spectroscopy. In the first years of the RIBF project, Ni and its vicinities, such as Ni, Co, Fe, Cr, Cu, Ga, Ge are planned to be investigated. They all have possible optical transitions in the ground states of neutral atoms with presently available laser systems. Some of them have so called recycle transitions which enhance the detection probabilities noticeably. Also the multistep resonance ionization (RIS) method can be applied to the isotopes of Ni as well as those of some other elements. The required minimum intensity for this method can be as low as 10 atoms per second.

We have built an off-line mass separator and a collinear fast beam apparatus with a large solid-angle fluorescence detector. A 617 nm transition of the metastable Ar<sup>+</sup> ion at 20 keV was measured with both collinear and anti-collinear geometry that allowed us to determine the absolute resonant frequency of the transition at rest with more than 10<sup>-8</sup> accuracy. Such high accuracy measurements for Ti and Ni isotopes are in progress.

*Head*

Masanori WAKASUGI

*Members*

Michiharu WADA

**Nuclear Physics Research Division  
Experimental Installations Development Group  
SAMURAI Team**

**1. Abstract**

This team is in charge of design, development and construction of the SAMURAI spectrometer that will be used for reaction experiments using RI beams at RI Beam Factory. SAMURAI consists of a large superconducting dipole magnet and a variety of detectors to detect charged particles and neutrons.

**2. Major Research Subjects**

Design, development and construction of the SAMURAI spectrometer at RI Beam Factory and its related research instruments.

**3. Summary of Research Activity**

This team is in charge of design, development and construction of the SAMURAI spectrometer at RI Beam Factory. Consisting of a large superconducting dipole magnet and a variety of detectors to detect charged particles and neutrons, SAMURAI will be used for various reaction studies with RI beams.

The research subjects may be summarized as follows:

- (1) Design, development and construction of a large superconducting dipole magnet that will be the main component of the SAMURAI spectrometer.
- (2) Design, development and construction of various detectors that are used for nuclear reaction experiments using the SAMURAI spectrometer.

*Team Leader*

Toshiyuki KUBO

*Members*

Hiromi SATO

*Senior Visiting Scientist*

Toshio KOBAYASHI (Tohoku University)

**Nuclear Physics Research Division  
Experimental Installations Development Group  
Polarized RI Beam Team**

**1. Abstract**

The team conducts the research and development on the production of spin-oriented radioactive-isotope beams (RIBs), and applies it to the research on nuclear physics, fundamental physics, and material science. The microscopic investigation of physical and chemical processes is performed based on nuclear techniques which takes the advantage of intrinsic nuclear properties and phenomena (spins, electromagnetic moments, decay modes etc.). In particular, the precession/resonance of a polarized/aligned nuclear spin under an external field is observed through a change in the angular distribution of radiation, for the study of nuclear structures via nuclear moments. The experimental methods and devices for fundamental physics research with polarized nuclei have been also developed. The same method, as well as the Moessbauer technique, are used for the investigation of condensed matter such as semiconductor, ferromagnets, fullerenes, systems with dilute magnetic impurities etc. by capitalizing radioactive nuclei as microscopic probes into them. All these research activities are to be extended to wide variety of unstable nuclei which RI Beam Factory (RIBF) provides. A method to produce beams of highly polarized radioactive nuclei, taking full advantage of RIBF, is being developed.

**2. Major Research Subjects**

- (1) Nuclear-moment measurements of unstable nuclei
- (2) RIPS upgrade and the development of highly polarized slow RI beams
- (3) Fundamental physics: Study of symmetry
- (4) Condensed matter studies using radioactive nuclear probes

**3. Summary of Research Activity**

- (1) Nuclear-moment measurements of unstable nuclei

It has been revealed in our earlier work that spin-oriented RIBs can be obtained as a function of their outgoing momentum in the projectile-fragmentation reaction. With the obtained spin-polarized nuclei, ground- and excited-state nuclear moments can be determined by means of the  $\beta$ -NMR and TDPAD methods, respectively. Based on these technique, we have recently been conducted the nuclear-moments measurement of neutron-rich *sd*-shell around the neutron magic number  $N=20$ . It has been proposed in this region that an inversion of amplitudes between the *sd* normal and the *pf* intruder configurations would lead to deformation of the ground states. Thus, the region of nuclei is called the *island of inversion*. The measured nuclear moments are expected to provide microscopic properties for those nuclei of interest. The sub-themes are the following:

- Nuclear structure study of neutron-rich aluminum isotopes  $^{30-32}\text{Al}$  on the border of the *island of inversion* and  $^{33-34}\text{Al}$  on/beyond it.
  - Investigation of a new *island of inversion* around  $N=28$ , the nuclear-moment measurements of neutron-rich isotopes.
  - The ground-state electric quadrupole moment measurements of  $^{23}\text{Al}$  for the study of the  $T=3/2$  mirror symmetry.
  - Study of nuclei around Fe region: isospin symmetry study by means of the magnetic moment of the  $10^+$  isomer in  $^{54}\text{Ni}$ , and the study of magicity in the vicinity of  $^{68}\text{Ni}$  through the quadrupole moment of the  $13/2^+$  isomeric state in  $^{69}\text{Cu}$ .
  - Development of a new method to produce highly spin-aligned RIBs and a superconducting-magnet TDPAD system.
- (2) RIPS upgrade and the development of highly polarized slow RI beams

The upgrade of RIPS has been proposed in the phase-II programs. In the cyclotron-cascade acceleration scheme, beams are accelerated up to the energy of  $E=115 A$  MeV with IRC. In this upgrade, the former fragment separator RIPS is equipped with a new beam line that delivers beams of  $115 A$  MeV heavy ions from the IRC cyclotron. RI beams produced by the primary beams at such an intermediate energy are high enough to produce RIBs via projectile-fragmentation reactions and suitably low in energy to be stopped in a sample material of limited thicknesses. Compared with the production yield of RIBs in the present AVF-RRC acceleration scheme, they are drastically increased. The design study of the upgrade program is in progress in our team. We noted that RIBs produced at  $E=115 A$  MeV can be spin-oriented so that the nuclear-moment measurements will be further conducted. Also, combining a new atomic-beam resonance method to combine with fragmentation-based RI beams, which is under development, to this program, highly spin-polarized RI beams will be produced in a low beam-energy region. Then, they could be useful not only for nuclear-moment measurements but also for spin-related subjects in nuclear physics, fundamental physics, and material sciences.

(3) Fundamental physics: Study of symmetry

Nuclear spins of stable and unstable isotopes sometimes play important roles in fundamental physics research. New experimental methods and devices have been developed for studies on the violation of time reversal symmetry ( $T$ -violation) using spin-polarized nuclei. These experiments aim detection of small frequency shift of the spin precession or measurement of the  $T$ -odd angular correlation in  $\beta$ -decay as  $T$ -violating signals arising from new mechanisms beyond the "Standard Model". Sub-themes are the following:

- Precision measurement of spin-precession frequency with a new type of the nuclear spin maser for atomic EDM (Electric Dipole Moment) search.
- Development of a new Mott polarimeter for  $T$ -violation experiment using  $\beta$ -decay of polarized unstable nuclei.

(4) Condensed matter studies using radioactive nuclear probes

Utilizing RI beams as a probe, online Mössbauer spectroscopy and online perturbed angular correlation experiments have been carried out through the  $\gamma$ -ray measurements. The microscopic structures, dynamics in ferromagnets, and properties of semiconductors have been investigated from the deduced internal local fields and the spin relaxation of the probe in materials. The  $\beta$ -NMR/NQR method is also utilized for these condensed matter studies. The methods and apparatus have been developed. Also, basic studies on the probe nuclei have been carried out. Sub-themes are the following:

- Study of "exotic" chemical states and the fast atomic-jump processes in solid with the online Mössbauer spectroscopy of implanted  $^{57}\text{Fe}$
- Development of the on-line perturbed angular-correlation method with  $^{19}\text{O}$  beams as a new probe
- Study of the diffusion and segregation of Fe impurity atoms in Si through in-beam Mössbauer experiment with a Coulomb excited, recoil implanted  $^{57}\text{Fe}$  nuclei.
- Study of the fast diffusion of Cu impurity atoms in Si through  $\beta$ -NMR/NQR with implanted  $^{58}\text{Cu}$ .

*Team Leader*

Masanori WAKASUGI

*Members*

Hideki UENO

Akihiro YOSHIMI

Yuichi ICHIKAWA

Yoshio KOBAYASHI

**Nuclear Physics Research Division**  
**Experimental Installations Development Group**  
**Rare RI-ring Team**

**1. Abstract**

We are developing the isochronous storage ring to measure the mass for rare radioactive isotopes (Rare RI ring). It is assumed that uranium is synthesized by neutron capture process after the supernovae explosion (r-process). To prove r-process, mass measurements for the rare RI are indispensable. To deduce the mass, we measure the circulation time (cyclotron frequency) for the rare RI inside the ring. RI beams produce in RIBF have some energy spread. To compensate the spread, isochronicity inside the ring is indispensable (isochronous storage ring). We will inject the rare RI one by one to the ring (individual injection) to identify the RI event-by-event. To perform the individual injection, we need a long injection line for the ring. The isochronous storage ring and the individual injection are very unique system.

**2. Major Research Subjects**

- (1) Developments of isochronous storage ring to measure mass of rare RI.
- (2) Developments of detectors for mass measurements and the related devices.

**3. Summary of Research Activity**

- (1) Developments of isochronous storage ring to measure mass of rare RI

We are improving conceptual designs for an isochronous storage ring, kicker magnets, and the injection line to the storage ring. The storage ring consists of six sector magnets. The edge angles of each sector magnets compensate the first order isochronism. For the kicker magnets, we fixed rough specifications. For the injection line, we performed the first order ion-optical calculations. Furthermore, we performed magnetic field measurements of a present sector magnet in BigRIPS by using NMR with high accuracy.

- (2) Developments of detectors for mass measurements and the related devices

Thin and fast timing detectors are developed. The group in Saitama University developed thin plastic-scintillators. They found that reasonably good timing resolution can be achieved even in the thin scintillator with 10 micron thickness. The group in University of Tsukuba developed Hybrid Photo Detector (HPD), which can replace with traditional Photo Multi Tube (PMT). Concerning to the related devices for the mass measurements, we started to develop cluster ion-source, that can be used for magnetic field calibrator in the storage ring.

*Team Leader*

Masanori WAKASUGI

*Research Associate*

Yoshitaka YAMAGUCHI

*JRA*

Shinpei NAKAJIMA (Saitama University)

Tetsuaki MORIGUCHI (University of Tsukuba)

*Visiting Scientists*

Akira OZAWA (Inst. Phys., Univ.of Tsukuba)

Yusuke YASUDA (Inst. Phys., Univ.of Tsukuba)

Ichiro ARAI (Inst. Phys., Univ.of Tsukuba)

Takeshi SUZUKI (Saitama University)

Takayuki YAMAGUCHI (Saitama University)  
Takashi OHTSUBO (Niirata University)  
Takashi KIKUCHI (Nagaoka University of Technology)

**Nuclear Physics Research Division**  
**Experimental Installations Development Group**  
**SCRIT Team**

**1. Abstract**

We aim at the investigation of internal nuclear structure of short-lived radioactive nuclei (RI) by means of electron scattering. Electron scattering for RI's has never been performed due to inability to make target of these nuclei. An electron-RI collider system, which requires a huge accelerator complex, has so far been unique solution to overcome the difficulty. We have developed a novel internal target system named SCRIT (Self-Confining RI Ion Target) in an electron storage ring to make the experiment easier with much compact experimental system. An electron accelerator system required in this experiment will be constructed in next year, and the SCRIT device will be completed within the next two years.

**2. Major Research Subjects**

Development of the SCRIT technology and electron scattering for unstable nuclei

**3. Summary of Research Activity**

Development of a novel internal target of unstable nuclei (SCRIT) in an electron storage ring for electron scattering experiment

(Wakasugi, Suda, Ito, Emoto, Nakamura, Kurita, Tamae, Noda, Shirai, Yano)

We have successfully developed a novel internal target system, which is to be used in an electron storage ring. This is named SCRIT (Self-Confining Radioactive Ion Target). This technology can localize specific ions on the electron beam axis using so-called "ion-trapping" phenomenon and form a fixed target of unstable nuclei. This will realize electron-scattering experiments for short-lived nuclei that have never been succeeded in. In the R&D study of the SCRIT at the KSR in Kyoto University, we confirmed that approximately  $10^7$  of  $^{133}\text{Cs}$  ions in the SCRIT device, and the angular distribution of elastically scattered electrons from the trapped Cs ions was measured. The collision luminosity was reached to be  $10^{26}$  / $\text{cm}^2/\text{s}$ , and the feasibility of electron scattering for unstable nuclei was completely demonstrated.

In last year, we moved the electron accelerator system, which consists of a 150-MeV microtron and an electron storage ring, to RIKEN from Sumitomo Heavy Industry Co. Ltd. They will be re-constructed and the SCRIT experimental system will be installed into the storage ring in 2009. We plan to start the electron scattering experiment for unstable nuclei from the beginning of 2011.

*Team Leader*

Masanori WAKASUGI

*Members*

Takashi EMOTO

**Nuclear Physics Research Division  
Experimental Installations Operation Group  
GARIS Team**

**1. Abstract**

Development and maintenance of devices related to study of the superheavy elements.

**2. Major Research Subjects**

- (1) Maintenance and development of a recoil separator.
- (2) Development of rapid chemistry devices.

**3. Summary of Research Activity**

- (1) Maintenance and development of recoil separator

A gas-filled recoil separator has been used as a main experimental device for the study of superheavy elements. We will develop and maintain the related devices. We will also offer user-support if a researcher wishes to use the devices for his/her own research program.

- (2) Development of devices for fast chemistry

We do research and development of devices for fast chemistry of superheavy elements. We also offer user-support for potential users.

*Team Leader*

Kouji MORIMOTO

*Members*

Kosuke MORITA

Daiya KAJI

Akira YONEDA

**Nuclear Physics Research Division  
Experimental Installations Operation Group  
BigRIPS Team**

**1. Abstract**

This team is in charge of design, construction, development and operation of BigRIPS in-flight separator and its related research instruments at RI beam factory (RIBF). They are employed not only for the production of RI beams but also the experimental studies using RI beams.

**2. Major Research Subjects**

Design, construction, development and operation of BigRIPS in-flight separator, RI-beam transport lines, and their related research instruments

**3. Summary of Research Activity**

This team is in charge of design, construction, development and operation of BigRIPS in-flight separator, RI-beam transport lines, and their related research instruments such as ZeroDegree spectrometer at RI beam factory (RIBF). They are employed not only for the production of RI beams but also various kinds of experimental studies using RI beams.

The research subjects may be summarized as follows:

- (1) General studies on RI-beam production using in-flight scheme.
- (2) Studies on ion-optics of in-flight separators, including particle identification of RI beams
- (3) Simulation and optimization of RI-beam production.
- (4) Development of beam-line detectors and their data acquisition system.
- (5) Experimental studies on production reactions and unstable nuclei.
- (6) Experimental studies of the limits of nuclear binding.
- (7) Development of superconducting magnets and their helium cryogenic systems.
- (8) Development of a high-power production target system.
- (9) Development of a high-power beam dump system.
- (10) Development of a remote maintenance and remote handling systems.
- (11) Operation, maintenance and improvement of BigRIPS separator system, RI-beam transport lines, and their related research instruments such as ZeroDegree spectrometer and so on.
- (12) Design and construction of high-resolution beam line at RIBF.

*Team Leader*

Toshiyuki KUBO

*Members*

Naohito INABE  
Atsushi YOSHIDA  
Koichi YOSHIDA  
Masao OHTAKE  
Yoshiyuki YANAGISAWA

*Contract Researchers*

Kensuke KUSAKA  
Tetsuya OHNISHI

*Research Associates*

Naoki FUKUDA  
Hiroyuki TAKEDA  
Daisuke KAMEDA  
Kanenobu TANAKA

*Part-time Staff*

Hidekazu KUMAGAI

*JRA*

Yoshiko SASAMOTO

*Student*

Masafumi MATSUSHITA

*Senior Visiting Scientist*

Susumu SHIMOURA (CNS, Grad. Sch. Sci., Univ. of Tokyo)

*Visiting Scientist*

Bradly SHERRILL (NSCL, Michigan State Univ., USA)  
Daniel BAZIN (NSCL, Michigan State Univ., USA)  
Anthony NETTLETON (NSCL, Michigan State Univ., USA)  
Hans GEISSEL (GSI, Germany)  
Martin WINKLER (GSI, Germany)  
Michael FAMIANO (Western Michigan Univ., USA)  
Shashikant MANIKONDA (Argonne National Lab., USA)  
Yutaka MIZOI (Osaka Electro-Communication Univ.)

**Nuclear Physics Research Division  
Experimental Installations Operation Group  
Computing and Network Team**

**1. Abstract**

Development, management and operation of the computing and network environment, mail server and data acquisition system and control of the information security of the Nishina Center for Accelerator-Based Science.

**2. Major Research Subjects**

- (1) Development, management and operation of the computing
- (2) Development, management and operation of the mail server
- (3) Development, management and operation of the data acquisition system
- (4) Development, management and operation of the network environment
- (5) Control of the information security

**3. Summary of Research Activity**

Development, management and operation of the computing and network environment, mail server and data acquisition system and control of the information security of the Nishina Center for Accelerator-Based Science

*Team Leader*

Takashi ICHIHARA

*Member*

Yasushi WATANABE

Hidetada BABA

**Nuclear Physics Research Division  
Experimental Installations Operation Group  
Detector Team**

**1. Abstract**

This team is in charge of organizing various detector developments performed at in-house laboratories and groups, in order to improve mutual share of knowledge and experience. The team is also in charge of development and operation of cryogenic target systems used for nuclear physics experiments.

**2. Major Research Subjects**

- (1) Development of delay-line PPAC.
- (2) Development of transmitter/receiver for fast signal transmission through optical fibers.
- (3) Design study of a micro strip silicon detector.
- (4) Development and operation of cryogenic hydrogen and helium targets.

**3. Summary of Research Activity**

This team is presently focusing on developments of delay-line PPAC and fast signal transmission system consisting of optical fiber and a pair of fast transmitter and receiver. These two developments are essential for particle identification at BigRIPS separator and ZeroDegree spectrometer at RI Beam Factory (RIBF). The team is also in charge of development and operation of cryogenic target systems.

(1) Delay-line PPAC

At BigRIPS and ZeroDegree, a purity of radioactive isotope (RI) beams is as low as 10% or less at medium and heavy mass region. Thus, development of detectors for high-rate use is one of goals in this team. With this respect, we have developed a position-sensitive Parallel Plate Avalanche Counter (PPAC). Delay-line read-out technique appropriate for high rate use is employed for position determination. This PPAC has two stripped-electrodes for both horizontal and vertical positions, and this configuration leads to high performance in terms of efficiency as well as position resolution. More than ten PPACs have been installed at BigRIPS and ZeroDegree, and successfully used for RI-beam production and experiments.

(2) Fast transmitter and receiver for optical fiber.

In general co-axial metal wires are used for fast signal transmission. Instead, we have developed a special circuit for fast signal transmission through optical fibers, which consists of a pair of fast transmitter and receiver with a semiconductor laser and photo diode. At RIBF, circuits for detectors are located at several focal planes of the BigRIPS and ZeroDegree, and distances between focal-planes and counting room are as long as 100 m. The use of optical fibers for signal transmission allows us to focus on a common ground at each focal plane and easily isolate the ground levels.

The circuit has a fast time response of more than 1GHz. Attenuation of signal amplitudes is negligibly small even at a long distance transmission of more than 100m. Many sets of transmitter/receiver with an optical fiber have been manufactured and installed for detectors at BigRIPS and ZeroDegree, and successfully used for RI-beam production and experiments. This fast signal transmission scheme will be standard at RIBF.

(3) Design study of a micro strip silicon detector that will be used for SAMURAI spectrometer.

(4) Development and operation of cryogenic targets for nuclear physics experiments.

Development and operation of cryogenic targets, such as liquid hydrogen and helium targets and a solid hydrogen target, are very important for nuclear physics experiments using RI beams at BigRIPS and RIBF.

*Team Leader*  
Toshiyuki KUBO

*Members*

Ken-ichiro YONEDA

*Contract Researcher*

Kanenobu TANAKA

Meiko UESAKA

*Senior Visiting Scientist*

Hirohiko SHIMIZU (Inst.of Materials Structure Sci., KEK)

**User Liaison and Support Division**  
**User Liaison and Support Group**  
**User Support Office**

**1. Abstract**

The RIKEN RI Beam Factory is the world preeminent facility providing the greatest opportunities for scientific researches. The facility, completed its construction in 2007, has started its full-scale operation in the end of the year 2008. It is our important mission to serve for a broad range of application of a large variety of researchers so that we bring out the best performance of the RI Beam Factory. We manage to facilitate the use of RI Beam Factory to the researchers both inside and outside of RIKEN, to support experiments using the accelerator complex, to exploit industrial application researches, and to promote the RI Beam Factory to interested researchers

**2. Major Research Subjects**

- (1) Facilitation of the use of the RI Beam Factory
- (2) Support of experiments in the RI Beam Factory
- (3) Promotion of the RI Beam Factory to interested researchers

**3. Summary of Research Activity**

In order to facilitate the use of RI Beam Factory to the researchers both inside and outside of RIKEN, we have organized international Program Advisory Committee, consisting of world leading scientists, to review proposals, purely based on their scientific merit and feasibility, in the fields of nuclear physics (NP) and material-and-life science (ML). The NP- and ML-PAC meetings are organized twice a year.

*Team Leader*

Toshimi SUDA

*Members*

Mieko KOGURE

*Technical Staff I*

Narumasa MIYAUCHI

*Assistant*

Tomoko IWANAMI

Yuri TSUBURAI

**User Liaison and Support Division  
User Liaison and Support Group  
Industrial Cooperation Team**

**1. Abstract**

The scope of the industrial cooperation team includes industrial application of RIBF facility and research and development for industrial application of accelerator associated technologies.

**2. Major Research Subjects**

Distribution of radioisotopes Zn-65 and Cd-109 produced at RIKEN AVF Cyclotron and investigation of novel industrial applications of the accelerator beam and its related technologies

**3. Summary of Research Activity**

(1) Charged distribution of radioisotopes

At RIBF, various specific radioisotopes for research have been produced with the cyclotrons and used for various research projects. Since October 2007, we have distributed radioisotopes Zn-65 and Cd-109, which are produced by the RI application team at the AVF cyclotron, to nonaffiliated users under a Material Transfer Agreement between Japan Radioisotope Association and RIKEN.

(2) Feasibility study of RI-beam application in industries

To study feasibility of application of RI beam to industrial fields, research collaboration is being arranged with a private company.

*Team Leader*

Tadashi KAMBARA

*Members*

Tomoko ABE

Hiroshige TAKEICHI

*Visiting Scientists*

Makiko KAGA (National Inst. of Mental Health, Natl. Ctr. Neurol. Psychiat.)

Atsuko GUNJI (National Inst. of Mental Health, Natl. Ctr. Neurol. Psychiat.)

Michiteru KITAZAKI (Res. Center for Future Vehicle. Toyohashi Univ. of Tech.)

*Student Trainees*

Kouta ARAI (Sakushin Gakuin Univ.)

Shinichiro HARIYAMA (Dept. of Knowledge-based Information Eng., Toyohashi Univ. of Tech.)

Shinichi ONIMARU (Dept. of Knowledge-based Information Eng., Toyohashi Univ. of Tech.)

## **Sub Nuclear System Research Division Radiation Laboratory**

### **1. Abstract**

Nucleons, such as protons and neutrons, are a bound state of constituent quarks glued together with gluons. The detail structure of nucleons, however, is not well understood yet. Especially the mechanism to build up the spin of proton, which is  $1/2$ , is a major problem in physics of the strong force. The research goal of Radiation Laboratory is to solve this fundamental question using the first polarized-proton collider, realized at RHIC, Brookhaven National Laboratory (BNL) in USA. RHIC stands for Relativistic Heavy Ion Collider, aiming also to create Quark Gluon Plasma, the state of Universe just after the Big Bang. RIKEN-BNL Research Center (RBRC) directed by N. Samios carries our core team at BNL for those exciting researches. Recent data analysis has shown that the proton spin carried by gluons is indeed small, which is a very striking finding beyond our expectations. We have been doing other pioneering researches at the domestic accelerators at SPring-8 and High Energy Accelerator Research Organization (KEK) which is now preceded to the new experiment at J-PARC. We are also performing technical developments such as novel ion sources, super conducting detectors, fine pitch pixel detectors and neutron optical devices.

### **2. Major Research subjects**

- 1) Spin physics with relativistic polarized-proton collisions at RHIC
- 2) Study of nuclear matter at high temperature and/or at high density
- 3) Technical developments on radiation detectors and accelerators

### **3. Summary of Research Activity**

- (1) Experimental study of spin structure of proton using RHIC polarized proton collider  
[See: RIKEN-BNL Research Center Experimental Group]
- (2) Experimental study of quark-gluon plasma RHIC heavy ion collider  
[See: RIKEN-BNL Research Center Experimental Group]
- (3) Study of properties of mesons and exotic hadrons with domestic accelerators

Hadrons with more than three quarks are of great interest and have been looked for over the past 30 years. The  $Q^+$  is a genuine exotic baryon with the minimum quark configuration of  $u, u, d, d$  and anti- $s$ . After the first report on the evidence of the  $Q^+$  at SPring-8/LEPS in 2002, evidence and counterevidence have been reported from all over the world, but its existence is not conclusive yet. We have made effort to establish the  $Q^+$  since our first report. This year we reported again the observation of the  $Q^+$  with clean and high statistics data at SPring-8/LEPS [Phys.Rev.C 79, 025210 (2009)]. In order to establish the  $Q^+$  and explore the world of multi-quark hadrons, R & D work is underway to construct LEPS-II, which is a new beam line and detectors at SPring-8.

Besides the  $Q^+$ , there is a long standing problem on the internal structure of the  $L(1405)$ , whether 3 quarks, meson-baryon molecule or 5 quarks. In 2008, we measured the cross section of  $L(1405)$  photoproduction for the first time in the world. The data show strong enhancement near production threshold, and may suggest contributions of exotic production mechanisms related to the meson-baryon molecular structure of the  $L(1405)$  [PRC 78, 035202 (2008)].

Preparation of the experiment E16 at J-PARC 50-GeV PS is ongoing to obtain the full approval by PAC. The experiment aims to perform the systematic study of the mass modification of low-mass vector mesons in nuclei to explore the chiral symmetry in nuclear matter. GEM tracker and hadron-blind Cherenkov counter are being developed for the experiment. Required position resolution, approximately 100 micro meters, was achieved with a newly-developed flexible read-out board in a beam test of the tracker.

- (4) Study of Accelerator and Ion source

To achieve highly polarized beams in RHIC it is necessary to understand the AGS (RHIC injector

synchrotron) spin dynamics. The normal-conducting partial-snake magnet, which we have developed for AGS years ago, is now in a stable operation with the other super-conducting snake magnet in AGS. After the departure of Researcher M. Okamura to BNL, this research category is moved to the collaborative work with BNL. Major equipments were transferred to BNL and became operational to continue the development of ion source with direct plasma injection scheme, with helps of two of our students.

#### (5) Detector development for PHENIX experiment

We have been developing the silicon vertex tracker (VTX) in order to enhance physics capability of the PHENIX detector at RHIC. It consists of two inner layers of pixel detectors and two outer layers of strip detectors. RIKEN Radiation Laboratory group is responsible for the ladder fabrication of the pixel detector. The production of high-signal-density low-material-budget flexible printed circuit board (bus) was started followed by a check procedure using dedicated test equipments. Prototype of the ladder was assembled on the fabricated bus and showed its functionality within the full PHENIX data acquisition chain. Also the assembly procedure with 10-micron accuracy was established

We also have been developing the momentum-sensitive trigger system for the PHENIX muon arms under the collaboration with KEK, Kyoto and Rikkyo University. About 200 circuit boards for the new trigger system were installed to a half of the muon arm acceptance and they are planned to be commissioned during the experiment in 2009.

#### (6) Research and development of superconductor radiation detectors

Superconductor radiation detectors are able to measure the energies of photons with a much better resolution than any type of conventional detectors. They are capable of detecting photons over a wide energy range and also charged particles. We have been developing superconducting tunnel junctions (STJs) as high-resolution radiation detectors. This year, we continued the collaborations between KEK and University of Tsukuba. With KEK, we succeeded in fabricating Aluminum-based-STJ (Al-STJ) which was free from a damage due to heat cycle. The sub-gap current of these STJs were almost uniform and they were consistent with calculated values from the BCS theorem. With Univ. of Tsukuba, we continued to study basic fabrication methods in order to make Hafnium-based-STJ (Hf-STJ). We found that Hf can be etched with ICP reactive etching method. An obtained etching speed was 31nm/min and this is enough to fabricate Hf film. We have started to make Hf-STJ structure. So far, unfortunately, we don't succeed in fabricating proper tunnel junctions.

We have decided to close this activity in Radiation Laboratory and transferred all the equipments to KEK. Our technologies to fabricate STJ are inherited by KEK and Univ. of Tsukuba.

#### (7) Neutron optics

Cold or thermal neutron beam is a high-sensitivity probe to study not only the structure of condensed matter, but also nuclear and particle physics. However, its realistic applications are still limited since the numbers of available neutron sources are small and their intensities are low. This project aims to enhance the efficiency in using those precious neutron beams by improving the neutron beam optics, in order to maximize scientific outputs within a short period of time. Base on the developed technologies, devices are fabricated and distributed to other laboratories and universities by "Riken Venture Company", Japan Neutron Optics Inc.

This year, we successfully observed the first signal for fundamental physics research in a new beam line at 1MW Pulse Spallation Neutron Source in J-PARC. This beam line was designed by applying our knowledge and technique of neutron optics. We also succeed to observe interference signals of cold neutrons using the Si crystal interferometer at JRR-3M. There, we are developing a new type of instrument for phase-difference imaging with use of the gratings developed by us. We are also planning to study neutron Electron Dipole Moment using a perfect crystal at the J-PARC beam line.

#### (8) Theoretical study of hadron physics

Nuclear matter at finite temperature and density was studied in lattice simulations of quantum chromodynamics (QCD) which is the first principle to describe the interactions of quarks and gluons. Several

experimental properties of a QCD phase transition from a hadronic matter to quark-gluon plasma, suggested by relativistic heavy-ion experiments at RHIC, were investigated with calculations of Polyakov-loop and quark number susceptibilities. A new approach to calculate the equation of state was derived and developed in the full-QCD simulations which include dynamical quarks of up, down and strange flavors.

Strong correlation in QGP was also studied in the lattice QCD simulation. Calculating correlation functions between Polyakov-loop operators, the free energy and potential between heavy quarks were extracted and confinement properties before and after the deconfinement transition and screening effects in the electric and magnetic sectors were investigated. Dissociation temperature of a charmonium bound state in QGP was also investigated in a multi-state variational analysis.

The fragmentation functions for the proton and the pion are studied using the Nambu-Jona-Lasinio (NJL) model. The Drell-Levy-Yan (DLY) relation, which connects the fragmentation functions with the quark distribution functions, is used to select the diagrams. The calculated fragmentation functions are  $Q^2$  evolved to be compared with the results of global analyses. The calculation gives too small fragmentation functions both for protons and pions. It is also found that the DLY relation could be violated by the cut-off procedure and the  $Q^2$  evolution may develop a singularity at  $x=1$ . Attempts to improve the choice of diagrams are now in progress.

In connection with the hot QCD, the particle emission and absorption in a uniformly accelerated frame are studied. The canonical quantization for the Maxwell field is formulated in general static space-time geometries and is applied to the case of the Rindler space-time corresponding to the uniformly accelerated frame. The Unruh effect is confirmed and its implications to RHIC physics are discussed. The effects of the uniform acceleration on the Coulomb potential are also studied and the possible ways of observing them in the hydrogen spectra are discussed.

*Head*

Hideto EN'YO

*Members*

Yasuyuki AKIBA

Yuji GOTO

Itaru NAKAGAWA

Yoshie OTAKE

Hiromi SATO

Atsushi TAKETANI

Yasushi WATANABE

Satoshi YOKKAICHI

*Special Postdoctoral Researchers*

Yoshinori FUKAO

Masayuki NIYAMA

*Contract Researchers*

Kazuya AOKI

Ryo ICHIMIYA

Kohei FUJIWARA

Maki MUROSAWA

Kenichi NAKANO

Tomoaki NAKAMURA

Yu MAESAWA

Yoshiyuki ONUKI  
Marco STRATMANN

*Research Consultant*  
Katsuya HIROTA

*Senior Visiting Scientists*

Ken-ichi IMAI (Grad. Sch. of Sci., Kyoto Univ.)  
Toshiaki SHIBATA (Grad. Sch. of Sci. and Eng., Tokyo Inst. of Tech. Sch. of Sci.)  
Hirohiko SHIMIZU (Inst. of Materials Structure Sci., KEK)  
Toshio SUZUKI (Grad. Sch. of Sci., Kanazawa Univ.)  
Koichi YAZAKI (Tokyo Woman's Christian Univ.)  
Takashi NAKANO (RCNP, Osaka Univ.)

*Visiting Scientists*

Tomohiro ADACHI (DAI-ICHI KIDEN CO.,LTD)  
Christine A. AIDALA (Univ. Massachusetts, Amherst, USA)  
Alexander BAZILEVSKY (BNL, USA)  
Wolfgang BENTZ (Tokai Univ.)  
Mickey CHIU (Univ. of Illinois at Urbana, USA)  
Ondrej CHVALA (Univ. of California at Riverside)  
Takumi DOI (University of Kentucky)  
Dipanwita DUTTA (Nuclear Physics Division, Bhabha Atomic Research Centre)  
Seishi DAIRAKU (Grad. Sch. of Sci., Kyoto Univ.)  
Waled EMAM (Univ. of California at Riverside, USA)  
Frank ELLINGHAUS (Univ. of Colorado, USA)  
Hirotsugu FUJII (Grad. Sch./College of Arts and Sciences, Univ. of Tokyo)  
Hisako FUJIMURA (Facul. Sci., Kyoto Univ.)  
Kenji FUKUSHIMA (YITP, Kyoto Univ.)  
Haruhiko FUNAHASHI (Grad. Sch. of Sci., Kyoto Univ.)  
Takashi HACHIYA (Private Company)  
Yuji HASEGAWA (Wien Inst. Tech.)  
Tetsuo HATSUDA (Grad. Sch. of Sci., Univ. of Tokyo)  
Toshiyuki HATTORI (Res. Lab. for Nuclear Reactors, Tokyo Inst. of Tech. Sch. of Sci.)  
Masashi HAZUMI (KEK)  
Takeo HIGUCHI (KEK)  
Masanori HIRAI (Grad. Sch. of Sci. and Eng., Tokyo Inst. of Tech.)  
Kensuke HONMA (Grad. Sch. of Sci., Hiroshima Univ.)  
Takuma HORAGUCHI (Grad. Sch. of Sci., Hiroshima Univ.)  
Kazuaki IKEDA (AIST)  
Katsuya ISHIGURO (Grad. Sch. of Natural Sci. & Tech., Kanazawa Univ.)  
Noriyoshi ISHII (Grad. Sch. of Pure and Applied Sci., Univ. of Tsukuba)  
Hirokazu ISHINO (Tokyo Inst. Tech.)  
Barbara JAGER (KEK)  
Robert JAMESON (Goethe Universitat Frankfurt, Germany)  
Takeshi KANESUE (Kyushu Univ.)  
Masashi KANETA (Grad. Sch. of Sci., Tohoku Univ.)  
Hirotsugu KASHIWAGI (Takasaki Advanced Radiation Res. Inst., JAEA)  
Takeo KAWASAKI (Grad. Sch. of Sci. and Tech., Niigata Univ.)

Akio KIYOMICHI (J-PARC, JAEA)  
Yuji KOIKE (Grad. Sch. of Sci. & Tech., Niigata Univ.)  
Dmitiri KOTCHETKOV (Univ. New Mexico, USA)  
Shunzo KUMANO (Inst. of Particle and Nuclear Studies, KEK)  
Teiji KUNIHURO (Yukawa Inst. for Theoretical Phys., Kyoto Univ.)  
Masahiko KURAKADO (Osaka Electro-Communication Univ.)  
Han LIU (Phys. Dept., New Mexico State Univ.)  
Ming XIONG LIU (Los Alamos Nat. Lab., USA)  
Yoshikazu MAEDA (RCNP, Osaka Univ.)  
Keisuke MAEHATA (Fac. of Eng., Kyushu Univ.)  
Yajun MAO (Peking Univ., China)  
Yasuo MIAKE (Grad. Sch. of Pure and Applied Sci., Univ. of Tsukuba)  
Tsutomu MIBE (KEK)  
Kenji MISHIMA (KEK)  
Yoshiyuki MIYACHI (Tokyo Inst. Tech.)  
Osamu MORIMATSU (Inst. of Particle and Nuclear Studies, KEK)  
Takahiro MORISHIMA (KEK)  
Hiroaki MYOREN (Grad. Sch. of Sci. & Eng., Saitama Univ.)  
Yoshifumi NAKAMURA (DESY, Germany)  
Atsushi NAKAMURA (Information Media Center, Hiroshima Univ.)  
Masashi OHNO (Sch. of Eng., Univ. of Tokyo)  
Munehisa OHTANI (Inst. fuer Theoretische Physik, Universitact Regensburg, Germany)  
Hiromi Okada (KEK)  
Masahiro OKAMURA (BNL, USA)  
Petra RIEDLER (CERN, Switzerland)  
Naohito SAITO (J-PARC, KEK)  
Shoichi SASAKI (Grad. Sch. of Sci., Univ. of Tokyo)  
Shin-ya SAWADA (Inst. of Particle and Nuclear Studies, KEK)  
Michiko SEKIMOTO (Inst. of Particle and Nuclear Studies, KEK)  
Kenta SHIGAKI (Grad. Sch. of Sci., Hiroshima Univ.)  
Prashant SHUKLA (Nuclear Physics Division, Bhabha Atomic Research Centre)  
Kazutaka SUDO (Inst. of Particle and Nuclear Studies, KEK)  
Toru SUGITATE (Grad. Sch. of Sci., Hiroshima Univ.)  
Mizuki SUMIHAMA (RCNP, Osaka Univ.)  
Kazutaka SUMISAWA (KEK)  
Toru TAINO (Grad. Sch. of Sci. & Eng., Saitama Univ.)  
Osamu TAJIMA (KEK)  
Junpei TAKANO (KEK)  
Manobu TANAKA (Inst. of Particle and Nuclear Studies, KEK)  
Kiyoshi TANIDA (Grad. Sch. of Sci., Kyoto Univ.)  
Kazuo TANIGUCHI (Fac. of Eng., Osaka Electro-Communication Univ.)  
Hisayuki TORII (Grad. Sch. of Sci., Hiroshima Univ.)  
Yutaka USIHIRODA (KEK)  
Shizui WATANABE (Tokyo Metropolitan College of Aeronautical Engineering)  
Imuran YOUNUS (Univ. of New Mexico, USA)

*Research Fellow*

Toru SEKIDO (Grad. Sch. of Natural Sci. & Tech., Kanazawa Univ.)

Yoshichika SEKI (Grad. Sch. of Sci., Kyoto Univ.)  
Seishi DAIRAKU (Grad. Sch. of Sci., Kyoto Univ.)

*Students*

*Junior Research Associate*

Yoki ARAMAKI (CNS, Univ. Tokyo)  
Masatoshi HAMADA (Fac. of Sci., Kyushu Univ.)  
Kimiaki HASHIMOTO (Fac. of Sci., Rikkyo Univ.)  
Kenichi KARATSU (Fac. of Sci., Kyoto Univ.)  
Kentaro MIKI (Inst. Phys., Univ. Tsukuba)  
Misaki OUCHIDA (Facul. Science, Facul. Sci. Hiroshima Univ.)  
Satoshi SANO (CNS, Univ. Tokyo)  
Kohei SHOJI (Grad. Sch. of Sci., Kyoto Univ.)  
Jun TAMURA (Grad. Sch. at Nagatsuta, Tokyo Inst. Technol.)  
Yorito YAMAGUCHI (CNS, Univ. Tokyo)

*Intern*

Hikaru KOUNO (Fac. of Sci., Rikkyo Univ.)  
Kazushi TSUKADA (Fac. of Sci., Rikkyo Univ.)

*Student Trainees*

Satoshi ADACHI  
Kazutaka AOKI (Grad. Sch. of Sci. & Eng., Saitama Univ.)  
Yosuke HAKI (Fac. of Sci., Rikkyo Univ.)  
Yusuke FUJISAWA (Grad. Sch. of Sci. & Eng., Saitama Univ.)  
Taku ITO (Grad. Sch. of Sci. and Eng., Tokyo Inst. of Tech.)  
Yoshihiro IWANAGA (Facul. Science, Facul. Sci. Hiroshima Univ.)  
Miki KASAI (Coll. Sci., Rikkyo Univ.)  
Yuuji KATOU (RCNP, Osaka Univ.)  
Kotaro KIJIMA (Grad. Sch. of Sci., Hiroshima Univ.)  
Kouichi MATSUBARA (Grad. Sch. of Sci. & Eng., Saitama Univ.)  
Nathan MEANS (Dept. of Physics, SUNY at Stony Brook)  
Shinji MOTOKI (Grad. Sch. of Biosphere Sci., Hiroshima Univ.)  
Yoshihide NAKAMIYA (Grad. Sch. of Sci., Hiroshima Univ.)  
Katsuro NAKAMURA (Facul. Sci., Kyoto Univ.)  
Masaya NIHASHI (Facul. Science, Facul. Sci. Hiroshima Univ.)  
Kentaro NISHIMURA (Univ. Tokyo)  
Atsushi OKAMURA (Facul. Sci., Kyoto Univ.)  
Koichi SAKASHITA (Tokyo Inst. Technol.)  
Shinkuro SATO (Inst. Phys., Univ. Tsukuba)  
Takahiro SAWADA (RCNP, Osaka Univ.)  
Maya SHIMOMURA (National Inst. of Advanced Industrial Sci. and Tech.)  
Satoru UEDA (Grad. Sch. of Pure and Applied Sciences, Univ. of Tsukuba)

*Technical Staff*

Junpei KANAYA

*Secretaries*

Noriko KIYAMA  
Yoko SAKUMA

## **Sub Nuclear System Research Division Advanced Meson Science Laboratory**

### **1. Abstract**

Particles like muons, pions, and kaons have finite life times, so they do not exist in natural nuclei or matters. Implanting these particles into nuclei/matters, exotic phenomena in varieties of objects can be studied from a new point of view.

Kaon is a second lightest meson which has strange-quark as a constituent quark. It is expected that if one embed a kaon into nuclei, the sizes of the nuclei become smaller and forms a high density object beyond the normal nuclear density. Study of this object could lead better understanding of the origin of the mass of the matter, and may reveal the quark degree of freedom beyond the quark-confinement. Those properties can be studied by precise heavy pionic atom research in different angle. The other example is the weak interaction in nuclear matter. It can only be studied by the weak decay of hypernuclei, which have Lambda particle in the nuclei,

Muon provides even wider variety of study from nuclear reaction to magnetism in matter. For instance, stopping positively charged muon in a material, we obtain information on the magnetic properties or the local field at the trapped site. Injecting negatively charged muon to mixture of deuterium and tritium, muon attracts surrounding atoms and is known to cause d-t fusions.

As is already clear, in our research we introduce different kind of impurities into nuclei/matters, and study new states of matter, new phenomena, or the object properties.

### **2. Major Research Subjects**

- (1) Study of meson property and interaction in nuclei
- (2) Origin of matter mass / quark degree of freedom in nuclei.
- (3) Condensed matter and material studies with muon
- (4) Nuclear physics via muon catalyzed fusion and muonic atoms

### **3. Summary of Research Activity**

#### **Hadron physics at J-PARC and RIKEN-RIBF**

Kaon and pion will shed a new insight to the nuclear physics. The recent discovery of deeply bound pionic atom enables us to investigate the properties of mesons in nuclear matter. At RIKEN-RIBF, we are preparing precise experimental study of the pionic atom. We are intensively preparing another next generation kaon experiments (E15 and E17) at J-PARC as day-one experiments. In these experiments, we are aiming at precise determination of the KN interaction, and clarify the nature of kaon in nuclei. By these experiments, we aim to be a world-leading scientific research group using these light meta-stable particles.

- 1) Deeply bound kaonic nuclei

We have performed a high precision and small ambiguity spectroscopy on the K-ppn system, strange tribaryon  $-S^{\circ}(3115)-$ , at KEK (High energy accelerator research organization). We measured the momenta of protons emitted in the reaction between negatively charged K mesons and helium nuclei. Compared to the previous experiment, the mass resolution was improved by a factor of 2 and the statistical accuracy by a factor of about 10. We have newly installed detectors exclusively used for the measurement of the protons and realized small-ambiguity experiment. As a result, no structure was observed, in the spectrum, associated to the strange tribaryon with the natural width of  $20 \text{ MeV}/c^2$ , and the result was contradictory to the previous experiment. Statistical evaluation tells that the previous results are rejected by 99% confidence level. The experiment also tells us that the difficulty of the bound state search using at rest reaction, in which non-mesonic two-nucleon absorption reactions produce huge energetic nucleon background in the energy region of interest. This two-nucleon absorption process also caused the absorption width of the kaonic bound state. Thus we proceed the search of the state in the simplest system K-pp at the kaon incident momentum of 1

GeV/c as a day-one experiment at J-PARC.

2) Deeply bound pionic and eta- nuclei

We made a spectroscopy experiment to measure deeply bound pionic states in several tin isotopes at the GSI, Germany, to investigate the pion-nucleus strong interaction. The results provided information on the iso-vector part of the strong interaction between pion and nucleus. More advanced discussion leads to the origin of the mass of matter, which is attributed to the quark condensation in the vacuum. Presently we have been working on preparation for the experimental study of pionic atoms at RIKEN-RIBF.

3) Precision X-ray measurement of kaonic atom

Simultaneously with the above experiment (1), we have performed an X-ray spectroscopy of atomic  $3d \rightarrow 2p$  transition of negatively charged K mesons captured by helium atoms. Many Kaonic atoms are known to be measured with various elements, however, there are very large deviations in the measured energy levels for the helium (and the oxygen) from the systematic expectations. The deviation originates in technical issues in old experiments, and new and high precision data have been long awaited for. Also, wave functions of the Kaonic atoms are expected to reflect the information on the existence of the inner structure, namely deeply bound Kaonic states. As a result of the experiment, we have succeeded in performing the spectroscopy and achieved the shift of  $2+2(\text{stat.}) +2(\text{syst.})$  eV. The obtained results reject older data beyond any doubt, and the above deviation is dissolved. Presently, aiming at the determination of the level width and yield, we are analyzing the data. To clarify the KN interaction strength, we are preparing another x-ray measurement of the kaonic helium-3 atom, which is another day-one experiment at J-PARC.

**Muon science at RIKEN-RAL branch**

The research area ranges over particle physics to condensed matter studies and life science. Our core activities are based on the RIKEN-RAL Muon Facility located at the Rutherford Appleton Laboratory (UK), which provides the most intense pulsed muon beam. We have variety of important research activities such as muon-catalyzed fusion (mCF) and condensed matter physics by muon spin rotation / relaxation / resonance (mSR).

(A) Condensed matter/materials studies with mSR

A major upgrade work for mSR facility is being carried out at RIKEN-RAL muon facility reflecting growing number of collaborations with other universities and research institutes in this field. A pulsed laser system, which consists of a Nd:YAG laser and an OPO laser, was installed under collaboration between the University of Yamanashi, KEK, and RIKEN. The laser system is now used for the mSR to study effects induced by intense photon field, such as spin polarization of conduction electrons in semiconductors. A new mSR spectrometer, which will enable us to study a sample under multiple-extreme condition, was built and is about to be installed in the beam area.

There are three topics of material sciences studied by the muon-spin relaxation method at the RIKEN-RAL Muon facility in 2008.

1) The dynamics of the charge transfer in an ion mixed-valence complex,  $(n\text{-C}_3\text{H}_7)_4\text{N}[\text{Fe}^{\text{II}}\text{Fe}^{\text{III}}(\text{dto})_3]$  ( $\text{dto}=\text{C}_2\text{O}_2\text{S}_2$ ), has been investigated. The oscillation of an electron with slow frequency of the order of kHz in between two iron sites has been firstly observed and quantitative value of the frequency has been achieved.

2) The dynamics of the internal field at the muon site in the high- $T_c$  superconducting oxide,  $\text{La}_{2-x}\text{Sr}_x\text{CuO}_4$ , has been investigated by precise mSR measurements. A change of the dynamics of the internal field at higher temperature than the superconducting and magnetic transition temperatures has been observed. A model-relationship with a spin-gap state which is important to describe the superconducting gap of high- $T_c$  oxides has been suggested.

3) A co-existing relationship between a magnetically ordered state and the superconducting state in a newly found Fe-based superconducting oxide has been clarified. An important role of the magnetism for the superconductivity has been suggested.

(B) Nuclear physics studies with muons, such as muon catalyzed fusion and muonic atoms

1) Muon catalyzed fusion (mCF)

We are studying the muon catalyzed fusion (mCF) processes in a wide range of hydrogen target conditions such as isotope mixtures and temperatures. This year we designed a test high pressure target, which will enable us to keep D<sub>2</sub> target in solid state up to 30 K, thus we will be able to study mCF in high density and high temperature solid target, where the mCF is expected to occur much faster than in liquid.

2) Development towards muonic atom formation with unstable nuclei

Stopping negative muons in the solid hydrogen with implanted unstable atoms, muons transfer efficiently to the implanted nuclei from muonic hydrogen to form the muonic atoms. By observing muonic X-rays at muonic atom formations, fundamental experiments on the nuclear charge density distribution are in progress. Using the newly installed surface ionization ion source, we carried out successfully the experiment to measure isotope energy shifts of muonic X-rays originated from muonic <sup>86</sup>Sr, <sup>88</sup>Sr, <sup>88</sup>Sr, <sup>138</sup>Ba, <sup>148</sup>Sm and <sup>152</sup>Sm atoms.

3) Generation of ultra slow positive muon beam

Low energy muon beam, whose kinetic energy is variable from a few keV to a few tens of keV, will extend the scope of mSR technique from a bulk material to surfaces and multi-layered materials. It is also expected that a very sharp beam of low energy muon may enable a new way of precision measurement of muon's anomalous gyro-magnetic ratio (*g*-2). Following the successful generation of slow muon beam by laser ionization of thermally emitted muonium in vacuum, we plan to increase the slow muon beam intensity by more than 100 times. For this purpose, we have started upgrading works on the slow muon beam such as a new intense laser system, more efficient muonium production targets, and new control system of the slow muon beam line.

*Head*

Masahiko IWASAKI

*Members*

Katsuhiko ISHIDA  
Kenta ITAHASHI  
Yoshio KOBAYASHI  
Teiichiro MATSUZAKI  
Hiroaki ONISHI  
Haruhiko OUTA  
Isao WATANABE

*Special Postdoctoral Researchers*

Masami IIO  
Kazuki OHISHI  
Fuminori SAKUMA

*Foreign Postdoctoral Researcher*

Risdiana

*Special Contract Researchers*

Masaharu SATO  
Kyo TSUKADA

*Contract Researchers*

Yasuyuki ISHII  
Takayuki KAWAMATA  
Takahisa KOIKE

Katsuya MIZUNO  
Takao SUZUKI  
Dai TOMONO

*Visiting Scientists*

Tadashi ADACHI (Grad. Sch. Eng., Tohoku Univ.)  
Yoshitami AJIRO (Grad. Sch. Sci., Kyoto Univ.)  
Jun AKIMITSU (Coll. Sci. Eng., Aoyama Gakuin Univ.)  
Shingo ARAKI (Grad. Sch. Sci., Osaka Univ.)  
Kunio AWAGA (Grad. Sch. Sci., Nagoya Univ.)  
George BEER (Univ. of Victoria, Canada)  
HyoungChan BHANG (Seoul National Univ., Korea)  
N. Ludmila BOGDANOVA (ITEP, Russia)  
Prasad Tara DAS (SUNY, USA)  
Truong DUAN (Grad. Sch. Sci., Osaka Univ.)  
Yasuaki EINAGA (Fac. Sci & Tech., Keio. Univ.)  
Masaya ENOMOTO (Grad. Sch. Arts and Sci., Univ of Tokyo)  
Mark FAYFMAN (Kurchatov Institute, Russia)  
Yutaka FUJII (Fac. Eng., Fukui Univ.)  
Hiroyuki FUJIOKA (Grad. Sch. Sci., Univ. of Tokyo)  
Masaki FUJITA (IMR, Tohoku Univ.)  
Hideto FUKAZAWA (Grad. Sch. Sci. & Tech., Chiba Univ.)  
Takayuki GOTO (Fac. Sci. & Tech., Sophia Univ.)  
Makoto HAGIWARA (Fac. Eng. Design, Kyoto Inst. Technol.)  
Kazuo HAYAKAWA (Fac of Sci. & Tech., Shizuoka Inst. Sci. & Tech.)  
Ryugo, S. HAYANO (Grad. Sch. Sci., Univ.of Tokyo)  
Wataru HIGEMOTO (Advanced Sci. Res. Center, JAEA)  
Masahiro HIRANO (JST)  
Kazuto HIRATA (NIMS)  
Satoru HIRENZAKI (Fac. Sci., Nara Women's Univ.)  
Masahiko HIROI (Fac. Sci., Kagoshima Univ.)  
Susumu IKEDA (KEK)  
Yutaka IKEDO (Toyota Central R&D Labs.)  
Takayuki ISHIDA (Fac. Elect. Commu., Univ. Elect. Commu.)  
Fumihiro ISHIKAWA (Grad. Sch. Sci. & Tech., Niigata Univ.)  
Shigeru ISHIMOTO (Inst. of Particle and Nuclear Studies, KEK)  
Tomoichi ISHIWATARI (SMI, Austria)  
Ryosuke KADONO (KEK)  
Yoichi KAMIHARA (JST)  
Toshiji KANAYA (Inst. For Chem. Research, Kyoto Univ.)  
Motomi KATADA (Grad. Sch. Sci. & Eng., Tokyo Met. Univ.)  
Mineo KATO (JAEA)  
Naritoshi KAWAMURA (KEK)  
Seiko KAWAMURA (JAEA)  
Hikomitsu KIKUCHI (Grad. Sch. Eng., Univ. of Fukii)  
Junggho KIM (Seoul National Univ., Korea)  
Yasushi KINO (Fac. Sci., Tohoku Univ.)  
Akihiro KODA (KEK)

Yoh KOHORI (Fac. Sci., Chiba Univ.)  
Yoji KOIKE (Grad. Sch. Eng., Tohoku Univ.)  
Norimichi KOJIMA (Grad. Sch. Arts and Sci., Univ of Tokyo)  
Kenya KUBO (Coll. Liberal Arts, ICU)  
Yoshitaka KUNO (Grad. Sch. Sci., Osaka Univ.)  
Takuya KURAHASHI (IMS)  
Chow LEE (UCF, USA)  
Shunsuke MAKIMURA (KEK)  
Goro MARUTA (Grad. Sch. Sci., Hokkaido Univ.)  
Satoru MATSUIISHI (FCRC, Tokyo Tech.)  
Yasuhiro MIYAKE (KEK)  
Hitoshi MIYASAKA (Grad. Sch. Sci., Tohoku Univ.)  
Jun MIYAZAKI (Fac. Sci. Div., Nihon Univ.)  
Soichiro MIZUSAKI (Coll.Sci. & Eng., Aoyama Gakuin Univ.)  
Tomoyuki MOCHIDA (Grad. Sch. Sci., Kobe Univ.)  
Kazuhiko MUKAI (Toyota Central R&D Labs.)  
Yujiro NAGATA (Coll. Sci. Eng., Aoyama Gakuin Univ.)  
Hiroyuki NAKAMURA (Grad. Sch. Eng., Univ. of Tokyo)  
Jin NAKAMURA (Fac. Elect. Commu., Univ. Elect. Commu.)  
Kazutaka NAKAHARA (KEK)  
Satoshi NAKAMURA (Grad. Sch. Sci., Tohoku Univ.)  
Takashi NAKAMURA (Tokyo Inst. of Tech., Particle-, Nuclear-, and Astro-Phys.)  
Takayoshi NAKAMURA (RIES, Hokkaido Univ.)  
Takehito NAKANO (Grad. Sch. Sci., Osaka Univ.)  
Saburoou NASU (Grad. Sch. Eng. & Sci., Osaka Univ.)  
Kazuhiko NINOMIYA (Grad. Sch. Sci., Osaka Univ.)  
Nobuhiko NISHIDA (Fac. Sci., Tokyo Tech.)  
Yoichi NISHIWAKI (Sch. Medi., TWUMU)  
Kusuo NISHIYAMA (KEK)  
Hiroshi NOZAKI (Toyota Central R&D Labs.)  
Yasuo NOZUE (Grad. Sch. Sci., Osaka Univ.)  
Agung NUGROHO (ITB, Indonesia)  
Masaaki OHBA (Grad. Sch. Eng., Kyoto Univ.)  
Yoshitaka OHKUBO (KURRI, Kyoto Univ.)  
Susumu OHYA (Fac. Sci., Niigata Univ.)  
Shinji OKADA (INF, Italy)  
Akira OSAWA (Fac. Sci. & Tech., Sophia Univ.)  
Vassili PEREVOZCHIKO (VNIEF, Russia)  
Leonid PONOMAREV (Kurchatov Institute, Russia)  
Francis PRATT (RAL, UK)  
Roland KAWAKAMI (UC Riverside, USA)  
Shin-ichi SAKAMOTO (JAEA)  
Kazuhiko SATO (Grad. Sch. Sci. & Eng., Saitama Univ.)  
Ralph SCHEICHER (MY, USA)  
Ryoichi SEKI (California State Univ. , Northridge, USA)  
Kouichiro SHIMOMURA (KEK)  
Ichiro SHIRAKI (Grad. Sch. Medi. & Eng. Sci., Univ. of Yamanashi)  
Vyacheslas STORCHAK (VNIIEF, Russia)

Patrick STRASSER (KEK)  
Hiroyuki SUGAI (JAEA)  
Jun SUGIYAMA (Toyota Central R&D Labs.)  
Haruhiko SUZUKI (Grad. Sch. Nat. Sic. & Tech., Kanazawa Univ.)  
Hiroyuki SUZUKI (NIMS)  
Soh SUZUKI (KEK)  
Takatoshi SUZUKI (Grad. Sch. Sci., Univ.of Tokyo)  
Yoshikazu TABATA (Grad, Sch. Eng. & Sci., Kyoto Univ.)  
Shigeru TAKAGI (Grad, Sch. Sci., Tohoku Univ.)  
Kazuyuki TAKAI (Grad. Sch. Sci. & Eng., Tokyo Tech.)  
Keiji TAKEDA (ISSP, Univ. of Tokyo)  
Soshi TAKESHITA (KEK)  
Hiroyuki TAKEYA (NIMS)  
Manobu TANAKA (Inst. of Particle and Nuclear Studies, KEK)  
Akihiro TANIGUCHI (KURRI, Kyoto Univ.)  
Takashi TANIGUCHI (Coll.Sci. & Eng., Aoyama Gakuin Univ.)  
Harry TOM (UC Riverside, USA)  
Eiko TORIKAI (Grad. Sch. Medi. & Eng. Sci., Univ. of Yamanashi)  
Akihisa TOYODA (KEK)  
Satoshi TSUTSUI (JASRI)  
Kazuo UEDA (ISSP, Univ. of Tokyo)  
Yun XUE (Grad. Sch. Nat. Sic. & Tech., Kanazawa Univ.)  
Eiichi YAGI (Fac. Sci. & Eng., Waseda Univ.)  
Kazuyoshi YAMADA (IMR, Tohoku Univ.)  
Yasuhiro YAMADA (Fac. Sci., Tokyo Univ. of Sci.)  
Yutaka YOSHIDA (Fac of Sci. & Tech., Shizuoka Inst. Sci. & Tech.)  
Arkady YUKHINCHUK (VNIIEF, Russia)  
Johann ZMESKAL (SMI, Austria)

*Research Consultants*

Yoshinori AKAISHI  
Masayasu KAMIMURA  
Atsuko ITO

*Students*

*Junior Reserch Associates*

Satoshi ITOH (Grad. Sch. Sci., Univ. of Tokyo)  
Toshihiko HIRAIWA (Grad. Sch. Sci., Univ. of Tokyo)

*Intern*

Yuya FUJIWARA (Grad. Sch. Sci. & Eng., Tokyo Tech.)

*Student Trainees*

Mika DOIZOE (Fac. Sci., Tokyo Univ. Sci.)  
Shun Enomoto (Grad, Sch. Sci., Osaka Univ.)  
Yuta HASAGAWA (Grad. Sch. Sci., Univ. of Tokyo)  
Masatoshi HIRAISHI (Sch. High Enegy Acce. Sci.,Sokendai)  
Toru HISAMATSU (Grad. Sch. Sci. & Eng., Tokyo Tech.)  
Naho IINUMA (Fac. Sci., Tokyo Univ. Sci.)  
Tomohiro KAMIMURA (Grad. Sch.Sci. & Eng., Shizuoka Inst. Sci. & Tech.)

Tomohiro KANIMURA (Grad. Sch. Sci. & Eng., Shizuoka Inst. Sci. & Tech.)  
Naoki KASE (Grad. Sch. Sci. & Eng., Aoyama Gakuin Univ.)  
Yu KAWAHARA (Fac. Sci., Tokyo Univ. Sci.)  
Noriyuki KIDA (Grad. Sch. Arts and Sci., Univ. of Tokyo)  
Naoyuki KONNO (Grad. Sch. Sci., Tokyo Univ. Sci.)  
Katsuhiro KOUNO (Grad. Sch. Sci., Tokyo Univ. Sci.)  
Yoko MANABE (Grad. Sch. Sci. & Eng., Saitama Univ.)  
Masanori MIYAZAKI (Sch. Phys. Sci., Sokendai)  
Yoshifumi NAGASAKI (Grad. Sch. Fac. Sci., Kanazawa Univ.)  
Reiko NAKAGAKI  
Mufti NANDANG (Nat. Sci., Univ. of Groningen, Indonesia)  
Masaru OYAMA (Grad. Sch. Sci., Toho Univ.)  
ROGER PINK (SUNY at Albany, USA)  
Ryuichi SUEHIRO (Grad. Sch. Sci., Osaka Univ.)  
Tomonori TAKAHASHI (Grad. Sch. Sci., Univ. of Tokyo)  
Yoichi TANABE (Grad. Sch. Eng., Tohoku Univ.)  
Masamitsu TANAKA (Grad. Sch. Medi. & Eng. Sci., Univ. of Yamanashi)  
Arisa TANIGUCHI (Grad. Sch. Sci. & Eng., Saitama Univ.)  
Hideyuki TATSUNO (Grad. Sch. Sci., Univ. of Tokyo)  
Makoto TOKUDA (Grad. Sch. Sci. & Eng., Tokyo Tech.)  
Maai UCHIKAWA (Grad. Sch. Sci., Univ. of Tokyo)  
Shin UEGAKI (Grad. Sch. Sci., Tokyo Univ. Sci.)  
Fumiko YAMADA (Grad. Sch. Sci. & Eng., Tokyo Tech.)  
Heejoong YIM (Seoul National Univ., Korea)  
Hiromi YOSHIDA (Grad. Sch. Sci., Tokyo Univ. Sci.)

*Secretaries*

Yoko FUJITA  
Kumiko INAGAKI

## **Sub Nuclear System Research Division Theoretical Physics Laboratory**

### **1. Abstract**

The aim of this laboratory is to reveal the laws of nature ranging from elementary particles to the universe. More precisely, the following three issues are pursued with their mutual relations emphasized: (1) Understanding the microscopic fundamental law of nature. In particular, trying to give a consistent definition of superstring and derive all the fundamental laws from one principle. (2) Understanding many-body systems. Both of the following two aspects are considered. One is the universal laws such as thermodynamics and the universality of spin systems, and the other is specific properties of individual systems such as hadrons, condensed matter, and the universe. (3) Computational science. Besides numerical analyses as an important tool for the above mentioned (1) and (2), aspects of fundamental mathematics are also pursued.

### **2. Major Research Subjects**

- (1) Constructive Definition of String Theory as Fundamental law of Physics
- (2) Fundamental aspects of Quantum Field Theory and its applications
- (3) High precision inspection of experimental and observational data

### **3. Summary of Research Activity**

The ability to understand nature at its most profound level is a basic human desire. Science is founded on accumulated and tremendous efforts driven by that aspiration. The objective of our laboratory is to participate in the endeavor to better understand nature by adding our contributions to theoretical physics. The present seems to be a particularly exciting time for this as many developments appear to be about to converge and allow formation of the ultimate theory of everything.

We organize our research activities into three segments: the pursuit of the microscopic fundamental laws of physics, the study of many-body systems, and the science and technology of computation. These three aspects have an inseparable interrelation and are investigated in an integrated manner throughout the research conducted within this laboratory.

(1) Understanding the fundamental law of nature through string theory.

- 1) Non-perturbative effect for non-critical string

The analysis of the nonperturbative effect in the  $c=0$  noncritical string theory defined by the one-matrix model is extended to the case of two-matrix models which provide nonperturbative definitions of  $c<1$  noncritical string theories. Then, universality of nonperturbative effects including their coefficients in a generic  $c<1$  noncritical string theory is achieved in the sense that they are independent of details of potentials of the two-matrix models.

- 2) Matrix models and curved space-time

Incorporating curved space time into matrix models is pursued. In particular, a method in which larger additional degrees of freedom is introduced to represent space-time symmetry, is proposed.

- 3) Domain Wall in string theory

We investigate a global structure of the moduli space of the BPS domain wall system. In particular, we are interested in the case where the dimensions of the moduli space is greater than those expected from the index theorem. We also study the T-duality between the vortices and domain walls from a string theoretical point of view. We explicitly construct a vortex solution in the Higgs phase of supersymmetric gauge theory and find an exact correspondence between the solution and D-brane configuration in the domain wall side.

- 4) Non BPS branes and supergravity

We investigate the correspondences between a class of classical solutions of Type II supergravity (the three-parameter solution) and D-branes in the superstring theory. In addition to the mass, the RR-charge, the solution also carries the so-called dilaton charge, whose physical meaning was unclear. We find that the

appearance of the dilaton charge is a consequence of deformations of the boundary condition from that of the boundary state for BPS D-branes. We also show that such deformed boundary states are realized as tachyonic and/or massive excitations of the open strings on D-brane systems.

#### 5) D-branes and instantons

We have investigated instantons of four-dimensional SUSY gauge theory from the view point of superstring theory. A general prescription to construct the instanton solutions is known as the ADHM (Atiyah-Drinfeld-Hitchin-Manin) construction. In terms of superstring theory, instanton is understood as a bound state of D3-branes and D (-1) -branes. We consider a system of D3-branes and anti-D3-branes to construct the bound state via a tachyon condensation. As a result, we found that the tachyon profile contains all information on the instanton and the ADHM construction can be understood as an outcome of the gauge equivalence of this system in the low energy limit. We also applied the same method to eight-dimensional gauge theory and showed that some solitonic solution of the eight-dimensional theory can be constructed by this method.

#### 6) Application of string theory to cosmology

Cosmological scenarios alternative to inflation motivated by string theories are known. In cyclic scenario, or ekpyrotic scenario, the universe is considered as branes sitting in higher dimensional space time. The universe is assumed to start out from a static Minkowskian space-time and experience the big-bang as the collision of pair of branes (bounce). From the observational point of view, it is of importance to study the time evolution of cosmological fluctuation through the time of big bang. We studied the problem from the point of view of local causality through the bounce. Assuming the local causality condition, we derived the most general matching condition for the fluctuation between before and after the bounce. Especially, we found it is impossible to generate scale invariant spectrum without introducing non-local causality throughout the bounce. This work made clear the physical problem to obtain the scale invariant spectrum in the bouncing cosmology. We have also studied a toy model inspired by a low-energy effective action of non-commutative field theory and estimated the range of parameters to obtain scale invariant spectrum.

Another subject pursued was the possibility of obtaining inflation due to the modification of the dispersion relation. When non-equilibrium dynamics is taken into account, we observed that the inflation can be easily realized when the energy is a decreasing function of the momentum in high-energy regime. This result provides alternative way of realizing inflation in the framework of unified theory.

#### 7) Application of string theory to Nuclear physics

Holographic QCD, which is the application of the AdS/CFT correspondence to QCD, turns out to be a very fruitful arena of research in string theory. Using holographic QCD technique, various quantities which are difficult to calculate by perturbative QCD, lattice QCD and conventional nuclear physics approach are investigated. For example, the decay rate of  $\rho(770)$  is calculated suggesting its connection to much sought glueballs.

### (2) Quantum field theory and physics of many body systems

#### 1) Lattice formulation of supersymmetric gauge theory

We proposed a lattice formulation of low dimensional supersymmetric gauge theories, aiming at practical implementation for numerical simulations.

#### 2) Lattice formulation of fermions coupled to gravity

We formulated lattice Dirac operator of the overlap-type that describes the propagation of a Dirac fermion in a gravitational field. We also analyzed global gauge anomalies associated with Majorana fermions in  $8k$  and  $8k+1$  dimensions.

#### 3) Mathematical aspects of 2-dimensional gauge theories and string.

We investigate a non-perturbative correction to the  $N=2$  supersymmetric Yang-Mills theory from the discrete matrix model point of view. We utilize the D-brane picture in superstring theory and localization theorem in order to derive the discrete matrix model from 2-dimensional Yang-Mills theory on a compact 2-cycles in the ALE space. We also find the relationship to the Dijkgraaf-Vafa theory in the continuum limit.

#### 4) Logarithmic Conformal Field Theory

The following topics are investigated: Free field representation for LCFT with boundary; The relation between Minimal String theory and LCFT; The relation between statistical models and LCFT.

#### 5) Quantum field theory over the deformed commutation relation

A quantum theory of free scalar field based on the deformed Heisenberg algebra which is the correction of stringy physics is constructed.

#### 6) Chern Simons Yang Mills Model

We have studied the Chern Simons Yang Mills Model. Non-commutative gauge theories on fuzzy spheres were obtained in such models. Fuzzy spheres look like dbrane configuration.  $k$  coincident fuzzy spheres generates the  $U(k)$  gauge group. In this direction, we are continuing effort to address some of the related issues.

### (3) High precision calculation of field theory and computational science

#### 1) High precision calculation of QED

We have announced the final result of our calculation of the electron anomalous magnetic moment. It contains up to the eighth-order of the perturbation theory of QED. The very reliable result was obtained by using high precision calculation on RIKEN's supercomputer system (RSCC).

We also succeeded in automating the calculation of the tenth-order of the perturbation theory, particularly in constructing the ultra-violet subtraction terms. This is an important step to accelerate our calculation of the entire tenth-order contribution.

The dominant contribution from the tenth order to the muon anomalous magnetic moment was also announced by us. In contrast to the electron, some specific Feynman diagrams give rise to the large contributions to the muon anomaly. We explicitly evaluated about 2000 Feynman diagrams which are possible to give the leading and next-to-leading contributions.

#### 2) Improved perturbation method and its applications

We apply improved perturbation method which is one of the variational schemes to Ising model in two-dimensions. It enables us to evaluate free energy and magnetization at strong coupling regions from weak coupling expansion even in the presence of the phase transition.

We determine approximated transition point in this scheme. In the presence of external magnetic field we can see not only stable physical states but metastable one. This reserach motivated by availability of this method to IIB matrix model which is expected to show a phase transition from 10-dimensional universe to 4-dimensional universe.

#### *Head*

Hikaru KAWAI

#### *Members*

Hiroshi SUZUKI

Koji HASHIMOTO

Tsukasa TADA

#### *Postdoctoral Researchers*

Issaku KANAMORI

Isao KISHIMOTO

Daisuke KADOH

Ta-sheng TAI

Koichi MURAKAMI

Yutaka SAKAMURA

Yutaka BABA

Yuuichirou SHIBUSA

*Contract Researchers*

Makiko MATSUKAWA

*Visiting Scientists*

Hajime AOKI (Fac. of Sci. and Eng., Saga Univ.)

Jiro ARAFUNE (National Inst. for Academic Degrees and Univ. Evaluation)

Zyun F. EZAWA (Grad. Sch. of Sci., Tohoku Univ.)

Kazuo FUJIKAWA (College of Sci. and Tech., Nihon Univ.)

Amihay HANANY (Massachusetts Inst. of Tech., USA)

Masashi HAYAKAWA (Grad. Sch. of Sci., Nagoya Univ.)

Takeo INAMI (Fac. of Sci. and Eng., Chuo Univ.)

Nobuyuki ISHIBASI (Grad. Sch. of Pure and Applied Sci., Univ. of Tsukuba,)

Satoshi ISO (High Energy Accelerator Res. Organization)

Hiroshi ITOYAMA (Grad. Sch. of Sci., Osaka City Univ.)

Toichiro KINOSHITA (Cornell Univ., USA)

Yoshihisa KITAZAWA (High Energy Accelerator Res. Organization)

Ivan KOSTOV (Service de Physique Theorique, CNRS, FRANCE)

Jnanadeva MAHARANA (Inst. of Phys., INDIA)

Jun NISHIMURA (High Energy Accelerator Res. Organization)

Fumihiko SUGINO (Okayama Inst. for Quantum Phys.)

Asato TSUCHIYA (Grad. Sch. of Sci., Osaka Univ.)

Tatsumi AOYAMA (KEK)

Shoichi MIDORIKAWA (Aomori Univ.)

Masanori HANADA (Weizmann Inst.)

*Research Consultants*

Keiji IGI

Hironari MIYAZAWA

Yoshio YAMAGUCHI

Masao NINOMIYA

*Junior Research Associate*

*Secretariy*

Yumi KURAMITSU

Yoko SAGIYA

## Sub Nuclear System Research Division Strangeness nuclear physics Laboratory

### 1. Abstract

We proposed accurate few-body calculational method called "Infinitesimally shifted Gaussian lobe method". Recently, we developed this method to four-body systems and five-body systems. This method is applicable for various three-and four-body systems. For example, we applied it to hypernuclear physics and clarified what is important and impressed. In fact, we applied this method to three kinds of hypernuclear experiments (KEK-E419, BNL-E930, and -E929) in the past, and we contributed to these experiments by discussing with experimentalists, analyzing the data, and interpreting the data.

### 2. Major Research Subjects

- (1) Hypernuclear structure from the view point of few-body problem
- (2) Structure of exotic hadron system
- (3) Baryon-baryon interaction based on lattice QCD

### 3. Summary of Research Activity

- (1) Detailed structure calculations in  $^{12}\text{Be}_{\Xi}$ ,  $^5\text{He}_{\Xi}$ ,  $^9\text{Li}_{\Xi}$ ,  $^7\text{H}_{\Xi}$  and  $^{10}\text{Li}_{\Xi}$  are performed within the framework of the microscopic two-and three-and four-body cluster models using Gaussian Expansion method.  $^7\text{H}_{\Xi}$  and  $^{10}\text{Li}_{\Xi}$  are predicted to have bound states. Then, we propose to observe the bound states in future (K-, K+) experiments using  $^7\text{Li}$  and  $^{10}\text{B}$  target after Day-1 experiment at J-PARC facility.
- (2) The potential between proton and  $\Xi$  are obtained using quenched lattice QCD simulation. As a result, we found that the central  $p\Xi^0$  potential has a strong (weak) repulsive core in the 1S0 (3S1) channel for  $r < 0.6\text{fm}$ .

#### *Head*

Emiko HIYAMA

#### *Contract Researchers*

Hidekatsu NEMURA

Atsushi UMEYA

#### *Visiting Scientists*

Yasuo YAMAMOTO (Tsuru University)

Taiichi YAMADA (Kanto Gakuin University)

Tetsuo HYODO (Tokyo Institute of Technology)

Makoto OKA (Tokyo Institute of Technology)

Tomokazu FUKUDA (Osaka Electro-Communication University)

Daisuke JIDO (YITP, Kyoto University)

#### *Student Trainees*

Henrik STEGEBY (Uppsala University, Sweden)

Jafar ESMAILI (Isfahan University of Technology, Iran)

Hitomi NODA (Nara Women's University)

Kaori HORII (RCNP, Osaka University)

Kei MIZUNO (Nara Women's University)

#### *Secretary*

Makiko OHISHI

**Accelerator Applications Research Division  
Accelerator Applications Research Group  
Radiation Biology Team**

**1. Abstract**

Radiation biology team studies various biological effects of fast heavy ions. It also develops new technique to breed plants by heavy-ion irradiations. Fast heavy ions can produce dense and localized ionizations in matters along their tracks, in contrast to photons (X rays and gamma rays) which produce randomly distributed isolated ionizations. These localized and dense ionization can cause double-strand breaks of DNA in cells which are not easily repaired and result in mutation more effectively than single-strand breaks. A unique feature of our experimental facility at the RIKEN Ring Cyclotron (RRC) is that we can irradiate living bodies in atmosphere or in bottles since the delivered heavy-ion beams have energies high enough to penetrate deep in matter. This team utilizes a dedicated beam line (E5B) of the RRC to irradiate cultivated cells, plants and animals with beams ranging from carbon to iron. Its research subjects cover physiological study of DNA repair, genome analyses of mutation, and development of mutation breeding of plants by heavy-ion irradiation. Some new cultivars have already been brought to the market.

**2. Major Research Subjects**

- (1) Study on the biological effects by heavy-ion irradiation
- (2) Studies on ion-beam breeding and genome analysis
- (3) New medical application of heavy-ion beams

**3. Summary of Research Activity**

We study biological effects of fast heavy ions from the RIKEN Ring Cyclotron using 135 MeV/N C, N, Ne ions, 95 MeV/N Ar ions and 90 MeV/N Fe ions. We also develop breeding technology of plants. Main subjects are:

- (1) Study and application of heavy-ion induced plant mutation

In contrast to X rays and gamma rays, fast heavy ions are found to be useful for plant breeding since they only cause localized damage on DNA and can induce mutations more effectively with lower dosage. Our team utilizes beams of fast heavy ions from the RIKEN Ring Cyclotron to develop heavy-ion breeding techniques. Genome analyses are performed to reveal the relation between genotype and phenotype.

- (2) Study of heavy ion-induced damage of DNA and its repair processes

We study the double-strand break of DNA induced by heavy-ion irradiation and its repair processes. DNA double strand break (DSB) is characteristic to heavy-ion irradiation and considered to be the characteristic lesion responsible for its biological effects. Cells have two pathways to repair DSB, non-homologous end-joining (NHEJ) and homologous recombination (HR), and it is unknown how the two pathways are involved in repairing the damage caused by heavy-ion irradiation. To elucidate it, we irradiate higher vertebrate cells lacking DNA repair proteins with C, Ar, or Fe ions and analyze them with colony formation assay and molecular biology methods.

*Team Leader*

Tomoko ABE

*Members*

Hiroyuki ICHIDA

Masako IZUMI

Yusuke KAZAMA

Hinako TAKEHISA  
Teruyo TSUKADA

*Part-time Staff I*

Hideo TOKAIRIN

*Technical Staff I*

Yoriko HAYASHI

*Technical Staff II*

Sumie OHBU

*Visiting Scientists*

Ryutaro AIDA (Natl. Inst. Floricult. Sci.)  
Mari AMINO (Tokai University Hospital)  
Chang-Hyu BAE (Sunchon Natl. Univ., Korea)  
Yasuhiro CHIMI (JAEA)  
Hiroyuki DAIMON (Osaka Pref. Univ.)  
Makoto FUJIWARA (Grad. Sch., Col. Arts Sci., Univ. of Tokyo)  
Eitaro FUKATSU (Forest tree breeding Cet.)  
Koji FURUKAWA (Mukoyama Orchids Co., Ltd.)  
Yoshiya FURUSAWA (Natl. Inst. Radiol. Sci.)  
Toshinari GODO (Botanic Gardens Toyama)  
Misako HAMATANI (Hiroshima City Agric. Forest. Promot. Cen.)  
Yasuhide HARA (Kanagawa Inst. Agric. Sci.)  
Masanori HATASHITA (Wakasa Wan Energy Res. Cen.)  
Atsushi HIGASHITANI (Grad. Sch. Life Sci., Tohoku Univ.)  
Ryoichi HIRAYAMA (Natl. Inst. Radiol. Sci.)  
Akiko HOKURA (Fac. Sci., Tokyo Univ. of Sci.)  
Ichiro HONDA (Natl. Agric. Res. Cen.)  
Mitsugu HORITA (Hokuren Agri. Res. Inst.)  
Yuji ITO (Natl. Agric. Res. Cen., Hokkaido Region)  
Akihiro IWASE (Grad. Sch. Engin., Osaka Pref. Univ.)  
Hiroshi KAGAMI (Shizuoka Citrus Exp. Station)  
Kensuke KAGEYAMA (Fac. Engin., Saitama Univ.)  
Takeshi KANAYA (Suntory Flowers, Ltd.)  
Si-Yong KANG (Dep. Rad. Plant Breed. Genet., KAERI, Korea)  
Tomojirou KOIDE (Riken Vitamin Co., Ltd.)  
Tsutomu KUBOYAMA (Ibaraki Univ.)  
Yutaka MIYAZAWA (Grad. Sch. Life Sci., Tohoku Univ.)  
Kazumitsu MIYOSHI (Fac. Bioresour. Sci., Akita Pref. Univ.)  
Toshikazu MORISHITA (Inst. Rad. Breeding, Natl. Inst. Agric. Res.)  
Koji MURAI (Fukui Pref. Univ.)  
Daisuke NAKADA (Ela Medical Japan Co. Ltd.)  
Ishikawa NORITO (JAEA)  
Mio OHNUMA (Inst. Mol. Cell. Biosci., Univ. Tokyo)  
Norihiko OHTSUBO (Natl. Inst. Floricult. Sci.)  
Fumihisa ONO (Grad. Sch. Natural Sci. & Tech., Okayama Univ.)  
Tomo OOMIYA (Hokkaido Ornamental Plants Veg. Res. Cen.)

Kenji OSAWA (Nagano Agric. Res. Cen.)  
Kouichi SAKAMOTO (YUKIGUNI AGURI Co., Ltd.)  
Tadashi SATO (Grad. Sch. Life Sci., Tohoku Univ.)  
Hiroaki SERIZAWA (Nagano Veg. Ornamental Crops Exp. Station)  
Takiko SHIMADA (Res. Inst. Agric. Resour., Ishikawa Agric. Coll.)  
Fumio SUGAWARA (Tokyo Univ. of Sci.)  
Masao SUGIYAMA (Hokko Chem. Ind. Co., Ltd.)  
Keita SUGIYAMA (Nat. Inst. Veg. Tea Sci.)  
Kazunori SUZUKI (Plant Biotech. Inst. Ibaraki Agric. Cen.)  
Masao SUZUKI (Natl. Inst. Radiol. Sci.)  
Kenichi SUZUKI (Suntory Flowers, Ltd.)  
Teruhiko TERAOKA (Hokko Chem. Ind. Co., Ltd.)  
Ken TOKUHARA (Dogashima Orchid Cen.)  
Masanori TOMITA (CRIEPI)  
Hisashi TSUJIMOTO (Fac. Agri., Tottori Univ.)  
Kozo TSUKADA (Nippon Veterinary and Life Sci. Univ.)  
Masao WATANABE (Fac. Agri., Tohoku Univ.)  
Takuji YOSHIDA (Takii Seed Co., Ltd.)  
Koichiro YOSHIOKA (Tokai University Hospital)

*Research Fellows*

Hideki ASAUMI (Ehime Agricultural Experiment Station)  
Eikou OYABU (Saga Pref. Agr. Res. Cen.)  
Takenori SAITO (Shizuoka Tea Exp. Station)  
Tsukasa SHIRAO (Kagoshima Biotechnology Inst.)  
Kei-ichiro UENO (Kagoshima Biotechnology Inst.)  
Fumiko HIDAKA (Kagoshima Pref. Inst. for Agric. Dev.)  
Masataka CHAYA (Nagasaki Agr. Forest. Exp. Station)  
Naotugu WAKITA (Wadomari Cho Agr. Exp. Station)  
Kyouzuke NIWA (Hyogo Pref. Res. Inst.)  
Keiichi TAKAGI (Wakasa-wan Energy Research Center)

*Consultant*

Hiroyuki SAITO

*Students*

*Junior Research Associate*

Kiyoshi NISHIHARA (Grad. Sch. Frontier Sci., Univ. of Tokyo)

*Student trainees*

Naoki FUKUDA (Fac. Sci., Tokyo Univ. of Sci.)  
Takayuki INOUE (Dept. Phys. Rikkyo Univ.)  
Teruhiko KASHIWABARA (Fac. Sci., Tokyo Univ. of Sci.)  
Nobuhiro MAEDA (Grad. Sch. Eng., Osaka Pref. Univ.)  
Yoshitaka MATSUMOTO (Grad. Sch. Medicine & Sch., Chiba Univ.)  
Sakiko MITSUO (Fac. Sci., Tokyo Univ. of Sci.)  
Kazuhiro SASAKI (Grad. Sch. Life Sci., Tohoku Univ.)  
Saori TAKADA (Fac. Sci., Tokyo Univ. of Sci.)  
Yuji YOSHII (Fac. Sci., Tokyo Univ. of Sci.)  
Wakiko YAMAOKA (Fac. Sci., Tokyo Univ. of Sci.)

**Accelerator Applications Research Division**  
**Accelerator Applications Research Group**  
**RI Applications Team**

**1. Abstract**

RI Applications Team performs following researches at the heavy ion accelerators of RIBF: (1) With proton from the RIKEN AVF Cyclotron, we produce radioisotopes for research of chemistry, biology, medicine, pharmaceutical and environmental sciences. The nuclides Zn-65 and Cd-109 are delivered to Japan Radioisotope Association for charged distribution to the general public in Japan. We also study the production and application of short-lived RI's. (2) We develop new technologies of mass spectrometry for the trace-element analyses using accelerator technology and apply them to the scientific research fields, such as cosmochemistry, environmental science, archaeology and so on.

**2. Major Research Subjects**

- (1) Production of radioisotopes Zn-65 and Cd-109 for charged distribution,
- (2) Research and development for new RI production at AVF cyclotron,
- (3) The development of trace element analysis, using the accelerator techniques, and its application to geo and environmental sciences

**3. Summary of Research Activity**

RI applications team utilizes RIBF heavy-ion accelerators for following research subjects:

(1) Production of radioisotopes

Using 14-MeV proton beam irradiations at the RIKEN AVF Cyclotron, we develop techniques of production and application of various radio-isotopes (RI's) for research in chemistry, biology, medicine, pharmaceutical and environmental sciences. We can produce RI's with wide range of lifetimes as short as seconds. Long-life (>a few days) RI's are produced in a target which is cooled by water and He gas, and short-life RI's are produced at a gas-jet system where RI atoms are recoiled out of thin foil targets, captured by KCl aerosols and transported to a hot lab by a flow of He carrier gas. These systems are in the same chamber and can operate in parallel with the same beam. Among the long-life RI's, Zn-65 ( $T_{1/2}=244$  days) and Cd-109 ( $T_{1/2}=463$  days) are delivered to Japan Radioisotope Association for charged distribution to the general public in Japan.

(2) R/D for RI production

We work to improve production procedure of the present Zn-65 and Cd-109 for stable supply and better quality. We also develop production techniques for other RI species which are demanded but lack supply sources. The collection efficiency of gas-jet system has been optimized for Zr-89m ( $T_{1/2}=4.16$ m), Nb-90m ( $T_{1/2}=18.8$ s) and Nd-141m ( $T_{1/2}=62$ s) nuclides.

(3) Trace element analyses with accelerator technologies

We have developed two new technologies of mass spectrometry for the trace-element analyses as an application of accelerator technology to various fields such as cosmochemistry, environmental science, archaeology and so on. One is a new type Accelerator Mass Spectrometry (AMS) at the RILAC equipped with an ECR ion source. This system is available for the measurements of trace-elements ( $10^{-14}$ - $10^{-15}$  level), and is expected to be especially effectible for the measurements of low electron-affinity elements such as  $^{26}\text{Al}$ ,  $^{41}\text{Ca}$ ,  $^{53}\text{Mn}$  and so on. As a preliminary study, the ECR ion source system has been evaluated and the basic data have been obtained for the detection and quantitative analysis of trace nuclides in archaeological samples (cinnabar) and functional metals. As another technology, we have attempted to customize a mass spectrometer equipped with a stand-alone ECR ion source for analyses of elemental and isotopic abundances.

*Team Leader*

Tadashi KAMBARA

*Members*

Hiromitsu HABA

Kazuya TAKAHASHI

Shuichi ENOMOTO

*Temporary Staff*

Yutaka EZAKI

*Visiting Scientists*

Hiroshi HIDAKA (Fac. Sci., Hiroshima Univ.)

Hiroshi SHIMIZU (Fac. Sci., Hiroshima Univ.)

Miho TAKAHASHI (Tokyo Univ. Marine Sci. and Tech.)

Shigekazu YONEDA (Natl. Sci. Museum)

Tokuko WATANABE (Aoyama Gakuin Women's Junior College)

Masayoshi TODA (Tokyo Univ. Marine Sci. and Tech.)

*Research Consultants*

Kuniko MAEDA

*Part-time Staffs*

Tatsuya URABE (Tokyo Univ. Marine Sci. and Tech.)

Yoko YANADA (Tokyo Univ. Sci.)

Tomohiro OIKAWA (Tokyo Univ. Marine Sci. and Tech.)

Atsushi HASEGAWA (Tokyo Univ. Marine Sci. and Tech.)

## **Safety Management Group**

### **1. Abstract**

The Nishina Center for Accelerator-Based Science possesses one of the biggest accelerator facilities in the world which consists of a heavy-ion linear accelerator and 5 cyclotrons. Uranium ions are accelerated here only in Japan. Our function is to keep the radiation level in and around the facility below the allowable limit and to control the exposure on the workers as low as reasonably achievable. We are also involved in the safety management of the Radioisotope Center where many types of experiments are performed with sealed and unsealed radioisotopes.

### **2. Major Research Subjects**

- (1) Safety management at radiation facilities of Nishina Center for Accelerator-Based Science
- (2) Safety management at Radioisotope Center
- (3) Radiation shielding design and development of accelerator safety systems

### **3. Summary of Research Activity**

Our most important task is to keep the personnel exposure as low as reasonably achievable, and to prevent an accident. Therefore, we daily patrol the facility, measure the ambient dose rates, maintain the survey meters, shield doors and facilities of exhaust air and wastewater, replenish the protective supplies, and manage the radioactive waste. Advice, supervision and assistance at major accelerator maintenance works are also our task.

We installed radiation safety interlock system at the newly built RIBF building, and are extending it along with the constructions of experimental facilities. The suffocation-safety interlock system was also installed at the BigRIPS tunnel of RIBF accelerator building where huge amount of liquid He is used for superconducting magnets. The radiation safety interlock system for Nishina building was recently replaced by a simple and reliable one with a new concept.

#### *Head*

Yoshitomo UWAMINO

#### *Members*

Rieko HIGURASHI HIRUNUMA

Hisao SAKAMOTO

#### *Technical Staff I*

Atsuko HIRIGOME

#### *Assistant*

Tomomi OKAYASU

#### *Contract Officer*

Hiroki MUKAI

Satoshi HASHIGUCHI

Hiroyuki FUKUDA

#### *Special Temporary Employee*

Shin FUJITA

*Visiting Scientists*

Koji OHISHI

*Secretary*

Tsutomu YAMAKI

Kazushiro NAKANO

Kimie IGARASHI

Satomi IIZUKA

Hiroko AISO

## **RIKEN-BNL Research Center Theory Group**

### **1. Abstract**

The RIKEN BNL Research Center (RBRC) was established in April 1997 at Brookhaven National Laboratory in New York, USA. The Center is dedicated to study of strong interactions, including hard QCD/spin physics, lattice QCD and RHIC physics through nurturing of a new generation of young physicists. The Theory Group activities are closely and intimately related to those of the Nuclear Theory, High Energy Theory and Lattice Gauge Theory Groups at BNL. The RBRC theory group carries out research in three areas: numerical lattice QCD, perturbative QCD and phenomenological QCD. It pioneered the use of the domain-wall fermion method in lattice QCD and has investigated various aspects of hadron physics including the calculation of neutral Kaon CP-violations that is relevant for checking the Cabibbo-Kobayashi-Maskawa theory. The perturbative QCD effort has developed various new methods required for studying hadron structures, especially in spin physics research. The group has pioneered phenomenological QCD researches of color superconductivity, isospin density, and small-x phenomena in extreme hadronic matters.

### **2. Major Research Subjects**

- (1) Perturbative QCD
- (2) Lattice QCD numerical research
- (3) Phenomenological QCD

### **3. Summary of Research Activity**

The RIKENBNL Research Center (RBRC) was established in 1997 to support the RIKEN activities at RHIC in BNL, and also to promote theoretical studies related to RHIC, i. e. theories of strong interaction. The center's first director was T. D. Lee (Columbia University), and in October 2003, the former director of BNL, N. P. Samios, succeeded to the post of director. H. En'yo, Chief scientist of RIKEN in Wako, is also associate director of RBRC. The center consists of a theory group lead by L. McLerran (BNL) and an experimental group lead by Y. Akiba of RIKEN, currently resident at BNL.

Research in the RBRC theory group focuses on a wide variety of phenomena caused by the strong interaction, one of the four fundamental interactions in nature. The strong interaction is described theoretically by Quantum Chromodynamics (QCD), and the research projects in the RBRC theory group aim to elucidate various phenomena brought about by the strong interaction from the principles of QCD. Major subjects of our research include studies (a) based on lattice QCD, (b) on spin physics based on perturbative QCD, and (c) on QCD in extreme conditions such as high temperature, high density or high energy. RBRC offers RHIC Physics Fellowships, allowing joint appointments with universities. These Fellowships enable a talented researcher to maintain a tenure track position at his/her university as well as a Fellow position at RBRC for a certain period of time. This system was established in order to increase the research potential of RBRC and to disseminate its research activities and results. At present, RBRC has cooperative agreements with Arizona State University, the City University of New York, Iowa State University, Purdue University, Pennsylvania State University, the State University of New York at Stony Brook, Texas A&M University, the University of Tsukuba, as well as with BNL and with Lawrence Berkeley National Laboratory.

#### **(1) Lattice QCD**

QCDOC (QCD on chip), a second-generation lattice-QCD computer, was developed in the collaboration amongst the RBRC group, Columbia University and IBM. Three units of such a machine with 10 teraflops computing power are in operation since 2005; two in BNL (RBRC and DOE) and one in Edinburgh (UK-QCD), and formed a world-wide strong collaboration for the lattice QCD studies. Such computing power enables us to perform precise calculations with 3 quark flavors with proper handling on the chiral symmetry breaking. Several projects are ongoing: flavor physics for Kaon and B-meson, electro-magnetic properties of

hadrons, proton decay, the nuclear force, nucleon form factors which relates to the proton spin problem, and QCD thermodynamics in finite temperature/density systems as is produced in RHIC heavy-ion collisions. R and D led by the Columbia University lattice group is also underway for a next generation RBRC lattice computer of about 200 teraflops sustained.

(2) Perturbative QCD and spin physics

The ongoing RHIC spin experiments have motivated much of the parallel theoretical developments at RBRC. In the area of transverse spin physics, novel predictions have been obtained for the single transverse-spin asymmetry in open charm production in pp collisions at RHIC. This asymmetry probes three gluon correlations in polarized proton. In addition, radiative QCD corrections to single-spin observables were investigated, providing the relevant evolution equations. Further work focused on hyperon production at RHIC, and on azimuthal asymmetries in the Drell-Yan process.

(3) Phenomenological QCD--QCD under extreme conditions--

To establish a detailed picture of relativistic heavy ion collisions, QCD-based theoretical approaches are in progress. Especially the idea of "color glass condensation (CGC)" can be a key to understand the initial condition of the heavy ion collision. Other phenomenological approaches are in progress to understand the characteristics of strongly interacting quark gluon plasma. A recent effort has been initiated to understand heavy ion elliptic flow in terms of viscous hydrodynamics. A new finite temperature effective field theory is being developed for the strongly interacting quark gluon plasma to explain the suppression of shear viscosity in the region of the phase transition.

*Group Leader*

Larry McLERRAN

*Deputy Group Leader*

Anthony J. BALTZ

*Members*

Yasumichi AOKI \*1  
Denes MOLNAR \*2  
Kirill TUCHIN \*2  
Rainer FRIES \*2  
Thomas BLUM \*2  
Tomomi ISHIKAWA \*3  
Feng YUAN \*2  
Adam LICHTL \*3  
Agnes MOCSY \*3  
Yoshimasa HIDAKA \*4  
Toru KOJO \*4  
Peter PETRECZKY \*2  
Taku IZUBUCHI \*1  
Sinya AOKI \*5  
Derek TEANEY \*2  
Adrian DUMITRU \*2  
Cecilia LUNARDINI \*2  
Anna STASTO \*2

*Visiting Members*

Norman CHRIST (Columbia Univ., USA)

Miklos GYULASSY (Columbia Univ., USA)  
Robert L. JAFFE (Massachusetts Inst. Technol., USA)  
Robert MAWHINNEY (Columbia Univ., USA)  
Edward SHURYAK (State Univ. New York, Stony Brook, USA)  
Kei IIDA (Kochi Univ.)  
Masakiyo KITAZAWA (Osaka Univ.)  
Testufumi HIRANO (U. Tokyo)  
Shigemi OHTA (KEK)

*Secretarial Staff*

Doris RUEGER (Secretary to Director N. P. Samios)  
Pamela ESPOSITO (Theory Group Secretary)  
Taeko ITO (Assistant to Account Manager for Administration)  
Susan FOSTER (Experimental Group Secretary)

*Administrative Staff / RIKEN Japan*

Masatoshi Moriyama, Deputy Director, Nishina Center Research Promotion Office  
Emiko ADACHI (RBRC Account Manager for Administration)  
Keiko SUSUKI (Japan)

\*1 RIKEN BNL Fellow   \*2 RHIC Physics Fellow,  
\*3 Research Associate,   \*4 Special Postdoctoral Researcher,  
\*5 RHIC visiting Fellow

## **RIKEN-BNL Research Center Experimental Group**

### **1. Abstract**

RIKEN BNL Research Center (RBRC) Experimental Group studies the strong interactions (QCD) using RHIC accelerator at Brookhaven National Laboratory, the world first heavy ion collider and polarized p+p collider. We have three major activities: Spin Physics at RHIC, Heavy ion physics at RHIC, and detector upgrades of PHENIX experiment at RHIC. We study the spin structure of the proton using the polarized proton-proton collisions at RHIC. This program has been promoted by RIKEN's leadership. The first focus of the research is to measure the gluon spin contribution to the proton spin. Our recent data analysis has shown that the proton spin carried by the gluons is small, which is a very striking finding beyond our expectations. The aim of Heavy ion physics at RHIC is to re-create Quark Gluon Plasma, the state of Universe just after the Big Bang. Two important discoveries, jet quenching effect and strong elliptic flows, have established that new state of dense matter is indeed produced in heavy ion collisions at RHIC. We are proceeding to understand the nature of the matter. We has major roles in detector upgrades of PHENIX experiment, namely, the silicon vertex tracker (VTX) and muon trigger upgrades.

### **2. Major Research Subjects**

- (1) Experimental Studies of the Spin Structure of the Nucleon
- (2) Study of Quark-Gluon Plasma at RHIC
- (3) PHENIX detector upgrades

### **3. Summary of Research Activity**

The RIKEN-BNL Research Center was established in 1997 to support the RIKEN activities at RHIC in BNL, and also to promote theoretical studies related to RHIC, i. e. theories of strong interaction. The center's first director was T. D. Lee (Columbia University), and in October 2003, the former director of BNL, N. P. Samios, succeeded to the post of the director. The center consists of a theory group lead by L. McLerran (BNL) and an experimental group lead by Y. Akiba, a vice chief scientist of RIKEN in Wako.

We study the strong interactions (QCD) using the RHIC accelerator at Brookhaven National Laboratory, the world first heavy ion collider and polarized p+p collider. We have three major activities: Spin Physics at RHIC, Heavy ion physics at RHIC, and detector upgrades of PHENIX experiment.

- (1) Experimental study of spin structure of proton using RHIC polarized proton collider

How is the spin of proton formed with 3 quarks and gluons? This is a very fundamental question in Quantum Chromodynamics (QCD), the theory of the strong nuclear forces. The RHIC Spin Project has been established as an international collaboration between RIKEN and Brookhaven National Laboratory (BNL) to solve this problem by colliding two polarized protons for the first time in history. This project also has extended the physics capabilities of RHIC.

The first goal of the RHIC spin physics program is to elucidate a contribution of the gluon spin in the proton spin. We have measured double-helicity asymmetries of neutral pions to study gluon polarization in proton. The most recent data from 2006 run have shown that the gluon polarization in the proton is small, and only about half of proton spin can be accounted by gluon spin in the measured region of gluon momentum in proton. The remaining part must be carried by gluons in lower momentum region where the measurement is not sensitive, and/or reside in the orbital-angular momentum of quarks and gluons.

To finalize the smallness of the gluon-spin contribution, we need to measure double helicity asymmetry in direct photon production. This process is dominated by a single and the simplest process, gluon Compton scattering, in perturbative QCD, and is the golden channel to determine the gluon density and the gluon polarization in the proton. We published a paper on direct photon cross section in p+p collisions at RHIC. Preliminary results on double-helicity asymmetry of direct photon from the 2006 run have been obtained.

We have also accumulating transversely-polarized proton collision data to measure single transverse-spin asymmetries of processes which are predicted to be sensitive to the orbital-angular momentum of quarks and gluons.

Since the RHIC operation in 2008 was shortened by the DOE budget problem there was a polarized-proton collisions for only about one-month long. The RHIC accelerator achieved  $2.3 \times 10^{31} / \text{cm}^2 / \text{s}$  of the average luminosity and 45% of the average beam polarization at the center-of-mass energy of 200 GeV. In 2008, we collected data with transversely-polarized proton collisions at 200 GeV to investigate single transverse-spin asymmetries. The PHENIX experiment recorded the data corresponding to 4.5 inverse picobarn of the integrated luminosity in 2008. All the physics data in the 2008 p+p run were transferred to RIKEN CC-J in almost real-time via the network between US and Japan. Event-reconstruction of the data has been completed at RIKEN CC-J.

In addition to the study of polarized p+p collisions at RHIC, we study quark fragmentation function. With collaboration with the BELLE experiment at High Energy Accelerator Research Organization (KEK), we discovered that the spin direction of a quark can be determined from its hadronic fragments. Precise data of the quark fragmentation function can be used to understand the cross sections and the spin dependences of particle production in polarized p+p collisions at RHIC. We continue the study of the quark fragmentation function at BELLE.

In 2009, we expect the first polarized p+p run at  $\sqrt{s}=500$  GeV. Main goal of the 500 GeV run is to measure single longitudinal spin asymmetry of W particle production. From this measurement, the polarization of the quarks and the anti-quarks in the proton can be determined.

## (2) Experimental study of Quark-Gluon Plasma using RHIC heavy-ion collider

The goal of high energy heavy ion physics at RHIC is study of QCD in extreme conditions i. e. at very high temperature and at very high energy density. Experimental results from RHIC have established that dense partonic matter is formed in Au+Au collisions at RHIC. The matter is very dense and opaque, and it has almost no viscosity and behaves like a perfect fluid. These conclusions are primarily based on the following two discoveries:

- Strong suppression of high transverse momentum hadrons in central Au+Au collisions (jet quenching)
- Strong elliptic flow

The focus of the research in heavy ion physics at RHIC is now to investigate the properties of the matter. RBRC have played the leading roles in some of the most important results from PHENIX in the study of the matter properties.

From the fall of 2007 to the spring of 2008, RHIC had its 8<sup>th</sup> year RUN (RUN8). The first part of RUN8 was deuteron + gold (d+Au) collision experiment. PHENIX recorded very high statistics d+Au data during RUN8, about 30 times of the previous d+Au run in year 2003. From the d+Au data we can study the cold nuclear matter effect, in particular that on J/Psi production, a key probe of Quark Gluon plasma.

Main results of PHENIX that are published in 2008 are as follows.

### 1) Measurements of electron pairs in p+p.

Electron pairs are measured in p+p collisions at  $\sqrt{s}=200$  GeV. The measured mass distribution is well explained by the contribution of light meson decays for the mass region less than 1 GeV. The mass spectrum above 1 GeV is dominated by correlated decay of charm and anti-charm mesons. From the yield of the electron pair continuum above 1 GeV, the total charm production cross section is deduced. The obtained cross section is in good agreement with the measurement from single electrons.

### 2) J/Psi measurements in d+Au and Cu+Cu

Cold nuclear matter effects in J/PSI production in d+Au collisions are studied. The d+Au data were re-analyzed and compared with higher statistics p+p data. From the comparison, J/Psi break-up cross section in cold nuclear matter is determined. The final results of J/Psi production in Cu+Cu collision from year 2005 run of RHIC has been published.

### 3) High pT pi0 measurement and constraints on theory.

PHENIX measured  $\pi^0$  production at high  $p_T$  in Au+Au collision at 200 GeV. The new measurement has more than 10 times of statistics of the previous published results and extend the measured  $p_T$  range to 20 GeV/c. The measurements shows that the  $\pi^0$  production is strongly suppressed, by about a factor of five, at high  $p_T$ . The suppression is consistent with that high  $p_T$  scattered quarks and gluons lose a significant amount of their energies in the dense matter formed in the collision. The suppression patterns are compared with the theory calculations of parton energy loss. Form the comparison, quantitative constraints on the parameters of the theories are obtained.

4) Measurement of low  $p_T$  direct photons through their internal conversion to  $e^+e^-$  pairs.

If the dense partonic matter formed at RHIC is thermalized, it should emit thermal photons. Observation of thermal photon is direct evidence of early thermalization, and we can determine the initial temperature of the matter. It is predicted that thermal photons from QGP phase is the dominant source of direct photons for  $1 < p_T < 3$  GeV/c at the RHIC energy. PHENIX measured the direct photon in this  $p_T$  region from measurements of quasi-real virtual photons that decays into low-mass  $e^+e^-$  pairs. Strong enhancement of direct photon yield in Au+Au over the scaled p+p data has been observed. Several hydrodynamical models can reproduce the central Au+Au data within a factor of two. These models assume formation of a hot system with initial temperature of  $T_{\text{init}}=300$  MeV to 600 MeV.

(3) PHENIX detector upgrade

The group has major roles in several PHENIX detector upgrades, namely, the silicon vertex tracker (VTX) and muon trigger upgrades.

VTX is 4 layers of silicon tracker, jointly funded by RIKEN and the US DOE. The inner two layers are silicon pixel detectors and the outer two layers are silicon strip detectors. The detector will be completed in 2010.

Muon trigger upgrades are needed for  $W \rightarrow \mu$  measurement at 500 GeV. New trigger electronics (Muon Trigger FEE) have been installed in one of muon arms and they will be commissioned in the 2009 run. After the 2009 run, the rest of the Muon Trigger FEE will be installed in PHENIX. Prototype of muon trigger detectors using MRPC technology have been installed for test during the 2009 run.

*Group Leader*

Yasuyuki AKIBA

*Deputy Group Leader*

Abhay DESHPANDE

*Members*

Yuji GOTO

Itaru NAKAGAWA

Takashi ICHIHARA

Atsushi TAKETANI

Yasushi WATANABE

Satoru YOKKAICHI

Kensuke OKADA \*1

Ralf-Christian SEIDL \*1

Stefan BATHE \*1

David KAWALL \*2

Kieran BOYLE \*3

Manabu TOGAWA \*4

Kohei SYOJI (Kyoto Univ.) \*5

Jun TAMURA (T. I. Tech) \*5

Yorito YAMAGUCHI (CNS-U-Tokyo) \*5  
Misaki OUCHIDA (Hiroshima Univ) \*5  
Kentaro MIKI (Tsukuba Univ) \*5  
Kenichi KARATSU (Kyoto Univ) \*5  
Yoki ARAMAKI (CNS-U-Tokyo) \*5

*Visiting Members*

Naohito SAITO (KEK)  
Zheng LEE (BNL)  
Kiyoshi TANIDA (Kyoto Univ.)  
Akio OGAWA (BNL)  
Masahiro OKAMURA (BNL)  
Seishi DAIRAKU (Kyoto Univ.) \*6  
Koichi SAKASHITA (T. I. Tech) \*7  
Takeshi KANESUE (Kyusyu Univ.) \*6

\*1RIKEN BNL Fellow, \*2 RHIC Physics Fellow,  
\*3 Research Associate, \*4 Special Postdoctoral Researcher,  
\*5 Junior Research Associate, \*6 JSPS Student, \*7 Student trainee

## **Center for Nuclear Study, Graduate School of Science, University of Tokyo.**

### **1. Abstract**

The Center for Nuclear Study (CNS) aims to elucidate the nature of nuclear system by producing the characteristic states where the Isospin, Spin and Quark degrees of freedom play central roles. These researches in CNS lead to the understanding of the matter based on common natures of many-body systems in various phases. We also aim at elucidating the explosion phenomena and the evolution of the universe by the direct measurements simulating nuclear reactions in the universe. In order to advance the nuclear science with heavy-ion reactions, we develop AVF upgrade, CRIB and SHARAQ facilities in the large-scale accelerators laboratories RIBF. We promote collaboration programs at RIBF as well as RHIC-PHENIX and ALICE-LHC with scientists in the world, and host international meetings and conferences. We also provide educational opportunities to young scientists in the heavy-ion science through the graduate course as a member of the department of physics in the University of Tokyo and through hosting the international summer school.

### **2. Major Research Subjects**

- (1) Accelerator Physics
- (2) Nuclear Astrophysics
- (3) Nuclear spectroscopy of exotic nuclei
- (4) Quark physics
- (5) Spin Physics
- (6) Nuclear Theory
- (7) SHARAQ project

### **3. Summary of Research Activity**

#### **(1) Accelerator Physics**

One of the Major tasks of the accelerator group is the AVF upgrade project which includes development of ion sources, upgrading the AVF cyclotron of RIKEN and the beam line to CRIB. A new heavy ion ECR source of CNS that use super-conducting magnet was successfully installed to the AVF cyclotron, and has been used to provide a variety heavy ion beams. Two CNS ECR sources now provide all the beams for the AVF cyclotron and support not only CRIB experiments but also a large number of RIBF experiments. A charge-breeding ECR source is also under development.

Two major works were advanced for upgrading the AVF cyclotron. One is the detailed design study of the central region of the cyclotron, which remedies insufficiencies for the transmission of the heavy ion beams through the cyclotron. A new central module will be made following the design in 2009. The second is a successful acceleration of heavy ion beams up to 11 MeV/u which was about 9.5 MeV/u before. Following the detailed simulation studies of the heavy ion beams through the cyclotron, beam acceleration tests were successfully performed for  $^{16}\text{O}$  and  $^6\text{Li}$  beams. These beams will be provided to new experimental projects at CRIB.

A non-destructive beam monitor was also successfully developed and installed just in front of the CRIB production target. It showed a sensitivity of about a few nA. This new beam monitor will become a powerful tool for all the RIBF facility.

#### **(2) Nuclear Astrophysics**

Major activity of the nuclear astrophysics group is to investigate experimentally nucleosynthesis of the universe, specifically of explosive phenomena in the universe such as novae and supernovae. High-intensity RI beams of light nuclei from the CNS low-energy RI beam separator CRIB provides a good opportunity to study stellar nuclear reactions under explosive conditions both by the direct method as well as by indirect methods. The research programs include investigations of  $\alpha$ -induced stellar reactions on  $^7\text{Li}$ ,  $^{14}\text{O}$  and  $^{21}\text{Na}$ .

The beta decay of  $^{46}\text{Cr}$  was also studied to learn the Gamow-Teller Transitions. Some beam developments were made for new RI beams, and an active target was also designed for studies of stellar reactions with low-cross sections.

Some technological development for the beam line as well as for the Wienfilter of CRIB were made in the past year.

### (3) Nuclear structure of exotic nuclei

The NUSPEQ (NUclear SPectroscopy for Extreme Quantum system) group studies exotic structures in high-isospin and/or high-spin states in nuclei. The CNS GRAPE (Gamma-Ray detector Array with Position and Energy sensitivity) is a major apparatus for high-resolution in-beam gamma-ray spectroscopy. In 2008, the following progress has been made.

Light neutron-rich nuclei have been studied by using nucleon transfer and inelastic scattering where the final states are identified by measuring de-excited gamma-rays. A low-lying proton intruder state has been found for the first time, which shows importance of a deformation effect in  $N \sim 8$  neutron-rich nuclei.

New high-spin states in  $^{49-51}\text{Ti}$  populated by fusion reactions of an RI beam have been found, which gives information on the  $N=28$  shell gap and the single particle energies in the fp-shell.

Upgrade of the readout system of the CNS GRAPE has started, where digital pulse data taken by sampling ADCs are analyzed by FPGAs on boards.

### (4) Quark Physics

Main goal of the CNS quark physics group is to understand the properties of hot and dense nuclear matter created by colliding heavy nuclei at relativistic energies. The group has been involved in the PHENIX experiment at Relativistic Heavy Ion Collider (RHIC) at Brookhaven

National Laboratory, and has also started active participation in the ALICE experiment at Large Hadron Collider (LHC) at CERN.

As for the RHIC PHENIX experiment, the group has been concentrating on the physics analysis with leptons and photons, which include study of charm and bottom production with the non-photonic single electrons, measurement of direct photon yield at low transverse momentum in p+p and A+A collisions using the virtual-gamma method, and determination of neutral pion yield as a function of azimuthal angle from the reaction plane in Au+Au collisions.

As for the LHC ALICE experiment, the group has been playing roles in the construction of the Transition Radiation Detector (TRD), and commissioning and calibration of Time Projection Chamber (TPC).

R&D of gas electron multiplier (GEM) and related techniques has been continuing. The major activities are; development of 2D-imaging prototype, and performance study of the thick-GEM prototypes with several different hole sizes.

### (5) Spin Physics

Development of the polarized solid proton target is being proceeded. We have examined how the proton polarization rate depends on pulse structure of excitation light and found that the polarization rate can be doubled for a duty factor of 20% and a repetition rate of 7.5 kHz, compared with the previous settings of 5% and 2.5 kHz. Higher proton polarization can be expected with this new settings.

### (6) Nuclear Theory

The nuclear theory group has been promoting the RIKEN-CNS collaboration project on large-scale nuclear structure calculations since 2001 and maintaining its parallel computing cluster. In 2008, we developed the effective interactions of various mass region based on the large-scale shell model calculation technique and discussed the "shell evolution" and the role of tensor force quantitatively in exotic nuclei, such as  $^{17}\text{C}$ ,  $^{48}\text{Ca}$ ,  $N=50$  isotones, Sm isotopes and so on.

### (7) SHARAQ project

Construction of the SHARAQ spectrometer and the dedicated high-resolution beamline are coming to the final phase. The magnetic field distribution in dipole magnets, D1 and D2, were precisely measured with the search coil method. A major part of the beamline has been constructed. Cathode readout drift chambers for

tracking detectors at the SHARAQ focal plane have been fabricated in GANIL and installed to SHARAQ in December 2008. It was also found that Low-pressure multiwire drift chambers (LP-MWDC) developed for beamline tracking detectors works well under pressure as low as 10 kPa with an isobutane gas.

*Director*

Takaharu OTSUKA

*Scientific Staff*

Susumu SHIMOURA (Professor)

Shigeru Kubono (Professor)

Hideki HAMAGAKI (Associate Professor)

Tomohiro UESAKA (Associate Professor)

Eiji IDEGUCHI (Lecturer)

Hironori IWASAKI (Research Associate (-Dec./31/2008))

Takahiro KAWABATA (Research Associate (-Jan./31/2009))

Hidetoshi YAMAGUCHI (Research Associate)

Shin'ichiro MICHIMASA (Research Associate)

Taku GUNJI (Research Associate)

*Guest Scientists*

Toshio SUZUKI (Guest Professor, Nihon Univ.)

Toshinori MITSUMOTO (Guest Associate Professor, Sumitomo Heavy Industries, Ltd.)

*Technical Staff*

Yukimitsu OHSHIRO

Norio YAMAZAKI

*Technical Assistants*

Shin-ichi WATANABE

Hiroshi KUREI

Hideaki NINOMIYA

Ryo YOSHINO

Shoichi YAMAKA

*Post Doctoral Associates*

Takashi ABE

Yohei SHIMIZU

Kosuke NAKANISHI

Takashi HASHIMOTO

Yashio WAKABAYASHI

Shinsuke OTA

Yuji TSUCHIMOTO (Mar./25/2009-)

*Graduate Students*

Megumi NIKURA

Yuhei MORINO

Yoshiko SASAMOTO

Satoshi SAKAGUCHI

Yorito YAMAGUCHI

Youki ARAMAKI  
Nguyen Binh DAM  
Satoshi SANO  
Seiya HAYAKAWA  
David. M KAHL (Oct./1/2008-)  
Akihisa TAKAHARA  
Yuzo KURIHARA  
Hiroyuki MIYA  
Ryoji AKIMOTO  
Kenshi OKADA  
Yasuto HORI  
Hiroshi TOKIEDA

*Administration Staff*

Midori HIRANO  
Ikuko YAMAMOTO  
Takako ENDO  
Yukino KISHI  
Toshiko ITAGAKI  
Ikuko ICHINOHE (-Jun./30/2008)  
Yuko SOMA (Jul./16/2008-)

## **TORIJIN**

### **(Todai-RIKEN Joint International Program for Nuclear Physics) Term**

#### **1. Abstract**

University of Tokyo and RIKEN agreed to cooperate with each other in the field of nuclear physics and established Todai-RIKEN Joint International Program for Nuclear Physics (TORIJIN) in June 2006. The aim of this organization is to promote the international collaborations, such as JUSTIPEN (Japan-US Theory Institute for Physics with Exotic Nuclei) and EFES (International Research Network for Exotic Femto Systems). JUSTIPEN was launched in June 2006 in order to facilitate collaborations between U. S. and Japanese scientists whose main research thrust is in the area of the physics of exotic nuclei. More than 40 nuclear scientists in U. S. have visited Japan in three years, and many collaborations are established. EFES was selected as one of the Core-to-Core Programs of Japan Society for the Promotion of Science (JSPS). This is the program to send Japanese nuclear scientists to U. S., Germany, France, Italy, Norway, and Finland and to promote the international collaborations in the field of nuclear study. Many joint workshops were held with the partner countries.

#### **2. Main activities**

Promote the international collaborations of both theoretical and experimental nuclear physicists under JUSTIPEN and EFES programs.

#### **3. Summary of Research Activity**

Under the JUSTIPEN program, 26 nuclear scientists visited in this fiscal year and many collaborations are established. Under the EFES program, we have carried out four types of activities: initiating the collaboration projects, organizing seminars with partner countries, sending researchers abroad, and sending/inviting young scientists to the summer schools. Regarding the collaborative works, we have carried out three projects. Many experimentalists and theoreticians have been sent abroad. As for the joint workshops, we have organized eight workshops and all of them were quite fruitful. Also, young scientists have been sent to partner countries for educational purpose and starting collaborations. As for the summer school, Japanese graduate students have been sent to the summer schools in Germany and USA, and we have invited students to CNS-EFES summer school from the partner countries.

##### *Leader*

Takaharu OTSUKA (University of Tokyo)

##### *Vice leader*

Tohru MOTOBAYASHI (RIKEN)

##### *Members*

Susumu SHIMOURA (University of Tokyo),

Hiroyoshi SAKURAI (RIKEN)

Takashi NAKATSUKASA (RIKEN)

Tomohiro UESAKA (University of Tokyo),

Naoyuki ITAGAKI (University of Tokyo),

**VI. LIST OF PUBLICATIONS  
& PRESENTATION**

## Accelerator Division

### Publications

#### [Journal]

(Original Papers) \*Subject to Peer Review

Aoki T., Stingelin L., Kamigaito O., Sakamoto N., Fukunishi N., Yokouchi S., Maie T., Kase M., Goto A., and Yano Y.: “Construction of a beam rebuncher for RIKEN RI-beam factory”, Nucl. Instrum. Methods Phys. Res. A **592**, No. 3, pp. 171–179 (2008). \*

#### [Book・Proceedings]

(Original Papers) \*Subject to Peer Review

Goto A., Fujimaki M., Fujinawa T., Fukunishi N., Hasebe H., Higurashi Y., Ikegami K., Ikezawa E., Inabe N., Kageyama T., Kamigaito O., Kase M., Kidera M., Kohara S., Komiyama M., Nagase M., Kumagai K., Maie T., Nakagawa T., Ohnishi J., Okuno H., Ryuto H., Sakamoto N., Wakasugi M., Watanabe T., Yamada K., Yokouchi S., and Yano Y.: “Commissioning of RIKEN RI Beam Factory”, Proceedings of 18th International Conference on Cyclotrons and Their Applications (Cyclotrons 2007), Giardini Naxos, Italy, 2007–9~10, , Giardini Naxos, pp. 3–8 (2007).

(Others)

Okuno H., Fukunishi N., Fujinawa T., Goto A., Higurashi Y., Ikezawa E., Kamigaito O., Kase M., Nakagawa T., Ohnishi J., Sato Y., Yano Y., and Ostroumov P.: “Heavy Ion Accelerators for RIKEN RI Beam Factory and Upgrade Plans”, 42nd ICFA Advanced Beam Dynamics Workshop on High-Intensity, High-Brightness Hadron Beams, Nashville, USA, 2008–8, ICFA, , p. (2009).

### Oral Presentations

(International Conference etc.)

Okuno H., Fukunishi N., Fujinawa T., Goto A., Higurashi Y., Ikezawa E., Kamigaito O., Kase M., Nakagawa T., Ohnishi J., Sato Y., Yano Y., and Ostroumov P.: “Heavy Ion Accelerators for RIKEN RI Beam Factory and Upgrade Plans”, 42nd ICFA Advanced Beam Dynamics Workshop on High-Intensity, High-Brightness Hadron Beams (HB2008), (Oakridge National Laboratory), Nashville, USA, Aug. (2008).

(Domestic Conference)

須田健嗣, 小山亮, 加瀬昌之, 上垣外修一, 坂本成彦, 福西暢尚, 藤巻正樹, 山田一成, 渡邊環: “RIBFにおける高周波系の安定度”, 第5回日本加速器学会年会/第33回リニアック技術研究会, 東広島, 8月(2008).

長谷部 裕雄, 奥野 広樹, 久保木 浩功, 龍頭 啓充, 福西 暢尚, 上垣外修一, 後藤彰, 加瀬昌之, 矢野安重: “理研 RIBF における長寿命炭素薄膜の開発状況”, 第5回日本加速器学会年会/第33回リニアック技術研究会, (広島大学), 広島, 8月(2008).

渡邊環, 藤巻正樹, 福西暢尚, 加瀬昌之, 山田一成, 坂本成彦, 須田健嗣, 込山美咲, 仲村武志, 小山亮, 小高康照, 上垣外

修一, 矢野安重: “RIBF におけるビーム診断系の高度化”, 第5回日本加速器学会年会/第33回リニアック技術研究会, (広島大学), 東広島, 8月(2008).

## Accelerator Development Group

### Publications

#### [Journal]

(Original Papers) \*Subject to Peer Review

Iwasa N., Motobayashi T., Sakurai H., Akiyoshi H., Ando Y., Aoi N., Baba H., Fukuda N., Fulop Z., Futakami U., Gomi T., Higurashi Y., Ieki K., Iwasaki H., Kubo T., Kubono S., Kinugawa H., Kumagai H., Kunibu M., Michimasa S., Minemura T., Murakami H., Sagara K., Saito A., Shimoura S., Takeuchi S., Yanagisawa Y., Yoneda K., and Ishihara M.: “In-beam  $\gamma$  spectroscopy of  $^{34}\text{Si}$  with deuteron inelastic scattering using reverse kinematics”, *Phys. Rev. C* **67**, 064315-1–064315-4 (2003). \*

Saito A., Shimoura S., Takeuchi S., Motobayashi T., Minemura T., Matsuyama Y., Baba H., Akiyoshi H., Ando Y., Aoi N., Fulop Z., Gomi T., Higurashi Y., Hirai M., Ieki K., Imai N., Iwasa N., Iwasaki H., Iwata Y., Kanno S., Kobayashi H., Kubono S., Kunibu M., Kurokawa M., Liu Z., Michimasa S., Nakamura T., Ozawa A., Sakurai H., Serata M., Takeshita E., Teranishi T., Ue K., Yamada K., Yanagisawa Y., and Ishihara M.: “Molecular states in neutron-rich beryllium isotopes”, *Nucl. Phys. A* **738**, 337–341 (2004). \*

Baba H., Shimoura S., Minemura T., Matsuyama Y., Saito A., Ryuto H., Aoi N., Gomi T., Higurashi Y., Ieki K., Imai N., Iwasa N., Iwasaki H., Kanno S., Kubono S., Kunibu M., Michimasa S., Motobayashi T., Nakamura T., Sakurai H., Serata M., Takeshita E., Takeuchi S., Teranishi T., Ue K., Yamada K., and Yanagisawa Y.: “Isoscalar compressional strengths in  $^{14}\text{O}$ ”, *Nucl. Phys. A* **788**, 188c–193c (2007). \*

Hasebe H., Ryuto H., Fukunishi N., Goto A., Kase M., and Yano Y.: “Polymer coating method developed for carbon stripper foils”, *Nucl. Instrum. Methods Phys. Res. A* **590**, 13–17 (2008). \*

Aoki T., Stingelin L., Kamigaito O., Sakamoto N., Fukunishi N., Yokouchi S., Maie T., Kase M., Goto A., and Yano Y.: “Construction of a beam rebuncher for RIKEN RI-beam factory”, *Nucl. Instrum. Methods Phys. Res. A* **592**, No. 3, pp. 171–179 (2008). \*

Yamaguchi Y., Ozawa A., Goto A., Arai I., Fujinawa T., Fukunishi N., Kikuchi T., Ohnishi T., Ohtsubo T., Sakurai H., Suzuki T., Wakasugi M., Yamaguchi T., Yasuda Y., and Yano Y.: “Rara-RI ring project at RIKEN RI beam factory”, *Nucl. Instrum. Methods Phys. Res. B* **266**, 4575–4578 (2008). \*

Tominaka T.: “Inductance calculation of twisted conductors by the broken line approximation”, *Cryogenics* **49**, 94–102 (2009). \*

(Others)

Nakajima S., Yamaguchi T., Suzuki T., Yamaguchi Y., Fujinawa T., Fukunishi N., Goto A., Ohnishi T., Sakurai

H., Wakasugi M., Yano Y., Arai I., Ozawa A., Yasuda Y., Kikuchi T., and Ohtsubo T.: “New scheme for precision mass measurements of rare isotopes produced at RI beam factory”, *Acta Phys. Pol. B* **39**, No. 2, pp. 457–462 (2008).

Okuno H., Yamada K., Ohnishi J., Fukunishi N., Yokouchi S., Hasebe H., Ikegami K., Kumagai K., Sakamoto N., Kamigaito O., Goto A., Kase M., Yano Y., and Maie T.: “Commissioning of the Superconducting Ring Cyclotron for the RIKEN RI Beam Factory”, *IEEE Trans. Appl. Supercond.* **18**, No. 2, pp. 226–231 (2008).

#### [Book • Proceedings]

(Original Papers) \*Subject to Peer Review

Goto A., Fujimaki M., Fujinawa T., Fukunishi N., Hasebe H., Higurashi Y., Ikegami K., Ikezawa E., Inabe N., Kageyama T., Kamigaito O., Kase M., Kidera M., Kohara S., Komiyama M., Nagase M., Kumagai K., Maie T., Nakagawa T., Ohnishi J., Okuno H., Ryuto H., Sakamoto N., Wakasugi M., Watanabe T., Yamada K., Yokouchi S., and Yano Y.: “Commissioning of RIKEN RI Beam Factory”, *Proceedings of 18th International Conference on Cyclotrons and Their Applications (Cyclotrons 2007)*, Giardini Naxos, Italy, 2007–9~10, Giardini Naxos, pp. 3–8 (2007).

Vorozhtsov S., Vorozhtsov A., Perepelkin E., Watanabe S., Kubono S., Mitsumoto T., and Goto A.: “Calculations of the beam transmission and quality in the RIKEN AVF cyclotron”, *Proceedings of RuPAC 2008, Zvenigorod, Russia, 2008–9~10, Russia, Russia*, pp. 51–53 (2008).

Ohnishi J., Okuno H., Fukunishi N., Yamada K., Goto A., and Yano Y.: “The magnetic field of the superconducting ring cyclotron”, *Proceedings of 18th International Conference on Cyclotrons and Their Applications (Cyclotrons 2007)*, Giardini Naxos, Italy, 2007–10, -, -, pp. 429–431 (2008).

Ohnishi J., Nakagawa T., Higurashi Y., Okuno H., Kusaka K., and Goto A.: “Construction and test of the superconducting coils for RIKEN SC-ECR ion source”, *Proceedings of the 11th European Particle Accelerator Conference (EPAC 2008)*, Genoa, 2008–6, The European Physical Society Accelerator Group, -, pp. 433–435 (2008).

(Others)

Yamaguchi T., Arai I., Fukunishi N., Goto A., Kikuchi T., Komatsubara T., Ohnishi T., Ohtsubo T., Okuno H., Ozawa A., Sasa K., Suzuki T., Tagisi Y., Takeda H., Wakasugi M., Yamaguchi M., Yamaguchi Y., and Yano Y.: “Mass measurements by an isochronous storage ring at the RIKEN RI beam factory”, *Proceedings of the 6th International Conference on Nuclear Physics at Storage Rings (STORI '05)*, Bonn, Germany, 2005–5, Forschungszentrum Julich, Julich, pp. 297–300 (2005).

Yamaguchi M., Arai I., Fukunishi N., Goto A., Kusaka K., Kikuchi T., Komatsubara T., Kubo T., Ohnishi T., Ohtsubo T., Okuno H., Ozawa A., Sasa K., Suzuki

- T., Tagisi Y., Takeda H., Wakasugi M., Yamaguchi T., Yamaguchi Y., and Yano Y.: “Design of an isochronous storage ring and an injection line for mass measurements at the RIKEN RI beam factory”, Proceedings of the 6th International Conference on Nuclear Physics at Storage Rings (STORI '05), Bonn, Germany, 2005–5, Forschungszentrum Julich, Julich, pp. 315–319 (2005).
- Kikuchi T., Horioka K., Ozawa A., Kawata S., Yamaguchi Y., Fukunishi N., Sakurai H., Wakasugi M., Yamaguchi M., Yamaguchi T., Arai I., Ohta H., Fujinawa T., Sasa K., Komatsubara T., Suzuki T., Ohtsubo T., Goto A., Ohnishi T., Okuno H., Takeda H., and Yano Y.: “Individual correction using induction modulator for mass measurements by isochronous ring in RIKEN RI beam factory”, Proceedings of the 2nd International Workshop on Recent Progress in Induction Accelerators (RPIA2006), Tsukuba, 2006–3, KEK, Tsukuba, pp. 127–131 (2006).
- Okuno H., Yamada K., Ohnishi J., Fukunishi N., Sakamoto N., Kamigaito O., Hasebe H., Kumagai K., Maie T., Yokouchi S., Ikegami K., Kase M., Goto A., and Yano Y.: “Hardware commissioning of the RIKEN superconducting ring cyclotron”, Proceedings of 18th International Conference on Cyclotrons and Their Applications (Cyclotrons 2007), Istituto Nazionale di Fisica Nucleare, Roma, pp. 18–20 (2007).
- Okuno H., Fukunishi N., Fujinawa T., Goto A., Higurashi Y., Ikezawa E., Kamigaito O., Kase M., Nakagawa T., Ohnishi J., Sato Y., Yano Y., and Ostroumov P.: “Heavy Ion Accelerators for RIKEN RI Beam Factory and Upgrade Plans”, 42nd ICFA Advanced Beam Dynamics Workshop on High-Intensity, High-Brightness Hadron Beams, Nashville, USA, 2008–8, ICFA, , p. (2009).
- 奥野広樹, 山田一成, 大西純一, 福西暢尚, 横内茂, 長谷部裕雄, 池上九三男, 熊谷桂子, 坂本成彦, 上垣外修一, 長瀬誠, 藤巻正樹, 込山美咲, 後藤彰, 加瀬昌之, 矢野安重, 真家武士: “理研超伝導リングサイクロトロンノ現状報告”, 第4回日本加速器学会年会・第32回リニアック技術研究会論文集, 和光, 2007–8, 日本加速器学会, 東京, pp. 46–48 (2007).
- A., Ohnishi T., Okuno H., Takeda H., and Yano Y.: “Individual correction using induction modulator for mass measurements by isochronous ring in RIKEN RI beam factory”, 2nd International Workshop on Recent Progress in Induction Accelerators (RPIA2006), (KEK , Tokyo Institute of Technology), Tsukuba, Mar. (2006).
- Baba H., Shimoura S., Minemura T., Matsuyama Y., Saito A., Ryuto H., Aoi N., Gomi T., Higurashi Y., Ieki K., Imai N., Iwasa N., Iwasaki H., Kanno S., Kubono S., Kunibu M., Michimasa S., Motobayashi T., Nakamura T., Sakurai H., Serata M., Takeshita E., Takeuchi S., Teranishi T., Ue K., Yamada K., and Yanagisawa Y.: “Isoscalar excitation in  $^{14}\text{O}$ ”, 5th International Workshop on Direct Reaction with Exotic Beams (DREB2007), (DREB2007 Committee), Wako, May–June (2006).
- Baba H., Shimoura S., Minemura T., Matsuyama Y., Saito A., Ryuto H., Aoi N., Gomi T., Higurashi Y., Ieki K., Imai N., Iwasa N., Iwasaki H., Kanno S., Kubono S., Kunibu M., Michimasa S., Motobayashi T., Nakamura T., Sakurai H., Serata M., Takeshita E., Takeuchi S., Teranishi T., Ue K., Yamada K., and Yanagisawa Y.: “Measurement of isoscalar monopole and dipole strengths in  $^{14}\text{O}$ ”, International Nuclear Physics Conference (INPC2007), Tokyo, June (2006).
- Hasebe H., Ryuto H., Fukunishi N., Goto A., Kase M., and Yano Y.: “Polymer coating method developed for carbon stripper foils”, 23rd World Conference of the INTDS, (High Energy Accelerator Research Organization (KEK)), Tsukuba, Oct. (2006).
- Arai I., Komatsubara T., Ozawa A., Sasa K., Yasuda Y., Fujinawa T., Fukunishi N., Goto A., Ohnishi T., Okuno H., Takeda H., Wakasugi M., Yamaguchi M., Yamaguchi Y., Yano Y., Kikuchi T., Suzuki T., Yamaguchi T., and Ohtsubo T.: “Isochronous ring at RIKEN”, Workshop on Advanced Laser and Mass Spectroscopy ALMAS-1: Innovative Physics Ideas, (Gesellschaft für Schwerionenforschung (GSI)), Darmstadt, Germany, Oct. (2006).
- Arai I., Komatsubara T., Ozawa A., Sasa K., Yasuda Y., Fujinawa T., Fukunishi N., Goto A., Ohnishi T., Okuno H., Takeda H., Wakasugi M., Yamaguchi M., Yamaguchi Y., Yano Y., Kikuchi T., Suzuki T., Yamaguchi T., and Ohtsubo T.: “Rare RI ring”, RIBF International Collaboration Workshop on Experiments at the RIBF, Wako, Nov. (2006).
- Yamaguchi Y., Fujinawa T., Fukunishi N., Goto A., Ohnishi T., Sakurai H., Wakasugi M., Yano Y., Ozawa A., Arai I., Yasuda Y., Suzuki T., Yamaguchi T., Kikuchi T., and Ohtsubo T.: “Rare-RI ring project at RI Beam factory in RIKEN”, 15th International Conference on Electromagnetic Isotope Separators and Techniques Related to their Applications (EMIS2007), (GANIL , IN2P3/CNRS , DSM/CEA), Deauville, France, June (2007).

### Oral Presentations

(International Conference etc.)

- Yamaguchi T., Ozawa A., Arai I., Komatsubara T., Sasa K., Tagisi Y., Yamaguchi M., Suzuki T., Ohtsubo T., Fukunishi N., Goto A., Ohnishi T., Okuno H., Takeda H., Wakasugi M., Yano Y., Yamaguchi Y., and Kikuchi T.: “Mass measurements in RIKEN”, 6th International Conference on Nuclear Physics at Storage Rings (STORI-05), (Research Center Julich), Bonn, Germany, May (2005).
- Kikuchi T., Horioka K., Ozawa A., Kawata S., Yamaguchi Y., Fukunishi N., Sakurai H., Wakasugi M., Yamaguchi M., Yamaguchi T., Arai I., Ohta H., Fujinawa T., Sasa K., Komatsubara T., Suzuki T., Ohtsubo T., Goto

- Ozawa A., Arai I., Fujinawa T., Fukunishi N., Goto A., Kikuchi T., Igarashi S., Komatsubara T., Ohtsubo T., Sakurai H., Sasa K., Suzuki T., Wakasugi M., Yamaguchi K., Yamaguchi T., Yamaguchi Y., Yano Y., and Yasuda Y.: “Mass measurements by isochronous storage ring in RI beam factory”, International Nuclear Physics Conference (INPC2007), (RIKEN and others), Tokyo, June (2007).
- Okuno H., Yamada K., Ohnishi J., Fukunishi N., Yokouchi S., Hasebe H., Ikegami K., Kumagai K., Sakamoto N., Kamigaito O., Goto A., Kase M., Yano Y., and Maie T.: “Commissioning of the Superconducting Ring Cyclotron for the RIKEN RI Beam Factory”, MT-20 The 20th biennial conference on magnet technology, Wako, Aug. (2007).
- Nakajima S., Suzuki T., Yamaguchi T., Fujinawa T., Fukunishi N., Goto A., Ohnishi T., Sakurai H., Wakasugi M., Yamaguchi Y., Yano Y., Ozawa A., Arai I., Yasuda Y., Kikuchi T., and Ohtsubo T.: “New scheme for precision mass measurement of rare isotopes produced at RI beam factory”, 30th Mazurian Lakes Conference on Physics : Nuclear Physics and the Fundamental Processes, (IPJ ; University of Warsaw ; Pro-Physica), Piaski, Poland, Sept. (2007).
- Goto A., Fujimaki M., Fujinawa T., Fukunishi N., Hasebe H., Higurashi Y., Ikegami K., Ikezawa E., Inabe N., Kageyama T., Kamigaito O., Kase M., Kidera M., Kohara S., Komiyama M., Nagase M., Kumagai K., Maie T., Nakagawa T., Ohnishi J., Okuno H., Ryuto H., Sakamoto N., Wakasugi M., Watanabe T., Yamada K., Yokouchi S., and Yano Y.: “Commissioning of RIKEN RI Beam Factory”, 18th International Conference on Cyclotrons and their Applications (Cyclotrons 2007), (Laboratori Nazionali del Sud, INFN), Giardini Naxos, Italy, Sept.–Oct. (2007).
- Yamada K., Fujimaki M., Fukunishi N., Goto A., Kase M., Komiyama M., Ohnishi J., Okuno H., Watanabe T., and Yano Y.: “Details of Beam Diagnostic System for RIKEN Superconducting Ring Cyclotron”, 18th International Conference on Cyclotrons and their Applications (Cyclotrons 2007), (Laboratori Nazionali del Sud), Giardini Naxos, Italy, Sept.–Oct. (2007).
- Okuno H., Yamada K., Ohnishi J., Fukunishi N., Yokouchi S., Hasebe H., Ikegami K., Kumagai K., Sakamoto N., Kamigaito O., Goto A., Kase M., Yano Y., and Maie T.: “Hardware commissioning of the RIKEN superconducting ring cyclotron”, 18th International Conference on Cyclotrons and their Applications (Cyclotrons 2007), Giardini Naxos, Italy, Sept.–Oct. (2007).
- Fukunishi N., Yamada K., Fujimaki M., Fujinawa T., Goto A., Hasebe H., Higurashi Y., Ikegami K., Ikezawa E., Inabe N., Kamigaito O., Kase M., Kohara S., Komiyama M., Kumagai K., Maie T., Nagase M., Nakagawa T., Ohnishi J., Okuno H., Ryuto H., Sakamoto N., Wakasugi M., Watanabe T., and Yano Y.: “Present performance and commissioning details of RIBF accelerator complex”, 18th International Conference on Cyclotrons and their Applications (Cyclotrons 2007), (Laboratori Nazionali del Sud), Giardini Naxos, Italy, Sept.–Oct. (2007).
- Yamaguchi T., Fujinawa T., Fukunishi N., Goto A., Ohnishi T., Sakurai H., Wakasugi M., Yamaguchi Y., Yano Y., Arai I., Moriguchi T., Ozawa A., Yasuda Y., Nakajima S., Kuboki T., Suzuki T., Kikuchi T., and Ohtsubo T.: “Storage-ring mass spectrometry”, ETC Workshop on Mass Olympics, (GSI , FIAS), Trento, Italy, May (2008).
- Okuno H., Fukunishi N., Fujinawa T., Goto A., Higurashi Y., Ikezawa E., Kamigaito O., Kase M., Nakagawa T., Ohnishi J., Sato Y., Yano Y., and Ostroumov P.: “Heavy Ion Accelerators for RIKEN RI Beam Factory and Upgrade Plans”, 42nd ICFA Advanced Beam Dynamics Workshop on High-Intensity, High-Brightness Hadron Beams (HB2008), (Oakridge National Laboratory), Nashville, USA, Aug. (2008).
- Yamaguchi T., Arai I., Ozawa A., Yasuda Y., Fujinawa T., Fukunishi N., Goto A., Hara K., Ohnishi T., Sakurai H., Wakasugi M., Yamaguchi Y., Yano Y., Kikuchi T., Suzuki T., and Ohtsubo T.: “Beam optics simulation for rare-RI ring at RI beam factory in RIKEN”, 7th International Conference on Nuclear Physics at Storage Rings STORI’08, (Institute of Modern Physics, Chinese Academy of Sciences, National Natural Foundation of China), Lanzhou, China, Sept. (2008).
- Yasuda Y., Ozawa A., Arai I., Fujinawa T., Fukunishi N., Goto A., Ohnishi T., Sakurai H., Wakasugi M., Yamaguchi Y., Yano Y., Suzuki T., Yamaguchi T., Kikuchi T., and Ohtsubo T.: “Present status of rare-RI ring project in RIKEN RIBF”, 7th International Conference on Nuclear Physics at Storage Rings STORI’08, (Institute of Modern Physics, Chinese Academy of Sciences, National Natural Foundation of China), Lanzhou, China, Sept. (2008).
- (Domestic Conference)
- 太田寛史, 新井一郎, 小沢顕, 小松原哲郎, 笹公和, 鈴木健, 山口貴之, 大坪隆, 山口充孝, 田岸義宏, 矢野安重, 後藤彰, 若杉昌徳, 奥野広樹, 福西暢尚, 大西哲哉, 山口由高, 菊池崇志: “Design of the isochronous storage ring for accurate mass measurement in RI beam factory”, 第2回日本加速器学会年会/第30回リニアック技術研究会, 鳥栖, 7月(2005).
- 太田寛史, 新井一郎, 小沢顕, 小松原哲郎, 笹公和, 鈴木健, 山口貴之, 大坪隆, 山口充孝, 田岸義宏, 矢野安重, 後藤彰, 奥野広樹, 福西暢尚, 大西哲哉, 山口由高, 菊池崇志: “等時性蓄積リングへの入射ラインとそのビーム光学”, 等時性蓄積リングによる不安定核の質量測定と宇宙元素合成, (筑波大学), つくば, 9月(2005).
- 山口由高, 若杉昌徳, 藤縄雅, 福西暢尚, 後藤彰, 大西哲哉, 奥野広樹, 櫻井博儀, 竹田浩之, 山口充孝, 矢野安重, 小沢顕, 新井一郎, 小松原哲郎, 笹公和, 菊池崇志, 鈴木健, 山口

- 貴之, 大坪隆: “等時性蓄積リングのためのキッカー電磁石及び入射スキームの検討”, 等時性蓄積リングによる不安定核の質量測定と宇宙元素合成, (筑波大学), つくば, 9月(2005).
- 山口由高, 小沢顕, 新井一郎, 安田裕介, 藤縄雅, 福西暢尚, 大西哲哉, 後藤彰, 奥野広樹, 櫻井博儀, 若杉昌徳, 矢野安重, 鈴木健, 山口貴之, 菊池崇志, 大坪隆: “等時性蓄積リングによる質量測定”, 国立天文台ワークショップ「Rプロセス元素組成の統合的理解: 量子ビームでさぐる宇宙進化の理解を目指して」, 三鷹, 3月(2007).
- 山田一成, 藤巻正樹, 福西暢尚, 後藤彰, 加瀬昌之, 込山美咲, 大西純一, 奥野広樹, 渡邊環, 矢野安重: “超伝導リングサイクロトロンビーム診断系の詳細”, 第4回日本加速器学会年会・第32回リニアック技術研究会, ( ), 和光, 8月(2007).
- 渡邊環, 若杉昌徳, 藤巻正樹, 加瀬昌之, 福西暢尚, 小高康照, 小山亮, 山田一成, 後藤彰, 矢野安重: “RIBFにおけるプラスチックシンチレーションモニターを用いたビームエネルギーと縦方向のビームプロファイルの測定”, 第4回日本加速器学会年会・第32回リニアック技術研究会, 和光, 8月(2007).
- 長谷部裕雄, 龍頭啓充, 福西暢尚, 後藤彰, 加瀬昌之, 矢野安重: “ポリマーコーティング炭素薄膜の制作”, 第4回日本加速器学会年会・第32回リニアック技術研究会, 和光, 8月(2007).
- 中川孝秀, 木寺正憲, 羽場宏光, 藍原利光, 加瀬昌之, 後藤彰, 矢野安重: “理研 ECR イオン源での多価ウランイオンの生成”, 第4回日本加速器学会年会・第32回リニアック技術研究会, 和光, 8月(2007).
- 安田裕介, 新井一郎, 小沢顕, 小松原哲郎, 笹公和, 大西哲哉, 後藤彰, 櫻井博儀, 福西暢尚, 藤縄雅, 矢野安重, 山口由高, 若杉昌徳, 鈴木健, 山口貴之, 大坪隆, 菊池崇志: “理研 RIBF における等時性蓄積リング計画”, 日本物理学会第62回年次大会, 札幌, 9月(2007).
- 山口由高, 大西哲哉, 後藤彰, 櫻井博儀, 福西暢尚, 藤縄雅, 矢野安重, 若杉昌徳, 新井一郎, 小沢顕, 小松原哲郎, 笹公和, 安田裕介, 鈴木健, 山口貴之, 菊池崇志, 大坪隆: “理研 RIBF における質量リング計画の現状”, 国立天文台研究会「Rプロセス元素合成の統合的理解-量子ビームで探る宇宙進化の理解を目指して-」, つくば, 3月(2008).
- 山口由高, 藤縄雅, 福西暢尚, 後藤彰, 大西哲哉, 櫻井博儀, 若杉昌徳, 矢野安重, 小沢顕, 新井一郎, 安田裕介, 菊池崇志, 大坪隆, 鈴木健, 山口貴之: “理研 RIBF における稀少 RI リング計画の現状”, 第5回日本加速器学会年会/第33回リニアック技術研究会, 東広島, 8月(2008).
- 長谷部裕雄, 奥野広樹, 久保木浩功, 龍頭啓充, 福西暢尚, 上垣外修一, 後藤彰, 加瀬昌之, 矢野安重: “理研 RIBF における長寿命炭素薄膜の開発状況”, 第5回日本加速器学会年会/第33回リニアック技術研究会, (広島大学), 広島, 8月(2008).
- 市川雄一, 久保敏幸, 青井考, Banerjee S. R., Chakrabarti A., 福田直樹, 岩崎弘典, 久保野茂, 本林透, 中林彩, 中村隆司, 中尾太郎, 奥村俊文, 王恵仁, 大西健夫, 鈴木大介, 鈴木賢, 山田一成, 山口英斉, 櫻井博儀: 第5回停止・低速不安定核ビームを用いた核分光研究会, (大阪大学), 豊中, 12月(2008).
- 市川雄一, 久保敏幸, 青井考, Banerjee S. R., Chakrabarti A., 福田直樹, 岩崎弘典, 久保野茂, 本林透, 中林彩, 中村隆司, 中尾太郎, 奥村俊文, 王恵仁, 大西健夫, 鈴木大介, 鈴木賢, 山田一成, 山口英斉, 櫻井博儀: 日本物理学会 2008 年秋季大会, 山形, 9月(2008).

## Accelerator Team

### Publications

#### [Journal]

(Original Papers) \*Subject to Peer Review

- Saito T., Sakai H., Ikeda T., Itoh K., Kawabata T., Kuboki H., Maeda Y., Matsui N., Sasano M., Satou Y., Sekiguchi K., Suda K., Tamii A., Uesaka T., and Yako K.: “Experimental Test of Bell’s Inequality via the  $^1\text{H}(d, ^2\text{He})n$  Reaction”, AIP Conf. Proc. **768**, 62–64 (2005). \*
- Takechi M., Fukuda M., Mihara M., Chinda T., Matsumasa T., Matsubara H., Nakashima Y., Matsuta K., Minamisono T., Koyama R., Shinosaki W., Takahashi M., Takisawa A., Ohtsubo T., Suzuki T., Momota S., Hatanaka K., Suda T., Sasaki M., Sato S., and Kitagawa A.: “Reaction cross-sections for stable nuclei and nucleon density distribution of proton drip-line nucleus  $8\text{B}$ ”, Eur. Phys. J. A **25**, No. s01, pp. 217–219 (2005). \*
- Hatano M., Sakai H., Wakui T., Uesaka T., Aoi N., Ichikawa Y., Ikeda T., Itoh K., Iwasaki H., Kawabata T., Kuboki H., Maeda Y., Matsui N., Ohnishi T., Ohnishi T., Saito T., Sakamoto N., Sasano M., Satou Y., Sekiguchi K., Suda K., Tamii A., Yanagisawa Y., and Yako K.: “First experiment of  $6\text{He}$  with a polarized proton target”, Eur. Phys. J. A **25**, No. s01, pp. 255–258 (2005). \*
- Sekiguchi K., Sakai H., Witala H., Glockle W., Golak J., Hatanaka K., Hatano M., Itoh K., Kamada H., Kuboki H., Maeda Y., Nogga A., Okamura H., Saito T., Sakamoto N., Sakemi Y., Sasano M., Shimizu Y., Suda T., Tamii A., Uesaka T., Wakasa T., and Yako K.: “Resolving the Discrepancy of 135 MeV  $pd$  Elastic Scattering Cross Sections and Relativistic Effects”, Phys. Rev. Lett. **95**, 162301-1–162301-4 (2005). \*
- Ladygin V., Uesaka T., Saito T., Hatano M., Isupov Y., Kato H., Ladygina N., Maeda Y., Malakhov A., Nishikawa J., Ohnishi T., Okumura H., Reznikov S., Sakai H., Sakamoto N., Sakoda S., Saito T., Sekiguchi K., Suda K., Tamii A., Uchigashima N., and Yako K.: “Tensor Analyzing Power  $T_{20}$  of the  $dd \rightarrow ^3\text{He}n$  and  $dd \rightarrow ^3\text{He}p$  Reactions at Zero Angle for Energies 140, 200, and 270 MeV”, Phys. At. Nucl. **69**, 1271–1278 (2006). \*
- Sakai H., Saito T., Ikeda T., Itoh K., Kawabata T., Kuboki H., Maeda Y., Matsui N., Rangacharyulu C., Sasano M., Sato Y., Sekiguchi K., Suda K., Tamii A., Uesaka T., and Yako K.: “Spin correlations of strongly interacting massive fermion pairs as a test of Bell’s inequality”, Phys. Rev. Lett. **97**, No. 15, pp. 150405-1–150405-4 (2006). \*
- Sakaguchi S., Uesaka T., Wakui T., Kawabata T., Aoi N., Hashimoto Y., Ichikawa M., Ichikawa Y., Itoh Y., Itoh M., Iwasaki H., Kawahara T., Kuboki H., Maeda Y., Matsuo R., Nakao T., Okamura H., Sakai H., Sakamoto N., Sasamoto Y., Sasano M., Satou Y., Sekiguchi K., Shinohara M., Suda K., Suzuki D., Takahashi Y., Tamii A., Yako K., and Yamaguchi M.: “Analyzing Power Measurement for Elastic Scattering of  $^6\text{He}$  on polarized protons”, AIP Conf. Proc. **915**, 833–836 (2007). \*
- Mardanpour H., Amir-Ahmadi H., Deltuva A., Itoh K., Kalantar N. N., Kawabata T., Kuboki H., Maeda Y., Messchendorp J. G., Sakaguchi S., Sakai H., Sakamoto N., Sasamoto Y., Sasano M., Sekiguchi K., Suda K., Takahashi Y., Uesaka T., Witala H., and Yako K.: “Precision Measurement of Vector and Tensor Analyzing Powers in Elastic Deuteron-Proton Scattering”, Eur. Phys. J. A **31**, 383–391 (2007). \*
- Miki K., Sakai H., Itoh K., Kawabata K., Kuboki H., Maeda Y., Noji S., Sakaguchi S., Sakamoto N., Sasamoto Y., Sasano M., Satou Y., Sekiguchi K., Suda K., Takahashi Y., Uesaka T., and Yako K.: “Measurement of the  $^2\text{H}(d, pn)$  Reaction at 0 degrees at 270 MeV”, Nucl. Phys. A **790**, 442c–445c (2007). \*
- Wakasa T., Ihara E., Fujita ., Funaki Y., Hatanaka K., Horiuchi H., Itoh M., Kamiya ., Roepke G., Sakaguchi H., Sakamoto ., Sakemi ., Schuck P., Shimizu Y., Takashina M., Terashima S., Suzuki A., Uchida M., Yoshida ., and Yosoi .: “New candidate for an alpha cluster condensed state in  $^{16}\text{O}$  ( $\alpha, \alpha'$ ) at 400 MeV”, Phys. Lett. B **653**, 173–177 (2007). \*
- Ladygin V., Uesaka T., Saito T., Janek M., Kiselev A., Kurilkin A., Vasiliev A., Hatano M., Isupov Y., Kato H., Ladygina N., Maeda Y., Malakhov A., Nishikawa J., Ohnishi T., Okamura H., Reznikov S., Sakai H., Sakoda S., Sakamoto N., Satou Y., Sekiguchi K., Suda K., Tamii A., Uchigashima N., and Yako K.: “Analyzing powers in the  $dd \rightarrow ^3\text{He}n(^3\text{He}p)$  reactions at intermediate energies”, AIP Conf. Proc. **1011**, 235–240 (2008). \*
- Kurilkin A., Saito T., Ladygin V., Uesaka T., Vasiliev T., Janek M., Hatano M., Isupov Y., Kato K., Ladygina N., Maeda Y., Malakhov A., Nishikawa J., Ohnishi T., Okamura H., Reznikov S., Sakai H., Sakamoto N., Sakoda S., Satou Y., Sekiguchi K., Suda K., Tamii A., Uchigashima N., and Yako K.: “Measurement of the vector  $A_y$  and tensor  $A_{yy}, A_{xx}, A_{xz}$  analyzing powers for the  $dd \rightarrow ^3\text{He}p$  reaction at 200 MeV”, Eur. Phys. J. Special Topics **162**, 133–136 (2008). \*
- Kiselev A., Ladygin V., Uesaka T., Vasiliev A., Janek M., Saito T., Hatano M., Isupov Y., Kato H., Ladygina N., Maeda Y., Malakhov A., Nishikawa J., Ohnishi T., Okamura H., Reznikov S., Sakai H., Sakamoto N., Sakoda S., Satou Y., Sekiguchi K., Suda K., Tamii A., Uchigashima N., and Yako K.: “Analyzing powers in the  $^{12}\text{C}(\vec{d}, p)^{13}\text{C}$  reaction at the energy  $T_d = 270$  MeV”, Eur. Phys. J. Special Topics **162**, 143–146 (2008). \*
- Hasebe H., Ryuto H., Fukunishi N., Goto A., Kase M., and Yano Y.: “Polymer coating method developed for carbon stripper foils”, Nucl. Instrum. Methods Phys.

Res. A **590**, 13–17 (2008). \*

Aoki T., Stingelin L., Kamigaito O., Sakamoto N., Fukunishi N., Yokouchi S., Maie T., Kase M., Goto A., and Yano Y.: “Construction of a beam rebuncher for RIKEN RI-beam factory”, Nucl. Instrum. Methods Phys. Res. A **592**, No. 3, pp. 171–179 (2008). \*

Sakaguchi S., Uesaka T., Wakui T., Kawabata T., Aoi N., Hashimoto Y., Ichikawa M., Itoh Y., Itoh M., Iwasaki H., Kawahara T., Kuboki H., Maeda Y., Matsuo R., Nakao T., Okamura H., Sakai H., Sakamoto N., Sasamoto Y., Sasano M., Satou Y., Sekiguchi K., Shinohara M., Suda K., Suzuki D., Takahashi Y., Tamii A., Yako K., and Yamaguchi M.: “Spin-orbit potential in  ${}^6\text{He}$  studied with polarized proton target”, Nucl. Phys. A **805**, 467–469 (2008). \*

Zegers R. G., Brown E. F., Akimune H., Austin S. M., van den Berg A. M., Brown B. A., Chamulak D. A., Fujita Y., Fujiwara M., Gales S., Harakeh M. N., Hashimoto H., Hayami R., Hitt G. W., Itoh M., Kawabata T., Kawase K., Kinoshita M., Nakanishi K., Nakayama S., Okumura S., Shimbara Y., Uchida M., Ueno H., Yamagata T., and Yosoi M.: “Gamow-Teller strength for the analog transitions to the first  $T = 1/2$ ,  $J^\pi = 3/2^-$  states in  ${}^{13}\text{C}$  and  ${}^{13}\text{N}$  and the implications for type Ia supernovae”, Phys. Rev. C **77**, 024307-1–024307-10 (2008). \*

(Others)

Okuno H., Yamada K., Ohnishi J., Fukunishi N., Yokouchi S., Hasebe H., Ikegami K., Kumagai K., Sakamoto N., Kamigaito O., Goto A., Kase M., Yano Y., and Maie T.: “Commissioning of the Superconducting Ring Cyclotron for the RIKEN RI Beam Factory”, IEEE Trans. Appl. Supercond. **18**, No. 2, pp. 226–231 (2008).

奥野広樹: “超伝導リングサイクロトロン (SRC) の概要”, 低温工学 **43**, No. 11, pp. 452–459 (2008).

#### [Book-Proceedings]

(Original Papers) \*Subject to Peer Review

Goto A., Fujimaki M., Fujinawa T., Fukunishi N., Hasebe H., Higurashi Y., Ikegami K., Ikezawa E., Inabe N., Kageyama T., Kamigaito O., Kase M., Kidera M., Kohara S., Komiyama M., Nagase M., Kumagai K., Maie T., Nakagawa T., Ohnishi J., Okuno H., Ryuto H., Sakamoto N., Wakasugi M., Watanabe T., Yamada K., Yokouchi S., and Yano Y.: “Commissioning of RIKEN RI Beam Factory”, Proceedings of 18th International Conference on Cyclotrons and Their Applications (Cyclotrons 2007), Giardini Naxos, Italy, 2007–9~10, , Giardini Naxos, pp. 3–8 (2007).

Ohnishi J., Okuno H., Fukunishi N., Yamada K., Goto A., and Yano Y.: “The magnetic field of the superconducting ring cyclotron”, Proceedings of 18th International Conference on Cyclotrons and Their Applications (Cyclotrons 2007), Giardini Naxos, Italy, 2007–10, -, -, pp. 429–431 (2008).

Ohnishi J., Nakagawa T., Higurashi Y., Okuno H., Kusaka

K., and Goto A.: “Construction and test of the superconducting coils for RIKEN SC-ECR ion source”, Proceedings of the 11th European Particle Accelerator Conference (EPAC 2008), Genoa, 2008–6, The European Physical Society Accelerator Group, -, pp. 433–435 (2008).

(Others)

Yamaguchi T., Arai I., Fukunishi N., Goto A., Kikuchi T., Komatsubara T., Ohnishi T., Ohtsubo T., Okuno H., Ozawa A., Sasa K., Suzuki T., Tagisi Y., Takeda H., Wakasugi M., Yamaguchi M., Yamaguchi Y., and Yano Y.: “Mass measurements by an isochronous storage ring at the RIKEN RI beam factory”, Proceedings of the 6th International Conference on Nuclear Physics at Storage Rings (STORI '05), Bonn, Germany, 2005–5, Forschungszentrum Julich, Julich, pp. 297–300 (2005).

Yamaguchi M., Arai I., Fukunishi N., Goto A., Kusaka K., Kikuchi T., Komatsubara T., Kubo T., Ohnishi T., Ohtsubo T., Okuno H., Ozawa A., Sasa K., Suzuki T., Tagisi Y., Takeda H., Wakasugi M., Yamaguchi T., Yamaguchi Y., and Yano Y.: “Design of an isochronous storage ring and an injection line for mass measurements at the RIKEN RI beam factory”, Proceedings of the 6th International Conference on Nuclear Physics at Storage Rings (STORI '05), Bonn, Germany, 2005–5, Forschungszentrum Julich, Julich, pp. 315–319 (2005).

Kikuchi T., Horioka K., Ozawa A., Kawata S., Yamaguchi Y., Fukunishi N., Sakurai H., Wakasugi M., Yamaguchi M., Yamaguchi T., Arai I., Ohta H., Fujinawa T., Sasa K., Komatsubara T., Suzuki T., Ohtsubo T., Goto A., Ohnishi T., Okuno H., Takeda H., and Yano Y.: “Individual correction using induction modulator for mass measurements by isochronous ring in RIKEN RI beam factory”, Proceedings of the 2nd International Workshop on Recent Progress in Induction Accelerators (RPIA2006), Tsukuba, 2006–3, KEK, Tsukuba, pp. 127–131 (2006).

Okuno H., Yamada K., Ohnishi J., Fukunishi N., Sakamoto N., Kamigaito O., Hasebe H., Kumagai K., Maie T., Yokouchi S., Ikegami K., Kase M., Goto A., and Yano Y.: “Hardware commissioning of the RIKEN superconducting ring cyclotron”, Proceedings of 18th International Conference on Cyclotrons and Their Applications (Cyclotrons 2007), Istituto Nazionale di Fisica Nucleare, Roma, pp. 18–20 (2007).

Okuno H., Fukunishi N., Fujinawa T., Goto A., Higurashi Y., Ikezawa E., Kamigaito O., Kase M., Nakagawa T., Ohnishi J., Sato Y., Yano Y., and Ostroumov P.: “Heavy Ion Accelerators for RIKEN RI Beam Factory and Upgrade Plans”, 42nd ICFA Advanced Beam Dynamics Workshop on High-Intensity, High-Brightness Hadron Beams, Nashville, USA, 2008–8, ICFA, , p. (2009).

奥野広樹, 山田一成, 大西純一, 福西暢尚, 横内茂, 長谷部裕雄, 池上九三男, 熊谷桂子, 坂本成彦, 上垣外修一, 長瀬誠, 藤巻

正樹, 込山美咲, 後藤彰, 加瀬昌之, 矢野安重, 真家武士: “理研超伝導リングサイクロトロン の現状報告”, 第4回日本加速器学会年会・第32回リニアック技術研究会論文集, 和光, 2007-8, 日本加速器学会, 東京, pp. 46-48 (2007).

### Oral Presentations

(International Conference etc.)

Yamaguchi T., Ozawa A., Arai I., Komatsubara T., Sasa K., Tagisi Y., Yamaguchi M., Suzuki T., Ohtsubo T., Fukunishi N., Goto A., Ohnishi T., Okuno H., Takeda H., Wakasugi M., Yano Y., Yamaguchi Y., and Kikuchi T.: “Mass measurements in RIKEN”, 6th International Conference on Nuclear Physics at Storage Rings (STORI-05), (Research Center Julich), Bonn, Germany, May (2005).

Kikuchi T., Horioka K., Ozawa A., Kawata S., Yamaguchi Y., Fukunishi N., Sakurai H., Wakasugi M., Yamaguchi M., Yamaguchi T., Arai I., Ohta H., Fujinawa T., Sasa K., Komatsubara T., Suzuki T., Ohtsubo T., Goto A., Ohnishi T., Okuno H., Takeda H., and Yano Y.: “Individual correction using induction modulator for mass measurements by isochronous ring in RIKEN RI beam factory”, 2nd International Workshop on Recent Progress in Induction Accelerators (RPIA2006), (KEK, Tokyo Institute of Technology), Tsukuba, Mar. (2006).

Sekiguchi K., Sakai H., Sakamoto N., Kuboki H., Sasano M., Takahashi Y., Yako K., Kawabata T., Maeda Y., Sakaguchi S., Sasamoto Y., Suda K., Uesaka T., Okamura H., Itoh K., and Wakasa T.: “Study of Spin Parts of Three Nucleon Forces via  $\bar{d}p$  Breakup Reactions at Intermediate Energies”, 18th International IUPAP Conference on Few-Body Problems in Physics, (Istituto de Fisica Teorica), Santos, Brazil, Aug. (2006).

Arai I., Komatsubara T., Ozawa A., Sasa K., Yasuda Y., Fujinawa T., Fukunishi N., Goto A., Ohnishi T., Okuno H., Takeda H., Wakasugi M., Yamaguchi M., Yamaguchi Y., Yano Y., Kikuchi T., Suzuki T., Yamaguchi T., and Ohtsubo T.: “Isochronous ring at RIKEN”, Workshop on Advanced Laser and Mass Spectroscopy ALMAS-1: Innovative Physics Ideas, (Gesellschaft für Schwerionenforschung (GSI)), Darmstadt, Germany, Oct. (2006).

Arai I., Komatsubara T., Ozawa A., Sasa K., Yasuda Y., Fujinawa T., Fukunishi N., Goto A., Ohnishi T., Okuno H., Takeda H., Wakasugi M., Yamaguchi M., Yamaguchi Y., Yano Y., Kikuchi T., Suzuki T., Yamaguchi T., and Ohtsubo T.: “Rare RI ring”, RIBF International Collaboration Workshop on Experiments at the RIBF, Wako, Nov. (2006).

Sekiguchi K., Sakai H., Sakamoto N., Kuboki T., Sasano M., Takahashi Y., Yako K., Kawabata T., Maeda Y., Sakaguchi S., Sasamoto Y., Suda K., Uesaka T., Okamura H., Itoh K., and Wakasa T.: “Three Nucleon Force Study via  $\bar{d}p$  Breakup Reactions at Intermediate Energies”, International Nuclear Physics Conference

(INPC2007), Tokyo, June (2007).

Okuno H., Yamada K., Ohnishi J., Fukunishi N., Yokouchi S., Hasebe H., Ikegami K., Kumagai K., Sakamoto N., Kamigaito O., Goto A., Kase M., Yano Y., and Maie T.: “Commissioning of the Superconducting Ring Cyclotron for the RIKEN RI Beam Factory”, MT-20 The 20th biennial conference on magnet technology, Wako, Aug. (2007).

Goto A., Fujimaki M., Fujinawa T., Fukunishi N., Hasebe H., Higurashi Y., Ikegami K., Ikezawa E., Inabe N., Kageyama T., Kamigaito O., Kase M., Kidera M., Kohara S., Komiyama M., Nagase M., Kumagai K., Maie T., Nakagawa T., Ohnishi J., Okuno H., Ryuto H., Sakamoto N., Wakasugi M., Watanabe T., Yamada K., Yokouchi S., and Yano Y.: “Commissioning of RIKEN RI Beam Factory”, 18th International Conference on Cyclotrons and their Applications (Cyclotrons 2007), (Laboratori Nazionali del Sud, INFN), Giardini Naxos, Italy, Sept.-Oct. (2007).

Yamada K., Fujimaki M., Fukunishi N., Goto A., Kase M., Komiyama M., Ohnishi J., Okuno H., Watanabe T., and Yano Y.: “Details of Beam Diagnostic System for RIKEN Superconducting Ring Cyclotron”, 18th International Conference on Cyclotrons and their Applications (Cyclotrons 2007), (Laboratori Nazionali del Sud), Giardini Naxos, Italy, Sept.-Oct. (2007).

Okuno H., Yamada K., Ohnishi J., Fukunishi N., Yokouchi S., Hasebe H., Ikegami K., Kumagai K., Sakamoto N., Kamigaito O., Goto A., Kase M., Yano Y., and Maie T.: “Hardware commissioning of the RIKEN superconducting ring cyclotron”, 18th International Conference on Cyclotrons and their Applications (Cyclotrons 2007), Giardini Naxos, Italy, Sept.-Oct. (2007).

Fukunishi N., Yamada K., Fujimaki M., Fujinawa T., Goto A., Hasebe H., Higurashi Y., Ikegami K., Ikezawa E., Inabe N., Kamigaito O., Kase M., Kohara S., Komiyama M., Kumagai K., Maie T., Nagase M., Nakagawa T., Ohnishi J., Okuno H., Ryuto H., Sakamoto N., Wakasugi M., Watanabe T., and Yano Y.: “Present performance and commissioning details of RIBF accelerator complex”, 18th International Conference on Cyclotrons and their Applications (Cyclotrons 2007), (Laboratori Nazionali del Sud), Giardini Naxos, Italy, Sept.-Oct. (2007).

Okuno H., Fukunishi N., Fujinawa T., Goto A., Higurashi Y., Ikezawa E., Kamigaito O., Kase M., Nakagawa T., Ohnishi J., Sato Y., Yano Y., and Ostroumov P.: “Heavy Ion Accelerators for RIKEN RI Beam Factory and Upgrade Plans”, 42nd ICFA Advanced Beam Dynamics Workshop on High-Intensity, High-Brightness Hadron Beams (HB2008), (Oakridge National Laboratory), Nashville, USA, Aug. (2008).

(Domestic Conference)

太田寛史, 新井一郎, 小沢顕, 小松原哲郎, 笹公和, 鈴木健, 山口貴之, 大坪隆, 山口充孝, 田岸義宏, 矢野安重, 後藤

彰, 若杉昌徳, 奥野広樹, 福西暢尚, 大西哲哉, 山口由高, 菊池崇志: “Design of the isochronous storage ring for accurate mass measurement in RI beam factory”, 第2回日本加速器学会年会/第30回リニアック技術研究会, 鳥栖, 7月(2005).

太田寛史, 新井一郎, 小沢顕, 小松原哲郎, 笹公和, 鈴木健, 山口貴之, 大坪隆, 山口充孝, 田岸義宏, 矢野安重, 後藤彰, 奥野広樹, 福西暢尚, 大西哲哉, 山口由高, 菊池崇志: “等時性蓄積リングへの入射ラインとそのビーム光学”, 等時性蓄積リングによる不安定核の質量測定と宇宙元素合成, (筑波大学), つくば, 9月(2005).

山口由高, 若杉昌徳, 藤縄雅, 福西暢尚, 後藤彰, 大西哲哉, 奥野広樹, 櫻井博儀, 竹田浩之, 山口充孝, 矢野安重, 小沢顕, 新井一郎, 小松原哲郎, 笹公和, 菊池崇志, 鈴木健, 山口貴之, 大坪隆: “等時性蓄積リングのためのキッカー電磁石及び入射スキームの検討”, 等時性蓄積リングによる不安定核の質量測定と宇宙元素合成, (筑波大学), つくば, 9月(2005).

山口由高, 小沢顕, 新井一郎, 安田裕介, 藤縄雅, 福西暢尚, 大西哲哉, 後藤彰, 奥野広樹, 櫻井博儀, 若杉昌徳, 矢野安重, 鈴木健, 山口貴之, 菊池崇志, 大坪隆: “等時性蓄積リングによる質量測定”, 国立天文台ワークショップ「Rプロセス元素組成の統合的理解: 量子ビームでさぐる宇宙進化の理解を目指して」, 三鷹, 3月(2007).

山田一成, 藤巻正樹, 福西暢尚, 後藤彰, 加瀬昌之, 込山美咲, 大西純一, 奥野広樹, 渡邊環, 矢野安重: “超伝導リングサイクロトロンビーム診断系の詳細”, 第4回日本加速器学会年会・第32回リニアック技術研究会, ( ), 和光, 8月(2007).

長谷部裕雄, 龍頭啓充, 福西暢尚, 後藤彰, 加瀬昌之, 矢野安重: “ポリマーコーティング炭素薄膜の制作”, 第4回日本加速器学会年会・第32回リニアック技術研究会, 和光, 8月(2007).

長谷部裕雄, 奥野広樹, 久保木浩功, 龍頭啓充, 福西暢尚, 上垣外修一, 後藤彰, 加瀬昌之, 矢野安重: “理研RIBFにおける長寿命炭素薄膜の開発状況”, 第5回日本加速器学会年会/第33回リニアック技術研究会, (広島大学), 広島, 8月(2008).

## Ion Source Team

### Publications

#### [Journal]

(Original Papers) \*Subject to Peer Review

- Gomi T., Motobayashi T., Yoneda K., Kanno S., Aoi N., Ando Y., Baba H., Demichi K., Fulop Z., Futakami U., Hasegawa H., Higurashi Y., Ieki K., Imai N., Iwasa N., Iwasaki H., Kubo T., Kubono S., Kunibu M., Matsuyama Y., Michimasa S., Minemura T., Murakami H., Nakamura T., Saito A., Sakurai H., Serata M., Shimoura S., Sugimoto T., Takeshita E., Takeuchi S., Ue K., Yamada K., Yanagisawa Y., Yoshida A., and Ishihara M.: “Coulomb Dissociation of  $^{23}\text{Al}$ ”, *Prog. Theor. Phys. Suppl.*, No. 146, pp. 557–558 (2002). \*
- Kanno S., Gomi T., Motobayashi T., Yoneda K., Aoi N., Ando Y., Baba H., Demichi K., Fulop Z., Futakami U., Hasegawa H., Higurashi Y., Ieki K., Imai N., Iwasa N., Iwasaki H., Kubo T., Kubono S., Kunibu M., Matsuyama Y., Michimasa S., Minemura T., Murakami H., Nakamura T., Saito A., Sakurai H., Serata M., Shimoura S., Sugimoto T., Takeshita E., Takeuchi S., Ue K., Yamada K., Yanagisawa Y., Yoshida A., and Ishihara M.: “Coulomb Excitation of  $^{24}\text{Si}$ ”, *Prog. Theor. Phys. Suppl.*, No. 146, pp. 575–576 (2002). \*
- Matsuyama Y., Motobayashi T., Shimoura S., Minemura T., Saito A., Baba H., Akiyoshi H., Aoi N., Ando Y., Gomi T., Higurashi Y., Ieki K., Imai N., Iwasa N., Iwasaki H., Kanno S., Kubono S., Kunibu M., Michimasa S., Murakami H., Nakamura T., Sakurai H., Serata M., Takeshita E., Takeuchi S., Teranishi T., Ue K., Yamada K., and Yanagisawa Y.: “Inelastic Scattering of  $^{12}\text{Be}$  with  $^4\text{He}$ ”, *Prog. Theor. Phys. Suppl.*, No. 146, pp. 593–594 (2002). \*
- Gomi T., Motobayashi T., Yoneda K., Kanno S., Aoi N., Ando Y., Baba H., Demichi K., Fulop Z., Futakami U., Hasegawa H., Higurashi Y., Ieki K., Imai N., Iwasa N., Iwasaki H., Kubo T., Kubono S., Kunibu M., Matsuyama Y., Michimasa S., Minemura T., Murakami H., Nakamura T., Saito A., Sakurai H., Serata M., Shimoura S., Sugimoto T., Takeshita E., Takeuchi S., Ue K., Yamada K., Yanagisawa Y., Yoshida A., and Ishihara M.: “Study of the  $^{22}\text{Mg}(p, \gamma)^{23}\text{Al}$  Reaction with the Coulomb-Dissociation Method”, *Nucl. Phys. A* **718**, 508c–509c (2003). \*
- Shimoura S., Saito A., Minemura T., Matsuyama Y., Baba H., Akiyoshi H., Aoi N., Gomi T., Higurashi Y., Ieki K., Imai N., Iwasa N., Iwasaki H., Kanno S., Kubono S., Kunibu M., Michimasa S., Motobayashi T., Nakamura T., Sakurai H., Serata M., Takeshita E., Takeuchi S., Teranishi T., Ue K., Yamada K., Yanagisawa Y., Ishihara M., and Itagaki N.: “Isomeric  $0^+$  state in  $^{12}\text{Be}$ ”, *Phys. Lett. B* **560**, 31–36 (2003). \*
- Gomi T., Motobayashi T., Ando Y., Aoi N., Baba H., Demichi K., Elekes Z., Fukuda N., Fulop Z., Futakami U., Hasegawa H., Higurashi Y., Ieki K., Imai N., Ishihara M., Ishikawa K., Iwasa N., Iwasaki H., Kanno S., Kondo Y., Kubo T., Kubono S., Kunibu M., Kurita K., Matsuyama Y., Michimasa S., Minemura T., Miura M., Murakami H., Nakamura T., Notani M., Ota S., Saito A., Sakurai H., Serata M., Shimoura S., Sugimoto T., Takeshita E., Takeuchi S., Ue K., Yamada K., Yanagisawa Y., Yoneda K., and Yoshida A.: “Study of the Stellar  $^{22}\text{Mg}(p, \gamma)^{23}\text{Al}$  Reaction using the Coulomb-Dissociation Method”, *Nucl. Phys. A* **734**, E77–E79 (2004).
- Gomi T., Motobayashi T., Ando Y., Aoi N., Baba H., Demichi K., Elekes Z., Fukuda N., Fulop Z., Futakami U., Hasegawa H., Higurashi Y., Ieki K., Imai N., Ishihara M., Ishikawa K., Iwasa N., Iwasaki H., Kanno S., Kondo Y., Kubo T., Kubono S., Kunibu M., Kurita K., Matsuyama Y., Michimasa S., Minemura T., Miura M., Murakami H., Nakamura T., Notani M., Ota S., Saito A., Sakurai H., Serata M., Shimoura S., Sugimoto T., Takeshita E., Takeuchi S., Togano Y., Ue K., Yamada K., Yanagisawa Y., Yoneda K., and Yoshida A.: “Coulomb dissociation experiment for explosive hydrogen burning: study of the  $^{22}\text{Mg}(p, \gamma)^{22}\text{Al}$  reaction”, *J. Phys. G* **31**, S1517–S1521 (2005).
- Togano Y., Gomi T., Motobayashi T., Ando Y., Aoi N., Baba H., Demichi K., Elekes Z., Fukuda N., Fulop Z., Futakami U., Hasegawa H., Higurashi Y., Ieki K., Imai N., Ishihara M., Ishikawa K., Iwasa N., Iwasaki H., Kanno S., Kondo Y., Kubo T., Kubono S., Kunibu M., Kurita K., Matsuyama Y., Michimasa S., Minemura T., Miura M., Murakami H., Nakamura T., Notani M., Ota S., Saito A., Sakurai H., Serata M., Shimoura S., Sugimoto T., Takeshita E., Takeuchi S., Ue K., Yamada K., Yanagisawa Y., Yoneda K., and Yoshida A.: “Study of  $^{26}\text{Si}(p, \gamma)^{27}\text{P}$  reaction using Coulomb dissociation method”, *Nucl. Phys. A* **758**, 182c–185c (2005). \*
- Iwasaki H., Motobayashi T., Sakurai H., Yoneda K., Gomi T., Aoi N., Fukuda N., Fulop Z., Futakami U., Gacsi Z., Higurashi Y., Imai N., Iwasa N., Kunibu M., Kubo T., Kurokawa M., Liu Z., Minemura T., Saito A., Serata M., Shimoura S., Takeuchi S., Watanabe Y., Yamada K., Yanagisawa Y., and Ishihara M.: “Quadrupole collectivity of  $^{28}\text{Ne}$  and the boundary of the island of inversion”, *Phys. Lett. B* **620**, 118–124 (2005). \*
- Togano Y., Gomi T., Motobayashi T., Ando Y., Aoi N., Baba H., Demichi K., Elekes Z., Fukuda N., Fulop Z., Futakami U., Hasegawa H., Higurashi Y., Ieki K., Imai N., Ishihara M., Ishikawa K., Iwasa N., Iwasaki H., Kanno S., Kondo Y., Kubo T., Kubono S., Kunibu M., Kurita K., Matsuyama Y., Michimasa S., Minemura T., Miura M., Murakami H., Nakamura T., Notani M., Ota S., Saito A., Sakurai H., Serata M., Shimoura S., Sugimoto T., Takeshita E., Takeuchi S., Ue K., Yamada K., Yanagisawa Y., Yoneda K., and Yoshida A.: “Study of the  $^{26}\text{Si}(p, \gamma)^{27}\text{P}$  reaction through Coulomb dissociation”, *Nucl. Phys. A* **758**, 182c–185c (2005). \*

tion of  $^{27}\text{P}$ ”, *Eur. Phys. J. A* **27**, No. s01, pp. 233–236 (2006). \*

Gomi T., Motobayashi T., Ando Y., Aoi N., Baba H., Demichi K., Elekes Z., Fukuda N., Fulop Z., Futakami U., Hasegawa H., Higurashi Y., Ieki K., Imai N., Ishihara M., Ishikawa K., Iwasa N., Iwasaki H., Kanno S., Kondo Y., Kubo T., Kubono S., Kunibu M., Kurita K., Matsuyama Y., Michimasa S., Minemura T., Miura M., Murakami H., Nakamura T., Notani M., Ota S., Saito A., Sakurai H., Serata M., Shimoura S., Sugimoto T., Takeshita E., Takeuchi S., Togano Y., Ue K., Yamada K., Yanagisawa Y., Yoneda K., and Yoshida A.: “Coulomb Dissociation of  $^{23}\text{Al}$  for the stellar  $^{22}\text{Mg}(p,\gamma)^{23}\text{Al}$  reaction”, *Nucl. Phys. A* **758**, 761c–764c (2006).

### [Book•Proceedings]

(Original Papers) \*Subject to Peer Review

Goto A., Fujimaki M., Fujinawa T., Fukunishi N., Hasebe H., Higurashi Y., Ikegami K., Ikezawa E., Inabe N., Kageyama T., Kamigaito O., Kase M., Kidera M., Kohara S., Komiyama M., Nagase M., Kumagai K., Maie T., Nakagawa T., Ohnishi J., Okuno H., Ryuto H., Sakamoto N., Wakasugi M., Watanabe T., Yamada K., Yokouchi S., and Yano Y.: “Commissioning of RIKEN RI Beam Factory”, *Proceedings of 18th International Conference on Cyclotrons and Their Applications (Cyclotrons 2007)*, Giardini Naxos, Italy, 2007–9~10, , Giardini Naxos, pp. 3–8 (2007).

Ohnishi J., Nakagawa T., Higurashi Y., Okuno H., Kusaka K., and Goto A.: “Construction and test of the superconducting coils for RIKEN SC-ECR ion source”, *Proceedings of the 11th European Particle Accelerator Conference (EPAC 2008)*, Genoa, 2008–6, The European Physical Society Accelerator Group, -, pp. 433–435 (2008).

(Others)

Okuno H., Fukunishi N., Fujinawa T., Goto A., Higurashi Y., Ikezawa E., Kamigaito O., Kase M., Nakagawa T., Ohnishi J., Sato Y., Yano Y., and Ostroumov P.: “Heavy Ion Accelerators for RIKEN RI Beam Factory and Upgrade Plans”, *42nd ICFA Advanced Beam Dynamics Workshop on High-Intensity, High-Brightness Hadron Beams*, Nashville, USA, 2008–8, ICFA, , p. (2009).

### Oral Presentations

(International Conference etc.)

Goto A., Fujimaki M., Fujinawa T., Fukunishi N., Hasebe H., Higurashi Y., Ikegami K., Ikezawa E., Inabe N., Kageyama T., Kamigaito O., Kase M., Kidera M., Kohara S., Komiyama M., Nagase M., Kumagai K., Maie T., Nakagawa T., Ohnishi J., Okuno H., Ryuto H., Sakamoto N., Wakasugi M., Watanabe T., Yamada K., Yokouchi S., and Yano Y.: “Commissioning of RIKEN RI Beam Factory”, *18th International Conference on*

*Cyclotrons and their Applications (Cyclotrons 2007)*, (Laboratori Nazionali del Sud, INFN), Giardini Naxos, Italy, Sept.–Oct. (2007).

Fukunishi N., Yamada K., Fujimaki M., Fujinawa T., Goto A., Hasebe H., Higurashi Y., Ikegami K., Ikezawa E., Inabe N., Kamigaito O., Kase M., Kohara S., Komiyama M., Kumagai K., Maie T., Nagase M., Nakagawa T., Ohnishi J., Okuno H., Ryuto H., Sakamoto N., Wakasugi M., Watanabe T., and Yano Y.: “Present performance and commissioning details of RIBF accelerator complex”, *18th International Conference on Cyclotrons and their Applications (Cyclotrons 2007)*, (Laboratori Nazionali del Sud), Giardini Naxos, Italy, Sept.–Oct. (2007).

Okuno H., Fukunishi N., Fujinawa T., Goto A., Higurashi Y., Ikezawa E., Kamigaito O., Kase M., Nakagawa T., Ohnishi J., Sato Y., Yano Y., and Ostroumov P.: “Heavy Ion Accelerators for RIKEN RI Beam Factory and Upgrade Plans”, *42nd ICFA Advanced Beam Dynamics Workshop on High-Intensity, High-Brightness Hadron Beams (HB2008)*, (Oakridge National Laboratory), Nashville, USA, Aug. (2008).

(Domestic Conference)

中川孝秀, 木寺正憲, 羽場宏光, 藍原利光, 加瀬昌之, 後藤彰, 矢野安重: “理研 ECR イオン源での多価ウランイオンの生成”, 第4回日本加速器学会年会・第32回リニアック技術研究会, 和光, 8月 (2007).

木寺正憲: “新しい微量元素分析技術 (ECRIS-MS) による生体内金属元素探査への応用”, 第1回メタロミクス研究フォーラム, (日本微量元素学会), 東京, 11月 (2008).

木寺正憲: “トキシコメタロミクス研究における新しい微量元素分析装置 (ECRIS-MS) の役割と可能性について”, 日本薬学会第129年会, (日本薬学会), 京都, 3月 (2009).

## Accelerator Operation Group

### Publications

#### [Journal]

(Original Papers) \*Subject to Peer Review

- Gomi T., Motobayashi T., Yoneda K., Kanno S., Aoi N., Ando Y., Baba H., Demichi K., Fulop Z., Futakami U., Hasegawa H., Higurashi Y., Ieki K., Imai N., Iwasa N., Iwasaki H., Kubo T., Kubono S., Kunibu M., Matsuyama Y., Michimasa S., Minemura T., Murakami H., Nakamura T., Saito A., Sakurai H., Serata M., Shimoura S., Sugimoto T., Takeshita E., Takeuchi S., Ue K., Yamada K., Yanagisawa Y., Yoshida A., and Ishihara M.: “Coulomb Dissociation of  $^{23}\text{Al}$ ”, *Prog. Theor. Phys. Suppl.*, No. 146, pp. 557–558 (2002). \*
- Kanno S., Gomi T., Motobayashi T., Yoneda K., Aoi N., Ando Y., Baba H., Demichi K., Fulop Z., Futakami U., Hasegawa H., Higurashi Y., Ieki K., Imai N., Iwasa N., Iwasaki H., Kubo T., Kubono S., Kunibu M., Matsuyama Y., Michimasa S., Minemura T., Murakami H., Nakamura T., Saito A., Sakurai H., Serata M., Shimoura S., Sugimoto T., Takeshita E., Takeuchi S., Ue K., Yamada K., Yanagisawa Y., Yoshida A., and Ishihara M.: “Coulomb Excitation of  $^{24}\text{Si}$ ”, *Prog. Theor. Phys. Suppl.*, No. 146, pp. 575–576 (2002). \*
- Matsuyama Y., Motobayashi T., Shimoura S., Minemura T., Saito A., Baba H., Akiyoshi H., Aoi N., Ando Y., Gomi T., Higurashi Y., Ieki K., Imai N., Iwasa N., Iwasaki H., Kanno S., Kubono S., Kunibu M., Michimasa S., Murakami H., Nakamura T., Sakurai H., Serata M., Takeshita E., Takeuchi S., Teranishi T., Ue K., Yamada K., and Yanagisawa Y.: “Inelastic Scattering of  $^{12}\text{Be}$  with  $^4\text{He}$ ”, *Prog. Theor. Phys. Suppl.*, No. 146, pp. 593–594 (2002). \*
- Gomi T., Motobayashi T., Yoneda K., Kanno S., Aoi N., Ando Y., Baba H., Demichi K., Fulop Z., Futakami U., Hasegawa H., Higurashi Y., Ieki K., Imai N., Iwasa N., Iwasaki H., Kubo T., Kubono S., Kunibu M., Matsuyama Y., Michimasa S., Minemura T., Murakami H., Nakamura T., Saito A., Sakurai H., Serata M., Shimoura S., Sugimoto T., Takeshita E., Takeuchi S., Ue K., Yamada K., Yanagisawa Y., Yoshida A., and Ishihara M.: “Study of the  $^{22}\text{Mg}(p, \gamma)^{23}\text{Al}$  Reaction with the Coulomb-Dissociation Method”, *Nucl. Phys. A* **718**, 508c–509c (2003). \*
- Shimoura S., Saito A., Minemura T., Matsuyama Y., Baba H., Akiyoshi H., Aoi N., Gomi T., Higurashi Y., Ieki K., Imai N., Iwasa N., Iwasaki H., Kanno S., Kubono S., Kunibu M., Michimasa S., Motobayashi T., Nakamura T., Sakurai H., Serata M., Takeshita E., Takeuchi S., Teranishi T., Ue K., Yamada K., Yanagisawa Y., Ishihara M., and Itagaki N.: “Isomeric  $0^+$  state in  $^{12}\text{Be}$ ”, *Phys. Lett. B* **560**, 31–36 (2003). \*
- Gomi T., Motobayashi T., Ando Y., Aoi N., Baba H., Demichi K., Elekes Z., Fukuda N., Fulop Z., Futakami U., Hasegawa H., Higurashi Y., Ieki K., Imai N., Ishihara M., Ishikawa K., Iwasa N., Iwasaki H., Kanno S., Kondo Y., Kubo T., Kubono S., Kunibu M., Kurita K., Matsuyama Y., Michimasa S., Minemura T., Miura M., Murakami H., Nakamura T., Notani M., Ota S., Saito A., Sakurai H., Serata M., Shimoura S., Sugimoto T., Takeshita E., Takeuchi S., Ue K., Yamada K., Yanagisawa Y., Yoneda K., and Yoshida A.: “Study of the Stellar  $^{22}\text{Mg}(p, \gamma)^{23}\text{Al}$  Reaction using the Coulomb-Dissociation Method”, *Nucl. Phys. A* **734**, E77–E79 (2004).
- Saito A., Shimoura S., Takeuchi S., Motobayashi T., Minemura T., Matsuyama Y., Baba H., Akiyoshi H., Ando Y., Aoi N., Fulop Z., Gomi T., Higurashi Y., Hirai M., Ieki K., Imai N., Iwasa N., Iwasaki H., Iwata Y., Kanno S., Kobayashi H., Kubono S., Kunibu M., Kurokawa M., Liu Z., Michimasa S., Nakamura T., Ozawa A., Sakurai H., Serata M., Takeshita E., Teranishi T., Ue K., Yamada K., Yanagisawa Y., and Ishihara M.: “Molecular states in neutron-rich beryllium isotopes”, *Nucl. Phys. A* **738**, 337–341 (2004). \*
- Yamada K., Motobayashi T., Aoi N., Baba H., Demichi K., Elekes Z., Gibelin J., Gomi T., Hasegawa H., Imai N., Iwasaki H., Kanno S., Kubo T., Kurita K., Matsuyama Y., Michimasa S., Minemura T., Notani M., Onishi T., Ong H., Ota S., Ozawa A., Saito A., Sakurai H., Shimoura S., Takeshita E., Takeuchi S., Tamaki M., Togano Y., Yanagisawa Y., Yoneda K., and Tanihata I.: “Reduced transition probabilities for the first  $2^+$  excited state in  $^{46}\text{Cr}$ ,  $^{50}\text{Fe}$ , and  $^{54}\text{Ni}$ ”, *Eur. Phys. J. A* **25**, No. s01, pp. 409–413 (2005).
- Gomi T., Motobayashi T., Ando Y., Aoi N., Baba H., Demichi K., Elekes Z., Fukuda N., Fulop Z., Futakami U., Hasegawa H., Higurashi Y., Ieki K., Imai N., Ishihara M., Ishikawa K., Iwasa N., Iwasaki H., Kanno S., Kondo Y., Kubo T., Kubono S., Kunibu M., Kurita K., Matsuyama Y., Michimasa S., Minemura T., Miura M., Murakami H., Nakamura T., Notani M., Ota S., Saito A., Sakurai H., Serata M., Shimoura S., Sugimoto T., Takeshita E., Takeuchi S., Togano Y., Ue K., Yamada K., Yanagisawa Y., Yoneda K., and Yoshida A.: “Coulomb dissociation experiment for explosive hydrogen burning: study of the  $^{22}\text{Mg}(p, \gamma)^{23}\text{Al}$  reaction”, *J. Phys. G* **31**, S1517–S1521 (2005).
- Togano Y., Gomi T., Motobayashi T., Ando Y., Aoi N., Baba H., Demichi K., Elekes Z., Fukuda N., Fulop Z., Futakami U., Hasegawa H., Higurashi Y., Ieki K., Imai N., Ishihara M., Ishikawa K., Iwasa N., Iwasaki H., Kanno S., Kondo Y., Kubo T., Kubono S., Kunibu M., Kurita K., Matsuyama Y., Michimasa S., Minemura T., Miura M., Murakami H., Nakamura T., Notani M., Ota S., Saito A., Sakurai H., Serata M., Shimoura S., Sugimoto T., Takeshita E., Takeuchi S., Ue K., Yamada K., Yanagisawa Y., Yoneda K., and Yoshida A.: “Study

- of  $^{26}\text{Si}(p, \gamma)^{27}\text{P}$  reaction using Coulomb dissociation method”, Nucl. Phys. A **758**, 182c–185c (2005). \*
- Iwasaki H., Motobayashi T., Sakurai H., Yoneda K., Gomi T., Aoi N., Fukuda N., Fulop Z., Futakami U., Gacsi Z., Higurashi Y., Imai N., Iwasa N., Kunibu M., Kubo T., Kurokawa M., Liu Z., Minemura T., Saito A., Serata M., Shimoura S., Takeuchi S., Watanabe Y., Yamada K., Yanagisawa Y., and Ishihara M.: “Quadrupole collectivity of  $^{28}\text{Ne}$  and the boundary of the island of inversion”, Phys. Lett. B **620**, 118–124 (2005). \*
- Ong H., Imai N., Aoi N., Sakurai H., Dombradi Z., Saito A., Elekes Z., Baba H., Demichi K., Fulop Z., Gibelin J., Gomi T., Hasegawa H., Ishihara M., Iwasaki H., Kanno S., Kawai S., Kubo T., Kurita K., Matsuyama Y., Michimasa S., Minemura T., Motobayashi T., Notani M., Ota S., Sakai H., Shimoura S., Takeshita E., Takeuchi S., Tamaki M., Togano Y., Yamada K., Yanagisawa Y., and Yoneda K.: “Inelastic proton scattering on  $^{16}\text{C}$ ”, Eur. Phys. J. A **25**, No. s01, pp. 347–348 (2006). \*
- Togano Y., Gomi T., Motobayashi T., Ando Y., Aoi N., Baba H., Demichi K., Elekes Z., Fukuda N., Fulop Z., Futakami U., Hasegawa H., Higurashi Y., Ieki K., Imai N., Ishihara M., Ishikawa K., Iwasa N., Iwasaki H., Kanno S., Kondo Y., Kubo T., Kubono S., Kunibu M., Kurita K., Matsuyama Y., Michimasa S., Minemura T., Miura M., Murakami H., Nakamura T., Notani M., Ota S., Saito A., Sakurai H., Serata M., Shimoura S., Sugimoto T., Takeshita E., Takeuchi S., Ue K., Yamada K., Yanagisawa Y., Yoneda K., and Yoshida A.: “Study of the  $^{26}\text{Si}(p, \gamma)^{27}\text{P}$  reaction through Coulomb dissociation of  $^{27}\text{P}$ ”, Eur. Phys. J. A **27**, No. s01, pp. 233–236 (2006). \*
- Gomi T., Motobayashi T., Ando Y., Aoi N., Baba H., Demichi K., Elekes Z., Fukuda N., Fulop Z., Futakami U., Hasegawa H., Higurashi Y., Ieki K., Imai N., Ishihara M., Ishikawa K., Iwasa N., Iwasaki H., Kanno S., Kondo Y., Kubo T., Kubono S., Kunibu M., Kurita K., Matsuyama Y., Michimasa S., Minemura T., Miura M., Murakami H., Nakamura T., Notani M., Ota S., Saito A., Sakurai H., Serata M., Shimoura S., Sugimoto T., Takeshita E., Takeuchi S., Togano Y., Ue K., Yamada K., Yanagisawa Y., Yoneda K., and Yoshida A.: “Coulomb Dissociation of  $^{23}\text{Al}$  for the stellar  $^{22}\text{Mg}(p, \gamma)^{23}\text{Al}$  reaction”, Nucl. Phys. A **758**, 761c–764c (2006).
- Elekes Z., Dombradi Z., Saito A., Aoi N., Baba H., Demichi K., Fulop Z., Gibelin J. D., Gomi T., Hasegawa H., Imai N., Ishihara M., Iwasaki H., Kanno S., Kawai S., Kishida T., Kubo T., Kurita K., Matsuyama Y., Michimasa S., Minemura T., Motobayashi T., Notani M., Ohnishi T., Ong H., Ota S., Ozawa A., Sakai H., Sakurai H., Shimoura S., Takeshita E., Takeuchi S., Tamaki M., Togano Y., Yamada K., Yanagisawa Y., and Yoneda K.: “Study of  $N=20$  shell gap with  $^1\text{H}(^{28}\text{Ne}, ^{27,28}\text{Ne})$  reactions”, Eur. Phys. J. Special Topics **150**, 99–102 (2007). \*
- Hasebe H., Ryuto H., Fukunishi N., Goto A., Kase M., and Yano Y.: “Polymer coating method developed for carbon stripper foils”, Nucl. Instrum. Methods Phys. Res. A **590**, 13–17 (2008). \*
- Aoki T., Stingelin L., Kamigaito O., Sakamoto N., Fukunishi N., Yokouchi S., Maie T., Kase M., Goto A., and Yano Y.: “Construction of a beam rebuncher for RIKEN RI-beam factory”, Nucl. Instrum. Methods Phys. Res. A **592**, No. 3, pp. 171–179 (2008). \*
- Ryuto H., Fukunishi N., Hayashi Y., Ichida H., Abe T., Kase M., and Yano Y.: “Heavy-ion beam irradiation facility for biological samples in RIKEN”, Plant Biotechnol. **25**, No. 1, pp. 119–122 (2008). \*
- Elekes Z., Dombradi Z., Aiba T., Aoi N., Baba H., Bemmerer D., Brown B., Furumoto T., Fulop Z., Iwasa N., Kiss A. B., Kobayashi T., Kondo Y., Motobayashi T., Nakabayashi T., Nannichi T., Sakuragi H., Sakurai H., Sohler D., Takashina M., Takeuchi S., Tanaka K., Togano Y., Yamada K., Yamaguchi M., and Yoneda K.: “Persistent decoupling of valence neutrons toward the dripline: study of  $^{20}\text{C}$  by  $\gamma$  spectroscopy”, Phys. Rev. C **79**, 011302-1–011302-5 (2009). \*
- (Others)
- Okuno H., Yamada K., Ohnishi J., Fukunishi N., Yokouchi S., Hasebe H., Ikegami K., Kumagai K., Sakamoto N., Kamigaito O., Goto A., Kase M., Yano Y., and Maie T.: “Commissioning of the Superconducting Ring Cyclotron for the RIKEN RI Beam Factory”, IEEE Trans. Appl. Supercond. **18**, No. 2, pp. 226–231 (2008).
- [Book • Proceedings]**
- (Original Papers) \*Subject to Peer Review
- Goto A., Fujimaki M., Fujinawa T., Fukunishi N., Hasebe H., Higurashi Y., Ikegami K., Ikezawa E., Inabe N., Kageyama T., Kamigaito O., Kase M., Kidera M., Kohara S., Komiyama M., Nagase M., Kumagai K., Maie T., Nakagawa T., Ohnishi J., Okuno H., Ryuto H., Sakamoto N., Wakasugi M., Watanabe T., Yamada K., Yokouchi S., and Yano Y.: “Commissioning of RIKEN RI Beam Factory”, Proceedings of 18th International Conference on Cyclotrons and Their Applications (Cyclotrons 2007), Giardini Naxos, Italy, 2007–9~10, , Giardini Naxos, pp. 3–8 (2007).
- (Others)
- Okuno H., Yamada K., Ohnishi J., Fukunishi N., Sakamoto N., Kamigaito O., Hasebe H., Kumagai K., Maie T., Yokouchi S., Ikegami K., Kase M., Goto A., and Yano Y.: “Hardware commissioning of the RIKEN superconducting ring cyclotron”, Proceedings of 18th International Conference on Cyclotrons and Their Applications (Cyclotrons 2007), Istituto Nazionale di Fisica Nucleare, Roma, pp. 18–20 (2007).
- Okuno H., Fukunishi N., Fujinawa T., Goto A., Higurashi Y., Ikezawa E., Kamigaito O., Kase M., Nakagawa

T., Ohnishi J., Sato Y., Yano Y., and Ostroumov P.: “Heavy Ion Accelerators for RIKEN RI Beam Factory and Upgrade Plans”, 42nd ICFA Advanced Beam Dynamics Workshop on High-Intensity, High-Brightness Hadron Beams, Nashville, USA, 2008–8, ICFA, p. (2009).

奥野広樹, 山田一成, 大西純一, 福西暢尚, 横内茂, 長谷部裕雄, 池上九三男, 熊谷桂子, 坂本成彦, 上垣外修一, 長瀬誠, 藤巻正樹, 込山美咲, 後藤彰, 加瀬昌之, 矢野安重, 真家武士: “理研超伝導リングサイクロトロン現状報告”, 第4回日本加速器学会年会・第32回リニアック技術研究会論文集, 和光, 2007–8, 日本加速器学会, 東京, pp. 46–48 (2007).

奥野広樹, 山田一成, 池上九三男, 加瀬昌之, 矢野安重, 真家武士: “Operational Status of the He Cooling System for RIKEN SRC”, 第4回日本加速器学会年会・第32回リニアック技術研究会論文集, Wako, 2007–8, 日本加速器学会, 東京, pp. 796–798 (2007).

### Oral Presentations

(International Conference etc.)

Imai N., Ong H., Aoi N., Sakurai H., Demichi K., Kawasaki H., Baba H., Dombradi Z., Elekes Z., Fukuda N., Fulop Z., Gelberg A., Gomi T., Hasegawa H., Ishikawa K., Iwasaki H., Kaneko E., Kanno S., Kishida T., Kondo Y., Kubo T., Kurita K., Michimasa S., Minemura T., Miura M., Motobayashi T., Nakamura T., Notani M., Onishi T., Saito A., Shimoura S., Sugimoto T., Suzuki M., Takeshita E., Takeuchi S., Tamaki M., Yamada K., Yoneda K., Watanabe H., and Ishihara M.: “The lifetime measurement of the first  $2^+$  state in  $^{12}\text{Be}$ ”, International Nuclear Physics Conference (INPC2007), Tokyo, June (2007).

Okuno H., Yamada K., Ohnishi J., Fukunishi N., Yokouchi S., Hasebe H., Ikegami K., Kumagai K., Sakamoto N., Kamigaito O., Goto A., Kase M., Yano Y., and Maie T.: “Commissioning of the Superconducting Ring Cyclotron for the RIKEN RI Beam Factory”, MT-20 The 20th biennial conference on magnet technology, Wako, Aug. (2007).

Goto A., Fujimaki M., Fujinawa T., Fukunishi N., Hasebe H., Higurashi Y., Ikegami K., Ikezawa E., Inabe N., Kageyama T., Kamigaito O., Kase M., Kidera M., Kohara S., Komiyama M., Nagase M., Kumagai K., Maie T., Nakagawa T., Ohnishi J., Okuno H., Ryuto H., Sakamoto N., Wakasugi M., Watanabe T., Yamada K., Yokouchi S., and Yano Y.: “Commissioning of RIKEN RI Beam Factory”, 18th International Conference on Cyclotrons and their Applications (Cyclotrons 2007), (Laboratori Nazionali del Sud, INFN), Giardini Naxos, Italy, Sept.–Oct. (2007).

Yamada K., Fujimaki M., Fukunishi N., Goto A., Kase M., Komiyama M., Ohnishi J., Okuno H., Watanabe T., and Yano Y.: “Details of Beam Diagnostic System for RIKEN Superconducting Ring Cyclotron”, 18th International Conference on Cyclotrons and their Applica-

tions (Cyclotrons 2007), (Laboratori Nazionali del Sud), Giardini Naxos, Italy, Sept.–Oct. (2007).

Okuno H., Yamada K., Ohnishi J., Fukunishi N., Yokouchi S., Hasebe H., Ikegami K., Kumagai K., Sakamoto N., Kamigaito O., Goto A., Kase M., Yano Y., and Maie T.: “Hardware commissioning of the RIKEN superconducting ring cyclotron”, 18th International Conference on Cyclotrons and their Applications (Cyclotrons 2007), Giardini Naxos, Italy, Sept.–Oct. (2007).

Fukunishi N., Yamada K., Fujimaki M., Fujinawa T., Goto A., Hasebe H., Higurashi Y., Ikegami K., Ikezawa E., Inabe N., Kamigaito O., Kase M., Kohara S., Komiyama M., Kumagai K., Maie T., Nagase M., Nakagawa T., Ohnishi J., Okuno H., Ryuto H., Sakamoto N., Wakasugi M., Watanabe T., and Yano Y.: “Present performance and commissioning details of RIBF accelerator complex”, 18th International Conference on Cyclotrons and their Applications (Cyclotrons 2007), (Laboratori Nazionali del Sud), Giardini Naxos, Italy, Sept.–Oct. (2007).

Okuno H., Fukunishi N., Fujinawa T., Goto A., Higurashi Y., Ikezawa E., Kamigaito O., Kase M., Nakagawa T., Ohnishi J., Sato Y., Yano Y., and Ostroumov P.: “Heavy Ion Accelerators for RIKEN RI Beam Factory and Upgrade Plans”, 42nd ICFA Advanced Beam Dynamics Workshop on High-Intensity, High-Brightness Hadron Beams (HB2008), (Oakridge National Laboratory), Nashville, USA, Aug. (2008).

(Domestic Conference)

今井伸明, 青井考, 王惠仁, 櫻井博儀, 出道仁彦, Kawasaki H., 馬場秀忠, Dombradi Z., Elekes Z., 福田直樹, Fulop Z., Gelberg A., 五味朋子, 長谷川浩一, 石川和宏, 岩崎弘典, 金子恵美, 菅野祥子, 岸田隆, 近藤洋介, 久保敏幸, 栗田和好, 道正新一郎, 峯村俊行, 三浦宗賢, 本林透, 中村隆司, 野谷将広, 大西健夫, 齋藤明登, 下浦享, 杉本崇, Suzuki M., 竹下英里, 武内聡, 玉城充, 山田一成, 米田健一郎, 渡邊寛, 石原正泰: “ $^{12}\text{Be}$  と  $^{16}\text{C}$  における第一励起状態から基底状態への換算転移確率”, 日本物理学会第58回年次大会, 仙台, 3月 (2003).

今井伸明, 王惠仁, 青井考, 櫻井博儀, 出道仁彦, Kawasaki H., 馬場秀忠, Dombradi Z., Elekes Z., 福田直樹, Fulop Z., Gelberg A., 五味朋子, 長谷川浩一, 石川和宏, 岩崎弘典, 金子恵美, 菅野祥子, 岸田隆, 近藤洋介, 久保敏幸, 栗田和好, 道正新一郎, 峯村俊行, 三浦宗賢, 本林透, 中村隆司, 野谷将広, 大西健夫, 齋藤明登, 下浦享, 杉本崇, Suzuki M., 竹下英里, 武内聡, 玉城充, 山田一成, 米田健一郎, 渡邊寛, 石原正泰: “Anomalously long lifetime of  $2^+$  state of  $^{16}\text{C}$ ”, A New Era of Nuclear Structure Physics, 新潟県黒川村, 11月 (2003).

今井伸明, 王惠仁, 青井考, 櫻井博儀, 出道仁彦, Kawasaki H., 馬場秀忠, Dombradi Z., Elekes Z., 福田直樹, Fulop Z., Gelberg A., 五味朋子, 長谷川浩一, 石川和宏, 岩崎弘典, 金子恵美, 菅野祥子, 岸田隆, 近藤洋介, 久保敏幸, 栗田和好, 道正新一郎, 峯村俊行, 三浦宗賢, 本林透, 中村隆司, 野谷将広, 大西健夫, 齋藤明登, 下浦享, 杉本崇, Suzuki

- M., 竹下英里, 武内聡, 玉城充, 山田一成, 米田健一郎, 渡邊寛, 石原正泰: “Experimental finding of the anomalous quadrupole collectivity in unstable nucleus  $^{16}\text{C}$ ”, 日本物理学会 2005 年秋季大会, (日本物理学会), 京田辺, 9 月 (2005).
- 今井伸明, 王惠仁, 青井考, 櫻井博儀, 出道仁彦, Kawasaki H., 馬場秀忠, Dombradi Z., Elekes Z., 福田直樹, Fulop Z., Gelberg A., 五味朋子, 長谷川浩一, 石川和宏, 岩崎弘典, 金子恵美, 菅野祥子, 岸田隆, 近藤洋介, 久保敏幸, 栗田和好, 道正新一郎, 峯村俊行, 三浦宗賢, 本林透, 中村隆司, 野谷将広, 大西健夫, 齋藤明登, 下浦亨, 杉本崇, Suzuki M., 竹下英里, 武内聡, 玉城充, 山田一成, 米田健一郎, 渡邊寛, 石原正泰: “Lifetime measurement of  $^{12}\text{Be}(2+1)$ ”, 日本物理学会 2005 年秋季大会, (日本物理学会), 京田辺, 9 月 (2005).
- 山田一成, 藤巻正樹, 福西暢尚, 後藤彰, 加瀬昌之, 込山美咲, 大西純一, 奥野広樹, 渡邊環, 矢野安重: “超伝導リングサイクロトロンでのビーム診断系の詳細”, 第 4 回日本加速器学会年会・第 32 回リニアック技術研究会, ( ), 和光, 8 月 (2007).
- 渡邊環, 若杉昌徳, 藤巻正樹, 加瀬昌之, 福西暢尚, 小高康照, 小山亮, 山田一成, 後藤彰, 矢野安重: “RIBF におけるプラスチックシンチレーションモニターを用いたビームエネルギーと縦方向のビームプロファイルの測定”, 第 4 回日本加速器学会年会・第 32 回リニアック技術研究会, 和光, 8 月 (2007).
- 長谷部裕雄, 龍頭啓充, 福西暢尚, 後藤彰, 加瀬昌之, 矢野安重: “ポリマーコーティング炭素薄膜の制作”, 第 4 回日本加速器学会年会・第 32 回リニアック技術研究会, 和光, 8 月 (2007).
- 中川孝秀, 木寺正憲, 羽場宏光, 藍原利光, 加瀬昌之, 後藤彰, 矢野安重: “理研 ECR イオン源での多価ウランイオンの生成”, 第 4 回日本加速器学会年会・第 32 回リニアック技術研究会, 和光, 8 月 (2007).
- 池沢英二, 加瀬昌之, 大木智則, 藍原利光, 山内啓資, 内山曉仁, 小山田和幸, 田村匡史: “理研重イオンリニアックの運転状況”, 第 5 回日本加速器学会年会/第 33 回リニアック技術研究会, (日本加速器学会), 東広島, 8 月 (2008).
- 須田健嗣, 小山亮, 加瀬昌之, 上垣外修一, 坂本成彦, 福西暢尚, 藤巻正樹, 山田一成, 渡邊環: “RIBF における高周波系の安定度”, 第 5 回日本加速器学会年会/第 33 回リニアック技術研究会, 東広島, 8 月 (2008).
- 長谷部裕雄, 奥野広樹, 久保木浩功, 龍頭啓充, 福西暢尚, 上垣外修一, 後藤彰, 加瀬昌之, 矢野安重: “理研 RIBF における長寿命炭素薄膜の開発状況”, 第 5 回日本加速器学会年会/第 33 回リニアック技術研究会, (広島大学), 広島, 8 月 (2008).
- 渡邊環, 藤巻正樹, 福西暢尚, 加瀬昌之, 山田一成, 坂本成彦, 須田健嗣, 込山美咲, 仲村武志, 小山亮, 小高康照, 上垣外修一, 矢野安重: “RIBF におけるビーム診断系の高度化”, 第 5 回日本加速器学会年会/第 33 回リニアック技術研究会, (広島大学), 東広島, 8 月 (2008).
- 市川雄一, 久保敏幸, 青井考, Banerjee S. R., Chakrabarti A., 福田直樹, 岩崎弘典, 久保野茂, 本林透, 中林彩, 中村隆司, 中尾太郎, 奥村俊文, 王惠仁, 大西健夫, 鈴木大介, 鈴木賢, 山田一成, 山口英斉, 櫻井博儀: 日本物理学会 2008 年秋季大会, 山形, 9 月 (2008).
- 市川雄一, 久保敏幸, 青井考, Banerjee S. R., Chakrabarti A., 福田直樹, 岩崎弘典, 久保野茂, 本林透, 中林彩, 中村隆司, 中尾太郎, 奥村俊文, 王惠仁, 大西健夫, 鈴木大介, 鈴木賢, 山田一成, 山口英斉, 櫻井博儀: 第 5 回停止・低速不安定核ビームを用いた核分光研究会, (大阪大学), 豊中, 12 月 (2008).

## RILAC Team

### Publications

#### [Book・Proceedings]

(Original Papers) \*Subject to Peer Review

Goto A., Fujimaki M., Fujinawa T., Fukunishi N., Hasebe H., Higurashi Y., Ikegami K., Ikezawa E., Inabe N., Kageyama T., Kamigaito O., Kase M., Kidera M., Kohara S., Komiyama M., Nagase M., Kumagai K., Maie T., Nakagawa T., Ohnishi J., Okuno H., Ryuto H., Sakamoto N., Wakasugi M., Watanabe T., Yamada K., Yokouchi S., and Yano Y.: “Commissioning of RIKEN RI Beam Factory”, Proceedings of 18th International Conference on Cyclotrons and Their Applications (Cyclotrons 2007), Giardini Naxos, Italy, 2007–9~10, Giardini Naxos, pp. 3–8 (2007).

Ohmori H., Lin W., Katahira K., Mizutani M., Naruse T., Uehara Y., Watanabe Y., Kameyama Y., Hachisu Y., Maekawa K., Sasaki C., Ito N., Yoshida K., Hirai S., Kasuga H., Mishima T., Asami M., Mitsuishi N., and Matsuzawa T.: “Developmental History and Variation of Precision and Efficient Machining assisted with Electrolytic Process Principle and Applications”, Proceedings of The World Advances in ELID-Grinding Technologies: Trends on High Efficiency and Essential Processing, Changsha, China, 2008–6, Hunan University, Changsha, pp. 1–5 (2008).

#### (Review)

Kasuga H., Ohmori H., Lin W., Watanabe Y., Mishima T., and Doi T.: “Efficient and smooth grinding characteristics of monocrystalline 4H-SiC wafer”, 1st International Conference on Nanomanufacturing (nanoMan2008), Singapore, Singapore, 2008–7, Center of MicroNano Manufacturing Technology, Singapore, pp. 1–6 (2008).

Ohmori H., Yoshida K., Hirai S., Watanabe Y., Uehara Y., Lin W., and Kwak T.: “Fabrication of SiC micro-lens mold for glass molding”, 8th International Joint Workshop on Micro Fabrication (IJWMF-2008), Kaohsiung, Taiwan, 2008–4, Metal Industries Research and Development Centre, Kaohsiung, pp. 9–12 (2008).

Kasuga H., Ohmori H., Watanabe Y., and Mishima T.: “Micro-grinding characteristics on alumina and zirconia ceramics for dental applications”, 8th International Joint Workshop on Micro Fabrication (IJWMF-2008), Kaohsiung, Taiwan, 2008–4, Metal Industries Research and Development Centre, Kaohsiung, pp. 13–17 (2008).

Kasuga H., Ohmori H., Lin W., Watanabe Y., Mishima T., and Doi T.: “Efficient super-smooth finishing characteristics of SiC materials through the use of fine-grinding”, International Conference on Smart Manufacturing Application, Gyeonggi-do, Korea, 2008–4, Institute of Control, Robotics, and Systems, Gyeonggi-do, pp. 5–8 (2008).

Kasuga H., Ohmori H., Watanabe Y., Mishima T., and Kwak T.: “Surface characteristics of efficient-

ground alumina and zirconia ceramics for dental applications”, Proceedings of The World Advances in ELID-Grinding Technologies: Trends on High Efficiency and Essential Processing, Changsha, China, 2008–6, Hunan University, Changsha, pp. 31–35 (2008).

大森整, 片平和俊, 林偉民, 上原嘉宏, 水谷正義, 渡邊裕, 森田晋也: “ELID 研削法による光学材料, 電子材料, キーパーツの加工効果”, 結晶加工と評価技術第 145 委員会第 115 回研究会資料, 東京, 2008–10, 独立行政法人日本学術振興会, 東京, pp. 10–15 (2008).

大森整, 森田晋也, 片平和俊, 上原嘉宏, 渡邊裕, 林偉民: “研削”, ガラスの加工技術と製品応用, 情報機構, 東京, pp. 101–108 (2009).

#### (Others)

Okuno H., Fukunishi N., Fujinawa T., Goto A., Higurashi Y., Ikezawa E., Kamigaito O., Kase M., Nakagawa T., Ohnishi J., Sato Y., Yano Y., and Ostroumov P.: “Heavy Ion Accelerators for RIKEN RI Beam Factory and Upgrade Plans”, 42nd ICFA Advanced Beam Dynamics Workshop on High-Intensity, High-Brightness Hadron Beams, Nashville, USA, 2008–8, ICFA, , p. (2009).

### Oral Presentations

(International Conference etc.)

Goto A., Fujimaki M., Fujinawa T., Fukunishi N., Hasebe H., Higurashi Y., Ikegami K., Ikezawa E., Inabe N., Kageyama T., Kamigaito O., Kase M., Kidera M., Kohara S., Komiyama M., Nagase M., Kumagai K., Maie T., Nakagawa T., Ohnishi J., Okuno H., Ryuto H., Sakamoto N., Wakasugi M., Watanabe T., Yamada K., Yokouchi S., and Yano Y.: “Commissioning of RIKEN RI Beam Factory”, 18th International Conference on Cyclotrons and their Applications (Cyclotrons 2007), (Laboratori Nazionali del Sud, INFN), Giardini Naxos, Italy, Sept.–Oct. (2007).

Fukunishi N., Yamada K., Fujimaki M., Fujinawa T., Goto A., Hasebe H., Higurashi Y., Ikegami K., Ikezawa E., Inabe N., Kamigaito O., Kase M., Kohara S., Komiyama M., Kumagai K., Maie T., Nagase M., Nakagawa T., Ohnishi J., Okuno H., Ryuto H., Sakamoto N., Wakasugi M., Watanabe T., and Yano Y.: “Present performance and commissioning details of RIBF accelerator complex”, 18th International Conference on Cyclotrons and their Applications (Cyclotrons 2007), (Laboratori Nazionali del Sud), Giardini Naxos, Italy, Sept.–Oct. (2007).

Kasuga H., Ohmori H., Lin W., Watanabe Y., Mishima T., Doi T., and Kwak T.: “Efficient grinding characteristics of 4H-SiC wafer”, 7th International Conference of High Speed Machining, (Technische Universit, Darmstadt, Germany, May (2008).

Kasuga H., Ohmori H., Mishima T., Watanabe Y., and Lin W.: “Investigation on mirror surface grinding characteristics of SiC materials”, International Symposium on

- New Frontier of Advanced Si-Based Ceramics and Composites (ISASC2008), (The Korean Ceramics Society), Jeju, Korea, June (2008).
- Yoshida K., Ohmori H., Katahira K., Henerichs M., Kloche F., Kwak T., Watanabe Y., and Hirai S.: “Ultra-precision ELID-Grinding of SiC Glass Mold Materials”, 1st International Conference on NanoManufacturing (nanoMan2008), Singapore, Singapore, July (2008).
- Okuno H., Fukunishi N., Fujinawa T., Goto A., Higurashi Y., Ikezawa E., Kamigaito O., Kase M., Nakagawa T., Ohnishi J., Sato Y., Yano Y., and Ostroumov P.: “Heavy Ion Accelerators for RIKEN RI Beam Factory and Upgrade Plans”, 42nd ICFA Advanced Beam Dynamics Workshop on High-Intensity, High-Brightness Hadron Beams (HB2008), (Oakridge National Laboratory), Nashville, USA, Aug. (2008).
- Kasuga H., Ohmori H., Watanabe Y., and Mishima T.: “Efficient grinding characteristics on alumina and zirconia ceramics for dental applications”, 8th International Conference on Frontiers of Design and Manufacturing, (Tianjin University), Tianjin, China, Sept. (2008).
- Kasuga H., Ohmori H., Watanabe Y., and Mishima T.: “Improvement in micro-grinding on alumina and zirconia ceramics for dental applications”, 6th International Workshop on Microfactories (IWMF 2008), (Northwestern University, University of Illinois), Evanston, USA, Oct. (2008).
- Kasuga H., Ohmori H., Lin W., Watanabe Y., Mishima T., Doi T., and Kwak T.: “Super-smooth machining of 4H-SiC wafer through the use of fine-grinding”, 2008 International Conference on Planarization/CMP Technology, (Chemical Mechanical Planarization User Group Taiwan), Hsinchu, Taiwan, Nov. (2008).
- (Domestic Conference)
- 込山美咲, 藤巻正樹, 内山暁仁, 山内啓資, 小田切淳一, 福西暢尚: “理研リニアックにおけるビーム診断機器制御への組み込み EPICS 搭載 F3RP61-2L の応用”, 第 5 回日本加速器学会年会/第 33 回リニアック技術研究会, (日本加速器学会, リニアック技術研究会), 東広島, 8 月 (2008).
- 池沢英二, 加瀬昌之, 大木智則, 藍原利光, 山内啓資, 内山暁仁, 小山田和幸, 田村匡史: “理研重イオンリニアックの運転状況”, 第 5 回日本加速器学会年会/第 33 回リニアック技術研究会, (日本加速器学会), 東広島, 8 月 (2008).
- 春日博, 林偉民, 渡邊裕, 三島健稔, 土肥俊郎, 大森整: “4H-SiC (0001) 面の高能率研削”, 2008 年度砥粒加工学会学術講演会 (ABTEC2008), (砥粒加工学会), 彦根, 9 月 (2008).
- 大森整, 林偉民, 森田晋也, 片平和俊, 上原嘉宏, 渡邊裕: “ガラス材のナノプレジジョン・メカニカルファブリケーション”, 第 26 回無機材料に関する最近の研究成果発表会—材料研究の最前線から—, (日本板硝子材料工学助成会), 東京, 1 月 (2009).

## Cyclotron Team

### Publications

#### [Journal]

(Original Papers) \*Subject to Peer Review

Aoki T., Stingelin L., Kamigaito O., Sakamoto N., Fukunishi N., Yokouchi S., Maie T., Kase M., Goto A., and Yano Y.: “Construction of a beam rebuncher for RIKEN RI-beam factory”, Nucl. Instrum. Methods Phys. Res. A **592**, No. 3, pp. 171–179 (2008). \*

(Others)

Okuno H., Yamada K., Ohnishi J., Fukunishi N., Yokouchi S., Hasebe H., Ikegami K., Kumagai K., Sakamoto N., Kamigaito O., Goto A., Kase M., Yano Y., and Maie T.: “Commissioning of the Superconducting Ring Cyclotron for the RIKEN RI Beam Factory”, IEEE Trans. Appl. Supercond. **18**, No. 2, pp. 226–231 (2008).

#### [Book・Proceedings]

(Original Papers) \*Subject to Peer Review

Goto A., Fujimaki M., Fujinawa T., Fukunishi N., Hasebe H., Higurashi Y., Ikegami K., Ikezawa E., Inabe N., Kageyama T., Kamigaito O., Kase M., Kidera M., Kohara S., Komiyama M., Nagase M., Kumagai K., Maie T., Nakagawa T., Ohnishi J., Okuno H., Ryuto H., Sakamoto N., Wakasugi M., Watanabe T., Yamada K., Yokouchi S., and Yano Y.: “Commissioning of RIKEN RI Beam Factory”, Proceedings of 18th International Conference on Cyclotrons and Their Applications (Cyclotrons 2007), Giardini Naxos, Italy, 2007–9~10, Giardini Naxos, pp. 3–8 (2007).

(Others)

Okuno H., Yamada K., Ohnishi J., Fukunishi N., Sakamoto N., Kamigaito O., Hasebe H., Kumagai K., Maie T., Yokouchi S., Ikegami K., Kase M., Goto A., and Yano Y.: “Hardware commissioning of the RIKEN superconducting ring cyclotron”, Proceedings of 18th International Conference on Cyclotrons and Their Applications (Cyclotrons 2007), Istituto Nazionale di Fisica Nucleare, Roma, pp. 18–20 (2007).

奥野広樹, 山田一成, 大西純一, 福西暢尚, 横内茂, 長谷部裕雄, 池上九三男, 熊谷桂子, 坂本成彦, 上垣外修一, 長瀬誠, 藤巻正樹, 込山美咲, 後藤彰, 加瀬昌之, 矢野安重, 真家武士: “理研超伝導リングサイクロトロン現状報告”, 第4回日本加速器学会年会・第32回リニアック技術研究会論文集, 和光, 2007–8, 日本加速器学会, 東京, pp. 46–48 (2007).

奥野広樹, 山田一成, 池上九三男, 加瀬昌之, 矢野安重, 真家武士: “Operational Status of the He Cooling System for RIKEN SRC”, 第4回日本加速器学会年会・第32回リニアック技術研究会論文集, Wako, 2007–8, 日本加速器学会, 東京, pp. 796–798 (2007).

### Oral Presentations

(International Conference etc.)

Okuno H., Yamada K., Ohnishi J., Fukunishi N., Yokouchi S., Hasebe H., Ikegami K., Kumagai K., Sakamoto N.,

Kamigaito O., Goto A., Kase M., Yano Y., and Maie T.: “Commissioning of the Superconducting Ring Cyclotron for the RIKEN RI Beam Factory”, MT-20 The 20th biennial conference on magnet technology, Wako, Aug. (2007).

Goto A., Fujimaki M., Fujinawa T., Fukunishi N., Hasebe H., Higurashi Y., Ikegami K., Ikezawa E., Inabe N., Kageyama T., Kamigaito O., Kase M., Kidera M., Kohara S., Komiyama M., Nagase M., Kumagai K., Maie T., Nakagawa T., Ohnishi J., Okuno H., Ryuto H., Sakamoto N., Wakasugi M., Watanabe T., Yamada K., Yokouchi S., and Yano Y.: “Commissioning of RIKEN RI Beam Factory”, 18th International Conference on Cyclotrons and their Applications (Cyclotrons 2007), (Laboratori Nazionali del Sud, INFN), Giardini Naxos, Italy, Sept.–Oct. (2007).

Yamada K., Fujimaki M., Fukunishi N., Goto A., Kase M., Komiyama M., Ohnishi J., Okuno H., Watanabe T., and Yano Y.: “Details of Beam Diagnostic System for RIKEN Superconducting Ring Cyclotron”, 18th International Conference on Cyclotrons and their Applications (Cyclotrons 2007), (Laboratori Nazionali del Sud), Giardini Naxos, Italy, Sept.–Oct. (2007).

Okuno H., Yamada K., Ohnishi J., Fukunishi N., Yokouchi S., Hasebe H., Ikegami K., Kumagai K., Sakamoto N., Kamigaito O., Goto A., Kase M., Yano Y., and Maie T.: “Hardware commissioning of the RIKEN superconducting ring cyclotron”, 18th International Conference on Cyclotrons and their Applications (Cyclotrons 2007), Giardini Naxos, Italy, Sept.–Oct. (2007).

Fukunishi N., Yamada K., Fujimaki M., Fujinawa T., Goto A., Hasebe H., Higurashi Y., Ikegami K., Ikezawa E., Inabe N., Kamigaito O., Kase M., Kohara S., Komiyama M., Kumagai K., Maie T., Nagase M., Nakagawa T., Ohnishi J., Okuno H., Ryuto H., Sakamoto N., Wakasugi M., Watanabe T., and Yano Y.: “Present performance and commissioning details of RIBF accelerator complex”, 18th International Conference on Cyclotrons and their Applications (Cyclotrons 2007), (Laboratori Nazionali del Sud), Giardini Naxos, Italy, Sept.–Oct. (2007).

(Domestic Conference)

山田一成, 藤巻正樹, 福西暢尚, 後藤彰, 加瀬昌之, 込山美咲, 大西純一, 奥野広樹, 渡邊環, 矢野安重: “超伝導リングサイクロトロンビーム診断系の詳細”, 第4回日本加速器学会年会・第32回リニアック技術研究会, ( ), 和光, 8月 (2007).

須田健嗣, 小山亮, 加瀬昌之, 上垣外修一, 坂本成彦, 福西暢尚, 藤巻正樹, 山田一成, 渡邊環: “RIBFにおける高周波系の安定度”, 第5回日本加速器学会年会/第33回リニアック技術研究会, 東広島, 8月 (2008).

渡邊環, 藤巻正樹, 福西暢尚, 加瀬昌之, 山田一成, 坂本成彦, 須田健嗣, 込山美咲, 仲村武志, 小山亮, 小高康照, 上垣外修一, 矢野安重: “RIBFにおけるビーム診断系の高度化”, 第5回日本加速器学会年会/第33回リニアック技術研究会

, (広島大学), 東広島, 8月 (2008).

## Beam Technology Team

### Publications

#### [Journal]

(Original Papers) \*Subject to Peer Review

Takechi M., Fukuda M., Mihara M., Chinda T., Matsumasa T., Matsubara H., Nakashima Y., Matsuta K., Minamisono T., Koyama R., Shinosaki W., Takahashi M., Takisawa A., Ohtsubo T., Suzuki T., Momota S., Hatanaka K., Suda T., Sasaki M., Sato S., and Kitagawa A.: “Reaction cross-sections for stable nuclei and nucleon density distribution of proton drip-line nucleus  $8\text{B}$ ”, *Eur. Phys. J. A* **25**, No. s01, pp. 217–219 (2005). \*

Hasebe H., Ryuto H., Fukunishi N., Goto A., Kase M., and Yano Y.: “Polymer coating method developed for carbon stripper foils”, *Nucl. Instrum. Methods Phys. Res. A* **590**, 13–17 (2008). \*

Aoki T., Stingelin L., Kamigaito O., Sakamoto N., Fukunishi N., Yokouchi S., Maie T., Kase M., Goto A., and Yano Y.: “Construction of a beam rebuncher for RIKEN RI-beam factory”, *Nucl. Instrum. Methods Phys. Res. A* **592**, No. 3, pp. 171–179 (2008). \*

Yamaguchi Y., Ozawa A., Goto A., Arai I., Fujinawa T., Fukunishi N., Kikuchi T., Ohnishi T., Ohtsubo T., Sakurai H., Suzuki T., Wakasugi M., Yamaguchi T., Yasuda Y., and Yano Y.: “Rara-RI ring project at RIKEN RI beam factory”, *Nucl. Instrum. Methods Phys. Res. B* **266**, 4575–4578 (2008). \*

Wakasugi M., Emoto T., Furukawa Y., Ishii K., Ito S., Koseki T., Kurita K., Kuwajima A., Masuda T., Morikawa A., Nakamura M., Noda A., Ohnishi T., Shirai T., Suda T., Takeda H., Tamae T., Tongu H., Wang S., and Yano Y.: “Novel Internal Target for Electron Scattering off Unstable Nuclei”, *Phys. Rev. Lett.* **100**, 164801-1–164801-4 (2008). \*

Kanaya T., Saito H., Hayashi Y., Fukunishi N., Ryuto H., Miyazaki K., Kusumi T., Abe T., and Suzuki K.: “Heavy-ion beam-induced sterile mutants of verbena (*Verbena × Hybrida*) with an improved flowering habit”, *Plant Biotechnol.* **25**, No. 1, pp. 91–96 (2008). \*

Kanaya T., Saito H., Hayashi Y., Fukunishi N., Ryuto H., Miyazaki K., Abe T., and Suzuki K.: “A Heavy-ion beam-induced mutant of *Verbena × Hybrida* and wild-type *V.peruviana* demonstrate different types of self-incompatibility”, *Plant Biotechnol.* **25**, No. 1, pp. 97–100 (2008). \*

Sugiyama M., Saito H., Ichida H., Hayashi Y., Ryuto H., Fukunishi N., Terakawa T., and Abe T.: “Biological effects of heavy-ion beam irradiation on cyclamen”, *Plant Biotechnol.* **25**, No. 1, pp. 101–104 (2008). \*

Kazama Y., Saito H., Yamamoto Y. Y., Hayashi Y., Ichida H., Ryuto H., Fukunishi N., and Abe T.: “LET-dependent effects of heavy-ion beam irradiation in *Arabidopsis thaliana*”, *Plant Biotechnol.* **25**, No. 1, pp.

113–117 (2008). \*

Ryuto H., Fukunishi N., Hayashi Y., Ichida H., Abe T., Kase M., and Yano Y.: “Heavy-ion beam irradiation facility for biological samples in RIKEN”, *Plant Biotechnol.* **25**, No. 1, pp. 119–122 (2008). \*

(Others)

Nakajima S., Yamaguchi T., Suzuki T., Yamaguchi Y., Fujinawa T., Fukunishi N., Goto A., Ohnishi T., Sakurai H., Wakasugi M., Yano Y., Arai I., Ozawa A., Yasuda Y., Kikuchi T., and Ohtsubo T.: “New scheme for precision mass measurements of rare isotopes produced at RI beam factory”, *Acta Phys. Pol. B* **39**, No. 2, pp. 457–462 (2008).

Okuno H., Yamada K., Ohnishi J., Fukunishi N., Yokouchi S., Hasebe H., Ikegami K., Kumagai K., Sakamoto N., Kamigaito O., Goto A., Kase M., Yano Y., and Maie T.: “Commissioning of the Superconducting Ring Cyclotron for the RIKEN RI Beam Factory”, *IEEE Trans. Appl. Supercond.* **18**, No. 2, pp. 226–231 (2008).

Sasaki K., Aida R., Niki T., Yamaguchi H., Narumi T., Nishijima T., Hayashi Y., Ryuto H., Fukunishi N., Abe T., and Ohtsubo N.: “High-efficiency improvement of transgenic torenia flowers by ion beam irradiation”, *Plant Biotechnol.* **25**, No. 1, pp. 81–89 (2008).

#### [Book-Proceedings]

(Original Papers) \*Subject to Peer Review

Goto A., Fujimaki M., Fujinawa T., Fukunishi N., Hasebe H., Higurashi Y., Ikegami K., Ikezawa E., Inabe N., Kageyama T., Kamigaito O., Kase M., Kidera M., Kohara S., Komiyama M., Nagase M., Kumagai K., Maie T., Nakagawa T., Ohnishi J., Okuno H., Ryuto H., Sakamoto N., Wakasugi M., Watanabe T., Yamada K., Yokouchi S., and Yano Y.: “Commissioning of RIKEN RI Beam Factory”, *Proceedings of 18th International Conference on Cyclotrons and Their Applications (Cyclotrons 2007)*, Giardini Naxos, Italy, 2007–9~10, Giardini Naxos, pp. 3–8 (2007).

Abe T., Kazama Y., Ichida H., Hayashi Y., Ryuto H., and Fukunishi N.: “Plant breeding using the ion beam irradiation in RIKEN”, *Proceedings of 18th International Conference on Cyclotrons and Their Applications (Cyclotrons 2007)*, Giardini Naxos, Italy, 2006–9~10, INFN, Giardini Naxos, pp. 222–224 (2008). \*

Hayashi Y., Takehisa H., Kazama Y., Ichida H., Ryuto H., Fukunishi N., Abe T., Kanba C., and Sato T.: “Effect of ion beam irradiation on mutation induction in rice”, *Proceedings of 18th International Conference on Cyclotrons and Their Applications (Cyclotrons 2007)*, Giardini Naxos, Italy, 2007–9~10, INFN, Giardini Naxos, pp. 237–239 (2008). \*

Ohnishi J., Okuno H., Fukunishi N., Yamada K., Goto A., and Yano Y.: “The magnetic field of the superconducting ring cyclotron”, *Proceedings of 18th International Conference on Cyclotrons and Their Applications (Cyclotrons 2007)*, Giardini Naxos, Italy, 2007–10, -, -, pp.

429–431 (2008).

(Others)

- Yamaguchi T., Arai I., Fukunishi N., Goto A., Kikuchi T., Komatsubara T., Ohnishi T., Ohtsubo T., Okuno H., Ozawa A., Sasa K., Suzuki T., Tagisi Y., Takeda H., Wakasugi M., Yamaguchi M., Yamaguchi Y., and Yano Y.: “Mass measurements by an isochronous storage ring at the RIKEN RI beam factory”, Proceedings of the 6th International Conference on Nuclear Physics at Storage Rings (STORI '05), Bonn, Germany, 2005–5, Forschungszentrum Julich, Julich, pp. 297–300 (2005).
- Yamaguchi M., Arai I., Fukunishi N., Goto A., Kusaka K., Kikuchi T., Komatsubara T., Kubo T., Ohnishi T., Ohtsubo T., Okuno H., Ozawa A., Sasa K., Suzuki T., Tagisi Y., Takeda H., Wakasugi M., Yamaguchi T., Yamaguchi Y., and Yano Y.: “Design of an isochronous storage ring and an injection line for mass measurements at the RIKEN RI beam factory”, Proceedings of the 6th International Conference on Nuclear Physics at Storage Rings (STORI '05), Bonn, Germany, 2005–5, Forschungszentrum Julich, Julich, pp. 315–319 (2005).
- Kikuchi T., Horioka K., Ozawa A., Kawata S., Yamaguchi Y., Fukunishi N., Sakurai H., Wakasugi M., Yamaguchi M., Yamaguchi T., Arai I., Ohta H., Fujinawa T., Sasa K., Komatsubara T., Suzuki T., Ohtsubo T., Goto A., Ohnishi T., Okuno H., Takeda H., and Yano Y.: “Individual correction using induction modulator for mass measurements by isochronous ring in RIKEN RI beam factory”, Proceedings of the 2nd International Workshop on Recent Progress in Induction Accelerators (RPIA2006), Tsukuba, 2006–3, KEK, Tsukuba, pp. 127–131 (2006).
- Okuno H., Yamada K., Ohnishi J., Fukunishi N., Sakamoto N., Kamigaito O., Hasebe H., Kumagai K., Maie T., Yokouchi S., Ikegami K., Kase M., Goto A., and Yano Y.: “Hardware commissioning of the RIKEN superconducting ring cyclotron”, Proceedings of 18th International Conference on Cyclotrons and Their Applications (Cyclotrons 2007), Istituto Nazionale di Fisica Nucleare, Roma, pp. 18–20 (2007).
- Kazama Y., Saito H., Hayashi Y., Ichida H., Ohbu S., Ryuto H., Fukunishi N., and Abe T.: “Effects of ion beam irradiation on mutation induction in *Arabidopsis thaliana*”, Proceedings of 18th International Conference on Cyclotrons and Their Applications (Cyclotrons 2007), Giardini Naxos, Italy, 2007–9~10, INFN, Giardini Naxos, pp. 240–242 (2008).
- Okuno H., Fukunishi N., Fujinawa T., Goto A., Higurashi Y., Ikezawa E., Kamigaito O., Kase M., Nakagawa T., Ohnishi J., Sato Y., Yano Y., and Ostroumov P.: “Heavy Ion Accelerators for RIKEN RI Beam Factory and Upgrade Plans”, 42nd ICFA Advanced Beam Dynamics Workshop on High-Intensity, High-Brightness Hadron Beams, Nashville, USA, 2008–8, ICFA, , p. (2009).

奥野広樹, 山田一成, 大西純一, 福西暢尚, 横内茂, 長谷部裕雄, 池上九三男, 熊谷桂子, 坂本成彦, 上垣外修一, 長瀬誠, 藤巻正樹, 込山美咲, 後藤彰, 加瀬昌之, 矢野安重, 真家武士: “理研超伝導リングサイクロトロン現状報告”, 第4回日本加速器学会年会・第32回リニアック技術研究会論文集, 和光, 2007–8, 日本加速器学会, 東京, pp. 46–48 (2007).

### Oral Presentations

(International Conference etc.)

- Yamaguchi T., Ozawa A., Arai I., Komatsubara T., Sasa K., Tagisi Y., Yamaguchi M., Suzuki T., Ohtsubo T., Fukunishi N., Goto A., Ohnishi T., Okuno H., Takeda H., Wakasugi M., Yano Y., Yamaguchi Y., and Kikuchi T.: “Mass measurements in RIKEN”, 6th International Conference on Nuclear Physics at Storage Rings (STORI-05), (Research Center Julich), Bonn, Germany, May (2005).
- Kikuchi T., Horioka K., Ozawa A., Kawata S., Yamaguchi Y., Fukunishi N., Sakurai H., Wakasugi M., Yamaguchi M., Yamaguchi T., Arai I., Ohta H., Fujinawa T., Sasa K., Komatsubara T., Suzuki T., Ohtsubo T., Goto A., Ohnishi T., Okuno H., Takeda H., and Yano Y.: “Individual correction using induction modulator for mass measurements by isochronous ring in RIKEN RI beam factory”, 2nd International Workshop on Recent Progress in Induction Accelerators (RPIA2006), (KEK, Tokyo Institute of Technology), Tsukuba, Mar. (2006).
- Uwamino Y., Sakamoto H., and Fukunishi N.: “Safety Design of the Radioactive Isotope Beam Facility (RIBF) at RIKEN”, Shielding Aspects of Accelerators, Targets and Irradiation Facilities 8th Meeting, (OECD/NEA), Pohang, Korea, May (2006).
- Hasebe H., Ryuto H., Fukunishi N., Goto A., Kase M., and Yano Y.: “Polymer coating method developed for carbon stripper foils”, 23rd World Conference of the INTDS, (High Energy Accelerator Research Organization (KEK)), Tsukuba, Oct. (2006).
- Arai I., Komatsubara T., Ozawa A., Sasa K., Yasuda Y., Fujinawa T., Fukunishi N., Goto A., Ohnishi T., Okuno H., Takeda H., Wakasugi M., Yamaguchi M., Yamaguchi Y., Yano Y., Kikuchi T., Suzuki T., Yamaguchi T., and Ohtsubo T.: “Isochronous ring at RIKEN”, Workshop on Advanced Laser and Mass Spectroscopy ALMAS-1: Innovative Physics Ideas, (Gesellschaft für Schwerionenforschung (GSI)), Darmstadt, Germany, Oct. (2006).
- Arai I., Komatsubara T., Ozawa A., Sasa K., Yasuda Y., Fujinawa T., Fukunishi N., Goto A., Ohnishi T., Okuno H., Takeda H., Wakasugi M., Yamaguchi M., Yamaguchi Y., Yano Y., Kikuchi T., Suzuki T., Yamaguchi T., and Ohtsubo T.: “Rare RI ring”, RIBF International Collaboration Workshop on Experiments at the RIBF, Wako, Nov. (2006).
- Yamaguchi Y., Fujinawa T., Fukunishi N., Goto A., Ohnishi T., Sakurai H., Wakasugi M., Yano Y., Ozawa

- A., Arai I., Yasuda Y., Suzuki T., Yamaguchi T., Kikuchi T., and Ohtsubo T.: “Rare-RI ring project at RI Beam factory in RIKEN”, 15th International Conference on Electromagnetic Isotope Separators and Techniques Related to their Applications (EMIS2007), (GANIL , IN2P3/CNRS , DSM/CEA), Deauville, France, June (2007).
- Ozawa A., Arai I., Fujinawa T., Fukunishi N., Goto A., Kikuchi T., Igarashi S., Komatsubara T., Ohtsubo T., Sakurai H., Sasa K., Suzuki T., Wakasugi M., Yamaguchi K., Yamaguchi T., Yamaguchi Y., Yano Y., and Yasuda Y.: “Mass measurements by isochronous storage ring in RI beam factory”, International Nuclear Physics Conference (INPC2007), (RIKEN and others), Tokyo, June (2007).
- Okuno H., Yamada K., Ohnishi J., Fukunishi N., Yokouchi S., Hasebe H., Ikegami K., Kumagai K., Sakamoto N., Kamigaito O., Goto A., Kase M., Yano Y., and Maie T.: “Commissioning of the Superconducting Ring Cyclotron for the RIKEN RI Beam Factory”, MT-20 The 20th biennial conference on magnet technology, Wako, Aug. (2007).
- Nakajima S., Suzuki T., Yamaguchi T., Fujinawa T., Fukunishi N., Goto A., Ohnishi T., Sakurai H., Wakasugi M., Yamaguchi Y., Yano Y., Ozawa A., Arai I., Yasuda Y., Kikuchi T., and Ohtsubo T.: “New scheme for precision mass measurement of rare isotopes produced at RI beam factory”, 30th Mazurian Lakes Conference on Physics : Nuclear Physics and the Fundamental Processes, (IPJ ; University of Warsaw ; Pro-Physica), Piaski, Poland, Sept. (2007).
- Goto A., Fujimaki M., Fujinawa T., Fukunishi N., Hasebe H., Higurashi Y., Ikegami K., Ikezawa E., Inabe N., Kageyama T., Kamigaito O., Kase M., Kidera M., Kohara S., Komiyama M., Nagase M., Kumagai K., Maie T., Nakagawa T., Ohnishi J., Okuno H., Ryuto H., Sakamoto N., Wakasugi M., Watanabe T., Yamada K., Yokouchi S., and Yano Y.: “Commissioning of RIKEN RI Beam Factory”, 18th International Conference on Cyclotrons and their Applications (Cyclotrons 2007), (Laboratori Nazionali del Sud, INFN), Giardini Naxos, Italy, Sept.–Oct. (2007).
- Yamada K., Fujimaki M., Fukunishi N., Goto A., Kase M., Komiyama M., Ohnishi J., Okuno H., Watanabe T., and Yano Y.: “Details of Beam Diagnostic System for RIKEN Superconducting Ring Cyclotron”, 18th International Conference on Cyclotrons and their Applications (Cyclotrons 2007), (Laboratori Nazionali del Sud), Giardini Naxos, Italy, Sept.–Oct. (2007).
- Okuno H., Yamada K., Ohnishi J., Fukunishi N., Yokouchi S., Hasebe H., Ikegami K., Kumagai K., Sakamoto N., Kamigaito O., Goto A., Kase M., Yano Y., and Maie T.: “Hardware commissioning of the RIKEN superconducting ring cyclotron”, 18th International Conference on Cyclotrons and their Applications (Cyclotrons 2007), Giardini Naxos, Italy, Sept.–Oct. (2007).
- Fukunishi N., Yamada K., Fujimaki M., Fujinawa T., Goto A., Hasebe H., Higurashi Y., Ikegami K., Ikezawa E., Inabe N., Kamigaito O., Kase M., Kohara S., Komiyama M., Kumagai K., Maie T., Nagase M., Nakagawa T., Ohnishi J., Okuno H., Ryuto H., Sakamoto N., Wakasugi M., Watanabe T., and Yano Y.: “Present performance and commissioning details of RIBF accelerator complex”, 18th International Conference on Cyclotrons and their Applications (Cyclotrons 2007), (Laboratori Nazionali del Sud), Giardini Naxos, Italy, Sept.–Oct. (2007).
- Yamaguchi T., Fujinawa T., Fukunishi N., Goto A., Ohnishi T., Sakurai H., Wakasugi M., Yamaguchi Y., Yano Y., Arai I., Moriguchi T., Ozawa A., Yasuda Y., Nakajima S., Kuboki T., Suzuki T., Kikuchi T., and Ohtsubo T.: “Storage-ring mass spectrometry”, ETC Workshop on Mass Olympics, (GSI , FIAS), Trento, Italy, May (2008).
- Okuno H., Fukunishi N., Fujinawa T., Goto A., Higurashi Y., Ikezawa E., Kamigaito O., Kase M., Nakagawa T., Ohnishi J., Sato Y., Yano Y., and Ostroumov P.: “Heavy Ion Accelerators for RIKEN RI Beam Factory and Upgrade Plans”, 42nd ICFA Advanced Beam Dynamics Workshop on High-Intensity, High-Brightness Hadron Beams (HB2008), (Oakridge National Laboratory), Nashville, USA, Aug. (2008).
- Yamaguchi T., Arai I., Ozawa A., Yasuda Y., Fujinawa T., Fukunishi N., Goto A., Hara K., Ohnishi T., Sakurai H., Wakasugi M., Yamaguchi Y., Yano Y., Kikuchi T., Suzuki T., and Ohtsubo T.: “Beam optics simulation for rare-RI ring at RI beam factory in RIKEN”, 7th International Conference on Nuclear Physics at Storage Rings STORI’08, (Institute of Modern Physics, Chinese Academy of Sciences, National Natural Foundation of China), Lanzhou, China, Sept. (2008).
- Yasuda Y., Ozawa A., Arai I., Fujinawa T., Fukunishi N., Goto A., Ohnishi T., Sakurai H., Wakasugi M., Yamaguchi Y., Yano Y., Suzuki T., Yamaguchi T., Kikuchi T., and Ohtsubo T.: “Present status of rare-RI ring project in RIKEN RIBF”, 7th International Conference on Nuclear Physics at Storage Rings STORI’08, (Institute of Modern Physics, Chinese Academy of Sciences, National Natural Foundation of China), Lanzhou, China, Sept. (2008).
- (Domestic Conference)
- 太田寛史, 新井一郎, 小沢顕, 小松原哲郎, 笹公和, 鈴木健, 山口貴之, 大坪隆, 山口充孝, 田岸義宏, 矢野安重, 後藤彰, 若杉昌徳, 奥野広樹, 福西暢尚, 大西哲哉, 山口由高, 菊池崇志: “Design of the isochronous storage ring for accurate mass measurement in RI beam factory”, 第2回日本加速器学会年会/第30回リニアック技術研究会, 鳥栖, 7月 (2005).
- 太田寛史, 新井一郎, 小沢顕, 小松原哲郎, 笹公和, 鈴木健, 山口貴之, 大坪隆, 山口充孝, 田岸義宏, 矢野安重, 後藤彰,

- 奥野広樹, 福西暢尚, 大西哲哉, 山口由高, 菊池崇志: “等時性蓄積リングへの入射ラインとそのビーム光学”, 等時性蓄積リングによる不安定核の質量測定と宇宙元素合成, (筑波大学), つくば, 9月(2005).
- 山口由高, 若杉昌徳, 藤縄雅, 福西暢尚, 後藤彰, 大西哲哉, 奥野広樹, 櫻井博儀, 竹田浩之, 山口充孝, 矢野安重, 小沢顕, 新井一郎, 小松原哲郎, 笹公和, 菊池崇志, 鈴木健, 山口貴之, 大坪隆: “等時性蓄積リングのためのキッカー電磁石及び入射スキームの検討”, 等時性蓄積リングによる不安定核の質量測定と宇宙元素合成, (筑波大学), つくば, 9月(2005).
- 山口由高, 小沢顕, 新井一郎, 安田裕介, 藤縄雅, 福西暢尚, 大西哲哉, 後藤彰, 奥野広樹, 櫻井博儀, 若杉昌徳, 矢野安重, 鈴木健, 山口貴之, 菊池崇志, 大坪隆: “等時性蓄積リングによる質量測定”, 国立天文台ワークショップ「Rプロセス元素組成の統合的理解: 量子ビームでさぐる宇宙進化の理解を目指して」, 三鷹, 3月(2007).
- 山田一成, 藤巻正樹, 福西暢尚, 後藤彰, 加瀬昌之, 込山美咲, 大西純一, 奥野広樹, 渡邊環, 矢野安重: “超伝導リングサイクロトロンビーム診断系の詳細”, 第4回日本加速器学会年会・第32回リニアック技術研究会, ( ), 和光, 8月(2007).
- 渡邊環, 若杉昌徳, 藤巻正樹, 加瀬昌之, 福西暢尚, 小高康熙, 小山亮, 山田一成, 後藤彰, 矢野安重: “RIBFにおけるプラスチックシンチレーションモニターを用いたビームエネルギーと縦方向のビームプロファイルの測定”, 第4回日本加速器学会年会・第32回リニアック技術研究会, 和光, 8月(2007).
- 長谷部裕雄, 龍頭啓充, 福西暢尚, 後藤彰, 加瀬昌之, 矢野安重: “ポリマーコーティング炭素薄膜の制作”, 第4回日本加速器学会年会・第32回リニアック技術研究会, 和光, 8月(2007).
- 安田裕介, 新井一郎, 小沢顕, 小松原哲郎, 笹公和, 大西哲哉, 後藤彰, 櫻井博儀, 福西暢尚, 藤縄雅, 矢野安重, 山口由高, 若杉昌徳, 鈴木健, 山口貴之, 大坪隆, 菊池崇志: “理研RIBFにおける等時性蓄積リング計画”, 日本物理学会第62回年次大会, 札幌, 9月(2007).
- 山口由高, 大西哲哉, 後藤彰, 櫻井博儀, 福西暢尚, 藤縄雅, 矢野安重, 若杉昌徳, 新井一郎, 小沢顕, 小松原哲郎, 笹公和, 安田裕介, 鈴木健, 山口貴之, 菊池崇志, 大坪隆: “理研RIBFにおける質量リング計画の現状”, 国立天文台研究会「Rプロセス元素合成の統合的理解-量子ビームで探る宇宙進化の理解を目指して-」, つくば, 3月(2008).
- 風間裕介, 齊藤宏之, 林依子, 市田裕之, 龍頭啓充, 福西暢尚, 阿部知子: “重イオンビーム照射において核種・LETが突然変異率へ与える影響”, 第5回イオンビーム育種研究会大会, 敦賀, 5月(2008).
- 込山美咲, 藤巻正樹, 内山暁仁, 山内啓資, 小田切淳一, 福西暢尚: “理研リニアックにおけるビーム診断機器制御への組み込みEPICS搭載F3RP61-2Lの応用”, 第5回日本加速器学会年会/第33回リニアック技術研究会, (日本加速器学会, リニアック技術研究会), 東広島, 8月(2008).
- 山口由高, 藤縄雅, 福西暢尚, 後藤彰, 大西哲哉, 櫻井博儀, 若杉昌徳, 矢野安重, 小沢顕, 新井一郎, 安田裕介, 菊池崇志, 大坪隆, 鈴木健, 山口貴之: “理研RIBFにおける稀少RIリング計画の現状”, 第5回日本加速器学会年会/第33回リニアック技術研究会, 東広島, 8月(2008).
- 須田健嗣, 小山亮, 加瀬昌之, 上垣外修一, 坂本成彦, 福西暢尚, 藤巻正樹, 山田一成, 渡邊環: “RIBFにおける高周波系の安定度”, 第5回日本加速器学会年会/第33回リニアック技術研究会, 東広島, 8月(2008).
- 長谷部裕雄, 奥野広樹, 久保木浩功, 龍頭啓充, 福西暢尚, 上垣外修一, 後藤彰, 加瀬昌之, 矢野安重: “理研RIBFにおける長寿命炭素薄膜の開発状況”, 第5回日本加速器学会年会/第33回リニアック技術研究会, (広島大学), 広島, 8月(2008).
- 渡邊環, 藤巻正樹, 福西暢尚, 加瀬昌之, 山田一成, 坂本成彦, 須田健嗣, 込山美咲, 仲村武志, 小山亮, 小高康熙, 上垣外修一, 矢野安重: “RIBFにおけるビーム診断系の高度化”, 第5回日本加速器学会年会/第33回リニアック技術研究会, (広島大学), 東広島, 8月(2008).
- 安田裕介, 新井一郎, 小沢顕, 森口哲朗, 大西哲哉, 櫻井博儀, 福西暢尚, 藤縄雅, 矢野安重, 山口由高, 若杉昌徳, 原かおる, 鈴木健, 山口貴之, 大坪隆, 菊池崇志: “理研稀少RIリング建設にむけての高精度磁場測定”, 日本物理学会2008年秋季大会, 盛岡, 9月(2008).
- 森下敏和, 清水明美, 山口博康, 出花幸之介, 六笠裕治, 相井城太郎, 長谷純宏, 鹿園直哉, 田中淳, 宮沢豊, 齊藤宏之, 林依子, 龍頭啓充, 福西暢尚, 阿部知子: “ガンマ線およびイオンビーム照射によって得られたダットンそば半矮性変異体の特性”, 日本育種学会第114回講演会, (日本育種学会), 彦根, 10月(2008).
- 渡邊環, 佐々木雄一朗: “高温超伝導電流センサーとSQUIDを用いたビーム電流モニターの実用化”, 2008年度秋季低温工学・超電導学会, (低温工学協会), 高知, 11月(2008).

## Cryogenic Technology Team

### Publications

#### [Journal]

(Original Papers) \*Subject to Peer Review

Aoki T., Stingelin L., Kamigaito O., Sakamoto N., Fukunishi N., Yokouchi S., Maie T., Kase M., Goto A., and Yano Y.: “Construction of a beam rebuncher for RIKEN RI-beam factory”, Nucl. Instrum. Methods Phys. Res. A **592**, No. 3, pp. 171–179 (2008). \*

(Others)

Okuno H., Yamada K., Ohnishi J., Fukunishi N., Yokouchi S., Hasebe H., Ikegami K., Kumagai K., Sakamoto N., Kamigaito O., Goto A., Kase M., Yano Y., and Maie T.: “Commissioning of the Superconducting Ring Cyclotron for the RIKEN RI Beam Factory”, IEEE Trans. Appl. Supercond. **18**, No. 2, pp. 226–231 (2008).

#### [Book・Proceedings]

(Original Papers) \*Subject to Peer Review

Goto A., Fujimaki M., Fujinawa T., Fukunishi N., Hasebe H., Higurashi Y., Ikegami K., Ikezawa E., Inabe N., Kageyama T., Kamigaito O., Kase M., Kidera M., Kohara S., Komiyama M., Nagase M., Kumagai K., Maie T., Nakagawa T., Ohnishi J., Okuno H., Ryuto H., Sakamoto N., Wakasugi M., Watanabe T., Yamada K., Yokouchi S., and Yano Y.: “Commissioning of RIKEN RI Beam Factory”, Proceedings of 18th International Conference on Cyclotrons and Their Applications (Cyclotrons 2007), Giardini Naxos, Italy, 2007–9~10, Giardini Naxos, pp. 3–8 (2007).

(Others)

Okuno H., Yamada K., Ohnishi J., Fukunishi N., Sakamoto N., Kamigaito O., Hasebe H., Kumagai K., Maie T., Yokouchi S., Ikegami K., Kase M., Goto A., and Yano Y.: “Hardware commissioning of the RIKEN superconducting ring cyclotron”, Proceedings of 18th International Conference on Cyclotrons and Their Applications (Cyclotrons 2007), Istituto Nazionale di Fisica Nucleare, Roma, pp. 18–20 (2007).

奥野広樹, 山田一成, 大西純一, 福西暢尚, 横内茂, 長谷部裕雄, 池上九三男, 熊谷桂子, 坂本成彦, 上垣外修一, 長瀬誠, 藤巻正樹, 込山美咲, 後藤彰, 加瀬昌之, 矢野安重, 真家武士: “理研超伝導リングサイクロトロン の現状報告”, 第4回日本加速器学会年会・第32回リニアック技術研究会論文集, 和光, 2007–8, 日本加速器学会, 東京, pp. 46–48 (2007).

奥野広樹, 山田一成, 池上九三男, 加瀬昌之, 矢野安重, 真家武士: “Operational Status of the He Cooling System for RIKEN SRC”, 第4回日本加速器学会年会・第32回リニアック技術研究会論文集, Wako, 2007–8, 日本加速器学会, 東京, pp. 796–798 (2007).

### Oral Presentations

(International Conference etc.)

Hasebe H., Ryuto H., Fukunishi N., Goto A., Kase M., and Yano Y.: “Polymer coating method developed for

carbon stripper foils”, 23rd World Conference of the INTDS, (High Energy Accelerator Research Organization (KEK)), Tsukuba, Oct. (2006).

Okuno H., Yamada K., Ohnishi J., Fukunishi N., Yokouchi S., Hasebe H., Ikegami K., Kumagai K., Sakamoto N., Kamigaito O., Goto A., Kase M., Yano Y., and Maie T.: “Commissioning of the Superconducting Ring Cyclotron for the RIKEN RI Beam Factory”, MT-20 The 20th biennial conference on magnet technology, Wako, Aug. (2007).

Goto A., Fujimaki M., Fujinawa T., Fukunishi N., Hasebe H., Higurashi Y., Ikegami K., Ikezawa E., Inabe N., Kageyama T., Kamigaito O., Kase M., Kidera M., Kohara S., Komiyama M., Nagase M., Kumagai K., Maie T., Nakagawa T., Ohnishi J., Okuno H., Ryuto H., Sakamoto N., Wakasugi M., Watanabe T., Yamada K., Yokouchi S., and Yano Y.: “Commissioning of RIKEN RI Beam Factory”, 18th International Conference on Cyclotrons and their Applications (Cyclotrons 2007), (Laboratori Nazionali del Sud, INFN), Giardini Naxos, Italy, Sept.–Oct. (2007).

Okuno H., Yamada K., Ohnishi J., Fukunishi N., Yokouchi S., Hasebe H., Ikegami K., Kumagai K., Sakamoto N., Kamigaito O., Goto A., Kase M., Yano Y., and Maie T.: “Hardware commissioning of the RIKEN superconducting ring cyclotron”, 18th International Conference on Cyclotrons and their Applications (Cyclotrons 2007), Giardini Naxos, Italy, Sept.–Oct. (2007).

Fukunishi N., Yamada K., Fujimaki M., Fujinawa T., Goto A., Hasebe H., Higurashi Y., Ikegami K., Ikezawa E., Inabe N., Kamigaito O., Kase M., Kohara S., Komiyama M., Kumagai K., Maie T., Nagase M., Nakagawa T., Ohnishi J., Okuno H., Ryuto H., Sakamoto N., Wakasugi M., Watanabe T., and Yano Y.: “Present performance and commissioning details of RIBF accelerator complex”, 18th International Conference on Cyclotrons and their Applications (Cyclotrons 2007), (Laboratori Nazionali del Sud), Giardini Naxos, Italy, Sept.–Oct. (2007).

## Nuclear Physics Research Division

### Publications

#### [Journal]

(Original Papers) \*Subject to Peer Review

Yamaguchi Y., Ozawa A., Goto A., Arai I., Fujinawa T., Fukunishi N., Kikuchi T., Ohnishi T., Ohtsubo T., Sakurai H., Suzuki T., Wakasugi M., Yamaguchi T., Yasuda Y., and Yano Y.: "Rara-RI ring project at RIKEN RI beam factory", Nucl. Instrum. Methods Phys. Res. B **266**, 4575–4578 (2008). \*

(Others)

Nakajima S., Yamaguchi T., Suzuki T., Yamaguchi Y., Fujinawa T., Fukunishi N., Goto A., Ohnishi T., Sakurai H., Wakasugi M., Yano Y., Arai I., Ozawa A., Yasuda Y., Kikuchi T., and Ohtsubo T.: "New scheme for precision mass measurements of rare isotopes produced at RI beam factory", Acta Phys. Pol. B **39**, No. 2, pp. 457–462 (2008).

#### [Book • Proceedings]

(Others)

Kikuchi T., Horioka K., Ozawa A., Kawata S., Yamaguchi Y., Fukunishi N., Sakurai H., Wakasugi M., Yamaguchi M., Yamaguchi T., Arai I., Ohta H., Fujinawa T., Sasa K., Komatsubara T., Suzuki T., Ohtsubo T., Goto A., Ohnishi T., Okuno H., Takeda H., and Yano Y.: "Individual correction using induction modulator for mass measurements by isochronous ring in RIKEN RI beam factory", Proceedings of the 2nd International Workshop on Recent Progress in Induction Accelerators (RPIA2006), Tsukuba, 2006–3, KEK, Tsukuba, pp. 127–131 (2006).

### Oral Presentations

(International Conference etc.)

Kikuchi T., Horioka K., Ozawa A., Kawata S., Yamaguchi Y., Fukunishi N., Sakurai H., Wakasugi M., Yamaguchi M., Yamaguchi T., Arai I., Ohta H., Fujinawa T., Sasa K., Komatsubara T., Suzuki T., Ohtsubo T., Goto A., Ohnishi T., Okuno H., Takeda H., and Yano Y.: "Individual correction using induction modulator for mass measurements by isochronous ring in RIKEN RI beam factory", 2nd International Workshop on Recent Progress in Induction Accelerators (RPIA2006), (KEK, Tokyo Institute of Technology), Tsukuba, Mar. (2006).

Yamaguchi Y., Fujinawa T., Fukunishi N., Goto A., Ohnishi T., Sakurai H., Wakasugi M., Yano Y., Ozawa A., Arai I., Yasuda Y., Suzuki T., Yamaguchi T., Kikuchi T., and Ohtsubo T.: "Rare-RI ring project at RI Beam factory in RIKEN", 15th International Conference on Electromagnetic Isotope Separators and Techniques Related to their Applications (EMIS2007), (GANIL, IN2P3/CNRS, DSM/CEA), Deauville, France, June (2007).

Ozawa A., Arai I., Fujinawa T., Fukunishi N., Goto

A., Kikuchi T., Igarashi S., Komatsubara T., Ohtsubo T., Sakurai H., Sasa K., Suzuki T., Wakasugi M., Yamaguchi K., Yamaguchi T., Yamaguchi Y., Yano Y., and Yasuda Y.: "Mass measurements by isochronous storage ring in RI beam factory", International Nuclear Physics Conference (INPC2007), (RIKEN and others), Tokyo, June (2007).

Nakajima S., Suzuki T., Yamaguchi T., Fujinawa T., Fukunishi N., Goto A., Ohnishi T., Sakurai H., Wakasugi M., Yamaguchi Y., Yano Y., Ozawa A., Arai I., Yasuda Y., Kikuchi T., and Ohtsubo T.: "New scheme for precision mass measurement of rare isotopes produced at RI beam factory", 30th Mazurian Lakes Conference on Physics : Nuclear Physics and the Fundamental Processes, (IPJ ; University of Warsaw ; Pro-Physica), Piaski, Poland, Sept. (2007).

Yamaguchi T., Fujinawa T., Fukunishi N., Goto A., Ohnishi T., Sakurai H., Wakasugi M., Yamaguchi Y., Yano Y., Arai I., Moriguchi T., Ozawa A., Yasuda Y., Nakajima S., Kuboki T., Suzuki T., Kikuchi T., and Ohtsubo T.: "Storage-ring mass spectrometry", ETC Workshop on Mass Olympics, (GSI, FIAS), Trento, Italy, May (2008).

Yamaguchi T., Arai I., Ozawa A., Yasuda Y., Fujinawa T., Fukunishi N., Goto A., Hara K., Ohnishi T., Sakurai H., Wakasugi M., Yamaguchi Y., Yano Y., Kikuchi T., Suzuki T., and Ohtsubo T.: "Beam optics simulation for rare-RI ring at RI beam factory in RIKEN", 7th International Conference on Nuclear Physics at Storage Rings STORI'08, (Institute of Modern Physics, Chinese Academy of Sciences, National Natural Foundation of China), Lanzhou, China, Sept. (2008).

Yasuda Y., Ozawa A., Arai I., Fujinawa T., Fukunishi N., Goto A., Ohnishi T., Sakurai H., Wakasugi M., Yamaguchi Y., Yano Y., Suzuki T., Yamaguchi T., Kikuchi T., and Ohtsubo T.: "Present status of rare-RI ring project in RIKEN RIBF", 7th International Conference on Nuclear Physics at Storage Rings STORI'08, (Institute of Modern Physics, Chinese Academy of Sciences, National Natural Foundation of China), Lanzhou, China, Sept. (2008).

(Domestic Conference)

山口由高, 若杉昌徳, 藤縄雅, 福西暢尚, 後藤彰, 大西哲哉, 奥野広樹, 櫻井博儀, 竹田浩之, 山口充孝, 矢野安重, 小沢顕, 新井一郎, 小松原哲郎, 笹公和, 菊池崇志, 鈴木健, 山口貴之, 大坪隆: "等時性蓄積リングのためのキッカー電磁石及び入射スキームの検討", 等時性蓄積リングによる不安定核の質量測定と宇宙元素合成, (筑波大学), つくば, 9月 (2005).

山口由高, 小沢顕, 新井一郎, 安田裕介, 藤縄雅, 福西暢尚, 大西哲哉, 後藤彰, 奥野広樹, 櫻井博儀, 若杉昌徳, 矢野安重, 鈴木健, 山口貴之, 菊池崇志, 大坪隆: "等時性蓄積リングによる質量測定", 国立天文台ワークショップ「Rプロセス元素組成の統合的理解: 量子ビームでさぐる宇宙進化の理解を目指して」, 三鷹, 3月 (2007).

安田裕介, 新井一郎, 小沢顕, 小松原哲郎, 笹公和, 大西哲哉, 後藤彰, 櫻井博儀, 福西暢尚, 藤縄雅, 矢野安重, 山口由高, 若杉昌徳, 鈴木健, 山口貴之, 大坪隆, 菊池崇志: “理研 RIBF における等時性蓄積リング計画”, 日本物理学会第 62 回年次大会, 札幌, 9 月 (2007).

山口由高, 大西哲哉, 後藤彰, 櫻井博儀, 福西暢尚, 藤縄雅, 矢野安重, 若杉昌徳, 新井一郎, 小沢顕, 小松原哲郎, 笹公和, 安田裕介, 鈴木健, 山口貴之, 菊池崇志, 大坪隆: “理研 RIBF における質量リング計画の現状”, 国立天文台研究会「r プロセス元素合成の統合的理解-量子ビームで探る宇宙進化の理解を目指して-」, つくば, 3 月 (2008).

山口由高, 藤縄雅, 福西暢尚, 後藤彰, 大西哲哉, 櫻井博儀, 若杉昌徳, 矢野安重, 小沢顕, 新井一郎, 安田裕介, 菊池崇志, 大坪隆, 鈴木健, 山口貴之: “理研 RIBF における稀少 RI リング計画の現状”, 第 5 回日本加速器学会年会/第 33 回リニアック技術研究会, 東広島, 8 月 (2008).

安田裕介, 新井一郎, 小沢顕, 森口哲朗, 大西哲哉, 櫻井博儀, 福西暢尚, 藤縄雅, 矢野安重, 山口由高, 若杉昌徳, 原かおる, 鈴木健, 山口貴之, 大坪隆, 菊池崇志: “理研稀少 RI リング建設にむけての高精度磁場測定”, 日本物理学会 2008 年秋季大会, 盛岡, 9 月 (2008).

## Heavy Ion Nuclear Physics Laboratory

### Publications

#### [Journal]

(Original Papers) \*Subject to Peer Review

- Otsu H., Kobayashi T., Matsuda Y., Kitayama M., Inafuku K., Ozawa A., Satou Y., Suda T., Yoshida K., and Sakaguchi H.: "Measurement of the H(38s,p') reaction at forward angles including 0 degree", Nucl. Phys. A **788**, 266c–270c (1997). \*
- Fukuda N., Nakamura T., Kobayashi T., Otsu H., Aoi N., Imai N., Iwasaki H., Kubo T., Mengoni A., Notani M., Sakurai H., Shimoura S., Teranishi T., Watanabe Y., Yoneda K., and Ishihara M.: "Coulomb Dissociation of Halo Nuclei", Prog. Theor. Phys. Suppl., No. 146, pp. 462–466 (2002).
- Gomi T., Motobayashi T., Yoneda K., Kanno S., Aoi N., Ando Y., Baba H., Demichi K., Fulop Z., Futakami U., Hasegawa H., Higurashi Y., Ieki K., Imai N., Iwasa N., Iwasaki H., Kubo T., Kubono S., Kunibu M., Matsuyama Y., Michimasa S., Minemura T., Murakami H., Nakamura T., Saito A., Sakurai H., Serata M., Shimoura S., Sugimoto T., Takeshita E., Takeuchi S., Ue K., Yamada K., Yanagisawa Y., Yoshida A., and Ishihara M.: "Coulomb Dissociation of  $^{23}\text{Al}$ ", Prog. Theor. Phys. Suppl., No. 146, pp. 557–558 (2002). \*
- Kanno S., Gomi T., Motobayashi T., Yoneda K., Aoi N., Ando Y., Baba H., Demichi K., Fulop Z., Futakami U., Hasegawa H., Higurashi Y., Ieki K., Imai N., Iwasa N., Iwasaki H., Kubo T., Kubono S., Kunibu M., Matsuyama Y., Michimasa S., Minemura T., Murakami H., Nakamura T., Saito A., Sakurai H., Serata M., Shimoura S., Sugimoto T., Takeshita E., Takeuchi S., Ue K., Yamada K., Yanagisawa Y., Yoshida A., and Ishihara M.: "Coulomb Excitation of  $^{24}\text{Si}$ ", Prog. Theor. Phys. Suppl., No. 146, pp. 575–576 (2002). \*
- Matsuyama Y., Motobayashi T., Shimoura S., Minemura T., Saito A., Baba H., Akiyoshi H., Aoi N., Ando Y., Gomi T., Higurashi Y., Ieki K., Imai N., Iwasa N., Iwasaki H., Kanno S., Kubono S., Kunibu M., Michimasa S., Murakami H., Nakamura T., Sakurai H., Serata M., Takeshita E., Takeuchi S., Teranishi T., Ue K., Yamada K., and Yanagisawa Y.: "Inelastic Scattering of  $^{12}\text{Be}$  with  $^4\text{He}$ ", Prog. Theor. Phys. Suppl., No. 146, pp. 593–594 (2002). \*
- Ideguchi E., Cederwall B., undefined u. u., Gono Y., Y.F. Y., Teranishi T., Aoi N., D. B., and Kishida T.: "Measurement of Depth of Interaction in a Segmented Planar Ge Detector", Nucl. Instrum. Methods Phys. Res. A **496**, 373–384 (2003). \*
- Gomi T., Motobayashi T., Yoneda K., Kanno S., Aoi N., Ando Y., Baba H., Demichi K., Fulop Z., Futakami U., Hasegawa H., Higurashi Y., Ieki K., Imai N., Iwasa N., Iwasaki H., Kubo T., Kubono S., Kunibu M., Matsuyama Y., Michimasa S., Minemura T., Murakami H., Nakamura T., Notani M., Ota S., Saito A., Sakurai H., Serata M., Shimoura S., Sugimoto T., Takeshita E., Takeuchi S., Togano Y., Ue K., Yamada K., Yanagisawa Y., Yoneda K., and Yoshida A.: "Study of the Stellar  $^{22}\text{Mg}(p, \gamma)^{23}\text{Al}$  Reaction with the Coulomb-Dissociation Method", Nucl. Phys. A **718**, 508c–509c (2003). \*
- Inakura T., Mizutori S., Yamagami M., and Matuyanagi K.: "Superdeformed Bands in Neutron-Rich Sulfur Isotopes suggested by Cranked Skyrme-Hartree-Fock Calculations", Nucl. Phys. A **728**, 52–64 (2003). \*
- Shimoura S., Saito A., Minemura T., Matsuyama Y., Baba H., Akiyoshi H., Aoi N., Gomi T., Higurashi Y., Ieki K., Imai N., Iwasa N., Iwasaki H., Kanno S., Kubono S., Kunibu M., Michimasa S., Motobayashi T., Nakamura T., Sakurai H., Serata M., Takeshita E., Takeuchi S., Teranishi T., Ue K., Yamada K., Yanagisawa Y., Ishihara M., and Itagaki N.: "Isomeric  $0^+$  state in  $^{12}\text{Be}$ ", Phys. Lett. B **560**, 31–36 (2003). \*
- Takashina M., Ito M., Kudo Y., Okabe S., and Sakuragi H.: " $^{12}\text{C}+^{12}\text{C}\rightarrow^8\text{Be}_{g.s.}+^{16}\text{O}_{g.s.}$  resonance reaction around  $E_{c.m.}=32.5$  MeV", Phys. Rev. C **67**, 014609-1–014609-6 (2003). \*
- Takashina M., Takagi S., Sakuragi H., and Iseri Y.: "A continuum discretized coupled channels study of  $^{11}\text{Be}\rightarrow^{10}\text{Be}+n$  breakup effect on the  $^{11}\text{Be}$  elastic scattering", Phys. Rev. C **67**, 037601-1–037601-4 (2003). \*
- Iwasa N., Motobayashi T., Sakurai H., Akiyoshi H., Ando Y., Aoi N., Baba H., Fukuda N., Fulop Z., Futakami U., Gomi T., Higurashi Y., Ieki K., Iwasaki H., Kubo T., Kubono S., Kinugawa H., Kumagai H., Kunibu M., Michimasa S., Minemura T., Murakami H., Sagara K., Saito A., Shimoura S., Takeuchi S., Yanagisawa Y., Yoneda K., and Ishihara M.: "In-beam  $\gamma$  spectroscopy of  $^{34}\text{Si}$  with deuteron inelastic scattering using reverse kinematics", Phys. Rev. C **67**, 064315-1–064315-4 (2003). \*
- Guimaraes V., Kubono S., F.C. B., M. H., S.C. J., Katayama I., Miyachi T., Nomura T., H.M. T., Fuchi Y., H. K., Kato S., Yun C., K. I., Orihara H., Terakawa A., Kishida T., Y. P., Hamada S., Hirai M., and Miyatake H.: "Structure of the Unbound  $^{11}\text{N}$  Nucleus by the ( $^3\text{He}$ ,  $^6\text{He}$ ) Reaction", Phys. Rev. C **67**, 064601-1–064601-8 (2003). \*
- Gomi T., Motobayashi T., Ando Y., Aoi N., Baba H., Demichi K., Elekes Z., Fukuda N., Fulop Z., Futakami U., Hasegawa H., Higurashi Y., Ieki K., Imai N., Ishihara M., Ishikawa K., Iwasa N., Iwasaki H., Kanno S., Kondo Y., Kubo T., Kubono S., Kunibu M., Kurita K., Matsuyama Y., Michimasa S., Minemura T., Miura M., Murakami H., Nakamura T., Notani M., Ota S., Saito A., Sakurai H., Serata M., Shimoura S., Sugimoto T., Takeshita E., Takeuchi S., Togano Y., Ue K., Yamada K., Yanagisawa Y., Yoneda K., and Yoshida A.: "Study of the Stellar  $^{22}\text{Mg}(p, \gamma)^{23}\text{Al}$  Reaction us-

- ing the Coulomb-Dissociation Method”, Nucl. Phys. A **734**, E77–E79 (2004).
- Ueno H., Asahi K., Ogawa H., Kameda D., Miyoshi H., Yoshimi A., Watanabe H., Shimada K., Sato W., Yoneda K., Imai N., Kobayashi Y., Ishihara M., and Wolf-Dieter S.: “Measurement of nuclear moments in the region of light neutron-rich nuclei”, Nucl. Phys. A **738**, 211–215 (2004). \*
- Saito A., Shimoura S., Takeuchi S., Motobayashi T., Minemura T., Matsuyama Y., Baba H., Akiyoshi H., Ando Y., Aoi N., Fulop Z., Gomi T., Higurashi Y., Hirai M., Ieki K., Imai N., Iwasa N., Iwasaki H., Iwata Y., Kanno S., Kobayashi H., Kubono S., Kunibu M., Kurokawa M., Liu Z., Michimasa S., Nakamura T., Ozawa A., Sakurai H., Serata M., Takeshita E., Teranishi T., Ue K., Yamada K., Yanagisawa Y., and Ishihara M.: “Molecular states in neutron-rich beryllium isotopes”, Nucl. Phys. A **738**, 337–341 (2004). \*
- Takashina M., Ito M., Kudo Y., Okabe S., and Sakuragi H.: “ $^{12}\text{C}+^{12}\text{C}\rightarrow^8\text{Be}_{\text{g.s.}}+^{16}\text{O}_{\text{g.s.}}$  resonance reaction and multi-cluster states of highly-excited  $^{24}\text{Mg}$  nucleus”, Nucl. Phys. A **738**, 352–356 (2004). \*
- Matsuzaki M., Shimizu Y., and Matuyanagi K.: “Nuclear Moment of Inertia and Wobbling Motions in Triaxial Superdeformed Nuclei”, Phys. Rev. C **69**, 034325-1–034325-10 (2004). \*
- Fukuda N., Nakamura T., Aoi N., Imai N., Ishihara M., Kobayashi T., Iwasaki H., Kubo T., Mengoni A., Notani M., Otsu H., Sakurai H., Shimoura S., Teranishi T., Watanabe Y., and Yoneda K.: “Coulomb and nuclear breakup of a halo nucleus  $^{11}\text{Be}$ ”, Phys. Rev. C **70**, 054606-1–054606-12 (2004). \*
- Imai N., Ong H., Aoi N., Sakurai H., Demichi K., Kawasaki H., Baba H., Dombradi Z., Elekes Z., Fukuda N., Fulop Z., Gelberg A., Gomi T., Hasegawa H., Ishikawa K., Iwasaki H., Kaneko E., Kanno S., Kishida T., Kondo Y., Kubo T., Kurita K., Michimasa S., Minemura T., Miura M., Motobayashi T., Nakamura T., Notani M., Ohnishi T., Saito A., Shimoura S., Sugimoto T., Suzuki M., Takeshita E., Takeuchi M., Tamaki M., Yoneda K., Watanabe H., and Ishihara M.: “Anomalous hindered  $E2$  Strength  $B(E2; 2_1^+ \rightarrow 0^+)$  in  $^{16}\text{C}$ ”, Phys. Rev. Lett. **92**, No. 6, pp. 062501-1–062501-4 (2004). \*
- Kobayasi M., Nakatsukasa T., Matsuo M., and Matuyanagi K.: “Collective Path Connecting the Oblate and Prolate Local Minima in  $^{68}\text{Se}$ ”, Prog. Theor. Phys. **112**, No. 2, pp. 363–368 (2004). \*
- Sekiguchi K.: “Exploring Three Nucleon Forces through  $dp$  Scattering at Intermediate Energies”, AIP Conf. Proc. **768**, 24–30 (2005). \*
- Saito T., Sakai H., Ikeda T., Itoh K., Kawabata T., Kuboki H., Maeda Y., Matsui N., Sasano M., Satou Y., Sekiguchi K., Suda K., Tamii A., Uesaka T., and Yako K.: “Experimental Test of Bell’s Inequality via the  $^1\text{H}(d, ^2\text{He})n$  Reaction”, AIP Conf. Proc. **768**, 62–64 (2005). \*
- Takechi M., Fukuda M., Mihara M., Chinda T., Matsumasa T., Matsubara H., Nakashima Y., Matsuta K., Minamisono T., Koyama R., Shinosaki W., Takahashi M., Takisawa A., Ohtsubo T., Suzuki T., Momota S., Hatanaka K., Suda T., Sasaki M., Sato S., and Kitagawa A.: “Reaction cross-sections for stable nuclei and nucleon density distribution of proton drip-line nucleus  $8\text{B}$ ”, Eur. Phys. J. A **25**, No. s01, pp. 217–219 (2005). \*
- Hatano M., Sakai H., Wakui T., Uesaka T., Aoi N., Ichikawa Y., Ikeda T., Itoh K., Iwasaki H., Kawabata T., Kuboki H., Maeda Y., Matsui N., Ohnishi T., Ohnishi T., Saito T., Sakamoto N., Sasano M., Satou Y., Sekiguchi K., Suda K., Tamii A., Yanagisawa Y., and Yako K.: “First experiment of  $6\text{He}$  with a polarized proton target”, Eur. Phys. J. A **25**, No. s01, pp. 255–258 (2005). \*
- Kannungo R., Chiba M., Abu-Ibrahim B., Adhikari S., Fang D., Iwasa N., Kimura K., Maeda K., Nishimura S., Ohnishi T., Ozawa A., Samanta C., Suda T., Suzuki T., Wang Q., Wu C., Yamaguchi Y., Yamada K., Yoshida A., Zheng T., and Tanihata I.: “A new view to the structure of  $^{19}\text{C}$ ”, Eur. Phys. J. A **25**, No. s01, pp. 261–262 (2005). \*
- Takashina M., Sakuragi H., and Iseri Y.: “Effect of halo structure on  $^{11}\text{Be}+^{12}\text{C}$  elastic scattering”, Eur. Phys. J. A **25**, No. s01, pp. 273–275 (2005). \*
- Yamada K., Motobayashi T., Aoi N., Baba H., Demichi K., Elekes Z., Gibelin J., Gomi T., Hasegawa H., Imai N., Iwasaki H., Kanno S., Kubo T., Kurita K., Matsuyama Y., Michimasa S., Minemura T., Notani M., Onishi T., Ong H., Ota S., Ozawa A., Saito A., Sakurai H., Shimoura S., Takeshita E., Takeuchi S., Tamaki M., Togano Y., Yanagisawa Y., Yoneda K., and Tanihata I.: “Reduced transition probabilities for the first  $2^+$  excited state in  $^{46}\text{Cr}$ ,  $^{50}\text{Fe}$ , and  $^{54}\text{Ni}$ ”, Eur. Phys. J. A **25**, No. s01, pp. 409–413 (2005).
- Gomi T., Motobayashi T., Ando Y., Aoi N., Baba H., Demichi K., Elekes Z., Fukuda N., Fulop Z., Futakami U., Hasegawa H., Higurashi Y., Ieki K., Imai N., Ishihara M., Ishikawa K., Iwasa N., Iwasaki H., Kanno S., Kondo Y., Kubo T., Kubono S., Kunibu M., Kurita K., Matsuyama Y., Michimasa S., Minemura T., Miura M., Murakami H., Nakamura T., Notani M., Ota S., Saito A., Sakurai H., Serata M., Shimoura S., Sugimoto T., Takeshita E., Takeuchi S., Togano Y., Ue K., Yamada K., Yanagisawa Y., Yoneda K., and Yoshida A.: “Coulomb dissociation experiment for explosive hydrogen burning: study of the  $^{22}\text{Mg}(p, \gamma)^{22}\text{Al}$  reaction”, J. Phys. G **31**, S1517–S1521 (2005).
- Togano Y., Gomi T., Motobayashi T., Ando Y., Aoi N., Baba H., Demichi K., Elekes Z., Fukuda N., Fulop Z.,

- Futakami U., Hasegawa H., Higurashi Y., Ieki K., Imai N., Ishihara M., Ishikawa K., Iwasa N., Iwasaki H., Kanno S., Kondo Y., Kubo T., Kubono S., Kunibu M., Kurita K., Matsuyama Y., Michimasa S., Minemura T., Miura M., Murakami H., Nakamura T., Notani M., Ota S., Saito A., Sakurai H., Serata M., Shimoura S., Sugimoto T., Takeshita E., Takeuchi S., Ue K., Yamada K., Yanagisawa Y., Yoneda K., and Yoshida A.: “Study of  $^{26}\text{Si}(p, \gamma)^{27}\text{P}$  reaction using Coulomb dissociation method”, *Nucl. Phys. A* **758**, 182c–185c (2005). \*
- Elekes Z., Dombradi Z., Kanungo R., Baba H., Fulop Z., Gibelin J. D., Horvath A., Ideguchi E., Ichikawa Y., Iwasa N., Iwasaki H., Kanno S., Kawai S., Kondo Y., Motobayashi T., Notani M., Ohnishi T., Ozawa A., Sakurai H., Shimoura S., Takeshita E., Takeuchi M., Tanihata I., Togano Y., Wu C., Yamaguchi Y., Yanagisawa Y., Yoshida A., and Yoshida K.: “Low-lying excited states in  $^{17,19}\text{C}$ ”, *Phys. Lett. B* **614**, 174–180 (2005). \*
- Iwasaki H., Motobayashi T., Sakurai H., Yoneda K., Gomi T., Aoi N., Fukuda N., Fulop Z., Futakami U., Gacsi Z., Higurashi Y., Imai N., Iwasa N., Kunibu M., Kubo T., Kurokawa M., Liu Z., Minemura T., Saito A., Serata M., Shimoura S., Takeuchi S., Watanabe Y., Yamada K., Yanagisawa Y., and Ishihara M.: “Quadrupole collectivity of  $^{28}\text{Ne}$  and the boundary of the island of inversion”, *Phys. Lett. B* **620**, 118–124 (2005). \*
- Dombradi Z., Elekes Z., Kanungo R., Baba H., Fulop Z., Gibelin J. D., Horvath A., Ideguchi E., Ichikawa Y., Iwasa N., Iwasaki H., Kanno S., Kawai S., Kondo Y., Motobayashi T., Notani M., Ohnishi T., Ozawa A., Sakurai H., Shimoura S., Takeshita E., Takeuchi S., Tanihata I., Togano Y., Wu C., Yamaguchi Y., Yanagisawa Y., Yoshida A., and Yoshida K.: “Decoupling of valence neutrons from the core in  $^{17}\text{B}$ ”, *Phys. Lett. B* **621**, 81–88 (2005). \*
- Kondo Y., Nakamura T., Aoi N., Baba H., Bazin D., Fukuda N., Gomi T., Hasegawa H., Imai N., Ishihara M., Kobayashi T., Kubo T., Miura M., Motobayashi T., Saito A., Sakurai H., Shimoura S., Sugimoto T., Watanabe K., Watanabe Y., Yakushiji T., Yanagisawa Y., and Yoneda K.: “In-beam  $\gamma$ -ray spectroscopy of the neutron-rich boron isotopes  $^{15,17}\text{B}$  via inelastic scattering on  $^{12}\text{C}$ ”, *Phys. Rev. C* **71**, 044611-1–044611-9 (2005). \*
- Onishi T., Gelberg A., Sakurai H., Yoneda K., Aoi N., Imai N., Baba H., Von Brentano P., Fukuda N., Ichikawa Y., Ishihara M., Iwasaki H., Kameda D., Kishida T., Lisetskiy A., Ong H., Osada M., Ohtsuka T., Suzuki M., Ue K., Utsuno Y., and Watanabe H.: “Gamow-Teller decay of the  $T = 1$  nucleus  $^{46}\text{Cr}$ ”, *Phys. Rev. C* **72**, No. 2, pp. 024308-1–024308-7 (2005). \*
- Sekiguchi K., Sakai H., Witala H., Glockle W., Golak J., Hatanaka K., Hatano M., Itoh K., Kamada H., Kuboki H., Maeda Y., Nogga A., Okamura H., Saito T., Sakamoto N., Sakemi Y., Sasano M., Shimizu Y., Suda T., Tamii A., Uesaka T., Wakasa T., and Yako K.: “Resolving the Discrepancy of 135 MeV pd Elastic Scattering Cross Sections and Relativistic Effects”, *Phys. Rev. Lett.* **95**, 162301-1–162301-4 (2005). \*
- Ong H., Imai N., Aoi N., Sakurai H., Dombradi Z., Saito A., Elekes Z., Baba H., Demichi K., Fulop Z., Gibelin J., Gomi T., Hasegawa H., Ishihara M., Iwasaki H., Kanno S., Kawai S., Kubo T., Kurita K., Matsuyama Y., Michimasa S., Minemura T., Motobayashi T., Notani M., Ota S., Sakai H., Shimoura S., Takeshita E., Takeuchi S., Tamaki M., Togano Y., Yamada K., Yanagisawa Y., and Yoneda K.: “Inelastic proton scattering on  $^{16}\text{C}$ ”, *Eur. Phys. J. A* **25**, No. s01, pp. 347–348 (2006). \*
- Togano Y., Gomi T., Motobayashi T., Ando Y., Aoi N., Baba H., Demichi K., Elekes Z., Fukuda N., Fulop Z., Futakami U., Hasegawa H., Higurashi Y., Ieki K., Imai N., Ishihara M., Ishikawa K., Iwasa N., Iwasaki H., Kanno S., Kondo Y., Kubo T., Kubono S., Kunibu M., Kurita K., Matsuyama Y., Michimasa S., Minemura T., Miura M., Murakami H., Nakamura T., Notani M., Ota S., Saito A., Sakurai H., Serata M., Shimoura S., Sugimoto T., Takeshita E., Takeuchi S., Ue K., Yamada K., Yanagisawa Y., Yoneda K., and Yoshida A.: “Study of the  $^{26}\text{Si}(p, \gamma)^{27}\text{P}$  reaction through Coulomb dissociation of  $^{27}\text{P}$ ”, *Eur. Phys. J. A* **27**, No. s01, pp. 233–236 (2006). \*
- Elekes Z., Dombradi Z., Bishop S., Fulop Z., Gibelin J., Gomi T., Hashimoto Y., Imai N., Iwasa N., Iwasaki H., Kalinka G., Kondo Y., Korshennikov A. A., Kurita K., Kurokawa M., Matsui N., Motobayashi T., Nakamura T., Nakao T., Nikolski E. Y., Ohnishi T., Okumura T., Ota S., Perera P., Saito A., Sakurai H., Satou Y., Sohler D., Sumikama T., Suzuki D., Suzuki M., Takeda H., Takeuchi S., Togano Y., and Yanagisawa Y.: “Testing of the RIKEN-ATOMKI CsI(Tl) array in the study of  $^{22,23}\text{O}$  nuclear structure”, *Eur. Phys. J. A* **27**, No. s01, pp. 321–324 (2006). \*
- Gomi T., Motobayashi T., Ando Y., Aoi N., Baba H., Demichi K., Elekes Z., Fukuda N., Fulop Z., Futakami U., Hasegawa H., Higurashi Y., Ieki K., Imai N., Ishihara M., Ishikawa K., Iwasa N., Iwasaki H., Kanno S., Kondo Y., Kubo T., Kubono S., Kunibu M., Kurita K., Matsuyama Y., Michimasa S., Minemura T., Miura M., Murakami H., Nakamura T., Notani M., Ota S., Saito A., Sakurai H., Serata M., Shimoura S., Sugimoto T., Takeshita E., Takeuchi S., Togano Y., Ue K., Yamada K., Yanagisawa Y., Yoneda K., and Yoshida A.: “Coulomb Dissociation of  $^{23}\text{Al}$  for the stellar  $^{22}\text{Mg}(p, \gamma)^{23}\text{Al}$  reaction”, *Nucl. Phys. A* **758**, 761c–764c (2006).
- Ladygin V., Uesaka T., Saito T., Hatano M., Isupov Y., Kato H., Ladygina N., Maeda Y., Malakhov A., Nishikawa J., Ohnishi T., Okumura H., Reznikov S.,

- Sakai H., Sakamoto N., Sakoda S., Saito T., Sekiguchi K., Suda K., Tamii A., Uchigashima N., and Yako K.: “Tensor Analyzing Power  $T_{20}$  of the  $dd \rightarrow {}^3\text{He}$  and  $dd \rightarrow {}^3\text{He}$  Reactions at Zero Angle for Energies 140, 200, and 270 MeV”, *Phys. At. Nucl.* **69**, 1271–1278 (2006). \*
- Schumann F., Typel S., Hammache F., Summerer K., Uhlig F., Bottcher I., Cortina D., Forster A., Gai M., Geissel H., Greife U., Gross E., Iwasa N., Koczon P., Kohlmeier B., Kulesa R., Kumagai H., Kurzu N., Menzel M., Motobayashi T., Oeshler H., Ozawa A., Ploskon M., Prokopowicz W., Schwab E., Senger P., Strieder F., Sturm C., Sun Z., Surowka G., Wagner A., and Walus W.: “Low-energy cross section of the  ${}^7\text{Be}(p,\gamma){}^8\text{B}$  solar fusion reaction from the Coulomb dissociation of  ${}^8\text{B}$ ”, *Phys. Rev. C* **73**, 015806-1–015806-13 (2006). \*
- Elekes Z., Dombradi Z., Saito A., Aoi N., Baba H., Demichi K., Fulop Z., Gibelin J., Gomi T., Hasegawa H., Imai N., Ishihara M., Iwasaki H., Kanno S., Kawai S., Kishida T., Kubo T., Kurita K., Matsuyama Y., Michimasa S., Minemura T., Motobayashi T., Notani M., Ohnishi T., Ong H., Ota S., Ozawa A., Sakai H., Sakurai H., Shimoura S., Takeshita E., Takeuchi S., Tamaki M., Togano Y., Yamada K., Yanagisawa Y., and Yoneda K.: “Proton inelastic scattering studies at the borders of the “island of inversion”: The  ${}^{30,31}\text{Na}$  and  ${}^{33,34}\text{Mg}$  case”, *Phys. Rev. C* **73**, 044314-1–044314-5 (2006). \*
- Yamaguchi M., Tagisi Y., Aoki Y., Iizuka T., Nagatomo T., Shinba t., Yoshimaru N., Yamato Y., Katabuchi T., and Tanifuji M.: “Analyzing powers of polarized deuterons in low-energy  ${}^6\text{Li}(d,\alpha){}^4\text{He}$  and  ${}^6\text{Li}(d,p_0){}^7\text{Li}$  reactions in a resonance region”, *Phys. Rev. C* **74**, No. 6, pp. 064606-1–064606-11 (2006). \*
- Elekes Z., Dombradi Z., Aoi N., Bishop S., Fulop Z., Gibelin J., Gomi T., Hashimoto Y., Imai N., Iwasa N., Iwasaki H., Kalinka G., Kondo Y., Korshennikov A. A., Kurita K., Kurokawa M., Matsui N., Motobayashi T., Nakamura T., Nakao T., Nikolski E. Y., Ohnishi T., Okumura T., Ota S., Perera P., Saito A., Sakurai H., Satou Y., Sohler D., Sumikama T., Suzuki D., Suzuki M., Takeda H., Takeuchi S., Togano Y., and Yanagisawa Y.: “Search for neutron decoupling in  ${}^{22}\text{O}$  via the  $(d, d'\gamma)$  reaction”, *Phys. Rev. C* **74**, 017306-1–017306-3 (2006). \*
- Yoneda K., Obertelli A., Gade A., Bazin D., Brown B. A., Campbell C. M., Cook J. M., Cottle P. D., Davies A. D., Dinca D. -, Glasmacher T., Hansen P. G., Hoagland T., Kemper K. W., Lecouey J. -, Mueller W. F., Reynolds R. R., Roeder B. T., Terry J. R., Tostevin J. A., and Zwahlen H.: “Two-neutron knockout from neutron-deficient  ${}^{34}\text{Ar}$ ,  ${}^{30}\text{S}$ , and  ${}^{26}\text{Si}$ ”, *Phys. Rev. C* **74**, 021303-1–021303-5 (2006). \*
- Furumoto T. and Sakuragi H.: “ Application of the Jeukenne-Lejeune-Mahaux folding model to  $\alpha$ -nucleus elastic scattering”, *Phys. Rev. C* **74**, 034606-1–034606-8 (2006). \*
- Yamaguchi T., Ohnishi T., Suzuki T., Becker T., Fukuda M., Geissel H., Hosoi M., Janik R., Kelic A., Kimura K., Mandel S., Muenzenberg G., Nakajima S., Ohtsubo T., Ozawa A., Prochazka A., Shindo M., Sitar B., Strmen P., Suda T., Summerer K., Sugawara K., Szarka I., Takechi M., Takisawa A., and Tanaka K.: “Production cross sections of isotopes formed by fragmentation of similar to 1A (GeVKr)-Kr-80 beam”, *Phys. Rev. C* **74**, 044608-1–044608-5 (2006). \*
- Takashina M. and Sakuragi H.: “ $\alpha+{}^{12}\text{C}$  inelastic angular distribution and nuclear size of  ${}^{12}\text{C}(0_2^+)$ ”, *Phys. Rev. C* **74**, 054606-1–054606-5 (2006). \*
- Dombradi Z., Elekes Z., Saito A., Aoi N., Baba H., Demichi K., Fulop Z., Gibelin J., Gomi T., Hasegawa H., Imai N., Ishihara M., Iwasaki H., Kanno S., Kawai S., Kishida T., Kubo T., Kurita K., Matsuyama Y., Michimasa S., Minemura T., Motobayashi T., Notani M., Ohnishi T., Ong H., Ota S., Ozawa A., Sakai H., Sakurai H., Shimoura S., Takeshita E., Takeuchi S., Tamaki M., Togano Y., Yamada K., Yanagisawa Y., and Yoneda K.: “Vanishing  $N = 20$  Shell Gap: Study of Excited States in  ${}^{27,28}\text{Ne}$ ”, *Phys. Rev. Lett.* **96**, 182501-1–182501-4 (2006). \*
- Nakamura T., Vinodkumar A., Sugimoto T., Aoi N., Baba H., Bazin D. P., Fukuda N., Gomi T., Hasegawa H., Imai N., Ishihara M., Kobayashi T., Kondo Y., Kubo T., Miura M., Motobayashi T., Otsu H., Saito A., Sakurai H., Shimoura S., Watanabe K., Watanabe Y., Yakushiji T., Yanagisawa Y., and Yoneda K.: “Observation of Strong Low-Lying E1 Strength in the Two-Neutron Halo Nucleus  ${}^{11}\text{Li}$ ”, *Phys. Rev. Lett.* **96**, 252502-1–252502-4 (2006). \*
- Sakai H., Saito T., Ikeda T., Itoh K., Kawabata T., Kuboki H., Maeda Y., Matsui N., Rangacharyulu C., Sasano M., Sato Y., Sekiguchi K., Suda K., Tamii A., Uesaka T., and Yako K.: “Spin correlations of strongly interacting massive fermion pairs as a test of Bell’s inequality”, *Phys. Rev. Lett.* **97**, No. 15, pp. 150405-1–150405-4 (2006). \*
- Motobayashi T.: “Nuclear structure studies far from stability using intermediate-energy RI beams”, *Phys. Scr.* **T125**, 41–44 (2006). \*
- Sekiguchi K.: “Three Nucleon Force Study via  $\vec{d}p$  Breakup Reactions at Intermediate Energies”, *AIP Conf. Proc.* **915**, 759–764 (2007). \*
- Sakaguchi S., Uesaka T., Wakui T., Kawabata T., Aoi N., Hashimoto Y., Ichikawa M., Ichikawa Y., Itoh Y., Itoh M., Iwasaki H., Kawahara T., Kuboki H., Maeda Y., Matsuo R., Nakao T., Okamura H., Sakai H., Sakamoto N., Sasamoto Y., Sasano M., Satou Y., Sekiguchi K., Shinohara M., Suda K., Suzuki D., Takahashi Y., Tamii A., Yako K., and Yamaguchi M.: “Analyzing Power

- Measurement for Elastic Scattering of  $^6\text{He}$  on polarized protons”, AIP Conf. Proc. **915**, 833–836 (2007). \*
- Sekiguchi K.: “ $Nd$  Scattering at Intermediate Energies: An Epoch-making Experimental Study of the Three Nucleon Force”, AIP Conf. Proc. **1011**, 23–32 (2007). \*
- Mardanpour H., Amir-Ahmadi H., Deltuva A., Itoh K., Kalantar N. N., Kawabata T., Kuboki H., Maeda Y., Messchendorp J. G., Sakaguchi S., Sakai H., Sakamoto N., Sasamoto Y., Sasano M., Sekiguchi K., Suda K., Takahashi Y., Uesaka T., Witala H., and Yako K.: “Precision Measurement of Vector and Tensor Analyzing Powers in Elastic Deuteron-Proton Scattering”, Eur. Phys. J. A **31**, 383–391 (2007). \*
- Elekes Z., Dombradi Z., Saito A., Aoi N., Baba H., Demichi K., Fulop Z., Gibelin J. D., Gomi T., Hasegawa H., Imai N., Ishihara M., Iwasaki H., Kanno S., Kawai S., Kishida T., Kubo T., Kurita K., Matsuyama Y., Michimasa S., Minemura T., Motobayashi T., Notani M., Ohnishi T., Ong H., Ota S., Ozawa A., Sakai H., Sakurai H., Shimoura S., Takeshita E., Takeuchi S., Tamaki M., Togano Y., Yamada K., Yanagisawa Y., and Yoneda K.: “Study of  $N=20$  shell gap with  $^1\text{H}(^{28}\text{Ne}, ^{27,28}\text{Ne})$  reactions”, Eur. Phys. J. Special Topics **150**, 99–102 (2007). \*
- Shimada K., Nagae D., Asahi K., Inoue T., Takase K., Kagami S., Hatakeyama N., Kobayashi Y., Ueno H., Yoshimi A., Kameda D., Nagatomo T., Sugimoto T., Kubono S., Yamaguchi H., Wakabayashi Y., Hayakawa S., Murata J., and Kawamura H.: “Production of spin-polarized  $^{17}\text{N}$  beam sing inverse-kinematics low-energy transfer reactions”, Hyperfine Interact. **180**, 43–47 (2007). \*
- Sakuragi H., Maenaka Y., and Furumoto T.: “Coupled-channels study of  $^{10}\text{Be}+^4\text{He}$  structure of highly-excited  $^{14}\text{C}$ ”, J. Phys.: Con. Ser. **111**, 012019-1–012019-6 (2007). \*
- Yamaguchi T., Suzuki T., Ohnishi T., Nummerer S., Becker F., Fukuda M., Geissel H., Hosoi M., Janike R., Kimura K., Mandal S., Munzenberg G., Nakajima S., Ohtsubo T., Ozawa A., Orochazka A., Shindo M., Strmen P., Suda T., Sugawara K., Szarka I., Takisawa A., Takechi M., and Tanaka K.: “Nuclear radii of neutron-deficient Kr isotopes studied via their interaction cross-sections at relativistic energies”, Nucl. Phys. A **787**, 471c–475c (2007). \*
- Baba H., Shimoura S., Minemura T., Matsuyama Y., Saito A., Ryuto H., Aoi N., Gomi T., Higurashi Y., Ieki K., Imai N., Iwasa N., Iwasaki H., Kanno S., Kubono S., Kunibu M., Michimasa S., Motobayashi T., Nakamura T., Sakurai H., Serata M., Takeshita E., Takeuchi S., Teranishi T., Ue K., Yamada K., and Yanagisawa Y.: “Isoscalar compressional strengths in  $^{14}\text{O}$ ”, Nucl. Phys. A **788**, 188c–193c (2007). \*
- Mardanpour H., Amir-Ahmadi H., Benard R., Biegun A., Eslami-Kalantari M., Kalantar N. N., Kis M., Kistryn S., Kozela A., Kuboki H., Maeda Y., Mahjour-Shafiei M., Messchendorp J. G., Miki K., Noji S., Ramazani A., Sakai H., Sasano M., Sekiguchi K., Stephen E., Sworst R., Takahashi Y., and Yako K.: “Study of Three-Nucleon Force Effects in  $\bar{p} + d$  Break-up with BINA”, Nucl. Phys. A **790**, 426c–429c (2007). \*
- Miki K., Sakai H., Itoh K., Kawabata K., Kuboki H., Maeda Y., Noji S., Sakaguchi S., Sakamoto N., Sasamoto Y., Sasano M., Satou Y., Sekiguchi K., Suda K., Takahashi Y., Uesaka T., and Yako K.: “Measurement of the  $^2\text{H}(d, pn)$  Reaction at 0 degrees at 270 MeV”, Nucl. Phys. A **790**, 442c–445c (2007). \*
- Wakasa T., Ihara E., Fujita ., Funaki Y., Hatanaka K., Horiuchi H., Itoh M., Kamiya ., Roepke G., Sakaguchi H., Sakamoto ., Sakemi ., Schuck P., Shimizu Y., Takashina M., Terashima S., Suzuki A., Uchida M., Yoshida ., and Yosoi .: “New candidate for an alpha cluster condensed state in  $^{16}\text{O}$  ( $\alpha, \alpha'$ ) at 400 MeV”, Phys. Lett. B **653**, 173–177 (2007). \*
- Nakatsukasa T., Inakura T., and Yabana K.: “Finite amplitude method for the solution of the random-phase approximation”, Phys. Rev. C **76**, 024318-1–024318-9 (2007). \*
- Fang D., Guo W., Ma. C., Wang K., Yang T., Ma. Y., Cai X., Shen W., Ren Z., Sun Z., Chen J., Tian W., Zhong C., Hosoi M., Izumikawa T., Kanungo R., Nakajima S., Ohnishi T., Ohtsubo T., Ozawa A., Suda T., Sugawara K., Suzuki T., Takisawa A., Tanaka K., Yamaguchi T., and Tanihata I.: “Examining the exotic structure of the proton-rich nucleus  $^{23}\text{Al}$ ”, Phys. Rev. C **76**, 031601-1–031601-5 (2007). \*
- Ladygin V., Uesaka T., Saito T., Janek M., Kiselev A., Kurilkin A., Vasiliev A., Hatano M., Isupov Y., Kato H., Ladygina N., Maeda Y., Malakhov A., Nishikawa J., Ohnishi T., Okamura H., Reznikov S., Sakai H., Sakoda S., Sakamoto N., Satou Y., Sekiguchi K., Suda K., Tamii A., Uchigashima N., and Yako K.: “Analyzing powers in the  $dd \rightarrow ^3\text{He}(^3\text{He})$  reactions at intermediate energies”, AIP Conf. Proc. **1011**, 235–240 (2008). \*
- Kobayashi T., Kato T., Matsuo Y., Nishimura M., Hayashizaki Y., and Kawai J.: “Temporal pulsewidth and the wavelength dependences of the product ions obtained by laser ablation of solid C60”, Appl. Phys. A **92**, 777–780 (2008). \*
- Kato T., Nishimura M., Kobayashi T., Oho Y., Sano T., Hayashizaki Y., Matsuo Y., and Kawai J.: “Ion extraction from the surface ablated materials in electric fields using an intense femtosecond laser pulse”, Appl. Phys. A **92**, 809–812 (2008). \*
- Kobayashi T., Kato T., Matsuo Y., Nishimura M., Hayashizaki Y., and Kawai J.: “Observation of the matrix effect due to the electron transfer in laser ablation plasma”, Appl. Phys. A **92**, 817–819 (2008). \*
- Matsuo Y., Nishimura M., Kobayashi T., Kato T., Oho Y., Sano T., Kawai J., and Hayashizaki Y.: “Substrate De-

- pendence of Ion Motion in Femtosecond Laser Ablation Cloud Observed by Planar Laser-Induced Fluorescence”, *Appl. Phys. A* **92**, 993–997 (2008). \*
- Nishimura M., Matsuo Y., Kobayashi T., Kato T., Hayashizaki Y., and Kawai J.: “Comparison of Plume Expansion in Femtosecond Laser Ablation on Oxidized and non-Oxidized Sm Surface”, *Appl. Phys. A* **92**, 1047–1050 (2008). \*
- Kurilkin A., Saito T., Ladygin V., Uesaka T., Vasiliev T., Janek M., Hatano M., Isupov Y., Kato K., Ladygina N., Maeda Y., Malakhov A., Nishikawa J., Ohnishi T., Okamura H., Reznikov S., Sakai H., Sakamoto N., Sakoda S., Satou Y., Sekiguchi K., Suda K., Tamii A., Uchigashima N., and Yako K.: “Measurement of the vector  $A_y$  and tensor  $A_{yy}$ ,  $A_{xx}$ ,  $A_{xz}$  analyzing powers for the  $dd \rightarrow {}^3\text{H}p$  reaction at 200 MeV”, *Eur. Phys. J. Special Topics* **162**, 133–136 (2008). \*
- Kiselev A., Ladygin V., Uesaka T., Vasiliev A., Janek M., Saito T., Hatano M., Isupov Y., Kato H., Ladygina N., Maeda Y., Malakhov A., Nishikawa J., Ohnishi T., Okamura H., Reznikov S., Sakai H., Sakamoto N., Sakoda S., Satou Y., Sekiguchi K., Suda K., Tamii A., Uchigashima N., and Yako K.: “Analyzing powers in the  ${}^{12}\text{C}(\vec{d}, p){}^{13}\text{C}$  reaction at the energy  $T_d = 270$  MeV”, *Eur. Phys. J. Special Topics* **162**, 143–146 (2008). \*
- Elekes Z., Dombradi Z., Aoi N., Baba H., Bishop S., Demichi K., Fulop Z., Gibelin J., Gomi T., Hasegawa H., Hashimoto Y., Imai N., Ishihara M., Iwasa N., Iwasaki H., Kalinka G., Kanno S., Kawai S., Kishida T., Kondo Y., Korshennikov A. A., Kubo T., Kurita K., Kurokawa M., Matsui N., Matsuyama Y., Michimasa S., Minemura T., Motobayashi T., Nakamura T., Nakao T., Nikolski E. Y., Notani M., Ohnishi T., Okumura T., Ong H., Ota S., Ozawa A., Perera P., Saito A., Sakai H., Sakurai H., Satou Y., Shimoura S., Sohler D., Sumikama T., Suzuki D., Suzuki M., Takeda H., Takeshita E., Takeuchi S., Tamaki M., Togano Y., Yamada K., Yanagisawa Y., and Yoneda K.: “The study of shell closures in light neutron-rich nuclei”, *J. Phys. G* **35**, 014038-1–014038-7 (2008).
- Kato T., Kobayashi T., Nishimura M., Oho Y., Sano T., Oyama R., Matsumura Y., Yamamoto H., Hayashizaki Y., Matsuo Y., and Kawai J.: “Time-of-flight detection of monoatomic ions generated by femtosecond laser ablation from large molecules”, *Nucl. Instrum. Methods Phys. Res. B* **266**, 992–997 (2008). \*
- Yamaguchi Y., Ozawa A., Goto A., Arai I., Fujinawa T., Fukunishi N., Kikuchi T., Ohnishi T., Ohtsubo T., Sakurai H., Suzuki T., Wakasugi M., Yamaguchi T., Yasuda Y., and Yano Y.: “Rara-RI ring project at RIKEN RI beam factory”, *Nucl. Instrum. Methods Phys. Res. B* **266**, 4575–4578 (2008). \*
- Nakajima S., Kuboki T., Yoshitake M., Hashizume Y., Kanazawa M., Kitagawa a., Kobayashi K., Moriguchi T., Ohtsubo T., Ozawa A., Sato S., Suzuki T., Yamaguchi Y., Yasuda Y., and Yamaguchi T.: “Development of a time-of-flight detector for the rare-RI ring project at RIKEN”, *Nucl. Instrum. Methods Phys. Res. B* **266**, 4621–4624 (2008). \*
- Sekiguchi K.: “Exploring Three Nucleon Forces with Nucleon-Deuteron Scattering”, *Nucl. Phys. A* **805**, 250c–259c (2008). \*
- Aoi N., Suzuki H., Takeshita E., Takeuchi S., Ota S., Baba H., Bishop S., Fukui T., Hashimoto Y., Ong H., Ideguchi E., Ieki K., Imai N., Iwasaki H., Kanno S., Kondo Y., Kubo T., Kurita K., Kusaka K., Minemura T., Motobayashi T., Nakabayashi T., Nakamura T., Nakao T., Niikura M., Okumura T., Ohnishi T., Sakurai H., Shimoura S., Sugo R., Suzuki D., Suzuki M., Tamaki M., Tanaka K., Togano Y., and Yamada K.: “Shape transition observed in neutron-rich pf-shell isotopes studied via proton inelastic scattering”, *Nucl. Phys. A* **805**, 400c–407c (2008).
- Sekiguchi K.: “Three Nucleon Force Study via  $\vec{d}p$  Breakup Reactions at Intermediate Energies”, *Nucl. Phys. A* **805**, 452–454 (2008). \*
- Sakaguchi S., Uesaka T., Wakui T., Kawabata T., Aoi N., Hashimoto Y., Ichikawa M., Itoh Y., Itoh M., Iwasaki H., Kawahara T., Kuboki H., Maeda Y., Matsuo R., Nakao T., Okamura H., Sakai H., Sakamoto N., Sasamoto Y., Sasano M., Satou Y., Sekiguchi K., Shinohara M., Suda K., Suzuki D., Takahashi Y., Tamii A., Yako K., and Yamaguchi M.: “Spin-orbit potential in  ${}^6\text{He}$  studied with polarized proton target”, *Nucl. Phys. A* **805**, 467–469 (2008). \*
- Suzuki D., Iwasaki H., Ong H., Imai N., Sakurai H., Nakao T., Aoi N., Baba H., Bishop S., Ichikawa Y., Ishihara M., Kondo Y., Kubo T., Kurita K., Motobayashi T., Nakamura T., Okumura T., Onishi T., Ota S., Suzuki M., Takeuchi S., Togano Y., and Yanagisawa Y.: “Lifetime measurements of excited states in  ${}^{17}\text{C}$ : Possible interplay between collectivity and halo effects”, *Phys. Lett. B* **666**, 222–227 (2008). \*
- Yamada T., Funaki Y., Horiuchi H., Roepke G., Schuck P., and Suzuki A.: “Criterion for Bose-Einstein condensation in traps and self-bound systems”, *Phys. Rev. A* **78**, 035603-1–035603-4 (2008). \*
- Dang N. D. and Nguyen H. Q.: “Pairing within the self-consistent quasiparticle random-phase approximation at finite temperature”, *Phys. Rev. C* **77**, No. 6, pp. 064315-1–064315-14 (2008). \*
- Zegers R. G., Brown E. F., Akimune H., Austin S. M., van den Berg A. M., Brown B. A., Chamulak D. A., Fujita Y., Fujiwara M., Gales S., Harakeh M. N., Hashimoto H., Hayami R., Hitt G. W., Itoh M., Kawabata T., Kawase K., Kinoshita M., Nakanishi K., Nakayama S., Okumura S., Shimbara Y., Uchida M., Ueno H., Yamagata T., and Yosoi M.: “Gamow-Teller strength for the analog transitions to the first  $T = 1/2$ ,  $J^\pi = 3/2^-$  states in  ${}^{13}\text{C}$  and  ${}^{13}\text{N}$  and the implications

- for type Ia supernovae”, *Phys. Rev. C* **77**, 024307-1–024307-10 (2008). \*
- Yamaguchi T., Suzuki T., Ohnishi T., Becker F., Fukuda M., Geissel H., Hosoi M., Janik R., Kimura K., Kuboki T., Mandel S., Matsuo M., Muenzenberg G., Nakajima S., Ohtsubo T., Ozawa A., Prochazka A., Shindo M., Sitar B., Strmen P., Suda T., Suemmerer K., Sugawara K., Szarka I., Takeuchi M., Takisawa A., Tanaka K., and Yamagami M.: “Nuclear matter radii of neutron-deficient Kr isotopes”, *Phys. Rev. C* **77**, 034315-1–034315-6 (2008). \*
- Funaki Y., Horiuchi H., Roepke G., Schuck P., Suzuki A., and Yamada T.: “Density-induced suppression of the  $\alpha$ -particle condensate in nuclear matter and the structure of  $\alpha$  cluster states in nuclei”, *Phys. Rev. C* **77**, 064312-1–064312-6 (2008). \*
- Furumoto T., Sakuragi H., and Yamamoto Y.: “New complex G-matrix interactions derived from two- and three-body forces and application to proton nucleus elastic scattering”, *Phys. Rev. C* **78**, No. 4, pp. 044610-1–044610-12 (2008). \*
- Nguyen H. Q. and Dang N. D.: “Pairing in hot rotating nuclei”, *Phys. Rev. C* **78**, No. 6, pp. 064315-1–064315-13 (2008). \*
- Ong H., Imai N., Suzuki D., Iwasaki H., Sakurai H., Onishi T., Suzuki M., Ota S., Takeuchi S., Nakao T., Togano Y., Kondo Y., Aoi N., Baba H., Bishop S., Ichikawa Y., Ishihara M., Kubo T., Kurita K., Motobayashi T., Nakamura T., Okumura T., and Yanagisawa Y.: “Lifetime measurements of first excited states in  $^{16,18}\text{C}$ ”, *Phys. Rev. C* **78**, 014308-1–014308-11 (2008). \*
- Wakasugi M., Emoto T., Furukawa Y., Ishii K., Ito S., Koseki T., Kurita K., Kuwajima A., Masuda T., Morikawa A., Nakamura M., Noda A., Ohnishi T., Shirai T., Suda T., Takeda H., Tamae T., Tongu H., Wang S., and Yano Y.: “Novel Internal Target for Electron Scattering off Unstable Nuclei”, *Phys. Rev. Lett.* **100**, 164801-1–164801-4 (2008). \*
- Funaki Y., Yamada T., Horiuchi H., Roepke G., Schuck P., and Suzuki A.: “ $\alpha$ -particle condensation in  $^{16}\text{O}$  studied with a full four-body orthogonality condition model calculation”, *Phys. Rev. Lett.* **101**, 082502-1–082502-4 (2008). \*
- Nakatsukasa T., Matsuo M., Matuyanagi K., and Hinojara N.: “Microscopic derivation of collective Hamiltonian by means of the adiabatic self-consistent collective coordinate method”, *Prog. Theor. Phys.* **119**, No. 1, pp. 59–101 (2008). \*
- Yamada T., Funaki Y., Horiuchi H., Ikeda K., and Suzuki A.: “Monopole Excitation to Cluster States”, *Prog. Theor. Phys.* **120**, 1139–1167 (2008). \*
- Elekes Z., Dombradi Z., Aiba T., Aoi N., Baba H., Bemmerer D., Brown B., Furumoto T., Fulop Z., Iwasa N., Kiss A. B., Kobayashi T., Kondo Y., Motobayashi T., Nakabayashi T., Nannichi T., Sakuragi H., Sakurai H., Sohler D., Takashina M., Takeuchi S., Tanaka K., Togano Y., Yamada K., Yamaguchi M., and Yoneda K.: “Persistent decoupling of valence neutrons toward the dripline: study of  $^{20}\text{C}$  by  $\gamma$  spectroscopy”, *Phys. Rev. C* **79**, 011302-1–011302-5 (2009). \*
- Furumoto T., Sakuragi H., and Yamamoto Y.: “Three-body-force effect on nucleus-nucleus elastic scattering”, *Phys. Rev. C* **79**, 011601-1–011601-4 (2009). \*
- Aoi N., Takeshita E., Suzuki H., Takeuchi S., Ota S., Baba H., Bishop S., Fukui T., Hashimoto Y., Ong H., Ideguchi E., Ieki K., Imai N., Ishihara M., Iwasaki H., Kanno S., Kondo Y., Kubo T., Kurita K., Kusaka K., Minemura T., Motobayashi T., Nakabayashi T., Nakamura T., Nakao T., Niikura M., Okumura T., Ohnishi T., Sakurai H., Shimoura S., Sugo R., Suzuki D., Suzuki M., Tamaki M., Tanaka K., Togano Y., and Yamada K.: “Development of Large Deformation in  $^{62}\text{Cr}$ ”, *Phys. Rev. Lett.* **102**, 012502-1–012502-4 (2009). \*
- (Review)
- Motobayashi T.: “Recent spectroscopic studies on light neutron-rich nuclei with fast exotic beams”, *AIP Conf. Proc.* **802**, 89–94 (2005).
- Funaki Y., Horiuchi H., Roepke G., Schuck P., Suzuki A., and Yamada T.: “Alpha particle condensation in nuclear systems”, *Nucl. Phys. News* **17**, No. 4, pp. 11–18 (2007).
- (Others)
- Nakajima S., Yamaguchi T., Suzuki T., Yamaguchi Y., Fujinawa T., Fukunishi N., Goto A., Ohnishi T., Sakurai H., Wakasugi M., Yano Y., Arai I., Ozawa A., Yasuda Y., Kikuchi T., and Ohtsubo T.: “New scheme for precision mass measurements of rare isotopes produced at RI beam factory”, *Acta Phys. Pol. B* **39**, No. 2, pp. 457–462 (2008).
- Yamada T., Funaki Y., Horiuchi H., Tohsaki A., Roepke G., and Schuck P.: “Dilute Alpha-Particle Condensation in  $^{12}\text{C}$  and  $^{16}\text{O}$ ”, *Int. J. Mod. Phys. B* **22**, No. 25/26, pp. 4545–4556 (2008).
- Yamada T., Horiuchi H., Ikeda K., Funaki Y., and Suzuki A.: “Monopole excitation to cluster states”, *J. Phys.: Con. Ser.* **111**, 012008-1–012014-6 (2008).
- Funaki Y., Yamada T., Horiuchi H., Roepke G., Schuck P., and Suzuki A.: “Alpha-cluster states and 4 alpha-particle Bose condensate in  $^{16}\text{O}$ ”, *J. Phys.: Con. Ser.* **111**, 012012-1–012018-6 (2008).
- Murata J., Akiyama T., Hata M., Hirayama Y., Ikeda Y., Ishii T., Kameda D., Kawamura H., Mitsuoka S., Miyatake H., Nagae D., Ninomiya K., Nitta M., Seitabashi E., and Toyoda T.: “R&D for a test of time reversal symmetry experiment using polarized nuclei”, *JAEA-Review* **2008-054**, 58–59 (2008).
- Funaki Y., Yamada T., Horiuchi H., Roepke G., Schuck P., and Suzuki A.: “Indication of  $4\alpha$ -particle Bose condensate in  $^{16}\text{O}$ ”, *Nucl. Phys. A* **805**, 236–238 (2008).
- [Book•Proceedings]

(Original Papers) \*Subject to Peer Review

Sekiguchi K.: “Results of Three Nucleon Experiments from RIKEN”, Proc. 5th International Workshop on Chiral Dynamics, Theory and Experiment (CHIRAL DYNAMICS 2006), Durham/Chatel Hill, USA, 2006–9, World Scientific, New Jersey, pp. 357–358 (2006). \*

Baba H., Ichihara T., Ohnishi T., Takeuchi S., Yoshida K., Watanabe Y., Ota S., and Shimoura S.: “The New DAQ System in RIKEN RIBF”, 2008 IEEE Nuclear Science Symposium Conference Record, Dresden, Germany, 2008–10, IEEE, Dresden, pp. 1384–1386 (2008). \*

Nguyen H. Q. and Dang N. D.: “Self-consistent quasi-particle RPA for multilevel pairing model”, Proceedings of the 9th International Spring Seminar on Nuclear Physics, Vico Equense, Italy, 2007–5, World Scientific, Singapore, pp. 503–510 (2008). \*

(Review)

Motobayashi T.: “Future nuclear physics in Japan”, Proceedings of the Memorial Symposium in Honor of D. Allan Bromley, World Scientific, Singapore, pp. 183–191 (2006).

Motobayashi T.: “RIKEN RI Beam Factory”, Proceedings of the Fourth International Conference on Fission and Properties of Neutron-Rich Nuclei, Sanibel Island, USA, 2007–11, World Scientific Publishing Co., Pte. Ltd, Singapore, pp. 145–154 (2008).

(Others)

Yamaguchi T., Arai I., Fukunishi N., Goto A., Kikuchi T., Komatsubara T., Ohnishi T., Ohtsubo T., Okuno H., Ozawa A., Sasa K., Suzuki T., Tagisi Y., Takeda H., Wakasugi M., Yamaguchi M., Yamaguchi Y., and Yano Y.: “Mass measurements by an isochronous storage ring at the RIKEN RI beam factory”, Proceedings of the 6th International Conference on Nuclear Physics at Storage Rings (STORI '05), Bonn, Germany, 2005–5, Forschungszentrum Julich, Julich, pp. 297–300 (2005).

Yamaguchi M., Arai I., Fukunishi N., Goto A., Kusaka K., Kikuchi T., Komatsubara T., Kubo T., Ohnishi T., Ohtsubo T., Okuno H., Ozawa A., Sasa K., Suzuki T., Tagisi Y., Takeda H., Wakasugi M., Yamaguchi T., Yamaguchi Y., and Yano Y.: “Design of an isochronous storage ring and an injection line for mass measurements at the RIKEN RI beam factory”, Proceedings of the 6th International Conference on Nuclear Physics at Storage Rings (STORI '05), Bonn, Germany, 2005–5, Forschungszentrum Julich, Julich, pp. 315–319 (2005).

Motobayashi T.: “Recent experimental studies of nuclear astrophysics”, Exotic Nuclei and Nuclear/Particle Astrophysics : Proceedings of the Carpathian Summer School of Physics 2005, Constanta, Romania, 2005–6, World Scientific, Singapore, pp. 297–306 (2006).

Kikuchi T., Horioka K., Ozawa A., Kawata S., Yamaguchi Y., Fukunishi N., Sakurai H., Wakasugi M., Yamaguchi M., Yamaguchi T., Arai I., Ohta H., Fujinawa T., Sasa K., Komatsubara T., Suzuki T., Ohtsubo T., Goto

A., Ohnishi T., Okuno H., Takeda H., and Yano Y.: “Individual correction using induction modulator for mass measurements by isochronous ring in RIKEN RI beam factory”, Proceedings of the 2nd International Workshop on Recent Progress in Induction Accelerators (RPIA2006), Tsukuba, 2006–3, KEK, Tsukuba, pp. 127–131 (2006).

Funaki Y., Yamada T., Schuck P., Horiuchi H., Suzuki A., and Roepke G.: “ $\alpha$ -cluster states and  $4\alpha$ -particle condensation in  $^{16}\text{O}$ ”, Physics of Unstable Nuclei: Proceedings of International Symposium on Physics of Unstable Nuclei (ISPUN07), Hoi An, Vietnam, 2007–7, World Scientific, Singapore, pp. 380–385 (2008).

**Oral Presentations**

(International Conference etc.)

Sugimoto S., Nakamura T., Fukuda N., Miura M., Kondo Y., Aoi N., Baba H., Bazin D. P., Gomi T., Hasegawa H., Hashimoto Y., Imai N., Kobayashi T., Kubo T., Motobayashi T., Shinohara M., Saito A., Sakurai H., Shimoura S., A.M. V., Watanabe K., Watanabe Y., T. Y., Yanagisawa Y., Yoneda K., and Ishihara M.: “Breakup Reactions of Halo Nuclei”, 1st Tokyo Tech Physics COE Symposium on Spin and Quantum Structure in Hadrons, Nuclei and Atoms (SQS04), Tokyo, Feb. (2004).

Korshennikov A. A.: “Recent Experimental Studies of Exotic Nuclei”, Workshop on Spectroscopic Factors, (European Centre for Theoretical Studies in Nuclear Physics and Related Areas), Trento, Italy, Mar. (2004).

Korshennikov A. A.: “Trends in Experimental Studies of Exotic Nuclei”, International Nuclear Physics Conference (INPC2004), (Chalmers University of Technology and Goteborgs University), Goteborg, Sweden, June–July (2004).

Kobayashi M., Nakatsukasa T., Matsuo M., and Matuyanagi K.: “Collective path connecting the oblate and prolate local minima in proton-rich  $N=Z$  nuclei around  $^{68}\text{Se}$ ”, 4th International Conference on Exotic Nuclei and Atomic Masses (ENAM 04), Georgia, USA, Sept. (2004).

Yamaguchi M., Arai I., Fukunishi N., Goto A., Kusaka K., Kikuchi T., Komatsubara T., Kubo T., Ohnishi T., Ohtsubo T., Okuno H., Ozawa A., Sasa K., Suzuki T., Tagisi Y., Takeda H., Wakasugi M., Yamaguchi T., Yamaguchi Y., and Yano Y.: “Design of an isochronous storage ring and an injection line from mass measurements at the RIKEN RI beam factory”, 6th International Conference on Nuclear Physics at Storage Rings (STORI-05), (Research Center Julich), Bonn, Germany, May (2005).

Yamaguchi T., Ozawa A., Arai I., Komatsubara T., Sasa K., Tagisi Y., Yamaguchi M., Suzuki T., Ohtsubo T., Fukunishi N., Goto A., Ohnishi T., Okuno H., Takeda H., Wakasugi M., Yano Y., Yamaguchi Y., and Kikuchi

- T.: “Mass measurements in RIKEN”, 6th International Conference on Nuclear Physics at Storage Rings (STORI-05), (Research Center Julich), Bonn, Germany, May (2005).
- Motobayashi T.: “Perspective of ”DREB” studies in RI Beam Factory”, Direct Reactions with Exotic Beams (DREB2005), (Michigan State University), East Lansing, USA, June (2005).
- Motobayashi T.: “Recent developments and future perspective of nuclear structure and nuclear astrophysics studies with fast exotic beams at RIKEN”, NSCL User Workshop 2005, (National Superconducting Cyclotron Laboratory, Michigan State University), Michigan, USA, Aug. (2005).
- Sugimoto S., Nakamura T., Fukuda N., Miura M., Kondo Y., Aoi N., Baba H., Bazin D. P., Gomi T., Hasegawa H., Hashimoto Y., Imai N., Kobayashi T., Kubo T., Motobayashi T., Shinohara M., Saito A., Sakurai H., Shimoura S., A.M. V., Watanabe K., Watanabe Y., T. Y., Yanagisawa Y., Yoneda K., and Ishihara M.: “Invariant-Mass Spectroscopy of  $^{14}\text{Be}$  with a Carbon Target at 68.1 AMeV”, 2nd Joint Meeting of the Nuclear Physics Divisions of the APS and JPS (Hawaii 2005), Maui, USA, Sept. (2005).
- Yoneda K., Hansen P. G., Bazin D., Brown B. A., Campbell C. M., Cook J. M., Dinca D. -, Gade A., Glasmacher T., Hoagland T. E., Lecouey J. -, Mueller W. F., Olliver H., Sherrill B. M., Terry J. R., Cottle P. D., Kemper K. W., Reynolds R. R., Roeder B. T., and Tostevin J. A.: “Two-neutron knockout reaction to final levels in the  $T_z = -2$  nuclei  $^{24}\text{Si}$ ,  $^{28}\text{S}$ , and  $^{32}\text{Ar}$ ”, 2nd Joint Meeting of the Nuclear Physics Divisions of the APS and JPS (Hawaii 2005), Hawaii, USA, Sept. (2005).
- Motobayashi T.: “Nuclear astrophysics studies using intermediate-energy exotic beams”, 3rd European Summer School on Experimental Nuclear Astrophysics, (LNS, Catania), Santa Tecla, Sicily, Italy, Oct. (2005).
- Yamaguchi M., Tagisi Y., Iizuka T., Aoki Y., Nagatomo T., Shinba T., Yoshimaru N., Yamato Y., Katabuchi T., and Tanifuji M.: “Extraction of fractions of the resonant component from analyzing powers in  $^6\text{Li}(d,\alpha)^4\text{He}$  and  $^6\text{Li}(d,p_0)^7\text{Li}$  reactions at very low incident energies”, International Symposium on Origin of Matter and Evolution of Galaxies (OMEG05): New Horizon of Nuclear Astrophysics and Cosmology, Tokyo, Nov. (2005).
- Sekiguchi K.: “Three Nucleon Force by  $\vec{d} + p$ ”, International Symposium on the 15 Years of Spectrometer SMART and New Turn to RIBF, Wako, Nov. (2005).
- Motobayashi T.: “RI Beam Factory: the upgraded RIKEN facility for exotic beams”, International Chemical Congress of Pacific Basin Societies (PACIFICHEM 2005), (American Chemical Society, Chemical Society of Japan and others), Honolulu, USA, Dec. (2005).
- Kikuchi T., Horioka K., Ozawa A., Kawata S., Yamaguchi Y., Fukunishi N., Sakurai H., Wakasugi M., Yamaguchi M., Yamaguchi T., Arai I., Ohta H., Fujinawa T., Sasa K., Komatsubara T., Suzuki T., Ohtsubo T., Goto A., Ohnishi T., Okuno H., Takeda H., and Yano Y.: “Individual correction using induction modulator for mass measurements by isochronous ring in RIKEN RI beam factory”, 2nd International Workshop on Recent Progress in Induction Accelerators (RPIA2006), (KEK , Tokyo Institute of Technology), Tsukuba, Mar. (2006).
- Takashina M.: “Inelastic scattering of light unstable nuclei”, International Workshop on “Nuclear Physics with RIBF”, Wako, Mar. (2006).
- Sakuragi H., Furumoto T., and Murakami E.: “Microscopic optical potential for nucleons and composite projectiles based on complex G-matrix interactions”, International Workshop on “Nuclear Physics with RIBF”, Wako, Mar. (2006).
- Kohama A., Iida K., and Oyamatsu K.: “Reaction cross section and nuclear radius in the black-sphere picture”, International Workshop on “Nuclear Physics with RIBF”, Wako, Mar. (2006).
- Baba H., Shimoura S., Minemura T., Matsuyama Y., Saito A., Ryuto H., Aoi N., Gomi T., Higurashi Y., Ieki K., Imai N., Iwasa N., Iwasaki H., Kanno S., Kubono S., Kunibu M., Michimasa S., Motobayashi T., Nakamura T., Sakurai H., Serata M., Takeshita E., Takeuchi S., Teranishi T., Ue K., Yamada K., and Yanagisawa Y.: “Isoscalar excitation in  $^{14}\text{O}$ ”, 5th International Workshop on Direct Reaction with Exotic Beams (DREB2007), (DREB2007 Committee), Wako, May–June (2006).
- Baba H., Shimoura S., Minemura T., Matsuyama Y., Saito A., Ryuto H., Aoi N., Gomi T., Higurashi Y., Ieki K., Imai N., Iwasa N., Iwasaki H., Kanno S., Kubono S., Kunibu M., Michimasa S., Motobayashi T., Nakamura T., Sakurai H., Serata M., Takeshita E., Takeuchi S., Teranishi T., Ue K., Yamada K., and Yanagisawa Y.: “Measurement of isoscalar monopole and dipole strengths in  $^{14}\text{O}$ ”, International Nuclear Physics Conference (INPC2007), Tokyo, June (2006).
- Miki K., Yako K., Itoh K., Kawabata T., Kuboki H., Maeda Y., Noji S., Sakaguchi S., Sakai H., Sakamoto N., Sasamoto Y., Sasano M., Sato Y., Sekiguchi K., Suda K., Takahashi Y., and Uesaka T.: “Measurement of the  $^2\text{H}(d, pn)$  reaction at 0 degrees at 270 MeV”, 18th International IUPAP Conference on Few-Body Problems in Physics, Santos, Brazil, Aug. (2006).
- Sekiguchi K., Sakai H., Sakamoto N., Kuboki H., Sasano M., Takahashi Y., Yako K., Kawabata T., Maeda Y., Sakaguchi S., Sasamoto Y., Suda K., Uesaka T., Okamura H., Itoh K., and Wakasa T.: “Study of Spin Parts of Three Nucleon Forces via  $\vec{d}p$  Breakup Reactions at Intermediate Energies”, 18th International IUPAP Conference on Few-Body Problems in Physics, (Istituto de Fisica Teorica), Santos, Brazil, Aug. (2006).

- Sekiguchi K.: “Three Nucleon Force Study via  $\bar{d}p$  Breakup Reactions at Intermediate Energies”, 17th International Spin Physics Symposium (SPIN2006), Kyoto, Oct. (2006).
- Arai I., Komatsubara T., Ozawa A., Sasa K., Yasuda Y., Fujinawa T., Fukunishi N., Goto A., Ohnishi T., Okuno H., Takeda H., Wakasugi M., Yamaguchi M., Yamaguchi Y., Yano Y., Kikuchi T., Suzuki T., Yamaguchi T., and Ohtsubo T.: “Isochronous ring at RIKEN”, Workshop on Advanced Laser and Mass Spectroscopy ALMAS-1: Innovative Physics Ideas, (Gesellschaft fur Schwerionenforschung (GSI)), Darmstadt, Germany, Oct. (2006).
- Sekiguchi K.: “Experimental Study on Three Nucleon Forces *via* Deuteron-Proton Scattering at RIKEN”, QCD and Few-Hadron Systems, 380th International Wilhelm und Else Heraeus Seminar, ( Helmholtz-Institut fuer Strahlen und Kernphysik, Universitaet Bonn), Bad Honnef, Germany, Nov. (2006).
- Arai I., Komatsubara T., Ozawa A., Sasa K., Yasuda Y., Fujinawa T., Fukunishi N., Goto A., Ohnishi T., Okuno H., Takeda H., Wakasugi M., Yamaguchi M., Yamaguchi Y., Yano Y., Kikuchi T., Suzuki T., Yamaguchi T., and Ohtsubo T.: “Rare RI ring”, RIBF International Collaboration Workshop on Experiments at the RIBF, Wako, Nov. (2006).
- Sekiguchi K.: “ $Nd$  Scattering as a Tool to Study  $3N$  Interactions”, TRIUMF workshop on Three-Nucleon Interactions from Few- to Many-Body Systems, Vancouver, Canada, Mar. (2007).
- Furumoto T., Sakuragi H., and Yamamoto Y.: “New complex G-matrix interactions and application to proton-nucleus scattering”, 5th International Workshop on Direct Reaction with Exotic Beams (DREB2007), Wako, May (2007).
- Sakuragi H., Yamamoto T., and Furumoto T.: “Analysis of polarized proton-6He elastic scattering based on an improved di-neutron model”, 5th International Workshop on Direct Reaction with Exotic Beams (DREB2007), Wako, May–June (2007).
- Iida K.: “Black sphere approach to proton elastic scattering and reaction cross section”, 5th International Workshop on Direct Reaction with Exotic Beams (DREB2007), Wako, May–June (2007).
- Maenaka Y., Furumoto T., and Sakuragi H.: “Coupled-channels study of  $10\text{Be}+\alpha$  structure of highly-excited  $^{14}\text{C}$ ”, 5th International Workshop on Direct Reaction with Exotic Beams (DREB2007), Wako, May–June (2007).
- Kondo Y., Nakamura T., Sato Y., Aoi N., Endo N., Fukuda N., Gomi T., Hashimoto Y., Ishihara M., Kawai S., Kitayama M., Kobayashi T., Matsuda Y., Matsui N., Motobayashi T., Nakabayashi T., Okumura T., Ong H., Onishi T., Otsu H., Sakurai H., Shimoura S., Shinohara M., Sugimoto T., Takeuchi S., Tamaki M., Togano Y., and Yanagisawa Y.: “Invariant mass spectroscopy of  $^{13}\text{Be}$  and  $^{14}\text{Be}$  via the proton-induced breakup reactions of  $^{14}\text{Be}$ ”, 5th International Workshop on Direct Reaction with Exotic Beams (DREB2007), Wako, May–June (2007).
- Kanno S., Aoi N., Bazin D., Bowen M. D., Campbell C. M., Cook J. M., Dinca D., Gade A., Glasmacher T., Iwasaki H., Kubo T., Kurita K., Motobayashi T., Mueller W. F., Nakamura T., Sakurai H., Suzuki H., Takeuchi S., Terry J. R., Yoneda K., and Zwahlen H.: “Weakening of  $Z=28$  shell closure in  $^{74}\text{Ni}$ ”, 5th International Workshop on Direct Reaction with Exotic Beams (DREB2007), (RIKEN Nishina Center, Kyushu University, Center for Nuclear Study (University of Tokyo)), wako, May–June (2007).
- Nakajima S., Kuboki T., Yoshitake M., Hashizume Y., Kanazawa M., Kitagawa a., Kobayashi K., Moriguchi T., Ohtsubo T., Ozawa A., Sato S., Suzuki T., Yamaguchi Y., Yasuda Y., and Yamaguchi T.: “Development of a time-of-flight detector for rare-RI ring project at RIKEN RIBF”, 15th International Conference on Electromagnetic Isotope Separators and Techniques Related to their Applications (EMIS2007), (GANIL , IN2P3/CNRS , DSM/CEA), Deauville, France, June (2007).
- Yamaguchi Y., Fujinawa T., Fukunishi N., Goto A., Ohnishi T., Sakurai H., Wakasugi M., Yano Y., Ozawa A., Arai I., Yasuda Y., Suzuki T., Yamaguchi T., Kikuchi T., and Ohtsubo T.: “Rare-RI ring project at RI Beam factory in RIKEN”, 15th International Conference on Electromagnetic Isotope Separators and Techniques Related to their Applications (EMIS2007), (GANIL , IN2P3/CNRS , DSM/CEA), Deauville, France, June (2007).
- Takeuchi S., Aoi N., Baba H., Fukui T., hashimoto ., Ieki K., Imai K., Iwasaki H., Kanno S., Kondo Y., Kubo T., Kurita K., Minemura T., Motobayashi T., Nakabayashi T., Nakamura T., Okumura T., Onishi T., Ota S., Sakurai H., Shimoura S., Sugo R., Suzuki D., Suzuki H., Suzuki M., Takeshita E., Tamaki M., Tanaka K., Togano Y., and Yamada K.: “Collectivity in  $^{32}\text{Mg}$  : a study of low-lying states”, International Nuclear Physics Conference (INPC2007), Tokyo, June (2007).
- Furukawa T., Matsuo Y., Hatakeyama A., Ito T., Fujikake K., Kobayashi T., and Shimoda T.: “Hyperfine structure of  $^{85,87}\text{Rb}$  and  $^{133}\text{Cs}$  atoms in superfluid helium”, International Nuclear Physics Conference (INPC2007), Tokyo, June (2007).
- Ozawa A., Arai I., Fujinawa T., Fukunishi N., Goto A., Kikuchi T., Igarashi S., Komatsubara T., Ohtsubo T., Sakurai H., Sasa K., Suzuki T., Wakasugi M., Yamaguchi K., Yamaguchi T., Yamaguchi Y., Yano Y., and Yasuda Y.: “Mass measurements by isochronous storage ring in RI beam factory”, International Nuclear Physics Conference (INPC2007), (RIKEN and others), Tokyo, June (2007).

- Nagatomo T., Matsuta K., Minamisono K., Levy C. D., Sumikama T., Mihara M., Ozawa A., Tagisi Y., Ogura M., Matsumiya R., Fukuda M., Yamaguchi M., Behr J. A., Jackson K. P., Yasuno T., Ohta H., Hashizume Y., Fujiwara H., Chiba A., and Minamisono T.: “Search for the  $G$  parity violating term in weak nucleon currents in mass 20 system”, International Nuclear Physics Conference (INPC2007), (Science Council of Japan, RIKEN and others), Tokyo, June (2007).
- Imai N., Ong H., Aoi N., Sakurai H., Demichi K., Kawasaki H., Baba H., Dombradi Z., Elekes Z., Fukuda N., Fulop Z., Gelberg A., Gomi T., Hasegawa H., Ishikawa K., Iwasaki H., Kaneko E., Kanno S., Kishida T., Kondo Y., Kubo T., Kurita K., Michimasa S., Minemura T., Miura M., Motobayashi T., Nakamura T., Notani M., Onishi T., Saito A., Shimoura S., Sugimoto T., Suzuki M., Takeshita E., Takeuchi S., Tamaki M., Yamada K., Yoneda K., Watanabe H., and Ishihara M.: “The lifetime measurement of the first  $2^+$  state in  $^{12}\text{Be}$ ”, International Nuclear Physics Conference (INPC2007), Tokyo, June (2007).
- Sekiguchi K., Sakai H., Sakamoto N., Kuboki T., Sasano M., Takahashi Y., Yako K., Kawabata T., Maeda Y., Sakaguchi S., Sasamoto Y., Suda K., Uesaka T., Okamura H., Itoh K., and Wakasa T.: “Three Nucleon Force Study via  $\vec{d}p$  Breakup Reactions at Intermediate Energies”, International Nuclear Physics Conference (INPC2007), Tokyo, June (2007).
- Kanno S., Aoi N., Bazin D., Bowen M. D., Campbell C. M., Cook J. M., Dinca D., Gade A., Glasmacher T., Iwasaki H., Kubo T., Kurita K., Motobayashi T., Mueller W. F., Nakamura T., Sakurai H., Suzuki H., Takeuchi S., Terry J. R., Yoneda K., and Zwahlen H.: “Weakening of  $Z=28$  shell closure in  $^{74}\text{Ni}$ ”, International Nuclear Physics Conference (INPC2007), (Science Council of Japan, RIKEN and others), Wako, June (2007).
- Kondo Y., Nakamura T., Sato Y., Aoi N., Endo N., Fukuda N., Gomi T., Hashimoto Y., Ishihara M., Kawai S., Kitayama M., Kobayashi T., Matsuda Y., Matsui N., Motobayashi T., Nakabayashi T., Okumura T., Ong H., Onishi T., Otsu H., Sakurai H., Shimoura S., Shinohara M., Sugimoto T., Takeuchi S., Tamaki M., Togano Y., and Yanagisawa Y.: “Invariant mass spectroscopy of  $^{13}\text{Be}$  and  $^{14}\text{Be}$  via the proton-induced breakup reactions”, International Symposium & School on Frontiers and Perspectives of Nuclear and Hadron Physics (FPNH07), (Tokyo Institute of Technology), Tokyo, June (2007).
- Maenaka Y., Furumoto T., and Sakuragi H.: “Coupled-channels study of  $^{10}\text{Be}+\alpha$  structure of highly-excited  $^{14}\text{C}$ ”, International Workshop on Nuclear Structure: New Pictures in the Extended Isospin Space (NS07), Kyoto, June (2007).
- Furukawa T., Matsuo Y., Hatakeyama A., Ito T., Fujikake K., Sasaki A., Kobayashi T., and Shimoda T.: “Laser spectroscopic study of atomic hyperfine structure in superfluid helium for the investigation of nuclear structure”, International Workshop on Nuclear Structure: New Pictures in the Extended Isospin Space (NS07), Kyoto, June (2007).
- Nagatomo T., Matsuta K., Minamisono K., Sumikama T., Mihara M., Ozawa A., Tagisi Y., Ogura M., Matsumiya R., Fukuda M., Yamaguchi M., Yasuno T., Ohta H., Hashizume Y., Fujiwara H., Chiba A., and Minamisono T.: “Beta-ray Angular Distribution from Purely Nuclear Spin Aligned  $^{20}\text{F}$  Nuclei”, 14th International Conference on Hyperfine Interactions and 18th International Symposium on Nuclear Quadrupole Interactions, (Universidad Nacional de La Plata/Instituto de Fisica de La Plata, CONICET), Iguassu Falls, Brazil, Aug. (2007).
- Nakatsukasa T., Yabana K., and Inakura T.: “Dipole response calculations with Skyrme TDDFT”, UNEDF Annual Workshop, (University of Washington), Pack Forest, USA, Aug. (2007).
- Nagatomo T., Matsuta K., Minamisono K., Levy C. D., Sumikama T., Mihara M., Ozawa A., Tagisi Y., Ogura M., Matsumiya R., Fukuda M., Yamaguchi M., Behr J. A., Jackson K. P., Yasuno T., Ohta H., Hashizume Y., Fujiwara H., Chiba A., and Minamisono T.: “Search for the  $G$  parity violating term in weak nucleon currents in mass 20 system”, 12th Int. Workshop on Polarized Sources, Targets & Polarimetry, (Brookhaven National Laboratory), Brookhaven, USA, Sept. (2007).
- Nakajima S., Suzuki T., Yamaguchi T., Fujinawa T., Fukunishi N., Goto A., Ohnishi T., Sakurai H., Wakasugi M., Yamaguchi Y., Yano Y., Ozawa A., Arai I., Yasuda Y., Kikuchi T., and Ohtsubo T.: “New scheme for precision mass measurement of rare isotopes produced at RI beam factory”, 30th Mazurian Lakes Conference on Physics : Nuclear Physics and the Fundamental Processes, (IPJ ; University of Warsaw ; Pro-Physica), Piaski, Poland, Sept. (2007).
- Funaki Y., Yamada T., Horiuchi H., Roepke G., Schuck P., and Suzuki A.: “ $\alpha$ -cluster states and  $4\alpha$ -particle Bose condensate in  $^{16}\text{O}$ ”, Clusters '07, Stratford upon Avon, UK, Sept. (2007).
- Nakatsukasa T., Inakura T., and Yabana K.: “Nuclear response function calculated with the time-dependent Skyrme density functional”, 3rd Japanese-German Workshop on Nuclear Structure and Astrophysics, (GSI), Chiemsee, Germany, Sept.–Oct. (2007).
- Kondo Y., Motobayashi T., Sakurai H., Aoi N., Otsu H., Yanagisawa Y., Fukuda N., Takeuchi S., Ishihara M., Baba H., Gomi T., Imai N., Kubo T., Yoneda K., Nakamura T., Sato Y., Sugimoto T., Matsui N., Attukalathil V. M., Okumura T., Hashimoto Y., Nakabayashi T., Shinohara M., Miura M., Kobayashi T., Matsuda Y., Endo N., Kitayama M., Watanabe K., Yakushiji T., Togano Y., Kawai S., Hasegawa H., Onishi

- T., Ong H., Shimoura S., Tamaki M., Saito A., Bazin D. P., and Watanabe Y.: “Breakup reactions of  $^{14}\text{Be}$ ”, Future Prospects for Spectroscopy and Direct Reactions 2008, (Michigan State University), East Lansing, USA, Feb. (2008).
- Takeuchi S., Aoi N., Baba H., Fukui T., hashimoto ., Ieki K., Imai K., Iwasaki H., Kanno S., Kondo Y., Kubo T., Kurita K., Minemura T., Motobayashi T., Nakabayashi T., Nakamura T., Okumura T., Onishi T., Ota S., Sakurai H., Shimoura S., Sugo R., Suzuki D., Suzuki H., Suzuki M., Takeshita E., Tamaki M., Tanaka K., Togano Y., and Yamada K.: “Low-lying states in  $^{32}\text{Mg}$ ”, Future Prospects for Spectroscopy and Direct Reactions 2008, East Lansing, USA, Feb. (2008).
- Baba H., Watanabe Y., Kawasaki Y., Takizawa Y., Hamada T., Ebisuzaki T., Uesaka M., Motobayashi T., Sato H., Hirota K., Shimizu H., Sato M., Fukuchi T., Ota S., and Shimoura S.: “RIBF DAQ and Ubiquitous detector”, TORIJIN-EFES-FJNSP LIA Joint Workshop on Next Generation Detector System for Nuclear Physics with RI Beams, (TORIJIN-EFES-FJNSP LIA ), Caen, France, Feb. (2008).
- Sakuragi H., Furumoto T., Okamoto S., and Takashina M.: “Collective deformation of neutron distribution in nuclei probed by proton inelastic scattering”, CNS-RIKEN Joint International Symposium on Frontier of gamma-ray spectroscopy and Perspectives for Nuclear Structure Studies (Gamma08), Wako, Apr. (2008).
- Dang N. D. and Nguyen H. Q.: “Nuclear pairing at finite temperature and angular momentum”, 1st Workshop on State of the Art in Nuclear Cluster Physics, (Institut Pluridisciplinaire Hubert Curien), Strasbourg, France, May (2008).
- Funaki Y., Yamada T., Horiuchi H., Roepke G., Schuck P., and Suzuki A.: “Present status of alpha-particle condensate states in self-conjugate  $4n$  nuclei”, 1st Workshop on State of the Art in Nuclear Cluster Physics (SOTANCP 2008), Strasbourg, France, May (2008).
- Yamaguchi T., Fujinawa T., Fukunishi N., Goto A., Ohnishi T., Sakurai H., Wakasugi M., Yamaguchi Y., Yano Y., Arai I., Moriguchi T., Ozawa A., Yasuda Y., Nakajima S., Kuboki T., Suzuki T., Kikuchi T., and Ohtsubo T.: “Storage-ring mass spectrometry”, ETC Workshop on Mass Olympics, (GSI , FIAS), Trento, Italy, May (2008).
- Dang N. D.: “Pairing in nuclei at finite temperature and angular momentum”, Seminar at Service de Physique Nucleaire, CEA Saclay, (Commissariat a l’Energie Atomique , Service de Physique Nucleaire), Saclay, France, May (2008).
- Sakuragi H., Furumoto T., and Yamamoto Y.: “Microscopic optical potentials for nucleon-nucleus (N-A) and nucleus-nucleus (A-A) systems-important role of three-body force-”, Hokudai-TORIJIN-JUSTIPEN-EFES Workshop & JUSTIPEN-EFES-Hokudai-UNEDF Meeting, Nanae-cho, Hokkaido Pref., July (2008).
- Dang N. D. and Nguyen H. Q.: “Nuclear pairing at finite temperature and angular momentum”, 13th International Symposium on Capture Gamma Ray Spectroscopy and Related Topics, (Institut fur Kernphysik, University of Cologne), Cologne, Germany, Aug. (2008).
- Matsuo Y., Nishimura M., Kobayashi T., Motobayashi T., Hayashizaki Y., and Kawai J.: “Dependence of Monoatomic Ion Production Rate using Femtosecond Laser Ablation for Solution Samples on Substrate”, 6th International Conference on Photo-Excited Processes and Applications (ICPEPA-6), Sapporo, Sept. (2008).
- Nishimura M., Kobayashi T., Hayashizaki Y., Matsuo Y., and Kawai J.: “Dynamics of Ablation Plasma induced by a Femtosecond Laser Pulse in Electric Fields”, 6th International Conference on Photo-Excited Processes and Applications (ICPEPA-6), Sapporo, Sept. (2008).
- Kobayashi T., Matsuo Y., Nishimura M., Hayashizaki Y., and Kawai J.: “Hydrogenation of the carbon fragments after femtosecond laser ablation of solid  $\text{C}_{60}$ ”, 6th International Conference on Photo-Excited Processes and Applications (ICPEPA-6), Sapporo, Sept. (2008).
- Yamaguchi T., Arai I., Ozawa A., Yasuda Y., Fujinawa T., Fukunishi N., Goto A., Hara K., Ohnishi T., Sakurai H., Wakasugi M., Yamaguchi Y., Yano Y., Kikuchi T., Suzuki T., and Ohtsubo T.: “Beam optics simulation for rare-RI ring at RI beam factory in RIKEN”, 7th International Conference on Nuclear Physics at Storage Rings STORI’08, (Institute of Modern Physics, Chinese Academy of Sciences, National Natural Foundation of China), Lanzhou, China, Sept. (2008).
- Yasuda Y., Ozawa A., Arai I., Fujinawa T., Fukunishi N., Goto A., Ohnishi T., Sakurai H., Wakasugi M., Yamaguchi Y., Yano Y., Suzuki T., Yamaguchi T., Kikuchi T., and Ohtsubo T.: “Present status of rare-RI ring project in RIKEN RIBF”, 7th International Conference on Nuclear Physics at Storage Rings STORI’08, (Institute of Modern Physics, Chinese Academy of Sciences, National Natural Foundation of China), Lanzhou, China, Sept. (2008).
- Funaki Y., Yamada T., Horiuchi H., Roepke G., Schuck P., and Suzuki A.: “ $\alpha$ -particle condensed state in  $^{16}\text{O}$ ”, Japanese French Symposium :New paradigms in Nuclear Physics, Paris, France, Sept.–Oct. (2008).
- Baba H., Ichihara T., Ohnishi T., Takeuchi S., Yoshida K., Watanabe Y., Ota S., and Shimoura S.: “The New DAQ System in RIKEN RIBF”, 2008 Nuclear Science Symposium, Medical Imaging Conference and 16th Room Temperature Semiconductor Detector Workshop, Dresden, Germany, Oct. (2008).
- Funaki Y., Yamada T., Horiuchi H., Roepke G., Schuck P., and Suzuki A.: “Alpha clustering and condensation in  $^{16}\text{O}$ ”, KGU Yokohama Autumn School of Nuclear Physics, Yokohama, Oct. (2008).
- Kondo Y., Nakamura T., Sato Y., Matsumoto T., Aoi

- N., Endo N., Fukuda N., Gomi T., Hashimoto Y., Ishihara M., Kawai S., Kitayama M., Kobayashi T., Matsuda Y., Matsui N., Motobayashi T., Nakabayashi T., Ogata K., Okumura T., Ong H., Onishi T., Otsu H., Sakurai H., Shimoura S., Shinohara M., Sugimoto T., Takeuchi S., Tamaki M., Togano Y., and Yanagisawa Y.: “Invariant-mass spectroscopy of neutron-rich Be isotopes”, Unbound Nuclei Workshop, (INFN), Pisa, Italy, Nov. (2008).
- Kondo Y., Nakamura T., Sato Y., Matsumoto T., Aoi N., Endo N., Fukuda N., Gomi T., Hashimoto Y., Ishihara M., Kawai S., Kitayama M., Kobayashi T., Matsuda Y., Matsui N., Motobayashi T., Nakabayashi T., Ogata K., Okumura T., Ong H., Onishi T., Otsu H., Sakurai H., Shimoura S., Shinohara M., Sugimoto T., Takeuchi S., Tamaki M., Togano Y., and Yanagisawa Y.: “Breakup reactions of  $^{14}\text{Be}$ ”, International Conference on Interfacing Structure and Reactions at the Centre of the Atom (Kernz08), (Livermore and University of Surrey), Queenstown, The Netherlands, Dec. (2008).
- Furumoto T., Sakuragi H., and Yamamoto Y.: “Importance of three-body forces for nucleus-nucleus scattering”, International Conference on Interfacing Structure and Reactions at the Centre of the Atom (Kernz08), Queenstown, New Zealand, Dec. (2008).
- (Domestic Conference)
- 今井伸明, 青井考, 王恵仁, 櫻井博儀, 出道仁彦, Kawasaki H., 馬場秀忠, Dombardi Z., Elekes Z., 福田直樹, Fulop Z., Gelberg A., 五味朋子, 長谷川浩一, 石川和宏, 岩崎弘典, 金子恵美, 菅野祥子, 岸田隆, 近藤洋介, 久保敏幸, 栗田和好, 道正新一郎, 峯村俊行, 三浦宗賢, 本林透, 中村隆司, 野谷将広, 大西健夫, 齋藤明登, 下浦享, 杉本崇, Suzuki M., 竹下英里, 武内聡, 玉城充, 山田一成, 米田健一郎, 渡邊寛, 石原正泰: “ $^{12}\text{Be}$  と  $^{16}\text{C}$  における第一励起状態から基底状態への換算転移確率”, 日本物理学会第 58 回年次大会, 仙台, 3 月 (2003).
- 杉本崇, 中村隆司, 福田直樹, 三浦元隆, 近藤洋介, 青井考, 今井伸明, 久保敏幸, 小林俊雄, 五味朋子, 齋藤明登, 櫻井博儀, 下浦享, Bazin D. P., 長谷川浩一, 馬場秀忠, A.M. V., 本林透, T. Y., 柳澤善行, 米田健一郎, 渡辺極之, 渡辺裕, 石原正泰: “ $^{17}\text{B}$  の分解反応 (2)”, 日本物理学会第 58 回年次大会, 仙台, 3 月 (2003).
- 武内聡: “高感度ガンマ線分析装置の開発”, 日本物理学会第 58 回年次大会, (東北学院大学), 仙台, 3 月 (2003).
- 武内聡: “NaI(Tl) シンチレータによる高感度ガンマ線分析装置の開発”, 先端科学計測研究センター 2002 年度成果報告会, (立教大学), 東京, 5 月 (2003).
- 今井伸明, 王恵仁, 青井考, 櫻井博儀, 出道仁彦, Kawasaki H., 馬場秀忠, Dombardi Z., Elekes Z., 福田直樹, Fulop Z., Gelberg A., 五味朋子, 長谷川浩一, 石川和宏, 岩崎弘典, 金子恵美, 菅野祥子, 岸田隆, 近藤洋介, 久保敏幸, 栗田和好, 道正新一郎, 峯村俊行, 三浦宗賢, 本林透, 中村隆司, 野谷将広, 大西健夫, 齋藤明登, 下浦享, 杉本崇, Suzuki M., 竹下英里, 武内聡, 玉城充, 山田一成, 米田健一郎, 渡邊寛, 石原正泰: “Anomalously long lifetime of  $2+_{1}$  state of  $^{16}\text{C}$ ”, A New Era of Nuclear Structure Physics, 新潟県黒川村, 11 月 (2003).
- 杉本崇, 中村隆司, 福田直樹, 三浦元隆, 近藤洋介, 青井考, 馬場秀忠, Bazin D. P., 五味朋子, 長谷川浩一, 橋本佳子, 今井伸明, 小林俊雄, 久保敏幸, 本林透, 篠原摩有子, 齋藤明登, 櫻井博儀, 下浦享, A.M. V., 渡辺極之, 渡辺裕, 薬師寺崇, 柳澤善行, 米田健一郎, 石原正泰: “Invariant-mass spectroscopy of  $^{13}\text{Be}$ ”, 日本物理学会第 59 回年次大会, 福岡, 3 月 (2004).
- 櫻木弘之: “核反応と核間相互作用: 現状と問題点”, 日本物理学会第 59 回年次大会, 福岡, 3 月 (2004).
- 杉本崇, 中村隆司, A.M. V., 福田直樹, 三浦元隆, 近藤洋介, 青井考, 馬場秀忠, Bazin D. P., 五味朋子, 長谷川浩一, 橋本佳子, 今井伸明, 小林俊雄, 久保敏幸, 本林透, 篠原摩有子, 齋藤明登, 櫻井博儀, 下浦享, 渡辺極之, 渡辺裕, 薬師寺崇, 柳澤善行, 米田健一郎, 石原正泰: “Invariant-Mass Spectroscopy of Unbound  $^{11}\text{Li}$ ,  $^{13}\text{Be}$ , and  $^{17}\text{B}$  Nuclei”, 東京工業大学 21 世紀 COE プログラム「量子ナノ物理学」第 1 回公開シンポジウム, 東京, 3 月 (2004).
- 高階正彰: “微視的な核反応分析を用いた不安定核構造研究の戦略”, RIBF-UEC/理研主催研究会「不安定核物理 この 10 年とこれから」, 和光, 6 月 (2004).
- 武内聡: “不安定核  $\gamma$  線検出器 DALI-2(160 個の NaI array)”, 高エネルギー宇宙・原子核交流促進  $\gamma$  線検出器ワークショップ, (埼玉大学), さいたま, 12 月 (2004).
- 武内聡: “高速 RI ビーム実験用の NaI(Tl) による高効率ガンマ線検出系”, 理研ワークショップ「放射線検出器と電子回路の課題と展望-光子検出器を中心に」, 和光, 5 月 (2005).
- 太田寛史, 新井一郎, 小沢顕, 小松原哲郎, 笹公和, 鈴木健, 山口貴之, 大坪隆, 山口充孝, 田岸義宏, 矢野安重, 後藤彰, 若杉昌徳, 奥野広樹, 福西暢尚, 大西哲哉, 山口由高, 菊池崇志: “Design of the isochronous storage ring for accurate mass measurement in RI beam factory”, 第 2 回日本加速器学会年会/第 30 回リニアック技術研究会, 鳥栖, 7 月 (2005).
- 太田寛史, 新井一郎, 小沢顕, 小松原哲郎, 笹公和, 鈴木健, 山口貴之, 大坪隆, 山口充孝, 田岸義宏, 矢野安重, 後藤彰, 奥野広樹, 福西暢尚, 大西哲哉, 山口由高, 菊池崇志: “等時性蓄積リングへの入射ラインとそのビーム光学”, 等時性蓄積リングによる不安定核の質量測定と宇宙元素合成, (筑波大学), つくば, 9 月 (2005).
- 山口由高, 若杉昌徳, 藤縄雅, 福西暢尚, 後藤彰, 大西哲哉, 奥野広樹, 櫻井博儀, 竹田浩之, 山口充孝, 矢野安重, 小沢顕, 新井一郎, 小松原哲郎, 笹公和, 菊池崇志, 鈴木健, 山口貴之, 大坪隆: “等時性蓄積リングのためのキッカー電磁石及び入射スキームの検討”, 等時性蓄積リングによる不安定核の質量測定と宇宙元素合成, (筑波大学), つくば, 9 月 (2005).
- 今井伸明, 王恵仁, 青井考, 櫻井博儀, 出道仁彦, Kawasaki H., 馬場秀忠, Dombardi Z., Elekes Z., 福田直樹, Fulop Z., Gelberg A., 五味朋子, 長谷川浩一, 石川和宏, 岩崎弘典, 金子恵美, 菅野祥子, 岸田隆, 近藤洋介, 久保敏幸, 栗田和好, 道正新一郎, 峯村俊行, 三浦宗賢, 本林透, 中村隆司, 野谷将広, 大西健夫, 齋藤明登, 下浦享, 杉本崇, Suzuki M., 竹下英里, 武内聡, 玉城充, 山田一成, 米田健一郎, 渡邊寛

- 寛, 石原正泰: “Experimental finding of the anomalous quadrupole collectivity in unstable nucleus  $^{16}\text{C}$ ”, 日本物理学会 2005 年秋季大会, (日本物理学会), 京田辺, 9 月 (2005).
- 今井伸明, 王患仁, 青井考, 櫻井博儀, 出道仁彦, Kawasaki H., 馬場秀忠, Dombardi Z., Elekes Z., 福田直樹, Fulop Z., Gelberg A., 五味朋子, 長谷川浩一, 石川和宏, 岩崎弘典, 金子恵美, 菅野祥子, 岸田隆, 近藤洋介, 久保敏幸, 栗田和好, 道正新一郎, 峯村俊行, 三浦宗賢, 本林透, 中村隆司, 野谷将広, 大西健夫, 齋藤明登, 下浦享, 杉本崇, Suzuki M., 竹下英里, 武内聡, 玉城充, 山田一成, 米田健一郎, 渡邊寛, 石原正泰: “Lifetime measurement of  $^{12}\text{Be}(2+)$ ”, 日本物理学会 2005 年秋季大会, (日本物理学会), 京田辺, 9 月 (2005).
- 櫻木弘之, 古本猛憲, 村上永理子: “Proton-nucleus optical potential with complex G-matrix ”JLM” and ”CEG””, 理研 RIBF 核反応理論研究会「不安定原子核-原子核/核子間相互作用の理論的分析へ向けて」, 和光, 2 月 (2006).
- 櫻木弘之: “複素 G 行列による  $\alpha$ -原子核および陽子-原子核散乱の研究”, 理研 RIBF 核反応理論研究会「不安定原子核-原子核/核子間相互作用の理論的分析へ向けて」, 和光, 2 月 (2006).
- 高階正彰: “Inelastic scattering of light unstable nuclei”, 日本物理学会第 61 回年次大会, (日本物理学会), 松山, 3 月 (2006).
- 須田利美: “Physics of electron-RI scattering”, Workshop on Nuclear Spectroscopy using Slow- and Stopped-RI Beams, 茨城県東海村, 3 月 (2006).
- 櫻木弘之: “Analysis of elastic scattering of polarized proton by  $^6\text{He}$  based on di-neutron model”, 理研ワークショップ「Theoretical description of elastic scattering of proton by unstable nuclei based on two-nucleon force」, 和光, 3 月 (2006).
- 古本猛憲, 櫻木弘之: “Microscopic proton-nucleus optical potentials based on the folding model with new complex G-matrix interactions”, 理研ワークショップ「Theoretical description of elastic scattering of proton by unstable nuclei based on two-nucleon force」, 和光, 3 月 (2006).
- 櫻木弘之: “Folding model approach to nucleus-nucleus interactions and applications to nuclear reaction studies”, 理研ワークショップ「Elastic scattering of unstable nuclei」, 和光, 6 月 (2006).
- 古本猛憲, 櫻木弘之: “Microscopic optical potential based on the folding model with complex G-matrix interactions: JLM and CEG”, 理研ワークショップ「Elastic scattering of unstable nuclei」, 和光, 6 月 (2006).
- 古本猛憲, 櫻木弘之: “複素 G 行列相互作用に基づく核反応研究 I”, 日本物理学会分科会, 奈良, 9 月 (2006).
- 須田利美: “Elastic electron scattering off exotic nuclei”, Workshop on Nuclear Structure Studied via Reaction Cross Section, 和光, 11 月 (2006).
- 須田利美: “Two nucleon correlation in  $^6\text{He}$ ”, Workshop on Cluster Phenomena in Many Body Systems, 大阪, 2 月 (2007).
- 山口由高, 小沢顕, 新井一郎, 安田裕介, 藤縄雅, 福西暢尚, 大西哲哉, 後藤彰, 奥野広樹, 櫻井博儀, 若杉昌徳, 矢野安重, 鈴木健, 山口貴之, 菊池崇志, 大坪隆: “等時性蓄積リングによる質量測定”, 国立天文台ワークショップ「R プロセス元素組成の統合的理解: 量子ビームでさぐる宇宙進化の理解を目指して」, 三鷹, 3 月 (2007).
- 久保本隆正, 小沢顕, 鈴木健, 山口貴之, 大坪隆, 山口由高, 金澤光高, 北川敦志, 小林圭, 佐藤眞二, 須田利美, 田中鐘信, 中島真平, 橋爪祐平, 森口哲朗, 安田裕介, 吉竹利織: “放医研 HIMAC に於ける TOF 検出器の分解能と荷電状態分布の測定”, 日本物理学会 2007 年春季大会, 八王子, 3 月 (2007).
- 古本猛憲, 櫻木弘之, 山本安夫: “複素 G 行列相互作用に基づく核反応研究 II”, 日本物理学会分科会, 東京, 3 月 (2007).
- 須田利美: “Two nucleon correlation via one-nucleon exchange reaction”, Workshop on Two Nucleon Correlation, 和光, 7 月 (2007).
- 安田裕介, 新井一郎, 小沢顕, 小松原哲郎, 笹谷和, 大西哲哉, 後藤彰, 櫻井博儀, 福西暢尚, 藤縄雅, 矢野安重, 山口由高, 若杉昌徳, 鈴木健, 山口貴之, 大坪隆, 菊池崇志: “理研 RIBF における等時性蓄積リング計画”, 日本物理学会第 62 回年次大会, 札幌, 9 月 (2007).
- 古本猛憲, 高階正彰, 櫻木弘之, 山本安夫: “複素 G 行列相互作用に基づく核反応研究 III”, 日本物理学会第 62 回年次大会, 札幌, 9 月 (2007).
- 須田利美: “SCRIT project: current status and perspectives”, Workshop on Nucleon Density Distributions in Exotic Nuclei using G-matrix, 和光, 12 月 (2007).
- 大西哲哉, 久保敏幸, 日下健祐, 吉田光一, 吉田敦, 大竹政雄, 竹田浩之, 溝井浩, 福田直樹, 柳澤善行, 青井考, 鈴木宏: “RIBF BigRIPS における PHITS の利用”, 第 4 回 PHITS ユーザー研究会, (日本原子力研究開発機構), 東海村, 2 月 (2008).
- 菅野祥子, 青井考, Bazin D., Bowen M. D., Campbell C. M., Cook J. M., Dinca D., Gade A., Glasmacher T., 岩崎弘典, 久保敏幸, 栗田和好, 本林透, Mueller W. F., 中村隆司, 櫻井博儀, 鈴木宏, 武内聡, Terry J. R., 米田健一郎, Zwahlen H.: “Proton core polarization in neutron-rich nucleus  $^{74}\text{Ni}$ ”, Workshop on Advance in Physics with ISOL-based/Fragmentation-based RI Beams, (TITECH), 東京, 2 月 (2008).
- 須田利美: “Probing two nucleons with electromagnetic probe”, Winter School for Strangeness Nuclear Physics, 秋田, 2-3 月 (2008).
- 馬場秀忠, 渡邊康, 川崎賀也, 滝澤慶之, 濱田剛, 戎崎俊一, 上坂明子, 本林透, 佐藤広海, 広田克也, 清水裕彦, 佐藤光輝, 福地知則, 大田晋輔, 下浦享: “ユビキタス検出器の開発: 検出器への自律性導入の試み”, 日本物理学会第 63 回年次大会, 東大阪, 3 月 (2008).
- 小濱洋央, 飯田圭, 親松和浩: “反陽子直接反応とくろたまモデル”, 日本物理学会第 63 回年次大会, 東大阪, 3 月 (2008).
- 近藤洋介, 中村隆司, 佐藤義輝, 杉本崇, 松井信行, 奥村俊文, 橋本佳子, 中林彩, 篠原摩有子, 青井考, 遠藤奈津美, 福田直樹, 五味朋子, 河合祥子, 來山益久, 小林俊雄, 松田洋平, 本林透, 王患仁, 大西健夫, 大津秀暁, 櫻井博儀, 下浦享, 武内聡, 玉城充, 榎野泰宏, 柳澤善行, 石原正泰: “ $^{18,19}\text{C}$

- の一中性子分離反応”, 日本物理学会第 63 回年次大会, 東大阪, 3 月 (2008).
- 岩崎照平, 堀内渉, 鈴木宜之, 小濱洋央: “酸素同位体の全反応断面積の系統的計算”, 日本物理学会第 63 回年次大会, 東大阪, 3 月 (2008).
- 森口哲朗, 橋爪祐平, 保谷毅, 小川賢一郎, 安田裕介, 原かおる, 小沢顕, 久保木隆正, 吉竹利織, 齊藤和哉, 三浦宗賢, 中島真平, 山口貴之, 鈴木健, 大坪隆, 山口由高, 金澤光高, 北川敦志, 佐藤眞二: “重イオンビームによる Hybrid Photo Detector の時間分解能の測定”, 日本物理学会第 63 回年次大会, 東大阪, 3 月 (2008).
- 久保木隆正, 山口貴之, 大坪隆, 小沢顕, 金澤光高, 北川敦志, 久保徹, 小林圭, 齊藤和哉, 佐藤眞二, 鈴木健, 須田利美, 田中鐘信, 中島真平, 橋爪祐平, 三浦宗賢, 森口哲朗, 安田裕介, 山口由高, 吉竹利織, 渡部亮太: “理研稀少 RI リングの為の TOF 検出器の開発”, 日本物理学会第 63 回年次大会, 東大阪, 3 月 (2008).
- 古本猛憲, 櫻木弘之, 山本安夫: “複素 G 行列有効核力を用いた核反応の研究 IV”, 日本物理学会第 63 回年次大会, 東大阪, 3 月 (2008).
- 堀井香織, 古本猛憲, 櫻木弘之: “偏極陽子+ $^8\text{B}$  散乱における  $^8\text{B}$ ,  $^7\text{Be}+p$  分解過程および  $^7\text{Be}$  核変形の効果”, 日本物理学会第 63 回年次大会, 東大阪, 3 月 (2008).
- 山口由高, 大西哲哉, 後藤彰, 櫻井博儀, 福西暢尚, 藤縄雅, 矢野安重, 若杉昌徳, 新井一郎, 小沢顕, 小松原哲郎, 笹公和, 安田裕介, 鈴木健, 山口貴之, 菊池崇志, 大坪隆: “理研 RIBF における質量リング計画の現状”, 国立天文台研究会「r プロセス元素合成の統合的理解-量子ビームで探る宇宙進化の理解を目指して-」, つくば, 3 月 (2008).
- 松尾由賀利: “レーザーでせまる物質の根源: 精密レーザー分光による原子核へのアプローチとレーザーアブレーションを用いた微量元素分析”, 東北大学サイクロトロン物理セミナー, 仙台核科学コロキウム, (東北大学 CYRIC), 仙台, 5 月 (2008).
- 古川武: “理研” OROCHI” 計画: 超流動ヘリウム中に導入されたエキゾチック RI 原子の新奇なレーザー核分光法”, 東北大学サイクロトロン物理セミナー, 仙台核科学コロキウム, (東北大学 CYRIC), 仙台, 5 月 (2008).
- 古川武, 松尾由賀利, 畠山温, 風戸正行, 星野紗代, 佐々木彩子, 涌井崇志, 上野秀樹, 吉見彰洋, 青井考, 武智麻耶, 梶野泰宏, 小林徹, 和田道治, 高峰愛子, 藤掛浩太郎, 松浦佑一, 小田原厚子, 下田正, 篠塚勉, 本林透: “超流動ヘリウム液体中に植え込まれた不安定同位体原子のレーザー分光実験” OROCHI”, 第 5 回 AMO 討論会, 八王子, 6 月 (2008).
- 佐々木彩子, 古川武, 藤掛浩太郎, 小林徹, 畠山温, 下田正, 小田島仁司, 松尾由賀利: “超流動ヘリウム中に植え込まれた In 原子の励起スペクトル”, 第 5 回 AMO 討論会, 八王子, 6 月 (2008).
- 林崎良英, 河合純, 西村美月, 小林徹, 松尾由賀利: “フェムト秒レーザーアブレーションで生成する炭素フラグメントの水素化反応”, 第 5 回 AMO 討論会, 東京, 6 月 (2008).
- 林崎良英, 加藤俊幸, 河合純, 西村美月, 小林徹, 松尾由賀利: “フェムト秒レーザーアブレーションによる単原子イオン放出プロセスの P-LIF 観察”, 第 5 回 AMO 討論会, 東京, 6 月 (2008).
- 山口由高, 藤縄雅, 福西暢尚, 後藤彰, 大西哲哉, 櫻井博儀, 若杉昌徳, 矢野安重, 小沢顕, 新井一郎, 安田裕介, 菊池崇志, 大坪隆, 鈴木健, 山口貴之: “理研 RIBF における稀少 RI リング計画の現状”, 第 5 回日本加速器学会年会/第 33 回リニアック技術研究会, 東広島, 8 月 (2008).
- 松尾由賀利, 古川武, 畠山温, 風戸正行, 星野紗代, 佐々木彩子, 涌井崇志, 上野秀樹, 青井考, 吉見彰洋, 武智麻耶, 梶野泰宏, 小林徹, 和田道治, 園田哲, 高峰愛子, 藤掛浩太郎, 松浦佑一, 小田原厚子, 下田正, 篠塚勉, 本林透: “超流動ヘリウム中エキゾチック RI 原子の新奇なレーザー分光法 (OROCHI 法): 不安定核 Rb 原子の超微細構造精密測定へ向けて”, 東北大学・CYRIC 研究会 Fundamental Physics using Atoms, (東北大学 CYRIC), 仙台, 8 月 (2008).
- 近藤洋介, 中村隆司, 佐藤義輝, 松本琢磨, 青井考, 遠藤奈津美, 福田直樹, 五味朋子, 橋本佳子, 石原正泰, 河合祥子, 來山益久, 小林俊雄, 松田洋平, 松井信行, 本林透, 中林彩, 緒方一介, 奥村俊文, 王恵仁, 大西健夫, 大津秀暁, 櫻井博儀, 下浦享, 篠原摩有子, 杉本崇, 武内聡, 玉城充, 梶野泰宏, 柳澤善行: “ $^{18,19}\text{C}$  の一中性子分離反応”, RCNP 研究会「RCNP における不安定核の研究: RCNP ビームラインの可能性を探る」, (大阪大学核物理研究センター), 大阪, 8 月 (2008).
- 古川武, 松尾由賀利, 畠山温, 風戸正行, 星野紗代, 佐々木彩子, 涌井崇志, 上野秀樹, 青井考, 吉見彰洋, 武智麻耶, 梶野泰宏, 小林徹, 和田道治, 園田哲, 高峰愛子, 藤掛浩太郎, 松浦佑一, 小田原厚子, 下田正, 篠塚勉, 本林透: “理研” OROCHI ” 実験計画: 超流動ヘリウムを利用した短寿命不安定核のレーザー核分光”, RCNP 研究会「RCNP における不安定核の研究: RCNP ビームラインの可能性を探る」, 茨木, 8 月 (2008).
- 南里朋洋, 荒木幹生, 西尾正樹, 羽場宏光, 江崎豊, 横山明彦: “Rf 溶液化学のための極微量濃度における TIOA を用いた逆相クロマトグラフィーの研究”, 2008 年日本放射化学学会年会/第 52 回放射化学討論会, (日本放射化学会), 広島, 9 月 (2008).
- 須田利美: “Probing two nucleons with electromagnetic probe”, RIBF ミニワークショップ「2 核子相関と不安定原子核」, 和光, 9 月 (2008).
- 安田裕介, 新井一郎, 小沢顕, 森口哲朗, 大西哲哉, 櫻井博儀, 福西暢尚, 藤縄雅, 矢野安重, 山口由高, 若杉昌徳, 原かおる, 鈴木健, 山口貴之, 大坪隆, 菊池崇志: “理研稀少 RI リング建設こむけての高精度磁場測定”, 日本物理学会 2008 年秋季大会, 盛岡, 9 月 (2008).
- 古川武, 松尾由賀利, 畠山温, 風戸正行, 星野紗代, 佐々木彩子, 涌井崇志, 上野秀樹, 青井考, 吉見彰洋, 武智麻耶, 梶野泰宏, 小林徹, 和田道治, 園田哲, 高峰愛子, 藤掛浩太郎, 松浦佑一, 小田原厚子, 下田正, 篠塚勉, 本林透: “超流動ヘリウム中における短寿命核のレーザー核分光実験計画『OROCHI』の現状”, 日本物理学会 2008 年秋季大会, (日本物理学会), 山形, 9 月 (2008).
- 市川雄一, 久保敏幸, 青井考, Banerjee S. R., Chakrabarti A., 福田直樹, 岩崎弘典, 久保野茂, 本林透, 中林彩, 中村隆司, 中尾太郎, 奥村俊文, 王恵仁, 大西健夫, 鈴木大介, 鈴木賢, 山田一成, 山口英齊, 櫻井博儀: 日本物理学会 2008 年秋季大会, 山形, 9 月 (2008).

- 高階正彰, 櫻木弘之: “ $^{16}\text{O}+^{16}\text{O}$  非弾性散乱における多段階効果”, 日本物理学会 2008 年秋季大会, 山形, 9 月 (2008).
- 長友侔, 南園啓, 松多健策, 三原基嗣, 松宮亮平, 小倉昌子, 福田光順, 小沢顕, 田岸義宏, 山口充孝, 安野琢磨, 太田寛史, 橋爪祐平, 炭竈聡之, Levy C. D., Behr J. A., Jackson K. P., 南園忠則: “質量数 20 体系の鏡映核対のベータ線角度分布の精密測定による  $G$  変換対称性の研究”, 日本物理学会 2008 年秋季大会, (山形大学, 日本物理学会), 山形, 9 月 (2008).
- 古本猛憲, 櫻木弘之, 山本安夫: “複素  $G$  行列有効核力を用いた Li-isotopes - 原子核反応の解析”, 日本物理学会 2008 年秋季大会, 山形, 9 月 (2008).
- 古本猛憲, 櫻木弘之, 山本安夫: “ $\Sigma$ -nucleus potential based on folding model with complex  $G$ -matrix interaction”, 文科省科研費補助金特定領域研究「ストレンジネスで探るクォーク多体系」研究会 2008, 山形, 9 月 (2008).
- 佐々木彩子, 星野紗代, 涌井崇志, 古川武, 風戸正行, 山口杏子, 小林徹, 畠山温, 藤掛浩太郎, 松浦佑一, 小田原厚子, 下田正, 篠塚勉, 松尾由賀利: “OROCHI 実験に向けた蛍光検出系の開発”, 第 5 回停止・低速不安定核ビームを用いた核分光研究会, 豊中, 12 月 (2008).
- 藤掛浩太郎, 古川武, 畠山温, 小林徹, 松浦佑一, 小田島仁司, 下田正, 松尾由賀利: “超流動ヘリウム中における光ポンピング法を用いた Ag 原子の高偏極生成”, 第 5 回停止・低速不安定核ビームを用いた核分光研究会, 豊中, 12 月 (2008).
- 松尾由賀利, 古川武, 畠山温, 風戸正行, 山口杏子, 星野紗代, 佐々木彩子, 涌井崇志, 上野秀樹, 青井考, 吉見彰洋, 武智麻耶, 梶野泰宏, 西村俊二, 小林徹, 和田道治, 園田哲, 高峰愛子, 藤掛浩太郎, 松浦佑一, 小田原厚子, 下田正, 篠塚勉, 本林透: “超流動ヘリウムを用いたレーザー核分光実験” OROCHI” - 第一回ビーム実験へ向けて -, 第 5 回停止・低速不安定核ビームを用いた核分光研究会, 豊中, 12 月 (2008).
- 川村広和, 秋山岳伸, 石井哲朗, 池田友樹, 亀田大輔, 聖代橋悦子, 豊田健司, 長江大輔, 新田稔, 二宮一史, 秦麻記, 平山賀一, 光岡真一, 宮武宇也, 村田次郎, 渡辺裕: “TRIAC における偏極不安定核を用いた時間反転対称性破れの探索”, 第 5 回停止・低速不安定核ビームを用いた核分光研究会, (大阪大学), 豊中, 12 月 (2008).
- 市川雄一, 久保敏幸, 青井考, Banerjee S. R., Chakrabarti A., 福田直樹, 岩崎弘典, 久保野茂, 本林透, 中林彩, 中村隆司, 中尾太郎, 奥村俊文, 王恵仁, 大西健夫, 鈴木大介, 鈴木賢, 山田一成, 山口英斉, 櫻井博儀: 第 5 回停止・低速不安定核ビームを用いた核分光研究会, (大阪大学), 豊中, 12 月 (2008).
- 佐々木彩子, 星野紗代, 涌井崇志, 古川武, 風戸正行, 山口杏子, 和田道治, 園田哲, 高峰愛子, 小林徹, 上野秀樹, 吉見彰洋, 青井考, 西村俊二, 梶野泰宏, 武智麻耶, 畠山温, 藤掛浩太郎, 松浦佑一, 小田原厚子, 下田正, 本林透, 篠塚勉, 松尾由賀利: “超流動ヘリウム中でのレーザー核分光に向けた蛍光検出系の開発”, 日本物理学会第 64 回年次大会, 東京, 3 月 (2009).
- 藤掛浩太郎, 古川武, 畠山温, 小林徹, 松浦佑一, 下田正, 小田島仁司, 松尾由賀利: “超流動ヘリウム中における Ag 原子の光ポンピング及び磁気共鳴”, 日本物理学会第 64 回年次大会, 東京, 3 月 (2009).
- 古川武, 藤掛浩太郎, 畠山温, 小林徹, 松浦佑一, 佐々木彩子, 星野紗代, 涌井崇志, 風戸正行, 山口杏子, 和田道治, 園田哲, 高峰愛子, 上野秀樹, 吉見彰洋, 青井考, 西村俊二, 梶野泰宏, 武智麻耶, 小田原厚子, 下田正, 篠塚勉, 本林透, 松尾由賀利: “超流動ヘリウム中での光ポンピング法を用いた Ag 原子の高偏極生成とレーザー核分光への応用”, 日本物理学会第 64 回年次大会, 東京, 3 月 (2009).
- 風戸正行, 古川武, 山口杏子, 梶野泰宏, 西村俊二, 佐々木彩子, 星野紗代, 涌井崇志, 畠山温, 藤掛浩太郎, 松浦佑一, 篠塚勉, 本林透, 小田原厚子, 下田正, 松尾由賀利: “超流動ヘリウム中における RI ビーム停止位置の精密制御”, 日本物理学会第 64 回年次大会, 東京, 3 月 (2009).
- 川村広和, 秋山岳伸, 秦麻記, 平山賀一, 池田友樹, 亀田大輔, 宮原直亮, 宮武宇也, 村田次郎, 中谷祐輔, 長江大輔, 二宮一史, 新田稔, 大西潤一, 聖代橋悦子, 豊田健司, 塚田和司, 渡辺裕: “TRIAC における偏極  $^8\text{Li}$  を用いた時間反転対称性破れの探索”, 日本物理学会第 64 回年次大会, 東京, 3 月 (2009).
- 堀井香織, 土岐博, 櫻木弘之, 高階正彰, 谷口億宇, 古本猛憲: “内部構造を考慮した  $^8\text{Be}+\gamma$  の陽子および  $^{12}\text{C}$  との弾性散乱”, 日本物理学会第 64 回年次大会, 東京, 3 月 (2009).

Publications

[Journal]

(Original Papers) \*Subject to Peer Review

- Otsu H., Kobayashi T., Matsuda Y., Kitayama M., Inafuku K., Ozawa A., Satou Y., Suda T., Yoshida K., and Sakaguchi H.: "Measurement of the H(38s,p') reaction at forward angles including 0 degree", Nucl. Phys. A **788**, 266c–270c (1997). \*
- Fukuda N., Nakamura T., Kobayashi T., Otsu H., Aoi N., Imai N., Iwasaki H., Kubo T., Mengoni A., Notani M., Sakurai H., Shimoura S., Teranishi T., Watanabe Y., Yoneda K., and Ishihara M.: "Coulomb Dissociation of Halo Nuclei", Prog. Theor. Phys. Suppl., No. 146, pp. 462–466 (2002).
- Gomi T., Motobayashi T., Yoneda K., Kanno S., Aoi N., Ando Y., Baba H., Demichi K., Fulop Z., Futakami U., Hasegawa H., Higurashi Y., Ieki K., Imai N., Iwasa N., Iwasaki H., Kubo T., Kubono S., Kunibu M., Matsuyama Y., Michimasa S., Minemura T., Murakami H., Nakamura T., Saito A., Sakurai H., Serata M., Shimoura S., Sugimoto T., Takeshita E., Takeuchi S., Ue K., Yamada K., Yanagisawa Y., Yoshida A., and Ishihara M.: "Coulomb Dissociation of  $^{23}\text{Al}$ ", Prog. Theor. Phys. Suppl., No. 146, pp. 557–558 (2002). \*
- Kanno S., Gomi T., Motobayashi T., Yoneda K., Aoi N., Ando Y., Baba H., Demichi K., Fulop Z., Futakami U., Hasegawa H., Higurashi Y., Ieki K., Imai N., Iwasa N., Iwasaki H., Kubo T., Kubono S., Kunibu M., Matsuyama Y., Michimasa S., Minemura T., Murakami H., Nakamura T., Saito A., Sakurai H., Serata M., Shimoura S., Sugimoto T., Takeshita E., Takeuchi S., Ue K., Yamada K., Yanagisawa Y., Yoshida A., and Ishihara M.: "Coulomb Excitation of  $^{24}\text{Si}$ ", Prog. Theor. Phys. Suppl., No. 146, pp. 575–576 (2002). \*
- Matsuyama Y., Motobayashi T., Shimoura S., Minemura T., Saito A., Baba H., Akiyoshi H., Aoi N., Ando Y., Gomi T., Higurashi Y., Ieki K., Imai N., Iwasa N., Iwasaki H., Kanno S., Kubono S., Kunibu M., Michimasa S., Murakami H., Nakamura T., Sakurai H., Serata M., Takeshita E., Takeuchi S., Teranishi T., Ue K., Yamada K., and Yanagisawa Y.: "Inelastic Scattering of  $^{12}\text{Be}$  with  $^4\text{He}$ ", Prog. Theor. Phys. Suppl., No. 146, pp. 593–594 (2002). \*
- Ideguchi E., Cederwall B., undefined u. u., Gono Y., Y.F. Y., Teranishi T., Aoi N., D. B., and Kishida T.: "Measurement of Depth of Interaction in a Segmented Planar Ge Detector", Nucl. Instrum. Methods Phys. Res. A **496**, 373–384 (2003). \*
- Gomi T., Motobayashi T., Yoneda K., Kanno S., Aoi N., Ando Y., Baba H., Demichi K., Fulop Z., Futakami U., Hasegawa H., Higurashi Y., Ieki K., Imai N., Iwasa N., Iwasaki H., Kubo T., Kubono S., Kunibu M., Matsuyama Y., Michimasa S., Minemura T., Murakami H., Nakamura T., Sakurai H., Serata M., Takeshita E., Takeuchi S., Teranishi T., Ue K., Yamada K., and Yanagisawa Y.: "Study of the H(38s,p') reaction at forward angles including 0 degree", Nucl. Phys. A **718**, 508c–509c (2003). \*
- Inakura T., Mizutori S., Yamagami M., and Matuyanagi K.: "Superdeformed Bands in Neutron-Rich Sulfur Isotopes suggested by Cranked Skyrme-Hartree-Fock Calculations", Nucl. Phys. A **728**, 52–64 (2003). \*
- Shimoura S., Saito A., Minemura T., Matsuyama Y., Baba H., Akiyoshi H., Aoi N., Gomi T., Higurashi Y., Ieki K., Imai N., Iwasa N., Iwasaki H., Kanno S., Kubono S., Kunibu M., Michimasa S., Motobayashi T., Nakamura T., Sakurai H., Serata M., Takeshita E., Takeuchi S., Teranishi T., Ue K., Yamada K., Yanagisawa Y., Ishihara M., and Itagaki N.: "Isomeric  $0^+$  state in  $^{12}\text{Be}$ ", Phys. Lett. B **560**, 31–36 (2003). \*
- Takashina M., Ito M., Kudo Y., Okabe S., and Sakuragi H.: " $^{12}\text{C}+^{12}\text{C}\rightarrow^8\text{Be}_{g.s.}+^{16}\text{O}_{g.s.}$  resonance reaction around  $E_{c.m.}=32.5$  MeV", Phys. Rev. C **67**, 014609-1–014609-6 (2003). \*
- Iwasa N., Motobayashi T., Sakurai H., Akiyoshi H., Ando Y., Aoi N., Baba H., Fukuda N., Fulop Z., Futakami U., Gomi T., Higurashi Y., Ieki K., Iwasaki H., Kubo T., Kubono S., Kinugawa H., Kumagai H., Kunibu M., Michimasa S., Minemura T., Murakami H., Sagara K., Saito A., Shimoura S., Takeuchi S., Yanagisawa Y., Yoneda K., and Ishihara M.: "In-beam  $\gamma$  spectroscopy of  $^{34}\text{Si}$  with deuteron inelastic scattering using reverse kinematics", Phys. Rev. C **67**, 064315-1–064315-4 (2003). \*
- Gomi T., Motobayashi T., Ando Y., Aoi N., Baba H., Demichi K., Elekes Z., Fukuda N., Fulop Z., Futakami U., Hasegawa H., Higurashi Y., Ieki K., Imai N., Ishihara M., Ishikawa K., Iwasa N., Iwasaki H., Kanno S., Kondo Y., Kubo T., Kubono S., Kunibu M., Kurita K., Matsuyama Y., Michimasa S., Minemura T., Miura M., Murakami H., Nakamura T., Notani M., Ota S., Saito A., Sakurai H., Serata M., Shimoura S., Sugimoto T., Takeshita E., Takeuchi S., Togano Y., Ue K., Yamada K., Yanagisawa Y., Yoneda K., and Yoshida A.: "Study of the Stellar  $^{22}\text{Mg}(p, \gamma)^{23}\text{Al}$  Reaction using the Coulomb-Dissociation Method", Nucl. Phys. A **734**, E77–E79 (2004).
- Ueno H., Asahi K., Ogawa H., Kameda D., Miyoshi H., Yoshimi A., Watanabe H., Shimada K., Sato W., Yoneda K., Imai N., Kobayashi Y., Ishihara M., and Wolf-Dieter S.: "Measurement of nuclear moments in the region of light neutron-rich nuclei", Nucl. Phys. A **738**, 211–215 (2004). \*
- Saito A., Shimoura S., Takeuchi S., Motobayashi T., Minemura T., Matsuyama Y., Baba H., Akiyoshi H., Ando Y., Aoi N., Fulop Z., Gomi T., Higurashi Y., Hirai M., Ieki K., Imai N., Iwasa N., Iwasaki H.,

- Iwata Y., Kanno S., Kobayashi H., Kubono S., Kunibu M., Kurokawa M., Liu Z., Michimasa S., Nakamura T., Ozawa A., Sakurai H., Serata M., Takeshita E., Teranishi T., Ue K., Yamada K., Yanagisawa Y., and Ishihara M.: “Molecular states in neutron-rich beryllium isotopes”, *Nucl. Phys. A* **738**, 337–341 (2004). \*
- Takashina M., Ito M., Ito Y., Okabe S., and Sakuragi H.: “ $^{12}\text{C}+^{12}\text{C}\rightarrow^8\text{Be}_{g.s.}+^{16}\text{O}_{g.s.}$  resonance reaction and multi-cluster states of highly-excited  $^{24}\text{Mg}$  nucleus”, *Nucl. Phys. A* **738**, 352–356 (2004). \*
- Fukuda N., Nakamura T., Aoi N., Imai N., Ishihara M., Kobayashi T., Iwasaki H., Kubo T., Mengoni A., Notani M., Otsu H., Sakurai H., Shimoura S., Teranishi T., Watanabe Y., and Yoneda K.: “Coulomb and nuclear breakup of a halo nucleus  $^{11}\text{Be}$ ”, *Phys. Rev. C* **70**, 054606-1–054606-12 (2004). \*
- Imai N., Ong H., Aoi N., Sakurai H., Demichi K., Kawasaki H., Baba H., Dombradi Z., Elekes Z., Fukuda N., Fulop Z., Gelberg A., Gomi T., Hasegawa H., Ishikawa K., Iwasaki H., Kaneko E., Kanno S., Kishida T., Kondo Y., Kubo T., Kurita K., Michimasa S., Minemura T., Miura M., Motobayashi T., Nakamura T., Notani M., Ohnishi T., Saito A., Shimoura S., Sugimoto T., Suzuki M., Takeshita E., Takeuchi M., Tamaki M., Yoneda K., Watanabe H., and Ishihara M.: “Anomalous hindered  $E2$  Strength  $B(E2; 2_1^+ \rightarrow 0^+)$  in  $^{16}\text{C}$ ”, *Phys. Rev. Lett.* **92**, No. 6, pp. 062501-1–062501-4 (2004). \*
- Takechi M., Fukuda M., Mihara M., Chinda T., Matsumasa T., Matsubara H., Nakashima Y., Matsuta K., Minamisono T., Koyama R., Shinosaki W., Takahashi M., Takisawa A., Ohtsubo T., Suzuki T., Momota S., Hatanaka K., Suda T., Sasaki M., Sato S., and Kitagawa A.: “Reaction cross-sections for stable nuclei and nucleon density distribution of proton drip-line nucleus  $8\text{B}$ ”, *Eur. Phys. J. A* **25**, No. s01, pp. 217–219 (2005). \*
- Hatano M., Sakai H., Wakui T., Uesaka T., Aoi N., Ichikawa Y., Ikeda T., Itoh K., Iwasaki H., Kawabata T., Kuboki H., Maeda Y., Matsui N., Ohnishi T., Ohnishi T., Saito T., Sakamoto N., Sasano M., Satou Y., Sekiguchi K., Suda K., Tamii A., Yanagisawa Y., and Yako K.: “First experiment of  $6\text{He}$  with a polarized proton target”, *Eur. Phys. J. A* **25**, No. s01, pp. 255–258 (2005). \*
- Kannungo R., Chiba M., Abu-Ibrahim B., Adhikari S., Fang D., Iwasa N., Kimura K., Maeda K., Nishimura S., Ohnishi T., Ozawa A., Samanta C., Suda T., Suzuki T., Wang Q., Wu C., Yamaguchi Y., Yamada K., Yoshida A., Zheng T., and Tanihata I.: “A new view to the structure of  $^{19}\text{C}$ ”, *Eur. Phys. J. A* **25**, No. s01, pp. 261–262 (2005). \*
- Yamada K., Motobayashi T., Aoi N., Baba H., Demichi K., Elekes Z., Gibelin J., Gomi T., Hasegawa H., Imai N., Iwasaki H., Kanno S., Kubo T., Kurita K., Matsuyama Y., Michimasa S., Minemura T., Notani M., Onishi T., Ong H., Ota S., Ozawa A., Saito A., Sakurai H., Shimoura S., Takeshita E., Takeuchi S., Tamaki M., Togano Y., Yanagisawa Y., Yoneda K., and Tanihata I.: “Reduced transition probabilities for the first  $2^+$  excited state in  $^{46}\text{Cr}$ ,  $^{50}\text{Fe}$ , and  $^{54}\text{Ni}$ ”, *Eur. Phys. J. A* **25**, No. s01, pp. 409–413 (2005).
- Gomi T., Motobayashi T., Ando Y., Aoi N., Baba H., Demichi K., Elekes Z., Fukuda N., Fulop Z., Futakami U., Hasegawa H., Higurashi Y., Ieki K., Imai N., Ishihara M., Ishikawa K., Iwasa N., Iwasaki H., Kanno S., Kondo Y., Kubo T., Kubono S., Kunibu M., Kurita K., Matsuyama Y., Michimasa S., Minemura T., Miura M., Murakami H., Nakamura T., Notani M., Ota S., Saito A., Sakurai H., Serata M., Shimoura S., Sugimoto T., Takeshita E., Takeuchi S., Togano Y., Ue K., Yamada K., Yanagisawa Y., Yoneda K., and Yoshida A.: “Coulomb dissociation experiment for explosive hydrogen burning: study of the  $^{22}\text{Mg}(p, \gamma)^{22}\text{Al}$  reaction”, *J. Phys. G* **31**, S1517–S1521 (2005).
- Togano Y., Gomi T., Motobayashi T., Ando Y., Aoi N., Baba H., Demichi K., Elekes Z., Fukuda N., Fulop Z., Futakami U., Hasegawa H., Higurashi Y., Ieki K., Imai N., Ishihara M., Ishikawa K., Iwasa N., Iwasaki H., Kanno S., Kondo Y., Kubo T., Kubono S., Kunibu M., Kurita K., Matsuyama Y., Michimasa S., Minemura T., Miura M., Murakami H., Nakamura T., Notani M., Ota S., Saito A., Sakurai H., Serata M., Shimoura S., Sugimoto T., Takeshita E., Takeuchi S., Ue K., Yamada K., Yanagisawa Y., Yoneda K., and Yoshida A.: “Study of  $^{26}\text{Si}(p, \gamma)^{27}\text{P}$  reaction using Coulomb dissociation method”, *Nucl. Phys. A* **758**, 182c–185c (2005). \*
- Elekes Z., Dombradi Z., Kanungo R., Baba H., Fulop Z., Gibelin J. D., Horvath A., Ideguchi E., Ichikawa Y., Iwasa N., Iwasaki H., Kanno S., Kawai S., Kondo Y., Motobayashi T., Notani M., Ohnishi T., Ozawa A., Sakurai H., Shimoura S., Takeshita E., Takeuchi M., Tanihata I., Togano Y., Wu C., Yamaguchi Y., Yanagisawa Y., Yoshida A., and Yoshida K.: “Low-lying excited states in  $^{17,19}\text{C}$ ”, *Phys. Lett. B* **614**, 174–180 (2005). \*
- Iwasaki H., Motobayashi T., Sakurai H., Yoneda K., Gomi T., Aoi N., Fukuda N., Fulop Z., Futakami U., Gacsi Z., Higurashi Y., Imai N., Iwasa N., Kunibu M., Kubo T., Kurokawa M., Liu Z., Minemura T., Saito A., Serata M., Shimoura S., Takeuchi S., Watanabe Y., Yamada K., Yanagisawa Y., and Ishihara M.: “Quadrupole collectivity of  $^{28}\text{Ne}$  and the boundary of the island of inversion”, *Phys. Lett. B* **620**, 118–124 (2005). \*
- Dombradi Z., Elekes Z., Kanungo R., Baba H., Fulop Z., Gibelin J. D., Horvath A., Ideguchi E., Ichikawa Y., Iwasa N., Iwasaki H., Kanno S., Kawai S., Kondo Y., Motobayashi T., Notani M., Ohnishi T., Ozawa A., Sakurai H., Shimoura S., Takeshita E., Takeuchi

- S., Tanihata I., Togano Y., Wu C., Yamaguchi Y., Yanagisawa Y., Yoshida A., and Yoshida K.: “Decoupling of valence neutrons from the core in  $^{17}\text{B}$ ”, *Phys. Lett. B* **621**, 81–88 (2005). \*
- Kondo Y., Nakamura T., Aoi N., Baba H., Bazin D., Fukuda N., Gomi T., Hasegawa H., Imai N., Ishihara M., Kobayashi T., Kubo T., Miura M., Motobayashi T., Saito A., Sakurai H., Shimoura S., Sugimoto T., Watanabe K., Watanabe Y., Yakushiji T., Yanagisawa Y., and Yoneda K.: “In-beam  $\gamma$ -ray spectroscopy of the neutron-rich boron isotopes  $^{15,17}\text{B}$  via inelastic scattering on  $^{12}\text{C}$ ”, *Phys. Rev. C* **71**, 044611-1–044611-9 (2005). \*
- Onishi T., Gelberg A., Sakurai H., Yoneda K., Aoi N., Imai N., Baba H., Von Brentano P., Fukuda N., Ichikawa Y., Ishihara M., Iwasaki H., Kameda D., Kishida T., Lisetskiy A., Ong H., Osada M., Ohtsuka T., Suzuki M., Ue K., Utsuno Y., and Watanabe H.: “Gamow-Teller decay of the  $T = 1$  nucleus  $^{46}\text{Cr}$ ”, *Phys. Rev. C* **72**, No. 2, pp. 024308-1–024308-7 (2005). \*
- Ong H., Imai N., Aoi N., Sakurai H., Dombradi Z., Saito A., Elekes Z., Baba H., Demichi K., Fulop Z., Gibelin J., Gomi T., Hasegawa H., Ishihara M., Iwasaki H., Kanno S., Kawai S., Kubo T., Kurita K., Matsuyama Y., Michimasa S., Minemura T., Motobayashi T., Notani M., Ota S., Sakai H., Shimoura S., Takeshita E., Takeuchi S., Tamaki M., Togano Y., Yamada K., Yanagisawa Y., and Yoneda K.: “Inelastic proton scattering on  $^{16}\text{C}$ ”, *Eur. Phys. J. A* **25**, No. s01, pp. 347–348 (2006). \*
- Togano Y., Gomi T., Motobayashi T., Ando Y., Aoi N., Baba H., Demichi K., Elekes Z., Fukuda N., Fulop Z., Futakami U., Hasegawa H., Higurashi Y., Ieki K., Imai N., Ishihara M., Ishikawa K., Iwasa N., Iwasaki H., Kanno S., Kondo Y., Kubo T., Kubono S., Kunibu M., Kurita K., Matsuyama Y., Michimasa S., Minemura T., Miura M., Murakami H., Nakamura T., Notani M., Ota S., Saito A., Sakurai H., Serata M., Shimoura S., Sugimoto T., Takeshita E., Takeuchi S., Ue K., Yamada K., Yanagisawa Y., Yoneda K., and Yoshida A.: “Study of the  $^{26}\text{Si}(p, \gamma)^{27}\text{P}$  reaction through Coulomb dissociation of  $^{27}\text{P}$ ”, *Eur. Phys. J. A* **27**, No. s01, pp. 233–236 (2006). \*
- Elekes Z., Dombradi Z., Bishop S., Fulop Z., Gibelin J., Gomi T., Hashimoto Y., Imai N., Iwasa N., Iwasaki H., Kalinka G., Kondo Y., Korshennikov A. A., Kurita K., Kurokawa M., Matsui N., Motobayashi T., Nakamura T., Nakao T., Nikolski E. Y., Ohnishi T., Okumura T., Ota S., Perera P., Saito A., Sakurai H., Satou Y., Sohler D., Sumikama T., Suzuki D., Suzuki M., Takeda H., Takeuchi S., Togano Y., and Yanagisawa Y.: “Testing of the RIKEN-ATOMKI CsI(Tl) array in the study of  $^{22,23}\text{O}$  nuclear structure”, *Eur. Phys. J. A* **27**, No. s01, pp. 321–324 (2006). \*
- Gomi T., Motobayashi T., Ando Y., Aoi N., Baba H., Demichi K., Elekes Z., Fukuda N., Fulop Z., Futakami U., Hasegawa H., Higurashi Y., Ieki K., Imai N., Ishihara M., Ishikawa K., Iwasa N., Iwasaki H., Kanno S., Kondo Y., Kubo T., Kubono S., Kunibu M., Kurita K., Matsuyama Y., Michimasa S., Minemura T., Miura M., Murakami H., Nakamura T., Notani M., Ota S., Saito A., Sakurai H., Serata M., Shimoura S., Sugimoto T., Takeshita E., Takeuchi S., Ue K., Yamada K., Yanagisawa Y., Yoneda K., and Yoshida A.: “Coulomb Dissociation of  $^{23}\text{Al}$  for the stellar  $^{22}\text{Mg}(p, \gamma)^{23}\text{Al}$  reaction”, *Nucl. Phys. A* **758**, 761c–764c (2006).
- Elekes Z., Dombradi Z., Saito A., Aoi N., Baba H., Demichi K., Fulop Z., Gibelin J., Gomi T., Hasegawa H., Imai N., Ishihara M., Iwasaki H., Kanno S., Kawai S., Kishida T., Kubo T., Kurita K., Matsuyama Y., Michimasa S., Minemura T., Motobayashi T., Notani M., Ohnishi T., Ong H., Ota S., Ozawa A., Sakai H., Sakurai H., Shimoura S., Takeshita E., Takeuchi S., Tamaki M., Togano Y., Yamada K., Yanagisawa Y., and Yoneda K.: “Proton inelastic scattering studies at the borders of the “island of inversion”: The  $^{30,31}\text{Na}$  and  $^{33,34}\text{Mg}$  case”, *Phys. Rev. C* **73**, 044314-1–044314-5 (2006). \*
- Elekes Z., Dombradi Z., Aoi N., Bishop S., Fulop Z., Gibelin J., Gomi T., Hashimoto Y., Imai N., Iwasa N., Iwasaki H., Kalinka G., Kondo Y., Korshennikov A. A., Kurita K., Kurokawa M., Matsui N., Motobayashi T., Nakamura T., Nakao T., Nikolski E. Y., Ohnishi T., Okumura T., Ota S., Perera P., Saito A., Sakurai H., Satou Y., Sohler D., Sumikama T., Suzuki D., Suzuki M., Takeda H., Takeuchi S., Togano Y., and Yanagisawa Y.: “Search for neutron decoupling in  $^{22}\text{O}$  via the  $(d, d'\gamma)$  reaction”, *Phys. Rev. C* **74**, 017306-1–017306-3 (2006). \*
- Yamaguchi T., Ohnishi T., Suzuki T., Becker T., Fukuda M., Geissel H., Hosoi M., Janik R., Kelic A., Kimura K., Mandel S., Muenzenberg G., Nakajima S., Ohtsubo T., Ozawa A., Prochazka A., Shindo M., Sitar B., Strmen P., Suda T., Summerer K., Sugawara K., Szarka I., Takechi M., Takisawa A., and Tanaka K.: “Production cross sections of isotopes formed by fragmentation of similar to 1A (GeVKr)-Kr-80 beam”, *Phys. Rev. C* **74**, 044608-1–044608-5 (2006). \*
- Dombradi Z., Elekes Z., Saito A., Aoi N., Baba H., Demichi K., Fulop Z., Gibelin J., Gomi T., Hasegawa H., Imai N., Ishihara M., Iwasaki H., Kanno S., Kawai S., Kishida T., Kubo T., Kurita K., Matsuyama Y., Michimasa S., Minemura T., Motobayashi T., Notani M., Ohnishi T., Ong H., Ota S., Ozawa A., Sakai H., Sakurai H., Shimoura S., Takeshita E., Takeuchi S., Tamaki M., Togano Y., Yamada K., Yanagisawa Y., and Yoneda K.: “Vanishing  $N = 20$  Shell Gap: Study of Excited States in  $^{27,28}\text{Ne}$ ”, *Phys. Rev. Lett.* **96**, 182501-1–182501-4 (2006). \*

- Nakamura T., Vinodkumar A., Sugimoto T., Aoi N., Baba H., Bazin D. P., Fukuda N., Gomi T., Hasegawa H., Imai N., Ishihara M., Kobayashi T., Kondo Y., Kubo T., Miura M., Motobayashi T., Otsu H., Saito A., Sakurai H., Shimoura S., Watanabe K., Watanabe Y., Yakushiji T., Yanagisawa Y., and Yoneda K.: “Observation of Strong Low-Lying E1 Strength in the Two-Neutron Halo Nucleus  $^{11}\text{Li}$ ”, *Phys. Rev. Lett.* **96**, 252502-1–252502-4 (2006). \*
- Yoshimi A., Ueno H., Kameda D., Asahi K., Nagae D., Takemura M., Shimada K., Takase K., Sugimoto T., Uchida M., Arai T., Inoue T., Murata J., and Kawamura H.: “Electric quadrupole moments of neutron rich Al isotope”, *AIP Conf. Proc.* **912**, 105–109 (2007). \*
- Murata J., Asahi K., Kameda D., Kawamura H., Nagae D., Narota K., Shimada K., Shimoyama T., Shuehiro T., Toyoda T., Uchida M., Ueno H., and Yoshimi A.: “Beta Neutrino Correlation and T-Violation Experiment in Nuclear Beta Decay”, *AIP Conf. Proc.* **915**, No. 1, pp. 218–221 (2007). \*
- Sakaguchi S., Uesaka T., Wakui T., Kawabata T., Aoi N., Hashimoto Y., Ichikawa M., Ichikawa Y., Itoh Y., Itoh M., Iwasaki H., Kawahara T., Kuboki H., Maeda Y., Matsuo R., Nakao T., Okamura H., Sakai H., Sakamoto N., Sasamoto Y., Sasano M., Satou Y., Sekiguchi K., Shinohara M., Suda K., Suzuki D., Takahashi Y., Tamii A., Yako K., and Yamaguchi M.: “Analyzing Power Measurement for Elastic Scattering of  $^6\text{He}$  on polarized protons”, *AIP Conf. Proc.* **915**, 833–836 (2007). \*
- Yoshimi A., Ueno H., Sugimoto T., Shimada K., Nagae D., Murata J., Kawamura H., Kameda D., and Asahi K.: “Developments of atomic beam resonance method with RI beams”, *AIP Conf. Proc.* **915**, 849–852 (2007). \*
- Kawamura H., Kameda D., Murata J., Narota K., Shimoyama T., Suehiro T., Toyoda T., and Uchida M.: “Development of a New Drift Chamber based Mott Polarimeter”, *AIP Conf. Proc.* **915**, 1105–1108 (2007). \*
- Elekes Z., Dombradi Z., Saito A., Aoi N., Baba H., Demichi K., Fulop Z., Gibelin J. D., Gomi T., Hasegawa H., Imai N., Ishihara M., Iwasaki H., Kanno S., Kawai S., Kishida T., Kubo T., Kurita K., Matsuyama Y., Michimasa S., Minemura T., Motobayashi T., Notani M., Ohnishi T., Ong H., Ota S., Ozawa A., Sakai H., Sakurai H., Shimoura S., Takeshita E., Takeuchi S., Tamaki M., Togano Y., Yamada K., Yanagisawa Y., and Yoneda K.: “Study of  $N=20$  shell gap with  $^1\text{H}(^{28}\text{Ne}, ^{27,28}\text{Ne})$  reactions”, *Eur. Phys. J. Special Topics* **150**, 99–102 (2007). \*
- Shimada K., Nagae D., Asahi K., Inoue T., Takase K., Kagami S., Hatakeyama N., Kobayashi Y., Ueno H., Yoshimi A., Kameda D., Nagatomo T., Sugimoto T., Kubono S., Yamaguchi H., Wakabayashi Y., Hayakawa S., Murata J., and Kawamura H.: “Production of spin-polarized  $^{17}\text{N}$  beam using inverse-kinematics low-energy transfer reactions”, *Hyperfine Interact.* **180**, 43–47 (2007). \*
- Yamaguchi T., Suzuki T., Ohnishi T., Nummerer S., Becker F., Fukuda M., Geissel H., Hosoi M., Janike R., Kimura K., Mandal S., Munzenberg G., Nakajima S., Ohtsubo T., Ozawa A., Orochazka A., Shindo M., Strmen P., Suda T., Sugawara K., Szarka I., Takisawa A., Takechi M., and Tanaka K.: “Nuclear radii of neutron-deficient Kr isotopes studied via their interaction cross-sections at relativistic energies”, *Nucl. Phys. A* **787**, 471c–475c (2007). \*
- Wakasa T., Ihara E., Fujita ., Funaki Y., Hatanaka K., Horiuchi H., Itoh M., Kamiya ., Roepke G., Sakaguchi H., Sakamoto ., Sakemi ., Schuck P., Shimizu Y., Takashina M., Terashima S., Suzuki A., Uchida M., Yoshida ., and Yosoi .: “New candidate for an alpha cluster condensed state in  $^{16}\text{O}$  ( $\alpha$ ,  $\alpha'$ ) at 400 MeV”, *Phys. Lett. B* **653**, 173–177 (2007). \*
- Fang D., Guo W., Ma. C., Wang K., Yang T., Ma. Y., Cai X., Shen W., Ren Z., Sun Z., Chen J., Tian W., Zhong C., Hosoi M., Izumikawa T., Kanungo R., Nakajima S., Ohnishi T., Ohtsubo T., Ozawa A., Suda T., Sugawara K., Suzuki T., Takisawa A., Tanaka K., Yamaguchi T., and Tanihata I.: “Examining the exotic structure of the proton-rich nucleus  $^{23}\text{Al}$ ”, *Phys. Rev. C* **76**, 031601-1–031601-5 (2007). \*
- Kameda D., Ueno H., Asahi K., Nagae D., Yoshimi A., Nagatomo T., Sugimoto T., Uchida M., Takemura M., Shimada K., Takase K., Inoue T., Kijima G., Arai T., Suda S., Murata J., Kawamura H., Kobayashi Y., Watanabe H., and Ishihara M.: “Production of spin-polarized radioactive ion beams via projectile fragmentation reaction”, *AIP Conf. Proc.* **980**, 283–288 (2008). \*
- Kameda D., Asahi K., Ueno H., Nagae D., Takemura M., Shimada K., Yoshimi A., Nagatomo T., Sugimoto T., Uchida M., Arai T., Takase K., Suda S., Inoue T., Murata J., Kawamura H., Watanabe H., Kobayashi Y., and Ishihara M.: “Electric quadrupole moments of neutron-rich nuclei  $^{32}\text{Al}$  and  $^{31}\text{Al}$ ”, *Hyperfine Interact.* **180**, 61–64 (2008). \*
- Yoshimi A., Inoue T., Uchida M., Hatakeyama N., and Asahi K.: “Optical-coupling nuclear spin maser under highly stabilized low static field”, *Hyperfine Interact.* **181**, 111–114 (2008). \*
- Sugimoto T., Asahi K., Kawamura H., Murata J., Nagae D., Shimada K., Ueno H., and Yoshimi A.: “Development of atomic-beam resonance method to measure the nuclear moments of unstable nuclei”, *Hyperfine Interact.* **181**, 141–144 (2008). \*
- Elekes Z., Dombradi Z., Aoi N., Baba H., Bishop S., Demichi K., Fulop Z., Gibelin J., Gomi T., Hasegawa H., Hashimoto Y., Imai N., Ishihara M., Iwasa N., Iwasaki H., Kalinka G., Kanno S., Kawai S., Kishida

- T., Kondo Y., Korshennikov A. A., Kubo T., Kurita K., Kurokawa M., Matsui N., Matsuyama Y., Michimasa S., Minemura T., Motobayashi T., Nakamura T., Nakao T., Nikolski E. Y., Notani M., Ohnishi T., Okumura T., Ong H., Ota S., Ozawa A., Perera P., Saito A., Sakai H., Sakurai H., Satou Y., Shimoura S., Sohler D., Sumikama T., Suzuki D., Suzuki M., Takeda H., Takeshita E., Takeuchi S., Tamaki M., Togano Y., Yamada K., Yanagisawa Y., and Yoneda K.: “The study of shell closures in light neutron-rich nuclei”, *J. Phys. G* **35**, 014038-1–014038-7 (2008).
- Sato W., Ueno H., Watanabe H., Miyoshi H., Yoshimi A., Kameda D., Ito T., Shimada K., Kaihara J., Suda S., Kobayashi Y., Shinohara A., Ohkubo Y., and Asahi K.: “Temperature-dependent behavior of impurity atoms implanted in highly oriented pyrolytic graphite –An application of a new online TDPAC method–”, *J. Phys. Soc. Jpn.* **77**, No. 9, pp. 095001-1–095001-2 (2008). \*
- Nagae D., Ueno H., Kameda D., Takemura M., Asahi K., Yoshimi A., Sugimoto T., Shimada K., Nagatomo T., Uchida M., Arai T., Inoue T., Kagami S., Hatakeyama N., Murata J., Kawamura H., and Narota K.: “Electric quadrupole moment of  $^{31}\text{Al}$ ”, *Nucl. Instrum. Methods Phys. Res. B* **266**, 4612–4615 (2008). \*
- Ueno H., Nagae D., Kameda D., Asahi K., Takemura M., Takase K., Yoshimi A., Sugimoto T., Shimada K., Nagatomo T., Uchida M., Arai T., Inoue T., Murata J., Kawamura H., and Narota K.: “Electric quadrupole moment of  $^{31}\text{Al}$ ”, *Nucl. Phys. A* **805**, 329–331 (2008). \*
- Aoi N., Suzuki H., Takeshita E., Takeuchi S., Ota S., Baba H., Bishop S., Fukui T., Hashimoto Y., Ong H., Ideguchi E., Ieki K., Imai N., Iwasaki H., Kanno S., Kondo Y., Kubo T., Kurita K., Kusaka K., Minemura T., Motobayashi T., Nakabayashi T., Nakamura T., Nakao T., Niikura M., Okumura T., Ohnishi T., Sakurai H., Shimoura S., Sugo R., Suzuki D., Suzuki M., Tamaki M., Tanaka K., Togano Y., and Yamada K.: “Shape transition observed in neutron-rich pf-shell isotopes studied via proton inelastic scattering”, *Nucl. Phys. A* **805**, 400c–407c (2008).
- Sakaguchi S., Uesaka T., Wakui T., Kawabata T., Aoi N., Hashimoto Y., Ichikawa M., Itoh Y., Itoh M., Iwasaki H., Kawahara T., Kuboki H., Maeda Y., Matsuo R., Nakao T., Okamura H., Sakai H., Sakamoto N., Sasamoto Y., Sasano M., Satou Y., Sekiguchi K., Shinohara M., Suda K., Suzuki D., Takahashi Y., Tamii A., Yako K., and Yamaguchi M.: “Spin-orbit potential in  $^6\text{He}$  studied with polarized proton target”, *Nucl. Phys. A* **805**, 467–469 (2008). \*
- Suzuki D., Iwasaki H., Ong H., Imai N., Sakurai H., Nakao T., Aoi N., Baba H., Bishop S., Ichikawa Y., Ishihara M., Kondo Y., Kubo T., Kurita K., Motobayashi T., Nakamura T., Okumura T., Onishi T., Ota S., Suzuki M., Takeuchi S., Togano Y., and Yanagisawa Y.: “Lifetime measurements of excited states in  $^{17}\text{C}$ : Possible interplay between collectivity and halo effects”, *Phys. Lett. B* **666**, 222–227 (2008). \*
- Mizuno T., Tsuchida H., Majima T., Nakai Y., and Itoh A.: “Multiple ionization of  $\text{C}_{60}$  by fast  $\text{Si}^{q+}$  ions”, *Phys. Rev. A* **78**, No. 5, pp. 053202-1–053202-6 (2008). \*
- Zegers R. G., Brown E. F., Akimune H., Austin S. M., van den Berg A. M., Brown B. A., Chamulak D. A., Fujita Y., Fujiwara M., Gales S., Harakeh M. N., Hashimoto H., Hayami R., Hitt G. W., Itoh M., Kawabata T., Kawase K., Kinoshita M., Nakanishi K., Nakayama S., Okumura S., Shimbara Y., Uchida M., Ueno H., Yamagata T., and Yosoi M.: “Gamow-Teller strength for the analog transitions to the first  $T = 1/2$ ,  $J^\pi = 3/2^-$  states in  $^{13}\text{C}$  and  $^{13}\text{N}$  and the implications for type Ia supernovae”, *Phys. Rev. C* **77**, 024307-1–024307-10 (2008). \*
- Yamaguchi T., Suzuki T., Ohnishi T., Becker F., Fukuda M., Geissel H., Hosoi M., Janik R., Kimura K., Kuboki T., Mandel S., Matsuo M., Muenzenberg G., Nakajima S., Ohtsubo T., Ozawa A., Prochazka A., Shindo M., Sitar B., Strmen P., Suda T., Suemmerer K., Sugawara K., Szarka I., Takechi M., Takisawa A., Tanaka K., and Yamagami M.: “Nuclear matter radii of neutron-deficient Kr isotopes”, *Phys. Rev. C* **77**, 034315-1–034315-6 (2008). \*
- Ong H., Imai N., Suzuki D., Iwasaki H., Sakurai H., Onishi T., Suzuki M., Ota S., Takeuchi S., Nakao T., Togano Y., Kondo Y., Aoi N., Baba H., Bishop S., Ichikawa Y., Ishihara M., Kubo T., Kurita K., Motobayashi T., Nakamura T., Okumura T., and Yanagisawa Y.: “Lifetime measurements of first excited states in  $^{16,18}\text{C}$ ”, *Phys. Rev. C* **78**, 014308-1–014308-11 (2008). \*
- Wakasugi M., Emoto T., Furukawa Y., Ishii K., Ito S., Koseki T., Kurita K., Kuwajima A., Masuda T., Morikawa A., Nakamura M., Noda A., Ohnishi T., Shirai T., Suda T., Takeda H., Tamae T., Tongu H., Wang S., and Yano Y.: “Novel Internal Target for Electron Scattering off Unstable Nuclei”, *Phys. Rev. Lett.* **100**, 164801-1–164801-4 (2008). \*
- Ito M., Itagaki N., Sakurai H., and Ikeda K.: “Coexistence of covalent superdeformation and molecular resonances in an unbound region of  $^{12}\text{Be}$ ”, *Phys. Rev. Lett.* **100**, 182502-1–182502-4 (2008). \*
- Nakai Y., Nakano Y., Azuma T., Hatakeyama A., Kondo C., Komaki K., Yamazaki Y., Takada E., and Murakami T.: “Dressed atoms in flight through a periodic crystal field: X-VUV double resonance”, *Phys. Rev. Lett.* **101**, No. 11, pp. 113201-1–113201-4 (2008). \*
- Nakatsukasa T., Matsuo M., Matuyanagi K., and Hinohara N.: “Microscopic derivation of collective Hamiltonian by means of the adiabatic self-consistent collective coordinate method”, *Prog. Theor. Phys.* **119**, No. 1, pp. 59–101 (2008). \*
- Elekes Z., Dombradi Z., Aiba T., Aoi N., Baba H.,

- Bemmerer D., Brown B., Furumoto T., Fulop Z., Iwasa N., Kiss A. B., Kobayashi T., Kondo Y., Motobayashi T., Nakabayashi T., Nannichi T., Sakuragi H., Sakurai H., Sohler D., Takashina M., Takeuchi S., Tanaka K., Togano Y., Yamada K., Yamaguchi M., and Yoneda K.: “Persistent decoupling of valence neutrons toward the dripline: study of  $^{20}\text{C}$  by  $\gamma$  spectroscopy”, *Phys. Rev. C* **79**, 011302-1–011302-5 (2009). \*
- Nagae D., Ueno H., Kameda D., Takemura M., Asahi K., Takase K., Yoshimi A., Sugimoto T., Shimada K., Nagatomo T., Uchida M., Arai T., Inoue T., Kagami S., Hatakeyama N., Kawamura H., Narota K., and Murata J.: “Ground-state electric quadrupole moment of  $^{31}\text{Al}$ ”, *Phys. Rev. C* **79**, 027301-1–027301-4 (2009). \*
- Aoi N., Takeshita E., Suzuki H., Takeuchi S., Ota S., Baba H., Bishop S., Fukui T., Hashimoto Y., Ong H., Ideguchi E., Ieki K., Imai N., Ishihara M., Iwasaki H., Kanno S., Kondo Y., Kubo T., Kurita K., Kusaka K., Minemura T., Motobayashi T., Nakabayashi T., Nakamura T., Nakao T., Niikura M., Okumura T., Ohnishi T., Sakurai H., Shimoura S., Sugo R., Suzuki D., Suzuki M., Tamaki M., Tanaka K., Togano Y., and Yamada K.: “Development of Large Deformation in  $^{62}\text{Cr}$ ”, *Phys. Rev. Lett.* **102**, 012502-1–012502-4 (2009). \*
- (Others)
- Murata J., Akiyama T., Hata M., Hirayama Y., Ikeda Y., Ishii T., Kameda D., Kawamura H., Mitsuoka S., Miyatake H., Nagae D., Ninomiya K., Nitta M., Seitaibashi E., and Toyoda T.: “R&D for a test of time reversal symmetry experiment using polarized nuclei”, *JAEA-Review* **2008-054**, 58–59 (2008).
- [Book • Proceedings]**
- (Original Papers) \*Subject to Peer Review
- Baba H., Ichihara T., Ohnishi T., Takeuchi S., Yoshida K., Watanabe Y., Ota S., and Shimoura S.: “The New DAQ System in RIKEN RIBF”, 2008 IEEE Nuclear Science Symposium Conference Record, Dresden, Germany, 2008–10, IEEE, Dresden, pp. 1384–1386 (2008). \*
- Oral Presentations**
- (International Conference etc.)
- Sugimoto S., Nakamura T., Fukuda N., Miura M., Kondo Y., Aoi N., Baba H., Bazin D. P., Gomi T., Hasegawa H., Hashimoto Y., Imai N., Kobayashi T., Kubo T., Motobayashi T., Shinohara M., Saito A., Sakurai H., Shimoura S., A.M. V., Watanabe K., Watanabe Y., T. Y., Yanagisawa Y., Yoneda K., and Ishihara M.: “Breakup Reactions of Halo Nuclei”, 1st Tokyo Tech Physics COE Symposium on Spin and Quantum Structure in Hadrons, Nuclei and Atoms (SQS04), Tokyo, Feb. (2004).
- Sugimoto S., Nakamura T., Fukuda N., Miura M., Kondo Y., Aoi N., Baba H., Bazin D. P., Gomi T., Hasegawa H., Hashimoto Y., Imai N., Kobayashi T., Kubo T., Motobayashi T., Shinohara M., Saito A., Sakurai H., Shimoura S., A.M. V., Watanabe K., Watanabe Y., T. Y., Yanagisawa Y., Yoneda K., and Ishihara M.: “Invariant-Mass Spectroscopy of  $^{14}\text{Be}$  with a Carbon Target at 68.1 AMeV”, 2nd Joint Meeting of the Nuclear Physics Divisions of the APS and JPS (Hawaii 2005), Maui, USA, Sept. (2005).
- Kondo Y., Nakamura T., Sato Y., Aoi N., Endo N., Fukuda N., Gomi T., Hashimoto Y., Ishihara M., Kawai S., Kitayama M., Kobayashi T., Matsuda Y., Matsui N., Motobayashi T., Nakabayashi T., Okumura T., Ong H., Onishi T., Otsu H., Sakurai H., Shimoura S., Shinohara M., Sugimoto T., Takeuchi S., Tamaki M., Togano Y., and Yanagisawa Y.: “Invariant mass spectroscopy of  $^{13}\text{Be}$  and  $^{14}\text{Be}$  via the proton-induced breakup reactions of  $^{14}\text{Be}$ ”, 5th International Workshop on Direct Reaction with Exotic Beams (DREB2007), Wako, May–June (2007).
- Kanno S., Aoi N., Bazin D., Bowen M. D., Campbell C. M., Cook J. M., Dinca D., Gade A., Glasmacher T., Iwasaki H., Kubo T., Kurita K., Motobayashi T., Mueller W. F., Nakamura T., Sakurai H., Suzuki H., Takeuchi S., Terry J. R., Yoneda K., and Zwahlen H.: “Weakening of  $Z=28$  shell closure in  $^{74}\text{Ni}$ ”, 5th International Workshop on Direct Reaction with Exotic Beams (DREB2007), (RIKEN Nishina Center, Kyushu University, Center for Nuclear Study (University of Tokyo)), wako, May–June (2007).
- Takeuchi S., Aoi N., Baba H., Fukui T., hashimoto ., Ieki K., Imai K., Iwasaki H., Kanno S., Kondo Y., Kubo T., Kurita K., Minemura T., Motobayashi T., Nakabayashi T., Nakamura T., Okumura T., Onishi T., Ota S., Sakurai H., Shimoura S., Sugo R., Suzuki D., Suzuki H., Suzuki M., Takeshita E., Tamaki M., Tanaka K., Togano Y., and Yamada K.: “Collectivity in  $^{32}\text{Mg}$  : a study of low-lying states”, International Nuclear Physics Conference (INPC2007), Tokyo, June (2007).
- Yoshimi A., Asahi K., Inoue T., Uchida M., and Hatakeyama N.: “Optical-coupling nuclear spin maser and search for an atomic EDM of  $^{129}\text{Xe}$ ”, International Nuclear Physics Conference (INPC2007), (Science Council of Japan, RIKEN and others), Tokyo, June (2007).
- Nagatomo T., Matsuta K., Minamisono K., Levy C. D., Sumikama T., Mihara M., Ozawa A., Tagisi Y., Ogura M., Matsumiya R., Fukuda M., Yamaguchi M., Behr J. A., Jackson K. P., Yasuno T., Ohta H., Hashizume Y., Fujiwara H., Chiba A., and Minamisono T.: “Search for the  $G$  parity violating term in weak nucleon currents in mass 20 system”, International Nuclear Physics Conference (INPC2007), (Science Council of Japan, RIKEN and others), Tokyo, June (2007).
- Kameda D., Ueno H., Asahi K., Nagae D., Takemura M., Yoshimi A., Shimada K., Uchida M., Kijima G., Arai T., Takase K., Suda S., Inoue T., Murata J., Kawamura H., Haseyama T., Kobayashi Y., Watanabe H., and Ishihara

- M.: “Small electric quadrupole moment of  $^{32}\text{Al}$ : Drastic shape transition between  $^{32}\text{Al}$  and  $^{31}\text{Mg}$ ”, International Nuclear Physics Conference (INPC2007), (Science Council of Japan, RIKEN and others), Tokyo, June (2007).
- Imai N., Ong H., Aoi N., Sakurai H., Demichi K., Kawasaki H., Baba H., Dombradi Z., Elekes Z., Fukuda N., Fulop Z., Gelberg A., Gomi T., Hasegawa H., Ishikawa K., Iwasaki H., Kaneko E., Kanno S., Kishida T., Kondo Y., Kubo T., Kurita K., Michimasa S., Minemura T., Miura M., Motobayashi T., Nakamura T., Notani M., Onishi T., Saito A., Shimoura S., Sugimoto T., Suzuki M., Takeshita E., Takeuchi S., Tamaki M., Yamada K., Yoneda K., Watanabe H., and Ishihara M.: “The lifetime measurement of the first  $2^+$  state in  $^{12}\text{Be}$ ”, International Nuclear Physics Conference (INPC2007), Tokyo, June (2007).
- Kanno S., Aoi N., Bazin D., Bowen M. D., Campbell C. M., Cook J. M., Dinca D., Gade A., Glasmacher T., Iwasaki H., Kubo T., Kurita K., Motobayashi T., Mueller W. F., Nakamura T., Sakurai H., Suzuki H., Takeuchi S., Terry J. R., Yoneda K., and Zwahlen H.: “Weakening of  $Z=28$  shell closure in  $^{74}\text{Ni}$ ”, International Nuclear Physics Conference (INPC2007), (Science Council of Japan, RIKEN and others), Wako, June (2007).
- Kondo Y., Nakamura T., Sato Y., Aoi N., Endo N., Fukuda N., Gomi T., Hashimoto Y., Ishihara M., Kawai S., Kitayama M., Kobayashi T., Matsuda Y., Matsui N., Motobayashi T., Nakabayashi T., Okumura T., Ong H., Onishi T., Otsu H., Sakurai H., Shimoura S., Shinohara M., Sugimoto T., Takeuchi S., Tamaki M., Togano Y., and Yanagisawa Y.: “Invariant mass spectroscopy of  $^{13}\text{Be}$  and  $^{14}\text{Be}$  via the proton-induced breakup reactions”, International Symposium & School on Frontiers and Perspectives of Nuclear and Hadron Physics (FPNH07), (Tokyo Institute of Technology), Tokyo, June (2007).
- Kameda D., Ueno H., Asahi K., Nagae D., Takemura M., Yoshimi A., Shimada K., Uchida M., Kijima G., Arai T., Takase K., Suda S., Inoue T., Murata J., Kawamura H., Haseyama T., Kobayashi Y., Watanabe H., and Ishihara M.: “Small electric quadrupole moment of  $^{32}\text{Al}$ ”, International Workshop on Nuclear Structure: New Pictures in the Extended Isospin Space (NS07), (Yukawa Institute for Theoretical Physics), Kyoto, June (2007).
- Nagatomo T., Matsuta K., Minamisono K., Sumikama T., Mihara M., Ozawa A., Tagisi Y., Ogura M., Matsumiya R., Fukuda M., Yamaguchi M., Yasuno T., Ohta H., Hashizume Y., Fujiwara H., Chiba A., and Minamisono T.: “Beta-ray Angular Distribution from Purely Nuclear Spin Aligned  $^{20}\text{F}$  Nuclei”, 14th International Conference on Hyperfine Interactions and 18th International Symposium on Nuclear Quadrupole Interactions, (Universidad Nacional de La Plata/Instituto de Fisica de La Plata, CONICET), Iguassu Falls, Brazil, Aug. (2007).
- Kameda D., Ueno H., Asahi K., Nagae D., Takemura M., Yoshimi A., Shimada K., Nagatomo T., Sugimoto T., Uchida M., Arai T., Takase K., Suda S., Inoue T., Murata J., Kawamura H., Watanabe H., Kobayashi Y., and Ishihara M.: “Electric quadrupole moments of neutron-rich nuclei  $^{32}\text{Al}$  and  $^{31}\text{Al}$ ”, 14th Int. Conf. on Hyperfine Interactions & 18th Int. Symp. on Nuclear Quadrupole Interactions, ( Universidad Nacional de La Plata), Iguassu Falls, Brazil, Aug. (2007).
- Kameda D., Ueno H., Asahi K., Nagae D., Yoshimi A., Nagatomo T., Sugimoto T., Uchida M., Takemura M., Shimada K., Takase K., Inoue T., Kijima G., Arai T., Suda S., Murata J., Kawamura H., Kobayashi Y., Watanabe H., and Ishihara M.: “Production of spin-polarized r/a beams via projectile fragmentation reaction”, 12th Int. Workshop on Polarized Sources, Targets & Polarimetry, (Brookhaven National Laboratory), Brookhaven, USA, Sept. (2007).
- Nagatomo T., Matsuta K., Minamisono K., Levy C. D., Sumikama T., Mihara M., Ozawa A., Tagisi Y., Ogura M., Matsumiya R., Fukuda M., Yamaguchi M., Behr J. A., Jackson K. P., Yasuno T., Ohta H., Hashizume Y., Fujiwara H., Chiba A., and Minamisono T.: “Search for the  $G$  parity violating term in weak nucleon currents in mass 20 system”, 12th Int. Workshop on Polarized Sources, Targets & Polarimetry, (Brookhaven National Laboratory ), Brookhaven, USA, Sept. (2007).
- Kondo Y., Motobayashi T., Sakurai H., Aoi N., Otsu H., Yanagisawa Y., Fukuda N., Takeuchi S., Ishihara M., Baba H., Gomi T., Imai N., Kubo T., Yoneda K., Nakamura T., Sato Y., Sugimoto T., Matsui N., Attukalathil V. M., Okumura T., Hashimoto Y., Nakabayashi T., Shinohara M., Miura M., Kobayashi T., Matsuda Y., Endo N., Kitayama M., Watanabe K., Yakushiji T., Togano Y., Kawai S., Hasegawa H., Onishi T., Ong H., Shimoura S., Tamaki M., Saito A., Bazin D. P., and Watanabe Y.: “Breakup reactions of  $^{14}\text{Be}$ ”, Future Prospects for Spectroscopy and Direct Reactions 2008, (Michigan State University), East Lansing, USA, Feb. (2008).
- Takeuchi S., Aoi N., Baba H., Fukui T., hashimoto ., Ieki K., Imai K., Iwasaki H., Kanno S., Kondo Y., Kubo T., Kurita K., Minemura T., Motobayashi T., Nakabayashi T., Nakamura T., Okumura T., Onishi T., Ota S., Sakurai H., Shimoura S., Sugo R., Suzuki D., Suzuki H., Suzuki M., Takeshita E., Tamaki M., Tanaka K., Togano Y., and Yamada K.: “Low-lying states in  $^{32}\text{Mg}$ ”, Future Prospects for Spectroscopy and Direct Reactions 2008, East Lansing, USA, Feb. (2008).
- Nakai Y., Majima T., Mizuno T., Tsuchida H., and Itoh A.: “Fragment ion formation of  $\text{C}_{60}$  induced by charge changing collisions of  $400\text{keV Au}^+$  ions”, 7th International Symposium Swift Heavy Ions in Matter (SHIM2008), (Universite Claude Bernard Lyon 1), Lyon,

- France, June (2008).
- Mizuno T., Yamada T., Nakai Y., Tsuchida H., and Itoh A.: “Ionization and fragmentation of CO molecule induced by charge-changing collisions of 2 MeV  $\text{Si}^{2+}$  ions”, 7th International Symposium Swift Heavy Ions in Matter (SHIM2008), (Universite Claude Bernard Lyon 1), Lyon, France, June (2008).
- Yoshimi A., Ueno H., Nagatomo T., Shimada K., Ichikawa Y., Kameda D., Sugimoto T., Sakurai H., Asahi K., Hasama Y., Takemura M., Kijima G., Nagae D., Uchida M., Arai T., Suda S., Takase T., Inoue T., Hatakeyama N., Kagami S., Murata J., and Kawamura H.: “Nuclear electromagnetic moments of neutron-rich Al isotopes”, Nuclear Structure 2008, (Michigan State University, NSCL at MSU), Michigan, USA, June (2008).
- Inoue T., Asahi K., Kagami S., Hatakeyama N., Uchida M., and Yoshimi A.: “Nuclear spin maser for  $^{129}\text{Xe}$  atomic EDM measurement -present status-”, 24th Advanced Studies Institute :Symmetries and Spin (SPIN-Praha-2008), (Charles University), Praha, Czech, July (2008).
- Kawamura H., Murata J., Toyoda T., Seitaibashi E., Nitta M., Hata M., Akiyama T., Ikeda Y., Ninomiya K., Kameda D., Nagae D., and Hirayama Y.: “The first T-violation experiment at KEK-TRIAC”, 24th Advanced Studies Institute :Symmetries and Spin (SPIN-Praha-2008), (Charles University in Prague, Faculty of Mathematics and Physics), Praha, Czech, July (2008).
- Nakano Y., Metoki K., Takano Y., Hatakeyama A., Nakai Y., Azuma T., Komaki K., Yamazaki Y., Takada E., and Murakami T.: “Selective formation of multiply excited states by resonant coherent excitation”, 14th International Conference on the Physics of Highly Charged Ions (HCI2008), (The University of Electro-Communications), Chofu, Sept. (2008).
- Mizuno T., Yamada T., Nakai Y., Tsuchida H., and Itoh A.: “Structure deformation dynamics of acetylene molecules following electron loss and capture collisions of 6MeV  $\text{O}^{4+}$  ions”, 14th International Conference on the Physics of Highly Charged Ions (HCI2008), (The University of Electro-Communications), Chofu, Sept. (2008).
- Yamaguchi T., Arai I., Ozawa A., Yasuda Y., Fujinawa T., Fukunishi N., Goto A., Hara K., Ohnishi T., Sakurai H., Wakasugi M., Yamaguchi Y., Yano Y., Kikuchi T., Suzuki T., and Ohtsubo T.: “Beam optics simulation for rare-RI ring at RI beam factory in RIKEN”, 7th International Conference on Nuclear Physics at Storage Rings STORI’08, (Institute of Modern Physics, Chinese Academy of Sciences, National Natural Foundation of China), Lanzhou, China, Sept. (2008).
- Yoshimi A., Asahi K., Inoue T., Uchida M., Hatakeyama N., and Kagami S.: “Nuclear spin maser at highly stabilized low magnetic field and search for an atomic EDM”, 18th International Symposium on Spin Physics (SPIN 2008), (University of Virginia), Charlottesville, USA, Oct. (2008).
- Asahi K.: “Nuclear Structure Studies with Polarized Radioactive Beams”, 18th International Symposium on Spin Physics (SPIN 2008), (University of Virginia), Charlottesville, USA, Oct. (2008).
- Baba H., Ichihara T., Ohnishi T., Takeuchi S., Yoshida K., Watanabe Y., Ota S., and Shimoura S.: “The New DAQ System in RIKEN RIBF”, 2008 Nuclear Science Symposium, Medical Imaging Conference and 16th Room Temperature Semiconductor Detector Workshop, Dresden, Germany, Oct. (2008).
- Kondo Y., Nakamura T., Sato Y., Matsumoto T., Aoi N., Endo N., Fukuda N., Gomi T., Hashimoto Y., Ishihara M., Kawai S., Kitayama M., Kobayashi T., Matsuda Y., Matsui N., Motobayashi T., Nakabayashi T., Ogata K., Okumura T., Ong H., Onishi T., Otsu H., Sakurai H., Shimoura S., Shinohara M., Sugimoto T., Takeuchi S., Tamaki M., Togano Y., and Yanagisawa Y.: “Invariant-mass spectroscopy of neutron-rich Be isotopes”, Unbound Nuclei Workshop, (INFN), Pisa, Italy, Nov. (2008).
- Kondo Y., Nakamura T., Sato Y., Matsumoto T., Aoi N., Endo N., Fukuda N., Gomi T., Hashimoto Y., Ishihara M., Kawai S., Kitayama M., Kobayashi T., Matsuda Y., Matsui N., Motobayashi T., Nakabayashi T., Ogata K., Okumura T., Ong H., Onishi T., Otsu H., Sakurai H., Shimoura S., Shinohara M., Sugimoto T., Takeuchi S., Tamaki M., Togano Y., and Yanagisawa Y.: “Breakup reactions of  $^{14}\text{Be}$ ”, International Conference on Interfacing Structure and Reactions at the Centre of the Atom (Kernz08), (Livermore and University of Surrey), Queenstown, The Netherlands, Dec. (2008).
- (Domestic Conference)
- 今井伸明, 青井考, 王惠仁, 櫻井博儀, 出道仁彦, Kawasaki H., 馬場秀忠, Dombradi Z., Elekes Z., 福田直樹, Fulop Z., Gelberg A., 五味朋子, 長谷川浩一, 石川和宏, 岩崎弘典, 金子恵美, 菅野祥子, 岸田隆, 近藤洋介, 久保敏幸, 栗田和好, 道正新一郎, 峯村俊行, 三浦宗賢, 本林透, 中村隆司, 野谷将広, 大西健夫, 齋藤明登, 下浦享, 杉本崇, Suzuki M., 竹下英里, 武内聡, 玉城充, 山田一成, 米田健一郎, 渡邊寛, 石原正泰: “ $^{12}\text{Be}$  と  $^{16}\text{C}$  における第一励起状態から基底状態への換算転移確率”, 日本物理学会第 58 回年次大会, 仙台, 3 月 (2003).
- 杉本崇, 中村隆司, 福田直樹, 三浦元隆, 近藤洋介, 青井考, 今井伸明, 久保敏幸, 小林俊雄, 五味朋子, 齋藤明登, 櫻井博儀, 下浦享, Bazin D. P., 長谷川浩一, 馬場秀忠, A.M. V., 本林透, T. Y., 柳澤善行, 米田健一郎, 渡辺極之, 渡辺裕, 石原正泰: “「 $^{17}\text{B}$  の分解反応 (2) 」”, 日本物理学会第 58 回年次大会, 仙台, 3 月 (2003).
- 今井伸明, 王惠仁, 青井考, 櫻井博儀, 出道仁彦, Kawasaki H., 馬場秀忠, Dombradi Z., Elekes Z., 福田直樹, Fulop Z., Gelberg A., 五味朋子, 長谷川浩一, 石川和宏, 岩崎弘典, 金子恵美, 菅野祥子, 岸田隆, 近藤洋介, 久保敏幸, 栗田和好, 道正新一郎, 峯村俊行, 三浦宗賢, 本林透, 中村隆司, 野谷将広, 大西健夫, 齋藤明登, 下浦享, 杉本崇, Suzuki M., 竹下

- 英里, 武内聡, 玉城充, 山田一成, 米田健一郎, 渡邊寛, 石原正泰: “Anomalously long lifetime of  $2+1$  state of  $^{16}\text{C}$ ”, A New Era of Nuclear Structure Physics, 新潟県黒川村, 11月(2003).
- 杉本崇, 中村隆司, 福田直樹, 三浦元隆, 近藤洋介, 青井考, 馬場秀忠, Bazin D. P., 五味朋子, 長谷川浩一, 橋本佳子, 今井伸明, 小林俊雄, 久保敏幸, 本林透, 篠原摩有子, 齋藤明登, 櫻井博儀, 下浦亨, A.M. V., 渡辺極之, 渡辺裕, 薬師寺崇, 柳澤善行, 米田健一郎, 石原正泰: “Invariant-mass spectroscopy of  $^{13}\text{Be}$ ”, 日本物理学会第59回年次大会, 福岡, 3月(2004).
- 杉本崇, 中村隆司, A.M. V., 福田直樹, 三浦元隆, 近藤洋介, 青井考, 馬場秀忠, Bazin D. P., 五味朋子, 長谷川浩一, 橋本佳子, 今井伸明, 小林俊雄, 久保敏幸, 本林透, 篠原摩有子, 齋藤明登, 櫻井博儀, 下浦亨, 渡辺極之, 渡辺裕, 薬師寺崇, 柳澤善行, 米田健一郎, 石原正泰: “Invariant-Mass Spectroscopy of Unbound  $^{11}\text{Li}$ ,  $^{13}\text{Be}$ , and  $^{17}\text{B}$  Nuclei”, 東京工業大学21世紀COEプログラム「量子ナノ物理学」第1回公開シンポジウム, 東京, 3月(2004).
- 今井伸明, 王患仁, 青井考, 櫻井博儀, 出道仁彦, Kawasaki H., 馬場秀忠, Dombardi Z., Elekes Z., 福田直樹, Fulop Z., Gelberg A., 五味朋子, 長谷川浩一, 石川和宏, 岩崎弘典, 金子恵美, 菅野祥子, 岸田隆, 近藤洋介, 久保敏幸, 栗田和好, 道正新一郎, 峯村俊行, 三浦宗賢, 本林透, 中村隆司, 野谷将広, 大西健夫, 齋藤明登, 下浦亨, 杉本崇, Suzuki M., 竹下英里, 武内聡, 玉城充, 山田一成, 米田健一郎, 渡邊寛, 石原正泰: “Experimental finding of the anomalous quadrupole collectivity in unstable nucleus  $^{16}\text{C}$ ”, 日本物理学会2005年秋季大会, (日本物理学会), 京田辺, 9月(2005).
- 今井伸明, 王患仁, 青井考, 櫻井博儀, 出道仁彦, Kawasaki H., 馬場秀忠, Dombardi Z., Elekes Z., 福田直樹, Fulop Z., Gelberg A., 五味朋子, 長谷川浩一, 石川和宏, 岩崎弘典, 金子恵美, 菅野祥子, 岸田隆, 近藤洋介, 久保敏幸, 栗田和好, 道正新一郎, 峯村俊行, 三浦宗賢, 本林透, 中村隆司, 野谷将広, 大西健夫, 齋藤明登, 下浦亨, 杉本崇, Suzuki M., 竹下英里, 武内聡, 玉城充, 山田一成, 米田健一郎, 渡邊寛, 石原正泰: “Lifetime measurement of  $^{12}\text{Be}(2+1)$ ”, 日本物理学会2005年秋季大会, (日本物理学会), 京田辺, 9月(2005).
- 菅野祥子, 青井考, Bazin D., Bowen M. D., Campbell C. M., Cook J. M., Dinca D., Gade A., Glasmacher T., 岩崎弘典, 久保敏幸, 栗田和好, 本林透, Mueller W. F., 中村隆司, 櫻井博儀, 鈴木宏, 武内聡, Terry J. R., 米田健一郎, Zwahlen H.: “Proton core polarization in neutron-rich nucleus  $^{74}\text{Ni}$ ”, Workshop on Advance in Physics with ISOL-based/Fragmentation-based RI Beams, (TITECH), 東京, 2月(2008).
- 近藤洋介, 中村隆司, 佐藤義輝, 杉本崇, 松井信行, 奥村俊文, 橋本佳子, 中林彩, 篠原摩有子, 青井考, 遠藤奈津美, 福田直樹, 五味朋子, 河合祥子, 來山益久, 小林俊雄, 松田洋平, 本林透, 王患仁, 大西健夫, 大津秀暁, 櫻井博儀, 下浦亨, 武内聡, 玉城充, 梶野泰宏, 柳澤善行, 石原正泰: “ $^{18,19}\text{C}$ の一中性子分離反応”, 日本物理学会第63回年次大会, 東大阪, 3月(2008).
- 山上雅之, 清水良文: “中性子スキンの陽子対相関への影響と対相関有効相互作用の拡張”, 日本物理学会第63回年次大会, 東大阪, 3月(2008).
- 森口哲朗, 橋爪祐平, 保谷毅, 小川賢一郎, 安田裕介, 原かおる, 小沢顕, 久保木隆正, 吉竹利織, 斎藤和哉, 三浦宗賢, 中島真平, 山口貴之, 鈴木健, 大坪隆, 山口由高, 金澤光高, 北川敦志, 佐藤眞二: “重イオンビームによる Hybrid Photo Detector の時間分解能の測定”, 日本物理学会第63回年次大会, 東大阪, 3月(2008).
- 中井陽一: “宇宙空間からの電離放射線の成層圏大気への影響: 実験室実験で何か判れるのか”, 「高度制御量子ビームによる応用研究の創出」- 2007年度UTTACの最新研究成果と動向-, (筑波大学), つくば, 3月(2008).
- 五十嵐誠, 望月優子, 高橋和也, 中井陽一, 本山秀明: “火山噴火記録から推定した南極ドームふじコアの堆積年代 1.1260AD~現在”, 日本地球惑星科学連合2008年大会, (日本地球惑星科学連合), 千葉, 5月(2008).
- 古川武, 松尾由賀利, 畠山温, 風戸正行, 星野紗代, 佐々木彩子, 涌井崇志, 上野秀樹, 吉見彰洋, 青井考, 武智麻耶, 梶野泰宏, 小林徹, 和田道治, 高峰愛子, 藤掛浩太郎, 松浦佑一, 小田原厚子, 下田正, 篠塚勉, 本林透: “超流動ヘリウム液体中に植え込まれた不安定同位体原子のレーザー分光実験”OROCHI”, 第5回AMO討論会, 八王子, 6月(2008).
- 市原卓, 渡邊康, 四日市悟, 中村智昭, 延與秀人: “GridFTPを使用したPHENX実験の日米間のデータ転送”, 広帯域ネットワーク利用に関するワークショップ(ADVNET2008), (ADVNET2008実行委員会, 国立情報学研究所 SINET), 東京, 7月(2008).
- 松尾由賀利, 古川武, 畠山温, 風戸正行, 星野紗代, 佐々木彩子, 涌井崇志, 上野秀樹, 青井考, 吉見彰洋, 武智麻耶, 梶野泰宏, 小林徹, 和田道治, 園田哲, 高峰愛子, 藤掛浩太郎, 松浦佑一, 小田原厚子, 下田正, 篠塚勉, 本林透: “超流動ヘリウム中エキゾチックRI原子の新奇なレーザー分光法(OROCHI法): 不安定核Rb原子の超微細構造精密測定へ向けて”, 東北大学・CYRIC研究会 Fundamental Physics using Atoms, (東北大学CYRIC), 仙台, 8月(2008).
- 近藤洋介, 中村隆司, 佐藤義輝, 松本琢磨, 青井考, 遠藤奈津美, 福田直樹, 五味朋子, 橋本佳子, 石原正泰, 河合祥子, 來山益久, 小林俊雄, 松田洋平, 松井信行, 本林透, 中林彩, 緒方一介, 奥村俊文, 王患仁, 大西健夫, 大津秀暁, 櫻井博儀, 下浦亨, 篠原摩有子, 杉本崇, 武内聡, 玉城充, 梶野泰宏, 柳澤善行: “ $^{18,19}\text{C}$ の一中性子分離反応”, RCNP研究会「RCNPにおける不安定核の研究: RCNPビームラインの可能性を探る」, (大阪大学核物理研究センター), 大阪, 8月(2008).
- 古川武, 松尾由賀利, 畠山温, 風戸正行, 星野紗代, 佐々木彩子, 涌井崇志, 上野秀樹, 青井考, 吉見彰洋, 武智麻耶, 梶野泰宏, 小林徹, 和田道治, 園田哲, 高峰愛子, 藤掛浩太郎, 松浦佑一, 小田原厚子, 下田正, 篠塚勉, 本林透: “理研”OROCHI”実験計画: 超流動ヘリウムを利用した短寿命不安定核のレーザー核分光”, RCNP研究会「RCNPにおける不安定核の研究: RCNPビームラインの可能性を探る」, 茨木, 8月(2008).
- 内田誠, 井上壮志, 旭耕一郎, 各務惣太, 畠山直人, 吉見彰洋: “核スピンメーザー開発の現状と今後の課題”, 東北大

- 学 CYRIC 研究会「Fundamental Physics using Atoms」, (東北大学 CYRIC), 仙台, 8 月 (2008).
- 吉見彰洋, 旭耕一郎, 内田誠, 井上壮志, 畠山直人, 各務惣太: “核スピンメーザーを用いた  $^{129}\text{Xe}$  原子 EDM の探索”, 東北大学 CYRIC 研究会「Fundamental Physics using Atoms」, (東北大学 CYRIC), 仙台, 8 月 (2008).
- 井上壮志, 吉見彰洋, 内田誠, 畠山直人, 旭耕一郎: “原子 EDM 測定のための  $^{129}\text{Xe}$  核スピンメーザーの開発”, 日本物理学会 2008 年秋季大会, (日本物理学会), 山形, 9 月 (2008).
- 島田健司, 長友傑, 旭耕一郎, Balabanski D. L., Daugas J. M., Depuydt M., De Rydt M., Gaudefroy L., Grevy S., 挾間優佳, 市川雄一, 亀田大輔, Morel P., Perrot L., Stodel C., Thomas J. C., Vanderheyolen W., Vermeulen N., Vingerhoets P., 吉見彰洋, Neyens G., 上野秀樹: “ $^{33}\text{Al}$  の電気四重極モーメント”, 日本物理学会 2008 年秋季大会, (山形大学, 日本物理学会), 山形, 9 月 (2008).
- 安田裕介, 新井一郎, 小沢顕, 森口哲朗, 大西哲哉, 櫻井博儀, 福西暢尚, 藤縄雅, 矢野安重, 山口由高, 若杉昌徳, 原かおる, 鈴木健, 山口貴之, 大坪隆, 菊池崇志: “理研希少 RI リング建設にむけての高精度磁場測定”, 日本物理学会 2008 年秋季大会, 盛岡, 9 月 (2008).
- 古川武, 松尾由賀利, 畠山温, 風戸正行, 星野紗代, 佐々木彩子, 涌井崇志, 上野秀樹, 青井考, 吉見彰洋, 武智麻耶, 梶野泰宏, 小林徹, 和田道治, 園田哲, 高峰愛子, 藤掛浩太郎, 松浦佑一, 小田原厚子, 下田正, 篠塚勉, 本林透: “超流動ヘリウム中における短寿命核のレーザー核分光実験計画『OROCHI』の現状”, 日本物理学会 2008 年秋季大会, (日本物理学会), 山形, 9 月 (2008).
- 豊田健司, 秋山岳伸, 秦麻記, 平山賀一, 池田友樹, 亀田大輔, 川村広和, 村田次郎, 長江大輔, 二宮一史, 新田稔, 聖代橋悦子: “TRIAC における時間反転対称性の破れ探索実験”, 日本物理学会 2008 年秋季大会, 山形, 9 月 (2008).
- 市川雄一, 久保敏幸, 青井考, Banerjee S. R., Chakrabarti A., 福田直樹, 岩崎弘典, 久保野茂, 本林透, 中林彩, 中村隆司, 中尾太郎, 奥村俊文, 王恵仁, 大西健夫, 鈴木大介, 鈴木賢, 山田一成, 山口英斉, 櫻井博儀: 日本物理学会 2008 年秋季大会, 山形, 9 月 (2008).
- 長友傑, 南園啓, 松多健策, 三原基嗣, 松宮亮平, 小倉昌子, 福田光順, 小沢顕, 田岸義宏, 山口充孝, 安野琢磨, 太田寛史, 橋爪祐平, 炭竈聡之, Levy C. D., Behr J. A., Jackson K. P., 南園忠則: “質量数 20 体系の鏡映核対のベータ線角度分布の精密測定による  $G$  変換対称性の研究”, 日本物理学会 2008 年秋季大会, (山形大学, 日本物理学会), 山形, 9 月 (2008).
- 岸田隆: “価値観の共有と科学コミュニケーション”, 総研大研究会, (総合研究大学院大学), 東京, 9 月 (2008).
- 五十嵐誠, 中井陽一, 望月優子, 高橋和也, 本山秀明, 牧島一夫: “火山噴火記録から推定した南極ドームふじ浅層コアの堆積年代: 1260 AD~現在”, 雪氷研究大会 (2008・東京), (日本雪氷学会), 東京, 9 月 (2008).
- 五十嵐誠, 高橋和也, 中井陽一, 望月優子, 本山秀明: “南極ドームふじ浅層コア中に含まれる極微量溶存成分の年変動”, 日本分析化学会第 57 年会, (日本分析化学会), 福岡, 9 月 (2008).
- 望月優子: “宇宙における元素創成の基礎知識”, 東京工業大  
学大学院「材料を知る」セミナー, (東京工業大学), 東京, 10 月 (2008).
- 五十嵐誠, 中井陽一, 高橋和也, 牧島一夫, 鈴木啓助, 本山秀明: “南極ドームふじ浅層コア中に含まれる極微量溶存成分の年変動”, 日本陸水学会第 73 回大会, (日本陸水学会), 札幌, 10 月 (2008).
- 松尾由賀利, 古川武, 畠山温, 風戸正行, 山口杏子, 星野紗代, 佐々木彩子, 涌井崇志, 上野秀樹, 青井考, 吉見彰洋, 武智麻耶, 梶野泰宏, 西村俊二, 小林徹, 和田道治, 園田哲, 高峰愛子, 藤掛浩太郎, 松浦佑一, 小田原厚子, 下田正, 篠塚勉, 本林透: “超流動ヘリウムを用いたレーザー核分光実験『OROCHI』-第一回ビーム実験へ向けて-, 第 5 回停止・低速不安定核ビームを用いた核分光研究会, 豊中, 12 月 (2008).
- 川村広和, 秋山岳伸, 石井哲朗, 池田友樹, 亀田大輔, 聖代橋悦子, 豊田健司, 長江大輔, 新田稔, 二宮一史, 秦麻記, 平山賀一, 光岡真一, 宮武宇也, 村田次郎, 渡辺裕: “TRIAC における偏極不安定核を用いた時間反転対称性破れの探索”, 第 5 回停止・低速不安定核ビームを用いた核分光研究会, (大阪大学), 豊中, 12 月 (2008).
- 市川雄一, 久保敏幸, 青井考, Banerjee S. R., Chakrabarti A., 福田直樹, 岩崎弘典, 久保野茂, 本林透, 中林彩, 中村隆司, 中尾太郎, 奥村俊文, 王恵仁, 大西健夫, 鈴木大介, 鈴木賢, 山田一成, 山口英斉, 櫻井博儀: 第 5 回停止・低速不安定核ビームを用いた核分光研究会, (大阪大学), 豊中, 12 月 (2008).
- 佐々木彩子, 星野紗代, 涌井崇志, 古川武, 風戸正行, 山口杏子, 和田道治, 園田哲, 高峰愛子, 小林徹, 上野秀樹, 吉見彰洋, 青井考, 西村俊二, 梶野泰宏, 武智麻耶, 畠山温, 藤掛浩太郎, 松浦佑一, 小田原厚子, 下田正, 本林透, 篠塚勉, 松尾由賀利: “超流動ヘリウム中でのレーザー核分光に向けた蛍光検出系の開発”, 日本物理学会第 64 回年次大会, 東京, 3 月 (2009).
- 古川武, 藤掛浩太郎, 畠山温, 小林徹, 松浦佑一, 佐々木彩子, 星野紗代, 涌井崇志, 風戸正行, 山口杏子, 和田道治, 園田哲, 高峰愛子, 上野秀樹, 吉見彰洋, 青井考, 西村俊二, 梶野泰宏, 武智麻耶, 小田原厚子, 下田正, 篠塚勉, 本林透, 松尾由賀利: “超流動ヘリウム中での光ポンピング法を用いた Ag 原子の高偏極生成とレーザー核分光への応用”, 日本物理学会第 64 回年次大会, 東京, 3 月 (2009).
- 風戸正行, 古川武, 山口杏子, 梶野泰宏, 西村俊二, 佐々木彩子, 星野紗代, 涌井崇志, 畠山温, 藤掛浩太郎, 松浦佑一, 篠塚勉, 本林透, 小田原厚子, 下田正, 松尾由賀利: “超流動ヘリウム中における RI ビーム停止位置の精密制御”, 日本物理学会第 64 回年次大会, 東京, 3 月 (2009).
- 川村広和, 秋山岳伸, 秦麻記, 平山賀一, 池田友樹, 亀田大輔, 宮原直亮, 宮武宇也, 村田次郎, 中谷祐輔, 長江大輔, 二宮一史, 新田稔, 大西潤一, 聖代橋悦子, 豊田健司, 塚田和司, 渡辺裕: “TRIAC における偏極  $^8\text{Li}$  を用いた時間反転対称性破れの探索”, 日本物理学会第 64 回年次大会, 東京, 3 月 (2009).
- 二宮一史, 秋山岳伸, 池田友樹, 小川成也, 川村広和, 関口雄太, 筒井亮丞, 秦麻記, 村田次郎: “NewtonII 号による等価原理検証を目指した近距離重力実験”, 日本物理学会第 64 回年次大会, 東京, 3 月 (2009).

Publications

[Journal]

(Original Papers) \*Subject to Peer Review

- Guimaraes V., Kubono S., F.C. B., M. H., S.C. J., Katayama I., Miyachi T., Nomura T., H.M. T., Fuchi Y., H. K., Kato S., Yun C., K. I., Orihara H., Terakawa A., Kishida T., Y. P., Hamada S., Hirai M., and Miyatake H.: “Structure of the Unbound  $^{11}\text{N}$  Nucleus by the ( $^3\text{He}$ ,  $^6\text{He}$ ) Reaction”, *Phys. Rev. C* **67**, 064601-1–064601-8 (2003). \*
- Elekes Z., Dombradi Z., Kanungo R., Baba H., Fulop Z., Gibelin J. D., Horvath A., Ideguchi E., Ichikawa Y., Iwasa N., Iwasaki H., Kanno S., Kawai S., Kondo Y., Motobayashi T., Notani M., Ohnishi T., Ozawa A., Sakurai H., Shimoura S., Takeshita E., Takechi M., Tanihata I., Togano Y., Wu C., Yamaguchi Y., Yanagisawa Y., Yoshida A., and Yoshida K.: “Low-lying excited states in  $^{17,19}\text{C}$ ”, *Phys. Lett. B* **614**, 174–180 (2005). \*
- Nakamura T., Vinodkumar A., Sugimoto T., Aoi N., Baba H., Bazin D. P., Fukuda N., Gomi T., Hasegawa H., Imai N., Ishihara M., Kobayashi T., Kondo Y., Kubo T., Miura M., Motobayashi T., Otsu H., Saito A., Sakurai H., Shimoura S., Watanabe K., Watanabe Y., Yakushiji T., Yanagisawa Y., and Yoneda K.: “Observation of Strong Low-Lying E1 Strength in the Two-Neutron Halo Nucleus  $^{11}\text{Li}$ ”, *Phys. Rev. Lett.* **96**, 252502-1–252502-4 (2006). \*
- Ishii Y., Toyoshima A., Tsukada K., Asai M., Toume H., Nishinaka I., Nagame Y., Miyashita S., Mori T., Sukanuma H., Haba H., Sakamaki M., Goto S., Kudo H., Akiyama K., Oura Y., Nakahara H., Tashiro T., Shinohara A., Schaedel M., Bruechle W., Pershina V., and Kratz J. V.: “Fluoride Complexation of Element 104, Rutherfordium (Rf), Investigated by Cation-exchange Chromatography”, *Chem. Lett.* **37**, No. 3, pp. 288–289 (2008). \*
- Haba H., Kikunaga H., Kaji D., Akiyama T., Morimoto K., Morita K., Nanri T., Ooe K., Sato N., Shinohara A., Suzuki D., Takabe T., Yamazaki I., Yokoyama A., and Yoneda A.: “Performance of the gas-jet transport system coupled to the RIKEN gas-filled recoil ion separator GARIS for the  $^{238}\text{U}(^{22}\text{Ne},^{5n})^{255}\text{No}$  reaction”, *J. Nucl. Radiochem. Sci.* **9**, No. 1, pp. 27–31 (2008). \*
- Sato W., Ueno H., Watanabe H., Miyoshi H., Yoshimi A., Kameda D., Ito T., Shimada K., Kaihara J., Suda S., Kobayashi Y., Shinohara A., Ohkubo Y., and Asahi K.: “Temperature-dependent behavior of impurity atoms implanted in highly oriented pyrolytic graphite –An application of a new online TDPAC method–”, *J. Phys. Soc. Jpn.* **77**, No. 9, pp. 095001-1–095001-2 (2008). \*
- Sakuma F., Enyo H., Fukao Y., Funahashi H., Hamagaki H., Kitaguchi M., Miwa K., Murakami T., Naruki M., Ozawa K., Sekimoto M., Tabaru T., Togawa M., Yokkaichi S., Chiba J., Kanda H., Ieiri M., Ishino M., Mihara S., Miyashita T., Muto R., Nakura T., Sasaki O., Tanaka K., Yamada S., and Yoshimura Y.: “Partial decay widths of the phi into  $e+e-$  and  $K+K-$  pairs in 12 GeV p+A reactions at KEK-PS E325”, *Mod. Phys. Lett. A* **23**, No. 27/30, pp. 2401–2404 (2008). \*
- Robinson A. P., Khoo T. L., Ahmad I., Tandel S. K., Kondev F. G., Nakatsukasa T., Asai M., Black B. B., Butler P. A., Carpenter M. P., Chowdhury P., Davids C. N., Eekhaudt S., Greene J. P., Greenlees P. T., Gros S., Heinz A., Herzberg R. D., Janssens R. V., Jones G. D., Lauritsen T., Lister C. J., Peterson D., Qian J., Reiter P., Seweryniak D., Tandel U., Wang X., and Zhu S.: “ $K^\pi = 8^-$  Isomers and  $K^\pi = 2^-$  Octupole Vibrations in  $N = 150$  shell-Stabilized Nuclei”, *Phys. Rev. C* **78**, 034308-1–034308-6 (2008). \*
- Toyoshima A., Haba H., Tsukada K., Asai M., Akiyama K., Goto S., Ishii Y., Nishinaka I., Sato T., Nagame Y., Sato W., Tani Y., Hasegawa H., Matsuo K., Saika D., Kitamoto Y., Shinohara A., Ito M., Saito J., Kudo H., Yokoyama A., Sakama M., Sueki K., Oura Y., Nakahara H., Schaedel M., Bruechle W., and Kratz J. V.: “Hexafluoro complex of rutherfordium in mixed HF/ $\text{HNO}_3$  solutions”, *Radiochim. Acta* **96**, 125–134 (2008). \*
- Toyoshima A., Kasamatu Y., Kitatsuji Y., Tsukada K., Haba H., Shinohara A., and Nagame Y.: “Development of an electrochemistry apparatus for the heaviest elements”, *Radiochim. Acta* **96**, 323–326 (2008). \*
- Kasamatu Y., Toyoshima A., Haba H., Toume H., Tsukada K., Akiyama K., Yoshimura T., and Nagame Y.: “Adsorption of Nb, Ta and Pa on anion-exchanger in HF and HF/ $\text{HNO}_3$  solutions: Model experiments for the chemical study of Db”, *J. Radioanal. Nucl. Chem.* **279**, 371–376 (2009). \*
- Tsukada K., Haba H., Asai M., Toyoshima A., Akiyama K., Kasamatu Y., Nishinaka I., Ichikawa S., Yasuda K., Miyamoto Y., Hashimoto K., Nagame Y., Goto S., Kudo H., Sato W., Shinohara A., Oura Y., Sueki K., Kikunaga H., Kinoshita N., Yokoyama A., Schaedel M., Bruechle W., and Kratz J. V.: “Adsorption of Db and its homologues Nb and Ta, and the pseudo-homologue Pa on anion-exchange resin in HF solution”, *Radiochim. Acta* **97**, 83–89 (2009). \*

(Review)

榎本秀一, 羽場宏光: “マルチレーザーの開発と利用”, *Isotope News*, pp. 9–15 (2008).

(Others)

Asai M., Tsukada K., Sakama M., Ishii Y., Toyoshima A., Ishii T., Nishinaka I., Nagame Y., Kasamatu Y., Shibata M., Hayashi H., Haba H., and Kojima Y.: “Alpha-gamma coincidence spectroscopy of  $^{259}\text{No}$ ”, *JAEA-Review* **2008-054**, 40–41 (2008).

Toyoshima A., Kasamatu Y., Tsukada K., Kitatsuji A., Haba H., Asai M., Ishii Y., Toume H., Akiyama K., Ooe

K., Sato W., Shinohara A., and Nagame Y.: "Oxidation of divalent nobelium (No) to the trivalent state using an electrochemistry apparatus", JAEA-Review **2008-054**, 63-64 (2008).

Kasamatu Y., Toyoshima A., Asai M., Tsukada K., Ishii Y., Toume H., Nishinaka I., Sato T., Nagame Y., Haba H., Kikunaga H., Akiyama K., Goto S., Ichikawa T., Kudo H., Sato W., Ooe K., Kuribayashi T., Shinohara A., Kinoshita N., Arai M., Yokoyama A., Sakama M., Qin Z., and Duellmann C. E.: "Adsorption of element 105, Db, on the anion-exchange resin in HF/HNO<sub>3</sub> media", JAEA-Review **2008-054**, 65-66 (2008).

### Oral Presentations

(International Conference etc.)

Toyoshima A., Kasamatu Y., Tsukada K., Kitatsuji A., Haba H., Asai M., Ishii Y., Toume H., Akiyama K., Ooe K., Sato W., Shinohara A., and Nagame Y.: "Electrochemical oxidation of element 102, nobelium", 2nd International Nuclear Chemistry Congress (2nd-INCC), (National University of Mexico), Cancun, Mexico, Apr. (2008).

Akiyama K., Haba H., Sueki K., Tsukada K., Asai M., Toyoshima A., Nagame Y., and Katada M.: "Metallofullerene Encapsulating <sup>225</sup>Ac", 2nd International Nuclear Chemistry Congress (2nd-INCC), (National University of Mexico), Cancun, Mexico, Apr. (2008).

Toyoshima A., Kasamatu Y., Tsukada K., Kitatsuji Y., Haba H., Ishii Y., Toume H., Asai M., Akiyama K., Ooe K., Sato W., Shinohara A., and Nagame Y.: "Characterization of heavy actinides with electrochemistry", Spring 2008 ACS National Meeting & Exposition, (American Chemical Society), USA, New Orleans, Apr. (2008).

Haba H.: "RIKEN GARIS for superheavy element chemistry", 7th Workshop on Recoil Separator for Superheavy Element Chemistry (TASCA 08), (GSI Helmholtzzentrum für Schwerionenforschung GmbH), Darmstadt, Germany, Oct. (2008).

(Domestic Conference)

中川孝秀, 木寺正憲, 羽場宏光, 藍原利光, 加瀬昌之, 後藤彰, 矢野安重: "理研 ECR イオン源での多価ウランイオンの生成", 第4回日本加速器学会年会・第32回リニアック技術研究会, 和光, 8月(2007).

羽場宏光: "超重元素化学研究に利用できる理研の実験設備", ワークショップ「超重元素化学研究の展望」, (Superheavy Element Laboratory), 和光, 8月(2007).

羽場宏光: "GARISを前段分離装置として用いた超重元素化学", ワークショップ「超重元素化学研究の展望」, (Superheavy Element Laboratory), 和光, 8月(2007).

佐藤望, 加治大哉, 森田浩介, 森本幸司, 羽場宏光, 米田晃, 菊永英寿, 市川隆敏, 秋山隆宏: "理研における新たな反跳分離装置の開発", 日本物理学会第62回年次大会, 札幌, 9月(2007).

佐藤望, 加治大哉, 森田浩介, 森本幸司, 羽場宏光, 米田晃, 菊永英寿, 市川隆敏, 秋山隆宏: "理研における新たな反跳

分離装置の開発", 第4回「停止・低速不安定核を用いた核分光研究」研究会, (東北大学, 理研仁科センター他), 仙台, 12月(2007).

羽場宏光: "超重元素化学研究に向けた理研加速器施設の準備状況", 京都大学原子炉実験所専門研究会「核化学・核物理の新領域としての重元素科学」, (京都大学原子炉実験所), 熊取, 12月(2007).

佐藤望, 加治大哉, 森田浩介, 森本幸司, 羽場宏光, 米田晃, 菊永英寿, 市川隆敏, 秋山隆宏: "理研における新たな反跳分離装置の開発", 京都大学原子炉実験所専門研究会「核化学・核物理の新領域としての重元素科学」, 大阪府熊取町, 12月(2007).

笠松良崇, 豊嶋厚史, 浅井雅人, 塚田和明, 羽場宏光, 石井康雄, 當銘勇人, 西中一朗, 秋山和彦, 菊永英寿, 後藤真一, 石川剛, 工藤久昭, 佐藤渉, 大江一弘, 栗林隆宏, 篠原厚, 木下哲一, 荒井美和子, 横山明彦, 阪間稔, 佐藤哲也, 永目諭一郎: "105番元素(Db)のHF/HNO<sub>3</sub>水溶液中での陰イオン交換樹脂への吸着挙動", 日本化学会第88春季年会, (The Chemical Society of Japan), 東京, 3月(2008).

大関和貴: "ヤング図形を用いたアイソスピン励起エネルギーの記述", RCNP研究会「RCNPにおける不安定核の研究: RCNPビームラインの可能性を探る」, (大阪大学核物理研究センター), 茨木, 8月(2008).

菊永英寿, 栗林隆宏, 吉村崇, 高橋成人, 篠原厚, 羽場宏光, 江崎豊, 榎本秀一, 三頭聡明: "α-HIBA/酢酸溶液中での電気泳動法によるランタニドおよびアメリカウム, キュリウム, カリホルニウムの錯安定度定数の導出と加速器実験への適用", 2008年日本放射化学学会年会/第52回放射化学討論会, (日本放射化学会), 広島, 9月(2008).

菊永英寿, 藤沢弘幸, 矢作亘, 篠原厚, 羽場宏光, 江崎豊, 笠松良崇, 廣瀬健太郎, 大槻勤: "ガスジェット運搬装置を用いた<sup>90m</sup>Nbの精密半減期測定", 2008年日本放射化学学会年会/第52回放射化学討論会, (日本放射化学会), 広島, 9月(2008).

工藤祐生, 羽場宏光, 大江一弘, 加治大哉, 森本幸司, 篠原厚, 森田浩介: "GARIS用回転式<sup>248</sup>Cm標的の作成", 2008年日本放射化学学会年会/第52回放射化学討論会, (日本放射化学会), 広島, 9月(2008).

大江一弘, 矢作亘, 小森有希子, 藤沢弘幸, 菊永英寿, 吉村崇, 佐藤渉, 高橋成人, 高久圭二, 羽場宏光, 工藤祐生, 江崎豊, 篠原厚: "106番元素シーボーギウムの化学実験に向けたタングステンの溶媒抽出挙動の研究", 2008年日本放射化学学会年会/第52回放射化学討論会, (日本放射化学会), 広島, 9月(2008).

南里朋洋, 荒木幹生, 西尾正樹, 羽場宏光, 江崎豊, 横山明彦: "Rf溶液化学のための極微量濃度におけるTIOAを用いた逆相クロマトグラフィーの研究", 2008年日本放射化学学会年会/第52回放射化学討論会, (日本放射化学会), 広島, 9月(2008).

藤沢弘幸, 大江一弘, 矢作亘, 小森有希子, 山玲央奈, 菊永英寿, 吉村崇, 高橋成人, 高久圭二, 羽場宏光, 江崎豊, 榎本秀一, 篠原厚: "<sup>238</sup>U(<sup>16</sup>O, 4n)<sup>250</sup>Fm反応によるFmの生成と溶媒抽出挙動", 2008年日本放射化学学会年会/第52回放射化学討論会, (日本放射化学会), 広島, 9月(2008).

佐藤望, 加治大哉, 森田浩介, 森本幸司, 羽場宏光, 米田晃,

菊永英寿, 大関和貴, 工藤祐生, 住田貴之: “理研における新たな反跳分離装置 GARIS-II の開発”, 日本物理学会 2008 年秋季大会, 山形, 9 月 (2008).

羽場宏光: “Present status of the superheavy element chemistry in the world -Reports on the TASC08 workshop-”, 理研超重元素化学ワークショップ 2008, 和光, 11 月 (2008).

羽場宏光: “RIKEN accelerator research facilities for superheavy element chemistry”, 理研超重元素化学ワークショップ 2008, 和光, 11 月 (2008).

羽場宏光: “Toward chemical studies of the superheavy elements”, アクチノイド元素実験棟利用研究会, 大洗, 2 月 (2009).

Publications

[Journal]

(Original Papers) \*Subject to Peer Review

- Otsu H., Kobayashi T., Matsuda Y., Kitayama M., Inafuku K., Ozawa A., Satou Y., Suda T., Yoshida K., and Sakaguchi H.: “Measurement of the H(38s,p’) reaction at forward angles including 0 degree”, Nucl. Phys. A **788**, 266c–270c (1997). \*
- Inakura T., Mizutori S., Yamagami M., and Matuyanagi K.: “Superdeformed Bands in Neutron-Rich Sulfur Isotopes suggested by Cranked Skyrme-Hartree-Fock Calculations”, Nucl. Phys. A **728**, 52–64 (2003). \*
- Kobayasi M., Nakatsukasa T., Matsuo M., and Matuyanagi K.: “Collective Path Connecting the Oblate and Prolate Local Minima in 68Se”, Prog. Theor. Phys. **112**, No. 2, pp. 363–368 (2004). \*
- Sakuragi H., Maenaka Y., and Furumoto T.: “Coupled-channels study of 10Be+4He structure of highly-excited 14C”, J. Phys.: Con. Ser. **111**, 012019-1–012019-6 (2007). \*
- Wakasa T., Ihara E., Fujita ., Funaki Y., Hatanaka K., Horiuchi H., Itoh M., Kamiya ., Roepke G., Sakaguchi H., Sakamoto ., Sakemi ., Schuck P., Shimizu Y., Takashina M., Terashima S., Suzuki A., Uchida M., Yoshida ., and Yosoi .: “New candidate for an alpha cluster condensed state in <sup>16</sup>O ( $\alpha$ ,  $\alpha'$ ) at 400 MeV”, Phys. Lett. B **653**, 173–177 (2007). \*
- Itagaki N., Kimura M., Kurokawa C., Ito M., and von Oertzen W.: “ $\alpha$  condensed state with a core nucleus”, Phys. Rev. C **75**, 0377303-1–0377303-4 (2007). \*
- Nakatsukasa T., Inakura T., and Yabana K.: “Finite amplitude method for the solution of the random-phase approximation”, Phys. Rev. C **76**, 024318-1–024318-9 (2007). \*
- Ito M. and Itagaki N.: “ $\alpha+^{6,8}\text{He}$  resonant scattering and exotic structures in <sup>10,12</sup>Be”, AIP Conf. Proc. **1016**, 199–204 (2008). \*
- Nakatsukasa T., Yabana K., and Ito M.: “Time-dependent approaches for reaction and response in unstable nuclei”, Eur. Phys. J. Special Topics **156**, 249–256 (2008). \*
- Ito M., Itagaki N., Sakurai H., and Ikeda K.: “Exotic molecular states in ht highly-excited states of <sup>10,12</sup>Be”, J. Phys.: Con. Ser. **111**, 012010-1–012010-6 (2008). \*
- Nakatsukasa T., Shinohara S., Ohta H., and Yabana K.: “Stochastic approach to correlation beyond the mean field with the Skyrme interaction”, Nucl. Phys. A **805**, 347–349 (2008). \*
- Yabana K., Ito M., and Nakatsukasa T.: “Time-dependent description for nuclear reaction dynamics in the continuum”, Nucl. Phys. A **805**, 428–430 (2008). \*
- Yamada T., Funaki Y., Horiuchi H., Roepke G., Schuck P., and Suzuki A.: “Criterion for Bose-Einstein condensation in traps and self-bound systems”, Phys. Rev. A **78**, 035603-1–035603-4 (2008). \*
- Otobe T., Yamagiwa M., Iwata J., Yabana K., Nakatsukasa T., and Bertsch G. F.: “First-principles electron dynamics simulation for optical breakdown of dielectrics under an intense laser field”, Phys. Rev. B **77**, 165104-1–165104-5 (2008). \*
- Sarhan B. A., Horiuchi W., Kohama A., and Suzuki Y.: “Reaction cross sections of carbon isotopes incident on a proton”, Phys. Rev. C **77**, No. 3, pp. 034607-1–034607-11 (2008). \*
- Yoshida K. and Yamagami M.: “Low-frequency  $K^\pi = 0^+$  modes in deformed neutron-rich nuclei: Pairing- and  $\beta$ -vibrational modes of neutrons”, Phys. Rev. C **77**, No. 4, pp. 044312-1–044312-9 (2008). \*
- Tanabe K. and Tanabe K. S.: “Selection rules for electromagnetic transitions in triaxially deformed odd-A nuclei”, Phys. Rev. C **77**, No. 6, pp. 064318-1–064318-11 (2008). \*
- Yamaguchi T., Suzuki T., Ohnishi T., Becker F., Fukuda M., Geissel H., Hosoi M., Janik R., Kimura K., Kuboki T., Mandel S., Matsuo M., Muenzenberg G., Nakajima S., Ohtsubo T., Ozawa A., Prochazka A., Shindo M., Sitar B., Strmen P., Suda T., Suemmerer K., Sugawara K., Szarka I., Takechi M., Takisawa A., Tanaka K., and Yamagami M.: “Nuclear matter radii of neutron-deficient Kr isotopes”, Phys. Rev. C **77**, 034315-1–034315-6 (2008). \*
- Itagaki N., Kokalova T., Ito M., Kimura M., and von Oertzen W.: “Coupling between  $\alpha$  condensed states and normal cluster states”, Phys. Rev. C **77**, 037301-1–037301-4 (2008). \*
- Funaki Y., Horiuchi H., Roepke G., Schuck P., Suzuki A., and Yamada T.: “Density-induced suppression of the  $\alpha$ -particle condensate in nuclear matter and the structure of  $\alpha$  cluster states in nuclei”, Phys. Rev. C **77**, 064312-1–064312-6 (2008). \*
- Yamagami M. and Shimizu Y.: “Pairing effects for rotational excitations unique to neutron-rich nuclei”, Phys. Rev. C **77**, 064319-1–064319-15 (2008). \*
- Itagaki N., Ito M., Milin M., Hashimoto T., Ishiyama H., and Miyatake H.: “Coexistence of  $\alpha+\alpha+n+n$  and  $\alpha+t+t$  cluster structures in <sup>10</sup>Be”, Phys. Rev. C **77**, 067301-1–067301-4 (2008). \*
- Yoshida K. and Nguyen V. G.: “Low-lying dipole resonance in neutron-rich Ne isotopes”, Phys. Rev. C **78**, No. 1, pp. 014305-1–014305-9 (2008). \*
- Furumoto T., Sakuragi H., and Yamamoto Y.: “New complex G-matrix interactions derived from two- and three-body forces and application to proton nucleus elastic scattering”, Phys. Rev. C **78**, No. 4, pp. 044610-1–044610-12 (2008). \*
- Kohama A., Iida K., and Oyamatsu K.: “Difference between interaction cross sections and reaction cross sections”, Phys. Rev. C **78**, No. 6, pp. 061601(R) -1–

- 061601(R) -5 (2008). \*
- Yoshida K. and Nguyen V.: “Deformed quasiparticle-random-phase approximation for neutron-rich nuclei using the Skyrme energy density functional”, *Phys. Rev. C* **78**, No. 6, pp. 064316-1–064316-10 (2008). \*
- Barbieri C., Caurier E., Langanke K., and Martinez-Pinedo G.: “Reply to ”Comment on ’Pygmy dipole response of proton-rich argon nuclei in random-phase approximation and no-core shell model’ ””, *Phys. Rev. C* **78**, No. 039802, (2008). \*
- Ito M. and Itagaki N.: “Covalent isomeric state in  $^{12}\text{Be}$  induced by two-neutron transfers”, *Phys. Rev. C* **78**, 011602(R)-1–011602(R)-5 (2008). \*
- Itagaki N., Ito M., Arai K., Aoyama S., and Kokalova T.: “Mixing of di-neutron components in  $^8\text{He}$ ”, *Phys. Rev. C* **78**, 017306-1–017306-4 (2008). \*
- Robinson A. P., Khoo T. L., Ahmad I., Tandel S. K., Kondev F. G., Nakatsukasa T., Asai M., Black B. B., Butler P. A., Carpenter M. P., Chowdhury P., Davids C. N., Eekhaudt S., Greene J. P., Greenlees P. T., Gros S., Heinz A., Herzberg R. D., Janssens R. V., Jones G. D., Lauritsen T., Lister C. J., Peterson D., Qian J., Reiter P., Seweryniak D., Tandel U., Wang X., and Zhu S.: “ $K^\pi = 8^-$  Isomers and  $K^\pi = 2^-$  Octupole Vibrations in  $N = 150$  hell-Stabilized Nuclei”, *Phys. Rev. C* **78**, 034308-1–034308-6 (2008). \*
- Ito M., Itagaki N., Sakurai H., and Ikeda K.: “Coexistence of covalent superdeformation and molecular resonances in an unboud region of  $^{12}\text{Be}$ ”, *Phys. Rev. Lett.* **100**, 182502-1–182502-4 (2008). \*
- Funaki Y., Yamada T., Horiuchi H., Roepke G., Schuck P., and Suzuki A.: “ $\alpha$ -particle condensation in  $^{16}\text{O}$  studied with a full four-body orthogonality condition model calculation”, *Phys. Rev. Lett.* **101**, 082502-1–082502-4 (2008). \*
- Nakatsukasa T., Matsuo M., Matuyanagi K., and Hinohara N.: “Microscopic derivation of collective Hamiltonian by means of the adiabatic self-consistent collective coordinate method”, *Prog. Theor. Phys.* **119**, No. 1, pp. 59–101 (2008). \*
- Ogasawara H., Yoshida K., Yamagami M., Mizutori S., and Matuyanagi K.: “Triaxiality dependence of octupole excitations on superdeformed states in  $^{44}\text{Ti}$ ”, *Prog. Theor. Phys.* **120**, No. 6, pp. 1169–1192 (2008). \*
- Yamada T., Funaki Y., Horiuchi H., Ikeda K., and Suzuki A.: “Monopole Excitation to Cluster States”, *Prog. Theor. Phys.* **120**, 1139–1167 (2008). \*
- Elekes Z., Dombradi Z., Aiba T., Aoi N., Baba H., Bemmerer D., Brown B., Furumoto T., Fulop Z., Iwasa N., Kiss A. B., Kobayashi T., Kondo Y., Motobayashi T., Nakabayashi T., Nannichi T., Sakuragi H., Sakurai H., Sohler D., Takashina M., Takeuchi S., Tanaka K., Togano Y., Yamada K., Yamaguchi M., and Yoneda K.: “Persistent decoupling of valence neutrons toward the dripline: study of  $^{20}\text{C}$  by  $\gamma$  spectroscopy”, *Phys. Rev. C* **79**, 011302-1–011302-5 (2009). \*
- Furumoto T., Sakuragi H., and Yamamoto Y.: “Three-body-force effect on nucleus-nucleus elastic scattering”, *Phys. Rev. C* **79**, 011601-1–011601-4 (2009). \*
- (Review)
- Funaki Y., Horiuchi H., Roepke G., Schuck P., Suzuki A., and Yamada T.: “Alpha particle condensation in nuclear systems”, *Nucl. Phys. News* **17**, No. 4, pp. 11–18 (2007).
- 中務孝: “人物・研究室紹介: 化学研究所仁科加速器研究センター原子核理論研究室”, *原子核研究* **53**, No. 2, pp. 3–10 (2008).
- (Others)
- Yamada T., Funaki Y., Horiuchi H., Tohsaki A., Roepke G., and Schuck P.: “Dilute Alpha-Particle Condensation in  $^{12}\text{C}$  and  $^{16}\text{O}$ ”, *Int. J. Mod. Phys. B* **22**, No. 25/26, pp. 4545–4556 (2008).
- Yamada T., Horiuchi H., Ikeda K., Funaki Y., and Suzuki A.: “Monopole excitation to cluster states”, *J. Phys.: Con. Ser.* **111**, 012008-1–012014-6 (2008).
- Funaki Y., Yamada T., Horiuchi H., Roepke G., Schuck P., and Suzuki A.: “Alpha-cluster states and 4 alpha-particle Bose condensate in  $^{16}\text{O}$ ”, *J. Phys.: Con. Ser.* **111**, 012012-1–012018-6 (2008).
- Funaki Y., Yamada T., Horiuchi H., Roepke G., Schuck P., and Suzuki A.: “Indication of  $4\alpha$ -particle Bose condensate in  $^{16}\text{O}$ ”, *Nucl. Phys. A* **805**, 236–238 (2008).
- Kohama A., Iida K., and Oyamatsu K.: “Reaction cross section and nuclear radius in the black-sphere picture”, *Nucl. Phys. A* **805**, 415–417 (2008).
- Horiuchi W., Sarhan B. A., Kohama A., and Suzuki Y.: “Reaction cross sections of carbon isotopes incident on proton and  $^{12}\text{C}$  target”, *Nucl. Phys. A* **805**, 418–420 (2008).
- Ito M. and Itagaki N.: “Nuclear Chemistry”, *Phys. Rev. Focus* **22**, No. Story 4, pp. 1–3 (2008).
- [Book • Proceedings]**
- (Original Papers) \*Subject to Peer Review
- Nakatsukasa T., Yabana K., and Inakura T.: “Linear response calculations with the time-dependent Skyrme density functional”, *Physics of Unstable Nuclei: Proceedings of International Symposium on Physics of Unstable Nuclei (ISPUN07)*, Hoi An, Vietnam, 2007–7, World Scientific, Singapore, pp. 195–200 (2008). \*
- (Others)
- Funaki Y., Yamada T., Schuck P., Horiuchi H., Suzuki A., and Roepke G.: “ $\alpha$ -cluster states and  $4\alpha$ -particle condensation in  $^{16}\text{O}$ ”, *Physics of Unstable Nuclei: Proceedings of International Symposium on Physics of Unstable Nuclei (ISPUN07)*, Hoi An, Vietnam, 2007–7, World Scientific, Singapore, pp. 380–385 (2008).
- Oral Presentations**
- (International Conference etc.)

- Kobayashi M., Nakatsukasa T., Matsuo M., and Matuyanagi K.: “Collective path connecting the oblate and prolate local minima in proton-rich  $N=Z$  nuclei around  $68\text{Se}$ ”, 4th International Conference on Exotic Nuclei and Atomic Masses (ENAM 04), Georgia, USA, Sept. (2004).
- Yamagami M.: “Di-neutron superfluidity and the collective motions in deformed weakly-bound nuclei”, International Workshop on Joint JUSTIPEN-LACM Meeting, (Oak Ridge National Laboratory), Oak Ridge, USA, Mar. (2007).
- Yamagami M.: “Rotational excitation of weakly-bound nuclei with di-neutron pairing”, ECT\* Sminars 2006: Many-body Open Quantum Systems: from Atomic Nuclei to Quantum Systems, Trento, Italy, May (2007).
- Yamagami M.: “Rotational motion in nuclei with di-neutron superfluidity”, International Nuclear Physics Conference (INPC2007), (Science Council of Japan, RIKEN and others), Tokyo, June (2007).
- Yamagami M.: “Di-neutron superfluidity and the collective motions in deformed unstable nuclei”, International Workshop on Nuclear Structure: New Pictures in the Extended Isospin Space (NS07), (Yukawa Institute for Theoretical Physics, Kyoto University), Kyoto, June (2007).
- Nakatsukasa T., Yabana K., and Inakura T.: “Dipole response calculations with Skyrme TDDFT”, UNEDF Annual Workshop, (University of Washington), Pack Forest, USA, Aug. (2007).
- Funaki Y., Yamada T., Horiuchi H., Roepke G., Schuck P., and Suzuki A.: “ $\alpha$ -cluster states and  $4\alpha$ -particle Bose condensate in  $^{16}\text{O}$ ”, Clusters '07, Stratford upon Avon, UK, Sept. (2007).
- Nakatsukasa T., Inakura T., and Yabana K.: “Nuclear response function calculated with the time-dependent Skyrme density functional”, 3rd Japanese-German Workshop on Nuclear Structure and Astrophysics, (GSI, Chiemsee, Germany, Sept.-Oct. (2007).
- Nakatsukasa T.: “Energy density functional in nuclei”, 1st FIDIPRO-JSPS Workshop on Energy Density Functional in Nuclei, (University of Jyvaskyla), Keurusselka, Finland, Oct. (2007).
- Nakatsukasa T.: “Photonuclear response studied with time-dependent methods”, Seminar at University of Surrey, (University of Surrey), Guildford, UK, Nov. (2007).
- Nakatsukasa T.: “Discussion Leader on Supercomputing in low-energy nuclear physics”, 2nd LACM-EFES-JUSTIPEN Workshop, (Oak Ridge National Laboratory), Oak Ridge, USA, Jan. (2008).
- Nakatsukasa T.: “Time-dependent approaches to nuclear many-body problems”, 2008 APCTP-BLTP JINR Joint Workshop on Quarks and Mesons in Nuclear Physics, (APCTP), Pohang, Korea, Apr. (2008).
- Yamagami M. and Shimizu Y.: “Continuum and pairing effects for rotational excitations in neutron rich nuclei”, CNS-RIKEN Joint International Symposium on Frontier of gamma-ray spectroscopy and Perspectives for Nuclear Structure Studies (Gamma08), Wako, Apr. (2008).
- Ito M. and Itagaki N.: “Unified studies of structural changes and nuclear reactions in  $^{10,12}\text{Be}$ ”, 1st Workshop on State of the Art in Nuclear Cluster Physics, Strasbourg I, France, May (2008).
- Funaki Y., Yamada T., Horiuchi H., Roepke G., Schuck P., and Suzuki A.: “Present status of alpha-particle condensate states in self-conjugate  $4n$  nuclei”, 1st Workshop on State of the Art in Nuclear Cluster Physics (SOTANCP 2008), Strasbourg, France, May (2008).
- Nakatsukasa T.: “Foundation and application of nuclear density functional theory”, Lecture at Department of Physics, Peking University, Beijing, China, May (2008).
- Nakatsukasa T.: “Nuclear Physics: Finite quantum many-body systems with strong interaction”, Lecture at Department of Physics, Peking University, Beijing, China, May (2008).
- Matsumoto T., Egami T., Ogata K., Iseri Y., and Yahiro M.: “Analyses for four-body breakup reactions of  $^6\text{He}$ ”, 50th Anniversary Symposium on Nuclear Sizes and Shapes, (University of Surrey), Surrey, UK, June (2008).
- Yoshida K.: “Low-lying excitation modes in deformed neutron-rich nuclei”, International Workshop on Nuclear Structure Physics, (China Nuclear Physics Society, Natural Science Foundation of China, Shanghai Jiao Tong University), Shanghai, China, June (2008).
- Barbieri C.: “Applications of propagator theory to atoms and nuclei”, Symposium on “50 Years of Coupled Cluster Theory”, (Institute for Nuclear theory), Seattle, USA, June–July (2008).
- Yamagami M. and Shimizu Y.: “Construction of pairing density functional for global description of pairing correlations”, Hokudai-TORIJIN-JUSTIPEN-EFES Workshop & JUSTIPEN-EFES-Hokudai-UNEDF Meeting, Nanae-cho, Hokkaido, July (2008).
- Matsumoto T., Egami T., Ogata K., Iseri Y., Yahiro M., and Kamimura M.: “Coupled-channel analyses of  $^6\text{He}$  breakup reactions”, Hokudai-TORIJIN-JUSTIPEN-EFES Workshop & JUSTIPEN-EFES-Hokudai-UNEDF Meeting, Sapporo, July (2008).
- Yoshida K.: “Deformed quasiparticle-random-phase approximation for neutron-rich nuclei using the Skyrme density functional”, Hokudai-TORIJIN-JUSTIPEN-EFES Workshop & JUSTIPEN-EFES-Hokudai-UNEDF Meeting, Morimachi, Hokkaido Pref., July (2008).
- Avogadro P., Barranco F. P., Broglia R. A., and Vigezzi E.: “Study of neutron vortices in the inner crust of a neutron star”, Hokudai-TORIJIN-JUSTIPEN-EFES Workshop & JUSTIPEN-EFES-Hokudai-UNEDF Meeting, (JUSTIPEN-EFES-Hokudai-UNEDF meeting, Hokudai-EFES-TORIJIN-JUSTIPEN meeting on Resonances and Continua), Nanae-cho, Hokkaido, July (2008).

- Barbieri C.: “Many-body correlations and exotic nuclei”, Hokudai-TORIJIN-JUSTIPEN-EFES Workshop: Perspectives in Resonances and Continua on Nuclei and JUSTIPEN-EFES-Hokudai-UNEDF Meeting, Hakodate, July (2008).
- Ito M. and Itagaki N.: “Covalent, Ionic, and Atomic Structures in  $^{10,12}\text{Be}$ ”, 4th Asia-Pacific Conference on Few-Body Problems in Physics (APFB08), (Universitas Indonesia), Depok, Indonesia, Aug. (2008).
- Nakatsukasa T.: “Time-dependent-density-functional theory”, 7th CNS-EFES Summer School (CNS-EFES08), (University of Tokyo), Wako, Aug.–Sept. (2008).
- Yoshida K.: “Self-consistent calculations for low-lying excitation modes in deformed neutron-rich nuclei using a Skyrme density functional”, 5th International Conference on Exotic Nuclei and Atomic Masses (ENAM 08), (University of Warsaw, Institute for Nuclear Studies, Swierk), Ryn, Poland, Sept. (2008).
- Ito M. and Itagaki N.: “Unified studies of the exotic structures of  $^{10,12}\text{Be}$  and the  $\alpha+^{6,8}\text{He}$  reactions”, Scientific Program for Fusion08, (Argonne National Laboratory), Chicago, USA, Sept. (2008).
- Funaki Y., Yamada T., Horiuchi H., Roepke G., Schuck P., and Suzuki A.: “ $\alpha$ -particle condensed state in  $^{16}\text{O}$ ”, Japanese French Symposium :New paradigms in Nuclear Physics, Paris, France, Sept.–Oct. (2008).
- Nakatsukasa T., Inakura T., and Yabana K.: “Response functions in the continuum of deformed nuclei studied with the time-dependent density-functional calculations”, Japanese French Symposium :New paradigms in Nuclear Physics, (JSPS-CNRS), Paris, France, Sept.–Oct. (2008).
- Funaki Y., Yamada T., Horiuchi H., Roepke G., Schuck P., and Suzuki A.: “Alpha clustering and condensation in  $^{16}\text{O}$ ”, KGU Yokohama Autumn School of Nuclear Physics, Yokohama, Oct. (2008).
- Matsumoto T., Egami T., Ogata K., Iseri Y., Yahiro M., and Kamimura M.: “Coupled-channel analyses of  $^6\text{He}$  breakup reactions”, KGU Yokohama Autumn School of Nuclear Physics, Yokohama, Oct. (2008).
- Nakatsukasa T.: “TDDFT approach to photoabsorption in even-even nuclei”, KGU Yokohama Autumn School on Nuclear Physics, (Kanto Gakuin University), Yokohama, Oct. (2008).
- Barbieri C.: “Asymmetry dependence of spectroscopic factors”, KGU(Kanto Gakuin University) Yokohama Autumn School of Nuclear Physics, (Kanto Gakuin University (KGU)), Yokohama, Oct. (2008).
- Ito M. and Itagaki N.: “Covalent Isomeric State in  $^{12}\text{Be}$  induced by Two-Neutron Transfers”, KGU(Kanto Gakuin University) Yokohama Autumn School of Nuclear Physics, (Kanto Gakuin University), Yokohama, Oct. (2008).
- Avogadro P., Barranco F. P., Broglia R. A., and Vigezzi E.: “Vortices in the inner crust of neutron stars”, KGU(Kanto Gakuin University) Yokohama Autumn School of Nuclear Physics, (KGU Kannai Media Center, Kanto Gakuin University (KGU)), Yokohama, Oct. (2008).
- Ito M.: “Unified description of structures and reactions based on microscopic models”, YIPQS International Molecule Workshop on “Alpha- and Dineutron-Correlation in Nuclear Many-Body Systems” Program, (Yukawa Institute of Theoretical Physics (YITP)), Kyoto, Oct. (2008).
- Barbieri C.: “Ab-initio Green’s Functions Calculations of Atoms”, 6th Japan-Italy Symposium on Heavy Ion Physics, (RICOTTI, Tokai), Tokai-mura, Ibaraki Pref., Nov. (2008).
- Avogadro P., Broglia R. A., Barranco F. P., and Vigezzi E.: “Interaction between neutron superfluid vortices and nuclei in neutron stars”, 6th Japan-Italy Symposium on Heavy-Ion Physics, Tokai-mura, Ibaraki Pref., Nov. (2008).
- Ito M.: “Exotic structures in  $^{12}\text{Be}$  and the  $\alpha+^8\text{He}$  resonant scattering”, Unbound Nuclei Workshop, (Istituto Nazionale di Fisica Nucleare, Sezione di Pisa), Pisa, Italy, Nov. (2008).
- Kondo Y., Nakamura T., Sato Y., Matsumoto T., Aoi N., Endo N., Fukuda N., Gomi T., Hashimoto Y., Ishihara M., Kawai S., Kitayama M., Kobayashi T., Matsuda Y., Matsui N., Motobayashi T., Nakabayashi T., Ogata K., Okumura T., Ong H., Onishi T., Otsu H., Sakurai H., Shimoura S., Shinohara M., Sugimoto T., Takeuchi S., Tamaki M., Togano Y., and Yanagisawa Y.: “Invariant-mass spectroscopy of neutron-rich Be isotopes”, Unbound Nuclei Workshop, (INFN), Pisa, Italy, Nov. (2008).
- Kondo Y., Nakamura T., Sato Y., Matsumoto T., Aoi N., Endo N., Fukuda N., Gomi T., Hashimoto Y., Ishihara M., Kawai S., Kitayama M., Kobayashi T., Matsuda Y., Matsui N., Motobayashi T., Nakabayashi T., Ogata K., Okumura T., Ong H., Onishi T., Otsu H., Sakurai H., Shimoura S., Shinohara M., Sugimoto T., Takeuchi S., Tamaki M., Togano Y., and Yanagisawa Y.: “Breakup reactions of  $^{14}\text{Be}$ ”, International Conference on Interfacing Structure and Reactions at the Centre of the Atom (Kernz08), (Livermore and University of Surrey), Queenstown, The Netherlands, Dec. (2008).
- Nakatsukasa T.: “Nuclear structure at the limits of rapid rotation, Large amplitude collective motion”, 20th Chris Engelbrecht Summer School in Theoretical Physics “Nuclei and Nucleonic Systems”, (National Institute for Theoretical Physics at Stellenbosch Institute for Advanced Study), Stellenbosch, South Africa, Jan. (2009).
- Barbieri C.: “Application of propagator theory to atoms and nuclei”, 1st EMMI-EFES Workshop on Neutron-Rich Nuclei (EENEN 09), (GSI), Darmstadt, Germany, Feb. (2009).

- Ito M.: "Future studies on nuclear structures and reactions with microscopic cluster model and UCOM", 1st EMMI-EFES Workshop on Neutron-Rich Nuclei (EENEN 09), (GSI Laboratory), Darmstadt, Germany, Feb. (2009).
- Yamagami M.: "Density functional for description of novel pairing properties in nuclei far from stability", 3rd LACM-EFES-JUSTIPEN Workshop, (Oak Ridge National Laboratory), Oak Ridge, USA, Feb. (2009).
- Barbieri C.: "Green's functions calculations of nuclei", 3rd LACM-EFES-JUSTIPEN Workshop, (Oak Ridge National Laboratory), Oak Ridge, USA, Feb. (2009).
- (Domestic Conference)
- 櫻木弘之, 古本猛憲, 村上永理子: "Proton-nucleus optical potential with complex G-matrix "JLM" and "CEG"", 理研 RIBF 核反応理論研究会「不安定原子核-原子核/核子間相互作用の理論的分析へ向けて」, 和光, 2月(2006).
- 古本猛憲, 櫻木弘之: "Microscopic proton-nucleus optical potentials based on the folding model with new complex G-matrix interactions", 理研ワークショップ「Theoretical description of elastic scattering of proton by unstable nuclei based on two-nucleon force」, 和光, 3月(2006).
- 古本猛憲, 櫻木弘之: "Microscopic optical potential based on the folding model with complex G-matrix interactions: JLM and CEG", 理研ワークショップ「Elastic scattering of unstable nuclei」, 和光, 6月(2006).
- 古本猛憲, 櫻木弘之: "複素 G 行列相互作用に基づく核反応研究 I", 日本物理学会分科会, 奈良, 9月(2006).
- 古本猛憲, 櫻木弘之, 山本安夫: "複素 G 行列相互作用に基づく核反応研究 II", 日本物理学会分科会, 東京, 3月(2007).
- 古本猛憲, 高階正彰, 櫻木弘之, 山本安夫: "複素 G 行列相互作用に基づく核反応研究 III", 日本物理学会第 62 回年次大会, 札幌, 9月(2007).
- 中務孝: "核構造大規模計算と密度汎関数法による数値シミュレーション", 日本物理学会第 63 回年次大会, 東大阪, 3月(2008).
- 飯田圭, 小濱洋央, 親松和浩: "反応断面積から探る原子核の中性子密度分布", 日本物理学会第 63 回年次大会, 東大阪, 3月(2008).
- 伊藤誠, 板垣直之: " $\alpha+^8\text{He}$  低エネルギー散乱における共鳴現象", 日本物理学会第 63 回年次大会, (日本物理学会), 東大阪, 3月(2008).
- 岩崎照平, 堀内渉, 鈴木宜之, 小濱洋央: "酸素同位体の全反応断面積の系統的計算", 日本物理学会第 63 回年次大会, 東大阪, 3月(2008).
- 古本猛憲, 櫻木弘之, 山本安夫: "複素 G 行列有効核力を用いた核反応の研究 IV", 日本物理学会第 63 回年次大会, 東大阪, 3月(2008).
- 堀井香織, 古本猛憲, 櫻木弘之: "偏極陽子+ $^8\text{B}$  散乱における  $^8\text{B}$ ,  $^7\text{Be}+p$  分解過程および  $^7\text{Be}$  核変形の効果", 日本物理学会第 63 回年次大会, 東大阪, 3月(2008).
- 中務孝: "Real-time representation of nuclear dynamics", 東京工業大学原子核理論研究室セミナー, (東京工業大学), 東京, 5月(2008).
- 吉田賢市: "Pairing and continuum effects on low-lying excitation modes in deformed neutron-rich nuclei", 筑波大学原子核理論研究室セミナー, つくば, 5月(2008).
- 伊藤誠: " $^{12}\text{Be}$  の連続エネルギー状態の構造と反応", 京都大学基礎物理学研究所研究会「原子核の分子的構造と低エネルギー反応」, (基礎物理学研究所), 京都, 7月(2008).
- 伊藤誠: "中重核及び不安定核における敷居値則と分子的構造", 京都大学基礎物理学研究所研究会「原子核の分子的構造と低エネルギー反応」, (基礎物理学研究所), 京都, 7月(2008).
- 吉田 賢市: "Low-lying excitation modes in deformed neutron-rich nuclei", Workshop on "Frontier in Unstable Nuclear Physics", (北海道大学), 札幌, 7月(2008).
- 近藤洋介, 中村隆司, 佐藤義輝, 松本琢磨, 青井考, 遠藤奈津美, 福田直樹, 五味朋子, 橋本佳子, 石原正泰, 河合祥子, 來山益久, 小林俊雄, 松田洋平, 松井信行, 本林透, 中林彩, 緒方一介, 奥村俊文, 王恵仁, 大西健夫, 大津秀暁, 櫻井博儀, 下浦享, 篠原摩有子, 杉本崇, 武内聡, 玉城充, 梶野泰宏, 柳澤善行: "18,19C の一中性子分離反応", RCNP 研究会「RCNP における不安定核の研究: RCNP ビームラインの可能性を探る」, (大阪大学核物理研究センター), 大阪, 8月(2008).
- 伊藤誠, 板垣直之: " $^{12}\text{Be}$  における単極遷移", 日本物理学会 2008 年秋季大会, (日本物理学会), 山形, 9月(2008).
- 山上雅之: "ダイニュートロン相関の探索へむけて", RIBF ミニワークショップ「ダイニュートロン相関をみる」, (RIKEN Nishina Center), 和光, 9月(2008).
- 小濱洋央, 飯田圭, 親松和浩: "不安定核反応へのくろたま模型適用可能性", 日本物理学会 2008 年秋季大会, 山形, 9月(2008).
- Barbieri C.: "Applications of self-consistent Green's function theory to nuclear response", 日本物理学会 2008 年秋季大会, (日本物理学会), 山形, 9月(2008).
- 松本琢磨, 江上智晃, 緒方一介, 井芹康統, 八尋正信, 上村正康: "中性子過剰核の分解反応断面積の計算", 日本物理学会 2008 年秋季大会, 盛岡, 9月(2008).
- 吉田賢市, Nguyen V.: "Deformed QRPA calculations using a Skyrme density functional", 日本物理学会 2008 年秋季大会, (日本物理学会), 山形, 9月(2008).
- 小笠原弘道, 吉田賢市, 水鳥正二郎, 山上雅之, 松柳研一: " $^{44}\text{Ti}$  の超変形状態に伴う 8 重極振動モードの非軸対称変形依存性", 日本物理学会 2008 年秋季大会, (日本物理学会), 山形, 9月(2008).
- 古本猛憲, 櫻木弘之, 山本安夫: "複素 G 行列有効核力を用いた Li-isotopes - 原子核反応の解析", 日本物理学会 2008 年秋季大会, 山形, 9月(2008).
- 中務孝: "Density functional calculation of E1 strength distribution in even-even nuclei", 第 1 回研究戦略ワークショップ「核物理から見た宇宙: r プロセスの新時代に向かへ」, 和光, 9月(2008).
- 吉田賢市: "中性子過剰不安定核に対する量子多体計算", 次世代スーパーコンピューティング・シンポジウム 2008, 東京, 9月(2008).
- 古本猛憲, 櫻木弘之, 山本安夫: " $\Sigma$ -nucleus potential based on folding model with complex G-matrix interaction", 文科省科研費補助金特定領域研究「ストレンジネスで探るクォーク多体系」研究会 2008, 山形, 9月(2008).

- 山上雅之, 清水良文: “高アイソスピン核の記述を目指した対相関密度汎関数の拡張”, 日本物理学会 2008 年秋季大会, (日本物理学会), 山形, 10 月 (2008).
- 吉田賢市: “対相関と変形相関の与える中性子過剰不安定核の集団運動への効果”, 千葉大学原子核理論研究室セミナー, 千葉, 10 月 (2008).
- 伊藤誠, 板垣直之: “軽い中性子過剰核の構造と反応の統一的研究”, 北大核物理の歴史と展望, (北海道大学), 札幌, 11 月 (2008).
- 伊藤誠: “ $\alpha+{}^8\text{He}$  共鳴散乱と  ${}^{12}\text{Be}$  の高励起状態”, 第 5 回停止・低速不安定核ビームを用いた核分光研究会, (大阪大学), 豊中, 12 月 (2008).
- 伊藤誠: “軽い中性子過剰核の構造と反応の統一的研究”, 「少数粒子系物理の現状と今後の展望」研究会, (大阪大学核物理研究センター), 茨木, 12 月 (2008).
- 中務孝: “密度汎関数法による核構造計算”, ワークショップ「計算科学による素粒子・原子核・宇宙の融合」, (筑波大学), つくば, 12 月 (2008).
- 山上雅之: “Density functional for description of novel pairing properties in nuclei far from beta-stability”, Aizu meeting 2009 on Spin Excitations and Exotic Degree of Freedom in Nuclei and Nuclear Matter, (会津大学), 会津若松, 2 月 (2009).
- 堀井香織, 土岐博, 櫻木弘之, 高階正彰, 谷口億宇, 古本猛憲: “内部構造を考慮した  ${}^8\text{Be}+\gamma$  の陽子および  ${}^{12}\text{C}$  との弾性散乱”, 日本物理学会第 64 回年次大会, 東京, 3 月 (2009).

## Experimental Installations Development Group

### Publications

#### [Journal]

(Original Papers) \*Subject to Peer Review

- Otsu H., Kobayashi T., Matsuda Y., Kitayama M., Inafuku K., Ozawa A., Satou Y., Suda T., Yoshida K., and Sakaguchi H.: “Measurement of the H(38s,p’) reaction at forward angles including 0 degree”, Nucl. Phys. A **788**, 266c–270c (1997). \*
- Fukuda N., Nakamura T., Kobayashi T., Otsu H., Aoi N., Imai N., Iwasaki H., Kubo T., Mengoni A., Notani M., Sakurai H., Shimoura S., Teranishi T., Watanabe Y., Yoneda K., and Ishihara M.: “Coulomb Dissociation of Halo Nuclei”, Prog. Theor. Phys. Suppl., No. 146, pp. 462–466 (2002).
- Ueno H., Asahi K., Ogawa H., Kameda D., Miyoshi H., Yoshimi A., Watanabe H., Shimada K., Sato W., Yoneda K., Imai N., Kobayashi Y., Ishihara M., and Wolf-Dieter S.: “Measurement of nuclear moments in the region of light neutron-rich nuclei”, Nucl. Phys. A **738**, 211–215 (2004). \*
- Saito A., Shimoura S., Takeuchi S., Motobayashi T., Minemura T., Matsuyama Y., Baba H., Akiyoshi H., Ando Y., Aoi N., Fulop Z., Gomi T., Higurashi Y., Hirai M., Ieki K., Imai N., Iwasa N., Iwasaki H., Iwata Y., Kanno S., Kobayashi H., Kubono S., Kunibu M., Kurokawa M., Liu Z., Michimasa S., Nakamura T., Ozawa A., Sakurai H., Serata M., Takeshita E., Teranishi T., Ue K., Yamada K., Yanagisawa Y., and Ishihara M.: “Molecular states in neutron-rich beryllium isotopes”, Nucl. Phys. A **738**, 337–341 (2004). \*
- Fukuda N., Nakamura T., Aoi N., Imai N., Ishihara M., Kobayashi T., Iwasaki H., Kubo T., Mengoni A., Notani M., Otsu H., Sakurai H., Shimoura S., Teranishi T., Watanabe Y., and Yoneda K.: “Coulomb and nuclear breakup of a halo nucleus  $^{11}\text{Be}$ ”, Phys. Rev. C **70**, 054606-1–054606-12 (2004). \*
- Kannungo R., Chiba M., Abu-Ibrahim B., Adhikari S., Fang D., Iwasa N., Kimura K., Maeda K., Nishimura S., Ohnishi T., Ozawa A., Samanta C., Suda T., Suzuki T., Wang Q., Wu C., Yamaguchi Y., Yamada K., Yoshida A., Zheng T., and Tanihata I.: “A new view to the structure of  $^{19}\text{C}$ ”, Eur. Phys. J. A **25**, No. s01, pp. 261–262 (2005). \*
- Yamada K., Motobayashi T., Aoi N., Baba H., Demichi K., Elekes Z., Gibelin J., Gomi T., Hasegawa H., Imai N., Iwasaki H., Kanno S., Kubo T., Kurita K., Matsuyama Y., Michimasa S., Minemura T., Notani M., Onishi T., Ong H., Ota S., Ozawa A., Saito A., Sakurai H., Shimoura S., Takeshita E., Takeuchi S., Tamaki M., Togano Y., Yanagisawa Y., Yoneda K., and Tanihata I.: “Reduced transition probabilities for the first  $2^+$  excited state in  $^{46}\text{Cr}$ ,  $^{50}\text{Fe}$ , and  $^{54}\text{Ni}$ ”, Eur. Phys. J. A **25**, No. s01, pp. 409–413 (2005).
- Dombradi Z., Elekes Z., Kanungo R., Baba H., Fulop Z., Gibelin J. D., Horvath A., Ideguchi E., Ichikawa Y., Iwasa N., Iwasaki H., Kanno S., Kawai S., Kondo Y., Motobayashi T., Notani M., Ohnishi T., Ozawa A., Sakurai H., Shimoura S., Takeshita E., Takeuchi S., Tanihata I., Togano Y., Wu C., Yamaguchi Y., Yanagisawa Y., Yoshida A., and Yoshida K.: “Decoupling of valence neutrons from the core in  $^{17}\text{B}$ ”, Phys. Lett. B **621**, 81–88 (2005). \*
- Onishi T., Gelberg A., Sakurai H., Yoneda K., Aoi N., Imai N., Baba H., Von Brentano P., Fukuda N., Ichikawa Y., Ishihara M., Iwasaki H., Kameda D., Kishida T., Lisetskiy A., Ong H., Osada M., Ohtsuka T., Suzuki M., Ue K., Utsuno Y., and Watanabe H.: “Gamow-Teller decay of the  $T = 1$  nucleus  $^{46}\text{Cr}$ ”, Phys. Rev. C **72**, No. 2, pp. 024308-1–024308-7 (2005). \*
- Schumann F., Typel S., Hammache F., Summerer K., Uhlig F., Bottcher I., Cortina D., Forster A., Gai M., Geissel H., Greife U., Gross E., Iwasa N., Koczon P., Kohlmeyer B., Kulesa R., Kumagai H., Kurzu N., Menzel M., Motobayashi T., Oeshler H., Ozawa A., Ploskon M., Prokopowicz W., Schwab E., Senger P., Strieder F., Sturm C., Sun Z., Surowka G., Wagner A., and Walus W.: “Low-energy cross section of the  $^7\text{Be}(p,\gamma)^8\text{B}$  solar fusion reaction from the Coulomb dissociation of  $^8\text{B}$ ”, Phys. Rev. C **73**, 015806-1–015806-13 (2006). \*
- Elekes Z., Dombradi Z., Saito A., Aoi N., Baba H., Demichi K., Fulop Z., Gibelin J., Gomi T., Hasegawa H., Imai N., Ishihara M., Iwasaki H., Kanno S., Kawai S., Kishida T., Kubo T., Kurita K., Matsuyama Y., Michimasa S., Minemura T., Motobayashi T., Notani M., Ohnishi T., Ong H., Ota S., Ozawa A., Sakai H., Sakurai H., Shimoura S., Takeshita E., Takeuchi S., Tamaki M., Togano Y., Yamada K., Yanagisawa Y., and Yoneda K.: “Proton inelastic scattering studies at the borders of the “island of inversion”: The  $^{30,31}\text{Na}$  and  $^{33,34}\text{Mg}$  case”, Phys. Rev. C **73**, 044314-1–044314-5 (2006). \*
- Yamaguchi T., Ohnishi T., Suzuki T., Becker T., Fukuda M., Geissel H., Hosoi M., Janik R., Kelic A., Kimura K., Mandel S., Muenzenberg G., Nakajima S., Ohtsubo T., Ozawa A., Prochazka A., Shindo M., Sitar B., Strmen P., Suda T., Summerer K., Sugawara K., Szarka I., Takechi M., Takisawa A., and Tanaka K.: “Production cross sections of isotopes formed by fragmentation of similar to 1A (GeVKr)-Kr-80 beam”, Phys. Rev. C **74**, 044608-1–044608-5 (2006). \*
- Dombradi Z., Elekes Z., Saito A., Aoi N., Baba H., Demichi K., Fulop Z., Gibelin J., Gomi T., Hasegawa H., Imai N., Ishihara M., Iwasaki H., Kanno S., Kawai S., Kishida T., Kubo T., Kurita K., Matsuyama Y., Michimasa S., Minemura T., Motobayashi T., Notani M., Ohnishi T., Ong H., Ota S., Ozawa A., Sakai H.,

- Sakurai H., Shimoura S., Takeshita E., Takeuchi S., Tamaki M., Togano Y., Yamada K., Yanagisawa Y., and Yoneda K.: “Vanishing  $N = 20$  Shell Gap: Study of Excited States in  $^{27,28}\text{Ne}$ ”, *Phys. Rev. Lett.* **96**, 182501-1–182501-4 (2006). \*
- Yoshimi A., Ueno H., Kameda D., Asahi K., Nagae D., Takemura M., Shimada K., Takase K., Sugimoto T., Uchida M., Arai T., Inoue T., Murata J., and Kawamura H.: “Electric quadrupole moments of neutron rich Al isotope”, *AIP Conf. Proc.* **912**, 105–109 (2007). \*
- Murata J., Asahi K., Kameda D., Kawamura H., Nagae D., Narota K., Shimada K., Shimoyama T., Shuehiro T., Toyoda T., Uchida M., Ueno H., and Yoshimi A.: “Beta Neutrino Correlation and T-Violation Experiment in Nuclear Beta Decay”, *AIP Conf. Proc.* **915**, No. 1, pp. 218–221 (2007). \*
- Yoshimi A., Ueno H., Sugimoto T., Shimada K., Nagae D., Murata J., Kawamura H., Kameda D., and Asahi K.: “Developments of atomic beam resonance method with RI beams”, *AIP Conf. Proc.* **915**, 849–852 (2007). \*
- Kawamura H., Kameda D., Murata J., Narota K., Shimoyama T., Suehiro T., Toyoda T., and Uchida M.: “Development of a New Drift Chamber based Mott Polarimeter”, *AIP Conf. Proc.* **915**, 1105–1108 (2007). \*
- Elekes Z., Dombradi Z., Saito A., Aoi N., Baba H., Demichi K., Fulop Z., Gibelin J. D., Gomi T., Hasegawa H., Imai N., Ishihara M., Iwasaki H., Kanno S., Kawai S., Kishida T., Kubo T., Kurita K., Matsuyama Y., Michimasa S., Minemura T., Motobayashi T., Notani M., Ohnishi T., Ong H., Ota S., Ozawa A., Sakai H., Sakurai H., Shimoura S., Takeshita E., Takeuchi S., Tamaki M., Togano Y., Yamada K., Yanagisawa Y., and Yoneda K.: “Study of  $N=20$  shell gap with  $^1\text{H}(^{28}\text{Ne}, ^{27,28}\text{Ne})$  reactions”, *Eur. Phys. J. Special Topics* **150**, 99–102 (2007). \*
- Shimada K., Nagae D., Asahi K., Inoue T., Takase K., Kagami S., Hatakeyama N., Kobayashi Y., Ueno H., Yoshimi A., Kameda D., Nagatomo T., Sugimoto T., Kubono S., Yamaguchi H., Wakabayashi Y., Hayakawa S., Murata J., and Kawamura H.: “Production of spin-polarized  $^{17}\text{N}$  beam sing inverse-kinematics low-energy transfer reactions”, *Hyperfine Interact.* **180**, 43–47 (2007). \*
- Yamaguchi T., Suzuki T., Ohnishi T., Nummerer S., Becker F., Fukuda M., Geissel H., Hosoi M., Janike R., Kimura K., Mandal S., Munzenberg G., Nakajima S., Ohtsubo T., Ozawa A., Orochazka A., Shindo M., Strmen P., Suda T., Sugawara K., Szarka I., Takisawa A., Takechi M., and Tanaka K.: “Nuclear radii of neutron-deficient Kr isotopes studied via their interaction cross-sections at relativistic energies”, *Nucl. Phys. A* **787**, 471c–475c (2007). \*
- Fang D., Guo W., Ma. C., Wang K., Yang T., Ma. Y., Cai X., Shen W., Ren Z., Sun Z., Chen J., Tian W., Zhong C., Hosoi M., Izumikawa T., Kanungo R., Nakajima S., Ohnishi T., Ohtsubo T., Ozawa A., Suda T., Sugawara K., Suzuki T., Takisawa A., Tanaka K., Yamaguchi T., and Tanihata I.: “Examining the exotic structure of the proton-rich nucleus  $^{23}\text{Al}$ ”, *Phys. Rev. C* **76**, 031601-1–031601-5 (2007). \*
- Kameda D., Ueno H., Asahi K., Nagae D., Yoshimi A., Nagatomo T., Sugimoto T., Uchida M., Takemura M., Shimada K., Takase K., Inoue T., Kijima G., Arai T., Suda S., Murata J., Kawamura H., Kobayashi Y., Watanabe H., and Ishihara M.: “Production of spin-polarized radioactive ion beams via projectile fragmentation reaction”, *AIP Conf. Proc.* **980**, 283–288 (2008). \*
- Kameda D., Asahi K., Ueno H., Nagae D., Takemura M., Shimada K., Yoshimi A., Nagatomo T., Sugimoto T., Uchida M., Arai T., Takase K., Suda S., Inoue T., Murata J., Kawamura H., Watanabe H., Kobayashi Y., and Ishihara M.: “Electric quadrupole moments of neutron-rich nuclei  $^{32}\text{Al}$  and  $^{31}\text{Al}$ ”, *Hyperfine Interact.* **180**, 61–64 (2008). \*
- Sugimoto T., Asahi K., Kawamura H., Murata J., Nagae D., Shimada K., Ueno H., and Yoshimi A.: “Development of atomic-beam resonance method to measure the nuclear moments of unstable nuclei”, *Hyperfine Interact.* **181**, 141–144 (2008). \*
- Elekes Z., Dombradi Z., Aoi N., Baba H., Bishop S., Demichi K., Fulop Z., Gibelin J., Gomi T., Hasegawa H., Hashimoto Y., Imai N., Ishihara M., Iwasa N., Iwasaki H., Kalinka G., Kanno S., Kawai S., Kishida T., Kondo Y., Korshennikov A. A., Kubo T., Kurita K., Kurokawa M., Matsui N., Matsuyama Y., Michimasa S., Minemura T., Motobayashi T., Nakamura T., Nakao T., Nikolski E. Y., Notani M., Ohnishi T., Okumura T., Ong H., Ota S., Ozawa A., Perera P., Saito A., Sakai H., Sakurai H., Satou Y., Shimoura S., Sohler D., Sumikama T., Suzuki D., Suzuki M., Takeda H., Takeshita E., Takeuchi S., Tamaki M., Togano Y., Yamada K., Yanagisawa Y., and Yoneda K.: “The study of shell closures in light neutron-rich nuclei”, *J. Phys. G* **35**, 014038-1–014038-7 (2008).
- Sato W., Ueno H., Watanabe H., Miyoshi H., Yoshimi A., Kameda D., Ito T., Shimada K., Kaihara J., Suda S., Kobayashi Y., Shinohara A., Ohkubo Y., and Asahi K.: “Temperature-dependent behavior of impurity atoms implanted in highly oriented pyrolytic graphite –An application of a new online TDPAC method–”, *J. Phys. Soc. Jpn.* **77**, No. 9, pp. 095001-1–095001-2 (2008). \*
- Yamaguchi Y., Ozawa A., Goto A., Arai I., Fujinawa T., Fukunishi N., Kikuchi T., Ohnishi T., Ohtsubo T., Sakurai H., Suzuki T., Wakasugi M., Yamaguchi T., Yasuda Y., and Yano Y.: “Rara-RI ring project at RIKEN RI beam factory”, *Nucl. Instrum. Methods Phys. Res. B* **266**, 4575–4578 (2008). \*

- Nagae D., Ueno H., Kameda D., Takemura M., Asahi K., Yoshimi A., Sugimoto T., Shimada K., Nagatomo T., Uchida M., Arai T., Inoue T., Kagami S., Hatakeyama N., Murata J., Kawamura H., and Narota K.: “Electric quadrupole moment of  $^{31}\text{Al}$ ”, Nucl. Instrum. Methods Phys. Res. B **266**, 4612–4615 (2008). \*
- Nakajima S., Kuboki T., Yoshitake M., Hashizume Y., Kanazawa M., Kitagawa a., Kobayashi K., Moriguchi T., Ohtsubo T., Ozawa A., Sato S., Suzuki T., Yamaguchi Y., Yasuda Y., and Yamaguchi T.: “Development of a time-of-flight detector for the rare-RI ring project at RIKEN”, Nucl. Instrum. Methods Phys. Res. B **266**, 4621–4624 (2008). \*
- Ueno H., Nagae D., Kameda D., Asahi K., Takemura M., Takase K., Yoshimi A., Sugimoto T., Shimada K., Nagatomo T., Uchida M., Arai T., Inoue T., Murata J., Kawamura H., and Narota K.: “Electric quadrupole moment of  $^{31}\text{Al}$ ”, Nucl. Phys. A **805**, 329–331 (2008). \*
- Yamaguchi T., Suzuki T., Ohnishi T., Becker F., Fukuda M., Geissel H., Hosoi M., Janik R., Kimura K., Kuboki T., Mandel S., Matsuo M., Muenzenberg G., Nakajima S., Ohtsubo T., Ozawa A., Prochazka A., Shindo M., Sitar B., Strmen P., Suda T., Suemmerer K., Sugawara K., Szarka I., Takechi M., Takisawa A., Tanaka K., and Yamagami M.: “Nuclear matter radii of neutron-deficient Kr isotopes”, Phys. Rev. C **77**, 034315-1–034315-6 (2008). \*
- Wakasugi M., Emoto T., Furukawa Y., Ishii K., Ito S., Koseki T., Kurita K., Kuwajima A., Masuda T., Morikawa A., Nakamura M., Noda A., Ohnishi T., Shirai T., Suda T., Takeda H., Tamae T., Tongu H., Wang S., and Yano Y.: “Novel Internal Target for Electron Scattering off Unstable Nuclei”, Phys. Rev. Lett. **100**, 164801-1–164801-4 (2008). \*
- Elekes Z., Dombradi Z., Aiba T., Aoi N., Baba H., Bemmerer D., Brown B., Furumoto T., Fulop Z., Iwasa N., Kiss A. B., Kobayashi T., Kondo Y., Motobayashi T., Nakabayashi T., Nannichi T., Sakuragi H., Sakurai H., Sohler D., Takashina M., Takeuchi S., Tanaka K., Togano Y., Yamada K., Yamaguchi M., and Yoneda K.: “Persistent decoupling of valence neutrons toward the dripline: study of  $^{20}\text{C}$  by  $\gamma$  spectroscopy”, Phys. Rev. C **79**, 011302-1–011302-5 (2009). \*
- Nagae D., Ueno H., Kameda D., Takemura M., Asahi K., Takase K., Yoshimi A., Sugimoto T., Shimada K., Nagatomo T., Uchida M., Arai T., Inoue T., Kagami S., Hatakeyama N., Kawamura H., Narota K., and Murata J.: “Ground-state electric quadrupole moment of  $^{31}\text{Al}$ ”, Phys. Rev. C **79**, 027301-1–027301-4 (2009). \*
- (Others)
- Nakajima S., Yamaguchi T., Suzuki T., Yamaguchi Y., Fujinawa T., Fukunishi N., Goto A., Ohnishi T., Sakurai H., Wakasugi M., Yano Y., Arai I., Ozawa A., Yasuda Y., Kikuchi T., and Ohtsubo T.: “New scheme for precision mass measurements of rare isotopes produced at RI beam factory”, Acta Phys. Pol. B **39**, No. 2, pp. 457–462 (2008).
- Murata J., Akiyama T., Hata M., Hirayama Y., Ikeda Y., Ishii T., Kameda D., Kawamura H., Mitsuoka S., Miyatake H., Nagae D., Ninomiya K., Nitta M., Seitabashi E., and Toyoda T.: “R&D for a test of time reversal symmetry experiment using polarized nuclei”, JAEA-Review **2008-054**, 58–59 (2008).
- [Book • Proceedings]**  
(Original Papers) \*Subject to Peer Review
- Goto A., Fujimaki M., Fujinawa T., Fukunishi N., Hasebe H., Higurashi Y., Ikegami K., Ikezawa E., Inabe N., Kageyama T., Kamigaito O., Kase M., Kidera M., Kohara S., Komiyama M., Nagase M., Kumagai K., Maie T., Nakagawa T., Ohnishi J., Okuno H., Ryuto H., Sakamoto N., Wakasugi M., Watanabe T., Yamada K., Yokouchi S., and Yano Y.: “Commissioning of RIKEN RI Beam Factory”, Proceedings of 18th International Conference on Cyclotrons and Their Applications (Cyclotrons 2007), Giardini Naxos, Italy, 2007–9~10, Giardini Naxos, pp. 3–8 (2007).
- (Others)
- Yamaguchi T., Arai I., Fukunishi N., Goto A., Kikuchi T., Komatsubara T., Ohnishi T., Ohtsubo T., Okuno H., Ozawa A., Sasa K., Suzuki T., Tagisi Y., Takeda H., Wakasugi M., Yamaguchi M., Yamaguchi Y., and Yano Y.: “Mass measurements by an isochronous storage ring at the RIKEN RI beam factory”, Proceedings of the 6th International Conference on Nuclear Physics at Storage Rings (STORI '05), Bonn, Germany, 2005–5, Forschungszentrum Julich, Julich, pp. 297–300 (2005).
- Yamaguchi M., Arai I., Fukunishi N., Goto A., Kusaka K., Kikuchi T., Komatsubara T., Kubo T., Ohnishi T., Ohtsubo T., Okuno H., Ozawa A., Sasa K., Suzuki T., Tagisi Y., Takeda H., Wakasugi M., Yamaguchi T., Yamaguchi Y., and Yano Y.: “Design of an isochronous storage ring and an injection line for mass measurements at the RIKEN RI beam factory”, Proceedings of the 6th International Conference on Nuclear Physics at Storage Rings (STORI '05), Bonn, Germany, 2005–5, Forschungszentrum Julich, Julich, pp. 315–319 (2005).
- Kikuchi T., Horioka K., Ozawa A., Kawata S., Yamaguchi Y., Fukunishi N., Sakurai H., Wakasugi M., Yamaguchi M., Yamaguchi T., Arai I., Ohta H., Fujinawa T., Sasa K., Komatsubara T., Suzuki T., Ohtsubo T., Goto A., Ohnishi T., Okuno H., Takeda H., and Yano Y.: “Individual correction using induction modulator for mass measurements by isochronous ring in RIKEN RI beam factory”, Proceedings of the 2nd International Workshop on Recent Progress in Induction Accelerators (RPIA2006), Tsukuba, 2006–3, KEK, Tsukuba, pp. 127–131 (2006).

#### Oral Presentations

(International Conference etc.)

- Yamaguchi T., Ozawa A., Arai I., Komatsubara T., Sasa K., Tagisi Y., Yamaguchi M., Suzuki T., Ohtsubo T., Fukunishi N., Goto A., Ohnishi T., Okuno H., Takeda H., Wakasugi M., Yano Y., Yamaguchi Y., and Kikuchi T.: “Mass measurements in RIKEN”, 6th International Conference on Nuclear Physics at Storage Rings (STORI-05), (Research Center Julich), Bonn, Germany, May (2005).
- Kikuchi T., Horioka K., Ozawa A., Kawata S., Yamaguchi Y., Fukunishi N., Sakurai H., Wakasugi M., Yamaguchi M., Yamaguchi T., Arai I., Ohta H., Fujinawa T., Sasa K., Komatsubara T., Suzuki T., Ohtsubo T., Goto A., Ohnishi T., Okuno H., Takeda H., and Yano Y.: “Individual correction using induction modulator for mass measurements by isochronous ring in RIKEN RI beam factory”, 2nd International Workshop on Recent Progress in Induction Accelerators (RPIA2006), (KEK, Tokyo Institute of Technology), Tsukuba, Mar. (2006).
- Arai I., Komatsubara T., Ozawa A., Sasa K., Yasuda Y., Fujinawa T., Fukunishi N., Goto A., Ohnishi T., Okuno H., Takeda H., Wakasugi M., Yamaguchi M., Yamaguchi Y., Yano Y., Kikuchi T., Suzuki T., Yamaguchi T., and Ohtsubo T.: “Isochronous ring at RIKEN”, Workshop on Advanced Laser and Mass Spectroscopy ALMAS-1: Innovative Physics Ideas, (Gesellschaft für Schwerionenforschung (GSI)), Darmstadt, Germany, Oct. (2006).
- Arai I., Komatsubara T., Ozawa A., Sasa K., Yasuda Y., Fujinawa T., Fukunishi N., Goto A., Ohnishi T., Okuno H., Takeda H., Wakasugi M., Yamaguchi M., Yamaguchi Y., Yano Y., Kikuchi T., Suzuki T., Yamaguchi T., and Ohtsubo T.: “Rare RI ring”, RIBF International Collaboration Workshop on Experiments at the RIBF, Wako, Nov. (2006).
- Kondo Y., Nakamura T., Sato Y., Aoi N., Endo N., Fukuda N., Gomi T., Hashimoto Y., Ishihara M., Kawai S., Kitayama M., Kobayashi T., Matsuda Y., Matsui N., Motobayashi T., Nakabayashi T., Okumura T., Ong H., Onishi T., Otsu H., Sakurai H., Shimoura S., Shinohara M., Sugimoto T., Takeuchi S., Tamaki M., Togano Y., and Yanagisawa Y.: “Invariant mass spectroscopy of  $^{13}\text{Be}$  and  $^{14}\text{Be}$  via the proton-induced breakup reactions of  $^{14}\text{Be}$ ”, 5th International Workshop on Direct Reaction with Exotic Beams (DREB2007), Wako, May–June (2007).
- Nakajima S., Kuboki T., Yoshitake M., Hashizume Y., Kanazawa M., Kitagawa a., Kobayashi K., Moriguchi T., Ohtsubo T., Ozawa A., Sato S., Suzuki T., Yamaguchi Y., Yasuda Y., and Yamaguchi T.: “Development of a time-of-flight detector for rare-RI ring project at RIKEN RIBF”, 15th International Conference on Electromagnetic Isotope Separators and Techniques Related to their Applications (EMIS2007), (GANIL, IN2P3/CNRS, DSM/CEA), Deauville, France, June (2007).
- Yamaguchi Y., Fujinawa T., Fukunishi N., Goto A., Ohnishi T., Sakurai H., Wakasugi M., Yano Y., Ozawa A., Arai I., Yasuda Y., Suzuki T., Yamaguchi T., Kikuchi T., and Ohtsubo T.: “Rare-RI ring project at RI Beam factory in RIKEN”, 15th International Conference on Electromagnetic Isotope Separators and Techniques Related to their Applications (EMIS2007), (GANIL, IN2P3/CNRS, DSM/CEA), Deauville, France, June (2007).
- Sugimoto T., Yoshimi A., Ueno H., Asahi K., Kawamura H., Murata J., Nagae D., and Shimada K.: “Development of ion guiding system for radio-isotope atomic-beam resonance measurements”, International Nuclear Physics Conference (INPC2007), (Science Council of Japan, RIKEN and others), Tokyo, June (2007).
- Ozawa A., Arai I., Fujinawa T., Fukunishi N., Goto A., Kikuchi T., Igarashi S., Komatsubara T., Ohtsubo T., Sakurai H., Sasa K., Suzuki T., Wakasugi M., Yamaguchi K., Yamaguchi T., Yamaguchi Y., Yano Y., and Yasuda Y.: “Mass measurements by isochronous storage ring in RI beam factory”, International Nuclear Physics Conference (INPC2007), (RIKEN and others), Tokyo, June (2007).
- Nagatomo T., Matsuta K., Minamisono K., Levy C. D., Sumikama T., Mihara M., Ozawa A., Tagisi Y., Ogura M., Matsumiya R., Fukuda M., Yamaguchi M., Behr J. A., Jackson K. P., Yasuno T., Ohta H., Hashizume Y., Fujiwara H., Chiba A., and Minamisono T.: “Search for the  $G$  parity violating term in weak nucleon currents in mass 20 system”, International Nuclear Physics Conference (INPC2007), (Science Council of Japan, RIKEN and others), Tokyo, June (2007).
- Kameda D., Ueno H., Asahi K., Nagae D., Takemura M., Yoshimi A., Shimada K., Uchida M., Kijima G., Arai T., Takase K., Suda S., Inoue T., Murata J., Kawamura H., Haseyama T., Kobayashi Y., Watanabe H., and Ishihara M.: “Small electric quadrupole moment of  $^{32}\text{Al}$ : Drastic shape transition between  $^{32}\text{Al}$  and  $^{31}\text{Mg}$ ”, International Nuclear Physics Conference (INPC2007), (Science Council of Japan, RIKEN and others), Tokyo, June (2007).
- Kondo Y., Nakamura T., Sato Y., Aoi N., Endo N., Fukuda N., Gomi T., Hashimoto Y., Ishihara M., Kawai S., Kitayama M., Kobayashi T., Matsuda Y., Matsui N., Motobayashi T., Nakabayashi T., Okumura T., Ong H., Onishi T., Otsu H., Sakurai H., Shimoura S., Shinohara M., Sugimoto T., Takeuchi S., Tamaki M., Togano Y., and Yanagisawa Y.: “Invariant mass spectroscopy of  $^{13}\text{Be}$  and  $^{14}\text{Be}$  via the proton-induced breakup reactions”, International Symposium & School on Frontiers and Perspectives of Nuclear and Hadron Physics (FPNH07), (Tokyo Institute of Technology), Tokyo, June (2007).
- Kameda D., Ueno H., Asahi K., Nagae D., Takemura M., Yoshimi A., Shimada K., Uchida M., Kijima G., Arai T.,

- Takase K., Suda S., Inoue T., Murata J., Kawamura H., Haseyama T., Kobayashi Y., Watanabe H., and Ishihara M.: “Small electric quadrupole moment of  $^{32}\text{Al}$ ”, International Workshop on Nuclear Structure: New Pictures in the Extended Isospin Space (NS07), (Yukawa Institute for Theoretical Physics), Kyoto, June (2007).
- Nagatomo T., Matsuta K., Minamisono K., Sumikama T., Mihara M., Ozawa A., Tagisi Y., Ogura M., Matsumiya R., Fukuda M., Yamaguchi M., Yasuno T., Ohta H., Hashizume Y., Fujiwara H., Chiba A., and Minamisono T.: “Beta-ray Angular Distribution from Purely Nuclear Spin Aligned  $^{20}\text{F}$  Nuclei”, 14th International Conference on Hyperfine Interactions and 18th International Symposium on Nuclear Quadrupole Interactions, (Universidad Nacional de La Plata/Instituto de Fisica de La Plata, CONICET), Iguassu Falls, Brazil, Aug. (2007).
- Kameda D., Ueno H., Asahi K., Nagae D., Takemura M., Yoshimi A., Shimada K., Nagatomo T., Sugimoto T., Uchida M., Arai T., Takase K., Suda S., Inoue T., Murata J., Kawamura H., Watanabe H., Kobayashi Y., and Ishihara M.: “Electric quadrupole moments of neutron-rich nuclei  $^{32}\text{Al}$  and  $^{31}\text{Al}$ ”, 14th Int. Conf. on Hyperfine Interactions & 18th Int. Symp. on Nuclear Quadrupole Interactions, ( Universidad Nacional de La Plata), Iguassu Falls, Brazil, Aug. (2007).
- Kameda D., Ueno H., Asahi K., Nagae D., Yoshimi A., Nagatomo T., Sugimoto T., Uchida M., Takemura M., Shimada K., Takase K., Inoue T., Kijima G., Arai T., Suda S., Murata J., Kawamura H., Kobayashi Y., Watanabe H., and Ishihara M.: “Production of spin-polarized r/a beams via projectile fragmentation reaction”, 12th Int. Workshop on Polarized Sources, Targets & Polarimetry, (Brookhaven National Laboratory), Brookhaven, USA, Sept. (2007).
- Nagatomo T., Matsuta K., Minamisono K., Levy C. D., Sumikama T., Mihara M., Ozawa A., Tagisi Y., Ogura M., Matsumiya R., Fukuda M., Yamaguchi M., Behr J. A., Jackson K. P., Yasuno T., Ohta H., Hashizume Y., Fujiwara H., Chiba A., and Minamisono T.: “Search for the  $G$  parity violating term in weak nucleon currents in mass 20 system”, 12th Int. Workshop on Polarized Sources, Targets & Polarimetry, (Brookhaven National Laboratory), Brookhaven, USA, Sept. (2007).
- Nakajima S., Suzuki T., Yamaguchi T., Fujinawa T., Fukunishi N., Goto A., Ohnishi T., Sakurai H., Wakasugi M., Yamaguchi Y., Yano Y., Ozawa A., Arai I., Yasuda Y., Kikuchi T., and Ohtsubo T.: “New scheme for precision mass measurement of rare isotopes produced at RI beam factory”, 30th Mazurian Lakes Conference on Physics : Nuclear Physics and the Fundamental Processes, (IPJ ; University of Warsaw ; Pro-Physica), Piaski, Poland, Sept. (2007).
- Kondo Y., Motobayashi T., Sakurai H., Aoi N., Otsu H., Yanagisawa Y., Fukuda N., Takeuchi S., Ishihara M., Baba H., Gomi T., Imai N., Kubo T., Yoneda K., Nakamura T., Sato Y., Sugimoto T., Matsui N., Attukulathil V. M., Okumura T., Hashimoto Y., Nakabayashi T., Shinohara M., Miura M., Kobayashi T., Matsuda Y., Endo N., Kitayama M., Watanabe K., Yakushiji T., Togano Y., Kawai S., Hasegawa H., Onishi T., Ong H., Shimoura S., Tamaki M., Saito A., Bazin D. P., and Watanabe Y.: “Breakup reactions of  $^{14}\text{Be}$ ”, Future Prospects for Spectroscopy and Direct Reactions 2008, (Michigan State University), East Lansing, USA, Feb. (2008).
- Yamaguchi T., Fujinawa T., Fukunishi N., Goto A., Ohnishi T., Sakurai H., Wakasugi M., Yamaguchi Y., Yano Y., Arai I., Moriguchi T., Ozawa A., Yasuda Y., Nakajima S., Kuboki T., Suzuki T., Kikuchi T., and Ohtsubo T.: “Storage-ring mass spectrometry”, ETC Workshop on Mass Olympics, (GSI , FIAS), Trento, Italy, May (2008).
- Yoshimi A., Ueno H., Nagatomo T., Shimada K., Ichikawa Y., Kameda D., Sugimoto T., Sakurai H., Asahi K., Hasama Y., Takemura M., Kijima G., Nagae D., Uchida M., Arai T., Suda S., Takase T., Inoue T., Hatakeyama N., Kagami S., Murata J., and Kawamura H.: “Nuclear electromagnetic moments of neutron-rich Al isotopes”, Nuclear Structure 2008, (Michigan State University, NSCL at MSU), Michigan, USA, June (2008).
- Kawamura H., Murata J., Toyoda T., Seitabashi E., Nitta M., Hata M., Akiyama T., Ikeda Y., Ninomiya K., Kameda D., Nagae D., and Hirayama Y.: “The first T-violation experiment at KEK-TRIAC”, 24th Advanced Studies Institute :Symmetries and Spin (SPIN-Praha-2008), (Charles University in Prague, Faculty of Mathematics and Physics), Praha, Czech, July (2008).
- Yamaguchi T., Arai I., Ozawa A., Yasuda Y., Fujinawa T., Fukunishi N., Goto A., Hara K., Ohnishi T., Sakurai H., Wakasugi M., Yamaguchi Y., Yano Y., Kikuchi T., Suzuki T., and Ohtsubo T.: “Beam optics simulation for rare-RI ring at RI beam factory in RIKEN”, 7th International Conference on Nuclear Physics at Storage Rings STORI’08, (Institute of Modern Physics, Chinese Academy of Sciences, National Natural Foundation of China), Lanzhou, China, Sept. (2008).
- Yasuda Y., Ozawa A., Arai I., Fujinawa T., Fukunishi N., Goto A., Ohnishi T., Sakurai H., Wakasugi M., Yamaguchi Y., Yano Y., Suzuki T., Yamaguchi T., Kikuchi T., and Ohtsubo T.: “Present status of rare-RI ring project in RIKEN RIBF”, 7th International Conference on Nuclear Physics at Storage Rings STORI’08, (Institute of Modern Physics, Chinese Academy of Sciences, National Natural Foundation of China), Lanzhou, China, Sept. (2008).
- Kondo Y., Nakamura T., Sato Y., Matsumoto T., Aoi N., Endo N., Fukuda N., Gomi T., Hashimoto Y., Ishihara M., Kawai S., Kitayama M., Kobayashi T., Matsuda Y., Matsui N., Motobayashi T., Nakabayashi T., Ogata K., Okumura T., Ong H., Onishi T., Otsu

- H., Sakurai H., Shimoura S., Shinohara M., Sugimoto T., Takeuchi S., Tamaki M., Togano Y., and Yanagisawa Y.: "Invariant-mass spectroscopy of neutron-rich Be isotopes", Unbound Nuclei Workshop, (INFN), Pisa, Italy, Nov. (2008).
- Kondo Y., Nakamura T., Sato Y., Matsumoto T., Aoi N., Endo N., Fukuda N., Gomi T., Hashimoto Y., Ishihara M., Kawai S., Kitayama M., Kobayashi T., Matsuda Y., Matsui N., Motobayashi T., Nakabayashi T., Ogata K., Okumura T., Ong H., Onishi T., Otsu H., Sakurai H., Shimoura S., Shinohara M., Sugimoto T., Takeuchi S., Tamaki M., Togano Y., and Yanagisawa Y.: "Breakup reactions of  $^{14}\text{Be}$ ", International Conference on Interfacing Structure and Reactions at the Centre of the Atom (Kernz08), (Livermore and University of Surrey), Queenstown, The Netherlands, Dec. (2008). (Domestic Conference)
- 太田寛史, 新井一郎, 小沢顕, 小松原哲郎, 笹公和, 鈴木健, 山口貴之, 大坪隆, 山口充孝, 田岸義宏, 矢野安重, 後藤彰, 若杉昌徳, 奥野広樹, 福西暢尚, 大西哲哉, 山口由高, 菊池崇志: "Design of the isochronous storage ring for accurate mass measurement in RI beam factory", 第2回日本加速器学会年会/第30回リニアック技術研究会, 鳥栖, 7月(2005).
- 太田寛史, 新井一郎, 小沢顕, 小松原哲郎, 笹公和, 鈴木健, 山口貴之, 大坪隆, 山口充孝, 田岸義宏, 矢野安重, 後藤彰, 奥野広樹, 福西暢尚, 大西哲哉, 山口由高, 菊池崇志: "等時性蓄積リングへの入射ラインとそのビーム光学", 等時性蓄積リングによる不安定核の質量測定と宇宙元素合成, (筑波大学), つくば, 9月(2005).
- 山口由高, 若杉昌徳, 藤縄雅, 福西暢尚, 後藤彰, 大西哲哉, 奥野広樹, 櫻井博儀, 竹田浩之, 山口充孝, 矢野安重, 小沢顕, 新井一郎, 小松原哲郎, 笹公和, 菊池崇志, 鈴木健, 山口貴之, 大坪隆: "等時性蓄積リングのためのキッカー電磁石及び入射スキームの検討", 等時性蓄積リングによる不安定核の質量測定と宇宙元素合成, (筑波大学), つくば, 9月(2005).
- 小沢顕: "Interaction cross section / mass measurement", Workshop on Nuclear Physics Collaboration between Germany and Japan, 和光, 9月(2005).
- 山口由高, 小沢顕, 新井一郎, 安田裕介, 藤縄雅, 福西暢尚, 大西哲哉, 後藤彰, 奥野広樹, 櫻井博儀, 若杉昌徳, 矢野安重, 鈴木健, 山口貴之, 菊池崇志, 大坪隆: "等時性蓄積リングによる質量測定", 国立天文台ワークショップ「Rプロセス元素組成の統合的理解: 量子ビームでさぐる宇宙進化の理解を目指して」, 三鷹, 3月(2007).
- 久保木隆正, 小沢顕, 鈴木健, 山口貴之, 大坪隆, 山口由高, 金澤光高, 北川敦志, 小林圭, 佐藤眞二, 須田利美, 田中鐘信, 中島真平, 橋爪祐平, 森口哲朗, 安田裕介, 吉竹利織: "放医研 HIMAC に於ける TOF 検出器の分解能と荷電状態分析の測定", 日本物理学会 2007 年春季大会, 八王子, 3月(2007).
- 安田裕介, 新井一郎, 小沢顕, 小松原哲郎, 笹公和, 大西哲哉, 後藤彰, 櫻井博儀, 福西暢尚, 藤縄雅, 矢野安重, 山口由高, 若杉昌徳, 鈴木健, 山口貴之, 大坪隆, 菊池崇志: "理研 RIBF における等時性蓄積リング計画", 日本物理学会第 62 回年次大会, 札幌, 9月(2007).
- 近藤洋介, 中村隆司, 佐藤義輝, 杉本崇, 松井信行, 奥村俊文, 橋本佳子, 中林彩, 篠原摩有子, 青井考, 遠藤奈津美, 福田直樹, 五味朋子, 河合祥子, 來山益久, 小林俊雄, 松田洋平, 本林透, 王恵仁, 大西健夫, 大津秀暁, 櫻井博儀, 下浦享, 武内聡, 玉城充, 梶野泰宏, 柳澤善行, 石原正泰: "18,19C の一中性子分離反応", 日本物理学会第 63 回年次大会, 東大阪, 3月(2008).
- 森口哲朗, 橋爪祐平, 保谷毅, 小川賢一郎, 安田裕介, 原かおる, 小沢顕, 久保木隆正, 吉竹利織, 齊藤和哉, 三浦宗賢, 中島真平, 山口貴之, 鈴木健, 大坪隆, 山口由高, 金澤光高, 北川敦志, 佐藤眞二: "重イオンビームによる Hybrid Photo Detector の時間分解能の測定", 日本物理学会第 63 回年次大会, 東大阪, 3月(2008).
- 久保木隆正, 山口貴之, 大坪隆, 小沢顕, 金澤光高, 北川敦志, 久保徹, 小林圭, 齊藤和哉, 佐藤眞二, 鈴木健, 須田利美, 田中鐘信, 中島真平, 橋爪祐平, 三浦宗賢, 森口哲朗, 安田裕介, 山口由高, 吉竹利織, 渡部亮太: "理研稀少 RI リングの為に TOF 検出器の開発", 日本物理学会第 63 回年次大会, 東大阪, 3月(2008).
- 山口由高, 大西哲哉, 後藤彰, 櫻井博儀, 福西暢尚, 藤縄雅, 矢野安重, 若杉昌徳, 新井一郎, 小沢顕, 小松原哲郎, 笹公和, 安田裕介, 鈴木健, 山口貴之, 菊池崇志, 大坪隆: "理研 RIBF における質量リング計画の現状", 国立天文台研究会「rプロセス元素合成の統合的理解-量子ビームで探る宇宙進化の理解を目指して-」, つくば, 3月(2008).
- 山口由高, 藤縄雅, 福西暢尚, 後藤彰, 大西哲哉, 櫻井博儀, 若杉昌徳, 矢野安重, 小沢顕, 新井一郎, 安田裕介, 菊池崇志, 大坪隆, 鈴木健, 山口貴之: "理研 RIBF における稀少 RI リング計画の現状", 第5回日本加速器学会年会/第33回リニアック技術研究会, 東広島, 8月(2008).
- 近藤洋介, 中村隆司, 佐藤義輝, 松本琢磨, 青井考, 遠藤奈津美, 福田直樹, 五味朋子, 橋本佳子, 石原正泰, 河合祥子, 來山益久, 小林俊雄, 松田洋平, 松井信行, 本林透, 中林彩, 緒方一介, 奥村俊文, 王恵仁, 大西健夫, 大津秀暁, 櫻井博儀, 下浦享, 篠原摩有子, 杉本崇, 武内聡, 玉城充, 梶野泰宏, 柳澤善行: "18,19C の一中性子分離反応", RCNP 研究会「RCNP における不安定核の研究: RCNP ビームラインの可能性を探る」, (大阪大学核物理研究センター), 大阪, 8月(2008).
- 島田健司, 長友傑, 旭耕一郎, Balabanski D. L., Daugas J. M., Depuydt M., De Rydt M., Gaudefroy L., Grevy S., 挾間優佳, 市川雄一, 亀田大輔, Morel P., Perrot L., Stodel C., Thomas J. C., Vanderheyolen W., Vermeulen N., Vingerhoets P., 吉見彰洋, Neyens G., 上野秀樹: " $^{33}\text{Al}$  の電気四重極モーメント", 日本物理学会 2008 年秋季大会, (山形大学・日本物理学会), 山形, 9月(2008).
- 安田裕介, 新井一郎, 小沢顕, 森口哲朗, 大西哲哉, 櫻井博儀, 福西暢尚, 藤縄雅, 矢野安重, 山口由高, 若杉昌徳, 原かおる, 鈴木健, 山口貴之, 大坪隆, 菊池崇志: "理研稀少 RI リング建設にむけての高精度磁場測定", 日本物理学会 2008 年秋季大会, 盛岡, 9月(2008).
- 豊田健司, 秋山岳伸, 秦麻記, 平山賀一, 池田友樹, 亀田大輔, 川村広和, 村田次郎, 長江大輔, 二宮一史, 新田稔, 聖代橋

- 悦子: “TRIAC における時間反転対称性の破れ探索実験”, 日本物理学会 2008 年秋季大会, 山形, 9 月 (2008).
- 長友侖, 南園啓, 松多健策, 三原基嗣, 松宮亮平, 小倉昌子, 福田光順, 小沢顕, 田岸義宏, 山口充孝, 安野琢磨, 太田寛史, 橋爪祐平, 炭竈聡之, Levy C. D., Behr J. A., Jackson K. P., 南園忠則: “質量数 20 体系の鏡映核対のベータ線角度分布の精密測定による  $G$  変換対称性の研究”, 日本物理学会 2008 年秋季大会, (山形大学、日本物理学会), 山形, 9 月 (2008).
- 長友侖: “Rutile 中  $^{13}\text{B}$  核のスピン整列制御と  $\beta$  線角度分布”, 平成 20 年度京都大学原子炉実験所専門研究会「短寿命核および放射線を用いた物性研究 (I)」研究会, 大阪府熊取町, 11 月 (2008).
- 長友侖: “Electric quadrupole moment of  $^{33}\text{Al}$ ”, 第 5 回停止・低速不安定核ビームを用いた核分光研究会, (大阪大学), 豊中, 12 月 (2008).
- 川村広和, 秋山岳伸, 石井哲朗, 池田友樹, 亀田大輔, 聖代橋悦子, 豊田健司, 長江大輔, 新田稔, 二宮一史, 秦麻記, 平山賀一, 光岡真一, 宮武宇也, 村田次郎, 渡辺裕: “TRIAC における偏極不安定核を用いた時間反転対称性破れの探索”, 第 5 回停止・低速不安定核ビームを用いた核分光研究会, (大阪大学), 豊中, 12 月 (2008).
- 川村広和, 秋山岳伸, 秦麻記, 平山賀一, 池田友樹, 亀田大輔, 宮原直亮, 宮武宇也, 村田次郎, 中谷祐輔, 長江大輔, 二宮一史, 新田稔, 大西潤一, 聖代橋悦子, 豊田健司, 塚田和司, 渡辺裕: “TRIAC における偏極  $^8\text{Li}$  を用いた時間反転対称性破れの探索”, 日本物理学会第 64 回年次大会, 東京, 3 月 (2009).
- 二宮一史, 秋山岳伸, 池田友樹, 小川成也, 川村広和, 関口雄太, 筒井亮丞, 秦麻記, 村田次郎: “NewtonII 号による等価原理検証を目指した近距離重力実験”, 日本物理学会第 64 回年次大会, 東京, 3 月 (2009).

## SLOWRI Team

### Publications

#### [Journal]

(Original Papers) \*Subject to Peer Review

Okada K., Wada M., Nakamura T., Takamine A., Lioubimov V., Schury P. H., Ishida Y., Sonoda T., Ogawa M., Yamazaki Y., Kanai Y., Kojima T., Katayama I., Ohtani S., Kubo T., and Yoshida A.: "Precision Measurement of the Hyperfine Structure of Laser-Cooled Radioactive  ${}^7\text{Be}^+$  Ions Produced by Projectile Fragmentation", *Phys. Rev. Lett.* **101**, 212502-1–212502-4 (2008). \*

(Review)

和田道治: "光学的手法による不安定原子核の精密分光", *光学* **37**, No. 7, pp. 383–390 (2008).

### Oral Presentations

(International Conference etc.)

Wada M.: "Precision hyperfine structure spectroscopy of  ${}^{11}\text{Be}$  and  ${}^7\text{Be}$ ", Hokudai-TORIJIN-JUSTIPEN-EFES Workshop & JUSTIPEN-EFES-Hokudai-UNEDF Meeting, Morimachi, Hokkaido Pref., July (2008).

Lioubimov V., Wada M., Takamine A., Nakamura T., Schury P. H., Imura H., Okada K., Schuch R. H., and Yamazaki Y.: "Precision Fast Ion Beam Laser Spectroscopy of  $\text{Ar}^+$ ", International Conference on Laser Probing 2008 (LAP 2008), (Nagoya University), Nagoya, Oct. (2008).

Wada M., Takamine A., Okada K., Sonoda T., Schury P. H., Lioubimov V., Yamazaki Y., Kanai Y., Kojima T., Kubo T., Imura H., Katayama I., Ohtani S., Wollnik H., and Schuch R. H.: "Universal Slow RI-Beam Facility at RIKEN RIBF for Laser Spectroscopy of Short-Lived Nuclei", International Conference on Laser Probing 2008 (LAP 2008), (Nagoya University), Nagoya, Oct. (2008).

(Domestic Conference)

古川武, 松尾由賀利, 畠山温, 風戸正行, 星野紗代, 佐々木彩子, 涌井崇志, 上野秀樹, 吉見彰洋, 青井考, 武智麻耶, 梶野泰宏, 小林徹, 和田道治, 高峰愛子, 藤掛浩太郎, 松浦佑一, 小田原厚子, 下田正, 篠塚勉, 本林透: "超流動ヘリウム液体中に植え込まれた不安定同位体原子のレーザー分光実験" OROCHI", 第5回 AMO 討論会, 八王子, 6月 (2008).

古川武, 松尾由賀利, 畠山温, 風戸正行, 星野紗代, 佐々木彩子, 涌井崇志, 上野秀樹, 青井考, 吉見彰洋, 武智麻耶, 梶野泰宏, 小林徹, 和田道治, 園田哲, 高峰愛子, 藤掛浩太郎, 松浦佑一, 小田原厚子, 下田正, 篠塚勉, 本林透: "理研" OROCHI "実験計画: 超流動ヘリウムを利用した短寿命不安定核のレーザー核分光", RCNP 研究会「RCNPにおける不安定核の研究: RCNP ビームラインの可能性を探る」, 茨木, 8月 (2008).

和田道治: "Be-11 の超微細構造異常と同位体効果による中性子ロー核の磁化半径, 荷電半径の研究", RCNP 研究会「RCNPにおける不安定核の研究: RCNP ビームラインの可能性を探る」, (RCNP), 茨木, 8月 (2008).

和田道治: "不安定ベリリウム同位体の精密レーザー分光と SLOWRI 施設の展望", 日本物理学会 2008 年秋季大会, (日本物理学会), 山形, 9月 (2008).

古川武, 松尾由賀利, 畠山温, 風戸正行, 星野紗代, 佐々木彩子, 涌井崇志, 上野秀樹, 青井考, 吉見彰洋, 武智麻耶, 梶野泰宏, 小林徹, 和田道治, 園田哲, 高峰愛子, 藤掛浩太郎, 松浦佑一, 小田原厚子, 下田正, 篠塚勉, 本林透: "超流動ヘリウム中における短寿命核のレーザー核分光実験計画『OROCHI』の現状", 日本物理学会 2008 年秋季大会, (日本物理学会), 山形, 9月 (2008).

## Polarized RI Beam Team

### Publications

#### [Journal]

(Original Papers) \*Subject to Peer Review

- Gomi T., Motobayashi T., Yoneda K., Kanno S., Aoi N., Ando Y., Baba H., Demichi K., Fulop Z., Futakami U., Hasegawa H., Higurashi Y., Ieki K., Imai N., Iwasa N., Iwasaki H., Kubo T., Kubono S., Kunibu M., Matsuyama Y., Michimasa S., Minemura T., Murakami H., Nakamura T., Saito A., Sakurai H., Serata M., Shimoura S., Sugimoto T., Takeshita E., Takeuchi S., Ue K., Yamada K., Yanagisawa Y., Yoshida A., and Ishihara M.: “Coulomb Dissociation of  $^{23}\text{Al}$ ”, *Prog. Theor. Phys. Suppl.*, No. 146, pp. 557–558 (2002). \*
- Kanno S., Gomi T., Motobayashi T., Yoneda K., Aoi N., Ando Y., Baba H., Demichi K., Fulop Z., Futakami U., Hasegawa H., Higurashi Y., Ieki K., Imai N., Iwasa N., Iwasaki H., Kubo T., Kubono S., Kunibu M., Matsuyama Y., Michimasa S., Minemura T., Murakami H., Nakamura T., Saito A., Sakurai H., Serata M., Shimoura S., Sugimoto T., Takeshita E., Takeuchi S., Ue K., Yamada K., Yanagisawa Y., Yoshida A., and Ishihara M.: “Coulomb Excitation of  $^{24}\text{Si}$ ”, *Prog. Theor. Phys. Suppl.*, No. 146, pp. 575–576 (2002). \*
- Gomi T., Motobayashi T., Yoneda K., Kanno S., Aoi N., Ando Y., Baba H., Demichi K., Fulop Z., Futakami U., Hasegawa H., Higurashi Y., Ieki K., Imai N., Iwasa N., Iwasaki H., Kubo T., Kubono S., Kunibu M., Matsuyama Y., Michimasa S., Minemura T., Murakami H., Nakamura T., Saito A., Sakurai H., Serata M., Shimoura S., Sugimoto T., Takeshita E., Takeuchi S., Ue K., Yamada K., Yanagisawa Y., Yoshida A., and Ishihara M.: “Study of the  $^{22}\text{Mg}(p, \gamma)^{23}\text{Al}$  Reaction with the Coulomb-Dissociation Method”, *Nucl. Phys. A* **718**, 508c–509c (2003). \*
- Prandolini M. J., Manzhur Y., Weber A., Potzger K., Bertschat H. H., Ueno H., Miyoshi H., and Dietrich M.: “Impurity-induced magnetic units embedded in ferromagnetic surfaces”, *Appl. Phys. Lett.* **85**, 76–78 (2004). \*
- Gomi T., Motobayashi T., Ando Y., Aoi N., Baba H., Demichi K., Elekes Z., Fukuda N., Fulop Z., Futakami U., Hasegawa H., Higurashi Y., Ieki K., Imai N., Ishihara M., Ishikawa K., Iwasa N., Iwasaki H., Kanno S., Kondo Y., Kubo T., Kubono S., Kunibu M., Kurita K., Matsuyama Y., Michimasa S., Minemura T., Miura M., Murakami H., Nakamura T., Notani M., Ota S., Saito A., Sakurai H., Serata M., Shimoura S., Sugimoto T., Takeshita E., Takeuchi S., Togano Y., Ue K., Yamada K., Yanagisawa Y., Yoneda K., and Yoshida A.: “Study of the Stellar  $^{22}\text{Mg}(p, \gamma)^{23}\text{Al}$  Reaction using the Coulomb-Dissociation Method”, *Nucl. Phys. A* **734**, E77–E79 (2004).
- Ueno H., Asahi K., Ogawa H., Kameda D., Miyoshi H., Yoshimi A., Watanabe H., Shimada K., Sato W., Yoneda K., Imai N., Kobayashi Y., Ishihara M., and Wolf-Dieter S.: “Measurement of nuclear moments in the region of light neutron-rich nuclei”, *Nucl. Phys. A* **738**, 211–215 (2004). \*
- Imai N., Ong H., Aoi N., Sakurai H., Demichi K., Kawasaki H., Baba H., Dombradi Z., Elekes Z., Fukuda N., Fulop Z., Gelberg A., Gomi T., Hasegawa H., Ishikawa K., Iwasaki H., Kaneko E., Kanno S., Kishida T., Kondo Y., Kubo T., Kurita K., Michimasa S., Minemura T., Miura M., Motobayashi T., Nakamura T., Notani M., Ohnishi T., Saito A., Shimoura S., Sugimoto T., Suzuki M., Takeshita E., Takeuchi M., Tamaki M., Yoneda K., Watanabe H., and Ishihara M.: “Anomalous hindered  $E2$  Strength  $B(E2; 2_1^+ \rightarrow 0^+)$  in  $^{16}\text{C}$ ”, *Phys. Rev. Lett.* **92**, No. 6, pp. 062501-1–062501-4 (2004). \*
- Gomi T., Motobayashi T., Ando Y., Aoi N., Baba H., Demichi K., Elekes Z., Fukuda N., Fulop Z., Futakami U., Hasegawa H., Higurashi Y., Ieki K., Imai N., Ishihara M., Ishikawa K., Iwasa N., Iwasaki H., Kanno S., Kondo Y., Kubo T., Kubono S., Kunibu M., Kurita K., Matsuyama Y., Michimasa S., Minemura T., Miura M., Murakami H., Nakamura T., Notani M., Ota S., Saito A., Sakurai H., Serata M., Shimoura S., Sugimoto T., Takeshita E., Takeuchi S., Togano Y., Ue K., Yamada K., Yanagisawa Y., Yoneda K., and Yoshida A.: “Coulomb dissociation experiment for explosive hydrogen burning: study of the  $^{22}\text{Mg}(p, \gamma)^{23}\text{Al}$  reaction”, *J. Phys. G* **31**, S1517–S1521 (2005).
- Togano Y., Gomi T., Motobayashi T., Ando Y., Aoi N., Baba H., Demichi K., Elekes Z., Fukuda N., Fulop Z., Futakami U., Hasegawa H., Higurashi Y., Ieki K., Imai N., Ishihara M., Ishikawa K., Iwasa N., Iwasaki H., Kanno S., Kondo Y., Kubo T., Kubono S., Kunibu M., Kurita K., Matsuyama Y., Michimasa S., Minemura T., Miura M., Murakami H., Nakamura T., Notani M., Ota S., Saito A., Sakurai H., Serata M., Shimoura S., Sugimoto T., Takeshita E., Takeuchi S., Ue K., Yamada K., Yanagisawa Y., Yoneda K., and Yoshida A.: “Study of  $^{26}\text{Si}(p, \gamma)^{27}\text{P}$  reaction using Coulomb dissociation method”, *Nucl. Phys. A* **758**, 182c–185c (2005). \*
- Onishi T., Gelberg A., Sakurai H., Yoneda K., Aoi N., Imai N., Baba H., Von Brentano P., Fukuda N., Ichikawa Y., Ishihara M., Iwasaki H., Kameda D., Kishida T., Lisetskiy A., Ong H., Osada M., Ohtsuka T., Suzuki M., Ue K., Utsuno Y., and Watanabe H.: “Gamow-Teller decay of the  $T = 1$  nucleus  $^{46}\text{Cr}$ ”, *Phys. Rev. C* **72**, No. 2, pp. 024308-1–024308-7 (2005). \*
- Togano Y., Gomi T., Motobayashi T., Ando Y., Aoi N., Baba H., Demichi K., Elekes Z., Fukuda N., Fulop Z., Futakami U., Hasegawa H., Higurashi Y., Ieki K., Imai N., Ishihara M., Ishikawa K., Iwasa N., Iwasaki H., Kanno S., Kondo Y., Kubo T., Kubono S., Kunibu M., Kurita K., Matsuyama Y., Michimasa S., Minemura

- T., Miura M., Murakami H., Nakamura T., Notani M., Ota S., Saito A., Sakurai H., Serata M., Shimoura S., Sugimoto T., Takeshita E., Takeuchi S., Ue K., Yamada K., Yanagisawa Y., Yoneda K., and Yoshida A.: “Study of the  $^{26}\text{Si}(p, \gamma)^{27}\text{P}$  reaction through Coulomb dissociation of  $^{27}\text{P}$ ”, *Eur. Phys. J. A* **27**, No. s01, pp. 233–236 (2006). \*
- Gomi T., Motobayashi T., Ando Y., Aoi N., Baba H., Demichi K., Elekes Z., Fukuda N., Fulop Z., Futakami U., Hasegawa H., Higurashi Y., Ieki K., Imai N., Ishihara M., Ishikawa K., Iwasa N., Iwasaki H., Kanno S., Kondo Y., Kubo T., Kubono S., Kunibu M., Kurita K., Matsuyama Y., Michimasa S., Minemura T., Miura M., Murakami H., Nakamura T., Notani M., Ota S., Saito A., Sakurai H., Serata M., Shimoura S., Sugimoto T., Takeshita E., Takeuchi S., Togano Y., Ue K., Yamada K., Yanagisawa Y., Yoneda K., and Yoshida A.: “Coulomb Dissociation of  $^{23}\text{Al}$  for the stellar  $^{22}\text{Mg}(p, \gamma)^{23}\text{Al}$  reaction”, *Nucl. Phys. A* **758**, 761c–764c (2006).
- Nakamura T., Vinodkumar A., Sugimoto T., Aoi N., Baba H., Bazin D. P., Fukuda N., Gomi T., Hasegawa H., Imai N., Ishihara M., Kobayashi T., Kondo Y., Kubo T., Miura M., Motobayashi T., Otsu H., Saito A., Sakurai H., Shimoura S., Watanabe K., Watanabe Y., Yakushiji T., Yanagisawa Y., and Yoneda K.: “Observation of Strong Low-Lying E1 Strength in the Two-Neutron Halo Nucleus  $^{11}\text{Li}$ ”, *Phys. Rev. Lett.* **96**, 252502-1–252502-4 (2006). \*
- Yoshimi A., Ueno H., Kameda D., Asahi K., Nagae D., Takemura M., Shimada K., Takase K., Sugimoto T., Uchida M., Arai T., Inoue T., Murata J., and Kawamura H.: “Electric quadrupole moments of neutron rich Al isotope”, *AIP Conf. Proc.* **912**, 105–109 (2007). \*
- Murata J., Asahi K., Kameda D., Kawamura H., Nagae D., Narota K., Shimada K., Shimoyama T., Shuehiro T., Toyoda T., Uchida M., Ueno H., and Yoshimi A.: “Beta Neutrino Correlation and T-Violation Experiment in Nuclear Beta Decay”, *AIP Conf. Proc.* **915**, No. 1, pp. 218–221 (2007). \*
- Yoshimi A., Ueno H., Sugimoto T., Shimada K., Nagae D., Murata J., Kawamura H., Kameda D., and Asahi K.: “Developments of atomic beam resonance method with RI beams”, *AIP Conf. Proc.* **915**, 849–852 (2007). \*
- Kawamura H., Kameda D., Murata J., Narota K., Shimoyama T., Suehiro T., Toyoda T., and Uchida M.: “Development of a New Drift Chamber based Mott Polarimeter”, *AIP Conf. Proc.* **915**, 1105–1108 (2007). \*
- Shimada K., Nagae D., Asahi K., Inoue T., Takase K., Kagami S., Hatakeyama N., Kobayashi Y., Ueno H., Yoshimi A., Kameda D., Nagatomo T., Sugimoto T., Kubono S., Yamaguchi H., Wakabayashi Y., Hayakawa S., Murata J., and Kawamura H.: “Production of spin-polarized  $^{17}\text{N}$  beam using inverse-kinematics low-energy transfer reactions”, *Hyperfine Interact.* **180**, 43–47 (2007). \*
- Kameda D., Ueno H., Asahi K., Nagae D., Yoshimi A., Nagatomo T., Sugimoto T., Uchida M., Takemura M., Shimada K., Takase K., Inoue T., Kijima G., Arai T., Suda S., Murata J., Kawamura H., Kobayashi Y., Watanabe H., and Ishihara M.: “Production of spin-polarized radioactive ion beams via projectile fragmentation reaction”, *AIP Conf. Proc.* **980**, 283–288 (2008). \*
- Kameda D., Asahi K., Ueno H., Nagae D., Takemura M., Shimada K., Yoshimi A., Nagatomo T., Sugimoto T., Uchida M., Arai T., Takase K., Suda S., Inoue T., Murata J., Kawamura H., Watanabe H., Kobayashi Y., and Ishihara M.: “Electric quadrupole moments of neutron-rich nuclei  $^{32}\text{Al}$  and  $^{31}\text{Al}$ ”, *Hyperfine Interact.* **180**, 61–64 (2008). \*
- Yoshimi A., Inoue T., Uchida M., Hatakeyama N., and Asahi K.: “Optical-coupling nuclear spin maser under highly stabilized low static field”, *Hyperfine Interact.* **181**, 111–114 (2008). \*
- Sugimoto T., Asahi K., Kawamura H., Murata J., Nagae D., Shimada K., Ueno H., and Yoshimi A.: “Development of atomic-beam resonance method to measure the nuclear moments of unstable nuclei”, *Hyperfine Interact.* **181**, 141–144 (2008). \*
- Sato W., Ueno H., Watanabe H., Miyoshi H., Yoshimi A., Kameda D., Ito T., Shimada K., Kaihara J., Suda S., Kobayashi Y., Shinohara A., Ohkubo Y., and Asahi K.: “Temperature-dependent behavior of impurity atoms implanted in highly oriented pyrolytic graphite—An application of a new online TDPAC method—”, *J. Phys. Soc. Jpn.* **77**, No. 9, pp. 095001-1–095001-2 (2008). \*
- Nagae D., Ueno H., Kameda D., Takemura M., Asahi K., Yoshimi A., Sugimoto T., Shimada K., Nagatomo T., Uchida M., Arai T., Inoue T., Kagami S., Hatakeyama N., Murata J., Kawamura H., and Narota K.: “Electric quadrupole moment of  $^{31}\text{Al}$ ”, *Nucl. Instrum. Methods Phys. Res. B* **266**, 4612–4615 (2008). \*
- Ueno H., Nagae D., Kameda D., Asahi K., Takemura M., Takase K., Yoshimi A., Sugimoto T., Shimada K., Nagatomo T., Uchida M., Arai T., Inoue T., Murata J., Kawamura H., and Narota K.: “Electric quadrupole moment of  $^{31}\text{Al}$ ”, *Nucl. Phys. A* **805**, 329–331 (2008). \*
- Suzuki D., Iwasaki H., Ong H., Imai N., Sakurai H., Nakao T., Aoi N., Baba H., Bishop S., Ichikawa Y., Ishihara M., Kondo Y., Kubo T., Kurita K., Motobayashi T., Nakamura T., Okumura T., Onishi T., Ota S., Suzuki M., Takeuchi S., Togano Y., and Yanagisawa Y.: “Lifetime measurements of excited states in  $^{17}\text{C}$ : Possible interplay between collectivity and halo effects”, *Phys. Lett. B* **666**, 222–227 (2008). \*
- Zegers R. G., Brown E. F., Akimune H., Austin S.

M., van den Berg A. M., Brown B. A., Chamulak D. A., Fujita Y., Fujiwara M., Gales S., Harakeh M. N., Hashimoto H., Hayami R., Hitt G. W., Itoh M., Kawabata T., Kawase K., Kinoshita M., Nakanishi K., Nakayama S., Okumura S., Shimbara Y., Uchida M., Ueno H., Yamagata T., and Yosoi M.: “Gamow-Teller strength for the analog transitions to the first  $T = 1/2$ ,  $J^\pi = 3/2^-$  states in  $^{13}\text{C}$  and  $^{13}\text{N}$  and the implications for type Ia supernovae”, *Phys. Rev. C* **77**, 024307-1–024307-10 (2008). \*

Nagae D., Ueno H., Kameda D., Takemura M., Asahi K., Takase K., Yoshimi A., Sugimoto T., Shimada K., Nagatomo T., Uchida M., Arai T., Inoue T., Kagami S., Hatakeyama N., Kawamura H., Narota K., and Murata J.: “Ground-state electric quadrupole moment of  $^{31}\text{Al}$ ”, *Phys. Rev. C* **79**, 027301-1–027301-4 (2009). \*

(Others)

Murata J., Akiyama T., Hata M., Hirayama Y., Ikeda Y., Ishii T., Kameda D., Kawamura H., Mitsuoka S., Miyatake H., Nagae D., Ninomiya K., Nitta M., Seitaibashi E., and Toyoda T.: “R&D for a test of time reversal symmetry experiment using polarized nuclei”, *JAEA-Review* **2008-054**, 58–59 (2008).

#### [Book • Proceedings]

(Original Papers) \*Subject to Peer Review

Ueno H.: “Status of RI Beam Factory Project at RIKEN”, *Changing Facets of Nuclear Structure: Proceedings of the 9th International Spring Seminar on Nuclear Physics*, Vico Equense, Italy, 2007–5, World Scientific Publishing, Singapore, pp. 13–21 (2008).

#### Oral Presentations

(International Conference etc.)

Sugimoto T., Yoshimi A., Ueno H., Asahi K., Kawamura H., Murata J., Nagae D., and Shimada K.: “Development of ion guiding system for radio-isotope atomic-beam resonance measurements”, *International Nuclear Physics Conference (INPC2007)*, (Science Council of Japan, RIKEN and others), Tokyo, June (2007).

Yoshimi A., Asahi K., Inoue T., Uchida M., and Hatakeyama N.: “Optical-coupling nuclear spin maser and search for an atomic EDM of  $^{129}\text{Xe}$ ”, *International Nuclear Physics Conference (INPC2007)*, (Science Council of Japan, RIKEN and others), Tokyo, June (2007).

Kameda D., Ueno H., Asahi K., Nagae D., Takemura M., Yoshimi A., Shimada K., Uchida M., Kijima G., Arai T., Takase K., Suda S., Inoue T., Murata J., Kawamura H., Haseyama T., Kobayashi Y., Watanabe H., and Ishihara M.: “Small electric quadrupole moment of  $^{32}\text{Al}$ : Drastic shape transition between  $^{32}\text{Al}$  and  $^{31}\text{Mg}$ ”, *International Nuclear Physics Conference (INPC2007)*, (Science Council of Japan, RIKEN and others), Tokyo, June (2007).

Imai N., Ong H., Aoi N., Sakurai H., Demichi K.,

Kawasaki H., Baba H., Dombradi Z., Elekes Z., Fukuda N., Fulop Z., Gelberg A., Gomi T., Hasegawa H., Ishikawa K., Iwasaki H., Kaneko E., Kanno S., Kishida T., Kondo Y., Kubo T., Kurita K., Michimasa S., Minemura T., Miura M., Motobayashi T., Nakamura T., Notani M., Onishi T., Saito A., Shimoura S., Sugimoto T., Suzuki M., Takeshita E., Takeuchi S., Tamaki M., Yamada K., Yoneda K., Watanabe H., and Ishihara M.: “The lifetime measurement of the first  $2^+$  state in  $^{12}\text{Be}$ ”, *International Nuclear Physics Conference (INPC2007)*, Tokyo, June (2007).

Kameda D., Ueno H., Asahi K., Nagae D., Takemura M., Yoshimi A., Shimada K., Uchida M., Kijima G., Arai T., Takase K., Suda S., Inoue T., Murata J., Kawamura H., Haseyama T., Kobayashi Y., Watanabe H., and Ishihara M.: “Small electric quadrupole moment of  $^{32}\text{Al}$ ”, *International Workshop on Nuclear Structure: New Pictures in the Extended Isospin Space (NS07)*, (Yukawa Institute for Theoretical Physics), Kyoto, June (2007).

Yoshimi A., Uchida M., Inoue T., and Hatakeyama N.: “Optical-coupling nuclear spin maser under highly stabilized low static field”, *14th International Conference on Hyperfine Interactions and 18th International Symposium on Nuclear Quadrupole Interactions*, (Universidad Nacional de La Plata etc.), Iguas, Brazil, Aug. (2007).

Kameda D., Ueno H., Asahi K., Nagae D., Takemura M., Yoshimi A., Shimada K., Nagatomo T., Sugimoto T., Uchida M., Arai T., Takase K., Suda S., Inoue T., Murata J., Kawamura H., Watanabe H., Kobayashi Y., and Ishihara M.: “Electric quadrupole moments of neutron-rich nuclei  $^{32}\text{Al}$  and  $^{31}\text{Al}$ ”, *14th Int. Conf. on Hyperfine Interactions & 18th Int. Symp. on Nuclear Quadrupole Interactions*, (Universidad Nacional de La Plata), Iguassu Falls, Brazil, Aug. (2007).

Kameda D., Ueno H., Asahi K., Nagae D., Yoshimi A., Nagatomo T., Sugimoto T., Uchida M., Takemura M., Shimada K., Takase K., Inoue T., Kijima G., Arai T., Suda S., Murata J., Kawamura H., Kobayashi Y., Watanabe H., and Ishihara M.: “Production of spin-polarized r/a beams via projectile fragmentation reaction”, *12th Int. Workshop on Polarized Sources, Targets & Polarimetry*, (Brookhaven National Laboratory), Brookhaven, USA, Sept. (2007).

Yoshimi A., Ueno H., Nagatomo T., Shimada K., Ichikawa Y., Kameda D., Sugimoto T., Sakurai H., Asahi K., Hasama Y., Takemura M., Kijima G., Nagae D., Uchida M., Arai T., Suda S., Takase T., Inoue T., Hatakeyama N., Kagami S., Murata J., and Kawamura H.: “Nuclear electromagnetic moments of neutron-rich Al isotopes”, *Nuclear Structure 2008*, (Michigan State University, NSCL at MSU), Michigan, USA, June (2008).

Inoue T., Asahi K., Kagami S., Hatakeyama N., Uchida M., and Yoshimi A.: “Nuclear spin maser for  $^{129}\text{Xe}$  atomic EDM measurement -present status-”, *24th Advanced Studies Institute :Symmetries and Spin (SPIN-*

- Praha-2008), (Charles University), Praha, Czech, July (2008).
- Kawamura H., Murata J., Toyoda T., Seitabashi E., Nitta M., Hata M., Akiyama T., Ikeda Y., Ninomiya K., Kameda D., Nagae D., and Hirayama Y.: "The first T-violation experiment at KEK-TRIAC", 24th Advanced Studies Institute :Symmetries and Spin (SPIN-Praha-2008), (Charles University in Prague, Faculty of Mathematics and Physics), Praha, Czech, July (2008).
- Yoshimi A., Asahi K., Inoue T., Uchida M., Hatakeyama N., and Kagami S.: "Nuclear spin maser at highly stabilized low magnetic field and search for an atomic EDM", 18th International Symposium on Spin Physics (SPIN 2008), (University of Virginia), Charlottesville, USA, Oct. (2008).
- (Domestic Conference)
- 今井伸明, 青井考, 王恵仁, 櫻井博儀, 出道仁彦, Kawasaki H., 馬場秀忠, Dombardi Z., Elekes Z., 福田直樹, Fulop Z., Gelberg A., 五味朋子, 長谷川浩一, 石川和宏, 岩崎弘典, 金子恵美, 菅野祥子, 岸田隆, 近藤洋介, 久保敏幸, 栗田和好, 道正新一郎, 峯村俊行, 三浦宗賢, 本林透, 中村隆司, 野谷将広, 大西健夫, 齋藤明登, 下浦享, 杉本崇, Suzuki M., 竹下英里, 武内聡, 玉城充, 山田一成, 米田健一郎, 渡邊寛, 石原正泰: "12Be と 16C における第一励起状態から基底状態への換算転移確率", 日本物理学会第 58 回年次大会, 仙台, 3 月 (2003).
- 今井伸明, 王恵仁, 青井考, 櫻井博儀, 出道仁彦, Kawasaki H., 馬場秀忠, Dombardi Z., Elekes Z., 福田直樹, Fulop Z., Gelberg A., 五味朋子, 長谷川浩一, 石川和宏, 岩崎弘典, 金子恵美, 菅野祥子, 岸田隆, 近藤洋介, 久保敏幸, 栗田和好, 道正新一郎, 峯村俊行, 三浦宗賢, 本林透, 中村隆司, 野谷将広, 大西健夫, 齋藤明登, 下浦享, 杉本崇, Suzuki M., 竹下英里, 武内聡, 玉城充, 山田一成, 米田健一郎, 渡邊寛, 石原正泰: "Anomalous long lifetime of 2+1 state of 16C", A New Era of Nuclear Structure Physics, 新潟県黒川村, 11 月 (2003).
- 今井伸明, 王恵仁, 青井考, 櫻井博儀, 出道仁彦, Kawasaki H., 馬場秀忠, Dombardi Z., Elekes Z., 福田直樹, Fulop Z., Gelberg A., 五味朋子, 長谷川浩一, 石川和宏, 岩崎弘典, 金子恵美, 菅野祥子, 岸田隆, 近藤洋介, 久保敏幸, 栗田和好, 道正新一郎, 峯村俊行, 三浦宗賢, 本林透, 中村隆司, 野谷将広, 大西健夫, 齋藤明登, 下浦享, 杉本崇, Suzuki M., 竹下英里, 武内聡, 玉城充, 山田一成, 米田健一郎, 渡邊寛, 石原正泰: "Experimental finding of the anomalous quadrupole collectivity in unstable nucleus 16C", 日本物理学会 2005 年秋季大会, (日本物理学会), 京田辺, 9 月 (2005).
- 今井伸明, 王恵仁, 青井考, 櫻井博儀, 出道仁彦, Kawasaki H., 馬場秀忠, Dombardi Z., Elekes Z., 福田直樹, Fulop Z., Gelberg A., 五味朋子, 長谷川浩一, 石川和宏, 岩崎弘典, 金子恵美, 菅野祥子, 岸田隆, 近藤洋介, 久保敏幸, 栗田和好, 道正新一郎, 峯村俊行, 三浦宗賢, 本林透, 中村隆司, 野谷将広, 大西健夫, 齋藤明登, 下浦享, 杉本崇, Suzuki M., 竹下英里, 武内聡, 玉城充, 山田一成, 米田健一郎, 渡邊寛, 石原正泰: "Lifetime measurement of 12Be(2+1)", 日本物理学会 2005 年秋季大会, (日本物理学会), 京田辺, 9 月 (2005).
- 上野 秀樹: "Nuclear-moment measurements utilizing fragmentation-induced spin-oriented RI beams at RIKEN", Workshop on Advance in Physics with ISOL-based/Fragmentation-based RI Beams, (東京工業大学), 東京, 2 月 (2008).
- 古川武, 松尾由賀利, 畠山温, 風戸正行, 星野紗代, 佐々木彩子, 涌井崇志, 上野秀樹, 吉見彰洋, 青井考, 武智麻耶, 梶野泰宏, 小林徹, 和田道治, 高峰愛子, 藤掛浩太郎, 松浦佑一, 小田原厚子, 下田正, 篠塚勉, 本林透: "超流動ヘリウム液体中に植え込まれた不安定同位体原子のレーザー分光実験" OROCHI", 第 5 回 AMO 討論会, 八王子, 6 月 (2008).
- 佐々木彩子, 古川武, 藤掛浩太郎, 小林徹, 畠山温, 下田正, 小田島仁司, 松尾由賀利: "超流動ヘリウム中に植え込まれた In 原子の励起スペクトル", 第 5 回 AMO 討論会, 八王子, 6 月 (2008).
- 松尾由賀利, 古川武, 畠山温, 風戸正行, 星野紗代, 佐々木彩子, 涌井崇志, 上野秀樹, 青井考, 吉見彰洋, 武智麻耶, 梶野泰宏, 小林徹, 和田道治, 園田哲, 高峰愛子, 藤掛浩太郎, 松浦佑一, 小田原厚子, 下田正, 篠塚勉, 本林透: "超流動ヘリウム中エキゾチック RI 原子の新奇なレーザー分光法 (OROCHI 法): 不安定核 Rb 原子の超微細構造精密測定へ向けて", 東北大学・CYRIC 研究会 Fundamental Physics using Atoms, (東北大学 CYRIC), 仙台, 8 月 (2008).
- 上野秀樹: "低・中間エネルギー RIB を用いた核モーメント測定", RCNP 研究会「RCNP における不安定核の研究: RCNP ビームラインの可能性を探る」, (大阪大学), 吹田, 8 月 (2008).
- 古川武, 松尾由賀利, 畠山温, 風戸正行, 星野紗代, 佐々木彩子, 涌井崇志, 上野秀樹, 青井考, 吉見彰洋, 武智麻耶, 梶野泰宏, 小林徹, 和田道治, 園田哲, 高峰愛子, 藤掛浩太郎, 松浦佑一, 小田原厚子, 下田正, 篠塚勉, 本林透: "理研" OROCHI "実験計画: 超流動ヘリウムを利用した短寿命不安定核のレーザー核分光", RCNP 研究会「RCNP における不安定核の研究: RCNP ビームラインの可能性を探る」, 茨木, 8 月 (2008).
- 内田誠, 井上壮志, 旭耕一郎, 各務惣太, 畠山直人, 吉見彰洋: "核スピンメーザー開発の現状と今後の課題", 東北大学 CYRIC 研究会「Fundamental Physics using Atoms」, (東北大学 CYRIC), 仙台, 8 月 (2008).
- 吉見彰洋, 旭耕一郎, 内田誠, 井上壮志, 畠山直人, 各務惣太: "核スピンメーザーを用いた 129Xe 原子 EDM の探索", 東北大学 CYRIC 研究会「Fundamental Physics using Atoms」, (東北大学 CYRIC), 仙台, 8 月 (2008).
- 大江一弘, 矢作亘, 小森有希子, 藤沢弘幸, 菊永英寿, 吉村崇, 佐藤渉, 高橋成人, 高久圭二, 羽場宏光, 工藤祐生, 江崎豊, 篠原厚: "106 番元素シーボーギウムの化学実験に向けたタンクステン溶媒抽出挙動の研究", 2008 年日本放射化学会年会/第 52 回放射化学討論会, (日本放射化学会), 広島, 9 月 (2008).
- 井上壮志, 吉見彰洋, 内田誠, 畠山直人, 旭耕一郎: "原子 EDM 測定のための 129Xe 核スピンメーザーの開発", 日本物理学会 2008 年秋季大会, (日本物理学会), 山形, 9 月 (2008).
- 島田健司, 長友傑, 旭耕一郎, Balabanski D. L., Daugas

- J. M., Depuydt M., De Rydt M., Gaudefroy L., Grevy S., 挾間 優佳, 市川 雄一, 亀田大輔, Morel P., Perrot L., Stodel C., Thomas J. C., Vanderheyolen W., Vermeulen N., Vingerhoets P., 吉見彰洋, Neyens G., 上野秀樹: “ $^{33}\text{Al}$  の電気四重極モーメント”, 日本物理学会 2008 年秋季大会, (山形大学, 日本物理学会), 山形, 9 月 (2008).
- 古川武, 松尾由賀利, 畠山温, 風戸正行, 星野紗代, 佐々木彩子, 涌井崇志, 上野秀樹, 青井考, 吉見彰洋, 武智麻耶, 梶野泰宏, 小林徹, 和田道治, 園田哲, 高峰愛子, 藤掛浩太郎, 松浦佑一, 小田原厚子, 下田正, 篠塚勉, 本林透: “超流動ヘリウム中における短寿命核のレーザー核分光実験計画『OROCHI』の現状”, 日本物理学会 2008 年秋季大会, (日本物理学会), 山形, 9 月 (2008).
- 豊田健司, 秋山岳伸, 秦麻記, 平山賀一, 池田友樹, 亀田大輔, 川村広和, 村田次郎, 長江大輔, 二宮一史, 新田稔, 聖代橋悦子: “TRIAC における時間反転対称性の破れ探索実験”, 日本物理学会 2008 年秋季大会, 山形, 9 月 (2008).
- 市川雄一, 久保敏幸, 青井考, Banerjee S. R., Chakrabarti A., 福田直樹, 岩崎弘典, 久保野茂, 本林透, 中林彩, 中村隆司, 中尾太郎, 奥村俊文, 王恵仁, 大西健夫, 鈴木大介, 鈴木賢, 山田一成, 山口英斉, 櫻井博儀: 日本物理学会 2008 年秋季大会, 山形, 9 月 (2008).
- 佐々木彩子, 星野紗代, 涌井崇志, 古川武, 風戸正行, 山口杏子, 小林徹, 畠山温, 藤掛浩太郎, 松浦佑一, 小田原厚子, 下田正, 篠塚勉, 松尾由賀利: “OROCHI 実験に向けた蛍光検出系の開発”, 第 5 回停止・低速不安定核ビームを用いた核分光研究会, 豊中, 12 月 (2008).
- 藤掛浩太郎, 古川武, 畠山温, 小林徹, 松浦佑一, 小田島仁司, 下田正, 松尾由賀利: “超流動ヘリウム中における光ポンピング法を用いた Ag 原子の高偏極生成”, 第 5 回停止・低速不安定核ビームを用いた核分光研究会, 豊中, 12 月 (2008).
- 松尾由賀利, 古川武, 畠山温, 風戸正行, 山口杏子, 星野紗代, 佐々木彩子, 涌井崇志, 上野秀樹, 青井考, 吉見彰洋, 武智麻耶, 梶野泰宏, 西村俊二, 小林徹, 和田道治, 園田哲, 高峰愛子, 藤掛浩太郎, 松浦佑一, 小田原厚子, 下田正, 篠塚勉, 本林透: “超流動ヘリウムを用いたレーザー核分光実験” OROCHI” -第一回ビーム実験へ向けて-, 第 5 回停止・低速不安定核ビームを用いた核分光研究会, 豊中, 12 月 (2008).
- 上野秀樹: “中性子過剰 Al 同位体の核モーメント”, 第 5 回停止・低速不安定核ビームを用いた核分光研究会, (大阪大学), 豊中, 12 月 (2008).
- 川村広和, 秋山岳伸, 石井哲朗, 池田友樹, 亀田大輔, 聖代橋悦子, 豊田健司, 長江大輔, 新田稔, 二宮一史, 秦麻記, 平山賀一, 光岡真一, 宮武宇也, 村田次郎, 渡辺裕: “TRIAC における偏極不安定核を用いた時間反転対称性破れの探索”, 第 5 回停止・低速不安定核ビームを用いた核分光研究会, (大阪大学), 豊中, 12 月 (2008).
- 市川雄一, 久保敏幸, 青井考, Banerjee S. R., Chakrabarti A., 福田直樹, 岩崎弘典, 久保野茂, 本林透, 中林彩, 中村隆司, 中尾太郎, 奥村俊文, 王恵仁, 大西健夫, 鈴木大介, 鈴木賢, 山田一成, 山口英斉, 櫻井博儀: 第 5 回停止・低速不安定核ビームを用いた核分光研究会, (大阪大学), 豊中, 12 月 (2008).
- 佐々木彩子, 星野紗代, 涌井崇志, 古川武, 風戸正行, 山口杏子, 和田道治, 園田哲, 高峰愛子, 小林徹, 上野秀樹, 吉見彰洋, 青井考, 西村俊二, 梶野泰宏, 武智麻耶, 畠山温, 藤掛浩太郎, 松浦佑一, 小田原厚子, 下田正, 本林透, 篠塚勉, 松尾由賀利: “超流動ヘリウム中でのレーザー核分光に向けた蛍光検出系の開発”, 日本物理学会第 64 回年次大会, 東京, 3 月 (2009).
- 藤掛浩太郎, 古川武, 畠山温, 小林徹, 松浦佑一, 下田正, 小田島仁司, 松尾由賀利: “超流動ヘリウム中における Ag 原子の光ポンピング及び磁気共鳴”, 日本物理学会第 64 回年次大会, 東京, 3 月 (2009).
- 古川武, 藤掛浩太郎, 畠山温, 小林徹, 松浦佑一, 佐々木彩子, 星野紗代, 涌井崇志, 風戸正行, 山口杏子, 和田道治, 園田哲, 高峰愛子, 上野秀樹, 吉見彰洋, 青井考, 西村俊二, 梶野泰宏, 武智麻耶, 小田原厚子, 下田正, 篠塚勉, 本林透, 松尾由賀利: “超流動ヘリウム中での光ポンピング法を用いた Ag 原子の高偏極生成とレーザー核分光への応用”, 日本物理学会第 64 回年次大会, 東京, 3 月 (2009).
- 風戸正行, 古川武, 山口杏子, 梶野泰宏, 西村俊二, 佐々木彩子, 星野紗代, 涌井崇志, 畠山温, 藤掛浩太郎, 松浦佑一, 篠塚勉, 本林透, 小田原厚子, 下田正, 松尾由賀利: “超流動ヘリウム中における RI ビーム停止位置の精密制御”, 日本物理学会第 64 回年次大会, 東京, 3 月 (2009).
- 川村広和, 秋山岳伸, 秦麻記, 平山賀一, 池田友樹, 亀田大輔, 宮原直亮, 宮武宇也, 村田次郎, 中谷祐輔, 長江大輔, 二宮一史, 新田稔, 大西潤一, 聖代橋悦子, 豊田健司, 塚田和司, 渡辺裕: “TRIAC における偏極  $^8\text{Li}$  を用いた時間反転対称性破れの探索”, 日本物理学会第 64 回年次大会, 東京, 3 月 (2009).
- 二宮一史, 秋山岳伸, 池田友樹, 小川成也, 川村広和, 関口雄太, 筒井亮丞, 秦麻記, 村田次郎: “NewtonII 号による等価原理検証を目指した近距離重力実験”, 日本物理学会第 64 回年次大会, 東京, 3 月 (2009).

## Rare RI-ring Team

### Publications

#### [Journal]

(Original Papers) \*Subject to Peer Review

Yamaguchi Y., Ozawa A., Goto A., Arai I., Fujinawa T., Fukunishi N., Kikuchi T., Ohnishi T., Ohtsubo T., Sakurai H., Suzuki T., Wakasugi M., Yamaguchi T., Yasuda Y., and Yano Y.: “Rara-RI ring project at RIKEN RI beam factory”, Nucl. Instrum. Methods Phys. Res. B **266**, 4575–4578 (2008). \*

Nakajima S., Kuboki T., Yoshitake M., Hashizume Y., Kanazawa M., Kitagawa a., Kobayashi K., Moriguchi T., Ohtsubo T., Ozawa A., Sato S., Suzuki T., Yamaguchi Y., Yasuda Y., and Yamaguchi T.: “Development of a time-of-flight detector for the rare-RI ring project at RIKEN”, Nucl. Instrum. Methods Phys. Res. B **266**, 4621–4624 (2008). \*

(Others)

Nakajima S., Yamaguchi T., Suzuki T., Yamaguchi Y., Fujinawa T., Fukunishi N., Goto A., Ohnishi T., Sakurai H., Wakasugi M., Yano Y., Arai I., Ozawa A., Yasuda Y., Kikuchi T., and Ohtsubo T.: “New scheme for precision mass measurements of rare isotopes produced at RI beam factory”, Acta Phys. Pol. B **39**, No. 2, pp. 457–462 (2008).

#### [Book•Proceedings]

(Others)

Yamaguchi T., Arai I., Fukunishi N., Goto A., Kikuchi T., Komatsubara T., Ohnishi T., Ohtsubo T., Okuno H., Ozawa A., Sasa K., Suzuki T., Tagisi Y., Takeda H., Wakasugi M., Yamaguchi M., Yamaguchi Y., and Yano Y.: “Mass measurements by an isochronous storage ring at the RIKEN RI beam factory”, Proceedings of the 6th International Conference on Nuclear Physics at Storage Rings (STORI '05), Bonn, Germany, 2005–5, Forschungszentrum Julich, Julich, pp. 297–300 (2005).

Yamaguchi M., Arai I., Fukunishi N., Goto A., Kusaka K., Kikuchi T., Komatsubara T., Kubo T., Ohnishi T., Ohtsubo T., Okuno H., Ozawa A., Sasa K., Suzuki T., Tagisi Y., Takeda H., Wakasugi M., Yamaguchi T., Yamaguchi Y., and Yano Y.: “Design of an isochronous storage ring and an injection line for mass measurements at the RIKEN RI beam factory”, Proceedings of the 6th International Conference on Nuclear Physics at Storage Rings (STORI '05), Bonn, Germany, 2005–5, Forschungszentrum Julich, Julich, pp. 315–319 (2005).

Kikuchi T., Horioka K., Ozawa A., Kawata S., Yamaguchi Y., Fukunishi N., Sakurai H., Wakasugi M., Yamaguchi M., Yamaguchi T., Arai I., Ohta H., Fujinawa T., Sasa K., Komatsubara T., Suzuki T., Ohtsubo T., Goto A., Ohnishi T., Okuno H., Takeda H., and Yano Y.: “Individual correction using induction modulator for mass measurements by isochronous ring in RIKEN RI beam factory”, Proceedings of the 2nd International

Workshop on Recent Progress in Induction Accelerators (RPIA2006), Tsukuba, 2006–3, KEK, Tsukuba, pp. 127–131 (2006).

### Oral Presentations

(International Conference etc.)

Yamaguchi T., Ozawa A., Arai I., Komatsubara T., Sasa K., Tagisi Y., Yamaguchi M., Suzuki T., Ohtsubo T., Fukunishi N., Goto A., Ohnishi T., Okuno H., Takeda H., Wakasugi M., Yano Y., Yamaguchi Y., and Kikuchi T.: “Mass measurements in RIKEN”, 6th International Conference on Nuclear Physics at Storage Rings (STORI-05), (Research Center Julich), Bonn, Germany, May (2005).

Kikuchi T., Horioka K., Ozawa A., Kawata S., Yamaguchi Y., Fukunishi N., Sakurai H., Wakasugi M., Yamaguchi M., Yamaguchi T., Arai I., Ohta H., Fujinawa T., Sasa K., Komatsubara T., Suzuki T., Ohtsubo T., Goto A., Ohnishi T., Okuno H., Takeda H., and Yano Y.: “Individual correction using induction modulator for mass measurements by isochronous ring in RIKEN RI beam factory”, 2nd International Workshop on Recent Progress in Induction Accelerators (RPIA2006), (KEK, Tokyo Institute of Technology), Tsukuba, Mar. (2006).

Arai I., Komatsubara T., Ozawa A., Sasa K., Yasuda Y., Fujinawa T., Fukunishi N., Goto A., Ohnishi T., Okuno H., Takeda H., Wakasugi M., Yamaguchi M., Yamaguchi Y., Yano Y., Kikuchi T., Suzuki T., Yamaguchi T., and Ohtsubo T.: “Isochronous ring at RIKEN”, Workshop on Advanced Laser and Mass Spectroscopy ALMAS-1: Innovative Physics Ideas, (Gesellschaft fur Schwerionenforschung (GSI)), Darmstadt, Germany, Oct. (2006).

Arai I., Komatsubara T., Ozawa A., Sasa K., Yasuda Y., Fujinawa T., Fukunishi N., Goto A., Ohnishi T., Okuno H., Takeda H., Wakasugi M., Yamaguchi M., Yamaguchi Y., Yano Y., Kikuchi T., Suzuki T., Yamaguchi T., and Ohtsubo T.: “Rare RI ring”, RIBF International Collaboration Workshop on Experiments at the RIBF, Wako, Nov. (2006).

Nakajima S., Kuboki T., Yoshitake M., Hashizume Y., Kanazawa M., Kitagawa a., Kobayashi K., Moriguchi T., Ohtsubo T., Ozawa A., Sato S., Suzuki T., Yamaguchi Y., Yasuda Y., and Yamaguchi T.: “Development of a time-of-flight detector for rare-RI ring project at RIKEN RIBF”, 15th International Conference on Electromagnetic Isotope Separators and Techniques Related to their Applications (EMIS2007), (GANIL, IN2P3/CNRS, DSM/CEA), Deauville, France, June (2007).

Yamaguchi Y., Fujinawa T., Fukunishi N., Goto A., Ohnishi T., Sakurai H., Wakasugi M., Yano Y., Ozawa A., Arai I., Yasuda Y., Suzuki T., Yamaguchi T., Kikuchi T., and Ohtsubo T.: “Rare-RI ring project at RI Beam factory in RIKEN”, 15th International Conference on Electromagnetic Isotope Separators and

- Techniques Related to their Applications (EMIS2007), (GANIL , IN2P3/CNRS , DSM/CEA), Deauville, France, June (2007).
- Ozawa A., Arai I., Fujinawa T., Fukunishi N., Goto A., Kikuchi T., Igarashi S., Komatsubara T., Ohtsubo T., Sakurai H., Sasa K., Suzuki T., Wakasugi M., Yamaguchi K., Yamaguchi T., Yamaguchi Y., Yano Y., and Yasuda Y.: “Mass measurements by isochronous storage ring in RI beam factory”, International Nuclear Physics Conference (INPC2007), (RIKEN and others), Tokyo, June (2007).
- Nakajima S., Suzuki T., Yamaguchi T., Fujinawa T., Fukunishi N., Goto A., Ohnishi T., Sakurai H., Wakasugi M., Yamaguchi Y., Yano Y., Ozawa A., Arai I., Yasuda Y., Kikuchi T., and Ohtsubo T.: “New scheme for precision mass measurement of rare isotopes produced at RI beam factory”, 30th Mazurian Lakes Conference on Physics : Nuclear Physics and the Fundamental Processes, (IPJ ; University of Warsaw ; Pro-Physica), Piaski, Poland, Sept. (2007).
- Yamaguchi T., Fujinawa T., Fukunishi N., Goto A., Ohnishi T., Sakurai H., Wakasugi M., Yamaguchi Y., Yano Y., Arai I., Moriguchi T., Ozawa A., Yasuda Y., Nakajima S., Kuboki T., Suzuki T., Kikuchi T., and Ohtsubo T.: “Storage-ring mass spectrometry”, ETC Workshop on Mass Olympics, (GSI , FIAS), Trento, Italy, May (2008).
- Yamaguchi T., Arai I., Ozawa A., Yasuda Y., Fujinawa T., Fukunishi N., Goto A., Hara K., Ohnishi T., Sakurai H., Wakasugi M., Yamaguchi Y., Yano Y., Kikuchi T., Suzuki T., and Ohtsubo T.: “Beam optics simulation for rare-RI ring at RI beam factory in RIKEN”, 7th International Conference on Nuclear Physics at Storage Rings STORI'08, (Institute of Modern Physics, Chinese Academy of Sciences, National Natural Foundation of China), Lanzhou, China, Sept. (2008).
- Yasuda Y., Ozawa A., Arai I., Fujinawa T., Fukunishi N., Goto A., Ohnishi T., Sakurai H., Wakasugi M., Yamaguchi Y., Yano Y., Suzuki T., Yamaguchi T., Kikuchi T., and Ohtsubo T.: “Present status of rare-RI ring project in RIKEN RIBF”, 7th International Conference on Nuclear Physics at Storage Rings STORI'08, (Institute of Modern Physics, Chinese Academy of Sciences, National Natural Foundation of China), Lanzhou, China, Sept. (2008).
- (Domestic Conference)
- 太田寛史, 新井一郎, 小沢顕, 小松原哲郎, 笹公和, 鈴木健, 山口貴之, 大坪隆, 山口充孝, 田岸義宏, 矢野安重, 後藤彰, 若杉昌徳, 奥野広樹, 福西暢尚, 大西哲哉, 山口由高, 菊池崇志: “Design of the isochronous storage ring for accurate mass measurement in RI beam factory”, 第2回日本加速器学会年会/第30回リニアック技術研究会, 鳥栖, 7月(2005).
- 太田寛史, 新井一郎, 小沢顕, 小松原哲郎, 笹公和, 鈴木健, 山口貴之, 大坪隆, 山口充孝, 田岸義宏, 矢野安重, 後藤彰, 奥野広樹, 福西暢尚, 大西哲哉, 山口由高, 菊池崇志: “等時性蓄積リングへの入射ラインとそのビーム光学”, 等時性蓄積リングによる不安定核の質量測定と宇宙元素合成, (筑波大学), つくば, 9月(2005).
- 山口由高, 若杉昌徳, 藤縄雅, 福西暢尚, 後藤彰, 大西哲哉, 奥野広樹, 櫻井博儀, 竹田浩之, 山口充孝, 矢野安重, 小沢顕, 新井一郎, 小松原哲郎, 笹公和, 菊池崇志, 鈴木健, 山口貴之, 大坪隆: “等時性蓄積リングのためのキッカー電磁石及び入射スキームの検討”, 等時性蓄積リングによる不安定核の質量測定と宇宙元素合成, (筑波大学), つくば, 9月(2005).
- 山口由高, 小沢顕, 新井一郎, 安田裕介, 藤縄雅, 福西暢尚, 大西哲哉, 後藤彰, 奥野広樹, 櫻井博儀, 若杉昌徳, 矢野安重, 鈴木健, 山口貴之, 菊池崇志, 大坪隆: “等時性蓄積リングによる質量測定”, 国立天文台ワークショップ「Rプロセス元素組成の統合的理解: 量子ビームでさぐる宇宙進化の理解を目指して」, 三鷹, 3月(2007).
- 久保木隆正, 小沢顕, 鈴木健, 山口貴之, 大坪隆, 山口由高, 金澤光高, 北川敦志, 小林圭, 佐藤眞二, 須田利美, 田中鐘信, 中島真平, 橋爪祐平, 森口哲朗, 安田裕介, 吉竹利織: “放医研 HIMAC に於ける TOF 検出器の分解能と荷電状態分布の測定”, 日本物理学会 2007 年春季大会, 八王子, 3月(2007).
- 安田裕介, 新井一郎, 小沢顕, 小松原哲郎, 笹公和, 大西哲哉, 後藤彰, 櫻井博儀, 福西暢尚, 藤縄雅, 矢野安重, 山口由高, 若杉昌徳, 鈴木健, 山口貴之, 大坪隆, 菊池崇志: “理研 RIBF における等時性蓄積リング計画”, 日本物理学会第 62 回年次大会, 札幌, 9月(2007).
- 森口哲朗, 橋爪祐平, 保谷毅, 小川賢一郎, 安田裕介, 原かおる, 小沢顕, 久保木隆正, 吉竹利織, 齊藤和哉, 三浦宗賢, 中島真平, 山口貴之, 鈴木健, 大坪隆, 山口由高, 金澤光高, 北川敦志, 佐藤眞二: “重イオンビームによる Hybrid Photo Detector の時間分解能の測定”, 日本物理学会第 63 回年次大会, 東大阪, 3月(2008).
- 久保木隆正, 山口貴之, 大坪隆, 小沢顕, 金澤光高, 北川敦志, 久保徹, 小林圭, 齊藤和哉, 佐藤眞二, 鈴木健, 須田利美, 田中鐘信, 中島真平, 橋爪祐平, 三浦宗賢, 森口哲朗, 安田裕介, 山口由高, 吉竹利織, 渡部亮太: “理研稀少 RI リングの為の TOF 検出器の開発”, 日本物理学会第 63 回年次大会, 東大阪, 3月(2008).
- 山口由高, 大西哲哉, 後藤彰, 櫻井博儀, 福西暢尚, 藤縄雅, 矢野安重, 若杉昌徳, 新井一郎, 小沢顕, 小松原哲郎, 笹公和, 安田裕介, 鈴木健, 山口貴之, 菊池崇志, 大坪隆: “理研 RIBF における質量リング計画の現状”, 国立天文台研究会「Rプロセス元素合成の統合的理解-量子ビームで探る宇宙進化の理解を目指して-」, つくば, 3月(2008).
- 山口由高, 藤縄雅, 福西暢尚, 後藤彰, 大西哲哉, 櫻井博儀, 若杉昌徳, 矢野安重, 小沢顕, 新井一郎, 安田裕介, 菊池崇志, 大坪隆, 鈴木健, 山口貴之: “理研 RIBF における稀少 RI リング計画の現状”, 第 5 回日本加速器学会年会/第 33 回リニアック技術研究会, 東広島, 8月(2008).
- 安田裕介, 新井一郎, 小沢顕, 森口哲朗, 大西哲哉, 櫻井博儀, 福西暢尚, 藤縄雅, 矢野安重, 山口由高, 若杉昌徳, 原かおる, 鈴木健, 山口貴之, 大坪隆, 菊池崇志: “理研稀少 RI リング建設にむけての高精度磁場測定”, 日本物理学会 2008 年秋

季大会, 盛岡, 9月 (2008).

## SCRIT Team

### Publications

#### [Journal]

(Original Papers) \*Subject to Peer Review

Yamaguchi Y., Ozawa A., Goto A., Arai I., Fujinawa T., Fukunishi N., Kikuchi T., Ohnishi T., Ohtsubo T., Sakurai H., Suzuki T., Wakasugi M., Yamaguchi T., Yasuda Y., and Yano Y.: “Rara-RI ring project at RIKEN RI beam factory”, Nucl. Instrum. Methods Phys. Res. B **266**, 4575–4578 (2008). \*

(Others)

Nakajima S., Yamaguchi T., Suzuki T., Yamaguchi Y., Fujinawa T., Fukunishi N., Goto A., Ohnishi T., Sakurai H., Wakasugi M., Yano Y., Arai I., Ozawa A., Yasuda Y., Kikuchi T., and Ohtsubo T.: “New scheme for precision mass measurements of rare isotopes produced at RI beam factory”, Acta Phys. Pol. B **39**, No. 2, pp. 457–462 (2008).

#### [Book • Proceedings]

(Others)

Yamaguchi T., Arai I., Fukunishi N., Goto A., Kikuchi T., Komatsubara T., Ohnishi T., Ohtsubo T., Okuno H., Ozawa A., Sasa K., Suzuki T., Tagisi Y., Takeda H., Wakasugi M., Yamaguchi M., Yamaguchi Y., and Yano Y.: “Mass measurements by an isochronous storage ring at the RIKEN RI beam factory”, Proceedings of the 6th International Conference on Nuclear Physics at Storage Rings (STORI '05), Bonn, Germany, 2005–5, Forschungszentrum Julich, Julich, pp. 297–300 (2005).

Yamaguchi M., Arai I., Fukunishi N., Goto A., Kusaka K., Kikuchi T., Komatsubara T., Kubo T., Ohnishi T., Ohtsubo T., Okuno H., Ozawa A., Sasa K., Suzuki T., Tagisi Y., Takeda H., Wakasugi M., Yamaguchi T., Yamaguchi Y., and Yano Y.: “Design of an isochronous storage ring and an injection line for mass measurements at the RIKEN RI beam factory”, Proceedings of the 6th International Conference on Nuclear Physics at Storage Rings (STORI '05), Bonn, Germany, 2005–5, Forschungszentrum Julich, Julich, pp. 315–319 (2005).

Kikuchi T., Horioka K., Ozawa A., Kawata S., Yamaguchi Y., Fukunishi N., Sakurai H., Wakasugi M., Yamaguchi M., Yamaguchi T., Arai I., Ohta H., Fujinawa T., Sasa K., Komatsubara T., Suzuki T., Ohtsubo T., Goto A., Ohnishi T., Okuno H., Takeda H., and Yano Y.: “Individual correction using induction modulator for mass measurements by isochronous ring in RIKEN RI beam factory”, Proceedings of the 2nd International Workshop on Recent Progress in Induction Accelerators (RPIA2006), Tsukuba, 2006–3, KEK, Tsukuba, pp. 127–131 (2006).

#### Oral Presentations

(International Conference etc.)

Yamaguchi T., Ozawa A., Arai I., Komatsubara T., Sasa

K., Tagisi Y., Yamaguchi M., Suzuki T., Ohtsubo T., Fukunishi N., Goto A., Ohnishi T., Okuno H., Takeda H., Wakasugi M., Yano Y., Yamaguchi Y., and Kikuchi T.: “Mass measurements in RIKEN”, 6th International Conference on Nuclear Physics at Storage Rings (STORI-05), (Research Center Julich), Bonn, Germany, May (2005).

Kikuchi T., Horioka K., Ozawa A., Kawata S., Yamaguchi Y., Fukunishi N., Sakurai H., Wakasugi M., Yamaguchi M., Yamaguchi T., Arai I., Ohta H., Fujinawa T., Sasa K., Komatsubara T., Suzuki T., Ohtsubo T., Goto A., Ohnishi T., Okuno H., Takeda H., and Yano Y.: “Individual correction using induction modulator for mass measurements by isochronous ring in RIKEN RI beam factory”, 2nd International Workshop on Recent Progress in Induction Accelerators (RPIA2006), (KEK , Tokyo Institute of Technology), Tsukuba, Mar. (2006).

Arai I., Komatsubara T., Ozawa A., Sasa K., Yasuda Y., Fujinawa T., Fukunishi N., Goto A., Ohnishi T., Okuno H., Takeda H., Wakasugi M., Yamaguchi M., Yamaguchi Y., Yano Y., Kikuchi T., Suzuki T., Yamaguchi T., and Ohtsubo T.: “Isochronous ring at RIKEN”, Workshop on Advanced Laser and Mass Spectroscopy ALMAS-1: Innovative Physics Ideas, (Gesellschaft fur Schwerionenforschung (GSI)), Darmstadt, Germany, Oct. (2006).

Arai I., Komatsubara T., Ozawa A., Sasa K., Yasuda Y., Fujinawa T., Fukunishi N., Goto A., Ohnishi T., Okuno H., Takeda H., Wakasugi M., Yamaguchi M., Yamaguchi Y., Yano Y., Kikuchi T., Suzuki T., Yamaguchi T., and Ohtsubo T.: “Rare RI ring”, RIBF International Collaboration Workshop on Experiments at the RIBF, Wako, Nov. (2006).

Yamaguchi Y., Fujinawa T., Fukunishi N., Goto A., Ohnishi T., Sakurai H., Wakasugi M., Yano Y., Ozawa A., Arai I., Yasuda Y., Suzuki T., Yamaguchi T., Kikuchi T., and Ohtsubo T.: “Rare-RI ring project at RI Beam factory in RIKEN”, 15th International Conference on Electromagnetic Isotope Separators and Techniques Related to their Applications (EMIS2007), (GANIL , IN2P3/CNRS , DSM/CEA), Deauville, France, June (2007).

Ozawa A., Arai I., Fujinawa T., Fukunishi N., Goto A., Kikuchi T., Igarashi S., Komatsubara T., Ohtsubo T., Sakurai H., Sasa K., Suzuki T., Wakasugi M., Yamaguchi K., Yamaguchi T., Yamaguchi Y., Yano Y., and Yasuda Y.: “Mass measurements by isochronous storage ring in RI beam factory”, International Nuclear Physics Conference (INPC2007), (RIKEN and others), Tokyo, June (2007).

Nakajima S., Suzuki T., Yamaguchi T., Fujinawa T., Fukunishi N., Goto A., Ohnishi T., Sakurai H., Wakasugi M., Yamaguchi Y., Yano Y., Ozawa A., Arai I., Yasuda Y., Kikuchi T., and Ohtsubo T.: “New scheme for precision mass measurement of rare isotopes

- produced at RI beam factory”, 30th Mazurian Lakes Conference on Physics : Nuclear Physics and the Fundamental Processes, (IPJ ; University of Warsaw ; Pro-Physica), Piaski, Poland, Sept. (2007).
- Goto A., Fujimaki M., Fujinawa T., Fukunishi N., Hasebe H., Higurashi Y., Ikegami K., Ikezawa E., Inabe N., Kageyama T., Kamigaito O., Kase M., Kidera M., Kohara S., Komiyama M., Nagase M., Kumagai K., Maie T., Nakagawa T., Ohnishi J., Okuno H., Ryuto H., Sakamoto N., Wakasugi M., Watanabe T., Yamada K., Yokouchi S., and Yano Y.: “Commissioning of RIKEN RI Beam Factory”, 18th International Conference on Cyclotrons and their Applications (Cyclotrons 2007), (Laboratori Nazionali del Sud, INFN), Giardini Naxos, Italy, Sept.–Oct. (2007).
- Fukunishi N., Yamada K., Fujimaki M., Fujinawa T., Goto A., Hasebe H., Higurashi Y., Ikegami K., Ikezawa E., Inabe N., Kamigaito O., Kase M., Kohara S., Komiyama M., Kumagai K., Maie T., Nagase M., Nakagawa T., Ohnishi J., Okuno H., Ryuto H., Sakamoto N., Wakasugi M., Watanabe T., and Yano Y.: “Present performance and commissioning details of RIBF accelerator complex”, 18th International Conference on Cyclotrons and their Applications (Cyclotrons 2007), (Laboratori Nazionali del Sud), Giardini Naxos, Italy, Sept.–Oct. (2007).
- Yamaguchi T., Fujinawa T., Fukunishi N., Goto A., Ohnishi T., Sakurai H., Wakasugi M., Yamaguchi Y., Yano Y., Arai I., Moriguchi T., Ozawa A., Yasuda Y., Nakajima S., Kuboki T., Suzuki T., Kikuchi T., and Ohtsubo T.: “Storage-ring mass spectrometry”, ETC Workshop on Mass Olympics, (GSI , FIAS), Trento, Italy, May (2008).
- (Domestic Conference)
- 太田寛史, 新井一郎, 小沢顕, 小松原哲郎, 笹公和, 鈴木健, 山口貴之, 大坪隆, 山口充孝, 田岸義宏, 矢野安重, 後藤彰, 若杉昌徳, 奥野広樹, 福西暢尚, 大西哲哉, 山口由高, 菊池崇志: “Design of the isochronous storage ring for accurate mass measurement in RI beam factory”, 第2回日本加速器学会年会/第30回リニアック技術研究会, 鳥栖, 7月(2005).
- 山口由高, 若杉昌徳, 藤縄雅, 福西暢尚, 後藤彰, 大西哲哉, 奥野広樹, 櫻井博儀, 竹田浩之, 山口充孝, 矢野安重, 小沢顕, 新井一郎, 小松原哲郎, 笹公和, 菊池崇志, 鈴木健, 山口貴之, 大坪隆: “等時性蓄積リングのためのキッカー電磁石及び入射スキームの検討”, 等時性蓄積リングによる不安定核の質量測定と宇宙元素合成, (筑波大学), つくば, 9月(2005).
- 山口由高, 小沢顕, 新井一郎, 安田裕介, 藤縄雅, 福西暢尚, 大西哲哉, 後藤彰, 奥野広樹, 櫻井博儀, 若杉昌徳, 矢野安重, 鈴木健, 山口貴之, 菊池崇志, 大坪隆: “等時性蓄積リングによる質量測定”, 国立天文台ワークショップ「Rプロセス元素組成の統合的理解: 量子ビームでさぐる宇宙進化の理解を目指して」, 三鷹, 3月(2007).
- 渡邊環, 若杉昌徳, 藤登正樹, 加瀬昌之, 福西暢尚, 小高康照, 小山亮, 山田一成, 後藤彰, 矢野安重: “RIBFにおけるプラスチックシンチレーションモニターを用いたビームエネルギーと縦方向のビームプロファイルの測定”, 第4回日本加速器学会年会・第32回リニアック技術研究会, 和光, 8月(2007).
- 安田裕介, 新井一郎, 小沢顕, 小松原哲郎, 笹公和, 大西哲哉, 後藤彰, 櫻井博儀, 福西暢尚, 藤縄雅, 矢野安重, 山口由高, 若杉昌徳, 鈴木健, 山口貴之, 大坪隆, 菊池崇志: “理研RIBFにおける等時性蓄積リング計画”, 日本物理学会第62回年次大会, 札幌, 9月(2007).
- 山口由高, 大西哲哉, 後藤彰, 櫻井博儀, 福西暢尚, 藤縄雅, 矢野安重, 若杉昌徳, 新井一郎, 小沢顕, 小松原哲郎, 笹公和, 安田裕介, 鈴木健, 山口貴之, 菊池崇志, 大坪隆: “理研RIBFにおける質量リング計画の現状”, 国立天文台研究会「rプロセス元素合成の統合的理解-量子ビームで探る宇宙進化の理解を目指して-」, つくば, 3月(2008).

Publications

[Journal]

(Original Papers) \*Subject to Peer Review

- Fukuda N., Nakamura T., Kobayashi T., Otsu H., Aoi N., Imai N., Iwasaki H., Kubo T., Mengoni A., Notani M., Sakurai H., Shimoura S., Teranishi T., Watanabe Y., Yoneda K., and Ishihara M.: “Coulomb Dissociation of Halo Nuclei”, *Prog. Theor. Phys. Suppl.*, No. 146, pp. 462–466 (2002).
- Gomi T., Motobayashi T., Yoneda K., Kanno S., Aoi N., Ando Y., Baba H., Demichi K., Fulop Z., Futakami U., Hasegawa H., Higurashi Y., Ieki K., Imai N., Iwasa N., Iwasaki H., Kubo T., Kubono S., Kunibu M., Matsuyama Y., Michimasa S., Minemura T., Murakami H., Nakamura T., Saito A., Sakurai H., Serata M., Shimoura S., Sugimoto T., Takeshita E., Takeuchi S., Ue K., Yamada K., Yanagisawa Y., Yoshida A., and Ishihara M.: “Coulomb Dissociation of  $^{23}\text{Al}$ ”, *Prog. Theor. Phys. Suppl.*, No. 146, pp. 557–558 (2002). \*
- Kanno S., Gomi T., Motobayashi T., Yoneda K., Aoi N., Ando Y., Baba H., Demichi K., Fulop Z., Futakami U., Hasegawa H., Higurashi Y., Ieki K., Imai N., Iwasa N., Iwasaki H., Kubo T., Kubono S., Kunibu M., Matsuyama Y., Michimasa S., Minemura T., Murakami H., Nakamura T., Saito A., Sakurai H., Serata M., Shimoura S., Sugimoto T., Takeshita E., Takeuchi S., Ue K., Yamada K., Yanagisawa Y., Yoshida A., and Ishihara M.: “Coulomb Excitation of  $^{24}\text{Si}$ ”, *Prog. Theor. Phys. Suppl.*, No. 146, pp. 575–576 (2002). \*
- Gomi T., Motobayashi T., Yoneda K., Kanno S., Aoi N., Ando Y., Baba H., Demichi K., Fulop Z., Futakami U., Hasegawa H., Higurashi Y., Ieki K., Imai N., Iwasa N., Iwasaki H., Kubo T., Kubono S., Kunibu M., Matsuyama Y., Michimasa S., Minemura T., Murakami H., Nakamura T., Saito A., Sakurai H., Serata M., Shimoura S., Sugimoto T., Takeshita E., Takeuchi S., Ue K., Yamada K., Yanagisawa Y., Yoshida A., and Ishihara M.: “Study of the  $^{22}\text{Mg}(p, \gamma)^{23}\text{Al}$  Reaction with the Coulomb-Dissociation Method”, *Nucl. Phys. A* **718**, 508c–509c (2003). \*
- Iwasa N., Motobayashi T., Sakurai H., Akiyoshi H., Ando Y., Aoi N., Baba H., Fukuda N., Fulop Z., Futakami U., Gomi T., Higurashi Y., Ieki K., Iwasaki H., Kubo T., Kubono S., Kinugawa H., Kumagai H., Kunibu M., Michimasa S., Minemura T., Murakami H., Sagara K., Saito A., Shimoura S., Takeuchi S., Yanagisawa Y., Yoneda K., and Ishihara M.: “In-beam  $\gamma$  spectroscopy of  $^{34}\text{Si}$  with deuteron inelastic scattering using reverse kinematics”, *Phys. Rev. C* **67**, 064315-1–064315-4 (2003). \*
- Gomi T., Motobayashi T., Ando Y., Aoi N., Baba H., Demichi K., Elekes Z., Fukuda N., Fulop Z., Futakami U., Hasegawa H., Higurashi Y., Ieki K., Imai N., Ishihara M., Ishikawa K., Iwasa N., Iwasaki H., Kanno S., Kondo Y., Kubo T., Kubono S., Kunibu M., Kurita K., Matsuyama Y., Michimasa S., Minemura T., Miura M., Murakami H., Nakamura T., Notani M., Ota S., Saito A., Sakurai H., Serata M., Shimoura S., Sugimoto T., Takeshita E., Takeuchi S., Togano Y., Ue K., Yamada K., Yanagisawa Y., Yoneda K., and Yoshida A.: “Study of the Stellar  $^{22}\text{Mg}(p, \gamma)^{23}\text{Al}$  Reaction using the Coulomb-Dissociation Method”, *Nucl. Phys. A* **734**, E77–E79 (2004).
- Fukuda N., Nakamura T., Aoi N., Imai N., Ishihara M., Kobayashi T., Iwasaki H., Kubo T., Mengoni A., Notani M., Otsu H., Sakurai H., Shimoura S., Teranishi T., Watanabe Y., and Yoneda K.: “Coulomb and nuclear breakup of a halo nucleus  $^{11}\text{Be}$ ”, *Phys. Rev. C* **70**, 054606-1–054606-12 (2004). \*
- Imai N., Ong H., Aoi N., Sakurai H., Demichi K., Kawasaki H., Baba H., Dombradi Z., Elekes Z., Fukuda N., Fulop Z., Gelberg A., Gomi T., Hasegawa H., Ishikawa K., Iwasaki H., Kaneko E., Kanno S., Kishida T., Kondo Y., Kubo T., Kurita K., Michimasa S., Minemura T., Miura M., Motobayashi T., Nakamura T., Notani M., Ohnishi T., Saito A., Shimoura S., Sugimoto T., Suzuki M., Takeshita E., Takeuchi M., Tamaki M., Yoneda K., Watanabe H., and Ishihara M.: “Anomalous hindered  $E2$  Strength  $B(E2; 2_1^+ \rightarrow 0^+)$  in  $^{16}\text{C}$ ”, *Phys. Rev. Lett.* **92**, No. 6, pp. 062501-1–062501-4 (2004). \*
- Yamada K., Motobayashi T., Aoi N., Baba H., Demichi K., Elekes Z., Gibelin J., Gomi T., Hasegawa H., Imai N., Iwasaki H., Kanno S., Kubo T., Kurita K., Matsuyama Y., Michimasa S., Minemura T., Notani M., Onishi T., Ong H., Ota S., Ozawa A., Saito A., Sakurai H., Shimoura S., Takeshita E., Takeuchi S., Tamaki M., Togano Y., Yanagisawa Y., Yoneda K., and Tanihata I.: “Reduced transition probabilities for the first  $2^+$  excited state in  $^{46}\text{Cr}$ ,  $^{50}\text{Fe}$ , and  $^{54}\text{Ni}$ ”, *Eur. Phys. J. A* **25**, No. s01, pp. 409–413 (2005).
- Gomi T., Motobayashi T., Ando Y., Aoi N., Baba H., Demichi K., Elekes Z., Fukuda N., Fulop Z., Futakami U., Hasegawa H., Higurashi Y., Ieki K., Imai N., Ishihara M., Ishikawa K., Iwasa N., Iwasaki H., Kanno S., Kondo Y., Kubo T., Kubono S., Kunibu M., Kurita K., Matsuyama Y., Michimasa S., Minemura T., Miura M., Murakami H., Nakamura T., Notani M., Ota S., Saito A., Sakurai H., Serata M., Shimoura S., Sugimoto T., Takeshita E., Takeuchi S., Togano Y., Ue K., Yamada K., Yanagisawa Y., Yoneda K., and Yoshida A.: “Coulomb dissociation experiment for explosive hydrogen burning: study of the  $^{22}\text{Mg}(p, \gamma)^{23}\text{Al}$  reaction”, *J. Phys. G* **31**, S1517–S1521 (2005).
- Togano Y., Gomi T., Motobayashi T., Ando Y., Aoi N., Baba H., Demichi K., Elekes Z., Fukuda N., Fulop Z., Futakami U., Hasegawa H., Higurashi Y., Ieki K., Imai N., Ishihara M., Ishikawa K., Iwasa N., Iwasaki H.,

- Kanno S., Kondo Y., Kubo T., Kubono S., Kunibu M., Kurita K., Matsuyama Y., Michimasa S., Minemura T., Miura M., Murakami H., Nakamura T., Notani M., Ota S., Saito A., Sakurai H., Serata M., Shimoura S., Sugimoto T., Takeshita E., Takeuchi S., Ue K., Yamada K., Yanagisawa Y., Yoneda K., and Yoshida A.: “Study of  $^{26}\text{Si}(p, \gamma)^{27}\text{P}$  reaction using Coulomb dissociation method”, *Nucl. Phys. A* **758**, 182c–185c (2005). \*
- Iwasaki H., Motobayashi T., Sakurai H., Yoneda K., Gomi T., Aoi N., Fukuda N., Fulop Z., Futakami U., Gacsi Z., Higurashi Y., Imai N., Iwasa N., Kunibu M., Kubo T., Kurokawa M., Liu Z., Minemura T., Saito A., Serata M., Shimoura S., Takeuchi S., Watanabe Y., Yamada K., Yanagisawa Y., and Ishihara M.: “Quadrupole collectivity of  $^{28}\text{Ne}$  and the boundary of the island of inversion”, *Phys. Lett. B* **620**, 118–124 (2005). \*
- Ong H., Imai N., Aoi N., Sakurai H., Dombradi Z., Saito A., Elekes Z., Baba H., Demichi K., Fulop Z., Gibelin J., Gomi T., Hasegawa H., Ishihara M., Iwasaki H., Kanno S., Kawai S., Kubo T., Kurita K., Matsuyama Y., Michimasa S., Minemura T., Motobayashi T., Notani M., Ota S., Sakai H., Shimoura S., Takeshita E., Takeuchi S., Tamaki M., Togano Y., Yamada K., Yanagisawa Y., and Yoneda K.: “Inelastic proton scattering on  $^{16}\text{C}$ ”, *Eur. Phys. J. A* **25**, No. s01, pp. 347–348 (2006). \*
- Togano Y., Gomi T., Motobayashi T., Ando Y., Aoi N., Baba H., Demichi K., Elekes Z., Fukuda N., Fulop Z., Futakami U., Hasegawa H., Higurashi Y., Ieki K., Imai N., Ishihara M., Ishikawa K., Iwasa N., Iwasaki H., Kanno S., Kondo Y., Kubo T., Kubono S., Kunibu M., Kurita K., Matsuyama Y., Michimasa S., Minemura T., Miura M., Murakami H., Nakamura T., Notani M., Ota S., Saito A., Sakurai H., Serata M., Shimoura S., Sugimoto T., Takeshita E., Takeuchi S., Ue K., Yamada K., Yanagisawa Y., Yoneda K., and Yoshida A.: “Study of the  $^{26}\text{Si}(p, \gamma)^{27}\text{P}$  reaction through Coulomb dissociation of  $^{27}\text{P}$ ”, *Eur. Phys. J. A* **27**, No. s01, pp. 233–236 (2006). \*
- Gomi T., Motobayashi T., Ando Y., Aoi N., Baba H., Demichi K., Elekes Z., Fukuda N., Fulop Z., Futakami U., Hasegawa H., Higurashi Y., Ieki K., Imai N., Ishihara M., Ishikawa K., Iwasa N., Iwasaki H., Kanno S., Kondo Y., Kubo T., Kubono S., Kunibu M., Kurita K., Matsuyama Y., Michimasa S., Minemura T., Miura M., Murakami H., Nakamura T., Notani M., Ota S., Saito A., Sakurai H., Serata M., Shimoura S., Sugimoto T., Takeshita E., Takeuchi S., Togano Y., Ue K., Yamada K., Yanagisawa Y., Yoneda K., and Yoshida A.: “Coulomb Dissociation of  $^{23}\text{Al}$  for the stellar  $^{22}\text{Mg}(p, \gamma)^{23}\text{Al}$  reaction”, *Nucl. Phys. A* **758**, 761c–764c (2006).
- Elekes Z., Dombradi Z., Saito A., Aoi N., Baba H., Demichi K., Fulop Z., Gibelin J., Gomi T., Hasegawa H., Imai N., Ishihara M., Iwasaki H., Kanno S., Kawai S., Kishida T., Kubo T., Kurita K., Matsuyama Y., Michimasa S., Minemura T., Motobayashi T., Notani M., Ohnishi T., Ong H., Ota S., Ozawa A., Sakai H., Sakurai H., Shimoura S., Takeshita E., Takeuchi S., Tamaki M., Togano Y., Yamada K., Yanagisawa Y., and Yoneda K.: “Proton inelastic scattering studies at the borders of the “island of inversion”: The  $^{30,31}\text{Ne}$  and  $^{33,34}\text{Mg}$  case”, *Phys. Rev. C* **73**, 044314-1–044314-5 (2006). \*
- Dombradi Z., Elekes Z., Saito A., Aoi N., Baba H., Demichi K., Fulop Z., Gibelin J., Gomi T., Hasegawa H., Imai N., Ishihara M., Iwasaki H., Kanno S., Kawai S., Kishida T., Kubo T., Kurita K., Matsuyama Y., Michimasa S., Minemura T., Motobayashi T., Notani M., Ohnishi T., Ong H., Ota S., Ozawa A., Sakai H., Sakurai H., Shimoura S., Takeshita E., Takeuchi S., Tamaki M., Togano Y., Yamada K., Yanagisawa Y., and Yoneda K.: “Vanishing  $N = 20$  Shell Gap: Study of Excited States in  $^{27,28}\text{Ne}$ ”, *Phys. Rev. Lett.* **96**, 182501-1–182501-4 (2006). \*
- Nakamura T., Vinodkumar A., Sugimoto T., Aoi N., Baba H., Bazin D. P., Fukuda N., Gomi T., Hasegawa H., Imai N., Ishihara M., Kobayashi T., Kondo Y., Kubo T., Miura M., Motobayashi T., Otsu H., Saito A., Sakurai H., Shimoura S., Watanabe K., Watanabe Y., Yakushiji T., Yanagisawa Y., and Yoneda K.: “Observation of Strong Low-Lying E1 Strength in the Two-Neutron Halo Nucleus  $^{11}\text{Li}$ ”, *Phys. Rev. Lett.* **96**, 252502-1–252502-4 (2006). \*
- Sakaguchi S., Uesaka T., Wakui T., Kawabata T., Aoi N., Hashimoto Y., Ichikawa M., Ichikawa Y., Itoh Y., Itoh M., Iwasaki H., Kawahara T., Kuboki H., Maeda Y., Matsuo R., Nakao T., Okamura H., Sakai H., Sakamoto N., Sasamoto Y., Sasano M., Satou Y., Sekiguchi K., Shinohara M., Suda K., Suzuki D., Takahashi Y., Tamii A., Yako K., and Yamaguchi M.: “Analyzing Power Measurement for Elastic Scattering of  $^6\text{He}$  on polarized protons”, *AIP Conf. Proc.* **915**, 833–836 (2007). \*
- Miki K., Sakai H., Itoh K., Kawabata K., Kuboki H., Maeda Y., Noji S., Sakaguchi S., Sakamoto N., Sasamoto Y., Sasano M., Satou Y., Sekiguchi K., Suda K., Takahashi Y., Uesaka T., and Yako K.: “Measurement of the  $^2\text{H}(d, pn)$  Reaction at 0 degrees at 270 MeV”, *Nucl. Phys. A* **790**, 442c–445c (2007). \*
- Elekes Z., Dombradi Z., Aoi N., Baba H., Bishop S., Demichi K., Fulop Z., Gibelin J., Gomi T., Hasegawa H., Hashimoto Y., Imai N., Ishihara M., Iwasa N., Iwasaki H., Kalinka G., Kanno S., Kawai S., Kishida T., Kondo Y., Korshennikov A. A., Kubo T., Kurita K., Kurokawa M., Matsui N., Matsuyama Y., Michimasa S., Minemura T., Motobayashi T., Nakamura T., Nakao T., Nikolski E. Y., Notani M., Ohnishi T., Okumura T., Ong H., Ota S., Ozawa A., Perera P., Saito A., Sakai H., Sakurai H., Satou Y., Shimoura S., Sohler D., Sumikama T., Suzuki D., Suzuki M., Takeda H.,

- Takeshita E., Takeuchi S., Tamaki M., Togano Y., Yamada K., Yanagisawa Y., and Yoneda K.: “The study of shell closures in light neutron-rich nuclei”, *J. Phys. G* **35**, 014038-1–014038-7 (2008).
- Yoshida A., Suda T., Ohtsuki T., Yuki H., and Kubo T.: “Status and overview of production target for BigRIPS separator at RIKEN”, *Nucl. Instrum. Methods Phys. Res. A* **590**, 204–212 (2008). \*
- Sakaguchi S., Uesaka T., Wakui T., Kawabata T., Aoi N., Hashimoto Y., Ichikawa M., Itoh Y., Itoh M., Iwasaki H., Kawahara T., Kuboki H., Maeda Y., Matsuo R., Nakao T., Okamura H., Sakai H., Sakamoto N., Sasamoto Y., Sasano M., Satou Y., Sekiguchi K., Shinohara M., Suda K., Suzuki D., Takahashi Y., Tamii A., Yako K., and Yamaguchi M.: “Spin-orbit potential in  $^6\text{He}$  studied with polarized proton target”, *Nucl. Phys. A* **805**, 467–469 (2008). \*
- Suzuki D., Iwasaki H., Ong H., Imai N., Sakurai H., Nakao T., Aoi N., Baba H., Bishop S., Ichikawa Y., Ishihara M., Kondo Y., Kubo T., Kurita K., Motobayashi T., Nakamura T., Okumura T., Onishi T., Ota S., Suzuki M., Takeuchi S., Togano Y., and Yanagisawa Y.: “Lifetime measurements of excited states in  $^{17}\text{C}$ : Possible interplay between collectivity and halo effects”, *Phys. Lett. B* **666**, 222–227 (2008). \*
- Ong H., Imai N., Suzuki D., Iwasaki H., Sakurai H., Onishi T., Suzuki M., Ota S., Takeuchi S., Nakao T., Togano Y., Kondo Y., Aoi N., Baba H., Bishop S., Ichikawa Y., Ishihara M., Kubo T., Kurita K., Motobayashi T., Nakamura T., Okumura T., and Yanagisawa Y.: “Lifetime measurements of first excited states in  $^{16,18}\text{C}$ ”, *Phys. Rev. C* **78**, 014308-1–014308-11 (2008). \*
- Okada K., Wada M., Nakamura T., Takamine A., Lioubimov V., Schury P. H., Ishida Y., Sonoda T., Ogawa M., Yamazaki Y., Kanai Y., Kojima T., Katayama I., Ohtani S., Kubo T., and Yoshida A.: “Precision Measurement of the Hyperfine Structure of Laser-Cooled Radioactive  $^7\text{Be}^+$  Ions Produced by Projectile Fragmentation”, *Phys. Rev. Lett.* **101**, 212502-1–212502-4 (2008). \*
- Aoi N., Takeshita E., Suzuki H., Takeuchi S., Ota S., Baba H., Bishop S., Fukui T., Hashimoto Y., Ong H., Ideguchi E., Ieki K., Imai N., Ishihara M., Iwasaki H., Kanno S., Kondo Y., Kubo T., Kurita K., Kusaka K., Minemura T., Motobayashi T., Nakabayashi T., Nakamura T., Nakao T., Niikura M., Okumura T., Ohnishi T., Sakurai H., Shimoura S., Sugo R., Suzuki D., Suzuki M., Tamaki M., Tanaka K., Togano Y., and Yamada K.: “Development of Large Deformation in  $^{62}\text{Cr}$ ”, *Phys. Rev. Lett.* **102**, 012502-1–012502-4 (2009). \*
- [Book Proceedings]**
- (Others)
- Yamaguchi M., Arai I., Fukunishi N., Goto A., Kusaka K., Kikuchi T., Komatsubara T., Kubo T., Ohnishi T., Ohtsubo T., Okuno H., Ozawa A., Sasa K., Suzuki T., Tagisi Y., Takeda H., Wakasugi M., Yamaguchi T., Yamaguchi Y., and Yano Y.: “Design of an isochronous storage ring and an injection line for mass measurements at the RIKEN RI beam factory”, *Proceedings of the 6th International Conference on Nuclear Physics at Storage Rings (STORI '05)*, Bonn, Germany, 2005–5, Forschungszentrum Julich, Julich, pp. 315–319 (2005).
- Oral Presentations**
- (International Conference etc.)
- Sugimoto S., Nakamura T., Fukuda N., Miura M., Kondo Y., Aoi N., Baba H., Bazin D. P., Gomi T., Hasegawa H., Hashimoto Y., Imai N., Kobayashi T., Kubo T., Motobayashi T., Shinohara M., Saito A., Sakurai H., Shimoura S., A.M. V., Watanabe K., Watanabe Y., T. Y., Yanagisawa Y., Yoneda K., and Ishihara M.: “Breakup Reactions of Halo Nuclei”, 1st Tokyo Tech Physics COE Symposium on Spin and Quantum Structure in Hadrons, Nuclei and Atoms (SQS04), Tokyo, Feb. (2004).
- Sugimoto S., Nakamura T., Fukuda N., Miura M., Kondo Y., Aoi N., Baba H., Bazin D. P., Gomi T., Hasegawa H., Hashimoto Y., Imai N., Kobayashi T., Kubo T., Motobayashi T., Shinohara M., Saito A., Sakurai H., Shimoura S., A.M. V., Watanabe K., Watanabe Y., T. Y., Yanagisawa Y., Yoneda K., and Ishihara M.: “Invariant-Mass Spectroscopy of  $^{14}\text{Be}$  with a Carbon Target at 68.1 AMeV”, 2nd Joint Meeting of the Nuclear Physics Divisions of the APS and JPS (Hawaii 2005), Maui, USA, Sept. (2005).
- Kanno S., Aoi N., Bazin D., Bowen M. D., Campbell C. M., Cook J. M., Dinca D., Gade A., Glasmacher T., Iwasaki H., Kubo T., Kurita K., Motobayashi T., Mueller W. F., Nakamura T., Sakurai H., Suzuki H., Takeuchi S., Terry J. R., Yoneda K., and Zwahlen H.: “Weakening of  $Z=28$  shell closure in  $^{74}\text{Ni}$ ”, 5th International Workshop on Direct Reaction with Exotic Beams (DREB2007), (RIKEN Nishina Center, Kyushu University, Center for Nuclear Study (University of Tokyo)), wako, May–June (2007).
- Takeuchi S., Aoi N., Baba H., Fukui T., hashimoto ., Ieki K., Imai K., Iwasaki H., Kanno S., Kondo Y., Kubo T., Kurita K., Minemura T., Motobayashi T., Nakabayashi T., Nakamura T., Okumura T., Onishi T., Ota S., Sakurai H., Shimoura S., Sugo R., Suzuki D., Suzuki H., Suzuki M., Takeshita E., Tamaki M., Tanaka K., Togano Y., and Yamada K.: “Collectivity in  $^{32}\text{Mg}$ : a study of low-lying states”, *International Nuclear Physics Conference (INPC2007)*, Tokyo, June (2007).
- Imai N., Ong H., Aoi N., Sakurai H., Demichi K., Kawasaki H., Baba H., Dombradi Z., Elekes Z., Fukuda N., Fulop Z., Gelberg A., Gomi T., Hasegawa H., Ishikawa K., Iwasaki H., Kaneko E., Kanno S., Kishida T., Kondo Y., Kubo T., Kurita K., Michimasa S., Minemura T., Miura M., Motobayashi T., Nakamura T.,

- Notani M., Onishi T., Saito A., Shimoura S., Sugimoto T., Suzuki M., Takeshita E., Takeuchi S., Tamaki M., Yamada K., Yoneda K., Watanabe H., and Ishihara M.: “The lifetime measurement of the first  $2^+$  state in  $^{12}\text{Be}$ ”, International Nuclear Physics Conference (INPC2007), Tokyo, June (2007).
- Kanno S., Aoi N., Bazin D., Bowen M. D., Campbell C. M., Cook J. M., Dinca D., Gade A., Glasmacher T., Iwasaki H., Kubo T., Kurita K., Motobayashi T., Mueller W. F., Nakamura T., Sakurai H., Suzuki H., Takeuchi S., Terry J. R., Yoneda K., and Zwahlen H.: “Weakening of  $Z=28$  shell closure in  $^{74}\text{Ni}$ ”, International Nuclear Physics Conference (INPC2007), (Science Council of Japan, RIKEN and others), Wako, June (2007).
- Kondo Y., Motobayashi T., Sakurai H., Aoi N., Otsu H., Yanagisawa Y., Fukuda N., Takeuchi S., Ishihara M., Baba H., Gomi T., Imai N., Kubo T., Yoneda K., Nakamura T., Sato Y., Sugimoto T., Matsui N., Attukalathil V. M., Okumura T., Hashimoto Y., Nakabayashi T., Shinohara M., Miura M., Kobayashi T., Matsuda Y., Endo N., Kitayama M., Watanabe K., Yakushiji T., Togano Y., Kawai S., Hasegawa H., Onishi T., Ong H., Shimoura S., Tamaki M., Saito A., Bazin D. P., and Watanabe Y.: “Breakup reactions of  $^{14}\text{Be}$ ”, Future Prospects for Spectroscopy and Direct Reactions 2008, (Michigan State University), East Lansing, USA, Feb. (2008).
- Takeuchi S., Aoi N., Baba H., Fukui T., hashimoto ., Ieki K., Imai K., Iwasaki H., Kanno S., Kondo Y., Kubo T., Kurita K., Minemura T., Motobayashi T., Nakabayashi T., Nakamura T., Okumura T., Onishi T., Ota S., Sakurai H., Shimoura S., Sugo R., Suzuki D., Suzuki H., Suzuki M., Takeshita E., Tamaki M., Tanaka K., Togano Y., and Yamada K.: “Low-lying states in  $^{32}\text{Mg}$ ”, Future Prospects for Spectroscopy and Direct Reactions 2008, East Lansing, USA, Feb. (2008).
- (Domestic Conference)
- 今井伸明, 青井考, 王惠仁, 櫻井博儀, 出道仁彦, Kawasaki H., 馬場秀忠, Dombradi Z., Elekes Z., 福田直樹, Fulop Z., Gelberg A., 五味朋子, 長谷川浩一, 石川和宏, 岩崎弘典, 金子恵美, 菅野祥子, 岸田隆, 近藤洋介, 久保敏幸, 栗田和好, 道正新一郎, 峯村俊行, 三浦宗賢, 本林透, 中村隆司, 野谷将広, 大西健夫, 齋藤明登, 下浦享, 杉本崇, Suzuki M., 竹下英里, 武内聡, 玉城充, 山田一成, 米田健一郎, 渡邊寛, 石原正泰: “ $^{12}\text{Be}$  と  $^{16}\text{C}$  における第一励起状態から基底状態への換算転移確率”, 日本物理学会第 58 回年次大会, 仙台, 3 月 (2003).
- 杉本崇, 中村隆司, 福田直樹, 三浦元隆, 近藤洋介, 青井考, 今井伸明, 久保敏幸, 小林俊雄, 五味朋子, 齋藤明登, 櫻井博儀, 下浦享, Bazin D. P., 長谷川浩一, 馬場秀忠, A.M. V., 本林透, T. Y., 柳澤善行, 米田健一郎, 渡辺極之, 渡辺裕, 石原正泰: “ $^{17}\text{B}$  の分解反応 (2)”, 日本物理学会第 58 回年次大会, 仙台, 3 月 (2003).
- 今井伸明, 王惠仁, 青井考, 櫻井博儀, 出道仁彦, Kawasaki H., 馬場秀忠, Dombradi Z., Elekes Z., 福田直樹, Fulop Z., Gelberg A., 五味朋子, 長谷川浩一, 石川和宏, 岩崎弘典, 金子恵美, 菅野祥子, 岸田隆, 近藤洋介, 久保敏幸, 栗田和好, 道正新一郎, 峯村俊行, 三浦宗賢, 本林透, 中村隆司, 野谷将広, 大西健夫, 齋藤明登, 下浦享, 杉本崇, Suzuki M., 竹下英里, 武内聡, 玉城充, 山田一成, 米田健一郎, 渡邊寛, 石原正泰: “Anomalously long lifetime of  $2^+$  state of  $^{16}\text{C}$ ”, A New Era of Nuclear Structure Physics, 新潟県黒川村, 11 月 (2003).
- 杉本崇, 中村隆司, 福田直樹, 三浦元隆, 近藤洋介, 青井考, 馬場秀忠, Bazin D. P., 五味朋子, 長谷川浩一, 橋本佳子, 今井伸明, 小林俊雄, 久保敏幸, 本林透, 篠原摩有子, 齋藤明登, 櫻井博儀, 下浦享, A.M. V., 渡辺極之, 渡辺裕, 薬師寺崇, 柳澤善行, 米田健一郎, 石原正泰: “Invariant-mass spectroscopy of  $^{13}\text{Be}$ ”, 日本物理学会第 59 回年次大会, 福岡, 3 月 (2004).
- 杉本崇, 中村隆司, A.M. V., 福田直樹, 三浦元隆, 近藤洋介, 青井考, 馬場秀忠, Bazin D. P., 五味朋子, 長谷川浩一, 橋本佳子, 今井伸明, 小林俊雄, 久保敏幸, 本林透, 篠原摩有子, 齋藤明登, 櫻井博儀, 下浦享, 渡辺極之, 渡辺裕, 薬師寺崇, 柳澤善行, 米田健一郎, 石原正泰: “Invariant-Mass Spectroscopy of Unbound  $^{11}\text{Li}$ ,  $^{13}\text{Be}$ , and  $^{17}\text{B}$  Nuclei”, 東京工業大学 21 世紀 COE プログラム「量子ナノ物理学」第 1 回公開シンポジウム, 東京, 3 月 (2004).
- 今井伸明, 王惠仁, 青井考, 櫻井博儀, 出道仁彦, Kawasaki H., 馬場秀忠, Dombradi Z., Elekes Z., 福田直樹, Fulop Z., Gelberg A., 五味朋子, 長谷川浩一, 石川和宏, 岩崎弘典, 金子恵美, 菅野祥子, 岸田隆, 近藤洋介, 久保敏幸, 栗田和好, 道正新一郎, 峯村俊行, 三浦宗賢, 本林透, 中村隆司, 野谷将広, 大西健夫, 齋藤明登, 下浦享, 杉本崇, Suzuki M., 竹下英里, 武内聡, 玉城充, 山田一成, 米田健一郎, 渡邊寛, 石原正泰: “Experimental finding of the anomalous quadrupole collectivity in unstable nucleus  $^{16}\text{C}$ ”, 日本物理学会 2005 年秋季大会, (日本物理学会), 京田辺, 9 月 (2005).
- 今井伸明, 王惠仁, 青井考, 櫻井博儀, 出道仁彦, Kawasaki H., 馬場秀忠, Dombradi Z., Elekes Z., 福田直樹, Fulop Z., Gelberg A., 五味朋子, 長谷川浩一, 石川和宏, 岩崎弘典, 金子恵美, 菅野祥子, 岸田隆, 近藤洋介, 久保敏幸, 栗田和好, 道正新一郎, 峯村俊行, 三浦宗賢, 本林透, 中村隆司, 野谷将広, 大西健夫, 齋藤明登, 下浦享, 杉本崇, Suzuki M., 竹下英里, 武内聡, 玉城充, 山田一成, 米田健一郎, 渡邊寛, 石原正泰: “Lifetime measurement of  $^{12}\text{Be}(2^+)$ ”, 日本物理学会 2005 年秋季大会, (日本物理学会), 京田辺, 9 月 (2005).
- 大竹政雄, 日下健祐, 久保敏幸, 矢野安重: “BigRIPS ヘリウム冷凍システムの運転状況”, 第 4 回日本加速器学会年会・第 32 回リニアック技術研究会, 和光, 8 月 (2007).
- 大西哲哉, 久保敏幸, 日下健祐, 吉田光一, 吉田敦, 大竹政雄, 竹田浩之, 溝井浩, 福田直樹, 柳澤善行, 青井考, 鈴木宏: “RIBF BigRIPS における PHITS の利用”, 第 4 回 PHITS ユーザー研究会, (日本原子力研究開発機構), 東海村, 2 月 (2008).
- 菅野祥子, 青井考, Bazin D., Bowen M. D., Campbell C. M., Cook J. M., Dinca D., Gade A., Glasmacher

T., 岩崎 弘典, 久保 敏幸, 栗田 和好, 本林 透, Mueller W. F., 中村 隆司, 櫻井 博儀, 鈴木 宏, 武内 聡, Terry J. R., 米田 健一郎, Zwahlen H.: “Proton core polarization in neutron-rich nucleus  $^{74}\text{Ni}$ ”, Workshop on Advance in Physics with ISOL-based/Fragmentation-based RI Beams, (TITECH), 東京, 2月 (2008).

市川 雄一, 久保敏幸, 青井考, Banerjee S. R., Chakrabarti A., 福田直樹, 岩崎弘典, 久保野茂, 本林透, 中林彩, 中村隆司, 中尾太郎, 奥村俊文, 王惠仁, 大西健夫, 鈴木大介, 鈴木賢, 山田一成, 山口英斉, 櫻井博儀: 日本物理学会 2008 年秋季大会, 山形, 9月 (2008).

市川 雄一, 久保敏幸, 青井考, Banerjee S. R., Chakrabarti A., 福田直樹, 岩崎弘典, 久保野茂, 本林透, 中林彩, 中村隆司, 中尾太郎, 奥村俊文, 王惠仁, 大西健夫, 鈴木大介, 鈴木賢, 山田一成, 山口英斉, 櫻井博儀: 第 5 回停止・低速不安定核ビームを用いた核分光研究会, (大阪大学), 豊中, 12月 (2008).

## **GARIS Team**

### **Publications**

#### **[Journal]**

(Original Papers) \*Subject to Peer Review

Haba H., Kikunaga H., Kaji D., Akiyama T., Morimoto K., Morita K., Nanri T., Ooe K., Sato N., Shinohara A., Suzuki D., Takabe T., Yamazaki I., Yokoyama A., and Yoneda A.: "Performance of the gas-jet transport system coupled to the RIKEN gas-filled recoil ion separator GARIS for the  $^{238}\text{U}(^{22}\text{Ne},5\text{n})^{255}\text{No}$  reaction", J. Nucl. Radiochem. Sci. **9**, No. 1, pp. 27–31 (2008). \*

## BigRIPS Team

### Publications

#### [Journal]

(Original Papers) \*Subject to Peer Review

- Fukuda N., Nakamura T., Kobayashi T., Otsu H., Aoi N., Imai N., Iwasaki H., Kubo T., Mengoni A., Notani M., Sakurai H., Shimoura S., Teranishi T., Watanabe Y., Yoneda K., and Ishihara M.: “Coulomb Dissociation of Halo Nuclei”, *Prog. Theor. Phys. Suppl.*, No. 146, pp. 462–466 (2002).
- Gomi T., Motobayashi T., Yoneda K., Kanno S., Aoi N., Ando Y., Baba H., Demichi K., Fulop Z., Futakami U., Hasegawa H., Higurashi Y., Ieki K., Imai N., Iwasa N., Iwasaki H., Kubo T., Kubono S., Kunibu M., Matsuyama Y., Michimasa S., Minemura T., Murakami H., Nakamura T., Saito A., Sakurai H., Serata M., Shimoura S., Sugimoto T., Takeshita E., Takeuchi S., Ue K., Yamada K., Yanagisawa Y., Yoshida A., and Ishihara M.: “Coulomb Dissociation of  $^{23}\text{Al}$ ”, *Prog. Theor. Phys. Suppl.*, No. 146, pp. 557–558 (2002). \*
- Kanno S., Gomi T., Motobayashi T., Yoneda K., Aoi N., Ando Y., Baba H., Demichi K., Fulop Z., Futakami U., Hasegawa H., Higurashi Y., Ieki K., Imai N., Iwasa N., Iwasaki H., Kubo T., Kubono S., Kunibu M., Matsuyama Y., Michimasa S., Minemura T., Murakami H., Nakamura T., Saito A., Sakurai H., Serata M., Shimoura S., Sugimoto T., Takeshita E., Takeuchi S., Ue K., Yamada K., Yanagisawa Y., Yoshida A., and Ishihara M.: “Coulomb Excitation of  $^{24}\text{Si}$ ”, *Prog. Theor. Phys. Suppl.*, No. 146, pp. 575–576 (2002). \*
- Gomi T., Motobayashi T., Yoneda K., Kanno S., Aoi N., Ando Y., Baba H., Demichi K., Fulop Z., Futakami U., Hasegawa H., Higurashi Y., Ieki K., Imai N., Iwasa N., Iwasaki H., Kubo T., Kubono S., Kunibu M., Matsuyama Y., Michimasa S., Minemura T., Murakami H., Nakamura T., Saito A., Sakurai H., Serata M., Shimoura S., Sugimoto T., Takeshita E., Takeuchi S., Ue K., Yamada K., Yanagisawa Y., Yoshida A., and Ishihara M.: “Study of the  $^{22}\text{Mg}(p, \gamma)^{23}\text{Al}$  Reaction with the Coulomb-Dissociation Method”, *Nucl. Phys. A* **718**, 508c–509c (2003). \*
- Gomi T., Motobayashi T., Ando Y., Aoi N., Baba H., Demichi K., Elekes Z., Fukuda N., Fulop Z., Futakami U., Hasegawa H., Higurashi Y., Ieki K., Imai N., Ishihara M., Ishikawa K., Iwasa N., Iwasaki H., Kanno S., Kondo Y., Kubo T., Kubono S., Kunibu M., Kurita K., Matsuyama Y., Michimasa S., Minemura T., Miura M., Murakami H., Nakamura T., Notani M., Ota S., Saito A., Sakurai H., Serata M., Shimoura S., Sugimoto T., Takeshita E., Takeuchi S., Togano Y., Ue K., Yamada K., Yanagisawa Y., Yoneda K., and Yoshida A.: “Study of the Stellar  $^{22}\text{Mg}(p, \gamma)^{23}\text{Al}$  Reaction using the Coulomb-Dissociation Method”, *Nucl. Phys. A* **734**, E77–E79 (2004).
- Ueno H., Asahi K., Ogawa H., Kameda D., Miyoshi H., Yoshimi A., Watanabe H., Shimada K., Sato W., Yoneda K., Imai N., Kobayashi Y., Ishihara M., and Wolf-Dieter S.: “Measurement of nuclear moments in the region of light neutron-rich nuclei”, *Nucl. Phys. A* **738**, 211–215 (2004). \*
- Fukuda N., Nakamura T., Aoi N., Imai N., Ishihara M., Kobayashi T., Iwasaki H., Kubo T., Mengoni A., Notani M., Otsu H., Sakurai H., Shimoura S., Teranishi T., Watanabe Y., and Yoneda K.: “Coulomb and nuclear breakup of a halo nucleus  $^{11}\text{Be}$ ”, *Phys. Rev. C* **70**, 054606-1–054606-12 (2004). \*
- Imai N., Ong H., Aoi N., Sakurai H., Demichi K., Kawasaki H., Baba H., Dombradi Z., Elekes Z., Fukuda N., Fulop Z., Gelberg A., Gomi T., Hasegawa H., Ishikawa K., Iwasaki H., Kaneko E., Kanno S., Kishida T., Kondo Y., Kubo T., Kurita K., Michimasa S., Minemura T., Miura M., Motobayashi T., Nakamura T., Notani M., Ohnishi T., Saito A., Shimoura S., Sugimoto T., Suzuki M., Takeshita E., Takeuchi M., Tamaki M., Yoneda K., Watanabe H., and Ishihara M.: “Anomalous hindered  $E2$  Strength  $B(E2; 2_1^+ \rightarrow 0^+)$  in  $^{16}\text{C}$ ”, *Phys. Rev. Lett.* **92**, No. 6, pp. 062501-1–062501-4 (2004). \*
- Hatano M., Sakai H., Wakui T., Uesaka T., Aoi N., Ichikawa Y., Ikeda T., Itoh K., Iwasaki H., Kawabata T., Kuboki H., Maeda Y., Matsui N., Ohnishi T., Ohnishi T., Saito T., Sakamoto N., Sasano M., Satou Y., Sekiguchi K., Suda K., Tamii A., Yanagisawa Y., and Yako K.: “First experiment of  $6\text{He}$  with a polarized proton target”, *Eur. Phys. J. A* **25**, No. s01, pp. 255–258 (2005). \*
- Kannungo R., Chiba M., Abu-Ibrahim B., Adhikari S., Fang D., Iwasa N., Kimura K., Maeda K., Nishimura S., Ohnishi T., Ozawa A., Samanta C., Suda T., Suzuki T., Wang Q., Wu C., Yamaguchi Y., Yamada K., Yoshida A., Zheng T., and Tanihata I.: “A new view to the structure of  $^{19}\text{C}$ ”, *Eur. Phys. J. A* **25**, No. s01, pp. 261–262 (2005). \*
- Gomi T., Motobayashi T., Ando Y., Aoi N., Baba H., Demichi K., Elekes Z., Fukuda N., Fulop Z., Futakami U., Hasegawa H., Higurashi Y., Ieki K., Imai N., Ishihara M., Ishikawa K., Iwasa N., Iwasaki H., Kanno S., Kondo Y., Kubo T., Kubono S., Kunibu M., Kurita K., Matsuyama Y., Michimasa S., Minemura T., Miura M., Murakami H., Nakamura T., Notani M., Ota S., Saito A., Sakurai H., Serata M., Shimoura S., Sugimoto T., Takeshita E., Takeuchi S., Togano Y., Ue K., Yamada K., Yanagisawa Y., Yoneda K., and Yoshida A.: “Coulomb dissociation experiment for explosive hydrogen burning: study of the  $^{22}\text{Mg}(p, \gamma)^{23}\text{Al}$  reaction”, *J. Phys. G* **31**, S1517–S1521 (2005).
- Togano Y., Gomi T., Motobayashi T., Ando Y., Aoi N., Baba H., Demichi K., Elekes Z., Fukuda N., Fulop Z., Futakami U., Hasegawa H., Higurashi Y., Ieki K., Imai

- N., Ishihara M., Ishikawa K., Iwasa N., Iwasaki H., Kanno S., Kondo Y., Kubo T., Kubono S., Kunibu M., Kurita K., Matsuyama Y., Michimasa S., Minemura T., Miura M., Murakami H., Nakamura T., Notani M., Ota S., Saito A., Sakurai H., Serata M., Shimoura S., Sugimoto T., Takeshita E., Takeuchi S., Ue K., Yamada K., Yanagisawa Y., Yoneda K., and Yoshida A.: “Study of  $^{26}\text{Si}(p, \gamma)^{27}\text{P}$  reaction using Coulomb dissociation method”, Nucl. Phys. A **758**, 182c–185c (2005). \*
- Elekes Z., Dombradi Z., Kanungo R., Baba H., Fulop Z., Gibelin J. D., Horvath A., Ideguchi E., Ichikawa Y., Iwasa N., Iwasaki H., Kanno S., Kawai S., Kondo Y., Motobayashi T., Notani M., Ohnishi T., Ozawa A., Sakurai H., Shimoura S., Takeshita E., Takeuchi M., Tanihata I., Togano Y., Wu C., Yamaguchi Y., Yanagisawa Y., Yoshida A., and Yoshida K.: “Low-lying excited states in  $^{17,19}\text{C}$ ”, Phys. Lett. B **614**, 174–180 (2005). \*
- Iwasaki H., Motobayashi T., Sakurai H., Yoneda K., Gomi T., Aoi N., Fukuda N., Fulop Z., Futakami U., Gacsi Z., Higurashi Y., Imai N., Iwasa N., Kunibu M., Kubo T., Kurokawa M., Liu Z., Minemura T., Saito A., Serata M., Shimoura S., Takeuchi S., Watanabe Y., Yamada K., Yanagisawa Y., and Ishihara M.: “Quadrupole collectivity of  $^{28}\text{Ne}$  and the boundary of the island of inversion”, Phys. Lett. B **620**, 118–124 (2005). \*
- Dombradi Z., Elekes Z., Kanungo R., Baba H., Fulop Z., Gibelin J. D., Horvath A., Ideguchi E., Ichikawa Y., Iwasa N., Iwasaki H., Kanno S., Kawai S., Kondo Y., Motobayashi T., Notani M., Ohnishi T., Ozawa A., Sakurai H., Shimoura S., Takeshita E., Takeuchi S., Tanihata I., Togano Y., Wu C., Yamaguchi Y., Yanagisawa Y., Yoshida A., and Yoshida K.: “Decoupling of valence neutrons from the core in  $^{17}\text{B}$ ”, Phys. Lett. B **621**, 81–88 (2005). \*
- Togano Y., Gomi T., Motobayashi T., Ando Y., Aoi N., Baba H., Demichi K., Elekes Z., Fukuda N., Fulop Z., Futakami U., Hasegawa H., Higurashi Y., Ieki K., Imai N., Ishihara M., Ishikawa K., Iwasa N., Iwasaki H., Kanno S., Kondo Y., Kubo T., Kubono S., Kunibu M., Kurita K., Matsuyama Y., Michimasa S., Minemura T., Miura M., Murakami H., Nakamura T., Notani M., Ota S., Saito A., Sakurai H., Serata M., Shimoura S., Sugimoto T., Takeshita E., Takeuchi S., Ue K., Yamada K., Yanagisawa Y., Yoneda K., and Yoshida A.: “Study of the  $^{26}\text{Si}(p, \gamma)^{27}\text{P}$  reaction through Coulomb dissociation of  $^{27}\text{P}$ ”, Eur. Phys. J. A **27**, No. s01, pp. 233–236 (2006). \*
- Gomi T., Motobayashi T., Ando Y., Aoi N., Baba H., Demichi K., Elekes Z., Fukuda N., Fulop Z., Futakami U., Hasegawa H., Higurashi Y., Ieki K., Imai N., Ishihara M., Ishikawa K., Iwasa N., Iwasaki H., Kanno S., Kondo Y., Kubo T., Kubono S., Kunibu M., Kurita K., Matsuyama Y., Michimasa S., Minemura T., Miura M., Murakami H., Nakamura T., Notani M., Ota S., Saito A., Sakurai H., Serata M., Shimoura S., Sugimoto T., Takeshita E., Takeuchi S., Ue K., Yamada K., Yanagisawa Y., Yoneda K., and Yoshida A.: “Coulomb Dissociation of  $^{23}\text{Al}$  for the stellar  $^{22}\text{Mg}(p, \gamma)^{23}\text{Al}$  reaction”, Nucl. Phys. A **758**, 761c–764c (2006).
- Ladygin V., Uesaka T., Saito T., Hatano M., Isupov Y., Kato H., Ladygina N., Maeda Y., Malakhov A., Nishikawa J., Ohnishi T., Okumura H., Reznikov S., Sakai H., Sakamoto N., Sakoda S., Saito T., Sekiguchi K., Suda K., Tamii A., Uchigashima N., and Yako K.: “Tensor Analyzing Power  $T_{20}$  of the  $dd \rightarrow ^3\text{He}$  and  $dd \rightarrow ^3\text{He}$  Reactions at Zero Angle for Energies 140, 200, and 270 MeV”, Phys. At. Nucl. **69**, 1271–1278 (2006). \*
- Yamaguchi T., Ohnishi T., Suzuki T., Becker T., Fukuda M., Geissel H., Hosoi M., Janik R., Kelic A., Kimura K., Mandel S., Muenzenberg G., Nakajima S., Ohtsubo T., Ozawa A., Prochazka A., Shindo M., Sitar B., Strmen P., Suda T., Summerer K., Sugawara K., Szarka I., Takechi M., Takisawa A., and Tanaka K.: “Production cross sections of isotopes formed by fragmentation of similar to 1A (GeVKr)-Kr-80 beam”, Phys. Rev. C **74**, 044608-1–044608-5 (2006). \*
- Nakamura T., Vinodkumar A., Sugimoto T., Aoi N., Baba H., Bazin D. P., Fukuda N., Gomi T., Hasegawa H., Imai N., Ishihara M., Kobayashi T., Kondo Y., Kubo T., Miura M., Motobayashi T., Otsu H., Saito A., Sakurai H., Shimoura S., Watanabe K., Watanabe Y., Yakushiji T., Yanagisawa Y., and Yoneda K.: “Observation of Strong Low-Lying E1 Strength in the Two-Neutron Halo Nucleus  $^{11}\text{Li}$ ”, Phys. Rev. Lett. **96**, 252502-1–252502-4 (2006). \*
- Elekes Z., Dombradi Z., Saito A., Aoi N., Baba H., Demichi K., Fulop Z., Gibelin J. D., Gomi T., Hasegawa H., Imai N., Ishihara M., Iwasaki H., Kanno S., Kawai S., Kishida T., Kubo T., Kurita K., Matsuyama Y., Michimasa S., Minemura T., Motobayashi T., Notani M., Ohnishi T., Ong H., Ota S., Ozawa A., Sakai H., Sakurai H., Shimoura S., Takeshita E., Takeuchi S., Tamaki M., Togano Y., Yamada K., Yanagisawa Y., and Yoneda K.: “Study of  $N=20$  shell gap with  $^1\text{H}(^{28}\text{Ne}, ^{27,28}\text{Ne})$  reactions”, Eur. Phys. J. Special Topics **150**, 99–102 (2007). \*
- Shimada K., Nagae D., Asahi K., Inoue T., Takase K., Kagami S., Hatakeyama N., Kobayashi Y., Ueno H., Yoshimi A., Kameda D., Nagatomo T., Sugimoto T., Kubono S., Yamaguchi H., Wakabayashi Y., Hayakawa S., Murata J., and Kawamura H.: “Production of spin-polarized  $^{17}\text{N}$  beam using inverse-kinematics low-energy transfer reactions”, Hyperfine Interact. **180**, 43–47 (2007). \*
- Yamaguchi T., Suzuki T., Ohnishi T., Summerer S., Becker F., Fukuda M., Geissel H., Hosoi M., Janik R., Kimura K., Mandel S., Muenzenberg G., Nakajima

- S., Ohtsubo T., Ozawa A., Orochazka A., Shindo M., Strmen P., Suda T., Sugawara K., Szarka I., Takisawa A., Takechi M., and Tanaka K.: “Nuclear radii of neutron-deficient Kr isotopes studied via their interaction cross-sections at relativistic energies”, Nucl. Phys. A **787**, 471c–475c (2007). \*
- Fang D., Guo W., Ma. C., Wang K., Yang T., Ma. Y., Cai X., Shen W., Ren Z., Sun Z., Chen J., Tian W., Zhong C., Hosoi M., Izumikawa T., Kanungo R., Nakajima S., Ohnishi T., Ohtsubo T., Ozawa A., Suda T., Sugawara K., Suzuki T., Takisawa A., Tanaka K., Yamaguchi T., and Tanihata I.: “Examining the exotic structure of the proton-rich nucleus  $^{23}\text{Al}$ ”, Phys. Rev. C **76**, 031601-1–031601-5 (2007). \*
- Ladygin V., Uesaka T., Saito T., Janek M., Kiselev A., Kurilkin A., Vasiliev A., Hatano M., Isupov Y., Kato H., Ladygina N., Maeda Y., Malakhov A., Nishikawa J., Ohnishi T., Okamura H., Reznikov S., Sakai H., Sakoda S., Sakamoto N., Satou Y., Sekiguchi K., Suda K., Tamii A., Uchigashima N., and Yako K.: “Analyzing powers in the  $dd \rightarrow {}^3\text{He}({}^3\text{He})$  reactions at intermediate energies”, AIP Conf. Proc. **1011**, 235–240 (2008). \*
- Kurilkin A., Saito T., Ladygin V., Uesaka T., Vasiliev T., Janek M., Hatano M., Isupov Y., Kato K., Ladygina N., Maeda Y., Malakhov A., Nishikawa J., Ohnishi T., Okamura H., Reznikov S., Sakai H., Sakamoto N., Sakoda S., Satou Y., Sekiguchi K., Suda K., Tamii A., Uchigashima N., and Yako K.: “Measurement of the vector  $A_y$  and tensor  $A_{yy}$ ,  $A_{xx}$ ,  $A_{xz}$  analyzing powers for the  $dd \rightarrow {}^3\text{He}p$  reaction at 200 MeV”, Eur. Phys. J. Special Topics **162**, 133–136 (2008). \*
- Kiselev A., Ladygin V., Uesaka T., Vasiliev A., Janek M., Saito T., Hatano M., Isupov Y., Kato H., Ladygina N., Maeda Y., Malakhov A., Nishikawa J., Ohnishi T., Okamura H., Reznikov S., Sakai H., Sakamoto N., Sakoda S., Satou Y., Sekiguchi K., Suda K., Tamii A., Uchigashima N., and Yako K.: “Analyzing powers in the  ${}^{12}\text{C}(\vec{d}, p){}^{13}\text{C}$  reaction at the energy  $T_d = 270$  MeV”, Eur. Phys. J. Special Topics **162**, 143–146 (2008). \*
- Kameda D., Asahi K., Ueno H., Nagae D., Takemura M., Shimada K., Yoshimi A., Nagatomo T., Sugimoto T., Uchida M., Arai T., Takase K., Suda S., Inoue T., Murata J., Kawamura H., Watanabe H., Kobayashi Y., and Ishihara M.: “Electric quadrupole moments of neutron-rich nuclei  ${}^{32}\text{Al}$  and  ${}^{31}\text{Al}$ ”, Hyperfine Interact. **180**, 61–64 (2008). \*
- Sato W., Ueno H., Watanabe H., Miyoshi H., Yoshimi A., Kameda D., Ito T., Shimada K., Kaihara J., Suda S., Kobayashi Y., Shinohara A., Ohkubo Y., and Asahi K.: “Temperature-dependent behavior of impurity atoms implanted in highly oriented pyrolytic graphite –An application of a new online TDPAC method–”, J. Phys. Soc. Jpn. **77**, No. 9, pp. 095001-1–095001-2 (2008). \*
- Yoshida A., Suda T., Ohtsuki T., Yuki H., and Kubo T.: “Status and overview of production target for BigRIPS separator at RIKEN”, Nucl. Instrum. Methods Phys. Res. A **590**, 204–212 (2008). \*
- Yamaguchi Y., Ozawa A., Goto A., Arai I., Fujinawa T., Fukunishi N., Kikuchi T., Ohnishi T., Ohtsubo T., Sakurai H., Suzuki T., Wakasugi M., Yamaguchi T., Yasuda Y., and Yano Y.: “Rara-RI ring project at RIKEN RI beam factory”, Nucl. Instrum. Methods Phys. Res. B **266**, 4575–4578 (2008). \*
- Nagae D., Ueno H., Kameda D., Takemura M., Asahi K., Yoshimi A., Sugimoto T., Shimada K., Nagatomo T., Uchida M., Arai T., Inoue T., Kagami S., Hatakeyama N., Murata J., Kawamura H., and Narota K.: “Electric quadrupole moment of  ${}^{31}\text{Al}$ ”, Nucl. Instrum. Methods Phys. Res. B **266**, 4612–4615 (2008). \*
- Ueno H., Nagae D., Kameda D., Asahi K., Takemura M., Takase K., Yoshimi A., Sugimoto T., Shimada K., Nagatomo T., Uchida M., Arai T., Inoue T., Murata J., Kawamura H., and Narota K.: “Electric quadrupole moment of  ${}^{31}\text{Al}$ ”, Nucl. Phys. A **805**, 329–331 (2008). \*
- Aoi N., Suzuki H., Takeshita E., Takeuchi S., Ota S., Baba H., Bishop S., Fukui T., Hashimoto Y., Ong H., Ideguchi E., Ieki K., Imai N., Iwasaki H., Kanno S., Kondo Y., Kubo T., Kurita K., Kusaka K., Minemura T., Motobayashi T., Nakabayashi T., Nakamura T., Nakao T., Niikura M., Okumura T., Ohnishi T., Sakurai H., Shimoura S., Sugo R., Suzuki D., Suzuki M., Tamaki M., Tanaka K., Togano Y., and Yamada K.: “Shape transition observed in neutron-rich pf-shell isotopes studied via proton inelastic scattering”, Nucl. Phys. A **805**, 400c–407c (2008).
- Yamaguchi T., Suzuki T., Ohnishi T., Becker F., Fukuda M., Geissel H., Hosoi M., Janik R., Kimura K., Kuboki T., Mandel S., Matsuo M., Muenzenberg G., Nakajima S., Ohtsubo T., Ozawa A., Prochazka A., Shindo M., Sitar B., Strmen P., Suda T., Suemmerer K., Sugawara K., Szarka I., Takechi M., Takisawa A., Tanaka K., and Yamagami M.: “Nuclear matter radii of neutron-deficient Kr isotopes”, Phys. Rev. C **77**, 034315-1–034315-6 (2008). \*
- Wakasugi M., Emoto T., Furukawa Y., Ishii K., Ito S., Koseki T., Kurita K., Kuwajima A., Masuda T., Morikawa A., Nakamura M., Noda A., Ohnishi T., Shirai T., Suda T., Takeda H., Tamae T., Tongu H., Wang S., and Yano Y.: “Novel Internal Target for Electron Scattering off Unstable Nuclei”, Phys. Rev. Lett. **100**, 164801-1–164801-4 (2008). \*
- Okada K., Wada M., Nakamura T., Takamine A., Lioubimov V., Schury P. H., Ishida Y., Sonoda T., Ogawa M., Yamazaki Y., Kanai Y., Kojima T., Katayama I., Ohtani S., Kubo T., and Yoshida A.: “Precision Measurement of the Hyperfine Structure of Laser-Cooled Radioactive  ${}^7\text{Be}^+$  Ions Produced by Projectile Fragmentation”, Phys. Rev. Lett. **101**, 212502-1–212502-4 (2008). \*

Nagae D., Ueno H., Kameda D., Takemura M., Asahi K., Takase K., Yoshimi A., Sugimoto T., Shimada K., Nagatomo T., Uchida M., Arai T., Inoue T., Kagami S., Hatakeyama N., Kawamura H., Narota K., and Murata J.: “Ground-state electric quadrupole moment of  $^{31}\text{Al}$ ”, *Phys. Rev. C* **79**, 027301-1–027301-4 (2009). \*

(Others)

Nakajima S., Yamaguchi T., Suzuki T., Yamaguchi Y., Fujinawa T., Fukunishi N., Goto A., Ohnishi T., Sakurai H., Wakasugi M., Yano Y., Arai I., Ozawa A., Yasuda Y., Kikuchi T., and Ohtsubo T.: “New scheme for precision mass measurements of rare isotopes produced at RI beam factory”, *Acta Phys. Pol. B* **39**, No. 2, pp. 457–462 (2008).

Murata J., Akiyama T., Hata M., Hirayama Y., Ikeda Y., Ishii T., Kameda D., Kawamura H., Mitsuoka S., Miyatake H., Nagae D., Ninomiya K., Nitta M., Seitabashi E., and Toyoda T.: “R&D for a test of time reversal symmetry experiment using polarized nuclei”, *JAEA-Review* **2008-054**, 58–59 (2008).

#### [Book • Proceedings]

(Original Papers) \*Subject to Peer Review

Baba H., Ichihara T., Ohnishi T., Takeuchi S., Yoshida K., Watanabe Y., Ota S., and Shimoura S.: “The New DAQ System in RIKEN RIBF”, 2008 IEEE Nuclear Science Symposium Conference Record, Dresden, Germany, 2008–10, IEEE, Dresden, pp. 1384–1386 (2008). \*

Ohnishi J., Nakagawa T., Higurashi Y., Okuno H., Kusaka K., and Goto A.: “Construction and test of the superconducting coils for RIKEN SC-ECR ion source”, *Proceedings of the 11th European Particle Accelerator Conference (EPAC 2008)*, Genoa, 2008–6, The European Physical Society Accelerator Group, -, pp. 433–435 (2008).

Yoshida A.: “Status of the target system for BigRIPS in-flight RI beam separator”, *PSI Proceedings 07-01*, Bad Zurzach, Switzerland, 2007–9, Paul Scherrer Institut (PSI), Villigen, pp. 81–83 (2008).

(Others)

Yamaguchi T., Arai I., Fukunishi N., Goto A., Kikuchi T., Komatsubara T., Ohnishi T., Ohtsubo T., Okuno H., Ozawa A., Sasa K., Suzuki T., Tagisi Y., Takeda H., Wakasugi M., Yamaguchi M., Yamaguchi Y., and Yano Y.: “Mass measurements by an isochronous storage ring at the RIKEN RI beam factory”, *Proceedings of the 6th International Conference on Nuclear Physics at Storage Rings (STORI '05)*, Bonn, Germany, 2005–5, Forschungszentrum Julich, Julich, pp. 297–300 (2005).

Yamaguchi M., Arai I., Fukunishi N., Goto A., Kusaka K., Kikuchi T., Komatsubara T., Kubo T., Ohnishi T., Ohtsubo T., Okuno H., Ozawa A., Sasa K., Suzuki T., Tagisi Y., Takeda H., Wakasugi M., Yamaguchi T., Yamaguchi Y., and Yano Y.: “Design of an isochronous storage ring and an injection line for mass measurements at the RIKEN RI beam factory”, *Proceedings of*

the 6th International Conference on Nuclear Physics at Storage Rings (STORI '05), Bonn, Germany, 2005–5, Forschungszentrum Julich, Julich, pp. 315–319 (2005).

Kikuchi T., Horioka K., Ozawa A., Kawata S., Yamaguchi Y., Fukunishi N., Sakurai H., Wakasugi M., Yamaguchi M., Yamaguchi T., Arai I., Ohta H., Fujinawa T., Sasa K., Komatsubara T., Suzuki T., Ohtsubo T., Goto A., Ohnishi T., Okuno H., Takeda H., and Yano Y.: “Individual correction using induction modulator for mass measurements by isochronous ring in RIKEN RI beam factory”, *Proceedings of the 2nd International Workshop on Recent Progress in Induction Accelerators (RPIA2006)*, Tsukuba, 2006–3, KEK, Tsukuba, pp. 127–131 (2006).

#### Oral Presentations

(International Conference etc.)

Yamaguchi T., Ozawa A., Arai I., Komatsubara T., Sasa K., Tagisi Y., Yamaguchi M., Suzuki T., Ohtsubo T., Fukunishi N., Goto A., Ohnishi T., Okuno H., Takeda H., Wakasugi M., Yano Y., Yamaguchi Y., and Kikuchi T.: “Mass measurements in RIKEN”, 6th International Conference on Nuclear Physics at Storage Rings (STORI-05), (Research Center Julich), Bonn, Germany, May (2005).

Kikuchi T., Horioka K., Ozawa A., Kawata S., Yamaguchi Y., Fukunishi N., Sakurai H., Wakasugi M., Yamaguchi M., Yamaguchi T., Arai I., Ohta H., Fujinawa T., Sasa K., Komatsubara T., Suzuki T., Ohtsubo T., Goto A., Ohnishi T., Okuno H., Takeda H., and Yano Y.: “Individual correction using induction modulator for mass measurements by isochronous ring in RIKEN RI beam factory”, 2nd International Workshop on Recent Progress in Induction Accelerators (RPIA2006), (KEK, Tokyo Institute of Technology), Tsukuba, Mar. (2006).

Arai I., Komatsubara T., Ozawa A., Sasa K., Yasuda Y., Fujinawa T., Fukunishi N., Goto A., Ohnishi T., Okuno H., Takeda H., Wakasugi M., Yamaguchi M., Yamaguchi Y., Yano Y., Kikuchi T., Suzuki T., Yamaguchi T., and Ohtsubo T.: “Isochronous ring at RIKEN”, *Workshop on Advanced Laser and Mass Spectroscopy ALMAS-I: Innovative Physics Ideas*, (Gesellschaft für Schwerionenforschung (GSI)), Darmstadt, Germany, Oct. (2006).

Arai I., Komatsubara T., Ozawa A., Sasa K., Yasuda Y., Fujinawa T., Fukunishi N., Goto A., Ohnishi T., Okuno H., Takeda H., Wakasugi M., Yamaguchi M., Yamaguchi Y., Yano Y., Kikuchi T., Suzuki T., Yamaguchi T., and Ohtsubo T.: “Rare RI ring”, *RIBF International Collaboration Workshop on Experiments at the RIBF*, Wako, Nov. (2006).

Kondo Y., Nakamura T., Sato Y., Aoi N., Endo N., Fukuda N., Gomi T., Hashimoto Y., Ishihara M., Kawai S., Kitayama M., Kobayashi T., Matsuda Y., Matsui N., Motobayashi T., Nakabayashi T., Okumura T., Ong H.,

- Onishi T., Otsu H., Sakurai H., Shimoura S., Shinohara M., Sugimoto T., Takeuchi S., Tamaki M., Togano Y., and Yanagisawa Y.: “Invariant mass spectroscopy of  $^{13}\text{Be}$  and  $^{14}\text{Be}$  via the proton-induced breakup reactions of  $^{14}\text{Be}$ ”, 5th International Workshop on Direct Reaction with Exotic Beams (DREB2007), Wako, May–June (2007).
- Yamaguchi Y., Fujinawa T., Fukunishi N., Goto A., Ohnishi T., Sakurai H., Wakasugi M., Yano Y., Ozawa A., Arai I., Yasuda Y., Suzuki T., Yamaguchi T., Kikuchi T., and Ohtsubo T.: “Rare-RI ring project at RI Beam factory in RIKEN”, 15th International Conference on Electromagnetic Isotope Separators and Techniques Related to their Applications (EMIS2007), (GANIL , IN2P3/CNRS , DSM/CEA), Deauville, France, June (2007).
- Kameda D., Ueno H., Asahi K., Nagae D., Takemura M., Yoshimi A., Shimada K., Uchida M., Kijima G., Arai T., Takase K., Suda S., Inoue T., Murata J., Kawamura H., Haseyama T., Kobayashi Y., Watanabe H., and Ishihara M.: “Small electric quadrupole moment of  $^{32}\text{Al}$ : Drastic shape transition between  $^{32}\text{Al}$  and  $^{31}\text{Mg}$ ”, International Nuclear Physics Conference (INPC2007), (Science Council of Japan, RIKEN and others), Tokyo, June (2007).
- Kondo Y., Nakamura T., Sato Y., Aoi N., Endo N., Fukuda N., Gomi T., Hashimoto Y., Ishihara M., Kawai S., Kitayama M., Kobayashi T., Matsuda Y., Matsui N., Motobayashi T., Nakabayashi T., Okumura T., Ong H., Onishi T., Otsu H., Sakurai H., Shimoura S., Shinohara M., Sugimoto T., Takeuchi S., Tamaki M., Togano Y., and Yanagisawa Y.: “Invariant mass spectroscopy of  $^{13}\text{Be}$  and  $^{14}\text{Be}$  via the proton-induced breakup reactions”, International Symposium & School on Frontiers and Perspectives of Nuclear and Hadron Physics (FPNH07), (Tokyo Institute of Technology), Tokyo, June (2007).
- Kameda D., Ueno H., Asahi K., Nagae D., Takemura M., Yoshimi A., Shimada K., Uchida M., Kijima G., Arai T., Takase K., Suda S., Inoue T., Murata J., Kawamura H., Haseyama T., Kobayashi Y., Watanabe H., and Ishihara M.: “Small electric quadrupole moment of  $^{32}\text{Al}$ ”, International Workshop on Nuclear Structure: New Pictures in the Extended Isospin Space (NS07), (Yukawa Institute for Theoretical Physics), Kyoto, June (2007).
- Nakajima S., Suzuki T., Yamaguchi T., Fujinawa T., Fukunishi N., Goto A., Ohnishi T., Sakurai H., Wakasugi M., Yamaguchi Y., Yano Y., Ozawa A., Arai I., Yasuda Y., Kikuchi T., and Ohtsubo T.: “New scheme for precision mass measurement of rare isotopes produced at RI beam factory”, 30th Mazurian Lakes Conference on Physics : Nuclear Physics and the Fundamental Processes, (IPJ ; University of Warsaw ; Pro-Physica), Piaski, Poland, Sept. (2007).
- Kondo Y., Motobayashi T., Sakurai H., Aoi N., Otsu H., Yanagisawa Y., Fukuda N., Takeuchi S., Ishihara M., Baba H., Gomi T., Imai N., Kubo T., Yoneda K., Nakamura T., Sato Y., Sugimoto T., Matsui N., Attukalathil V. M., Okumura T., Hashimoto Y., Nakabayashi T., Shinohara M., Miura M., Kobayashi T., Matsuda Y., Endo N., Kitayama M., Watanabe K., Yakushiji T., Togano Y., Kawai S., Hasegawa H., Onishi T., Ong H., Shimoura S., Tamaki M., Saito A., Bazin D. P., and Watanabe Y.: “Breakup reactions of  $^{14}\text{Be}$ ”, Future Prospects for Spectroscopy and Direct Reactions 2008, (Michigan State University), East Lansing, USA, Feb. (2008).
- Yamaguchi T., Fujinawa T., Fukunishi N., Goto A., Ohnishi T., Sakurai H., Wakasugi M., Yamaguchi Y., Yano Y., Arai I., Moriguchi T., Ozawa A., Yasuda Y., Nakajima S., Kuboki T., Suzuki T., Kikuchi T., and Ohtsubo T.: “Storage-ring mass spectrometry”, ETC Workshop on Mass Olympics, (GSI , FIAS), Trento, Italy, May (2008).
- Yoshimi A., Ueno H., Nagatomo T., Shimada K., Ichikawa Y., Kameda D., Sugimoto T., Sakurai H., Asahi K., Hasama Y., Takemura M., Kijima G., Nagae D., Uchida M., Arai T., Suda S., Takase T., Inoue T., Hatakeyama N., Kagami S., Murata J., and Kawamura H.: “Nuclear electromagnetic moments of neutron-rich Al isotopes”, Nuclear Structure 2008, (Michigan State University, NSCL at MSU), Michigan, USA, June (2008).
- Kawamura H., Murata J., Toyoda T., Seitabashi E., Nitta M., Hata M., Akiyama T., Ikeda Y., Ninomiya K., Kameda D., Nagae D., and Hirayama Y.: “The first T-violation experiment at KEK-TRIAC”, 24th Advanced Studies Institute :Symmetries and Spin (SPIN-Praha-2008), (Charles University in Prague, Faculty of Mathematics and Physics), Praha, Czech, July (2008).
- Yamaguchi T., Arai I., Ozawa A., Yasuda Y., Fujinawa T., Fukunishi N., Goto A., Hara K., Ohnishi T., Sakurai H., Wakasugi M., Yamaguchi Y., Yano Y., Kikuchi T., Suzuki T., and Ohtsubo T.: “Beam optics simulation for rare-RI ring at RI beam factory in RIKEN”, 7th International Conference on Nuclear Physics at Storage Rings STORI’08, (Institute of Modern Physics, Chinese Academy of Sciences, National Natural Foundation of China), Lanzhou, China, Sept. (2008).
- Yasuda Y., Ozawa A., Arai I., Fujinawa T., Fukunishi N., Goto A., Ohnishi T., Sakurai H., Wakasugi M., Yamaguchi Y., Yano Y., Suzuki T., Yamaguchi T., Kikuchi T., and Ohtsubo T.: “Present status of rare-RI ring project in RIKEN RIBF”, 7th International Conference on Nuclear Physics at Storage Rings STORI’08, (Institute of Modern Physics, Chinese Academy of Sciences, National Natural Foundation of China), Lanzhou, China, Sept. (2008).
- Baba H., Ichihara T., Ohnishi T., Takeuchi S., Yoshida K., Watanabe Y., Ota S., and Shimoura S.: “The New DAQ System in RIKEN RIBF”, 2008 Nuclear Science Sym-

- Onishi T., Otsu H., Sakurai H., Shimoura S., Shinohara M., Sugimoto T., Takeuchi S., Tamaki M., Togano Y., and Yanagisawa Y.: “Invariant mass spectroscopy of  $^{13}\text{Be}$  and  $^{14}\text{Be}$  via the proton-induced breakup reactions of  $^{14}\text{Be}$ ”, 5th International Workshop on Direct Reaction with Exotic Beams (DREB2007), Wako, May–June (2007).
- Yamaguchi Y., Fujinawa T., Fukunishi N., Goto A., Ohnishi T., Sakurai H., Wakasugi M., Yano Y., Ozawa A., Arai I., Yasuda Y., Suzuki T., Yamaguchi T., Kikuchi T., and Ohtsubo T.: “Rare-RI ring project at RI Beam factory in RIKEN”, 15th International Conference on Electromagnetic Isotope Separators and Techniques Related to their Applications (EMIS2007), (GANIL , IN2P3/CNRS , DSM/CEA), Deauville, France, June (2007).
- Kameda D., Ueno H., Asahi K., Nagae D., Takemura M., Yoshimi A., Shimada K., Uchida M., Kijima G., Arai T., Takase K., Suda S., Inoue T., Murata J., Kawamura H., Haseyama T., Kobayashi Y., Watanabe H., and Ishihara M.: “Small electric quadrupole moment of  $^{32}\text{Al}$ : Drastic shape transition between  $^{32}\text{Al}$  and  $^{31}\text{Mg}$ ”, International Nuclear Physics Conference (INPC2007), (Science Council of Japan, RIKEN and others), Tokyo, June (Domestic Conference)
- Kondo Y., Nakamura T., Sato Y., Aoi N., Endo N., Fukuda N., Gomi T., Hashimoto Y., Ishihara M., Kawai S., Kitayama M., Kobayashi T., Matsuda Y., Matsui N., Motobayashi T., Nakabayashi T., Okumura T., Ong H., Onishi T., Otsu H., Sakurai H., Shimoura S., Shinohara M., Sugimoto T., Takeuchi S., Tamaki M., Togano Y., and Yanagisawa Y.: “Invariant mass spectroscopy of  $^{13}\text{Be}$  and  $^{14}\text{Be}$  via the proton-induced breakup reactions”, International Symposium & School on Frontiers and Perspectives of Nuclear and Hadron Physics (FPNH07), (Tokyo Institute of Technology), Tokyo, June (2007).
- Kameda D., Ueno H., Asahi K., Nagae D., Takemura M., Yoshimi A., Shimada K., Uchida M., Kijima G., Arai T., Takase K., Suda S., Inoue T., Murata J., Kawamura H., Haseyama T., Kobayashi Y., Watanabe H., and Ishihara M.: “Small electric quadrupole moment of  $^{32}\text{Al}$ ”, International Workshop on Nuclear Structure: New Pictures in the Extended Isospin Space (NS07), (Yukawa Institute for Theoretical Physics), Kyoto, June (2007).
- Nakajima S., Suzuki T., Yamaguchi T., Fujinawa T., Fukunishi N., Goto A., Ohnishi T., Sakurai H., Wakasugi M., Yamaguchi Y., Yano Y., Ozawa A., Arai I., Yasuda Y., Kikuchi T., and Ohtsubo T.: “New scheme for precision mass measurement of rare isotopes produced at RI beam factory”, 30th Mazurian Lakes Conference on Physics : Nuclear Physics and the Fundamental Processes, (IPJ ; University of Warsaw ; Pro-Physica), Piaski, Poland, Sept. (2007).
- Kondo Y., Motobayashi T., Sakurai H., Aoi N., Otsu H., Yanagisawa Y., Fukuda N., Takeuchi S., Ishihara M., Baba H., Gomi T., Imai N., Kubo T., Yoneda K., Nakamura T., Sato Y., Sugimoto T., Matsui N., Attukalathil V. M., Okumura T., Hashimoto Y., Nakabayashi T., Shinohara M., Miura M., Kobayashi T., Matsuda Y., Endo N., Kitayama M., Watanabe K., Yakushiji T., Togano Y., Kawai S., Hasegawa H., Onishi T., Ong H., Shimoura S., Tamaki M., Saito A., Bazin D. P., and Watanabe Y.: “Breakup reactions of  $^{14}\text{Be}$ ”, Future Prospects for Spectroscopy and Direct Reactions 2008, (Michigan State University), East Lansing, USA, Feb. (2008).
- Yamaguchi T., Fujinawa T., Fukunishi N., Goto A., Ohnishi T., Sakurai H., Wakasugi M., Yamaguchi Y., Yano Y., Arai I., Moriguchi T., Ozawa A., Yasuda Y., Nakajima S., Kuboki T., Suzuki T., Kikuchi T., and Ohtsubo T.: “Storage-ring mass spectrometry”, ETC Workshop on Mass Olympics, (GSI , FIAS), Trento, Italy, May (2008).
- Yoshimi A., Ueno H., Nagatomo T., Shimada K., Ichikawa Y., Kameda D., Sugimoto T., Sakurai H., Asahi K., Hasama Y., Takemura M., Kijima G., Nagae D., Uchida M., Arai T., Suda S., Takase T., Inoue T., Hatakeyama N., Kagami S., Murata J., and Kawamura H.: “Nuclear electromagnetic moments of neutron-rich Al isotopes”, Nuclear Structure 2008, (Michigan State University, NSCL at MSU), Michigan, USA, June (2008).
- Kawamura H., Murata J., Toyoda T., Seitabashi E., Nitta M., Hata M., Akiyama T., Ikeda Y., Ninomiya K., Kameda D., Nagae D., and Hirayama Y.: “The first T-violation experiment at KEK-TRIAC”, 24th Advanced Studies Institute :Symmetries and Spin (SPIN-Praha-2008), (Charles University in Prague, Faculty of Mathematics and Physics), Praha, Czech, July (2008).
- Yamaguchi T., Arai I., Ozawa A., Yasuda Y., Fujinawa T., Fukunishi N., Goto A., Hara K., Ohnishi T., Sakurai H., Wakasugi M., Yamaguchi Y., Yano Y., Kikuchi T., Suzuki T., and Ohtsubo T.: “Beam optics simulation for rare-RI ring at RI beam factory in RIKEN”, 7th International Conference on Nuclear Physics at Storage Rings STORI’08, (Institute of Modern Physics, Chinese Academy of Sciences, National Natural Foundation of China), Lanzhou, China, Sept. (2008).
- Yasuda Y., Ozawa A., Arai I., Fujinawa T., Fukunishi N., Goto A., Ohnishi T., Sakurai H., Wakasugi M., Yamaguchi Y., Yano Y., Suzuki T., Yamaguchi T., Kikuchi T., and Ohtsubo T.: “Present status of rare-RI ring project in RIKEN RIBF”, 7th International Conference on Nuclear Physics at Storage Rings STORI’08, (Institute of Modern Physics, Chinese Academy of Sciences, National Natural Foundation of China), Lanzhou, China, Sept. (2008).
- Baba H., Ichihara T., Ohnishi T., Takeuchi S., Yoshida K., Watanabe Y., Ota S., and Shimoura S.: “The New DAQ System in RIKEN RIBF”, 2008 Nuclear Science Sym-

鈴木賢, 山田一成, 山口英斉, 櫻井博儀: 日本物理学会 2008 年秋季大会, 山形, 9 月 (2008).

川村広和, 秋山岳伸, 石井哲朗, 池田友樹, 亀田大輔, 聖代橋悦子, 豊田健司, 長江大輔, 新田稔, 二宮一史, 秦麻記, 平山賀一, 光岡真一, 宮武宇也, 村田次郎, 渡辺裕: “TRIAC における偏極不安定核を用いた時間反転対称性破れの探索”, 第 5 回停止・低速不安定核ビームを用いた核分光研究会, (大阪大学), 豊中, 12 月 (2008).

市川雄一, 久保敏幸, 青井考, Banerjee S. R., Chakrabarti A., 福田直樹, 岩崎弘典, 久保野茂, 本林透, 中林彩, 中村隆司, 中尾太郎, 奥村俊文, 王恵仁, 大西健夫, 鈴木大介, 鈴木賢, 山田一成, 山口英斉, 櫻井博儀: 第 5 回停止・低速不安定核ビームを用いた核分光研究会, (大阪大学), 豊中, 12 月 (2008).

川村広和, 秋山岳伸, 秦麻記, 平山賀一, 池田友樹, 亀田大輔, 宮原直亮, 宮武宇也, 村田次郎, 中谷祐輔, 長江大輔, 二宮一史, 新田稔, 大西潤一, 聖代橋悦子, 豊田健司, 塚田和司, 渡辺裕: “TRIAC における偏極  $^8\text{Li}$  を用いた時間反転対称性破れの探索”, 日本物理学会第 64 回年次大会, 東京, 3 月 (2009).

## Computing and Network Team

### Publications

#### [Journal]

(Original Papers) \*Subject to Peer Review

Suzuki D., Iwasaki H., Ong H., Imai N., Sakurai H., Nakao T., Aoi N., Baba H., Bishop S., Ichikawa Y., Ishihara M., Kondo Y., Kubo T., Kurita K., Motobayashi T., Nakamura T., Okumura T., Onishi T., Ota S., Suzuki M., Takeuchi S., Togano Y., and Yanagisawa Y.: "Life-time measurements of excited states in  $^{17}\text{C}$ : Possible interplay between collectivity and halo effects", *Phys. Lett. B* **666**, 222–227 (2008). \*

#### [Book·Proceedings]

(Original Papers) \*Subject to Peer Review

Baba H., Ichihara T., Ohnishi T., Takeuchi S., Yoshida K., Watanabe Y., Ota S., and Shimoura S.: "The New DAQ System in RIKEN RIBF", 2008 IEEE Nuclear Science Symposium Conference Record, Dresden, Germany, 2008–10, IEEE, Dresden, pp. 1384–1386 (2008). \*

### Oral Presentations

(International Conference etc.)

Kondo Y., Motobayashi T., Sakurai H., Aoi N., Otsu H., Yanagisawa Y., Fukuda N., Takeuchi S., Ishihara M., Baba H., Gomi T., Imai N., Kubo T., Yoneda K., Nakamura T., Sato Y., Sugimoto T., Matsui N., Attukalathil V. M., Okumura T., Hashimoto Y., Nakabayashi T., Shinohara M., Miura M., Kobayashi T., Matsuda Y., Endo N., Kitayama M., Watanabe K., Yakushiji T., Togano Y., Kawai S., Hasegawa H., Onishi T., Ong H., Shimoura S., Tamaki M., Saito A., Bazin D. P., and Watanabe Y.: "Breakup reactions of  $^{14}\text{Be}$ ", Future Prospects for Spectroscopy and Direct Reactions 2008, (Michigan State University), East Lansing, USA, Feb. (2008).

Baba H., Ichihara T., Ohnishi T., Takeuchi S., Yoshida K., Watanabe Y., Ota S., and Shimoura S.: "The New DAQ System in RIKEN RIBF", 2008 Nuclear Science Symposium, Medical Imaging Conference and 16th Room Temperature Semiconductor Detector Workshop, Dresden, Germany, Oct. (2008).

## Detector Team

### Publications

#### [Journal]

(Original Papers) \*Subject to Peer Review

Iwasaki H., Motobayashi T., Sakurai H., Yoneda K., Gomi T., Aoi N., Fukuda N., Fulop Z., Futakami U., Gacsi Z., Higurashi Y., Imai N., Iwasa N., Kunibu M., Kubo T., Kurokawa M., Liu Z., Minemura T., Saito A., Serata M., Shimoura S., Takeuchi S., Watanabe Y., Yamada K., Yanagisawa Y., and Ishihara M.: “Quadrupole collectivity of  $^{28}\text{Ne}$  and the boundary of the island of inversion”, *Phys. Lett. B* **620**, 118–124 (2005). \*

Yamaguchi T., Suzuki T., Ohnishi T., Becker F., Fukuda M., Geissel H., Hosoi M., Janik R., Kimura K., Kuboki T., Mandel S., Matsuo M., Muenzenberg G., Nakajima S., Ohtsubo T., Ozawa A., Prochazka A., Shindo M., Sitar B., Strmen P., Suda T., Suemmerer K., Sugawara K., Szarka I., Takechi M., Takisawa A., Tanaka K., and Yamagami M.: “Nuclear matter radii of neutron-deficient Kr isotopes”, *Phys. Rev. C* **77**, 034315-1–034315-6 (2008). \*

### Oral Presentations

(International Conference etc.)

Wada M., Takamine A., Okada K., Sonoda T., Schury P. H., Lioubimov V., Yamazaki Y., Kanai Y., Kojima T., Kubo T., Iimura H., Katayama I., Ohtani S., Wollnik H., and Schuch R. H.: “Universal Slow RI-Beam Facility at RIKEN RIBF for Laser Spectroscopy of Short-Lived Nuclei”, International Conference on Laser Probing 2008 (LAP 2008), (Nagoya University), Nagoya, Oct. (2008).

(Domestic Conference)

久保木隆正, 小沢顕, 鈴木健, 山口貴之, 大坪隆, 山口由高, 金澤光高, 北川敦志, 小林圭, 佐藤眞二, 須田利美, 田中鐘信, 中島真平, 橋爪祐平, 森口哲朗, 安田裕介, 吉竹利織: “放医研 HIMAC に於ける TOF 検出器の分解能と荷電状態分析の測定”, 日本物理学会 2007 年春季大会, 八王子, 3 月 (2007).

久保木隆正, 山口貴之, 大坪隆, 小沢顕, 金澤光高, 北川敦志, 久保徹, 小林圭, 齊藤和哉, 佐藤眞二, 鈴木健, 須田利美, 田中鐘信, 中島真平, 橋爪祐平, 三浦宗賢, 森口哲朗, 安田裕介, 山口由高, 吉竹利織, 渡部亮太: “理研稀少 RI リングの為に TOF 検出器の開発”, 日本物理学会第 63 回年次大会, 東大阪, 3 月 (2008).

有吉誠一郎, 大谷知行, Dobroiu A., 佐藤広海, 田井野徹, 松尾宏, 清水裕彦: “超伝導トンネル接合素子を用いたテラヘルツ波検出器アレイの開発とイメージング応用”, 2008 年度春季低温工学・超電導学会, (低温工学会), 日野, 5 月 (2008).

有吉誠一郎, 大谷知行, Dobroiu A., 佐藤広海, 田井野徹, 松尾宏, 清水裕彦: “超伝導検出器 2 次元アレイを用いたテラヘルツイメージング”, 理研シンポジウム「第 7 回理研・分子研合同シンポジウム: エクストリームフォトニクス研究」, 和光, 5 月 (2008).

## User Liaison and Support Group

### Publications

#### [Journal]

(Original Papers) \*Subject to Peer Review

Otsu H., Kobayashi T., Matsuda Y., Kitayama M., Inafuku K., Ozawa A., Satou Y., Suda T., Yoshida K., and Sakaguchi H.: “Measurement of the H(38s,p’) reaction at forward angles including 0 degree”, Nucl. Phys. A **788**, 266c–270c (1997). \*

Takechi M., Fukuda M., Mihara M., Chinda T., Matsumasa T., Matsubara H., Nakashima Y., Matsuta K., Minamisono T., Koyama R., Shinosaki W., Takahashi M., Takisawa A., Ohtsubo T., Suzuki T., Momota S., Hatanaka K., Suda T., Sasaki M., Sato S., and Kitagawa A.: “Reaction cross-sections for stable nuclei and nucleon density distribution of proton drip-line nucleus 8B”, Eur. Phys. J. A **25**, No. s01, pp. 217–219 (2005). \*

Kannungo R., Chiba M., Abu-Ibrahim B., Adhikari S., Fang D., Iwasa N., Kimura K., Maeda K., Nishimura S., Ohnishi T., Ozawa A., Samanta C., Suda T., Suzuki T., Wang Q., Wu C., Yamaguchi Y., Yamada K., Yoshida A., Zheng T., and Tanihata I.: “A new view to the structure of 19C”, Eur. Phys. J. A **25**, No. s01, pp. 261–262 (2005). \*

Yamaguchi T., Ohnishi T., Suzuki T., Becker T., Fukuda M., Geissel H., Hosoi M., Janik R., Kelic A., Kimura K., Mandel S., Muenzenberg G., Nakajima S., Ohtsubo T., Ozawa A., Prochazka A., Shindo M., Sitar B., Strmen P., Suda T., Summerer K., Sugawara K., Szarka I., Takechi M., Takisawa A., and Tanaka K.: “Production cross sections of isotopes formed by fragmentation of similar to 1A (GeVKr)-Kr-80 beam”, Phys. Rev. C **74**, 044608-1–044608-5 (2006). \*

Fang D., Guo W., Ma C., Wang K., Yang T., Ma Y., Cai X., Shen W., Ren Z., Sun Z., Chen J., Tian W., Zhong C., Hosoi M., Izumikawa T., Kanungo R., Nakajima S., Ohnishi T., Ohtsubo T., Ozawa A., Suda T., Sugawara K., Suzuki T., Takisawa A., Tanaka K., Yamaguchi T., and Tanihata I.: “Examining the exotic structure of the proton-rich nucleus 23Al”, Phys. Rev. C **76**, 031601-1–031601-5 (2007). \*

Yamaguchi T., Suzuki T., Ohnishi T., Becker F., Fukuda M., Geissel H., Hosoi M., Janik R., Kimura K., Kuboki T., Mandel S., Matsuo M., Muenzenberg G., Nakajima S., Ohtsubo T., Ozawa A., Prochazka A., Shindo M., Sitar B., Strmen P., Suda T., Summerer K., Sugawara K., Szarka I., Takechi M., Takisawa A., Tanaka K., and Yamagami M.: “Nuclear matter radii of neutron-deficient Kr isotopes”, Phys. Rev. C **77**, 034315-1–034315-6 (2008). \*

### Oral Presentations

(International Conference etc.)

Suda T.: “A novel ion trap for electron scattering off short-lived unstable nuclei”, Gordon conference on photonuclear reactions 2008, Tilton, USA, Aug. (2008).

Suda T.: “Electron scattering from short-lived exotic nuclei using a novel internal target : SCRIT”, JLAB workshop on Lead Radius Experiment (PREX), Newport News, USA, Aug. (2008).

## User Support Office

### Publications

#### [Journal]

(Original Papers) \*Subject to Peer Review

Yamaguchi T., Suzuki T., Ohnishi T., Nummerer S., Becker F., Fukuda M., Geissel H., Hosoi M., Janike R., Kimura K., Mandal S., Munzenberg G., Nakajima S., Ohtsubo T., Ozawa A., Orochazka A., Shindo M., Strmen P., Suda T., Sugawara K., Szarka I., Takisawa A., Takechi M., and Tanaka K.: “Nuclear radii of neutron-deficient Kr isotopes studied via their interaction cross-sections at relativistic energies”, Nucl. Phys. A **787**, 471c–475c (2007). \*

Yoshida A., Suda T., Ohtsuki T., Yuki H., and Kubo T.: “Status and overview of production target for BigRIPS separator at RIKEN”, Nucl. Instrum. Methods Phys. Res. A **590**, 204–212 (2008). \*

### Oral Presentations

(International Conference etc.)

久保木隆正, 小沢顕, 鈴木健, 山口貴之, 大坪隆, 山口由高, 金澤光高, 北川敦志, 小林圭, 佐藤眞二, 須田利美, 田中鐘信, 中島真平, 橋爪祐平, 森口哲朗, 安田裕介, 吉竹利織: “放医研 HIMAC に於ける TOF 検出器の分解能と荷電状態分布の測定”, 日本物理学会 2007 年春季大会, 八王子, 3 月 (2007).

久保木隆正, 山口貴之, 大坪隆, 小沢顕, 金澤光高, 北川敦志, 久保徹, 小林圭, 斉藤和哉, 佐藤眞二, 鈴木健, 須田利美, 田中鐘信, 中島真平, 橋爪祐平, 三浦宗賢, 森口哲朗, 安田裕介, 山口由高, 吉竹利織, 渡部亮太: “理研稀少 RI リングの為に TOF 検出器の開発”, 日本物理学会第 63 回年次大会, 東大阪, 3 月 (2008).

## Experiment Support Team

### Publications

#### [Book・Proceedings]

(Others)

Okuno H., Fukunishi N., Fujinawa T., Goto A., Higurashi Y., Ikezawa E., Kamigaito O., Kase M., Nakagawa T., Ohnishi J., Sato Y., Yano Y., and Ostroumov P.: “Heavy Ion Accelerators for RIKEN RI Beam Factory and Upgrade Plans”, 42nd ICFA Advanced Beam Dynamics Workshop on High-Intensity, High-Brightness Hadron Beams, Nashville, USA, 2008-8, ICFA, , p. (2009).

### Oral Presentations

(International Conference etc.)

Hasebe H., Ryuto H., Fukunishi N., Goto A., Kase M., and Yano Y.: “Polymer coating method developed for carbon stripper foils”, 23rd World Conference of the INTDS, (High Energy Accelerator Research Organization (KEK)), Tsukuba, Oct. (2006).

Okuno H., Fukunishi N., Fujinawa T., Goto A., Higurashi Y., Ikezawa E., Kamigaito O., Kase M., Nakagawa T., Ohnishi J., Sato Y., Yano Y., and Ostroumov P.: “Heavy Ion Accelerators for RIKEN RI Beam Factory and Upgrade Plans”, 42nd ICFA Advanced Beam Dynamics Workshop on High-Intensity, High-Brightness Hadron Beams (HB2008), (Oakridge National Laboratory), Nashville, USA, Aug. (2008).

(Domestic Conference)

藤縄雅: “理研 RIBF の交流電源の設計と建設”, 第 5 回日本加速器学会年会/第 33 回リニアック技術研究会, (日本加速器学会), 東広島, 8 月 (2008).

## Industrial Cooperation Team

### Publications

#### [Journal]

(Original Papers) \*Subject to Peer Review

竹市博臣, 寺尾敦, 竹内文也, 豊澤悠子, 小山幸子: “m 系列変調法を用いた談話理解評価に関係する脳領域の fMRI による同定”, 認知神経科学 **10**, No. 1, pp. 99–108 (2008). \*

(Review)

神原正: “理研 RI ビームファクトリー利用の現状”, 放射線と産業, No. 117, pp. 26–30 (2008).

竹市博臣, 小山幸子, 松本秀彦, 諸富隆: “ランダムプローブ法と談話理解の脳内機構”, 臨床脳波 **50**, No. 9, pp. 524–530 (2008).

(Technical Document)

井上康之, 小川昭利, 荒井宏太, 松本秀彦, 豊巻敦人, 竹市博臣, 大森隆司, 小山幸子, 諸富隆, 北崎充晃: “統計的識別による聴覚誘発電位の特徴分析”, 信学技報, No. NC2007-94(2008-1), pp. 43–48 (2008).

### Oral Presentations

(International Conference etc.)

Takeichi H., Koyama S., Foster B. L., and Liley D.: “A Coherence analysis of EEG response to speech modulated by m-sequence”, Cognitive Neuroscience Society (CNS) 2008 Annual Meeting, San Francisco, USA, Apr. (2008).

Inoue Y., Ogawa A., Arai K., Matsumoto H., Toyomaki A., Takeichi H., Omori T., Koyama S., Morotomi T., and Kitazaki M.: “Feature Analysis of Event-related Brain Potentials by Statistical Classification: Application of Naive Bayes Method and Principal Component Analysis to Predicting Auditory Stimuli”, 14th Annual Meeting of the Organization for Human Brain Mapping, Melbourne, Australia, June (2008).

Takeuchi F., Takeichi H., Koyama S., and Cichocki A.: “A new technique for accessing verbal comprehension using magnetoencephalography”, 16th International Conference on Biomagnetism (BIOMAG 2008), (Japan Biomagnetism and Bioelectromagnetics Society), Sapporo, Aug. (2008).

Koyama S., Inoue Y., Toyomaki A., Toyosawa Y., Ogawa A., Takeuchi F., Takeichi H., Omori T., Kitazaki M., and Kuriki S.: “Evoked magnetic responses to short temporal gaps between sounds”, 16th International Conference on Biomagnetism (BIOMAG 2008), (Japan Biomagnetism and Bioelectromagnetics Society), Sapporo, Aug. (2008).

Takeichi H., Dumoulin S. O., Wandell B. A., Masuda Y., Shigemasu H., Kitazaki M., and Nakadomari S.: “Different responses of human V1 and V2 to stereoscopic stimulus: an application of visual field mapping”, 38th Annual Meeting of Society for Neuroscience (Neuroscience 2008), Washington DC, USA, Nov. (2008).

Koyama S., Takeichi H., Gunji A., Kaga M., Cichocki A.,

Okada H., and Omori T.: “EEG responses associated with verbal comprehension in school age children: A new technique using m-sequence modulation”, 38th Annual Meeting of Society for Neuroscience (Neuroscience 2008), Washington DC, USA, Nov. (2008).

Tamura T., Gunji A., Koyama S., Kitazaki M., Shigemasu H., Matsuzaki N., and Takeichi H.: “Speech-related rhythmic activities in the motor cortex”, 38th Annual Meeting of Society for Neuroscience (Neuroscience 2008), Washington DC, USA, Nov. (2008).

Takeichi H., Koyama S., Foster B. L., and Liley D.: “A coherence analysis of independent-component electroencephalogram”, 10th RIES-Hokudai International Symposium on aya, (RIES, Hokkaido University), Sapporo, Dec. (2008).

(Domestic Conference)

田村健, 軍司敦子, 北崎充晃, 繁舩博昭, 松崎直幸, 竹市博臣, 小山幸子: “EEG rhythm changes associated with speech-related movements”, 第 31 回日本神経科学大会 (Neuroscience 2008), 東京, 7 月 (2008).

竹市博臣, 小山幸子: “Volterra Series Analysis of Scalp EEG Responses to Spoken Sentences Modulated by M-Sequence”, 第 31 回日本神経科学大会 (Neuroscience 2008), 東京, 7 月 (2008).

竹市博臣, 寺尾敦, 竹内文也, 小山幸子, 室橋春光: “劣化 (m 系列変調) 音声に対する fMRI 応答”, 日本心理学会第 72 回大会, 札幌, 9 月 (2008).

竹市博臣, 小山幸子, 寺尾敦, 竹内文也, 豊澤悠子, 室橋春光: “M 系列変調劣化音声を用いた談話理解の神経機構のニューロイメージング”, 日本音響学会 2008 年秋季研究発表会, 福岡, 9 月 (2008).

## Radiation Laboratory

### Publications

#### [Journal]

(Original Papers) \*Subject to Peer Review

- Gomi T., Motobayashi T., Yoneda K., Kanno S., Aoi N., Ando Y., Baba H., Demichi K., Fulop Z., Futakami U., Hasegawa H., Higurashi Y., Ieki K., Imai N., Iwasa N., Iwasaki H., Kubo T., Kubono S., Kunibu M., Matsuyama Y., Michimasa S., Minemura T., Murakami H., Nakamura T., Saito A., Sakurai H., Serata M., Shimoura S., Sugimoto T., Takeshita E., Takeuchi S., Ue K., Yamada K., Yanagisawa Y., Yoshida A., and Ishihara M.: “Coulomb Dissociation of  $^{23}\text{Al}$ ”, *Prog. Theor. Phys. Suppl.*, No. 146, pp. 557–558 (2002). \*
- Kanno S., Gomi T., Motobayashi T., Yoneda K., Aoi N., Ando Y., Baba H., Demichi K., Fulop Z., Futakami U., Hasegawa H., Higurashi Y., Ieki K., Imai N., Iwasa N., Iwasaki H., Kubo T., Kubono S., Kunibu M., Matsuyama Y., Michimasa S., Minemura T., Murakami H., Nakamura T., Saito A., Sakurai H., Serata M., Shimoura S., Sugimoto T., Takeshita E., Takeuchi S., Ue K., Yamada K., Yanagisawa Y., Yoshida A., and Ishihara M.: “Coulomb Excitation of  $^{24}\text{Si}$ ”, *Prog. Theor. Phys. Suppl.*, No. 146, pp. 575–576 (2002). \*
- Matsuyama Y., Motobayashi T., Shimoura S., Minemura T., Saito A., Baba H., Akiyoshi H., Aoi N., Ando Y., Gomi T., Higurashi Y., Ieki K., Imai N., Iwasa N., Iwasaki H., Kanno S., Kubono S., Kunibu M., Michimasa S., Murakami H., Nakamura T., Sakurai H., Serata M., Takeshita E., Takeuchi S., Teranishi T., Ue K., Yamada K., and Yanagisawa Y.: “Inelastic Scattering of  $^{12}\text{Be}$  with  $^4\text{He}$ ”, *Prog. Theor. Phys. Suppl.*, No. 146, pp. 593–594 (2002). \*
- Gomi T., Motobayashi T., Yoneda K., Kanno S., Aoi N., Ando Y., Baba H., Demichi K., Fulop Z., Futakami U., Hasegawa H., Higurashi Y., Ieki K., Imai N., Iwasa N., Iwasaki H., Kubo T., Kubono S., Kunibu M., Matsuyama Y., Michimasa S., Minemura T., Murakami H., Nakamura T., Saito A., Sakurai H., Serata M., Shimoura S., Sugimoto T., Takeshita E., Takeuchi S., Ue K., Yamada K., Yanagisawa Y., Yoshida A., and Ishihara M.: “Study of the  $^{22}\text{Mg}(p, \gamma)^{23}\text{Al}$  Reaction with the Coulomb-Dissociation Method”, *Nucl. Phys. A* **718**, 508c–509c (2003). \*
- Iwasa N., Motobayashi T., Sakurai H., Akiyoshi H., Ando Y., Aoi N., Baba H., Fukuda N., Fulop Z., Futakami U., Gomi T., Higurashi Y., Ieki K., Iwasaki H., Kubo T., Kubono S., Kinugawa H., Kumagai H., Kunibu M., Michimasa S., Minemura T., Murakami H., Sagara K., Saito A., Shimoura S., Takeuchi S., Yanagisawa Y., Yoneda K., and Ishihara M.: “In-beam  $\gamma$  spectroscopy of  $^{34}\text{Si}$  with deuteron inelastic scattering using reverse kinematics”, *Phys. Rev. C* **67**, 064315-1–064315-4 (2003). \*
- Morishima T. and Shimizu H.: “Hamiltonian of a free neutron in curved spacetime on the Earth”, *Nucl. Instrum. Methods Phys. Res. A* **529**, 187–189 (2004). \*
- Gomi T., Motobayashi T., Ando Y., Aoi N., Baba H., Demichi K., Elekes Z., Fukuda N., Fulop Z., Futakami U., Hasegawa H., Higurashi Y., Ieki K., Imai N., Ishihara M., Ishikawa K., Iwasa N., Iwasaki H., Kanno S., Kondo Y., Kubo T., Kubono S., Kunibu M., Kurita K., Matsuyama Y., Michimasa S., Minemura T., Miura M., Murakami H., Nakamura T., Notani M., Ota S., Saito A., Sakurai H., Serata M., Shimoura S., Sugimoto T., Takeshita E., Takeuchi S., Togano Y., Ue K., Yamada K., Yanagisawa Y., Yoneda K., and Yoshida A.: “Study of the Stellar  $^{22}\text{Mg}(p, \gamma)^{23}\text{Al}$  Reaction using the Coulomb-Dissociation Method”, *Nucl. Phys. A* **734**, E77–E79 (2004).
- Saito A., Shimoura S., Takeuchi S., Motobayashi T., Minemura T., Matsuyama Y., Baba H., Akiyoshi H., Ando Y., Aoi N., Fulop Z., Gomi T., Higurashi Y., Hirai M., Ieki K., Imai N., Iwasa N., Iwasaki H., Iwata Y., Kanno S., Kobayashi H., Kubono S., Kunibu M., Kurokawa M., Liu Z., Michimasa S., Nakamura T., Ozawa A., Sakurai H., Serata M., Takeshita E., Teranishi T., Ue K., Yamada K., Yanagisawa Y., and Ishihara M.: “Molecular states in neutron-rich beryllium isotopes”, *Nucl. Phys. A* **738**, 337–341 (2004). \*
- Gomi T., Motobayashi T., Ando Y., Aoi N., Baba H., Demichi K., Elekes Z., Fukuda N., Fulop Z., Futakami U., Hasegawa H., Higurashi Y., Ieki K., Imai N., Ishihara M., Ishikawa K., Iwasa N., Iwasaki H., Kanno S., Kondo Y., Kubo T., Kubono S., Kunibu M., Kurita K., Matsuyama Y., Michimasa S., Minemura T., Miura M., Murakami H., Nakamura T., Notani M., Ota S., Saito A., Sakurai H., Serata M., Shimoura S., Sugimoto T., Takeshita E., Takeuchi S., Togano Y., Ue K., Yamada K., Yanagisawa Y., Yoneda K., and Yoshida A.: “Coulomb dissociation experiment for explosive hydrogen burning: study of the  $^{22}\text{Mg}(p, \gamma)^{23}\text{Al}$  reaction”, *J. Phys. G* **31**, S1517–S1521 (2005).
- Heuser J.: “A Silicon VertexTracker upgrade for the PHENIX experiment at RHIC”, *Nucl. Instrum. Methods Phys. Res. A* **546**, 60–66 (2005).
- Makii H., Mishima K., Segawa M., Sano E., Ueda H., Shima T., Nagai Y., Igashira M., and Osaki T.: “Measurement system of the  $\gamma$ -ray angular distributions of the  $^{12}\text{C}(\alpha, \gamma)^{16}\text{O}$  reaction”, *Nucl. Instrum. Methods Phys. Res. A* **547**, 411–423 (2005). \*
- Togano Y., Gomi T., Motobayashi T., Ando Y., Aoi N., Baba H., Demichi K., Elekes Z., Fukuda N., Fulop Z., Futakami U., Hasegawa H., Higurashi Y., Ieki K., Imai N., Ishihara M., Ishikawa K., Iwasa N., Iwasaki H., Kanno S., Kondo Y., Kubo T., Kubono S., Kunibu M., Kurita K., Matsuyama Y., Michimasa S., Minemura T., Miura M., Murakami H., Nakamura T., Notani M.,

- Ota S., Saito A., Sakurai H., Serata M., Shimoura S., Sugimoto T., Takeshita E., Takeuchi S., Ue K., Yamada K., Yanagisawa Y., Yoneda K., and Yoshida A.: “Study of  $^{26}\text{Si}(p, \gamma)^{27}\text{P}$  reaction using Coulomb dissociation method”, Nucl. Phys. A **758**, 182c–185c (2005). \*
- Makii H., Nagai Y., Shima T., Segawa M., Ueda H., Masaki T., Mishima K., Igashira M., Osaki T., and Okabe S.: “Measurement of the  $^{12}\text{C}(\alpha, \gamma)^{16}\text{O}$  reaction cross section using pulsed  $\alpha$  beams”, Nucl. Phys. A **758**, 371c–374c (2005). \*
- Togano Y., Gomi T., Motobayashi T., Ando Y., Aoi N., Baba H., Demichi K., Elekes Z., Fukuda N., Fulop Z., Futakami U., Hasegawa H., Higurashi Y., Ieki K., Imai N., Ishihara M., Ishikawa K., Iwasa N., Iwasaki H., Kanno S., Kondo Y., Kubo T., Kubono S., Kunibu M., Kurita K., Matsuyama Y., Michimasa S., Minemura T., Miura M., Murakami H., Nakamura T., Notani M., Ota S., Saito A., Sakurai H., Serata M., Shimoura S., Sugimoto T., Takeshita E., Takeuchi S., Ue K., Yamada K., Yanagisawa Y., Yoneda K., and Yoshida A.: “Study of the  $^{26}\text{Si}(p, \gamma)^{27}\text{P}$  reaction through Coulomb dissociation of  $^{27}\text{P}$ ”, Eur. Phys. J. A **27**, No. s01, pp. 233–236 (2006). \*
- Gomi T., Motobayashi T., Ando Y., Aoi N., Baba H., Demichi K., Elekes Z., Fukuda N., Fulop Z., Futakami U., Hasegawa H., Higurashi Y., Ieki K., Imai N., Ishihara M., Ishikawa K., Iwasa N., Iwasaki H., Kanno S., Kondo Y., Kubo T., Kubono S., Kunibu M., Kurita K., Matsuyama Y., Michimasa S., Minemura T., Miura M., Murakami H., Nakamura T., Notani M., Ota S., Saito A., Sakurai H., Serata M., Shimoura S., Sugimoto T., Takeshita E., Takeuchi S., Togano Y., Ue K., Yamada K., Yanagisawa Y., Yoneda K., and Yoshida A.: “Coulomb Dissociation of  $^{23}\text{Al}$  for the stellar  $^{22}\text{Mg}(p, \gamma)^{23}\text{Al}$  reaction”, Nucl. Phys. A **758**, 761c–764c (2006).
- Akiba Y. and PHENIX C.: “Probing the properties of dense partonic matter at RHIC”, Nucl. Phys. A **774**, 403–408 (2006). \*
- Ladygin V., Uesaka T., Saito T., Hatano M., Isupov Y., Kato H., Ladygina N., Maeda Y., Malakhov A., Nishikawa J., Ohnishi T., Okumura H., Reznikov S., Sakai H., Sakamoto N., Sakoda S., Saito T., Sekiguchi K., Suda K., Tamii A., Uchigashima N., and Yako K.: “Tensor Analyzing Power  $T_{20}$  of the  $dd \rightarrow ^3\text{He}$  and  $dd \rightarrow ^3\text{He}$  Reactions at Zero Angle for Energies 140, 200, and 270 MeV”, Phys. At. Nucl. **69**, 1271–1278 (2006). \*
- Naitou S., Nagai Y., Shima T., Makii H., Mishima K., Tamura K., Toyokawa H., Ohgaki H., Golak J., Shibinski R., Witala H., Glockle W., Nogga A., and Kamada H.: “New data for total  $^3\text{He}(\gamma, p)\text{D}$  and  $^3\text{He}(\gamma, pp)\text{n}$  cross sections compared to current theory”, Phys. Rev. C **73**, No. 3, pp. 034003-1–034003-10 (2006). \*
- Okada H., Bunce G. M., Jinnouchi O., Nakagawa I., Saito N., Alekseev I., Bravar A., Dhawan S., Eyser K. O., Gill R., Haeberli W., Huang H., Makdisi Y. I., Nass A., Stephenson E., Sviridia D., Wise T., Wood J., and Zelenski A.: “Measurements of single and double spin asymmetry in pp elastic scattering in the CNI region with polarized hydrogen gas jet target”, AIP Conf. Proc. **915**, 681–684 (2007).
- Huang H., Ahrens L. A., Bai M., Bravar A., Brown K., Courant E. D., Gardner C. J., Glenn J. W., Lin F., Luccio A. U., MacKay W. W., Okamura M., Ptitsyn V., Roser T., Takano J., Tepikian S., Tsoupas N., Wood J., Yip K., Zelenski A., and Zeno K.: “Polarized proton acceleration in the AGS with two helical partial snakes”, AIP Conf. Proc. **915**, 900–903 (2007). \*
- Takano J., Ahrens L. A., Bai M., Brown K., Courant E. D., Gardner C. J., Glenn J. W., Hattori T., Huang H., Lin F., Luccio A. U., MacKay W. W., Okamura M., Roser T., Tepikian S., Tsoupas N., Yip K., Zelenski A., and Zeno K.: “Multiple partial siberian snakes in the AGS”, AIP Conf. Proc. **915**, 904–907 (2007). \*
- Blumlein J. and Kawamura H.: “Universal higher order singlet QED corrections to unpolarized lepton scattering”, Eur. Phys. J. C **51**, 317–333 (2007). \*
- Iida K. and Fukushima K.: “Instability of a Gapless Color Superconductor with Respect to Inhomogeneous Fluctuations”, Nucl. Phys. A **785**, 118c–121c (2007). \*
- Kawamura H., Tanaka K., and Kodaira J.: “Soft gluon corrections to double transverse-spin asymmetries for small-Q(T) dilepton production at RHIC and J-PARC”, Nucl. Phys. B **777**, 203–225 (2007). \*
- Yoon C., Akiakawa H., Aoki K., Fukao Y., Funahashi H., Hayata M., Imai K., Miwa K., Okada H., Saito N., Sato H., Shoji K., Takahashi H., Taketani K., Asai J., Kurosawa M., Ieiri M., Hayakawa T., Kishimoto T., Sato A., Shimizu Y., Yamamoto K., Yoshida T., Hibi T., Nakazawa K., Ahn J., Choi B., Kim S., Kim S., Park B., Park I., Song J., Yoon C., Tanida K., and Oonishi A.: “Search for the  $H$ -dibaryon resonance in  $^{12}\text{C}(K^-, K^+\Lambda\Lambda X)$ ”, Phys. Rev. C **75**, 022201-1–022201-5 (2007). \*
- Makii H., Nagai Y., Mishima K., Segawa M., Shima T., and Igashira M.: “Neutron-induced reactions using a  $\gamma$ -ray detector in a  $^{12}\text{C}(\alpha, \gamma)^{16}\text{O}$  reaction study”, Phys. Rev. C **76**, No. 2, pp. 022801-1–022801-5 (2007). \*
- Fukushima K.: “Initial fields and instabilities in the classical model of relativistic heavy-ion collisions”, Phys. Rev. C **76**, 021902-1–021902-5 (2007). \*
- Bozzi G., Jager B., Oleari C., and Zeppenfeld D.: “Next-to-leading order QCD corrections to  $W^+ Z$  and  $W^- Z$  production via vector-boson fusion”, Phys. Rev. D **75**, 073004-1–073004-7 (2007). \*
- Fukushima K. and Iida K.: “Larkin-Ovchinnikov-Fulde-Ferrell state in two-color quark matter”, Phys. Rev. D **76**, 054004-1–054004-10 (2007). \*
- Blum T. C., Doi T., Hayakawa M., Izubushi T.,

- and Yamada N.: “Determination of Light Quark Masses From the Electromagnetic Splitting of Pseudoscalar Meson Masses Computed with Two Flavors of Domain Wall Fermions”, *Phys. Rev. D* **76**, 114508-1–114508-16 (2007). \*
- Huang H., Ahrens L., Bai M., Brown K., Courant E. D., Gardner C., Glenn J. W., Lin F., Luccio A. U., MacKay W. W., Okamura M., Ptitsyn V., Roser T., Takano J., Tepikian S., Tsoupas N., Zelenski A., and Zeno K.: “Overcoming depolarizing resonances with dual helical partial siberian snakes”, *Phys. Rev. Lett.* **99**, 154801-1–154801-4 (2007). \*
- Lin F., Ahrens L. A., Bai M., Brown K., Courant E. D., Gardner C., Glenn J. W., Huang H., Lee S. Y., Luccio A., MacKay W. W., Ptitsyn V., Roser T., Takano J., Tepikian S., Tsoupas N., Zelenski A., and Zeno K.: “Exploration of horizontal intrinsic spin resonances with two partial siberian snakes”, *Phys. Rev. Spec. Top.: Accel. Beams* **10**, No. 4, pp. 044001-1–044001-6 (2007). \*
- Oku T., Yamada S., Shinohara T., Suzuki J., Mishima K., Hirota K., Sato H., and Shimiuzu H. M.: “Highly polarized cold neutron beam obtained by using a quadrupole magnet”, *Physica B* **397**, 188–191 (2007). \*
- Kawamura H., Tanaka K., and Kodaira J.: “Transversely Polarized Drell-Yan Process and Soft Gluon Resummation in QCD”, *Prog. Theor. Phys.* **118**, No. 4, pp. 581–656 (2007). \*
- Okada H., Bunce G. M., Jinnouchi O., Nakagawa I., Saito N., Alekseev I., Bravar A., Dhawan S., Eyser K. O., Gill R., Haeberli W., Huang H., Makdisi Y. I., Nass A., Stephenson E., Sviridia D., Wise T., Wood J., and Zelenski A.: “Absolute polarimetry at RHIC”, *AIP Conf. Proc.* **980**, 370–379 (2008).
- Ladygin V., Uesaka T., Saito T., Janek M., Kiselev A., Kurilkin A., Vasiliev A., Hatano M., Isupov Y., Kato H., Ladygina N., Maeda Y., Malakhov A., Nishikawa J., Ohnishi T., Okamura H., Reznikov S., Sakai H., Sakoda S., Sakamoto N., Satou Y., Sekiguchi K., Suda K., Tamii A., Uchigashima N., and Yako K.: “Analyzing powers in the  $dd \rightarrow {}^3\text{He}({}^3\text{He})$  reactions at intermediate energies”, *AIP Conf. Proc.* **1011**, 235–240 (2008). \*
- Kurilkin A., Saito T., Ladygin V., Uesaka T., Vasiliev T., Janek M., Hatano M., Isupov Y., Kato K., Ladygina N., Maeda Y., Malakhov A., Nishikawa J., Ohnishi T., Okamura H., Reznikov S., Sakai H., Sakamoto N., Sakoda S., Satou Y., Sekiguchi K., Suda K., Tamii A., Uchigashima N., and Yako K.: “Measurement of the vector  $A_y$  and tensor  $A_{yy}$ ,  $A_{xx}$ ,  $A_{xz}$  analyzing powers for the  $dd \rightarrow {}^3\text{He}p$  reaction at 200 MeV”, *Eur. Phys. J. Special Topics* **162**, 133–136 (2008). \*
- Kiselev A., Ladygin V., Uesaka T., Vasiliev A., Janek M., Saito T., Hatano M., Isupov Y., Kato H., Ladygina N., Maeda Y., Malakhov A., Nishikawa J., Ohnishi T., Okamura H., Reznikov S., Sakai H., Sakamoto N., Sakoda S., Satou Y., Sekiguchi K., Suda K., Tamii A., Uchigashima N., and Yako K.: “Analyzing powers in the  ${}^{12}\text{C}(\vec{d}, p){}^{13}\text{C}$  reaction at the energy  $T_d = 270$  MeV”, *Eur. Phys. J. Special Topics* **162**, 143–146 (2008). \*
- Sakuma F., Enyo H., Fukao Y., Funahashi H., Hamagaki H., Kitaguchi M., Miwa K., Murakami T., Naruki M., Ozawa K., Sekimoto M., Tabaru T., Togawa M., Yokkaichi S., Chiba J., Kanda H., Ieiri M., Ishino M., Mihara S., Miyashita T., Muto R., Nakura T., Sasaki O., Tanaka K., Yamada S., and Yoshimura Y.: “Partial decay widths of the phi into  $e+e-$  and  $K+K-$  pairs in 12 GeV p+A reactions at KEK-PS E325”, *Mod. Phys. Lett. A* **23**, No. 27/30, pp. 2401–2404 (2008). \*
- Miwa K., Dairaku S., Nakajima D., Ajimura S., Arvieux J., Fujimura H., Fujioka H., Fukuda T., Funahashi H., Hayata M., Hicks K., Imai K., Ishimoto S., Kameyama T., Kamigaito S., Kinoshita S., Koike T., Ma Y., Maruta T., Miura Y., Miyabe M., Nagae T., Nakano T., Nakazawa K., Naruki M., Noumi H., Niiyama M., Saito N., Sato Y., Sawada S., Seki Y., Sekimoto M., Senzaka K., Shirotori K., Shoji K., Suzuki S., Takahashi H., Takahashi T., Takahashi T., Tamura H., Tanaka N., Tanida K., Toyoda A., Watanabe T., Yosoi M., and Zavislak R.: “Search for  $\Theta^+$  via the  $K^+p \rightarrow \pi^+X$  reaction with a 1.2 GeV/c  $K^+$  beam”, *Phys. Rev. C* **77**, 045203-1–045203-10 (2008). \*
- Suzuki T., Ishiguro K., Koma Y., and Sekido T.: “Gauge-independent Abelian mechanism of color confinement in gluodynamics”, *Phys. Rev. D* **77**, 034502-1–034502-5 (2008). \*
- Lin H., Blum T., Ohta S., Sasaki S., and Yamazaki T.: “Nucleon structure with two flavors of dynamical domain-wall fermions”, *Phys. Rev. D* **78**, 014505-1–014505-29 (2008). \*
- Fukushima K. and Warringa H. J.: “Color Superconducting Matter in a Magnetic Field”, *Phys. Rev. Lett.* **100**, 032007-1–032007-4 (2008). \*
- Yamazaki T., Aoki Y., Blum T. C., Lin H., Lin M., Ohta S., Sasaki S., Tweedie R. J., and Zanotti J. M.: “Nucleon Axial Charge in (2+1)-Flavor Dynamical-Lattice QCD with Domain-Wall Fermions”, *Phys. Rev. Lett.* **100**, 171602-1–171602-4 (2008). \*
- Toyoshima A., Haba H., Tsukada K., Asai M., Akiyama K., Goto S., Ishii Y., Nishinaka I., Sato T., Nagame Y., Sato W., Tani Y., Hasegawa H., Matsuo K., Saika D., Kitamoto Y., Shinohara A., Ito M., Saito J., Kudo H., Yokoyama A., Sakama M., Sueki K., Oura Y., Nakahara H., Schaedel M., Bruechle W., and Kratz J. V.: “Hexafluoro complex of rutherfordium in mixed HF/HNO<sub>3</sub> solutions”, *Radiochim. Acta* **96**, 125–134 (2008). \*
- (Review)
- Akiba Y.: “Experimental Study of Dense Matter at RHIC”, *Prog. Theor. Phys. Suppl.*, No. 174, pp. 88–102 (2008).
- (Others)
- Bhang H. C., Ajimura S., Aoki K., Banu A., Fukuda T.,

Hashimoto O., Hwang J., Kameoka S., Kang B., Kim E., Kim J., Kim M., Maruta T., Miura Y., Miyake Y., Nagae T., Nakamura M., Nakamura S. N., Noumi H., Okada S., Okayasu Y., Ota H., Park H., Saha P. K., Sato Y., Sekimoto M., Shin S., Takahashi T., Tamura H., Tanida K., Toyota A., Tsukada K., Watanabe T., and Yim H.: “The quenching of nucleon yields in the nonmesonic weak decay of  $\Lambda$ -hypernuclei and the three-body weak decay process”, *Eur. Phys. J. A* **33**, No. 3, pp. 259–263 (2007).

Murata J., Akiyama T., Hata M., Hirayama Y., Ikeda Y., Ishii T., Kameda D., Kawamura H., Mitsuoka S., Miyatake H., Nagae D., Ninomiya K., Nitta M., Seitabashi E., and Toyoda T.: “R&D for a test of time reversal symmetry experiment using polarized nuclei”, *JAEA-Review* **2008-054**, 58–59 (2008).

### [Book-Proceedings]

(Original Papers) \*Subject to Peer Review

Kawamura H., Tanaka K., and Kodaira J.: “Soft gluon resummation and a novel asymptotic formula for double-spin asymmetries in dilepton production at small transverse momentum”, Munich 2007, Deep-inelastic scattering, vol. 1, Munich, 2007–4, Verlag Deutsches Elektronen-Synchrotron, Munich, pp. 615–618 (2007).

Tamura J., Okamura M., and Kanesue T.: “Use of solidified gas target to laser ion source.”, *Proceedings of 22nd Biennial Particle Accelerator Conference (PAC07)*, IEEE, Piscataway, pp. 1535–1537 (2007).

Baba H., Ichihara T., Ohnishi T., Takeuchi S., Yoshida K., Watanabe Y., Ota S., and Shimoura S.: “The New DAQ System in RIKEN RIBF”, 2008 IEEE Nuclear Science Symposium Conference Record, Dresden, Germany, 2008–10, IEEE, Dresden, pp. 1384–1386 (2008). \*

(Technical Document)

Ariyoshi S., Otani C., Dobroiu A., Sato H., Taino T., Matsuo H., and Shimizu H.: “Terahertz Imaging with a Two-dimensional Array Detector Based on Superconducting Tunnel Junctions”, *Proceedings of 33rd International Conference on Infrared, Millimeter, and Terahertz Waves (IRMMW-THz 2008)*, Pasadena, USA, 2008–9, California Institute of Technology, Pasadena, p. 1681 (2008).

### Oral Presentations

(International Conference etc.)

Heuser J., Enyo H., Onishi H., and NA60 C.: “The NA60 experiment: results and perspectives”, 8th Conference on the Intersections of Particle and Nuclear Physics (CIPANP 2003), New York, USA, May (2003).

Akiba Y.: “Single- and Dileptons from Open Charm at RHIC”, *Electromagnetic Probes of Hot and Dense Matter*, (ECT\*, Trento, Italy), Trento, Italy, June (2005).

Akiba Y. and PHENIX C.: “Probing the properties of dense partonic matter at RHIC”, 18th International

Conference on Ultra-Relativistic Nucleus-Nucleus Collisions (Quark Matter 2005), (Conseil Européen pour la Recherche Nucleaire and others), Budapest, Hungary, Aug. (2005).

Taketani K., Funahashi H., Seki Y., Hino M., Kitaguchi M., Maruyama R., Otake Y., and Shimizu H.: “Development of Mach-Zehnder Interferometer and “coherent beam steering” technique for cold neutron”, 8th International Symposium on Foundations of Quantum Mechanics in the Light of New Technology (ISQM-Tokyo’05), (Advanced Research Laboratory Hitachi Ltd.), Hatoyama-cho, Saitama Pref., Aug. (2005).

Kawamura S., Kaneko J., Otake Y., Fujimoto H., Fujita F., Sawamura T., Pavel M., and Furusaka M.: “Deformation experiment of piezoelectric single-crystals for neutron-optical-devices”, *International Conference on Neutron Scattering (ICNS2005)*, (Australian Neutron Beam User Group), Sydney, Australia, Nov.–Dec. (2005).

Mishima K., Hirota K., Shimizu H., Shinohara T., Suzuki J., Yamada S., Oku T., Sato H., and Morishima T.: “Development of measurement system of neutron  $\beta$  decay”, *International Conference on Neutron Scattering (ICNS2005)*, (ANSTO), Sydney, Australia, Nov.–Dec. (2005).

Taketani K., Funahashi H., Seki Y., Hino M., Kitaguchi M., Otake Y., and Shimizu H.: “Moire fringes of cold neutron with large divergence angle”, *International Conference on Neutron Scattering (ICNS2005)*, (Australian Neutron Beam users Group), Sydney, Australia, Nov.–Dec. (2005).

Takeuchi S., Aoi N., Baba H., Fukui T., hashimoto ., Ieki K., Imai K., Iwasaki H., Kanno S., Kondo Y., Kubo T., Kurita K., Minemura T., Motobayashi T., Nakabayashi T., Nakamura T., Okumura T., Onishi T., Ota S., Sakurai H., Shimoura S., Sugo R., Suzuki D., Suzuki H., Suzuki M., Takeshita E., Tamaki M., Tanaka K., Togano Y., and Yamada K.: “Collectivity in  $^{32}\text{Mg}$  : a study of low-lying states”, *International Nuclear Physics Conference (INPC2007)*, Tokyo, June (2007).

Aoki K.: “Spin physics program at RHIC-PHENIX”, *International Nuclear Physics Conference (INPC2007)*, Tokyo, June (2007).

Takeuchi S., Aoi N., Baba H., Fukui T., hashimoto ., Ieki K., Imai K., Iwasaki H., Kanno S., Kondo Y., Kubo T., Kurita K., Minemura T., Motobayashi T., Nakabayashi T., Nakamura T., Okumura T., Onishi T., Ota S., Sakurai H., Shimoura S., Sugo R., Suzuki D., Suzuki H., Suzuki M., Takeshita E., Tamaki M., Tanaka K., Togano Y., and Yamada K.: “Low-lying states in  $^{32}\text{Mg}$ ”, *Future Prospects for Spectroscopy and Direct Reactions 2008*, East lansing, USA, Feb. (2008).

Baba H., Watanabe Y., Kawasaki Y., Takizawa Y., Hamada T., Ebisuzaki T., Uesaka M., Motobayashi T., Sato H., Hirota K., Shimizu H., Sato M., Fukuchi T.,

- Ota S., and Shimoura S.: "RIBF DAQ and Ubiquitous detector", TORIJIN-EFES-FJNSP LIA Joint Workshop on Next Generation Detector System for Nuclear Physics with RI Beams, (TORIJIN-EFES-FJNSP LIA ), Caen, France, Feb. (2008).
- Sato T., Furusaka M., Mikula P., Tanabe K., Sasaki Y., Homma A., Kawamura Y., Asami T., Otake Y., Sugiyama M., Naito S., and Fukunaga T.: "Development of a high intensity monochromator for Mini-Focusing SANS", 1st J-PARC International Symposium on Pulsed Neutron and Muon Sciences (IPS 08), (J-Parc Center), Mito, Mar. (2008).
- Yokkaichi S.: "Measurements of the low mass di-electron spectra at J-PARC", 4th International Workshop on Nuclear and Particle Physics at J-PARC (NP08), (J-PARC Center, Science Council of Japan, The Physical Society of Japan), Mito, Mar. (2008).
- Akiba Y.: "Experimental Study of high density matter at RHIC", YITP International Symposium Fundamental Problems in Hot and/or Dense QCD, (YITP, Kyoto University), Kyoto, Mar. (2008).
- Akiba Y.: "Experimental study of properties of quark gluon plasma via heavy quarks and EM probes", 2008 APS April Meeting and HEDP/HEDLA Meeting, St. Louis, USA, Apr. (2008).
- Toyoshima A., Kasamatu Y., Tsukada K., Kitatsuji A., Haba H., Asai M., Ishii Y., Toume H., Akiyama K., Ooe K., Sato W., Shinohara A., and Nagame Y.: "Electrochemical oxidation of element 102, nobelium", 2nd International Nuclear Chemistry Congress (2nd-INCC), (National University of Mexico), Cancun, Mexico, Apr. (2008).
- Akiyama K., Haba H., Sueki K., Tsukada K., Asai M., Toyoshima A., Nagame Y., and Katada M.: "Metallofullerene Encapsulating  $^{225}\text{Ac}$ ", 2nd International Nuclear Chemistry Congress (2nd-INCC), (National University of Mexico), Cancun, Mexico, Apr. (2008).
- Yokkaichi S.: "Low mass dielectron measurement at J-PARC", J-PARC Meeting for Spin and Hadron Physics (2008), Wako, Apr. (2008).
- Toyoshima A., Kasamatu Y., Tsukada K., Kitatsuji Y., Haba H., Ishii Y., Toume H., Asai M., Akiyama K., Ooe K., Sato W., Shinohara A., and Nagame Y.: "Characterization of heavy actinides with electrochemistry", Spring 2008 ACS National Meeting & Exposition, (American Chemical Society), USA, New Orleans, Apr. (2008).
- Akiba Y.: "PHENIX Results and Perspectives", RHIC and AGS Annual User's Meeting, (RHIC and AGS User's Organization), Upton, USA, May (2008).
- Akiba Y.: "Highlight from BNL: RHIC", International School of Subnuclear Physics, 46th Course: Predicted and totally unexpected in the energy frontier opened by LHC, (Ettore Majorana Foundation), Erice, Italy, Aug.–Sept. (2008).
- Ariyoshi S., Otani C., Dobroiu A., Sato H., Taino T., Matsuo H., and Shimizu H.: "Terahertz Imaging with a Two-dimensional Array Detector Based on Superconducting Tunnel Junctions", 33rd International Conference on Infrared, Millimeter, and Terahertz Waves (IRMMW-THz 2008), Pasadena, USA, Sept. (2008).
- Baba H., Ichihara T., Ohnishi T., Takeuchi S., Yoshida K., Watanabe Y., Ota S., and Shimoura S.: "The New DAQ System in RIKEN RIBF", 2008 Nuclear Science Symposium, Medical Imaging Conference and 16th Room Temperature Semiconductor Detector Workshop, Dresden, Germany, Oct. (2008).
- Akiba Y.: "Overview of Experimental Results from RHIC", 2nd Asian Triangle Heavy Ion Conference (ATHIC 2008), (Tsukuba University), Tsukuba, Oct. (2008).
- Akiba Y.: "Heavy Ion Physics at RHIC", 6th Japan-Italy Symposium on Heavy-Ion Physics, Tokai-mura, Ibaraki Pref., Nov. (2008).
- (Domestic Conference)
- 小貫良行: "PHENIX 実験におけるシリコンピクセル検出器ラダーの組立てに関する研究", 日本物理学会第 61 回年次大会, 松山, 3 月 (2006).
- 谷田聖: "RHIC-PHENIX 実験における、重心系エネルギー 200GeV での偏極陽子衝突からの  $\pi$  中間子生成のスピンの非対称性の測定", 日本物理学会 2007 年春季大会, 八王子, 3 月 (2007).
- 小貫良行: "PHENIX 実験用シリコンピクセル検出器のための量産組立て手順の開発", 日本物理学会 2007 年春季大会, 八王子, 3 月 (2007).
- 小貫良行: "工作プラネタリウムを利用した科学広報活動報告", 日本物理学会第 62 回年次大会, 札幌, 9 月 (2007).
- 森田晋也, 上原嘉宏, 渡邊裕, 大森整, 広田克也, 池田一昭, 大竹豊, 林偉民, 加瀬究, 金井崇: "中性子ミラー開発技術の研究 第 1 報: V-Cam を援用した評価手法の考察", 2007 年度精密工学会秋季大会学術講演会, 旭川, 9 月 (2007).
- 有吉誠一郎, 大谷知行, Dobroiu A., 佐藤広海, 田井野徹, 松尾宏, 清水裕彦: "超伝導検出器 2 次元アレイを用いたテラヘルツイメージング", 第 55 回応用物理学関係連合講演会, (応用物理学会), 船橋, 3 月 (2008).
- 渡邊穰, 山下将嗣, 田井野徹, 明連広昭, 高田進, 大谷知行: "非開口型走査近接場テラヘルツ顕微鏡の開発", 第 55 回応用物理学関係連合講演会, (応用物理学会), 船橋, 3 月 (2008).
- 小貫良行: "PHENIX シリコンピクセル検出器におけるボンディングワイヤの磁場中での共振現象と封止法", 日本物理学会第 63 回年次大会, 東大阪, 3 月 (2008).
- 馬場秀志, 渡邊康, 川崎賀也, 滝澤慶之, 濱田剛, 戎崎俊一, 上坂明子, 本林透, 佐藤広海, 広田克也, 清水裕彦, 佐藤光輝, 福地知則, 大田晋輔, 下浦享: "ユビキタス検出器の開発: 検出器への自律性導入の試み", 日本物理学会第 63 回年次大会, 東大阪, 3 月 (2008).
- 笠松良崇, 豊嶋厚史, 浅井雅人, 塚田和明, 羽場宏光, 石井康雄, 當銘勇人, 西中一朗, 秋山和彦, 菊永英寿, 後藤真一, 石川剛, 工藤久昭, 佐藤渉, 大江一弘, 栗林隆宏, 篠原厚, 木下哲一, 荒井美和子, 横山明彦, 阪間稔, 佐藤哲也, 永目諭一郎: "105 番元素 (Db) の HF/HNO<sub>3</sub> 水溶液中での陰イオン交

- 換樹脂への吸着挙動”, 日本化学会第 88 春季年会, (The Chemical Society of Japan), 東京, 3 月 (2008).
- 有吉誠一郎, 大谷知行, Dobroiu A., 佐藤広海, 田井野徹, 松尾宏, 清水裕彦: “超伝導トンネル接合素子を用いたテラヘルツ波検出器アレイの開発とイメージング応用”, 2008 年度春季低温工学・超電導学会, (低温工学会), 日野, 5 月 (2008).
- 有吉誠一郎, 大谷知行, Dobroiu A., 佐藤広海, 田井野徹, 松尾宏, 清水裕彦: “超伝導検出器 2 次元アレイを用いたテラヘルツイメージング”, 理研シンポジウム「第 7 回理研・分子研合同シンポジウム: エクストリームフォトニクス研究」, 和光, 5 月 (2008).
- 市原卓, 渡邊康, 四日市悟, 中村智昭, 延與秀人: “GridFTP を使用した PHENX 実験の日米間のデータ転送”, 広帯域ネットワーク利用に関するワークショップ (ADVNET2008), (ADVNET2008 実行委員会, 国立情報学研究所 SINET), 東京, 7 月 (2008).
- 四日市悟: “カイラル対称性の回復と中間子の質量変化 @ J-PARC”, KEK 研究会「J-PARC の物理: ハドロン・原子核研究の新しい局面」, Tsukuba, 8 月 (2008).
- 後藤雄二: “Measurements of the proton spin structure with polarized proton-proton collision”, 日本物理学会 2008 年秋季大会, (日本物理学会), 山形, 9 月 (2008).
- 北口雅暁, 日野正裕, 關義親, 舟橋春彦, 三島賢二, 猪野隆, 竹谷薫, 吉岡瑞樹, 武藤豪, 森嶋隆裕, 清水 (M) 裕彦, 嶋達志, 佐藤広海, 広田克也, 大竹淑恵, 酒井健二: “J-PARC パルス中性子を用いた中性子干渉実験”, 日本物理学会 2008 年秋季大会, (日本物理学会), 山形, 9 月 (2008).
- 猪野隆, 三島賢二, 竹谷薫, 吉岡瑞樹, 武藤豪, 森嶋隆裕, 清水 (M) 裕彦, 嶋達志, 舟橋春彦, 北口雅暁, 日野正裕, 關義親, 佐藤広海, 広田克也, 大竹淑恵, 酒井健二, 鈴木淳市, 篠原武尚: “J-PARC 中性子基礎物理実験装置”, 日本物理学会 2008 年秋季大会, (日本物理学会), 山形, 9 月 (2008).
- 三島賢二, 猪野隆, 竹谷薫, 吉岡瑞樹, 武藤豪, 森嶋隆裕, 清水 (M) 裕彦, 嶋達志, 佐藤広海, 広田克也, 大竹淑恵, 酒井健二, 佐貫智行, 鈴木善明, 舟橋春彦, 北口雅暁, 日野正裕, 關義親, 岩下芳久, 山田雅子: “J-PARC パルス中性子を用いた中性子崩壊寿命測定実験”, 日本物理学会 2008 年秋季大会, (日本物理学会), 山形, 9 月 (2008).
- 山田雅子, 岩下芳久, 市川雅浩, 頓宮拓, 藤澤博, 杉本貴則, 清水 (M) 裕彦, 猪野隆, 三島賢二, 竹谷薫, 吉岡瑞樹, 武藤豪, 森嶋隆裕, 奥隆之, 鈴木淳市, 篠原武尚, 酒井健二, 佐藤広海, 広田克也, 大竹淑恵, 關義親, 川崎真介, 駒宮幸男, 神谷好郎, 音野瑛俊, 山下了: “パルス冷中性子収束用の強度変調型永久六極磁石の開発 II”, 日本物理学会 2008 年秋季大会, (日本物理学会), 山形, 9 月 (2008).
- 關義親, 北口雅暁, 日野正裕, 舟橋春彦, 三島賢二, 猪野隆, 竹谷薫, 吉岡瑞樹, 武藤豪, 森嶋隆裕, 清水 (M) 裕彦, 佐貫智行, 鈴木善明, 嶋達志, 佐藤広海, 広田克也, 大竹淑恵, 川崎真介, 駒宮幸男, 神谷好郎, 酒井健二, 音野瑛俊, 山下了: “極冷中性子干渉計の開発”, 日本物理学会 2008 年秋季大会, (日本物理学会), 山形, 9 月 (2008).
- 竹谷薫, 三島賢二, 猪野隆, 吉岡瑞樹, 武藤豪, 森嶋隆裕, 清水 (M) 裕彦, 嶋達志, 舟橋春彦, 北口雅暁, 日野正裕, 關義親, 佐藤広海, 広田克也, 大竹淑恵, 酒井健二, 鈴木淳市, 奥隆之, 篠原武尚: “高偏極中性子生成実験”, 日本物理学会 2008 年秋季大会, (日本物理学会), 山形, 9 月 (2008).
- 川村広和, 秋山岳伸, 石井哲朗, 池田友樹, 亀田大輔, 聖代橋悦子, 豊田健司, 長江大輔, 新田稔, 二宮一史, 秦麻記, 平山賀一, 光岡真一, 宮武宇也, 村田次郎, 渡辺裕: “TRIAC における偏極不安定核を用いた時間反転対称性破れの探索”, 第 5 回停止・低速不安定核ビームを用いた核分光研究会, (大阪大学), 豊中, 12 月 (2008).
- 四日市悟: “Chiral symmetry in nuclear matter - from KEK-PS E325 to J-PARC E16 -”, 研究会「多彩なフレーバーで探る新しいハドロン存在形態」, (名古屋大学), 名古屋, 12 月 (2008).
- 有吉誠一郎, 大谷知行, 佐藤広海, 大嶋重利, 中島健介, 齊藤敦, 田井野徹, 松尾宏, 野口卓, 清水裕彦: “THz 帯・薄膜マッチング型 STJ 検出器の開発 他”, 「超伝導カメラと関連技術」研究会, (「超伝導カメラと関連技術」研究会), つくば, 2 月 (2009).
- 川村広和, 秋山岳伸, 秦麻記, 平山賀一, 池田友樹, 亀田大輔, 宮原直亮, 宮武宇也, 村田次郎, 中谷祐輔, 長江大輔, 二宮一史, 新田稔, 大西潤一, 聖代橋悦子, 豊田健司, 塚田和司, 渡辺裕: “TRIAC における偏極<sup>8</sup>Li を用いた時間反転対称性破れの探索”, 日本物理学会第 64 回年次大会, 東京, 3 月 (2009).
- 二宮一史, 秋山岳伸, 池田友樹, 小川成也, 川村広和, 関口雄太, 筒井亮丞, 秦麻記, 村田次郎: “NewtonII 号による等価原理検証を目指した近距離重力実験”, 日本物理学会第 64 回年次大会, 東京, 3 月 (2009).

Publications

[Journal]

(Original Papers) \*Subject to Peer Review

- Ueno H., Asahi K., Ogawa H., Kameda D., Miyoshi H., Yoshimi A., Watanabe H., Shimada K., Sato W., Yoneda K., Imai N., Kobayashi Y., Ishihara M., and Wolf-Dieter S.: “Measurement of nuclear moments in the region of light neutron-rich nuclei”, *Nucl. Phys. A* **738**, 211–215 (2004). \*
- Sekiguchi K., Sakai H., Witala H., Glockle W., Golak J., Hatanaka K., Hatano M., Itoh K., Kamada H., Kuboki H., Maeda Y., Nogga A., Okamura H., Saito T., Sakamoto N., Sakemi Y., Sasano M., Shimizu Y., Suda T., Tamii A., Uesaka T., Wakasa T., and Yako K.: “Resolving the Discrepancy of 135 MeV pd Elastic Scattering Cross Sections and Relativistic Effects”, *Phys. Rev. Lett.* **95**, 162301-1–162301-4 (2005). \*
- Fujiwara M., Andresen G., Bertsche W., Boston A., Bowe P. D., Cesar C. L., Chapman S., Charlton M., Chartier M., Deutsch A., Fajans J., Funakoshi R., Gill D. R., Gomboroff K., Hangst J. S., Hardy W. N., Hayano R., Hydromako R., Jenkins M. J., Jorgensen L. V., Kurchaninov L., Madsen N., Nolan P., Olchanski K., Olin A., Page R. D., Povilus A., Robicheaux F., Sarid E., Silveira D. M., Storey J. W., Thompson R. I., van der Werf D. P., Wurtele J. S., Yamazaki Y., and ALPHA Collaboration.: “Towards antihydrogen confinement with the ALPHA antihydrogen trap”, *Hyperfine Interact.* **172**, 81–89 (2006).
- Zurlo N., Amoretti M., Amsler C., Bonomi G., Carraro C., Cesar C. L., Charlton M., Doser M., Fontana A., Funakoshi R., Genova P., Hayano R., Jorgensen L. V., Kellerbauer A., Lagomarsino V., Landua R., Lodi Rizzini E., Macri M., Madsen N., Manuzio G., Mitchard D., Montagna P., Posada L. G., Pruys H., Regenfus C., Rotondi A., Testera G., Van der Werf D. P., Variola A., Venturelli L., and Yamazaki Y.: “Production of slow protonium in vacuum”, *Hyperfine Interact.* **172**, 97–105 (2006).
- Bertsche W., Boston A., Bowe P. D., Cesar C. L., Chapman S., Charlton M., Chartier M., Deutsch A., Fajans J., Fujiwara M., Funakoshi R., Gomboroff K., Hangst J. S., Hayano R., Jenkins M. J., Jorgensen L. V., Ko P., Madsen N., Nolan P., Page R. D., Posada L. G., Povilus A., Sarid E., Silveira D. M., van der Werf D. P., Yamazaki Y., Parker B., Escallier J., and Ghosh A.: “A magnetic trap for antihydrogen confinement”, *Nucl. Instrum. Methods Phys. Res.* **566**, 746–756 (2006). \*
- Amoretti M., Amsler C., Bonomi G., Bowe P. D., Canali C., Carraro C., Cesar C. L., Charlton M., Doser M., Fontana A., Fujiwara M., Funakoshi R., Genova P., Hangst J. S., Hayano R., Johnson I., Jorgensen L. V., Kellerbauer A., Lagomarsino V., Landua R., Lodi Rizzini E., Macri M., Madsen N., Manuzio G., Mitchard D., Montagna P., Pruys H., Regenfus C., Rotondi A., Testera G., Variola A., Venturelli L., Van der Werf D. P., Yamazaki Y., and ZURLO N.: “Progress with cold antihydrogen”, *Nucl. Instrum. Methods Phys. Res. B* **247**, 133–137 (2006). \*
- Kellerbauer A., Amoretti M., Bonomi G., Bowe P. D., Canali C., Carraro C., Cesar C. L., Charlton M., Doser M., Fontana A., Fujiwara M., Funakoshi R., Genova P., Hayano R., Johnson I., Jorgensen L. V., Lagomarsino V., Landua R., Lodi Rizzini E., Macri M., Madsen N., Mitchard D., Montagna P., Posada L. G., Rotondi A., Testera G., Variola A., Venturelli L., van der Werf D. P., Yamazaki Y., and Zurlo N.: “Sideband cooling of ions in a non-neutral buffer gas”, *Phys. Rev. A* **73**, 062508-1–062508-9 (2006). \*
- Shimada K., Nagae D., Asahi K., Inoue T., Takase K., Kagami S., Hatakeyama N., Kobayashi Y., Ueno H., Yoshimi A., Kameda D., Nagatomo T., Sugimoto T., Kubono S., Yamaguchi H., Wakabayashi Y., Hayakawa S., Murata J., and Kawamura H.: “Production of spin-polarized  $^{17}\text{N}$  beam using inverse-kinematics low-energy transfer reactions”, *Hyperfine Interact.* **180**, 43–47 (2007). \*
- Venturelli L., Amoretti M., Amsler C., Bonomi G., Carraro C., Cesar C. L., Charlton M., Doser M., Fontana A., Funakoshi R., Genova P., Hayano R., Jorgensen L. V., Kellerbauer A., Lagomarsino V., Landua R., Lodi Rizzini E., Macri M., Madsen N., Manuzio G., Mitchard D., Montagna P., Posada L. G., Pruys H., Regenfus C., Rotondi A., Testera G., Van der Werf D. P., Variola A., Yamazaki Y., Zurlo N., and ATHENA C.: “Protonium production in ATHENA”, *Nucl. Instrum. Methods Phys. Res. B* **261**, 40–43 (2007).
- Andresen G., Bertsche W., Boston A., Bowe P. D., Cesar C. L., Chapman S., Charlton M., Chartier M., Deutsch A., Fajans J., Fujiwara M., Funakoshi R., Gill D. R., Gomboroff K., Hangst J. S., Hayano R., Hydromako R., Jenkins M. J., Jorgensen L. V., Kurchaninov L., Madsen N., Nolan P., Olchanski K., Olin A., Povilus A., Robicheaux F., Sarid E., Silveira D. M., Storey J. W., Telle H. H., Thompson R. I., van der Werf D. P., Wurtele J. S., and Yamazaki Y.: “Antimatter Plasmas in a Multipole Trap for Antihydrogen”, *Phys. Rev. Lett.* **98**, 023402-1–023402-4 (2007). \*
- Kameda D., Ueno H., Asahi K., Nagae D., Yoshimi A., Nagatomo T., Sugimoto T., Uchida M., Takemura M., Shimada K., Takase K., Inoue T., Kijima G., Arai T., Suda S., Murata J., Kawamura H., Kobayashi Y., Watanabe H., and Ishihara M.: “Production of spin-polarized radioactive ion beams via projectile fragmentation reaction”, *AIP Conf. Proc.* **980**, 283–288 (2008). \*

- Ladygin V., Uesaka T., Saito T., Janek M., Kiselev A., Kurilkin A., Vasiliev A., Hatano M., Isupov Y., Kato H., Ladygina N., Maeda Y., Malakhov A., Nishikawa J., Ohnishi T., Okamura H., Reznikov S., Sakai H., Sakoda S., Sakamoto N., Satou Y., Sekiguchi K., Suda K., Tamii A., Uchigashima N., and Yako K.: “Analyzing powers in the  $dd \rightarrow {}^3\text{He}({}^3\text{He})$  reactions at intermediate energies”, AIP Conf. Proc. **1011**, 235–240 (2008). \*
- Kiselev A., Ladygin V., Uesaka T., Vasiliev A., Janek M., Saito T., Hatano M., Isupov Y., Kato H., Ladygina N., Maeda Y., Malakhov A., Nishikawa J., Ohnishi T., Okamura H., Reznikov S., Sakai H., Sakamoto N., Sakoda S., Satou Y., Sekiguchi K., Suda K., Tamii A., Uchigashima N., and Yako K.: “Analyzing powers in the  ${}^{12}\text{C}(\vec{d}, p){}^{13}\text{C}$  reaction at the energy  $T_d = 270$  MeV”, Eur. Phys. J. Special Topics **162**, 143–146 (2008). \*
- Kameda D., Asahi K., Ueno H., Nagae D., Takemura M., Shimada K., Yoshimi A., Nagatomo T., Sugimoto T., Uchida M., Arai T., Takase K., Suda S., Inoue T., Murata J., Kawamura H., Watanabe H., Kobayashi Y., and Ishihara M.: “Electric quadrupole moments of neutron-rich nuclei  ${}^{32}\text{Al}$  and  ${}^{31}\text{Al}$ ”, Hyperfine Interact. **180**, 61–64 (2008). \*
- Andresen G. B., Bertsche W., Boston A., Bowe P. D., Cesar C. L., Chapman S., Charlton M., Chartier M., Deutsch A., Fajans J., Fujiwara M., Funakoshi R., Gill D. R., Gomboroff K., Hangst J. S., Hayano R., Hydromako R., Jenkins M. J., Jorgensen L. V., Kurchaninov L., Madsen N., Nolan P., Olchanski K., Olin A., Page R. D., Povilus A., Robicheaux F., Sarid E., Silveira D. M., Storey J. W., Thompson R. I., Van der Werf D. P., Wurtele J. S., and Yamazaki Y.: “Production of antihydrogen at reduced magnetic field for anti-atom trapping”, J. Phys. B **41**, 011001-1–011001-5 (2008).
- Kawamata T., Takahashi N., Adachi T., Noji T., Kudo K., Kobayashi N., and Koike Y.: “Evidence for Ballistic Thermal Conduction in the One-Dimensional  $S = 1/2$  Heisenberg Antiferromagnetic Spin System  $\text{Sr}_2\text{CuO}_3$ ”, J. Phys. Soc. Jpn. **77**, No. 3, pp. 034607-1–034607-6 (2008). \*
- Yagi E., Hirabayashi K., Murakami Y., Koike S., Higami N., Hayashi T., Takebayashi A., Yoshida T., Sugi C., Sugawara T., Shishido T., and Ogiwara K.: “Site change of hydrogen in Nb due to interaction with oxygen”, J. Phys. Soc. Jpn. **77**, No. 5, pp. 054802-1–054802-8 (2008). \*
- Sato W., Ueno H., Watanabe H., Miyoshi H., Yoshimi A., Kameda D., Ito T., Shimada K., Kaihara J., Suda S., Kobayashi Y., Shinohara A., Ohkubo Y., and Asahi K.: “Temperature-dependent behavior of impurity atoms implanted in highly oriented pyrolytic graphite –An application of a new online TDPAC method–”, J. Phys. Soc. Jpn. **77**, No. 9, pp. 095001-1–095001-2 (2008). \*
- Yagi E., Sakuma K., Higami N., Hagiwara S., Mori K., Yoshii M., Koike S., Hayashi T., and Ogiwara K.: “Irradiation-induced site change of hydrogen in niobium”, J. Phys. Soc. Jpn. **77**, No. 12, pp. 124602-1–124602-7 (2008). \*
- Koike T. and Harada T.: “Formation of the deeply-bound  $K^-pp$  state in  ${}^3\text{He}(\text{in-flight } K^-, n)$  spectrum”, Mod. Phys. Lett. A **23**, No. 27-30, pp. 2540–2543 (2008). \*
- Sakuma F., Enyo H., Fukao Y., Funahashi H., Hamagaki H., Kitaguchi M., Miwa K., Murakami T., Naruki M., Ozawa K., Sekimoto M., Tabaru T., Togawa M., Yokkaichi S., Chiba J., Kanda H., Ieiri M., Ishino M., Mihara S., Miyashita T., Muto R., Nakura T., Sasaki O., Tanaka K., Yamada S., and Yoshimura Y.: “Partial decay widths of the phi into  $e+e-$  and  $K+K-$  pairs in 12 GeV p+A reactions at KEK-PS E325”, Mod. Phys. Lett. A **23**, No. 27/30, pp. 2401–2404 (2008). \*
- Koike T. and Harada T.: “Isospin properties of  $(K^-, N)$  reactions for the formation of deeply-bound antikaonic nuclei”, Nucl. Phys. A **804**, 231–273 (2008). \*
- Mitrovic V., Julien M., Vaulx C., Horvatic M., Berthier C., Suzuki T., and Yamada K.: “Similar glassy features in the  ${}^{139}\text{La}$  NMR response of pure and disordered  $\text{La}_{1.88}\text{Sr}_{0.12}\text{CuCO}_4$ ”, Phys. Rev. B **78**, 014504-1–014504-7 (2008). \*
- Goto T., Suzuki T., Kanada K., Saito T., Osawa A., Watanabe I., and Manaka H.: “Muon spin relaxation detection of the soft mode toward the exotic magnetic ground state in the bond-disordered quantum spin system  $\text{IPA-Cu}(\text{Cl}_{0.35}\text{Br}_{0.65})_3$ ”, Phys. Rev. B **78**, 054422-1–054422-6 (2008). \*
- Yamada F., Ishii Y., Suzuki T., Matsuzaki T., and Tanaka H.: “Pressure-induced reentrant oblique antiferromagnetic phase in the spin-dimer system  $\text{TlCuCl}_3$ ”, Phys. Rev. B **78**, 224405-1–224405-6 (2008). \*
- Hiyama E., Yamamoto Y., Motoba T., Thomas R., and Kamimura M.: “Light  $\Xi$  hypernuclei in four-body cluster models”, Phys. Rev. C **78**, 054316-1–054316-13 (2008). \*
- Andresen G. B., Bertsche W., Bowe P. D., Bray C. C., Butler E., Cesar C. L., Chapman S., Charlton M., Fajans J., Fujiwara M., Funakoshi R., Gill D. R., Hangst J. S., Hardy W. N., Hayano R., Hayden M. E., Hydromako R., Jenkins M. J., Jorgensen L. V., Kurchaninov L., Lambo R., Madsen N., Nolan P., Olchanski K., Olin A., Povilus A., Pusa P., Robicheaux F., Sarid E., Seif EI Nasr S., Silveira D. M., Storey J. W., Thompson R. I., van der Werf D. P., Wurtele J. S., and Yamazaki Y.: “Compression of Antiproton Clouds for Antihydrogen Trapping”, Phys. Rev. Lett. **100**, No. 20, pp. 203401-1–203401-5 (2008). \*
- Suzuki T., Yamada F., Watanabe I., Goto T., Osawa A., and Tanaka H.: “Bond-randomness effect on the quantum spin system  $\text{Tl}_{1-x}\text{K}_x\text{CuCl}_3$  probed by muon-spin-relaxation method”, Physica B **404**, 590–593 (2009). \*

Goto T., Suzuki T., Watanabe I., Kanada K., Saito T., Osawa A., and Manaka H.: “ $\mu$ SR-detected soft mode toward a possible phase transition in a disordered spin-gap system,  $(\text{CH}_3)_2\text{CHNH}_3\text{-Cu}(\text{Cl}_x\text{Br}_{1-x})_3$ ”, *Physica B* **404**, 594–596 (2009). \*

(Review)

川股隆行, 小池洋二: “低次元量子スピン系物質におけるスピンによる熱伝導”, *応用物理* **77**, No. 5, pp. 525–529 (2008).

(Others)

Bhang H. C., Ajimura S., Aoki K., Banu A., Fukuda T., Hashimoto O., Hwang J., Kameoka S., Kang B., Kim E., Kim J., Kim M., Maruta T., Miura Y., Miyake Y., Nagae T., Nakamura M., Nakamura S. N., Noumi H., Okada S., Okayasu Y., Outa H., Park H., Saha P. K., Sato Y., Sekimoto M., Shin S., Takahashi T., Tamura H., Tanida K., Toyota A., Tsukada K., Watanabe T., and Yim H.: “The quenching of nucleon yields in the nonmesonic weak decay of  $\Lambda$ -hypernuclei and the three-body weak decay process”, *Eur. Phys. J. A* **33**, No. 3, pp. 259–263 (2007).

#### [Book • Proceedings]

(Original Papers) \*Subject to Peer Review

Koike T. and Harada T.: “The formation of the deeply-bound  $K^-pp$  state in  $^3\text{He}(\text{in-flight } K^-, n)$  reaction spectrum”, *International Conference on Muon Catalyzed Fusion and Related topics ( $\mu\text{CF-07}$ )*, Dubna, Russia, 2007–6, Joint Institute for Nuclear Research, Dubna, pp. 222–229 (2008).

#### Oral Presentations

(International Conference etc.)

Heuser J., Enyo H., Onishi H., and NA60 C.: “The NA60 experiment: results and perspectives”, 8th Conference on the Intersections of Particle and Nuclear Physics (CIPANP 2003), New York, USA, May (2003).

Kameda D., Ueno H., Asahi K., Nagae D., Takemura M., Yoshimi A., Shimada K., Uchida M., Kijima G., Arai T., Takase K., Suda S., Inoue T., Murata J., Kawamura H., Haseyama T., Kobayashi Y., Watanabe H., and Ishihara M.: “Small electric quadrupole moment of  $^{32}\text{Al}$ : Drastic shape transition between  $^{32}\text{Al}$  and  $^{31}\text{Mg}$ ”, *International Nuclear Physics Conference (INPC2007)*, (Science Council of Japan, RIKEN and others), Tokyo, June (2007).

Kameda D., Ueno H., Asahi K., Nagae D., Takemura M., Yoshimi A., Shimada K., Uchida M., Kijima G., Arai T., Takase K., Suda S., Inoue T., Murata J., Kawamura H., Haseyama T., Kobayashi Y., Watanabe H., and Ishihara M.: “Small electric quadrupole moment of  $^{32}\text{Al}$ ”, *International Workshop on Nuclear Structure: New Pictures in the Extended Isospin Space (NS07)*, (Yukawa Institute for Theoretical Physics), Kyoto, June (2007).

Kameda D., Ueno H., Asahi K., Nagae D., Takemura M., Yoshimi A., Shimada K., Nagatomo T., Sugimoto

T., Uchida M., Arai T., Takase K., Suda S., Inoue T., Murata J., Kawamura H., Watanabe H., Kobayashi Y., and Ishihara M.: “Electric quadrupole moments of neutron-rich nuclei  $^{32}\text{Al}$  and  $^{31}\text{Al}$ ”, 14th Int. Conf. on Hyperfine Interactions & 18th Int. Symp. on Nuclear Quadrupole Interactions, (Universidad Nacional de La Plata), Iguassu Falls, Brazil, Aug. (2007).

Kameda D., Ueno H., Asahi K., Nagae D., Yoshimi A., Nagatomo T., Sugimoto T., Uchida M., Takemura M., Shimada K., Takase K., Inoue T., Kijima G., Arai T., Suda S., Murata J., Kawamura H., Kobayashi Y., Watanabe H., and Ishihara M.: “Production of spin-polarized r/a beams via projectile fragmentation reaction”, 12th Int. Workshop on Polarized Sources, Targets & Polarimetry, (Brookhaven National Laboratory), Brookhaven, USA, Sept. (2007).

Suzuki T., Yamada F., Watanabe I., Goto T., Osawa A., and Tanao H.: “Bond-randomness effect on the quantum spin system  $\text{Ti}_{1-x}\text{K}_x\text{CuCl}_3$  probed by muon-spin-relaxation method”, 11th International Conference on Muon Spin Rotation, Relaxation and Resonance ( $\mu\text{SR2008}$ ), (JAEA, KEK, RIKEN), Tsukuba, July (2008).

Ishii Y., Watanabe I., Suzuki T., Kawamata T., and Kato R.: “Effect of pressure on conductive anion-radical salt,  $(\text{DMe-DCNQI})_2\text{Cu}$ ”, 11th International Conference on Muon Spin Rotation, Relaxation and Resonance ( $\mu\text{SR2008}$ ), Tsukuba, July (2008).

Yamada I., Koda A., Saha S. R., Higemoto W., Kadono R., Kojima K. M., Azuma M., and Takano M.: “Field-induced magnetism in cuprate superconductor  $\text{Ca}_{2-x}\text{Na}_x\text{CuO}_2\text{Cl}_2$ ”, 11th International Conference on Muon Spin Rotation, Relaxation and Resonance ( $\mu\text{SR2008}$ ), Tsukuba, July (2008).

Heffner R. H., Spehling J., MacDougall G. J., Ito T. U., Higemoto W., Amato A., Andreica D., Nieuwenhuys G., Klauss H. H., Luke G. M., Thompson J. D., Bianchi A. D., and Fisk Z.: “Magnetism and superconductivity in heavy fermion superconductor  $\text{CeCo}(\text{In}_{1-x}\text{Cd}_x)_5$ ”, 11th International Conference on Muon Spin Rotation, Relaxation and Resonance ( $\mu\text{SR2008}$ ), Tsukuba, July (2008).

Matsumoto T., Egami T., Ogata K., Iseri Y., Yahiro M., and Kamimura M.: “Coupled-channel analyses of  $^6\text{He}$  breakup reactions”, *Hokudai-TORIJIN-JUSTIPEN-EFES Workshop & JUSTIPEN-EFES-Hokudai-UNEDF Meeting*, Sapporo, July (2008).

Kawamata T., Sugawara N., Uesaka M., Kaneko N., Kajiwara T., Yamane H., Koyama K., Kudo K., Kobayashi N., and Koike Y.: “ $\text{Pb}_2\text{V}_3\text{O}_9$  and the bose-einstein condensed state of triplons studied by thermal conductivity and specific heat measurements”, 25th International Conference on Low Temperature Physics (LT25), Amsterdam, Netherland, Aug. (2008).

Uesaka M., Kawamata T., Sugawara N., Kaneko N.,

- Kudo K., Kobayashi N., and Koike Y.: “Single-Crystal Growth and Thermal Conductivity of the Quasi One-Dimensional Spin System  $\text{Sr}_2\text{V}_3\text{O}_9$ ”, 25th International Conference on Low Temperature Physics (LT25), Amsterdam, Netherland, Aug. (2008).
- Koike Y., Haidar S. M., Adachi T., Kawamata T., Sugawara N., Kaneko N., Uesaka M., Sato H., Tanabe Y., Noji T., Kudo K., and Kobayashi N.: “Thermal-conductivity study on the electronic state in the overdoped regime of  $\text{La}_{2-x}\text{Sr}_x\text{CuO}_4$ : Phase separation and anomaly at  $x \sim 0.21$ ”, 25th International Conference on Low Temperature Physics (LT25), Amsterdam, Netherland, Aug. (2008).
- Koike T. and Harada T.: “ $^3\text{He}(\text{in-flight } K^-, n)$  reaction spectrum near the  $\bar{K}N \rightarrow \pi\Sigma$  decay threshold and the deeply-bound  $K^-pp$  state”, 4th Asia-Pacific Conference on Few-Body Problems in Physics (APFB08), (University of Indonesia), Depok, Indonesia, Aug. (2008).
- Koike T. and Harada T.: “The  $\bar{K}N \rightarrow \pi\Sigma$  decay threshold effect in  $^3\text{He}(\text{in-flight } K^-, n)$  reaction spectrum”, International Conference on Exotic Atoms and Related Topics (EXA 08), (Stefan Meyer Institute for subatomic Physics, Austrian Academy of Science), Vienna, Australia, Sept. (2008).
- Sakuma F.: “The search for deeply-bound kaonic nuclear states at J-PARC”, 19th International Baldin Seminar on High Energy Physics Problems: Relativistic Nuclear Physics and Quantum Chromodynamics, (JINR), Dubna, Russia, Sept.-Oct. (2008).
- Matsumoto T., Egami T., Ogata K., Iseri Y., Yahiro M., and Kamimura M.: “Coupled-channel analyses of  $^6\text{He}$  breakup reactions”, KGU Yokohama Autumn School of Nuclear Physics, Yokohama, Oct. (2008).
- Kawamata T., Uesaka M., Sugawara N., Kaneko N., Koyama K., Kudo K., Kobayashi N., and Koike Y.: “Single-Crystal Growth and Thermal Conductivity of the Alternating Chain System  $\text{Pb}_2\text{V}_3\text{O}_9$  and Uniform Chain System  $\text{Sr}_2\text{V}_3\text{O}_9$ ”, 2nd International Symposium on Anomalous Quantum Materials (ISAQM2008) and the 7th Asia-Pacific Workshop, (Grant-in-Aid for Scientific Research on Priority Areas), Tokyo, Nov. (2008). (Domestic Conference)
- 鈴木栄男, 山田文子, 渡邊功雄, 大沢明, 後藤貴行, 田中秀数: “ $\text{Tl}(\text{Cu}_{1-x}\text{Mg}_x)\text{Cl}_3$  ( $x = 0.0047$ ) における  $\mu\text{SR}$  法で見たスピン揺らぎ”, 日本物理学会第 63 回年次大会, (日本物理学会), 東大阪, 3 月 (2008).
- 石田勝彦, 今尾浩士, 松田恭幸, 河村成肇, 豊田晃久, 岩崎雅彦, 永嶺謙忠: “負ミュオン移行率の温度依存性で見る固体トリチウム中の  $^3\text{He}$  の挙動”, 日本物理学会第 63 回年次大会, 東大阪, 3 月 (2008).
- Haidar S. M., 足立 匡, 川股 隆行, 菅原 直樹, 佐藤 秀孝, 田邊 洋一, 野地 尚, 工藤 一貴, 小林 典男, 小池 洋二: “ $\text{La}_{2-x}\text{Sr}_x\text{CuO}_4$  の オーバードープ 領域における 磁場中熱伝導と  $1/4$  異常”, 日本物理学会第 63 回年次大会, (日本物理学会), 東大阪, 3 月 (2008).
- 菅原直樹, 川股隆行, Haidar S. M., 金子直人, 上坂正憲, 工藤一貴, 小林典男, 小池洋二: “1 次元スピン-ダイマー系  $\text{Pb}_2\text{V}_3\text{O}_9$  におけるトリブロンポーズ・アインシュタイン凝縮相転移”, 日本物理学会第 63 回年次大会, (日本物理学会), 東大阪, 3 月 (2008).
- 川股隆行, 菅原直樹, Haidar S. M., 野地尚, 小池洋二, 工藤一貴, 小林典男, 藤井裕, 菊池彦光, 千葉明朗, Petrakovskii G., Popov M., Bezmaternikh L.: “熱伝導からみた  $\text{CuB}_2\text{O}_4$  の磁気秩序移”, 日本物理学会第 63 回年次大会, (日本物理学会), 東大阪, 3 月 (2008).
- 川股隆行, 菅原直樹, Haidar S. M., 金子直人, 上坂正憲, 小山佳一, 工藤一貴, 小林典男, 小池洋二: “熱伝導, 比熱, 磁化からみた  $\text{Pb}_2\text{V}_3\text{O}_9$  単結晶におけるトリブロンポーズ・アインシュタイン凝縮相転移”, 文部科学省科学研究補助金特定領域研究「フラストレーションが創る新しい物性」第 2 回トピカルミーティング「フラストレーションとマルチフェロイクス」, (文部科学省科学研究費補助金特定領域研究「フラストレーションが創る新しい物性」), 宇治, 6 月 (2008).
- 川股隆行, 金子直人, 上坂正憲, 工藤一貴, 小林典男, 小池洋二: “ $\text{Sr}_2\text{CuO}_3, \text{SrCuO}_2$  におけるスピンによる巨大熱伝導”, 第 69 回応用物理学会学術講演会, (応用物理学会), 春日井, 9 月 (2008).
- 鈴木栄男, 渡邊功雄, 後藤貴行, 山田文子, 田中秀数: “量子スピン系  $\text{Tl}_{1-x}\text{K}_x\text{CuCl}_3$  ( $x = 0.20, 0.44, 0.58$ ) におけるミュオンスピン緩和 ( $\mu\text{SR}$ ) 測定”, 日本物理学会 2008 年秋季大会, (日本物理学会), 盛岡, 9 月 (2008).
- 松本琢磨, 江上智晃, 緒方一介, 井芹康統, 八尋正信, 上村正康: “中性子過剰核の分解反応断面積の計算”, 日本物理学会 2008 年秋季大会, 盛岡, 9 月 (2008).
- 髭本亘, Heffner R. H., Spehling J., MacDougall G. J., 伊藤孝, Amato A., Andreica D., Nieuwenhuys G., Klauss H. H., Luke G. M., Thompson J. D., Bianchi A. D., Fisk Z.: “ $\mu\text{SR}$  から眺めた  $\text{CeCo}(\text{In}, \text{Cd})_5$  の磁性と超伝導”, 日本物理学会 2008 年秋季大会, (日本物理学会), 盛岡, 9 月 (2008).
- 上坂正憲, 川股隆行, 金子直人, 菅原直樹, 工藤一貴, 小林典男, 小池洋二: “1 次元量子スピン系  $\text{Sr}_2\text{V}_3\text{O}_9$  単結晶の育成とスピンによる熱伝導”, 日本物理学会 2008 年秋季大会, 盛岡, 9 月 (2008).
- 金子直人, 川股隆行, 上坂正憲, 小池洋二: “1 次元量子スピン系  $\text{SrCuO}_2$  単結晶におけるスピンによる熱伝導のアニール効果”, 日本物理学会 2008 年秋季大会, 盛岡, 9 月 (2008).
- 小池貴久, 原田融: “結合チャンネル DWIA による  $^3\text{He}(\text{in-flight } K^-, n)$  反応計算”, 日本物理学会 2008 年秋季大会, (日本物理学会), 山形, 9 月 (2008).
- 小池洋二, 川股隆行, 高橋伸雄, 金子直人, 上坂正憲, 足立匡, 野地尚, 工藤一貴, 小林典男: “低次元量子スピン系物質におけるスピンによる熱伝導”, 日本熱物性学会第 10 回「マイクロナノスケールの熱物性とシステムデザイン」研究会, 東京, 9 月 (2008).
- 石田勝彦: “理研 RAL ミュオン施設の概要”, RCNP 研究会「ミュオン科学と加速器研究」, (大阪大学), 茨木, 10 月 (2008).
- 川股隆行, 金子直人, 上坂正憲, 工藤一貴, 小林典男, 小池洋二:

“1次元量子スピン系 SrCuO<sub>2</sub>, Sr<sub>2</sub>V<sub>3</sub>O<sub>9</sub> におけるスピンによる熱伝導”, 物性科学領域横断研究会「スピンの拓く物性科学の最前線」, 東京, 11-12月(2008).

佐久間史典: “J-PARC E15 実験における TGEM-TPC の開発@理研”, 第5回「マイクロパターンガス検出器 (MPGD) 研究会」, (東大 CNS), 和光, 12月(2008).

上坂正憲, 川股隆行, 金子直人, 佐藤光秀, 菅原直樹, 工藤一貴, 小林典男, 小池洋二: “1次元量子スピン系 Sr<sub>2</sub>V<sub>3</sub>O<sub>9</sub> 単結晶のスピンによる熱伝導”, 日本物理学会第64回年次大会, 東京, 3月(2009).

大久保晋, 日野俊一, 藤澤真士, 太田仁, 川股隆行, 小池洋二: “ボンド交替系 Pb<sub>2</sub>V<sub>3</sub>O<sub>9</sub> 単結晶試料の強磁場 ESR 測定”, 日本物理学会第64回年次大会, 東京, 3月(2009).

小池貴久, 原田融: “結合チャンネル DWIA による <sup>3</sup>He(in-flight *K*<sup>-</sup>, *n*) 反応計算 II”, 日本物理学会第64回年次大会, (日本物理学会), 東京, 3月(2009).

川股隆行, 上坂正憲, 菅原直樹, 佐藤光秀, 金子直人, 小山佳一, 工藤一貴, 小林典男, 小池洋二: “比熱と磁化からみた Pb<sub>2</sub>V<sub>3</sub>O<sub>9</sub> 単結晶のボース・アインシュタイン凝縮相転移”, 日本物理学会第64回年次大会, 東京, 3月(2009).

## Theoretical Physics Laboratory

### Publications

#### [Journal]

(Original Papers) \*Subject to Peer Review

- Fukuma M., Kawai H., and Ninomiya M.: “Limiting temperature, limiting curvature and the cyclic universe”, *Int. J. Mod. Phys. A* **19**, 4367–4385 (2004). \*
- Kawai H., Kuroki T., and Morita T.: “Supersymmetric large  $N$  reduced model with multiple matter”, *Nucl. Phys. B* **683**, 27–47 (2004). \*
- Kimura Y.: “Myers effect and tachyon condensation”, *Nucl. Phys. B* **692**, 394–416 (2004). \*
- Hasebe K. and Kimura Y.: “Dimensional hierarchy in quantum Hall effects on fuzzy spheres”, *Phys. Lett. B* **602**, 255–260 (2004). \*
- Ishibashi N., Kuroki T., and Yamaguchi A.: “Universality of nonperturbative effects in  $c \neq 1$  noncritical string theory”, *J. High Energy Phys.* **0509**, 043-1-043-15 (2005). \*
- Kawai H., Kuroki T., and Matsuo Y.: “Universality of nonperturbative effect in type 0 string theory”, *Nucl. Phys. B* **711**, 253–274 (2005). \*
- Kawai H., Kuroki T., Morita T., and Yoshida K.: “Direct derivation of the Veneziano-Yankielowicz superpotential from matrix model”, *Phys. Lett. B* **611**, 269–278 (2005). \*
- Igi K. and Ishida M.: “On the discrepancy of  $pp$ ,  $\bar{p}p$  total cross sections at  $\sqrt{s} = 1.8$  TeV between E710, E811 and CDF”, *Prog. Theor. Phys.* **115**, No. 3, pp. 601–609 (2005). \*
- Alig C., Drees M., and Oda K.: “QCD effects in the decays of TeV black holes”, *J. High Energy Phys.* **0612**, 049-1-049-26 (2006). \*
- Shibusa Y. and Matsuo T.: “Quantization of fields based on generalized uncertainty principle”, *Mod. Phys. Lett. A* **21**, 1285–1296 (2006). \*
- Shibusa Y.: “Supersymmetric field theory based on generalized uncertainty principle”, *Int. J. Mod. Phys. A* **22**, 5279–5286 (2007). \*
- Furuta K., Hanada M., Kawai H., and Kimura Y.: “Field equations of massless fields in the new interpretation of the matrix model”, *Nucl. Phys. B* **767**, 82–99 (2007). \*
- Aoyama T., Hayakawa M., Kinoshita T., and Nio M.: “Revised value of the eighth-order contribution to the electron  $g-2$ ”, *Phys. Rev. Lett.* **99**, 110406-1–110406-4 (2007). \*
- D’Adda A., Kanamori I., Kawamoto N., and Nagata K.: “Lattice formulation of the  $N=4$   $D=3$  twisted super Yang-Mills”, *Proceedings of Science LAT2007*, 271-1–271-7 (2007).
- Ishikawa T., Azeyanagi T., Hanada M., and Hirata T.: “Phase structure of twisted Eguchi-Kawai model”, *Proceedings of Science*, No. 054, pp. 1–7 (2007). \*
- Baba Y., Ishibashi N., and Murakami K.: “D-brane states and annulus amplitudes in  $OSp$  invariant closed string field theory”, *J. High Energy Phys.* **0807**, 046-1–046-12 (2008). \*
- Hashimoto K., Hirayama T., Lin F., and Yee H.: “Quark mass deformation of holographic massless QCD”, *J. High Energy Phys.* **0807**, 089-1–089-26 (2008). \*
- Ohta K. and Tai T.: “Extended MQCD and SUSY/non-SUSY duality”, *J. High Energy Phys.* **0809**, No. 033, pp. 033-1–033-13 (2008). \*
- Kawai H. and Suyama T.: “AdS/CFT correspondence as a consequence of scale invariance”, *Nucl. Phys. B* **789**, 209–224 (2008). \*
- Kawai H. and Suyama T.: “Some Implications of Perturbative Approach to AdS/CFT Correspondence.”, *Nucl. Phys. B* **794**, 1–12 (2008). \*
- Aoyama T., Hayakawa M., Kinoshita T., and Nio M.: “Automated Calculation Scheme for  $\alpha^n$  Contributions of QED to Lepton  $g-2$ : New Treatment of Infrared Divergence for Diagrams without Lepton Loops”, *Nucl. Phys. B* **796**, 184–210 (2008). \*
- D’Adda A., Kanamori I., Kawamoto N., and Nagata K.: “Exact Extended Supersymmetry on a Lattice: Twisted  $N=4$  Super-Yang-Mills in Three Dimensions”, *Nucl. Phys. B* **798**, 168–183 (2008). \*
- Kawano T., Kishimoto I., and Takahashi T.: “Gauge invariant overlaps for classical solutions in open string field theory”, *Nucl. Phys. B* **803**, 135–165 (2008). \*
- Kanamori I. and Suzuki H.: “Restoration of supersymmetry on the lattice: Two-dimensional  $\mathcal{N} = (2, 2)$  supersymmetric Yang-Mills theory”, *Nucl. Phys. B* **811**, No. 3, pp. 420–437 (2008). \*
- Kawai H. and Sato M.: “Perturbative Vacua from IIB Matrix Model”, *Phys. Lett. B* **659**, 712–717 (2008). \*
- Kawano T., Kishimoto I., and Takahashi T.: “Schnabl’s solution and boundary states in open string field theory”, *Phys. Lett. B* **669**, 357–358 (2008). \*
- Aoyama T., Hayakawa M., Kinoshita T., and Nio M.: “Revised value of the eighth-order QED contribution to the anomalous magnetic moment of the electron”, *Phys. Rev. D* **77**, No. 5, pp. 053012-1–053012-24 (2008). \*
- Hashimoto K., Terashima S., and Tan C.: “Glueball decay in holographic QCD”, *Phys. Rev. D* **77**, 086001-1–086001-14 (2008). \*
- Kanamori I., Sugino F., and Suzuki H.: “Euclidean lattice simulation for dynamical supersymmetry breaking”, *Phys. Rev. D* **77**, 091502(R)-1–091502(R)-5 (2008). \*
- Aoyama T., Hayakawa M., Kinoshita T., Nio M., and Watanabe N.: “Eighth-order vacuum-polarization function formed by two light-by-light-scattering diagrams and its contribution to the tenth-order electron  $g-2$ ”, *Phys. Rev. D* **78**, No. 5, pp. 053005-1–053005-14 (2008). \*
- Aoyama T., Hayakawa M., Kinoshita T., and Nio M.: “Tenth-order lepton anomalous magnetic moment:

- Second-order vertex containing two vacuum polarization subdiagrams, one within the other”, *Phys. Rev. D* **78**, No. 11, pp. 113006-1–113006-7 (2008). \*
- Hosotani Y., Oda K., Ohnuma T., and Sakamura Y.: “Dynamical electroweak symmetry breaking in  $SO(5) \times U(1)$  gauge-Higgs unification with top and bottom quarks”, *Phys. Rev. D* **78**, 096002-1–096002-16 (2008). \*
- Kanamori I., Sugino F., and Suzuki H.: “Observing dynamical supersymmetry breaking with euclidean lattice simulations”, *Prog. Theor. Phys.* **119**, 797–827 (2008). \*
- Kishimoto I.: “Comments on gauge invariant overlaps for marginal solutions in open string field theory”, *Prog. Theor. Phys.* **120**, No. 5, pp. 875–886 (2008). \*
- Hashimoto K., Sakai T., and Sugimoto S.: “Holographic baryons: Static properties and form factors from gauge/string duality”, *Prog. Theor. Phys.* **120**, 1093–1137 (2008). \*
- Kanamori I. and Suzuki H.: “Some physics of the two-dimensional  $\mathcal{N} = (2, 2)$  supersymmetric Yang-Mills theory: Lattice Monte Carlo study”, *Phys. Lett. B* **672**, No. 3, pp. 307–311 (2009). \*
- Abe H. and Sakamura Y.: “Flavor structure with multi-moduli in 5D supergravity”, *Phys. Rev. D* **79**, 045005-1–045005-16 (2009). \*
- (Review)
- 橋本幸士: “超弦理論から原子核へ: ホログラフィック QCD”, *パリティ* **23**, No. 1, pp. 44–45 (2008).
- 橋本幸士: “コスミックストリングの逆襲—宇宙に横たわる巨大なスーパーストリング”, *パリティ* **23**, No. 8, pp. 39–45 (2008).
- 橋本幸士: “D ブレーンの力学からゲージ重力対応へ”, *数理科学*, No. 536, pp. 15–21 (2008).
- 鈴木博: “場の量子論の考え方”, *数理科学*, No. 541, pp. 6–11 (2008).
- (Others)
- Abe H. and Sakamura Y.: “Moduli stabilization and flavor structure in 5D SUGRA with multi moduli”, *AIP Conf. Proc.* **1078**, 414–416 (2008).
- Kanamori I.: “RHMC simulation of two-dimensional  $N=(2,2)$  super Yang-Mills with exact supersymmetry”, *Proceedings of Science* **232**, 1–7 (2008).
- structure in 5D SUGRA with multi moduli”, 16th International Conference on Supersymmetry and the Unification of Fundamental Interactions, (KIAS, CQUEST, KPS), Seoul, Korea, June (2008).
- Kanamori I.: “Observing dynamical SUSY breaking with lattice simulation”, 16th International Conference on Supersymmetry and Unification of Fundamental Interactions (SUSY08), (SUSY08 organizing committee), Seoul, Korea, June (2008).
- Abe H. and Sakamura Y.: “Moduli stabilization and flavor structure in 5D SUGRA with multi moduli”, *PASCOS’ 08*, (Perimeter Institute), Waterloo, Canada, June (2008).
- Kanamori I.: “RHMC simulation of two-dimensional  $N=(2,2)$  super Yang-Mills with exact supersymmetry”, *Lattice 2008*, 26th International Symposium on Lattice Field Theory, (Lattice 2008 Local Organizing Committee), Williamsburg, USA, July (2008).
- Suzuki H.: “2d  $\mathcal{N} = (2, 2)$  SYM in the machine”, *Lattice supersymmetry and beyond*, (Niels Bohr International Academy), Copenhagen, Denmark, Nov. (2008).
- (Domestic Conference)
- 鈴木博: “Note on massless bosonic states in two-dimensional field theories”, 2006 年度基礎物理学研究所研究会「場の量子論の基礎的諸問題と応用」, (京都大学基礎物理学研究所), 京都, 12 月 (2006).
- 深谷英則, 金森逸作, 鈴木博, 瀧見知久: 日本物理学会第 62 回年次大会, 札幌, 9 月 (2007).
- 金森逸作: “超対称性の自発的破れの格子シミュレーションによる測定”, 理研シンポジウム「量子場の理論と対称性」, 和光, 12 月 (2007).
- 橋本幸士: “ADHM construction of instantons and D-branes”, 素粒子原子核四国セミナー 2007, (四国学院大学, 京都大学基礎物理学研究所), 高松, 12 月 (2007).
- 橋本幸士: “超弦理論における D ブレーン”, 14th ICEPP Symposium, (東京大学), 長野県白馬村, 2 月 (2008).
- 川野輝彦, 岸本功, 九後汰一郎, 高橋智彦: “Schnabl 解に対するあるゲージ不変量の計算”, 日本物理学会第 63 回年次大会, 東大阪, 3 月 (2008).
- 橋本幸士: “QCD String as Vortex String in Seiberg-Dual Theory”, 日本物理学会第 63 回年次大会, (日本物理学会), 東大阪, 3 月 (2008).
- 金森逸作, 鈴木博, 杉野文彦: “超対称性の自発的破れの格子シミュレーションによる測定”, 日本物理学会第 63 回年次大会, 東大阪, 3 月 (2008).
- 川野輝彦, 岸本功, 高橋智彦: “Gauge invariant overlaps for classical solutions in open string field theory”, 基研研究会「量子場理論と弦理論の発展」, 京都, 7 月 (2008).
- 金森逸作: “超対称性の自発的破れの格子シミュレーションによる測定”, 基研研究会「量子場理論と弦理論の発展」, 京都, 7 月 (2008).
- 馬場裕, 石橋延幸, 村上公一: “ $OSp$  不変な超弦の場の理論”, 基研研究会「量子場理論と弦理論の発展」, (京都大学基礎物理学研究所), 京都, 7 月 (2008).
- 橋本幸士: “Quark Mass in Holographic QCD”, 基研研究会

- 「量子場理論と弦理論の発展」, (京都大学基礎物理学研究所), 京都, 7月 (2008).
- 安倍博之, 阪村豊: “Moduli stabilization and flavor structure in 5D SUGRA with multi moduli”, 基研研究会「量子場の理論と弦理論の発展」, (基礎物理学研究所), 京都, 7-8月 (2008).
- 太田和俊, 戴大盛: “Extended MQCD and SUSY/non-SUSY duality”, 基研研究会「量子場理論と弦理論の発展」, (京都大学基礎物理学研究所), 京都, 8-1月 (2008).
- 金森逸作, 鈴木博: “Lattice simulation of super Yang-Mills model with scalar mass term added”, 日本物理学会 2008 年秋季大会, (日本物理学会), 山形, 9月 (2008).
- 岸本功, 高橋智彦: “浅野-加藤ゲージにおけるゲージ不変量の数値計算”, 日本物理学会 2008 年秋季大会, 山形, 9月 (2008).
- 馬場裕, 石橋延幸, 村上公一: “OSp 不変な超弦の場の理論の NS セクター”, 日本物理学会 2008 年秋季大会, 山形, 9月 (2008).
- 馬場裕, 石橋延幸, 村上公一: “OSp 不変な超弦の場の理論の R セクター”, 日本物理学会 2008 年秋季大会, 山形, 9月 (2008).
- 安倍博之, 阪村豊: “Moduli stabilization and flavor structure in 5D SUGRA with multi moduli”, 日本物理学会 2008 年秋季大会, (日本物理学会), 山形, 9-9月 (2008).
- 橋本幸士: “Toward a Proof of Montonen-Olive Duality via Multiple M2-branes”, KEK Workshop “Heterotic String and M-theory”, (高エネルギー加速器研究機構), つくば, 12月 (2008).
- 馬場裕, 石橋延幸, 村上公一: “OSp 不変な閉弦場の理論における D-brane 状態と円環振幅”, 理研シンポジウム「場と弦の理論の新展開に向けて」, 和光, 12月 (2008).
- 橋本幸士: “Holographic Nuclei”, 理研シンポジウム「場と弦の理論の新展開に向けて」, 和光, 12月 (2008).
- 岸本功, 高橋智彦: “a-ゲージにおけるゲージ不変量の数値計算”, 理研シンポジウム「場と弦の理論の新展開に向けて」, 和光, 12月 (2008).
- 仁尾真紀子: “レプトン  $g-2$  の QED 高次補正”, ワークショップ「計算科学による素粒子・原子核・宇宙の融合」, (科研費新学術領域「素核宇宙融合による計算科学に基づいた重層的物質構造の解明」), つくば, 12月 (2008).
- 金森逸作: “Is lattice simulation of two-dimensional super Yang-Mills possible?”, Sapporo Winter School 2009, (Sapporo Winter School 2009 世話人), 札幌, 1月 (2009).
- 岸本功, 高橋智彦: “Numerical evaluation of gauge invariants in open string field theory”, Sapporo Winter School 2009, 札幌, 1月 (2009).
- 金森逸作: “超対称ゲージ理論の格子シミュレーション”, 日本物理学会第 64 回年次大会, 東京, 3月 (2009).

## Strangeness Nuclear Physics Laboratory

### Publications

#### [Journal]

(Original Papers) \*Subject to Peer Review

Hiyama E., Yamamoto Y., Motoba T., Thomas R., and Kamimura M.: “Light  $\Xi$  hypernuclei in four-body cluster models”, Phys. Rev. C **78**, 054316-1–054316-13 (2008). \*

### Oral Presentations

(International Conference etc.)

Hiyama E.: “Four and five-body calculation of exotic hadron systems”, 2008 APCTP-BLTP JINR Joint Workshop on Quarks and Mesons in Nuclear Physics, Pohang, Korea, Apr. (2008).

Hiyama E.: “Three- and four-body structure of light hypernuclear physics”, 3rd China-Japan-Korea Hadron and Nuclear Physics 2008 Symposium, Lanzhou, China, June (2008).

Hiyama E.: “Few-body aspects of hypernuclear physics”, Japanese French Symposium :New paradigms in Nuclear Physics, (JSPS), Paris, France, Sept. (2008).

Hiyama E.: “Four and five-body calculation of exotic hadron systems”, Workshop on Hadron Dynamics, Almunecar, Spain, Sept. (2008).

Hiyama E.: “Recent progress in strangeness nuclear physics”, Asia Science Seminar on Frontier Science at High-Intensity Proton Accelerators, (JSPS, Tohoku Univ. CIAE, IHEP-CAS), Beijing, China, Oct. (2008).

Hiyama E.: “Recent progress in hypernuclear physics”, International Symposium on Heavy Ion Physics 2008 (ISHIP2008), (HIC for FAIR, EMMI, HGS-HIRe, GSI), Darmstadt, Germany, Nov. (2008).

Hiyama E.: “Four-body structure of  $\Xi$  hypernuclei”, Sendai International Symposium on Strangeness in Nuclear and Hadronic Systems (SENDAI08), (Tohoku University), Sendai, Dec. (2008).

(Domestic Conference)

堀井香織, 古本猛憲, 櫻木弘之: “偏極陽子+ $^8\text{B}$  散乱における  $^8\text{B}$ ,  $^7\text{Be}+p$  分解過程および  $^7\text{Be}$  核変形の効果”, 日本物理学会第 63 回年次大会, 東大阪, 3 月 (2008).

堀井香織, 土岐博, 櫻木弘之, 高階正彰, 谷口億宇, 古本猛憲: “内部構造を考慮した  $^8\text{Be}+\gamma$  の陽子および  $^{12}\text{C}$  との弾性散乱”, 日本物理学会第 64 回年次大会, 東京, 3 月 (2009).

## Publications

## [Journal]

(Original Papers) \*Subject to Peer Review

Stolterfoht N., Hellhammer R., Bundesmann J., Fink D., Kanai Y., Hoshino M., Kambara T., Ikeda T., and Yamazaki Y.: "Guiding of slow  $\text{Ne}^{7+}$  ions through nanocapillaries in insulating polyethylene terephthalate: incident current dependence", *Phys. Rev. A* **76**, 022712-1-022712-10 (2007). \*

Kazama Y., Saito H., Miyagai M., Takehisa H., Ichida H., Miyazawa Y., Mishiba K., Kanaya T., Suzuki K., Bae C., Miyoshi K., Mii M., and Abe T.: "Effect of heavy ion-beam irradiation on plant growth and mutation induction in *Nicotiana tabacum*", *Plant Biotechnol.* **25**, No. 1, pp. 105-111 (2008). \*

Kazama Y., Saito H., Yamamoto Y. Y., Hayashi Y., Ichida H., Ryuto H., Fukunishi N., and Abe T.: "LET-dependent effects of heavy-ion beam irradiation in *Arabidopsis thaliana*", *Plant Biotechnol.* **25**, No. 1, pp. 113-117 (2008). \*

Kanai Y., Hoshino M., Kambara T., Ikeda T., Hellhammer ., Stolterfoht N., and Yamazaki Y.: "Dynamic features of ion guiding by nanocapillaries in an insulating polymer", *Phys. Rev. A* **79**, 012711-1-012711-5 (2009). \*

## [Book・Proceedings]

(Others)

Kazama Y., Saito H., Hayashi Y., Ichida H., Ohbu S., Ryuto H., Fukunishi N., and Abe T.: "Effects of ion beam irradiation on mutation induction in *Arabidopsis thaliana*", *Proceedings of 18th International Conference on Cyclotrons and Their Applications (Cyclotrons 2007)*, Giardini Naxos, Italy, 2007-9~10, INFN, Giardini Naxos, pp. 240-242 (2008).

## Oral Presentations

(International Conference etc.)

Koizumi A., Nishihara K., Yamanaka K., Ishii K., Kazama Y., Abe T., and Kawano S.: "Asexual and bisexual mutants caused by defective sex-chromosomes in the dioecious plant, *Silene latifolia*", 20th International Congress of Genetics, (The International Genetics Federation), Berlin, Germany, July (2008).

Nishihara K., Kazama Y., Fujiwara M., Koizumi A., Abe T., and Kawano S.: "Roles of *SUPERMAN* and *WUSCHEL* in the female differentiation of the dioecious plant *Silene latifolia*", 20th International Congress of Genetics, (The International Genetics Federation), Berlin, Germany, July (2008).

Honda I., Nishihara K., Kikuchi K., Matsuo S., Fukuda M., Kazama Y., Kawano S., and Abe T.: "Physiological analysis of pepper dwarf mutants induced by heavy-ion-irradiation", NARO International Symposium on Solanaceae Genomics to Agriculture and Food Research;

Aiming for Effective and Efficient Application, (National Institute of Vegetable and Tea Science), Tsu, Mar. (2009).

(Domestic Conference)

風間裕介, 齊藤宏之, 林依子, 市田裕之, 龍頭啓充, 福西暢尚, 阿部知子: "重イオンビーム照射において核種・LETが突然変異率へ与える影響", 第5回イオンビーム育種研究会大会, 敦賀, 5月(2008).

竹久妃奈子, 風間裕介, 林依子, 市田裕之, 大部登江, 三吉一光, 阿部知子: "炭素イオンビームで誘発したタバコホメオティック変異体の解析", 日本植物形態学会第19回総会・大会, 高知, 9月(2008).

小泉綾子, 西原潔, 山中香, 石井公太郎, 風間裕介, 阿部知子, 河野重行: "雌雄異株植物ヒロハノマンテマにおける性染色体欠失により引き起こされた無性花変異体と両性花変異体", 日本植物形態学会第19回総会・大会, 高知, 9月(2008).

風間裕介, 竹久妃奈子, 市田裕之, 宮沢豊, 金谷健至, 鈴木賢一, 藤原誠, 林依子, 阿部知子: "重イオンビーム照射で作出したタバコ白花変異体は *DFR* 遺伝子に欠失変異をもつ", 第26回日本植物細胞分子生物学学会大会・シンポジウム, 吹田, 9月(2008).

風間裕介, 藤原誠, 竹久妃奈子, 市田裕之, 金谷健至, 鈴木賢一, 林依子, 阿部知子: "タバコ複二倍体ゲノムに生じた重イオンビーム誘発変異の解析", 日本植物学会第72回大会, 高知, 9月(2008).

金澤悠, 池田時浩, Flores Carrasco M., 小島隆夫, 岩井良夫, 金井保之, Tribedi L. C., 神原正, 小林知洋, 星野正光, 田中大, 山崎泰規: "ガラスキャピラリーを用いた低速多価イオンによるナノファブリケーション(2)", 日本物理学会2008年秋季大会, 山形, 9月(2008).

西原潔, 風間裕介, 藤原誠, 阿部知子, 河野重行: "PCR-SSPを用いた雌雄異株植物ヒロハノマンテマのX染色体連鎖遺伝子のマッピング", 日本育種学会第114回講演会, (日本育種学会), 彦根, 10月(2008).

風間裕介, 藤原誠, 西原潔, 小泉綾子, 石井公太郎, 河野重行, 阿部知子: "雌雄異株植物ヒロハノマンテマの雌花特異的に発現する遺伝子 *SISUP* の解析", 日本育種学会第114回講演会, 彦根, 10月(2008).

西原 潔, 風間 裕介, 藤原 誠, 河野 重行, 阿部 知子: "A *WUSCHEL* homologue is exclusively linked to the X chromosome in the dioecious plant *Silene latifolia*", 理研植物科学研究センター(PSC), かずさDNA研究所, 横浜市立大学木原生物学研究所 Joint Retreat 2008, 木更津, 10月(2008).

今尾浩士, 下山拓也, 満汐孝治, Hassan T. A., 金井保之, 榎本嘉範, 黒田直史, 檜垣浩之, 吉良健太郎, 毛利明博, 鳥居寛之, 永田祐吾, 豊田寛, 長嶋泰之, 斎藤晴彦, 山崎泰規: "反水素合成・トラップに向けた陽電子源の開発", 日本物理学会第64回年次大会, (日本物理学会), 東京, 3月(2009).

## Radiation Biology Team

### Publications

#### [Journal]

(Original Papers) \*Subject to Peer Review

Tanigawa N., Kashiwabara T., Hokura A., Abe T., Shibata M., and Nakayama M.: “A peculiar yellow flower coloration of camellia using aluminum-flavonoid interaction”, *J. Jpn. Soc. Hort. Sci.* **77**, No. 4, pp. 402–407 (2008). \*

Fukuda N., Hokura A., Kitajima N., Terada Y., Saito H., Abe T., and Nakai I.: “Micro X-ray fluorescence imaging and micro X-ray absorption spectroscopy of cadmium hyper-accumulating plant, *Arabidopsis helleri* ssp. *gemmifera*, using high-energy synchrotron radiation”, *Journal of Analytical Atomic Spectrometry* **23**, 1068–1075 (2008). \*

Kanaya T., Saito H., Hayashi Y., Fukunishi N., Ryuto H., Miyazaki K., Kusumi T., Abe T., and Suzuki K.: “Heavy-ion beam-induced sterile mutants of verbena (*Verbena × Hybrida*) with an improved flowering habit”, *Plant Biotechnol.* **25**, No. 1, pp. 91–96 (2008). \*

Kanaya T., Saito H., Hayashi Y., Fukunishi N., Ryuto H., Miyazaki K., Abe T., and Suzuki K.: “A Heavy-ion beam-induced mutant of *Verbena × Hybrida* and wild-type *V. peruviana* demonstrate different types of self-incompatibility”, *Plant Biotechnol.* **25**, No. 1, pp. 97–100 (2008). \*

Sugiyama M., Saito H., Ichida H., Hayashi Y., Ryuto H., Fukunishi N., Terakawa T., and Abe T.: “Biological effects of heavy-ion beam irradiation on cyclamen”, *Plant Biotechnol.* **25**, No. 1, pp. 101–104 (2008). \*

Kazama Y., Saito H., Miyagai M., Takehisa H., Ichida H., Miyazawa Y., Mishiba K., Kanaya T., Suzuki K., Bae C., Miyoshi K., Mii M., and Abe T.: “Effect of heavy ion-beam irradiation on plant growth and mutation induction in *Nicotiana tabacum*”, *Plant Biotechnol.* **25**, No. 1, pp. 105–111 (2008). \*

Kazama Y., Saito H., Yamamoto Y. Y., Hayashi Y., Ichida H., Ryuto H., Fukunishi N., and Abe T.: “LET-dependent effects of heavy-ion beam irradiation in *Arabidopsis thaliana*”, *Plant Biotechnol.* **25**, No. 1, pp. 113–117 (2008). \*

Ryuto H., Fukunishi N., Hayashi Y., Ichida H., Abe T., Kase M., and Yano Y.: “Heavy-ion beam irradiation facility for biological samples in RIKEN”, *Plant Biotechnol.* **25**, No. 1, pp. 119–122 (2008). \*

Hirayama R., Ito A., Tomita M., Tsukada T., Yatagai F., Noguchi M., Matsumoto Y., Kase Y., Ando K., Okayasu R., and Furusawa Y.: “Contributions of direct and indirect actions in cell killing by high-LET radiations”, *Radiat. Res.* **171**, 212–218 (2009). \*

(Review)

Kazama Y. and Matsunaga S.: “The use of repetitive DNA in cytogenetic studies of plant sex chromosomes”, *Cyto-*

*genet. Genome Res.* **120**, No. 3/4, pp. 247–254 (2008).  
阿部知子: “桜の新品種「仁科蔵王」誕生物語”, *Isotope News*, No. 648, pp. 13–15 (2008).

阿部知子: “イオンビームを用いて新しい花を創る一理化学研究所の挑戦(その1)”, *NL だより*, No. 369, p. 3 (2008).

阿部知子: “イオンビームを用いて新しい花を創る一理化学研究所の挑戦(その2)”, *NL だより*, No. 372, p. 3 (2008).

杉山正夫, 寺川輝彦, 林依子, 阿部知子: “重イオンビームと組織培養技術を利用したシクラメンの新品種育成への取り組み”, *放射線と産業* **119**, 4–8 (2008).

大坪憲弘, 間竜太郎, 阿部知子: “遺伝子組み換えと重イオンビーム照射の組み合わせによる高品位花き育成の試み”, *放射線と産業* **119**, 13–17 (2008).

阿部知子: “イオンビームを用いて新しい花を創る一理化学研究所の挑戦(その3)”, *NL だより*, No. 373, p. 3 (2009).

(Others)

Sasaki K., Aida R., Niki T., Yamaguchi H., Narumi T., Nishijima T., Hayashi Y., Ryuto H., Fukunishi N., Abe T., and Ohtsubo N.: “High-efficiency improvement of transgenic torenia flowers by ion beam irradiation”, *Plant Biotechnol.* **25**, No. 1, pp. 81–89 (2008).

白尾吏, 上野敬一郎, 松山知樹, 市田裕之, 阿部知子: “秋輪ギク品種「新神」のDNAマーカーによる品種識別”, *九州沖縄農業研究情報* **22**, 245–246 (2007).

大坪憲弘, 間竜太郎, 阿部知子: “遺伝子組替と重イオンビーム照射の組み合わせによる高品位花き育成の試み”, *放射線と産業*, No. 119, pp. 13–17 (2008).

(Technical Document)

Kazama Y. and Kawano S.: “Detection of pseudo autosomal region in the *Silene latifolia* Y chromosome by FISH analysis of chromosomal distal end satellite DNAs”, *Cytologia* **73**, No. 2, pp. 2–2 (2008).

#### [Book・Proceedings]

(Original Papers) \*Subject to Peer Review

Abe T., Kazama Y., Ichida H., Hayashi Y., Ryuto H., and Fukunishi N.: “Plant breeding using the ion beam irradiation in RIKEN”, *Proceedings of 18th International Conference on Cyclotrons and Their Applications (Cyclotrons 2007)*, Giardini Naxos, Italy, 2006–9~10, INFN, Giardini Naxos, pp. 222–224 (2008). \*

Hayashi Y., Takehisa H., Kazama Y., Ichida H., Ryuto H., Fukunishi N., Abe T., Kanba C., and Sato T.: “Effect of ion beam irradiation on mutation induction in rice”, *Proceedings of 18th International Conference on Cyclotrons and Their Applications (Cyclotrons 2007)*, Giardini Naxos, Italy, 2007–9~10, INFN, Giardini Naxos, pp. 237–239 (2008). \*

(Review)

白尾吏, 上野敬一郎, 松山知樹, 阿部知子: “イオンビーム育種により育成した秋輪ギク「今神」の品種識別”, *DNA 多型* Vol.16, 日本DNA多型学会, 東京, pp. 108–110 (2008).

阿部知子: “サイクロトロンを使った新しい植物誕生物語”, *仁科芳雄博士記念科学講演会講演録* 第18巻, 里庄町, 2007–8, 大内恒章, 岡山県里庄町, pp. 29–61 (2008).

阿部知子: “重イオンビーム育種で「日本ブランド」を創

る”, 第 43 回 RI・放射線利用促進セミナー抄録集, 名古屋, 2008-2, (社) 日本原子力産業協会 中部原子力懇談会, 名古屋, pp. 11-20 (2008).

(Others)

Kazama Y., Saito H., Hayashi Y., Ichida H., Ohbu S., Ryuto H., Fukunishi N., and Abe T.: “Effects of ion beam irradiation on mutation induction in *Arabidopsis thaliana*”, Proceedings of 18th International Conference on Cyclotrons and Their Applications (Cyclotrons 2007), Giardini Naxos, Italy, 2007-9~10, INFN, Giardini Naxos, pp. 240-242 (2008).

### Oral Presentations

(International Conference etc.)

Ikeda T., Kojima T., Iwai Y., Kanai Y., Kambara T., Nebiki T., Narusawa T., and Yamazaki Y.: “Production of a nm sized slow HCI beam with a guiding effect”, 13th International Conference on the Physics of Highly Charged Ions (HCI 2006), Belfast, UK, Aug.-Sept. (2006).

Saito T., Tabayashi A., Kazama Y., Abe T., and Hayashi Y.: “The effect of heavy ion beam on the tea plant”, 3rd International Conference on O-CHA (Tea) Culture and Science, Shizuoka, Nov. (2007).

Takehisa H., Fukuta Y., Yamaya T., Abe T., and Sato T.: “Epistatic interaction of *qLb-3* and *qLb-11* controlling leaf-bronzing in rice (*Oryza sativa* L.) grown in reduced soil”, 9th Conference of the International Society for Plant Anaerobiosis (ISPA): Molecular, Physiological and Ecological Adaptations to Flooded Conditions by Crops and Native Plants, Sendai, Nov. (2007).

Kazama Y., Ohbu S., Hayashi Y., Matsuyama T., and Abe T.: “New technology for inducing deletion mutants in *Arabidopsis thaliana*”, 19th International Conference on Arabidopsis Research, (The North American Arabidopsis Steering Committee), Montreal, Canada, July (2008).

Koizumi A., Nishihara K., Yamanaka K., Ishii K., Kazama Y., Abe T., and Kawano S.: “Asexual and bisexual mutants caused by defective sex-chromosomes in the dioecious plant, *Silene latifolia*”, 20th International Congress of Genetics, (The International Genetics Federation), Berlin, Germany, July (2008).

Nishihara K., Kazama Y., Fujiwara M., Koizumi A., Abe T., and Kawano S.: “Roles of *SUPERMAN* and *WUSCHEL* in the female differentiation of the dioecious plant *Silene latifolia*”, 20th International Congress of Genetics, (The International Genetics Federation), Berlin, Germany, July (2008).

Ishii K., Amanai Y., Kazama Y., Sugiyama R., and Kawano S.: “Three BAC clones containing distal regions of sex chromosomes in the dioecious plant, *Silene latifolia*”, 20th International Congress of Genetics, (The International Genetics Federation), Berlin, Germany, July (2008).

Niwa K., Hayashi Y., Abe T., and Aruga Y.: “Induc-

tion and isolation of pigmentation mutants of *Porphyra yezoensis* (Bangiales, Rhodophyta) by heavy-ion beam irradiation”, 5th Asian Pacific Phycological Forum, Wellington, New Zealand, Nov. (2008).

Murai K. and Abe T.: “Chromatin deletion mutants in einkorn wheat induced by ion-beam irradiation”, 3rd Asian Chromosome Colloquium 2008, Suita, Dec. (2008).

Ichida H.: “Heavy-ion irradiation and in silico RLGS – new technologies to induce and detect bacterial mutations”, Brookhaven National Laboratory Biology Seminar, (Biology Department, Brookhaven National Laboratory), Upton, USA, Dec. (2008).

Honda I., Nishihara K., Kikuchi K., Matsuo S., Fukuda M., Kazama Y., Kawano S., and Abe T.: “Physiological analysis of pepper dwarf mutants induced by heavy-ion-irradiation”, NARO International Symposium on Solanaceae Genomics to Agriculture and Food Research; Aiming for Effective and Efficient Application, (National Institute of Vegetable and Tea Science), Tsu, Mar. (2009).

Imanishi S., Suzuki T., Noguchi A., Hatakeyama R., Nagata M., Abe T., and Honda I.: “Resources and tools for tomato functional genomics developed by NIVTS/NARO: Libraries of ‘Micro-Tom’ tomato mutations induced by heavy-ion bombardment and “whole gene” microarray”, NARO International Symposium on Solanaceae Genomics to Agriculture and Food Research; Aiming for Effective and Efficient Application, Tsu, Mar. (2009).

(Domestic Conference)

阿部知子: “理研の重イオンビーム育種の取り組み”, 平成 18 年度明日の和泊農業を考える会講演会, (明日の和泊農業を考える会), 鹿児島県和泊町, 1 月 (2007).

阿部知子: “花き分野でのイオンビーム育種の活用について”, 平成 18 年度農家育種家育成研修 洋ラン・草花育種研究会 合同研修会, (長崎県), 雲仙, 2 月 (2007).

阿部知子: “イオンビームの育種への応用”, 農林業先端技術講演会, (長崎県総合農林試験場), 長崎, 2 月 (2007).

阿部知子: “農業分野におけるイオンビーム育種の可能性と最新技術”, イオンビーム育種に関する勉強会, (埼玉県農林総合研究センター), 久喜, 2 月 (2007).

阿部知子: “イオンビーム照射技術の基本的理論”, 平成 18 年度研究人材活性化対策事業研究推進支援研修, (神奈川県農業技術センター), 平塚, 3 月 (2007).

阿部知子: “イオンビーム照射技術を利用した植物育種への応用”, 平成 18 年度研究人材活性化対策事業研究推進支援研修, (神奈川県農業技術センター), 平塚, 3 月 (2007).

阿部知子: “加速器を使って植物の新品種を創る”, 第 4 回日本加速器学会年会・第 32 回リニアック技術研究会, (日本加速器学会年会), 和光, 8 月 (2007).

阿部知子: “サイクロトロンを使った新しい植物誕生物語”, 第 16 回理化学研究所里庄セミナー, (科学振興仁科財団), 岡山県里庄町, 8 月 (2007).

阿部知子: “イオンビームによる地球環境・食糧問題を解決す

- る高機能植物の創出”, 理化学研究所と親しむ会第 13 回セミナー, (理研と親しむ会), 東京, 11 月 (2007).
- 阿部知子: “理研における重イオン加速器を用いた植物科学の取組み”, 理研シンポジウム「重イオン加速器を用いた植物科学の革新」, 和光, 1 月 (2008).
- 阿部知子: “重イオンビーム育種で「日本ブランド」を創る—高機能植物の創出—”, 第 43 回 RI・放射線利用促進セミナー, ((社)日本原子力産業協会 中部原子力懇談会), 名古屋, 2 月 (2008).
- 阿部知子: “加速器を使って新しい植物を創る: 江戸時代の園芸植物を復活”, 第 7 回環境まちづくりフォーラム・埼玉, (埼玉県地球温暖化対策西部地域協議会連絡会), 和光, 2 月 (2008).
- 仲條真介, 長谷川聡, 漆原昌二, 阿部知子, 藤田智美, 阿部陽, 大清水保見: “半矮性・低アミロースヒエ新系統の育成”, 日本育種学会第 113 回講演会, (日本育種学会), 川崎, 3 月 (2008).
- 竹久妃奈子, 安田美智子, 福田善通, 小林伸也, 林長生, 仲下英雄, 佐藤雅志, 阿部知子: “インド型イネ品種カサラスの新規いもち病抵抗性遺伝子の検出”, 日本育種学会第 113 回講演会, 川崎, 3 月 (2008).
- 谷川奈津, 柏原輝彦, 保倉明子, 阿部知子, 柴田道夫, 中山真義: “キンカチャの黄色花色の発現におけるアルミニウムの関与”, 園芸学会平成 20 年度春季大会, 厚木, 3 月 (2008).
- 保坂ふみ子, 寺上伸吾, 西谷千佳子, 澤村豊, 高田教臣, 阿部知子, 松山知樹, 山本俊哉: “DNA マーキングによるナシの品種・産地判別技術の開発 1. レトロトランスポゾン領域での DNA 多型”, 園芸学会平成 20 年度春季大会, 厚木, 3 月 (2008).
- 阿部知子: “イオンビーム育種技術の要素”, 理研-KEK ワークショップ「重イオンビームを用いた微生物育種」, 和光, 4 月 (2008).
- 竹久妃奈子, 林依子, 風間裕介, 市田裕之, 三吉一光, 阿部知子: “重イオンビーム照射により誘導されたタバコ (*Nicotiana tabacum* L.) 突然変異 “Meshibedarake” の解析”, 第 5 回イオンビーム育種研究会大会, 敦賀, 5 月 (2008).
- 風間裕介, 齊藤宏之, 林依子, 市田裕之, 龍頭啓充, 福西暢尚, 阿部知子: “重イオンビーム照射において核種・LET が突然変異率へ与える影響”, 第 5 回イオンビーム育種研究会大会, 敦賀, 5 月 (2008).
- 玉木克知, 山中正仁, 小山佳彦, 林依子, 阿部知子: “イオンビーム照射によるキクの花色素変異体の作出”, 第 5 回イオンビーム育種研究会大会, (イオンビーム育種研究会), 敦賀, 5 月 (2008).
- 村井耕二, 阿部知子: “イオンビーム変異体を用いたコムギの生殖成長関連遺伝子の同定と機能解析”, 第 5 回イオンビーム育種研究会大会, (イオンビーム育種研究会), 敦賀, 5 月 (2008).
- 阿部知子: “イオンビーム育種技術の開発と微生物育種への応用”, KEK ワークショップ, (高エネルギー加速器研究機構), つくば, 7 月 (2008).
- 阿部知子: “重イオンビームを用いた「日本ブランド」品種育成技術の開発”, 若狭湾エネルギー研究センター加速器将来計画に関するワークショップ, (若狭湾エネルギーセンター), 敦賀, 7 月 (2008).
- 阿部知子: “重イオンビーム育種技術の開発と新品種”, 第 6 回花部会セミナー「花の新品種育成の魅力—具体的な事例(4)—», (全国新品種育成者の会), 東京, 8 月 (2008).
- 阿部知子: “重イオンビームによる育種技術の開発とその広がり”, 平成 20 年度原子力平和利用連絡協議会講演会, (原子力平和利用連絡協議会), 仙台, 8 月 (2008).
- 阿部知子: “重イオンビーム育種法を用いた「日本ブランド」花き植物の新品種育成”, 平成 20 年度花き研究所研究成果発表会, (農業・食品産業技術総合研究機構 花き研究所), つくば, 8 月 (2008).
- 阿部知子: “重イオンビーム育種による新品種育成”, 東北原子力懇談会講演会, (東北原子力懇談会), 仙台, 8 月 (2008).
- 竹久妃奈子, 風間裕介, 林依子, 市田裕之, 大部登江, 三吉一光, 阿部知子: “炭素イオンビームで誘発したタバコホメオティック変異体の解析”, 日本植物形態学会第 19 回総会・大会, 高知, 9 月 (2008).
- 小泉綾子, 西原潔, 山中香, 石井公太郎, 風間裕介, 阿部知子, 河野重行: “雌雄異株植物ヒロハノマンテマにおける性染色体欠失により引き起こされた無性花変異体と両性花変異体”, 日本植物形態学会第 19 回総会・大会, 高知, 9 月 (2008).
- 菅原慎太郎, 高木宏樹, 齊藤宏之, 阿部知子, 中野優: “ホトギス (*Tricyrtis hirta*) における重イオンビームを照射したエンブリオジェニックカルスからの再生個体の形質調査”, 園芸学会平成 20 年度秋季大会, 津, 9 月 (2008).
- 竹久妃奈子, 風間裕介, 市田裕之, 林依子, 宮沢豊, 三吉一光, 阿部知子: “重イオンビーム照射によるタバコの効率的な変異誘発法の開発と変異体の解析”, 第 26 回日本植物細胞分子生物学会大会・シンポジウム, 吹田, 9 月 (2008).
- 風間裕介, 竹久妃奈子, 市田裕之, 宮沢豊, 金谷健至, 鈴木賢一, 藤原誠, 林依子, 阿部知子: “重イオンビーム照射で作出したタバコ白花変異体は *DFR* 遺伝子に欠失変異をもつ”, 第 26 回日本植物細胞分子生物学会大会・シンポジウム, 吹田, 9 月 (2008).
- 風間裕介, 藤原誠, 竹久妃奈子, 市田裕之, 金谷健至, 鈴木賢一, 林依子, 阿部知子: “タバコ複二倍体ゲノムに生じた重イオンビーム誘発変異の解析”, 日本植物学会第 72 回大会, 高知, 9 月 (2008).
- 村井耕二, 鈴木隆之, 阿部知子: “VRN1/WAP1 欠失変異体の解析からみたコムギ花成遺伝子ネットワーク”, 日本遺伝学会第 80 回大会, 名古屋, 9 月 (2008).
- 阿部知子: “Development of ion irradiation technique for mutation breeding”, RCNP 特別セミナー「重イオンビームを用いた育種技術」, (大阪大学核物理研究センター), 吹田, 9 月 (2008).
- 風間裕介, 阿部知子: “重イオンビームの変異誘導作用における LET 効果の解析”, RCNP 特別セミナー「重イオンビームを用いた育種技術」, (大阪大学核物理研究センター), 大阪, 9 月 (2008).
- 阿部知子: “重イオンビーム照射による組換え花卉高品位技術の開発”, 先端技術を活用した農林水産研究高度化事業成果発表会 2008, (農林水産省), 東京, 9 月 (2008).
- 金會澤, 保坂ふみ子, 寺上伸吾, 西谷千佳子, 澤村豊, 高田教臣, 阿部知子, 松山知樹, 山本俊哉: “DNA マーキングによるナシの品種・産地判別技術の開発 2. RAPD 由来バンドの STS(Sequence Tagged-Site) マーカー化.”, 園芸学会

- 平成 20 年度秋季大会, (園芸学会), 津, 9 月 (2008).
- 竹久妃奈子, 風間裕介, 市田裕之, 林依子, 三吉一光, 阿部知子: “重イオンビーム照射による栽培タバコの組織感受性差異と変異体の解析”, 日本育種学会第 114 回講演会, 彦根, 10 月 (2008).
- 杉山正夫, 風間裕介, 林依子, 寺川輝彦, 阿部知子: “重イオンビーム照射による白花ナデシコ新品種の育成”, 日本育種学会第 114 回講演会, (日本育種学会), 彦根, 10 月 (2008).
- 森下敏和, 清水明美, 山口博康, 出花幸之介, 六笠裕治, 相井城太郎, 長谷純宏, 鹿園直哉, 田中淳, 宮沢豊, 齊藤宏之, 林依子, 龍頭啓充, 福西暢尚, 阿部知子: “ガンマ線およびイオンビーム照射によって得られたダッタンそば半矮性変異体の特性”, 日本育種学会第 114 回講演会, (日本育種学会), 彦根, 10 月 (2008).
- 鈴木隆之, 阿部知子, 村井耕二: “mvp 変異体の解析から明らかとなった WAP1/VRN1 と WFT との関係”, 日本育種学会第 114 回講演会, (日本育種学会), 彦根, 10 月 (2008).
- 林依子, 竹久妃奈子, 風間裕介, 大部澄江, 東海林英夫, 林祐子, 佐藤雅志, 阿部知子: “炭素イオンビーム照射によるイネの突然変異誘発に対する LET の影響”, 日本育種学会第 114 回講演会, (日本育種学会), 彦根, 10 月 (2008).
- 西原潔, 風間裕介, 藤原誠, 阿部知子, 河野重行: “PCR-SSP を用いた雌雄異株植物ヒロハノマンテマの X 染色体連鎖遺伝子のマッピング”, 日本育種学会第 114 回講演会, (日本育種学会), 彦根, 10 月 (2008).
- 風間裕介, 藤原誠, 西原潔, 小泉綾子, 石井公太郎, 河野重行, 阿部知子: “雌雄異株植物ヒロハノマンテマの雌花特異的に発現する遺伝子 *SISUP* の解析”, 日本育種学会第 114 回講演会, 彦根, 10 月 (2008).
- 阿部知子: “イオンビームによる植物育種”, 第 15 回放射線利用技術セミナー「豊かな暮らしを創る放射線の利用」, (文部科学省), 松江, 10 月 (2008).
- 阿部知子: “重イオンビーム育種技術の開発とそれを用いた新品種育成”, 日本アイソトープ協会第 15 回中国・四国支部主任者研修会, ((社) 日本アイソトープ協会), 岡山, 10 月 (2008).
- 阿部知子: “量子ビームを用いて新しい植物を創る”, 平成 20 年度 農業・工業原材料生産と光技術研究会, (光科学技術研究振興財団), 浜松, 10 月 (2008).
- 西原 潔, 風間 裕介, 藤原 誠, 河野 重行, 阿部 知子: “A *WUSCHEL* homologue is exclusively linked to the X chromosome in the dioecious plant *Silene latifolia*”, 理研植物科学研究センター (PSC), かずさ DNA 研究所, 横浜市立大学木原生物学研究所 Joint Retreat 2008, 木更津, 10 月 (2008).
- 風間裕介, 大部澄江, 林依子, 林祐子, 藤原誠, 松山知樹, 阿部知子: “Heavy-ion beam irradiation effectively induces deletion mutations in *Arabidopsis thaliana*”, 理研植物科学研究センター (PSC), かずさ DNA 研究所, 横浜市立大学木原生物学研究所 Joint Retreat 2008, 木更津, 10 月 (2008).
- 竹久妃奈子, 安田美智子, 福田善通, 小林伸也, 林長生, 仲下英雄, 佐藤雅志, 阿部知子: “Identification of novel blast resistant genes in Indica-type rice, Kasalath, using new differential system and mapping population”, 理研植物科学研究センター (PSC), かずさ DNA 研究所, 横浜市立大学木原生物学研究所 Joint Retreat 2008, (RIKEN PSC), 木更津, 10 月 (2008).
- 谷川奈津, 柏原輝彦, 保倉明子, 阿部知子, 柴田道夫, 中山真義: “キンカチャの黄色花色発現”, 植物色素研究会 20 周年記念大会, 熊本, 11 月 (2008).
- 網野真理, 吉岡公一郎, 藤林大輔, 橋田匡史, 島牧義, 藤井敏晴, 田辺晃久, 古澤佳也, 神原正, 児玉逸雄: “イヌ心筋梗塞モデルに対する重粒子線単回照射による心室内遅延電位の長期的改善効果”, 第 25 回日本心電学会学術集会, (日本心電学会), 新潟, 11 月 (2008).
- 泉雅子, 柳憲一郎, 水野武, 今本尚子, 花岡文雄: “複製開始反応におけるヒト Mcm10 の機能”, 第 31 回日本分子生物学会年会・第 81 回日本生化学会大会合同大会 (BMB2008), (日本分子生物学会・日本生化学会), 神戸, 12 月 (2008).
- 阿部知子: “バイオクロストーク機能研究”, 物質の創成研究第一期シンポジウム, 和光, 12 月 (2008).
- 阿部知子: “重イオンビームを用いた植物研究”, 放射線業務従事者教育, (若狭湾エネルギー研究センター), 敦賀, 1 月 (2009).
- 阿部知子: “植物の七変化”, 科学宅配塾 三鷹ネットワーク大学「理化学研究所シリーズ: いま, 科学研究の最先端では…」, (NPO 三鷹ネットワーク大学推進機構), 三鷹, 2 月 (2009).
- 風間裕介, Liu Y., 大部澄江, 林依子, 松山知樹, 阿部知子: “シロイヌナズナの炭素イオンビーム照射で生じる DNA 変異”, 日本育種学会第 115 回講演会, つくば, 3 月 (2009).
- 竹久妃奈子, 林依子, 市田裕之, 宮沢豊, 東海林英夫, 長村吉晃, 佐藤雅志, 阿部知子: “イネ重イオンビーム照射突然変異系統の迅速な変異解析法の検討”, 日本育種学会第 115 回講演会, つくば, 3 月 (2009).
- 藤原誠, 本山高幸, 山口勇, 阿部知子, 伊藤竜一: “シロイヌナズナ珠皮におけるミトコンドリア形態解析”, 日本農芸化学会 2009 年度大会, (日本農芸化学会), 福岡, 3 月 (2009).
- 二羽恭介, 林依子, 阿部知子, 有賀祐勝: “重イオンビーム照射によるスサビノリの人為突然変異体の誘発”, 平成 21 年度日本水産学会春季大会, 東京, 3 月 (2009).
- 井関光太郎, 田中朋之, 阿部知子, 本間香貴, 白岩立彦: “重イオンビーム照射により得られたイネ zebra 突然変異体の特性解析”, 日本作物学会第 227 回講演会, つくば, 3 月 (2009).
- 藤原誠, 伊藤竜一, 森山崇, 丹羽康夫, 佐藤直樹, 阿部知子, 吉田茂男: “シロイヌナズナ葉緑体分裂異常変異体におけるストロミュールを介したアミロプラス複製”, 第 50 回日本植物生理学会年会, (日本植物生理学会), 名古屋, 3 月 (2009).
- 佐々木克友, 山口博康, 間竜太郎, 四方雅仁, 小松拓真, 阿部知子, 大坪憲弘: “第 2 ウォールが萼化したトレンニア変異体を用いた解析 変異表現型の原因遺伝子の解明に向けて”, 第 50 回日本植物生理学会年会, 名古屋, 3 月 (2009).
- 村井耕二, 鈴木隆之, 嶋田早苗, 北川哲, 阿部知子: “コムギの葉における花成関連遺伝子ネットワーク: AP1/FUL-like 遺伝子が FT 遺伝子の上流に位置する”, 第 50 回日本植物生理学会年会, 名古屋, 3 月 (2009).

## RI Applications Team

### Publications

#### [Journal]

(Original Papers) \*Subject to Peer Review

Takechi M., Fukuda M., Mihara M., Chinda T., Matsumasa T., Matsubara H., Nakashima Y., Matsuta K., Minamisono T., Koyama R., Shinosaki W., Takahashi M., Takisawa A., Ohtsubo T., Suzuki T., Momota S., Hatanaka K., Suda T., Sasaki M., Sato S., and Kitagawa A.: “Reaction cross-sections for stable nuclei and nucleon density distribution of proton drip-line nucleus  $8\text{B}$ ”, *Eur. Phys. J. A* **25**, No. s01, pp. 217–219 (2005). \*

Ishii Y., Toyoshima A., Tsukada K., Asai M., Toume H., Nishinaka I., Nagame Y., Miyashita S., Mori T., Suganuma H., Haba H., Sakamaki M., Goto S., Kudo H., Akiyama K., Oura Y., Nakahara H., Tashiro T., Shinohara A., Schaedel M., Bruechle W., Pershina V., and Kratz J. V.: “Fluoride Complexation of Element 104, Rutherfordium (Rf), Investigated by Cation-exchange Chromatography”, *Chem. Lett.* **37**, No. 3, pp. 288–289 (2008). \*

Haba H., Kikunaga H., Kaji D., Akiyama T., Morimoto K., Morita K., Nanri T., Ooe K., Sato N., Shinohara A., Suzuki D., Takabe T., Yamazaki I., Yokoyama A., and Yoneda A.: “Performance of the gas-jet transport system coupled to the RIKEN gas-filled recoil ion separator GARIS for the  $^{238}\text{U}(^{22}\text{Ne},5\text{n})^{255}\text{No}$  reaction”, *J. Nucl. Radiochem. Sci.* **9**, No. 1, pp. 27–31 (2008). \*

Takahashi M. and Takahashi K.: “Estimation of silica Species’ concentrations in lithium and magnesium chloride solutions from the peak intensities observed by FAB-MS”, *J. Solution Chem.* **37**, 1187–1195 (2008). \*

Toyoshima A., Haba H., Tsukada K., Asai M., Akiyama K., Goto S., Ishii Y., Nishinaka I., Sato T., Nagame Y., Sato W., Tani Y., Hasegawa H., Matsuo K., Saika D., Kitamoto Y., Shinohara A., Ito M., Saito J., Kudo H., Yokoyama A., Sakama M., Sueki K., Oura Y., Nakahara H., Schaedel M., Bruechle W., and Kratz J. V.: “Hexafluoro complex of rutherfordium in mixed HF/HNO<sub>3</sub> solutions”, *Radiochim. Acta* **96**, 125–134 (2008). \*

Toyoshima A., Kasamatu Y., Kitatsuji Y., Tsukada K., Haba H., Shinohara A., and Nagame Y.: “Development of an electrochemistry apparatus for the heaviest elements”, *Radiochim. Acta* **96**, 323–326 (2008). \*

Kasamatu Y., Toyoshima A., Haba H., Toume H., Tsukada K., Akiyama K., Yoshimura T., and Nagame Y.: “Adsorption of Nb, Ta and Pa on anion-exchanger in HF and HF/HNO<sub>3</sub> solutions: Model experiments for the chemical study of Db”, *J. Radioanal. Nucl. Chem.* **279**, 371–376 (2009). \*

Tsukada K., Haba H., Asai M., Toyoshima A., Akiyama K., Kasamatu Y., Nishinaka I., Ichikawa S., Yasuda K., Miyamoto Y., Hashimoto K., Nagame Y., Goto S., Kudo

H., Sato W., Shinohara A., Oura Y., Sueki K., Kikunaga H., Kinoshita N., Yokoyama A., Schaedel M., Bruechle W., and Kratz J. V.: “Adsorption of Db and its homologues Nb and Ta, and the pseudo-homologue Pa on anion-exchange resin in HF solution”, *Radiochim. Acta* **97**, 83–89 (2009). \*

Takahashi M., Urabe T., Oikawa T., Nagashima H., and Nemoto M.: “First application of the depth profile of silica species as a tracer by fast-atom bombardment mass spectrometry: investigation of the circulation of seawater and silica uptake by diatoms”, *Rapid Commun. Mass Spectrom.* **23**, 698–704 (2009). \*

(Others)

Asai M., Tsukada K., Sakama M., Ishii Y., Toyoshima A., Ishii T., Nishinaka I., Nagame Y., Kasamatu Y., Shibata M., Hayashi H., Haba H., and Kojima Y.: “Alpha-gamma coincidence spectroscopy of  $^{259}\text{No}$ ”, *JAEA-Review* **2008-054**, 40–41 (2008).

Toyoshima A., Kasamatu Y., Tsukada K., Kitatsuji A., Haba H., Asai M., Ishii Y., Toume H., Akiyama K., Ooe K., Sato W., Shinohara A., and Nagame Y.: “Oxidation of divalent nobelium (No) to the trivalent state using an electrochemistry apparatus”, *JAEA-Review* **2008-054**, 63–64 (2008).

Kasamatu Y., Toyoshima A., Asai M., Tsukada K., Ishii Y., Toume H., Nishinaka I., Sato T., Nagame Y., Haba H., Kikunaga H., Akiyama K., Goto S., Ichikawa T., Kudo H., Sato W., Ooe K., Kuribayashi T., Shinohara A., Kinoshita N., Arai M., Yokoyama A., Sakama M., Qin Z., and Duellmann C. E.: “Adsorption of element 105, Db, on the anion-exchange resin in HF/HNO<sub>3</sub> media”, *JAEA-Review* **2008-054**, 65–66 (2008).

### Oral Presentations

(International Conference etc.)

Toyoshima A., Kasamatu Y., Tsukada K., Kitatsuji A., Haba H., Asai M., Ishii Y., Toume H., Akiyama K., Ooe K., Sato W., Shinohara A., and Nagame Y.: “Electrochemical oxidation of element 102, nobelium”, 2nd International Nuclear Chemistry Congress (2nd-INCC), (National University of Mexico), Cancun, Mexico, Apr. (2008).

Akiyama K., Haba H., Sueki K., Tsukada K., Asai M., Toyoshima A., Nagame Y., and Katada M.: “Metallofullerene Encapsulating  $^{225}\text{Ac}$ ”, 2nd International Nuclear Chemistry Congress (2nd-INCC), (National University of Mexico), Cancun, Mexico, Apr. (2008).

Toyoshima A., Kasamatu Y., Tsukada K., Kitatsuji Y., Haba H., Ishii Y., Toume H., Asai M., Akiyama K., Ooe K., Sato W., Shinohara A., and Nagame Y.: “Characterization of heavy actinides with electrochemistry”, Spring 2008 ACS National Meeting & Exposition, (American Chemical Society), USA, New Orleans, Apr. (2008).

(Domestic Conference)

笠松良崇, 豊嶋厚史, 浅井雅人, 塚田和明, 羽場宏光, 石井康雄,

- 富銘勇人, 西中一朗, 秋山和彦, 菊永英寿, 後藤真一, 石川剛, 工藤久昭, 佐藤渉, 大江一弘, 栗林隆宏, 篠原厚, 木下哲一, 荒井美和子, 横山明彦, 阪間稔, 佐藤哲也, 永目諭一郎: “105 番元素 (Db) の HF/HNO<sub>3</sub> 水溶液中での陰イオン交換樹脂への吸着挙動”, 日本化学会第 88 春季年会, (The Chemical Society of Japan), 東京, 3 月 (2008).
- 五十嵐誠, 望月優子, 高橋和也, 中井陽一, 本山秀明: “火山噴火記録から推定した南極ドームふじコアの堆積年代 1. 1260AD~現在”, 日本地球惑星科学連合 2008 年大会, (日本地球惑星科学連合), 千葉, 5 月 (2008).
- 江崎豊, 神原正, 高橋和也, 宮本寛: “理研 AVF サイクロトロンによる <sup>65</sup>Zn と <sup>109</sup>Cd の製造と有償頒布”, 第 45 回アイソトープ・放射線研究発表会, (日本アイソトープ協会), 東京, 7 月 (2008).
- 菊永英寿, 栗林隆宏, 吉村崇, 高橋成人, 篠原厚, 羽場宏光, 江崎豊, 榎本秀一, 三頭聰明: “α-HIBA/酢酸溶液中での電気泳動法によるランタニドおよびアメリシウム, キュリウム, カリホルニウムの錯安定度定数の導出と加速器実験への適用”, 2008 年日本放射化学会年会/第 52 回放射化学討論会, (日本放射化学会), 広島, 9 月 (2008).
- 菊永英寿, 藤沢弘幸, 矢作亘, 篠原厚, 羽場宏光, 江崎豊, 笠松良崇, 廣瀬健太郎, 大槻勤: “ガスジェット運搬装置を用いた <sup>90m</sup>Nb の精密半減期測定”, 2008 年日本放射化学会年会/第 52 回放射化学討論会, (日本放射化学会), 広島, 9 月 (2008).
- 江崎豊, 神原正, 羽場宏光, 高橋和也: “理研 AVF サイクロトロンによる RI の製造と有償頒布”, 2008 年日本放射化学会年会/第 52 回放射化学討論会, (日本放射化学会), 広島, 9 月 (2008).
- 大江一弘, 矢作亘, 小森有希子, 藤沢弘幸, 菊永英寿, 吉村崇, 佐藤渉, 高橋成人, 高久圭二, 羽場宏光, 工藤祐生, 江崎豊, 篠原厚: “106 番元素シーボーギウムの化学実験に向けたタングステンの溶媒抽出挙動の研究”, 2008 年日本放射化学会年会/第 52 回放射化学討論会, (日本放射化学会), 広島, 9 月 (2008).
- 南里朋洋, 荒木幹生, 西尾正樹, 羽場宏光, 江崎豊, 横山明彦: “Rf 溶液化学のための極微量濃度における TIOA を用いた逆相クロマトグラフィーの研究”, 2008 年日本放射化学会年会/第 52 回放射化学討論会, (日本放射化学会), 広島, 9 月 (2008).
- 藤沢弘幸, 大江一弘, 矢作亘, 小森有希子, 山玲央奈, 菊永英寿, 吉村崇, 高橋成人, 高久圭二, 羽場宏光, 江崎豊, 榎本秀一, 篠原厚: “<sup>238</sup>U(<sup>16</sup>O,4n)<sup>250</sup>Fm 反応による Fm の生成と溶媒抽出挙動”, 2008 年日本放射化学会年会/第 52 回放射化学討論会, (日本放射化学会), 広島, 9 月 (2008).
- 五十嵐誠, 中井陽一, 望月優子, 高橋和也, 本山秀明, 牧島一夫: “火山噴火記録から推定した南極ドームふじ浅層コアの堆積年代: 1260 AD~現在”, 雪氷研究大会 (2008・東京), (日本雪氷学会), 東京, 9 月 (2008).
- 五十嵐誠, 高橋和也, 中井陽一, 望月優子, 本山秀明: “南極ドームふじ浅層コア中に含まれる極微量溶存成分の年変動”, 日本分析化学会第 57 年会, (日本分析化学会), 福岡, 9 月 (2008).
- 五十嵐誠, 中井陽一, 高橋和也, 牧島一夫, 鈴木啓助, 本山秀明: “南極ドームふじ浅層コア中に含まれる極微量溶存成分の年変動”, 日本陸水学会第 73 回大会, (日本陸水学会), 札幌, 10 月 (2008).
- 川畑俊明, 中嶋将太, 鳥山保, 小野田充, 高木靖雄, 川崎克則, 実吉啓二, 長谷川賢一, 前田邦子, 小栗慶之: “波長分散型粒子線誘起 X 線分光システムによる固体高分子型燃料電池中の硫黄の分析”, 第 27 回法政大学イオンビーム工学研究所シンポジウム, (法政大学イオンビーム工学研究所), 小金井, 12 月 (2008).

## Safety Management Group

### Publications

#### [Journal]

(Original Papers) \*Subject to Peer Review

Takamiya K., Ota Y., Akamine M., Shibata S., Shibata T., Ito Y., Imamura M., Uwamino Y., Nogawa N., Baba M., Iwasaki S., and Matsuyama S.: "Excitation function for  $^{63}\text{Cu}(n,p)^{63}\text{Ni}$  reaction in neutron energy range up to 15 MeV", *Appl. Radiat. Isot.* **66**, No. 10, pp. 1321–1324 (2008). \*

Takamiya K., Imanaka T., Ota Y., Akamine M., Shibata S., Shibata T., Ito Y., Imamura M., Uwamino Y., Nogawa N., Baba M., Iwasaki S., and Matsuyama S.: "Nickel-63 production in copper samples exposed to the Hiroshima atomic bomb: estimation based on an excitation function obtained by neutron irradiation experiments", *Radiat. Environ. Biophys.* **47**, 343–348 (2008). \*

(Others)

上義義明: "加速器施設における放射線管理 II. 理研 RI ビームファクトリーの放射線管理", *Radioisotopes* **57**, No. 4, pp. 261–266 (2008).

### Oral Presentations

(International Conference etc.)

Uwamino Y., Sakamoto H., and Fukunishi N.: "Safety Design of the Radioactive Isotope Beam Facility (RIBF) at RIKEN", *Shielding Aspects of Accelerators, Targets and Irradiation Facilities 8th Meeting*, (OECD/NEA), Pohang, Korea, May (2006).

## Publications

## [Journal]

(Original Papers) \*Subject to Peer Review

- Aoki Y., Blum T. C., Christ N. H., Dawson C., Izubuchi T., Mawhinney R. D., Noaki J., Ohta S., Orginos K., Soni A., and Yamada N.: “Kaon B-parameter from quenched domain-wall QCD”, *Phys. Rev. D* **73**, 094507-1–094507-33 (2006). \*
- Patricia L.: “Extraction of  $\Delta G/G$  from HERMES data on Inclusive Charged Hadrons”, *AIP Conf. Proc.* **915**, 331–334 (2007). \*
- Okada H., Bunce G. M., Jinnouchi O., Nakagawa I., Saito N., Alekseev I., Bravar A., Dhawan S., Eyser K. O., Gill R., Haeberli W., Huang H., Makdisi Y. I., Nass A., Stephenson E., Sviridia D., Wise T., Wood J., and Zelenski A.: “Measurements of single and double spin asymmetry in pp elastic scattering in the CNI region with polarized hydrogen gas jet target”, *AIP Conf. Proc.* **915**, 681–684 (2007).
- Samios N. P.: “RHIC: The early years”, *J. Phys. G* **34**, S181–S189 (2007). \*
- Vogelsang W. and Yuan F.: “Hadronic Dijet imbalance and Transverse-Momentum Dependent Parton Distributions”, *Phys. Rev. D* **76**, 094013-1–094013-6 (2007). \*
- Aoki Y. and Wennekens J.: “Heavy-light matrix elements in static limit with domain wall fermions”, *Proceedings of Science*, No. 345, pp. 1–7 (2007). \*
- Albertus C., Aoki Y., Boyle P. A., Christ N. H., Del Debbio L., Dumitrescu T. T., Flynn J. M., Izubuchi T., Loktik O., Sachrajda C. T., Soni A., and Wennekens J.: “ $B - \bar{B}$ -mixing with domain wall fermions in the static approximation”, *Proceedings of Science*, No. 376, pp. 1–7 (2007). \*
- Okada H., Bunce G. M., Jinnouchi O., Nakagawa I., Saito N., Alekseev I., Bravar A., Dhawan S., Eyser K. O., Gill R., Haeberli W., Huang H., Makdisi Y. I., Nass A., Stephenson E., Sviridia D., Wise T., Wood J., and Zelenski A.: “Absolute polarimetry at RHIC”, *AIP Conf. Proc.* **980**, 370–379 (2008).
- Sakuma F., Enyo H., Fukao Y., Funahashi H., Hamagaki H., Kitaguchi M., Miwa K., Murakami T., Naruki M., Ozawa K., Sekimoto M., Tabaru T., Togawa M., Yokkaichi S., Chiba J., Kanda H., Ieiri M., Ishino M., Mihara S., Miyashita T., Muto R., Nakura T., Sasaki O., Tanaka K., Yamada S., and Yoshimura Y.: “Partial decay widths of the phi into  $e+e-$  and  $K+K-$  pairs in 12 GeV p+A reactions at KEK-PS E325”, *Mod. Phys. Lett. A* **23**, No. 27/30, pp. 2401–2404 (2008). \*
- Koike Y., Vogelsang W., and Yuan F.: “On the Relation Between Mechanisms for Single-Transverse-Spin Asymmetries”, *Phys. Lett. B* **659**, 878–884 (2008). \*
- Aoki Y., Boyle P. A., Cooney P., Del Debbio L., Kenway R. D., Maynard C. M., Soni A., and Tweedie R. J.: “Proton lifetime bounds from chirally symmetric lattice QCD”, *Phys. Rev. D* **78**, 054505-1–054505- (2008). \*
- Aoki Y., Boyle P. A., Christ N. H., Dawson C., Donnellan M. A., Izubuchi T., Juttner A., Li S., Mawhinney R. D., Noaki J., Sachrajda C. T., Soni A., Tweedie R. J., and Yamaguchi A.: “Nonperturbative renormalization of quark bilinear operators and  $B_K$  using domain wall fermions”, *Phys. Rev. D* **78**, 054510-1–054510-28 (2008). \*
- Allton C., Antonio D. J., Aoki Y., Blum T. C., Boyle P. A., Christ N. H., Clark M. A., Cohen S. D., Dawson C., Donnellan M. A., Flynn J. M., Hart A., Izubuchi T., Jung C., Juttner A., Kennedy A. D., Kenway R. D., Li M., Li S., Lin M., Mawhinney R. D., Maynard C. M., Ohta S., Pendleton B. J., Sachrajda C. T., Sasaki S., Scholtz E. E., Soni A., Tweedie R. J., Wennekens J., Yamazaki T., and Zanotti J. M.: “Physical results from 2+1 flavor domain wall QCD and SU(2) chiral perturbation theory”, *Phys. Rev. D* **78**, 114509-1–114509-60 (2008). \*
- Boyle P. A., Juttner A., Kenway R. D., Sachrajda C. T., Sasaki S., Tweedie R. J., Soni A., and Zanotti J. M.: “ $K_{13}$  semileptonic form-factor from 2+1 flavour lattice QCD”, *Phys. Rev. Lett.* **100**, 141601-1–141601-4 (2008). \*
- Yamazaki T., Aoki Y., Blum T. C., Lin H., Lin M., Ohta S., Sasaki S., Tweedie R. J., and Zanotti J. M.: “Nucleon Axial Charge in (2+1)-Flavor Dynamical-Lattice QCD with Domain-Wall Fermions”, *Phys. Rev. Lett.* **100**, 171602-1–171602-4 (2008). \*

## Oral Presentations

(International Conference etc.)

- Okada K. and PHENIX C.: “Probing spin-structure of proton with the PHENIX Central Arm Detectors”, 11th Workshop on High Energy Spin Physics, (Joint Institute for Nuclear Research ), Dubna, Russia, Sept.–Oct. (2005).
- Kohama A., Iida K., and Oyamatsu K.: “Reaction cross section and nuclear radius in the black-sphere picture”, International Workshop on “Nuclear Physics with RIBF”, Wako, Mar. (2006).
- Aoki Y., Dawson C., Noaki J., and Soni A.: “Proton decay matrix elements with domain-wall fermions”, Joint Meeting of Pacific Region Particle Physics Communities (DPF2006+JPS2006) , Honolulu, USA, Oct.–Nov. (2006).
- Aoki Y. and RBC/UKQCD c.: “Heavy-light matrix elements in static limit with  $N_f = 2 + 1$  domain wall fermions”, Lattice 2007, 25th International Symposium on Lattice Field Theory, (Physics Department, University of Regensburg), Regensburg, Germany, July–Aug. (2007).
- Aoki Y.: “Nucleon decay matrix elements on the lattice”, Workshop on Next Generation Nucleon Decay and Neu-

trino Detectors 2007 (NNN07-Hamamatsu), (ICRR and KEK), Hamamatsu, Oct. (2007).

Aoki Y.: “Lattice calculations of EOS using stout staggered action”, Hydrodynamics in Heavy Ion Collisions and QCD Equation of State, (RIKEN BNL Research Center), Upton, USA, Apr. (2008).

Aoki Y.: “Quark mass renormalization with non-exceptional momenta”, Lattice 2008, 26th International Symposium on Lattice Field Theory, (College of William and Mary), Williamsburg, USA, July (2008).

(Domestic Conference)

青木保道: “ $B^0 - \bar{B}^0$  mixing in static limit with 2+1 flavor domain wall fermions”, 日本物理学会第 62 回年次大会, 札幌, 9 月 (2007).

青木保道: “Hadronic matrix elements with domain wall fermions”, 筑波大学素粒子論セミナー, つくば市, 9 月 (2007).

青木保道: “クォーク質量非摂動繰り込みスキームの改良”, 日本物理学会 2008 年秋季大会, 山形, 9 月 (2008).

青木保道: “格子上のくりこみの話題”, ワークショップ「計算科学による素粒子・原子核・宇宙の融合」, (筑波大学), つくば, 12 月 (2008).

## Theory Group

### Publications

#### [Journal]

(Original Papers) \*Subject to Peer Review

- Lappi T. and McLerran L.: “Some features of the glasma”, Nucl. Phys. A **772**, 200–212 (2006). \*
- Aoki Y., Blum T. C., Christ N. H., Dawson C., Izubuchi T., Mawhinney R. D., Noaki J., Ohta S., Orginos K., Soni A., and Yamada N.: “Kaon B-parameter from quenched domain-wall QCD”, Phys. Rev. D **73**, 094507-1–094507-33 (2006). \*
- McLerran L.: “Summary Talk for ISMD 06”, Brazilian Journal of Physics **37**, 861–866 (2007).
- Aoki S. and Bar O.: “WChPT Analysis of Twisted Mass Lattice Data”, Eur. Phys. J. A **31**, 781–783 (2007).
- Mocsy A.: “The  $\eta_c$  above deconfinement”, J. Phys. G **34**, 745–748 (2007).
- Fries R.: “Early time evolution of high-energy heavy-ion collisions”, J. Phys. G **34**, S851–S854 (2007). \*
- Armesto N., McLerran L., and Pajares C.: “Long Range Forward-Backward Correlations and the Color Glass Condensate”, Nucl. Phys. A **781**, 201–208 (2007). \*
- Iida K. and Fukushima K.: “Instability of a Gapless Color Superconductor with Respect to Inhomogeneous Fluctuations”, Nucl. Phys. A **785**, 118c–121c (2007). \*
- Fukushima K., Gelis F., and McLerran L.: “Initial Singularity of the Little Bang”, Nucl. Phys. A **786**, 107–130 (2007). \*
- McLerran L.: “The Color Glass Condensate to the Strongly Interacting Quark Gluon Plasma: Theoretical Development”, Nucl. Phys. A **787**, 1c–8c (2007).
- Iancu E. and McLerran L.: “Liouville field theory for gluon saturation in QCD at high energy”, Nucl. Phys. A **793**, 96–127 (2007). \*
- Marquet C.: “Forward Inclusive Dijet Production and Azimuthal Correlations in pA Collisions”, Nucl. Phys. A **796**, 41–60 (2007). \*
- McLerran L. and Pisarski R. D.: “Phases of Dense Quarks at Large  $N_c$ ”, Nucl. Phys. A **796**, 83–100 (2007). \*
- Qiu J., Vogelsang W., and Yuan F.: “Asymmetric di-jet production in polarized hadronic collisions”, Phys. Lett. B **650**, 373–378 (2007). \*
- Aoki Y., Dawson C., Noaki J., and Soni A.: “Proton decay matrix elements with domain-wall fermions”, Phys. Rev. D **75**, 014507-1–014507-24 (2007). \*
- Bomhof C. J., Mulders P. J., Vogelsang W., and Yuan F.: “Single-Transverse Spin Asymmetry in dijet correlation at hadron colliders”, Phys. Rev. D **75**, 074019-1–074019-7 (2007). \*
- Li Y. and Kirill T. L.: “Gluon recombination in high parton density QCD: Inclusive pion production”, Phys. Rev. D **75**, 074022-1–074022-13 (2007). \*
- Maezawa Y., Ukita N., Aoki S., Ejiri S., Ishii N., and Kanaya K.: “Heavy-quark free energy, Debye mass, and spatical string tension at finite temperature in two flavor lattice QCD with Wilson quark action”, Phys. Rev. D **75**, 074501-1–074501-23 (2007). \*
- Marquet C., Peschanski R., and Soyez G.: “Exclusive vector meson production at HERA from QCD with saturation”, Phys. Rev. D **76**, 034011-1–034011-10 (2007). \*
- Fukushima K. and Iida K.: “Larkin-Ovchinnikov-Fulde-Ferrell state in two-color quark matter”, Phys. Rev. D **76**, 054004-1–054004-10 (2007). \*
- Qiu J., Vogelsang W., and Yuan F.: “Single transverse-spin asymmetry in hadronic dijet production”, Phys. Rev. D **76**, 074029-1–074029-30 (2007). \*
- Basak S., Edwards R. G., Fleming G. T., Juge K. J., Morningstar C., Lichtl A., Richard D. G., Sato I., and Wallace S. J.: “Lattice QCD Determination of Patterns of Excited Baryon States”, Phys. Rev. D **76**, 074504-1–074504-14 (2007). \*
- Vogelsang W. and Yuan F.: “Hadronic Dijet imbalance and Transverse-Momentum Dependent Parton Distributions”, Phys. Rev. D **76**, 094013-1–094013-6 (2007). \*
- Marquet C.: “Unified Description of Diffractive Deep Inelastic Scattering with Saturation”, Phys. Rev. D **76**, 094017-1–094017-12 (2007).
- Aoki S., Fukugita M., Ishikawa K., Ishizuka N., Kanaya K., Kuramashi Y., Namekawa Y., Okawa M., Sasaki K., Ukawa A., and Yoshie T.: “Lattice QCD Calculation of the  $\rho$  Meson Decay Width”, Phys. Rev. D **76**, 094506-1–094506-8 (2007). \*
- Blum T. C., Doi T., Hayakawa M., Izubuchi T., and Yamada N.: “Determination of Light Quark Masses From the Electromagnetic Splitting of Pseudoscalar Meson Masses Computed with Two Flavors of Domain Wall Fermions”, Phys. Rev. D **76**, 114508-1–114508-16 (2007). \*
- Avakian H., Brodsky S. J., Deur A., and Yuan F.: “Effect of Orbital Angular Momentum on Valence-Quark Helicity Distributions”, Phys. Rev. Lett. **99**, 082001-1–082001-4 (2007). \*
- Mocsy A.: “Color Screening Melts Quarkonium”, Phys. Rev. Lett. **99**, 211602-1–211602-4 (2007). \*
- Ishikawa T., Azeyanagi T., Hanada M., and Hirata T.: “Phase structure of twisted Eguchi-Kawai model”, Proceedings of Science, No. 054, pp. 1–7 (2007). \*
- Mocsy A.: “Describing Charmonium Correlation Functions in Euclidean Time”, Eur. Phys. J. Special Topics **155**, 101–106 (2008). \*
- Petreczky P.: “Properties of quark gluon plasma from lattice calculations”, Eur. Phys. J. Special Topics **155**, 123–130 (2008). \*
- Azeyanagi T., Hirata T., Hanada M., and Ishikawa T.: “Phase structure of twisted Eguchi-Kawai model”, J. High Energy Phys. **0801**, No. 025, pp. 1–17 (2008). \*

- Petreczky P.: “Progress in finite temperature lattice QCD”, *J. Phys. G* **35**, 044033-1–044033-7 (2008).
- McLerran L.: “From AGS-SPS and onwards to the LHC”, *J. Phys. G* **35**, 104001-1–12 (2008). \*
- Kirill T. L.: “Forward Hadron Production in High Energy  $pA$  Collisions: From RHIC to LHC”, *Nucl. Phys. A* **798**, 61–73 (2008). \*
- Dmitri K. E., McLerran L., and Warringa H. J.: “The Effects of Topological Charge Change in Heavy Ion Collisions: “Event by event P and CP Violation””, *Nucl. Phys. A* **803**, 227–253 (2008). \*
- Dumitru A., Gelis F., McLerran L., and Venugopalan R.: “Glasma flux tubes and the near side ridge phenomenon at RHIC”, *Nucl. Phys. A* **810**, 91–108 (2008). \*
- Karsch F., Kharzeev D. E., and Kirill T. L.: “Universal Properties of Bulk Viscosity Near the QCD Phase Transition”, *Phys. Lett. B* **663**, 217–221 (2008). \*
- Mocsy A. and Petreczky P.: “Can Quarkonia Survive Deconfinement?”, *Phys. Rev. D* **77**, 014501-1–014501-20 (2008). \*
- Cheng M., Christ N. H., Datta S., Heide J. V., Kaczmarek O., Laermann E., Mawhinney R. D., Miao C., Petreczky P., Petrov K., Schmidt C., Soeldner W., and Umeda T.: “The QCD Equation of State with Almost Physical Quark Mass”, *Phys. Rev. D* **77**, 014511-1–014511-20 (2008). \*
- Ishikawa T., Aoki S., Fukugita M., Hashimoto S., Ishikawa K., Ishizuka N., Iwasaki Y., Kanaya K., Kaneko T., Okawa M., Taniguchi Y., Tsutsui N., Ukawa A., Yamada N., and Yoshie T.: “Light-quark masses from unquenched lattice QCD”, *Phys. Rev. D* **78**, No. 011502(R), pp. 011502-1–011502-5 (2008). \*
- Lin H., Blum T., Ohta S., Sasaki S., and Yamazaki T.: “Nucleon structure with two flavors of dynamical domain-wall fermions”, *Phys. Rev. D* **78**, 014505-1–014505-29 (2008). \*
- Aoki Y., Boyle P. A., Christ N. H., Dawson C., Donnellan M. A., Izubuchi T., Juttner A., Li S., Mawhinney R. D., Noaki J., Sachrajda C. T., Soni A., Tweedie R. J., and Yamaguchi A.: “Nonperturbative renormalization of quark bilinear operators and  $B_K$  using domain wall fermions”, *Phys. Rev. D* **78**, 054510-1–054510-28 (2008). \*
- Allton C., Antonio D. J., Aoki Y., Blum T. C., Boyle P. A., Christ N. H., Clark M. A., Cohen S. D., Dawson C., Donnellan M. A., Flynn J. M., Hart A., Izubuchi T., Jung C., Juttner A., Kennedy A. D., Kenway R. D., Li M., Li S., Lin M., Mawhinney R. D., Maynard C. M., Ohta S., Pendleton B. J., Sachrajda C. T., Sasaki S., Scholtz E. E., Soni A., Tweedie R. J., Wennekers J., Yamazaki T., and Zanotti J. M.: “Physical results from 2+1 flavor domain wall QCD and SU(2) chiral perturbation theory”, *Phys. Rev. D* **78**, 114509-1–114509-60 (2008). \*
- Antonio D. J., Boyle P. A., Blum T. C., Christ N. H., Cohen S. D., Dawson C., Izubuchi T., Kenway R. D., Jung C., Li S., Lin M. F., Mawhinney R. D., Noaki J., Ohta S., Pendleton B. J., Scholz E. E., Soni A., Tweedie R. J., and Yamaguchi A.: “Neutral-Kaon Mixing from (2+1)-Flavor Domain-Wall QCD”, *Phys. Rev. Lett.* **100**, 032001-1–032001-4 (2008). \*
- Yuan F.: “Asymmetric azimuthal distribution of hadrons inside a jet at hadron-hadron collisions”, *Phys. Rev. Lett.* **100**, 032003-1–032003-14 (2008). \*
- Yamazaki T., Aoki Y., Blum T. C., Lin H., Lin M., Ohta S., Sasaki S., Tweedie R. J., and Zanotti J. M.: “Nucleon Axial Charge in (2+1)-Flavor Dynamical-Lattice QCD with Domain-Wall Fermions”, *Phys. Rev. Lett.* **100**, 171602-1–171602-4 (2008). \*
- Nawa K., Suganuma H., and Kojo T.: “Brane-induced Skyrmion on  $S^3$ : Baryonic matter in holographic QCD”, *Phys. Rev. D* **79**, 026005-1–026005-25 (2009). \*
- Bulava J. M., Edwards R. G., Engelson E., Foley J., Joo B., Lichtl A., Lin H., Mathur N., Morningstar C., Richards D. G., and Wallace S. J.: “Excited state nucleon spectrum with two flavors of dynamical fermions”, *Phys. Rev. D* **79**, 034505-1–034505-17 (2009). \*
- Ohta S. and Yamazaki T.: “Nucleon structure with dynamical (2+1)-flavor domain wall fermions lattice QCD.”, *Proceedings of Science*, No. 168, pp. 1–14 (2009). \*
- Ishikawa T. and RBC and UKQCD Collab.: “Perturbative  $O(\alpha_s a)$  matching in static heavy and domain-wall light quark system”, *Proceedings of Science*, No. 277, pp. 1–7 (2009). \*
- (Others)
- Kojo T. and Jido D.: “QCD Sum Rules and  $1/N(c)$  expansion”, *Prog. Theor. Phys. Suppl.*, No. 174, pp. 258–261 (2008).
- Nawa K., Suganuma H., and Kojo T.: “Baryonic Matter in Holographic QCD”, *Prog. Theor. Phys. Suppl.*, No. 174, pp. 347–352 (2008).

### Oral Presentations

(International Conference etc.)

- Aoki Y., Dawson C., Noaki J., and Soni A.: “Proton decay matrix elements with domain-wall fermions”, *Joint Meeting of Pacific Region Particle Physics Communities (DPF2006+JPS2006)*, Honolulu, USA, Oct.–Nov. (2006).
- Ishikawa T.: “Phase structure of twisted Eguchi-Kawai model”, *Lattice 2007, 25th International Symposium on Lattice Field Theory*, Regensburg, Germany, July–Aug. (2007).
- Kojo T. and Jido D.: “QCD Sum Rules and  $1/N(c)$  expansion: On the low energy dominance and separation of scattering backgrounds”, *Hadron Structure and QCD: from Low to High energies (HSQCD 2008)*, (St. Petersburg Nuclear Physics Institute), Gatchina, Russia, June–July (2008).

Ishikawa T.: “B meson decay constant in static approximation with domain wall fermion and perturbative  $O(\alpha_s a)$  matching”, Lattice 2008, 26th International Symposium on Lattice Field Theory, Williamsburg, USA, July (2008).

(Domestic Conference)

石川智己: “B meson decay constant in static approximation with 2+1 flavor dynamical domain-wall fermion and perturbative  $O(a)$  matching”, 日本物理学会 2008 年秋季大会, 山形, 9 月 (2008).

## Experimental Group

### Publications

#### [Journal]

(Original Papers) \*Subject to Peer Review

- Abhay D.: “Exploring the Nucleon Helicity Structure with pp collision”, AIP Conf. Proc. **915**, 76–81 (2007). \*
- Samuel A. H. and Abhay D.: “The Future of Spin Physics at BNL”, AIP Conf. Proc. **915**, 184–196 (2007). \*
- Bunce G. M.: “The muon g-2 Experiment at Brookhaven: Past and Future”, AIP Conf. Proc. **915**, 234–239 (2007). \*
- Okada H., Bunce G. M., Jinnouchi O., Nakagawa I., Saito N., Alekseev I., Bravar A., Dhawan S., Eyser K. O., Gill R., Haeberli W., Huang H., Makdisi Y. I., Nass A., Stephenson E., Sviridia D., Wise T., Wood J., and Zelenski A.: “Measurements of single and double spin asymmetry in pp elastic scattering in the CNI region with polarized hydrogen gas jet target”, AIP Conf. Proc. **915**, 681–684 (2007).
- Makdisi Y., Alekseev I., Bellavia S., Bravar A., Bunce G. M., Chapman M. A., Dhawan S., Eyser K., Gasner D., Gill R., Haeberli W., Li Z., Khodinov A., Kponou A., Meng W., Nass A., Okada H., Saito N., Resica S., Stephenson E., Svirida D., Trbojevic D., Tsang T., Wise T., Zelenski A., and Zubets V.: “Status and Operational Experience with the Polarized Hydrogen Jet at RHIC”, AIP Conf. Proc. **915**, 975–978 (2007). \*
- Okada H., Bunce G. M., Jinnouchi O., Nakagawa I., Saito N., Alekseev I., Bravar A., Dhawan S., Eyser K. O., Gill R., Haeberli W., Huang H., Makdisi Y. I., Nass A., Stephenson E., Sviridia D., Wise T., Wood J., and Zelenski A.: “Absolute polarimetry at RHIC”, AIP Conf. Proc. **980**, 370–379 (2008).

### Oral Presentations

(Domestic Conference)

- 岡田謙介, PHENIX C.: “RHIC-PHENIX 実験における高い横運動量光子生成の検出”, 日本物理学会第 62 回年次大会, 札幌, 9 月 (2007).
- 岡田謙介: “Study of proton helicity structure in polarized p+p collisions at RHIC”, 日本物理学会第 62 回年次大会, 札幌, 9 月 (2007).
- 岡田謙介, PHENIX C.: “PHENIX セントラルアームにおける  $\sqrt{s}=500\text{GeV}$ (偏極) 陽子衝突の物理”, 日本物理学会 2008 年秋季大会, 山形, 9 月 (2008).

## RIKEN Facility Office at RAL

### Publications

#### [Journal]

(Original Papers) \*Subject to Peer Review

Yamada F., Ishii Y., Suzuki T., Matsuzaki T., and Tanaka H.: "Pressure-induced reentrant oblique antiferromagnetic phase in the spin-dimer system  $\text{TlCuCl}_3$ ", Phys. Rev. B **78**, 224405-1–224405-6 (2008). \*

### Oral Presentations

(Domestic Conference)

松崎禎市郎: "理研-RAL ミュオン施設におけるミュオン科学の展開", 鹿児島大学理学部物理科学科セミナー, 鹿児島, 5月 (2008).

松崎禎市郎: "理研-RAL 支所ミュオン施設におけるミュオン科学研究", 上智大学大学院理工学研究科理工学専攻物理学領域セミナー, 東京, 6月 (2008).

松崎禎市郎: "ミュオン触媒  $t$ - $t$  核融合で見る  $t+t$  反応の粒子相関", RIBF ミニワークショップ「ダイニュートロン相関をみる」, (仁科加速器研究センター), 和光, 9月 (2008).

**Publications**

**[Journal]**

(Original Papers) \*Subject to Peer Review

- Yamaguchi H., Wakabayashi Y., Amadio G., Hayakawa S., Fujikawa H., Kubono S., He J. J., Kim A., and Binh D. N.: “Development of a cryogenic gas target system for intense radioisotope beam production at CRIB”, Nucl. Instrum. Methods. Phys. Res. A **589**, 150–156 (2008).\*
- Yamaguchi H., Wakabayashi Y., Kubono S., Amadio G., Fujikawa H., Teranishi T., Saito A., He J. J., Nishimura S., Togano Y., Kwon Y. K., Niikura M., Iwasa N., Inafuku K., and Khiem L. H.: “Low-lying non-normal parity states in  $^8\text{B}$  measured by proton elastic scattering on  $^7\text{Be}$ ”, Phys. Lett. B **672**, 230–234 (2009).\*
- He J. J., Kubono S., Teranishi T., Notani M., Baba H., Nishimura S., Moon J. Y., Nishimura M., Michimasa S., Iwasaki H., Yanagisawa Y., Hokoiwa N., Kibe M., Lee J. H., Kato S., Gono Y., and Lee C. S.: “A study of the proton resonant property in  $^{22}\text{Mg}$  by elastic scattering of  $^{21}\text{Na} + p$  and its astrophysical implication in the  $^{18}\text{Ne}(\alpha, p)^{21}\text{Na}$  reaction rate”, Eur. Phys. J. A **36**, 1–5 (2008).\*
- Kwon Y. K., Lee C. S., Moon J. Y., Lee J. H., Kim J. Y., Cheoun M. K., Kubono S., Iwasa N., Inafuku K., Yamaguchi H., He J. J., Saito A., Wakabayashi Y., Fujikawa H., Amadio G., Khiem L. H., Tanaka M., Chen A. A., Kato S., Fuchi Y., and Fukunishi N.: “Astrophysically Important  $^{26}\text{Si}$  States Studied with the  $^{28}\text{Si}(^4\text{He}, ^6\text{He})^{26}\text{Si}$  Reaction”, J. Korean Phys. Soc. **53**, 1141 (2008).\*
- Suzuki T., and Otsuka T.: “Exotic magnetic properties in  $^{17}\text{C}$ ”, Phys. Rev. C **78**, 061301(R) 1–5, (2008).\*
- Yoshida T., Suzuki T., Chiba S., Kajino T., Yokomura H., Kimura K., Takamura A., and Hartmann D. H.: “Neutrino-nucleus reaction cross sections for light element synthesis in supernova explosions”, The Astrophysical Journal **686**, 448–466 (2008).\*
- Adcox K. *et al.* (PHENIX Collaboration): “PHENIX detector overview”, Nucl. Instrum. Methods. A **499**, 469–479 (2003).\*
- Adare A. *et al.* for the PHENIX Collaboration: “Inclusive cross section and double helicity asymmetry for  $\pi^0$  production in  $p + p$  collisions at  $\sqrt{s} = 62.4$  GeV”, Phys. Rev. D **79**, 012003 (2009).\*
- Adare A. *et al.* for the PHENIX Collaboration: “Dilepton mass spectra in  $p + p$  collisions at and the contribution from open charm”, Phys. Lett. B **670**, 313 (2009).\*
- Adare A. *et al.* for the PHENIX Collaboration: “Charged hadron multiplicity fluctuations in Au+Au and Cu+Cu collisions from  $\sqrt{s_{NN}} = 22.5$  to 200 GeV”, Phys. Rev. C **78**, 044902 (2008).\*
- Adare A. *et al.* for the PHENIX Collaboration: “Dihadron azimuthal correlations in Au+Au collisions at  $\sqrt{s_{NN}} = 200$  GeV”, Phys. Rev. C **78**, 014901 (2008).\*
- Adare A. *et al.* for the PHENIX Collaboration: “Onset of  $\pi^0$  Suppression Studied in Cu+Cu collisions at  $\sqrt{s_{NN}} = 22.4, 62.4, \text{ and } 200$  GeV”, Phys. Rev. Lett. **101**, 162301 (2008).
- Adare A. *et al.* for the PHENIX Collaboration: “Suppression Pattern of Neutral Pions at High Transverse Momentum in Au+Au Collisions at  $\sqrt{s_{NN}} = 200$  GeV and Constraints on Medium Transport Coefficients”, Phys. Rev. Lett. **101**, 232301 (2008).\*
- Adare A. *et al.* for the PHENIX Collaboration: “Quantitative constraints on the transport properties of hot partonic matter from semi-inclusive single high transverse momentum pion suppression in Au+Au collisions at  $\sqrt{s_{NN}} = 200$  GeV”, Phys. Rev. C **77**, 064907 (2008).\*
- Adare A. *et al.* for the PHENIX Collaboration: “ $J/\psi$  Production in  $\sqrt{s_{NN}} = 200$  GeV Cu+Cu Collisions”, Phys. Rev. Lett. **101**, 122301 (2008).\*
- Afanasiev S. *et al.* for the PHENIX Collaboration: “Particle-Species Dependent Modification of Jet-Induced Correlations in Au+Au Collisions at  $\sqrt{s_{NN}} = 200$  GeV”, Phys. Rev. Lett. **101**, 082301 (2008).\*
- Afanasiev S. *et al.* for the PHENIX Collaboration: “Source Breakup Dynamics in Au+Au Collisions at  $\sqrt{s_{NN}} = 200$  GeV via Three-Dimensional Two-Pion Source Imaging”, Phys. Rev. Lett. **100**, 232301 (2008).\*
- Imai N., Aoi N., Ong H. J., Sakurai H., Demichi K., Kawasaki H., Baba H., Dombradi Zs., Elekes Z., Fukuda N., Fulop Zs., Gelberg A., Gomi T., Hasegawa H., Ishikawa K., Ishihara M., Iwasaki H., Kaneko E., Kanno S., Kishida T., Kondo Y., Kubo T., Kurita K., Michimasa S., Minemura T., Miura M., Motobayashi T., Nakamura T., Notani M., Ohnishi T. K., Saito A., Shimoura S., Sugimoto T., Suzuki M. K., Takeshita E., Takeuchi S., Tamaki M., Watanabe H., and Yoneda K.: “First lifetime measurement of  $2_1^+$  state in  $^{12}\text{Be}$ ”, Phys. Lett. B **673**, 179–182 (2004).\*
- Elekes Z., Dombradi Z., Aoi N., Baba H., Bishop S., Demichi K., Fulop Z., Gibelin J., Gomi T., Hasegawa H., Hashimoto Y., Imai N., Ishihara M., Iwasa N., Iwasaki H., Kalinka G., Kanno S., Kawai S., Kishida T., Kondo Y., Korshennikov A. A., Kubo T., Kurita K., Kurokawa M., Matsui N., Matsuyama Y., Michimasa S., Minemura T., Motobayashi T., Nakamura T., Nakao T., Nikolskii E. Y., Notani M., Ohnishi T. K., Okumura T., Ong H. J., Ota S., Ozawa A., Perera A., Saito A., Sakai H. K., Sakurai H., Satou Y., Shimoura S., Sohler D., Sumikama T., Suzuki D., Suzuki M., Takeda H., Takeshita E., Takeuchi S., Tamaki M., Togano Y., Yamada K., Yanagisawa Y., and Yoneda K.: “The study of shell closures in light neutron-rich nuclei”, J.Phys.(London) **G35**, 014038 (2008).\*
- Ota S., Shimoura S., Iwasaki H., Kurokawa M., Michimasa S., Aoi N., Baba H., Demichi K., Elekes Z., Fukuchi T., Gomi T., Kanno S., Kubono S., Kurita K., Hasegawa

- H., Ideguchi E., Iwasa N., Matsuyama Y. U., Yurkewicz K. L., Minemura T., Motobayashi T., Murakami T., Notani M., Odahara A., Saito A., Sakurai H., Takeshita E., Takeuchi S., Tamaki M., Teranishi T., Yanagisawa Y., Yamada K., and Ishihara M.: “Low-lying proton intruder state in  $^{13}\text{B}$ ”, *Phys. Lett. B* **666**, 311–314 (2008).\*
- Iwasaki H., Michimasa S., Niikura M., Tamaki M., Aoi N., Sakurai H., Shimoura S., Takeuchi S., Ota S., Honma M., Onishi T. K., Takeshita E., Ong H. J., Baba H., Elekes Z., Fukuchi T., Ichikawa Y., Ishihara M., Iwasa N., Kanno S., Kanungo R., Kawai S., Kubo T., Kurita K., Motobayashi T., Saito A., Satou Y., Suzuki H., Suzuki M. K., Togano Y., and Yanagisawa Y.: “Persistence of the  $N=50$  shell closure in the neutron-rich isotope  $^{80}\text{Ge}$ ”, *Phys. Rev. C* **78**, 021304(R) (2008).\*
- Iwasa N., Motobayashi T., Bishop S., Elekes Z., Gibelin J., Hosoi M., Ieki K., Ishikawa K., Iwasaki H., Kawai S., Kubono S., Kurita K., Kurokawa M., Matsui N., Minemura T., Morikawa H., Nakamura T., Niikura M., Notani M., Ota S., Saito A., Sakurai H., Shimoura S., Sugawara K., Sugimoto T., Suzuki H., Suzuki T., Tanihata I., Takeshita E., Teranishi T., Togano Y., Yamada K., Yamaguchi K., and Yanagisawa Y.: “Large proton contribution to the  $2^+$  excitation in  $^{20}\text{Mg}$  studied by intermediate energy inelastic scattering”, *Phys. Rev. C* **78**, 024306 (2008).\*
- Aoi N., Takeshita E., Suzuki H., Takeuchi S., Ota S., Baba H., Bishop S., Fukui T., Hashimoto Y., Ong H. J., Ideguchi E., Ieki K., Imai N., Ishihara M., Iwasaki H., Kanno S., Kondo Y., Kubo T., Kurita K., Kusaka K., Minemura T., Motobayashi T., Nakabayashi T., Nakamura T., Nakao T., Niikura M., Okumura T., Ohnishi T. K., Sakurai H., Shimoura S., Sugo R., Suzuki D., Suzuki M. K., Tamaki M., Tanaka K., Togano Y., and Yamada K.: “Development of Large Deformation in  $^{62}\text{Cr}$ ”, *Phys. Rev. Lett.* **102**, 012502 (2009).\*
- Kondo Y., Nakamura T., Satou Y., Matsumoto T., Aoi N., Endo N., Fukuda N., Gomi T., Hashimoto Y., Ishihara M., Kawai S., Kitayama M., Kobayashi T., Matsuda Y., Matsui N., Motobayashi T., Nakabayashi T., Ogata K., Okumura T., Ong H. J., Onishi T. K., Otsu H., Sakurai H., Shimoura S., Shinohara M., Sugimoto T., Takeuchi S., Tamaki M., Togano Y., and Yanagisawa Y.: “One-neutron removal reactions of  $^{18}\text{C}$  and  $^{19}\text{C}$  on a proton target”, *Phys. Rev. C* **79**, 014602 (2009).\*
- Kaji D., Morimoto K., Sato N., Ichikawa T., Ideguchi E., Ozeki K., Haba H., Koura H., Kudou Y., Ozawa A., Sumita T., Yamaguchi T., Yoneda A., Yoshida A., and Morita K., “Production and Decay Properties of  $^{263}\text{Hs}$ ”, *J. Phys. Soc. Jpn.* **78**, 035003 (2009).\*
- Nakamura T., Fukuda N., Aoi N., Imai N., Ishihara M., Iwasaki H., Kobayashi T., Kubo T., Mengoni A., Motobayashi T., Notani M., Otsu H., Sakurai H., Shimoura S., Teranishi T., Watanabe Y. X., and Yoneda K.: “Neutron capture cross section of  $^{14}\text{C}$  of astrophysical interest studied by Coulomb breakup of  $^{15}\text{C}$ ”, *Phys. Rev. C* **79**, 035805 (2009).\*
- Shizuma T., Ishii T., Makii H., Hayakawa T., Matsuda M., Shigematsu S., Ideguchi E., Zheng Y., Liu M., Morikawa T., and Oi M.: “One-quasiparticle bands in neutron-rich  $^{187}\text{W}$ ”, *Phys. Rev. C*, **77**, 047303 (2008).\*
- Janek M., Ladygin V. P., Azhgirey L. S., Uesaka T., Gurchin Yu. V., Hatano M., Itoh K., Yu. Isupov A., Karachuk J. T., Kato H., Kawabata T., Krasnov V. A., Khrenov A. N., Kiselev A. S., Kizka V. A., Kliman J., Kurilkin A. K., Kurilkin P. K., Ladygina N. B., Livanov A. N., Maeda Y., Malakhov A. I., Matousek V., Morhach M., Nishikawa J., Pilipenko Yu. K., Ohnishi T., Okamura H., Piyadin S. M., Reznikov S. G., Saito T., Sakaguchi S., Sakai H., Sakamoto N., Sakoda S., Sasamoto Y., Satou Y., Sekiguchi K., Suda K., Shikhalev M. A., Tamii A., Turzo I., Uchigashima N., Vasiliev T. A., Yako K., and Zolin L. S.: “Status of the investigation of the spin structure of  $d$ ,  $^3\text{H}$ , and  $^3\text{He}$  at VBLHE using polarized and unpolarized deuteron beam”, *Phys. Atomic Nuclei* **71**, 1495 (2008).\*
- [Book•Proceedings]**  
(Original Papers) \*Subject to Peer Review
- Yamaguchi H., Wakabayashi Y., Hayakawa S., Amadio G., Kubono S., Fujikawa H., Saito A., He J. J., Teranishi T., Kwon Y. K., Nishimura S., Togano Y., Iwasa N., Inafuku K., Niikura M., Binh D. N., and Khiem L. H.: “Nuclear Structure of  $^8\text{B}$  Studied by Proton Resonance Scatterings on  $^7\text{Be}$ ”, *Origin of Matter and Evolution of Galaxies*, AIP conference proceeding, **1016**, 307–312 (2008).\*
- Yamaguchi H., Wakabayashi Y., Amadio G., Hayakawa S., Fujikawa H., Kubono S., Teranishi T., He J. J., Saito A., Nishimura S., Togano Y., Kwon Y. K., Kim A., Niikura M., Iwasa N., Inafuku K., Khiem L. H., and Binh D.N.: “Nuclear astrophysics studies using low-energy  $^7\text{Be}$  beams at CRIB”, *Nucl. Phys. A.*, **805**, 546–548 (2008).\*
- Togano Y., Gomi T., Motobayashi T., Ando Y., Aoi N., Baba H., Demichi K., Elekes Z., Fukuda N., Fulop Zs., Futakami U., Hasegawa H., Higurashi Y., Ieki K., Imai N., Ishihara M., Ishikawa K., Iwasa N., Iwasaki H., Kanno S., Kondo Y., Kubo T., Kubono S., Kunibu M., Kurita K., Matsuyama Y. U., Michimasa S., Minemura T., Miura M., Murakami H., Nakamura T., Notani M., Ota S., Saito A., Sakurai H., Serata M., Shimoura S., Sugimoto T., Takeshita E., Takeuchi S., Ue K., Yamada K., Yanagisawa Y., Yoneda K., and Yoshida A.: “Investigation of Stellar  $^{26}\text{Si}(p,\gamma)^{27}\text{P}$  Reaction via Coulomb Dissociation”, *Proc. 10th, Int. Sym. on Origin of Matter and Evolution of Galaxies 2007 (OMEG07)*, AIP Conf. Proc. **1016**, 193–198 (2008).\*
- Kwon Y. K., Lee C. S., Moon J. Y., Lee J. H., Kim J. Y., Cheoun M. K., Kubono S., Iwasa N., Inafuku

- K., Yamaguchi H., He J. J., Saito A., Wakabayashi Y., Fujikawa H., Amadio G., Khiem L. H., Tanaka M., Chen A. A., Kato S., Fuchi Y., and Fukunishi N.: “Astrophysically Important  $^{26}\text{Si}$  States Studied with the  $^{28}\text{Si}(^4\text{He}, ^6\text{He})^{26}\text{Si}$  Reaction”, *J. Korean Phys. Soc.* **53**, 1141–1145 (2008).\*
- Yamaguchi H., Wakabayashi Y., Hayakawa S., Binh D. N., Kahl D., Kurihara Y., Kubono S., Teranishi T., He J. J., Kwon Y. K., Nishimura S., Togano Y., Iwasa N., Niikura M., and Khiem L. H.: “Nuclear Astrophysical studies using low-energy RI beams at CRIB”, *Proc. of the 6th Japan-Italy Symposium on Heavy-Ion Physics, AIP Conf. Proc.*, **1120**, 189–193 (2009).\*
- Spitaleri C., Romano S., Lamia L., Puglia S. M. R., Del Szanto M. G., Carlin N., Munhoz M. G., Kroha V., Kubono S., Somoryai E., Szanto de Toledo A., Cherubini S., Crucill V., Gulino M., Kiss G., La Cognata M., Li Chengbo, Neto R. Liguori, De Moura M. M., Pizzone R. G., Rapisarda G. G., Sergi M. L., Souza F. A., Suaide A. A. P., Szanto E., Tabacaru G., Tudisco S., Tumino A., Wakabayashi Y., Wen Qungang, and Yamaguchi H.: “New results on the Trojan Horse Method applied to the  $^{10,11}\text{B}+p$  reactions”, *Proc. of the 6th Japan-Italy Symposium on Heavy-Ion Physics, AIP Conf. Proc.*, **1120**, 171 - 176 (2009).\*
- Teranishi T., Kubono S., Yamaguchi H., He J. J., Saito A., Fujikawa H., Amadio G., Niikura M., Shimoura S., Wakabayashi Y., Nishimura S., Nishimura M., Moon J. Y., Lee C. S., Odahara A., Sohler D., Khiem L. H., Li Z.H., Lian G., and Liu W.P.: “Spectroscopy of resonance levels in  $^{14}\text{O}$  by  $^{13}\text{N}+p$ ”, *Proc. of the 23rd International Nuclear Physics Conference (INPC07)*, Volume 2, pp. 305–307 (2008).\*
- Yamaguchi H., Wakabayashi Y., Amadio G., Hayakawa S., Fujikawa H., Kubono S., Teranishi T., He J. J., Saito A., Nishimura S., Togano Y., Kwon Y. K., Kim A., Niikura M., Iwasa N., Inafuku S., Khiem L. H., and Binh D. N.: “Nuclear astrophysics studies using low-energy  $^7\text{Be}$  beams at CRIB”, *Proc. of the 23rd International Nuclear Physics Conference (INPC07)*, Volume 2, pp. 546–548 (2008).\*
- Cherubini S., Spitaleri C., Crucillà V., Gulino M., La Cognata M., Lamia L., Pizzone R. G., Romano S., Kubono S., Yamaguchi H., Wakabayashi Y., Hayakawa S., Iwasa N., Kato S., Komatsubara H., Teranishi T., Coc A., De Séréville N., and Hammache F.: “The study of  $^{18}\text{F}+p$  reaction at astrophysical energies”, *Proc. of the 6th Japan-Italy Symposium on Heavy-Ion Physics, AIP Conf. Proc.*, **1120**, 294–297 (2009).\*
- Morino Y. for the PHENIX Collaboration: “Measurement of charm and bottom production in p+p collisions at  $\sqrt{s} = 200$  GeV at RHIC-PHENIX”, *Proc. of the 20th International Conference on Ultra-Relativistic Nucleus-Nucleus Collisions (QM2008)*, *J. Phys. G*, **35**, 104116 (2008).\*
- Gunji T., Hamagaki H., Hatsuda T., Hirano T., and Akamatsu Y.: “Onset of  $J/\psi$  melting in quark-gluon fluid at RHIC” *Proc. of the 20th International Conference on Nucleus Nucleus Collisions (QM2008)*, *J.Phys. G: Nucl. Part. Phys.*, **35**, 104137 (2008).\*
- Yamaguchi Y. L. for the PHENIX collaboration: “Dielectron Continuum at PHENIX”, *Proc. of the 43th Recontres de Moriond, Conference Record* (2008).
- Yamaguchi Y. L. for the PHENIX collaboration: “Measurements of low pT direct photons in PHENIX”, *Proc. of the 24th Winter Workshop on Nuclear Dynamics, Conference Record*, (2008).
- Sakaguchi S., Uesaka T., Wakui T., Kawabata T., Aoi N., Hashimoto Y., Ichikawa M., Ichikawa Y., Itoh K., Itoh M., Iwasaki H., Kawahara T., Kuboki H., Maeda Y., Matsuo R., Nakao T., Okamura H., Sakai H., Sakamoto N., Sasamoto Y., Sasano M., Satou Y., Sekiguchi K., Shinohara M., Suda K., Suzuki D., Takahashi Y., Tamii A., Yako K., and Yamaguchi M.: “Spin-orbit potential in  $^6\text{He}$  studied with polarized proton target”, *Proc. of International Nuclear Physics Conference 2007 (INPC2007)*, *Nucl. Phys. A*, **805**, 467–469 (2008).\*
- Sakaguchi S., Uesaka T., Wakui T., Kawabata T., Aoi N., Hashimoto Y., Ichikawa M., Ichikawa Y., Itoh K., Itoh M., Iwasaki H., Kawahara T., Kuboki H., Maeda Y., Matsuo R., Nakao T., Okamura H., Sakai H., Sakamoto N., Sasamoto Y., Sasano M., Satou Y., Sekiguchi K., Shinohara M., Suda K., Suzuki D., Takahashi Y., Tamii A., Yako K., and Yamaguchi M.: “Analyzing power measurement for proton elastic scattering on  $^6\text{He}$ ”, *Proc. of the International Symposium on Physics of Unstable Nuclei (ISPUN07)*, *World Scientific*, 245–248 (2008).\*
- Shimoura S.: “Light Neutron-Rich Nuclei Studied by Alpha-Induced Reactions”, *Proc. of the International Symposium on Physics of Unstable Nuclei (ISPUN07)*, 230–237, (2007).
- Aoi N., Suzuki H., Takeshita E., Takeuchi S., Ota S., Baba H., Bishop S., Fukui T., Hashimoto Y., Ong H. J., Ideguchi E., Ieki K., Imai N., Iwasaki H., Kanno S., Kondo Y., Kubo T., Kurita K., Kusaka K., Minemura T., Motobayashi T., Nakabayashi T., Nakamura T., Nakao T., Niikura M., Okumura T., Ohnishi T. K., Sakurai H., Shimoura S., Sugo R., Suzuki D., Suzuki M. K., Tamaki M., Tanaka K., Togano Y., and Yamada K.: “Shape transition observed in neutron-rich  $pf$ -shell isotopes studied via proton inelastic scattering”, *Proc. of the 23rd International Nuclear Physics Conference (INPC07)*, *Nucl. Phys. A*, **805**, 400c–407c (2008).\*
- Shimoura S., Ota S., Iwasaki H., Kurokawa M., Michimasa S., Kubono S., Teranishi T., Notani M., Tamaki M., Murakami T., Iwasa N., Motobayashi T., Yanagisawa Y., Minemura T., Takeuchi S., Gomi T., Yamada K., Saito A., Baba H., Matsuyama Y. U., Kanno S., Takeshita E., Demichi K., Hasegawa K., Kurita K., Sakurai H., Aoi N., Ideguchi E., Odahara A., Fukuchi T.,

- Miller K., Elekes Z., and Ishihara M.: “Lifetime of the low-lying isomeric  $0^+$  state in  $^{12}\text{Be}$ ”, Proc. of the 23rd International Nuclear Physics Conference (INPC07), Volume 2, pp. 365–367 (2008).\*
- Imai N., Aoi N., Ong H. J., Sakurai H., Demichi K., Kawasaki H., Baba H., Dombrádi Zs., Elekes Z., Fukuda N., Fülöp Zs., Gelberg A., Gomi T., Hasegawa H., Ishikawa K., Iwasaki H., Kaneko E., Kanno S., Kishida T., Kondo Y., Kubo T., Kurita K., Michimasa S., Minemura T., Miura M., Motobayashi T., Nakamura T., Notani M., Ohnishi T. K., Saito A., Shimoura S., Sugimoto T., Suzuki M. K., Takeshita E., Takeuchi S., Tamaki M., Watanabe H., Yoneda K., and Ishihara M.: “The lifetime measurement of the first  $2^+$  state of  $^{12}\text{Be}$ ”, Proceedings of the 23rd International Nuclear Physics Conference (INPC07), Volume 2, pp. 245–247 (2008).\*
- Satou Y., Nakamura T., Fukuda N., Sugimoto T., Kondo Y., Matsui N., Hashimoto Y., Nakabayashi T., Okumura T., Shinohara M., Motobayashi T., Yanagisawa Y., Aoi N., Takeuchi S., Gomi T., Togano Y., Kawai S., Sakurai H., Ong H. J., Ohnishi T. K., Shimoura S., Tamaki M., Kobayashi T., Otsu H., Matsuda Y., Endo N., Kitayama M., and Ishihara M.: “Unbound excited states in  $^{19,17}\text{C}$ ”, Proc. of the 23rd International Nuclear Physics Conference (INPC07), Volume 2, pp. 248–250 (2008).\*
- Imai N., Aoi N., Ong H.J., Sakurai H., Demichi K., Kawasaki H., Baba H., Dombrádi Zs., Elekes Z., Fukuda N., Fülöp Zs., Gelberg A., Gomi T., Hasegawa H., Ishikawa K., Ishihara M., Iwasaki H., Kaneko E., Kanno S., Kishida T., Kondo Y., Kubo T., Kurita K., Michimasa S., Minemura T., Miura M., Motobayashi T., Nakamura T., Notani M., Ohnishi T. K., Saito A., Shimoura S., Sugimoto T., Suzuki M. K., Takeshita E., Takeuchi S., Tamaki M., Watanabe H., and Yoneda K.: “Application of Doppler-shift attenuation method to the de-excitation  $\gamma$  rays from the in-flight  $^{12}\text{Be}$  beam”, Proc. of the 6th Japan-Italy Symposium on Heavy-Ion Physics, AIP Conf. Proc., **1120**, 265–269 (2009).\*
- Shimoura S.: “SHARAQ spectrometer and GRAPE”, Proc. the XVth International Conference on Electromagnetic Isotope Separators and Techniques Related to their Applications, Nucl. Instrum. Methods. Phys. Res. B, **266**, 4131–4136 (2008).\*
- Kawabata T., Berg G. P. A., Kubo T., Sakai H., Shimoura S., and Uesaka T.: “High resolution beam line for the SHARAQ spectrometer”, Proc. the XVth International Conference on Electromagnetic Isotope Separators and Techniques Related to their Applications, Nucl. Instrum. Methods. Phys. Res. B, **266**, 4201–4204 (2008).\*
- Uesaka T., Shimoura S., Sakai H., Berg G. P. A., Nakanishi K., Sasamoto Y., Saito A., Michimasa S., Kawabata T., and Kubo T.: “The high resolution SHARAQ spectrometer”, Proc. the XVth International Conference on Electromagnetic Isotope Separators and Techniques Related to their Applications, Nucl. Instrum. Methods. Phys. Res. B, **266**, 4218–4222 (2008).\*
- Shimoura S.: “High-resolution spectroscopy using direct reactions of RI beams”, Proc. of the 6th Japan-Italy Symposium on Heavy-Ion Physics, AIP Conf. Proc., **1120**, 59–63 (2009).\*
- Kiselev A. S., Ladygin V. P., Uesaka T., Vasiliev T. A., Janek M., Saito T., Hatano M., Isupov A. Yu., Kato H., Ladygina N. B., Maeda Y., Malakhov A. I., Nishikawa J., Ohnishi T., Okamura H., Reznikov S. G., Sakai H., Sakamoto N., Sakoda S., Satou Y., Sekiguchi K., Suda K., Tamii A., Uchigashima N., and Yako K.: “Analyzing powers in the  $^{12}\text{C}(d\rightarrow p)^{13}\text{C}$  reaction at the energy  $T_d = 270$  MeV”, Eur. Phys. J. Special Topics, **162**, 143 (2008).\*
- Kurilkin A. K., Saito T., Ladygin V. P., Uesaka T., Vasiliev T. A., Janek M., Hatano M., Isupov A. Yu., Kato H., Ladygina N. B., Maeda Y., Malakhov A. I., Nishikawa J., Ohnishi T., Okamura H., Reznikov S. G., Sakai H., Sakamoto N., Sakoda S., Satou Y., Sekiguchi K., Suda K., Tamii A., Uchigashima N., and Yako K.: “Measurement of the vector  $A_y$  and tensor  $A_{yy}$ ,  $A_{xx}$ ,  $A_{xz}$  analyzing powers for the  $dd \rightarrow {}^3\text{H} p$  reaction at 200 MeV”, Eur. Phys. J. Special Topics, **162**, 133 (2008).\*
- Kurilkin P. K., Suda K., Uesaka T., Ladygin V.P., Gurchin Yu. V., Isupov A. Yu., Itoh K., Janek M., Karachuk J. T., Kawabata T., Khrenov A. N., Kiselev A. S., Kizka V. A., Kliman J., Krasnov V. A., Ladygina N. B., Livanov A. N., Maeda Y., Malakhov A. I., Matoucek V., Morhac M., Reznikov S. G., Sakaguchi S., Sakai H., Sasamoto Y., Sekiguchi K., Shikhalev M. A., Turzo I., Vasiliev T. A., and Witala H.: “Measurement of the vector and tensor analyzing powers in dp elastic scattering at the energy of 880 MeV”, Eur. Phys. J. Special Topics, **162**, 137 (2008).\*
- Tameshige Y., Hatanaka K., Sagara K., Dozono M., Fujita K., Ihara E., Kaneda T., Kato M., Kawabata T., Kuroita S., Maeda Y., Matsubara H., Okamura H., Sakemi Y., Sekiguchi K., Shimizu Y., Sugimoto T., Tamii A., and Wakasa T.: “Measurement of  $A_{zz}$  of pd radiative capture at  $E_d=196$  MeV”, Few-Body Systems, **44**, 179 (2008).

### Oral Presentations

(International Conference etc.)

- Yamaguchi H., Wakabayashi Y., Hayakawa S., Binh D. N., Kahl D., Kurihara Y., and Kubono S.: “Nuclear Astrophysical Studies Using Low-energy RI Beams at CRIB”, 6th Italy-Japan Symposium on Heavy Ion Physics, Tokai, Ibaraki, Japan, Nov. (2008).
- Yamaguchi H., Wakabayashi Y., Hashimoto T., Hayakawa S., Binh D. N., Kahl D., Kurihara Y., and Kubono S.: “Measurement of proton and alpha resonance scattering using  ${}^7\text{Be}$  beam, at CRIB”, Workshop on Competition of hydrogen burning with  $\nu$  p-process and

- r*-process in explosive nucleosynthesis, Nishina Hall, RIKEN, Saitama, Japan, Feb. (2009).
- Hayakawa S.: “Breakout from the *pp*-chain region through an alternative path  $^{11}\text{C}(\alpha, p)^{14}\text{N}$ ”, Workshop on Competition of hydrogen burning with  $\nu$  *p*-process and *r*-process in explosive nucleosynthesis, Nishina Hall, RIKEN, Saitama, Japan, Feb. (2009).
- Yamaguchi H., Wakabayashi Y., Hashimoto T., Hayakawa S., Binh D. N., Kahl D., Kurihara Y., and Kubono S.: “Current status of nuclear astrophysical studies using RI beams at CRIB”, Workshop on studies of isotope abundances and origin of elements, by means of astronomical observation, analysis on meteorites, and nuclear astrophysics, National Astronomical Observatory of Japan, Tokyo, Japan, Feb. (2009).
- Kubono S.: “Study of Explosive Burning Process with RI Beams”, The 2008 APCTP-BLTP-RIKEN Joint Workshop on Quarks and Mesons in Nuclear Physics, Pohang, Korea Apr. (2008).
- Kubono S.: “The Low Energy RI Beam Facility CRIB and the Activities”, Workshop on Low-energy RI beam facility at MSU, East Lansing, USA, Aug. (2008).
- Kubono S.: “Nuclear Astrophysics with RI Beams”, Workshop on Frontiers in Nuclear Astrophysics, Osaka, Japan, Jan. (2008).
- Kubono S.: “Nuclear Astrophysics with Low Energy RI Beams at CRIB”, Workshop on the strategic approach to the *r*-process, Wako, Japan, Sept. (2008).
- Kubono S.: “Nuclear Astrophysics Programs with Low Energy RI Beams at CRIB”, SSRI workshop, Osaka, Japan, Dec. (2008).
- Kubono S.: “Future of the JAEA Tandem Accelerator Facility”, The memorial workshop on the 100 thousand-our operation of the JAEA tandem operation, Tokai, Ibaraki, Japan, Jan., (2009).
- Kubono S.: “ $\nu p$ -process in Type II Supernovae”, Workshop on *r*-process, Tsukuba, Ibaraki, Japan, Mar. (2009).
- Suzuki T.: “Structure of Light Exotic Nuclei”, The 3rd LACM-EFES-JUSTIPEN Workshop, Oak Ridge, USA, Feb. (2009).
- Suzuki T., and Otsuka T.: “Exotic Electromagnetic Transitions in Neutron-Rich Carbon Isotopes”, Franco-Japanese Symposium on New Paradigms in Nuclear Physics, Paris, France, Sept. (2008).
- Suzuki T., and Otsuka T.: “Electromagnetic Properties of Neutron-Rich Li and C Isotopes”, The 5th International Conference on Exotic Nuclei and Atomic Masses (ENAM08), Ryn, Poland, Sept. (2008).
- Suzuki T.: “Spin Modes, Neutrino-induced Reactions and Nucleosynthesis in Stars”, International Conference on Nuclear Physics and Astrophysics: From Stable Beams to Exotic Nuclei, Cappadocia, Turkey, Jun. (2008).
- Suzuki T.: “Nuclear Structure and Nucleosynthesis”, Theoretical Issues in Nuclear Astrophysics, Orsay, France, Apr. (2008).
- Michimasa S., Gangnant P., Kawabata T., Kurei H., Libin J.F., Miki K., Miya H., Nakanishi K., Ota S., Roussel-Chomaz P., Saito A., Sakai H., Sasamoto Y., Shimoura S., Spitaels C., Tokieda H., and Uesaka T.: “Low-pressure tracking detectors for SHARAQ spectrometer”, ICHOR-EFES International Symposium on New Facet of Spin-Isospin Responses (SIR08), RIKEN, Wako, Japan, Oct. (2008).
- Nakanishi K.: “Ion optical design and current status of SHARAQ spectrometer”, ICHOR-EFES International Symposium on New Facet of Spin-Isospin Responses - Toward the Commissioning of SHARAQ Spectrometer - (SIR2008), RIKEN, Wako, Japan, Oct. (2008).
- Morino Y. for the PHENIX Collaboration: “Measurements of charm and bottom production in pp collisions in PHENIX” 24th Winter Workshop on Nuclear Dynamics, South Padre Island, USA, Apr. (2008).
- Morino Y. for the PHENIX Collaboration “Measurements of charm and bottom production at RHIC-PHENIX” 13th International Conference on Strangeness in Quark Matter, Beijing, China, Oct. (2008).
- Sano S., Hamagaki H., Tanaka Y., Fusayasu T., and Gunji T.: “Development of a Readout Circuit for 2D-Imaging Using GEM” IEEE 2008 Nuclear Science Symposium, Medical Imaging Conference and 16th Room Temperature Semiconductor Detector Workshop, N23-4, Dresden, Germany, Aug. (2008).
- Abe T., and Seki R.: “Hadronic lattice calculation of thermal properties of low-density neutron matter with pionless *NN* effective field theory”, Hokudai-TORJIN-EFES Workshop “Perspectives in Resonances and Continua on Nuclei” & JUSTIPEN-EFES-Hokudai-UNEDF Meeting, Onuma, Hokkaido, Japan, Jul. (2008).
- Abe T., and Seki R.: “Lattice calculation of thermal properties of low-density neutron matter with pionless effective field theory”, EENEN 09, First EMMI-EFES Workshop on Neutron-Rich Nuclei, (GSI), Germany, Feb. (2009).
- Abe T., and Seki R.: “Lattice calculation of thermal properties of low-density neutron matter with pionless effective field theory”, The 2nd LACM-EFES Workshop, (Joint Institute for Heavy Ion Research, Oak Ridge National Laboratory), Oak Ridge, Tennessee, USA, Feb. (2009).
- Niikura M.: Ideguchi E., Michimasa S., Ohnishi T., Onishi T. K., Ota S., Shimoura S., Suzuki H., Suzuki D., Wakabayashi Y., Yoshida K., Zheng Y., Aoi N., Baba H., Fukuchi T., Ichikawa Y., Iwasaki H., Kubo T., Kurokawa M., and Liu M.: “Study of High-spin States in  $^{49-51}\text{Ti}$ ”, CNS-RIKEN Joint Int. Symp. on Frontier of gamma-ray spectroscopy and Perspectives for Nuclear Structure Studies (gamma08), Wako, Saitama, Japan, Apr. (2008).
- Ideguchi E., Shimoura S., Baba H., Fukuchi T., Kurokawa

- M., Michimasa S., Niikura M., and Ota S.: “Development of CNS GRAPE and experiments at RIBF”, CNS-RIKEN Joint Int. Symp. on Frontier of gamma-ray spectroscopy and Perspectives for Nuclear Structure Studies (gamma08), Wako, Saitama, Japan, Apr. (2008).
- Ota S.: “Proton intruder state in the neutron-rich nucleus  $^{13}\text{B}$ ”, Conference on Nuclear Structure 2008 (NS2008), East Lansing, Michigan, USA, Jun., (2008).
- Ideguchi E.: “Gamma-ray spectroscopy instruments in Japan (Present status and future perspectives)”, 7th AGATA Week, Uppsala, Sweden, Jul. (2008).
- Saito A.: “Alpha+ $^8\text{He}$  cluster states in  $^{12}\text{Be}$  via  $\alpha$ -inelastic scattering”, Frontier in Unstable Nuclear Physics, Hokkaido University, Sapporo, Japan, Jul. (2008).
- Shimoura S.: “High-resolution spectroscopy using RI beams — SHARAQ project”, Japanese French Symposium on New paradigms in Nuclear Physics, Institut Henri Poincaré, Paris, France, September 29 – October 2.
- Shimoura S.: “High-resolution spectroscopy using direct reactions of RI beams”, 6th Italy-Japan Symposium on Heavy Ion Physics, Tokai, Ibaraki, Japan, Nov. (2008).
- Ideguchi E.: “Study of High-Spin States by Using Degraded RI Beam at RIBF”, Joint ANL-EFES Workshop for a Compton-Suppressed Ge Clover Array for Stopped and Energy Degraded Exotic Beams at RIKEN, (ANL), Argonne, IL, USA, Dec. (2008).
- Shimoura S.: “Digital electronics for GRAPE”, Joint ANL-EFES Workshop for a Compton-Suppressed Ge Clover Array for Stopped and Energy Degraded Exotic Beams at RIKEN, (ANL), Argonne, IL, USA, Dec. (2008).
- Ideguchi E.: “Study of high-spin states in mass 30 region”, JAEA tandem accelerator workshop, JAEA, Japan, Jan. (2009).
- Shimoura S.: “Proton single-particle states in neutron-rich nuclei”, The 3rd LACM-EFES-JUSTIPEN Workshop, (Oak Ridge National Laboratory), Tennessee, USA, Feb. (2009).
- Ideguchi E.: “Collective band structure in  $^{40}\text{Ar}$ ”, The 3rd LACM-EFES-JUSTIPEN Workshop, (Oak Ridge National Laboratory), Tennessee, USA, Feb. (2009).
- Niikura M.: “In-beam Spectroscopy in  $^{49-51}\text{Ti}$  via Fusion Reaction of RI Beam”, LIA-EFES Workshop on Low-energy collective excitations in exotic nuclei, (GANIL), Caen, France, Mar. (2009).
- Hamagaki H.: “Charmonium and Heavy Quarks – experimental overview –”, 10th Tamura Symposium on Heavy Ion Physics, (University of Texas), Austin, USA, Nov. (2008).
- Hamagaki H.: “Gluon PDF at LHC”, The workshop on Photons and Jets with ALICE, (Central China Normal University), Wuhan, China, Dec. (2008).
- Hamagaki H.: “A Forward Electromagnetic Calorimeter (F-CAL) for the ALICE Experiment”, The workshop on Photons and Jets with ALICE, (Central China Normal University), Wuhan, China, Dec. (2008).
- Gunji T.: “Heavy Quark and Quarkonia Production at RHIC”, The 2nd Asian Triangle Heavy Ion Conference (ATHIC2008), University of Tsukuba, Ibaraki, Japan, Oct. (2008).
- Gunji T.: “Quarkonia Production in High Energy Heavy Ion Collisions at RHIC”, International Conference on Strangeness in Quark Matter 2008, Tsinghua University, Beijing, China, Oct. (2008).
- Morino Y. for the PHENIX Collaboration: “Measurements of charm and bottom production at RHIC-PHENIX”, International Conference on Strangeness in Quark Matter 2008, Tsinghua University, Beijing, China, Oct. (2008).
- Aramaki Y. for the PHENIX Collaboration: “Reaction plane dependence of neutral pion production in center-of-mass energy of 200 GeV Au+Au collisions at RHIC-PHENIX”, The International Conference on Particles And Nuclei (PANIC08), Eilat, Israel, Nov.. (2008).
- Aramaki Y. for the PHENIX Collaboration: “Electromagnetic Particle Production at PHENIX”, Rencontres de Moriond, La Thuile, Italy, Mar. (2009).
- Yamaguchi Y. L. for the PHENIX collaboration: “Measurements of low pT direct photons in PHENIX”, The 24th Winter Workshop on Nuclear Dynamics (WWND2008), South Padre Island, Texas, USA, Apr. (2008).
- Yamaguchi Y. L. for the PHENIX collaboration: “Direct photon in PHENIX”, The 2nd Asian Triangle Heavy Ion Conference (ATHIC2008), University of Tsukuba, Ibaraki, Japan, Oct. (2008).
- Yamaguchi Y. L. for the PHENIX collaboration: “Measurements of Soft and Intermediate pT Photons from Hot and Dense Matter at RHIC-PHENIX”, The 21st International Conference on Ultra-Relativistic Nucleus Nucleus Collisions (Quark Matter 2009), Knoxville, Tennessee, USA, Mar.-Apr. (2009).
- Sano S., Hamagaki H., Tanaka Y., Fusayasu T., and Gunji T.: “Development of a Readout Circuit for 2D-Imaging Using GEM” IEEE 2008 Nuclear Science Symposium, Medical Imaging Conference and 16th Room Temperature Semiconductor Detector Workshop, N23-4, Dresden, Germany, Aug. (2008).
- Gunji T.: “Heavy Quark and Quarkonia Measurement at RHIC & LHC”, The workshop on Photons and Jets with ALICE, Central China Normal University, Wuhan, China, Dec. (2008).
- Uesaka T.: “Spin Polarization in QFS experiments with RI beams”, 1st International Workshop on Quasi-free Scattering with Radioactive Ion Beams, Trento, Italy, Apr. (2008).
- Uesaka T.: “New facets of nuclear spin-isospin responses:

- challenge with the SHARAQ spectrometer”, ICHOR-EFES International Symposium on New Facet of Spin-Isospin Responses, RIKEN, Wako, Saitama, Japan, Oct. (2008).
- Sasamoto Y.: ”High resolution beam line for SHARAQ”, ICHOR-EFES International Symposium on New Facet of Spin-Isospin Responses, RIKEN, Wako, Saitama, Japan, Oct. (2008).
- (Domestic Conference)
- 清水陽平, 上坂友洋, 川畑貴裕, 伊藤圭介, 坂口聡志, 笹本良子, 河原朋美, 時枝紘史, 酒井英行, 矢向謙太郎, 笹野匡紀, 畑中吉治, 岡村弘之, 民井淳, 松原礼明, 野呂哲夫, 若狭智嗣, 堂園昌伯, 山田由希子, 涌井崇志, 吉田英智, 前田幸重: “ $^3\text{He}(p, 2p)$  反応を用いた  $^3\text{He}$  のスピン依存スペクトル関数の研究”, 日本物理学会 2009 年春季大会, 東京, 3 月 (2009).
- 坂口聡志, 上坂友洋, 涌井崇志, 川畑貴裕, 河原朋美, 青井考, 市川雄一, 伊藤圭介, 伊藤正俊, 久保木浩功, 酒井英行, 笹野匡紀, 笹本良子, 島村智之, 清水陽平, 関口仁子, 中尾太郎, 中村隆司, 中山佳晃, 野地俊平: “陽子-He 同位体間のスピン軌道ポテンシャル”, 日本物理学会 2009 年春季大会, 東京, 3 月 (2009).
- 宮裕之, 下浦享, 斎藤明登, 川畑貴裕, 道正新一郎, 大田晋輔, 中西康介, 笹本良子, 三木謙二郎, 樽井博, 上坂友洋, 酒井英行: “低圧動作型多芯線ドリフトチェンバーの性能評価”, 日本物理学会 2009 年春季大会, 東京, 3 月 (2009).
- 時枝 紘史, 上坂 友洋, 下浦 享, 酒井 英行, 道正 新一郎, Roussel-Chomaz P., 大田晋輔, Libin J-F., Gangnant P., Spitaels C.: “SHARAQ 最終焦点面検出器 CRDC 開発”, 日本物理学会 2009 年春季大会, 東京, 3 月 (2009).
- 早川勢也, 山口英斉, 若林泰生, 栗原佑蔵, 久保野茂, 西村俊二, 加治大哉, 森本幸司: “位置読み出し型 MCP ビームモニターの性能評価”, 日本物理学会 2008 年秋季大会, 山形, 9 月 (2008).
- 下浦享: “SHARAQ スペクトロメータの現状と不安定核誘起荷電交換反応実験” 日本物理学会 2008 年秋季大会, 山形, 9 月 (2008).
- 新倉潤, 井手口栄治, 青井考, 馬場秀忠, 福地知則, 市川雄一, 岩崎弘典, 久保敏幸, 黒川明子, Liu M., 道正新一郎, 大西哲也, 大西健夫, 大田晋輔, 下浦享, 鈴木宏, 鈴木大介, 若林泰生, 吉田光一, Zheng Y.: “RI ビームの核融合反応による  $^{49-51}\text{Ti}$  の高スピン核分光”, 日本物理学会 2009 年春季大会, 東京, 3 月 (2009).
- 井手口栄治, 大田晋輔, 森川恒安, 静間俊行, 大島真澄, 小泉光生, 藤嶋輔, 初川雄一, 木村敦, 古高和禎, 中村詔司, 北谷文人, 原田秀郎, 菅原昌彦, 渡辺裕, 平山賀一, 宮武宇也, “ $^{40}\text{Ar}$  の高スピン状態の研究”, 日本物理学会 2009 年春季大会, 東京, 3 月 (2009).
- 浜垣秀樹: “高エネルギー重イオン物理”, 日本物理学会 2008 年秋季大会, 山形, 9 月 (2008).
- Gunji T. for the ALICE Collaboration: “ALICE Performance for the Measurement of Heavy Quarkonia via dielectron decays”, 日本物理学会 2008 年秋季大会, 山形, 9 月 (2008).
- Aramaki Y. for the PHENIX Collaboration: “Measurement of neutral pion production at  $\sqrt{s_{NN}}=200$  GeV Au+Au collisions at RHIC-PHENIX”, 日本物理学会 2008 年秋季大会, 山形, 9 月 (2008).
- 佐野哲, 浜垣秀樹, 郡司卓, Ivanov M., Wiechula J.: “LHC における TPC を用いた粒子多重度測定”, 日本物理学会 2009 年春季大会, 東京, 3 月 (2009).
- 秋元亮二, 浜垣秀樹, 郡司卓, 山口頼人: “Thick GEM の基礎特性”, 日本物理学会 2009 年春季大会, 東京, 3 月 (2009).
- 堀泰斗, 浜垣秀樹, 郡司卓, 佐野哲: “GEM を使った中性子 2 次元 imaging のための DAQ”, 日本物理学会 2009 年春季大会, 東京, 3 月 (2009).
- Takahara A. for the ALICE collaboration “Momentum dependence of the electron identification capability of the ALICE-TRD”, 日本物理学会 2008 年秋季大会, 山形, 9 月 (2008).

# TORIJIN

## Publications

### [Journal]

(Original papers) \*Subject to Peer Review

- N. Itagaki and M. Kimura M.Kimura “Cluster structure stabilized by  $s^2$  neutrons in light neutron-rich nuclei” Phys. Rev. C **79** 034312 1-4 (2009).
- T. Yoshida, N. Itagaki, and T. Otsuka “Appearance of cluster states in  $^{13}\text{C}$ ” Phys. Rev. C **79** 034308 1-6 (2008).
- N. Itagaki, M. Ito, K. Arai, S. Aoyama and Tz. Kokalova “Mixing of di-neutron components in  $^8\text{He}$ ” Phys. Rev. C **78** 017306 1-4 (2008).
- N. Itagaki, M. Ito, M. Milin, T. Hashimoto, H. Ishiyama and H. Miyatake “Coexistence of alpha+alpha+n+n and alpha+t+t cluster structures in  $^{10}\text{Be}$ ” Phys. Rev. C **77** 067301 1-4 (2008).

### Book Proceedings

(Original papers) \*Subject to Peer Review

- N. Itagaki, M. Kimura, M. Ito, S. Aoyama, and Y. Hirata “Application of THSR wave function using Monte Carlo technique” Int. J. Modern Physics Letters A **24** Issue: 11 2019-2026 (2009).
- Y. Iwata, T. Otsuka, J. A. Maruhn, and N. Itagaki “Reduced charge equilibration in heavy-ion collisions at higher energies” AIP Conf. Proc. **1098** 308-312 (2009).
- T. Yoshida, N. Itagaki, and T. Otsuka “Alpha cluster structure in  $^{13}\text{C}$ ” Int. J. Modern Physics E **17** No. 10 2076-2080 (2008).
- T. Yoshida, N. Itagaki, and T. Otsuka “E0 transition strength and cluster structure in  $^{13}\text{C}$ ” AIP Conf. Proc. **1016** 451-453 (2008).

### Oral Presentations

(International Conference etc.)

- N. Itagaki, “ Multi cluster correlations studied with UCOM-like treatment”, First EMMI-EFES workshop on neutron-rich exotic nuclei “Realistic effective nuclear forces for neutron-rich nuclei” 9-11 Feb., GSI, Germany

N. Itagaki, “Cluster-like correlations in light nuclei”, The 3rd LACM-EFES-JUSTIPEN workshop, 23-25 Feb., Oak Ridge National Lab., USA  
(Domestic Conference)

- N. Itagaki, M. Ito, M. Milin, T. Hashimoto, H. Ishiyama, H. Miyatake, “ $\alpha+\alpha+t$  structure in  $^{10}\text{Be}$ ”, 2008 Japan Physical Society Meeting, Yamagata, Sep. 2008
- N. Itagaki, “Exotic structure in the excited states of neutron-rich nuclei”, 64-th Japan Physical Society Meeting, Tokyo, Mar. 2009

## **VII. LIST OF PREPRINTS**

1. Y. Satou, T. Nakamura, N. Fukuda, T. Sugimoto, Y. Kondo, N. Matsui, Y. Hashimoto, T. Nakabayashi, T. Okumura, M. Shinohara, T. Motobayashi, Y. Yanagisawa, N. Aoi, S. Takeuchi, T. Gomi, Y. Togano, S. Kawai, H. Sakurai, H. J. Ong, T. K. Onishi, S. Shimoura, M. Tamaki, T. Kobayashi, H. Otsu, Y. Matsuda, N. Endo, M. Kitayama, and M. Ishihara : “ Unbound excited states in  $^{19}\text{F}$  ”
2. M. Yamagami, and Y. R. Shimizu : “ Spatial structure of neutron Cooper pairs in deformed neutron-rich nuclei ”
3. A. Kohama, K. Iida, and K. Oyamatsu : “ Difference between interaction cross sections and reaction cross sections ”
4. T. Ohnishi, T. Kubo, K. Kusaka, A. Yoshida, K. Yoshida, N. Fukuda, M. Ohtake, Y. Yanagisawa, H. Takeda, D. Kameda, Y. Yamaguchi, N. Aoi, K. Yoneda, H. Otsu, S. Takeuchi, T. Sugimoto, Y. Kondo, H. Scheit, Y. Gono, H. Sakurai, T. Motobayashi, H. Suzuki, T. Nakao, H. Kimura, Y. Mizoi, M. Matsushita, K. Ieki, T. Kuboki, T. Yamaguchi, T. Suzuki, A. Ozawa, T. Moriguchi, Y. Yasuda, T. Nakamura, T. Nannichi, T. sumikama, Y. Nakayama, H. Geissel, H. Weick, J. A. Nolen, O. B. Tarasov, A. S. Nettleton, D. P. Bazin, B. M. Sherrill, D. J. Morrissey, and W. Mittig : “ Identification of New Isotopes  $^{125}\text{Pd}$  and  $^{126}\text{Pd}$  produced by In-flight Fission of  $^{238}\text{U}$ : First Results from the RIKEN RI Beam Factory ”
5. N. Iwasa, T. Motobayashi, S. Bishop, Z. Elekes, J. Gibelin, M. Hosoi, K. Ieki, K. Ishikawa, H. Iwasaki, S. Kawai, S. Kubono, K. Kurita, M. Kurokawa, N. Matsui, T. Minemura, H. Morikawa, T. Nakamura, M. Niikura, M. Notani, S. Ota, A. Saito, H. Sakurai, S. Shimoura, K. Sugawara, T. Sugimoto, H. Suzuki, T. Suzuki, I. Tanihata, E. Takeshita, T. Teranishi, Y. Togano, K. Yamada, K. Yamaguchi, and Y. Yanagisawa : “ Large proton contribution to the  $2^+$  excitation in  $^{20}\text{Mg}$  studied by intermediate energy inelastic scattering ”
6. D. Suzuki, H. Iwasaki, H. J. Ong, N. Imai, H. Sakurai, T. Nakao, N. Aoi, H. Baba, S. Bishop, Y. Ichikawa, M. Ishihara, Y. Kondo, T. Kubo, K. Kurita, T. Motobayashi, T. Nakamura, T. Okumura, T. K. Onishi, S. Ota, M. K. Suzuki, S. Takeuchi, Y. Togano, and Y. Yanagisawa: “Lifetime measurements of excited states in  $^{17}\text{C}$  : possible interplay between collectivity and halo effects ”
7. S. Ota, S. Shimoura, H. Iwasaki, M. Kurokawa, S. Michimasa, N. Aoi, H. Baba, K. Demichi, Z. Elekes, T. Fukuchi, T. Gomi, S. Kanno, S. Kubono, K. Kurita, H. Hasegawa, E. Ideguchi, N. Iwasa, Y. U. Matsuyama, K. L. Yurkewicz, T. Minemura, T. Motobayashi, T. Murakami, M. Notani, A. Odahara, A. Saito, H. Sakurai, E. Takeshita, S. Takeuchi, M. Tamaki, T. Teranishi, Y. Yanagisawa, K. Yamada, and M. Ishihara : “ Low-Iying Proton Intruder State in  $^{13}\text{B}$  ”

8. Z. Elekes, N. Aoi, Zs. Dombrádi, Zu. Fülöp, T. Motobayashi, and H. Sakurai : “ Inelastic Scattering studies of  $^{16}\text{C}$  revisited ”
9. M. Ito, N. Itagaki, H. Sakurai, and K. Ikeda : “ Coexistence of covalent superdeformation and molecular resonances in an unbound region of  $^{12}\text{Be}$  ”
10. M. Ito and N. Itagaki : “ Covalent isomeric state in  $^{12}\text{Be}$  induced by two-neutron transfers ”
11. M. Yamagami, and Y. R. Shimizu, and T. Nakatsukasa : “ Optimal pair density functional for description of nuclei with large neutron excess ”
12. J. Gibelin, D. Beaumel, T. Motobayashi, Y. Blumenfeld, N. Aoi, H. Baba, Z. Elekes, S. Fortier, N. Francaria, N. Fukuda, T. Gomi, K. Ishikawa, Y. Kondo, T. Kudo, V. Lima, T. Nakamura, A. Saito, Y. Satou, J. -A. Scarpaci, E. Takeshita, S. Takeuchi, T. Teranishi, Y. Togano, A. M. Vinodkumar, Y. Yanagisawa, and K. Yoshida : “Decay Pattern of Pygmy States Observed in neutron-Rich  $^{26}\text{Ne}$  ”
13. T. Suda, M. Wakasugi, T. Emoto, K. Ishii, S. Ito, K. Kurita, A. Kuwajima, A. Noda, T. Shirai, T. Tamae, H. Tongu, S. Wang, and Y. Yano : “ First Demonstration of Electron Scattering using a Novel Target Developed for Short-Lived Nuclei ”
14. N. Imai, N. Aoi, H. J. Ong, H. Sakurai, K. Demich, H. Kawasaki, H. Baba, Zs. Dombradi, Z. Elekes, N. Fukuda, Zs. Fulop, A. Gelberg, T. Gomi, H. Hasegawa, K. Ishikawa, M. Ishihara, H. Iwasaki, E. Kaneko, S. Kanno, T. Kishida, Y. Kondo, T. Kubo, K. Kurita, S. Michimasa, T. Minemura, M. Miura, T. Motobayashi, T. Nakamura, M. Notani, T. K. Ohnishi, A. Saito, S. Shimoura, T. Sugimoto, M. K. Suzuki, E. Takeshita, S. Takeuchi, M. Tamaki, H. Watanabe, and K. Yoneda : “ First lifetime measurement of  $2+1$  state in  $^{12}\text{Be}$  ”

RIKEN- NC- AC  
(2008 Jan. ~ 2009 Mar.)

1. T. Fujisawa: “ Impedance Matching in Radio-Frequency Circuits ”

#### CNS-REP

1. S.Ota, S.Shimoura, H.Iwasaki, M.Kurokawa, S.Michimasa, N.Aoi, H.Baba, K.Demichi, Z.Elekes, T.Fukuchi, T.Gomi, S.Kanno, S.Kubono, K.Kurita, H.Hasegawa, E.Ideguchi, N.Iwasa, Y.U.Matsuyama, K.L.Yurkewicz, T.Minemura, T.Motobayashi, T.Murakami, M.Notani, A.Odahara, A.Saito, H.Sakurai, E.Takeshita, S.Takeuchi, M.Tamaki, T.Teranishi, Y.Yanagisawa, K.Yamada, and M.Ishihara:  
“Low-lying Proton Intruder State in  $^{13}\text{B}$ ”
2. H.Yamaguchi, Y.Wakabayashi, S.Kubono, G.Amadio, H.Fujikawa, T.Teranishi, A.Saito, J.J.He, S.Nishimura, Y.Togano, Y.K.Kwon, M.Niikura, Niwasa, K.Inafuku, and L.H.Khirm:  
“Low-lying non-normal parity states in  $^8\text{B}$  measured by proton elastic scattering on  $^7\text{Be}$ ”

## **VIII. LIST OF SYMPOSIA**

(2008 Apr. ~ 2009 Mar.)

1. SAKURA Workshop “International Workshop on Materials and Life Science using Nuclear Probes from High-energy Accelerators” 1-3 Apr. Advanced Meson Science Laboratory
2. CNS-RIKEN Joint International Symposium on Frontier of gamma-ray spectroscopy and Perspectives for Nuclear Structure Studies (gamma08)" 3-5 Apr. CNS, Univ. Tokyo, & RIKEN
3. RIKEN Workshop “Mutation breeding for microorganisms using heavy ion beams” 8 Apr. Radiation Biology Team RIKEN & KEK
4. Riken BNL Workshop “Hydrodynamics in Heavy Ion Collisions and QCD equation of state” 21-22 Apr. RBRC
5. Riken BNL Workshop “Understanding QGP through spectral functions and Euclidean Correlators” 23-25 Apr. RBRC
6. Brookhaven Symposium “Neutrino Helicity at 50: A Celebration of the Goldhaber-Grodzins-Sunyar Experiment” RBRC
7. Workshop “Plant biotechnology for flower breeding in Thailand” 21 May Radiation Biology Team RIKEN
8. Workshop “Mutation breeding for salt tolerant rice” 9 Jun. Radiation Biology Team RIKEN
9. The Frontier of Isotope Science (from nuclear physics to nuclear medicine) 1 Jul. RIKEN & JRIA
10. Joint Illinois-MIT-RBRC Workshop on “Gluon Polarization in the Nucleon” in Urbana 16-17 Jun. RBRC
11. PKU-RBRC Workshop on “Transverse Spin Physics” in Beijing 30 Jun. RBRC
12. Hokudai-TORIJIN JUSTIPEN-EFES workshop “Perspective in Resonances and Continua on nuclei & JUSTIPEN-EFES-Hokkaido-UNEDF meeting”, 21-25 July, Onuma, Hokkaido, EFES, TORIJIN, JUSTIPEN, Hokkaido University
13. Spin Fest lectures August 4-5, Introduction to pQCD by George Sterman (Stony Brook) August 6-7, Transverse Spin Structure of the Nucleon by Mauro Anselmino (Torino) August 7, Acceleration of Polarized Protons by Mei Bai (BNL) August 8, Nucleon Structure and Lattice QCD by John Negele (MIT) RBRC
14. Workshop on the future of hadron physics at J-PARC 1-2 Sep. Strangeness Nuclear Physics Laboratory & Advanced Meson Science Laboratory RIKEN
15. STAR Workshop “Workshop on the Ridge” 22-24 Sep. RBRC
16. 1st JaFNA Workshop on Research Strategy: Program “New Era of Nuclear Physics in the Cosmos -the r-process nucleosynthesis” 25-26 Sep.
17. Japanese-French Symposium “New Paradigms in Nuclear Physics”, 29 Sep. – 2 Oct., Paris, France, EFES, CNRS, IN2P3, RIKEN, IPN, GANIL
18. RSC meeting in Stony Brook 3 Oct. RBRC
19. Special Stony Brook Workshop “Celebration of Edward Shuryak's 60th Birthday” 2-3 Oct.

RBRC

20. ATHIC2008 TSUKUBA 13-15 Oct. CCS, Univ. Tsukuba & RIKEN Nishina Center & CNS, Univ. Tokyo
21. BNL Workshop “UDiG workshop” 16-17 Oct. RBRC
22. International Symposium on New Facet of Spin-Isospin Responses ~ Toward the Commissioning of SHARAQ Spectrometer ~ 29 Oct. CNS, Univ. Tokyo & RIKEN
23. ICHOR-EFES International Symposium on New Facet of Spin-Isospin Responses, 29-31 Oct., Wako, RIKEN, ICHOR program, EFES, RIKEN, CNS University of Tokyo
24. Special High Energy Workshop “Terra Incognita: From LHC to Cosmology” 6-8 Nov. RBRC
25. The 6th Japan-Italy symposium on Heavy Ion Physics, 11-15 Nov., Tokai, JAEA, KEK, RIKEN, NAO, CNS University of Tokyo, EFES
26. Workshop on Superheavy Element Chemistry 2008 12 Nov. Superheavy Element Laboratory RIKEN
27. Special BNL Workshop “Symposium for Gerry Bunce: Celebrating 32 Years of Spin Physics Research at Brookhaven” 19 Nov. RBRC
28. Workshop on Giant Resonances with Inverse Kinematics and Missing Mass Techniques 25 Nov. Nuclear Physics Research Division RIKEN
29. Workshop on Future perspectives in nuclear physics 26-27 Nov. Strangeness Nuclear Physics Laboratory & Theoretical Nuclear Physics Laboratory RIKEN
30. Joint ANL-EFES Workshop for a Compton-Suppressed Ge Clover Array for Stopped and Energy Degraded Exotic Beams at RIKEN, 4-5 Dec., Argonne National Lab., USA, EFES, Argonne National Lab.
31. Workshop on the recent progress and future of physics on few-body problem 23-25 Dec. Strangeness Nuclear Physics Laboratory RIKEN
32. RIKEN Workshop “The use of ion beam for mutation induction in plants and animal cells” 9 Jan. Radiation Biology Team RIKEN & The Wakasa Wan Energy Research Center
33. A Planning of Synchrotron X-ray Use of RIBF at Wako RIKEN 13 Jan. Nishina Center RIKEN
34. Workshop “The use of ion beam for mutation induction in plants and microorganisms” 28 Jan. Radiation Biology Team RIKEN
35. First EMMI-EFES workshop on neutron-rich exotic nuclei “Realistic effective nuclear forces for neutron-rich nuclei” 9-11 Feb., GSI, Germany, EMMI, GSI, EFES
36. Workshop on Competition of hydrogen burning with vp-process and r-process in explosive nucleosynthesis, 19-20 Feb., Nishina Hall, RIKEN, CNS University of Tokyo, RIKEN, JSPS.
37. The 3rd LACM-EFES-JUSTIPEN workshop, 23-25 Feb., Oak Ridge National Lab., USA, EFES, JUSTIPEN, Oak Ridge National Lab.
38. CATHIE-RIKEN Workshop “Critical Assessment of Theory and Experiment on Correlations

at RHIC “ 25-26 Feb. RBRC

39. Workshop on the study of hypernuclear physics and neutron star 1 Mar. Strangeness Nuclear Physics Laboratory RIKEN
40. First LIA-EFES workshop “Low-energy collective motion of exotic nuclei”, 2-4 Mar., GANIL, France, LIA, EFES, GANIL
41. Joint Theory/Experimental Workshop “Early Physics at the LHC “ 16 Mar. RBRC

## **IX. LIST OF SEMINAR**

(2008 Apr. ~ 2009 Mar.)

## Accelerator Division

- 1 Jacques Cherix (PSI) 16 Apr. [PSI National Research Center in Switzerland]
- 2 Jacques Cherix (PSI) 16 Apr. [The RF of the PSI Cyclotron, Specifically LLRF]
- 3 Jameson (BNL) 23 May [Discussion on Comparison of Design and Simulation Codes for RFQs]
- 4 H. Sakaki (Japan Atomic Energy Agency) 11 Jun. [Statistical analysis and control of beam energy for electron linear accelerator]
- 5 T. Shirai (National Institute of Radiological Sciences) 25 Jul. [Ultra Cold Ion Beam Experiments by Electron and Laser Cooling at Ion Storage Ring, S-LSR]
- 6 I. Yamane (KEK) 23 Jan. [Magnetic Neutralizer for cw beam-splitting of high energy H-beam and possibility of Laser Neutralizer option]
- 7 P. Ostroumov (Argonne National Laboratory) 3 Mar. [Development of superconducting heavy-ion accelerators at ANL]
- 8 F. Marti (MSU) 6 Mar. [From NSCL to FRIB, challenges and opportunities.]
- 9 I. Sugai (KEK) 6 Mar. [Development of hybrid long-lived carbon foils with high heat resistance even at 1800 K.]
- 10 N. Nakamura (ILS) 13 Mar. [Principle and application of an electron beam ion source/trap (EBIS/T)]

## Nuclear Physics Research Division

- 1 S. G. Frauendorf (Research Center Dresden-Rossendorf and Univ. of Notre Dame) 8 Apr. RIBF Nuclear Physics Seminar [Dynamic and static chirality of rotating triaxial nuclei]
- 2 Y. Nagai (Japan Atomic Energy Agency) 15 Apr. Monthly Colloquium [Nuclear Astrophysics studied with neutron, alpha, and gamma-ray]
- 3 M. Oi (Physics Department, University of Surrey) 23 Apr. RIBF Nuclear Physics Seminar [Superdeformation of  $^{40}\text{Ca}$ ]
- 4 A. Schwenk (TRIUMF) 25 Apr. RIBF Nuclear Physics Seminar [Frontiers in understanding matter at the extremes]
- 5 H. Murayama (IPMU, Tokyo University) 13 May Monthly Colloquium [The Next Twenty Years in Particle Physics]
- 6 S. Shimoura (CNS, Univ. of Tokyo) 27 May Lecture Series IV-1 [Practical nuclear reaction theory for experimentalists (3rd)]
- 7 T. Nakatsukasa (RIKEN Nishina Center) 10 Jun. RIBF Nuclear Physics Seminar [Nuclear structure studied with the Skyrme density functional approach]
- 8 H. Toki (RCNP, Osaka University) 17 Jun. Monthly Colloquium [Tensor optimized shell model and role of pion in nuclear physics]
- 9 P. Doornenbal (RIKEN Nishina Center) 24 Jun. RIBF Nuclear Physics Seminar [Probing nuclear structure far-off stability with RISING-Gamma-ray spectroscopy with Radioactive Beams at GSI]
- 10 K. Nakai (KEK) 2 Jul. RIBF Nuclear Physics Seminar [UNuclear physics to NUclear physics]
- 11 T. Nishio (Research Center for Innovative Oncology, National Cancer Center) 15 Jul. Monthly Colloquium [Imaging of the irradiated volume using positron-emitting nuclei generated in a patient body by the target nuclear fragment reaction for proton therapy]
- 12 P. Avogadro (RIKEN Nishina Center) 16 Jul. RIBF Nuclear Physics Seminar [Vortices and nuclei in the inner crust of a neutron star]
- 13 M. Takashina (RCNP, Osaka University), *et al* 16 Jul. RIBF Mini-workshop [Analysis of inelastic proton scattering on unstable nuclei using single-folding model with JLM potential]
- 14 M. Yamagami, *et al* 3 Sep. RIBF Mini-workshop [Probing dineutron correlations in RIBF experiment]
- 15 S. Bishop (Technische Universitaet Muenchen) 21 Oct. RIBF Nuclear Physics Seminar [Elastic Scattering of  $^7\text{Be}$ ,  $^8\text{B}$  and a Roadmap to a Self-Consistent Approach to the  $^7\text{Be}$  (p, gamma) Solar S-Factor]
- 16 M. Takechi (RIKEN Nishina Center) 28 Oct. RIBF Nuclear Physics Seminar [Study of Total Reaction Cross Sections]

at Intermediate Energies]

- 17 M. Kamimura (RIKEN Nishina Center) 6 Nov. Monthly Colloquium [Big-bang nucleosynthesis reactions catalyzed by SUSY particle stau.]
- 18 K. Langanke (GSI) 17 Nov. Lecture Series VII-1 [Nuclear Astrophysics (1st)]
- 19 A. Masaike (Kyoto University) 9 Dec. Monthly Colloquium [Perspective of High Energy Physics, Challenge in US and Japan]
- 20 Z. Fulop (ATOMKI) 16 Dec. RIBF Nuclear Physics Seminar [Cross section data for the astrophysical p-process]
- 21 Betty Tsang (NSCL, Michigan State University) and 8 other authors 16-17 Dec. Mini-workshop [Nuclear Collisions and Nuclear Matter]
- 22 P. Moller (Theoretical Division, Los Alamos National Laboratory) 19 Dec. RIBF Nuclear Physics Seminar [FISSION AT THE END OF THE NUCLEAR CHART]
- 23 A. N. Andreyev (IKS, KU Leuven, Belgium) 19 Dec. RIBF Nuclear Physics Seminar [Electron-capture delayed fission (ECDF) in the lead region]
- 24 I. Hamamoto (Lund University) 24 Dec. Lecture Series V-3 [One-particle motion in nuclear many-body problem]
- 25 Ma. Hori (Group leader, Max Planck Institute of Quantum Optics) 8 Jan. RIBF Nuclear Physics Seminar [High precision spectroscopy of antiprotonic atoms—new techniques to manipulate antimatter.]
- 26 H. Oigawa (Japan Atomic Energy Agency) 22 Jan. Monthly Colloquium [Nuclear transmutation technology for ? long-lived radioactive nuclides]
- 27 M. Wada (RIKEN Nishina Center) 29 Jan. RIBF Nuclear Physics Seminar [Precision optical spectroscopy of Be isotopes]
- 28 M. Lantz (RIKEN Nishina Center) 17 Feb. RIBF Nuclear Physics Seminar [FLUKA - A Monte Carlo code for physics and applications]
- 29 M. Ito (RIKEN Nishina Center) 17 Feb. RIBF Nuclear Physics Seminar [Unified studies of structures and reactions in light neutron-rich nuclei---Present analysis of  $^{10,12}\text{Be}$  and future perspectives---
- 30 M. Schadel (GSI) 2 Mar. RIBF Nuclear Physics Seminar [Superheavy element research at GSI]
- 31 K. Muto (TITECH), *et al* 18-19 Mar. [Explorative investigation for the measurement of Gamow-Teller transition strength for neutron rich nuclei]
- 32 S. Chiba (JAEA), *et al* 25-26 Mar. Mini-workshop [Nuclear data and nuclear theory]

#### Theoretical Nuclear Physics Laboratory

- 1 Y. M. Zhao (Shanghai Jiao Tong Univ.) 21 May 7th Nuclear Theory Seminar [Approximate approach of obtaining eigenvalues of given matrices]
- 2 L. Guo (Univ. Tokyo) 11 Jun. 8th Nuclear Theory Seminar [Boost-invariant TDHF theory and the nuclear Landau-Zener effect]
- 3 Y. Iwata (Univ. Tokyo) 9 Jul. 9th Nuclear Theory Seminar [Reduced charge equilibration in heavy-ion collision at higher energy and synthesis of neutron-rich nuclei]
- 4 G. Watanabe (Univ. Trento) 6 Aug. 10th Nuclear Theory Seminar [Nuclear pasta phases in supernovae and neutron stars: Quantum molecular dynamics approach and future prospects]
- 5 H. Schulz (INFN, Universita di Catania) 7 Jan. 11th Nuclear Theory Seminar "Pairing Gaps in Neutron Star Matter"
- 6 W. Long (Peking University and Technischen Universitat Munchen) 18 Feb. 12th Nuclear Theory Seminar [Relativistic Hartree-Fock-Bogoliubov theory with Density Dependent Meson-Nucleon Couplings]

#### Radiation Laboratory

- 1 Dr. O. Sasaki (KEK Associate Professor) 15 May Experience for development and construction of ATLAS TGC

readout

- 2 Prof. Frieder Lenz (The Univ. Erlangen-Nurnberg), *et al* 13 Nov. Lab. Seminar Physics Discussions with Frieder Lenz

### Advanced Meson Science Laboratory

- 1 M. Iwasaki (Graduate School of Science, University of Tokyo) 25 Jun. Lab. Seminar [Study of B-meson rare decays at the Belle experiment]
- 2 K. Ohishi (RIKEN Nishina Center) 27 Aug. Lab. Seminar [Influence of self-irradiation in superconducting PuCoGa5 probed by uSR]
- 3 Risdiana (RIKEN Nishina Center) 27 Aug. Lab. Seminar [ $\mu$ SR study of Cu-Spin Fluctuations in Hole and Electron-Doped High-Tc Superconducting Cuprates]
- 4 M. Arai (Materials and Life Science Division, J-PARC) 21 Jan. Lab. Seminar [Neutron scattering approach on strongly correlated electron systems]
- 5 K. Hashimoto (RIKEN Nishina Center) 19 Mar. Lab. Seminar [Superstring theory]

### Theoretical Physics Laboratory

- 1 Y. Tachikawa (School of Natural Sciences, Institute for Advanced Study, USA) 4 Apr. RIKEN Seminar [New Developments in  $d=4$ ,  $N=2$  Superconformal Field Theory]
- 2 F. Nori (Digital Materials Lab.) 14 Apr. Colloquium [Quantum Circuits as Artificial Atoms]
- 3 A. Tsuchiya (Shizuoka University) 18 Apr. RIKEN Seminar [Fiber Bundles and Matrix Models]
- 4 S. Matuura (Niels Bohr Institute, Denmark) 25 Apr. RIKEN Seminar [Relation among supersymmetric lattice gauge theories and matrix theories]
- 5 Y. Matsuo (Department of Physics, Faculty of Science, University of Tokyo) 27 May RIKEN Seminar [Lie 3-algebra and multiple M2 branes]
- 6 D. Yamada (Racah Institute of Physics, The Hebrew University of Jerusalem, Israel) 10 Jun. RIKEN Seminar [Phase Diagrams of  $N=4$  SYM in Strong and Weak Couplings]
- 7 C. Albertsson (Yukawa Institute for Theoretical Physics, Kyoto University) 17 Jun. RIKEN Seminar [D-branes in doubled geometry]
- 8 K. Hashimoto (RIKEN Nishina Center) 18 Jun. Colloquium [The Frontiers of Superstring Theory : “D-branes” and new perspective of our world]
- 9 M. Passera (INFN) 27 Jun. RIKEN Seminar [The muon  $g-2$  and the bounds on the Higgs boson mass]
- 10 N. Maru (Department of Physics, Kobe University) 8 Jul. RIKEN Seminar [Direct Gauge Mediation of Metastable Supersymmetry Breaking]
- 11 Y. Koichi (Graduate School of Science, Kyoto University) 15 Jul. RIKEN Seminar [Detection of neutrino from extra dimensions]
- 12 N. Jokela (Helsinki Institute of Physics, Finland) 22 Jul. RIKEN Seminar [Rolling tachyons, random matrices, and Coulomb gas thermodynamics]
- 13 A. D’adda (I. N. F. N. Sezione di Torino, Italy) 29 Sep. “New Era of Nuclear Physics in the Cosmos -the r-process nucleosynthesis”
- 14 W. Vinci (University of Pisa) 6 Oct. RIKEN Seminar [New Developments on Non-Abelian Vortices]
- 15 H. Kawai (RIKEN Nishina Center) 17 Oct. [Seminar to introduce the Nobel prize in physics 2008 for novices]
- 16 Y. Sugita (Theoretical Biochemistry Laboratory) 20 Oct. Colloquium [All-atom molecular dynamics simulations of membrane proteins in lipid bilayer]
- 17 T. Yamashita (E-ken, Theoretical Particle Physics Group Department of Physics, Graduate School of Science Nagoya University) 20 Oct. RIKEN Seminar [Gauge-Higgs Dark Matter]

- 18 Prof. Deog-Ki Hong (Department of Physics, Pusan National University, Korea) 20 Oct. RIKEN Seminar [Holographic QCD and Baryons]
- 19 T. Onogi (Yukawa Institute for Theoretical Physics, Kyoto University) 1 Nov. RIKEN Seminar [Lattice study of the conformal window in QCD with many flavors]
- 20 J. Nishimura (KEK) 1 Nov. RIKEN Seminar [Simulating Superstrings inside a Black Hole]
- 21 A. Tsuchiya (Department of Physics, Shizuoka University) 1 Nov. RIKEN Seminar [N=4 Super Yang-Mills from the Plane Wave Matrix Model]
- 22 T. Kimura (Yukawa Institute for Theoretical Physics, Kyoto University) 1 Nov. RIKEN Seminar [Supergravity on generalized geometry]
- 23 K. Nagata (Graduate School of Science, Hokkaido University) 14 Nov. RIKEN Seminar [Non-commutative product formulation of Exact Lattice Supersymmetry at Large N]
- 24 G. Kirilin (Budker Institute of Nuclear Physics) 5 Dec. RIKEN Seminar [Effective theories from diagrams]
- 25 Y. Kawamura (Department of Physics, Faculty of Science, Shinshu University) 6 Dec. RIKEN Seminar [Beyond Grand Unified Theories on  $Z_2$  Orbifold]
- 26 M. Sakamoto (Physics Department, Graduate School of Science, Kobe University) 6 Dec. RIKEN Seminar [Supersymmetry in Gauge/Gravity Theories with Extra Dimensions]
- 27 M. Tanabashi (Department of Physics, Nagoya University) 6 Dec. RIKEN Seminar [General Sum Rules for WW scattering in Higgsless Models]
- 28 K. Oda (Graduate School of Science/ School of Science, Osaka University) 19 Jan. RIKEN Seminar [A consistent AdS/CFT dual for time-dependent finite temperature system]
- 29 A. Hanany (Imperial College London, UK) 19 Jan. RIKEN Seminar [Brane Tilings, M2 Branes, and CS Theories]
- 30 M. Nitta (Faculty of Business and Commerce, Keio University) 23 Jan. RIKEN Seminar [Non-Abelian Vortices - Five Years Since the Discovery]
- 31 A. FURUSAKI (RIKEN NishinaCenter) 4 Feb. Colloquium [Topological Insulators]
- 32 S. Moriyama (Graduate School of Mathematics, Nagoya University) 13 Mar. RIKEN Seminar [Serre Relation and Higher Grade Generators of the AdS/CFT Yangian Symmetry]

#### Strangeness Nuclear Physics Laboratory

- 1 T. Myo (Osaka Institute of Technology) 17 Jul. Lab. Seminar [Study of role of tensor correlation in light nuclei based on the tensor-optimized shell model]
- 2 T. Nagae (Kyoto University) and others 3-6 Aug. [Summer school on exotic nuclei]
- 3 T. R. Saito, GSI and Mainz University beams at GSI (HypHI) 19 Dec. SNP Seminar [Recent progress on the hypernuclear spectroscopy with heavy ion]
- 4 H. J. Schulze (INFN, Universita di Catania) 8 Jan. Strangeness Nuclear Physics (SNP) Seminar [Hypernuclei with a Microscopic Lambda-Nucleon Force]
- 5 E. Hiyama (RIKEN Nishina Center), *et al* 27-28 Feb. [Workshop on the future of physics on quark many-body system]
- 6 S. Ishikawa (Hosei University) 16-19 Mar. Lab. Seminar [Three-body force effects in three-nucleon scattering process]

#### Accelerator Applications Research Division

- 1 K. Takagi (The Wakasa Wan Energy Research Center) 13 Jun. RIKEN Seminar [Biological effects of proton-beam irradiation]
- 2 H. Takehisa (RIKEN Nishina Center), F-S Che (Nagahama Institute of Bio-Science and Technology) 18 Jul. Radiation Biology Seminar [Mutated gene analysis using array-comparative genomic hybridization]

- 3 T. Sato (Tohoku Univ.), Y. Okumoto (Kyoto Univ.) 29 Aug. Radiation Biology Seminar [Mutant selection in paddy field is important]
- 4 Y. Kodaira (Fukushima Pref. Soma High school) Y. Kazama (RIKEN Nishina Center) 16 Sep. Radiation Biology Seminar [Educational materials for genetics using Arabidopsis mutants]
- 5 R. Sugiyama (Ajinomoto) T. Abe (RIKEN Nishina Center) 24 Oct. Radiation Biology Seminar [Potential use of heavy ion breeding for functional food factors]
- 6 A. Ferjani (Department of Education, Tokyo Gakugei University) 10 Mar. RIKEN Seminar [FUGU5/AVP1 Activity Is Essential For Early Seedling Development And Organ-Size Control In Arabidopsis]

#### RIKEN BNL Research Center

- 1 Howard Georgi (Harvard University) 23 Apr. "The Unparticle Scale"
- 2 Mikhail Shifman (University of Minnesota) 19 Nov. "From Vortices in Superconductivity to Quark Confinement"
- 3 Michele Papucci (IAS, Princeton) 25 Feb. "Dark Matter Sees the Light"

#### JUSTIPEN

- 1 Anatoli Afanasjev (Department of Physics and Astronomy, Mississippi State University) 12 May The next frontier : hyperdeformation
- 2 Carlos Bertulani (Texas A&M) 9 Jun. Pairing strength and odd-even mass differences
- 3 Betty Tsang (NSCL, Michigan State University) 18 Dec. Systematics of neutron spectroscopic factors

#### CNS

- 1 P. Roussel-Chomaz (GANIL) 2 Apr. Status of the SPIRAL 2 project at GANIL
- 2 T. Abe (CNS, University of Tokyo) 24 Jun. Lattice Calculation of Thermal Properties of Low-Density Neutron Matter with NN Effective Field Theory
- 3 P. Schuck (Orsay) 8 Oct. Alpha-particle condensation in nuclei
- 4 T. Hashimoto (CNS, University of Tokyo) 28 Oct. Direct measurements of the astrophysical nuclear reaction rates with radioactive nuclear beams
- 5 J. Miyamoto (Weizmann Institute) 30 Jan. The Thick Gas Electron Multiplier: its performance and applications
- 6 J. J. He (IMP, Lanzhou, China) 12 Mar. Some Results and Progress in Nuclear Astrophysics Research

## AUTHOR INDEX

- ABE Akira 阿部陽 288  
ABE Tomoko 阿部知子 xi, xx, 274, 277, 278, 279, 280, 281,  
282, 283, 284, 285, 286, 287, 288  
ABU-IBRAHIM Badawy 42  
ADACHI Satoshi 足立智 216  
AIDA Ryutaro 間竜太郎 281, 282  
AIHARA Toshimitsu 藍原利光 117, 118, 126, 291, 296  
AKIBA Yasuyuki 秋葉康之 68, 201, 203, 205, 207, 209, 212,  
214  
AKIYAMA Kazuhiko 秋山和彦 270  
AKIYAMA Takahiro 秋山隆宏 15  
AKIYAMA Takashi 秋山岳伸 25, 216, 221  
AL-BATAINEH Hisham 70  
ALLTON Chris 87  
AL-TA'ANI Hussein 66  
AMADIO Guilherme 21  
AMANO Ryohei 天野良平 264  
AMATO Alex 248  
ANTONIO Dave 87  
AOI Nori 青井考 3, 4, 5, 6, 7, 8, 9, 10, 11, 12, 14, 182  
AOKI Sinya 青木慎也 60  
AOKI Yasumichi 青木保道 86, 87, 88  
APADULA Nicole 4, 207  
ARAI Ichiro 新井一郎 197  
ARAMAKI Yoki 荒卷陽紀 71  
ARIYOSHI Kingo 有吉欽吾 257  
ASAHI Koichiro 旭耕一郎 22, 23, 24, 195  
ASAI Masato 浅井雅人 268  
ASANO Hidemitsu 浅野秀光 216  
AVOGADRO Paolo 50, 57  
BABA Hidetada 馬場秀忠 viii, xv, 3, 4, 6, 8, 10, 11, 12, 14,  
29, 159, 198, 199  
BABA Yutaka 馬場裕 96  
BAKULE Pavel 233, 234, 235, 236  
BALABANSKI Dimiter 22  
BARBIERI Carlo 51, 52  
BAUER Eric 238  
BAZILEVSKY Alexander 63  
BAZIN Daniel 3  
BENNETT Robert 31, 63  
BENTZ Wolfgang 80, 81  
BINH Dam 20  
BISHOP Shawn 8, 10, 11, 13, 14  
BISTA Deepak 205, 207  
BLUM Thomas 87, 88  
BLUNDELL Stephen 255  
BOYLE Kieran 34, 35  
BOYLE Peter 87  
BROWN Alex 45  
CAI Xiangzhou 11, 12, 14  
CASSANO Nicole 201, 203  
CHEN Alan 20, 21  
CHEN Jingen 12  
CHEN Jun 陈俊 20, 21  
CHERUBINI Sivio 21  
CHIBA Junsei 千葉順成 viii, xv, 29, 159, 183, 184  
CHIBA Toshiya 千葉利哉 124  
CHIBA Yoshiaki 千葉好明 124  
CHOLLET Simon 201, 203, 207  
CHRIST Norman 87  
CIANCIOLO Vince 201, 214  
CLARK Michael 87  
CLOET Ian 80, 81  
COHEN Saul 87  
DAIRAKU Seishi 37  
DAM Binh 19  
DANG NGUYEN Dinh 53, 54  
DANTSUKA Tomoyuki 段塚知志 305, 307, 311  
DATTA Amaresh 36  
DAUGAS Jean-Michel 22  
DAWSON Chris 87  
DE RYDT Marieke 22  
DEEPAK Bista 201, 203  
DEGUCHI Shigeki 出口茂樹 viii, xv, 4, 29, 159, 163  
DEPUYDT Maarten 22  
DESHPANDE Abhay 201, 214  
DION Alan 214  
DOI Kenichi 土井憲一 239  
DOMBRÁDI Zsolt 9  
DONNELLAN Michael 87  
DOORNENBAL Pieter 3, 11, 14, 182  
DRAPIER Oliver 201, 203, 207  
DREES Axel 201, 203, 207, 212  
DUAN Truong 248  
DUMITRU Adrian 85  
EBATA Shuichiro 江幡修一郎 49  
EBESU Shoichiro 胡子昇一郎 28, 216  
EGAMI Tomoaki 江上智晃 41  
ELEKES Zoltán 9, 13  
EMOTO Takashi 江本隆 xii, 196  
ENDO Natsumi 遠藤奈津美 7  
ENOKIZONO Akitomo 榎園昭智 214  
ENOMOTO Shuichi 榎本秀一 264, 268  
ENRICO Vigezzi 57

- EN'YO Hideto 延與秀人 201, 203, 205, 209, 212, 223  
 EZAKI Yutaka 江崎豊 263, 267, 268, 269, 295  
 FAMIANO Michael viii, xv, 29, 159  
 FANG Deqing 11, 12, 14  
 FITRILAWATI 256  
 FLEMING Donald 236  
 FLORES Marcos 229  
 FLYNN Jonathan 87  
 FRANCISCO Barranco 57  
 FRANCISCONI Patricia 34, 35  
 FRIES Rainer 61  
 FUJIKAKE Kotaro 藤掛浩太郎 193, 194, 231  
 FUJIKAWA Hisashi 藤川尚志 21  
 FUJIMAKI Masaki 藤巻正樹 ix, xviii, 105, 122, 148, 150, 152, 291, 296, 298  
 FUJIMORI Yasuyuki 藤森康之 i  
 FUJINAWA Tadashi 藤縄雅 150, 152, 289  
 FUJISAWA Hiroshi 藤澤博 126  
 FUJISAWA Hiroyuki 藤沢弘幸 263, 268, 269  
 FUJITA Shin 藤田新 302  
 FUJITA Yoshitaka 藤田佳孝 19  
 FUJIWARA Kohei 藤原康平 201, 203, 205, 207, 209, 212, 214  
 FUKAO Yoshinori 深尾祥紀 216, 217, 218, 221  
 FUKUDA Hiroyuki 福田弘幸 141, 302, 304  
 FUKUDA Machiko 福田真知子 283  
 FUKUDA Mitsunori 福田光順 5, 24  
 FUKUDA Naoki 福田直樹 viii, xv, 3, 4, 5, 7, 29, 157, 159, 163, 309  
 FUKUI Toshiaki 福井利晃 6, 8  
 FUKUNISHI Nobuhisa 福西暢尚 xi, xviii, 75, 105, 107, 109, 111, 113, 122, 131, 133, 135, 137, 143, 148, 150, 152, 281, 282, 284, 285, 288, 291, 293, 296, 298  
 FUKUZAWA Seiji 福澤聖児 109, 143, 293, 296  
 FÜLÖP Zsolt 9  
 FUNAKI Yasuro 船木靖郎 xvi  
 FURUKAWA Takeshi 古川武 11, 14, 187, 193, 194, 231  
 GANGNANT Patrice 177  
 GARABATOS Chilo 74  
 GASTALDI Franck 201, 203, 212  
 GAUDEFROY Laurent 22  
 GEISSEL Hans 3, 5, 75  
 GERNHÄUSER Roman 3  
 GIBELIN Julien 3, 4, 13  
 GOMI Tomoko 五味朋子 7  
 GONO Yasuyuki 郷農靖之 viii, xv, 19, 29, 159  
 GOTO Akira 後藤彰 ix, 105, 107, 115, 117, 118, 120, 126, 127, 133, 135, 147, 148, 150, 152, 291, 293, 296  
 GOTO Shin'ichi 後藤真一 i, 15, 267  
 GOTO Takayuki 後藤貴行 239, 240, 241  
 GOTO Yuji 後藤雄二 63, 223  
 GRANIER DE CASSAGNAC Raphael 201, 203, 207  
 GRÉVY Stéphane 22  
 GROSSE-PERDEKAMP Matthias 32, 33, 34, 35, 219  
 GUMPLINGER Peter 236  
 GUNJI Taku 郡司卓 68, 74  
 GUO Wei 12  
 HABA Hiromitsu 羽場宏光 i, xiii, 15, 16, 181, 263, 264, 265, 266, 267, 268, 269, 270, 271, 295  
 HACHIUMA Isao 八馬功 viii, xv, 5, 24, 29, 163  
 HAKI Yosuke 羽木洋介 201, 203, 205, 207, 212, 216  
 HAMAGAKI Hideki 浜垣秀樹 68, 74, 223  
 HAMAGAKI Manabu 浜垣学 273  
 HAMANAKA Makoto 濱仲誠 293, 296, 298  
 HARA Kaoru 原かおる 197  
 HARA Yuta 原裕太 3, 12, 14  
 HART Alistair 87  
 HASAMA Yuka 挟間優佳 22, 23, 195  
 HASEBE Hiroo 長谷部裕雄 105, 133, 135, 291, 293, 296  
 HASEBE Hisashi 長谷部尚志 203, 205  
 HASEGAWA Ken 長谷川謙 203, 205  
 HASEGAWA Satoshi 長谷川聡 288  
 HASEGAWA Taichi 長谷川太一 267  
 HASHIMOTO Kimiaki 橋本公瑛 201, 203, 207, 212  
 HASHIMOTO Koichi 橋本耕一 89  
 HASHIMOTO Koji 橋本幸士 xvii, 77, 78, 95  
 HASHIMOTO Takashi 橋本尚志 19, 20, 184  
 HASHIMOTO Yoshiko 橋本佳子 6, 7, 8  
 HASHIMOTO Yukio 橋本幸男 49, 55  
 HASUKO Kazumi 蓮子和己 33  
 HATA Maki 秦麻記 25, 216, 221  
 HATAKEYAMA Atsushi 畠山温 193, 194, 231  
 HATAKEYAMA Shin 畠山晋 277  
 HATSUDA Tetsuo 初田哲男 60  
 HAYAKAWA Seiya 早川勢也 19, 20, 21, 26  
 HAYANO Ryugo 早野龍五 75  
 HAYASHI Yoriko 林依子 xi, 274, 279, 280, 281, 282, 284, 285  
 HAYASHI Tatuya 林達也 228  
 HE Jianjun 21  
 HEFFNER Robert 238  
 HEMMI Masatake 逸見政武 xviii  
 HIDAYAT Rahmat 256  
 HIGAMI Naota 樋上直太 228  
 HIGEMOTO Wataru 髭本亘 238

- HIGURASHI Rieko 日暮(蛭沼)利江子 302  
HIGURASHI Yoshihide 日暮祥英 ix, 105, 107, 115, 117, 118, 148, 150, 152, 291, 293, 296
- HINKE Christoph 3  
HINOHARA Nobuo 日野原伸生 47  
HIRABAYASHI Kazuhiro 平林和紘 228  
HIRAYAMA Takayuki 平山貴之 78  
HIRAYAMA Yoshikazu 平山賀一 24, 25  
HIRAYAMA Yuzo 平山雄三 237  
HIROI Masahiko 廣井政彦 246  
HIROSE Kentarou 廣瀬健太郎 263  
HISAMATSU Toru 久松徹 246  
HIYAMA Emiko 肥山詠美子 59  
HJORTH-JENSEN Morten 43  
HONDA Ichiro 本多一郎 283  
HONDA Takashige 本多崇成 12, 14  
HONMA Michio 本間道雄 43, 45  
HORIBATA Takatoshi 堀端孝俊 55  
HORIGOME Atsuko 堀米敦子 302, 304  
HORIYAMA Daisuke 堀川大輔 24  
HORIUCHI Hisashi 堀内昶 xvi  
HORIUCHI Wataru 堀内渉 42  
HOSHINO Sayo 星野紗代 193  
HOSOI Motooki 細井基興 13  
HOSOTANI Yutaka 細谷裕 100  
HU Zhengguo 12  
HUYSE Mark 187  
HYODO Toshio 兵頭俊夫 226, 227  
ICHIDA Hiroyuki 市田裕之 277, 278, 279, 280, 284  
ICHIHARA Takashi 市原卓 viii, xv, 29, 159, 198, 199, 223  
ICHIKAWA Takatoshi 市川隆敏 i, xiii, 16, 56  
ICHIKAWA Yuichi 市川雄一 10, 22, 23, 24, 195  
ICHIMIYA Ryo 一宮亮 201, 203, 205, 207, 209, 212  
IDEGUCHI Eiji 井手口栄治 i, viii, xiii, xv, 8, 15, 16, 29, 159  
IEKI Kazuo 家城和夫 viii, xv, 6, 8, 11, 12, 13, 14, 28, 29, 159, 183  
IGARASHI Kimie 五十嵐きみ江 302  
IIDA Kei 飯田圭 58  
IJIMA Hiroaki 飯島裕章 23  
IIMURA Hideki 飯村秀紀 xiv, 187  
IIZUKA Satomi 飯塚里美 302  
IKEDA Naomi 池田直美 225  
IKEDA Tokihiro 池田時浩 261, 273  
IKEDA Yuki 池田友樹 25, 28, 216, 221  
IKEDO Yutaka 池戸豊 258  
IKEGAMI Kumio 池上九三男 311  
IKEZAWA Eiji 池沢英二 ix, 105, 107, 126, 131, 143, 148, 150, 152, 291, 296, 300
- IMAI Ken'ichi 今井憲一 216  
IMAI Nobuaki 今井伸明 6, 8, 10  
IMAMOTO Naoko 今本尚子 273  
INABE Naohito 稲辺尚人 viii, xv, 3, 4, 5, 29, 157, 159  
INAKURA Tsunenori 稲倉恒法 48, 49  
INOUE Hirokazu 井上弘一 277  
INOUE Rintaro 井上倫太郎 251  
INOUE Takeshi 井上壮志 23  
ISHI Naoko 石尚子 xx  
ISHIBASHI Nobuyuki 石橋延幸 96  
ISHIBASHI Yoko 石橋陽子 5, 12, 23, 24, 186  
ISHIDA Katsuhiko 石田勝彦 234, 235, 237, 259, 260, 261, 290  
ISHIDA Takayuki 石田尚行 252  
ISHIDA Yoshihisa 石田佳久 18  
ISHIHARA Masayasu 石原正泰 4, 7, 10  
ISHII Chihiro 石井千尋 viii, xv, 29, 159, 183, 184  
ISHII Ken'ichi 石井健一 xii, 196  
ISHII Kotaro 石井公太郎 xx  
ISHII Noriyoshi 石井理修 60  
ISHII Shigehisa 石井重久 xi  
ISHII Tetsuro 石井哲朗 25  
ISHII Yasuyuki 石井康之 240, 246, 253, 254  
ISHIKAWA Fumihiko 石川文洋 247  
ISHIKAWA Kazuhiro 石川和宏 13  
ISHIKAWA Shigeru 石川盛 293, 296  
ISHIKAWA Tomomi 石川智己 91  
ISHIMOTO Shigeru 石元茂 186  
ISONO Hiroshi 磯野裕 94  
ITAGAKI Naoyuki 板垣直之 39  
ITAHASHI Kenta 板橋健太 3, 75  
ITO Hiromasa 伊藤寛昌 309  
ITO Makoto 伊藤誠 39, 40  
ITO Sachiko 伊藤祥子 196  
ITO Takashi 伊藤孝 238  
ITO Takuya 伊藤拓也 80, 81  
ITO Yuta 伊藤由太 5, 12, 24, 186  
ITOH Satoshi 伊藤聖 3, 75  
IVANOV Marian 74  
IWAI Yoshio 岩井良夫 261, 273  
IWAMOTO Akira 岩本昭 56  
IWASA Naohito 岩佐直仁 11, 12, 13, 14, 21, 26  
IWASAKI Hironori 岩崎弘典 6, 8, 10, 13  
IWASAKI Masahiko 岩崎雅彦 237, 259, 261  
IWASAKI Shohei 岩崎照平 42  
IZUBUCHI Taku 出渕卓 87, 89  
IZUMI Masako 泉雅子 274, 275, 276  
IZUMIKAWA Takuji 泉川卓司 24  
JUNG Chulwoo 87

- JUTTNER Andreas 87
- KAGEYAMA Tadashi 影山正 105, 291, 293, 296, 300
- KAHL David 19, 20, 21
- KAJI Daiya 加治大哉 i, xiii, 15, 16, 179, 181, 265, 266
- KAKUTANI Nobukazu 角谷暢一 309
- KAMBARA Tadashi 神原正 225, 226, 227, 295
- KAMEDA Daisuke 亀田大輔 viii, xv, 3, 4, 5, 22, 25, 29, 157, 159
- KAMIGAITO Osamu 上垣外修一 ix, xviii, 105, 107, 113, 117, 118, 120, 122, 124, 126, 133, 135, 148, 150, 152, 291, 293, 296, 305
- KAMIMURA Masayasu 上村正康 59
- KANADA-EN'YO Yoshiko 延與佳子 47
- KANAI Yasuyuki 金井保之 xiv, 17, 18, 229, 273
- KANAMORI Issaku 金森逸作 101, 102, 103
- KANAYA Junpei 金谷淳平 201, 203, 205, 207
- KANAYA Toshiji 金谷利治 251
- KANAZAWA Yuu 金澤悠 261
- KANEKO Wakako 兼子和佳子 255
- KANESUE Takeshi 金末猛 155, 154
- KANNO Shouko 菅野祥子 3, 6, 8, 11, 12, 14
- KARATSU Ken'ichi 唐津謙一 216, 218, 221
- KASAI Miki 河西実希 201, 203, 205, 207, 209, 212, 214
- KASAMATSU Yoshitaka 笠松良崇 i, 263, 270, 271
- KASE Masayuki 加瀬昌之 ix, xviii, 105, 107, 109, 111, 113, 117, 118, 120, 122, 126, 127, 129, 131, 133, 135, 137, 139, 141, 143, 148, 150, 152, 225, 289, 291, 293, 296, 298, 300, 305, 307, 311
- KATAYAMA Ichiro 片山一郎 xiv, 17, 18, 187
- KATO Reizo 加藤礼三 254
- KATO Tetsuya 加藤徹也 243
- KATORI Kenji 鹿取謙二 i, 15
- KAWABATA Takahiro 川畑貴裕 11, 12, 14, 26, 27, 165, 169, 171, 173, 175
- KAWADA Yosuke 河田鷹介 viii, xv, 3, 4, 29, 159, 163
- KAWAI Shoko 河合祥子 7, 13
- KAWAKAMI Roland 234, 235
- KAWALL David 36
- KAWAMATA Takayuki 川股隆行 237, 241, 243, 245, 248, 249, 253, 254
- KAWAMURA Hirokazu 川村広和 23, 25, 28
- KAWANO Shigeyuki 河野重行 xx, 283, 284
- KAWANO Teruhiko 川野輝彦 97, 98
- KAWASHIMA Motohiro 川嶋基敬 203, 209
- KAWASUMI Masaya 川角昌弥 258
- KAZAMA Yusuke 風間裕介 xx, 274, 277, 279, 280, 283, 284, 285
- KAZATO Masayuki 風戸正行 193
- KENNEDY Anthony 87
- KENWAY Richard 87
- KHIEM LE Hong 21
- KIDERA Masanori 木寺正憲 ix, 105, 117, 118, 291, 293, 296
- KIKUCHI Akihiro 菊地晶裕 249
- KIKUCHI Kaori 菊地郁 283
- KIKUNAGA Hidetoshi 菊永英寿 263, 268, 269
- KIM Aram 20
- KIMURA Hitomi 木村仁美 12
- KISHIDA Takashi 岸田隆 135
- KISHIMOTO Isao 岸本功 97, 98, 99
- KITAGAWA Susumu 北川進 255
- KITATSUJI Yoshihiro 北辻章浩 271
- KITAYAMA Mitsuhisa 來山益久 7
- KOBA Takato 木庭卓人 278
- KOBAYASHI Kiyoshi 小林清志 293, 296
- KOBAYASHI Nobuyuki 小林信之 viii, xv, 3, 4, 11, 14, 29, 159
- KOBAYASHI Tohru 小林徹 193, 194, 231
- KOBAYASHI Tomohiro 小林知洋 226, 273
- KOBAYASHI Toshio 小林俊雄 7, 26
- KOBAYASHI Yoshio 小林義男 24, 260, 290
- KOBAYASHI-KOMIYAMA Misaki 小林-込山美咲 ix, 105, 145, 291, 293, 296, 298
- KOHAMA Akihisa 小濱洋央 42, 58
- KOHARA Takao 小原孝夫 250
- KOIKE Shigetoshi 小池茂年 228
- KOIKE Yoji 小池洋二 245
- KOIZUMI Ayako 小泉綾子 xx, 284
- KOJIMA Takao 小島隆夫 xiv, 17, 18, 261, 273
- KOJO Toru 古城徹 82
- KOMATSU Takuma 小松拓真 281
- KOMORI Yukiko 小森有希子 i, 266, 269
- KONDO Yosuke 近藤洋介 viii, xv, 3, 4, 6, 7, 8, 10, 11, 12, 14, 29, 159, 163
- KONO Hikaru 河野光瑠 221
- KOSHIDA Haruka 越田晴香 264
- KOTAKA Yasuteru 小高康熙 293, 296
- KOURA Hiroyuki 小浦寛之 i, xiii, 15, 16
- KOYAMA Ryo 小山亮 xviii, 120, 122, 139, 293, 296
- KOYAMA Takehide 小山岳秀 250
- KRÜCKEN Reiner 3
- KUBO Kenya 久保謙哉 260
- KUBO Toru 久保徹 24

- KUBO Toshiyuki 久保敏幸 viii, xiv, xv, 3, 4, 5, 6, 8, 10, 17, 18, 26, 29, 157, 159, 161, 165, 169, 187, 309
- KUBOKI Hironori 久保木浩功 105, 133, 135, 291, 293, 296
- KUBOKI Takamasa 久保木隆正 5, 11, 14, 24, 163
- KUBONO Shigeru 久保野茂 13, 19, 20, 21, 147, 184
- KUBOYAMA Satoshi 久保山智司 26
- KUDO Hisaaki 工藤久昭 i, 15, 267
- KUDOU Yuki 工藤祐生 i, xiii, 16, 181, 265, 266, 268, 269
- KUDRYAVTSEV Yuri 187
- KUMAGAI Keiko 熊谷桂子 105, 109, 111, 143, 296
- KUME Naoto 久米直人 11, 14
- KUREI Hiroshi 樽井博 165, 167, 171, 173, 175
- KURIHARA Yuzo 栗原佑蔵 19, 20, 21
- KURITA Kazuyoshi 栗田和好 xii, 6, 8, 10, 11, 12, 13, 14, 196, 201, 203, 205, 207, 209, 212, 214, 216
- KUROKAWA Meiko 黒川明子 11, 12, 13, 14
- KUROSAWA Maki 黒澤真城 201, 202, 203, 205, 207, 209, 211, 212, 214
- KUSAKA Kensuke 日下健祐 viii, ix, xv, 3, 4, 5, 8, 26, 29, 115, 157, 159, 300, 309
- KUWAJIMA Atsuhiko 桑島淳宏 xii, 196
- KWON YOUNG Kwan 21
- KYLE Gary 66
- LA COGNATA Marco 21
- LANCASTER Tom 255
- LANTZ Mattias 5, 163
- LEBEDEV Alexander 201
- LEE Nam 20
- LEITGAB Martin 34, 35
- LI Kuoang 李闊昂 3, 14
- LI Min 87
- LIBIN Jean-François 177
- LIN Feng-Li 78
- LIN Huey-Wen 88
- LIN Mei-Feng 87
- LIOUBIMOV Vladimir 17, 18, 191
- LIU Han 刘涵 65, 66, 70
- LIU Mingxiong 柳明雄 65, 66, 70
- LIU Wei 61
- MA LiQiu 馬立秋 277
- MA Yugang 11, 12, 14
- MAEDA Yukie 前田幸重 27
- MAESHIMA Kazuhiro 前島一博 273
- MAIE Takeshi 眞家武士 105, 109, 111, 291, 293, 296, 300, 311
- MANAKA Hirotaka 眞中浩貴 239
- MANIKONDA Shashi viii, xv, 29, 159
- MANNEL Eric 201, 203, 212, 214
- MANO Daisuke 眞野大輔 226
- MÅNSSON Martin 257
- MARU Akifumi 丸明史 225
- MATSUDA Yasuyuki 松田恭幸 233, 234, 235, 236, 259, 261
- MATSUDA Yohei 松田洋平 7
- MATSUI Nobuyuki 松井信行 7, 13
- MATSUKAWA Kazuhito 松川和人 24
- MATSUMOTO Jun 松本淳 248
- MATSUMOTO Takuma 松本琢磨 7, 41
- MATSUMURA Hiroshi 松村宏 260
- MATSUO Satoshi 松尾哲 283
- MATSUO Yukari 松尾由加利 11, 187, 193, 194, 231
- MATSUSHITA Akiyuki 松下明行 247
- MATSUSHITA Masafumi 松下昌史 viii, xv, 11, 14, 28, 29, 159, 183
- MATSUTA Kensaku 松多健策 23, 24
- MATSUURA Yuichi 松浦佑一 193, 194
- MATSUYAMA Tomoki 松山知樹 278
- MATSUZAKI Teichiro 松崎禎市郎 237, 244, 247, 251, 254, 259, 260, 261
- MAWHINNEY Robert 87
- MAYNARD Chris 87
- MENGONI Alberto 4
- MEREDITH Beau 32
- MIBE Tsutomu 三部勉 216, 218, 221
- MICHIMASA Shin'ichiro 道正新一郎 3, 14, 20, 165, 167, 171, 173, 175, 177
- MIHARA Mototsugu 三原基嗣 5, 23, 24
- MIKI Kenjiro 三木謙二郎 27, 165, 167, 171, 173, 175
- MINAMISONO Tadanori 南園忠則 23, 24
- MINEMURA Toshiyuki 峯村俊行 6, 8, 13
- MITSUOKA Shinichi 光岡真一 25
- MIURA Taichi 三浦太一 260
- MIYA Hiroyuki 宮裕之 165, 167, 171, 173, 175
- MIYAKE Kazuo 三宅和生 293, 296
- MIYAMOTO Hiroshi 宮本寛 295
- MIYAMOTO Sakiko 宮本咲紀子 285
- MIYASHITA Yuuki 宮下雄樹 5, 183, 184
- MIYOSHI Kazumitsu 三吉一光 279
- MIZOI Yutaka 溝井浩 29, 159
- NISHIMURA Mizuki-Kurata 西村美月 183
- MIZUSAKI Takahiro 水崎高浩 43, 45
- MÖLLER Peter 56
- MOMOSE Takamasa 百瀬孝昌 236
- MOMOTA Sadao 百田佐多生 5, 24
- MOON JUN Young 21
- MOREL Pascal 22
- MORIGUCHI Tetsuaki 森口哲朗 viii, xv, 5, 12, 23, 24, 29,

- 159, 186
- MORIKAWA Hitoshi 森川齊 13
- MORIMOTO Kouji 森本幸司 i, xiii, 15, 16, 179, 181, 265, 266
- MORITA Kosuke 森田浩介 i, xiii, 15, 16, 179, 181, 265, 266
- MORREALE Astrid 73
- MOTObA Toshio 元場俊雄 59
- MOTOBAYASHI Tohru 本林透 viii, xv, 3, 4, 6, 7, 8, 9, 10, 11, 12, 13, 14, 26, 29, 157, 159, 182
- MOTOHASHI Kenji 本橋健次 229
- MUFTI Nandang 242
- MUKAI Hiroki 向井弘樹 302, 304
- MUKAI Kazuhiko 向和彦 257
- MURAKAMI Hiroyuki 村上浩之 11, 12, 14
- MURAKAMI Koichi 村上公一 96
- MURAKAMI Testuya 村上哲也 26, 28, 184, 216
- MURAKAMI Yoichi 村上洋一 228
- MURATA Jiro 村田次郎 25, 28, 216, 221
- MUTOH Hideaki 武藤英明 225
- NAGAE Daisuke 長江大輔 25
- NAGAME Yuichiro 永目諭一郎 268, 270, 271
- NAGAMINE Kanetada 永嶺謙忠 233, 234, 235, 259
- NAGASE Makoto 長瀬誠 105, 143, 291, 293, 296
- NAGASHIMA Yasuyuki 長嶋泰之 226, 227
- NAGATANI Takeshi 長谷健 286, 287
- NAGATOMO Takashi 長友傑 22, 23, 24, 195
- NAKABAYASHI Takumi 中林彩 6, 7, 8
- NAKAGAKI Reiko 中垣麗子 260
- NAKAGAWA Itaru 中川格 216, 218, 221
- NAKAGAWA Takahide 中川孝秀 ix, 105, 107, 115, 117, 118, 148, 150, 152, 291, 293, 296
- NAKAI Yoichi 中井陽一 26, 28
- NAKAJIMA Saori 中島紗織 239
- NAKAJIMA Tsukasa 中島司 197
- NAKAJO Shinsuke 仲條眞介 288
- NAKAMURA Hiroyuki 中村裕之 250
- NAKAMURA Katsuro 中村克朗 216, 218, 221
- NAKAMURA Masato 中村仁音 141, 311
- NAKAMURA Risa 中村梨沙 264
- NAKAMURA Takashi 中村隆司 viii, xv, 3, 4, 6, 7, 8, 10, 11, 13, 14, 26, 29, 159
- NAKAMURA Takashi 中村貴志 17, 18, 298
- NAKAMURA Takeshi 仲村武志 223, 293, 296
- NAKAMURA Tomoaki 中村智昭 173
- NAKANISHI Kohsuke 中西康介 165, 167, 171, 175, 216
- NAKANISHI Reona 中西怜央奈 302
- NAKANO Kazushiro 中野和城 201
- NAKANO Kenichi 中野健一 203, 205, 207, 209, 211, 212, 226
- NAKANO Nobuo 中野信夫 248
- NAKANO Takehito 中野岳仁 10
- NAKAO Taro 中尾太郎 viii, xv, 3, 8, 29, 49, 159
- NAKATSUKASA Takashi 中務孝 28, 46, 48, 50
- NAKAYA Yusuke 中谷祐輔 163
- NAMIHIRA Kousuke 波平晃佑 5, 24
- NAMIKI Yuichi 並木祐一 273
- NARUSAWA Tadashi 成沢忠 60
- NEMURA Hidekatsu 根村英克 viii
- NETTELETON Anthony xv, 22, 29, 159
- NEYENS Gerda 212
- NIIKURA Megumi 新倉潤 8, 13, 25
- NINOMIYA Kazufumi 二宮一史 216, 221, 260
- NINOMIYA Kazuhiko 二宮和彦 129
- NISHIDA Minoru 西田稔 127, 283, 293, 296
- NISHIHARA Kiyoshi 西原潔 xx, 5, 284
- NISHIMURA Daiki 西村太樹 21, 24
- NISHIMURA Shunji 西村俊二 viii, xv, 3, 19, 20, 21, 28, 29, 159, 212, 243
- NISHIWAKI Youichi 西脇洋一 25
- NITTA Minori 新田稔 28, 216, 221, 309
- NOBUTOKI Minoru 信時実 27
- NOJI Shumpei 野地俊平 viii, 165, 167, 171, 175, 177
- NOLEN Jerry xv, 13, 29, 159
- NOTANI Masahiro 野谷将広 214
- NOUICER Rachid 201, 257
- NOZAKI Hiroshi 野崎洋 248, 258
- NOZUE Yasuo 野末泰夫 242
- NUGROHO Agustinus 100
- ODA Kin-ya 尾田欣也 298
- ODAGIRI Jun-ichi 小田切淳一 21
- ODAHARA Atsuko 小田原厚子 193, 231
- ODASHIMA Hitoshi 小田島仁司 41
- OGATA Kazuyuki 緒方一介 7, 33
- OGAWA Akio 小川暁生 5, 34, 35
- OGAWA Ken-ichiro 小川賢一郎 186, 201
- OGILVIE Craig 273
- OGIWARA Kiyoshi 荻原清 228, 255
- OHBA Masaaki 大場正昭 255
- OHBU Sumie 大部澄江 279, 280, 284, 285
- OHIRA-KAWAMURA Seiko 河村聖子 238
- OHISHI Kazuki 大石一城 126, 234, 235, 240, 246
- OHKI Tomonori 大木智則 5, 291, 296
- OHKUMA Yuki 大熊悠希 201
- OHNISHI Hiroaki 大西宏明 115, 203
- OHNISHI Jun-ichi 大西純一 ix, 4, 26, 105, 107, 113, 148, 150, 152, 296

- OHNISHI Tetsuya 大西哲哉 viii, xv, 3, 5, 29, 100, 157, 159,  
161, 163, 199, 309
- OHNUMA Toshihiko 大沼俊彦 296
- OHSHIRO Yukimitsu 大城幸光 93, 293
- OHTA Kazutoshi 太田和俊 87
- OHTA Shigemi 太田滋生 4, 88
- OHTAKE Masao 大竹政雄 viii, xiv, xv, 3, 5, 29, 157, 159,  
309
- OHTANI Shunsuke 大谷俊介 17, 18, 187, 230, 281
- OHTSUBO Norihiro 大坪憲弘 viii, 282
- OHTSUBO Takashi 大坪隆 xv, 5, 29, 159, 259, 263
- OHTSUKI Tsutomu 大槻勤 225
- OHYA Susumu 大矢進 257
- OHZONO Hironobu 大園浩之 12
- OHZUKU Tsutomu 小槻勉 218
- OISHI Hiroto 大石寛人 31
- OKADA Hiromi 岡田裕美 64
- OKADA Kensuke 岡田謙介 xiv, 14, 11, 12, 230
- OKADA Kunihiro 岡田邦宏 17, 18, 27, 187, 191, 226
- OKAMURA Hiroyuki 岡村弘之 154
- OKAMURA Kei 岡村圭 155
- OKAMURA Masahiro 岡村昌宏 10, 252
- OKAMURA Yoshitomo 岡村祥有 8
- OKUMURA Toshifumi 奥村俊文 6, 7, 115, 311
- OKUNO Hiroki 奥野広樹 ix, 10, 26, 105, 107, 113, 127, 129,  
133, 135, 148, 150, 152, 212, 291,  
293, 296, 300, 305, 307
- ONG Hooi Jin 王惠仁 7, 8, 10
- ONISHI Takeo 大西健夫 6, 7, 201, 203
- ONUKE Yoshiyuki 小貫良行 205, 207, 209, 212, 263, 266
- OOE Kazuhiro 大江一弘 i, 265, 268, 269, 286, 287
- OOE Masakazu 大江正和 5, 186
- OOISHI Hiroto 大石寛人 3, 24, 288
- ORR Nigel 10, 21
- OSHIMIZU Yasumi 大清水保見 13
- OTA Shinsuke 大田晋輔 4, 6, 8, 11, 12, 14, 26, 29, 159, 165,  
167, 171, 173, 175, 199
- OTSU Hideaki 大津秀暁 viii, xv, 3, 7, 29, 43, 45, 159, 163
- OTSUKA Takaharu 大塚孝治 20, 72
- OUCHIDA Misaki 大内田美沙紀 75
- OUELLET Christian 131
- OUTA Haruhiko 應田治彦 126
- OYAMADA Kazuyuki 小山田和幸 16, 58, 291, 296
- OYAMATSU Kazuhiro 親松和浩 viii
- OZAWA Akira 小沢顕 i, xiii, xv, 5, 12, 15, 16, 23, 24, 29,  
159, 186, 197, 266
- OZEKI Kazutaka 大関和貴 i, xiii, 15, 163, 181, 201, 203
- PAK Robert 201, 242
- PALSTRA THEODORAS Marie 203
- PANCAKE Charles 21, 207, 212, 214
- PEARSON Jonty 87
- PEI Hua 147
- PENDLETON Brian 22
- PEREPELKIN Evgeny 84
- PERROT Luc 21
- PETRECKZY Peter 248
- PIZZONE Rosario 253
- PRATT Francis 53, 57, 233, 234, 235, 236, 255
- QUANG HUNG Nguyen 54, 201
- RICARDO Broglia 203
- RIEDLER Petra 59, 256
- RIJKEN Thomas 240
- RISDIANA xvi, 177, 242
- RÖPKE Gerd xi
- ROUSSEL-CHOMAZ Patricia 288
- RYUTO Hiromichi 龍頭啓充 87, 135, 216, 281, 282, 284
- SACHRAJDA Chris 21
- SADA Yuta 佐田優太 13
- SAITO Akito 齋藤明登 xv, 4, 29, 159, 165, 167, 171, 173,  
175, 226, 227
- SAITO Fuminori 齋藤文修 286, 287
- SAITO Hiroyuki 齋藤宏之 216, 221
- SAITO Naohito 齋藤直人 27, 218
- SAKAGUCHI Satoshi 坂口聡志 177
- SAKAI Hideyuki 酒井英行 xvii, 165, 169, 171, 173, 175, 304
- SAKAI Tadakatsu 酒井忠勝 302
- SAKAMOTO Hisao 坂本久雄 27, 124
- SAKAMOTO Naruhiko 坂本成彦 xviii, 64, 100, 105, 113,  
120, 122, 126, 127, 129,  
291, 293, 296
- SAKAMURA Yutaka 阪村豊 28
- SAKASHITA Kohichi 坂下耕一 9
- SAKO Masami 酒向正己 10
- SAKURAI Hiroyoshi 櫻井博儀 viii, xv, 3, 4, 6, 7, 8, 12, 13,  
26, 28, 29, 69, 74, 157, 159,  
182, 183
- SANO Satoshi 佐野哲 231
- SARSOUR Murad 193
- SASAKI Ayako 佐々木彩子 194, 281, 282
- SASAKI Katsutomo 佐々木克友 87, 88
- SASAKI Shoichi 佐々木勝一 137, 309
- SASAKI Tomoyuki 佐々木知之 27
- SASAKI Yuichiro 佐々木雄一郎 159
- SASAMOTO Yoshiko 笹本良子 24, 26, 29, 165, 167, 169,  
171, 173, 175
- SATO Hiromi 佐藤広海 309
- SATO Kazuhiko 佐藤一彦 83
- SATO Kiyokazu 佐藤潔和 266

- SATO Koichi 佐藤弘一 16
- SATO Nozomi 佐藤望 i, xiii, 15, 152, 179, 181, 285
- SATO Tadashi 佐藤雅志 ix
- SATO Yoichi 佐藤洋一 107, 148, 150, 225
- SATOH Yohei 佐藤洋平 14
- SATOU Yoshiteru 佐藤義輝 viii, xv, 3, 4, 7, 11, 14, 29, 159, 182
- SCHEIT Heiko 3, 87, 249
- SCHEUERMANN Robert 54
- SCHOLZ Enno xvi
- SCHUCK Peter xiv, 230
- SCHUESSLER Hans xiv, 17, 18, 187, 189, 191
- SCHURY Peter 17, 18, 32, 187, 191, 219
- SEIDL Ralf 25, 33, 34, 35, 216
- SEITAIBASHI Etsuko 聖代橋悦子 27, 184
- SEKIGUCHI Kimiko 関口仁子 111, 201, 203
- SEKIMOTO Michiko 関本美知子 20, 201, 205, 207, 209, 212
- SETOODEH NIA Kiana 203
- SHAFTO Eugene viii, 183, 207
- SHERRILL Bradley xv, 29, 64, 226
- SHIBATA Toshiaki 柴田利明 281
- SHIGA Yuichiro 志賀雄一朗 282
- SHIKATA Masahito 四方雅仁 22, 195
- SHIMADA Kenji 島田健司 5, 225
- SHIMADA Osamu 島田修 46
- SHIMBARA Yoshihiro 新原佳弘 231
- SHIMIZU Yoshifumi 清水良文 193
- SHIMODA Tadashi 下田正 194, 233, 234
- SHIMOMURA Koichiro 下村浩一郎 13, 14, 235
- SHIMOURA Susumu 下浦享 3, 4, 6, 7, 8, 11, 12, 29, 159, 165, 167, 169, 171, 173, 175, 177, 199, 266, 271
- SHINOHARA Atsushi 篠原厚 7, 187, 260, 263, 265, 268, 269
- SHINOHARA Mayuko 篠原摩有子 193
- SHINOZUKA Tsutomu 篠塚勉 11, 14
- SHIODA Ryota 塩田良太 12, 234, 235
- SHIRAKI Ichiro 白木一郎 viii, 159
- SHIRAKI Yasutsugu 白木恭嗣 xv, 29, 183, 184, 216, 228
- SHISHIDO Toetsu 宍戸統悦 67
- SHOJI Kohei 庄司幸平 183, 184
- SIGNORINI Cosimo 201
- SONDHEIM Walter 87, 189, 212
- SONI Amarjit xiv
- SONODA Tetsu 園田哲 17, 69, 177, 187, 191
- SPITAEELS Charles 79
- STAR Collaboration 22
- STASTO Anna 249
- STÖDEL Christelle 259
- STOYKOV Alexey 124
- STRASSER Patrick xviii
- SUDA Kenji 須田健嗣 xii, 105, 113, 120, 122, 126, 196, 291, 293, 296
- SUDA Toshimi 須田利美 5, 19, 248, 289, 290
- SUEHIRO Ryuichi 末廣龍一 13
- SUGA Masaki 壽賀正城 228
- SUGAWARA Kosuke 菅原浩介 228
- SUGAWARA Takamasa 菅原孝昌 xvii
- SUGI Chika 杉千花 13
- SUGIMOTO Shigeki 杉本茂樹 7
- SUGIMOTO Takashi 杉本崇 257, 258
- SUGIYAMA Jun 杉山純 6, 8
- SUGO Ryohei 須合亮平 47, 236
- SUHARA Tadahiro 須原唯広 4
- SUKHORUKOV Oleksander viii
- SUMIKAMA Toshiyuki 炭竈聡之 xv, 3, 5, 16, 23, 29, 159, 181, 183, 184
- SUMITA Takayuki 住田貴之 i, xiii, 8, 10
- SUZUKI Daisuke 鈴木大介 6, 102, 103
- SUZUKI Hiroshi 鈴木博 13, 27
- SUZUKI Hiroshi 鈴木宏 6, 8, 23, 111, 244
- SUZUKI Hiroyuki 鈴木博之 24
- SUZUKI Kunifumi 鈴木都文 8, 10
- SUZUKI Masaru 鈴木賢 6, 248, 253
- SUZUKI Takao 鈴木栄男 13, 14, 238, 239, 240, 241, 244, 245, 246, 247, 249, 254
- SUZUKI Takeshi 鈴木健 viii, xv, 5, 24, 29, 42, 159, 226
- SUZUKI Yasuyuki 鈴木宜之 227
- SUZUKI Yoshiaki 鈴木嘉昭 5, 250
- SUZUKI Shinji 鈴木伸司 203
- TABATA Yoshikazu 田畑吉計 93
- TABUKI Masahiro 榊木正博 94
- TAI Ta-Sheng 戴大盛 28, 95, 285
- TAKADA Eiichi 高田栄一 274
- TAKADA Saori 高田沙織 244
- TAKAGI Keiichi 高城啓一 226
- TAKAGI Shigeru 高木滋 295
- TAKAHASHI Katsuo 高橋勝緒 269
- TAKAHASHI Kazuya 高橋和也 268
- TAKAHASHI Naruto 高橋成人 97, 98
- TAKAHASHI Tomohiko 高橋智彦 xiv, 189
- TAKAMINE Aiko 高峰愛子 xiv, 17, 18, 24, 187, 191
- TAKASHINA Masaaki 高階正彰 6
- TAKAYAMA Reona 高山玲央奈 263, 268
- TAKAYANAGI Toshinobu 高柳俊暢 230
- TAKEBAYASHI Akiko 武林昭子 228
- TAKECHI Maya 武智麻耶 viii, xv, 4, 5, 24, 29, 159, 163, 186
- TAKEDA Hiroyuki 竹田浩之 viii, xv, 3, 4, 5, 29, 157, 159

- TAKEHISA Hinako 竹久妃奈子 279, 280, 285  
TAKENOSHITA Yoshihisa 竹之下佳久 286, 287  
TAKESHITA Eri 竹下英里 3, 4, 6, 8, 12, 13  
TAKETANI Atsushi 竹谷篤 201, 203, 205, 207, 209, 212,  
214, 216, 218, 221  
TAKEUCHI Satoshi 武内聡 3, 4, 6, 7, 8, 10, 11, 12, 14, 182,  
199  
TAMAE Tadaaki 玉江忠明 xii, 196  
TAMAKI Mitsuru 玉城充 6, 7, 8  
TAMII Atsushi 民井淳 27  
TAMURA Jun 田村潤 154, 155  
TAMURA Masashi 田村匡史 117, 118, 126, 291, 296  
TAN Chung-I 77  
TANABE Yoichi 田邊洋一 245  
TANAKA Hidekazu 田中秀数 240, 241  
TANAKA Kana 田中佳奈 viii, xv, 3, 4, 11, 14, 29, 159  
TANAKA Kanenobu 田中鐘信 viii, xv, 3, 4, 5, 6, 8, 14, 29,  
157, 159, 161, 186  
TANAKA Naoki 田中直樹 viii, xv, 4, 29, 159  
TANAKA Shuuitsu 田中秀逸 277  
TANIDA Kiyoshi 谷田聖 216  
TANIGUCHI Akihiro 谷口秋洋 259  
TANIHATA Isao 谷畑勇夫 13  
TATSUMI Toshitaka 巽敏隆 83  
TEANEY Derek 92  
TERANISHI Takashi 寺西高 13, 21  
TERASHIMA Seiji 寺嶋靖治 77, 95  
TESHIMA Yuta 手嶋祐太 203  
THOMAS Anthony 80, 81  
THOMAS Jean-Charles 22  
TIAN Wendong 11, 14  
TJIA MAY On 242  
TOGANO Yasuhiro 梅野泰宏 3, 4, 6, 7, 8, 10, 11, 12, 13, 14,  
21, 26  
TOGAWA Manabu 外川学 201, 203, 205, 207, 209, 211,  
212, 214  
TOHSAKI Akihiro 東崎昭弘 xvi  
TOKAIRIN Hideo 東海林英夫 285  
TOKANAI Fuyuki 門叶冬樹 i, 15  
TOKIEDA Hiroshi 時枝紘史 165, 167, 171, 175, 177  
TOM Harry 233, 234, 235  
TOMITA Masanori 富田雅典 276  
TOMONO Dai 友野大 237, 261  
TORII Chihiro 鳥居千寛 xx  
TORIKAI Eiko 鳥養映子 233, 234, 235, 236  
TOYODA Takeshi 豊田健司 25, 28  
TOYOSHIMA Atsushi 豊嶋厚史 268, 270, 271  
TSUCHIHASHI Takahiro 土橋隆博 309  
TSUKADA Kazuaki 塚田和明 i, 270, 271  
TSUKADA Kazushi 塚田和司 221  
TSUKADA Teruyo 塚田晃代 274, 276  
TSUKIORI Noritoshi 月居憲俊 293, 296  
TWEEDIE Robert 87, 88  
UCHIDA Makoto 内田誠 23  
UCHIKOSHI Syouichi 打越祥一 226  
UCHIYAMA Akito 内山暁仁 126, 145, 291, 296, 298  
UEMATSU Nobuya 植松暢矢 viii, xv, 29, 159, 183, 184  
UENO Hideki 上野秀樹 viii, xv, 22, 23, 24, 29, 159, 195  
UESAKA Tomohiro 上坂友洋 27, 29, 159, 165, 167, 169,  
171, 173, 175, 177  
URUSHIBARA Shoji 漆原昌二 288  
UTSUNO Yutaka 宇都野穰 45  
UWAMINO Yoshitomo 上藁義朋 302, 304  
VAN DUPPEN Piet 187  
VAN NECK Dimitri 52  
VANDERHEYJDEN Wannes 22  
VERMEULEN Nele 22  
VINGERHOETS Pieter 22  
VOROZHTSOV Alexey 147  
VOROZHTSOV Serge 147  
VOSSSEN Anselm 34, 35  
WADA Michiharu 和田道治 xiv, 17, 18, 187, 189, 191, 230,  
273  
WAKABAYASHI Yasuo 若林泰生 19, 20, 21, 184  
WAKASUGI Masanori 若杉昌徳 xii, 196  
WAKUI Takashi 涌井崇志 187, 193  
WANG He 王赫 3  
WANG Hongwei 11, 12, 14  
WANG Jiansong 11, 12, 14  
WANG Shuo 王碩 xii, 196  
WANG Xiaorong 王曉榮 65, 66, 70  
WASHIYAMA Kohshin 鷺山幸信 264  
WATANABE Hiroshi 渡辺博 105, 139, 143  
WATANABE Hiroshi 渡邊寛 viii, xv, 29, 159, 183, 184  
WATANABE Isao 渡邊功雄 237, 239, 240, 241, 242, 243,  
244, 245, 246, 247, 248, 249,  
250, 251, 252, 253, 254, 255,  
256, 257, 258  
WATANABE Shin-ichi 渡邊伸一 139, 147  
WATANABE Shizui 渡辺静意 201, 203, 205  
WATANABE Tamaki 渡邊環 xviii, 105, 122, 137, 291, 296  
WATANABE Yasushi 渡邊康 198, 199, 223  
WATANABE Yutaka 渡邊裕 ix, 25, 107, 109, 111, 148,  
150, 152, 291, 300  
WATANABE Ryota 渡部亮太 5  
WEICK Helmut 75  
WEN Wen-Yu 温文金玉 94  
WENDONG Tian 12

WENNEKERS Jan 87  
 WIECHULA Jens 74  
 WINKLER Martin 3, 5  
 WOLLNIK Hermann 187, 189  
 YABANA Kazuhiro 矢花一浩 48, 49  
 YADOMI Kazuyoshi 矢富一慎 127, 129, 143, 293, 296  
 YAGI Eiichi 八木栄一 228  
 YAHAGI Wataru 矢作亘 263, 268, 269  
 YAHIRO Masanobu 八尋正信 41  
 YAKO Kentaro 矢向謙太郎 27  
 YAMADA Fumiko 山田文子 240, 241  
 YAMADA Kazunari 山田一成 xviii, 6, 8, 11, 12, 13, 14, 23,  
 24, 105, 111, 113, 122, 126,  
 127, 129, 141, 291, 293, 296,  
 298, 305  
 YAMADA Taiichi 山田泰一 xvi  
 YAMADA Yuh 山田裕 247  
 YAMADA Yusuke 山田雄介 11, 12, 14  
 YAMAGAMI Masayuki 山上雅之 46  
 YAMAGUCHI Hidetoshi 山口英斉 19, 20, 21, 184  
 YAMAGUCHI Hiroyasu 山口博康 281, 282  
 YAMAGUCHI Koji 山口考司 13  
 YAMAGUCHI Kyoko 山口杏子 193  
 YAMAGUCHI Takayuki 山口貴之 i, viii, xiii, xv, 5, 15, 16,  
 24, 29, 159  
 YAMAGUCHI Yorito 山口頼人 68  
 YAMAGUCHI Yoshitaka 山口由高 viii, xv, 29, 159, 161,  
 197  
 YAMAKA Shoichi 山家捷一 293  
 YAMAKI Tsutomu 八巻務 302  
 YAMAMOTO Yasuo 山本安夫 59  
 YAMAMOTO Yoshihiro 山本純太 209  
 YAMANAKA Kahori 山中香 xx, 284  
 YAMAUCHI Hiromoto 山内啓資 126, 291, 296, 298  
 YAMAZAKI Norio 山崎則夫 165, 167, 169  
 YAMAZAKI Takeshi 山崎剛 87, 88  
 YAMAZAKI Yasunori 山崎泰規 xiv, 17, 18, 187, 189, 229,  
 261, 273  
 YANAGISAWA Yoshiyuki 柳澤善行 viii, xv, 3, 4, 5, 7, 10,  
 13, 29, 157, 159, 161,  
 165, 169, 309  
 YANO Yasushige 矢野安重 ix, xviii, 1, 126, 133, 135, 137,  
 150, 152, 157, 196, 291, 293,  
 296, 305, 309  
 YASUDA Yusuke 安田裕介 5, 12, 186, 197  
 YEE Ho-Ung 78  
 YOKKAICHI Satoshi 四日市悟 223  
 YOKOUCHI Shigeru 横内茂 105, 113, 127, 129, 131, 135,  
 150, 152, 291, 293, 296  
 YOKOYAMA Koji 横山幸司 233, 234, 235  
 YONEDA Akira 米田晃 i, xiii, 15, 16, 181, 266  
 YONEDA Ken-ichiro 米田健一郎 3, 4, 11, 12, 14, 26  
 YOSHIDA Atsushi 吉田敦 i, viii, xiii, xiv, xv, 3, 4, 5, 15, 16,  
 17, 18, 29, 157, 159, 161, 179,  
 187, 304, 309  
 YOSHIDA Hiroshi 吉田宏 288  
 YOSHIDA Kenichi 吉田賢市 44  
 YOSHIDA Koichi 吉田光一 viii, xv, 3, 4, 5, 29, 157, 159,  
 199, 304, 309  
 YOSHIDA Tomohiro 吉田知紘 165, 171, 175  
 YOSHIDA Toru 吉田徹 228  
 YOSHII Hideakira 吉井秀彬 viii, xv, 29, 159, 183, 184  
 YOSHIMI Akihiro 吉見彰洋 viii, xv, 22, 23, 24, 29, 159, 195  
 YOSHIMURA Takashi 吉村崇 268, 269, 270  
 YOSHINAGA Kenta 吉永健太 viii, xv, 5, 29, 159, 183, 184  
 YOSHINO Akira 吉野亮 165, 167, 169  
 ZANOTTI James 87, 88

## RIKEN Accelerator Progress Report vol. 42

独立行政法人理化学研究所加速器年次報告 第42巻 (2009)

---

印刷 平成21年 (2009) 9月30日  
発行 平成21年 (2009) 9月30日

発行者 独立行政法人理化学研究所 仁科加速器研究センター

代表者 矢野安重

〒351-0198 埼玉県和光市広沢2番1号  
電話 (048) 462-1111

編集者 独立行政法人理化学研究所 仁科加速器研究センター  
加速器年次報告編集委員会

印刷所 藤庄印刷株式会社

〒990-0821 山形県山形市北町一丁目3-1

---